Astro

MAR 2 2 1984

VOLUME 22 / NUMBER 3
FEBRUARY 8, 1984
ACC. NOS. N84-12027 TO N84-13135

ASTRONOMY
TL
501
.S42
V.22
NO3

ROOM USE ONLY

STAR
AN ABSTRACT JOURNAL

Scientific and Technical Aerospace Reports

The University of Michigan Astronomy Library

The University of Michigan Astronomy

PRODUCED BY THE SCIENTIFIC AND TECHNICAL INFORMATION BRANCH

NASA

NATIONAL AERONAUTICS AND SPACE ADMINISTRATION

WHAT YOU CAN DO FOR *STAR*

All users of this abstract service are urged to forward reports to be considered for announcement in *STAR*. This will aid NASA in its efforts to provide the fullest possible coverage of all scientific and technical publications that might support aeronautics and space research and development. If you have prepared relevant reports (other than those that you will transmit to NASA, DoD, or DOE through the usual contract- or grant-reporting channels), please send them for consideration to the NASA Scientific and Technical Information Facility, P.O. Box 8757, B.W.I. Airport, Maryland 21240.

Reprints of journal articles, book chapters, and conference papers are also welcome. These will be considered for announcement in *STAR's* companion journal, *International Aerospace Abstracts*.

You may specify a particular source to be included in a report announcement if you wish; otherwise the report will be placed on public sale at the National Technical Information Service. Copyrighted publications will be announced but not distributed or sold.

PURCHASE OF *STAR*

The semimonthly issues are available postpaid on subscription and in single copy from the Superintendent of Documents, United States Government Printing Office, Washington, D.C. 20402, United States of America.

Semimonthly issues...

Annual subscription rates: $90.00 domestic; $112.00 foreign. Price per single copy: $4.75 domestic; $5.95 foreign.

Annual index issues...

Pricing based upon pagination.

Domestic subscription rates...

Apply to the United States, Canada, Mexico, and all Central and South American countries, except as noted below.

Foreign subscription rates...

Apply to Argentina, Brazil, French Guiana, Guyana, Surinam, Belize, and all other countries throughout the world.

Payment should be by check, money order, or document coupons, and must accompany order. Remittances from foreign countries should be made by international money order or draft on an American bank, payable to the Superintendent of Documents, or by UNESCO book coupons.

PUBLISHED BY:

UNITED STATES GOVERNMENT
NATIONAL AERONAUTICS AND SPACE ADMINISTRATION
SCIENTIFIC AND TECHNICAL INFORMATION BRANCH
Scientific and Technical Aerospace Reports, Volume 22, is prepared by the NASA Scientific and Technical Information Facility operated for the National Aeronautics and Space Administration by PRC Government Information Systems.

The Administrator of the National Aeronautics and Space Administration has determined that the publication of this periodical is necessary in the transaction of the public business required by law of this Agency. Use of funds for printing this periodical has been approved by the Director of the Office of Management and Budget through February 28, 1985.

US ISSN 0036-8741

INTRODUCTION

Scientific and Technical Aerospace Reports (STAR) is a major component of a comprehensive National Aeronautics and Space Administration information system covering aeronautics, space, and supporting disciplines. *STAR* is issued on the 8th and 23rd of each month and announces current publications of the following types:

- NASA, NASA contractor, and NASA grantee reports
- Reports issued by other U.S. Government agencies, domestic and foreign institutions, universities, and private firms
- Translations in report form
- NASA-owned patents and patent applications
- Dissertations and theses

Cumulative index volumes are published annually.

Journal, book, and conference literature, cover-to-cover journal translations, and certain foreign dissertations are announced in a companion journal, *International Aerospace Abstracts (IAA)*, available on subscription from the American Institute of Aeronautics and Astronautics, Technical Information Service, 555 West 57th Street, 12th Floor, New York, New York 10019.

SUBJECT SCOPE

Subject scope of *STAR*, and *IAA* includes all aspects of aeronautics and space research and development, supporting basic and applied research, and applications. Aerospace aspects of earth resources, energy development, conservation, oceanography, environmental protection, urban transportation, and other topics of high national priority are also covered.

OTHER NASA PUBLICATIONS

Other NASA publications and information services are described in the publication, *The NASA Scientific and Technical Information System ... and How to Use It*, available without charge from the NASA Scientific and Technical Information Facility, P.O. Box 8757, B.W.I. Airport, Maryland 21240.

10_{84} 291AA2 $_2$ 013_1 XL_3 2713

HOW TO USE *STAR* SUBJECT CATEGORIES

STAR is categorized by 10 major subject divisions divided into 74 specific subject categories and one general category/division. The major subject divisions are listed in the Table of Contents, together with a note for each that defines its scope and provides any cross-references. For example:

AERONAUTICS

Includes aeronautics (general); aerodynamics; air transportation and safety; aircraft communications and navigation; aircraft design, testing and performance; aircraft instrumentation; aircraft propulsion and power; aircraft stability and control; and research and support facilities (air).

For related information see also *Astronautics*.

Each major division is further divided into as many as nine specific categories, which are identified by category numbers.

Abstracts in *STAR* are grouped by specific category, the categories appearing in sequential order. Category breaks in the abstract section are identified by the category number and title, and a scope note. Cross-references to other categories are provided as appropriate. For example:

02 AERODYNAMICS

Includes aerodynamics of bodies, combinations, wings, rotors, and control surfaces; and internal flow in ducts and turbomachinery.

For related information see also *34 Fluid Mechanics and Heat Transfer*.

CROSS-REFERENCES

Individual *STAR* abstracts are not ordinarily cross-referenced, except for certain conference reports or book translations that have had separate abstracts written for their component papers or chapters. Citations and abstracts of the components follow immediately after those of the parent document. When the subject content of a component differs sufficiently from the general content of the parent, a cross-reference citation also is printed at the end of the category to which it normally would have been assigned if it were independent.

DOCUMENTS ON MICROFICHE

Documents on microfiche(1) are designated by a pound sign (#) following the accession number. The pound sign is used without regard to the source or quality of the microfiche.

AVAILABILITIES

One or more sources from which a document announced in *STAR* is available to the public is given in each citation. The most commonly indicated sources and their acronyms or abbreviations are listed below. If the publication is available from a source other than those listed, the publisher and his address will be displayed on the availability line or in combination with the corporate source line.

(1) A microfiche is a transparent sheet of film, 105 by 148 mm in size, containing as many as 60 to 98 pages of information reduced to micro images (not to exceed 26:1 reduction).

Avail: NTIS. Sold by the National Technical Information Service. Prices for hard copy (HC) and microfiche (MF) are indicated by a price code following the letters HC or MF in the *STAR* citation. Current values for the price codes are given in the tables on page vii.

Initially distributed microfiche under the NTIS SRIM (Selected Research in Microfiche) is available at greatly reduced unit prices. For this service and for information concerning subscription to NASA printed reports, consult the NTIS Subscription Section, Springfield, Va. 22161.

NOTE ON ORDERING DOCUMENTS: When ordering NASA publications (those followed by the * symbol), use the N accession number. NASA patent applications (only the specifications are offered) should be ordered by the US-Patent-Appl-SN number. Non-NASA publications (no asterisk) should be ordered by the AD, PB, or other *report* number shown on the last line of the citation, not by the N accession number. It is also advisable to cite the title and other bibliographic identification.

Avail: SOD (or GPO). Sold by the Superintendent of Documents, U.S. Government Printing Office, in hard copy. The current price and order number are given following the availability line. (NTIS will fill microfiche requests, as indicated above, for those documents identified by a # symbol.)

Avail: NASA Public Document Rooms. Documents so indicated may be examined at or purchased from the National Aeronautics and Space Adminstration, Public Documents Room (Room 126), 600 Independence Ave., S.W., Washington, D.C. 20546, or public document rooms located at each of the NASA research centers, the NASA Space Technology Laboratories, and the NASA Pasadena Office at the Jet Propulsion Laboratory.

Avail: DOE Depository Libraries. Organizations in U.S. cities and abroad that maintain collections of Department of Energy reports, usually in microfiche form, are listed in *Energy Research Abstracts*. Services available from the DOE and its depositories are described in a booklet, *DOE Technical Information Center - Its' Functions and Services* (TID-4660), which may be obtained without charge from the DOE Technical Information Center.

Avail: Univ. Microfilms. Documents so indicated are dissertations selected from *Dissertation Abstracts* and are sold by University Microfilms as xerographic copy (HC) and microfilm. All requests should cite the author and the Order Number as they appear in the citation.

Avail: USGS. Originals of many reports from the U.S. Geological Survey, which may contain color illustrations, or otherwise may not have the quality of illustrations preserved in the microfiche or facsimile reproduction, may be examined by the public at the libraries of the USGS field offices whose addresses are listed in this Introduction. The libraries may be queried concerning the availability of specific documents and the possible utilization of local copying services, such as color reproduction.

Avail: HMSO. Publications of Her Majesty's Stationery Office are sold in the U.S. by Pendragon House, Inc. (PHI), Redwood City, California. The U.S. price (including a service and mailing charge) is given, or a conversion table may be obtained from PHI.

Avail: BLL (formerly NLL): British Library Lending Division, Boston Spa, Wetherby, Yorkshire, England. Photocopies available from this organization at the price shown. (If none is given, inquiry should be addressed to the BLL.)

Avail: Fachinformationszentrum, Karlsruhe. Sold by the Fachinformationszentrum Energie, Physik, Mathematik GMBH, Eggenstein Leopoldshafen, Federal Republic of Germany, at the price shown in deutschmarks (DM).

Avail: Issuing Activity, or Corporate Author, or no indication of availability. Inquiries as to the availability of these documents should be addressed to the organization shown in the citation as the corporate author of the document.

Avail: U.S. Patent and Trademark Office. Sold by Commissioner of Patents and Trademarks, U.S. Patent and Trademark Office, at the standard price of 50 cents each, postage free. (See discussion of patents and patent applications below.)

Avail: ESDU. Pricing information on specific data items, computer programs, and details on ESDU topic categories can be obtained from ESDU International Ltd. Requesters in North America should use the Virginia address while all other requesters should use the London address, both of which are on page vi.

NASA PATENTS AND PATENT APPLICATIONS

Patents and patent applications owned by NASA are announced in *STAR* under appropriate subject categories and are referenced in the *STAR* indexes. In the Report/Accession Number Index, patents are indexed by the NASA Case Number (which appears in lieu of the report number in other indexes), the U.S. Patent Number, the U.S. Patent Application Serial Number, and the U.S. Patent Class. Patent applications for which patents have not yet been issued are indexed by the NASA Case Number and the U.S. Patent Application Serial Number.

NASA *patent application specifications* are sold in paper copy by the National Technical Information Service at price code A02 ($7.00 domestic; $14.00 foreign). Microfiche are sold at price code A01 ($4.50 domestic; $9.00 foreign). The US-Patent-Appl-SN- number should be used in ordering either paper copy or microfiche from NTIS. Printed copies of *patents* (which are not microfiched) are available for purchase at 50 cents per copy from:

Commissioner of Patents and Trademarks
U.S. Patent and Trademark Office
Washington, D.C. 20231

When ordering patents, the U.S. Patent Number should be used, and payment must be remitted in advance, preferably by money order or check payable to the Commissioner of Patents and Trademarks. Prepaid purchase coupons for ordering are also available from the Patent and Trademark Office. The patents and patent applications announced in *STAR* are owned by NASA and are available for royalty-free licensing. Requests for licensing terms and further information should be addressed to:

Assistant General Counsel for Patent Matters/Code GP-1
National Aeronautics and Space Administration
Washington, D.C. 20546

ELIGIBILITY AND REGISTRATION FOR NASA INFORMATION PRODUCTS AND SERVICES

A variety of services is available to organizations of the following types that have registered with NASA to receive specific services or products:

1. NASA offices, research centers, contractors, subcontractors, grantees, and consultants;
2. Other U.S. Government agencies and their contractors;
3. Libraries in the United States that have arrangements with NASA to maintain collections of NASA documents for public reference;
4. Other organizations in the United States having a need for NASA documents in work related to aeronautics and space research;
5. Organizations abroad that have established reciprocal document exchange arrangements with NASA.

Only the central service points or central points of document acquisition and control within qualified organizations are eligible to register for NASA products and services. Domestic organizations that may be eligible to receive various classes of NASA publications and services should address their requests for registration or for further information to:

NASA Scientific and Technical Information Facility
ATTN: Registration Activity
P.O. Box 8757
B.W.I. Airport, Maryland 21240

Organizations abroad should direct requests to the same address, but to the attention of: International Exchange Program.

AVAILABILITY OF *STAR* ABSTRACTS ON MICROFICHE

Microfiche of the abstract sections of this issue and other issues of *STAR* are available on annual subscription from NTIS, Attn: Subscriptions, 5285 Port Royal Road, Springfield, Virginia 22161. Annual subscription rates are $60.00 North America; $120 00 foreign. Abstract sections for previous years retroactive to 1964 are available at the current rates. Microfiche for individual *STAR* issue abstract sections are not available.

ADDRESSES OF ORGANIZATIONS

American Institute of Aeronautics and Astronautics
Technical Information Service
555 West 57th Street, 12th Floor
New York, New York 10019

British Library Lending Division,
Boston Spa, Wetherby, Yorkshire,
England

Commissioner of Patents and Trademarks
U.S. Patent and Trademark Office
Washington, D.C. 20231

Department of Energy
Technical Information Center
P.O. Box 62
Oak Ridge, Tennessee 37830

ESA-Information Retrieval Service
ESRIN
Via Galileo Galilei
00044 Frascati (Rome) Italy

ESDU International, Ltd.
1495 Chain Bridge Road
McLean, Virginia 22101

ESDU International, Ltd.
251-259 Regent Street
London, W1R 7AD, England

Fachinformationszentrum Energie, Physik, Mathematik GMBH
7514 Eggenstein Leopoldshafen
Federal Republic of Germany

Her Majesty's Stationery Office
P.O. Box 569, S.E. 1
London, England

NASA Scientific and Technical Information Facility
P.O. Box 8757
B.W.I. Airport, Maryland 21240

National Aeronautics and Space Administration
Scientific and Technical Information Branch (NIT-1)
Washington, D.C. 20546

National Technical Information Service
5285 Port Royal Road
Springfield, Virginia 22161

Pendragon House, Inc.
899 Broadway Avenue
Redwood City, California 94063

Superintendent of Documents
U.S. Government Printing Office
Washington, D.C. 20402

University Microfilms
A Xerox Company
300 North Zeeb Road
Ann Arbor, Michigan 48106

University Microfilms, Ltd.
Tylers Green
London, England

U.S. Geological Survey Library
National Center – MS 950
12201 Sunrise Valley Drive
Reston, Virginia 22092

U.S. Geological Survey Library
2255 North Gemini Drive
Flagstaff, Arizona 86001

U.S. Geological Survey
345 Middlefield Road
Menlo Park, California 94025

U.S. Geological Survey Library
Box 25046
Denver Federal Center, MS 914
Denver, Colorado 80225

NTIS PRICE SCHEDULES

Schedule A

STANDARD PAPER COPY PRICE SCHEDULE

(Effective January 1, 1983)

Price Code	Page Range	North American Price	Foreign Price
A01	Microfiche	$ 4.50	$ 9.00
A02	001-025	7.00	14.00
A03	026-050	8.50	17.00
A04	051-075	10.00	20.00
A05	076-100	11.50	23.00
A06	101-125	13.00	26.00
A07	126-150	14.50	29.00
A08	151-175	16.00	32.00
A09	176-200	17.50	35.00
A10	201-225	19.00	38.00
A11	226-250	20.50	41.00
A12	251-275	22.00	44.00
A13	276-300	23.50	47.00
A14	301-325	25.00	50.00
A15	326-350	26.50	53.00
A16	351-375	28.00	56.00
A17	376-400	29.50	59.00
A18	401-425	31.00	62.00
A19	426-450	32.50	65.00
A20	451-475	34.00	68.00
A21	476-500	35.50	71.00
A22	501-525	37.00	74.00
A23	526-550	38.50	77.00
A24	551-575	40.00	80.00
A25	576-600	41.50	83.00
A99	601-up	-- 1	-- 2

1/ Add $1.50 for each additional 25 page increment or portion thereof for 601 pages up.

2/ Add $3.00 for each additional 25 page increment or portion thereof for 601 pages and more.

Schedule E

EXCEPTION PRICE SCHEDULE

Paper Copy & Microfiche

Price Code	North American Price	Foreign Price
E01	$ 6.50	$ 13.50
E02	7.50	15.50
E03	9.50	19.50
E04	11.50	23.50
E05	13.50	27.50
E06	15.50	31.50
E07	17.50	35.50
E08	19.50	39.50
E09	21.50	43.50
E10	23.50	47.50
E11	25.50	51.50
E12	28.50	57.50
E13	31.50	63.50
E14	34.50	69.50
E15	37.50	75.50
E16	40.50	81.50
E17	43.50	88.50
E18	46.50	93.50
E19	51.50	102.50
E20	61.50	123.50
E-99 - Write for quote		
N01	35.00	45.00

VOLUME 22 NUMBER 3/FEBRUARY 8, 1984

TABLE OF CONTENTS

AERONAUTICS

Includes aeronautics (general); aerodynamics; air transportation and safety; aircraft communications and navigation; aircraft design, testing and performance; aircraft instrumentation; aircraft propulsion and power; aircraft stability and control; and research and support facilities (air).

For related information see also *Astronautics*.

01 AERONAUTICS (GENERAL) 311

02 AERODYNAMICS 319

Includes aerodynamics of bodies, combinations, wings, rotors, and control surfaces; and internal flow in ducts and turbomachinery.

For related information see also *34 Fluid Mechanics and Heat Transfer*

03 AIR TRANSPORTATION AND SAFETY 328

Includes passenger and cargo air transport operations; and aircraft accidents.

For related information see also *16 Space Transportation* and *85 Urban Technology and Transportation.*

04 AIRCRAFT COMMUNICATIONS AND NAVIGATION 329

Includes digital and voice communication with aircraft; air navigation systems (satellite and ground based); and air traffic control.

For related information see also *17 Spacecraft Communications, Command and Tracking* and *32 Communications.*

05 AIRCRAFT DESIGN, TESTING AND PERFORMANCE 330

Includes aircraft simulation technology.

For related information see also *18 Spacecraft Design, Testing and Performance* and *39 Structural Mechanics.*

06 AIRCRAFT INSTRUMENTATION 332

Includes cockpit and cabin display devices; and flight instruments.

For related information see also *19 Spacecraft Instrumentation* and *35 Instrumentation and Photography.*

07 AIRCRAFT PROPULSION AND POWER 333

Includes prime propulsion systems and systems components, e.g., gas turbine engines and compressors; and on-board auxiliary power plants for aircraft.

For related information see also *20 Spacecraft Propulsion and Power, 28 Propellants and Fuels,* and *44 Energy Production and Conversion.*

08 AIRCRAFT STABILITY AND CONTROL 336

Includes aircraft handling qualities; piloting; flight controls; and autopilots.

09 RESEARCH AND SUPPORT FACILITIES (AIR) 338

Includes airports, hangars and runways; aircraft repair and overhaul facilities; wind tunnels; shock tube facilities; and engine test blocks.

For related information see also *14 Ground Support Systems and Facilities (Space).*

ASTRONAUTICS

Includes astronautics (general); astrodynamics; ground support systems and facilities (space); launch vehicles and space vehicles; space transportation; spacecraft communications, command and tracking; spacecraft design, testing and performance; spacecraft instrumentation; and spacecraft propulsion and power.

For related information see also *Aeronautics*

12 ASTRONAUTICS (GENERAL) 338

For extraterrestrial exploration see *91 Lunar and Planetary Exploration.*

13 ASTRODYNAMICS N.A.

Includes powered and free-flight trajectories; and orbit and launching dynamics.

14 GROUND SUPPORT SYSTEMS AND FACILITIES (SPACE) 339

Includes launch complexes, research and production facilities; ground support equipment, e.g., mobile transporters; and simulators.

For related information see also *09 Research and Support Facilities (Air).*

15 LAUNCH VEHICLES AND SPACE VEHICLES 340

Includes boosters; manned orbital laboratories; reusable vehicles; and space stations.

16 SPACE TRANSPORTATION 341

Includes passenger and cargo space transportation, e.g., shuttle operations; and rescue techniques.

For related information see also *03 Air Transportation and Safety* and *85 Urban Technology and Transportation.*

17 SPACECRAFT COMMUNICATION, COMMAND AND TRACKING N.A.

Includes telemetry; space communications networks; astronavigation; and radio blackout.

For related information see also *04 Aircraft Communications and Navigation* and *32 Communications.*

18 SPACECRAFT DESIGN, TESTING AND PERFORMANCE 341

Includes spacecraft thermal and environmental control; and attitude control.

For life support systems see *54 Man/System Technology and Life Support.* For related information see also *05 Aircraft Design, Testing and Performance* and *39 Structural Mechanics.*

19 SPACECRAFT INSTRUMENTATION 342

For related information see also *06 Aircraft Instrumentation* and *35 Instrumentation and Photography.*

20 SPACECRAFT PROPULSION AND POWER 343

Includes main propulsion systems and components, e.g., rocket engines; and spacecraft auxiliary power sources.

For related information see also *07 Aircraft Propulsion and Power, 28 Propellants and Fuels,* and *44 Energy Production and Conversion.*

CHEMISTRY AND MATERIALS

Includes chemistry and materials (general); composite materials; inorganic and physical chemistry; metallic materials; nonmetallic materials; and propellants and fuels.

23 CHEMISTRY AND MATERIALS (GENERAL) 346
Includes biochemistry and organic chemistry.

24 COMPOSITE MATERIALS 347
Includes laminates.

25 INORGANIC AND PHYSICAL CHEMISTRY 348
Includes chemical analysis, e.g., chromatography; combustion theory; electrochemistry; and photochemistry.
For related information see also *77 Thermodynamics and Statistical Physics.*

26 METALLIC MATERIALS 352
Includes physical, chemical, and mechanical properties of metals, e.g., corrosion; and metallurgy.

27 NONMETALLIC MATERIALS 355
Includes physical, chemical, and mechanical properties of plastics, elastomers, lubricants, polymers, textiles, adhesives, and ceramic materials.

28 PROPELLANTS AND FUELS 357
Includes rocket propellants, igniters, and oxidizers; storage and handling; and aircraft fuels.
For related information see also *07 Aircraft Propulsion and Power, 20 Spacecraft Propulsion and Power,* and *44 Energy Production and Conversion.*

ENGINEERING

Includes engineering (general); communications; electronics and electrical engineering; fluid mechanics and heat transfer; instrumentation and photography; lasers and masers; mechanical engineering; quality assurance and reliability; and structural mechanics.
For related information see also *Physics.*

31 ENGINEERING (GENERAL) 358
Includes vacuum technology; control engineering; display engineering; and cryogenics.

32 COMMUNICATIONS 359
Includes land and global communications; communications theory; and optical communications.
For related information see also *04 Aircraft Communications and Navigation* and *17 Spacecraft Communications, Command and Tracking.*

33 ELECTRONICS AND ELECTRICAL ENGINEERING 366
Includes test equipment and maintainability; components, e.g., tunnel diodes and transistors; microminiaturization; and integrated circuitry.
For related information see also *60 Computer Operations and Hardware* and *76 Solid-State Physics.*

34 FLUID MECHANICS AND HEAT TRANSFER 370
Includes boundary layers; hydrodynamics; fluidics; mass transfer; and ablation cooling.
For related information see also *02 Aerodynamics* and *77 Thermodynamics and Statistical Physics.*

35 INSTRUMENTATION AND PHOTOGRAPHY 375
Includes remote sensors; measuring instruments and gages; detectors; cameras and photographic supplies; and holography.
For aerial photography see *43 Earth Resources.* For related information see also *06 Aircraft Instrumentation* and *19 Spacecraft Instrumentation.*

36 LASERS AND MASERS 378
Includes parametric amplifiers.

37 MECHANICAL ENGINEERING 382
Includes auxiliary systems (non-power); machine elements and processes; and mechanical equipment.

38 QUALITY ASSURANCE AND RELIABILITY 385
Includes product sampling procedures and techniques; and quality control.

39 STRUCTURAL MECHANICS 386
Includes structural element design and weight analysis; fatigue; and thermal stress.
For applications see *05 Aircraft Design, Testing and Performance* and *18 Spacecraft Design, Testing and Performance.*

GEOSCIENCES

Includes geosciences (general); earth resources; energy production and conversion; environment pollution; geophysics; meteorology and climatology; and oceanography.
For related information see also *Space Sciences.*

42 GEOSCIENCES (GENERAL) N.A.

43 EARTH RESOURCES 392
Includes remote sensing of earth resources by aircraft and spacecraft; photogrammetry; and aerial photography.
For instrumentation see *35 Instrumentation and Photography.*

44 ENERGY PRODUCTION AND CONVERSION 403
Includes specific energy conversion systems, e.g., fuel cells and batteries; global sources of energy; fossil fuels; geophysical conversion; hydroelectric power; and wind power.
For related information see also *07 Aircraft Propulsion and Power, 20 Spacecraft Propulsion and Power, 28 Propellants and Fuels,* and *85 Urban Technology and Transportation.*

45 ENVIRONMENT POLLUTION 406
Includes air, noise, thermal and water pollution; environment monitoring; and contamination control.

46 GEOPHYSICS 406
Includes aeronomy; upper and lower atmosphere studies; ionospheric and magnetospheric physics; and geomagnetism.
For space radiation see *93 Space Radiation.*

47 METEOROLOGY AND CLIMATOLOGY 409
Includes weather forecasting and modification.

48 OCEANOGRAPHY 413
Includes biological, dynamic and physical oceanography; and marine resources.

LIFE SCIENCES

Includes sciences (general); aerospace medicine; behavioral sciences; man/system technology and life support; and planetary biology.

51 LIFE SCIENCES (GENERAL) **413**
Includes genetics.

52 AEROSPACE MEDICINE **415**
Includes physiological factors; biological effects of radiation; and weightlessness.

53 BEHAVIORAL SCIENCES **416**
Includes psychological factors; individual and group behavior; crew training and evaluation; and psychiatric research.

54 MAN/SYSTEM TECHNOLOGY AND LIFE SUPPORT **417**
Includes human engineering; biotechnology; and space suits and protective clothing.

55 PLANETARY BIOLOGY **N.A.**
Includes exobiology; and extraterrestrial life.

MATHEMATICAL AND COMPUTER SCIENCES

Includes mathematical and computer sciences (general); computer operations and hardware; computer programming and software; computer systems; cybernetics; numerical analysis; statistics and probability; systems analysis; and theoretical mathematics.

59 MATHEMATICAL AND COMPUTER SCIENCES (GENERAL) **417**

60 COMPUTER OPERATIONS AND HARDWARE **418**
Includes computer graphics and data processing.
For components see *33 Electronics and Electrical Engineering.*

61 COMPUTER PROGRAMMING AND SOFTWARE **419**
Includes computer programs, routines, and algorithms.

62 COMPUTER SYSTEMS **423**
Includes computer networks.

63 CYBERNETICS **423**
Includes feedback and control theory.
For related information see also *54 Man/System Technology and Life Support.*

64 NUMERICAL ANALYSIS **424**
Includes iteration, difference equations, and numerical approximation.

65 STATISTICS AND PROBABILITY **427**
Includes data sampling and smoothing; Monte Carlo method; and stochastic processes.

66 SYSTEMS ANALYSIS **428**
Includes mathematical modeling; network analysis; and operations research.

67 THEORETICAL MATHEMATICS **N.A.**
Includes topology and number theory.

PHYSICS

Includes physics (general); acoustics; atomic and molecular physics; nuclear and high-energy physics; optics; plasma physics; solid-state physics; and thermodynamics and statistical physics.
For related information see also *Engineering.*

70 PHYSICS (GENERAL) **429**
For geophysics see *46 Geophysics.* For astrophysics see *90 Astrophysics.* For solar physics see *92 Solar Physics.*

71 ACOUSTICS **430**
Includes sound generation, transmission, and attenuation.
For noise pollution see *45 Environment Pollution.*

72 ATOMIC AND MOLECULAR PHYSICS **432**
Includes atomic structure and molecular spectra.

73 NUCLEAR AND HIGH-ENERGY PHYSICS **437**
Includes elementary and nuclear particles; and reactor theory.
For space radiation see *93 Space Radiation.*

74 OPTICS **440**
Includes light phenomena.

75 PLASMA PHYSICS **443**
Includes magnetohydrodynamics and plasma fusion.
For ionospheric plasmas see *46 Geophysics.* For space plasmas see *90 Astrophysics.*

76 SOLID-STATE PHYSICS **451**
Includes superconductivity.
For related information see also *33 Electronics and Electrical Engineering* and *36 Lasers and Masers.*

77 THERMODYNAMICS AND STATISTICAL PHYSICS **456**
Includes quantum mechanics; and Bose and Fermi statistics.
For related information see also *25 Inorganic and Physical Chemistry* and *34 Fluid Mechanics and Heat Transfer.*

SOCIAL SCIENCES

Includes social sciences (general); administration and management; documentation and information science; economics and cost analysis; law and political science; and urban technology and transportation.

80 SOCIAL SCIENCES (GENERAL) **457**
Includes educational matters.

81 ADMINISTRATION AND MANAGEMENT **457**
Includes management planning and research.

82 DOCUMENTATION AND INFORMATION SCIENCE 458
Includes information storage and retrieval technology; micrography; and library science.
For computer documentation see *61 Computer Programming and Software.*

83 ECONOMICS AND COST ANALYSIS 460
Includes cost effectiveness studies.

84 LAW AND POLITICAL SCIENCE 460
Includes space law; international law; international cooperation; and patent policy.

85 URBAN TECHNOLOGY AND TRANSPORTATION 461
Includes applications of space technology to urban problems; technology transfer; technology assessment; and surface and mass transportation.
For related information see *03 Air Transportation and Safety, 16 Space Transportation,* and *44 Energy Production and Conversion.*

SPACE SCIENCES

Includes space sciences (general); astronomy; astrophysics; lunar and planetary exploration; solar physics; and space radiation.
For related information see also *Geosciences.*

88 SPACE SCIENCES (GENERAL) N.A.

89 ASTRONOMY 461
Includes radio and gamma-ray astronomy; celestial mechanics; and astrometry.

90 ASTROPHYSICS 462
Includes cosmology; and interstellar and interplanetary gases and dust.

91 LUNAR AND PLANETARY EXPLORATION 464
Includes planetology; and manned and unmanned flights.
For spacecraft design see *18 Spacecraft Design, Testing and Performance.* For space stations see *15 Launch Vehicles and Space Vehicles.*

92 SOLAR PHYSICS 465
Includes solar activity, solar flares, solar radiation and sunspots.

93 SPACE RADIATION 476
Includes cosmic radiation; and inner and outer earth's radiation belts.
For biological effects of radiation see *52 Aerospace Medicine.* For theory see *73 Nuclear and High-Energy Physics.*

GENERAL

99 GENERAL 476

Note: N.A. means that no abstracts were assigned to this category for this issue.

SUBJECT INDEX I-1
PERSONAL AUTHOR INDEX I-59
CORPORATE SOURCE INDEX I-69
CONTRACT NUMBER INDEX I-83
REPORT / ACCESSION NUMBER INDEX I-87

TYPICAL CITATION AND ABSTRACT

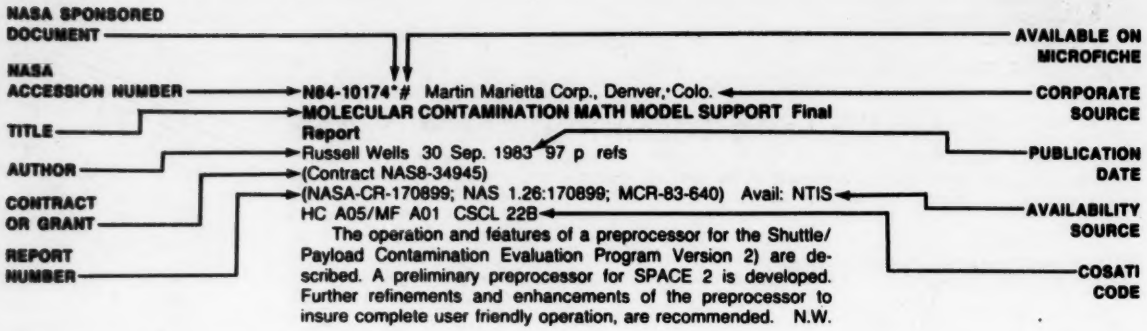
NASA SPONSORED DOCUMENT
NASA ACCESSION NUMBER
TITLE
AUTHOR
CONTRACT OR GRANT
REPORT NUMBER
AVAILABLE ON MICROFICHE
CORPORATE SOURCE
PUBLICATION DATE
AVAILABILITY SOURCE
COSATI CODE
N84-10174*# Martin Marietta Corp., Denver, Colo.
MOLECULAR CONTAMINATION MATH MODEL SUPPORT Final Report
Russell Wells 30 Sep. 1983 97 p refs
(Contract NAS8-34945)
(NASA-CR-170899; NAS 1.26:170899; MCR-83-640) Avail: NTIS
HC A05/MF A01 CSCL 22B
The operation and features of a preprocessor for the Shuttle/ Payload Contamination Evaluation Program Version 2) are described. A preliminary preprocessor for SPACE 2 is developed. Further refinements and enhancements of the preprocessor to insure complete user friendly operation, are recommended. N.W.

VOLUME 22 NUMBER 3/FEBRUARY 8, 1984

Scientific and Technical Aerospace Reports

A Semimonthly Publication of the National Aeronautics and Space Administration

01 AERONAUTICS (GENERAL)

N84-12027* National Aeronautics and Space Administration, Washington, D. C.
AERONAUTICAL ENGINEERING: A CONTINUING BIBLIOGRAPHY WITH INDEXES (SUPPLEMENT 166)
Oct. 1983 152 p
(NASA-SP-7037(166); NAS 1.21:7037(166)) Avail: NTIS HC $5.00 CSCL 01A

This bibliography lists 558 reports, articles and other documents introduced into the NASA scientific and technical information system in September 1983. Author

N84-12028*# Iowa State Univ. of Science and Technology, Ames. Engineering Research Inst.
LOAD DEFLECTION CHARACTERISTICS OF INFLATED STRUCTURES Final Report
Joseph R. Baumgarten Oct. 1983 48 p refs
(Grant NsG-1605)
(NASA-CR-174585; NAS 1.26:174585; ISU-ERI-a84414) Avail: NTIS HC A03/MF A01 CSCL 01B

A single, closed form relationship to relate load to the deformed dimensions of the horizontal torus was developed. Wall elasticity was included in the analysis, and special care was taken to predict the final footprint area of the loaded structure. The test fixture utilized is shown. The tori used for the bulk of the testing were rubber inner tubes for a 32 and 160 pneumatic tire. The inner tube being tested was plumbed, to a mercury-filled manometer, which had a 50 inch measurement capacity, by use of a special adapter. The adapter fit over the valve stem and allowed air to be added from a shop-air source and to be bled through the standard valve mechanism. In this fashion, tests requiring the maintenance of a constant indication of air pressure could be run with little difficulty. S.L.

N84-12029*# National Aeronautics and Space Administration. Langley Research Center, Hampton, Va.
CONTROLS, DISPLAYS, AND INFORMATION TRANSFER FOR GENERAL AVIATION IFR OPERATIONS
Hugh P. Bergeron, ed. and John D. Shaughnessy, ed. Washington Oct. 1983 272 p refs Workshop held in Hampton, Va., 30-31 Aug. 1982
(NASA-CP-2279; L-15649; NAS 1.55:2279) Avail: NTIS HC A12/MF A01 CSCL 01B

The purpose of the workshop was to review and evaluate the work performed under the NASA Single Pilot IFR (SPIFR) program, to highlight and disseminate major research findings, and to provide a forum for industry, universities, and government to interact and discuss the future thrust of research in the SPIFR program. The presentations selected represent key elements of the SPIFR program. These elements are classified into five disciplinary areas: program definition, controls, displays, information transfer, and research simulation facilities. Emphasis is also placed on aircraft accident investigation. For individual titles, see N84-12030 through N84-12049.

N84-12030*# National Aeronautics and Space Administration. Langley Research Center, Hampton, Va.
SINGLE PILOT IFR PROGRAM OVERVIEW AND STATUS
John D. Shaughnessy *In its* Controls, Displays and Inform. Transfer for Gen. Aviation IFR Operations Oct. 1983 p 19-24 (For primary document see N84-12029 03-01)
Avail: NTIS HC A12/MF A01 CSCL 01B

The history of the General Aviation Single Pilot IFR research program at NASA LaRC was discussed in general terms. The program objective, justification, and technical approach were given. The facilities used to conduct the research were discussed briefly. A general overview of recent accomplishments, present activities and near term plans were given. B.W.

N84-12031*# Spectrum Technology, Inc., Virginia Beach, Va. **c03**
SINGLE PILOT IFR ACCIDENT DATA ANALYSIS
David F. Harris *In* NASA. Langley Research Center Controls, Displays and Inform. Transfer for Gen. Aviation IFR Operations Oct. 1983 p 25-31 refs (For primary document see N84-12029 03-01)
Avail: NTIS HC A12/MF A01 CSCL 01C

The aircraft accident data recorded by the National Transportation and Safety Board (NTSR) for 1964-1979 were analyzed to determine what problems exist in the general aviation (GA) single pilot instrument flight rule (SPIFR) environment. A previous study conducted in 1978 for the years 1964-1975 provided a basis for comparison. This effort was generally limited to SPIFR pilot error landing phase accidents but includes some SPIFR takeoff and enroute accident analysis as well as some dual pilot IFR accident analysis for comparison. Analysis was performed for 554 accidents of which 39% (216) occurred during the years 1976-1979. Author

N84-12032*# Ohio State Univ., Columbus. **c03**
STUDY TO DETERMINE THE IFR OPERATIONAL PROFILE AND PROBLEMS TO THE GENERAL AVIATION PILOT
Stacy Weislogel *In* NASA. Langley Research Center Controls, Displays and Inform. Transfer for Gen. Aviation IFR Operations Oct. 1983 p 33-55 refs (For primary document see N84-12029 03-01)
Avail: NTIS HC A12/MF A01 CSCL 01C

A study of the general aviation single pilot operating under instrument flight rules (GA SPIFR) has been conducted for NASA Langley Research Center. The objectives of the study were to (1) develop a GA SPIFR operational profile, (2) identify problems experienced by the GA SPIFR pilot, and (3) identify research tasks which have the potential for eliminating or reducing the severity of the problems. To obtain the information necessary to accomplish these objectives, a mail questionnaire survey of instrument rated pilots was conducted. Complete questionnaire data is reported in NASA CR-165805, 'Statistical Summary: Study to Determine the IFR Operational Profile and Problems of the General Aviation Single Pilot'-Based upon the results of the GA SPIFR survey, this final report presents the general aviation IFR single pilot operational

profile, illustrates selected data analysis, examples, identifies the problems which he is experiencing, and recommends further research. Author

N84-12033*# National Aeronautics and Space Administration. Langley Research Center, Hampton, Va.
ANALYSIS OF GENERAL AVIATION SINGLE-PILOT IFR INCIDENT DATA OBTAINED FROM THE NASA AVIATION SAFETY REPORTING SYSTEM **c03**
Hugh P. Bergeron *In its* Controls, Displays and Inform. Transfer for Gen. Aviation IFR Operations Oct. 1983 p 57-63 refs (For primary document see N84-12029 03-01)
Avail: NTIS HC A12/MF A01 CSCL 01C

An analysis of incident data obtained from the NASA Aviation Safety Reporting System (ASRS) has been made to determine the problem areas in general aviation single-pilot IFR (SPIFR) operations. The Aviation Safety Reporting System data base is a compilation of voluntary reports of incidents from any person who has observed or been involved in an occurrence which was believed to have posed a threat to flight safety. This paper examines only those reported incidents specifically related to general aviation single-pilot IFR operations. The frequency of occurrence of factors related to the incidents was the criterion used to define significant problem areas and, hence, to suggest where research is needed. The data was cataloged into one of five major problem areas: (1) controller judgment and response problems, (2) pilot judgment and response problems, (3) air traffic control (ATC) intrafacility and interfacility conflicts, (4) ATC and pilot communication problems, and (5) IFR-VFR conflicts. In addition, several points common to all or most of the problems were observed and reported. These included human error, communications, procedures and rules, and work load. B.W.

N84-12034*# Ohio State Univ., Columbus.
A SUMMARY AND INTEGRATION OF RESEARCH CONCERNING SINGLE PILOT IFR OPERATIONAL PROBLEMS **c03**
G. Courtney Chapman *In* NASA. Langley Research Center Controls, Displays and Inform. Transfer for Gen. Aviation IFR Operations Oct. 1983 p 65-84 refs (For primary document see N84-12029 03-01)
Avail: NTIS HC A12/MF A01 CSCL 01C

A review of seven research studies pertaining to Single Pilot IFR (SPIFR) operations was performed. Two studies were based on questionnaire surveys, two were based on National Transportation Safety Board (NTSB) reports, two were based on Aviation Safety Reporting System (ASRS) incident reports, and one report used event analysis and statistics to forecast problems. The results obtained in each study were extracted and integrated. Results were synthesized and key issues pertaining to SPIFR operations problems were identified. The research that was recommended by the studies and that addressed the key issues is cataloged for each key issue. Author

N84-12035*# National Aeronautics and Space Administration. Langley Research Center, Hampton, Va.
GENERAL AVIATION SINGLE PILOT IFR AUTOPILOT STUDY **c08**
Hugh P. Bergeron *In its* Controls, Displays and Inform. Transfer for Gen. Aviation IFR Operations Oct. 1983 p 85-96 refs (For primary document see N84-12029 03-01)
Avail: NTIS HC A12/MF A01 CSCL 01C

Five levels of autopilot complexity were flown in a single engine IFR simulation for several different IFR terminal operations. A comparison was made of the five levels of complexity ranging from no autopilot to a fully coupled lateral and vertical guidance mode to determine the relative benefits versus complexity/cost of state-of-the-art autopilot capability in the IFR terminal area. Of the five levels tested, the heading select mode made the largest relative difference in decreasing workload and simplifying the approach task. It was also found that the largest number of blunders was detected with the most highly automated mode. The data also showed that, regardless of the autopilot mode, performance during an IFR approach was highly dependent on the type of approach being flown. These results indicate that automation can be useful when making IFR approaches in a high workload environment, but also that some disturbing trends are associated with some of the higher levels of automation found in state-of-the-art autopilots. Author

N84-12036*# National Aeronautics and Space Administration. Langley Research Center, Hampton, Va.
FLIGHT TEST VALIDATION OF A DESIGN PROCEDURE FOR DIGITAL AUTOPILOTS **c08**
Wayne H. Bryant *In its* Controls, Displays and Inform. Transfer for Gen. Aviation IFR Operations Oct. 1983 p 97-110 refs (For primary document see N84-12029 03-01)
Avail: NTIS HC A12/MF A01 CSCL 01C

Commercially available general aviation autopilots are currently in transition from an analogue circuit system to a computer implemented digital flight control system. Well known advantages of the digital autopilot include enhanced modes, self-test capacity, fault detection, and greater computational capacity. A digital autopilot's computational capacity can be used to full advantage by increasing the sophistication of the digital autopilot's chief function, stability and control. NASA's Langley Research Center has been pursuing the development of direct digital design tools for aircraft stabilization systems for several years. This effort has most recently been directed towards the development and realization of multi-mode digital autopilots for GA aircraft, conducted under a SPIFR-related program called the General Aviation Terminal Operations Research (GATOR) Program. This presentation focuses on the implementation and testing of a candidate multi-mode autopilot designed using these newly developed tools. Author

N84-12037*# National Aeronautics and Space Administration. Langley Research Center, Hampton, Va.
A SIMULATOR EVALUATION OF AN AUTOMATIC TERMINAL APPROACH SYSTEM **c04**
David A. Hinton *In its* Controls, Displays and Inform. Transfer for Gen. Aviation IFR Operations Oct. 1983 p 111-120 (For primary document see N84-12029 03-01)
Avail: NTIS HC A12/MF A01 CSCL 17G

The automatic terminal approach system (ATAS) is a concept for improving the pilot/machine interface with cockpit automation. The ATAS can automatically fly a published instrument approach by using stored instrument approach data to automatically tune airplane avionics, control the airplane's autopilot, and display status information to the pilot. A piloted simulation study was conducted to determine the feasibility of an ATAS, determine pilot acceptance, and examine pilot/ATAS interaction. Seven instrument-rated pilots each flew four instrument approaches with a base-line heading select autopilot mode. The ATAS runs resulted in lower flight technical error, lower pilot workload, and fewer blunders than with the baseline autopilot. The ATAS status display enabled the pilots to maintain situational awareness during the automatic approaches. The system was well accepted by the pilots. Author

N84-12038*# Kansas Univ., Lawrence.
PILOT CONTROLS AND SPIRF FLIGHT **c08**
D. R. Downing *In* NASA. Langley Research Center Controls, Displays and Inform. Transfer for Gen. Aviation IFR Operations Oct. 1983 p 121-140 refs (For primary document see N84-12029 03-01)
Avail: NTIS HC A12/MF A01 CSCL 01C

A study was performed to determine the relative advantages and disadvantages of four candidate pilot control devices for use by a single pilot flying a general aviation aircraft in instrument meteorological conditions. Only the pitch and roll axes were considered. The control devices examined were the wheel-yoke, center-stick, Brolley handles, and side-arm controller. Qualitative evaluation criteria were established that included instrument panel visibility, control sensitivity, pilot comfort, and space requirement behind the instrument panel. The results of the study indicated that the side-arm controller offered the possibility of an improve-

ment, but further research was necessary to determine its feasibility. Author

N84-12039*# National Aeronautics and Space Administration. Langley Research Center, Hampton, Va.
ADVANCED SYMBOLOGY FOR GENERAL AVIATION APPROACH TO LANDING DISPLAYS **c06**
Wayne H. Bryant *In its* Controls, Displays and Inform. Transfer for Gen. Aviation IFR Operations Oct. 1983 p 141-153 refs (For primary document see N84-12029 03-01)
Avail: NTIS HC A12/MF A01 CSCL 01D

A set of flight tests designed to evaluate the relative utility of candidate displays with advanced symbology for general aviation terminal area instrument flight rules operations are discussed. The symbology was previously evaluated as part of the NASA Langley Research Center's Terminal Configured Vehicle Program for use in commercial airlines. The advanced symbology included vehicle track angle, flight path angle and a perspective representation of the runway. These symbols were selectively drawn on a cathode ray tube (CRT) display along with the roll attitude, pitch attitude, localizer deviation and glideslope deviation. In addition to the CRT display, the instrument panel contained standard turn and bank, altimeter, rate of climb, airspeed, heading, and engine instruments. The symbology was evaluated using tracking performance and pilot subjective ratings for an instrument landing system capture and tracking task. R.J.F.

N84-12040*# National Aeronautics and Space Administration. Langley Research Center, Hampton, Va.
PILOT RESPONSE WITH CONVENTIONAL DISPLAYS **c54**
James J. Adams *In its* Controls, Displays and Inform. Transfer for Gen. Aviation IFR Operations Oct. 1983 p 155-157 (For primary document see N84-12029 03-01)
Avail: NTIS HC A12/MF A01 CSCL 05H

A critical examination of pilot-aircraft-display system response was conducted for conventional displays. The system frequency and damping both by visual examination of system responses to initial errors and by pilot model analysis was studied. Examples of system response at two points in a flight are shown. The long periods and the occasional loss of system damping in these responses are a matter of concern. These system characteristics can be duplicated with the pilot model given on the pilot-model-aircraft system block diagram. The responses obtained with the pilot model are also shown, together with the pilot model gains used in obtaining these responses. The factors that determine what these gains will be are the requirements for system stability, the sensitivity of the displays, and the scanning required in looking at the displays. The effects of scanning on system response can be determined with the test set-up given. Using this test equipment, it was found that separating bank angle information from heading information caused a noticeable degradation in system response. R.J.F.

N84-12041*# National Aeronautics and Space Administration. Langley Research Center, Hampton, Va.
SINGLE PILOT SCANNING BEHAVIOR IN SIMULATED INSTRUMENT FLIGHT **c54**
Jack E. Pennington *In its* Controls, Displays and Inform. Transfer for Gen. Aviation IFR Operations Oct. 1983 p 159-169 refs (For primary document see N84-12029 03-01)
Avail: NTIS HC A12/MF A01 CSCL 05H

Results from a simulation of general aviation instrument flight tasks in which the pilot's scan pattern and lookpoint were measured along with control inputs and state variables are given. The objective was to provide a baseline for comparing results from later studies of advanced avionics. Some of the scanning parameters measured are described, and conclusions from this and subsequent studies are presented. R.J.F.

N84-12042*# National Aeronautics and Space Administration. Langley Research Center, Hampton, Va.
A SIMULATOR EVALUATION OF A RATE-ENHANCED INSTRUMENT LANDING SYSTEM DISPLAY **c06**
David A. Hinton *In its* Controls, Displays and Inform. Transfer for Gen. Aviation IFR Operations Oct. 1983 p 171-180 (For primary document see N84-12029 03-01)
Avail: NTIS HC A12/MF A01 CSCL 01D

A piloted simulation study was conducted to evaluate the effect on instrument landing system tracking performance of integrating localizer error rate information with the raw localizer error display. The resulting display was named the pseudo command tracking indicator (PCTI) because it provides an indication of any changes of heading required to track the localizer. Eight instrument-rated pilots each flew five instrument approaches with the PCTI and five instrument approaches with a conventional course deviation indicator. The results show good overall pilot acceptance of the PCTI and a significant reduction in localizer tracking error. Author

N84-12043*# National Aeronautics and Space Administration. Langley Research Center, Hampton, Va.
DISPLAY RESEARCH: PILOT RESPONSE WITH THE "FOLLOW-ME" BOX DISPLAY **c54**
James J. Adams *In its* Controls, Displays and Inform. Transfer for Gen. Aviation IFR Operations Oct. 1983 p 181-188 (For primary document see N84-12029 03-01)
Avail: NTIS HC A12/MF A01 CSCL 05H

A study of display configurations and their effect on pilot-aircraft system response was undertaken. An examination of conventional displays was done to provide a set of data that can be used for comparison with advanced displays. An examination of an advanced display design that includes the use of a digital computer and a cathode ray tube to provide a drawing of a three dimensional box is done. The results show the improvement in system performance that can be obtained with the advanced display. Studies were conducted using the General Aviation Simulator, but verification of the results with the advanced display was also obtained from flight tests. R.J.F.

N84-12044*# Systems Technology, Inc., Hawthorne, Calif.
CONTROL/DISPLAY TRADE-OFF STUDY FOR SINGLE-PILOT INSTRUMENT FLIGHT RULE OPERATIONS **c06**
Roger Hoh (Milco Intern.) *In* NASA. Langley Research Center Controls, Displays and Inform. Transfer for Gen. Aviation IFR Operations Oct. 1983 p 189-199 ref (For primary document see N84-12029 03-01)
Avail: NTIS HC A12/MF A01 CSCL 01D

The objectives were to determine minimum autopilot functions and displays required to keep pilot workload at an acceptable level; to determine what constitutes an acceptable level of workload; to identify critical tasks; and to suggest specific experiments required to refine conclusions. It was determined that workload relief is derived from basic stability augmentation; that complex autopilots can lead to serious blunders; and that displays need to enhance positional awareness and minimize the likelihood of false hypothesis. R.J.F.

N84-12045*# Ohio Univ., Athens. Avionics Engineering Center.
WEATHER DATA COMMUNICATION AND UTILIZATION **c32**
Richard H. McFarland, James D. Nickum, and Daryl L. McCall *In* NASA. Langley Research Center Controls, Displays and Inform. Transfer for Gen. Aviation IFR Operations Oct. 1983 p 201-210 refs (For primary document see N84-12029 03-01)
Avail: NTIS HC A12/MF A01 CSCL 17B

The communication of weather data to aircraft is discussed. Problems encountered because of the great quantities of data available and the limited capacity to transfer this via radio link to an aircraft are discussed. Display devices are discussed. R.J.F.

N84-12046*# BioTechnology, Inc., Falls Church, Va.
A FLIGHT INVESTIGATION OF SIMULATED DATA LINK COMMUNICATIONS DURING SINGLE-PILOT IFR FLIGHT **c32**
James F. Parker, Jack W. Duffy, and D. G. Christensen *In* NASA. Langley Research Center Controls, Displays and Inform. Transfer for Gen. Aviation IFR Operations Oct. 1983 p 211-224 (For primary document see N84-12029 03-01)
Avail: NTIS HC A12/MF A01 CSCL 17B

A Flight Data Console (FDC) was developed to allow simulation of a digital communications link to replace the current voice communication system used in air traffic control (ATC). The voice system requires manipulation of radio equipment, read-back of clearances, and mental storage of critical information items, all contributing to high workload, particularly during single-pilot operations. This was an inflight study to determine how a digital communications system might reduce cockpit workload, improve flight proficiency, and be accepted by general aviation pilots. Results show that instrument flight, including approach and landing, can be accomplished quite effectively using a digital data link system for ATC communications. All pilots expressed a need for a back-up voice channel. When included, this channel was used sparingly and principally to confirm any item of information about which there might be uncertainty. R.J.F.

N84-12047*# National Aeronautics and Space Administration. Langley Research Center, Hampton, Va.
PROPOSED STUDY TO DETERMINE POTENTIAL FLIGHT APPLICATIONS AND HUMAN FACTORS DESIGN GUIDELINES OF VOICE RECOGNITION/SYNTHESIS SYSTEMS c54
Hugh P. Bergeron *In its* Controls, Displays and Inform. Transfer for Gen. Aviation IFR Operations Oct. 1983 p 225-227 (For primary document see N84-12029 03-01)
Avail: NTIS HC A12/MF A01 CSCL 05H

An effort to evaluate the human factors aspects and potential of voice recognition/synthesis techniques and the application of present and near-future (5 years) voice recognition/synthesis systems as a pilot/aircraft cockpit interface capability in an operational environment is discussed. The analysis will emphasize applications for single pilot instrument flight rules operations but will also include applications for other categories of aircraft with various levels of complexity. R.J.F.

N84-12048*# Honeywell, Inc., St. Louis Park, Minn.
NASA DEMONSTRATION ADVANCED AVIONICS SYSTEM (DAAS) c06
Eric M. Peterson *In* NASA. Langley Research Center Controls, Displays and Inform. Transfer for Gen. Aviation IFR Operations Oct. 1983 p 229-240 refs (For primary document see N84-12029 03-01)
Avail: NTIS HC A12/MF A01 CSCL 01D

The Demonstration Advanced Avionics Systems (DAAS) integrates a comprehensive set of general aviation avionics functions into an advanced system architecture for demonstration in a Cessna 402 aircraft. A cursory functional description of the DAAS complex is given. Microprocessors, computer architecture, and display devices are discussed. R.J.F.

N84-12049*# National Aeronautics and Space Administration. Ames Research Center, Moffett Field, Calif.
AN OVERVIEW OF THE DEMONSTRATION ADVANCED AVIONICS SYSTEM GUEST PILOT EVALUATION CONDUCTED AT AMES RESEARCH CENTER c06
George P. Callas, G. H. Hardy, and D. G. Denery *In* NASA. Langley Research Center Controls, Displays and Inform. Transfer for Gen. Aviation IFR Operations Oct. 1983 p 241-265 refs (For primary document see N84-12029 03-01)
Avail: NTIS HC A12/MF A01 CSCL 01D

The guest pilot flight evaluation of the Demonstration Advanced Avionics System (DAAS) is discussed. The results are based on the fifty-nine questionnaires that were completed by the participants. The primary purpose of the pilot evaluation was to expose the Demonstration Advanced Avionics System to the various segments of the general aviation community and solicit comments in order to determine the effectiveness of integrated avionics for general aviation. Segments of the community that were represented in the evaluation are listed. A total of sixty-four (64) flights were conducted in which one hundred and seventeen (117) pilots and observers participated. It was felt that the exposure each subject had with the DAAS was too short to adequately assess the training requirements, pilot workload, and the reconfiguration concept of the DAAS. It is recommended that an operational evaluation of the DAAS be made to assess: the training requirements or varying experience levels, the pilot workload in the ATC environment with unplanned route changes, and the viability of the reconfiguration concept for failures. R.J.F.

N84-12050# Advisory Group for Aerospace Research and Development, Neuilly-Sur-Seine (France).
SOME TRENDS IN AIRSHIP TECHNOLOGY DEVELOPMENTS
L. Balis Crema (Ist. di Tecnologia Aerospaziale, Rome) and A. Castellani (Ist. di Tecnologia Aerospaziale, Rome) [1982] 12 p refs Presented at the 56th Meeting of the Struct. and Mater. Panel, London, 10-15 Apr. 1983
(AGARD-R-717; ISBN-92-835-1458-0) Avail: NTIS HC A02/MF A01

Recent advances in aerospace technology, and in particular the application of new materials and novel structures, have special relevance to the development of dirigibles. Significant reductions in structure weight, it is demonstrated, can be achieved through the use of, for example, carbon fiber composites. Corresponding improvements in operational performance are shown. Author

N84-12051# Synergy, Inc., Washington, D. C.
DEVELOP A NORMATIVE OR DESCRIPTIVE MODEL OF THE INTERNATIONAL/DOMESTIC CIVIL AVIATION INDUSTRY, VOLUME 3 Final Report
Lee H. Dymond, Debrah L. Denemark, and Karl E. Olsoni 30 Sep. 1982 382 p 3 Vol.
(Contract F49642-81-C-0237)
(AD-A131878) Avail: NTIS HC A17/MF A01 CSCL 01/2

This appendix deals with the regulatory environment that the civilian air fleet has faced in the past and will likely face in the future. A brief history of the different regulatory agencies involved with civilian air travel is presented first, followed by a more in-depth analysis of the changing regulatory environment brought about by the Airline Deregulation Act of 1978, and its possible consequences on the structure of the civilian air fleet in the future. GRA

N84-12052# Synergy, Inc., Washington, D. C.
DEVELOP A NORMATIVE OR DESCRIPTIVE MODEL OF THE INTERNATIONAL/DOMESTIC CIVIL AVIATION INDUSTRY, VOLUME 2 Final Report
Lee H. Dymond, Debrah L. Denemark, and Karl E. Olsoni 30 Sep. 1982 89 p 3 Vol.
(Contract F49642-81-C-0237)
(AD-A131877) Avail: NTIS HC A05/MF A01 CSCL 01/2

Volume 2 is composed of four major sections that provide the bulk of the analysis. The first section deals with the regulatory framework, followed by a section dealing with the association framework, and a third section that deals with the industry components and demographics. The fourth section addresses the financial performance of the industry. GRA

N84-12053# Synergy, Inc., Washington, D. C.
DEVELOP A NORMATIVE OR DESCRIPTIVE MODEL OF THE INTERNATIONAL/DOMESTIC CIVIL AVIATION INDUSTRY. VOLUME 1: EXECUTIVE SUMMARY Final Report
Lee H. Dymond, Debrah L. Denemark, and Karl E. Olsoni 30 Sep. 1982 31 p 3 Vol.
(Contract F49642-81-C-0237)
(AD-A131876) Avail: NTIS HC A03/MF A01 CSCL 01/2

Volume 1 of this report provides an overview of the U.S. civil aviation industry, focusing on the immediate term and the future. Its purpose is to provide a summary for identifying the implications of the projected future aircraft fleet mix on the civil/military airlift system in the 1990 time period. The project is a direct result of the current turbulence in the airline industry and the uncertainty of the future airlift system. The results of the study provide a foundation to support the development of an analytical modeling system of the Air Staff to project alternative future configurations of the civil air fleet given alternative scenarios of future conditions in the industry. This particular phase of the effort focuses on four areas including: the regulatory framework existing in the industry and that projected to exist in the future; the association network

that has developed for the civil aviation industry and its importance to the development of future air industry structure; the components of the industry itself, including the number and types of airframes, engines, support functions within the industry such as travel agents, air freight forwarders, etc.; and the industry demographics, including operating behavior, route competition, fares, etc. GRA

N84-12054# Air Force Wright Aeronautical Labs., Wright-Patterson AFB, Ohio.
AFWAL FY82 TECHNICAL ACCOMPLISHMENTS Final Report
Russell S. Hoff, Jr. Jun. 1983 72 p
(AD-A131839; AFWAL-TR-83-0001) Avail: NTIS HC A04/MF A01 CSCL 14/2

This report contains highlights of significant technical achievements made during FY 82. The document exemplifies the broad range of R&D activities being undertaken within AFWAL and the significance of the technological contributions being made to enhance Air Force operational capabilities. The accomplishments have been grouped by Laboratory to assist the reader in understanding the technologies covered. The Air Force Wright Aerodynamical Laboratories are: (1) Aero Propulsion Laboratory; (2) Avionics Laboratory; (3) Flight Dynamics Laboratory, and (4) Materials Laboratory. GRA

N84-12055# Air Force Systems Command, Wright-Patterson AFB, Ohio. Foreign Technology Div.
ACTA AERONAUTICA ET ASTRONAUTICA SINICA
28 Jul. 1983 193 p Transl. into ENGLISH of Hang Kong Xuebao (China), v. 3, no. 4, Dec. 1982 108 p
(AD-A131828; FTD-ID(RS)T-0266-83) Avail: NTIS HC A09/MF A01 CSCL 20/4

In this paper, the available state space aeroelastic models are reviewed, and several suggestions for improvement are proposed. A new state space aeroelastic model is also proposed. Flutter calculation is carried out on two types of wings. These examples show that the new state space aeroelastic model is one of high accuracy and low order. A method is presented by which the modals can be automatically identified and the flutter point automatically determined during the course of flutter calculation using state space aeroelastic modeling. GRA

N84-12056# Advisory Group for Aerospace Research and Development, Neuilly-Sur-Seine (France).
INTEGRATION OF FIRE CONTROL, FLIGHT CONTROL AND PROPULSION CONTROL SYSTEMS
Loughton, England Aug. 1983 194 p refs In ENGLISH and FRENCH Symp. held in Toulouse, 17-20 May 1983
(AGARD-CP-349; ISBN-92-835-0335-X) Avail: NTIS HC A09/MF A01

The potential and problems of integrating mission critical and flight critical systems are examined. Fuel conservation, attack performance, combat survivability, and flight safety are addressed. For individual titles, see N84-12057 through N84-12071.

N84-12057# Federal Ministry for Defence, Bonn (West Germany).
INTEGRATION OF FIRE, FLIGHT AND PROPULSION CONTROL SYSTEMS: AN OVERVIEW, RETROSPECTIVE AND PROSPECTIVE **c05**
Werner M. Fraedrich *In* AGARD Integration of Fire Control, Flight Control and Propulsion Control Systems Aug. 1983 12 p refs (For primary document see N84-12056 03-01)
Avail: NTIS HC A09/MF A01

A brief historical review of aviation control technology is presented and topics related to digital data processing are discussed in detail. Problems which may arise with a totally integrated system are demonstrated through the use of examples and strategies for avoiding such problems are suggested. M.G.

N84-12058# Air Force Armament Lab., Eglin AFB, Fla. Hypervelocity Missile Branch.
HYPERVELOCITY MISSILE: BASED ON THE CONCEPT OF AIRCRAFT/MISSILE INTEGRATION FOR MAXIMUM FIREPOWER **c15**
T. C. Aden *In* AGARD Integration of Fire Control, Flight Control and Propulsion Control Systems Aug. 1983 14 p (For primary document see N84-12056 03-01)
Avail: NTIS HC A09/MF A01

The conventional approach to weapons for the close air support/battlefield interdiction (CAS/BI) missions has not provided NATO forces with affordable, effective firepower of the order required to defeat armored thrusts. The conventional approach has led to weapons that are either too expensive for stockpile and training purposes or too expensive to go to war. It has also failed to provide NATO strike aircraft assigned to the CAS/BI missions with the ability to achieve a large number of kills per pass or kills per sortie. The hypervelocity missile concept integrates current and emerging flight control system (FCS) technology with a low cost, lightweight missile to provide NATO forces with a significant firepower improvement. The U.S. Air Force has completed a series of ground launched flight tests that have successfully resolved all technical issues critical to missile guidance, control and accuracy questions. This series of successful demonstrations permits immediate continuation into an air launch flight test environment to demonstrate the integration of the three critical elements -- the aircraft, the FCS, and the missile. Author

N84-12059# Norwegian Defence Research Establishment, Kjeller.
F-16 PENGUIN ANTI-SHIP MISSILE INTEGRATION **c15**
E. Brodersen *In* AGARD Integration of Fire Control, Flight Control and Propulsion Control Systems Aug. 1983 7 p (For primary document see N84-12056 03-01)
Avail: NTIS HC A09/MF A01

Integration of the Norwegian Penguin Mk3 antiship missile for operation on the F-16 aircraft is discussed. Due to the inherent flexibility of both the aircraft and the missile system, no hardware changes are required on the aircraft. Software changes are designed such that the pilot can operate the weapon to its full performance by using existing cockpit controls and displays in a way quite similar to other air to ground missions. M.G.

N84-12060# Marconi Avionics Ltd., Rochester (England). Airborne Display Div.
INTEGRATION OF FIRE CONTROL, NAVIGATION SYSTEM AND HEAD UP DISPLAY **c06**
G. M. Barling *In* AGARD Integration of Fire Control, Flight Control and Propulsion Control Systems Aug. 1983 18 p (For primary document see N84-12056 03-01)
Avail: NTIS HC A09/MF A01

The inclusion of a sophisticated navigation function in a head up display/weapon aiming computer (HUD)/(WAC) is described together with integration of the resultant subsystem into an overall navigation/attack system. A growing trend in airborne systems computing is highlighted. Author

N84-12061# Northrop Corp., Hawthorne, Calif. Aircraft Div.
APPLICATION OF FLIGHT CONTROLS TECHNOLOGY TO ENGINE CONTROL SYSTEMS **c08**
Rudolf J. Seemann and J. L. Lockenour *In* AGARD Integration of Fire Control, Flight Control and Propulsion Control Systems Aug. 1983 26 p refs (For primary document see N84-12056 03-01)
Avail: NTIS HC A09/MF A01

A system design approach is outlined and some considerations for the design of electronically implemented control laws are discussed. A typical redundancy management concept, based on digital flight control techniques, for a quadruplex engine control system is described. This is followed by an analysis methodology to determine the probability of control system failure. Some implications that the use of probability theory has on the control system design requirements are discussed. M.G.

N84-12062# Societe Nationale d'Etudes et de Construction de Moteurs d'Aviation, Moissy-Cramayel (France).
THE RELATIONS BETWEEN THE NUMERICAL CONTROL OF THE ENGINE AND OTHER AIRCRAFT FUNCTIONS [LIENS

ENTRE LA REGULATION NUMERIQUE DU MOTEUR ET LES AUTRES FONCTIONS DE L'AVION] c08
D. Rambach *In* AGARD Integration of Fire Control, Flight Control and Propulsion Control Systems Aug. 1983 9 p In FRENCH (For primary document see N84-12056 03-01)
Avail: NTIS HC A09/MF A01

Numerical control opens the door to a larger integration of the aircraft engine by means of dialog with the pilot and other aircraft systems, either to provide new functions or to improve actual services. The objectives aimed for cover better performance, a nontotal optimization, and a greater ease in piloting. To accomplish this, several systems must dialog. A number of structures permit this. A method is proposed for choosing a structure that preserves to each important system its autonomy in case of difficulty while always benefitting from the advantage of integration. The functions are analyzed and regrouped in a pyramid so as to respect a nonpropagation of engine trouble. The objective is to preserve a distinct and controllable organization in the integrated system. This nonoptimal organization gives priority to reliability on the one hand, and an unambiguous division of responsibilities on the other. A.R.H.

N84-12063# British Aerospace Public Ltd. Co., Lancashire (England). Advanced Control Systems Group.
INTEGRATED POWERPLANT CONTROL SYSTEMS AND POTENTIAL PERFORMANCE BENEFITS c07
A. G. Seabridge and R. A. Edwards *In* AGARD Integration of Fire Control, Flight Control and Propulsion Control Systems Aug. 1983 10 p refs (For primary document see N84-12056 03-01)
Avail: NTIS HC A09/MF A01

Three aspects of integration in which the powerplant control system was integrated with the aircraft systems were examined. It is shown that the powerplant control system can be progressively integrated into the aircraft systems architecture by a distributed computing system for utility systems management. It is shown that the powerplant control system is a candidate for further improvement as a result of the integration and the ready availability of off take load related data. Some of the advantages of integration with flight control are discussed. E.A.K.

N84-12064# Dowty and Smith Industries Controls Ltd., Cheltenham (England).
FULL AUTHORITY DIGITAL ELECTRONIC ENGINE CONTROLS AND THEIR INTEGRATION WITH FLIGHT CONTROL SYSTEMS IN VSTOL AIRCRAFT c07
E. S. Eccles *In* AGARD Integration of Fire Control, Flight Control and Propulsion Control Systems Aug. 1983 10 p refs (For primary document see N84-12056 03-01)
Avail: NTIS HC A09/MF A01

The architecture and construction of the system applied to the Pegasus engine and aimed at the AV8B application are described. The system's architecture was determined by the requirements of a single engined VSTOL aircraft. It is essentially a dual-dual system. This architecture was chosen to provide reliable and positive detection of failure with rapid reaction and no degradation of performance. The likely extension of this system to the control of plenum chamber burning (PCB) is discussed. E.A.K.

N84-12065# Air Force Flight Dynamics Lab., Wright-Patterson AFB, Ohio.
DESIGN AND DEVELOPMENT OF THE MULTIFUNCTION FLIGHT CONTROL REFERENCE SYSTEM c06
John T. Young, John M. Perdzock, David L. Sebring (McDonnell Douglas Corp.), and Les Edinger (Honeywell Inc.) *In* AGARD Integration of Fire Control, Flight Control and Propulsion Control Systems Aug. 1983 10 p refs (For primary document see N84-12056 03-01)
Avail: NTIS HC A09/MF A01

The multifunction flight control reference system (MFCRS) concept which uses a minimum number of inertial sensors in a survivable configuration to provide inertial data for flight control, navigation, weapon delivery, cockpit displays, and sensor stabilization is discussed. The MFCRS program was initiated to verify, through flight test, the key issues of redundancy management and flight control. A redundancy management system based on parity equations was designed. It was shown which noise levels were higher than predicted. Additional filtering was required for MFCRS to prevent false alarms and high frequency actuator response. This filtering affected the flight control stability and performance and the flight control design was modified. It is found that integration of inertial data for fire control, flight control, and propulsion control will require close coupling and coordination between functional groups to resolve performance conflicts and compromises. E.A.K.

N84-12066# Ferranti Ltd., Edinburgh (Scotland).
SOME ASPECTS OF FLIGHT TRAJECTORY CONTROL IN FUTURE AVIONIC SYSTEMS FOR COMBAT AIRCRAFT c06
W. H. McKinlay *In* AGARD Integration of Fire Control, Flight Control and Propulsion Control Systems Aug. 1983 11 p ref (For primary document see N84-12056 03-01)
Avail: NTIS HC A09/MF A01

Some of the reasons for increased integration with the emphasis on flight profile control in combat aircraft, largely in the ground attack role are considered. Some of the reasons for further integration involving flight control are examined and the various phases of flight and particular problems are considered. It is suggested that future work will consist of developing particular capabilities, concentrating on the relationship between pilot and total system, learning how to control the design of such a closely coupled system and handling the important problems of testing, reliability, maintainability and the attainment of minimum economic configurations which will satisfy all these goals. The need for flexibility in any system which combines automation with a high degree of pilot participation is stressed. E.A.K.

N84-12067# Deutsche Forschungs- und Versuchsanstalt fuer Luft- und Raumfahrt, Brunswick (West Germany). Inst. fuer Flugfuehrung.
A DIAGNOSIS SCHEME FOR SENSORS OF A FLIGHT CONTROL SYSTEM USING ANALYTIC REDUNDANCY c06
Norbert Stuckenberg *In* AGARD Integration of Fire Control, Flight Control and Propulsion Control Systems Aug. 1983 12 p refs (For primary document see N84-12056 03-01)
Avail: NTIS HC A09/MF A01

A diagnosis scheme for sensors of a flight control system is presented. Based on analytic redundancy a duplex sensor configuration provides the fail operational capability of a conventional triplex sensor system. This is achieved by using deterministic observers. The feasibility of the presented concept is demonstrated. E.A.K.

N84-12068# Avions Marcel Dassault, Saint-Cloud (France).
EFFECTS OF INTEGRATED MAINTENANCE ON THE DEFINITIONS OF ONBOARD EQUIPMENTS [REPERCUSSIONS DE LA MAINTENANCE INTEGREE SUR LA DEFINITION DES EQUIPMENTS EMBARQUES] c05
Michel Coutois *In* AGARD Integration of Fire Control, Flight Control and Propulsion Control Systems Aug. 1983 13 p In FRENCH (For primary document see N84-12056 03-01)
Avail: NTIS HC A09/MF A01

Equipments for the Mirage 2000 aircraft are related among themselves by a numeric bus centrally controlled by a single tactical (principal) computer. The integrated maintenance of these systems encompasses that realized during the functional operation of the weapon system and is based on permanent surveillance of the equipment operation and the recording of anomalies during flight. In addition, there is a maintenance realized during the particular operation of the weapon system which permits more in-depth tests of the equipment and verifies all information exchanges made by the numeric bus or by point-to-point analog or digital relations. During the maintenance operation, the weapon system no longer provides an operational function. The material and logic implications of the maintainability function accomplished by the equipments are described by distinguishing those arrangements used during

functional operation and those used during maintenance. The software for integrated maintenance at the level of the principal computer which controls the numeric bus is described.
Transl. by A.R.H.

N84-12069# Bodenseewerk Geraetetechnik G.m.b.H., Ueberlingen (West Germany).
AN INTEGRATED AFCS FOR THE "PROFILE"-MODE **c08**
P. Wuest and W. Alles *In* AGARD Integration of Fire Control, Flight Control and Propulsion Control Systems Aug. 1983 11 p refs (For primary document see N84-12056 03-01)
Avail: NTIS HC A09/MF A01

The structure of the integrated control system and the appropriate parameter design method using the AIRBUS A300 as an example is described. The structure of the system is characterized by: (1) a mixture of feedforward and feedback control thus allowing to separate the design of the command disturbance characteristics; and (2) decoupling speed and height loop. The control system design relies on the knowledge of aircraft and engine characteristics, both known to the FMC or similar devices. To ease the analytic parameter design, the relevant aircraft dynamic is simplified by the incorporation of well proven basic loops such as pitch attitude feedback and N1/EPR-control. Within the scope of this simplification eigenvalues of the entire system are prescribed. Energy-saving aspects by the reduction of throttle lever excursions is considered using this approach. E.A.K.

N84-12070# British Aerospace Aircraft Group, Brough (England). ACT Design Group.
THE INTEGRATION OF FLIGHT AND ENGINE CONTROL FOR VSTOL AIRCRAFT **c08**
N. P. Pattinson *In* AGARD Integration of Fire Control, Flight Control and Propulsion Control Systems Aug. 1983 7 p refs (For primary document see N84-12056 03-01)
Avail: NTIS HC A09/MF A01

A control philosophy appropriate to future jet VSTOL aircraft which leads naturally to the integration of flight and engine control system is discussed. The potential benefits of this class of system are stated and integration aspects, both in terms of control laws and at the hardware level, are considered. The areas surrounding this approach to VSTOL control which require deeper study are outlined. E.A.K.

N84-12071# Office National d'Etudes et de Recherches Aerospatiales, Paris (France).
A NONLINEAR CONTROL LAW FOR PILOTING AIRCRAFT IN THE AIR-TO-GROUND ATTACK PHASE [SUR UNE LOI DE COMMANDE NON-LINEAIRE POUR LE PILOTAGE DES AVIONS EN PHASE D'ATTAQUE AIR-SOL] **c08**
B. Dang Vu and O. L. Mercier *In* AGARD Integration of Fire Control, Flight Control and Propulsion Control Systems Aug. 1983 10 p refs In FRENCH; ENGLISH summary (For primary document see N84-12056 03-01)
Avail: NTIS HC A09/MF A01

With focus on the control configured vehicle concept, a manual and non-conventional aircraft control law is presented which provides an improved target tracking in air-to-ground gunnery. The system architecture which integrates a weapon system, a fire control system and a flight control system is analyzed. In comparison to classical flight control systems, improvements come mainly from the elaborate processing of the pilot steering commands. The application of modern nonlinear control techniques to the design of the control law makes it otherwise well-suited for aircraft alignment maneuvers of large magnitude. The controllability of a linear version of the control law was demonstrated on a manned simulator. Author

N84-12072# Advisory Group for Aerospace Research and Development, Neuilly-Sur-Seine (France).
SPECIAL COURSE ON SUBSONIC/TRANSONIC AERODYNAMIC INTERFERENCE FOR AIRCRAFT
Loughton, England Jul. 1983 286 p refs In ENGLISH and FRENCH Course held in Rhode-Saint-Genese, Belgium, 2-6 May 1983 and in Dayton, Ohio, 16-20 May 1983
(AGARD-R-712; ISBN-92-835-0332-5) Avail: NTIS HC A13/MF A01

The emphasis of the course was on the configuration optimization in the transonic regime where both military and commercial aircraft must maneuver in an agile but stable manner. The course material has been updated and was presented in a more structured fashion emphasizing the fluid dynamic interference mechanisms that are the keys to the optimization. In additon some aspects of subcritical interference were also covered including those arising in the takeoff and landing phase of the flight with high lift devices deployed. Background material is given describing the computational and testing. The wide range of interference phenomena is covered arising in the optimization of both military and commercial aircraft starting from the simple airfoil and wing and extending to the complete configuration. For individual titles, see N84-12073 through N84-12086.

N84-12073# Boeing Co., Seattle, Wash.
SUBSONIC/TRANSONIC AERODYNAMIC INTERFERENCE FOR AIRCRAFT: INTRODUCTORY REMARKS **c02**
H. Yoshihara *In* AGARD Spec. Course on Subsonic/Transonic Aerodyn. Interference for Aircraft Jul. 1983 5 p (For primary document see N84-12072 03-01)
Avail: NTIS HC A13/MF A01

These introductory remarks provide examples of important subsonic and transonic fluid dynamic mechanisms that make up interference concepts used in aircraft optimization. The rationale for the lecture topic selection and the course outline are then given. Author

N84-12074# National Aerospace Lab., Amsterdam (Netherlands). Theoretical Aerodynamics Dept.
COMPUTATIONAL METHODS FOR SUBSONIC AND TRANSONIC AERODYNAMIC DESIGN **c02**
J. W. Slooff *In* AGARD Spec. Course on Subsonic/Transonic Aerodyn. Interference for Aircraft Jul. 1983 40 p refs (For primary document see N84-12072 03-01)
Avail: NTIS HC A13/MF A01

An overview is provided of computational methods that can be used in solving the design problem of aerodynamics; i.e., the problem of finding the detailed shape of (parts of) configurations of which the gross geometric characteristics have already been determined in a preliminary, overall design process, and that, subject to certain constraints, have to meet given aerodynamic requirements. Attention is focussed on methods for solving the classical inverse problem of aerodynamics and on approaches using optimization techniques. Both methods limited to subsonic flow utilizing panel method technology as well as methods based on finite difference/volume formulations for compressible, transonic flow are covered. In conclusion a discussion is presented of the relative merits of the various computational approaches to the problem of aerodynamic design. Author

N84-12075# Boeing Co., Seattle, Wash.
SUBSONIC/TRANSONIC VISCOUS INTERACTIONS **c02**
H. Yoshihara *In* AGARD Spec. Course on Subsonic/Transonic Aerodyn. Interference for Aircraft Jul. 1983 14 p refs (For primary document see N84-12072 03-01)
Avail: NTIS HC A13/MF A01

Significant viscous interactions arising at transonic cruise and maneuver conditions and low speed/high lift conditions are described for airfoils and swept wings. Consequences on the performance and stability of fighter and airlift aircraft are briefly sketched. Computational methods using the integral boundary layer/wake equations are then described in a narrative fashion.
Author

N84-12076*# National Aeronautics and Space Administration. Langley Research Center, Hampton, Va.
TRANSONIC AIRFOIL DEVELOPMENT **c02**
Richard T. Whitcomb *In* AGARD Spec. Course on Subsonic/Transonic Aerodyn. Interference for Aircraft Jul. 1983 9 p refs

(For primary document see N84-12072 03-01)
Avail: NTIS HC A13/MF A01 CSCL 01A

This lecture consists of three parts, in which discussions are presented of the current state of development of transonic or supercritical airfoils designed for fully turbulent boundary layers on the surfaces, previous research on subcritical airfoils designed to achieve laminar boundary layers on all or parts of the surfaces, and current research on supercritical airfoils designed to achieve laminar boundary layers. In the first part the use of available two dimensional computer codes in the development of supercritical airfoils and the general trends in the design of such airfoils with turbulent boundary layers are discussed. The second part provides the necessary background on laminar boundary layer phenomena. The last part, which constitutes the major portion of the lecture, covers research by NASA on supercritical airfoils utilizing both decreasing pressure gradients and surface suction for stabilizing the laminar boundary layer. An investigation of the former has been recently conducted in fight using gloves on the wing panels of the U.S. Air Force F111 TACT airplane, research on the later is currently being conducted in a transonic wind tunnel which has been modified to greatly reduce the stream turbulence and noise levels in the tests section. Author

N84-12077# Boeing Commercial Airplane Co., Seattle, Wash. Aero Research and Development.
AERODYNAMIC DESIGN FOR OVERALL VEHICLE PERFORMANCE **c05**
I. H. Rettie *In* AGARD Spec. Course on Subsonic/Transonic Aerodyn. Interference for Aircraft Jul. 1983 10 p (For primary document see N84-12072 03-01)
Avail: NTIS HC A13/MF A01

The process by which a wing is designed and integrated into an aircraft configuration is examined in detail. The way in which the characteristics of the design are matched to the size of the aircraft and to the critical segments of typical missions is described with some examples. High-speed computers are used routinely today to determine optimum dimensions for the vehicle. Their growing use in Computational Fluid Dynamics for aerodynamic design prior to wind tunnel testing is examined particularly as regards the capability this offers to tailor a single component such as the wing leading edge to obtain improvements in more than one flight regime by one modification to the aircraft. Author

N84-12078# National Aerospace Lab., Amsterdam (Netherlands).
APPLICATION OF COMPUTATIONAL PROCEDURES IN AERODYNAMIC DESIGN **c05**
J. W. Slooff *In* AGARD Spec. Course on Subsonic/Transonic Aerodyn. Interference for Aircraft Jul. 1983 23 p refs (For primary document see N84-12072 03-01)
Avail: NTIS HC A13/MF A01

Examples are discussed on the application of computational methods in aerodynamic design problems involving interference. Amongst these are: subsonic wing-body, sting support, pylon-nacelle and pylon-store interference, high-lift devices, induced drag minimization through constrained optimization in the Trefftz-plane and transonic wing-fuselage design and analysis. In addition a discussion is given on the problem of optimal usage of aerodynamic soft-ware in analyses and design, requiring an integrated systems approach. Author

N84-12079*# National Aeronautics and Space Administration. Langley Research Center, Hampton, Va.
TRANSONIC EMPIRICAL CONFIGURATION DESIGN PROCESS **c05**
Richard T. Whitcomb *In* AGARD Spec. Course on Subsonic/Transonic Aerodyn. Interference for Aircraft Jul. 1983 9 p refs (For primary document see N84-12072 03-01)
Avail: NTIS HC A13/MF A01

This lecture describes some of the experimental research pertaining to transonic configuration development conducted by the Transonic Aerodynamics Branch of the NASA Langley Research Center. Discussions are presented of the following: use of florescent oil films for the study of surface boundary layer flows; the severe effect of wind tunnel wall interference on the measured configuration drag rise near the speed of sound as determined by a comparison between wind tunnel and free air results; the development of a near sonic transport configuration incorporating a supercritical wing and an indented fuselage, designed on the basis of the area rule with a modification to account for the presence of local supersonic flow above the wing; a device for improving the transonic pitch up of swept wings with very little added drag at the cruise condition; a means for reducing the large transonic aerodynamic interference between the wing, fuselage, nacelle and pylon for a for a fuselage mounted nacelle having the inlet above the wing; and methods for reducing the transonic interference between flows over a winglet and the wing. Author

N84-12080# Aircraft Research Association Ltd., Bedford (England).
AERODYNAMIC INTERFERENCE: A GENERAL OVERVIEW **c02**
A. B. Haines *In* AGARD Spec. Course on Subsonic/Transonic Aerodyn. Interference for Aircraft Jul. 1983 52 p refs (For primary document see N84-12072 03-01)
Avail: NTIS HC A13/MF A01

A general survey is given of the sources of aerodynamic interference and of how adverse interference can be avoided and favorable interference exploited in the optimisation of the design of complete configurations for modern civil transport and military combat aircraft. The basic nature of wing-body interference is discussed at some length since these effects are at the root of much of what is to follow. There is considerable emphasis on means to reduce profile, vortex and transonic wave drag but it is also stressed that favorable interference concepts can be employed to improve lift for manoeuvere and to optimise stability and control characteristics at high incidence. R.J.F.

N84-12081# Messerschmitt-Boelkow-Blohm/Entwicklungspring Nord, Bremen (West Germany).
TRANSONIC CONFIGURATION DESIGN **c05**
G. Krenz *In* AGARD Spec. Course on Subsonic/Transonic Aerodyn. Interference for Aircraft Jul. 1983 26 p refs (For primary document see N84-12072 03-01)
Avail: NTIS HC A13/MF A01

General design aspects as well as specific criteria for a transonic wing lay-out are described and some special problems inherent in any transonic wing design are discussed on the basis of wind tunnel measurements. Aerodynamic wing concepts are considered, following two different design strategies by model tests in the transonic wind-tunnel. It was found that the shock development on the upper wing surface has a strong effect on both the design and off-design performance of the wing in terms of lift-drag. Potential flow methods used in transonic wing designs are discussed. R.J.F.

N84-12082# British Aerospace Aircraft Group, Preston (England).
TRANSONIC CONFIGURATION DESIGN (FIGHTER) **c05**
D. E. Shaw *In* AGARD Spec. Course on Subsonic/Transonic Aerodyn. Interference for Aircraft Jul. 1983 21 p refs (For primary document see N84-12072 03-01)
Avail: NTIS HC A13/MF A01

Current design procedures with special reference to aerodynamic interference and the associated use of computational fluid dynamics are discussed. A number of illustrations of various interference phenomena that play a major part in the optimisation of a new design are given. Specifically, the examples given are: the detailed effects of twin fins versus single fin; the flap taileron effects on laterals; wing stores; the effects of vortices; and wind tunnel effects with vortices included. R.J.F.

N84-12083# Aircraft Research Association Ltd., Bedford (England).
EXTERNAL STORES INTERFERENCE **c02**
A. B. Haines *In* AGARD Spec. Course on Subsonic/Transonic Aerodyn. Interference for Aircraft Jul. 1983 20 p refs (For

primary document see N84-12072 03-01)
Avail: NTIS HC A13/MF A01

External store installations are frequently a source of considerable adverse aerodynamic interference giving large increases in drag, reductions in usable lift and poor store release characteristics. This adverse interference can be greatly alleviated or even transformed into favorable interference. Some of the available evidence for a wide variety of arrangements is given. The nature of the interference, both adverse and favorable, is described, particular emphasis being placed on the major adverse interference in standard multiple carriers and in some underwing installations. The possible benefits of wing tip carriage and carefully arranged underfuselage arrays are noted. Throughout, stress is laid on the fact that dramatic improvements might be possible by adopting a radical approach to store carriage. R.J.F.

N84-12084# Boeing Commercial Airplane Co., Seattle, Wash. Aero Research and Development.
INTERFERENCE PROBLEMS IN AIRCRAFT DESIGN c02
I. H. Rettie *In* AGARD Spec. Course on Subsonic/Transonic Aerodyn. Interference for Aircraft Jul. 1983 10 p (For primary document see N84-12072 03-01)
Avail: NTIS HC A13/MF A01

The nature of aerodynamic interference among the components of an aircraft is examined. Some of the flow mechanisms involved are studied with the help of theoretical flow models with the objective of identifying design guidelines for the avoidance of performance or other penalties. The possible achievement of favorable interference in some cases is also discussed. Emphasis is placed upon the growing capability of computational methods which allow the designer to explore interference effects during the early phase of a design prior to wind tunnel tests. Author

N84-12085# Messerschmitt-Boelkow-Blohm/Entwicklungspring Nord, Bremen (West Germany).
ENGINE/AIRFRAME INTERFERENCE c02
G. Krenz *In* AGARD Spec. Course on Subsonic/Transonic Aerodyn. Interference for Aircraft Jul. 1983 17 p refs (For primary document see N84-12072 03-01)
Avail: NTIS HC A13/MF A01

A short review about typical aircraft representatives with different types of engine housing is given. The reasons why current commercial transport aircraft designed for the transonic flight regime prefer conventional engine locations under the wing are given. On first sight type of configuration rarely changed over the past 25 years. However, the strength of flow interference was increased considerably due to the rapid progress in engine as well as wing technology. On the engine side mainly the enlarged massflow and fan diameter contribute to the stronger interaction, while the wing tends to thicker leading to higher loaded designs with supercritical flow in the transonic flight regime. The increasing effects of wing/engine interference were studied in several transonic wind-tunnels. Results including those of varying engine distances from the transonic wing are presented. R.J.F.

N84-12086# British Aerospace Aircraft Group, Preston (England).
ENGINE-AIRFRAME INTERFERENCE EFFECTS c02
Alan Vint *In* AGARD Spec. Course on Subsonic/Transonic Aerodyn. Interference for Aircraft Jul. 1983 21 p refs (For primary document see N84-12072 03-01)
Avail: NTIS HC A13/MF A01

The various types of interference between a turbo-jet or turbo-fan engine and the airframe as applicable to military aircraft are described in detail. Examples of the effects on overall aircraft aerodynamics are given, including, where possible, simple means for their evaluation. It is shown that the interference may give either significant benefits or penalties and that relatively minor geometric changes can have profound effects. Above all it is shown that the effects of all aspects of engine airframe interference must be known early in the design process so tht pitfalls can be avoided or beneficial effects included in the initial aircraft design. R.J.F.

02 AERODYNAMICS

Includes aerodynamics of bodies, combinations, wings, rotors, and control surfaces; and internal flow in ducts and turbomachinery.

For related information see also *34 Fluid Mechanics and Heat Transfer.*

N84-12087 Wichita State Univ., Kans.
AN EXPERIMENTAL INVESTIGATION OF SEPARATED THREE DIMENSIONAL FLOW ON GENERAL AVIATION TWIN-ENGINE AIRCRAFT Ph.D. Thesis
Cyrus Ostowari 1982 131 p
Avail: Univ. Microfilms Order No. DA8308658

Force measurements, surface flow patterns and wake total pressure surveys have been obtained for a wing, wing-body, wing-nacelle and wing-body-nacelle configuration at typical pre- and post-stall angle of attack (10 deg and 16 deg), for a general aviation twin-engine airplane. The data includes separated regions and tentative flow field models. Special total pressure survey instrumentation was designed, manufactured and utilized, to measure the extent of separated regions in a minimum amount of time. The results indicate the presence of highly three dimensional separated regions above and beyond the surface at post-stall condition. The present tests reveal that when separation occurs the viscous layers are displaced vertically, creating a much wider wake than for cases without separation. Based upon the present experimental data, combined flow field models have been proposed for each of the configurations, at the pre-stall (10 deg) and post-stall (16 deg) angle of attack condition. In all cases, the flow is shown to be forming steady three dimensional separation bubbles. Dissert. Abstr.

N84-12088 Tennessee Univ., Knoxville.
ACOUSTIC STREAMING AS A MECHANISM OF THE RANQUE-HILSCH EFFECT Ph.D. Thesis
Joseph Quang Chu 1982 99 p
Avail: Univ. Microfilms Order No. DA8313285

The Ranque-Hilsch effect of the vortex tube effect is a striking phenomenon observed in swirling flows where air injected tangentially into a single pipe, separates spontaneously into two streams: the colder stream near the tube centerline and the hotter stream near its periphery. In spite of the simplicity of the Ranque-Hilsch tube, the mechanism of the total temperature separation, in the absence of any apparent external work, has not satisfactorily been resolved. Previously the mechanism has been purported to be due to the turbulent motion. However, if this were the mechanism, one could not explain why, in other turbulent swirling devices, the turbulence does not separate the total temperature in the same manner. Here experiments are conducted to substantiate a theory that acoustic streaming induced by the pure tone, a spinning wave present in swirling flows, deforms the base Rankine vortex into a forced vortex, resulting in total temperature separation in the radial direction. Dissert. Abstr.

N84-12089 Royal Aircraft Establishment, Farnborough (England).
RECENT ADVANCES IN PARACHUTE TECHNOLOGY
D. R. Dennis 18 May 1983 28 p refs Lecture for Royal Aeron. Soc., London, 10 Mar. 1983
(RAE-TM-FS(F)-514; BR88700) Copyright. Avail: Issuing Activity

Advances in the prediction of parachute inflation loads, in formulating design rules for ram air gliding parachutes, and in parachute construction materials are summarized. Test techniques, including aircraft launched parachute test vehicles are outlined. Stability analysis and techniques for obtaining basic data are described. Author (ESA)

N84-12090*# United Technologies Corp., East Hartford, Conn.
HELICOPTER ROTOR WAKE GEOMETRY AND ITS INFLUENCE IN FORWARD FLIGHT. VOLUME 1: GENERALIZED WAKE GEOMETRY AND WAKE EFFECT ON ROTOR AIRLOADS AND PERFORMANCE Final Report
T. Alan Egolf and Anton J. Landgrebe Oct. 1983 222 p refs

2 Vol.
(Contract NAS1-14568)
(NASA-CR-3726; NAS 1.26:3726; R83-912666-58) Avail: NTIS HC A10/MF A01 CSCL 01A

An analytical investigation to generalize the wake geometry of a helicopter rotor in steady level forward flight and to demonstrate the influence of wake deformation in the prediction of rotor airloads and performance is described. A first level generalized wake model is presented which is based on theoretically predicted tip vortex geometries for a selected representative blade design. The tip vortex distortions are generalized in equation form as displacements from the classical undistorted tip vortex geometry in terms of vortex age, blade azimuth, rotor advance ratio, thrust coefficient, and number of blades. These equations were programmed in a computer module to provide distorted wake coordinates at very low cost for use in rotor airflow and airloads prediction analyses. The sensitivity of predicted rotor airloads, performance, and blade bending moments to the modeling of the tip vortex distortion are demonstrated for low to moderately high advance ratios for a representative rotor and the H-34 rotor. Comparisons with H-34 rotor test data demonstrate the effects of the classical, predicted distorted, and the newly developed generalized wake models on airloads and blade bending moments. S.L.

N84-12091*# United Technologies Research Center, East Hartford, Conn.
HELICOPTER ROTOR WAKE GEOMETRY AND ITS INFLUENCE IN FORWARD FLIGHT. VOLUME 2: WAKE GEOMETRY CHARTS Final Report
T. Alan Egolf and Anton J. Landgrebe Washington NASA Oct. 1983 204 p 2 Vol.
(Contract NAS1-14568)
(NASA-CR-3727; NAS 1.26:3727; R83-912666-58) Avail: NTIS HC A10/MF A01 CSCL 01A

Isometric and projection view plots, inflow ratio nomographs, undistorted axial displacement nomographs, undistorted longitudinal and lateral coordinates, generalized axial distortion nomographs, blade/vortex passage charts, blade/vortex intersection angle nomographs, and fore and aft wake boundary charts are discussed. Example condition, in flow ratio, undistorted axial location, longitudinal and lateral coordinates, axial coordinates distortions, blade/tip vortex intersections, angle of intersection, and fore and aft wake boundaries are also discussed. N.W.

N84-12092*# National Aeronautics and Space Administration. Langley Research Center, Hampton, Va.
GEOMETRIES FOR ROUGHNESS SHAPES IN LAMINAR FLOW Patent Application
Bruce J. Holmes, Glenn L. Martin (Kentron Intern., Hampton, Va.), Christopher S. Domack (Kentron Intern., Hampton, Va.), Clifford J. Obara (Kentron Intern., Hampton, Va.), and Ahmed A. Hassan, inventors (to NASA) (Arizona State Univ., Tempe) Filed 10 Nov. 1983 18 p
(NASA-Case-LAR-13255-1; US-Patent-Appl-SN-550681) Avail: NTIS HC A02/MF A01 CSCL 01A

A passive interface mechanism between upper and lower skin structures, and a leading edge structure of a laminar flow airfoil is described. The interface mechanism takes many shapes. All are designed to be different than the sharp orthogonal arrangement prevalent in the prior art. The shapes of the interface structures are generally of two types: steps away from the centerline of the airfoil with a sloping surface directed toward the trailing edge and, the other design has a gap before the sloping surface. By properly shaping the step, the critical step height is increased by more than 50% over the orthogonal edged step. NASA

N84-12093# Air Force Geophysics Lab., Hanscom AFB, Mass. Aerospace Instrumentation Div.
A BALLOON DESIGN FOR 9000 POUNDS AT 90,000 FEET: RECOMMENDATIONS BASED ON HEAVY-LOAD BALLOON HISTORY Final Scientific Report
James F. Dwyer 9 Mar. 1983 41 p
(AF Proj. 7659)
(AD-A131987; AD-F000018; AFGL-TR-83-0062; AFGL-IP-315) Avail: NTIS HC A03/MF A01 CSCL 04/2

The history of the development of free balloons to carry heavy payloads into the stratosphere is reviewed with the objective of developing a design based on existing technologies for a balloon to carry 9000 lb to 90,000 ft. Reinforced polyester balloons, in tandem balloon configurations, are discussed with respect to materials, design criteria, and performance. The problem of launch dynamics for single cell polyethylene balloons is also discussed and it is concluded that a capped single cell polyethylene balloon can be dynamically launched, successfully, with the 9000-lb payload. Further, it is concluded that the single cell polyethylene balloon is the best means to meet the objective. Specifications for such a balloon are provided. GRA

N84-12094# Ballistic Research Labs., Aberdeen Proving Ground, Md.
A THEORETICAL AND EXPERIMENTAL INVESTIGATION OF A TRANSONIC PROJECTILE FLOW FIELD Final Report
Charles J. Nietubicz, James E. Danberg, and George R. Inger (West Virginia Univ.) Jul. 1983 32 p Supersedes IMR-712
(Grant DAAG29-78-G-0057; DA Proj. 1L1-61102-AH-43)
(AD-A131938; AD-F300295; ARBRL-MR-03291; ARBRL-IMR-712) Avail: NTIS HC A03/MF A01 CSCL 20/4

The transonic flow field about a secant-ogive-cylinder-boattail with a turbulent boundary layer has been studied. A joint theoretical and experimental effort is presented which compares the results of a generalized axisymmetric Navier-Stokes code, a composite inviscid boundary-layer/shock interaction solution method, and experiment. The experimental longitudinal pressure distribution at M= 0.94, and 0.97 for alpha = 0.0 degree are generally well predicted by both theoretical techniques although the Navier-Stokes solutions are shown to be superior in describing the detail, such as, upstream effects of expansion corners and the position and magnitude of minimum pressure regions. Both theoretical solutions predict the boundary layer velocity profiles very well in all cases with the largest differences occurring just downstream of the boattail corner. Comparisons of displacement thickness and skin friction distributions are also presented. GRA

N84-12095# Kentucky Univ., Lexington. Dept. of Mechanical Engineering.
STABILITY OF A PAIR OF STATIONARY VORTICES IN THE LEEWARD SIDE OF A CYLINDER IN A POTENTIAL FLOWFIELD Final Technical Report, May - Sep. 1981
Shiva N. Singh Wright-Patterson AFB, Ohio AFWAL May 1983 24 p
(Contract F33615-79-C-3030; AF Proj. 2307)
(AD-A131917; AFWAL-TR-83-3067) Avail: NTIS HC A02/MF A01 CSCL 20/4

In this report the steady state flow of an incompressible inviscid fluid past a circular cylinder is considered when a pair of asymmetrical stationary vortices are situated in the rear of the cylinder. Complex potential for this flow is obtained with the help of Milne-Thompson's circle theorem. The condition that the vortex centers have zero induced velocity determines the positions of the stationary vortices. This condition is determined for the various combination of the free stream velocity, the radius of the cylinder, and the strengths of the vortices by the secant routine on the computer. Asymmetrical disturbances are introduced and a stability analysis of the system is performed. And finally for the stable systems, the lift force acting on the cylinder is calculated and compared with the experimental results. GRA

N84-12096*# Vought Corp., Dallas, Tex.
IMPROVED WAVE DRAG PREDICTIONS USING MODIFIED LINEAR THEORY Final Technical Report, 7 Dec. 1981 - 7 Dec. 1982
R. T. Stancil 7 Dec. 1982 85 p Sponsored by NASA. Langley Research Center
(Contract N00167-82-C-0023)
(NASA-CR-174494; NAS 1.26:174494; AD-A131634; Rept-2-55110/2R-53299; DTNSRDC/ASED-CR-1-83) Avail: NTIS

HC A05/MF A01 CSCL 20/4

The wave drag prediction method is based on a modified supersonic linear theory computer technique. The modified linear theory differs from ordinary linear theory in that it uses the exact, boundary condition, it uses th exact pressure coefficient equation, and it uses characteristic tracing to determine regions of influence. The theoretical and numerical techniques are described in detail. A computer user's manual is included which provides a detailed description of the inputs and outputs of the computer routine, including recommended guidelines for preparing the geometric input. Comparisons between predictions of drag or pressures using the modified linear theory are made for five cases with wind tunnel data or other theories. These comparisons verify the improved accuracy of the modified linear theory relative to ordinary linear theory, particularly for high Mach numbers and high surface slopes. GRA

N84-12097# Texas Technological Univ., Lubbock. Dept. of Mechanical Engineering.

DYNAMIC-STALL REGULATION OF THE DARRIEUS TURBINE

J. W. Oler, J. H. Strickland, B. J. Im, and G. H. Graham Aug. 1983 180 p refs

(Contract DE-AC04-76DP-00789)

(DE83-017994; SAND-83-7029) Avail: NTIS HC A09/MF A01

A two dimensional unsteady airfoil analysis is described which utilizes a doublet panel method to model the airfoil surface, an integral boundary scheme to model the viscous attached flow, and discrete vortices to model the detached boundary layers which form the airfoil wake region. This model has successfully predicted steady lift and drag coefficients as well as pressure distributions for several airfoils with both attached and detached boundary layers. Unsteady calculations were limited to attached flow situations. Instantaneous pressure distributions were also obtained on a single bladed rotor operating in a tow tank in order to provide experimental data for eventual comparison with analytical predictions. DOE

N84-12098# National Aerospace Lab., Amsterdam (Netherlands). Fluid Dynamics Div.

ENGINE/AIRFRAME INTERFERENCE DRAG AT CRUISE CONDITIONS, USING PROPULSION SIMULATION

G. Doornbos and W. B. Dewolf Feb. 1982 31 p refs

(NLR-TR-82012-U) Avail: NTIS HC A03/MF A01

A wind tunnel test procedure to determine from the thrust minus drag measurements the aircraft drag and engine/airframe interference drag at cruise conditions is described. Engine thrust simulation is provided by a calibrated turbofan powered simulator (TPS). The use of a blown nacelle as propulsion simulator is described and compared with the simulation by a TPS. It is concluded that TPS engines are valuable test tools, simulating the aircraft engine closely, but the blown nacelle can not be totally replaced by the TPS nacelle. Author (ESA)

N84-12099# Advisory Group for Aerospace Research and Development, Neuilly-Sur-Seine (France).

AERODYNAMICS OF VORTICAL TYPE FLOWS IN THREE DIMENSIONS

Loughton, England Jul. 1983 557 p refs In ENGLISH and FRENCH Symp. held in Rotterdam, Netherlands, 25-28 Apr. 1983

(AGARD-CP-342; ISBN-92-835-0334-1) Avail: NTIS HC A24/MF A01

Separations which are frequently associated with vortical type flows are discussed. The trailing vortex system behind a lifting wing where the separation occurs at the trailing edge is noted. The use of large sweep angles with vortical flows is associated with separations forward of the trailing edge. A feature of such three dimensional flows are frequently well ordered with a defined stable structure and designers have increasingly sought to exploit them in meeting the growing speed and maneuver demands on modern aircraft. The following topics are discussed: (1) fundamentals, generation and structure of vortical flows; (2) interaction of vortical flows with surfaces; (3) modelling and computing; (4) stability and breakdown of vortical flows; (5) control and exploration of vortical flows. For individual titles, see N84-12100 through N84-12133.

N84-12100*# National Aeronautics and Space Administration. Ames Research Center, Moffett Field, Calif.

ON ISSUES CONCERNING FLOW SEPARATION AND VORTICAL FLOWS IN THREE DIMENSIONS

David J. Peake and Murray Tobak *In* AGARD Aerodyn. of Vortical Type Flows in Three Dimensions Jul. 1983 31 p refs (For primary document see N84-12099 03-02)

Avail: NTIS HC A24/MF A01 CSCL 01A

Vortical flows in three dimensional configurations that are of typical interest to aerodynamicists and researchers in fluid mechanics are reviewed. A list of 10 issues was compiled to understanding complex vortical flows. E.A.K.

N84-12101# Deutsche Forschungs- und Versuchsanstalt fuer Luft- und Raumfahrt, Goettingen (West Germany).

THE VORTEX SKELETON MODEL FOR THREE-DIMENSIONAL STEADY FLOWS

H. G. Hornung *In* AGARD Aerodyn. of Vortical Type Flows in Three Dimensions Jul. 1983 12 p refs (For primary document see N84-12099 03-02)

Avail: NTIS HC A24/MF A01

The essential concepts of two dimensional separation were extened to three dimensional steady flow, and the vortex skeleton model and electromagnetic analogy are introduced. The model gives a simple topological rule by which the vortex skeleton of a flow can be established from the structure of the wall streamline pattern. The important question of the occurrence of smoothly starting separation without zeros in the wall shear stress, is examined because of a new local solution of the Navier-Stokes and continuity equations. E.A.K.

N84-12102# Stanford Univ., Calif. Joint Inst. for Aeronautics and Acoustics.

ON THE STRUCTURE OF THE TURBULENT VORTEX

Leonard Roberts *In* AGARD Aerodyn. of Vortical Type Flows in Three Dimensions Jul. 1983 11 p refs (For primary document see N84-12099 03-02)

Avail: NTIS HC A24/MF A01

The trailing vortex generated by a lifting surface, the structure of its turbulent core and the influence of axial flow within the vortex on its initial persistence and on its subsequent decay are described. Similarity solutions of the turbulent diffusion equation are given in closed form and results are expressed in sufficiently simple terms that the influence of the lifting surface parameters on the length of persistence and the rate of decay of the vortex can be evaluated. E.A.K.

N84-12103# Imperial Coll. of Science and Technology, London (England). Dept. of Aeronautics.

INSTABILITIES IN TRAILING VORTICES: FLOW VISUALIZATION USING HOT-WIRE ANEMOMETRY

C. Strange and J. K. Harvey *In* AGARD Aerodyn. of Vortical Type Flows in Three Dimensions Jul. 1983 11 p refs (For primary document see N84-12099 03-02)

Avail: NTIS HC A24/MF A01

Trailing vortices often break up after the formation of disc shaped disturbances. A flow visualization experiment was performed in which similar strongly dissipative disturbances were produced in the laboratory. Details of the origin and development of this instability are discussed. An experiment using hot wire anemometry and a conditional sampling technique was set up. Data are presented on a solitary wave like disturbance which was found on the outer edge of the core and convected downstream at about the same velocity as the ambient fluid. It is found that the perturbation flow field associated with this disturbance is not axisymmetric. E.A.K.

N84-12104# Office National d'Etudes et de Recherches Aerospatiales, Paris (France).

INTERACTION BETWEEN A SHOCK-WAVE AND A VORTEX FLOW

J. Delery and E. Horowitz *In* AGARD Aerodyn. of Vortical Type Flows in Three Dimensions Jul. 1983 19 p refs In FRENCH; ENGLISH summary (For primary document see N84-12099 03-02)
Avail: NTIS HC A24/MF A01

The interaction between a vortex and a shock-wave normal to the streamwise axis of the vortex was studied both experimentally and theoretically. Measurements were made for four values of the upstream Mach number ranging from 1.6 to 2.28. They allowed the characterization of the shock effect on the vortical flow structure when breakdown does not occur. They also led to the definition of a breakdown limit function of the two parameters: normal shock strength - vortex swirl/ratio. Two flow configurations associated respectively with interaction without and with vortex bursting were carefully probed by using a two-color laser Doppler velocimeter system. When breakdown occurs, the mean meridian motion comprises a recirculating bubble near the axis of the structure. A flow model was developed in the framework of the Euler equations. As long as the vortex does not burst, the calculations give a faithfull description of flow phenomena. They also predict a limit for vortex breakdown which agrees satisfactorily with experiment. M.G.

N84-12105# Cranfield Inst. of Tech., Bedfordshire (England). Div. of Aerodynamics.

ON THE GENERATION AND SUBSEQUENT DEVELOPMENT OF SPIRAL VORTEX FLOW OVER A SWEPT-BACK WING

D. I. A. Poll *In* AGARD Aerodyn. of Vortical Type Flows in Three Dimensions Jul. 1983 14 p refs (For primary document see N84-12099 03-02)
Avail: NTIS HC A24/MF A01

An experimental investigation was performed to study the formation and development of spiral vortex flow over a swept-back wing. An aerofoil section with three alternative leading edge shapes was tested at sweep angles ranging from 0 to 56 deg for unit Reynolds number of 1,000,000/m and 2,000,000/m. The principal diagnostic tool was the surface oil-flow visualization technique supplemented by pressure distribution measurements in certain cases. No spiral vortex flow was observed for sweep angles of 0 and 15 deg but at higher sweep angles the oil-flows indicated that there were three different mechanisms for the formation of spiral vortices. The angle of incidence at the onset of vortex flow, and the mechanism responsible for its formation, were found to depend upon the sweep angle, the leading edge shape and the Reynolds number. It was also noted that the larger the leading edge radius the greater the dependence upon Reynolds number. However, comparison with other work suggests that Reynolds number, incidence and sweep angle alone are insufficient to determine the type of spiral vortex flow occurring on a given wing. M.G.

N84-12106# Technische Hogeschool, Delft (Netherlands). Dept. of Aerospace Engineering.

AN EXPERIMENTAL INVESTIGATION OF THE VORTEX FLOW OVER DELTA AND DOUBLE-DELTA WINGS AT LOW SPEED

N. G. Verhaagen *In* AGARD Aerodyn. of Vortical Type Flows in Three Dimensions Jul. 1983 16 p refs (For primary document see N84-12099 03-02)
Avail: NTIS HC A24/MF A01

A wind tunnel investigation was performed to study, by employing a laserlight-sheet and oil-flow visualization technique, the flow above and behind a sharp-edged 76 deg delta wing and two sharp-edged double-delta wing models (76/60 and 76/40 deg, kink at midchord). In addition, balance measurements were performed to determine lift, drag and pitching moment. The tests were carried out for angles of attack from 5 to 25 deg and at a free-stream velocity of 30 m/sec, corresponding to a Reynolds number of 1,400,000, based on centerline chord. Above both double-delta wings a single-branched strake vortex is formed by vorticity from the strake leading edge. Downstream of the leading-edge kink a wing vortex is formed which is conjectured to be single-branched at about 5 deg angle of attack and double branched at angles of 10 deg, and beyond. The flow pattern downstream of the trailing edge of the 76/60 deg double-delta wing was observed to be similar to that behind the delta wing. Above the 76/40 deg double-delta wing breakdown of both the wing and strake vortices took place ahead of the trailing edge. M.G.

N84-12107# Office National d'Etudes et de Recherches Aerospatiales, Paris (France).

VISUALIZATION OF VORTICAL TYPE FLOWS IN THREE DIMENSIONS

H. Werle *In* AGARD Aerodyn. of Vortical Type Flows in Three Dimensions Jul. 1983 20 p refs In FRENCH; ENGLISH summary Previously announced as A83-44312 (For primary document see N84-12099 03-02)
Avail: NTIS HC A24/MF A01

Turbulence structures that have been made visible by various means are outlined. Natural occurrences such as hurricanes, whirlpools, and island wakes have been photographed by satellite, from aircraft, and from the ground. Laboratory trials with wind and water tunnels have permitted photography of flows around helicopter blades, models, airfoils at various angles of attack, and around diversely shaped and oriented objects. Smoke streamlines have been generated with titanium tetrachloride wires, kerosene, and oil vapor, or by water condensed over liquid nitrogen. Colored dyes have been released from the surface of the model and pressure distributions have been translated into lighted regions. Gases and liquids, colored or fluorescent, have served for visualizations in water channels. Spiral structures, point vortices on swept wings, bursting vortices, vortices shed from cylindrical and ellipsoidal bodies, as well as in unsteady flows have been visualized during trials in applied aerodynamics. Numerous photographic examples are provided. M.S.K. (IAA)

N84-12108# Von Karman Inst. for Fluid Dynamics, Rhode-Saint-Genese (Belgium).

LASER VELOCIMETRY STUDY OF COMPRESSIBILITY EFFECTS ON THE FLOW FIELD OF A DELTA WING

G. Vorropoulos and J. F. Wendt *In* AGARD Aerodyn. of Vortical Type Flows in Three Dimensions Jul. 1983 13 p refs (For primary document see N84-12099 03-02)
Avail: NTIS HC A24/MF A01

Compressibility effects on the lee-side vortical flow field of a delta wing at incidence were studied using laser Doppler velocimetry. The tests covered the Mach number range from 0.18 to 0.80; both axial and circumferential velocity components were measured. It was found that the axial velocity excess observed at low Mach numbers became an axial velocity deficit at Mach numbers above 0.6. Strong asymmetry was observed in the circumferential velocity distribution at the higher Mach numbers. A flow picture including an embedded shock wave is proposed as physical explanation of observed compressibility effects. Author

N84-12109*# National Aeronautics and Space Administration. Langley Research Center, Hampton, Va.

RECENT STUDIES AT NASA-LANGLEY OF VORTICAL FLOWS INTERACTING WITH NEIGHBORING SURFACES

John E. Lamar and James F. Campbell *In* AGARD Aerodyn. of Vortical Type Flows in Three Dimensions Jul. 1983 32 p refs Previously announced as A83-33972 (For primary document see N84-12099 03-02)
Avail: NTIS HC A24/MF A01 CSCL 01A

The importance of leading edge vortical flows, which occur near and interact with neighboring surfaces, is stressed. Research in this area conducted or sponsored by the NASA Langley Research Center since 1978 is surveyed. Particular attention is given to the cumulative results of a number of theoretical and experimental studies. It is noted that these studies have been carried out in order to understand and use this kind of flow. Much of the work has been devoted to improving the lift-to-drag ratio and pitch characteristics for wings in this flow, although work has also been done on examining the unsteady and lateral characteristics.Author

N84-12110*# National Aeronautics and Space Administration. Langley Research Center, Hampton, Va.

EXPERIMENTAL INVESTIGATION OF FOREBODY AND WING LEADING-EDGE VORTEX INTERACTIONS AT HIGH ANGLES OF ATTACK

Gary E. Erickson (Northrop Corp.) and William P. Gilbert *In* AGARD Aerodyn. of Vortical Type Flows in Three Dimensions Jul. 1983 20 p refs (For primary document see N84-12099 03-02)
(Contract NAS1-16617)
Avail: NTIS HC A24/MF A01 CSCL 01A

An experimental investigation was conducted to assess the vortex flow-field interactions on an advanced, twin-jet fighter aircraft configuration at high angles of attack. Flow-field surveys were conducted on a small-scale model in the Northrop 0.41 - by 0.60-meter water tunnel and, where appropriate, the qualitative observations were correlated with low-speed wind tunnel data trends obtained on a large-scale model of the advanced fighter in the NASA Langley Research Center 30- by 60-foot (9.1- by 18.3-meter) facility. Emphasis was placed on understanding the interactions of the forebody and LEX-wing vortical flows, defining the effects on rolling moment variation with sideslip, and identifying modifications to control or regulate the vortex interactions at high angles of attack. The water tunnel flow visualization results and wind tunnel data trend analysis revealed the potential for strong interactions between the forebody and LEX vortices at high angles of attack. In particular, the forebody flow development near the nose could be controlled by means of carefully-positioned radome strakes. The resultant strake-induced flow-field changes were amplified downstream by the more powerful LEX vortical motions with subsequent large effects on wing flow separation characteristics. Author

N84-12111# Royal Aircraft Establishment, Bedford (England). Aerodynamics Dept.

SOME RESULTS FROM A PROGRAMME OF RESEARCH INTO THE STRUCTURE OF VORTEX FLOW FIELDS AROUND MISSILE SHAPES

T. R. Byram, A. Petersen (British Aerospace PLC), and S. T. Kitson *In* AGARD Aerodyn. of Vortical Type Flows in Three Dimensions Jul. 1983 20 p refs (For primary document see N84-12099 03-02)
Avail: NTIS HC A24/MF A01

Wind tunnel tests were performed to measure the leeside flow field of a generalized missile model at an angle of attack of 14 degrees and freestream Mach numbers of 0.7 and 1.8. Flow field data are presented for a station towards the rear of the model showing the flow structure for the body alone and the effects of mounting a cruciform set of delta fins near to the nose and near to the base. The data presented include vector plots of the components of velocity in the cross flow plane, the distributions of local total pressure, local Mach number and vorticity. The presence of the set of forward mounted fins and its roll orientation was found to have a significant effect on the development of the body vortices. Fins mounted towards the rear of the body were found to disrupt the body vortex feeding region but had little effect on the vortex centers unless these lay in or very close to the plane of the fins. R.J.F.

N84-12112*# Analytical Methods, Inc., Bellevue, Wash.

PREDICTING AERODYNAMIC CHARACTERISTICS OF VORTICAL FLOWS ON THREE-DIMENSIONAL CONFIGURATIONS USING A SURFACE-SINGULARITY PANEL METHOD

B. Maskew *In* AGARD Aerodyn. of Vortical Type Flows in Three Dimensions Jul. 1983 12 p refs (For primary document see N84-12099 03-02)
(Contracts NAS2-8788; N00014-78-C-0128; N00014-82-C-0354; DAAG29-81-C-0032)
Avail: NTIS HC A24/MF A01 CSCL 01A

A general low-order surface-singularity panel method is used to predict the aerodynamic characteristics of a problem where a wing-tip vortex from one wing closely interacts with an aft mounted wing in a low Reynolds Number flow; i.e., 125,000. Nonlinear effects due to wake roll-up and the influence of the wings on the vortex path are included in the calculation by using a coupled iterative wake relaxation scheme. The interaction also affects the wing pressures and boundary layer characteristics: these effects are also considered using coupled integral boundary layer codes and preliminary calculations using free vortex sheet separation modelling are included. Calculated results are compared with water tunnel experimental data with generally remarkably good agreement. Author

N84-12113# Deutsche Forschungs- und Versuchsanstalt fuer Luft- und Raumfahrt, Goettingen (West Germany). Inst. for Experimental Fluid Mechanics.

SEPARATION AND VORTICAL-TYPE FLOW AROUND A PROLATE SPHEROID: EVALUATION OF RELEVANT PARAMETERS

H. Vollmers, H.-P. Kreplin, and H. U. Meier *In* AGARD Aerodyn. of Vortical Type Flows in Three Dimensions Jul. 1983 14 p refs (For primary document see N84-12099 03-02)
Avail: NTIS HC A24/MF A01

The definition of some special lines in a flow field is discussed and a criterion for the identification of axes of local rotation is given. A preferred direction is introduced in space using the local direction of the velocity. A surface is constructed locally such that at any point the surface is normal to the velocity field. For a (normalized) direction field of the velocity, the components of the gradient tensor on this surface can be regarded as being equivalent to the curvature tensor of the surface. The behavior of the curvature is discussed. The surface is partitioned into hyperbolic and elliptic regions by the sign of the Gaussian curvature. It is found that the special points are associated with regions of extremely steep variations of the Gaussian curvature. Experimental evidence to this effect is provided by measurements of wall shear stress vectors and velocity vectors in the flow field around an inclined prolate spheroid. The above procedure is shown to be a tool for revealing some properties of the vortex skeleton of a flow field. Several other parameters of the measured flow field are also evaluated and presented. Author

N84-12114# Ministry of National Defence, Athens (Greece). Defence Industry Directorate.

ON THE GENERATION OF VORTICAL FLOW AT HYPERSONIC SPEEDS OVER ELLIPTICAL CONES

Panajotis Evangelou *In* AGARD Aerodyn. of Vortical Type Flows in Three Dimensions Jul. 1983 9 p refs (For primary document see N84-12099 03-02)
Avail: NTIS HC A24/MF A01

A method for calculating the hypersonic slip flow around slender elliptic cones at slight angle of attack is developed. The governing equations are derived from the Navier-Stokes equations and the energy equation by an order of magnitude analysis. There results a system of partial nonlinear parabolic differential equations for the flow variables of the shock formation regime. The system is integrated by means of an explicit finite-difference scheme and the results so obtained are compared with experimental data. Finally the influence of the elliptic cross section geometry as well as the influence of the angle of attack on the flow field properties with particular attention on the cross flow are investigated. Author

N84-12115# National Aeronautical Establishment, Ottawa (Ontario). Low Speed Aerodynamic Lab.

VISCOUS THREE-DIMENSIONAL FLOW SEPARATIONS FROM HIGH-WING PROPELLER-TURBINE NACELLE MODELS

R. H. Wickens *In* AGARD Aerodyn. of Vortical Type Flows in Three Dimensions Jul. 1983 29 p refs (For primary document see N84-12099 03-02)
Avail: NTIS HC A24/MF A01

This paper describes an investigation of viscous three dimensional flows on high-wing nacelle configurations which are typical of current commuter aircraft. Flow visualization on two nacelle configurations was used to depict the viscous vortex separations in the underwing junction, the nacelle afterbody, and the wing upper surface over the central region. The surface shear stress patterns, although complex, were composed of combinations

of elementary three dimensional viscous flows and free vortices which stream downwind. A strong vortex flow was produced over the top of the wing by the use of leading edge extensions along the forward portion of the nacelle. Observations were also made of the effects of a propeller slip-stream and the distortion of this propulsive flow by the mutual interference of the wing and nacelle. Author

N84-12116# Royal Aircraft Establishment, Farnborough (England). Aerodynamics Dept.
THEORETICAL MODELLING OF THREE-DIMENSIONAL VORTEX FLOWS IN AERODYNAMICS
J. H. B. Smith *In* AGARD Aerodyn. of Vortical Type Flows in Three Dimensions Jul. 1983 21 p refs (For primary document see N84-12099 03-02)
Avail: NTIS HC A24/MF A01

A unified account is presented of the various inviscid models used to represent three dimensional vortex flows in aerodynamics; essentially those relying on vortex sheets and line-vortices. Recent developments in extending the scope, accuracy, and stability of these models are described. An evaluation of their relative strengths and weaknesses suggests that the different models all have continuing roles to play. It is claimed that vortex modelling has come of age, in the sense that we can now learn about the real world from the behavior of models, after decades of trying to make the models conform with reality. Author

N84-12117# National Aerospace Lab., Amsterdam (Netherlands). Fluid Dynamics Div.
COMPUTATIONAL VORTEX FLOW AERODYNAMICS
H. W. M. Hoeijmakers *In* AGARD Aerodyn. of Vortical Type Flows in Three Dimensions Jul. 1983 35 p refs Sponsored in part by Royal Netherlands Air Force (For primary document see N84-12099 03-02)
Avail: NTIS HC A24/MF A01

A review is presented of computational methods for the determination of the characteristics of vortical type flows occurring in aircraft aerodynamics. The review covers primarily computational methods for computing the downstream development of vortex wakes and methods for computing the characteristics of configurations with leading-edge and strake vortices. The various computational methods in use at present are discussed in some detail. The possibilities and limitations of the methods are indicated and results of different methods are compared and discussed. Author

N84-12118# Messerschmitt-Boelkow-Blohm G.m.b.H., Ottobrunn (West Germany).
VORTEX FLOW SIMULATIONS PAST WINGS USING THE EULER-EQUATIONS
Claus Weiland *In* AGARD Aerodyn. of Vortical Type Flows in Three Dimensions Jul. 1983 12 p refs (For primary document see N84-12099 03-02)
Avail: NTIS HC A24/MF A01

Flow fields with vortex separation play an important role in the aerodynamics of missiles and for airplanes. Investigations carried out recently have shown that such flow fields can be computed by means of solutions of the Euler-equations. In the present paper results are presented for flow fields around delta-wings with freestream Mach number larger than 1. The range of the angle of attack is up to alpha = 15 deg. The Euler-equations are integrated by using a space-marching finite-difference method. The delta-wings have got sharp and blunted leading edges. At the sharp leading edge a condition is prescribed which produces a tangential discontinuity by means of which vorticity is introduced into the flow field. The formulation of the governing equations, the boundary conditions and the initial data is discussed. The results shown are the contours of the bow shock, the isobars, the lines of constant total pressure and the velocity vectors of the cross flow. The wave drag is determined by evaluating the integral for the momentum in an adequate surface in the flow field. Author

N84-12119# Office National d'Etudes et de Recherches Aerospatiales, Paris (France).
SIMULATION OF TURBULENT FLOWS WITH A POINT VORTEX METHOD
S. Huberson *In* AGARD Aerodyn. of Vortical Type Flows in Three Dimensions Jul. 1983 8 p refs Previously announced as A83-44313 (For primary document see N84-12099 03-02)
Avail: NTIS HC A24/MF A01

Turbulent flows are modelled by the method defined by Rehbach (1977) for treating three dimensional, incompressible flows of a perfect fluid. The Helmholtz equation is used to calculate the temporal evolution of the vortices, the rotational velocity field, and the continuity equation. The velocity field is then obtained as a function of the Biot-Savart integral and the vortex field is discretized in terms of vortex particles, with the flow described by two fields of discrete vectors: vortices and temporal position. The formulation allows the use of a very fine mesh, with the number of grid points chosen limited by the amount of computing power and time available. A technique is defined for determining the magnitude of the error associated with the total number of grid points used. Examples are provided for turbulence in two dimensional flows. The technique is demonstrated to represent well deformation and elongation of the vortex eddies. M.S.K. (IAA)

N84-12120# Aeronautical Research Inst. of Sweden, Bromma.
NUMERICAL SOLUTIONS OF THE EULER EQUATIONS SIMULATING VORTEX FLOWS AROUND WINGS
Arthur Rizzi, Lars-Erik Eriksson, Wolfgang Schmidt, and Stephan Hitzel *In* AGARD Aerodyn. of Vortical Type Flows in Three Dimensions Jul. 1983 14 p refs Prepared in cooperation with Dornier G.m.b.H., Friedrichshafen, West Germany (For primary document see N84-12099 03-02)
Avail: NTIS HC A24/MF A01

The Euler equations was established as an appropriate model for inviscid vortex flow. The range of this model's applicability is demonstrated by presentation of flowfields computed around a number of different wings with either sharp or rounded edges and at subsonic, transonic, and supersonic speeds. The emphasis here is on the physics of the flow model rather than the numerical aspects of the solution method. The results display both expected as well as unexpected vortex phenomena and indicate the value of this computational tool. Particular attention is paid to the wake regions. Author

N84-12121*# Tennessee Univ. Space Inst., Tullahoma.
THE TREATMENT OF CONVECTED VORTICES IN COMPRESSIBLE POTENTIAL FLOW
John Steinhoff, K. Ramachandran, and K. Suryanarayanan *In* AGARD Aerodyn. of Vortical Type Flows in Three Dimensions Jul. 1983 12 p refs Sponsored in part by NASA-Ames (For primary document see N84-12099 03-02)
Avail: NTIS HC A24/MF A01

A method is described for incorporating line vortices into the three dimensional compressible potential flow equation. A modified Biot-Savart law is used to compute a vortical velocity field, which is added to the gradient of the potential to form a total velocity. A rapidly converging approximate factorization (AFZ) scheme is then used to compute a potential such that the modified potential flow equation as well as the appropriate boundary conditions, based on total velocity, are satisfied. As part of a coupled iteration procedure, the positions of the line vortices are computed so that they convect with the total flow. The method is used to compute the field due to a single line vortex convecting past a wing. This represents an approximation of the effect of a canard or other lifting surface ahead of the wing, which sheds a tip vortex. It is seen that the flow field is substantially modified by the passage of the vortex. Unlike Euler equation schemes, which are also used to compute these flows, the solutions exhibit no numerical diffusion: The convected vortices retain their initial upstream width. Euler solutions, on the other hand, involve a vorticity which is numerically convected in an Eulerian frame and, unless extensive adaptive grid refinement is used they result in vortices with spread as they convect. Also, the potential flow method requires approximately two orders of magnitude less computing time and much less computer storage than the Euler methods. Author

N84-12122# Cornell Univ., Ithaca, N.Y. School of Mechanical and Aerospace Engineering.
VORTEX STABILITY AND BREAKDOWN
Sidney Leibovich *In* AGARD Aerodyn. of Vortical Type Flows in Three Dimensions Jul. 1983 22 p refs (For primary document see N84-12099 03-02)
(Grant NSF CME-79-19817)
Avail: NTIS HC A24/MF A01

Theoretical and experimental results, some quite recent, on the instability and breakdown of concentrated vortices at high Reynolds numbers are reviewed. Wave related theories of the vortex breakdown phenomenon are treated in some detail; these appear to provide a qualitative description of the response of vortex breakdown to variations in swirl or flow rate, and Benjamin's criticality classification, a wave-based concept, is consistent with experiment data. Known general criteria for the stability or instability of inviscid columnar vortices are reviewed, together with numerical studies of an inviscid vortex model that provides an excellent analytical fit to measured velocity profiles in vortices that experience breakdown. A new analysis of experimental data on vortex breakdown flows sheds light on the interplay between criticality and instability. The flows sufficiently far upstream of breakdowns to be unaffected by them are supercritical and stable, but they are generally closer to marginal instability than they are to criticality. The wakes are both subcritical and unstable. A conceptual framework for vortex breakdown, incorporating nonlinear wave theory and instability to three dimensional disturbances, is suggested based on information derived from the experimental studies. Author

N84-12123# Trondheim Univ. (Norway). Inst. for Mekanikk.
THE BREAK-UP MECHANISM OF A STREAMWISE DIRECTED VORTEX
Leif N. Persen *In* AGARD Aerodyn. of Vortical Type Flows in Three Dimensions Jul. 1983 5 p refs (For primary document see N84-12099 03-02)
Avail: NTIS HC A24/MF A01

The possible break-up mechanism of a vortex with its axis parallel to the direction of the mean flow is considered. Such streamwise directed vortices were considered first of all by G. I. Taylor in his investigation of the stability of the flow between two concentric cylinders. H. Gortler has made studies of streamwise directed vortices along a concave wall. In both these cases the vortices created seem to be very stable in the side-wise direction. However the G. I. Taylor vortices do not change in the direction of the mean flow, and thus do not exhibit any breakup mechanisms. In very many cases encountered under different flow conditions the breakup of a stream-wise directed vortex occurs after a certain distance downstream, and a possible mechanism whereby such a break-up can occur is presented. This mechanism is inherent in the basic equations of the flow, and as such is also exhibited on the equations of motion a non-viscous fluid. Author

N84-12124# Brown Boveri Research Center, Baden (Switzerland).
VORTEX BREAKDOWN: A TWO-STAGE TRANSITION
M. P. Escudier and J. J. Keller *In* AGARD Aerodyn. of Vortical Type Flows in Three Dimensions Jul. 1983 8 p refs (For primary document see N84-12099 03-02)
Avail: NTIS HC A24/MF A01

It is demonstrated that a large-scale isentropic transition between conjugate swirling flow states can occur with no change in the flow force and that both flow states are supercritical. It is argued that such a transition represents the first stage of vortex breakdown in a tube, the second stage being a non-isentropic transition in the nature of a hydraulic jump to the downstream subcritical state. The intermediate (supercritical) state consists of a zone of stagnant fluid surrounded by a region of potential flow. These two zones are separated by a layer of rotational fluid originating in the upstream flow modelled as a Rankine vortex. It is found that for any ratio of core-to-tube radii, breakdown (i.e. the first transition) occurs for a unique value of the swirl number. In the limiting case of an infitesimally small core, the value is the square root of 2 compared with the critical value 2.405. It is argued that this limit cannot represent free breakdown, which in consequence must have a different character from the tube-flow breakdowns generally observed. Author

N84-12125# Technische Hochschule, Aachen (West Germany). Aeridynamisches Inst.
A CONTRIBUTION TO THE PROBLEM OF VORTEX BREAKDOWN
E. Krause *In* AGARD Aerodyn. of Vortical Type Flows in Three Dimensions Jul. 1983 4 p refs (For primary document see N84-12099 03-02)
Avail: NTIS HC A24/MF A01

Associated with the breakdown process is the formation of a stagnation point on the axis of the vortex. This requires the deceleration of the axial velocity component, which must be enforced by a positive axial pressure gradient. An analysis is presented which shows how the pressure gradient along the axis of the vortex is influenced by the radial and azimuthal velocity components. An explicit expression for delta p/delta x(x,0) can be obtained by integration of the momentum equation for the radial velocity component with respect to the radial and subsequent differentiation of the integral with respect to the axial direction. In an order of magnitude analysis, it is then demonstrated that for large Reynolds numbers one component of the frictional force in the azimuthal direction cannot be neglected. In order to obtain an estimate for the pressure gradient rigid body rotation is assumed for the vortex core, and a distribution similar to that of a potential vortex, for the outer portion. The estimate shows that a positive axial pressure gradient can exist only, if the radial velocity component is positive and if the exponent is less than unity. It is also verified that a potential vortex cannot support an axial pressure gradient, that the pressure gradient in magnitude is directly proportional to the square of the maximum of the azimuthal velocity, referenced to the freestream velocity. Author

N84-12126# National Aeronautics and Space Administration. Ames Research Center, Moffett Field, Calif.
NUMERICAL SIMULATION OF VORTEX BREAKDOWN BY THE VORTEX-FILAMENT METHOD
Y. Nakamura, A. Leonard, and P. R. Spalart *In* AGARD Aerodyn. of Vortical Type Flows in Three Dimensions Jul. 1983 13 p refs (For primary document see N84-12099 03-02)
Avail: NTIS HC A24/MF A01 CSCL 01A

The vortex-filament method was applied to the simulation of vortex breakdown. The principal vortex region was represented by multiple filaments, and an axial velocity component was induced by a spiral winding of the filaments. An accuracy check was performed for a cylindrical swirling flow with simple analytical expressions for the axial and theta velocities. The result suggests that the flow field can be simulated to any accuracy by increasing the number of filaments. An axisymmetric-type vortex breakdown was simulated, with experimental data serving as upstream conditions. The calculated axial- and theta-velocity contours show the breakdown of the vortex, including a rapid change in the vortex core, followed axially by a recovery zone and then a second breakdown. When three dimensional initial data are used the second breakdown appears to be of the spiral type in correspondence with experimental observations. The present method can easily be used to simulate other types of vortex breakdown or other vortex flows with axial velocity. Author

N84-12127# Office National d'Etudes et de Recherches Aerospatiales, Paris (France).
EXPERIMENTATION WITH TURBULENT FLOWS EXPERIENCING THE EFFECTS OF AN ADVERSE PRESSURE GRADIENT
J. L. Solignac and O. Leuchter *In* AGARD Aerodyn. of Vortical Type Flows in Three Dimensions Jul. 1983 25 p refs In FRENCH; ENGLISH summary Previously announced as A83-44314 (For primary document see N84-12099 03-02)
Avail: NTIS HC A24/MF A01

Experiments were performed to examine the effects on turbulent structures produced by the adverse pressure gradients around a delta wing and about symmetric wings. Laser tomoscopy

visualized the flows, and measurements were taken of the static pressure distributions and the flow velocities (using LDV techniques). The flow velocities were 14.5 and 32 m/sec for the delta wing and winglets, respectively. Attention was focused on the leading edge vortex for the delta wing and the turbulence generated by the two NACA 0012 winglets, which were mounted at opposite angles of attack. The resulting turbulence differed mainly in velocity profiles. M.S.K. (IAA)

N84-12128# Grenoble Univ. (France). Inst. de Mecanique.
WAVES ON VORTEX CORES AND THEIR RELATION TO VORTEX BREAKDOWN
T. Maxworthy (Univ. of Southern California), M. Mory, and E. J. Hopfinger *In* AGARD Aerodyn. of Vortical Type Flows in Three Dimensions Jul. 1983 13 p refs (For primary document see N84-12099 03-02)
(Contracts N00014-82-K-0084; DRET-82-468)
Avail: NTIS HC A24/MF A01

The conjective by Hopfinger, Browand and Gagne (1982) that travelling, large amplitude "kink" waves, observed in rotating, turbulent fluid might be at the ori,in of vortex breakdown and small scale turbulence production motivated a study of such waves on isolated vortices under controlled conditions. Their characteristics are interpreted in terms of theories based on the localized induction equation. It is found that these kink waves remain stable and exhibit soliton interaction properties. Axisymmetric travelling waves, on the contrary, cause breakdown when their amplitude exceeds a certain magnitude. Benjamin's (1967) theory was used to calculate the critical phase speed and the velocity perturbation inside a wave of finite amplitude. The theoretical results show that the axial velocity changes rapidly become large so that, according to instability considerations, growth of spiral disturbances is possible. Breakdown caused by axisymmetric waves and possibly by combined, axisymmetric and kink waves, is demonstrated experimentally. A.R.H.

N84-12129*# Vigyan Research Associates, Inc., Hampton, Va.
VORTICAL FLOW MANAGEMENT FOR IMPROVED CONFIGURATION AERODYNAMICS: RECENT EXPERIENCES
Dhanvada M. Rao *In* AGARD Aerodyn. of Vortical Type Flows in Three Dimensions Jul. 1983 14 p refs Sponsored in part by NASA-Langley (For primary document see N84-12099 03-02)
Avail: NTIS HC A24/MF A01 CSCL 01A

Recent progress in vortex-control applications for alleviating the adverse consequences of three dimensional separation and vortical interactions on slender body/swept wing configurations is reported. Examples include helical separation trip to alleviate the side force due to forebody vortex asymmetry; hinged strakes to avoid vortex breakdown effects; compartmentation of swept leading edge separation to delay the pitch-up instability; under wing vortex trip and vortex trip and vortex flaps for drag reduction at high lift; and an apex-flap trimmer to fully utilize the lift capability of trailing-edge flaps for take off and landing of delta wings. Experimental results on generic wind-tunnel models are presented to illustrate the vortex-management concepts involved and to indicate their potential for enhancing the subsonic aerodynamics of supersonic-cruise type vehicles. Author

N84-12130# Cranfield Inst. of Tech., Bedfordshire (England). Dept. of Applied Aerodynamics.
THE EFFECTS OF WING TIP DEVICES ON THE PERFORMANCE OF THE BAe JETSTREAM
M. J. Fell (British Aerospace PLC) and J. J. Spillman *In* AGARD Aerodyn. of Vortical Type Flows in Three Dimensions Jul. 1983 11 p refs (For primary document see N84-12099 03-02)
Avail: NTIS HC A24/MF A01

A measurable drag reduction for a Jetstream fitted with tip devices over the range of operational lift coefficients is demonstrated. The increase in wing root blending moment due to either device in order to compare their relative moments with simple tip extensions is estimated. N.W.

N84-12131# Cranfield Inst. of Tech., Bedfordshire (England). Dept. of Applied Aerodynamics.
THE EFFECT OF WING TIP DEVICES ON THE FAR-FIELD WAKE OF A PARIS AIRCRAFT
J. J. Spillman *In* AGARD Aerodyn. of Vortical Type Flows in Three Dimensions Jul. 1983 9 p refs (For primary document see N84-12099 03-02)
Avail: NTIS HC A24/MF A01

Studies made of the flow about the wing-tip of a wind tunnel model showed that the vortex-type flow generally associated with the rolled-up vortex sheet well behind the tip existed just behind the trailing edge and seemed to be forming over the top of the wing-tip itself. As a result small cambered aerofoils were attached to the wing-tip to redirect the flow locally in such a way that each experienced a force with a significant thrust component. The effect is similar to that generated by the sail of a close-hauled yacht; consequently these small tip extensions were called sails. The original windtunnel and the preliminary flight tests of sails mounted from the tip tanks of the Paris aircraft of the Cranfield Institute of Technology are described. These initial tests showed that a considerable reduction in the lift-dependent drag resulted from fitting the sails but there was a marked scatter in the results which detracted from their credibility. Author

N84-12132# Politecnico di Milano (Italy). Dipt. di Ingegneria Aerospaziale.
BOUNDARY LAYER SEGMENTATION ON SHARP HIGHLY SWEPT LEADING EDGES AND ITS EFFECTS ON SECONDARY VORTICES
A. Baron and S. DePonte *In* AGARD Aerodyn. of Vortical Type Flows in Three Dimensions Jul. 1983 7 p refs (For primary document see N84-12099 03-02)
Avail: NTIS HC A24/MF A01

Pressure measurements were performed on an unslotted delta wing model, which enabled to determine the location of the secondary separation line, as a function of the angle of attack. A slotted delta wing model was then built and tests were carried on, showing a remarkable shift of the location of the secondary separation line. In addition, the secondary vortex flow was investigated by means of a tracing gas technique, based on the injection of Helium on the upper surface of the wing and measurements of its concentration in the flow downstream. Boundary layer segmentation appears to be a useful tool in preventing large secondary separations and allows higher lift coefficients to be obtained. It is reasonable to suppose that results similar to those reached for this delta wing could be expected also for conventional highly swept wings. Author

N84-12133*# National Aeronautics and Space Administration. Ames Research Center, Moffett Field, Calif.
AUGMENTATION OF FIGHTER-AIRCRAFT PERFORMANCE BY SPANWISE BLOWING OVER THE WING LEADING EDGE
Arnan Seginer (Technion-Israel Inst. of Technology) and Meir Salomon (SAL Engineering) *In* AGARD Aerodyn. of Vortical Type Flows in Three Dimensions Jul. 1983 26 p refs (For primary document see N84-12099 03-02)
Avail: NTIS HC A24/MF A01 CSCL 01A

Spanwise blowing over the wing and canard of a 1:35 model of a close-coupled-canard fighter-airplane configuration (similar to the Kfir-C2) was investigated experimentally in low-speed flow. Tests were conducted at airspeeds of 30 m/sec (Reynolds number of 1.8 x 10 to the 5th power based on mean aerodynamic chord) with angle-of-attack sweeps from -8 deg to 60 deg, and yaw-angle sweeps from -8 deg to 36 deg at fixed angles of attack 0 deg, 10 deg, 20 deg, 25 deg, 30 deg, and 35 deg. Significant improvement in lift-curve slope, maximum lift, drag polar and lateral/directional stability was found, enlarging the flight envelope beyond its previous low-speed/maximum-lift limit. In spite of the highly swept (60 deg) leading edge, the efficiency of the lift augmentation by blowing was relatively high and was found to increase with increasing blowing momentum on the close-coupled-canard configuration. Interesting possibilities of obtaining much higher efficiencies with swirling jets were indicated. Author

N84-12134 Wichita State Univ., Kans.
A STUDY OF WING-BODY AERODYNAMIC INTERFERENCE OF A LIGHT TWIN AIRCRAFT UTILIZING A PANEL METHOD POTENTIAL FLOW PROGRAM Ph.D. Thesis
William George Thomson 1982 112 p
Avail: Univ. Microfilms Order No. DA8308657

An analytical and experimental study of wing-body aerodynamic interference has been conducted for a general aviation light twin aircraft. The analysis method used a panel methods potential flow computer program. Although the inviscid method used did not yield quantitative changes in drag, it was found to be useful in designing shapes for reducing pressure gradients, thus reducing the tendency for boundary layer growth and separation. Both the influence of the wing on the body and the influence of the body on the wing are considered. While information from this analysis can be used to reduce the number of experimental parametric studies, it does not eliminate the need for experiments for tuning and verification. Dissert. Abstr.

N84-12135 Georgia Inst. of Tech., Atlanta.
STUDY OF AN ASYMPTOTIC METHOD FOR HELICOPTER ROTOR BLADE AERODYNAMIC LOADS Ph.D. Thesis
Vaidyanathan Ramabhadran Anand 1982 193 p
Avail: Univ. Microfilms Order No. DA8310651

A study has been conducted of Van Holten's approach to airload calculation for a helicopter rotor blade in forward flight. The airloads are systematically determined using a matched asymptotic expansion technique in an acceleration potential formulation. For a straight wing in steady flow, the method is equivalent to either simple or extended lifting line theory, depending on the order of the solution. Results for a pitching wing compare well with Reissner's analysis. Under the assumptions of incompressible flow and small disturbances, Van Holten's approach is found to be basically valid for a rotor in forward flight. Measured airloads for a two-bladed teetering model rotor and a four-bladed articulated full-scale rotor are compared with computations using Van Holten's method, Willmer's method, an actuator disk method and a discrete vortex wake method. Better agreement is obtained for the two-bladed rotor, possibly due to greater rotor/wake interaction for the four-bladed rotor. Of the computations, the asymptotic method and the discrete vortex wake method are generally found to yield the best results. Dissert. Abstr.

N84-12136 Stanford Univ., Calif.
STEADY AND UNSTEADY FLOW MODELS FOR AIRFOILS WITH SPOILER Ph.D. Thesis
Ahmed OmarAmrani 1983 154 p
Avail: Univ. Microfilms Order No. DA8307195

The study of the complex problem of spoiler aerodynamics can be divided into three main categories: (1) mean flow characteristics; (2) spoiler actuation; (3) wake vortex shedding. The first part of this work was consequently concerned with the steady state flow around the airfoil/spoiler system. A separated flow model for a multi-component airfoil with spoiler has been developed. The method uses a surface vorticity analysis to compute the potential flow in conjunction with an integral boundary layer method to predict separation. An iterative approach has been selected for the estimate of the wake geometry. The second part was concerned with the unsteady flow due to a fast spoiler deflection. A non-linear inviscid flow model was formulated. The method utilizes a distributed-singularities analysis for the computation of the flow. The wake formation and spoiler motion effects can be modelled separately which allows for a geometric approximation of the wake region. Dissert. Abstr.

N84-12073# Boeing Co., Seattle, Wash.
SUBSONIC/TRANSONIC AERODYNAMIC INTERFERENCE FOR AIRCRAFT: INTRODUCTORY REMARKS
H. Yoshihara *In* AGARD Spec. Course on Subsonic/Transonic Aerodyn. Interference for Aircraft Jul. 1983 5 p (For primary document see N84-12072 03-01)
Avail: NTIS HC A13/MF A01

N84-12074# National Aerospace Lab., Amsterdam (Netherlands). Theoretical Aerodynamics Dept.
COMPUTATIONAL METHODS FOR SUBSONIC AND TRANSONIC AERODYNAMIC DESIGN
J. W. Slooff *In* AGARD Spec. Course on Subsonic/Transonic Aerodyn. Interference for Aircraft Jul. 1983 40 p refs (For primary document see N84-12072 03-01)
Avail: NTIS HC A13/MF A01

N84-12075# Boeing Co., Seattle, Wash.
SUBSONIC/TRANSONIC VISCOUS INTERACTIONS
H. Yoshihara *In* AGARD Spec. Course on Subsonic/Transonic Aerodyn. Interference for Aircraft Jul. 1983 14 p refs (For primary document see N84-12072 03-01)
Avail: NTIS HC A13/MF A01

N84-12076*# National Aeronautics and Space Administration. Langley Research Center, Hampton, Va.
TRANSONIC AIRFOIL DEVELOPMENT
Richard T. Whitcomb *In* AGARD Spec. Course on Subsonic/Transonic Aerodyn. Interference for Aircraft Jul. 1983 9 p refs (For primary document see N84-12072 03-01)
Avail: NTIS HC A13/MF A01 CSCL 01A

N84-12080# Aircraft Research Association Ltd., Bedford (England).
AERODYNAMIC INTERFERENCE: A GENERAL OVERVIEW
A. B. Haines *In* AGARD Spec. Course on Subsonic/Transonic Aerodyn. Interference for Aircraft Jul. 1983 52 p refs (For primary document see N84-12072 03-01)
Avail: NTIS HC A13/MF A01

N84-12083# Aircraft Research Association Ltd., Bedford (England).
EXTERNAL STORES INTERFERENCE
A. B. Haines *In* AGARD Spec. Course on Subsonic/Transonic Aerodyn. Interference for Aircraft Jul. 1983 20 p refs (For primary document see N84-12072 03-01)
Avail: NTIS HC A13/MF A01

N84-12084# Boeing Commercial Airplane Co., Seattle, Wash. Aero Research and Development.
INTERFERENCE PROBLEMS IN AIRCRAFT DESIGN
I. H. Rettie *In* AGARD Spec. Course on Subsonic/Transonic Aerodyn. Interference for Aircraft Jul. 1983 10 p (For primary document see N84-12072 03-01)
Avail: NTIS HC A13/MF A01

N84-12085# Messerschmitt-Boelkow-Blohm/Entwicklungspring Nord, Bremen (West Germany).
ENGINE/AIRFRAME INTERFERENCE
G. Krenz *In* AGARD Spec. Course on Subsonic/Transonic Aerodyn. Interference for Aircraft Jul. 1983 17 p refs (For primary document see N84-12072 03-01)
Avail: NTIS HC A13/MF A01

N84-12086# British Aerospace Aircraft Group, Preston (England).
ENGINE-AIRFRAME INTERFERENCE EFFECTS
Alan Vint *In* AGARD Spec. Course on Subsonic/Transonic Aerodyn. Interference for Aircraft Jul. 1983 21 p refs (For primary document see N84-12072 03-01)
Avail: NTIS HC A13/MF A01

N84-12813# Office National d'Etudes et de Recherches Aerospatiales, Paris (France).
RANDOM EDDIES IN WAKES AND MIXING LAYERS
R. Legendre *In its* La Rech, Aerospatiale, Bimonthly Bull. No. 1983-1/212, Jan.-Feb. 1983 (ESA-TT-814) Jul. 1983 p 77-78 Transl. into ENGLISH from La Rech. Aerospatiale, Bull. Bimensuel (Paris), no. 1983-1/212, Jan.-Feb. 1983 (For primary document see N84-12810 03-70)
Avail: NTIS HC A05/MF A01; HC in ENGLISH available at ONERA, Paris FF 60; original report in FRENCH available at ONERA, Paris FF 60

03 AIR TRANSPORTATION AND SAFETY

Includes passenger and cargo air transport operations; and aircraft accidents.

For related information see also *16 Space Transportation* and *85 Urban Technology and Transportation.*

N84-12137# Army Safety Center, Fort Rucker, Ala.
LESSONS LEARNED FROM FY82 US ARMY AVIATION MISHAPS
Grover D. Lindsey, Matilda J. Reeder, Cecil Smith, and Darvin S. Ricketson, Jr. Jul. 1983 53 p
(AD-A131725; USASC-TR-83-7) Avail: NTIS HC A04/MF A01 CSCL 01/2

US Army aviation mishap data (96 cases) for FY 82 were analyzed. Lessons learned and corrective actions are identified and presented in Section 1. Section 2 details the results of a survey of three US Army aviation battalion/squadron organization with good safety records. Observation on the factors contributing to their successful safety efforts are provided. Author (GRA)

N84-12138# Federal Aviation Administration, Atlantic City, N.J. Technical Center.
CORRELATION OF LABORATORY-SCALE FIRE TEST METHODS FOR SEAT BLOCKING LAYER MATERIALS WITH LARGE-SCALE TEST RESULTS Final Report, Aug. 1981 - Jun. 1982
Louis J. Brown, Jr. and Richard M. Johnson Jun. 1983 65 p
(AD-A131666; FAA-CT-83-29) Avail: NTIS HC A04/MF A01 CSCL 01/3

An interlaboratory study was conducted to determine the adaptability of various laboratory fire test devices to measure aircraft seat cushion blocking layer effectiveness. Full scale tests conducted by the FAA have shown blocking layers to be an effective means of delaying aircraft seat cushion fire involvement when exposed to a large external fuel fire. Large scale tests conducted in the Douglas Aircraft Company Cabin Fire Simulator (CFS) have also shown similar findings. Such findings are fostering development of new candidate materials. However, it is more practical to evaluate these materials in a suitable laboratory test device rather than continuously performing expensive full or large scale tests. Several such devices were determined to be satisfactory when operated under specific conditions and when certain parameters are measured. The satisfactory devices are the Ohio State University (OSU) Rate of Heat Release Apparatus operated at 5.0 Watts/centimeter squared, the FAA Standard two gallon/hour burner operated for a 2 minute exposure, and the Lockheed Aircraft Company Meeker burner. For a series of blocking layer material candidates, test measurements obtained with the above devices exhibit comparable rankings with weight loss or percent weight loss from larger scale CFS tests. Author (GRA)

N84-12139# Deutsche Lufthansa Aktiengesellschaft, Frankfurt am Main (West Germany).
[ACTIVITIES REPORT OF THE AEROSPACE INDUSTRY IN WEST GERMANY] Annual Report, 1980 [DEUTSCHE LUFTHANSA AKTIENGESELLSCHAFT GESCHAEFTSBEREICHT 1980]
7 May 1981 58 p refs In GERMAN Original contains color illustrations
Avail: NTIS HC A04/MF A01

Surveys by the board of directors, comments on the annual statement of accounts, profit and loss account, capital conservation and investment program, technical progress, and Lufthansa group report are presented. Author (ESA)

N84-12140# Deutsche Lufthansa Aktiengesellschaft, Frankfurt am Main (West Germany).
[ACTIVITIES REPORT OF THE AEROSPACE INDUSTRY IN WEST GERMANY] Annual Report, 1981 [DEUTSCHE LUFTHANSA AKTIENGESELLSCHAFT GESCHAEFTSBEREICH 1981]
11 Dec. 1982 67 p refs In GERMAN Original contains color illustrations
Avail: NTIS HC A04/MF A01

Surveys by the board of directors, comments on the annual statement of accounts, profit and loss account, capital conservation and investment program, technical progress, and Lufthansa group report are presented. Author (ESA)

N84-12141# Deutsche Forschungs- und Versuchsanstalt fuer Luft- und Raumfahrt, Cologne (West Germany). Abt. Flugverkehrswissenschaft.
DOMESTIC SCHEDULED AIR TRANSPORT FOR THE YEAR 2000. FINANCIAL AND CAPACITY RELATED EFFECTS OF SUPPLY ALTERNATIVES, CONSIDERING, ALSO, THE COOPERATION WITH HIGH SPEED RAIL TRANSPORT SERVICES Ph.D. Thesis - Technische Hocschule, Aachen
Rolf Juergen Haupt Dec. 1982 88 p refs In GERMAN; ENGLISH summary Report will also be announced as translation (ESA-TT-828)
(DFVLR-FB-83-03) Avail: NTIS HC A05/MF A01; DFVLR, Cologne DM 28.60

Various alternatives of available offers in domestic scheduled air transport are presented and evaluated. A forecast of passenger demand serves as a basis for a specially adapted cost/benefit-calculation model and is used to estimate financial and capacity effects on an air carrier and on airports (differences of financial results due to airport take-off charges). Passengers load factors of 61 %, 66 % and 71 % are discussed. Substitutional effects by high speed rail transport are also presented. Substitution of air trafic offers by an increase of mean rail speed up to 160 km/h, 225 km/h and 280 km/h is discussed on the basis of a travel time difference of 40 to 45 minutes. Author (ESA)

N84-12142# National Transportation Safety Board, Washington, D. C. Bureau of Technology.
SAFETY REPORT: GENERAL AVIATION CRASHWORTHINESS PROJECT, PHASE 1 Report, 1972 - 1981
27 Jun. 1983 94 p
(PB83-917004; NTSB/SR-83/01) Avail: NTIS HC A05/MF A01; HC also available on subscription, North American Continent $90.00 per year, all others write for quote CSCL 01B

As part of its ongoing work in the area of general aviation crashworthiness, the Safety Board has undertaken a special program of investigation that will provide the real-world data necessary to establish an envelope of typical general aviation accident impact deceleration loads and to describe crash scenarios for a range of general aviation accidents for which design for passenger survivability is feasible. This report, the first of a projected series, explains the Safety Board's crashworthiness program, its objective, and its goals. It presents a description of the crashworthiness analysis methodology used, demonstrates its validity, and provides an example demonstrating its application. GRA

N84-12031*# Spectrum Technology, Inc., Virginia Beach, Va.
SINGLE PILOT IFR ACCIDENT DATA ANALYSIS
David F. Harris *In* NASA. Langley Research Center Controls, Displays and Inform. Transfer for Gen. Aviation IFR Operations Oct. 1983 p 25-31 refs (For primary document see N84-12029 03-01)
Avail: NTIS HC A12/MF A01 CSCL 01C

N84-12032*# Ohio State Univ., Columbus.
STUDY TO DETERMINE THE IFR OPERATIONAL PROFILE AND PROBLEMS TO THE GENERAL AVIATION PILOT
Stacy Weislogel *In* NASA. Langley Research Center Controls, Displays and Inform. Transfer for Gen. Aviation IFR Operations Oct. 1983 p 33-55 refs (For primary document see N84-12029 03-01)
Avail: NTIS HC A12/MF A01 CSCL 01C

N84-12033*# National Aeronautics and Space Administration. Langley Research Center, Hampton, Va.
ANALYSIS OF GENERAL AVIATION SINGLE-PILOT IFR IN-

CIDENT DATA OBTAINED FROM THE NASA AVIATION SAFETY REPORTING SYSTEM
Hugh P. Bergeron *In its* Controls, Displays and Inform. Transfer for Gen. Aviation IFR Operations Oct. 1983 p 57-63 refs (For primary document see N84-12029 03-01)
Avail: NTIS HC A12/MF A01 CSCL 01C

N84-12034*# Ohio State Univ., Columbus.
A SUMMARY AND INTEGRATION OF RESEARCH CONCERNING SINGLE PILOT IFR OPERATIONAL PROBLEMS
G. Courtney Chapman *In* NASA. Langley Research Center Controls, Displays and Inform. Transfer for Gen. Aviation IFR Operations Oct. 1983 p 65-84 refs (For primary document see N84-12029 03-01)
Avail: NTIS HC A12/MF A01 CSCL 01C

N84-12147# Office of Technology Assessment, Washington, D.C.
AVIATION GROWTH SCENARIOS
In its Airport and Air Traffic Control System Jan. 1982 p 45-63 (For primary document see N84-12143 03-04)
Avail: SOD HC $6.00 as 052-003-00873-4

04 AIRCRAFT COMMUNICATIONS AND NAVIGATION

Includes digital and voice communication with aircraft; air navigation systems (satellite and ground based); and air traffic control.

For related information see also *17 Spacecraft Communications, Command, and Tracking* and *32 Communications.*

N84-12143# Office of Technology Assessment, Washington, D.C.
AIRPORT AND AIR TRAFFIC CONTROL SYSTEM
Jan. 1982 148 p refs
(OTA-STI-175; LC-82-600545) Avail: SOD HC $6.00 as 052-003-00873-4

Needed improvements in the United States Air Traffic Control (ATC) system are discussed. Included are: scenarios of future growth in air transportation, alternative ways to increase airport and terminal capacity, technological and economic alternatives to the AIC system modification, and alternatives to the ATC process. For individual titles, see N84-12144 through N84-12150.

N84-12144# Office of Technology Assessment, Washington, D.C.
AIRPORT AND AIR TRAFFIC CONTROL SYSTEM. EXECUTIVE SUMMARY
In its Airport and Air Traffic Control System Jan. 1982 p 3-6 (For primary document see N84-12143 03-04)
Avail: SOD HC $6.00 as 052-003-00873-4

Four major topics are examined including: scenarios of future growth in air transportation; alternative ways to increase airport and terminal area capacity; technological and economical alternatives to the air traffic control (ATC) system modifications proposed by FAA; and alternatives to the present ATC process. Author

N84-12145# Office of Technology Assessment, Washington, D.C.
AIRPORT AND AIR TRAFFIC CONTROL SYSTEM. INTRODUCTION AND OVERVIEW
In its Airport and Air Traffic Control System Jan. 1982 p 9-22 refs (For primary document see N84-12143 03-04)
Avail: SOD HC $6.00 as 052-003-00873-4

The National Airspace System (NAS) includes about 6,500 public-use airports serving nearly all cities and small communities in the United States. Connecting these airports is a network of air routes, defined by navigational aids, that channel the flow of traffic. The growth of air transportation over the remainder of this century is considered. Improvements on the ATC system that affect the safety and capacity of terminal airspace are assessed. Policy options and alternative development plans are identified and analyzed. B.G.

N84-12146# Office of Technology Assessment, Washington, D.C.
THE NATIONAL AIRSPACE SYSTEM
In its Airport and Air Traffic Control System Jan. 1982 p 25-42 refs (For primary document see N84-12143 03-04)
Avail: SOD HC $6.00 as 052-003-00873-4

The National Airspace System (NAS) is a large and complex network of airports, airways, and air traffic control (ATC) facilities that exists to support the commercial, private, and military use of aircraft in the United States. The major parts of the system are examined, both to see how the system operates and to identify factors that may shape its future development. For explanatory purposes, first the goals of the system are considered, and then the system under three major headings: airports, air traffic services, and airspace users. Author

N84-12147# Office of Technology Assessment, Washington, D.C.
AVIATION GROWTH SCENARIOS **c03**
In its Airport and Air Traffic Control System Jan. 1982 p 45-63 (For primary document see N84-12143 03-04)
Avail: SOD HC $6.00 as 052-003-00873-4

The main focus is on the procedures and assumptions underlying the aviation forecasts on which FAA will base its 1982 system plan. Some sense of the range of possible future demand for aviation facilities and services are provided, in order to assist Congress in making its decisions about long-lived investments in both airports and ATC equipment. Author

N84-12148# Office of Technology Assessment, Washington, D.C.
TECHNOLOGY AND THE FUTURE EVOLUTION OF THE ATC SYSTEM
In its Airport and Air Traffic Control System Jan. 1982 p 67-98 refs (For primary document see N84-12143 03-04)
Avail: SOD HC $6.00 as 052-003-00873-4

An overview of some of the technologies and technological issues that are of concern in decisions that will soon be made about the future development of the ATC system are presented. It is not a detailed treatment of the technological and engineering complexities of the subject, nor does it attempt to resolve any of the related economic and funding controversies. Instead, this discussion is intended to provide decision makers and the public with useful information about the implications of some of the advances in technology that have occurred or which are on the horizon. This information forms a background against which to assess FAA's 1982 revision of the National Airspace System (NAS) Plan. Author

N84-12149# Office of Technology Assessment, Washington, D.C.
AIRPORT CAPACITY ALTERNATIVES **c09**
In its Airport and Air Traffic Control System Jan. 1982 p 101-122 refs (For primary document see N84-12143 03-04)
Avail: SOD HC $6.00 as 052-003-00873-4

The airport components in the operation of a typical airport are described. The major factors which influence or limit airside capacity are reviewed. The problem of delay, alternate methods for reducing delay or increasing the airside capacity is discussed. These include changing the pattern of traffic demand, expanding the runway system, or modifying the terminal area air traffic control procedures and equipment. Author

N84-12150# Office of Technology Assessment, Washington, D.C.
POLICY IMPLICATIONS
In its Airport and Air Traffic Control System Jan. 1982 p 125-141 refs (For primary document see N84-12143 03-04)
Avail: SOD HC $6.00 as 052-003-00873-4

The letter from the House Committee on Appropriations requesting an assessment indicated the following areas of concern: scenarios of future air transportation growth; alternative ways to increase airport and terminal capacity; proposed modifications of air traffic control (ATC) system technology; and alternatives to the present ATC process. The major points emerging and their implications in terms of congressional interests are summarized and examined. The intent is to highlight those aspects of air system evolution that may be of particular concern to the Congress in

evaluating the Federal Aviation Administration's (FAA) 1982 National Airspace System (NAS) Plan. Author

N84-12151*# National Aeronautics and Space Administration. Pasadena Office, Calif.
HIGH DYNAMIC GLOBAL POSITIONING SYSTEM RECEIVER Patent Application
William J. Hurd, inventor (to NASA) (JPL, California Inst. of Tech., Pasadena) Filed 31 Oct. 1983 31 p
(Contract NAS7-100)
(NASA-Case-NPO-16171-1-CU; US-Patent-Appl-SN-551536) Avail: NTIS HC A03/MF A01 CSCL 17G

A Global Positioning System (GPS) receiver having a number of channels, receives an aggregate of pseudorange code time division modulated signals. The aggregate is converted to baseband and then to digital form for separate processing in the separate channels. A fast Fourier transform processor computes the signal energy as a function of Doppler frequency for each correlation lag, and a range and frequency estimator computes estimates of pseudorange, and frequency. Raw estimates from all channels are used to estimate receiver position, velocity, clock offset and clock rate offset in a conventional navigation and control unit, and based on the total solution, that unit computes smoothed estimates, for the next measurement interval. NASA

N84-12152# Air Force Wright Aeronautical Labs., Wright-Patterson AFB, Ohio.
A COMPARISON OF MANUAL AND VOCAL RESPONSE MODES FOR THE CONTROL OF AIRCRAFT SUBSYSTEMS Final Report, 1 Jan. - 30 Nov. 1982
Anthony J. Aretz Mar. 1983 132 p
(AF Proj. 2403)
(AD-A132048; AFWAL-TR-83-3005) Avail: NTIS HC A07/MF A01 CSCL 14/2

The objective of this study was to determine how a vocal response mode compared to a manual response mode for data entry in a fighter cockpit simulator. Specifically, both vocal and manual response modes were compared in single and dual task conditions on the basis of pilot flight performance, response time, and errors while accomplishing several communication, navigation, and weapons tasks. The results indicated that the manual response mode was more effective than the vocal response mode in terms of response time data; however, the vocal response mode was more effective in terms of flying performance data. These results pointed to a trade off strategy used by the pilots as a function of their current workload. In the dual task manual condition the pilots concentrated on the manual data entry task and flying performance suffered, whereas, in the dual task vocal condition, the pilots kept their attention on the flying task and entered data while maintaining good flight control. As a result, in future fighter aircraft both manual and vocal control should be provided to the pilot for his selection. This conclusion was also supported by questionnaire results in which the pilots favored the implementation of both manual and vocal control. Author (GRA)

N84-12153# European Space Agency, Paris (France).
FLIGHT TESTS FOR A STRAPDOWN SYSTEM (MSS): THE RESULTS OF A SPECIAL FLIGHT TEST
Hans-Juergen Hotop Jul. 1982 42 p refs Transl. into ENGLISH of "Flugerprobung eines Strapdown-System (MSS): Darstellung der Ergebnisse am Beispiel eines Versuchsfluges" DFVLR-Mitt-83-02, Brunswick, West Germany, Oct. 1982
(ESA-TT-818; DFVLR-Mitt-83-02) Avail: NTIS HC A03/MF A01; original German version available from DFVLR, Cologne DM 16,60

The instruments and data evaluation procedure for the flight testing of the modular strapdown system are described. Reference data based on an inertial navigation system and optimal smoothing techniques are presented for a test flight of an HFB 320 aircraft. Overall position error is 10 km/hr maximum. Maximum velocity deviation is 8 m/sec; attitude errors are < 0.4 deg; heading error drift is 0.4 deg/hr. Alignment error in heading cannot be given since the system was aligned with the aid of the azimuth of the LN3-2A system throughout the test flight series. The MSS system operated without major faults, apart from the switch-overs of the gyroscope measuring ranges, which produce large errors in the heading and attitude during stationary runs. Author (ESA)

N84-12037*# National Aeronautics and Space Administration. Langley Research Center, Hampton, Va.
A SIMULATOR EVALUATION OF AN AUTOMATIC TERMINAL APPROACH SYSTEM
David A. Hinton *In its* Controls, Displays and Inform. Transfer for Gen. Aviation IFR Operations Oct. 1983 p 111-120 (For primary document see N84-12029 03-01)
Avail: NTIS HC A12/MF A01 CSCL 17G

05 AIRCRAFT DESIGN, TESTING AND PERFORMANCE

Includes aircraft simulation technology.

For related information see also *18 Spacecraft Design, Testing and Performance* and *39 Structural Mechanics.*

N84-12154* National Aeronautics and Space Administration. Langley Research Center, Hampton, Va.
SOLAR POWERED AIRCRAFT Patent
William H. Phillips, inventor (to NASA) Issued 15 Nov. 1983 5 p Filed 15 May 1981 Supersedes N81-32138 (19 - 23, p 3148)
(NASA-Case-LAR-12615-1; US-Patent-4,415,133;
US-Patent-Appl-SN-263829; US-Patent-Class-244-53R;
US-Patent-Class-244-13; US-Patent-Class-244-45R;
US-Patent-Class-244-91; US-Patent-Class-244-55) Avail: US Patent and Trademark Office CSCL 01C

A cruciform wing structure for a solar powered aircraft is disclosed. Solar cells are mounted on horizontal wing surfaces. Wing surfaces with spanwise axis perpendicular to surfaces maintain these surfaces normal to the Sun's rays by allowing aircraft to be flown in a controlled pattern at a large bank angle. The solar airplane may be of conventional design with respect to fuselage, propeller and tail, or may be constructed around a core and driven by propeller mechanisms attached near the tips of the airfoils. Official Gazette of the U.S. Patent and Trademark Office

N84-12155 Princeton Univ., N. J.
THE TRACKED WING IN GROUND-EFFECT (TWIG) Ph.D. Thesis
Mithra M. K. V. Sankrithi 1982 480 p
Avail: Univ. Microfilms Order No. DA8305909

The Tracked Wing In Group-Effect (TWIG) is a track-guided aerodynamically levitated vehicle for high speed intercity transportation. This study develops and applies methodologies for the aerodynamic, dynamic, and economic analysis and evaluation of TWIGs. The study starts by outlining some objectives of TWIG design and presenting some alternative TWIG design concepts. Preliminary designs of two roadable TWIGs are made. These comprise a five seat 'TWIGcar' and a forty passenter 'TWIGbus'. An extensive series of aerodynamic theories are developed for the flow between the guideway and the lower surface of a fairly arbitrary TWIG configuration. These treat the lower surface flow as either 2-D or 1-D incompressible potential flow, with account taken of 'Winglet gap leakage flow' around the vehicle sides. Steady and unsteady perturbation solutions are developed. Extensions are made to TWIGs with underbody keels. The aerodynamic theories collectively permit the prediction of frequency dependent longitudinal and lateral aerodynamic generalized stability derivatives, as well as trim and drag characteristics of TWIGs. Dissert. Abstr.

N84-12156# McDonnell Aircraft Co., St. Louis, Mo.
V/STOL (VERTICAL/SHORT TAKEOFF AND LANDING) LOW SPEED AND TRANSITION EQUIVALENT SYSTEMS ANALYSIS Final Report, 20 Sep. 1981 - 20 Sep. 1982
Carl G. Carpenter and John Hodgkinson Dec. 1982 193 p
(Contract N62269-81-C-0726)

(AD-A131955; NADC-81104-60) Avail: NTIS HC A09/MF A01 CSCL 01/3

A fixed base manned V/STOL handling qualities simulation was performed to investigate (1) classification criteria of attitude and rate command systems in hover and low-speed flight; (2) control system blending schemes for transition from approach dynamics to hover dynamics and vice versa, and (3) the amount of control usage. Pilot ratings and comments showed that a time response criterion discriminated well between attitude and rate systems; blending schemes for transition correlated well with earlier NASA results and; pilot's command gain had a strong effect on piloting characteristics and the amount of control usage.

Author (GRA)

N84-12157# Dayton Univ., Ohio.

AIRCRAFT TRANSPARENCY TESTING METHODOLOGY AND EVALUATION CRITERIA. PART 2: METHODOLOGY DEVELOPMENT FOR IMPROVED DURABILITY Final Report, 18 Jan. 1982 - 18 Feb. 1983

Kenneth I. Clayton and Blaine S. West Apr. 1983 51 p

(Contract F33615-81-C-3421; AF Proj. 2402)

(AD-A131928; UDR-TR-83-25-Pt-2; AFWAL-TR-83-3045-Pt-2) Avail: NTIS HC A04/MF A01 CSCL 01/3

A methodology and criteria for testing and evaluating the durability of high performance aircraft transparencies through the use of simulated in-service environments are defined. A realistic and cost-effective durability evaluation criteria is presented for monolithic stretched acrylic, coated monolithic polycarbonate, and acrylic faced/polycarbonate laminate configurations. M.G.

N84-12158# Dayton Univ., Ohio.

AIRCRAFT TRANSPARENCY TESTING METHODOLOGY AND EVALUATION CRITERIA. PART 1: TEST METHODS AND INFORMATION ANALYSIS Final Report, 18 Jan. 1982 - 18 Feb. 1983

Kenneth I. Clayton and Blaine S. West Apr. 1983 68 p

(Contract F33615-81-C-3421; AF Proj. 2402)

(AD-A131927; UDR-TR-83-25-Pt-1; AFWAL-TR-83-3045-Pt-1) Avail: NTIS HC A04/MF A01 CSCL 01/3

A methodology and criteria for testing and evaluating the durability of high performance aircraft transparencies through the use of simulated in-service environments are defined. Relevant information on applicable operational environments, candidate test methods, and previously used simulation/testing techniques are presented and analyzed. Appropriate corrective action is recommended to circumvent knowledge voids and/or test method deficiencies. M.G.

N84-12159# Dayton Univ., Ohio.

ALTERNATE T-38 TRANSPARENCY DEVELOPMENT. PART 4: PARAMETRIC STUDIES Final Report, Jan. 1980 - Feb. 1981

Richard A. Nash and Blaine S. West Wright-Patterson AFB, Ohio AFWAL Jun. 1983 108 p

(Contracts F33615-76-C-3103; F33615-80-C-3401; AF Proj. 2202; AF Proj. 1926)

(AD-A131904; UDR-TR-82-25-Pt-4; AFWAL-TR-80-3132-Pt-4) Avail: NTIS HC A06/MF A01 CSCL 01/3

Studies conducted to examine the effect of structural parameter variations on the nonlinear, dynamic response of the T-38 student windshield/support structure system to bird impact are described. The studies were conducted using the materially and geometrically nonlinear analysis (MAGNA) finite element computer program. Both static and transient dynamic analyses were conducted, examining the effects of changes to the transparency and support structure stiffness, intensity of the applied load both coupled and uncoupled, and duration of the impact event. Significant results of the finite element analysis include transparency deflection, peak load versus transparency stiffness, and resultant force plots both along the aft arch and around the impact area. A discussion of application of the finite element method to the birdstrike problem is also presented. Author (GRA)

N84-12160# Massachusetts Inst. of Tech., Cambridge. Aeroelastic and Structures Research Labs.

REVIEW OF AIRCRAFT CRASH STRUCTURAL RESPONSE RESEARCH Final Report, Aug. 1981 - Aug. 1982

Emmett A. Witmer and David J. Steigmann Aug. 1982 136 p

(Contract F33615-77-C-5155)

(AD-A131696; ASRL-TR-198-1; FAA-CT-82-152) Avail: NTIS HC A07/MF A01 CSCL 11/4

A review of aircraft crash structural response research has been carried out by studying the literature, discussions with researchers working in that area, and visits to facilitates/personnel involved in conducting and/or monitoring aircraft crash structural response investigations. Aircraft structures consisting of conventional built-up metallic construction and those consisting of advanced composite materials were of interest. The latter type of material and construction is of particular interest since their use is expanding rapidly, and crashworthiness of such structures is of increasing importance. Some recent theoretical and experimental studies of the behavior of composite-material structures subjected to severe static, dynamic, and/or impact conditions are noted. Such topics as crashworthiness testing of composite fuselage structures, the impact resistance of graphite and hybrid configurations, and the effects of elastomeric additives on the mechanical properties of epoxy resin and composite systems are reviewed. A review is made of some current and planned research to investigate experimentally the mechanical failure, postfailure, and energy-absorbing behavior of a sequence of composite-material structural elements and structural assemblages subjected to static loads or to simulated crash-impact loads. GRA

N84-12161# Dayton Univ., Ohio. Research Inst.

LONG TERM EVALUATION OF THE EFFECTS OF SHALE OIL PRODUCED JP-4 ON AIRCRAFT CONSTRUCTION MATERIALS Interim Technical Report, Mar. 1980 - Apr. 1982

B. H. Wilt and J. N. Dues Wright-Patterson AFB, Ohio AFWAL Apr. 1983 53 p

(Contract F33615-82-C-5039; AF Proj. 2421)

(AD-A131665; UDR-TR-83-20; AFWAL-TR-83-4046) Avail: NTIS HC A04/MF A01 CSCL 01/3

Various fuel system materials including elastomers, structural adhesives, and tank coatings were subjected to accelerated agings in both petroleum produced and shale oil produced JP-4 fuels. Comparisons were made of the test results in the different fuels. There was no significant difference in the test results for most materials. There was, however, significantly more deterioration of buna-N and polyurethane elastomers in shale oil JP-4 than in petroleum derived JP-4. Repeat tests in a second supply of shale oil JP-4 did not result in the buna-N and polyurethane deterioration. The results indicate that the first batch of shale oil JP-4 was contaminated although the contaminant could not be identified. Subsequent testing will be done with future batches of shale oil JP-4 to insure there is not a problem. GRA

N84-12162# Army Research and Technology Labs., Moffett Field, Calif. Aeromechanics Lab.

DESIGN CONSIDERATIONS FOR BEARINGLESS ROTOR HUBS

William G. Bousman, Robert A. Ormiston, and Paul H. Mirick 1983 28 p

(AD-A131660) Avail: NTIS HC A03/MF A01 CSCL 01/3

Five studies were performed under contract for concept definition of the integrated technology rotor/flight research rotor (ITR/FRR) Project. The purpose of these studies was to examine numerous hub design concepts with the potential of meeting the technical goals and specifications set for the ITR/FRR. Thirty three concepts were proposed, including 21 bearingless designs. Although the level of effort in these studies was not equivalent to a preliminary design, many important design issues for advanced rotor hubs were examined, particularly with respect to bearingless rotor designs. This paper summarizes the critical aspects of bearingless hub design; they include the design of the flexbeam, the design of a torque structure for pitch control, and the means of augmenting rotor lead lag damping. Representative designs

from the concept definition studies are used to illuminate these design aspects. The capability of the designs to meet the ITR/FRR technical goals is also discussed. GRA

N84-12163# Air Force Wright Aeronautical Labs., Wright-Patterson AFB, Ohio.
FLIGHTLINE THERMAL ENVIRONMENT TESTING OF F-111 TRANSPARENCIES Final Technical Report, 1 Nov. 1979 - 20 Aug. 1981
Robert J. Simmons Jul. 1983 51 p
(AF Proj. 1926)
(AD-A131642; AFWAL-TR-83-3062) Avail: NTIS HC A04/MF A01 CSCL 01/3

The objective of this effort was to simulate delamination failures occurring on F-111 aircraft located at Cannon AFB, New Mexico. The approach used was to simulate the flightline environment at Cannon AFB using existing laboratory test facilities. Test procedures and results of the tests are discussed. Test results indicated excellent correlation between visible degradation observed in the laboratory specimens and transparencies removed from field service. A design modification to combat the delamination failures was tested and proved to be successful. Results of bird impact testing of the laboratory tested specimens is presented. GRA

N84-12057# Federal Ministry for Defence, Bonn (West Germany).
INTEGRATION OF FIRE, FLIGHT AND PROPULSION CONTROL SYSTEMS: AN OVERVIEW, RETROSPECTIVE AND PROSPECTIVE
Werner M. Fraedrich *In* AGARD Integration of Fire Control, Flight Control and Propulsion Control Systems Aug. 1983 12 p refs (For primary document see N84-12056 03-01)
Avail: NTIS HC A09/MF A01

N84-12068# Avions Marcel Dassault, Saint-Cloud (France).
EFFECTS OF INTEGRATED MAINTENANCE ON THE DEFINITIONS OF ONBOARD EQUIPMENTS [REPERCUSSIONS DE LA MAINTENANCE INTEGREE SUR LA DEFINITION DES EQUIPMENTS EMBARQUES]
Michel Coutois *In* AGARD Integration of Fire Control, Flight Control and Propulsion Control Systems Aug. 1983 13 p In FRENCH (For primary document see N84-12056 03-01)
Avail: NTIS HC A09/MF A01

N84-12077# Boeing Commercial Airplane Co., Seattle, Wash. Aero Research and Development.
AERODYNAMIC DESIGN FOR OVERALL VEHICLE PERFORMANCE
I. H. Rettie *In* AGARD Spec. Course on Subsonic/Transonic Aerodyn. Interference for Aircraft Jul. 1983 10 p (For primary document see N84-12072 03-01)
Avail: NTIS HC A13/MF A01

N84-12078# National Aerospace Lab., Amsterdam (Netherlands).
APPLICATION OF COMPUTATIONAL PROCEDURES IN AERODYNAMIC DESIGN
J. W. Slooff *In* AGARD Spec. Course on Subsonic/Transonic Aerodyn. Interference for Aircraft Jul. 1983 23 p refs (For primary document see N84-12072 03-01)
Avail: NTIS HC A13/MF A01

N84-12079*# National Aeronautics and Space Administration. Langley Research Center, Hampton, Va.
TRANSONIC EMPIRICAL CONFIGURATION DESIGN PROCESS
Richard T. Whitcomb *In* AGARD Spec. Course on Subsonic/Transonic Aerodyn. Interference for Aircraft Jul. 1983 9 p refs (For primary document see N84-12072 03-01)
Avail: NTIS HC A13/MF A01

N84-12081# Messerschmitt-Boelkow-Blohm/Entwicklungspring Nord, Bremen (West Germany).
TRANSONIC CONFIGURATION DESIGN
G. Krenz *In* AGARD Spec. Course on Subsonic/Transonic Aerodyn. Interference for Aircraft Jul. 1983 26 p refs (For primary document see N84-12072 03-01)
Avail: NTIS HC A13/MF A01

N84-12082# British Aerospace Aircraft Group, Preston (England).
TRANSONIC CONFIGURATION DESIGN (FIGHTER)
D. E. Shaw *In* AGARD Spec. Course on Subsonic/Transonic Aerodyn. Interference for Aircraft Jul. 1983 21 p refs (For primary document see N84-12072 03-01)
Avail: NTIS HC A13/MF A01

06 AIRCRAFT INSTRUMENTATION

Includes cockpit and cabin display devices; and flight instruments.

For related information see also *19 Spacecraft Instrumentation* and *35 Instrumentation and Photography.*

N84-12164*# National Aeronautics and Space Administration. Langley Research Center, Hampton, Va.
EVALUATION OF A TOTAL ENERGY-RATE SENSOR ON A TRANSPORT AIRPLANE
Aaron J. Ostroff, Richard M. Hueschen, R. F. Hellbaum, Christine M. Belcastro, and J. F. Creedon Nov. 1983 48 p refs
(NASA-TP-2212; NAS 1.60:2212; L-15461) Avail: NTIS HC A03/MF A01 CSCL 01D

A sensor that measures the rate of change of total energy of an airplane with respect to the airstream has been evaluated. The sensor consists of two cylindrical probes located on the fuselage of a transport airplane, an in line acoustic filter, and a pressure sensing altitude rate transducer. Sections of this report include the sensor description and experimental configuration, frequency response tests, analytical model development, and flight test results for several airplane maneuvers. The results section includes time history comparisons between data generated by the total energy rate sensor and calculated data derived from independent sources. Author

N84-12165# Army Test and Evaluation Command, Aberdeen Proving Ground, Md.
TEST OPERATIONS PROCEDURE: ABSOLUTE ALTIMETERS Final Report
1 Sep. 1983 32 p
(AD-A131746; TOP-6-2-013) Avail: NTIS HC A03/MF A01 CSCL 14/2

This test operations procedure (TOP) delineates general test and specific subtest procedure required to determine the technical performance of absolute altimeters. Absolute altimeters which are used to measure vertical separation between the aircraft and the surface of the Earth, may also be referred to as Radio or Radar altimeters as they determine absolute terrain clearance by measuring the time interval required for a radio frequency signal to travel from the aircraft to the terrain and back again. The TOP is limited to the listed tests which are applicable only to absolute altimeters. The tests will determine: Warm-up-Time; Primary Voltage Sensitivity; Mutual Interference; Low Altitude Accuracy and Resolution; Failsafe, Pitch and Roll; Accuracy and Range; Terrain Tracking; Performance in adverse weather; over icecaps and snow, and under continuous operation. GRA

N84-12039*# National Aeronautics and Space Administration. Langley Research Center, Hampton, Va.
ADVANCED SYMBOLOGY FOR GENERAL AVIATION APPROACH TO LANDING DISPLAYS
Wayne H. Bryant *In its* Controls, Displays and Inform. Transfer for Gen. Aviation IFR Operations Oct. 1983 p 141-153 refs (For primary document see N84-12029 03-01)
Avail: NTIS HC A12/MF A01 CSCL 01D

N84-12042*# National Aeronautics and Space Administration. Langley Research Center, Hampton, Va.
A SIMULATOR EVALUATION OF A RATE-ENHANCED INSTRUMENT LANDING SYSTEM DISPLAY

David A. Hinton *In its* Controls, Displays and Inform. Transfer for Gen. Aviation IFR Operations Oct. 1983 p 171-180 (For primary document see N84-12029 03-01)
Avail: NTIS HC A12/MF A01 CSCL 01D

N84-12044*# Systems Technology, Inc., Hawthorne, Calif.
CONTROL/DISPLAY TRADE-OFF STUDY FOR SINGLE-PILOT INSTRUMENT FLIGHT RULE OPERATIONS
Roger Hoh (Milco Intern.) *In* NASA. Langley Research Center Controls, Displays and Inform. Transfer for Gen. Aviation IFR Operations Oct. 1983 p 189-199 ref (For primary document see N84-12029 03-01)
Avail: NTIS HC A12/MF A01 CSCL 01D

N84-12048*# Honeywell, Inc., St. Louis Park, Minn.
NASA DEMONSTRATION ADVANCED AVIONICS SYSTEM (DAAS)
Eric M. Peterson *In* NASA. Langley Research Center Controls, Displays and Inform. Transfer for Gen. Aviation IFR Operations Oct. 1983 p 229-240 refs (For primary document see N84-12029 03-01)
Avail: NTIS HC A12/MF A01 CSCL 01D

N84-12049*# National Aeronautics and Space Administration. Ames Research Center, Moffett Field, Calif.
AN OVERVIEW OF THE DEMONSTRATION ADVANCED AVIONICS SYSTEM GUEST PILOT EVALUATION CONDUCTED AT AMES RESEARCH CENTER
George P. Callas, G. H. Hardy, and D. G. Denery *In* NASA. Langley Research Center Controls, Displays and Inform. Transfer for Gen. Aviation IFR Operations Oct. 1983 p 241-265 refs (For primary document see N84-12029 03-01)
Avail: NTIS HC A12/MF A01 CSCL 01D

N84-12060# Marconi Avionics Ltd., Rochester (England). Airborne Display Div.
INTEGRATION OF FIRE CONTROL, NAVIGATION SYSTEM AND HEAD UP DISPLAY
G. M. Barling *In* AGARD Integration of Fire Control, Flight Control and Propulsion Control Systems Aug. 1983 18 p (For primary document see N84-12056 03-01)
Avail: NTIS HC A09/MF A01

N84-12065# Air Force Flight Dynamics Lab., Wright-Patterson AFB, Ohio.
DESIGN AND DEVELOPMENT OF THE MULTIFUNCTION FLIGHT CONTROL REFERENCE SYSTEM
John T. Young, John M. Perdzock, David L. Sebring (McDonnell Douglas Corp.), and Les Edinger (Honeywell Inc.) *In* AGARD Integration of Fire Control, Flight Control and Propulsion Control Systems Aug. 1983 10 p refs (For primary document see N84-12056 03-01)
Avail: NTIS HC A09/MF A01

N84-12066# Ferranti Ltd., Edinburgh (Scotland).
SOME ASPECTS OF FLIGHT TRAJECTORY CONTROL IN FUTURE AVIONIC SYSTEMS FOR COMBAT AIRCRAFT
W. H. McKinlay *In* AGARD Integration of Fire Control, Flight Control and Propulsion Control Systems Aug. 1983 11 p ref (For primary document see N84-12056 03-01)
Avail: NTIS HC A09/MF A01

N84-12067# Deutsche Forschungs- und Versuchsanstalt fuer Luft- und Raumfahrt, Brunswick (West Germany). Inst. fuer Flugfuehrung.
A DIAGNOSIS SCHEME FOR SENSORS OF A FLIGHT CONTROL SYSTEM USING ANALYTIC REDUNDANCY
Norbert Stuckenberg *In* AGARD Integration of Fire Control, Flight Control and Propulsion Control Systems Aug. 1983 12 p refs (For primary document see N84-12056 03-01)
Avail: NTIS HC A09/MF A01

07 AIRCRAFT PROPULSION AND POWER

Includes prime propulsion systems and systems components, e.g., gas turbine engines and compressors; and on-board auxiliary power plants for aircraft.

For related information see also *20 Spacecraft Propulsion and Power, 28 Propellants and Fuels,* and *44 Energy Production and Conversion.*

N84-12166*# National Aeronautics and Space Administration. Lewis Research Center, Cleveland, Ohio.
A GENERALIZED COMPUTER CODE FOR DEVELOPING DYNAMIC GAS TURBINE ENGINE MODELS (DIGTEM)
Carl J. Daniele Nov. 1983 18 p refs To be presented at the Aerospace Conf., San Diego, Calif., 2-3 Feb. 1984
(NASA-TM-83508; NAS 1.15:83508; E-1853) Avail: NTIS HC A02/MF A01 CSCL 21E

This paper describes DIGTEM (digital turbofan engine model), a computer program that simulates two spool, two stream (turbofan) engines. DIGTEM was developed to support the development of a real time multiprocessor based engine simulator being designed at the Lewis Research Center. The turbofan engine model in DIGTEM contains steady state performance maps for all the components and has control volumes where continuity and energy balances are maintained. Rotor dynamics and duct momentum dynamics are also included. DIGTEM features an implicit integration scheme for integrating stiff systems and trims the model equations to match a prescribed design point by calculating correction coefficients that balance out the dynamic equations. It uses the same coefficients at off design points and iterates to a balanced engine condition. Transients are generated by defining the engine inputs as functions of time in a user written subroutine (TMRSP). Closed loop controls can also be simulated. DIGTEM is generalized in the aerothermodynamic treatment of components. This feature, along with DIGTEM's trimming at a design point, make it a very useful tool for developing a model of a specific turbofan engine. B.W.

N84-12167# Ames Lab., Iowa.
PROGRESS ON ULTRASONIC FLAW SIZING IN TURBINE-ENGINE ROTOR COMPONENTS: BORE AND WEB GEOMETRIES
James H. Rose, T. A. Gray, R. B. Thompson, and J. L. Opsal (California Univ., Lawrence Livermore Lab.) 1983 31 p refs Presented at the Conf. on Quantitative NDE, Santa Cruz, Calif., 7-12 Aug. 1983
(Contract W-7405-eng-82)
(DE83-018081; IS-M-445; CONF-830811-9) Avail: NTIS HC A03/MF A01

The application of generic flaw-sizing techniques to specific components generally involves difficulties associated with geometrical complexity and simplifications arising from a knowledge of the expected flaw distribution. This paper is concerned with the case of ultrasonic flaw sizing in turbine-engine rotor components. The sizing of flat penny-shaped cracks in the web geometry discussed and new crack-sizing algorithms based on the Born and Kirchhoff approximations are introduced. Additionally, we propose a simple method for finding the size of a flat, penny-shaped crack given only the magnitude of the scattering amplitude. The bore geometry is discussed with primary emphasis on the cylindrical focusing of the incident beam. Important questions which are discussed include the effects of diffraction and the position of the flaw with respect to the focal line. The appropriate deconvolution procedures to account for these effects are introduced. Generic features of the theory are compared with experiment. Finally, the effects of focused transducers on the Born inversion algorithm are discussed. DOE

N84-12168# Advisory Group for Aerospace Research and Development, Neuilly-Sur-Seine (France).
AUXILIARY POWER SYSTEMS
Loughton, England Sep. 1983 228 p refs In ENGLISH and

FRENCH Meeting held in Copenhagen, 30-31 May 1983
(AGARD-CP-352; ISBN-92-835-0339-2) Avail: NTIS HC A11/MF A01

The state-of-the-art of aircraft auxiliary power systems for electrical, hydraulic, and pneumatic subsystems is reviewed. The advantages and problems associated with such systems are defined and future design improvements are identified. For individual titles, see N84-12169 through N84-12186.

N84-12169# Bundesministerium der Verteidigung, Bonn (West Germany).
AUXILIARY POWER REQUIREMENTS: THEIR ROLE IN AIRCRAFT PERFORMANCE
E. W. Eckert *In* AGARD Auxiliary Power Systems Sep. 1983 17 p (For primary document see N84-12168 03-07)
Avail: NTIS HC A11/MF A01

Based on the historical development and the actual status of requirements, the trends of essential parameters are analyzed, physical and technical possibilities are assessed and a prognosis is offered. Increasing demands for secondary power for subsystems and more powerful engines have led to stronger secondary power components, thus creating a mass problem. Energy losses add a thermal problem. Complexity rises rapidly with the number of inputs and outputs. All of this, together with such aspects as redundancy, reliability, safety, maintainability and life cycle cost, composes today's auxiliary power system. The future system, in response to high performance requirements and budgetary and personnel restrictions, should aim at less complexity and more efficiency.
Author

N84-12170# Societe Microturbo, Toulouse (France).
AUXILLIARY POWER SYSTEMS WITH GAS TURBINES [GROUPES AUXILIAIRES A TURBINE A GAZ]
A. Romier and P. Calmels *In* AGARD Auxiliary Power Systems Sep. 1983 8 p In FRENCH (For primary document see N84-12168 03-07)
Avail: NTIS HC A11/MF A01

Gas turbine auxilliary power systems were developed to meet the demand for aircraft autonomy during their use for checklist, conditioning from the ground, and main engine starting. Solutions developed in the military and civil domains for a short operational pure start system are examined as well as an auxilliary system with continued operation. Present trends on modern aircraft where the starting system is capable of continued operation are considered. Future needs that can be predicted as a function of the growing complexity of onboard weapons systems which require ground conditioning, the development of principal reactors imposing ever more important starting power, and operation as a help in the flight domain with extremely reduced time of use are explored.
Transl. by A.R.H.

N84-12171# KHD Luftfahrttechnik G.m.b.H., Oberursel (West Germany).
SECONDARY POWER SYSTEMS FOR FIGHTER AIRCRAFT EXPERIENCES TODAY AND REQUIREMENTS FOR A NEXT GENERATION
Walter Hausmann, Manfred Pucher, and Thomas Weber *In* AGARD Auxiliary Power Systems Sep. 1983 15 p refs (For primary document see N84-12168 03-07)
Avail: NTIS HC A11/MF A01

The necessary of a continuous increase of fighting efficiency of weapon systems sets forth a number of new requirements for the next generation of military aircraft in particular regarding the distribution and use of the onboard auxiliary power. Energy conversion methods have to be applied which are readily adaptable to operation requirements and also favour the thermal balance of the aircraft. As an example of the pneumatic energy conversion the efficiency of an auxiliary system is presented together with a listing of those factors which play a role in its optimization. Design concepts and options available for future systems are presented. Experience derived from a modern fighter aircraft system serves as a basis for discussion of advanced requirements and design features.
Author

N84-12172# Solar Turbines International, San Diego, Calif. Turbomach.
SMALL AUXILIARY POWER UNIT DESIGN CONSTRAINTS
Colin Rodgers *In* AGARD Auxiliary Power Systems Sep. 1983 19 p refs (For primary document see N84-12168 03-07)
Avail: NTIS HC A11/MF A01

Self-sufficiency for military aircraft operating from remote advanced bases can be attained with small on-board air breathing gas turbine auxiliary power units (APUs) supplying main engine start and aircraft secondary power. The small, fixed shaft, gas turbine configuration comprising the single-stage radial compressor and radial inflow turbine, mounted back-to-back, and overhung from a cold end bearing capsule has found favor in providing this duty due to inherent attributes of low costs, simplicity and high power-to-weight ratio. Extensive experience with these APUs has led to the formulation of several major design constraints, within the objective of minimum life cycle costs, that enhance development of both modified and derivative versions. Some of these design constraints are discussed and advantageous areas of research and development for future APUs are identified. Author

N84-12173# KLM Royal Dutch Airlines, Amsterdam (Netherlands).
APU IN COMMERCIAL AIRLINE OPERATION
H. W. C. L. Schoevers and A. Booy *In* AGARD Auxiliary Power Systems Sep. 1983 9 p (For primary document see N84-12168 03-07)
Avail: NTIS HC A11/MF A01

Advantages and disadvantages of incorporating auxiliary power units in commercial aircraft are discussed. Reliability, maintenance and weight costs, and fuel savings are specifically addressed. The auxiliary power unit (APU) provides pneumatic and electrical power on the ground for operation of the air conditioning and electrical systems and for starting the main engines. Operation and control are fully automatic after start initiation, making a better use of the manpower available. Since the airplane's air packs are run, the APU can provide a cooler aircraft at boarding time on hot days than ground equipment. Moreover, individual temperature control of the cabin sections is possible. The APU reduces dependence on ground equipment availability and reliability, thus enhancing on-time performance. It reduces the quantity of required ramp equipment, thus reducing ramp congestion and consequently turn-around time. Even a water system may fall in this category. On some aircraft availability of the APU may be used to replace a failing engine generator during specific flight phases.
M.G.

N84-12174# ABG-Semca S.A., Toulouse (France).
AUXILIARY POWER UNITS FOR WIDE-BODY AIRCRAFT
S. Riazuelo, M. Cenival (Turbomeca, Bizanos, France), and M. Eglem *In* AGARD Auxiliary Power Systems Sep. 1983 14 p (For primary document see N84-12168 03-07)
Avail: NTIS HC A11/MF A01

Existing auxiliary power units for wide body aircraft are described with individual consideration given to the power section, accessory gear box, load compressor, and digital electronic regulation modules. Requirements for future designs of such systems are identified.
M.G.

N84-12175# British Aerospace Aircraft Group, Brough (England).
SECONDARY POWER SUPPLIES FOR A SMALL SINGLE ENGINE COMBAT AIRCRAFT
G. Jones *In* AGARD Auxiliary Power Systems Sep. 1983 7 p (For primary document see N84-12168 03-07)
Avail: NTIS HC A11/MF A01

A possible secondary power supply system for a small single engined combat aircraft is described along with the way in which reliability, survivability and installation problems influence the type of system which is proposed for such an aircraft. The particular constraints imposed by the use of a Pegasus vectored thrust engine in a short take off vertical landing (STOVL) aircraft are also discussed. The proposed system consists of a conventional engine driven accessory gearbox to provide hydraulic and electrical power in flight. A remotely mounted auxiliary power unit (APU) is used to start the engine by means of a pneumatic link from a load

compressor. The APU drives a separate standby hydraulic pump and generator for ground operation and emergency power in flight. Possible areas of future research and development which would lead to improved efficiency and reduced weight are also discussed. M.G.

N84-12176# Avions Marcel Dassault, Saint-Cloud (France). Dept. au Bureau d'Etudes Serie.
HYDRAULIC GENERATION OF AUXILLIARY POWER FOR THE MIRAGE 2000 AIRCRAFT [GENERATION HYDRAULIQUE DE SECOURS DU MIRAGE 2000]
P. Atlan *In* AGARD Auxiliary Power Systems Sep. 1983 6 p In FRENCH (For primary document see N84-12168 03-07)
Avail: NTIS HC A11/MF A01

The auxiliary hydraulic power system of the Mirage 2000 aircraft is described and justified. The system was designed to respond to a particular problem that is specific to that aircraft. A source of energy was found and a means of putting it to work to assure the operation of the aircraft flight control hydraulic servocommand in the case of a dead engine and in the tail slide maneuver flight phase was developed. Transl. by A.R.H.

N84-12177# British Aerospace Aircraft Group, Preston (England).
OPTIMIZATION OF ENGINE POWER OFFTAKE BY SECONDARY POWER SYSTEM DESIGN
J. R. Hopkins *In* AGARD Auxiliary Power Systems Sep. 1983 15 p refs (For primary document see N84-12168 03-07)
Avail: NTIS HC A11/MF A01

The configuration constraints presented to a systems engineer when designing a secondary power system are examined with particular reference to the minimizing of engine power offtake. The effects of power offtake on the engine and current solutions available to the systems designer are discussed. A secondary power system which is optimized for a twin engined, agile, combat aircraft is defined. M.G.

N84-12178# Rocket Research Corp., Redmond, Wash.
HOT GAS APU STARTER FOR ADVANCED AIRCRAFT APPLICATIONS
B. W. Schmitz, L. D. Galbraith, W. E. Jorgenson, and D. A. Pahl *In* AGARD Auxiliary Power Systems Sep. 1983 14 p refs (For primary document see N84-12168 03-07)
(Contract F33615-76-C-2148)
Avail: NTIS HC A11/MF A01

A hot gas rotary vane motor for aircraft APU starting over the environmental temperature range of -65 F to +130 F was tested. Problems with excessive gas consumption and binding of parts due to differential expansion are indicated. The effect of friction coefficient, vane weight, venting, and blade linking on overall internal friction are shown. Design approaches evolved to minimize overall friction and loads on the vanes. A motor successfully demonstrated operation at environmental temperatures down to -65 F and as repeated restart capability are solved. Design criteria allow application of the rotary vane motor to specific aircraft starting requirements. E.A.K.

N84-12179# Teledyne CAE, Toledo, Ohio. Advanced Development and Technical Planning.
A JET FUEL STARTER FOR LOWEST SYSTEM LIFE CYCLE COST
Ray Smith *In* AGARD Auxiliary Power Systems Sep. 1983 11 p refs (For primary document see N84-12168 03-07)
(Contract F33657-76-C-2055)
Avail: NTIS HC A11/MF A01

A modular Jet Fuel Starter design employing an Expendable Gasifier (EG) concept indicates a substantial life cycle cost savings over a conventional overhauled unit. To achieve these savings, a low cost gasifier is a mandatory requirement. The EG does this by maximizing cast to hear net shape components, using aluminum cold end castings and by minimizing the use of expensive high temperature alloys. Gasifier performance parameters, specific power, compressor pressure ratio, cycle temperature and fuel consumption, were selected to minimize component stress and sensitivity to refined dimensions. The gasifier interfaces were established to fit optional JFS and auxilarily power unit installations, and include turbojets and turbofans suitable for unmaned vehicles. E.A.K.

N84-12180# Lufthansa G.m.b.H., Hamburg (West Germany).
COST EFFICIENT ON BOARD POWER FOR AIRLINE OPERATION
Klaus Mose *In* AGARD Auxiliary Power Systems Sep. 1983 12 p (For primary document see N84-12168 03-07)
Avail: NTIS HC A11/MF A01

Airline experience with auxiliary power units (APU), influenced by the fuel crisis was reviewed. Typical APU design features and performance outputs, supplying bleed air and/or electrical power on board the airplane are presented. It is suggested that the economical impact on APU operation are tue to fuel cost increase and high level of APU maintenance cost. Remedy actions are proposed by: incorporation of fuel saving modification programs and reduction of APU operating time which will effect the operating procedures. The utilization of alternative power sources on the ground, providing on board power, by mobile or stationary systems for electrical and pneumatic supply with respect to: system compatibility with on board power requirements and availability and necessary cost investments are proposed. E.A.K.

N84-12181# Messerschmitt-Boelkow-Blohm G.m.b.H., Hamburg (West Germany).
APU OPERATIONAL EFFICIENCY
Werner Hoose *In* AGARD Auxiliary Power Systems Sep. 1983 15 p (For primary document see N84-12168 03-07)
Avail: NTIS HC A11/MF A01

Exprience with a new generation on Auxiliary Power Unit (APU) installed in a commercial transport aircraft is presented. Operational requirements and efficiency of the APU in the Various operating modes are outlined. The factors determining the APU performance characteristics with respect to a cost effective are emphasized. Future development trends seen from the point of view of the aircraft manufacturer is considered. E.A.K.

N84-12182# Vereinigte Flugtechnische Werke G.m.b.H., Bremen (West Germany).
GROUND AND INFLIGHT OPERATIONAL EFFECTS OF APU'S
J. H. Renken *In* AGARD Auxiliary Power Systems Sep. 1983 17 p (For primary document see N84-12168 03-07)
Avail: NTIS HC A11/MF A01

The Airbus APU which has a deliver well defined quantities of bleed air and electrical power under two very different conditions on ground and inflight was examined. The on ground operation is essentially governed by problems like noise generation and emission, and ingestion of hot gas, constraining the possible range of intake and exhaust position. The infight operation is dominated by the external fuselage flow conditions intake and exhaust are exposed to and which may effect significantly the installation pressure-ratio and with that the infight restart envelope and infight performance. Depending on fuselage surface pressures and boundary layer conditions, intake and exhaust geometries and ducting have to be designed so that a favourable IPR is provided during APU starting as well as APU operation, keeping at the same time negative effects on the aircraft as for instance drag increase at a minimum. The effect of these environmental conditions on the APU performance is discussed. E.A.K.

N84-12183# Rocketdyne, Canoga Park, Calif.
SUPER INTEGRATED POWER UNIT FOR FIGHTER AIRCRAFT
Armando D. Lucci, James A. Williams, Earl C. Beder, and Buryl L. McFadden (AFAPL, Wright-Patterson AFB, Ohio) *In* AGARD Auxiliary Power Systems Sep. 1983 6 p (For primary document see N84-12168 03-07)
Avail: NTIS HC A11/MF A01

The SIPU concept the designs of the demonstrator, and each of its subsystems are described. An SIPU is a multifunctional aircraft power unit capable of providing (1) electrical, pneumatic, and hydraulic power for ground maintenance and standby operations,

(2) normal and emergency main engine start power, and (3) emergency electrical and hydraulic power. Power is obtained either from jet fuel combustion with air for ground operations and normal engine starts, from a gas generator system using onboard stored propellants for emergency functions, or from the aircraft main engine compressor air for the emergency electrical and hydraulic power function. The benefits resulting from the use of an SIPU are pesented. E.A.K.

N84-12184# Rolls-Royce Ltd., Bristol (England).
ALL-ELECTRIC ACCESSORY DRIVE SYSTEMS: IMPLICATIONS ON ENGINE DESIGN AND PERFORMANCE
G. B. Toyne and G. S. Hodges *In* AGARD Auxiliary Power Systems Sep. 1983 8 p (For primary document see N84-12168 03-07)
Avail: NTIS HC A11/MF A01

All-electric accessory power systems were studied. The effects on engine design and performance are outlined. In the all-electric proposal, all accessory power requirements are generated and distributed electrically. Air bleeds for environmental control systems are replaced by increased shaft power offtake. The concept which is considered for a large subsonic offers the prospect of simplification and weight reduction in the engines. For supersonic combat aircraft, the concept is not recommended; with relatively higher levels of shaft power offtake, additional handing problems will be created. The effects on the engine and aircraft weight and systems as a whole consideration. E.A.K.

N84-12185# Sundstrand Advanced Technology Group, Rockford, Ill.
IMPLEMENTING MICROPROCESSOR TECHNOLOGY IN AIRCRAFT ELECTRICAL POWER GENERATING SYSTEM CONTROL
Greg Ruffner, Byron Menl, and Susan Lorenz *In* AGARD Auxiliary Power Systems Sep. 1983 15 p refs (For primary document see N84-12168 03-07)
Avail: NTIS HC A11/MF A01

The implementation of microprocessor technology of most control protection, and build on test functions, the aircraft electrical power generating systems is described. The design implementation process used in current system is highlighted. With the adaptation of advanced microprocessor systems in the next generation of aircraft electric systems, additional functions can be implemented. Microprocessor control of generator paralleling and voltage regulation coupled with more effectie builtin test capabilities will result in significant improvements in system performance. E.A.K.

N84-12186# Auxilec S.A., Colombus (France). Electro-Technics Dept.
THE 400 Hz GENERATORS EVOLUTION, EFFECTS ON INSTALLATION ARRANGEMENTS
Claude Jacques *In* AGARD Auxiliary Power Systems Sep. 1983 11 p (For primary document see N84-12168 03-07)
Avail: NTIS HC A11/MF A01

The need for 400 Hz electric power which keeps on increasing on airplanes is discussed. Up to now the way to obtain constant frequency from variable speed drive is either hydro or electro mechanical. New conversion systems are arising: they take benefits from the most recent improvements and developments in high speed electrotechnics and power electronics. Rotational speeds running at more than 2400 r.p.m. are accessible to the onboard generator and a significant improvement of power to weight ratio is obtained. The installation of such a generator on aircraft entails an high speed gear whic can be combined with it or, installed in the accessory gearbox. The cooling of the whole system is realized by air or, by oil, electronic components included. Optimum design leads to share the oil circuit of the gearbox with the generator cooling system. E.A.K.

N84-12187 Wichita State Univ., Kans.
ANALYTICAL DESIGN OF A LIQUID HYDROGEN FUELED TURBOFAN-RAMJET ENGINE FOR FLIGHT MACH NUMBERS ZERO TO FIVE Ph.D. Thesis
Sompol Suwanprasert 1982 291 p
Avail: Univ. Microfilms Order No. DA8308656

The analytical design of a hydrogen fueled, dual-cycle engine having either an annular "wraparound" turboramjet or side-by-side turbofan-ramjet has been conducted. The typical flight profile was assumed with altitude ranging from sea level to 90,000 ft and Mach number from 0 to 5. The overall performances evaluated for both engines are presented in the form of the engine thrust, drag and thrust specific fuel consumption. The corresponding weights and lengths of the engines are also determined. The side-of-side turbofan-ramjet, which is lighter and shorter than the wraparound turboramjet, emerges as an optimum engine configuration. It yields considerably higher overall performance over the entire prescribed flight profile. However, this optimum design requires a side-by-side combustion chamber for ramjet and turbofan afterburner with a variable position wall between the two chambers. The optimum operating mode of the side-by-side turbofan-ramjet is then defined. Dissert. Abstr.

N84-12188 California Univ., Berkeley.
COMBUSTION JET IGNITION Ph.D. Thesis
Daih Yeou Chen 1982 139 p
Avail: Univ. Microfilms Order No. DA8312780

A combustion jet ignitior system was developed to generate turbulent jets of combustion products containing free radicals and to discharge them as ignition sources into a combustible medium. In order to understand the ignition and the inflammation processes caused by combustion jets, the study of the fluid mechanical properties of turbulent jets with and without combustion were conducted theoretically and experimentally. Experiments using a specially designed igniter, with a prechamber to build up and control the stagnation pressure upstream of the orifice, were conducted to investigate the formation processes of turbulent jets of combustion products. The penetration speed of combustion jets has been found to be constant initially and then decreases monotonically as turbulent jets of combustion products travel closer to the wall. This initial penetration speed of combustion jets is proportional to the initial stagnation pressure upstream of the orifice for the same stoichiometric mixture. Dissert. Abstr.

N84-12063# British Aerospace Public Ltd. Co., Lancashire (England). Advanced Control Systems Group.
INTEGRATED POWERPLANT CONTROL SYSTEMS AND POTENTIAL PERFORMANCE BENEFITS
A. G. Seabridge and R. A. Edwards *In* AGARD Integration of Fire Control, Flight Control and Propulsion Control Systems Aug. 1983 10 p refs (For primary document see N84-12056 03-01)
Avail: NTIS HC A09/MF A01

N84-12064# Dowty and Smith Industries Controls Ltd., Cheltenham (England).
FULL AUTHORITY DIGITAL ELECTRONIC ENGINE CONTROLS AND THEIR INTEGRATION WITH FLIGHT CONTROL SYSTEMS IN VSTOL AIRCRAFT
E. S. Eccles *In* AGARD Integration of Fire Control, Flight Control and Propulsion Control Systems Aug. 1983 10 p refs (For primary document see N84-12056 03-01)
Avail: NTIS HC A09/MF A01

08 AIRCRAFT STABILITY AND CONTROL

Includes aircraft handling qualities; piloting; flight controls; and autopilots.

N84-12189 Kansas Univ., Lawrence.
A FAULT-TOLERANT DISTRIBUTED COMPUTER NETWORK DESIGN AND ANALYSIS FOR AN INTEGRATED FLIGHT CONTROL SYSTEM Ph.D. Thesis
David Piang-Wen Jiang 1982 262 p
Avail: Univ. Microfilms Order No. DA8309353

A Fault-Tolerant Distributed Computer (FTDC) Network for an integrated flight control system was designed for real time control applications requiring good reliability, availability, and survivability characteristics. A Maximally Connect Minimum Diameter topology with node connection degree 4 (MCMD-4) is proposed which minimized the average message time delay. Realization MCMD-4 graphs with diameter 2 and 3 are given. A comparison of graph diameter and fault tolerant capability of MCMD-4 graphs with other topologies is included. Network reliability bounds were obtained which included four paths between any two nodes for MCMD-4 networks and Harary-Hakimi networks. Network hardware design for a seven node network was completed and tested. Each node was designed with a node connection degree of four where the communication processor handled data at 2 MBPS on each of the four channels into a node and on each of the four channels out of a node for a total node capacity of 16 MBPS.

Dissert. Abstr.

N84-12190*# National Aeronautics and Space Administration. Langley Research Center, Hampton, Va.

SIMULATOR STUDY OF FLIGHT CHARACTERISTICS OF A LARGE TWIN-FUSELAGE CARGO TRANSPORT AIRPLANE DURING APPROACH AND LANDING

William D. Grantham, Perry L. Deal, Gerald L. Keyser, Jr., and Paul M. Smith (Kentron International, Inc.) Nov. 1983 87 p refs (NASA-TP-2183; L-15505; NAS 1.60:2183) Avail: NTIS HC A05/MF A01 CSCL 01C

A six degree-of-freedom, ground-based simulator study was conducted to evaluate the low speed flight characteristics of a twin fuselage cargo transport airplane and to compare these characteristics with those of a large, single fuselage (reference) transport configuration which was similar to the Lockheed C-5C airplane. The primary piloting task was the approach and landing. The results indicated that in order to achieve 'acceptable' low speed handling qualities on the twin fuselage concept, considerable stability and control augmentation was required, and although the augmented airplane could be landed safely under adverse conditions, the roll performance of the aircraft had to be improved appreciably before the handling qualities were rated as being 'satisfactory.' These ground-based simulation results indicated that a value of t sub phi = 30 (time required to bank 30 deg) less than 6 sec should result in 'acceptable' roll response characteristics, and when t sub phi = 30 is less than 3.8 sec, 'satisfactory' roll response should be attainable on such large and unusually configured aircraft as the subject twin fuselage cargo transport concept. S.L.

N84-12191# Air Force Wright Aeronautical Labs., Wright-Patterson AFB, Ohio. Aeroelastic Group.

DEVELOPMENT AND FLIGHT TEST OF AN ACTIVE FLUTTER SUPPRESSION SYSTEM FOR THE F-4F WITH STORES. PART 3. FLIGHT DEMONSTRATION OF THE ACTIVE FLUTTER SUPPRESSION SYSTEM Final Report, Mar. - Dec. 1980

H. Hoenlinger, D. Mussman, R. Manser, and Lawrence J. Huttsell Jun. 1983 66 p Prepared in cooperation with Messerschmitt-Blohm-Blohm GmbH, Ottobrunn (West Germany)
(AF Proj. 2401)
(AD-A131972; AFWAL-TR-82-3040-Pt-3) Avail: NTIS HC A04/MF A01 CSCL 01/3

A flutter suppression system was developed and flight tested on an F-4F aircraft. The control law was designed by MBB (Messerschmitt-Bolkow-Blohm GmbH) using optimal control theory to minimize the control surface motion and to provide the required stability margins. During the test it was found that the dynamic behavior of the wing-pylon-store changed considerably with excitation amplitude due to free play and preload. The active flutter suppression system worked well and provided an increase in flutter speed. GRA

N84-12035*# National Aeronautics and Space Administration. Langley Research Center, Hampton, Va.

GENERAL AVIATION SINGLE PILOT IFR AUTOPILOT STUDY

Hugh P. Bergeron *In its* Controls, Displays and Inform. Transfer for Gen. Aviation IFR Operations Oct. 1983 p 85-96 refs (For primary document see N84-12029 03-01)
Avail: NTIS HC A12/MF A01 CSCL 01C

N84-12036*# National Aeronautics and Space Administration. Langley Research Center, Hampton, Va.

FLIGHT TEST VALIDATION OF A DESIGN PROCEDURE FOR DIGITAL AUTOPILOTS

Wayne H. Bryant *In its* Controls, Displays and Inform. Transfer for Gen. Aviation IFR Operations Oct. 1983 p 97-110 refs (For primary document see N84-12029 03-01)
Avail: NTIS HC A12/MF A01 CSCL 01C

N84-12038*# Kansas Univ., Lawrence.

PILOT CONTROLS AND SPIRF FLIGHT

D. R. Downing *In* NASA. Langley Research Center Controls, Displays and Inform. Transfer for Gen. Aviation IFR Operations Oct. 1983 p 121-140 refs (For primary document see N84-12029 03-01)
Avail: NTIS HC A12/MF A01 CSCL 01C

N84-12061# Northrop Corp., Hawthorne, Calif. Aircraft Div.

APPLICATION OF FLIGHT CONTROLS TECHNOLOGY TO ENGINE CONTROL SYSTEMS

Rudolf J. Seemann and J. L. Lockenour *In* AGARD Integration of Fire Control, Flight Control and Propulsion Control Systems Aug. 1983 26 p refs (For primary document see N84-12056 03-01)
Avail: NTIS HC A09/MF A01

N84-12062# Societe Nationale d'Etudes et de Construction de Moteurs d'Aviation, Moissy-Cramayel (France).

THE RELATIONS BETWEEN THE NUMERICAL CONTROL OF THE ENGINE AND OTHER AIRCRAFT FUNCTIONS [LIENS ENTRE LA REGULATION NUMERIQUE DU MOTEUR ET LES AUTRES FONCTIONS DE L'AVION]

D. Rambach *In* AGARD Integration of Fire Control, Flight Control and Propulsion Control Systems Aug. 1983 9 p In FRENCH (For primary document see N84-12056 03-01)
Avail: NTIS HC A09/MF A01

N84-12069# Bodenseewerk Geraetetechnik G.m.b.H., Ueberlingen (West Germany).

AN INTEGRATED AFCS FOR THE "PROFILE"-MODE

P. Wuest and W. Alles *In* AGARD Integration of Fire Control, Flight Control and Propulsion Control Systems Aug. 1983 11 p refs (For primary document see N84-12056 03-01)
Avail: NTIS HC A09/MF A01

N84-12070# British Aerospace Aircraft Group, Brough (England). ACT Design Group.

THE INTEGRATION OF FLIGHT AND ENGINE CONTROL FOR VSTOL AIRCRAFT

N. P. Pattinson *In* AGARD Integration of Fire Control, Flight Control and Propulsion Control Systems Aug. 1983 7 p refs (For primary document see N84-12056 03-01)
Avail: NTIS HC A09/MF A01

N84-12071# Office National d'Etudes et de Recherches Aerospatiales, Paris (France).

A NONLINEAR CONTROL LAW FOR PILOTING AIRCRAFT IN THE AIR-TO-GROUND ATTACK PHASE [SUR UNE LOI DE COMMANDE NON-LINEAIRE POUR LE PILOTAGE DES AVIONS EN PHASE D'ATTAQUE AIR-SOL]

B. Dang Vu and O. L. Mercier *In* AGARD Integration of Fire Control, Flight Control and Propulsion Control Systems Aug. 1983 10 p refs In FRENCH; ENGLISH summary (For primary document see N84-12056 03-01)
Avail: NTIS HC A09/MF A01

09 RESEARCH AND SUPPORT FACILITIES (AIR)

Includes airports, hangars and runways; aircraft repair and overhaul facilities; wind tunnels; shock tube facilities; and engine test blocks.

For related information see also *14 Ground Support Systems and Facilities (Space).*

N84-12192*# Southampton Univ. (England). Dept. of Aeronautics and Astronautics.
PERFORMANCE MEASUREMENTS OF A PILOT SUPERCONDUCTING SOLENOID MODEL CORE FOR A WIND TUNNEL MAGNETIC SUSPENSION AND BALANCE SYSTEM Contractor Report, Oct. 1982 - Jul. 1983
M. J. Goodyer and C. P. Britcher Nov. 1983 31 p refs
(Grant NsG-7523)
(NASA-CR-172243; NAS 1.26:172243) Avail: NTIS HC A03/MF A01 CSCL 14B

The results of experimental demonstrations of a superconducting solenoid model core in the Southampton University Magnetic Suspension and Balance System are detailed. Technology and techniques relevant to large-scale wind tunnel MSBSs comprise the long term goals. The magnetic moment of solenoids, difficulties peculiar to superconducting solenoid cores, lift force and pitching moment, dynamic lift calibration, and helium boil-off measurements are discussed. N.W.

N84-12193*# National Aeronautics and Space Administration. Ames Research Center, Moffett Field, Calif.
VISUAL ACCOMMODATION TRAINER-TESTER Patent Application
Robert J. Randle, Jr., Inventor (to NASA) Filed 12 Aug. 1983 20 p
(NASA-Case-ARC-11426-1; US-Patent-Appl-SN-526741) Avail: NTIS HC A02/MF A01 CSCL 14B

An apparatus for training of the human visual accommodation system is presented, specifically, useful for training a person to volitionally control his focus to his far point (normaly infinity) from a position of myopia due to functional causes. The functional causes could be due, for example, to a behavioral accommodative spasm or the effects of an empty field. The device may also be used to measure accommodation, the accommodation resting position and the near and far points of vision. NASA

N84-12194# Ballistic Research Labs., Aberdeen Proving Ground, Md.
EXPERIMENTAL AND COMPUTATIONAL MODELING OF RAREFACTION WAVE ELIMINATORS SUITABLE FOR THE BRL 2.44 M SHOCK TUBE Final Report
George A. Coulter, Gerald Bulmash, and Charles N. Kingery Jun. 1983 117 p
(DA Proj. 1L1-62618-AH-80)
(AD-A131894; AD-F300292; ARBRL-TR-02503) Avail: NTIS HC A06/MF A01 CSCL 19/4

Three general types of rarefaction wave eliminators, RWEs (solid plate, vented plate, and lattice) were tested on a 1/48th scale model of the BRL 2.44 m shock tube. Pressures were monitored along the test section with piezoelectric transducers to determine effectiveness of the RWEs tested. All types were found to be equally effective in reducing the rarefactions but the lattice type was most difficult to use. The solid plate and vented plate RWEs would both be suitable for the 2.44 m shock tube. Predictions are produced using the NASA-Ames one dimensional computer hydrocode. The hydrocode can be used effectively to model a RWE for the 2.44 m shock tube. Experimental and computational results are compared. GRA

N84-12195# BDM Corp., McLean, Va.
RAPID RUNWAY REPAIR PROGRAM SUBTASK 1.07 - RAPID CONCRETE CUTTING Final Technical Report, Mar. 1982 - Jan. 1983
R. K. Moats, F. D. Wang, William Dears (Air Force Engineering and Services Center, Tyndall AFB, Fla.), and G. G. Yie (Fluidyne Corp., Auburn, Wash.) Tyndall AFB, Fla. Air Force Engineering and Services Center Jun. 1983 197 p
(Contract F08635-80-C-0206; AF Proj. 2673)
(AD-A131771; BDM/W-82-770-TR; AFESC/ESL-TR-83-09) Avail: NTIS HC A09/MF A01 CSCL 13/2

Two concrete-cutting technologies utilizing high-pressure waterjets have been investigated to assess their feasibility in achieving rapid cutting rates (30 sq ft/min) to facilitate bomb damage repair to runways. The current cutting rate of abrasive waterjets was established as 0.25 sq ft/min for a 60 hp system. Present scaling information indicates that for the near term the technology cannot feasibly achieve the desired cutting rate without a major technical breakthrough. Data from laboratory tests of linear cutting with a single carbide pick assisted with a waterjet indicate that high cutting rates are feasible with that technology. The waterjet-assisted mechanical cutting technology, however, has not been developed as a concrete cutting system. Prototype concepts are proposed in this report and an estimate is made of the power requirement to achieve the desired cutting rate (250 hp to cut 30 sq ft/min). GRA

N84-12149# Office of Technology Assessment, Washington, D.C.
AIRPORT CAPACITY ALTERNATIVES
In its Airport and Air Traffic Control System Jan. 1982 p 101-122 refs (For primary document see N84-12143 03-04)
Avail: SOD HC $6.00 as 052-003-00873-4

12 ASTRONAUTICS (GENERAL)

For extraterrestrial exploration see *91 Lunar and Planetary Exploration.*

N84-12196*# National Aeronautics and Space Administration. Marshall Space Flight Center, Huntsville, Ala.
MATERIALS PROCESSING IN SPACE PROGRAM TASKS-SUPPLEMENT
Elizabeth Pentecost, comp. Oct. 1983 60 p
(NASA-TM-82548; NAS 1.15:82548) Avail: NTIS HC A04/MF A01 CSCL 22A

An overview of the program scope for managers and scientists in industry, university, and government communities is provided. An introductory description of the program, its history, strategy, and overall goals; identification of the organizational structures and people involved; and a description of each research task, together with a list of recent publications are included. The tasks are grouped into six categories: crystal growth; solidification of metals, alloys, and composites; fluids, transports, and chemical processes; and ultrahigh vacuum and containerless processing technologies; combustion experiments; and experimental technology. S.L.

13 ASTRODYNAMICS

Includes powered and free-flight trajectories; and orbit and launching dynamics.

No abstracts in this category.

14 GROUND SUPPORT SYSTEMS AND FACILITIES (SPACE)

Includes launch complexes, research and production facilities; ground support equipment, e.g., mobile transporters; and simulators.

For related information see also *09 Research Support Facilities (Air).*

N84-12197# European Space Agency, Paris (France).
SPACECRAFT VIBRATION TESTING USING MULTI-AXIS HYDRAULIC VIBRATION SYSTEMS
W. R. Burke, comp. Jul. 1983 179 p refs Proc. of Workshop, Noordwijk, Netherlands, 3-4 May 1983
(ESA-SP-197; ISSN-0379-6566) Avail: NTIS HC A09/MF A01

Test philosophy; test specifications; and facility requirements for multiaxis vibration testing of spacecraft were discussed. Hydraulic hardware; control of multiaxis vibration systems; and mathematical modeling and simulation of tests were treated. For individual titles, see N84-12198 through N84-12207.

N84-12198# Technische Hochschule, Aachen (West Germany). Inst. fuer Leichtbau.
THE HYDRAULIC MULTIAXES VIBRATOR: ITS CAPABILITIES TO SIMULATE REAL MECHANICAL ENVIRONMENTS AND TO VERIFY AEROSPACE STRUCTURES
H. Oery, E. Hornung (Erno Raumfahrttechnik G.m.b.H.), and K. Eckhardt (Erno Raumfahrttechnik G.m.b.H.) *In* ESA Spacecraft Vibration Testing using Multiaxis Hydraul. Vibration Systems Jul. 1983 p 5-10 refs (For primary document see N84-12197 03-14)
Avail: NTIS HC A09/MF A01

For the realistic dynamic verification and structural qualification of large modern spacecraft prototypes as well as for the acceptance of the corresponding flight units, a test philosophy was defined. After a review of the dynamic environments to be simulated, it is concluded that a multiaxis vibrator system (MAVIS) fulfills these requirements with six degrees of freedom up to a frequency of 100 Hz. A further increase of this frequency margin causes serious technical difficulties. The MAVIS tests can also simulate realistic dynamic environments for spacecrafts having more than one interface. They also permit the simultaneous application of quasistatic and dynamic loads. The MAVIS facilities are a development of earthquake simulators. Author (ESA)

N84-12199# Technische Hochschule, Aachen (West Germany). Inst. fuer Leichtbau.
PRACTICAL EXPERIENCE DURING INSTALLATION OF THE LARGE MULTIAXES VIBRATION TEST FACILITY SAMSON
A. Kleine-Tebbe (Hochtemperatur Reaktorbau G.m.b.H.) and G. Hirsch *In* ESA Spacecraft Vibration Testing using Multiaxis Hydraul. Vibration Systems Jul. 1983 p 13-23 refs (For primary document see N84-12197 03-14)
Avail: NTIS HC A09/MF A01

A three-axis test facility (SAMSON) whose vibration test platform, a steel box structure of 5 x 5 x 1,2 m, is designed for testing specimens of up to 25 tons mass is presented. The platform can be moved in both horizontal axes by two pairs of hydraulic actuators and in vertical axes by one main actuator and four additional actuators used for counteracting the pitch motion. It is possible to reproduce simultaneous and independent motions in three axes in the frequency range 0.5 to 100 Hz with a maximum acceleration of 20 m/sec/sec (15 tons). Installations and acceptance tests are reported. A test specimen with adjustable stiffness was designed to check the performance of the control system.
Author (ESA)

N84-12200# National Engineering Lab., East Kilbride (Scotland).
THE DEVELOPMENT OF A MULTI-AXIS HYDRAULIC VIBRATION TEST FACILITY AT THE NATIONAL ENGINEERING LABORATORY, SCOTLAND
J. Fairbairn *In* ESA Spacecraft Vibration Testing using Multiaxis Hydraul. Vibration Systems Jul. 1983 p 25-28 (For primary document see N84-12197 03-14)
Avail: NTIS HC A09/MF A01

For seismic qualification of nuclear power plant components, three servohydraulic shaker table test facilities were designed and constructed. Components up to 20 tons mass can be tested at frequencies up to 70 Hz. In addition to seismic qualification work, techniques for the simulation of vibrations during transportation, where rotational degrees of freedom are significant, are described. Author (ESA)

N84-12201# Industrieanlagen-Betriebsgesellschaft m.b.H., Ottobrunn (West Germany).
HYDRAULIC ACTUATORS AND ASSOCIATED COMPONENTS SUITED FOR MULTIAXIS VIBRATION SYSTEMS
W. Raasch *In* ESA Spacecraft Vibration Testing using Multiaxis Hydraul. Vibration Systems Jul. 1983 p 31-53 refs (For primary document see N84-12197 03-14)
Avail: NTIS HC A09/MF A01

The influence of the arrangement of the cylinders and the test table on vibration simulator performance data is discussed. Different joints between cylinder and table are compared for stiffness, weight, friction torque and cost. Problems of seismic foundations are discussed. It is shown that two types of three-stage servovalves meet the performance requirements of the test facility. Author (ESA)

N84-12202# Industrieanlagen-Betriebsgesellschaft m.b.H., Ottobrunn (West Germany).
CONCEPT OF A SAFETY SYSTEM FOR A SERVOHYDRAULIC TEST FACILITY
H. Hahn *In* ESA Spacecraft Vibration Testing using Multiaxis Hydraul. Vibration Systems Jul. 1983 p 55-72 refs (For primary document see N84-12197 03-14)
(Contract ESA-3807/78/NL-HP(SC))
Avail: NTIS HC A09/MF A01

A safety system for a one degree of freedom hydraulic test facility which serves as a basis for protecting hydraulic multidegree of freedom vibration facilities for large Ariane and Spacelab payloads from malfunctions liable to damage the test object or test facility was developed and analyzed. Collection, analysis and classification of possible and serious failures in the system; hardware design of a safety system; and hardware simulation of serious failure are discussed. The structure of the system is defined by the redundancy concept of electronic and hydraulic components. The safety system proposed governs all serious failures except interruption of the feedback loop of the inner control loop. Author (ESA)

N84-12203# Dynatest, Munich (West Germany). Mehraxiale Prueftechnik.
CONTROL OF MULTIAXIS VIBRATION SYSTEMS
A. Schmidt *In* ESA Spacecraft Vibration Testing using Multiaxis Hydraul. Vibration Systems Jul. 1983 p 75-89 refs (For primary document see N84-12197 03-14)
Avail: NTIS HC A09/MF A01

Hardware and software to generate control functions for different load history types, to provide acquisition of test plant variables and to manage test supervision and documentation during vibration testing is proposed. The system is based on a desktop computer, linked to modules which enable each actuator to generate an individual control history. Signal frequency, bandwidth and amplitude are programmable. Phase relations and a second signal history can be handled. Sine sweep level control (predicted by a time variable reference level) and phase control (e.g., for 90 deg resonance feedback) are possible. Vibration level acquisition (accelerations, forces, displacements) occupies a third module frame. Author (ESA)

N84-12204# Industrieanlagen-Betriebsgesellschaft m.b.H., Ottobrunn (West Germany).
MATHEMATICAL MODELING AND SIMULATION OF MULTIAXIS HYDRAULIC TEST FACILITIES
H. Hahn *In* ESA Spacecraft Vibration Testing using Multiaxis

Hydraul. Vibration Systems Jul. 1983 p 93-117 refs (For primary document see N84-12197 03-14)
(Contracts ESA-3879/79/NL-MS; ESA-5179/82/NL-PP(SC))
Avail: NTIS HC A09/MF A01

Detailed mathematical models of a servohydraulic actuator system which serve as a basis for numerical models and for a theoretical analysis of hydraulic test facilities for large spacecraft were developed. The theoretical and numerical models use the network concept and the program design language MOSES. A variety of constraints which must be met by servohydraulic actuators of the hydraulic test facilities considered are derived. Electronic control systems for multiaxis test facilities are considered. Author (ESA)

N84-12205# SDRC Engineering Services Ltd., Herts (England).
CALCULATION OF FORCED RESPONSE TO BASE EXCITATION USING EXPERIMENTALLY DERIVED MODAL PARTICIPATION FACTORS **c39**
J. Cory, J. M. OKeefe, and K. L. Howard *In* ESA Spacecraft Vibration Testing using Multiaxis Hydraul. Vibration Systems Jul. 1983 p 119-122 (For primary document see N84-12197 03-14)
Avail: NTIS HC A09/MF A01

A method for calculating the forced response of a structure due to base excitation using experimentally derived modal data is presented. A method of extracting modal participation factors (MPF's) purely from a test data base is described. The MPF's are used to create a computer model of the structure which can be used for simulation studies. Tests with cantilever and simply supported beams show that modal participation factor results obtained from MPF compare within 10% of the results obtained by analysis when a sufficient number of dynamic degrees of freedom are used for the calculations. As the number of data points is decreased the procedure underestimates the modal participation factor, since the calculation of modal participation factors is a summation. Author (ESA)

N84-12206# Industrieanlagen-Betriebsgesellschaft m.b.H., Ottobrunn (West Germany).
SIMULATION OF ELECTRO-SERVO-HYDRAULIC ACTUATOR FOR HIGH QUALITY TESTING
H. Hahn and D. Krenz *In* ESA Spacecraft Vibration Testing using Multiaxis Hydraul. Vibration Systems Jul. 1983 p 129-157 refs (For primary document see N84-12197 03-14)
Avail: NTIS HC A09/MF A01

Simulation results of an electroservohydraulic actuator are presented together with information on the system analysis and synthesis program package (SAS) used to derive the simulation models and to perform the simulation runs. Using frequency response methods and root locus plots, the influence of various cross couplings and the parameter sensitivity of the subsystems are investigated. Subsystems discussed are: electronic power amplifier; nozzle flapper valve; spool valve; total actuator (without controllers); and total feedback controlled actuator. The controllers used are not optimized. The results serve as a basis for optimization of controlled electroservohydraulic actuators used in test facilities for space vehicles. Author (ESA)

N84-12207# Industrieanlagen-Betriebsgesellschaft m.b.H., Ottobrunn (West Germany).
SIMULATION OF MECHANICAL CROSS COUPLING OF MULTIAXES VIBRATION FACILITIES
H. Hahn and K. Keller *In* ESA Spacecraft Vibration Testing using Multiaxis Hydraul. Vibration Systems Jul. 1983 p 159-173 refs (For primary document see N84-12197 03-14)
(Contract ESA-81-IG-28-R3-61)
Avail: NTIS HC A09/MF A01

Simulation results of the coupling phenomena of a three axis vibration test facility mechanics are presented. The simulation is based on a rigid body test facility of six degrees of freedom controlled by eight drastically reduced servohydraulic actuator models. The test facility model is set up by the program TOPAS, whose structure function and handling are sketched. Author (ESA)

15 LAUNCH VEHICLES AND SPACE VEHICLES

Includes boosters; manned orbital laboratories; reusable vehicles; and space stations.

N84-12208# Committee on Commerce, Science, and Transportation (U. S. Senate).
US WEATHER SATELLITES AND SERVICES
Washington GPO 1983 79 p Hearing before the Comm. on Com., Sci. and Transportation, 98th Congr., 1st Sess., 22 Aug. 1983
(GPO-25-753) Avail: Committee on Commerce, Science and Transportation

The weather satellites and services of the National Weather Service of the National Oceanic and Atmospheric Administration are discussed. The economy and public safety of Washington State, monitoring of the extreme weather conditions around Mount St. Helens and search and rescue satellites are included. N.W.

N84-12209# Air Force Geophysics Lab., Hanscom AFB, Mass.
PRELIMINARY DATA PROCESSING PLAN FOR THE THERMAL PLASMA EXPERIMENT ON THE HILAT SATELLITE Instrumentation Papers
F. J. Rich and R. A. Heelis 31 Mar. 1983 43 p
(AF Proj. 7601)
(AD-A132017; AFGL-TR-83-0091; AFGL-IP-317) Avail: NTIS HC A03/MF A01 CSCL 05/2

The thermal plasma experiment is one of five experiments to be flown on the HILAT satellite in a polar orbit. The experiment consists of an ion drift-meter, an ion retarding potential analyzers and a spherical electron Langmuir probe. The details of the instruments are described. The calibrations and conversion factor to change from telemetry units to scientific units are given. Algorithms for converting the raw data into the parameters of interest are given. These algorithms are intended for obtaining quick-look information. Refinements to the algorithm will be required before the final results are released. Author (GRA)

N84-12210# Emmanuel Coll., Boston, Mass.
TECHNIQUE FOR PRODUCING A COHERENT SUM OF THE DATA FROM P78-1, F2, AND F4 SATELLITES Progress Report, 1 Apr. 1982 - 31 Mar. 1983
Ernest G. Holeman Hanscom AFB, Mass. AFGL May 1983 47 p
(Contract F19628-82-K-0039; AF Proj. 7601)
(AD-A131965; AFGL-TR-83-0130; SR-2) Avail: NTIS HC A03/MF A01 CSCL 22/2

Vertically incident data from the P78-1 J sensor was made available during the first quarter of 1983. It was sorted into a grid and time frame compatible with the F2 and F4 statfile data. In order to produce a coherent sum of the data from the three satellites into a final statfile product a consensus solution to several problems was agreed to. Author (GRA)

N84-12211# Analytical Systems Engineering Corp., Burlington, Mass.
ENGINEERING SERVICES IN SUPPORT OF THE AFGL SOUNDING ROCKET PROGRAM Final Report, 1 Aug. 1980 - 25 Mar. 1983
Roger Kozuma, Emmett Cox, Herbert Engel, Walter Greenwood, and Robert Hamann Hanscom AFB, Mass. AFGL 25 Mar. 1983 71 p
(Contract F19628-80-C-0125; AF Proj. 2127)
(AD-A131929; ASECR-83-126; AFGL-TR-83-0127) Avail: NTIS HC A04/MF A01 CSCL 05/1

During the 32 months' period of performance on this contract, ASEC has actively participated in numerous sounding rocket projects, balloon projects and a space shuttle project. The system engineering support rendered to various AFGL science and engineering branches included engineering design, design analysis, test planning and test management and reporting, field engineering,

equipment fabrication and installation, and development and production of program documentation. A central data depository was maintained to record the technical activities in each project. Through co-location of the majority of the ASEC support team within AFGL facilities, daily communication was efficiently and quickly executed. The minimization of distribution time for multiple iteration of various documentation maximized productivity for the both AFGL and ASEC personnel. GRA

N84-12212# Air Force Systems Command, Wright-Patterson AFB, Ohio. Foreign Technology Div.
JOURNAL OF THE CHINESE SOCIETY OF ASTRONAUTICS (SELECTED ARTICLES)
21 Jul. 1983 69 p Transl. into ENGLISH from Yuhang Xuebao (China), no. 1, 1982 p 18-29, 63-73, 98-103 and 104-107
(AD-A131881; FTD-ID(RS)T-0898-83) Avail: NTIS HC A04/MF A01 CSCL 21/8

The operation principle and regulation process of a bipropellant variable thrust rocket engine with a variable area injector that uses a solenoid valve control are discussed. The mathematical models of each link are given. The transfer function method is used to analyze the dynamic and steady performances of engine control systems. The use of concrete numerical calculations further shows the factors influencing the dynamic performance and steady errors for the engine control system. R.J.F.

N84-12058# Air Force Armament Lab., Eglin AFB, Fla. Hypervelocity Missile Branch.
HYPERVELOCITY MISSILE: BASED ON THE CONCEPT OF AIRCRAFT/MISSILE INTEGRATION FOR MAXIMUM FIREPOWER
T. C. Aden *In* AGARD Integration of Fire Control, Flight Control and Propulsion Control Systems Aug. 1983 14 p (For primary document see N84-12056 03-01)
Avail: NTIS HC A09/MF A01

N84-12059# Norwegian Defence Research Establishment, Kjeller.
F-16 PENGUIN ANTI-SHIP MISSILE INTEGRATION
E. Brodersen *In* AGARD Integration of Fire Control, Flight Control and Propulsion Control Systems Aug. 1983 7 p (For primary document see N84-12056 03-01)
Avail: NTIS HC A09/MF A01

16 SPACE TRANSPORTATION

Includes passenger and cargo space transportation, e.g., shuttle operations; and rescue techniques.

For related information see also *03 Air Transportation and Safety* and *85 Urban Technology and Transportation.*

N84-12213*# Systems Dynamics, Inc., Gainesville, Fla.
SPACE SHUTTLE PROPULSION PARAMETER ESTIMATION USING OPTIMAL ESTIMATION TECHNIQUES, VOLUME 1
Interim Final Technical Report
19 Nov. 1983 93 p refs
(Contract NAS8-35324)
(NASA-CR-170935; NAS 1.26:170935) Avail: NTIS HC A05/MF A01 CSCL 20H

The mathematical developments and their computer program implementation for the Space Shuttle propulsion parameter estimation project are summarized. The estimation approach chosen is the extended Kalman filtering with a modified Bryson-Frazier smoother. Its use here is motivated by the objective of obtaining better estimates than those available from filtering and to eliminate the lag associated with filtering. The estimation technique uses as the dynamical process the six degree equations-of-motion resulting in twelve state vector elements. In addition to these are mass and solid propellant burn depth as the "system" state elements. The "parameter" state elements can include aerodynamic coefficient, inertia, center-of-gravity, atmospheric wind, etc. deviations from referenced values. Propulsion parameter state elements have been included not as options just discussed but as the main parameter states to be estimated. The mathematical developments were completed for all these parameters. Since the systems dynamics and measurement processes are nonlinear functions of the states, the mathematical developments are taken up almost entirely by the linearization of these equations as required by the estimation algorithms. Author

N84-12214*# National Aeronautics and Space Administration, Washington, D. C.
STS-9 SPACELAB 1 PRESS KIT
Nov. 1983 83 p
(P83-10209) Avail: NTIS HC A05/MF A01 CSCL 22A

Press information on the STS-9/SPACELAB 1 mission is provided. Launch preparations, launch window, flight objectives, experiments, life sciences baseline data collection, SPACELAB 1 payload operations and control crew and specialists, and tracking and data management are among the topics explained. N.W.

N84-12215# Calspan Field Services, Inc., Arnold Air Force Station, Tenn.
SPACE SHUTTLE EXTERNAL INTERFERENCE HEATING TEST
Final Report, Aug. - Dec. 1982
William K. Crain and Kenneth W. Nutt AEDC Dec. 1982 56 p Sponsored by Air Force
(AD-A131688; AD-E750775; AEDC-TSR-83-V2) Avail: NTIS HC A04/MF A01 CSCL 20/13

Interference heating data were obtained on the 0.0175 scale 60-OTS Integrated Space Shuttle Vehicle in the AEDC Aerothermal (M=4) Tunnel C Facility. The data were obtained at M = 4.0, Re/ft = 400,000 to 6,600,000 TW/TT =approx. 0.3 to 0.8 at angles of attack of -5 to +5 degrees and -3 to +3 degrees angle of sideslip. The purpose of the tests was to obtain External Tank Interference heating data at higher total temperatures (lower TW/TT) for assessment of the validity of interference heating data previously obtained in the AEDC Tunnel A. A second objective was to obtain data at conditions comparable to STS1-4 flight data. Author (GRA)

17 SPACECRAFT COMMUNICATIONS, COMMAND AND TRACKING

Includes telemetry; space communications networks; astronavigation; and radio blackout.

For related information see also *04 Aircraft Communications and Navigation* and *32 Communications.*

No abstracts in this category.

18 SPACECRAFT DESIGN, TESTING AND PERFORMANCE

Includes spacecraft thermal and environmental control; and attitude control.

For life support systems see *54 Man/System Technology and Life Support.* For related information see also *05 Aircraft Design, Testing and Performance* and *39 Structural Mechanics.*

N84-12216*# National Aeronautics and Space Administration. Goddard Space Flight Center, Greenbelt, Md.
SHUTTLE MEASURED CONTAMINANT ENVIRONMENT AND MODELING FOR PAYLOADS. PRELIMINARY ASSESSMENT OF THE SPACE TELESCOPE ENVIRONMENT IN THE SHUTTLE BAY
John J. Scialdone Dec. 1983 13 p refs
(NASA-TM-85111; NAS 1.15:85111) Avail: NTIS HC A02/MF A01 CSCL 22B

A baseline gaseous and particulate environment of the Shuttle bay was developed based on the various measurements which were made during the first four flights of the Shuttle. The environment is described by the time dependent pressure, density, scattered molecular fluxes, the column densities and including the transient effects of water dumps, engine firings and opening and closing of the bay doors. The particulate conditions in the ambient and on surfaces were predicted as a function of the mission time based on the available data. This basic Shuttle environment when combined with the outgassing and the particulate contributions of the payloads, can provide a description of the environment of a payload in the Shuttle bay. As an example of this application, the environment of the Space Telescope in the bay, which may be representative of the environment of several payloads, was derived. Among the many findings obtained in the process of modeling the environment, one is that the payloads environment in the bay is not substantially different or more objectionable than the self-generated environment of a large payload or spacecraft. It is, however, more severe during ground facilities operations, the first 15 to 20 hours of the flight, during and for a short period after ater was dumped overboard, and the reaction control engines are being fired. S.L.

N84-12217*# Chrysler Corp., New Orleans, La. Structures and Mechanics Dept.
TEST REPORT FOR MSFC TEST 83-2. PRESSURE SCALED WATER IMPACT TEST OF A 12.5 INCH DIAMETER MODEL OF THE SPACE SHUTTLE SOLID ROCKET BOOSTER FILAMENT WOUND CASE AND EXTERNAL TVC POD
Sep. 1983 99 p refs
(Contract NAS8-35017)
(NASA-CR-174601; NAS 1.26:174601; TM-SM-83-12) Avail: NTIS HC A05/MF A01 CSCL 22B

Water impact using a 12.5 inch diameter model representing a 8.56 percent scale of the space shuttle solid rocket booster configurations were conducted. Cavity collapse applied pressure distributions for the 8.56 percent rigid body scale model FWC pressure magnitudes were obtained as a function of full scale initial impact conditions at vertical velocities from 65 to 85 ft/sec, horizontal velocities from 0 to 45 ft/sec, and angles from -10 to +10 degrees. Rigid body applied pressures on the TVC pod and aft skirt internal stiffener rings at initial impact and cavity collapse loading events were also obtained. In addition, nozzle loads were measured. Full scale vertical velocities of 65 to 85 ft/sec, horizontal velocities of 0 to 45 ft/sec, and impact angles from -10 to +10 degrees simulated. S.L.

N84-12218# Air Force Geophysics Lab., Hanscom AFB, Mass. Aerospace Instrumentation Div.
ORBITING GEOPHYSICS LABORATORY EXPERIMENT Interim Scientific Report
Francesco L. Bacchialoni (Lowell Univ.) 25 Oct. 1982 20 p
(AF Proj. 7659)
(AD-A131950; AFGL-TR-83-0083; AFGL-SR-234) Avail: NTIS HC A02/MF A01 CSCL 22/2

This document reports the investigation on the potential utility and technical feasibility of a new self-contained support system to be utilized repeatedly for different AFGL experiments in space, using the Space Transportation System (Shuttle) for launch and retrieval. This support system is designed to operate independently of both the STS and ground stations, therefore, stores data rather than transmitting them by telemetry. Angular pointing is the only maneuver planned; no propulsion is designed into this system. GRA

N84-12219# Dornier-Werke G.m.b.H., Friedrichshafen (West Germany).
SYSTEM DEFINITION ROENTGENSATELLIT, PHASE B 1.2 Final Report, Nov. 1981
Edgar Bachor and Karl Frankenbach Bonn Bundesministerium fuer Forschung und Technologie Jun. 1983 53 p In GERMAN, ENGLISH summary Sponsored by Bundesministerium fuer Forschung und Technologie
(BMFT-FB-W-83-010; ISSN-0170-1339) Avail: NTIS HC A04/MF A01; Fachinformationszentrum, Karlsruhe, West Germany DM 11

A satellite for research on X ray sources in space is described. Its total weight is 2121 kg and it comprises a fixed solar generator, a triaxial stabilization system, a propulsion system to enter the orbit and the maximum experimental data rate is 251 Mbit/day. The telescope aperture is 83 cm, the angle resolution is five angular sec for a wave range of 70100 A. It is a Spacelab payload and the orbit determination gives a retrieval option of two and a half years, but the mission duration is one year. The following additional options were considered: inclusion of a "Wide Field Soft X-ray Camera", NASA participation and 28 deg. orbit, NASA participation with "High Resolution Imager", retrieval with the Space Shuttle and the use of Ariane as launch vehicle. After one year of work on the system definition, the project appears fully compatible with the settled requirements. Author (ESA)

N84-12220# European Space Operations Center, Darmstadt (West Germany).
SPACECRAFT INTERFACE DESIGN AND ITS IMPACT ON OPERATIONAL SUPPORT
D. Wilkins, W. Wimmer, and M. Barrett Aug. 1983 42 p
(ESA-STR-211; ISSN-00379-4067) Avail: NTIS HC A03/MF A01

The impact of spacecraft interface design on the post-launch operational support insofar as this affects mission and spacecraft control is discussed. Operationally undesirable characteristics are summarized. Experience gained in the in-orbit control of the ESRO-4, Cos-B, EXOSAT, OTS, MARECS and METEOSAT missions is outlined. Author (ESA)

N84-12221# European Space Agency, Paris (France).
THE OTS: FIFTH YEAR IN ORBIT Progress Report
Aug. 1983 116 p
Avail: NTIS HC A06/MF A01

The OTS orbital test program status and satellite utilization for European television transmission are described. The repeater, antenna, attitude control, power, and thermal control susbsystems are discussed. The satellite continues to function well, both as a laboratory in its own right and as a means for payload exploitation. Author (ESA)

N84-12222 Stanford Univ., Calif.
CONTROL OF FLEXIBLE SPACECRAFT BY OPTIMAL MODEL FOLLOWING Ph.D. Thesis
Jeffery Allan Quirk 1983 244 p
Avail: Univ. Microfilms Order No. DA8307199

Spacecraft flexibility resulting from increased size and lightweight design techniques significantly increases the interaction between the structural bending modes and the vehicle control system. The subject of this thesis is the use of the unique properties of Optimal Model Following (OMF) to simplify the controller design process for flexible spacecraft. Model following controllers force the plant states to follow the dynamics of a model which incorporates the system performance specifications. OMF, model following using a linear quadratic cost function, trades off the degree of dynamics matching with the control effort utilized. As part of this thesis, an OMF controller design program was developed. OMF controllers were designed for three examples: altitude control of a flexible spacecraft, pointing of a camera package on a flexible appendage, and control of a spacecraft based on the Galileo vehicle. The performance characteristics of the OMF designs were compared to those of optimal controllers. Dissert. Abstr.

19 SPACECRAFT INSTRUMENTATION

For related information see also *06 Aircraft Instrumentation* and *35 Instrumentation and Photography.*

N84-12223*# Smithsonian Astrophysical Observatory, Cambridge, Mass.

HIGH RESOLUTION IMAGER (HRI) FOR THE ROENTGEN SATELLITE (ROSAT) DEFINITION STUDY Final Report, 16 Aug. 1982 - 15 Feb. 1983
Sep. 1983 52 p refs
(Grant NAGw-365)
(NASA-CR-174598; NAS 1.26:174598) Avail: NTIS HC A03/MF A01 CSCL 22B

The design of the high resolution imager (HRI) on HEAO 2 was modified for use in the instrument complement of the Roentgen Satellite (ROSAT). Mechanical models of the front end assembly, central electronics assembly, and detector assembly were used to accurately represent the HRI envelope for both fit checks and focal plane configuration studies. The mechanical and electrical interfaces were defined and the requirements for electrical ground support equipment were established. A summary description of the ROSAT telescope and mission is included. A.R.H.

N84-12224# European Space Agency, Paris (France).
LAYOUT OF A SAR SENSOR FOR SPACELAB AND SATELLITE. PART 1: DESIGN CONSIDERATIONS FOR FUNDAMENTAL SAR PARAMETERS
N. Bartsch, C. Boesswetter, and A. P. Wolfram Jul. 1983 89 p ref Translated into ENGLISH of "Die Auslegung eines SAR-Sensors fuer Spacelab u. Satellit: Entwurfs-Ueberlegungen fuer die wichtigsten SAR-Parameter" rept. DFVLR-Manuskript-8A-Pt-1 DFVLR, Oberpfaffenhofen, West Germany, 1983
(ESA-TT-802; DFVLR-Manuskript-8A-Pt-1) Avail: NTIS HC A05/MF A01

Boundary conditions and design specifications for a Spacelab or satellite-borne C and X band radar are outlined. Ground resolution is 100 X 100 m for C band, 60 x 60 m for X band. Radiometric resolution is 1 dB for both. The Earth is initially assumed to be flat and stationary. Antenna length should be as large as possible so that the power budget is always favorable. Multilook processing is suggested, to increase radiometric resolution and image quality. The effects of azimuth and range ambiguities, beam width and complete coverage requirements on pulse repetition frequency are analyzed. Power budget for surface and point targets, with and without processing are discussed. The power budget for altitude line echo should enable a measure of the suppression required in the nadir direction to be estimated.
Author (ESA)

20 SPACECRAFT PROPULSION AND POWER

Includes main propulsion systems and components, e.g., rocket engines; and spacecraft auxiliary power sources.

For related information see also *07 Aircraft Propulsion, 28 Propellants and Fuels,* and *44 Energy Production and Conversion.*

N84-12225*# United Technologies Corp., East Hartford, Conn.
DEPOSIT FORMATION AND HEAT TRANSFER IN HYDROCARBON ROCKET FUELS Final Progress Report, Jul. 1982 - May 1983
Anthony J. Giovanetti, Louis J. Spadaccini, and Eugene J. Szetela Oct. 1983 170 p refs
(Contract NAS3-23344)
(NASA-CR-168277; NAS 1.26:168277; R83-956152-10) Avail: NTIS HC A08/MF A01 CSCL 21H

An experimental research program was undertaken to investigate the thermal stability and heat transfer characteristics of several hydrocarbon fuels under conditions that simulate high-pressure, rocket engine cooling systems. The rates of carbon deposition in heated copper and nickel-plated copper tubes were determined for RP-1, propane, and natural gas using a continuous flow test apparatus which permitted independent variation and evaluation of the effect on deposit formation of wall temperature, fuel pressure, and fuel velocity. In addition, the effects of fuel additives and contaminants, cryogenic fuel temperatures, and extended duration testing with intermittent operation were examined. Parametric tests to map the thermal stability characteristics of RP-1, commercial-grade propane, and natural gas were conducted at pressures of 6.9 to 13.8 MPa, bulk fuel velocities of 30 to 90 m/s, and tube wall temperatures in the range of 230 to 810 K. Also, tests were run in which propane and natural gas fuels were chilled to 230 and 160 K, respectively. Corrosion of the copper tube surface was detected for all fuels tested. Plating the inside of the copper tubes with nickel reduced deposit formation and eliminated tube corrosion in most cases. The lowest rates of carbon deposition were obtained for natural gas, and the highest rates were obtained for propane. For all fuels tested, the forced-convection heat transfer film coefficients were satisfactorily correlated using a Nusselt-Reynolds-Prandtl number equation.
Author

N84-12226*# Boeing Aerospace Co., Seattle, Wash.
STUDY OF AUXILIARY PROPULSION REQUIREMENTS FOR LARGE SPACE SYSTEMS. VOLUME 1: EXECUTIVE SUMMARY
W. W. Smith and G. W. Machles Sep. 1983 22 p
(Contract NAS3-23248)
(NASA-CR-168193; NAS 1.26:168193; D180-27728-1) Avail: NTIS HC A02/MF A01 CSCL 21H

An insight into auxiliary propulsion systems (APS) requirements for large space systems (LSS) launchable by a single shuttle is presented. In an effort to scope the APS requirements for LSS, a set of generic LSSs were defined. For each generic LSS class a specific structural configuration, representative of that most likely to serve the needs of the 1980's and 1990's was defined. The environmental disturbance forces and torques which would be acting on each specific structural configuration in LEO and GEO orbits were then determined. Auxiliary propulsion requirements were determined as a function of: generic class specific configuration, size and openness of structure, orbit, angle of orientation, correction frequency, duty cycle, number and location of thrusters and direction of thrusters and APS/LSS interactions. The results of this analysis were used to define the APS characteristics of: (1) number and distribution of thrusters, (2) thruster modulation, (3) thrust level, (4) mission energy requirements, (5) total APS mass component breakdown, and (6) state of the art adequacy/deficiency.
S.L.

N84-12227*# GT-Devices, Alexandria, Va.
INVESTIGATION OF A PULSED ELECTROTHERMAL THRUSTER
R. L. Burton, S. A. Goldstein, B. K. Hilko, D. A. Tidman, and N. K. Winsor 1 Oct. 1983 45 p refs
(Contract NAS3-23779)
(NASA-CR-168266; NAS 1.26:168266; GTD-83-10) Avail: NTIS HC A03/MF A01 CSCL 21C

Exhaust velocity and thrust measurements are performed on a pulsed electrothermal thruster using polyethylene and Teflon propellants. The results verify theoretical predictions of equilibrium flow in the nozzle, resulting in substantial recovery of the energy of dissociation and ionization. The thruster is tested in an unsteady mode (15 micro sec current pulse and 15 cm discharge length) and in a quasi-steady mode (48 micro sec current pulse and 5 cm discharge length). All tests are run at 2 kJ. The exhaust velocity of the propellant mass exiting during the current pulse is measured with two types of time of flight probes, and the impulse bit is measured on a thrust stand. It is inferred from both theory and experiment that an additional amount of mass is exhausted after the pulse. The measured thrust to power ratio for polyethylene is $T/P = 0.10$ NkW at 21 km/sec in the unsteady mode, and $T/P = .053$ N/kW at 27 km/sec in the quasi-steady mode, where the velocities are measured by the time-of-flight probes. For Teflon propellant, $T/P = .20$ N/kW at 15 km/sec (unsteady mode) and 0.090 N/kW at 20 km/sec (quasi-steady mode). The discharge pressure and temperature predicted by a computational model for polyethylene are consistent with the measured thrust and discharge resistance.
S.L.

N84-12228*# National Aeronautics and Space Administration. Langley Research Center, Hampton, Va.
INTEGRATED FLYWHEEL TECHNOLOGY, 1983
Claude R. Keckler, ed., Guillermo E. Rodriguez, ed. (NASA. Goddard Space Flight Center), and Nelson J. Groom, ed. Washington Dec. 1983 205 p refs Workshop held in Greenbelt, Md., 2-3 Aug. 1983
(NASA-CP-2290; L-15707; NAS 1.55:2290) Avail: NTIS HC A10/MF A01 CSCL 10C

Topics of discussion included: technology assessment of the integrated flywheel systems, potential of system concepts, identification of critical areas needing development and, to scope and define an appropriate program for coordinated activity. For individual titles, see N84-12229 through N84-12247.

N84-12229*# National Aeronautics and Space Administration. Langley Research Center, Hampton, Va.
INTEGRATED POWER/ATTITUDE CONTROL SYSTEM (IPACS)
C. R. Keckler *In* NASA. Langley Research Center Integrated Flywheel Technol., 1983 Dec. 1983 p 5-21 refs (For primary document see N84-12228 03-20)
Avail: NTIS HC A10/MF A01 CSCL 22B

During orbit day, solar energy collected by the solar cell arrays and transformed into electrical energy is used to power the spacecraft subsystems, including the control system. In conventional spacecraft designs, a portion of the energy collected during the light portion of the orbit is stored in a set of batteries for use during orbit night. In the Integrated Power/Attitude Control System (IPACS) approach, that energy is stored in the rotating flywheel in the form of kinetic energy. Umbra electrical power demands are satisfied by attaching a generator to the wheel shaft and despinning the rotor. Through this approach, the battery system is no longer required and thus is eliminated. Author

N84-12230*# National Aeronautics and Space Administration. Goddard Space Flight Center, Greenbelt, Md.
GSFC FLYWHEEL STATUS
G. E. Rodriguez *In* NASA. Langley Research Center Integrated Flywheel Technol., 1983 Dec. 1983 p 23-34 refs (For primary document see N84-12228 03-20)
Avail: NTIS HC A10/MF A01 CSCL 10C

The assessment of flywheel energy storage for spacecraft power system is based on the conceptual flywheel design. This conceptual design of an integrated flywheel is based on the Mechanical Capacitor which evolved from development of magnetic bearings and permanent magnet ironless-brushless DC motors. The mechanical capacitor is based on three key technologies: (1) a composite rotor with a low ID to OD ratio for high energy density (weight and volume); (2) magnetic suspension close to the geometric center of the rotating mass to minimize loads normally encountered on the ends of a shaft, a no-wear mechanism in a vacuum environment, and to minimize losses at high rotational speeds; (3) permanent magnet ironless-brushless DC motor/generator for high efficiency of conversion and low losses at high rotational speeds. The complete system would include the necessary electronics for the motor/generator, containment, and counterrotating wheels for attitude control compatibility. Author

N84-12231*# Oak Ridge National Lab., Tenn.
OVERVIEW OF STATE-OF-THE-ART FLYWHEEL TECHNOLOGY
Mitchell Olszewski *In* NASA. Langley Research Center Integrated Flywheel Technol., 1983 Dec. 1983 p 35-46 (For primary document see N84-12228 03-20)
Avail: NTIS HC A10/MF A01 CSCL 10C

The technology and applications evaluation task focuses on defining performance and cost requirements for flywheels in the various areas of application. To date the DOE program has focused on automotive applications. The composite materials effort entails the testing of new commercial composites to determine their engineering properties. The rotor and containment development work uses data from these program elements to design and fabricate flywheels. The flywheels are then tested and their performance is evaluated to indicate possible areas for improvement. Once a rotor was fully developed it is transferred to the private sector. Author

N84-12232*# National Aeronautics and Space Administration. Marshall Space Flight Center, Huntsville, Ala.
ELECTRICAL POWER TRADE-OFFS
Bob Giudici *In* NASA. Langley Research Center Integrated Flywheel Technol., 1983 Dec. 1983 p 49-56 (For primary document see N84-12228 03-20)
Avail: NTIS HC A10/MF A01 CSCL 10C

Electrical power trade studies were initiated in September 1982 supporting the Space Station Systems Definition activity. Responsibility for performing the electrical power trade studies (Power Data Base) was divided between the NASA Centers. Center representatives and their respective subjects are identified in the accompanying chart. The data base material was used to conduct a general storage trade study. When the results appeared to favor the flywheel option, effort was focused on a comparative flywheel investigation wherein a range of flywheel performance and cost possibilities was compared with optimistic projections of competing options. Author

N84-12233*# National Aeronautics and Space Administration. Lyndon B. Johnson Space Center, Houston, Tex.
SPACE STATION ENERGY SIZING
Robert R. Rice *In* NASA. Langley Research Center Integrated Flywheel Technol., 1983 Dec. 1983 p 57-62 (For primary document see N84-12228 03-20)
Avail: NTIS HC A10/MF A01 CSCL 22B

A general schematic for a space station power system is described. The major items of interest in the power system are the solar array, transfer devices, energy storage, and conversion equipment. Each item will have losses associated with it and must be utilized in any sizing study, and can be used as a checklist for itemizing the various system components. Author

N84-12234*# National Aeronautics and Space Administration. Marshall Space Flight Center, Huntsville, Ala.
SPACE STATION ATTITUDE CONTROL SYSTEM CONCEPT AND REQUIREMENTS
P. D. Nicaise *In* NASA. Langley Research Center Integrated Flywheel Technol., 1983 Dec. 1983 p 63-69 ref (For primary document see N84-12228 03-20)
Avail: NTIS HC A10/MF A01 CSCL 22B

There is currently no single Space Station configuration which is accepted as a baseline. However, the latest approach is toward symmetry in both geometry and mass distribution. This minimizes aerodynamic and gravity gradient torques. Solar arrays and radiators drive the configuration strongly. One axis of the solar arrays needs to be perpendicular to the orbit plane, and the geometric and principal axis should remain common along this axis to minimize secular torques. The need for both inertial and earth-fixed modes drives the structure of the Station toward a disk-like shape in the orbital plane. Author

N84-12235*# National Aeronautics and Space Administration. Lyndon B. Johnson Space Center, Houston, Tex.
THE BOEING FLYWHEEL STUDY
Robert R. Rice *In* NASA. Langley Research Center Integrated Flywheel Technol., 1983 Dec. 1983 p 71-76 ref (For primary document see N84-12228 03-20)
Avail: NTIS HC A10/MF A01 CSCL 10C

The major features of the history of the Boeing flywheel were studied. The analysis of the regenerative fuel cell was started as an outgrowth of the original Boeing study of the Space Operations Center, and was completed in November 1982 with the publication of the final report number D180-27160-1. The current flywheel effort attempts to study the integrated flywheel using the same ground rules that were used on the fuel cell study. Author

N84-12236*# National Aeronautics and Space Administration. Lyndon B. Johnson Space Center, Houston, Tex.

SPACE STATION CONTROL REQUIREMENTS AND FLYWHEEL SYSTEM WEIGHTS FOR COMBINED MOMENTUM AND ENERGY STORAGE

Frank M. Elam *In* NASA. Langley Research Center Integrated Flywheel Technol., 1983 Dec. 1983 p 77-92 refs (For primary document see N84-12228 03-20)

Avail: NTIS HC A10/MF A01 CSCL 10C

The specifications of the flywheel system for momentum storage and vehicle torquing are somewhat dependent upon the attitude control requirements of the space station in orbit. As a ground rule, the flywheel system will be sized large enough to provide all attitude maneuvers, if practical, to avoid or minimize turning on the reaction control system (RCS). The RCS, whenever used, expels expensive mass and tends to contaminate optical surfaces of the vehicle. The vehicle rate and acceleration specifications of 0.10 deg/sec and 0.01 deg/square sec are tentative, and may be reduced if lesser values are more practical for flywheel design. For local vertical attitude hold, the average attitude error should be zero, and not the classical 1 degree, since control moment gyro (CMG) gimbal angles provide an exact reference feedback for gravity gradient momentum. Docking presents a problem for docking transients and attitude alignment which will require use of the RCS. Author

N84-12237*# National Aeronautics and Space Administration. Goddard Space Flight Center, Greenbelt, Md.

COMBINED ATTITUDE CONTROL AND ENERGY STORAGE

Henry Hoffman *In* NASA. Langley Research Center Integrated Flywheel Technol., 1983 Dec. 1983 p 93-98 (For primary document see N84-12228 03-20)

Avail: NTIS HC A10/MF A01 CSCL 10C

The effect on attitude control by multiple wheels (used for energy storage) is described. B.G.

N84-12238*# National Aeronautics and Space Administration. Marshall Space Flight Center, Huntsville, Ala.

IPACS ATTITUDE CONTROL TECHNOLOGY CONSIDERATIONS

L. Brandon *In* NASA. Langley Research Center Integrated Flywheel Technol., 1983 Dec. 1983 p 99-104 (For primary document see N84-12228 03-20)

Avail: NTIS HC A10/MF A01 CSCL 22B

Larger facilities or the Space Station and its evolutionary versions are considered for the control bandwidth which will evolve to lower values, probably in the 0.01 to 0.1 hertz range. An integrated power attitude control systems (IPACS) unit that incorporates conventional mechanical bearings to have a bandwidth of 4-10 hertz is expected. If the IPACS unit incorporates the advanced technology magnetic bearing, a bandwidth of 1.2 hertz is expected. It is found that for the Space Station or even the Space Platform, either of the above IPACS concepts are adequate. E.A.K.

N84-12239*# National Aeronautics and Space Administration. Marshall Space Flight Center, Huntsville, Ala.

FLYWHEEL ELECTRONICS

Frank Nola *In* NASA. Langley Research Center Integrated Flywheel Technol., 1983 Dec. 1983 p 105-116 (For primary document see N84-12228 03-20)

Avail: NTIS HC A10/MF A01 CSCL 09C

Requirements of the flywheel electronic system are to accelerate the momentum wheel to a fixed maximum speed when solar energy is available and to maintain a constant voltage on the spacecraft bus under varying loads when solar energy is not available. Requirements, energy flow control, types of motors considered, type of electronic control, and efficiency considerations, are outlined. E.A.K.

N84-12240*# National Aeronautics and Space Administration. Langley Research Center, Hampton, Va.

IPACS ELECTRONICS: COMMENTS ON THE ORIGINAL DESIGN AND CURRENT EFFORTS AT LANGLEY RESEARCH CENTER

Joe C. Gowdey *In its* Integrated Flywheel Technol., 1983 Dec. 1983 p 117-122 ref (For primary document see N84-12228 03-20)

Avail: NTIS HC A10/MF A01 CSCL 09C

The development of the integrated power altitude control system (IPACS) is described. The power bridge was fabricated, and all major parts are in hand. The bridge was tested with a 1/4 HP motor for another program. The PWM, Control Logic, and upper bridge driver power supply are breadboarded and are debugged prior to starting testing on a passive load. The Hall sensor circuit for detecting rotor position is in design. E.A.K.

N84-12241*# National Aeronautics and Space Administration. Langley Research Center, Hampton, Va.

ANNULAR MOMENTUM CONTROL DEVICE (AMCD)

Nelson J. Groom *In its* Integrated Flywheel Technol., 1983 Dec. 1983 p 123-132 refs (For primary document see N84-12228 03-20)

Avail: NTIS HC A10/MF A01 CSCL 09C

The Annular Momentum Control Device (AMCD) concept, applications, and advantages as a momentum storage device are discussed. A laboratory test model AMCD was designed and built. The laboratory model AMCD is described and the results of the laboratory model test phase are presented. The efforts required to complete the AMCD laboratory model test phase are outlined. E.A.K.

N84-12242*# National Aeronautics and Space Administration. Goddard Space Flight Center, Greenbelt, Md.

MAGNETIC BEARINGS FOR INERTIAL ENERGY STORAGE

Philip A. Studer *In* NASA. Langley Research Center Integrated Flywheel Technol., 1983 Dec. 1983 p 133-140 refs (For primary document see N84-12228 03-20)

Avail: NTIS HC A10/MF A01 CSCL 10C

The selection of a noncontacting bearing technique with no wear out phenomena and which is vacuum compatible which is the decisive factor in selecting magnetic bearings for kinetic energy storage was investigated. Unlimited cycle life without degradation is a primary goal. Storage efficiency is a key parameter which is defined as the ratio of the energy remaining to energy stored after a fixed time interval at no load conditions. Magnetic bearings, although noncontacting, are not perfectly frictionless in that magnetic losses due to eddy currents and hysteresis can occur. Practical magnetic bearings, however, deviate from perfect symmetry and have discontinuities and asymmetric flux paths either by design or when controlled in the presence of disturbances, which cause losses. These losses can be kept smaller in the bearings than in a high power motor/generator, however, are a significant factor in selecting the magnetic bearing type. E.A.K.

N84-12243*# National Aeronautics and Space Administration. Langley Research Center, Hampton, Va.

ADVANCED CONTROL AND POWER SYSTEM (ACAPS) TECHNOLOGY PROGRAM

C. R. Keckler and Nelson J. Groom *In its* Integrated Flywheel Technol., 1983 Dec. 1983 p 141-156 refs (For primary document see N84-12228 03-20)

Avail: NTIS HC A10/MF A01 CSCL 22B

The advanced control and power system (ACAPS) program is to establish the technology necessary to satisfy space station and related large space structures requirements for efficient, reliable, and cost effective energy storage and attitude control. Technology advances in the area of integrated flywheel systems capable of performing the dual functions of energy storage and attitude control are outlined. E.A.K.

N84-12244*# National Aeronautics and Space Administration. Marshall Space Flight Center, Huntsville, Ala.

POWER SYSTEM CONSIDERATIONS AND TEST ACTIVITIES

Jim Miller *In* NASA. Langley Research Center Integrated Flywheel Technol., 1983 Dec. 1983 p 157-164 (For primary document see N84-12228 03-20)

Avail: NTIS HC A10/MF A01 CSCL 22B

The potential benefits of an IPACS system compared to NiCd

and/or Regen Fuel Cell systems are summarized. The benefits are: (1) significant life cycle cost savings; (2) total weight to orbit savings (30 yrs) as much as 10 times; (3) end to end efficiency increase results in approximately 10 kW reduction in array size(6%); (4) motor/generator controller regulation during discharge simplifies distribution system; and (5) momentum stored for attitude control increased by 4 times. E.A.K.

N84-12245*# National Aeronautics and Space Administration. Marshall Space Flight Center, Huntsville, Ala.
IPACS GUIDANCE NAVIGATION AND CONTROL SYSTEM CONSIDERATIONS AND TEST ACTIVITIES
H. J. Buchanan *In* NASA. Langley Research Center Integrated Flywheel Technol., 1983 Dec. 1983 p 165-168 (For primary document see N84-12228 03-20)
Avail: NTIS HC A10/MF A01 CSCL 17G

The MSFC facility proposed for the Space Station Attitude Control Simulator which consists of a large three degree of freedom table driven by computer controlled hydraulic actuators designed to give high bandwidth and extremely fine control through large angles is outlined. The facility includes star and solar simulators providing collimated light with the spectral content and intensity typical of Earth orbit. E.A.K.

N84-12246*# National Aeronautics and Space Administration. Goddard Space Flight Center, Greenbelt, Md.
ASSESSMENT OF POTENTIAL FOR BATTERIES IN SPACE APPLICATIONS
F. E. Ford *In* NASA. Langley Research Center Integrated Flywheel Technol., 1983 Dec. 1983 p 171-174 (For primary document see N84-12228 03-20)
Avail: NTIS HC A10/MF A01 CSCL 10C

Different battery technologies for energy storage in space missions were examined. One of the best ways of the possibilities of high energy density batteries were determined by looking at more conventional batteries (i.e., lead-acid, nickel-cadmium, nickel-hydrogen, etc.). The theoretical specific energy density for state of the art batteries and the usable energy density for a reasonable life expectancy are outlined. The most mature of these couples is lead acid, which achieves nearly 20% of its theoretical capacity. The nickel-cadmium couple, has matured to where the active capacity is 17% of its theoretical capacity. The achievements are used to measure the practicality of more advanced batteries and to estimate what is needed for future high power space systems. E.A.K.

N84-12247*# National Aeronautics and Space Administration. Lewis Research Center, Cleveland, Ohio.
SOME COMMENTS ON LONGEVITY BY A TECHNOLOGIST
Larry H. Thaller *In* NASA. Langley Research Center Integrated Flywheel Technol., 1983 Dec. 1983 p 175-185 (For primary document see N84-12228 03-20)
Avail: NTIS HC A10/MF A01 CSCL 12B

The durability of flywheels was investigated. Since only composite flywheels possess the potential for system energy densities in the range of 20 to 40 W hr/kg, and they are not yet at a level of maturity where a comfortable data base exists, the longevity aspects of the yet to be developed devices is still a speculation. The general methodologies that have been used in some of the more established technology areas to establish some degree of credibility in the ability to predict the upper limits of expected useful life based on the current limiting decay mechanism are outlined. E.A.K.

N84-12248*# Software and Engineering Associates, Inc., Santa Ana Heights, Calif.
IMPROVED TWO-DIMENSIONAL KINETICS (TDK) COMPUTER PROGRAM Final Report
Gary R. Nickerson and Lanh D. Dang Oct. 1983 114 p refs
(Contract NAS8-35046)
(NASA-CR-170922; NAS 1.26:170922; SN-54) Avail: NTIS HC A06/MF A01 CSCL 21H

Fluid properties, the boundary layer module, and regenerative cooling are discussed. Chemistry, low density flow effects, test cases, input and output for TDK, and documentation are also discussed. Author

N84-12249# Forward (Robert L.), Oxnard, Calif.
ALTERNATE PROPULSION ENERGY SOURCES
Robert L. Forward Jun. 1983 99 p
(Contract F04611-83-C-0013)
(AD-A131939; AFRPL-TR-83-039) Avail: NTIS HC A05/MF A01 CSCL 10/1

This report summarizes the results of the first phase of the referenced contract. The task was to survey the entire field of advanced propulsion to uncover and carry out a technical assessment of any concept that showed promise of leading to a major advance in available energy sources for space power and propulsion in the next century. In general we were to consider any concept that might derive energy from the space environment, as well as any unconventional methods of storing energy in a compact form that may have applicability to space power and propulsion. The best of these were to be selected for investigation in Phase 2 of the contract. We uncovered 62 concepts, carried out technical assessments on 26 of the more promising concepts, and recommended that four concepts be considered for more detailed study in Phase 2. The concepts recommended were solid metastable helium, solar pumped plasmas, perforated solar sails, and antiproton annihilation propulsion. Of these, the Air Force selected two concepts to receive the major portion of the Phase 2 effort, solar pumped plasmas and antiproton annihilation. GRA

23 CHEMISTRY AND MATERIALS (GENERAL)

Includes biochemistry and organic chemistry.

N84-12250# Rutgers - The State Univ., New Brunswick, N. J. Dept. of Chemistry.
IONIC CONDUCTIVITY IN LITHIUM HEXAOXOMETALLATE SOLID SOLUTIONS
E. Nomura and M. Greenblatt 26 Jul. 1983 22 p
(Contract N00014-82-K-0317)
(AD-A131842; TR-1) Avail: NTIS HC A02/MF A01 CSCL 07/4

Lithium ion conductivity in solid solutions formed between Li7Ta06, Li7 M sub V06 (M sub V = Nb, Bi) and Li8Zr06 has been measured as a function of temperature and composition using complex impedance method. The samples prepared were Li7Ta1-xNbx06, Li7Ta1-xBix06 and Li7+xTa1-xZr06. At 200 C, the conductivities of Li7Ta0.7Nb0.306, Li7Ta0.4Bi0.6Bi0.406 and Li7.4Ta0.6Zr0.406 are 4.3 x 10-4 (Omega cm)-1,3.0x10-4 (Omega cm) and 4.0 x 10-4 (Omega cm)-1, respectively. GRA

N84-12251# Stanford Univ., Calif. High Temperature Gasdynamics Lab.
ADVANCED DIAGNOSTICS AND INSTRUMENTATION FOR CHEMICALLY REACTIVE FLOW SYSTEMS Final Scientific Report, 1 Sep. 1980 - 30 Sep. 1982
R. K. Hanson, D. Baganoff, C. T. Bowman, R. L. Byer, and B. J. Cantwell Nov. 1982 89 p Original contains color illustrations
(Contract F49620-80-C-0091; AF Proj. 2308)
(AD-A131814; AFOSR-83-0705TR) Avail: NTIS HC A05/MF A01 CSCL 20/5

Progress is reported at the completion of 2 years of an interdisciplinary program to investigate and establish modern diagnostic techniques for application to reacting flows. Project areas include: (1) optical probes for species measurements employing tunable ultraviolet, visible and infrared laser sources; (2) coherent anti-Stokes Raman spectroscopy (CARS) for temperature and velocity measurements in a supersonic jet; (3) computed absorption tomography for species measurements in a plane; (4) particle sizing techniques, especially for rocket exhausts; (5) fast response temperature monitor, based on line reversal concepts; (6) quantitative flow visualization, including temporally and spatially

resolved species measurements in a plane using laser induced fluorescence; (7) multiple point velocity visualization; (8) application of modern diagnostics to a two dimensional reacting shear layer; (9) development of measurement techniques and a novel facility for investigations of droplet evaporation in turbulent flows; (10) holographic display techniques for 3 D visualization of flow field data; (11) spatially resolved laser absorption spectroscopy using optical Stark shifting; and (12) fast scanning dye laser for measurements of species, temperature and fundamental spectral parameters. Author (GRA)

N84-12252# Ames Lab., Iowa.
PISTON-DISPLACEMENT EQUATIONS OF STATE FOR SODIUM, POTASSIUM, AND RUBIDIUM METALS TO 20 KBAR FROM 300 K TO 4 K
C. A. Swenson and M. S. Anderson 1983 4 p refs Presented at the 9th AIRAPT Conf., Albany, N.Y., 24-29 Jul. 1983
(Contract W-7405-eng-82)
(DE83-018079; IS-M-453; CONF-830763-15) Avail: NTIS HC A02/MF A01

The equations of state of sodium, potassium and rubidium metals to 20 kbar at temperatures to 4 K were studied. Some of the general features of the results are summarized. The summary is presented in terms of the Rb results, since comparable data for this metal were not available previously. It is found that considerable similarities exist between the equations of state of the three metals. DOE

N84-12253# California Univ., Livermore. Lawrence Livermore Lab.
LITHIUM EQUATION-OF-STATE
James A. Blink Sep. 1983 15 p refs
(Contract W-7405-eng-48)
(DE83-017988; UCID-19890; E&MA-82-176) Avail: NTIS HC A02/MF A01

An equation-of-state (EOS) for lithium was established. This EOS was used in AFTON calculations of the HYLIFE inertial fusion reactor hydrodynamics. In this paper, Young's Development of the EOS is summarized and a computer program (MATHSY) that plots isotherms, isentropes and constant energy lines on a P-V diagram is demonstrated. DOE

N84-12254# Argonne National Lab., Ill. Materials Science and Technology Div.
NEW APPROACH TO THE GENERATION OF METAL-BEARING, MEDIUM-PORE, SHAPE-SELECTIVE ZEOLITES FOR FISCHER-TROPSCH CATALYSIS: SPECTROSCOPIC STUDIES OF ZEOLITES
Lennox E. Iton, Richard B. Beal (Univ. of South Florida), and David T. Hodul 1983 53 p refs Presented at the 4th Intern. Symp. on Relations Between Hemogeneous and Heterogeneous Catalysis, Asilomar, Calif., 2-5 Oct. 1983
(Contract W-31-109-eng-38)
(DE83-014344; CONF-8310120-1) Avail: NTIS HC A04/MF A01

Two developments in zeolite synthesis and modification were successfully combined to demonstrate a new approach to the generation of metal-bearing, medium-pore, shape-selective zeolites for use as catalysts in Fischer-Tropsch conversions. The steps are: (1) synthesis of an aluminoferrisilicate zeolite having the ZSM-5-type structure; (2) removal of the organic base template incorporated in the channel system during synthesis; (3) formation of a polycyano inclusion compound in the AFS zeolite; and (4) reduction of the inclusion compound by hydrogen at approx. 400 C. Photoacoustic and electron paramagnetic resonance spectroscopy were used to establish that the as-synthesized AFS zeolite contains Fe(3+) ions in both framework and non-framework sites. Ferromagnetic resonance (FMR) spectroscopy was used to confirm the formation of the metallic (Fe) and bimetallic (Fe/Ru and Fe/Co) particles as products of the reduction of the inclusion compounds by hydrogen. The application of other spectroscopic techniques in studies of cations, complexes, and metal particles in zeolites is reviewed: high-resolution solid-state NMR, nuclear-spin-relaxation studies, FMR, EXAFS, and XANES. DOE

N84-12255# California Univ., Berkeley. Lawrence Berkeley Lab. Materials and Molecular Research Div.
RESEARCH ACTIVITIES IN MATERIALS AND MOLECULAR RESEARCH Annual Report for 1982
Alan W. Searcy May 1983 311 p refs
(Contract DE-AC03-76SF-00098)
(DE83-015005; LBL-15150) Avail: NTIS HC A14/MF A01

Materials sciences, chemical sciences, nuclear sciences, fossil energy, advanced isotope separation technology (AISI), energy storage, magnetic fusion energy (MFE), nuclear waste management, and work for others (WFO are examined. Separate abstracts were prepared for all except AIST, MFE, and WFO. DOE

N84-12256# Brookhaven National Lab., Upton, N. Y. Process Sciences Div.
ADVANCED TECHNOLOGIES FOR THE RECOVERY, DISPOSAL, AND REUSE OF CARBON DIOXIDE FOR ATMOSPHERIC CONTROL
Meyer Steinberg Jul. 1983 33 p refs Presented at the Am. Inst. of Chem. Engr. Fall Ann. Meeting, Washington, 30 Oct. - 4 Nov. 1983
(Contract DE-AC02-76CH-00016)
(DE83-016371; BNL-33441; CONF-831063-3) Avail: NTIS HC A03/MF A01

Several technologies for controlling CO2 content in the atmosphere, which are useful in mitigating the possible CO global greenhouse effect are examined. These relate to recovery of CO2 from the atmosphere, removal of CO2 from fossil fuel burning plants, the disposal of CO2 in the ocean and in depleted wells and salt domes, and the use of CO2 for the production of synthetic fuels. Evaluation of some of these systems are presented in terms of energy costs. DOE

24 COMPOSITE MATERIALS

Includes laminates.

N84-12257*# Rensselaer Polytechnic Inst., Troy, N. Y.
COMPOSITE STRUCTURAL MATERIALS Semiannual Progress Report, 30 Sep. 1982 - 10 Apr. 1983
George S. Ansell, Robert G. Loewy, and Stephen E. Wiberley Jul. 1983 140 p refs
(Grant NGL-33-018-003)
(NASA-CR-174597; NAS 1.26:174597; SAR-44) Avail: NTIS HC A07/MF A01 CSCL 11D

Transverse properties of fiber constituents in composites, fatigue in composite materials, matrix dominated properties of high performance composites, numerical investigation of moisture effects, numerical investigation of the micromechanics of composite fracture, advanced analysis methods, compact lug design, and the RP-1 and RP-2 sailplanes projects are discussed. N.W.

N84-12258# Oklahoma Univ., Norman.
THREE-DIMENSIONAL ANALYSIS OF COMPOSITE PLATES WITH MATERIAL NONLINEARITY Interim Report
T. Kuppusamy, A. Nanda, and J. N. Reddy Aug. 1983 24 p
(Contract N00014-78-C-0647)
(AD-A131884; AD-E950422; TR-34) Avail: NTIS HC A02/MF A01 CSCL 12/1

The study deals with a fully three dimensional analysis of laminated composite plates accounting for material nonlinearity. The finite-element method with trilinear interpolation of the three displacements is used to model layers of the laminate (both in the plane of laminae and through the thickness of the laminate). The modified Romberg-Osgood material constitutive relations is used to update the principal moduli in the plane of the laminate. The elastic-plastic model with Hill's criteria for anisotropic criteria is also used to analyze laminates. The shear deformable plate-theory element is also used in the study. Author (GRA)

N84-12259# Ames Lab., Iowa.
AMORPHOUS SILICON-CARBON FILMS

H. R. Shanks, J. F. Ward, and C. Carlone (Sherbrook Univ., Quebec) 1983 4 p refs Presented at the 10th Intern. Conf. on Amorphous and Liquid Semiconductors, Tokyo, 22-26 Aug. 1983
(Contract W-7405-eng-82)
(DE83-018077; IS-M-450; CONF-830895-7) Avail: NTIS HC A02/MF A01

Thin films of amorphous silicon carbon hydrogen were prepared by reactive RF sputtering in an argon propane atmosphere. AES and NMR were used to determine the film composition. IR measurements show that the SiH stretching mode at 2087/cm is present in addition to an admixture of the Si-CH3 wagging mode near 780/cm and the Si-C stretching mode at approx. 700 cm(+1). Optical density measurements were used to determine that the optical gap energy appears to vary between 2.0 and 2.2 eV. A series of isochronal annealing steps were performed on the aSiC:H films and the changes in hydrogen bonding and optical gap energy are observed. Photoluminescence was also measured on the aSiC:H films. DOE

N84-12260# Aeronautical Research Inst. of Sweden, Stockholm. Structures Dept.
FATIGUE OF FIBER COMPOSITES
Anders F. Blom Jun. 1983 49 p refs
(Contract FMV-F-FL-82223-80-001-21-001; FFA Proj. HU-2302)
(FFA-TN-1983-30) Avail: NTIS HC A03/MF A01

Basic fatigue mechanisms and fatigue characteristics of unidirectional and multidirectional composites are discussed for tensile and compressive fatigue loading. It is emphasized that the matrix properties, rather than the fiber properties, determine the long life behavior. It is pointed out that compressive loading is more detrimental than tensile loading, contradictory to metals, due to local buckling of fibers and plies. Author (ESA)

N84-12261 Syracuse Univ., N. Y.
MULTIPLANE FINITE ELEMENT METHOD: APPLICATIONS TO FIBER REINFORCED MATERIAL Ph.D. Thesis
Steven Charles Pack 1982 134 p
Avail: Univ. Microfilms Order No. DA8310466

Study of the micromechanical aspects of crack growth in a fiber reinforced composite material is an essential step in evaluating the potential structural applications and limitations of such a material. Knowledge of the mechanism of failure is required to establish a rational basis for modification of material design or fabrication technique when striving to improve the mechanical properties and reliability of the composite material. The combination of crack tip stress singularities, multiphase material interaction and three dimensional morphology hinder the development of closed form solutions of practical application. Use of three dimensional finite element analysis is restricted by excessive demands upon computational resources. To overcome these analytical restrictions, a finite element model is developed which considers the composite to be composed of a series of laminae parallel to the plane of loading. Dissert. Abstr.

25 INORGANIC AND PHYSICAL CHEMISTRY

Includes chemical analysis, e.g., chromatography; combustion theory; electrochemistry; and photochemistry.

For related information see also *77 Thermodynamics and Statistical Physics.*

N84-12262* National Aeronautics and Space Administration. Pasadena Office, Calif.
PHOTOELECTROCHEMICAL ELECTRODES Patent
Roger M. Williams (JPL, California Inst. of Tech., Pasadena) and Alan Rembaum, inventors (to NASA) (JPL, California Inst. of Tech., Pasadena) Issued 8 Nov. 1983 13 p Filed 10 May 1982 Supersedes N83-25587 (21 - 14, p 2327) Sponsored by NASA
(NASA-Case-NPO-15458-1; US-Patent-4,414,060;
US-Patent-Appl-SN-376306; US-Patent-Class-204-129;
US-Patent-Class-204-242; US-Patent-Class-204-278;
US-Patent-Class-204-290R; US-Patent-Class-204-DIG.3;
US-Patent-Class-427-443.2; US-Patent-Class-429-111) Avail: US Patent and Trademark Office CSCL 07D

The surface of a moderate band gap semiconductor such as p-type molybdenum sulfide is modified to contain an adherent film of charge mediating ionene polymer containing an electroactive unit such as bipyridimium. Electron transport between the electrode and the mediator film is favorable and photocorrosion and recombination processes are suppressed. Incorporation of particles of catalyst such as platinum within the film provides a reduction in overvoltage. The polymer film is readily deposited on the electrode surface and can be rendered stable by ionic or addition crosslinking. Catalyst can be predispersed in the polymer film or a salt can be impregnated into the film and reduced therein.
Official Gazette of the U.S. Patent and Trademark Office

N84-12263*# Garrett Turbine Engine Co., Phoenix, Ariz.
EXECUTIVE SUMMARY, AEROTHERMAL MODELING PROGRAM, PHASE 1
R. Srinivasan, R. Reynolds, I. Ball, R. Berry, K. Johnson, and H. Mongia Aug. 1983 54 p
(Contract NAS3-23523)
(NASA-CR-174602; NAS 1.26:174602; Garrett-21-4766) Avail: NTIS HC A04/MF A01 CSCL 21B

Submodels used in the combustor analytical models that were successfully used in designing advanced technology combustors were assessed. Specific recommendations for further improvement of model accuracy for combustor design purposes were made. Based upon an exhaustive literature survey, a number of test cases were selected to assess accuracy of submodels of turbulence, turbulence/chemistry interaction, spray combustion, and dilution jet mixing processes within a confined cross-stream. These test cases included simple flows and complex flows with and without swirl. Nonrecirculating and recirculating, and nonreactive and reactive flows were investigated. It was concluded that the current models give qualitative trends for the recirculating secondary flows (as encountered in a gas turbine combustor primary zone), but the predictions are good for the dilution zone. S.L.

N84-12264*# Garrett Turbine Engine Co., Phoenix, Ariz.
AEROTHERMAL MODELING PROGRAM, PHASE 1 Final Report
R. Srinivasan, R. Reynolds, I. Ball, R. Berry, K. Johnson, and H. Mongia Aug. 1983 327 p
(NASA-CR-168243-Vol-1; NAS 1.26:168243-Vol-1;
Garrett-21-4742-1) Avail: NTIS HC A15/MF A01 CSCL 21B

Aerothermal submodels used in analytical combustor models are analyzed. The models described include turbulence and scalar transport, gaseous full combustion, spray evaporation/combustion, soot formation and oxidation, and radiation. The computational scheme is discussed in relation to boundary conditions and convergence criteria. Also presented is the data base for benchmark quality test cases and an analysis of simple flows. S.L.

N84-12265*# Garrett Turbine Engine Co., Phoenix, Ariz.
AEROTHERMAL MODELING PROGRAM, PHASE 1
R. Srinivasan, R. Reynolds, I. Ball, R. Berry, K. Johnson, and H. Mongia Aug. 1983 351 p refs
(Contract NAS3-23523)
(NASA-CR-168243-Vol-2; NAS 1.26:168243-Vol-2;
Garrett-21-4742-2) Avail: NTIS HC A16/MF A01 CSCL 21B

The combustor performance submodels for complex flows are evaluated. The benchmark test cases for complex nonswirling flows are identified and analyzed. The introduction of swirl into the flow creates much faster mixing, caused by radial pressure gradients and increase in turbulence generation. These phenomena are more difficult to predict than the effects due to geometrical streamline curvatures, like the curved duct, and sudden expansion. Flow fields with swirl, both confined and unconfined are studied. The role of the dilution zone to achieve the turbine inlet radial profile plays an important part, therefore temperature field measurements were made in several idealized dilution zone configurations. S.L.

N84-12266# Santa Barbara Research Center, Goleta, Calif.
HgCdTe SURFACE STUDY PROGRAM Final Technical Report
Jerry A. Wilson, Joel Silberman, Per Morgen, and W. E. Spicer Sep. 1982 70 p
(Contract MDA903-80-C-0496; ARPA Order 3985)
(AD-A132071) Avail: NTIS HC A04/MF A01 CSCL 07/4

This report presents the conclusions of a 2 year study of the surface of HgCdTe conducted jointly by Santa Barbara Research Center and Stanford University. Photoemission spectroscopy (PES) of HgCdTe cleaved in UHV has indicated a surface which is very stable against Hg loss. The surface has shown a tendency to type convert (p to n) due to defects in the surface region stressed by cleaving. Type conversion has been confirmed by independent electrolytic electroreflectance (EER) measurements. Photoemission has also been used to probe the bulk band structure and indicates a fundamental difference in bonding of Cd and Hg in the lattice. A breakdown of the virtual crystal approximation is noted and an improved computation for the alloy is discussed. Oxygen chemistry has been studied using PES; results show the undamaged surface is inert to unexcited molecular oxygen. Oxidation proceeds with exposure to excited oxygen and is preceded by a loss of Hg from the surface. The oxide formed does not contain Hg. Differences in oxidation between HgTe and HgCdTe indicate Cd plays a role in the oxidation. GRA

N84-12267# Ballistic Research Labs., Aberdeen Proving Ground, Md.
LASER SPECTROSCOPY OF PROPELLANT-LIKE FLAMES Final Report
Richard A. Beyer, John A. Vanderhoff, and Mark A. DeWilde Jul. 1983 23 p
(DA Proj. 1L1-61102-AH-43)
(AD-A132042; ARBRL-TR-02507) Avail: NTIS HC A02/MF A01 CSCL 20/5

The laser-based techniques Coherent Anti-Stokes Raman Spectroscopy (CARS) and Spontaneous Raman Scattering have been applied to studies of the detailed chemistry of premixed flames. The status of this research effort and its future goals in gun propulsion research are discussed. Author (GRA)

N84-12268# Illinois Univ., Urbana.
THERMOLYSIS OF 4-METHYL-4-PHENYL MALONYL PEROXIDE: A NEW OXYGEN DEPENDENT CHEMILUMINESCENT REACTION
Judith E. Porter and Gary B. Schuster 8 Aug. 1983 25 p
(Contract N00014-76-C-0745)
(AD-A131863; AD-E850387) Avail: NTIS HC A02/MF A01 CSCL 07/3

Thermolysis of 4-methyl-4-phenyl malonyl peroxide in acetonitrile is accelerated by electron donors, such as perylene. When both the perylene and oxygen are present in solution the reaction gives acetophenone and a small amount of light. Investigation of the mechanism of light generation reveals that it involves formation and fragmentation of a tetraoxide. The chemically initiated electron-exchange luminescence mechanism (CIEEL) appears to be responsible for light generation. Author (GRA)

N84-12269# South Australian Inst. of Tech., Adelaide. School of Chemical Technology.
INFRARED CHARACTERISTICS OF GAS PLUMES
A. Steven and G. T. Wilkinson Aug. 1982 50 p
(AD-A131796; Rept-82-2) Avail: NTIS HC A03/MF A01 CSCL 21/2

This report describes the results of a research program undertaken at the S.A. Institute of Technology, School of Chemical Technology to study the infra-red characteristics of high temperature gas plumes containing particulate material. The program involved: a critical survey of the open literature and identification of significant gaps in the data base, the design and construction of a hot gas test rig for investigating the infra-red characteristics of turbulent flames, and preliminary experimental work to establish the reliability of the rig. The first part of the report contains the literature review. This is then followed by the results of the preliminary experimental program. A complete list of literature surveyed is given in the bibliography. GRA

N84-12270# Rockwell International Corp., Anaheim, Calif. Autonetics Strategic Systems Div.
MECHANISMS AND KINETICS OF DIPHTHALOCYANINE ELECTRODE PROCESSES Final Report, 1 May 1980 - 31 Mar. 1983
M. M. Nicholson, T. P. Weismuller, and F. A. Pizzarello Jul. 1983 31 p Submitted for publication
(Contract F49620-80-C-0060; AF Proj. 2303)
(AD-A131726; C83-522/201; AFOSR-83-0721TR) Avail: NTIS HC A03/MF A01 CSCL 09/1

Redox processes of lutetium diphthalocyanine were investigated by chemical, electrochemical, and optical spectroscopic methods. Oxidized films of the dye slowly reverted from the red to the green state on standing in moist air. The rate of this color change depended on the nature of the anion that had been incorporated during the oxidation. The feasibility of faster chemical switching and of color cycling by indirect coulometry was demonstrated. Slow-scan cyclic voltammetry of film specimens on tin oxide electrodes provided evidence of incipient phase transitions in blue reduced forms of the dye. The current-voltage curves could be interpreted on the basis of a model in which the electron-transfer processes were assumed to be much faster than the phase transitions. Finally, the role of oxygen in the dye system was elucidated through discovery of a reversible oxygen reaction with lutetium diphthalocyanine in dimethylformamide solution. This information explains some apparent discrepancies in the chemistry of rare-earth diphtalocyanines and provides an important link in the formulation of a unified redox reaction scheme. Author (GRA)

N84-12271# Louisiana State Univ., Baton Rouge. , Dept. of Chemical Engineering.
SOOT FORMATION FROM POLYCYCLIC AROMATICS Final Report, 1 Sep. 1980 - 31 Aug. 1982
M. Frenklach Dec. 1982 32 p refs
(Contract DE-FG22-80PC-30247)
(DE83-009750; DOE/PC-30247/T4) Avail: NTIS HC A03/MF A01

Knowledge of the mechanism of soot formation and the ability to predict the soot yield under various conditions is of great importance to combustor design. The present work for the first time, offers a consistent approach to empirical modeling of soot formation during the pyrolysis of aromatic hydrocarbons. Understanding and adequate modeling of the pyrolysis of aromatic hydrocarbons are necessary steps towards the prediction of sooting in flames. Soot formation in toluene-argon mixtures has been investigated behind reflected shock waves by monitoring attenuation of a laser beam in the visible (632.8 nm) and the infrared (3.39 (SIGMA)m) regions of the spectrum. The experimental data indicated a strong pressure effect on soot formation which cannot be rationalized within Graham's model. A new model for soot formation was proposed that not only explains the observed phenomena but also unifies the various experimental facts which previously had been considered to be contradictory. The size of soot particles formed during the shock tube pyrolysis of toluene was measured by laser Doppler velocimetry. DOE

N84-12272# California Univ., Livermore. Lawrence Livermore Lab.
EROSIVE PARTICLE KINEMATICS IN THE TURBULENT COMBUSTION BOUNDARY LAYER CONTACTING A SOLID WALL
A. C. Buckingham and W. J. Siekhaus 15 Apr. 1983 10 p refs Presented at 6th Intern. Conf. on Erosion by Liquid and Solid Impact, Cambridge, England, 4 Sep. 1983
(Contract W-7405-eng-48)
(DE83-010594; UCRL-88178; CONF-8301059-4) Avail: NTIS HC A02/MF A01

Measurements and numerical modeling are applied to observe and predict the interactive influence of sub-micron gas borne particles in an erosive turbulent combustion wall boundary layer. Some of the experiments and computations discussed are directed

to study of turbulent free shear layers. Others emphasize wall boundary layers. The common purpose is to generate information on the particle interaction mechanisms active in alteration and reduction of the turbulent transport and the consequent reduction of the erosive heat and mass transfer. Primary emphasis here is given to analysis of erosive two phase wall boundary layers encountered in solid propellant combustion situations. Examples are gun barrel, rocket nozzle, and coal-fired gas turbine combustions flow fields. DOE

N84-12273# Ames Lab., Iowa.
PHONON DISPERSION OF TRANSVERSE BASAL-PLANE MODES IN ALKALI-GRAPHITE COMPOUNDS
W. A. Kamitakahara, H. Zabel (Illinois Univ., Urbana), and R. M. Nicklow (ORNL, Tenn.) 1982 6 p refs Presented at the Mater. Res. Soc. Ann. Meeting, Boston, 16 Nov. 1982
(Contracts DE-AC02-76ER-01198; W-7405-eng-82; W-7405-eng-26)
(DE83-003910; DOE/ER-01198/1394; CONF-821185-2) Avail: NTIS HC A02/MF A01

Dispersion curves for low frequency transverse modes propagating in the basal plane were measured in the compounds KC8, KC24 and RbC24 by neutron inelastic scattering. The acoustic branches show at low q a behavior (NU) (2) = Aq(2) + Bq(4) characteristic of layered materials. The optical branches are derived qualitatively from graphite like optical branches hybridized with new alkali like branches. In stage two compounds, the shear constant C44, is appreciably smaller than in stage-one compounds or in pure graphite. It is noted in KC24 that a frequency gap in the acoustic branch opens up near q = 0.6 A(+1) at low temperature, corresponding to the Brillouin zone boundary of the low temperature alkali superstructure. DOE

N84-12274# Argonne National Lab., Ill.
HIGH-SENSITIVITY MASS SPECTROMETRY WITH A TANDEM ACCELERATOR
Walter Henning 1983 13 p refs Presented at the Intern. Symp. on Nucl. Phys. at Large Tandem Accelerators, Legnaro-Padova, Italy, 15 Mar. 1983 Prepared in cooperation with Technische Univ., Munich, West Germany
(Contract W-31-109-eng-38)
(DE83-017914; CONF-830384-2) Avail: NTIS HC A02/MF A01

The characteristic features of accelerator mass spectroscopy are discussed. The current status of mass spectrometry with high energy (MeV/nucleon) heavy ion accelerators is reviewed. Studies with tandem accelerators and on future mass spectrometry of heavier isotopes with the new generation of higher voltage tandems are emphasized. DOE

N84-12275# Language Services, Knoxville, Tenn.
FORMATION OF FREE HYDROGEN DURING RADIOLYSIS IN A BED OF CLAY
Trygve Eriksen (Royal Inst. of Tech., Stockholm) and Johan Lind (Royal Inst. of Tech., Stockholm) 1983 20 p refs Transl. into ENGLISH from a Swedish Report Prepared for Brookhaven National Lab., Upton, N.Y.
(Contract DE-AC02-76CH-00016)
(DE83-017724; BNL-tr-1000) Avail: NTIS HC A02/MF A01

The amount of molecular hydrogen formed radiolytically in (BETA)-irradiated sodium bentonite with varying water content were measured. The 0.1 to 5 MPa Ar pressure and 2 to 5 MPa mechanical pressure applied to the bentonite was studied. It is shown that a water content and pressure dependent equilibrium is obtained with hydrogen concentrations well below the hydrogen solubility in water. Tritrations of slurries of 10 q irradiated and unirradiated bentonite in 100 g water with NaOH show a dose dependent increase in the surface acidity of the benetonite. DOE

N84-12276# California Univ., Berkeley. Lawrence Berkeley Lab. Applied Science Div.
INFLUENCE OF HEAT-TREATMENT AND PHYSICOCHEMICAL PROPERTIES ON THE ELECTROCHEMICAL OXIDATION OF CARBON BLACKS IN PHOSPHORIC ACID
K. Kinoshita Aug. 1983 19 p refs Presented at the Workshop on the Electrochem. of Carbon, Cleveland, 17-19 Aug. 1983 Submitted for publication
(Contract DE-AC03-76SF-00098)
(DE83-017744; LBL-16514; CONF-8308116-1) Avail: NTIS HC A02/MF A01

Electrochemical oxidation of carbon blacks in concentrated phosphoric acid at 135 to 1600C were studied. The electrochemical oxidation mechanism and the influence of physiochemical properties on the oxidation rate of carbon blacks was investigated. The effects of heat treatment on the surface area and crystal structure of carbon black and electrochemical oxidation rate is discussed. DOE

N84-12277# Pennsylvania State Univ., University Park. Dept. of Chemistry.
FREE-RADICAL AND ION CHEMISTRY OF VOLATILE SILANES, GERMANES, AND PHOSPHINES Technical Progress Report, 1 Aug. 1982 - 31 Jul. 1983
F. W. Lampe 1983 7 p
(Contract DE-AC02-76ER-03416)
(DE83-016389; DOE/ER-03416/T1) Avail: NTIS HC A02/MF A01

Brief summaries are presented of research on: infrared multiphoton decomposition of PH3 and SiH4-PH3 sensitized by SiF4, spectroscopic detection of SiH2 in the infrared multiphoton decomposition of SiH4, infrared laser photochemistry of SiH4-HCl mixtures, reactions of C2H3 ions with CH4, and reactions of SiH3 ions with chloromethanes. DOE

N84-12278# McGill Univ., Montreal (Quebec). Shock Wave Physics Research Lab.
HYDROGEN-AIR DETONATIONS
J. H. S. Lee, R. Knystautas, C. Guirao, W. B. Benedick (Sandia National Labs.), and J. E. Shepherd (Sandia National Labs.) 1983 46 p refs Presented at the 2nd Intern. Workshop on the Impact of Hydrogen on Water Reactor Safety, Albuquerque, N. Mex., 3 Oct. 1983
(Contract DE-AC04-76DP-00789)
(DE83-009289; SAND-82-1864C; CONF-831003-1) Avail: NTIS HC A03/MF A01

General gaseous detonation propagation phenomena are briefly discussed. The importance of cellular structure and cell size to detonation initiation, transmission and failure is emphasized. Experimental measurements of cell size lambda for hydrogen-air-carbon dioxide mixtures are presented; the hydrogen/air volume ratios range between 0.16 and 1.5 and the carbon dioxide mole fractions are 0, 0.05, 0.10 and 0.15. Cell sizes are a minimum for both diluted and undiluted hydrogen-air mixtures near stoichiometric (i.e., hydrogen/air = 0.4). Minimum cell sizes for carbon dioxide mole fractions of 0, 0.05, 0.10 and 0.15 are 1.51, 2.05, 4.2 and 15.0 cm, respectively. Results of large and small scale critical tube diameter (d/sub c/) measurements are presented and show good agreement with the empirical scaling law, d/sub c/ = 13 lambda. Mean detonation velocities and pressures were measured and compared to the theoretical Chapman-Jouquet values. DOE

N84-12279# California Univ., Berkeley. Lawrence Berkeley Lab.
PHOTOTHERMAL DISPLACEMENT SPECTROSCOPY OF SURFACES AND THIN FILMS
Nabil M. Amer, Marjorie A. Olmstead, Daniele Fournier (Ecole Superieure de Physique et de Chimie), and A. Claude Boccara (Ecole Superieure de Physique et de Chimie) Jan. 1983 7 p Presented at the 3rd Intern. Meeting on Photoacoustic and Photothermal Spectry., Paris, 5 Apr. 1983
(Contract DE-AC03-76SF-00098)
(DE83-015957; LBL-15545; CONF-8304113-1) Avail: NTIS HC A02/MF A01

A new technique, photothermal displacement spectroscopy, was developed for studying the optical and thermal properties of surfaces. Photothermal displacement spectroscopy is based on optical detection of the thermal expansion of a sample as it is

heated by absorption of electromagnetic radiation. Details of the experimental configuration are shown. An optical absorption spectrum is generated as an intensity modulated, tunable light beam (pump beam) is focussed onto the sample, and, depending on the optical cross section, some fraction of the radiation is absorbed. As the excited electrons decay nonradiatively, the sample is heated. The illuminated surface is then displaced as the sample expands. A probe beam reflected from the surface is deflected by the slope of the surface displacement. This deflection is measured by a position sensitive photodiode whose output is then amplified by a phase sensitive lock-in amplifier referenced to the pump beam modulation. Thermal information can be obtained by measuring the shape and phase of the photothermal displacement relative to the illumination as a function of the modulation frequency. DOE

N84-12280# Ames Lab., Iowa.
EQUATIONS OF STATE FOR THE ALKALI METALS, WITH GENERALIZATIONS TO NaCl
C. A. Swenson and M. S. Anderson 1983 4 p refs Presented at the Am. Phys. Soc. Meeting on Shodk Waves in Condensed Media, Santa Fe, N. Mex., 18-21 Jul. 1983
(Contract W-7405-eng-82)
(DE83-018075; IS-M-454; CONF-830719-51) Avail: NTIS HC A02/MF A01

Recent 20 kbar P-V-T data for the alkali metals cover a wide range of relative pressures and temperatures and are sufficiently accurate to provide guidelines for testing empirical equation of state relations. Data for rubidium, as typical for these metals, are presented in terms of a modification of the ME-2 relation, the MME, at room temperature, and thermal pressures for the other isotherms. These ideas are shown to apply to previous NaCl data to 30 kbar and from 200C to 5000C. A generalization of the MME is applied the 250C shock-wave isotherm for NaCl to 250 kbar to obtain a representation which is consistent with existing high quality P-V data for NaCl at room temperature. DOE

N84-12281# Exxon Research and Engineering Co., Bayton, Tex. Research and Development Div.
COMBUSTION OF EDS MID-DISTILLATE AND REFINED SHALE-OIL RESIDUAL FUEL IN A GAS TURBINE WITH LARGE SINGLE-COMBUSTION CHAMBER
1983 27 p refs
(Contract DE-FC05-77ET-10069)
(DE83-017700; DOE/ET-10069/T41) Avail: NTIS HC A03/MF A01

The test fuels included a coal derived mid distillate recycle liquid from the EDS coal liquefaction process, produced by Exxon, and a hydroprocessed residual Paraho shale oil fraction originating from a US Government sponsored program. A BBC Brown Boveri Co. (BBC) type 9 fully equipped 35 MW capacity gas turbine, located at BBC's test facilities near Basel, Switzerland, was utilized. The objective of the combustion test was to establish whether these alternate fuels can be fired in large single combustor turbines without deleterious effects to the turbine or environment. Nitrogen in the shale oil was on the order of 0.4 wt% while the EDS distillate contained slightly less than 10 wt% hydrogen. The test program entailed the firing of 600 barrels of each test fuel at varying turbine loads and a comparison of the results with those from a base case petroleum diesel fuel. Fuel bound nitrogen was not found to contribute significantly to NO sub x emissions in contrast to other work reported earlier in subscale gas turbine tests. Water injection at 0.6 to 0.7 water to fuel mass ratios was effective in meeting requirements. DOE

N84-12282# Ames Lab., Iowa.
ATMOSPHERIC-PRESSURE ARGON AFTERGLOWS AS A DETECTOR FOR GAS CHROMATOGRAPHY
G. W. Rice, A. P. DSilva, and V. A. Fassel 1983 2 p refs Presented at the Conf. on Anal. Chem. and Appl. Spectry., Atlantic City, 6 Mar. 1983
(Contract W-7405-eng-82)
(DE83-017695; IS-M-436; CONF-830388-2) Avail: NTIS HC A02/MF A01

Ames was involved in developing an atmospheric pressure, active nitrogen (APAN) afterglow as an excitation source for analytical emission spectroscopy and as an element specific, multielemental gas chromatography detector. The same type of discharges and afterglows can be produced from both helium and argon. The argon afterglow was evaluated as an element selective detector for gas chromatography by monitoring atomic spectral lines arising from S, P, C, N, Cl, Br, and I containing species. Limits of detection ranged from 0.08 ng for P to 50 ng for Br. DOE

N84-12283# Materials Quality Assurance Directorate, London (England).
MULTI-DETECTOR GEL PERMEATION CHROMATOGRAPHY AND ITS APPLICATION TO THE ANALYSIS OF INDUSTRIAL SAMPLES
A. W. J. Brough and D. E. Hillman Mar. 1982 20 p refs
(MQAD-808; BR85803) Avail: NTIS HC A02/MF A01

The use of a standardized gel permeation chromatography system for the characterization of industrial samples consisting mainly of components of molecular weight of a few hundred is described. A microparticulate styrene-divinylbenzene column system was used with tetrahydrofuran as solvent to give elution of all components of the sample within preset elution volumes. A differential refractometer was used to give universal detection for an overall fingerprint characterization. Selective detectors coupled in series were used to show the presence of specific components and for their quantitative determination. Applications to plasticizers, fuel and oil additives, hydraulic fluids and natural resins are shown. Author (ESA)

N84-12284# Bend Research, Inc., Oreg.
NOVEL COMPOSITE MEMBRANES
Eric K. L. Lee, W. C. Babcock, R. P. Barss, P. A. Bresnahan, and M. B. Chidlaw Apr. 1983 52 p refs
(Contract DI-14-34-0001-1449)
(PB83-243170; W83-03678; OWRT-C-10004-S(1449)(1)) Avail: NTIS HC A04/MF A01 CSCL 07A

A serious limitation of most high performance composite reverse osmosis (RO) membranes is their sensitivity to chlorine attack. Membranes with good desalination performance and improved chlorine resistance were developed. The probable mechanisms of chlorine attack in polyamide membranes and the likely identity of the reacting species are summarized. GRA

N84-12285 Purdue Univ., Lafayette, Ind.
COMBUSTION MODELING OF COMPOSITE SOLID PROPELLANTS Ph.D. Thesis
John Paul Renie 1982 272 p
Avail: Univ. Microfilms Order No. DA8310853

A theoretical model for the combustion of composite solid propellants is described. This model, the Petite Ensemble Model (PEM) is based upon a combination of a unique statistical treatment of the burning surface of a composite solid propellant and a comprehensive, multiple flame, physio-chemical combustion model. Due to this statistical treatment, the PEM accounts for both oxidizer particle size and size distribution effects on propellant burning rate behavior. A scenario for the behavior of aluminum particles burning within the surface/near surface environment of a composite solid propellant is postulated. Calculations indicate the importance of considering aluminum particle size distribution within the framework of this aluminum PEM, or ALPEM. The augmentation of propellant burning rate due to an imposed acceleration field is shown to have an aluminum particle size dependency.
Dissert. Abstr.

26 METALLIC MATERIALS

Includes physical, chemical, and mechanical properties of metals, e.g., corrosion; and metallurgy.

N84-12286 Wisconsin Univ., Madison.
SOLIDIFICATION OF ALUMINUM AND ALUMINUM ALLOYS AT

HIGH LEVELS OF UNDERCOOLING Ph.D. Thesis
Stephen Edward LeBeau 1982 338 p
Avail: Univ. Microfilms Order No. DA8304953

Under most practical conditions, the crystallization of bulk metals is initiated by a heterogeneous catalyst which restricts the observed liquid undercooling to only a few degrees. An effective experimental method that may be applied to yield large liquid undercoolings involves the slow cooling from the melt of a dispersion of stabilized fine liquid droplets. Substantial undercooling levels (160 C) were measured by differential thermal analysis for slowly cooled (30 C/min) droplet emulsions of high purity aluminum. Commercial purity melts of Al dispersed into droplet form, either by emulsification in a molten salt or by commercial atomization processes, also exhibit substantial undercoolings. The observed level of undercooling of Al droplet samples was examined as a function of the sample droplet size distribution, the externally applied cooling rate and the melt superheating temperature. The maximum leel of undercooling measured for pure Al in the present studies occurs in the finest droplets and appears to be limited by the catalytic influence of the droplet coating. Dissert. Abstr.

N84-12287*# National Aeronautics and Space Administration. Lewis Research Center, Cleveland, Ohio.
SOLID IMPINGEMENT EROSION MECHANISMS AND CHARACTERIZATION OF EROSION RESISTANCE OF DUCTILE METALS
Veerabhadra P. Rao (Cleveland State Univ., Ohio) and Donald H. Buckley [1982] 21 p refs To be presented at the Fluids, Eng. Conf., New Orleans, 11-17 Feb. 1984; sponsored by ASME
(NASA-TM-83492; E-1823; NAS 1.15:83492) Avail: NTIS HC A02/MF A01 CSCL 11F

Experimental results pertaining to spherical glass bead and angular crushed glass particle impingement are presented. A concept of energy adsorption to explain the failure of material is proposed. The erosion characteristics of several pure metals were correlated with the proposed energy parameters and with other properties. Correlations of erosion and material properties were also carried out with these materials to study the effect of the angle of impingement. Analyses of extensive erosion data indicate that surface energy, strain energy, melting point, bulk modulus, hardness, ultimate resilience, atomic volume and product of linear coefficient of thermal expansion, bulk modulus, and temperature rise required for melting, and ultimate resilience, and hardness exhibit the best correlations. It appears that both energy and thermal properties contribute to the total erosion. Author

N84-12288*# National Aeronautics and Space Administration, Washington, D. C.
CONTAINERLESS ELECTROMAGNETIC LEVITATION MELTING OF Cu-Fe AND Ag-Ni ALLOYS
G. J. Abbaschian (Florida Univ.) and E. C. Ethridge Sep. 1983 19 p refs
(NASA-TM-82553; NAS 1.15:82553) Avail: NTIS HC A02/MF A01 CSCL 11F

The feasibility of producing silver or copper alloys containing finely dispersed nickel or iron particles, respectively, by utilizing containerless electromagnetic levitation casting techniques was investigated. A levitation coil was designed to successfully levitate and melt a variety of alloys including Nb-Ge, Cu-Fe, Fe-C, and Ag-Ni. Samples of 70 Cu-30 Fe and 80 Ag-20 Ni (atomic %), prepared by mechanical pressing of the constituent powders, were levitated and heated either to the solid plus liquid range of the alloys or to the fully liquid region. The samples were then solidified by passing helium gas into the bell jar or they were dropped into a quenching oil. The structure of the samples which were heated to the solid plus liquid range consists of uniform distribution of Fe or Ni particle in their respective matrices. A considerable amount of entrapped gas bubbles were contained. Upon heating for longer periods or to higher temperatures, the bubbles coalesced and burst, causing the samples to become fragmented and usually fall out of the coil. Author

N84-12289*# National Aeronautics and Space Administration. Pasadena Office, Calif.
CORROSION RESISTANT COATING Patent Application
Satish K. Khanna (JPL, California Inst. of Tech., Pasadena), Anilkumar Thakoor (JPL, California Inst. of Tech., Pasadena), and Roger M. Williams, inventors (to NASA) (JPL, California Inst. of Tech., Pasadena) Filed 30 Sep. 1983 14 p
(Contract NAS7-100)
(NASA-CASE-NPO-15928-1; US-Patent-Appl-SN-537616) Avail: NTIS HC A02/MF A01 CSCL 11F

A highly corrosive resistant coating for substrates, such as glasses and metal is provided. Amorphous metals are deposited on the substrate by the magnetron sputtering process which is conducted at a very low pressure, such as two micrometers of mercury, to provide on the surface of the substrate a thin, uniformly thick, pinhole-free film of the metal. NASA

N84-12290# Dayton Univ., Ohio. Research Inst.
MECHANICAL PROPERTY EVALUATION OF P/M (POWDER-METALLURGY) ALUMINUM 7090-T7E71 PLATE Interim Technical Report, Jun. - Dec. 1982
John J. Ruschau Aug. 1983 26 p
(Contract F33615-82-C-5039; AF Proj. 2418)
(AD-A132058; UDR-TR-83-19; AFWAL-TR-83-4074) Avail: NTIS HC A03/MF A01 CSCL 11/6

Mechanical property data were obtained for a single plate of powder-metallurgy (P/M) produced aluminum 7090-T7E71. Properties examined are tensile, compression, shear, bearing, smooth and notched fatigue, fatigue crack growth rate, and fracture toughness. Comparisons are made to other 7000-series ingot-metallurgy (I/M) produced aluminum alloys, more particularly, aluminum 7050. Results show the test material to be superior in strength, bearing, and shear properties than the majority of I/M 7000-series alloys. Improvements in both smooth and notched fatigue resistance are also realized over I/M aluminums 7050 and 7075 in their respective corrosion resistant tempers. Toughness and fatigue crack growth rate properties are inferior to several I/M produced 7000-series structural aluminum alloys.
Author (GRA)

N84-12291# Technische Univ., Vienna (Austria). Inst. of Applied and Technical Physics.
ANISOTROPY AND MICROSTRUCTURE OF Sm2(Co, Fe, Cu, Zr)17 MAGNETIC MATERIALS Final Report, Jan. 1982 - Jan. 1983
Josef Fidler, Roland Grossinger, Hans Kirchmayr, and Peter Skalicky May 1983 135 p
(Contract DAJA37-82-C-0050; DA Proj. 1T1-61102-BH-57)
(AD-A131961; AD-E750837) Avail: NTIS HC A07/MF A01 CSCL 07/4

The present report is divided into two parts, the anisotropy measurements and the microstructural investigations of Sm2(Co,Fe, Cu,Zr)17 magnetic materials. Section I shows that the pulsed field technique is a versatile extension of a static magnetometer. Beside the possibility of generating fields up to 280 k theta e it can be used as an instrument with specific possibilities. An example for this is the SPD-technique which delivers even for polycrystalline samples - a value for the anisotropy field Ha. Up to now no clear correlation between the magnetic parameters like coercivity or energy product and the absolute value of Ha is possible. However, the knowledge of Ha allows the application of models which may help to understand the occurrence of these parameters. The temperature dependence of Ha should be mainly determined by the temperature dependence of the magnetization of the Sm sublattice. If this is known the validity of the One Ion Model can be tested. The role of the partly substituted Co sublattice is not so clear. More accurate M(T) measurements should be done. The influence of the inter-atomic distance on Ha(T), which should exist according to to an extended One Ion model, necessitates the knowledge of the thermal expansion. GRA

N84-12292# Drexel Univ., Philadelphia, Pa. Dept. of Materials Engineering.
COLD SINTERING: A NEW POWDER CONSOLIDATION PROCESS
E. Y. Gutmanas and A. Lawley Jul. 1983 17 p
(Contract N00014-81-K-0039)
(AD-A131687; AD-E750775) Avail: NTIS HC A02/MF A01 CSCL 11/6

The plastic deformation of powder particles in a high pressure gradient at ambient temperature results in green densities close to theoretical. Physical contact of freshly formed oxide-free surfaces leads to strong particle-particle bonding; this phenomenon is called cold sintering. High strength levels can be obtained in metals, alloys, composites, ionic and ionic-covalent solids by cold sintering. Subsequent heat treatment of cold sintered material, at temperatures significantly lower than those used in conventional sintering, results in excellent combinations of strength and ductility. Thus, cold sintering offers the potential for retaining metastable constituents, fine-scale microstructures and small precipitates in rapidly solidified powders. Interface reactions or dissolution of phases in metal matrix composites can also be reduced or eliminated. Details of the compacting response, microstructure and mechanical properties of cold sintered and heat treated high speed tool steel and super-alloy powders are presented. Cold sintering characteristics are understood in terms of the interplay of particle shape and particle deformation. Possible cold sintering processing routes of commercial interest are discussed and the limitations of this new technology considered. Author (GRA)

N84-12293# Sandia Labs., Albuquerque, N. Mex.
EVALUATION OF THE KINEMATIC VARIABLE (BACK STRESS) RESPONSE OF METALS
Wendell B. Jones and R. W. Rohde 1983 8 p refs Presented at the 7th Intern. Conf. on Structural Mech. in Reactor Technol., Chicago, 22 Aug. 1983
(Contract DE-AC04-76DP-00789)
(DE83-008381; SAND-82-1778C; CONF-830805-6) Avail: NTIS HC A02/MF A01

The desire to develop unified creep plasticity (UCP) models comes from the necessity to design advanced nuclear reactor components for service under conditions which include combined creep and low cycle fatigue. An approach to UCP modeling centers on the hypothesis that the inelastic strain rate is determined by a balance between the competing processes of work hardening and recovery. One class of UCP models is characterized by a power law relationship between strain rate and stess. In order to treat unloading or reverse loading conditions, several models also include a kinematic hardening variable which is also allowed to evolve according to a balance of work hardening and recovery. The measured response of 316SS and A800 indicates that the kinematic variable must, in steady state, be taken as a constant fraction (about 0.8) of the applied stress. This experimental result makes it impossible for the simple power law type expression to properly predict the commonly observed power law breakdown behavior in most metals and alloys. It is proposed that an expression for total inelastic strain rate involving the sum of two separate strain rate contributions is more appropriate. DOE

N84-12294# Argonne National Lab., Ill. Materials Science and Technology Div.
STUDY OF CHROMIUM-FREE AND CHROMIUM-REDUCED STEELS
T. C. Wiencek and H. R. Thresh May 1983 24 p refs
(Contract W-31-109-eng-38)
(DE83-016717; ANL-82-43) Avail: NTIS HC A02/MF A01

The goal was to develop an iron based alloy, similar to Type 316 stainless steel in mechanical and corrosion properties but with a reduced Cr content or, ideally, no Cr. A total of twenty-six 225-g ingots and ten 2.5 to 12 kg ingots of various compositions in the Fe-Si-Mn-Ni-C system were prepared. All ingots contained from 5 to 11 w/o silicon and drew their corrosion resistance primarily from this component. The composition ranges of the remaining major alloying elements were (in w/o) 0-24 Mn, 0-35 Ni, and 0.08 to 0.95 C. Most of the alloys were reduced to sheet, demonstrating the hot fabricability of these high silicon alloys. The mechanical and corrosion properties of these alloys are attractive. Tensile tests showed yield strengths of 303 to 379 Mpa (44 to 55 ksi), ultimate tensile strengths of 731 to 882 MPa (106 to 128 ksi), and elongations of 34 to 77%. Air oxidation rates were lower than those of 300 series stainless steels at 10000C. Salt water corrosion rates for these alloys fall between those of stainless steels and plain carbon steels and are 5 to 10 times lower than the rates for plain carbon steels. DOE

N84-12295# Oak Ridge Y-12 Plant, Tenn. Metals and Ceramics Dept.
DEGRADATION OF SHAPE MEMORY EFFECT
R. A. Vandermeer 19 Jul. 1983 9 p refs Presented at the Intern. Conf. on Martensitic Transformations, ICOMAT-82, Leuven, Belgium, 9-13 Aug. 1983 Submitted for publication
(Contract W-7405-eng-26)
(DE83-016586; Y/DV-203; CONF-820898-3) Avail: NTIS HC A02/MF A01

The elucidation of metallurgical factors that cause degradation of heat activated recovery strain, E/sub R/ was studied. Two manifestations of degradation identified in near monotectoid uranium niobium alloys are described. The first was associated with the onset of plastic deformation of the martensite beyond the reversible strain limit, E/sub L/; a reduction of E/sub R/ from 5.25% at 8% total strain, i.e., E/sub L/, to 2.9% at 12% total strain was observed. A second type of degradation depended strongly on the heating rate during reversion; the E/sub R/ for an imposed strain of 6.95% was reduced from a value of 5.25% to 1.3% when the heating rate was decreased from 400/sec to 0.050/sec. Degradation is attributed to a change in the transformation path and the interjection of time dependent, low temperature aging reactions. DOE

N84-12296# Sandia Labs., Albuquerque, N. Mex.
ACCELERATED COMPATIBILITY TESTING USING CORROSION FATIGUE TECHNIQUES
R. Salzbrenner and J. A. Ruppen 1983 7 p ref Presented at the 11th Ann. DOE Compatibility Meeting, Livermore, Calif., 18-20 Oct. 1983
(Contract DE-AC04-76DP-00789)
(DE83-015104; SAND-83-1381C; CONF-8310111-1) Avail: NTIS HC A02/MF A01

A corrosion fatigue test procedure based on fracture mechanics which is a severe test of materials compatibility is presented. Fatigue type tests can be used to demonstrate an accelerated cracking behavior. Care must be taken, however, when comparing fatigue crack growth behavior between two alloys and extrapolating to behavior under static loads. DOE

N84-12297# Argonne National Lab., Ill. Materials Science and Technology Div.
CORROSION BEHAVIOR OF Fe-Cr-Ni-Zr ALLOYS IN AGGRESSIVE ENVIRONMENTS AT HIGH TEMPERATURES
D. J. Baxter and K. Natesan May 1983 3 p refs Presented at the Symp. on High-Temp. Corrosion and Erosion, Electrochem. Soc. Fall Meeting, Washington, D.C., 9-14 Oct. 1983
(Contract W-31-109-eng-38)
(DE83-014735; CONF-831086-4) Avail: NTIS HC A02/MF A01

The influences of Zr on the scaling behavior of Fe-Cr-Ni alloys were observed. The following influences were noted: (1) additions of 1 to 6% Zr promote protective oxide scale formation on the 12% Cr alloy in air; (2) a concentration of $>$ 3% Zr is required to promote protective oxide scale formation on 12% Cr alloys in a S-free, low-p/sub O2/ environment; and (3) in mixed gas environments, Zr reduces surface scale thickness, generally reduces sulfur penetration into the alloy, and shifts the threshold boundary to lower p/sub O2/ for the 25% Cr alloy. DOE

N84-12298# California Univ., Livermore. Lawrence Livermore Lab.
EVALUATION OF SEVERAL HIGH-STRENGTH COPPER SHEET

ALLOYS
E. N. C. Dalder, W. Ludemann, and B. Schumacher 21 Jul. 1983 57 p refs Presented at the Am. Soc. for Metals Conf. on Copper and Copper Alloys, Philadelphia, 3-6 Oct. 1983
(Contract W-7405-eng-48)
(DE83-015612; UCRL-88919; CONF-8310129-1) Avail: NTIS HC A04/MF A01

The effects of the thermal treatments used during diffusion bonding, forming, and tritiding 50-cm-dia RTNS-II targets on the room temperature tensile properties of Amzirc, MZC, Elbrodur RS, and Glid-Cop copper alloy sheets of 0.04-in. thickness were determined. DOE

N84-12299# Argonne National Lab., Ill. Materials Science and Technology Div.
BREAKAWAY CORROSION IN MIXED-GAS ENVIRONMENTS
K. Natesan and D. J. Baxter May 1983 3 p refs Presented at the Symp. on High-Temp. Corrosion and Erosion at the Electrochem. Soc. Fall Meeting, Washington, D.C., 9-14 Oct. 1983
(Contract W-31-109-eng-38)
(DE83-014704; CONF-831086-2) Avail: NTIS HC A02/MF A01

Incology 800 was preoxidized for approx. 165 h in a low oxygen environment at 8750C. Subsequently, the specimens were exposed for approx. 165 h to either H2-H2S or CO-CO2-CH4-H2-H2S gas mixtures with a wide range of oxygen and sulfur partial pressures. It is shown that in atmospheres with p-Sub S2/ values below that required for base metal sulfidation and above threshold p/sub O2/ values, negligible adsorption of sulfur by the Cr rich oxide scale is noted. Any transport of sulfur across the oxide scale leads to the formation of Cr sulfide particles at grain boundary locations. Under these conditions, the alloy can weaken owing to grain boundary embrittlement but the sulfidation wastage will be small. The same conclusions can apply even if the atmosphere has a p/sub S2/ value above that required for base metal sulfidation and an above threshold p-sub O2/ value. As p/sub O2/ decreases below the threshold value, significant adsorption of sulfur by the scale and establishment of sulfur channels occur; these processes aid in the transport of Fe and Ni to the gas/scale interface for reaction to form fast growing sulfides, which lead to breakaway corrosion. DOE

N84-12300# Hanford Engineering Development Lab., Richland, Wash.
MINIATURE CHARPY-IMPACT TEST RESULTS FOR THE IRRADIATED FERRITIC ALLOYS HT-9 AND MODIFIED 9Cr-1Mo
W. L. Hu and D. S. Gelles May 1983 35 p refs Presented at the TMS/AIMEA Topical Conf. on Ferritic Alloys for Use in Nucl. Energy Technol., Snowbird, Utah, 19 Jun. 1983
(Contract DE-AC06-76FF-02170)
(DE83-016935; HEDL-21-2788-FP; CONF-830659-12) Avail: NTIS HC A03/MF A01

Impact tests of irradiated Charpy specimens made of ferritic alloys were conducted at temperatures from -650C to 2500C. The specimens involve four different material stocks, HT-9 base metal, HT-9 weld metal, HT-9 heat affected zone (HAZ) and modified 9Cr-1Mo base metal. The specimens were irradiated in EBR-II to a peak exposure of approximately 13 dpa at temperatures of 390, 450, 500 and 5500C. Specimens made of unirradiated HT-9 base metal and modified 9Cr-1Mo base metal were also tested. DOE

N84-12301# Du Pont de Nemours (E. I.) and Co., Aiken, S.C. Hydrogen and Ceramic Technology Div.
HYDROGEN COMPATIBILITY HANDBOOK FOR STAINLESS STEELS
George R. Caskey, Jr. Jun. 1983 151 p refs
(Contract DE-AC09-76SR-00001)
(DE83-017051; DP-1643) Avail: NTIS HC A08/MF A01

Data on the effects of hydrogen on the mechanical properties of stainless steels are compiled. This data is discussed within the context of current understanding of hydrogen compatibility of metals. All of the tabulated data derives from continuing studies of hydrogen effects on materials that were conducted at the Savannah River Laboratory over the past fifteen years. Supplementary data from other sources are included in the discussion. Austenitic, ferritic, martensitic, and precipitation hardenable stainless steels were studied. Damage caused by helium generated from decay of tritium is a distinctive effect that occurs in addition to the hydrogen isotopes protium and deuterium. The scope of our current knowledge of hydrogen effects in stainless steels is defined, serving as a guide to selection of stainless steels for service in hydrogen. DOE

N84-12302# Illinois Univ., Chicago. Dept. of Civil Engineering, Mechanics, and Metallurgy.
FORMATION OF SURFACE LAYERS DURING OXIDATION OF A Fe-Mn-Si ALLOY
J. M. Oh, Wayne King (ANL), and M. J. McNallan 1983 3 p Presented at the 163rd Electrochem. Soc. Meeting, San Francisco, 8 May 1983
(Contract W-31-109-eng-38; Grant NSF DMR-79-21210)
(DE83-009495; CONF-830508-23) Avail: NTIS HC A02/MF A01

The selective oxidation of Mn from Fe-16.7 Mn-6.6 Si-2.1 Ni was studied by electron microscopy. Nearly all the MnO scale formed spalls during cooling. Two layers are apparent, one being very low in Mn. The growth rate of the oxidation-induced ferrite layer is parabolic with time. DOE

N84-12303# Oak Ridge National Lab., Tenn. Metals and Ceramics Div.
RADIATION DAMAGE AND PHASE INSTABILITY IN IRRADIATED STAINLESS STEEL
Edward A. Kenik and Earl H. Lee 1983 3 p Presented at the Electron Microscopy Society of American Ann. Meeting, Phoenix, Ariz., 6 Aug. 1983
(Contract W-7405-eng-26)
(DE83-017190; CONF-830871-8) Avail: NTIS HC A02/MF A01

A 316 stainless steel, LS1A, with greater than nominal levels of silicon and titanium was developed which exhibits high resistance to swelling under ion irradiation. The origin of this swelling resistance and the roles of silicon and titanium were investigated. DOE

N84-12304# Oak Ridge National Lab., Tenn. Metals and Ceramics Div.
COMPARISON OF DAMAGE MICROSTRUCTURES IN NEUTRON-IRRADIATED VANADIUM AND IRON
L. L. Horton and K. Farrell 1983 3 p Presented at the Electron Microscopy Society of American Ann. Meeting, Phoenix, Ariz., 6 Aug. 1983
(Contract W-7405-eng-26)
(DE83-017189; CONF-830871-6) Avail: NTIS HC A02/MF A01

The cavity morphology and dislocation loop geometry in bcc vanadium are compared with the previously reported observations for neutron-irradiated iron. The specimens were vanadium with 100 wppM of interstitial impurities and vanadium with boron carbide additions which were irradiated to approx. 1 dpa in the same Oak Ridge Research Reactor capsules as the iron specimens. DOE

N84-12305# Kentucky Univ., Lexington. Dept. of Metallurgical Engineering.
STRUCTURAL CHARACTERIZATION OF DISPERSED METAL CATALYSTS Progress Report, 1 Sep. 1982 - 31 Aug. 1983
P. J. Reucroft, R. J. DeAngelis, and J. Bentley (ORNL, Tenn.) 1983 35 p refs
(Contract W-7405-eng-26; DE-AS05-82ER-12098)
(DE83-017145; DOE/ER-12098/1) Avail: NTIS HC A03/MF A01

Analytical electron microscopy characterization techniques were developed to investigate the structural features of small metal particles (50 to 100 angstroms) in porous media. In the first phase of the project, bright and dark field imaging techniques were emphasized. High quality images were obtained in both bright field and dark field and earlier characterization studies on three catalyst systems were confirmed and extended. Particle size growth (sintering) at low temperatures is much greater in the AU/SiO2 system, indicating a weak metal-support interaction. A more uniform and generally smaller particle size distribution is observed in

Ni/MgSiO3 compared to Ni/SiO2. The nickel particles in Ni/SiO2 show contrast effects which indicate that the particles contain faults or twins. DOE

N84-12306# Argonne National Lab., Ill. Fusion Power Program Office.
SELF-PUMPING IMPURITY BY IN-SITU METAL DEPOSITION
J. N. Brooks and R. F. Mattas Jul. 1983 24 p refs Presented at the Symp. on Energy Removal and Particle Control and Toroidal Fusion Devices, Princeton, N.J., 26-29 Jul. 1983
(Contract W-31-109-eng-38)
(DE83-017937; CONF-830795-3) Avail: NTIS HC A02/MF A01

A system for in-situ removal of helium trapping in freshly deposited metal surface layers of a limiter or divertor was studied. The system would trap helium on a limiter front surface, or a divertor plate, at low plasma edge temperatures, or in a limiter slot region, at high edge temperatures. Fresh material, introduced to the plasma and/or scrape-off zone, would be added at a rate of about five times the alpha production rate. The material would be reprocessed periodically, e.g. once a year. Possible materials are nickel, vanadium, niobium, and tantalum. Advantages of a self-pumping system are the absence of vacuum ducts and pumps, and the minimization of tritium processing and inventory. DOE

N84-12307# Ames Lab., Iowa.
LIFE PREDICTION UNDER STRESS CORROSION CONDITIONS BELOW K SUB ISCC
R. Ranjan and O. Buck 1983 8 p refs Presented at the Conf. on Quantitative NDE, Santa Cruz, Calif., 7-12 Aug. 1983
(Contract W-7405-eng-82)
(DE83-018074; IS-M-455; CONF-830811-12) Avail: NTIS HC A02/MF A01

Under stress corrosion conditions, the major portion of the useful life of a structure, originally free of defects, is spent during incubation and growth of microcracks. On the other hand, microcrack initiation is one of the least-well-understood phenomena and a prediction of the remaining life of a component in service is very difficult. Therefore, a physical model was developed which, at the present time, is specific to stress-corrosion cracking (SCC) OF CU-30Zn brass in a nontarnishing ammoniacal solution. The predictions of the model in terms of time to initiation were tested using experimental data of the effects of applied stress on crack initiation. Metallographic observations and scanning electron microscopy provided information on the transition from corrosion pitting to microcrack initiation. This transition occurs at a critical pit size of about (SIGMA)m, which will increase with decreasing stress. Implications of this research on nondestructive evaluation of SCC in the microcrack-initiation regime are briefly discussed. DOE

N84-12308# Sandia Labs., Albuquerque, N. Mex.
STRAIN RATE EFFECTS ON DUCTILE/BRITTLE TRANSITIONS IN STEELS
G. A. Knorovsky 1983 54 p refs Presented at the 16th Natl. Symp. on Fracture Mech., Columbus, Ohio, 15 Aug. 1983
(Contract DE-AC04-76DP-00789)
(DE83-016906; SAND-83-2917C; CONF-830820-2) Avail: NTIS HC A04/MF A01

A recently-implemented fracture control plan for structural steel highway bridges makes use of a linear relation to describe the effect of strain rate on the ductile/brittle transition temperature as a function of yield strength. Literature data show the predictions of the above-mentioned relation are not general. An alternate analysis is offered along with a qualitative model for understanding the phenomenon. Results of an experimental program investigating microstructural effects on the ductile/brittle strain rate dependence are also presented. The results exhibit linear behavior of (RADICAL)T sub db vs. (RADICAL)sigma/sigma, where (RADICAL)T sub db is the transition temperature shift, sigma is the yield stress, and (RADICAL)sigma is the change in yield stress due to strain rate. The magnitude of the temperature shift, however, is dependent upon the test specimen used. Factors discussed include microstructure, type of test specimen. crack initiation vs crack propagation, and implications for regulatory bodies. DOE

N84-12309# Du Pont de Nemours (E. I.) and Co., Aiken, S.C. Savannah River Lab.
HELIUM DAMAGE IN AUSTENITIC STAINLESS STEELS
George R. Caskey, Jr., David A. Mezzanotte, Jr., and David E. Rawl, Jr. 1983 21 p refs Presented at the TMS/AIME Meeting, Atlanta, 6-10 Mar. 1983
(Contract DE-AC09-76SR-00001)
(DE83-017494; DP-MS-82-55; CONF-830317-3) Avail: NTIS HC A02/MF A01

Helium produced by tritium decay was first shown to embrittle austenitic stainless steel at ambient temperature in tensile specimens of Nitronic-40 steel. A long term study of helium damage in five austenitic alloys was initiated. Results from this study were analyzed by the J-integral technique and show a decrease in ductile fracture toughness with increasing He-3 concentration. Sustained-load cracking tests indicate that the stress intensity required to initiate and propagate a crack also decreases with increasing He-3 concentration. DOE

27 NONMETALLIC MATERIALS

Includes physical, chemical, and mechanical properties of plastics, elastomers, lubricants, polymers, textiles, adhesives, and ceramic materials.

N84-12310 Royal Aircraft Establishment, Farnborough (England).
SOME CONSIDERATIONS OF THE EFFICIENCY OF SEWN LAP JOINTS IN A NYLON WEBBING
M. Webb 17 Jan. 1983 27 p refs
(RAE-TR-83009; RAE-Mat/Struct-29; BR88457) Copyright. Avail: Issuing Activity

The strength of lap joints sewn in a circularly-woven nylon webbing with an undyed nylon thread in a 3-point double W stitching pattern was studied at 20 C and after heating, storage, or weather exposure. Maximum seam efficiency was considered as the optimum combination of stitches/cm with the minimum length of overlap to ensure webbing breaks. Such seams were near the edge of a seam strength plateau or ridge. Heating, particularly at 170 C, or exposure to full, natural weathering for 6 months or longer affects the position of the edge and the height of the ridge. Author (ESA)

N84-12311*# Thiokol Corp., Brigham City, Utah.
REPLACEMENT OF PBNA IN HB AND HC POLYMERS USED IN SRM PROPELLANT AND LINER
M. L. Levinthal, R. D. Law, and D. C. Suisse 1 Jul. 1981 92 p refs
(Contract NAS8-30490)
(NASA-CR-170936; NAS 1.26:170936; TWR-13009) Avail: NTIS HC A05/MF A01 CSCL 11G

The antioxidant phenyl-beta-naphthylamine (PBNA) was used in both HB and HC polymers. The sole (domestic) supplier of PBNA has withdrawn this product from the market, primarily because of suspected health hazards. Commercially available substitute(s) were selected and qualified for use in the two polymers. Author

N84-12312*# Pratt and Whitney Aircraft Group, East Hartford, Conn. Engineering Div.
DEVELOPMENT OF STRAIN TOLERANT THERMAL BARRIER COATING SYSTEMS, TASKS 1 - 3
Neal P. Anderson and Keith D. Sheffler Sep. 1983 117 p refs
(Contract NAS3-22548)
(NASA-CR-168251; NAS 1.26:168251; PWA-5777-29) Avail: NTIS HC A06/MF A01 CSCL 11B

Insulating ceramic thermal barrier coatings can reduce gas turbine airfoil metal temperatures as much as 170 C (about 300 F), providing fuel efficiency improvements greater than one percent and durability improvements of 2 to 3X. The objective was to

increase the spalling resistance of zirconia based ceramic turbine coatings. To accomplish this, two baseline and 30 candidate duplex (layered MCrAlY/zirconia based ceramic) coatings were iteratively evaluated microstructurally and in four series of laboratory burner rig tests. This led to the selection of two candidate optimized 0.25 mm (0.010 inch) thick plasma sprayed partially stabilized zirconia ceramics containing six weight percent yttria and applied with two different sets of process parameters over a 0.13 mm (0.005 inch) thick low pressure chamber sprayed MCrAlY bond coat. Both of these coatings demonstrated at least 3X laboratory cyclic spalling life improvement over the baseline systems, as well as cyclic oxidation life equivalent to 15,000 commercial engine flight hours. M.G.

N84-12313*# National Aeronautics and Space Administration. Ames Research Center, Moffett Field, Calif.
POLYMERS OF PHOSPHONYLMETHYL-2,4- AND -2,6-DIAMINO BENZENES AND THE LIKE Patent Application
John A. Mikroyannidis (NAS-NRC, Washington, D.C.) and Demetrius A. Kourtides, inventors (to NASA) Filed 12 Aug. 1983 14 p Sponsored by NASA
(NASA-ARC-11506-1; US-Patent-Appl-SN-522629) Avail: NTIS HC A02/MF A01 CSCL 11I

Epoxy polymers resulting from the curing of epoxy materials with diamines such as m-phenylene diamine are deficient with respect to fire and heat resistance. A phosphonyl-methylbenzene is provided and polymerized with a monomer such as an epoxide, or a dianhydride. The resulting polymers combine one or more properties of heat resistance, low flammability and high char yield with good mechanical properties such as high tensile strength. NASA

N84-12314# Akron Univ., Ohio. Inst. of Polymer Science.
FAILURE PROCESSES IN ELASTOMERS AT OR NEAR A RIGID SPHERICAL INCLUSION
A. N. Gent and Byoungkyeu Park Sep. 1983 42 p
(Contract N00014-76-C-0408)
(AD-A132060; AD-E750778; TR-29) Avail: NTIS HC A03/MF A01 CSCL 11/9

A systematic experimental study has been carried out of two distinct failure phenomena, cavitation and debonding, in an elastomer containing a rigid spherical inclusion. Several elastomers were employed containing glass beads of various diameters, ranging from 60 micrometer to 5000 micrometer, and with chemically different surfaces. The critical stress for cavitation was found to depend upon Young's modulus-E of the elastomer and upon the diameter of the bead. By extrapolation, it was found that the stress for cavitation near an infinitely large bead is given by 5E/12, as predicted by theory. In contrast, the critical stress for debonding decreased somewhat with increasing Young's modulus of the elastomer. This is attributed to a concomitant decrease in the strength of adhesion between the elastomer and the bead surface, due to rheological effects. The stresses for both cavitation and for debonding were found to vary approximately with the negative half power of the bead diameter. This suggests that a similar Griffith mechanism governs both failure processes when the bead size is small. GRA

N84-12315# Massachusetts Univ., Amherst. Materials Research Lab.
RADIOLYSIS OF RESIST POLYMERS. 1: POLY(METHYL-ALPHA-HALOACRYLATES) AND COPOLYMERS WITH METHYLMETHACRYLATE
G. N. Babu, A. Narula, S. L. Hsu, and James C. W. Chien Aug. 1983 45 p Submitted for publication
(Contract N00014-81-K-0611)
(AD-A131864; AD-E850387; TR-1) Avail: NTIS HC A03/MF A01 CSCL 11/9

Methyl alpha-chloroacrylate (MCA) and methyl alpha-bromoacrylate (MBA) were copolymerized with methyl methacrylate (MMA) over a broad range of composition. The copolymers were exposed to gamma-radiation to determine chain scission susceptibility. The mechanisms of degradation of copolymers towards radiation was suggested from product analysis. The radiolysis of copolymers of MMA with MCA and MBA are dominated by the alpha-halogenated monomers. Author (GRA)

N84-12316# Lake Shore Cryotronics, Inc., Westerville, Ohio.
ENTHALPY - IMPROVED DIELECTRIC INSULATION FOR SUPERCONDUCTING WIRES Final Report, Jun. 1980 - Mar. 1982
W. N. Lawless, C. F. Clark, and R. W. Arenz Wright-Patterson AFB, Ohio AFWAL May 1982 150 p
(Contract F33615-80-C-2022; AF Proj. 2301)
(AD-A131857; AFWAL-TR-82-2056) Avail: NTIS HC A07/MF A01 CSCL 11/2

The purpose of this study was to investigate for the first time dielectric materials for enthalpy stabilization, the broad picture being that these materials would also serve as the dielectric-insulation coating. These new, inorganic materials resulted from basic research by the author into the specific heats of ferroelectric-type materials at low and glass which leads to enhanced specific-heat properties in several cases. In a particularly noteworthy case (60% SC-1C ceramic + 40% 7570 glass), the composite has a much larger specific heat (approx. = 0.07 J/cu cm/K) than the bulk ceramic alone below 7 K. There is evidence that the low thermal conductivities of all the composites are due to Kapitza resistance, and suggestions are made for improving these conductivities.GRA

N84-12317# Army Troop Support and Aviation Materiel Readiness Command, Corpus Christi, Tex. Power Plants Section.
150 HOUR ENGINE TEST OF CORROSION INHIBITED MIL-L-23699C OIL
Billy G. Wilson Jun. 1983 24 p
(AD-A131633; MRDP-6297-1) Avail: NTIS HC A02/MF A01 CSCL 11/8

A modified version of MIL-L-23699 oil with a corrosion inhibitor additive was evaluated. The CCAD test cell lubrication system is massive in comparison to an aircraft lubrication system such a system could not produce realistic test results. A simulated aircraft lubrication system was designed, fabricated, and used to recently engine tests an on-line ferrograph analyzer. The system was patterned after the UH-III aircraft, which has the same oil capacity and uses the same oil cooler and oil tank. E.A.K.

N84-12318# Sandia Labs., Albuquerque, N. Mex.
IN-SITU PERMEATION TESTS OF ELASTOMERIC O-RING SEALS
W. B. Leisher, F. B. Burns, P. J. Rodacy, and A. A. Trujillo 1983 6 p refs Presented at 7th Intern. Symp. on Packaging and Transport. of Radioactive Mater., New Orleans, 15 May 1983
(Contract DE-AC04-76DP-00789)
(DE83-015622; SAND-82-2237C; CONF-830528-50) Avail: NTIS HC A02/MF A01

A series of in-situ permeation tests are being conducted to determine permeation coefficients and breakthrough and saturation times for certain elastomeric o-rings with various gases that might be used as leak test tracers. The work is directed towards developing more effective and efficient nuclear material shipping packaging leak test procedures. The tests are in progress. DOE

N84-12319# Argonne National Lab., Ill.
ENGINEERING HOT-CELL WINDOWS FOR RADIATION PROTECTION
K. R. Ferguson and J. C. Courtney (Louisiana State Univ.) 1983 5 p refs Presented at the Am. Nucl. Soc. Winter Meeting, San Francisco, 30 Oct. - 3 Nov. 1983
(Contract W-31-109-eng-38)
(DE83-014675; CONF-831047-27) Avail: NTIS HC A02/MF A01

Radiation protection considerations in the design and construction of hot-cell windows are discussed. The importance of evaluating the potential gamma spectra and neutron source terms is stressed. DOE

N84-12320# Centec Consultants, Inc., Reston, Va.
ASSESSMENT OF ENERGY-EFFICIENCY IMPROVEMENTS FOR

PAINT SPRAY BOOTHS
Mar. 1983 73 p refs
(Contract DE-AC01-80CS-40402)
(DE83-016680; DOE/CS-40402/16) Avail: NTIS HC A04/MF A01

The economic and technical benefits achievable through spray booth control are discussed. A discussion of the energy use and potential for conservation in spray booths is presented. Descriptions, costs, and payback potentials of several spray booth control system concepts are provided. In addition, the technological barriers and the research and development needs to overcome these barriers are identified and discussed. DOE

N84-12321# Pacific Northwest Lab., Richland, Wash.
DISPARATE CHANGES IN THE PHYSICAL PROPERTIES OF GRAPHITE
W. C. Morgan Jul. 1983 3 p refs Presented at the 16th Am. Carbon Soc. Biennial Conf., La Jolla, Calif., 18-22 Jul. 1983
(Contract DE-AC06-76RL-01830)
(DE83-015986; PNL-SA-10923; CONF-830711-6) Avail: NTIS HC A02/MF A01

The strength of graphite is rapidly degraded by small amounts of oxidation; thus, where graphite is used as a structural material (such as the core-support components of a High Temperature Gas-Cooled Reactor) it is highly desirable that the strength of these components can be assessed by nondestructive means. It is shown that large disparate changes (either increases or decreases) in ultrasonic velocities, elastic moduli, and/or compressive strength can occur during the initial stages of oxidation; thereafter, the continued changes with oxidation are best-fit as a linear function of density. The disparate changes in the elastic moduli and compressive strength of oxidized graphite samples functions of density are examined. DOE

N84-12322# Sandia Labs., Albuquerque, N. Mex.
CHEMICAL PROPERTIES OF METALLIC GLASSES
Ronald B. Diegle 1983 13 p refs Presented at the 5th Intern. Conf. on Liquid and Amorphous Metals, Los Angeles, 15 Aug. 1983
(Contract DE-AC04-76DP-00789)
(DE83-017353; SAND-83-1273C; CONF-830888-8) Avail: NTIS HC A02/MF A01

Research into chemical properties of metallic glasses has revealed promising behavior in the areas of corosion resistance and catalysis. Metallic glasses containing a film-forming element exhibit resistance to uniform and localized corrosion that is superior to that of many crystalline stainless steels. This resistance is due to the presence of passive films that are enriched in the film-forming element. Cr is particularly effective, especially if P is present as in transition metal-Cr-P glasses. Protective coatings are an obvious application of metallic glasses. Metallic glasses also show promise as catalysts and electrocatalysts. Some glasses containing Pd and P offer better reactivity and resistance to corrosion than crystalline noble elements for electrolytic chlorine production. Others have demonstrated an ability as catalysts to oxidize methanol for fuel cell application, and also for hydrogenation of carbon monoxide. The very uniform structure and unique meta-stable compositions characteristics of metallic glasses are keys to understanding the chemical behavior of this exciting class of materials. DOE

N84-12323# Kernforschungsanlage, Juelich (West Germany). Inst. fuer Reaktorwerkstoffe.
INVESTIGATION OF INHOMOGENEITY IN CERAMIC REACTOR MATERIALS USING LASER-LOCALIZED EMISSION SPECTROSCOPY Thesis - Technische Hochschule, Aachen
R. Siechau, M. Mazurkiewicz, and H. Nickel Mar. 1983 157 p refs In GERMAN; ENGLISH summary
(JUEL-1834; ISSN-0366-0885) Avail: NTIS HC A08/MF A01

Using laser-localized emission spectroscopy, a method was developed for the determination of elemental inhomogeneity within the grains of three coarse-grained ceramic materials : mullite-based Duritals M70 and E90 and silica-based Masrock. Results for Durital E90 show that the large grains consist of very pure mullite and the fine grained regions contain small particles of mullite, corundom and binder, the impurities in the binder being concentrated at the grain boundaries. In Durital M70, the coarse and fine grained regions consist principally of mullite, the impurities introduced during manufacture being evenly distributed in both regions. Analyses of the Masrock material show a concentration of impurities in the fine grained regions with a very inhomogeneous distribution. The large grains consist of nearly pure SiO2. The distribution of impurity elements on the fracture surfaces of ceramics show that the fracture behavior is mainly influenced by the physical properties of the materials and not by the chemical properties of the phases present in the materials. Author (ESA)

N84-12324# Kernforschungsanlage, Juelich (West Germany). Inst. fuer Festkoerperforschung.
INVESTIGATION OF THE STATISTICAL MECHANICS OF LINEAR POLYMERS FOR VARIOUS PHYSICAL CONDITIONS Thesis - Cologne Univ. [UNTERSUCHUNGEN ZUR STATISTISCHEN MECHANIK VON LINEAREN POLYMEREN UNTER VERSCHIEDENEN PHYSIKALISCHEN BEDINGUNGEN]
K. Kremer Mar. 1983 222 p refs In GERMAN; ENGLISH summary
(JUEL-1832) Avail: NTIS HC A10/MF A01

The statistical mechanics of chain molecules were investigated, using the self avoiding walk (SAW) model on a diamond lattice. The investigation of the collapse transition of a single polymer for the whole crossover region results in a temperature scaling analysis and an estimation of the inner chain density in agreement with simulations. A chain on a randomly diluted lattice is investigated and a crossover is constructed for the case that the dilution is so strong that the SAW is placed on a critical percolating cluster. The investigation of the adsorption transition of a single chain at a hard wall with short range attractive force results in a complete energy scaling analysis, the mean squared gyration radius and end-to-end distance, and the free free energy. Using the dynamic simulation technique, obeying the Rouse dynamics for tandom walks, the statics and dynamics of polymeric melts were investigated. Even for the case of small static entanglement lengths there is no reptation onset, either for the mean square inner monomer displacements, or for the time dependent structure function. Author (ESA)

28 PROPELLANTS AND FUELS

Includes rocket propellants, igniters, and oxidizers; storage and handling; and aircraft fuels.

For related information see also *07 Aircraft Propulsion and Power, 20 Spacecraft Propulsion and Power,* and *44 Energy Production and Conversion.*

N84-12325# Naval Surface Weapons Center, White Oak, Md. Research and Technology Dept.
MICROSTRUCTURAL ORIGINS OF HOT SPOTS IN RDX EXPLOSIVE AND SEVERAL REFERENCE INERT MATERIALS Annual Progress Report, 30 Dec. 1981 - 30 Sep. 1982
W. L. Elban, C. S. Coffey, R. W. Armstrong, K.-C. Yoo, and R. G. Rosemeier Mar. 1983 41 p Prepared in cooperation with Maryland Univ., College Park
(Contracts N00014-82-K-0263; N00014-82-WR-20129; NR Proj. 659-797; NR Proj. 659-798; RR02402OD)
(AD-A132056; NSWC-MP-83-116; APR-1) Avail: NTIS HC A03/MF A01 CSCL 19/1

Hardness testing is being used to locally deform RDX explosive and several selected reference inert crystals in a controlled manner in order to investigate the microstructural origins of hot spots. The plastic deformation in RDX was found to be very inhomogeneous. The strain fields around Knoop hardness impressions in a reasonably perfect laboratory-grown crystal were studied using surface reflection Berg-Barrett topography. Highly localized strain fields were observed, and a considerable anisotropy in Knoop hardness number was measured. A substantial variation in Vickers

hardness numbers was obtained for several Holsten production-grade Class D RDX crystals. This is indicative of this material's inhomogeneous internal structure; perhaps most notable is the presence of numerous pores observed by microscopic examination. Spherical ball hardness experiments at various applied loads were performed on a single crystal of MgO. Examination of the strain fields surrounding the resultant impressions by surface reflection Berg-Barrett topography revealed that, for increasing applied loads, the size of the strain fields was controlled by cracking. The strain fields around hardness indentations placed in a single crystal of NaCl were also investigated, in collaboration with other researchers, by synchrotron X-Ray topography.
Author (GRA)

N84-12326# California Univ., Livermore. Lawrence Livermore Lab.
USING AN X-RAY-SENSITIVE VIDICON AND REMOTE-CONTROL STAGE MECHANISM TO OBTAIN CRITICAL RADIOGRAPHIC ALIGNMENT OF SMALL EXPLOSIVE DEVICES
Richard H. Bossi and Ross Hoblitzell 1983 5 p Presented at the 14th Symp. of Nondestructive Evaluation, San Antonio, Tex., 19 Apr. 1983
(Contract W-7405-eng-48)
(DE83-012846; UCRL-88963; CONF-830430-2) Avail: NTIS HC A02/MF A01

A novel approach for the radiography of small electro-explosive devices to determine the presence or absence of gaps has been developed. Image resolution and part alignment were the main obstacles to be overcome. The required resolution for the inspection was 25 microns. Fine grain X-ray film was found to meet the resolution requirement. The alignment problem was overcome by using an X-ray sensitive vidicon camera and remote control stage mechanism. The input field of view of the camera is 9.5 mm x 12.7 mm. This results in enlargement of 20 to 30 times when viewed on a television monitor. By rotating the electro-explosive device on the remote control stage and observing the monitor, proper alignment for imaging gaps could be obtained. This system can readily detect gaps less than 0.02 mm (0.0001 inch). DOE

N84-12327# Ricardo & Co., Engineers (1927) Ltd., Shoreham-by-Sea (England).
EVALUATION OF UNTHROTTLED COMBUSTION SYSTEM OPTIONS FOR LIGHT DUTY APPLICATIONS WITH FUTURE SYNCRUDE DERIVED FUELS
J. R. Needham, B. M. Cooper, and S. R. Norris-Jones Dec. 1982 104 p refs
(Contract DE-AC01-80CS-50021)
(DE83-017047; DOE/CS-50021/3) Avail: NTIS HC A06/MF A01

An experimental program examining the interaction between several fuel and light duty automotive engine combinations is detailed. Combustion systems addressed covered indirect and direct injection diesel and spark ignited stratified charge. Fuels primarily covered D2, naphtha and intermediate broadcut blends. Low ignition quality diesel fuels were also evaluated. The results indicate the baseline fuel tolerance of each combustion system and enable characteristics of the systems to be compared. Performance, gaseous and particulate emissions aspects were assessed. The data obtained assists in the selection of candidate combustion systems for potential future fuels. Performance and environmental penalties as appropriate are highlighted relative to the individual candidates. Areas of further work for increased understanding are also reviewed. DOE

N84-12328# Illinois Univ., Urbana. Dept. of Aeronautical and Astronautical Engineering.
FLAME ACCELERATION MECHANISMS UNDER CONDITIONS OF PARTIAL CONFINEMENT Annual Report, Feb. 1982 - Jan. 1983
Roger A. Strehlow, A. I. Ormsbee, T. W. Gary Yip, and Mike Adlasor 23 Feb. 1983 42 p refs Sponsored by Gas Research Inst.
(PB83-244012; GRI-82/0054; AR-2) Avail: NTIS HC A03/MF A01 CSCL 21D

Studies in the 3-D channel were discontinued because the complex flow that was observed there makes interpretation of the results difficult. Experiments in the 2-D channel have identified the fact that obstacles placed ahead of the flame shed vortices in the impulsive flow generated by the flame and that these vortices are liminar when produced and subsequently break down to form turbulent vortices. Qualitatively it was observed that the violence of the flame vortex interctions increases markedly when the vortex is turbulent. DOE

N84-12329# SRI International Corp., Menlo Park, Calif.
REDUCTION OF CO2 TO METHANOL AND METHANE BY PHOTO AND DARK REACTIONS ON SEMICONDUCTOR ELECTRODES Annual Report, Feb. 1982 - Feb. 1983
K. W. Frese, Jr. and Duane Canfield Mar. 1983 62 p refs Sponsored by Gas Research Inst.
(PB83-249490; GRI-81/0162) Avail: NTIS HC A04/MF A01 CSCL 21D

Electrochemical mechanism of reduction of CO2 or carbonate species to useful fuels e.g., methanol and methane by means of sunlight and semiconductor electrodes was investigated. Carbon dioxide is an abundant raw material that is used as a source of inorganic carbon. By suitable electrochemical processes this inorganic carbon is converted to organic carbon in the form of methanol and methane, which could be used as a fuel. Such electrochemical conversions are made to occur at semiconductor electrodes. In addition, semiconductor electrodes absorb light, and this light is converted to a voltage that causes the electrochemical transformations of interest. By combining the CO2, water, semiconductor, and sunlight, we can store solar energy in the fuel. The end result is a method to upgrade the products of ordinary combustion, namely CO2 and H2O, by returning them to useful fuels. The electrochemical and solid state aspects of the conversion of CO2 to fuels at semiconductor electrodes was studied. GRA

31 ENGINEERING (GENERAL)

Includes vacuum technology; control engineering; display engineering; and cryogenics.

N84-12330 California Univ., Berkeley.
SYSTEM IDENTIFICATION OF STRUCTURES WITH JOINT ROTATION Ph.D. Thesis
Jerry Samuel Dimsdale 1982 144 p
Avail: Univ. Microfilms Order No. DA8312798

The role of joint behavior in the identification of frame models from dynamic response data caused by seismic forcing functions is investigated. Including joint rotation and deformation in the mathematical model for even simple structures significantly affects the distribution of stiffness, and the accuracy with which response can be predicted. An optical method was deviced for accurately measuring joint rotation of a structure during earthquake excitation. This method was applied to a simple six story frame in which the columns have approximately the same stiffness as the griders. Response data were collected for a variety of base motion histories. Also studied are data previously collected from a three story frame in which joint rotation information was inferred from strain measurements. A number of different mathemtical models of these structures are evaluated using system identification. Each mathematical model depends on a number of parameters related to the characteristics of the structure. An iterative method is applied to calculate the values of these parameters which best reproduce the measured response of the structure. Dissert. Abstr.

N84-12331# Army Cold Regions Research and Engineering Lab., Hanover, N. H.
DETECTION OF CAVITIES UNDER CONCRETE PAVEMENT
Austin Kovacs and Rexford M. Morey Jul. 1983 50 p
(Contracts MIPR-CES-82-3; MIPR-CES-82-3A)
(AD-A131851; CRREL-83-18) Avail: NTIS HC A03/MF A01 CSCL

17/9

An evaluation of an impulse radar system for detecting cavities under concrete pavement is discussed, and field results are presented. It was found that a dual antenna mode of surveying was ideal for void detection. In this mode one antenna operated in a transceive mode and a second, offset from the first, operated in a receive-only mode. This arrangement allowed a refraction-type profile survey to be performed, which enabled subpavement voids to be easily detected. Field trails were held at Plattsburgh Air Force Base, where 28 cavities were detected and mapped. Drilling of holes verified that a cavity existed and allowed cavity depth to be measured. The cavities varied from 1.5 in. to 23 in, depth and were up to 20 ft. long. Author (GRA)

N84-12332# National Bureau of Standards, Washington, D.C. National Engineering Lab.

PERFORMANCE OF ADD-ON-TYPE HEAT PUMP WATER HEATERS USING TWO DIFFERENT TEST METHODS

James E. Harris Jun. 1983 34 p refs Sponsored in part by Department of Energy

(PB83-222703; NBSIR-83-2723) Avail: NTIS HC A03/MF A01 CSCL 13A

Two different makes of add-on (without tank) heat pump water heaters (HPWH) were tested. Each of the HPWH's was subjected to a series of recovery tests similar to the Department of Energy (DOE) recovery test for conventional electric water heaters. The results of the tests (recovery efficiency, standby loss, input power, storage tank capacity and energy used) were used to compute an energy factor which could be used to calculate the estimated annual operating cost of such HPWH's. The energy factor was also determined by a series of simulated use tests consisting of four equal draws totaling 64.3 gallons of hot water per day. Author (GRA)

N84-12333# Battelle Columbus Labs., Ohio.

WALK-THROUGH SURVEY REPORT: CONTROL TECHNOLOGY FOR INTEGRATED CIRCUIT FABRICATION, XEROX CORPORATION, EL SEGUNDO, CALIFORNIA

Gary J. Mihlan, Leslie J. Ungers (PEDCO-Environmental, Inc., Cincinnati, Ohio), Russell K. Smith, Ralph I. Mitchell, and James H. Jones (NIOSH, Cincinnati, Ohio) 31 May 1983 49 p refs Sponsored by NIOSH and EPA

(PB83-239053; Rept-115-12A) Avail: NTIS HC A03/MF A01 CSCL 06J

A preliminary control technology assessment survey was conducted at the facility which manufactures N-channel metal oxide semiconductor (NMOS) integrated circuits. The facility has industrial hygiene review procedures for evaluating all new and existing process equipment. Employees are trained in safety, use of personal protective equipment, and emergency response. Workers potentially exposed to arsenic are monitored for urinary arsenic levels. The facility should be considered a candidate for detailed study based on the diversity of process operations encountered and the use of state-of-the-art technology and process equipment. GRA

N84-12334# Michigan Univ., Ann Arbor. Dept. of Industrial and Operations Engineering.

BIBLIOGRAPHY OF COEFFICIENT OF FRICTION LITERATURE RELATING TO SLIP TYPE ACCIDENTS

James M. Miller Feb. 1983 15 p Sponsored in part by Occupational Safety and Health Administration

(PB83-243626; IOE/CE-83-01) Avail: NTIS HC A02/MF A01 CSCL 13L

Over 300 references are listed which address various aspects of coefficient of friction (COF) as it relates to slip type accidents. Friction measurement machines, floor slipperiness, shoe sole COF values, and required COF for walking and a few work type tasks are covered. The references were collected as cited from among over thirty-five publications which appeared over the past fifty years. GRA

32 COMMUNICATIONS

Includes land and global communications; communications theory; and optical communications.

For related information see also *04 Aircraft Communications and Navigation* and *17 Spacecraft Communications, Command and Tracking.*

N84-12335 Oklahoma Univ., Norman.

THE EFFECTS OF CHANNEL TORTUOSITY ON ELECTROMAGNETIC RADIATIONS FROM LIGHTNING RETURN STROKES Ph.D. Thesis

Yueh-ping Liaw 1982 163 p

Avail: Univ. Microfilms Order No. DA8306723

The analysis of radiation form a lightning return stroke requires both channel geometry and the current waveform that propagates along the channel. Analysis and interpretation in the past have been performed with simplified channel geometries or simplified current models. A numerical solution of Maxwell's equations was developed and used to examine the impact of channel tortuosity on calculated electric field waveforms using artificial channel geometries and two different return stroke current models (compound exponential transmission line and the modified model of Lin et al.). Simultaneous channel geometries and electric field waveforms were recorded in Oklahoma and Florida. Two flashes from each location were used to compare measured electric field waveforms with calculated waveforms for reconstructed tortuous and and equivalent linear channels. It is concluded that the magnitude of the effect due to tortuosity is highly dependent upon the current model and the range of the lightning flash.

Dissert. Abstr.

N84-12336*# New Mexico State Univ., Las Cruces.

SPEED-DEPENDENT COLLISION EFFECTS ON RADAR BACKSCATTERING FROM THE IONOSPHERE Final Report

Yugal K. Behl and Otto H. Theimer Dec. 1982 63 p refs (Grant NsG-7622)

(NASA-CR-173077; NAS 1.26:173077) Avail: NTIS HC A04/MF A01 CSCL 20N

The question whether the differences between fluctuation spectra for linearly speed-dependent and speed-independent collision frequencies could account for disagreements between rocket and incoherent scatter estimate was addressed. The basic theory used for computing the fluctuation spectrum is outlined. The speed-dependence of the charge-neutral collision frequency is discussed, with special emphasis on its derivation from the mobility measurements. Various developments of the computer code used for the computation of the fluctuation spectrum are described. The range of values of input parameters typical to the collision-dominated ionosphere are briefly described. The computational results are presented, and the significance and limitation of these results and the future scope of the research are discussed. N.W.

N84-12337# Instituto de Pesquisas Espaciais, Sao Jose dos Campos (Brazil).

SATELLITE COMMUNICATION, PART 1

Vishwanath Sinha Oct. 1983 14 p refs Submitted for publication

(INPE-2893-PRE/417) Avail: NTIS HC A02/MF A01

Satellite communication at an introductory level is discussed and communication aspects of a satellite link are covered. The parameters involved in a link calculation are discussed. An example, illustrating typical values, is given. Author

N84-12338# Air Force Systems Command, Wright-Patterson AFB, Ohio. Foreign Technology Div.

TRENDS IN THE DEVELOPMENT OF TELEINFORMATICS

Wladyslaw Majewski 18 Jul. 1983 8 p refs Transl. into ENGLISH from Przeglad Telekomun. (Poland), v. 52, no. 4, 1979 p 97-98

(AD-A131067; FTD-ID(RS)T-0854-83) Avail: NTIS HC A02/MF A01 CSCL 17/2

Modern informatics is characterized by space structures.

Computing centers with local access are gradually being replaced by centers with remote access. Isolated centers give way to groups of centers divided into space and located throughout the country. Of course, these centers are mutually interconnected by telecommunication, forming so-called computer networks. These networks also contain preprocessors, utilized for preliminary data processing. The computer networks make it possible to realize spatially distributed informatic systems, so-called teleinformatic systems. Thus the role of telecommunication in the development of modern informatics is exceedingly important. GRA

N84-12339# Mission Research Corp., San Diego, Calif.
ION-ION RECOMBINATION RATE IN THE EMP SOURCE REGION
J. G. Chervenak and V. A. J. VanLint 10 Feb. 1982 32 p refs
(Contract DNA001-81-C-0175; DNA Proj. X99-QAXV)
(AD-A131148; AD-E301203; DNA-TR-81-83; MRC/SD-R-98) Avail: NTIS HC A03/MF A01 CSCL 20/14

The ion-ion recombination coefficient in air was measured to be 7.0 + or - 0.4 x 10 to the 7th power cu cm/s using an ion chamber at HIFX. The difference between this and previously measured values may be due to air purity or a dose dependence. GRA

N84-12340# Spectron Development Labs, Inc., Seattle, Wash.
INVESTIGATION OF THE RAYLEIGH CRITICAL ANGLE PHENOMENON FOR THE CHARACTERIZATION OF SURFACE PROPERTIES Final Report, Nov. 1982 - Feb. 1983
B. P. Hildebrand, G. L. Fitzpatrick, and A. J. Boland Apr. 1983 59 p refs
(Contract F49620-81-C-0040; ARPA Order 4109; AF Proj. 2306)
(AD-A131530; AFOSR-83-0678TR; SDL-82-2188-14F) Avail: NTIS HC A04/MF A01 CSCL 20/14

Rayleigh type acoustic critical angle experiments on a variety of samples ranging from single crystals to polycrystalline alloy and glasses have been performed. Two conclusions can be drawn from this work: (1) simple linear equations of motion, which include anisotropy, suffice for an approximate description of the observations; (2) certain observations at and near the critical angle, involving the production of anomalous harmonics, imply that the nonlinear characteristics of the water, and possibly the solid, cannot be ignored and need further study. Moreover, the new measuring apparatus, using an acoustic lens, has the following desirable features: (a) it allows local measurements of the solid properties to be made, and (b) except for problems associated with phase measurements of the reflected waves, experimental results are essentially consistent with the work of others who used a different experimental approach. We conclude that our goal of using a device in practical flaw imaging work is reasonable and holds promise of being a quantitative flaw imaging technique. GRA

N84-12341# Electronics Engineering Group (1842nd), Scott AFB, Ill.
PROTOTYPE FIBER OPTIC SYSTEM TO REMOTE TRACALS RADAR Final Technical Report
Jacob A. Radcliff and Kenneth E. Becker 30 Jun. 1983 50 p Revised
(AD-A132073; Rept-1842-EEG/EEIT-TR-16-EZ) Avail: NTIS HC A03/MF A01 CSCL 17/9

This report details the installation, acceptance testing and operational testing of a prototype fiber optic remoting system for TRACALS radars. GRA

N84-12342# Naval Research Lab., Washington, D. C.
TECHNIQUES FOR LOCATING A REMOTE HF TRANSMITTER FROM SINGLE-SITE MEASUREMENTS Memorandum Report
M. H. Reilly 11 Aug. 1983 24 p
(AD-A132014; NRL-MR-5145) Avail: NTIS HC A02/MF A01 CSCL 17/3

Techniques are developed for the location of a remote HF transmitter from single-site DF measurements on the incoming wavefront, coupled with ionospheric data. A simple method is detailed, which utilizes the Breit-Tuve and Martyn equivalent path theorems in a flat ionosphere approximation. It is shown to break down in this application only for high elevation angles and frequencies. Curved ionosphere generalizations of these theorems are developed to remove this breakdown. These generalizations are found to be remarkably accurate within the context of the neglect of magnetic field and non-spherical ionosphere effects, and are shown to applicable to the present problem. GRA

N84-12343# Lincoln Lab., Mass. Inst. of Tech., Lexington. Group 47.
EFFECT OF FREQUENCY-AVERAGING ON ESTIMATION OF CLUTTER STATISTICS USED IN SETTING CFAR DETECTION THRESHOLDS
Thomas H. Einstein 9 Nov. 1982 67 p
(Contract F19628-80-C-0002; ARPA Order 3391; AF Proj. 3G10)
(AD-A131947; TT-60; ESD-TR-83-031) Avail: NTIS HC A04/MF A01 CSCL 12/1

Incoherent averaging of radar returns measured at different frequencies has been shown to be an effective method of improving fixed target detection performance. This improvement results from the fact that frequency-averaging narrows the amplitude probability distributions of both the target and clutter returns(after averaging), thereby allowing returns from targets to the more easily distinguished from those of clutter. This report examines the effect of frequency averaging on decreasing the variance of the estimated clutter reflectivity. The attainable reduction in clutter sample variance that results from frequency-averaging is shown to be strongly dependent upon the spatial non-uniformity of the clutter. The more non-uniform the clutter, the less effective frequency-averaging is in reducing the clutter sample variance and corresponding CFAR (Constant False Alarm Rate) threshold setting. An analytic expression is derived for the amount of sample variance reduction provided by frequency averaging, as a function of spatial standard deviation of mean clutter reflectivity and the number of frequencies averaged. The amount of variance reduction predicted by this expression is confirmed by experimental measurements (at Ku band) of clutter returns, at 16 and 32 different frequencies, for a variety of different clutter types. Author (GRA)

N84-12344# City Coll. of the City Univ. of New York. Communications Systems Lab.
ACQUISITION, IMAGE AND DATA COMPRESSION Final Technical Report, 1 Mar. 1981 - 28 Feb. 1983
Donald L. Schilling and George Eichmann 30 Apr. 1983 109 p Presented at MILCOM 1983, Opt. Soc. 1983, SPIE 1983, and Opt. Computing Conf. 1983
(Grant AF-AFOSR-0169-81; AF Proj. 2305)
(AD-A131923; AFOSR-83-0505TR) Avail: NTIS HC A06/MF A01 CSCL 17/2

This report discusses the following subjects: (1) A new technique to achieve a fast PN Acquisition scheme; (2) A comparison of schemes for coarse acquisition of frequency-hopped spread-spectrum signals; (3) Investigation of the tracking of frequency hopped spread spectrum signals in adverse environments; (4) Coherent optical production of the Hough transform; (5) Estimation of the closely spaced frequencies buried in white noise using linear programming; (6) Restoration of discrete Fourier spectra using linear programming; (7) Two-dimensional optical filtering of 1-D signals; (8) Random TDMA Access Protocol with application to multi beam satellites; and (9) A reservations scheme of multiple access for local networks. GRA

N84-12345# Naval Research Lab., Washington, D.C. Electromagnetics Branch.
PERFORMANCE ANALYSIS OF A THREE-DIMENSIONAL MICROWAVE LENS IN A CYLINDRICAL ARRAY SCANNING APPLICATION Interim Report
H. Paris Coleman and J. Paul Shelton 29 Jul. 1983 17 p
(RR0210543)
(AD-A131891; AD-E000538; NRL-8713) Avail: NTIS HC A02/MF A01 CSCL 09/1

The calculated performance of a scanning cylindrical antenna array using a three dimensional lens system as the feed system

is discussed. Nominal specifications of 4 deg beamwidth, 0.l deg pointing accuracy and 25 dB sidelobe level were established. The system was designed to scan through a full 360 deg of azimuth using associate phase shifters and sector switching matrix. It is shown that the evaluated lens system is unable to meet the sidelobe specification and suffers in this regard, and with regard to overall system loss, when compared to a more conventional matrix feed system. GRA

N84-12346# Air Force Systems Command, Wright-Patterson AFB, Ohio. Foreign Technology Div.
TELECOMMUNICATIONS (SELECTED ARTICLES)
Marek Palacz, Ryszard Jankowski, Stefan Kijak, Jerzy Blaszyk, and Antoni Krysztofiak 21 Jul. 1983 50 p Transl. into ENGLISH from Przeglad Telekomun. (Poland), v. 52, no. 9, 1979 p 266-271, 272-274 and 275-278
(AD-A131872; AD-E850387; FTD-ID(RS)T-0818-83) Avail: NTIS HC A03/MF A01 CSCL 17/2

Topics of discussion include: the E-10 automaated international telephone exchange; the use of modems and converters by the Telkom-Teletra plant; and the EACT-200 electronic subscriber central telephone exchange. B.G.

N84-12347# Rome Air Development Center, Griffiss AFB, N.Y.
SIMULTANEOUS NULLING IN THE SUM AND DIFFERENCE PATTERNS OF A MONOPULSE ANTENNA
Randy L. Haupt Oct. 1982 108 p
(DA Proj. 4600)
(AD-A131865; AD-E850387; RADC-TR-82-274) Avail: NTIS HC A06/MF A01 CSCL 09/5

Most adaptive array research neglects the problem of nulling in a monopulse antenna. Placing a null in the sum pattern does not automatically place a null in the difference pattern and vice versa. Nulls may be placed in the two patterns by having separate adaptive weights and controls for each channel, however, this method uses two sets of adaptive hardware for one antenna. This paper develops a technique for simultaneous nulling in the sum and difference patterns of a monopulse phased array using one set of adaptive weights shared by both channels. First, the technique is used for amplitude and phase nulling then for phase-only nulling. In each case, the ability to simultaneously null in both channels with one set of weights, chosen to place a null at a particular location, is theoretically demonstrated.
Author (GRA)

N84-12348# Weissman (David E.), Northport, N.Y.
THE DEPENDENCE OF THE RADAR MODULATION TRANSFER FUNCTION ON ENVIRONMENTAL CONDITIONS AND WAVE PARAMETERS Final Report, Jun. - Aug. 1983
David E. Weissman Aug. 1983 27 p
(Contract N00014-83-M-0081)
(AD-A131858; DEW-83-1) Avail: NTIS HC A03/MF A01 CSCL 20/14

Recent measurements of ocean wave-radar modulation transfer function (MTF) from fixed ocean platforms, over a period of several years, have demonstrated that the loval hydrodynamic modulation of short centimetric waves is affected by the air-sea interaction. Results from widely separated ocean regions also show different individual properties, that make detailed measurements necessary. An X-band radar with vertical polarization was mounted on a platform in the Gulf of Mexico during Nov.-Dec. 1978. The data set is computer stored and was processed. A selective study of this data has been conducted on the separate, independent influence of wind speed, air-sea temperature difference and wave slope on the MTF and the average radar cross section. Dependence on all these parameters was observed. Data from other experiments agree with these results. Variations of the coherence function for the modulation transfer function imply that other mechanisms must be found for these modulation effects other than hydrodynamic (wave-wave) interactions. An important conclusion of this study is that the surface stress depends not only on wind speed, but also on air-sea temperature difference and wave slope. Author (GRA)

N84-12349# Naval Ocean Systems Center, San Diego, Calif.
NETWORK DESIGN TOOL FOR EHF SATELLITE COMMUNICATIONS NETWORKS Final Report, Jan. - Sep. 1982
Sally Norvell and G. J. Brown Jun. 1983 157 p
(AD-A131812; NOSC/TR-839) Avail: NTIS HC A08/MF A01 CSCL 05/1

This document describes the design concept of the network design tool. The network design tool (NDT) is a collection of analytical techniques, algorithms and simulation methods that may be used to characterize the performance of a computer communication network. Much work has been done over the past several years in network performance analysis and many techniques have been developed or proposed. Each of these methods applies to a particular aspect of the network design and is based on a particular modeling point of view. We define the computer communication network and then describe the different ways the network may be modeled. Each network model is related to the particular design problem being addressed. The various analytical approaches are briefly described and their relationship to the network models discussed. Chapter 2 is a survey of the major approaches to specific network design problems while chapters 3 and 4 discuss two fairly well defined areas of network analysis: topological design/optimization and protocol validation. Chapter 5 is a survey of network design tools presently available locally or on the advanced research projects agency network (ARPANET). Finally, chapter 6 presents an outline of the NDT specification. GRA

N84-12350# ALPHATECH, Inc., Burlington, Mass.
TRACKING THEORY FOR AIRBORNE SURVEILLANCE RADARS Final Technical Report
J. R. Delaney, A. S. Willsky, A. L. Blitz, and J. Korn Feb. 1983 139 p
(Contract N00019-81-C-0182)
(AD-A131792; TR-142) Avail: NTIS HC A07/MF A01 CSCL 12/1

This report describes the development of an advanced multitarget tracking algorithm for surveillance radars. The approach is based on the development of mathematical models relating targets, the environment, and radar parameters to the measurements supplied to the tracking algorithm. The fundamentals of the surveillance and tracking algorithm are based on adaptive hypothesis testing techniques, and specifically, on the multiple model adaptive estimation approach. The algorithm was developed, computer-programmed, and exercised on several hypothetical but realistic surveillance/tracking scenarios. Author (GRA)

N84-12351# Paris XI Univ., Orsay (France). Lab. d'Optique des Solides.
RESEARCH AND DEVELOPMENT FOR INVESTIGATIONS OF METALLIC ADSORPTIONS ON METAL SURFACES BY OPTICAL TECHNIQUES COMPLEMENTED BY dc RESISTIVITY AND AUGER SPECTROSCOPY Final Technical Report
F. Abeles, T. Lopez-Rios, Y. Borensztein, and G. Vuye Jun. 1983 57 p
(Contract DAJA37-79-C-0516; DA Proj. 1T1-61102-BH-57)
(AD-A131739) Avail: NTIS HC A04/MF A01 CSCL 07/4

Differential reflectivity delta R/R measurements between a smooth Ag surface and the same surface covered by silver deposits of various thicknesses were performed in ultra high vacuum over the 1.5-5 eV spectral range for different Ag substrate temperatures in order to examine roughness effects on the electromagnetic field. GRA

N84-12352# Polytechnic Inst. of New York, Brooklyn.
RESEARCH IN NET MANAGEMENT TECHNIQUES FOR TACTICAL DATA NETWORKS Semiannual Technical Report, No. 3, 1 Sep. 1981 - 28 Feb. 1982
Robert Boorstyn and Aaron Kershenbaum Sep. 1982 97 p
(Contract DAAK80-80-K-0579; DA Proj. 1L1-61102-AH-48)
(AD-A131674; CECOM-80-0579-3; SATR-3) Avail: NTIS HC A05/MF A01 CSCL 17/2

This report is the third semi-annual report covering research in Packet Radio communication networks design and analysis.

Presented herein is an approach for the throughput analysis of arbitrary multi-hop packet radio networks a teleprocessing network design technique, and a mathematical technique for combinational organization problems. GRA

N84-12353# Ames Lab., Iowa. Applied Mathematical Sciences.
EFFECTS OF DISSIPATION IN ONE-DIMENSIONAL INVERSE PROBLEMS
J. P. Corones, M. E. Davison, and R. J. Krueger (Nebraska Univ., Lincoln) 1983 14 p refs Presented at the Soc. of Photo-Opt. Instr. Engr. Conf., Arlington, Va., 4-8 Apr. 1983
(Contract W-7405-eng-82)
(DE83-017692; IS-M-434; CONF-830420-5) Avail: NTIS HC A02/MF A01

Consider the problem of determining the permittivity as a function of depth in a one dimensional medium. If the incident field is a transverse electric plane wave then the permittivity can be determined by using the resulting reflected field in an appropriate inversion algorithm, assuming the conductivity of the medium is known. However, if the conductivity is only known approximately, use of such inversion techniques can result in erroneous estimates of the permittivity. How the performance of an inversion algorithm is altered by misrepesenting the dissipative effects of the medium is examined. Two cases are of interest: (1) the assumed dissipative effects differ slightly from the actual dissipative effects throughout the medium, e.g., assuming no dissipation in a medium which in fact has small, non-zero conductivity, and (2) ignoring conductivity in a narrow region of the medium. DOE

N84-12354# Prakla-Seismos G.m.b.H., Hannover (West Germany).
NUMERICAL MODELING TECHNIQUES ACCORDING TO THE WAVE EQUATION AND THE RAY METHOD Final Report, Apr. 1982
Joerg Schneider and Dietrich Ristow Bonn Bundesministerium fuer Forschung und Technologie Jul. 1983 149 p refs In GERMAN; ENGLISH summary Sponsored by Bundesministerium fuer Forschung und Technologie
(BMFT-FB-T-83-136; ISSN-0340-7608) Avail: NTIS HC A07/MF A01; Fachinformationszentrum, Karlsruhe, West Germany DM 31,50

Computer programs were developed to solve the elastic or acoustic wave equation. They provide partial solutions according to the method of asymptotic series approximations to the elastic wave equation (ray methods), the three dimensional image-ray method, and the two dimensional finite difference method in the time-distance domain. In exploration seismics these numerical modeling techniques can be used to evaluate the recording quality of field measurements, to acquire information about suitable processing parameters, or to check the interpretation of survey areas. Author (ESA)

N84-12355# Erno Raumfahrttechnik G.m.b.H., Bremen (West Germany).
PHASE A STUDY FOR A TEST SATELLITE FOR PROPAGATION AND TRANSMISSION EXPERIMENTS IN THE 20/30 GHz FREQUENCY BAND Final Report, Oct. 1980
Gerhard Schneider Bonn Bundesministerium fuer Forschung und Technologie Jul. 1983 219 p In GERMAN; ENGLISH summary Sponsored by Bundesministerium fuer Forschung und Technologie
(BMFT-FB-W-83-009; ISSN-0170-1339) Avail: NTIS HC A10/MF A01; Fachinformationszentrum, Karlsruhe, West Germany DM 38,50

A test satellite reusing the platform of the European Communication Satellite (ECS) with a 20/30 GHz communications payload is proposed. A satellite concept was elaborated and the technical problems were identified. The repeater comprises two transponders for the transmission experiment and two beacan transmitters for the coverage experiment. The antenna module is made up of one double-offset Cassegrain antenna (transmission) and two parabolic antennas (coverage). The satellite subsystem incorporates a priority select and interface unit (PSIU). A time schedule and a first cost estimate were established. The study shows that a test satellite launched by the Space Shuttle/payload assist module D (PAM-D) is feasible. Author (ESA)

N84-12356# European Space Agency, Paris (France).
L BAND SATELLITE COMMUNICATION EXPERIMENT IN THE ANTARTIC
Daniel T. Salzer Jul. 1983 32 p refs Transl. into ENGLISH of "L-Band-Satellitekommun.- Expt. in der Antarktis" rept. DFVLR-FB-82-24 DFVLR, Oberpfaffenhofen, West Germany, Aug. 1982 Original report in GERMAN
(ESA-TT-805; DFVLR-FB-82-24) Avail: NTIS HC A03/MF A01; original German version available from DFVLR, Cologne DM 16

Satellite communication with the Antarctic was studied, using a ground station and the L band beacon signal from Marisat (positioned over the Atlantic Ocean). The elevation angle to the satellite was 3 deg. The results show unexpectedly strong influences exerted by propagation medium effects, highly prejudicial to a satellite link with this Antarctic region. The daily and seasonal variations in the amplitude and frequency of the received signal indicate the ionosphere as a source of these phenomena.
Author (ESA)

N84-12357# European Space Agency, Paris (France).
PULSE SIGNALS IN HETERODYNE AND HOMODYNE DETECTION
Friedrich Malota Jul. 1983 26 p refs Transl. into ENGLISH of "Impulssignale beim Heterodyn- u. Homodynempfung" rept. DFVLR-Mitt-82-13 DFVLR, Oberpfaffenhofen, West Germany, Aug. 1982 Original report in GERMAN
(ESA-TT-809; DFVLR-Mitt-82-13) Avail: NTIS HC A03/MF A01; original German version available from DFVLR, Cologne DM 13,40

The signal levels which result in a detector when transmitted pulses are superimposed with the CW wave form of a local oscillator are calculated for a heterodyne detector. Modulating CW transmitter, CW-LO; pulse transmitter, CW-LO; and pulse transmitter, pulse CW combinations are dealt with for heterodyne and homodyne detectors. Results are in the form of heterodyne and homodyne currents, whose magnitude was validated experimentally.
Author (ESA)

N84-12358# Istituto di Ricerca e Tecnologia per lo Studio del Plasma Nello Spazio, Frascati (Italy).
RADIO SCINTILLATIONS AT LARGE ELONGATION ANGLES: CONTRIBUTIONS OF WAVES VERSUS DISCONTINUITIES
L. less (Pavia Univ.), M. Dobrowolny, and B. Bertotti (Pavia Univ.) Mar. 1982 41 p refs
(IFSI-82-4) Avail: NTIS HC A03/MF A01

Formulas for the phase fluctuation of an electromagnetic wave moving though a random time dependent medium, which generalize existing theory by including retardation effects due to the finite time of propagation of radio signals are presented. Formulas to compute the phase correlation in a complete round trip Doppler link between Earth and a spacecraft are given. Formulas for statistics of phase fluctuations are separately applied to the case of discontinuities and two MHD waves, with reasonable assumption on their wavelength spectra. Numerical results are shown, and the role of waves versus discontinuities in the correlation spectrum of phase fluctuation is discussed as a function of elongation angle and of frequency. Author (ESA)

N84-12359# Istituto di Ricerca e Tecnologia per lo Studio del Plasma Nello Spazio, Frascati (Italy).
ANALYSIS OF SOME FILTERING AND DATA ANALYSIS METHODS FOR GRAVITATIONAL WAVE ANTENNAS WITH RESONANT TRANSDUCERS
G. V. Pallottino Sep. 1982 34 p refs
(IFSI-82-11) Avail: NTIS HC A03/MF A01

The signal, noise, and noise temperature of phase sensitive detectors (PSD's) driven at the initial bar resonance frequency (omega R); PSD's driven at omega R cascaded with PSD's driven

at the beat frequency (omega b); and PSD's driven at the resonance frequency of the two modes arising from the interaction of the bar and the transducer are derived. Going from the single oscillator to the double oscillator the signal power is reduced by a factor of two, as the brownian and back reaction noise, and the wideband noise is increased by a factor of two, because of the doubling of the bandwidth. This gives a factor of four for the product wideband-narrowband noise. Author (ESA)

N84-12360# Istituto di Ricerca e Tecnologia per lo Studio del Plasma Nello Spazio, Frascati (Italy).
DATA ANALYSIS FOR GRAVITATIONAL WAVE ANTENNA WITH RESONANT TRANSDUCERS
G. V. Pallottino and G. Pizzella (Rome Univ.) Oct. 1982 15 p refs
(IFSI-82-12) Avail: NTIS HC A02/MF A01

It is shown that data analysis procedures for antennas with nonresonant transducers can be applied to a single mode of gravitational wave antennas (GWA) with resonant transducers. The signal to noise ratio is reduced by a factor of two, since by selecting only one Fourier component of the resonant transducer signal one half of the signal power is discarded. The factor of two can be recovered by using a second electronic line which selects the other Fourier component and then by combining together the four output quantities, i.e., the in phase and the in quadrature components. With this method, GWA's could be used to detect supernovae in the Virgo cluster. Author (ESA)

N84-12361# Istituto di Ricerca e Tecnologia per lo Studio del Plasma Nello Spazio, Frascati (Italy).
GUIDANCE OF ELECTROMAGNETIC WAVES IN THE IONOSPHERE AND MAGNETOSPHERE
M. Dobrowolny Dec. 1982 175 p refs
(IFSI-82-15) Avail: NTIS HC A08/MF A01

Classical theory of guiding of electromagnetic waves along magnetic field lines is introduced for waves at frequencies below the electron cyclotron frequency (essentially to whistlers and low frequency hydromagnetic waves). Dielectric tensor and wave branches of a cold magnetoplasma; VLF and ELF waves; energy propagation of waves in anisotropic dispersive media; energy propagation of ELF-VLF waves in a homogeneous magnetoplasma; ray tracing; mode theory of guided wave theory; Bookers mode theory of electromagnetic wave guidance in the magnetosphere; and guidance of whistlers are treated. Author (ESA)

N84-12362# Istituto di Ricerca e Tecnologia per lo Studio del Plasma Nello Spazio, Frascati (Italy).
CORRELATION BETWEEN TWO SPACECRAFT IN THE DOPPLER DETECTION OF A GRAVITATIONAL BACKGROUND RADIATION
B. Bertotti (Pavia Univ., Italy) and L. Iess Jun. 1983 21 p ref
(IFSI-83-7) Avail: NTIS HC A02/MF A01

The cross spectrum of Doppler signals from two spacecraft due to an isotropic background of gravitational radiation, characterized by the energy density spectrum is calculated. The calculation confirms that the filter function has three characteristic scales of frequency variations, one of which appears only as a periodic modulation factor of modulus one. Data from two spacecraft provide four different functions of frequency to be discriminated against noise: the spectra of the two spacecraft and the real and imaginary part of the cross correlation spectrum. Thus in the case of a constant energy spectral density of the gravitational wave background, the signatures of the observables are much richer and more easily recognizable. Author (ESA)

N84-12363# Deutsche Forschungs- und Versuchsanstalt fuer Luft- und Raumfahrt, Oberpfaffenhofen (West Germany). Abt. Nachrichtentheorie.
THE SIMULATION OF A FREQUENCY SHIFT KEYING (FSK) DIVERSITY SYSTEM
Jinrong Sun Jan. 1983 18 p refs
(DFVLR-FB-83-22) Avail: NTIS HC A02/MF A01; DFVLR, Cologne DM 9

A simulation of FSK with diversity, which shows that threshold decoding for the convolutional code with interleaving improves the communication quality of FSK with diversity over the Rayleigh fading channel is presented. The improvement is 6 dB at a bit error rate of 0.01 and 10 dB at 0.001 with diversity degree = 5. The modulating frequencies should be orthogonal of each other, the signals and noise in the branches independent. Author (ESA)

N84-12364# Institute for Telecommunication Sciences, Boulder, Colo.
OPTIMUM RECEPTION IN NON-GAUSSIAN ELECTROMAGNETIC INTERFERENCE ENVIRONMENTS. PART 2: OPTIMUM AND SUBOPTIMUM THRESHOLD SIGNAL DETECTION IN CLASS A AND B NOISE
David Middleton and A. D. Spaulding May 1983 348 p refs
(PB83-241141; NTIA/Rept-83-120) Avail: NTIS HC A15/MF A01 CSCL 09D

The general theory of optimum and suboptimum detection of threshold (i.e., weak) signals in highly nongaussian interference environments is developed. Both signal processing algorithms and performance measures are obtained canonicaly, and specifically for both narrowband and broadband interference environments. Suboptimum systems are also treated and a number of numerical examples are included which illustrate the determination of performance and performance comparisons. An extensive set of appendices contains many of the analytic details developed and presented here as well as the required computational algorithms. GRA

N84-12365# Institute for Telecommunication Sciences, Boulder, Colo.
ALTERNATIVE TRANSMISSION MEDIA FOR THIRD-GENERATION INTERFACE STANDARDS
J. A. Hull, A. G. Hanson, and L. R. Bloom May 1983 89 p refs
(PB83-238345; NTIA/Rept-83-121) Avail: NTIS HC A05/MF A01 CSCL 17B

A review of EIA and CCITT data interface standards identifies three generations, namely: first (1960's), second (1970's), and third (1980's and beyond). The User/Network physical interface for the pending Integrated Services Digital Network is an example of third generation standards. Wideband channel requirements under discussion by the CCITT will be limited by transmission media in the implementation of future interchange circuits. Conventional wire pairs and coaxial cables used in such interchange circuits are limited in the transmission rate and distance combinations by pulse distortion. Author (GRA)

N84-12366# National Telecommunications and Information Administration, Washington, D.C.
INTERNATIONAL TELECOMMUNICATION STANDARDS: ISSUES AND IMPLICATIONS FOR THE '80'S Summary Report
D. M. Cerni and E. M. Gray May 1983 200 p refs Workshop held in Boulder, Colo., 21-22 Jul. 1982
(PB83-241471; NTIA-SP-83-15) Avail: NTIS HC A09/MF A01 CSCL 17B

International telecommunication standards and their effects on the U.S. telecommunication industry were considered at a 2-day workshop entitled International Standards--Issues and Implications for the '80's. Papers presented at the conference are summarized. The speakers addressed the importance of standards, the international organizations responsible for their development (including U.S. participation in that process), and the standards-building process itself. Two major efforts in international standards development--the Integrated Services Digital Network and the Open Systems Interconnection Reference Model are discussed. The status of other standards work, including videotex and Signalling System No. 7, is also reviewed. GRA

N84-12367# Advisory Group for Aerospace Research and Development, Neuilly-Sur-Seine (France).
THE PERFORMANCE OF ANTENNAS IN THEIR OPERATIONAL ENVIRONMENT
Loughton, England Sep. 1983 243 p refs Lecture ser. held in

Ankara, Turkey, 19-20 Oct. 1983, in Athens, 24-25 Oct. 1983, and in Brussels, 27-28 Oct. 1983
(AGARD-LS-131; ISBN-92-835-1461-0) Avail: NTIS HC A11/MF A01

Antennas provide gain in any direction, and the effect of the operational environment on this parameter is fundamentally important for the performance of radio systems. Yet the effect of the environment on antennas is often overlooked. The design of the antenna is often specified in terms of its operation over a perfectly conducting flat ground plane, which if the antenna is to be used on three dimensional bodies or in a complex environment, has little to recommend it except cost. The Lecture Series will cover: techniques for measurement/prediction of antenna performance (experimental modeling and in situ measurements); performance of fixed and transportable antennas (terrain effects, masts, building effects, re-radiation by supporting towers); performance of mobile antennas (effects of supporting platforms such as automobiles, ships, aircraft); non-linear scatterers; and performance of antennas in plasmas. For individual titles, see N84-12368 through N84-12377.

N84-12368# Communications Research Centre, Ottawa (Ontario).
SCALE MODELLING AND FULL SCALE MEASUREMENT TECHNIQUES WITH PARTICULAR REFERENCE TO ANTENNAS IN THEIR OPERATIONAL ENVIRONMENTS
John S. Belrose *In* AGARD The Performance of Antennas in their Operational Environ. Sep. 1983 25 p refs (For primary document see N84-12367 03-32)
Copyright. Avail: NTIS HC A11/MF A01

Recent advances in antenna design and the need for more accurate prediction of performance of antennas in their operational environment has increased the need for improved electrical measurements, and there was a significant accompanying development in antenna metrology. Some of these developments, those relevant to the theme of these lectures, are reviewed here. Author

N84-12369# Communications Satellite Corp., Clarksburg, Md.
CALCULATION OF GROUND WAVE ATTENUATION OVER IRREGULAR, INHOMOGENEOUS, LAYERED MEDIA USING PROGRAM WAGNER
R. H. Ott *In* AGARD The Performance of Antennas in their Operational Environ. Sep. 1983 17 p refs (For primary document see N84-12367 03-32)
Copyright. Avail: NTIS HC A11/MF A01

A method for calculating the ground wave field over irregular, inhomogeneous terrain was developed, and comparisons with alternative analytical methods were made for idealized terrain profiles such as concave parabolas, sea-land-sea paths, and single Gaussian ridges. This method employs a numerically efficient algorithm, PROGRAM WAGNER, based on an integral equation. PROGRAM WAGNER appears the only method general enough for calculating ground wave attenuation along detailed paths. The fundamentals of PROGRAM WAGNER to the user seeking to make path loss calculations are explained. A users guide, the complete FORTRAN IV program listing, and sample input and output are included. Comparisons of computed field strengths are presented, with measured values over a path in the Netherlands at 10 frequencies from 2 to 30 MHz. Also, PROGRAM WAGNER at 5 and 30 MHz is compared with a method based on scattering from multiple knife edges. Finally, reciprocity is shown to provide necessary and useful criteria for spacing the observation points along the terrain profile. Author

N84-12370# California Univ., Livermore. Lawrence Livermore Lab.
PHYSICAL MODELING OF EM PROPAGATION OVER NONHOMOGENEOUS TERRAIN
R. J. King *In* AGARD The Performance of Antennas in their Operational Environ. Sep. 1983 19 p refs (For primary document see N84-12367 03-32)
(Contract W-7405-eng-48)
Copyright. Avail: NTIS HC A11/MF A01

To obtain experimental data for comparison with the theoretical results obtained from mathematical groundwave propagation models, it is often expedient to conduct experiments on laboratory models using microwaves. Besides the obvious convenience and reduced cost, practical difficulties encountered in full scale experiments are avoided (e.g., weather and other uncontrolled parameters such as path nonhomogeneities, earth curvature, buildings, right-of-ways, etc.). There is no need to use exact similitude scaling; the media and geometries are generally chosen to test the limits of the theory's validity. The design of several much models in the frequency range of 405 GHz is discussed, and the experimental results are compared with the corresponding theory. Specific examples are propagation over planar and curved surfaces (including stratified media, e.g., layered earth, sea ice, etc.), mixed paths (including media having abrupt discontinuities such as land-sea boundaries, gradual nonuniformities such as sloping beaches, off-path such as land-sea boundaries, gradual nonuniformities such as sloping beaches, off-path discontinuities such as islands, lakes and peninsulas), uniaxially anisotropic media, and media having an index of refraction near unity such as heavy vegetation. Author

N84-12371# Bundeswehr Munich Univ., Neubiberg (West Germany).
INTERACTION OF ANTENNAS WITH MASTS UNDER SPECIAL CONSIDERATION OF THE SENSITIVITY AND NONLINEAR EFFECTS IN SHIP BORNE RECEIVING SYSTEMS
H. K. Lindenmeier *In* AGARD The Performance of Antennas in their Operational Environ. Sep. 1983 17 p refs (For primary document see N84-12367 03-32)
Copyright. Avail: NTIS HC A11/MF A01

The minimum height of active and passive rod antennas is presented as a function of the environmental noise. A high linearity of the system is necessary to suppress intermodulation and crossmodulation effects generated by high level signals radiation from the transmitters on the ship. In many cases this problem only is solved by selective means at the front end of a receiving system. An appropriate solution is found in a fast tunable active receiving antenna. The effective height, the antenna impedance and the vertical pattern of an antenna mounted on top of a mast are influenced in an undesired way. The available dynamic of the receiving system is reduced considerably by the interaction of the mast and the antenna. Due to the resonant effects of the mast-antenna structure this reduction factor is frequency dependent and increases with increasing height of the mast. In addition there is a severe disturbing influence of the mast on the vertical diagrams of the rod antenna on this mast. Passive broadband rod antennas should not be mounted on a mast at all. With an active antenna however the effect of the mast on the antenna properties are reduced. In contrary to rod antennas loop antennas are advantageously decoupled from the mast by symmetrical mounting on top of a rotationally symmetrical mast. Author

N84-12372# Royal Aircraft Establishment, Farnborough (England). Radio and Navigation Dept.
INFLUENCE OF THE AIRFRAME ON THE PERFORMANCE OF ANTENNAS FOR AVIONICS
M. J. Sidford *In* AGARD The Performance of Antennas in their Operational Environ. Sep. 1983 15 p refs (For primary document see N84-12367 03-32)
Copyright. Avail: NTIS HC A11/MF A01

The performance of antennas mounted on airframes is an important factor in the design of airborne radio systems, and is considered at an early stage in the study and definition of the system requirements for any particular aircraft and associated operational scenario. This is becoming critical as the number of systems and their complexity increases, and as the number of associated antennas required is further multiplied in the application of such techniques as adaptive array signal processing. The infuences of the airframe environment on antenna properties such as radiation pattern, gain, impedance, polarization and coupling, and means of quantifying such influences are discussed. Related electromagnetic structure-dependent effects due to non-linear junctions, and the use of carbon fiber composite materials are

also considered. The limitations of system performance resulting from airframe-antenna interaction are difficult to quantify, since detailed knowledge of particular system parameters, associated hardware, and operational scenarios is required. Author

N84-12373# California Univ., Livermore. Lawrence Livermore Lab. Electronics Engineering Dept.
NUMERICAL MODELING TECHNIQUES FOR ANTENNAS
E. K. Miller *In* AGARD The Performance of Antennas in their Operational Environ. Sep. 1983 29 p refs (For primary document see N84-12367 03-32)
(Contract W-7405-eng-48)
Copyright. Avail: NTIS HC A11/MF A01

An overview of wire-antenna computer modeling is given for infinite media and half-space type problems. The formulation and numerical solution methods are summarized, and applications are demonstrated with numerous examples. Author

N84-12374# California Univ., Livermore. Lawrence Livermore Lab.
NUMERICAL MODELING TECHNIQUES FOR HALF-SPACE (GROUND) PROBLEMS
E. K. Miller, G. J. Burke, R. J. King, and N. C. Mathur (Illinois Univ., Chicago) *In* AGARD The Performance of Antennas in their Operational Environ. Sep. 1983 33 p refs (For primary document see N84-12367 03-32)
(Contract W-7405-eng-48)
Avail: NTIS HC A11/MF A01

In the frequency range below a few hundred MHz, the earth-air interface significantly affected are: the object's current distribution and input impedance (if an antenna); and the near and far fields that it produces. The problem of modeling both the object-ground near-field interaction and the ground screens used to reduce or control this interaction is discussed here. The basic model (Part 1) employed for the object-ground interaction uses a thin wire approximation to the electric-field integral equation in which the kernel includes the interface effect via the usual Sommerfeld integrals. Both the reflected and transmitted fields are accounted for so that objects on both sides of the interface, or even penetrating the interface, are modeled. Another approach (Part 2) to modeling a ground system uses the surface impedance Z (subs) to represent the boundary conditions at the interface. To permit applications to generic set of problems, Z (subs)(rho) is permitted to vary arbitrarily in the radial direction. A one dimensional integral equation is first used to solve for the tangential magnetic field on the interface. This field is then used in a two dimensional integral to find the radiation patterns for arrays of vertical dipoles over ground screens. Author

N84-12375# Concordia Univ., Loyola Campus, Montreal (Quebec). Dept. of Electrical Engineering.
NUMERICAL MODELLING METHODS FOR PREDICTING ANTENNA PERFORMANCE ON AIRCRAFT
Stanley J. Kubina *In* AGARD The Performance of Antennas in their Operational Environ. Sep. 1983 38 p refs (For primary document see N84-12367 03-32)
Copyright. Avail: NTIS HC A11/MF A01

Typical case studies that involve the application of Moment Methods to the prediction of the radiation characteristics of antennas in the HF frequency band are examined. The examples consist of the analysis of a shorted transmission line HF antenna on a CHSS-2/Sea King helicopter, wire antennas on the CP-140/Aurora patrol aircraft and a long dipole antenna on the Space Shuttle Orbiter spacecraft. In each of these cases the guidelines for antenna modeling by the use of the program called the Numerical Electromagnetic Code are progressively applied and results are compared to measurements made by the use of scale-model techniques. In complex examples of this type comparisons based on individual radiation patterns are insufficient for the validation of computer models. A volumetric method of radiation pattern comparison is used based on criteria that result from pattern integration and that are related to communication system performance. This is supplemented by hidden-surface displays of an entire set of conical radiation patterns resulting from measurements and computations. Antenna coupling considerations are discussed for the case of the dual HF installation on the CP-140/Aurora aircraft. Author

N84-12376# Los Alamos Scientific Lab., N. Mex.
EFFECTS OF NONLINEAR LOADS ON ANTENNAS AND SCATTERERS
J. A. Landt *In* AGARD The Performance of Antennas in their Operational Environ. Sep. 1983 22 p refs (For primary document see N84-12367 03-32)
Copyright. Avail: NTIS HC A11/MF A01

Nonlinear loads on antennas are used to advantage or degrade the performance of a communications system. Nonlinear elements are routinely used to protect sensitive receivers from high-power signals including high-power microwaves and EMP (electromagnetic pulse). Time-varying loading of antennas are used to modulate the radar backscatter cross section to produce sidebands at the modulation frequency. Nonlinear elements are used to detect the electromagnetic energy incident on an antenna, and thus used as a measurement technique. Nonlinear loads are also used for pulse shaping of the fields radiated by pulse-excited antennas. Active loads are used to increase the performance of electrically small antennas and closely coupled arrays. Alternatively, undesired semiconducting junctions on structures near antennas produce intermodulation products that seriously degrade performance (this is often called the "rusty-bolt" effect). The techniques available for analyzing these effects are reviewed and representative examples given. A time-stepping procedure is treated in detail. Author

N84-12377# Toronto Univ. (Ontario). Dept. of Electrical Engineering.
PERFORMANCE OF ANTENNAS IN PLASMA
K. G. Balmain *In* AGARD The Performance of Antennas in their Operational Environ. Sep. 1983 19 p refs (For primary document see N84-12367 03-32)
Copyright. Avail: NTIS HC A11/MF A01

The Waves in Space Plasmas (WISP) facility is expected to be flown on the Space Shuttle in 1987. The payload will include Spacelab, a 300 m tip-to-tip dipole antenna for wave launching and reception, and a small subsatellite for remote signal reception and plasma diagnostics. The objectives are to study wave injection and propagation in the ionospheric plasma, and to use these phenomena to probe the structure and morphology of the ionosphere. To achieve these objectives, it is essential to understand how much the properties of a long dipole antenna are affected by the surrounding anisotropic plasma medium. The WISP project with emphasis on antenna-related aspected is summarized, and the state of the art on the subject of antennas in plasmas is reviewed. Author

N84-12045*# Ohio Univ., Athens. Avionics Engineering Center.
WEATHER DATA COMMUNICATION AND UTILIZATION
Richard H. McFarland, James D. Nickum, and Daryl L. McCall *In* NASA. Langley Research Center Controls, Displays and Inform. Transfer for Gen. Aviation IFR Operations Oct. 1983 p 201-210 refs (For primary document see N84-12029 03-01)
Avail: NTIS HC A12/MF A01 CSCL 17B

N84-12046*# BioTechnology, Inc., Falls Church, Va.
A FLIGHT INVESTIGATION OF SIMULATED DATA LINK COMMUNICATIONS DURING SINGLE-PILOT IFR FLIGHT
James F. Parker, Jack W. Duffy, and D. G. Christensen *In* NASA. Langley Research Center Controls, Displays and Inform. Transfer for Gen. Aviation IFR Operations Oct. 1983 p 211-224 (For primary document see N84-12029 03-01)
Avail: NTIS HC A12/MF A01 CSCL 17B

N84-12575*# Kansas Univ. Center for Research, Inc., Lawrence. Telecommunications and Information Sciences Lab.
THE INFLUENCE OF SENSOR AND FLIGHT PARAMETERS ON TEXTURE IN RADAR IMAGES Final Report
V. S. Frost, K. S. Shanmugan, and J. C. Holtzman *In* Texas A and M Univ. Proc. of the NASA Symp. on Math. Pattern Recognition and Image Analysis 1983 p 577-608 refs Original contains imagery. Original photography may be purchased from the EROS Data Center, Sioux Falls, S.D. ERTS (For primary document see N84-12557 03-43)
Avail: NTIS HC A99/MF A01 CSCL 17I

33 ELECTRONICS AND ELECTRICAL ENGINEERING

Includes test equipment and maintainability; components, e.g., tunnel diodes and transistors; microminiaturization; and integrated circuitry.

For related information see also *60 Computer Operations and Hardware* and *76 Solid-State Physics.*

N84-12378 Royal Signals and Radar Establishment, Malvern (England).
NOISE REDUCTION AND SEGMENTATION OF IR IMAGES USING CO-MEDIAN FILTERS
S. M. Peeling Jun. 1983 24 p refs
(RSRE-3582; BR89250) Copyright. Avail: Issuing Activity

A method of separating targets from background in thermal images is described. The picture passes through a 2-dimensional 3 x 3 spatial median filter to reduce noise and then a 31 x 31 median filter to provide a background estimator. The outputs from these two are then compared and the result passed to a border following routine which finds the minimum and maximum coordinates of the target, which are then passed to a classifier. The system was successfully tested on infrared databases and on digitized photographs. It can be applied to conventional TV images where target sizes are smaller than background features, irrespective of gray level histogram. Author (ESA)

N84-12379 Royal Signals and Radar Establishment, Malvern (England).
DIELECTRIC LOSS MEASUREMENT AT MILLIMETRE WAVE FREQUENCIES USING AN UNTUNED CAVITY
D. J. Gunton Jun. 1983 10 p refs
(RSRE-3597; BR89248) Copyright. Avail: Issuing Activity

The theoretical basis of the untuned cavity method, especially for high permittivity samples, is outlined, and experimental hardware is described. The lid of the cavity opens to introduce a sample or to replace one of the solid sealing disks by one with a circular hole for calibration. The input signal is switched at 11 Hz with a pin diode in a waveguide, to serve as a reference for the two-channel lock-in voltameter which measures output signals from a power detector. An attenuator enables linearity checks to be performed. For very small changes in power at the output of the cavity, an offset facility on the lock-in together with a chart recorder to ease interpretation of the measured changes, enables values of r as low as 0.002 to be detected. These values occur for small volumes of very low loss materials, or when absorption by semiconductor surfaces is measured, if an estimate of reflection coefficient (and hence conductivity) is required. Author (ESA)

N84-12380# Air Force Systems Command, Wright-Patterson AFB, Ohio. Foreign Technology Div.
FROM LAUNCHING CARRIER ROCKETS TOWARDS THE PACIFIC ON THE ACCOMPLISHMENTS AND PROBLEMS OF ELECTRONIC TECHNOLOGIES IN OUR COUNTRY
Zeng-Pei Gu 12 Jul. 1983 12 p Transl. into ENGLISH from Dianzi Kexue Jishu (China), no. 11, 1981 p 43-44
(AD-A131088; FTD-ID(RS)T-0518-83) Avail: NTIS HC A02/MF A01 CSCL 17/2

From launching carrier rockets towards the Pacific on the accomplishments and problems of electronic technologies in our country. GRA

N84-12381# Air Force Systems Command, Wright-Patterson AFB, Ohio. Foreign Technology Div.
SCIENTIFIC-TECHNICAL CONFERENCE ON ACYCLIC ELECTRIC MACHINES
B. L. Aliyevskiy 12 Aug. 1983 10 p Transl. into ENGLISH from Izv. Vyssh. Ucheb. Zaved. Elektromekhan. (USSR), no. 7, Jul. 1969 p 802-804
(AD-A131880; FTD-ID(RS)T-0721-83) Avail: NTIS HC A02/MF A01 CSCL 10/2

The theory and design of acyclic electric machines, movable electric contacts, and electromagnetic fields in acyclic machines are discussed. Homopolar generators, superconducting magnets, and magnetohydrodynamics are some of the topics discussed. R.J.F.

N84-12382# Air Force Systems Command, Wright-Patterson AFB, Ohio. Foreign Technology Div.
SYNCHRONOUS GENERATORS WITH SUPERCONDUCTIVE EXCITATION WINDINGS
Wladyslaw Paszek and Adam Rozycki 27 Jul. 1983 26 p Transl. into ENGLISH from Gospodarka Paliwami i Energia (Poland), v. 24, no. 4(263), 1976 p 12-17
(AD-A131832; FTD-ID(RS)T-1087-83) Avail: NTIS HC A03/MF A01 CSCL 20/3

Possibilities for taking advantage of superconductivity in the design of synchronous generator windings are presented. Parameters of designed and built experimental models are listed. The concept of the structure of a synchronous generator with a superconductive excitation winding is discussed and specific characteristics of its design are presented. It is shown that an increase in magnetic induction and elimination of the ferromagnetic from the magnetic circuit alloys one to reduce the dimensions, weight, and cost of the machine. E.A.K.

N84-12383# Air Force Systems Command, Wright-Patterson AFB, Ohio. Foreign Technology Div.
UNIPOLAR MACHINE WITH SUPERCONDUCTIVE EXCITATION WINDING
Wladyslaw Paszek, Adam Rozycki, and Zbigniew Pawelec 26 Jul. 1983 19 p Transl. into ENGLISH from Gospodarka Paliwami i Energia (Poland), v. 23, no. 2(249), 1975 p 22-26
(AD-A131820; FTD-ID(RS)T-1086-83) Avail: NTIS HC A02/MF A01 CSCL 09/3

The problem of building unipolar machines with superconductive excitation winding is presented. Methods for increasing the unit power and unit voltage of these machines by increasing the induction of the excitation field are discussed. A survey of structural designs in which an increase in the rated voltage of unipolar machines was obtained is presented. E.A.K.

N84-12384# Los Alamos Scientific Lab., N. Mex.
MEGAVOLT PULSE TRANSFORMER POWERED BY A FAST PLATE GENERATOR
D. J. Erickson, R. S. Caird, C. M. Fowler, B. L. Freeman, W. B. Garn, and J. H. Goforth 1983 24 p refs Presented at 3rd Intern. Conf. on Magagauss Magnetic Field Generation and Related Topics, Novosibirsk, USSR, 13 Jun. 1983
(Contract W-7405-eng-36)
(DE83-014189; LA-UR-83-1671; CONF-830606-12) Avail: NTIS HC A02/MF A01

A compact air-core resistive impedances > 20 (DAMEDA) when powered by fast explosive plate generators. The step-up transformer features many of the techniques employed in the tape wound transformers. The primary windng of the transformer is a discrete, single-turn coil. The multiturn secondary coil is fabricated separately, encapsulted in a thin-walled container, and vacuum impregnated with dielectric grading fluid. Once assembled, the transformer is immersed in oil. This transformer has a 0.8 coupling coefficient. Transformers of this type are especially attractive for single shot applictions because of their simplicity and ease of construction. DOE

N84-12385# Sandia Labs., Albuquerque, N. Mex.
HIGH-AVERAGE-POWER REP RATE SYSTEMS
M. Buttram 1983 8 p refs Presented at IEEE Power Electron. Specialists Conf., Albuquerque, N. Mex., 6 Jun. 1983
(Contract DE-AC04-76DP-00789)
(DE83-013769; SAND-83-0228C; CONF-830621-23) Avail: NTIS HC A02/MF A01

Insulation, switching, voltage amplification, and beam generation, all of these aspects of pulsed power which offer new challenges as systems move from single pulses to repetitive operation are discussed. The status of each is reviewed. DOE

N84-12386# Brookhaven National Lab., Upton, N. Y. National Synchrotron Light Source.
A HIGH-PERFORMANCE DIGITAL TRIGGERING SYSTEM FOR PHASE-CONTROLLED RECTIFIERS
R. E. Olsen 1983 4 p refs Presented at the 1983 Particle Accelerator Conf., Santa Fe., N. Mex., 21-23 Mar. 1983
(Contract DE-AC02-76CH-00016)
(DE83-012217; BNL-32777; CONF-830311-148) Avail: NTIS HC A02/MF A01

A 12-pulse, phase control system whose digital signal processing techniques that essentially eliminates subharmonic ripple was constructed. The larger power supplies used to power accelerator magnets are most commonly polyphase rectifiers using phase control. While this method is capable of handling impressive amounts of power, it suffers from one serious disadvantage of subharmonic ripple. The stability of the stored beam depends on the regulation of the current in the bending magnets, subharmonic ripple, especially that of low frequency, and can have a detrimental effect. DOE

N84-12387# Argonne National Lab., Ill. Chemical Technology Div.
DIFFUSION MASS TRANSFER OF KOH THROUGH Ni/Zn BATTERY MEMBRANE SEPARATORS
David S. Poa, Glenn M. Cook, and N. P. Yao Jan. 1983 34 p refs
(Contract W-31-109-eng-38)
(DE83-014551; ANL/OEPM-83-4) Avail: NTIS HC A03/MF A01

Three elements that influence KOH electrolyte diffusion fluxes through nickel/zinc battery separators are discussed: (1) concentration gradient; (2) temperature dependence; and (3) ordering of multilayer membranes. The KOH diffusion fluxes through three different Ni/Zn battery separators (193 PUDO cellophane, Celgard 3401 and 3501, and Permion P-2291 40/30) increase linearly with an increasing KOH concentration gradient from 10 to 40 wt%. The flux approaches a constant value as the concentration gradient is further increased from 45 to 60 wt%. This increase in diffusion mass transfer resistance, in the 45 to 60 wt% KOH concentration range, was analyzed by the modified Wilson plots and found to be related to an increase in the phase boundary resistance. It is shown that the temperature dependences of the KOH diffusion fluxes through these three separators are not the same and they do not always explicitly follow liquid phase diffusion theory. In the case of two layer composite membrane separators, in which one layer bears fixed negative charges and the other layer is an ideal Fickian membrane the KOH diffusion flux is higher when the charge bearing layer faces the concentrated side of the diffusion cell. DOE

N84-12388# Los Alamos Scientific Lab., N. Mex.
PROGRESS IN DEVELOPING REPETITIVE PULSE SYSTEMS UTILIZING INDUCTIVE ENERGY STORAGE
E. M. Honig 1983 5 p refs Presented at the 4th IEEE Pulsed Power Conf., Albuquerque, N. Mex., 6-8 Jun. 1983
(Contract W-7405-eng-36)
(DE83-015167; LA-UR-83-1585; CONF-830621-33) Avail: NTIS HC A02/MF A01

High power, fast recovery vacuum switches were used in a new repetitive counterpulse and transfer circuit to deliver a 5 kHz pulse train with a peak power of 75 MW (at 8.6 kA) to a 1-(LAMBDA) load, resulting in the first demonstration of fully controlled, high power, high repetition rate operation of an inductive energy storage and transfer system with nondestructive switches. New circuits, analytical and experimental results, and feasibility of 100 kV repetitive pulse generation are discussed. A switching concept for railgun loads is presented. DOE

N84-12389# Argonne National Lab., Ill.
CHARGE CHARACTERISTICS OF Ni/Fe TRACTION CELLS
W. H. DeLuca, R. Biwer, A. F. Tummillo, and N. P. Yao 1983 6 p Presented at the 18th Intersoc. Energy Conversion Eng. Conf., Orlando, Fla., 21 Aug. 1983
(Contract W-31-109-eng-38)
(DE83-014205; CONF-830812-34) Avail: NTIS HC A02/MF A01

In a series of tests performed on 6-V Ni/Fe modules, a range of recharge levels and charge rates were examined for three charge methods. The results show that higher discharge capacities are achieved at higher recharge Ah levels, but at lower Ah and Wh cycling efficiencies. However, when the modules are continuously cycled at any recharge level, repeatable module performance is obtained. Consequently, the optimum combination of module discharge capacity and cycle efficiency can be obtained for any given application by proper selection of the recharge level. It was also observed that at a fixed recharge level, module charge acceptance is virtually independent of the charge method. The tested modules also exhibited a self-discharge loss in capacity that was directly related to the length of the open-circuit stand time after charging and module state-of-charge. This paper describes the test procedures used, presents the data, and discusses the results obtained. DOE

N84-12390# California Univ., Livermore. Lawrence Livermore Lab.
STRUCTURE AND VIBRATIONAL SPECTRA OF A MODEL OF a-Si:H WITH PERIODIC BOUNDARY CONDITIONS
K. Winer and F. Wooten (California Univ., Davis) 1983 6 p refs Presented at the 10th Intern. Conf. on Amorphous and Liquid Semiconductors, Tokyo, 22 Aug. 1983
(Contract W-7405-eng-48)
(DE83-015245; UCRL-89444; CONF-830895-1) Avail: NTIS HC A02/MF A01

A ball and stick model of a Si:H with periodic boundary conditions was constructed. A computer replica of the structure was relaxed and the density, radial distribution function and vibrational spectra calculated. DOE

N84-12391# Los Alamos Scientific Lab., N. Mex.
NOVEL OPTICAL PIN USING MICROBALLOONS
R. F. Benjamin 1983 3 p refs Presented at the 9th AIRAPT Conf., Albany, 24-29 Aug. 1983
(DE83-015222; LA-UR-83-2147; CONF-830763-8) Avail: NTIS HC A02/MF A01

The design, fabrication and application of an optical probe for detecting a shock front or moving surface are described. The probe is a gas-filled microballoon affixed to an optical fiber. The probe has significant technical and economic advantages over other methods. DOE

N84-12392# California Univ., Berkeley. Lawrence Berkeley Lab.
SELF-CORRECTION COIL: OPERATION MECHANISM OF SELF-CORRECTION COIL
Kenji Hosoyama (National Lab. for High Energy Phys.) Jun. 1983 43 p refs
(Contract DE-AC03-76SF-00098)
(DE83-016324; LBL-16304) Avail: NTIS HC A03/MF A01

The operation mechanism of self-correction coil is extended with a simple model. For the ideal self-correction coil case, The self-inductance L of the self-correction coil is calculated. This calculation method is extended to a non-ideal self-correction coil case. For measure of completeness of self-correction coil is measured by the ratio of induced magnetic field by the self-correction coil and error field. Examples are L, M and N calculated for two cases; one is a single block approximation of self-correction coil winding and the other is a two block approximation case. By

choosing the adequate angles of self-correction coil winding, one can get about 98% efficiency for single block approximation case and 99.8% for two block approximation case. DOE

N84-12393# Sandia Labs., Albuquerque, N. Mex.
POWER-LOADING EFFECTS IN GAS-DISCHARGE MODELS
L. C. Pitchford 1983 6 p refs Presented at the US-FRG Joint Seminar on Diffuse Discharges, Bad Honneff, West Germany, 15-18 Aug. 1983
(Contract DE-AC04-76DP-00789)
(DE83-016504; SAND-83-1769C; CONF-830810-2) Avail: NTIS HC A02/MF A01

The effect of the large discharge currents in the switch conduction stage on the transport and rate coefficients which appear in the rate equation for the electron density, the basic element in a discharge model was examined. It is indicated that for the current levels of interest there will be significant heating. The related changes due to enhanced populations in the high energy states of the gas molecules: modified rates for translational gas heating and for excitation, dissociation, and perhaps ioinization. It is concluded that the high energy tail of the electron energy distribution is affected. Rate coefficients are more sensitive to power loading of the gas than are the drift velocity, average electron energy, and diffusion rate. In terms of model predictions of switch performance, knowledge of the source function from the e-beam is important in calculations of switch current gain and for conductivities. These will be underestimated with the neglect of ionization produced by secondaries. The distribution function is modified at the high energies from its form characterized by E/N in the presence of the e-beam source. The subsequent changes in the rate coefficients due to the e-beam source and the excited state populations can affect the turn on time of the switch. DOE

N84-12394# Argonne National Lab., Ill.
SPALLATION AND 14-MeV NEUTRON IRRADIATION OF STABILIZED NbTI SUPERCONDUCTORS
P. Hahn (Atominstitute der Osterreichichen Univ., Vienna), B. S. Brown, H. W. Weber, and M. W. Guinan (California Univ., Lawrence Livermore Lab.) Aug. 1983 9 p refs Presented at the Cryog. Eng. Conf. and Intern. Cryog. Mater. Conf., Colorado Springs, 15-19 Aug. 1983 Sponsored in part by the Federal Ministry of Science and Research, Vienna
(Contract W-31-109-eng-38)
(DE83-017973; CONF-830841-13) Avail: NTIS HC A02/MF A01

The results on 5 K irradiation available are summarized as follows: (1) increases of j-sub c/ following neutron irradiation occur only in conductors which are far from the optimal metallurgical treatments, (2) The changes of j/sub c/ following neutron irradiation and a thermal cycle to room temperature are small and in most cases comparable to the results obtained after 77 K irradiation, (3) The data available so far indicate that the degradation of j/sub c/ at 8 T is larger by about 5 to 10% than the corresponding changes at 5 T at a neutron fluence of 1.3 x 10 22nd power m(+2) (E > 0.1 MeV), (4) The increase of Cu resistivity is significant even after a thermal cycle to room temperature and requires design changes for a stable magnet operation. DOE

N84-12395# Argonne National Lab., Ill. Chemical Technology Div.
COMPARATIVE RESPONSE OF LEAD-ACID AND NICKEL-IRON BATTERIES TO PULSED AND CONSTANT-CURRENT LOADS
W. H. DeLuca, A. F. Tummillo, T. L. Biwer, C. C. Christianson, F. Hornstra, and N. P. Yao 1983 10 p refs Presented at the Elec. Vehicle Council Symp. and EXPO '83, Dearborn, Mich., 4-6 Oct. 1983
(Contract W-31-109-eng-38)
(DE83-017939; CONF-831020-2) Avail: NTIS HC A02/MF A01

Improved lead acid and nickel iron batteries were developed for use in electric vehicles. The response of these batteries to given discharge conditions differs according to characteristics of each system. The discharge capacity of the lead acid system is reduced at increased discharge rates and its internal resistance is a function of both depth of discharge (DOD) and discharge rate. Open circuit stand times at DOD levels > 50% reduce the internal resistance of the lead acid system and provide a corresponding increase in its availability capacity. The discharge capacity and internal resistance of the nickel/iron system are virtually independent of both discharge rate and open circuit stand times during discharge. With pulsed current loads, the available energy and power output of both battery systems are always less than those obtained with equivalent constant current loads due to increased internal power losses. The nickel-iron system exhibits an internal inductance that is significantly greater than that for the lead acid system thereby causing potentially damaging voltage transients. The test procedures and system employed, test data, and methods for predicting battery response are described. DOE

N84-12396# Argonne National Lab., Ill.
SOLID-OXIDE FUEL-CELL PERFORMANCE
D. C. Fee, S. A. Zwick, and J. P. Ackerman 1983 10 p refs Presented at the 2nd Solid Oxide Fuel Cell Workshop, Upton, N.Y., 16 Aug. 1983
(Contract W-31-109-eng-38)
(DE83-017926; CONF-8308120-1) Avail: NTIS HC A02/MF A01

Two models were developed to describe the performance of solid oxide fuel cells: (1) a cell model which calculates cell performance for various conditions of temperature, current density, and gas composition, and (2) a systems model which performs detailed heat and mass balances around each component in a power plant. The cell model provides insight into the performance tradeoffs in cell design. Further, the cell model provides the basis for predicting fuel cell performance in a power plant environment as necessary for the systems code. Using these two tools, analysis of an atmospheric pressure, natural gas fueled, internally reforming power plant confirms the simplicity and increased efficiency of a solid oxide fuel cell system compared to existing plants. DOE

N84-12397# California Univ., Livermore. Lawrence Livermore Lab.
ADVANCED HIGH-FIELD COIL DESIGNS: 20 TESLA
R. W. Hoard, D. N. Cornish, R. M. Scanlan, J. P. Zbasnik, R. L. Leber, R. B. Hickman, and J. D. Lee 1983 11 p refs Presented at the Advan. in Cryogenic Eng., Cryogenic Eng. Conf., Colorado Springs, 15-19 Aug. 1983
(Contract W-7405-eng-48)
(DE83-017368; UCRL-88811; CONF-830841-11) Avail: NTIS HC A02/MF A01

The technology required for producing large high field coils has shown that, with some extensions to the technological base, feasible designs are achievable. The resulting magnets could well make a paramount contribution to the national mirror fusion endeavor. DOE

N84-12398# California Univ., Berkeley. Lawrence Berkeley Lab. Electronics Research and Development Group.
EVALUATION OF THE BEIJING INSTRUMENT FACTORY GDB-44F PHOTOMULTIPLIER
Eric Young and C. C. Lo (Beijing Comprehensive Instrument Factory) 15 Dec. 1982 21 p refs
(Contract DE-AC03-76SF-00098)
(DE84-000849; LBL-16248) Avail: NTIS HC A02/MF A01

Characteristics were measured for the GDB-44F 2 inch diameter photomultiplier. Some typical photomultiplier characteristics, such as gain, dark current, anode output current, transit and rise times as a function of voltage between anode and cathode, and photoelectron pulse height spectrum, the quantum efficiency and the single electron transit time spread were measured. Descriptions of the measuring systems are given. DOE

N84-12399# Brookhaven National Lab., Upton, N. Y. Office of the National Synchrotron Light Source.
PROBLEM OF MAGNET RAMPING
Eva S. Bozoki 1983 5 p refs Presented at the EPS Conf. on Computing in Accelerator Design and Operation, Berlin, West Germany, 20-23 sep. 1983
(Contract DE-AC02-76CH-00016)

(DE83-014054; BNL-33651; CONF-8309144-2) Avail: NTIS HC A02/MF A01

The ramping function and its implementation in a microprocessor controlled function generator is discussed. In the accelerator rings, the momentum of the beam is changed. It is necessary to ramp all magnets in the ring in perfect synchronism and precisely according to a desired ramping function to prevent beam losses or unwanted changes in the beam characteristics. DOE

N84-12400# Sandia Labs., Albuquerque, N. Mex.
STRESS PRODUCTION AND RELIEF IN THE GOLD/SILICON EUTECTIC DIE-ATTACH PROCESS
T. D. Hund and S. N. Burchett 1983 14 p refs Presented at the Internatl. Soc. for Hybrid Microelectronics Conf., Philadelphia, 31 Oct. 1983
(Contract DE-AC04-76DP-00789)
(DE83-015230; SAND-83-0412C; CONF-8310108-1) Avail: NTIS HC A02/MF A01

Eutectic braze thickness and package cooling rate for stress relief in eutectically bonded die were evaluated. Two package types, a 30 pin leadless chip carrier and a 28 pin flat pack were used as models in finite element stress calculations to study these parameters on the maximum principal stress, maximum circumferential stress, and maximum shear stress. Bonding temperature, creep rate, silicon tensile strength, and the effects of surface defects on silicon tensile strength were studied to evaluate their effects on stresses in the die. It is indicated that with a thicker eutectic braze and a slower cooling rate, die can be eutectically attached without excessive stress. DOE

N84-12401# California Univ., Berkeley. Lawrence Berkeley Lab. Lighting Systems Research Dept.
COMPARISON OF TECHNOLOGIES FOR NEW ENERGY-EFFICIENT LAMPS
R. R. Verderber and F. R. Rubinstein Jun. 1983 6 p refs Presented at the IEEE/IAS Glass Industry Comm. Meeting, Mexico City, 3-7 Oct. 1983
(Contract DE-AC03-76SF-00098)
(DE83-015949; LBL-16225; CONF-831070-4) Avail: NTIS HC A02/MF A01

Energy efficient light bulbs are developed to replace the incandescent lamp where they can satisfy the design criteria and be used in sockets that have long hours of annual use. Four technologies are discussed which include: the compact fluorescent lamp, coated filament lamp, electrodeless fluorescent lamp, and compact high intensity discharge lamp. The systems demonstrate efficacy improvements of two to four times that of their incandescent counterparts. The new lamps required considerable advances in lamp technology. They offer the potential for achieving efficacies close to 80 lumens per watt. The new lamps will reduce the energy used annually by incandescent lamps (190 BkWh) by more than 50% in the 1990s, at which times they will be commonly employed. DOE

N84-12402# Sandia Labs., Albuquerque, N. Mex.
THE PERFORMANCE OF THE PERFLUOROCARBON LIQUID/PLASTIC-FILM CAPACITOR TECHNOLOGY IN PULSE-POWER SERVICE. A CURRENT STATUS REPORT
G. H. Mauldin, W. C. Nunnally (Los Alamos National Lab.), M. C. Thompson (Los Alamos National Lab.), and W. J. Sarjeant (State Univ. of New York, Buffalo) 1983 8 p refs Presented at the Conf. on Elec. Insulation and Dielec. Phenomena, Buck Hill Falls, Pa., 16 Oct. 1983
(Contract DE-AC04-76DP-00789)
(DE83-014606; SAND-83-0260C; CONF-8310135-2) Avail: NTIS HC A02/MF A01

Data are presented from a program to evaluate the perfluorocarbon liquid/plastic film capacitor technology. It is indicated the lives of 10(7) cycles at 1 kHz for polysulfone performed without failure to 7x10(6) cycles at 4.7 kV/mil before the test was halted. It is concluded that this capacitor system permits at least an order of magnitude increase in energy density over current systems in repetitive discharge service, particularly for long life at high reliability. DOE

N84-12403# Exxon Research and Engineering Co., Linden, N.J.
MICROPROCESSOR-BASED CONTROL SYSTEM FOR FLOWING-ELECTROLYTE ZINC-BROMINE BATTERY SYSTEMS
P. A. Malachesky, L. S. Chang, C. E. Elspass, and R. J. Bellows 1983 7 p Presented at the Electrochem. Soc. Fall Meeting, Washington, D.C., 9 Oct. 1983
(Contract DE-AC04-76DP-00789)
(DE83-012506; SAND-83-7091C; CONF-831086-1) Avail: NTIS HC A02/MMF A01

The zinc bromine battery system under development which is based on a bipolar, circulating electrolyte design concept is discussed. Such circulating electrolyte systems require a controller to operate and monitor system auxiliaries such as valves and pumps. A 1.2 kWh zinc bromine battery system controller was constructed using a single board computer. The design and operation of this controller are discussed. DOE

N84-12404# Johnson Controls, Inc., Milwaukee, Wis.
EFFECT OF ANTIMONY ON LEAD-ACID BATTERY NEGATIVE ELECTRODE
B. Mahato, J. Strebe, D. Wilkinson, and K. Bullock 1983 27 p refs Presented at the Electrochem. Soc. Fall Meeting, Washington, D.C., 9 Oct. 1983
(Contract W-31-109-eng-38)
(DE83-014680; CONF-831086-5) Avail: NTIS HC A03/MF A01

The lead electrode charge efficiency was related to antimony concentration to analyze. The effect of the interaction of antimony and lignin-expander on the head-electrode behavior was analyzed and the critical lead-electrode potential necessary to purge antimony was determined. Pasted type and small Plante' type lead-electrodes were prepared and tested to determine the effect of antimony by cathodic linear potential sweep charging. Antimony and/or lignin-expander were included either in electrolyte or in paste matrix. Results showed a significant contribution of antimony in decreasing charge efficiency and an overwhelming role of expander in suppressing the effect of antimony on charge efficiency. The critical lead-electrode potential for purging antimony from the electrode is close to -1.275 V (vs. Hq/Hq2/SO4). DOE

N84-12405# National Bureau of Standards, Washington, D.C. National Engineering Lab.
CENTER FOR ELECTRONICS AND ELECTRICAL ENGINEERING TECHNICAL PROGRESS BULLETIN COVERING SIGNALS AND SYSTEMS PROGRAM, APRIL 1982 - SEPTEMBER 1982
J. Franklin Mayo-Wells May 1983 20 p
(PB83-241158; NBSIR-83-2719-2) Avail: NTIS HC A02/MF A01 CSCL 09C

This is the second issue of an abstract bulletin to be issued quarterly by the Center for Electronics and Electrical Engineering, National Bureau of Standards. The issue covers the work of the Center's Signals and Systems Program for the second half of Federal fiscal year 1982. Abstracts are provided by technical area for both published papers and papers approved by NBS for publication. GRA

N84-12568*# Jet Propulsion Lab., California Inst. of Tech., Pasadena.
SAR SPECKLE NOISE REDUCTION USING WIENER FILTER Final Report
Tae H. Joo and Daniel N. Held *In* Texas A and M Univ. Proc. of the NASA Symp. on Math. Pattern Recognition and Image Analysis 1983 p 295-310 refs Original contains imagery. Original photography may be purchased from the EROS Data Center, Sioux Falls, S.D. 57198 ERTS (For primary document see N84-12557 03-43)
Avail: NTIS HC A99/MF A01 CSCL 09C

34 FLUID MECHANICS AND HEAT TRANSFER

Includes boundary layers; hydrodynamics; fluidics; mass transfer; and ablation cooling.

For related information see also *02 Aerodynamics* and *77 Thermodynamics and Statistical Physics.*

N84-12406* National Aeronautics and Space Administration. Marshall Space Flight Center, Huntsville, Ala.
CONSTANT-OUTPUT ATOMIZER Patent
Jack Y. Dea, inventor (to NASA) (Nevada Univ. System, Reno) Issued 8 Nov. 1983 4 p Filed 2 Oct. 1981 Supersedes N82-10360 (20 - 01, p 0053) Sponsored by NASA
(NASA-Case-MFS-25631-1; US-Patent-4,413,784; US-Patent-Appl-SN-308203; US-Patent-Class-239-426) Avail: US Patent and Trademark Office CSCL 20D

A constant-output atomizer includes a body which has a generally frustoconical expansion nozzle for producing an air jet when a supply of pressurized air is connected to the nozzle upstream of the throat of the nozzle. A liquid feed line supplies liquid to be atomized by the air jet, and the body includes a groove which opens into the diffuser section of the nozzle downstream of the throat for conducting liquid from the feed line to the nozzle. The groove which extends in a direction perpendicular to the axis of the nozzle, and radially with respect to it, has a depth approximately equal to half the axial length of the nozzle. Liquid, conducted by capillary action in the groove to the nozzle, is atomized into a fine mist by the air jet in the nozzle; and the groove eliminates fluctuations in spray order.

Official Gazette of the U.S. Patent and Trademark Office

N84-12407# Polish Academy of Sciences, Warsaw. Dept. of Fluid Dynamics.
THE SHOCK WAVE STRUCTURE IN ONE-COMPONENT GAS AND IN BINARY GAS MIXTURE
Magdalena Bratos and Ryszard Herczynski 1983 82 p refs
(ISSN-0208-5658) Avail: Issuing Activity

The variational method of solving Boltzmann equations, showing the forms of functionals, trial functions (generalized Mott-Smith distribution functions) and Euler equations for a single-component gas as well as for a mixture of gases, is considered. The details concerning the calculations of collision integrals, especially the dynamics of molecular collision, are discussed. The numerical characteristics of shock wave structures are considered. Relaxation parameters are also considered. Numerical methods used in the calculations, in particular the methods of solving Euler equations, are dealt with. The results relating to the shock wave structures in a single-component gas and in a binary gas mixture are discussed. The relation between the dimensionless shock wave thickness and Mach number in front of the shock wave is considered. N.W.

N84-12408 Syracuse Univ., N. Y.
THERMAL STRESS ANALYSIS OF ANNULAR GLASS-TO-METAL SEALS UNDER THERMAL SHOCK Ph.D. Thesis
Klod Kokini 1982 234 p
Avail: Univ. Microfilms Order No. DA8310459

The effect of the thermal shock test on glass-to-metal seals is analyzed by evaluating the transient thermal stresses that develop in the glass as a result of large temperature gradients. A lower bound for the strength of the glass-to-metal interface is estimated using an experimental procedure. The thermal stress analysis is performed on a model which considers the lead, the glass seal, and the base as three concentric cylinders. The transient temperature distribution in the three components is calculated by solving the two dimensional axisymmetric heat conduction equation for the glass using a finite difference method. The temperature distribution in the glass varies in the radial and axial directions. The temperature distribution is input into the thermal stress model to evaluate the transient thermal stresses in the glass using a finite element method. Dissert. Abstr.

N84-12409 California Univ., Berkeley.
THEORETICAL AND EXPERIMENTAL INVESTIGATION OF TURBULENT PREMIXED FLAMES Ph.D. Thesis
Medhat T. F. Azzazy 1982 103 p
Avail: Univ. Microfilms Order No. DA8312748

A model is proposed to describe the propagation of a plane oblique flame into a turbulent flow of premixed reactants. The model incorporates a transport equation for the single or joint PDF's of passive scalers, in addition to the conservation equations of mass, momentum, energy and K.E. of turbulence. In the first phase of developing the model, the reaction mechanism was treated as a single step irreversible exothermic reaction. In this case, the PDF of the progress variable was parameterized and solved with the conservation equations. The second phase considered a two step reaction mechanism in an attempt to explore the role played by the radicals in the propagation of turbulent premixed flames. For both the two phases, the flame speed and angle are eigenvalues of the solution. Laser induced fluorescence spectroscopy (LIFS) was used to measure the PDF of OH concentration in a laboratory scale burner simulating the flame studied by the model. The premixed methane-air flame is stabilized on a rod flame holder downstream of a turbulence producing grid. The experimentally observed PDF's of the hydroxil radical concentration, and the statistical moments, used to describe and compare the PDF's and moments of the two reaction model. Dissert. Abstr.

N84-12410 Ruhr Univ., Bochum (West Germany). Inst. fuer Konstruktionstechnik.
CALCULATION OF UNSTEADY FLOW IN TUBES OF COMBUSTION ENGINES WITH SPECIAL REGARD TO MULTIPLE BRANCHING [BERECHNUNG INSTATIONAER STROEMUNGSVORGAENGE IN RONRLEITUNGEN AN VERBRENNUNGSMOTOREN UNTER BESONDERER BERUECKSICHTUGUNG DER MEHRFACHVERZWEIGUNG]
Karl Alfred Goerg 1982 191 p refs In GERMAN; ENGLISH summary
(Rept-82.8) Copyright. Avail: Issuing Activity

A theoretical basis for numerical analysis of unsteady flow in internal combustion engines is suggested. By a general study of an arbitrary throttle point as control volume, only two flow conditions-inlet flow and outlet flow-have to be computed. The throttle-point function is reduced to linking tube parts in a logical way. The convergence criteria of the solution methods used (Lax-Wendroff, Hartree, Predictor Corrector, and fixed point method) guarantee that the solutions are unequivocal. Limiting value studies lead to the formulation of an algorithm, which allows the computation of the throttle flow by multiple branching.

Author (ESA)

N84-12411*# Naval Research Lab., Washington, D. C. Lab. for Computational Physics.
NUMERICAL SIMULATIONS OF FUEL DROPLET FLOWS USING A LAGRANGIAN TRIANGULAR MESH Final Report
M. J. Fritts, D. E. Fyfe, and E. S. Oran Aug. 1983 56 p refs
(NASA-CR-168263; NAS 1.26:168263) Avail: NTIS HC A04/MF A01 CSCL 20D

The incompressible, Lagrangian, triangular grid code, SPLISH, was converted for the study of flows in and around fuel droplets. This involved developing, testing and incorporating algorithms for surface tension and viscosity. The major features of the Lagrangian method and the algorithms are described. Benchmarks of the algorithms are given. Several calculations are presented for kerosene droplets in air. Finally, extensions which make the code compressible and three dimensional are discussed. S.L.

N84-12412*# National Aeronautics and Space Administration. Langley Research Center, Hampton, Va.
ANALYTICAL PREDICTION OF AEROTHERMAL ENVIRONMENT IN A WING-ELEVON COVE
Kim S. Bey Nov. 1983 10 p refs Proposed for presentation at the 5th Symp. of Finite Elements in Flow Problems, Texas, 23-26 Jan. 1984

(NASA-TM-85711; NAS 1.15:85711) Avail: NTIS HC A02/MF A01 CSCL 20D

The fluid/thermal environment in the cove between the wing and elevon surfaces was a concern throughout the design and initial operational phases of the space shuttle. Experimenal and analytical investigations provided some understanding of the environmental in the wing-elevon cove. An incompressible finite element analysis of flow through straight parallel walls and curved parallel walls to determine the effects of cove geomtry on the fluid/thermal environment is described. Results from this analysis agree qualitatively with experimental data. The centerline gas temperatures and cold wall heating rates are virtually identical for the two cases indicating that the slight curvature has little effect on the overall thermal environment. Author

N84-12413*# Precision Devices Ltd., Huntsville, Ala.
LOW GRAVITY EXPERIMENT FOR STUDYING A ROTATING FLUID HAVING A FREE SURFACE Final Report
O. C. Holderer 29 Oct. 1983 33 p
(Contract NAS8-35481)
(NASA-CR-170923; NAS 1.26:170923; DCN-1-3-ES-26516) Avail: NTIS HC A03/MF A01 CSCL 20D

Electrical, mechanical, and operational aspects of a test cell assembly for studying rotating fluids with a free surface are described. Results of a stress analysis prepared to document the structural adequacy for safe use on the KC-135 aircraft are presented along with results of a single load proof test of the most critical load case. Engineering drawings are included. A.R.H.

N84-12414*# National Aeronautics and Space Administration. Ames Research Center, Moffett Field, Calif.
COMPUTATION OF TURBULENT FLOWS OVER BACKWARD-FACING STEP
N. N. Mansour (Stanford Univ., Calif.), J. Kim, and P. Moin Oct. 1983 20 p refs
(NASA-TM-85851; A-9508; NAS 1.15:85851) Avail: NTIS HC A02/MF A01 CSCL 20D

A numerical method for computing incompressible turbulent flows is presented. The method is tested by calculating laminar recirculating flows and is applied in conjunction with a modified Kappa-epsilon model to compute the flow over a backward-facing step. In the laminar regime, the computational results are in good agreement with the experimental data. The turbulent flow study shows that the reattachment length is underpredicted by the standard Kappa-epsilon model. The addition of a term to the standard model that accounts for the effects of rotation on turbulent flow improves the results in the recirculation region and increases the computed reattachment length. S.L.

N84-12415*# Clarkson Coll. of Technology, Potsdam, N.Y. Dept. of Mechanical and Industrial Engineering.
THE AGCE RELATED STUDIES OF BAROCLINIC FLOWS IN SPHERICAL GEOMETRY Final Report
J. M. Hyun Nov. 1983 12 p refs
(Contract NAS8-34750)
(NASA-CR-170934; NAS 1.26:170934) Avail: NTIS HC A02/MF A01 CSCL 20D

Steady state, axisymmetric motions of a Boussineaq fluid continued in rotating spherical anmulus are considered. The motions are driven by latitudinally varying temperature gradient at the shells. Linearized formulations for a narrow gap are derived and the flow field is divided into the Ekman layers and the geostrophic interior. The Ekman layer flows are consistent with the known results for cylindrical geometries. Within the framework of rather restrictive assumptions, the interior flows are solved by a series of associated Legendre polynomials. The solutions show qualitative features valid at midlatitudes. Author

N84-12416# Toronto Univ. (Ontario).
INITIAL DECAY OF FLOW PROPERTIES OF PLANAR, CYLINDRICAL AND SPHERICAL BLAST WAVES
H. S. I. Sadek and J. J. Gottlieb Oct. 1983 92 p refs
(UTIAS-TN-244; ISSN-0082-5263) Avail: NTIS HC A05/MF A01

Analytical expressions are presented for the initial decay of all major flow properties just behind planar, cylindrical, and spherical shock wave fronts whose trajectories are known as a function of either distance versus time or shock overpressure versus distance. These expressions give the time and/or distance derivatives of the flow properties not only along constant time and distance lines but also along positive and negative characteristic lines and a fluid-particle path. Conventional continuity, momentum and energy equations for the nonstationary motion of an inviscid, non-heat conducting, compressible gas are used in their derivation, along with the equation of state of a perfect gas. All analytical expressions are validated by comparing the results to those obtained indirectly from known self-similar solutions for planar, cylindrical and spherical shock-wave flows generated both by a sudden energy release and by a moving piston. Futhermore, time derivatives of pressure and flow velocity are compared to experimental data from trinitrotoluene (TNT), pentolite, ammonium nitrate-fuel oil (ANFO) and propane-oxygen explosions, and good agreement is obtained. M.G.

N84-12417# Harry Diamond Labs., Adelphi, Md.
TOPICALLY CLASSIFIED BIBLIOGRAPHY ON SHAPES OF FALLING DROPS, DROPS IN ELECTRIC FIELDS AND RELATED TOPICS
Clyde A. Morrison, Richard P. Leavitt, and Amanda F. Hansen Jun. 1983 57 p
(DA Proj. 1L1-61101-A-91A)
(AD-A131134; HDL-SR-83-8) Avail: NTIS HC A04/MF A01 CSCL 05/2

We report results of an extensive literature search on shapes of falling drops, drops in electric fields, and related topics. Numerous references to the literature from the late nineteenth century through the present are given. Author (GRA)

N84-12418# Stanford Univ., Calif. Dept. of Mathematics.
RISING BUBBLES Progress Report, 16 Mar. - 31 Dec. 1982
Joseph B. Keller Dec. 1982 17 p
(Grant AF-AFOSR-034-79; AF Proj. 2304)
(AD-A131572; AFOSR-83-0676TR) Avail: NTIS HC A02/MF A01 CSCL 05/2

This progress report lists publications supported by AFOSR through March 16, 1982 - December 31, 1982. GRA

N84-12419# Naval Surface Weapons Center, White Oak, Md. Underwater Systems Dept.
WATER ENTRY IMPACT SHOCK ON FLAT FACED CYLINDRICAL MISSILES Final Report, FY82
S. Van Denk and Charles W. Smith 2 Sep. 1982 68 p
(SR0230100)
(AD-A131937; AD-F500193; NSWC/TR-82-438) Avail: NTIS HC A04/MF A01 CSCL 20/4

Impact shock dynamics, including shock force and impulse as functions of time, are described for a flat faced cylindrical missile striking a smooth water surface with the missile's axis either normal or oblique to the water's surface. Shock dynamics calculations were facilitated by the development of a computer program, IMPACT, the use of which is described and a code listing given. GRA

N84-12420# Ballistic Research Labs., Aberdeen Proving Ground, Md.
UNSTEADY COMPRESSIBLE LAMINAR BOUNDARY-LAYER FLOW WITHIN AN EXPANSION WAVE Final Report
Lang-Mann Chang Jul. 1983 33 p
(DA Proj. 1L1-61102-AH-43)
(AD-A131889; AD-F300296; ARBRL-TR-02511) Avail: NTIS HC A03/MF A01 CSCL 20/4

Numerical solutions are presented for the unsteady compressible laminar boundary-layer flow developing within a centered expansion wave for two wall thermal conditions, namely, isothermal and adiabatic. The solutions are obtained using Howarth's transformation, a similarity transformation via one-parameter groups, and a series expansion. The expansion in terms of a

dimensionless similarity variable is carried up to second-order terms and it improves Hall's zero-order solution for the temperature distribution in the boundary layer. It is shown that both velocity and temperature boundary layers grow rapidly behind the expansion wavefront but attenuate further down stream. If the wall temperature is held at the undisturbed temperature, the heat transfer occurs from the wall to the expanding gas. The rate of heat transfer increases from the wavefront to approximately x =0.35 behind the wave where maximum heat transfer is observed, x being a dimensionless distance from the expansion wavefront. The isothermal wall temperature is found to be higher than the adiabatic wall temperature by a factor of (1 + 0.335x). GRA

N84-12421# Purdue Univ., Lafayette, Ind. School of Mechanical Engineering.
LASER VELOCIMETER MEASUREMENTS AND ANALYSIS IN TURBULENT FLOWS WITH COMBUSTION, PART 2 Interim Report, 1 Jan. - 31 Dec. 1982
Warren H. Stevenson, H. Doyle Thompson, and R. D. Gould Wright-Patterson AFB, Ohio AFWAL Jul. 1983 172 p
(Contract F33615-81-K-2003; AF Proj. 2308)
(AD-A131882; AFWAL-TR-82-2076-Pt-2) Avail: NTIS HC A08/MF A01 CSCL 21/2

Laser velocimeter measurements in the highly turbulent flow field following an axisymmetric sudden expansion have been carried out for both isothermal and reacting flows. Mean streamwise velocity and turbulence intensity profiles covering the region from the sudden expansion to well beyond shear layer reattachment are presented. A study of velocity bias conducted as part of this investigation reconfirmed the effectiveness of the experimental bias elimination technique used in earlier studies. Numerical predictions of the isothermal flow field using the k-epsilon turbulence model were made and compared to experimental measurements. Significant differences in the mean velocity profiles were found to exist, with measured velocities in the central part of the flow being consistently higher than those predicted. Combustion was found to increase mean velocities in regions beyond the combustion zone as expected and to significantly alter the structure of the shear layer. Significant reductions in turbulence intensity were observed throughout most of the flow in the reacting flow case.
Author (GRA)

N84-12422# Air Force Systems Command, Wright-Patterson AFB, Ohio. Foreign Technology Div.
ACTA MECHANICA SINICA (SELECTED ARTICLES)
Sund-gao Wang and Chi Kao 21 Jul. 1983 22 p Transl. into ENGLISH from Lixue Xuebao (China), no. 6, 1982 p 595-600; 606-611
(AD-A131871; AD-E850387; FTD-ID(RS)T-0284-83) Avail: NTIS HC A02/MF A01 CSCL 20/4

Topics of discussion include: problems in the design of the tube wind tunnel, simplified Navier-Stokes equations, and combined solution of nonviscuous and boundary layer equations. B.G.

N84-12423# School of Aerospace Medicine, Brooks AFB, Tex.
A LABORATORY COMPARISON OF PORTABLE COOLING SYSTEMS FOR WORKERS EXPOSED TO TWO LEVELS OF HEAT STRESS Final Report, Aug. 1981 - Jan. 1982
David M. Terrian and Sarah A. Nunneley Jul. 1983 23 p
(AF Proj. 2729)
(AD-A131848; SAM-TR-83-14) Avail: NTIS HC A02/MF A01 CSCL 06/19

Two commercially available liquid cooling systems (LCSs) were tested on subjects wearing the current USAF groundcrew chemical defense ensemble and working in the heat. Each cooling system consisted of an ice-water heat sink, a pump, and a vest or vest-and-cap through which cool water circulated. Subjects walked on a treadmill to produce a time-weighted metabolic rate of about 480 W. Environmental conditions were: hot = 45/31C and warm = 32/22C. Under the hot conditions neither LCS produced and difference from the uncooled control, and all subjects were forced to stop within 40-50 min because of high temperatures, excessive heat rates, or exhaustion. Under the warm condition the LCS did allow T sub re to equilibrate; one system which could be recharged with ice enabled subjects to continue work to the 160-min limit of the protocol. Discussion covers logistics problems and reliability of the two systems. The conclusion is the LCSs are a viable concept for USAF operations, but that better heat sinks must be found and field tested before acceptance. GRA

N84-12424# Sandia Labs., Albuquerque, N. Mex.
NUMERICAL SIMULATION OF PLASTIC FLUIDS
D. K. Gartling 1983 12 p refs Presented at 3rd Intern. Conf. on Numerical Methods in Laminar and Turbulent Flow, Seattle, 8 Aug. 1983
(DE83-007911; SAND-83-0462C; CONF-830803-4) Avail: NTIS HC A02/MF A01

A finite element numerical procedure is outlined for the solution of flow problems involving fluids with a yield stress. Such materials, termed plastic or viscoplastic fluids, complicate the usual numerical procedures through the introduction of a material nonlinearity. In the present work a specific form for the viscoplastic fluids, complicate the usual numerical procedures through the introduction of a material nonlinearity. In the present work a specific form for the viscoplastic constitutive relation is described that is amenable to numerical solution. A hypermatrix technique is outlined for incorporating the deformation dependent fluid viscosity into the finite element formulation. Two example problems are presented that illustrate the numerical method and the behavior of viscoplastic fluids in complex flows. DOE

N84-12425# Oak Ridge Gaseous Diffusion Plant, Tenn. Separation Systems Div.
A GAS-FLOW TRACING TECHNIQUE APPLICABLE TO ROTATING SYSTEMS BOUNDARY LAYER ON A ROTATING DISK
J. J. Keyes, Jr., B. L. Johnson, Sr., and J. E. Park 1983 36 p refs Presented at the 5th Intern. Workshop on Gases in Strong Rotation, Charlottesville, Va., 6 Jun. 1983
(Contract W-7405-eng-26)
(DE83-012761; K/TS-10-997; CONF-830642-1) Avail: NTIS HC A03/MF A01

A sensitive flow tracing technique applicable to remote rotating systems for a disk rotating in air is described. The technique is based on the formation of a plume of silver iodide by reaction of iodine trace vapor, convected by the air flow relative to the disk, with silver foil attached to the surface. The plume is in effect an image of the flow made visible by the colored interference fringe pattern due to the optically thin silver iodide. By the use of a delayed iodine release technique this flow tracing method can be extended to remote geometries. The experimentally observed patterns are compared with computer generated patterns based on T. von Karman's analytical solution coupled with a numerical model for the three dimensional transport of iodine vapor. The applicability of von Karman's solution is verified, and the usefulness of the experimental method for correlating speeds of air relative to the disk is demonstrated. DOE

N84-12426# Oak Ridge Gaseous Diffusion Plant, Tenn. Theory Development Group.
PRACTICAL COMPUTATION OF MULTIDIMENSIONAL THERMAL FLOWS IN A GAS CENTRIFUGE
M. H. Berger Dec. 1982 14 p refs Presented at the 3rd Intern. Conf. on Numerical Methods in Laminar and Turbulent Flow, Seattle, 8-11 Aug. 1983
(Contract W-7405-eng-26)
(DE83-005697; K/OA-5325; CONF-830803-1) Avail: NTIS HC A02/MF A01

A finite element theory for Onsager's two dimensional equation which approximates the steady, viscous, gas motion in a high speed centrifuge was derived. A new high order tensor product element is proposed to make the computations easy. The method of weighted residuals is used to construct the stiffness matrix, associated boundary integrals, and load vectors. It is shown that Ekman suction conditions along horizontal surfaces are natural boundary conditions of the weak approximation. A class of pure boundary value problems are solved for the field variables of

interest. The effect of Ekman suction on the flow by computing with and without suction was evaluated. The case of pure two dimensional flow where the azimuthal velocity perturbation is presumed to vanish is evaluated. The effect of this simplifying assumption on the end to end temperature difference necessary for a given circulation is discussed. It is shown that the streamfunction must be graphed in physical coordinates for the isolines to be streamlines. Only in this form do the velocity vectors lie tangent to the contours and the radial velocity is redefined for graphical purposes. DOE

N84-12427# Brookhaven National Lab., Upton, N. Y. Solar and Renewables Div.

GROUND COUPLED HEAT-PUMP-SYSTEM EXPERIMENTAL RESULTS

Phillip D. Metz 1983 22 p refs Presented at ASHRAE Conf., Washington, D.C., 26-29 Jun. 1983

(Contract W-7405-eng-26)

(DE83-014011; CONF-830640-6) Avail: NTIS HC A02/MF A01

Since October 1980, a small house in Upton, Long Island, New York has been heated and cooled by a liquid source heat pump using a shallow serpentine earth coil as a heat source/sink. After a brief introduction and system description, system performance data are presented, for the winter of 1981-82 and the summer of 1982, followed by a discussion of these results. The experimental test house is a 104 m(2) (1120 ft(2)) 3 bedroom ranch of energy saving construction with a heating load of 7.8 x 10 to the 6th power J/0C-day (4.1 x 10 to the 3rd power Btu/0F-day). The heat pump used during most of the period reported on here is a commercially available water to air unit sized to just meet the building design heating load with no auxiliary heat. The earth coil contains 155 m (507 ft) of nominal 1-1/2 in. medium density polyethylene pipe, and is approximately 25% ethylene glycol in water, is employed to permit subfreezing earth coil operation. Two independent data acquisition systems, a datalogger microcomputer system backed up by a Btu meter, monitor the space conditioning system performance. DOE

N84-12428# Sandia Labs., Albuquerque, N. Mex. Photovoltaic Concentrator Research Div.

USE OF SUPERPOSITION IN CALCULATING COOLING REQUIREMENTS FOR CIRCUIT CARDS CONTAINING ARRAYS OF ELECTRONIC COMPONENTS

Dan E. Arvizu and Robert J. Moffat (Stanford Univ., Calif.) Jun. 1983 53 p refs

(Contract DE-AC04-76DP-00789; Grant NSF-79-06337)

(DE83-016091; SAND-82-0002) Avail: NTIS HC A04/MF A01

The work reported here describes heat-transfer and fluid-friction behavior on surfaces populated with arrays of heat-dissipating components and relates to cooling problems now being faced by the electronics industry. A superposition approach has been developed for calculating the temperature distribution in a regular array of arbitrarily heated cubical elements on an adiabatic wall in a channel. Heat-transfer coefficient and temperature-superposition kernel functions have been determined as a function of position downstream of a single heated element in an array over a range of velocities and channel heights for two different array densities. The measured superposition kernel functions allow prediction of temperature distribution. Furthermore, with the introduction of concepts of array-velocity and array-density parameters, the heat-transfer behavior of the family of in-line cubical elements can be predicted from a relatively small set of input information. These concepts, when applied to other regular arrays, will allow heat-transfer behavior to be predicted over a wide range of flows and passage heights with minimal testing specific to the array in question. DOE

N84-12429# Sandia Labs., Albuquerque, N. Mex.

EXPERIMENTAL MIXED-CONVECTION HEAT TRANSFER FROM A LARGE, VERTICAL SURFACE IN A HORIZONTAL FLOW

Dennis L. Siebers, Richard G. Schwind (Nielen Engineering and Research, Inc., Mountain View, Calif.), and Robert J. Moffat (Stanford Univ.) Jul. 1983 218 p

(Contract DE-AC04-76DP-00789)

(DE83-016419; SAND-83-8225) Avail: NTIS HC A10/MF A01

The convective heat transfer from and the boundary layer flow on a vertical, 3-m-square surface parallel to a horizontal air flow were studied. The test conditions ranged from pure forced convection driven by a horizontal inertial force induced by the horizontal free-stream flow, to combined forced and free convection (i.e., mixed convection) driven by orthogonal forces, the horizontal inertial force and a vertical buoyant force generated by the heated vertical wall, to pure free convection driven by the vertical buoyant force. The emphasis was on mixed convection. Surface temperatures and free-stream velocities ranged from 40 to 600 C and 0 to 6.0 m/s, respectively, resulting in Reynolds numbers (Re) and Grashof numbers (Gr) up to 2 x 10(6) and 2 x 10(12), respectively. Convective heat-transfer and boundary-layer profiles of mean velocity, flow angle, and temperature were measured. The heat-transfer results showed the range of conditions for which the heat transfer was characterized either as forced, mixed, or free convection. DOE

N84-12430# Oak Ridge National Lab., Tenn. Atomic, Molecular, and High Voltage Physics Group.

ISOTOPE DEPENDENCE OF THE BREAKDOWN STRENGTH OF GASES

L. G. Christophorou, R. A. Mathis, and D. R. James 1983 3 p refs Presented at the 16th Intern. Conf. on Phenomena in Ionized Gases, Duesseldorft, 29 Aug. 1983

(Contract W-7405-eng-26)

(DE83-017272; CONF-8308108-1) Avail: NTIS HC A02/MF A01

It was found that while the highly nonuniform direct current breakdown voltages, V-sub s/, of H2 and NH3 exceed, respectively, those of D2 and ND3, the V/sub s/ of CH4 is substantially lower than that of CD4. The former isotope effect may be attributed to the higher ionization coefficients for the deuterated species compared with the nondeuterated, and the latter isotope effect may result from differences in the electron impact induced dissociation processes of the isotopic pairs of molecules. DOE

N84-12431# Sandia Labs., Livermore, Calif.

ZERO-DIMENSIONAL MODEL OF COMPRESSIBLE GAS FLOW IN NETWORKS OF PRESSURE VESSELS: PROGRAM TRIC

G. L. Clark Jul. 1983 93 p refs

(Contract DE-AC04-76DP-00789)

(DE83-017121; SAND-83-8226) Avail: NTIS HC A05/MF A01

A computational tool that models the flow of real gases of arbitrary equation of state in networks of pressure vessels connected by various flow components is described. The conservation equations in zero dimensions are applied to the vessels, which are treated as either constant or deformable control volumes, to produce a set of time dependent, ordinary differential equations. A flow model is developed for an isentropic process, appropriate to nozzles and short orifices, with the flow rate modified by a flow coefficient. For long ducts, the code solves the boundary value problem resulting from the one dimensional conservation equations. Friction and heat transfer in the duct are included in this flow model and a loss of total pressure is predicted, obviating a flow coefficient. DOE

N84-12432# Illinois Univ., Urbana. Dept. of Chemistry.

TRANSPORT AND RELAXATION PROCESSES IN SUPERCRITICAL FLUIDS Technical Progress Report, 1 Apr. - 30 Jun. 1983

Jiri Jonas 1983 9 p

(Contract DE-FG22-82PC-50800)

(DE83-015966; DOE/PC-50800/T3) Avail: NTIS HC A02/MF A01

Self-diffusion coefficients in supercritical toluene was measured. Equipment developed for proton NMR studies of relaxation in supercritical compressed steam was rejuvenated, reassembled, and tested. Design changes were made to allow NMR observation of deuterium nuclei. DOE

N84-12433# National Aerospace Lab., Amsterdam (Netherlands). Fluid Dynamics Div.
ASPECTS OF SECOND- AND THIRD-ORDER PANEL METHODS DEMONSTRATED FOR THE TWO-DIMENSIONAL FLAT PLATE PROBLEM
H. W. M. Hoeijmakers 14 Jan. 1983 55 p refs
(NLR-TR-81074-U) Avail: NTIS HC A04/MF A01

Characteristics of three second order and two third order panel method formulations for the incompressible flow about a flat plate at incidence are investigated. The second-order methods employ quadratic representations for the doublet distribution, based on quadratic B-splines or on a combination of a Taylor series expansion and finite difference formulas. The third order methods are based on cubic B-splines or on cubic Hermite polynomials. The integral equation resulting from imposing the stream surface condition at the flat plate is written in the vorticity formulation. Higher order accuracy is achieved by employing mode functions which extract the singular behavior of the doublet distribution near the leading and trailing edge to sufficient degree. It is demonstrated that for computational efficiency the third-order methods are superior, with cubic Hermite polynomials being most efficient.
Author (ESA)

N84-12434# National Aerospace Lab., Amsterdam (Netherlands). Fluid Dynamics Div.
RESULTS OF A NEW VERSION OF THE LTRAN2-NLR (LTRANV) FOR UNSTEADY VISCOUS TRANSONIC FLOW COMPUTATIONS
R. Houwink 14 Jan. 1983 42 p refs Sponsored by Netherlands Agency for Aerospace Programs (NIVR)
(NLR-TR-81078-U) Avail: NTIS HC A03/MF A01

A computer program for coupled unsteady transonic flow/turbulent boundary layer computations is presented. It is a combination of the LTRAN2-NLR program and Green's lag-entrainment method. Theoretical and experimental results for the NACA64A006 airfoil with oscillating flap in subsonic and transonic flow are compared. Accounting for the effect of the boundary layer on the airfoil yields a reduction of the magnitude of unsteady airloads by 10 to 35% and a phase shift of 2 to 7 deg, giving better agreement with experimental data. Considerable differences between theory and experiment at low reduced frequency are likely, due to strong wall interference effects and underestimation of the boundary layer effect. The use of a steady boundary layer method instead of an unsteady one is acceptable. Author (ESA)

N84-12435# Imperial Coll. of Science and Technology, London (England). Computational Fluid Dynamics Unit.
TURBULENCE MODELLING: A STATE-OF-THE-ART REVIEW
D. Brian Spalding 1983 17 p refs
(CFD/83/3) Avail: NTIS HC A02/MF A01

Traditional and multiphase flow turbulance models are reviewed. Traditional models neglect intermittency, and periodicity, and postulate only gradient induced diffusion, whereas other diffusion-promoting mechanisms exist. Multifluid models permit different fluids to exist and interact in the same space. A complete multiphase mathematical model requires formulation of expressions for: fragment-size growth and diminution; interphase mass transfer (entrainment); interphase momentum transfer (friction); interphase heat transfer; phase-fragment migration (diffusion). Author (ESA)

N84-12436# Imperial Coll. of Science and Technology, London (England). Computational Fluid Dynamics Unit.
A REVISED TWO-EQUATION MODEL OF TURBULENCE Ph.D. Thesis
J. O. Ilegbusi May 1983 346 p refs Sponsored by Ibadan Univ., Nigeria and by UK Commonwealth Scholarships Commission
(CFD/83/5) Avail: NTIS HC A15/MF A01

Modifications to a transport model which characterizes turbulence by the specific kinetic energy of the fluctuating motion and the time-mean square of the vorticity fluctuations (W) are described. Partial differential equations expressing the conservation of these quantities are solved numerically, along with those for the momentum and enthalpy. Modeling of the near-wall region is emphasized. Unlike the earlier version of the model, the same set of the asymptotic high Reynolds-number values of the model constants is used in all calculations. Predictions of fluid flow and heat transfer are compared with experimental data and predictions based on the earlier model. The model performs as well as, or better than, the original version, and does not need the near-wall fix of the latter. Agreement with experiment is at least as good as that of the model in which dissipation rate of the turbulence energy is used in place of W. Author (ESA)

N84-12437 Minnesota Univ., Minneapolis.
TURBULENT TUBE-FLOW HEAT TRANSFER COEFFICIENTS IN THE PRESENCE OF FLOW IMBALANCE IN THE TUBES OF A PARALLEL ARRAY Ph.D. Thesis
Majid Molki 1982 216 p
Avail: Univ. Microfilms Order No. DA8308100

Experiments were performed to study the effects of a controlled flow imbalance on the heat transfer coefficients in the entrance region of a tube situated in an array of parallel tubes. The array was modeled by two parallel tubes which were set into a large baffle plate to form a sharp-edged inlet, with air being drawn into the tube inlets from a large upstream plenum chamber. Quasi-local heat transfer coefficients were determined at various axial and circumferential locations along the length of the test section tube. A preselected, fixed Reynolds number was established in the test section tube while that of the other was varied systematically. Both Reynolds numbers ranged from 5000 to 88000. The separation distance between the tubes varied from 1.5 to 4.5 tube diameters. It was found that high degrees of flow imbalance played a decisive role in shaping the axial and circumferential distributions of the heat transfer coefficient in the thermal entrance region. Dissert. Abstr.

N84-12438 California Univ., Berkeley.
CONVECTION IN HORIZONTAL POROUS MEDIA WITH DIFFERENT END TEMPERATURES Ph.D. Thesis
Masoud Haajizadeh 1982 125 p
Avail: Univ. Microfilms Order No. DA8312831

This work consists of a combined theoretical and experimental study of natural and forced convection in horizontal porous layer with different end temperatures and adiabatic horizontal walls. The first part of this work is concerned with two dimensional thermally driven flow in a rectangular porous cavity with one permeable end-wall. Connected to a constant temperature tank the permeable end allows for natural recharge and discharge of the saturating fluid. The other vertical end-wall is impermeable and maintained at a constant but higher temperature, thus inducing a thermally driven flow. The theoretical study includes an asymptotic analysis developed for a shallow cavity with one permeable end-wall and the numerical solutions of the power-law difference representation of the full governing equations. The experimental system consists of water-saturated glass beads packed in a rectangular cavity with the length-to-height aspect ratio of 3.17, and the Rayleigh number can vary up to 120. Measurements were made of the steady-state temperature distribution in the cavity and the heat transfer rate from the impermeable end-wall. Dissert. Abstr.

N84-12439 Howard Univ., Washington, D. C.
NUMERICAL CALCULATIONS OF TURBULENT RECIRCULATING HEAT TRANSFER BEYOND TWO-DIMENSIONAL BACK-STEPS AND SUDDEN PIPE EXPANSIONS Ph.D. Thesis
Arthur Maignauth Gooray 1982 236 p
Avail: Univ. Microfilms Order No. DA8311431

Extensive results of numerical calculations for turbulent recirculating flow with heat transfer are presented. The geometries studied were two dimensional flows over rearward (backward)--facing steps and sudden pipe expansions. The computations described were performed using the k-epsilon, two equation model of turbulence. To yield better predictions of heat transfer, the standard model was improved, by developing algebraic approximations for Reynolds stresses and scalar fluxes, so as to account

for the effects of streamline curvature, pressure-strain and variation of turbulent Prandtl number in the flow field. In addition, the low-Reynolds-number version of the standard k-epsilon model was employed in the redeveloping region. In order to apply the low-Reynolds-number model to the redeveloping region, a two pass procedure was developed to partition the flow field into separated and reattached regions. Dissert. Abstr.

N84-12440 Pittsburgh Univ., Pa.
COMPUTATION OF THREE-DIMENSIONAL UNSTEADY FLOW IN RIGID AND DEFORMABLE CURVED TUBES Ph.D. Thesis
Weng-Sheng Cheng 1982 239 p
Avail: Univ. Microfilms Order No. DA8312498

A computational analysis and a computer code were developed to calculate three dimensional pulsatile flow through the rigid and deformable coiled and curved tubes. For pulsating flow in a coiled tube, the effects of distensibility of the tube wall on flow rate, pressure and the shear stress on the wall, the velocity field and the temporal and spatial development of boundary layer were studied. In order to simulate large velocity gradients near the wall, an irregular mesh along the radial direction was used with small meshes in the wall region and coarse meshes in the core region of a cross section. However, the calculation was proceeded with regular meshes (elements) in a transformed coordinate system. Numerical solutions for flow establishment from rest in a rigid coiled tube were obtained; they were somewhat similar to the experimental data of Hawes for a radius of curvature equal to ten diameters. Numerical results of pulsatile flow in a rigid coiled tube were compared with those of a deformable tube. Dissert. Abstr.

N84-12441 California Univ., Berkeley.
STEADY LAMINAR NATURAL CONVECTION IN OPEN RECTANGULAR CAVITIES Ph.D. Thesis
Yuk Lun Chan 1982 140 p
Avail: Univ. Microfilms Order No. DA8312776

A combined numerical and experimental investigation on natural convection in a two dimensional open cavity was performed. The cavity is rectangular with one vertical heated wall facing a vertical opening; the two horizontal walls are insulated. Numerical studies for both the square cavity with Rayleigh numbers up to 10 and the shallow cavity with height-to-length aspect ratio of 0.143 for Rayleigh numbers up to 10 under the laminar, steady flow conditions were carried out. The flow inside the cavity was solved through numerical modeling by imposing reasonable boundary conditions around an outer region near the opening. Computed flow patterns and heat transfer results illustrate the effect of the open boundary. A simplified modeling at this open boundary was then tested and computations were performed strictly inside the cavity. Good heat transfer results were obtained at a smaller computation cost by omitting the whole outside flow field. Experimental work using laser Doppler velocimetry was carried out with water as the working fluid in a shallow cavity. Heat transfer results were also obtained by measuring the electrical power input into the heater. Dissert. Abstr.

N84-12442 North Carolina State Univ., Raleigh.
NUMERICAL SOLUTION OF THE TWO-PHASE, THREE DIMENSIONAL BOUNDARY LAYER IN LAMINAR FILM CONDENSATION OVER A CURVED SURFACE Ph.D. Thesis
Abdul Rahim Abdul Jabbar AlAnsari 1982 335 p
Avail: Univ. Microfilms Order No. DA8308527

An analysis is performed to study the effects of the body force on the heat transfer characteristics of laminar filmwise condensation over curved surface, which is either maintained at a uniform temperature or subjected to a uniform heat flux. The governing equations describing the boundary layers are transformed to nondimensional forms and then solved by a two-point implicit finite difference method. Numerical results for the velocity and temperature distributions, the local mass transfer in both the streamwise and crosswise directions, the local Nusselt number and the local skin friction are represented for Pradtl numbers of 0.00346 and 1.74 with three values of the body force and for two values of temperature potentials across the liquid film. Generally, it is found that for both surface heating conditions, the local mass transfer in the crosswise direction, the crosswise velocity and the local Nusselt number increases with an increase in the body force. In addition, an increase in the body force results in control of the liquid layer thickness and thus an improvement in the condensation heat transfer. Dissert. Abstr.

35 INSTRUMENTATION AND PHOTOGRAPHY

Includes remote sensors; measuring instruments and gages; detectors; cameras and photographic supplies; and holography.

For aerial photography see *43 Earth Resources.* For related information see also *06 Aircraft Instrumentation,* and *19 Spacecraft Instrumentation.*

N84-12443* National Aeronautics and Space Administration. Flight Research Center, Edwards, Calif.
INFLATABLE DEVICE FOR INSTALLING STRAIN GAGE BRIDGES Patent
Clarence E. Cook, Glynn E. Smith, and Richard C. Monaghan, inventors (to NASA) Issued 4 Oct. 1983 7 p Filed 17 Nov. 1981 Supersedes N82-24473 (20 - 15, p 2086)
(NASA-Case-FRC-11068-1; US-Patent-4,407,686;
US-Patent-Appl-SN-322314; US-Patent-Class-156-215;
US-Patent-Class-156-71; US-Patent-Class-156-230;
US-Patent-Class-156-235; US-Patent-Class-156-294;
US-Patent-Class-156-391; US-Patent-Class-156-423;
US-Patent-Class-156-540; US-Patent-Class-338-2) Avail: US Patent and Trademark Office CSCL 14B

Methods and devices for installing in a tubular shaft multiple strain gages are disclosed with focus on a method and a device for pneumatically forcing strain gages into seated engagement with the internal surfaces of a tubular shaft in an installation of multiple strain gages in a tubular shaft. The strain gages or other electron devices are seated in a template-like component which is wrapped about a pneumatically expansible body. The component is inserted into a shaft and the body is pneumatically expanded after a suitable adhesive was applied to the surfaces.

Official Gazette of the U.S. Patent and Trademark Office

N84-12444* National Aeronautics and Space Administration. Langley Research Center, Hampton, Va.
LOW ENERGY ELECTRON MAGNETOMETER USING A MONOENERGETIC ELECTRON BEAM Patent
Jag J. Singh (Univ. of Southern Mississippi, Hattiesburg), George M. Wood (Univ. of Southern Mississippi, Hattiesburg), Grayson H. Rayborn (Univ. of Southern Mississippi, Hattiesburg), and Frederick A. White, inventors (to NASA) (Univ. of Southern Mississippi, Hattiesburg) Issued 8 Nov. 1983 9 p Filed 26 Nov. 1980 Supersedes N81-19428 (19 - 10, p 1350) Sponsored by NASA
(NASA-Case-LAR-12706-1; US-Patent-4,414,509;
US-Patent-Appl-SN-210498; US-Patent-Class-324-250;
US-Patent-Class-328-230; US-Patent-Class-372-74) Avail: US Patent and Trademark Office CSCL 14B

A low energy electron beam magnetometer utilizes near-monoenergetic electrons thereby reducing errors due to electron energy spread and electron nonuniform angular distribution. In a first embodiment, atoms in an atomic beam of an inert gas are excited to a Rydberg state and then electrons of near zero energy are detached from the Rydberg atoms. The near zero energy electrons are then accelerated by an electric field V(acc) to form the electron beam. In a second embodiment, a filament emits electrons into an electrostatic analyzer which selects electrons at a predetermined energy level within a very narrow range. These selected electrons make up the electron beam that is subjected to the magnetic field being measured.

Official Gazette of the U.S. Patent and Trademark Office

N84-12445* National Aeronautics and Space Administration. Langley Research Center, Hampton, Va.
RIDE QUALITY METER Patent
Jack D. Leatherwood, Thomas K. Dempsey, Sherman A. Clevenson, and David G. Stephens, inventors (to NASA) Issued 8 Nov. 1983 11 p Filed 22 May 1981 Supersedes N81-31848 (19 - 22, p 3107)
(NASA-Case-LAR-12882-1; US-Patent-4,413,522; US-Patent-Appl-SN-267179; US-Patent-Class-73-646; US-Patent-Class-73-658; US-Patent-Class-364-415) Avail: US Patent and Trademark Office CSCL 14B

A ride quality meter is disclosed that automatically transforms vibration and noise measurements into a single number index of passenger discomfort. The noise measurements are converted into a noise discomfort value. The vibrations are converted into single axis discomfort values which are then converted into a combined axis discomfort value. The combined axis discomfort value is corrected for time duration and then summed with the noise discomfort value to obtain a total discomfort value.
Official Gazette of the U.S. Patent and Trademark Office

N84-12446# Instituto de Pesquisas Espaciais, Sao Jose dos Campos (Brazil).
DIGITAL IMAGE REGISTRATION BY SEQUENTIAL ANALYSIS
Jose Antonio Goncalves Pereira and Nelson D. A. Mascarenhas Oct. 1983 28 p refs Submitted for publication
(INPE-2940-PHE/429) Avail: NTIS HC A03/MF A01

An approach to translational image registration problems, based on the theory of sequential test of hypotheses (S.T.H.) is proposed. This leads to the development of two different methods. The first one is based on the Gaussian assumption and uses the fact that the variance of the error between two images to be registered tends to be low on the registration point. The second method uses binary images derived from the original ones. The statistical model for the resulting accumulated error is a binomial distribution and the registration position is characterized by a low probability of the binary error being one. In both methods two sequences of thresholds are employed: one leading to the rejection of the point and the other one to the eventual acceptance of it. Experimental results with both methods are presented. They include registration of a LANDSAT image against noisy versions of it, matching of different channels of the same multispectral image as well as matching of segments of two images taken at different dates. Successful registration was achieved in most cases even in low signal to noise ratio conditions, with a modest amount of computational effort. M.G.

N84-12447*# National Aeronautics and Space Administration. Lewis Research Center, Cleveland, Ohio.
A MULTISTAGE SPENT PARTICLE COLLECTOR AND A METHOD FOR MAKING SAME Patent Application
B. T. Ebihara, inventor (to NASA) Filed 30 Sep. 1983 12 p
(NASA-CASE-LEW-13914-1; US-Patent-Appl-SN-537615) Avail: NTIS HC A02/MF A01 CSCL 14B

A spent particle collector is comprised of one or more axisymmetric stages, each stage comprising a subassembly having an inner pyrolytic graphite ring, a transition ring, a ceramic insulator ring, and an outer metal ring which forms part of the wall of the collector. Each transition ring is of a ductile metal having high thermal conductivity and is provided with an annual sputter shield wall extending toward the source of spent particles and, where necessary, a trough in the other surface to enclose the sputter shield of the next adjacent transition ring. Radial extending slots are provided in a transition ring to form segments which are retained in their position by the sputter shield. This arrangement with the ceramic ring outwardly of the transition ring keeps the latter in contact with the inner pyrolytic graphite ring. This multistage collector can be assembled with high accuracy. The collector is attached by welding to a flange attached to a source of spent particles such as a traveling wave tube. NASA

N84-12448*# National Aeronautics and Space Administration. Wallops Flight Center, Wallops Island, Va.
THIN FILM STRAIN TRANSDUCER Patent Application
James L. Rand, inventor (to NASA) (Southwest Research Inst., San Antonio, Tex.) Filed 26 Aug. 1983 13 p Sponsored by NASA
(NASA-WLP-10055-2; US-Patent-Appl-SN-526770) Avail: NTIS HC A02/MF A01 CSCL 14B

On a beryllium-copper ring are four strain gages which are electrically connected in Wheatstone bridge fashion to output instrumentation. Tabs are bonded to a balloon or like surface where strain on the surface causes bending of the ring. An electrical signal is provided through the gages proportional to the surface strain. A one-half ring segment, as placed on a sheet of beryllium-copper for chem-mill etch formation prior to bending and welding of a pair of the segments to form a ring structure, is illustrated.
NASA

N84-12449# Deutsche Forschungs- und Versuchsanstalt fuer Luft- und Raumfahrt, Brunswick (West Germany). Abt. Kreiselgeraete und Traegheitshavigation.
EVALUATION OF THE STOCHASTIC DRIFT OF RATE INTEGRATING GYROS AS PREPARATION FOR THE ANALYSIS OF LASER GYRO DRIFT MEASUREMENTS
Norbert Fuerstenau Jan. 1983 38 p refs In GERMAN; ENGLISH summary Report will also be announced as translation (ESA-TT-827)
(DFVLR-Mitt-83-04; ESA-TT-827) Avail: NTIS HC A03/MF A01; DFVLR, Cologne DM 16

A method for evaluating long term drift measurements with inertial sensors was developed for stability tests of laser gyros. Data acquisition and mathematical techniques for analyzing stochastic drifts are described. The interrelation of autocorrelation functions with mean squared fluctuations and physically explainable dissipative constants is emphasized. The method of evaluation was tested with stability tests of the rate integrating gyros of a strapdown system. The limits of this method are discussed, employing characteristic results. It resulted that the limits of the stability test system are conditioned by the process data mass (that determines storage requirements and calculating time) and the applicability of the mathematical procedures used.
Author (ESA)

N84-12450# Arnold Engineering Development Center, Arnold Air Force Station, Tenn.
DETERMINATION OF THE UNCERTAINTY OF EXPERIMENTAL HEAT-FLUX CALIBRATIONS Final Report, 1 Oct. 1981 - 30 Sep. 1982
C. T. Kidd Aug. 1983 62 p
(AD-A131918; AEDC-TR-83-13) Avail: NTIS HC A04/MF A01 CSCL 20/13

A description and the results of a study of the uncertainty associated with experimental calibration of heat-flux transducers/gages performed at the Arnold Engineering Development Center (AEDC) are given. Determination of an overall or total calibration uncertainty was achieved by combining the results of different groups of experimental calibrations performed at the AEDC and the National Bureau of Standards (NBS), respectively. The first group of calibration data was obtained by calibrating six heat-flux transducers fabricated in-house at the AEDC versus calibration standard slug calorimeters also fabricated at the AEDC. The radiant heat source used in the calibrations was a nine-unit (1-kw max/unit) quartz tube lamp bank. A classical precision term was calculated for each of the six transducers from the results of these experimental calibrations. Acquisition of the second group of calibration data was achieved by sending the same six transducers to the Fire Research Center of the NBS in Washington, D.C. for experimental calibration services. Thus, traceability to NBS heat-flux standards was achieved. A radiant heat source was also used by the NBS and the calibrations were performed in a manner similar to the procedures employed at the AEDC. Calibration data obtained at the AEDC and the NBS were compared to determine a bias value for each of the six transducers. A total uncertainty value for each transducer was calculated by combining the precision and bias terms. The average total uncertainty calculated

for the six transducers was nominally plus or minus percent.
Author (GRA)

N84-12451# Air Force Systems Command, Wright-Patterson AFB, Ohio. Foreign Technology Div.
DISCUSSION OF STATIC PRESSURE LIQUID-FLOATED GYROS
Zhang Guoan 3 Aug. 1983 9 p Transl. into ENGLISH from Hankong Zhishi (China), no. 10, Oct. 1982 p 20-21
(AD-A131874; FTD-ID(RS)T-0015-83) Avail: NTIS HC A02/MF A01 CSCL 17/7

Improvement in air floated gyro technology resulted in the replacement of gas by thin oil. The oil is continuously pumped to the bearings supporting the gimbal shaft by a miniature pump incorporated in the gyroscope itself. The oil circulates inside the housing and a self-feed type static pressure liquid floated gyro is formed. Author

N84-12452# Northeastern Univ., Boston, Mass. Electronics Research Lab.
GSE FOR BALLOON-BORNE I.M.S.: DECOMMUTATOR AND D/A UNITS
Raimundas Sukys and J. S. Rochefort Oct. 1982 52 p
(Contract F19628-81-C-0162; AF Proj. 2310)
(AD-A131845; SCIENTIFIC-1; AFGL-TR-83-0095) Avail: NTIS HC A04/MF A01 CSCL 09/6

Two ground based units to support data processing and control operations during the flight of a Balloon-Borne Ion Bass Spectrometer (BBIMS) are described. One of the units decommutated the incoming PCM data and presented that data upon request to a computer for further processing. The data was available through IEEE-488 compatible interface and/or in parallel form as 16 and/or 8 bit words. Communications interface for commands and messages to and from the airborne instrumentation was also provided. The second unit converted the digital data, supplied by the computer, into analog signals for display and recording. An IEEE-488 compatible interface was used for data transfer.
Author (GRA)

N84-12453# California Inst. of Tech., Pasadena.
THE OWENS VALLEY FREQUENCY-AGILE INTERFEROMETER
G. J. Hurford Hanscom AFB, Mass. AFGL Mar. 1983 24 p
(Contract F19628-82-K-0033; AF Proj. 2311)
(AD-A131825; SR-1; AFGL-TR-83-0108) Avail: NTIS HC A02/MF A01 CSCL 20/6

The solar microwave spectrum encodes significant information on plasma parameters, magnetic field strengths and characteristics of accelerated electrons in solar flares and active regions. The solar interferometer of the Owens Valley Radio Observatory has recently been converted to frequency agile operation to effectively become a high resolution, interferometric spectrometer. The interferometer uses two moveable, 27 m diameter parabolic antennas equipped with frequency agile receivers. These receivers are capable of switching their observing frequency in less than 50 ms between any of 86 different frequencies in the range 1 to 18 GHz. All data are absolutely calibrated with respect to cosmic sources. In 1981, observations with one frequency agile receiver were conducted and high resolution spectra of many flares were obtained. One unexpected aspect of such spectra were narrow band bursts, which featured sharp high and low frequency cutoffs and a relatively narrow bandwidth. GRA

N84-12454# Army Research and Technology Labs., Moffett Field, Calif. Aeromechanics Lab.
APPLICATION OF THE SMALL BODY PRESSURE TRANSDUCER
Robert E. George 1983 26 p
(AD-A131733) Avail: NTIS HC A03/MF A01 CSCL 14/2

The small body pressure transducers were used in both fixed-wing and rotary-wing scale models to measure dynamic and static pressures. These models were then tested under controlled wind tunnel conditions and the transducer signals recorded for either on- or off-line analyses. One experiment using the small body pressure transducers was conducted in the American Aeromechanics Wind Tunnel in order to compare different geometrically shaped rotary-wing airfoil sections under dynamic stall conditions. An additional application for the small body pressure transducer was a series of tests conducted in both the French Tunnel, Saclay, France and the Dutch-German Amsterdam, The Netherlands wind tunnel. During the foreign tests, data were obtained on helicopter rotor noise generated by blade pressure disturbances due to helicopter blade-vortex interaction. Both the acoustic signature and the blade pressure transducer outputs were recorded simultaneously. GRA

N84-12455# Air Force Wright Aeronautical Labs., Wright-Patterson AFB, Ohio.
UTILITY OF THE CORTICAL EVOKED RESPONSE AS A MEASURE OF PHOTOGRAPHIC IMAGE QUALITY Final Report, 1 Oct. 1979 - 31 Jan. 1980
Robert D. ODonnell, Thomas Stanzione, Lloyd G. Clark, Edward L. Gliatti, and Robert Love Jun. 1983 44 p
(AD-A131679; AFWAL-TR-83-1025) Avail: NTIS HC A03/MF A01 CSCL 14/5

This report covers the results of investigation by AMRL into the use of Cortical-Evoke Potentials to measure Photographic Image Quality. This work was sponsored by the Avionics Laboratory using Laboratory Director's Funds. Cortical Evoked Response (ER) procedures (both steady-state and transient) were tested for their utility and sensitivity in indexing the focus level of various kinds of targets. Four studies investigated the ERs generated by presentation of Air Force tri-bar photographs, checkerboard patterns, and complex real imagery. Neither low nor high frequency steady-state ER amplitudes showed sensitivity to defocusing of any type of imagery, although contrast ration clearly produced differences. The phase delay of the fundamental steady-state ER changed significantly with focus of a single tri-bar target. Transient evoked responses showed systematic changes in amplitude as a function of focus. A negative going peak between 90 and 170 msec. after the stimulus appeared to diminish in amplitude with increasingly poorer focus of both checkerboard and complex imagery. Results indicate that, under conditions tested, the steady-state ER does not appear to be a promising technique for assessing image focus, while the transient ER seems considerably more reliable and valid. GRA

N84-12456# Massachusetts Inst. of Tech., Cambridge. Dept. of Nuclear Engineering.
DESIGN AND OPERATION OF A LIGHT-SCATTERING DEVICE FOR SIZING AND VELOCIMETRY OF LARGE DROPLETS Interim Report
W. J. Glantschnig, M. W. Golay, S. H. Chen, and F. R. Best May 1983 163 p refs Sponsored by Electric Power Research Inst.
(DE83-902641; EPRI-CS-3098) Avail: NTIS HC A08/MF A01

The design and operation of a light scattering device for sizing and velocimetry of large droplets are presented. This device was for use as a laboratory standard instrument to compare alternative cooling tower drift measurement methods. The instrument consists of coupled optical and electronic subsystems. Novel beam shaping methods are employed and electronic modules are incorporated into the signal processing chain. The instrument is also capable of droplet velocity measurements, and it is equipped with a fast, online, data reduction capability. The theory of light scattering by large water droplets and instrument calibration procedures are described. DOE

N84-12457# Sandia Labs., Albuquerque, N. Mex.
AUTOMATED DATA REDUCTION FOR OPTICAL INTERFEROMETRIC DATA
Ronald D. Boyd, David J. Miller, and Dennis C. Ghiglia 1983 6 p refs Presented at the 3rd Intern. Symp. on Flow Visualization, Ann Arbor, Mich., 6-9 Sep. 1983
(Contract DE-AC04-76DP-00789)
(DE83-012075; SAND-82-2300C; CONF-830926-1) Avail: NTIS HC A02/MF A01

The potential for significant progress in understanding many

transport processes exists through the use of a rapid and automated data reduction process of optical interferometric data. Natural convection in a horizontal annulus is used to demonstrate that the accuracy possible in automated techniques is better than 99.9%. DOE

N84-12458# Sandia Labs., Livermore, Calif. Standards and Calibration and Photography Section.
GAUGE BLOCK LASOMETER DEVELOPMENT
Robert D. Pilkey Sep. 1983 17 p refs
(Contract DE-AC04-76DP-00789)
(DE83-018288; SAND-83-8025) Avail: NTIS HC A02/MF A01

Automated dimensional measurement and calibration systems which require gauging apparatus capable of transferring measurement data to appropriate computing devices is discussed. The upgrading a formerly obsolete dimensional measuring instrument to interface with a desktop computer is described thereby giving it current technological capability. DOE

N84-12459# Sandia Labs., Albuquerque, N. Mex. Centrifuge, Climatic and Radiant Heat Div.
TRANSIENT TEMPERATURE RESPONSE OF STRAIN GAGES, REVISION 1
P. H. Adams Jul. 1983 15 p refs
(Contract DE-AC04-76DP-00789)
(DE83-017514; SAND-80-2689-REV-1) Avail: NTIS HC A02/MF A01

The use of electrical resistance strain gages for measuring strain under transient temperatures which presents the problem of determining the thermal output or apparent strain of the gages accurately enough for satisfactory results was examined. Various circuit temperature compensation techniques were used but little data exist about the accuracy of those techniques under transient temperatures. In particular, published data are limited to temperature changes less than or equal to 300F/s. In preparation for a specific measurement problem, the thermal response of one model of AilTech high temperature weldable strain gages was determined for a temperature rise rate of 1000F/s. DOE

N84-12460# TRW Defense and Space Systems Group, Redondo Beach, Calif. Systems Engineering and Development Div.
DEVELOPMENT OF INSTRUMENTATION FOR MONITORING CARBON FIBER EMISSION Final Report, 1 Sep. 1979 - 1 Feb. 1982
D. L. Tague Jul. 1983 77 p refs
(Contract EPA-68-02-3273)
(PB83-233726; EPA-600/3-83-056) Avail: NTIS HC A05/MF A01 CSCL 14B

This document reports the design of an electrical instrument which utilizes a variable capacitance in one leg of an R-C feedback network to provide discriminatory information regarding the air stream particulate materials. Sufficient testing was performed on the breadboard to validate system concept. The current instrument is counting fiber mass and indicating fiber diameters to yield an approximate count of individual fibers. Its operational range has a lower limit of 10000 fiber/cu m and an upper limit internally restricted for this breadboard state of 2 x 10 to the 8th power fibers/cu m. The program scope did not allow completion of a prototype design; therefore, emphasis is placed on recommendations to complete design efforts. Author (GRA)

N84-12461# California Univ., Berkeley. Lawrence Berkeley Lab.
DEVELOPMENT OF A CONTINUOUS MONITOR FOR DETECTION OF TOXIC ORGANIC COMPOUNDS Final Report, Oct. 1981 - Oct. 1982
T. Hadeishi, R. McLaughlin, J. Millaud, and M. Pollard Jul. 1983 91 p refs
(Contract EPA-IAG-AD-89-F-2A008)
(PB83-234922; EPA-600/4-83-034) Avail: NTIS HC A05/MF A01 CSCL 14B

The goal of the present program was the design, construction, and delivery to EMSL/RTP of a small continuous monitor for benzene and other organic compounds based upon Tunable Atomic Line Molecular Spectroscopy. The most limiting design factor was found to be the detection limit of the instrument. To improve this limiting factor, some new developments were investigated. These developments have improved the sensitivity of the TALMS benzene monitor by a factor of 100 to a detection limit of 3 ppm-v benzene. The instrument that was delivered to EMSL/RTP is compact in size (41 inches in length) and weight (75 lbs.) and requires a modest amount of power (125 watts). It was supplied with a permanent magnet of field strength 7 kG (0.7T) and utilizes the Hg 253.6 nm line. Author (GRA)

36 LASERS AND MASERS

Includes parametric amplifiers.

N84-12462*# Illinois Univ., Urbana. Aeronomy Lab.
DESIGN AND IMPLEMENTATION OF A PREPROCESSING SYSTEM FOR A SODIUM LIDAR
D. G. Voelz and C. F. Sechrist, Jr. 1 Sep. 1983 186 p refs Sponsored by NSF
(NASA-CR-174593; NAS 1.26:174593; ISSN-0568-0581; AR-112) Avail: NTIS HC A09/MF A01 CSCL 20E

A preprocessing system, designed and constructed for use with the University of Illinois sodium lidar system, was developed to increase the altitude resolution and range of the lidar system and also to decrease the processing burden of the main lidar computer. The preprocessing system hardware and the software required to implement the system are described. Some preliminary results of an airborne sodium lidar experiment conducted with the preprocessing system installed in the sodium lidar are presented. Author

N84-12463*# National Aeronautics and Space Administration. Pasadena Office, Calif.
LASER ACTIVATED MTOS MICROWAVE DEVICE Patent Application
Joseph Maserjian, inventor (to NASA) (JPL, California Inst. of Tech., Pasadena) Filed 14 Oct. 1983 13 p
(Contract NAS7-100)
(NASA-CASE-NPO-16112-1; US-Patent-Appl-SN-542232) Avail: NTIS HC A02/MF A01 CSCL 20E

A light-activated semiconductor device usable as an opto-electronic switch, pulse generator or optical detector is provided. A semiconductor device is disclosed which provides back-to-back metal-thin oxide-silicon (MTOS) capacitors. Each capacitor includes a thin, light-absorptive aluminum electrode which overlies a thin oxide layer and a lightly doped region implanted in an intrinsic silicon substrate. NASA

N84-12464# Polytechnic Inst. of New York, Farmingdale. Microwave Research Inst.
LASER INTERACTION WITH METALLIC SURFACES Final Technical Report, 1 Sep. 1978 - 31 Aug. 1981
William T. Walter Dec. 1982 34 p refs
(Contract N00014-78-C-0678)
(AD-A126269; POLY-MRI-1425-82) Avail: NTIS HC A03/MF A01 CSCL 20/5

Direct real-time measurements of a target material's optical properties with subnanosecond resolution may provide crucial, process-revealing signatures in following the interaction of an intense laser beam with a metal as the surface progressively undergoes heating, plastic deformation, slip, vaporization, ejection of liquid metal, plasma formation, etc. Three classes of physical processes have been proposed to account for a substantial decrease in reflectance observed during the interaction of an intense laser pulse with a metal surface: (1) deformation of the surface, (2) plasma formation, and (3) a nonlinear process causing enhanced absorption within the metal. Thus far we may conclude that specular reflectance is a sensitive indicator of surface deformation. Total reflectance measurements, on the other hand, indicate that until the surface temperature of a metal target reaches

the vicinity of the boiling point, the total reflectance does not differ significantly from that given by a Drude-type free-electron model. The reflectivity decrease of a Drude model for a metal heated from room temperature to a liquid at the boiling point is not large enough to account for the substantial reflectance decrease observed experimentally. Author (GRA)

N84-12465# Air Force Systems Command, Wright-Patterson AFB, Ohio. Foreign Technology Div.
LASER JOURNAL (SELECTED ARTICLES)
27 Jul. 1983 15 p Transl. into ENGLISH from Jiguang (China), v. 9, no. 9, 1982 p 600-602 and 613-614
(AD-A131886; AD-E950422; FTD-ID(RS)T-0603-83) Avail: NTIS HC A02/MF A01 CSCL 20/5

An effective and convenient method for branch selection that will keep the intensities of two waves that travel in opposite directions in a ring cavity fundamentally the same, so that one has the choice of making use of any one of several competing effects is discussed. A method is suggested and the beam parameters for the cavity are calculated. R.J.F.

N84-12466# City Coll. of the City Univ. of New York.
SEMICONDUCTORS INVESTIGATED BY TIME RESOLVED RAMAN ABSORPTION AND PHOTOLUMINESCENCE SPECTROSCOPY USING FEMTOSECOND AND PICOSECOND LASER TECHNIQUES Final Report, 1 Dec. 1979 - 30 Nov. 1982
Robert R. Alfano and Apostolos G. Doukas 5 May 1983 71 p
(Grant AF-AFOSR-0079-80; AF Proj. 2305)
(AD-A131860; 05423-F; AFOSR-83-0694TR) Avail: NTIS HC A04/MF A01 CSCL 20/5

This report summarizes the research progress achieved in the period 1979-1982 in the research effort supported by AFOSR 80-0079. Two main areas of research are: picosecond and subpicosecond laser development and application and time-resolved studies of semiconductors. In the subpicosecond laser development program we investigated a variety of cavities of different physical parameters. A stable and reliable oscillator, which produces 200 fsec pulses, has been developed using a ring configuration. The first generation amplifier system has been completed with a gain of 10 to the sixth power. We have produce continuum by focusing the amplified pulses in a CC14 cell; and have invented a femtosecond luminescence technique (called population mixing) for probing semiconductor processes.
Author (GRA)

N84-12467# Illinois Univ., Chicago. Dept. of Physics.
STUDIES OF COLLISIONAL AND NONLINEAR RADIATIVE PROCESSES FOR DEVELOPMENT OF COHERENT UV AND XUV SOURCES Final Report, 1 Oct. 1981 - 30 Nov. 1982
Charles K. Rhodes, Herbert Pummer, and Hans Egger Sep. 1982 69 p
(Grant AF-AFOSR-0130-79; AF Proj. 2301)
(AD-A131837; AFOSR-83-0713TR) Avail: NTIS HC A04/MF A01 CSCL 20/14

High spectral brightness rare gas halogen (RGH) sources can be used to generate coherent extreme ultraviolet radiation by either harmonic generation mechanisms or direct multiquantum excitation of appropriate gain media. In order to demonstrate the basic characteristics of these two approaches, recent comparative measurements have been made. With the use of a 4 GW 193 nm (ArF*) system operating at a pulse duration of 10 ps, harmonic generation has been studied in several atomic and molecular media and used to generate 20 kW at 64.3 nm and 200 W at 38.6 nm. In addition, stimulated emission in molecular hydrogen on both the Lyman and Werner bands excited by two quantum absorption at 193 nm, has resulted in the generation of radiation as short as 117.6 nm at an efficiency of conversion approaching one percent. It has been concluded that the latter method is superior for the generation of short wavelength radiation. Extension of these results to both shorter wavelengths and higher power levels requires the ultraviolet. Recent studies of collision-free multiply-charged ion production with irradiation at 193 nm point to an anomalously strong coupling to high Z materials with processes involving as many as 99 quanta being observed. These multiquantum processes in the 40 - 80 eV range in certain atomic systems can be generated with existing laser instrumentation. Author (GRA)

N84-12468# Air Force Weapons Lab., Kirtland AFB, N. Mex.
PULSED POWER BIBLIOGRAPHY. VOLUME 2: ANNOTATED BIBLIOGRAPHY Final Report
J. Bernesderfer, ed., R. L. Druce, ed., B. Frantz, ed., A. H. Guenther, ed., M. Kristiansen, ed., J. P. OLoughlin, ed., and W. K. Pendleton, ed. Aug. 1983 273 p 2 Vol.
(AF Proj. 9993)
(AD-A131753; AFWL-TR-83-74-Vol-2) Avail: NTIS HC A12/MF A01 CSCL 20/5

Pulsed power and high-voltage technologies are playing an ever increasing role in weapons' effects simulation, fusion power research, power distribution, materials processing and medical research. It is a rapidly expanding field of applied physics as evidenced by the growth in published literature. Three years ago, the Air Force Weapons Laboratory (AFWL) initiated a project to compile a computerized data base of pulsed power research papers. The data base is stored on our IBM System 2000. This AFWL Technical Report is the first release of the bibliography to date. It contains about 2,500 full bibliographic citations, original sources, availability, key words and abstracts. There are three indices: Subject, Personal Author, and Corporate. There are 30 main subject headings, from Breakdown Studies to Switching. Volume II contains the citations. In addition to these entries, the data base contains about 7,500 additional titles. As these titles are added to the full bibliography, they will be published. GRA

N84-12469# Air Force Weapons Lab., Kirtland AFB, N. Mex.
PULSED POWER BIBLIOGRAPHY. VOLUME 1: INDICES Final Report
J. Bernesderfer, ed., R. L. Druce, ed., B. Frantz, ed., A. H. Guenther, ed., M. Kristiansen, ed., J. P. OLoughlin, ed., and W. K. Pendleton, ed. Aug. 1983 304 p 2 Vol.
(AF Proj. 9993)
(AD-A131752; AFWL-TR-83-74-Vol-1) Avail: NTIS HC A14/MF A01 CSCL 20/5

Pulsed power and high-voltage technologies are playing an ever increasing role in weapons' effects simulation, fusion power research, power distribution, materials processing and medical research. It is a rapidly expanding field of applied physics as evidenced by the growth in published literature. Three years ago, the Air Force Weapons Laboratory (AFWL) initiated a project to compile a computerized data base of pulsed power research papers. The data base is stored on our IBM System 2000. This AFWL Technical Report is the first release of the bibliography to date. It contains about 2,500 full bibliographic citations, original sources, availability, key words and abstract. There are three indices: Subject, Personal Author, and Corporate Author. There are 30 main subject headings, from Breakdown Studies to Switching. The indices are contained in Volume 1. GRA

N84-12470# Stanford Univ., Calif. Physics Lab.
LASER PHYSICS AND LASER SPECTROSCOPY Final Technical Report, 15 Mar. 1981 - 14 Apr. 1983
Robert L. Byer Jun. 1983 83 p
(Contract F49620-81-C-0047; AF Proj. 2301)
(AD-A131720; SU-GL-3598; AFOSR-83-0733TR) Avail: NTIS HC A05/MF A01 CSCL 20/5

During the past year a theoretical study of laser ionization mass spectroscopy has been completed. The study evaluated laser ionization combined with Fourier transform mass spectroscopy. A second generation single crystal fiber growth machine has been completed and high quality fibers of sapphire have been grown. Rapid progress in the growth and evaluation of small diameter single crystal fibers for nonlinear optical device application is being made. Theoretical model studies for laser plasma pumping of indium ion for a vacuum ultraviolet laser source have been carried out. Experiments have been initiated. The laser produced plasma X-ray source to other X-ray sources such as synchrotron and rotating anodes have been studied and compared. It is clear that the

laser plasma X-ray source has an important role to play in soft X-ray spectroscopy, X-ray lithography and X-ray microscopy. GRA

N84-12471# Boston Coll., Chestnut Hill, Mass. Dept. of Chemistry.
CHEMILUMINESCENCE AND LASER INDUCED FLUORESCENCE OF BORON ATOM REACTIONS Final Progress Report
Paul Davidovits 30 Jun. 1983 21 p
(Grant AF-AFOSR-0061-80; AF Proj. 2303)
(AD-A131709; AFOSR-83-0717TR) Avail: NTIS HC A02/MF A01 CSCL 20/5

The purpose of the work sponsored by grant AFOSR 80-0061 was to study the highly exoergic gas phase reactions of boron atoms. The main goal of these studies is to obtain a basic understanding of exoergic reactions of non metal atoms. These types of reactions play a fundamental role in fields such as combustion, plasma chemistry, laser induced chemistry and chemical lasers. We have completed rate and chemiluminescence studies of boron atom reactions with most of the important oxygen containing molecules of interest. From the results of these studies we are now able to suggest a qualitative model that may explain the nature of these reactions. GRA

N84-12472# California Univ., Livermore. Lawrence Livermore Lab.
DAMAGE THRESHOLDS OF THIN FILM MATERIALS AND HIGH REFLECTORS AT 248 nm
F. Rainer, W. H. Lowdermilk, D. Milam, C. K. Carniglia, T. T. Hart, and T. L. Lichtenstein 1982 10 p refs Presented at the Boulder Damage Symp., Colo., 15-17 Nov. 1982 Prepared in cooperation with Optical Coating Lab., Inc., Santa Rosa, Calif.
(Contract W-7405-eng-48)
(DE83-012663; UCRL-89097; CONF-821194-1) Avail: NTIS HC A02/MF A01

Twenty-ns, 248-nm KrF laser pulses were used to measure laser damage thresholds for halfway-thick layers of 15 oxide and fluoride coating materials, and for high reflectance coatings made with 13 combinations of these materials. The damage thresholds of the reflectors and single-layer films were compared to measurements of several properties of the halfway-thick films to determine whether measurements of these properties of single-layer films to determine whether measurements of these properties of single-layer films were useful for identifying materials for fabrication of damage resistant coatings. DOE

N84-12473# California Univ., Livermore. Lawrence Livermore Lab.
WINDOWS AND MIRRORS NEEDED FOR A LASER-DRIVEN PHOTONEUTRALIZER
J. H. Fink (Negion, Inc.) 22 Jun. 1983 14 p refs
(Contract W-7405-eng-48)
(DE83-013582; UCID-19788) Avail: NTIS HC A02/MF A01

Rough estimates of the neutral fraction obtainable from a photoneutralizer and the power required to operate are presented as functions of the window and mirror performance. DOE

N84-12474# Los Alamos Scientific Lab., N. Mex.
SUBHARMONIC BUNCHER FOR THE LOS ALAMOS FREE-ELECTRON LASER OSCILLATOR EXPERIMENT
John S. Fraser 1983 10 p refs Presented at the Soc. of Photo-Optical Instrumentation Engr. Conf., Bellingham, Wash., 26 Jun. 1983
(Contract W-7405-eng-36)
(DE83-015220; LA-UR-83-2151; CONF-830693-1) Avail: NTIS HC A02/MF A01

A high efficiency free electron laser oscillator experiment is constructed. A buncher system was designed to deliver 30 ps, 5 nC electron bunches to a 20 MeV standing wave linac at the 60th subharmonic of the 1300 MHz accelerator frequency. The first 108.3 MHz buncher cavity accepts a 5 ns, 5 A peak current pulse from a triode gun. Following a 120 cm drift space, a second 108.3 MHz cavity is used, primarily to enhance the bunching of the trailing half of the bunch. A 1300 MHz cavity with 20 cm drift spaces at the each end completes the beamline components. The bunching process continues into the linac's first three accelerating cells. Two thin iron shielded lenses and several large diameter solenoids provide axial magnetic fields for radial focusing. DOE

N84-12475# Burkes (T. R.), Inc., Lubbock, Tex. Pulse Power Engineering.
SOLID STATE COPPER VAPOR LASER MODULATOR Final Report
3 Dec. 1982 32 p refs
(Contract W-7405-eng-48)
(DE83-015837; UCRL-15538) Avail: NTIS HC A03/MF A01

The theory of operation, design, and efficiency calculations, circuit trade-off, and construction recommendations for an advanced pulse generator to meet the drive requirements for a copper vapor laser are described. This circuit employs thyratrons as switches and is essentially a 'capacitor discharge' with a peaking capacitor and inverse protection for the switches. The copper vapor laser represents a nonlinear load so that 'matched operation' in the classical sense is very difficult. Nontheless, satisfactory operation of the laser is obtained using this circuit and the approach taken in this design and analysis will essentially be to replace the thyratrons with magnetic devices and add sufficient circuits to interface with solid state switches. DOE

N84-12476# California Univ., Livermore. Lawrence Livermore Lab.
EXPERIMENTS TO STUDY THE FEASIBILITY OF MAKING AN X-RAY LASER AT THE NOVETTE LASER FACILITY
D. L. Matthews, P. Hagelstein, R. Kauffman, C. Wang, G. Leipelt, J. Wengert, G. Heaton, R. Price, G. Tirsell, P. Lee et al 17 May 1983 7 p Presented at the Conf. on Lasers and Electro-Optics, Baltimore, 17 May 1983
(Contract W-7405-eng-48)
(DE83-015615; UCRL-89541; CONF-830569-2) Avail: NTIS HC A02/MF A01

A set of experiments which are designed to study approaches to and search for the existence of amplified spontaneous emission at photon energies of 42.3, 53.6, 119.0, and 153.0 eV are discussed. The schemes utilize pumping from the Novette laser operated with cylindrical optics at 5 TW/beam and 100 psec. DOE

N84-12477# Helionetics, Inc., San Diego, Calif.
SEMICONDUCTOR PROCESSING WITH EXCIMER LASERS
R. T. Young, J. Narayan (ORNL, Tenn.), W. H. Christie (ORNL, Tenn), G. A. vanderLeeden, D. E. Rothe, and L. J. Cheng (JPL, California Inst. of Tech., Pasadena) Jan. 1983 14 p refs Presented at the Topical Meeting on Opt. Tech. for Remote Probing of the Atmosphere, Incline Village, Nev., 10 Jan. 1983 Sponsored in part by SERI
(Contract W-7405-eng-26)
(DE83-007509; CONF-830109-3) Avail: NTIS HC A02/MF A01

The advantages of pulsed excimer lasers for semiconductor processing are reviewed. Extensive comparisons of the quality of annealing of ion implanted Si obtained with XeCl and ruby lasers have been made. It is indicated that irrespective of the large difference in the optical properties of Si at UV and visible wavelengths, the efficiency of usage of the incident energy for annealing is comparable for the two lasers. However, because of the excellent optical beam quality, the XeCl laser can provide superior control of the surface melting and the resulting junction depth. The concentrations of electrically active point defects in the XeCl laser annealed region are 2 to 3 orders of magnitude lower than that obtained from ruby or Nd:YAG lasers. It is suggested that XeCl lasers should be suitable for fabricating the more advanced device structures required for VLSI or VHSIC applications. DOE

N84-12478# California Univ., Livermore. Lawrence Livermore Lab.
INERTIAL EFFECTS IN LASER-DRIVEN ABLATION
Robert J. Harrach, Abraham Szoeke, and W. Michael Howard

18 Aug. 1983 8 p refs Presented at the Am. Phys. Soc. Meeting on Shock Waves in Condensed Media, Santa Fe, N. Mex., 18-21 Jul. 1983
(Contract W-7405-eng-48)
(DE83-016941; UCRL-88682-Rev-1; CONF-830719-44-Rev-1) Avail: NTIS HC A02/MF A01

The gasdynamic partial differential equations (PDE's) governing the motion of an ablatively accelerated target contain an inertial force term that arises mathematically from acceleration of the reference frame in which the PDE's are written, and more physically from the requirement that part of the ablated mass (the deflagration wave zone) needs to be accelerated along with the unablated mass (payload). This effect is described, and its magnitude and parametric dependences by means of approximate analytical formulas inferred from the computer hydrocode calculation is estimated. The inertial term problems in laser fusion and laser equation of state studies found to reduce the attainable hydrodynamic efficiency of acceleration and implosion by up to 25% for typical conditions. DOE

N84-12479# Naval Research Lab., Washington, D. C. Laser Physics Branch.
RF CONDITIONED dc DISCHARGES FOR EXCITATION OF RARE GAS HALIDE LASERS Final Report
Jan. 1983 17 p refs
(Contract DE-AI01-82NE-50004)
(DE83-016537; DOE/NE-50004/T1) Avail: NTIS HC A02/MF A01

High power microwave sources for laser discharge switching and preionization are described. It is found that significant preionization using microwaves is possible. Ability to switch the discharge and operate a laser were demonstrated. It is recommended that experiments with the microwaves better concentrated between the electrodes should be performed. The best way to accomplish this appears to be using the side feed geometry; however, a large expansion of the microwaves should occur and then a cylindrical lens should be used to focus the microwaves between the electrodes. DOE

N84-12480# Los Alamos Scientific Lab., N. Mex.
INFRARED-LASER SPECTROSCOPY USING A LONG-PATHLENGTH ABSORPTION CELL
K. C. Kim and R. A. Briesmeister 1983 16 p refs Presented at the 26th ORNL-DOE Conf. on Anal. Chem. in Energy Technol., Knoxville, Tenn., 11-13 Oct. 1983
(Contract W-7405-eng-36)
(DE83-014197; LA-UR-83-1568; CONF-831025-1) Avail: NTIS HC A02/MF A01

The absorption measurements in an ordinary cell may require typically a few torr pressure of sample gas. At these pressures the absorption lines are usually pressure-broadened and, therefore, closely spaced transitions are poorly resolved even at diode-laser resolution. This situation is greatly improved in Doppler-limited spectroscopy at extremely low sample pressures. Two very long pathlength absorption cells were developed to be used in conjunction with diode lasers. They were designed to operate at controlled temperatures with the optical pathlength variable up to approx. 1.5 km. Not only very low sample pressures are used for studies with such cells but also the spectroscopic sensitivity is enhanced over conventional methods by a factor of 1000 to 10,000, improving the analytical capability of measuring particle densities to the order of 10 sq. in. molecules/cu cm. Some analytical aspects of the diode laser spectroscopy using the long-pathlength absorption cells in the areas of absorption line widths, pressure broadening coefficients, isotope composition measurements and trace impurity analysis are presented. Author

N84-12481# Los Alamos Scientific Lab., N. Mex.
ELECTRON-BEAM DIAGNOSTICS FOR THE LOS ALAMOS FREE-ELECTRON OSCILLATOR EXPERIMENT
R. L. Sheffield, W. E. Stein, A. Lumpkin, R. W. Warren, and J. S. Fraser 1983 6 p refs Presented at the Soc. of Photo-Optical Instrumentation Engr. Conf., Bellingham, Wash., 27 Jun. - 1 Jul. 1983
(Contract W-7405-eng-36)
(DE83-017230; LA-UR-83-2383; CONF-830693-2) Avail: NTIS HC A02/MF A01

Electron beam diagnostics for the Los Alamos free electron laser oscillator experiment were designed to measure the time dependence of the electron energy distribution with time intervals ranging from 30 ps to 200 (SIGMA)s. The electron beam consists of macropulses that have a 100 (SIGMA)s duration and a 1-Hz repetition rate. Each macropulse consists of a series of micropulses that have approx. 30 ps duration, approx. 50 A peak current, and approx. 50 ns separation. The primary purposes of the electron beam diagnostics is twofold: (1) optimization of the bunching system to provide a maximum peak current in the micropulses; and (2) measurement of the time dependence of the electron energy distribution during build up of the photon field in the oscillator. Because the exact time of build up is uncertain, provisions are made to allow the observation window to be varied from 10 to 100 (SIGMA)s and to be delayed by times up to 100 (SIGMA)S. DOE

N84-12482# California Univ., Livermore. Lawrence Livermore Lab.
FEASIBILITY OF A LASER OR CHARGED-PARTICLE-BEAM FUSION-REACTOR CONCEPT WITH DIRECT ELECTRIC GENERATION BY MAGNETIC-FLUX COMPRESSION
George Patrick Lasche Jun. 1983 210 p refs
(Contract W-7405-eng-48)
(DE83-015735; UCRL-53434) Avail: NTIS HC A10/MF A01

A new concept for an inertial-confinement fusion reactor is described which, because of its fundamentally different approach to blanket geometry and energy conversion, makes possible a unique combination of high efficiency, high power density, and low radioactivity. The conventional blanket is replaced with a liquid-density mass of lithium contiguously surrounding the fusion yield. This compact blanket configuration produces the maximum shock-induced kinetic energy metal and the maximum neutron absorption per unit mass. The shock-induced kinetic energy of the liquid lithium is converted directly to electricity with high efficiency by work done against a pulsed normal-conducting magnetic field applied to the exterior of the lithium. DOE

N84-12483# Los Alamos Scientific Lab., N. Mex.
SELECTIVE LASER IONIZATION FOR MASS-SPECTRAL ISOTOPIC ANALYSIS
C. M. Miller, N. S. Nogar, and S. W. Downey 1983 6 p refs Presented at the 5th Laser-Based Ultrasensitive Spectry. and Detection Conf., San Diego, Calif., 23 Aug. 1983
(Contract W-7405-eng-36)
(DE83-017303; LA-UR-83-2319; CONF-8308114-1) Avail: NTIS HC A02/MF A01

Resonant enhancement of the ionization process can provide a high degree of interference problem. In addition, extension of this method to isotopically selective ionization has the potential for greatly increasing the range of isotope ratios that can be determined experimentally. This gain can be realized by reducing or eliminating the tailing of the signal from the high-abundance isotope into that of the low-abundance isotope, augmenting the dispersion of the mass spectrometer. The hardware and techniques used in both the pulsed and cw RIMS experiments are discussed. Results are presented for both cw ionization experiments on Lu/Yb mixtures, and spectroscopic studies of multicolor RIMS of Tc. DOE

N84-12484# Los Alamos Scientific Lab., N. Mex.
EVOLUTION OF LONG PULSES IN A TAPERED WIGGLER FREE-ELECTRON LASER
John C. Goldstein 1983 10 p refs Presented at the Soc. of Photo-Optical Instrumentation Engr. DARPA Free-Electron Laser Conf., Eastsound, Wash., 27 Jun. - 1 Jul. 1983
(Contract W-7405-eng-36)
(DE83-017235; LA-UR-83-2411; CONF-8306121-2) Avail: NTIS HC A02/MF A01

The evolution of a long pulse in a tapered wiggler free electron laser is studied by numerical solution of the 1-D theoretical model for a realistic set of magnet, electron beam, and optical resonator parameter values. Single pass gain curves are calculated for low and high light intensity. It is found that an initial, low amplitude, incoherent pulse grows into a coherent pulse whose growth rate agrees with the calculated small signal gain. The transient evolution of coherent pulses is calculated for several different cavity length detunings, and a quasi steady state desynchronism curve is given. The frequency changing behavior of the optical pulse is shown to occur through sideband generation associated with synchrotron oscillations. Pulse evolution with an ideal intracavity high pass optical filter is calculated. DOE

N84-12485# Los Alamos Scientific Lab., N. Mex.
THE LOS ALAMOS FREE-ELECTRON-LASER OSCILLATOR EXPERIMENT: PLANS AND PRESENT STATUS
R. W. Warren, J. S. Fraser, W. E. Stein, J. G. Winston, T. A. Swann, A. Lumpkin, R. L. Sheffield, J. E. Sollid, B. E. Newnam, C. A. Brau et al 1983 8 p refs Presented at the 4th Workshop on Free-Electron Laser Devices, Eastsound, Wash., 27 Jun. - 1 Jul. 1983
(Contract W-7405-eng-36)
(DE83-017290; LA-UR-83-2443; CONF-8306121-3) Avail: NTIS HC A02/MF A01

The free electron laser amplifier experiment to allow its use as an oscillator at 10.6 microns was outlined. Major changes were required, all of which are completed. The necessity for these changes and the details of their fulfillment are discussed. DOE

N84-12486# California Univ., Livermore. Lawrence Livermore Lab.
CREATION OF ULTRA-HIGH-PRESSURE SHOCKS BY THE COLLISION OF LASER-ACCELERATED DISKS: EXPERIMENT AND THEORY
M. D. Rosen, D. W. Phillion, R. H. Price, E. M. Campbell, S. P. Obenschain, R. R. Whitlock, E. A. McLean, and B. H. Ripin 24 Aug. 1983 11 p refs Presented at the Am. Phys. Soc. Topical Conf. on Shock Waves in Condensed Matter, Santa Fe, N. Mex., 18-21 Jul. 1983 Prepared in cooperation with Naval Research Lab.
(Contract W-7405-eng-48)
(DE83-017366; UCRL-89750; CONF-830719-49) Avail: NTIS HC A02/MF A01

The SHIVA laser system was used to accelerate carbon disks to speeds in excess of 100 km/sec. The 3KJ/3 ns pulse, on a 1 mm diameter spot of a single disk produced a conventional shock of about 5 MB. The laser energy can, however, be stored in kinetic motion of this accelerated disk and delivered, reconverted to thermal energy, upon impact with another carbon disk. This collision occurs in a time much shorter than the 3 ns pulse, thus acting as a power amplifier. The shock pressures measured upon impact are estimated to be in the 20 MB range, which demonstrates the amplification power of this colliding disk technique in creating ultrahigh pressures. Theory and computer simulations of this process are discussed. DOE

N84-12487# California Univ., Los Angeles. Dept. of Chemistry.
TIME-RESOLVED LASER STUDIES ON THE ENERGY TRANSFER AND THE CONFIGURATION CHANGES IN BACTERIOHODOPSIN Progress Report, 1 Dec. 1982 - 30 Nov. 1983
M. A. El-Sayed 1983 7 p
(Contract DE-AT03-76ER-70278)
(DE83-015708; UCLA-34P278-39) Avail: NTIS HC A02/MF A01

Transient picosecond Raman methods, time-resolved fluorescence protein techniques and a method based on retinal-protein photoselection were developed. Detailed Raman studies on the nano-and picosecond time domain were carried out on bacteriorhodopsin in H2O and D2O. A detailed study of the cycle under dried and different humidities was carried out using resonance Raman techniques. Combining our results together with those of other workers, a cycle for the primary processes based on the retinal vibrational behavior can be written down. Polarized photochemistry techniques were used to study the polarization characteristics of the photolysis laser at different wavelengths of excitation relative to the daughter retinal absorption transition moment (along the retinal axis). The results are not only useful in assigning the absorption characteristics of the retinal but also indicative of the energy transfer processes occurring between the different aromatic molecules of the protein. DOE

N84-12488# Los Alamos Scientific Lab., N. Mex.
PROCEEDINGS OF THE 16TH LAMPF USERS-GROUP MEETING
James N. Bradbury, comp., Kit Ruminer, ed., and Beverly Talley, ed. Apr. 1983 156 p refs Meeting held at Los Alamos, N. Mex., 1-2 Nov. 1982
(Contract W-7405-eng-36)
(DE83-013215; LA-9767-C; CONF-821191) Avail: NTIS HC A08/MF A01

The status and operation of the Los Alamos Meson Physics Facility are discussed as well as prospects for future activities in U.S. nuclear science. Other topics covered include low energy strong interactions; parity violations in nuclei and other results from the pion spectrometer. The Triumpf kaon factory plans, and physics at the facility are also explored. A.R.H.

N84-12489# Stanford Linear Accelerator Center, Calif.
FREE-ELECTRON-LASER RESEARCH
P. L. Morton Aug. 1983 4 p refs Presented at the 12th Intern. Conf. on High Energy Accelerators, Batavia, Ill., 11-16 Aug. 1983
(Contract DE-AC03-76SF-00515)
(DE83-016957; SU-SLAC-Pub-3176; CONF-830822-16) Avail: NTIS HC A02/MF A01

A simple description and schematic representation of a free electron laser is given. The evolution of the electron energy distribution is demonstrated as well as the extraction efficiency as a function of optical power. The major restriction in free electron laser research appears to be the need for good quality electron beams. Research on achieving such electron beams and accelerator technology is being advanced. A.R.H.

N84-12490# European Space Agency, Paris (France).
Y03: PREQUALIFICATION OF SURFACE TREATMENT. MEASUREMENT OF LASER REFLECTING POWER
M. Dinguirard and B. Duchenne Sep. 1983 16 p Transl. into ENGLISH of "Y03: Prequalification du Traitement de Surface. Mesure du Pouvoir Reflecteur Laser", ONERA, Toulouse Report CERT-2/6035-DERO, Mar. 1977
(ESA-TT-791; CERT-2/6035-DERO) Avail: NTIS HC A02/MF A01

The reflecting power of aluminum mirrors thermally protected by a thick film dielectric coating was measured with a dye laser in the spectral range 5900 to 6100. Destructive interference occurs in the case of polarization perpendicular to the plane of incidence. This can reduce the reflecting power by 26%. Author (ESA)

37 MECHANICAL ENGINEERING

Includes auxiliary systems (non-power); machine elements and processes; and mechanical equipment.

N84-12491* National Aeronautics and Space Administration. Goddard Space Flight Center, Greenbelt, Md.
HOLDING FIXTURE FOR A HOT STAMPING PRESS Patent
Raymond P. Harris, inventor (to NASA) Issued 19 Jul. 1983 6 p Filed 16 Jan. 1981 Supersedes N81-16470 (19 - 07, p 0918)
(NASA-Case-GSC-12619-1; US-Patent-4,393,777;
US-Patent-Appl-SN-225499; US-Patent-Class-101-407BP;
US-Patent-Class-269-3) Avail: US Patent and Trademark Office CSCL 13I

A hand held guide for manually positioning a work piece between the anvil rib and tool of a hot die stamping press is described. A groove completed by interchangeable cover plates attached at one end of the guide conforms to a cross sectional dimension common to similar workpieces and, with a force fit,

retentively holds each of the workpieces.
Official Gazette of the U.S. Patent and Trademark Office

N84-12492* National Aeronautics and Space Administration. Goddard Space Flight Center, Greenbelt, Md.
UNIDIRECTIONAL FLEXURAL PIVOT Patent
Hossein Bahiman, inventor (to NASA) Issued 20 Sep. 1983 5 p Filed 16 Mar. 1981 Supersedes N81-22359 (19 - 13, p 1762)
(NASA-Case-GSC-12622-1; US-Patent-4,405,184; US-Patent-Appl-SN-243684; US-Patent-Class-308-2A) Avail: US Patent and Trademark Office CSCL 13I

A pair of generally coaxial mutually rotatable cylindrical outer ring members are held in spaced-apart relationship by three parallelogram-shaped, relatively thin, flexible, flat planar spring elements. These spring elements are substantially inextensible in length and are joined to the inside of the outer ring members and held in position by arcuate inner ring segments, three for each outer ring members, which respectively span an arc of substantially 120. The parallelogram shape of the spring elements provides a slanted interconnection between the outer ring members. The direction of slant, moreover, determines in which direction the spring elements can flex or bend unidirectionally to relieve the compression stress imparted thereto by any mutual angular rotation of the outer ring members.
Official Gazette of the U.S. Patent and Trademark Office

N84-12493* National Aeronautics and Space Administration. Langley Research Center, Hampton, Va.
VERTICAL SHAFT WINDMILL Patent
David C. Grana and Spencer V. Inge, Jr., inventors (to NASA) Issued 15 Nov. 1983 4 p Filed 28 May 1982 Supersedes N82-29713 (20 - 20, p 2849)
(NASA-Case-LAR-12923-1; US-Patent-4,415,311; US-Patent-Appl-SN-383063; US-Patent-Class-416-117; US-Patent-Class-416-132B) Avail: US Patent and Trademark Office CSCL 13I

A vertical shaft has several equally spaced blades mounted. Each blade consists of an inboard section and an outboard section skew hinged to the inboard section. The inboard sections automatically adjust their positions with respect to the fixed inboard sections with changes in velocity of the wind. This windmill design automatically governs the maximum rotational speed of shaft.
Official Gazette of the U.S. Patent and Trademark Office

N84-12494 Ruhr Univ., Bochum (West Germany). Inst. fuer Konstruktionstechnik.
USE OF THE ONE-DIMENSIONAL THEORY OF THE FILAMENT OF FLOW FOR THE INTERPRETATION AND SYNTHESIS OF MUFFLERS IN EXHAUST PIPES OF INTERNAL COMBUSTION ENGINES [ANWENDUNG DER EINDIMENSIONALEN STROMFADENTHEORIE ZUR AUSLEGUNG UND SYNTHESE VON SCHALLDAEMPFERN IN AUSPUFFLEITUNGEN VON VERBRENNUNGSMOTOREN]
Abdel G. Sadek 1981 210 p refs In GERMAN; ENGLISH summary
(Rept-81.4) Copyright. Avail: Issuing Activity

To calculate and optimize muffler systems of internal combustion engines, the interactive computer program ASDE-1 was conceived. It is based on one-dimensional wave propagation, considering the medium flow velocity and different temperatures in the exhaust pipe system. To test the limits of the precision of the theory of one-dimensional wave propagation, the computer program ASDZ-2 was developed. It is based on the axially symmetrical two-dimensional theory of the propagation of waves and the finite element method. The formulation of the finite elements used is general and can be applied to mufflers with arbitrary geometrical boundaries. A way to reduce the influences of the two-dimensional theory of wave propagation on the one-dimensional one is suggested. The tuning and adaptation of the muffler system of a 6-cylinder otto engine with regard to an optimum of output and reduction of noise, using the PROMO program, is shown. Author (ESA)

N84-12495*# Texas A&M Univ., College Station. Turbomachinery Labs.
THE SSME SEAL TEST PROGRAM: LEAKAGE TESTS FOR HELICALLY-GROOVED SEALS Progress Report
Dara W. Childs 1 Nov. 1983 95 p refs
(Contract NAS8-33716)
(NASA-CR-170921; NAS 1.26:170921; Seal-3-83) Avail: NTIS HC A05/MF A01 CSCL 11A

Helically grooved annular seal configurations were tested in highly turbulent flow to determine if reduced leakage and enhanced stability would result from the pumping action of the seal. It was found that: (1) leakage of a helically grooved seals decreases with running speed; (2) leakage reduction due to increased running speed is greater at lower values of R sub a; (3) an asymptote for leakage reduction is indicated with increasing running speed; (4) leakage is reduced by reducing the ridge (minimum) and average clearances; (5) leakage increases with increasing pitch angles and with increasing groove depth. Plain seals with smooth rotors and stators will leak more than a helically grooved seal. It was also found that plain seals with a rough rotor and a rough stator leak less than a properly designed helically grooved seal. A properly designed helically grooved seal consumes at least twice as much power as a conventional annular seal. A.R.H.

N84-12496# Albany International Corp., Dedham, Mass.
SEAMLESS COLLAPSIBLE FUEL TANKS Final Report, Mar. 1982 - Mar. 1983
Norman J. Abbott and Robert E. Erlandson Jul. 1983 15 p
(Contract DAAK70-80-C-0045)
(AD-A131933; AD-E850386; G80143) Avail: NTIS HC A02/MF A01 CSCL 13/4

Twenty-Three by twenty foot (lay flat) pieces of tubular fabric were coated with polyurethane and fabricated into two 7500-gallon fuel tanks. The tanks were shipped to Arizona for filling and exposure testing. Author (GRA)

N84-12497# General Electric Co., Philadelphia, Pa. Space Systems Div.
NEW DEVELOPMENTS IN COMPOSITE-FLYWHEEL CONTAINMENT
Anthony P. Coppa 1983 17 p refs Presented at the 2nd European Symp. on Flywheel Energy Storage, Turin, 9-13 May 1983
(Contract W-7405-eng-26)
(DE83-012583; CONF-830503-3) Avail: NTIS HC A02/MF A01

Composite construction is increasingly applied to the development of efficient flywheel rotors for vehicular energy storage systems. New developments in understanding and quantifying composite rotor burst containment behavior are contributing to advancing the practicality of such systems. Some of these developments are discussed, as well as overall design requirements for containment housings. A novel analysis of composite rotor burst containment action is described. The analysis considers fragmentation released from a failed composite rotor as undergoing a progressive crushing process during containment. The process is characterized by a constant parameter called the apparent fragment crushing strength, which is the ability of initially released fragmentation to resist progressive breakdown under the applied containment forces. The analysis was successfully applied to correlating the containment test behavior of a variety of high performance composite rotors. Burst containment weight estimates based on the analysis are also presented for several containment ring constructions. Containment considerations and test correlation for a loose rotor spinning in the housing interior are also discussed. DOE

N84-12498# Air Force Systems Command, Wright-Patterson AFB, Ohio. Foreign Technology Div.
STEAM TURBINE AS UNIPOLAR GENERATOR
Ye. G. Oleynikov 30 Jun. 1983 12 p refs Transl. into ENGLISH from Energ. Mashinostr. (USSR0, no. 14, 1972 p 106-112
(AD-A131142; FTD-ID(RS)T-0398-83) Avail: NTIS HC A02/MF A01 CSCL 10/2

The technological process in which magnetization of parts occurs in order to prevent these parts from going into the assembled turbine without preliminary demagnetization was determined. A program was outlined for measuring the magnetization of parts and turbine assemblies during operation. GRA

N84-12499# Dave (Sharad M.), Farmington Hills, Mich.
CONTROLLED COMBUSTION ENGINE EVALUATION Final Report
Sharad M. Dave 1983 29 p refs
(Contract DE-FG01-81CS-15040)
(DE83-011245; DOE/CS-15040/T1) Avail: NTIS HC A03/MF A01

The Controlled Combustion Engine (CCE) theory somewhat follows a shrouded valve concept in that the intake valve mechanism acts as a variable restrictor and turbulence inducer to the flowing fuel/air charge. By adjustment of the shroud ring from a retracted to extended position it may be possible to increase compression ratio (CR), lower pumping loss by leaner operation, and improve idle quality by control of exhaust residual. All testing was performed on a used (13,000 miles) 1979 Ford 2.3 litre over head cam engine with 2 bbl. feedback Holly/Weber carburetor. Production data was obtained at a 9 to 1 CR. CCE configuration utilized the production short block and a production cylinder head modified for the shroud mechanism. The CCE head was later milled to provide a CR increase to 11 to 1. DOE

N84-12500# Oak Ridge National Lab., Tenn.
DYNAMIC ANALYSIS OF THE FLUIDYNE
C. D. West 1983 27 p refs Presented at the 18th Intersoc. Energy Conversion Eng. Conf., Orlando, Fla., 21-26 Aug. 1983
(Contract W-7405-eng-26)
(DE83-017283; CONF-830812-49) Avail: NTIS HC A03/MF A01

The dynamic behavior of the liquid piston Stirling engine is analyzed using the vector or phasor method of representing the motions of coupled systems. The result is a simple physical explanation of the feedback mechanism most frequently employed in these machines. In addition, the method leads to an easy derivation of certain results already known from experiment or from more complex analyses. DOE

N84-12501# Oak Ridge National Lab., Tenn.
EFFECTS OF PRESSURE-DROP CORRELATIONS ON STIRLING-ENGINE PREDICTED PERFORMANCE
Norbert C. J. Chen and Fred P. Griffin 1983 6 p refs Presented at the 18th Intersoc. Energy Conversion Eng. Conf., Orlando, Fla., 21 Aug. 1983
(Contract W-7405-eng-26)
(DE83-017279; CONF-830812-52) Avail: NTIS HC A02/MF A01

Pressure drop correlations for Stirling engine applications were studied from three perspectives: (1) sensitivity studies of their effects on predicted engine performance; (2) presentation of an improved correlation for steady unidirectional flow through wire screen matrices; and (3) a theoretical analysis of friction factors for oscillating laminar flow through circular tubes. The sensitivity studies of two reference engines show significant effects of regenerator pressure drop on engine performance. The improved friction factor correlation for steady unidirectional flow fits the data satisfactorily with an uncertainty of about + or - 10%. It is shown that the derived friction factor for oscillating flow is characterized by two Reynolds numbers: steady and kinetic. When this friction factor is compared with the one for steady unidirectional flow, no significant difference is observed when the kinetic Reynolds number is small, but there is a considerable increase at high kinetic Reynolds numbers. DOE

N84-12502# Fermi National Accelerator Lab., Batavia, Ill.
SATELLITE REFRIGERATOR COMPRESSORS WITH THE OIL AND MOISTURE REMOVAL SYSTEMS
J. A. Satti Aug. 1983 18 p
(Contract DE-AC02-76CH-03000)
(DE83-016079; FERMILAB/TM-1198) Avail: NTIS HC A02/MF A01

The piping and the components schematic for four Mycom compressor skids per building with each having an independent oil and moisture removal system is shown. The Mycom skids each consist of an oil injected screw compressor of 750 SCFM capacity with a 350 hp motor, oil pump, oil cooler, and oil separator. Helium gas returning from the heat exchanger train is compressed from 1 atm to 20 atm in the compressor. The compressed gas is then passed through the three coalescer demister where oil mist is separated from the helium gas. The helium gas then flows through the charcoal adsorber and molecular sieve where any residual oil vapor and water vapor are removed. The final stage of purification is the final filter which removers any remaining particulates from the compressed helium gas. The end product of this system is compressed and purified helium gas ready to be cooled down to cryogenic temperatures. DOE

N84-12503# Sandia Labs., Albuquerque, N. Mex.
HERMETICALLY SEALED MICROMINIATURE MULTISOCKET CONNECTOR
Paul J. Konnick 1983 7 p Presented at the Electron. Connector Study Group Symp., Philadelphia, 14 Nov. 1983
(Contract DE-AC04-76DP-00789)
(DE83-017484; SAND-83-0665C; CONF-831182-1) Avail: NTIS HC A02/MF A01

A hermetic microminiature multisocket connector was designed as a means of interfacing with a sealed component package in a weapon system to ensure a controlled environment. The connector is characterized by glass sealing of a high density contact pattern, a weldable mounting flange, and by microminiature size. This glass to metal sealing method, using individual glass beads, requires 51 holes on 50 mil centers in the web portion of the shell. As an alternative to the glass to metal method, the connector contacts and shell were redesigned for compatability with ceramic to metal sealing techniques. In this method, the metal web of the shell is replaced with a ceramic web containing 51 metallized holes on 50 mil centers. The design requirements for the hermetic microminiature multisocket connector are presented. The physical and electrical characteristics and the electrical and environmental test program are described. DOE

N84-12504# Martini Engineering, Richland, Wash.
REVISED ISOTHERMAL ANALYSIS PROGRAM FOR STIRLING ENGINES
W. R. Martini 1983 7 p refs Presented at the 18th Intersoc. Energy Conversion Eng. Conf., Orlando, Fla., 21-26 Aug. 1983 Sponsored in part by ORNL
(Contract W-7405-eng-26)
(DE83-017276; CONF-830812-51) Avail: NTIS HC A02/MF A01

An isothermal analysis, which was described in the literature previously, was improved and made more versatile. Some of the heat and power loss equations were changed and the effect of the adiabatic spaces on the power and the heat input is included. The Stirling cycle machine operating can be considered as either a heat engine or a heat pump. It is suggested that engine data agreed well with the program and the other did not. The program should be used with care. DOE

N84-12505# Maschinenfabrik Augsburg-Nuernberg A.G., Munich (West Germany). Bereich Neue Technologie.
CONSTRUCTION OF TWO WIND TURBINES AEROMAN 11/11 FOR INDONESIA Final Report, Aug. 1982
Hans Martin Thiele Bonn Bundesministerium fuer Forschung und Technologie Jul. 1983 39 p refs In GERMAN; ENGLISH summary Sponsored by Bundesministerium fuer Forschung und Technologie
(BMFT-FB-T-83-143; ISSN-0340-7608) Avail: NTIS HC A03/MF A01; Fachinformationszentrum, Karlsruhe, West Germany DM 8

An ice making machine based an wind turbine technology was developed. The machine runs without an electrical storage system. The turbine consists of a double-bladed glass-reinforced plastic rotor with a variable blade angle of 90 deg and a two stage spur gear. The rotor diameter is 11.6 m, the number of

revolutions is 77 r.p.m. and it is lee side mounted on a 10 m high mast. The step up gear ratio is 1 to 19.5 and the synchronous generator voltage is 220/380 V for a power output of 11 kw. The ice making machine consists of an air cooled condenser, a compressor, a freezing cylinder and a feed screw. A specific ice production of 9 kg/kWh is reported for a test run of 72 hours. Author (ESA)

N84-12506# Environmental Protection Agency, Ann Arbor, Mich. Control Technology Assessment and Characterization Branch.
A STUDY OF THE RELATIONSHIP BETWEEN EXHAUST EMISSIONS AND FUEL ECONOMY
Jensen P. Cheng, Larry C. Landman, and Robert D. Wagner May 1983 582 p
(PB83-235564; EPA/AA/CTAB/TA/83-2) Avail: NTIS HC A25/MF A01 CSCL 13F

The relationship between exhaust emissions and fuel economy of automobiles is discussed. Examined are vehicle characteristics such as driveability, performance, costs, octane requirements, and production lead time. Also included is past EPA reports on fuel economy and exhaust emissions and a literature search identifying other pertinent reports. Finally, the 1981 automobile fleet was examined and its fuel economy and exhaust emissions performance were assessed. Author (GRA)

N84-12507# Ricardo & Co., Engineers (1927) Ltd., Shoreham-by-Sea (England).
OPTIMUM ENGINE FOR METHANOL UTILIZATION Final Report
Apr. 1983 178 p refs
(Contract EPA-68-03-1647)
(PB83-239459; EPA-460/3-83-005) Avail: NTIS HC A09/MF A01 CSCL 21G

The design, construction, and calibration of an engine for methanol utilization incorporating a high compression ratio, compact chamber combustion system are described. Recommendations for further work are included. GRA

38 QUALITY ASSURANCE AND RELIABILITY

Includes product sampling procedures and techniques; and quality control.

N84-12508 Defence Research Information Centre, Orpington (England).
NON-DESTRUCTIVE TESTING OF NON-METALLIC MATERIALS USING MICROWAVES
G. Wittig Jul. 1983 19 p refs Transl. into ENGLISH of Materialpruefung (West Germany), v. 19, no. 4, 1977 p 137-143 (DRIC-T-6974; BR88807) Copyright. Avail: Issuing Activity

The problems connected with practical applications of microwaves to nondestructive testing were investigated in the frequency band from 26.5 to 40 GHz. A test apparatus for measuring transmission and reflection is described. The effects of antenna arrangement on sensitivity of detection of inhomogeneities were also investigated. Tests were conducted on objects with artificial defects to determine the manner of signal scattering. Measurements on reinforced plastics, concrete, and fine sand with differing quantities of water, to determine moisture content, are described. Author (ESA)

N84-12509# Air Force Wright Aeronautical Labs., Wright-Patterson AFB, Ohio. Metals Behavior Branch.
IMPROVING NDE (NON-DESTRUCTIVE EVALUATION) CAPABILITY THROUGH MULTIPLE INSPECTION WITH APPLICATION TO GAS TURBINE ENGINE DISKS Final Report, Feb. - Aug. 1982
Jann N. Yang (George Washington Univ., Washington, D.C.) and Robert C. Donath Jun. 1983 96 p
(AF Proj. 2307)
(AD-A131762; AFWAL-TR-82-4111) Avail: NTIS HC A05/MF A01 CSCL 14/2

Techniques are not capable of repeatedly producing correct indications when applied to flaws of the same length. As a result, the probability of detection (POD) for all cracks of a given length has been used to define the capability of a particular NDE system in a given environment. Thus the NDE reliability consists of two types of errors. For safety-critical components in airframe structures, Type I error is of major concern. According to the damage tolerant requirement, the inspection limit or the reset crack size should be the crack length associated with a 90% detection probability and 95% confidence level. On the other hand the main criterion used for analysis of the retirement-for-cause of gas turbine engine components is the minimization of the life cycle cost. The objectives of this report are to: (1) formulate and derive mathematically the resulting POD curve for multiple inspection systems; (2) investigate quantitatively the benefit and advantage of multiple inspection procedures; (3) establish the direction in which the NDE capability should be improved under certain mission requirements; (4) establish the strategy and sequence for multiple inspection procedures to reduce either Type I or Type II errors or both; (5) determine the POD curve for a disk from the POD curve of an NDE system; (6)determine the inspection reliability of engine disks; and (7) evaluate the benefit of multiple inspections for engine disks. GRA

N84-12510# Hanford Engineering Development Lab., Richland, Wash.
QUALITY IS NOT A DIRTY WORD
V. A. Coston 1983 6 p Presented at the Am. Soc. for Quality Control Conf., Richland, Wash., 17-19 Apr. 1983
(Contract DE-AC06-76FF-02170)
(DE83-012166; HEDL-SA-2890-FP; CONF-830475-2) Avail: NTIS HC A02/MF A01

There is a great deal of emphasis today on management's commitment to quality. Yet with all the hue and cry about this commitment do we find much more happening than just lip service. Are quality professionals aiding and abetting the nonacceptance of quality organizations, resulting in their exclusion from the management. Quality professionals must recognize they cannot divorce themselves from cost and schedule. They must recognize they are not policemen with omnipotent authority. Self-recognition must occur and be acted upon for changes in attitudes and opinions of others to be affected. There are, of course, other factors involved. But in searching for the root cause of the problem, does the evidence of those other factors again point back to the Quality professionals. Quality is not a dirty word. We must convince ourselves before we can convince others. DOE

N84-12511# Argonne National Lab., Ill.
DEVELOPMENT IN RELIABILITY MODELS AND METHODS
J. K. Vaurio 1983 6 p refs Presented at the Am. Nucl. Soc. Winter Meeting, San Francisco, 30 Oct. - 4 Nov. 1983
(Contract W-31-109-eng-38)
(DE83-014683; CONF-831047-35) Avail: NTIS HC A02/MF A01

Analytical developments in modeling reliability characteristics for components and systems were analyzed. Modeling involves definition of failure modes, relevant probability and timing parameters for the modes, and derivation of explicit equations for component and system unavailabilities and failure intensities. DOE

N84-12512# Ames Lab., Iowa.
INVERSE BORN APPROXIMATION: EXACT DETERMINATION OF SHAPE OF CONVEX VOIDS
James H. Rose and Jon L. Opsal (California Univ., Lawrence Livermore Lab.) 1983 11 p refs Presented at the Conf. on Quantitative NDE, Santa Cruz, Calif., 7-12 Aug. 1983
(Contract W-7405-eng-82)
(DE83-017685; IS-M-440; CONF-830811-5) Avail: NTIS HC A02/MF A01

The Inverse Born Approximation (IBA) to the elastic wave inverse scattering problem is known to give highly accurate results for the shape of complex voids. This paper presents an argument

demonstrating that the IBA is, in fact, exact for determining the size, shape and orientation of a wide class of these scatterers given infinite bandwidth and unlimited aperture information. Essentially, the argument demonstrates how the IBA algorithm picks out the singular contribution to the impulse response function and correctly relates it to the shape of the scatterer. Some specific examples are used to illustrate the more intuitive aspects of the discussion. DOE

N84-12513# Ames Lab., Iowa.
ELASTIC-WAVE INVERSE SCATTERING IN NON-DESTRUCTIVE EVALUATION
James H. Rose 1983 16 p refs
(Contract W-7405-eng-82)
(DE83-017683; IS-M-433; CONF-8309135-1) Avail: NTIS HC A02/MF A01

Ultrasonic detection and characterization of flaws in metals and ceramics is of considerable technological interest. Scattering and inverse scattering theories were applied to these tasks in a systematic manner and considerable progress has resulted. The development of scattering and inverse scattering methods in the AF/DARPA Program in Quantitative Non-destructive Evaluation are reviewed. The inverse Born approximation, is discussed. Progress is reviewed and the ability of the method to distinguish volumetric and cracklike flaws is demonstrated. DOE

N84-12514# Messerschmitt-Boelkow-Blohm G.m.b.H., Ottobrunn (West Germany). Betriebsbereich.
QUALITY CONTROL AND SAMPLE COMPARISON BY DIFFERENTIAL MODAL ANALYSIS [QUALITAETSKONTROLLE UND MUSTERVERGLEICH MITTELS DIFFERENTIELLER MODALANALYSE]
O. Bschorr and J. Mittmann 12 Apr. 1983 12 p refs In GERMAN
(MBB-BB-543-83-OE) Avail: NTIS HC A02/MF A01

A differential modal analysis measurement system is presented. It was developed for final controls in series production in order to check dimensional stability and errors of the different components. The method consists in measuring the eigenfrequencies of the components and comparing them with those of a standard specimen. The modal analysis deduces magnitude and position of the error with high accuracy. An exciting force of 10 to the power -4 of the sample weight is sufficient for the frequency measurement. A frequency accuracy better than 0.1% is obtained for measuring times of 100 vibration periods. An example using a bending beam is given. Author (ESA)

N84-12515# Maschinenfabrik Augsburg-Nuernberg A.G., Munich (West Germany). Abt. Werkstofftechnik.
DEVELOPMENT OF AN ULTRASONIC TESTING PROCEDURE FOR ELECTRON BEAM WELDED PARTS FOR AEROSPACE APPLICATIONS Final Report, Apr. 1980
Peter Salfner and Eberhard Wagner Bonn Bundesministerium fuer Forschung und Technologie Jun. 1983 83 p In GERMAN; ENGLISH summary Sponsored by Bundesministerium fuer Forschung und Technologie
(BMFT-FB-W-72-011; ISSN-0170-1339) Avail: NTIS HC A05/MF A01; Fachinformationszentrum, Karlsruhe, West Germany DM 17,50

Improved quality control of weld seams by means of a nondestructive testing method based on the ultrasonic impulse echo is covered. The procedure is designed to reduce production costs of the Ariane rocket turbopump wheels. The use of turbine blades made from rolled profiles and joining to gearbody by electron beam welding are proposed. Using the immersion method with single and dual probes natural defects of less than 0.2 mm in length were detected, proving the method to be applicable for general use. Mechanized test procedure and simultaneous documentation of defects reduce the inspection time. Acceptance criteria for weld seams were determined and test specifications for the routine procedure were established. Author (ESA)

N84-12516# Aeronautical Research Inst. of Sweden, Stockholm. Structures Dept.
AN X-RAY RADIOGRAPHY STUDY OF DELAMINATION GROWTH IN NOTCHED CARBON/EPOXY LAMINATES
T. Mohlin, L. Carlsson, and A. F. Blom Jun. 1983 24 p refs Presented at Intern. Conf. on Testing, Evaluation and Quality Control of Composites (TEQC83), Guildford, England, Sep. 1983
(Contract FMV-F-FL-82223-80-183-21-001)
(FFA-TN-1983-29) Avail: NTIS HC A02/MF A01

Nondestructive investigation of damage growth in a notched carbon/epoxy composite laminate subjected to compression fatigue loading is described. Coupon specimens were fatigue loaded in compression at different constant load amplitudes in an ambient laboratory environment. Damage was determined at certain intervals of load cycles using tetrabromoethane enhanced X-ray radiography. Under continued cyclic loading the major damage growth is growth of delaminations as stable cracks. In order to quantify the extent of delamination growth during cyclic loading the delaminated area was determined by a measuring microscope. Results show that delamination initiates at stress levels as low as half the static compression strength. A large amount of scatter is inherent in all fatigue data, probably related to the surface roughness of the drilled hole. It is therefore important to control the quality of holes or cut-outs in structures subjected to compression fatigue. Author (ESA)

N84-12517# National Bureau of Standards, Washington, D.C. National Measurement Lab.
NONDESTRUCTIVE EVALUATION PUBLICATIONS, 1981
Leonard Mordfin, ed. Jul. 1983 47 p
(PB83-239574; NBSIR-83-2741) Avail: NTIS HC A03/MF A01 CSCL 14B

This fifth in a series of bibliographies of NBS publications on nondestructive evaluation provides citations, with selected abstracts, for 172 publications that appeared in the open literature, primarily during calendar year 1981. A subject index is included as well as information on how copies of many of the publications may be obtained. GRA

N84-12518# Texas A&M Univ., College Station. Dept. of Mechanical Engineering.
OPTIMIZATION OF ULTRASONIC FLAW DETECTION IN RAILROAD RAIL Final Report, 1 Jun. 1980 - 30 Nov. 1982
D. E. Bray, M. Najm, and L. R. Cornwell Feb. 1983 135 p refs
(Contract DTRS56-80-C-00032)
(PB83-236919; DOT/RSPA/DMA-50/83/18) Avail: NTIS HC A07/MF A01 CSCL 13F

Factors affecting the propagation of ultrasonic waves in railroad rail were studied in a collection of over forty new and used rail. Velocities were obtained for critically refractured longitudinal and shear waves and Rayleigh waves propagating along the rail head upper surface, and for bulk longitudinal and shear waves propagating in the head. Experimental results show that the typical inspection (refracted shear) beam is diverted due to the anisotropy of the cold worked zone. Moreover, the rate of development of the cold worked zone appears to be related to several factors, particularly the weight of the rail and whether it was manufactured by a control cooled or noncontrol cooled process. Metallurgical investigations of the coldworked zone included texture and hardness determination. Mathematical analysis was used to develop a model for the probability of detection of a flaw for rail parameters as seen in the sample. The use of other wave forms in rail flaw detection is discussed. GRA

39 STRUCTURAL MECHANICS

Includes structural element design and weight analysis; fatigue; and thermal stress.

For applications see *05 Aircraft Design, Testing and Performance* and *18 Spacecraft Design, Testing and Performance.*

N84-12519 Brown Univ., Providence, R. I.
A PRESSURE-SHEAR EXPERIMENT FOR STUDYING THE

DYNAMIC PLASTIC RESPONSES OF METALS AT SHEAR STRAIN RATES OF 10 TO THE 5TH POWER s(-1) Ph.D. Thesis
Li Chin-Ho 1982 183 p refs
Avail: Univ. Microfilms Order No. DA8228291

A thin specimen attached to an elastic anvil was subjected to pressure-shear loading by impact of an elastic flyer inclined to the direction of approach. After several wave reverberations between the two elastic plates, the state of stress in the specimen is essentially homogeneous. The strain rate can then be obtained as the velocity difference between the two faces of the specimen divided by the thickness of the specimen. The stresses in the specimen can be inferred from the particle velocity at the free surface of the anvil by means of elastic wave theory. The normal and transverse components of particle velocity are measured with a laser normal velocity interferometer and a laser transverse displacement interferomter. Experimental results for 1100-0 aluminum, 6061-T6 aluminum and OFHC copper are discussed. Tungsten carbide, because of its high elastic impedances and its high yield strength, is shown to be a good material for the two elastic plates that bound the specimen. Dissert. Abstr.

N84-12520 Wayne State Univ., Detroit, Mich.
BENDING OF TRANSVERSALLY LOADED ORTHOTROPIC RECTANGULAR AND SECTOR PLATES Ph.D. Thesis
Issam Elias Harik 1982 177 p
Avail: Univ. Microfilms Order No. DA8306886

An approximate solution for the bending of polar orthotropic pie or ring-shaped sector plates under the action of distributed transverse loads is presented. The deflection expression is assumed to be a single series solution of the product of two functions, one in the radial and the other in the angular direction. The function in the angular direction satisfying the boundary conditions of the radial edges is substituted into governing differential equation for bending of the circular plate. By a suitable transformation, an ordinary differential equation is obtained. The resulting equation is solved for the deflection expression of the circular plate. Results for the deflection, moments, shears and reactions, are presented for isotropic and orthotropic pieshaped sector plates having clamped and/or simply supported radial edges. Excellent agreement was obtained wherever comparisons with previously published results were possible. The analytical procedure developed in this study is first tested and proven valid by its application to the isotropic and orthotropic rectangular plates. Dissert. Abstr.

N84-12521 Brown Univ., Providence, R. I.
PLASTIC DEFORMATIONS OF A PORTABLE FRAME UNDER SHORT PULSE LOADING ON ONE COLUMN BY AN APPROXIMATE METHOD INCLUDING EFFECTS OF ELASTICITY AND PLASTIC RATE SENSITIVITY Ph.D. Thesis
Jean Laurent Raphanel 1982 164 p
Avail: Univ. Microfilms Order No. DA8228321

The proposed method aims to provide estimates of maximum and final deflections of portal frames subjected to a short pulse loading on one column. The response is purely flexural and we do not consider stability or local failure. The basic concept of the method is to include elastic effects but to separate the response into a wholly elastic and a wholly plastic part. The initial stage, wholly elastic is treated by an aproximate model involving appropriate stiffness and mass matrices. Elastic displacements, velocities, bending moments and curvature rates are evaluated at selected points. Dissert Abstr.

N84-12522 Georgia Inst. of Tech., Atlanta.
INTERACTION OF STRESS WAVES AND CRACKS USING A SECOND ORDER ACCURATE FINITE DIFFERENCE METHOD Ph.D. Thesis
Ralph Leonard Latham 1982 283 p
Avail: Univ. Microfilms Order No. DA8310654

A numerical procedure is developed for the solution of the stress wavecrack interaction problem. An explicit, second order accurate finite difference scheme for the solution of the equations of linear elastodynamics is used. For the crack interaction problem the Williams series is incorporated through the use of a high-order singular finite element. The equations of motion are expressed as a first order hyperbolic system to allow the application of the two step forms of the Lax-Wendroff scheme, namely the Richtmyer and MacCormack schemes. The one dimensional forms of these difference schemes are used with a Strang type of time splitting to solve two and three dimensional problems. This has the advantage of optimum stability, and greater efficiency than the equivalent two or three dimensional Lax-Wendroff scheme. A non-reflecting boundary condition is also developed and implemented for use in linear elastodynamics. Dissert. Abstr.

N84-12523 Purdue Univ., Lafayette, Ind.
BUCKLED PLATE VIBRATIONS, LARGE AMPLITUDE VIBRATIONS AND NONLINEAR FLUTTER OF ELASTIC PLATES USING HIGH-ORDER TRIANGULAR FINITE ELEMENTS Ph.D. Thesis
An-Dong Han 1982 112 p
Avail: Univ. Microfilms Order No. DA8310758

A high-order triangular membrane finite element is combined with a fully conforming triangular plate bending element to solve the geometrically nonlinear problems of plates where the membrane and flexural behavior are coupled and the effect of the inplane boundary conditions is as significant as the flexural boundary conditions. Each of the three orthogonal displacement components is represented by a two dimensional polynomial of quintic order with no bias against one or the other giving the element a total of 54 degrees of freedom. The nonlinear stiffness matrices are formulated and an iterative procedure is used. Examples include the plane stress analyses of a parabolically loaded square plate, large deflections of a square plate under lateral pressure, postbuckling of a square plate, linear free vibration of a square plate with and without inplane stresses. Various flexural and inplane boundary conditions are considered. Dissert. Abstr.

N84-12524 California Univ., Berkeley.
SOME BIFURCATION TOPICS IN NON-LINEAR ELASTOSTATICS Ph.D. Thesis
Juan Carlos Simo-Muerza 1982 144 p
Avail: Univ. Microfilms Order No. DA8312973

Development of nonlinear theories of rods and plates suitable for the systematic consideration of bifurcation and instability phenomena is discussed. The framework of general nonlinear elastostatics is adopted throughout, and emphasis is placed on the derivation of formulations consistent within this framework. Phenomena such as the warping effect due to shear deformations are systematically accounted for an proven to have an important effect in the structure of the resulting equations and in stability considerations. Dissert. Abstr.

N84-12525 California Univ., Berkeley.
MECHANICAL RESPONSE OF FLUID-FILLED POROELASTIC SOLIDS Ph.D. Thesis
Noriko Katsube 1982 184 p
Avail: Univ. Microfilms Order No. DA8312865

The problem of fluid flow through porous media is approached from different points of view. There is the phenomenological theory of Biot which was applied with considerable success. The continuum theory of mixtures provides a more fundamental description of the interaction of the fluid and the solid constituents. Each point of space is assumed occupied by a fluid particle and a solid particle, and the systems of equations were developed to describe the mechanical response of each constituent and their interactions. In applying mixture theory to problems of flow through porous geological materials, some conceptual difficulties are encountered due to the fact that porosity does not appear as a kinematic variable. This difficulty is avoided by treating fluid-filled porous material as a mixture whose constituents are a porous solid and a porous fluid. The mechanical behavior is based on averaging procedures applied to the representative volume element

and their interaction is described by the conventional mixture theory. Dissert. Abstr.

N84-12526 National Physical Lab., Teddington (England). Div. of Materials Applications.
AN INTERACTIVE COMPUTER PROGRAM FOR ANALYSIS OF ULTRASONIC MODULUS DATA ON ANISTROPIC MATERIALS
A. Woolf Jun. 1983 32 p refs
(NPL-DMA(A)68; ISSN-0143-7313) Copyright. Avail: Issuing Activity

A FORTRAN program that computes stiffness components, compliances and engineering elastic constants for composite materials, using velocity measurements taken from the ultrasonic immersion method is described. The method is applicable to transversely isotropic, tetragonal and orthotropic materials. The program is interactive with prompts for the input data. It runs on an ICL 2972 computer. A fully worked example (carbon fiber reinforced plastic) is included. Author (ESA)

N84-12527*# George Washington Univ., Washington, D.C. School of Engineering and Applied Science.
VIBRATION RESPONSE OF GEOMETRICALLY NONLINEAR ELASTIC BEAMS TO PULSE AND IMPACT LOADING Progress Report
H. Liebowitz 7 Oct. 1983 33 p refs
(Grant NAG1-158)
(NASA-CR-174495; NAS 1.26:174495) Avail: NTIS HC A03/MF A01 CSCL 20K

The governing equations for the geometrically nonlinear deformation of elastic beams subjected to dynamic bending loads are developed and solved for various initial conditions. Of primary interest is the response to pulse loading and simulated impact. Both transient and several cycle solutions are generated for the free vibration response to pulse loading. The results obtained are compared to a first mode analysis approximation. A model is developed to simulate impact loading by the distribution of additional mass to the elastic system and subjecting it to a velocity pulse. The governing equations are solved using second order finite differences in space and time. The solutions obtained are in reasonable agreement with experimental results. S.L.

N84-12528*# Kentron International, Inc., Hampton, Va.
NONLINEAR DYNAMICS AND CONTROL OF A VIBRATING RECTANGULAR PLATE
John V. Shebalin NASA. Langley Research Center Oct. 1983 41 p refs
(Contract NAS1-16000)
(NASA-CR-172215; NAS 1.26:172215) Avail: NTIS HC A03/MF A01 CSCL 20K

The von Karman equations of nonlinear elasticity are solved for the case of a vibrating rectangular plate by means of a Fourier spectral transform method. The amplification of a particular Fourier mode by nonlinear transfer of energy is demonstrated for this conservative system. The multi-mode system is reduced to a minimal (two mode) system, retaining the qualitative features of the multi-mode system. The effect of a modal control law on the dynamics of this minimal nonlinear elastic system is examined. Author

N84-12529*# National Aeronautics and Space Administration. Langley Research Center, Hampton, Va.
THE DUGDALE MODEL FOR THE COMPACT SPECIMEN
S. Mall (Missouri Univ., Rolla) and J. C. Newman, Jr. Oct. 1983 31 p refs Presented at the ASTM 16th Natl. Symp. on Fracture Mech., Columbus, Ohio, 15-18 Aug. 1983
(NASA-TM-85714; NAS 1.15:85714) Avail: NTIS HC A03/MF A01 CSCL 20K

Plastic zone size and crack tip opening displacement (CTOD) equations were developed. Boundary collocation analyses were used to analyze the compact specimen subjected to various loading conditions (pin loads, concentrated forces, and uniform pressure acting on the crack surface). Stress intensity factor and crack surface displacement equations for some of these loadings were developed and used to obtain the Dugdale model. The results from the equations for plastic zone size and CTOD agreed well with numerical values calculated by Terada for crack length to width ratios greater than 0.4. Author

N84-12530*# United Technologies Research Center, East Hartford, Conn.
AEROELASTIC ANALYSIS FOR PROPELLERS - MATHEMATICAL FORMULATIONS AND PROGRAM USER'S MANUAL Final Report
R. L. Bielawa, S. A. Johnson, R. M. Chi, and S. T. Gangwani Washington NASA Dec. 1983 255 p refs
(Contract NAS3-22753)
(NASA-CR-3729; NAS 1.26:3729; UTRC83-6) Avail: NTIS HC A12/MF A01 CSCL 20K

Mathematical development is presented for a specialized propeller dedicated version of the G400 rotor aeroelastic analysis. The G400PROP analysis simulates aeroelastic characteristics particular to propellers such as structural sweep, aerodynamic sweep and high subsonic unsteady airloads (both stalled and unstalled). Formulations are presented for these expanded propeller related methodologies. Results of limited application of the analysis to realistic blade configurations and operating conditions which include stable and unstable stall flutter test conditions are given. Sections included for enhanced program user efficiency and expanded utilization include descriptions of: (1) the structuring of the G400PROP FORTRAN coding; (2) the required input data; and (3) the output results. General information to facilitate operation and improve efficiency is also provided. Author

N84-12531*# National Aeronautics and Space Administration. Langley Research Center, Hampton, Va.
VERTICAL DROP TEST OF A TRANSPORT FUSELAGE CENTER SECTION INCLUDING THE WHEEL WELLS
M. Susan Williams and Robert J. Hayduk Oct. 1983 59 p refs
(NASA-TM-85706; NAS 1.15:85706) Avail: NTIS HC A04/MF A01 CSCL 20K

A Boeing 707 fuselage section was drop tested to measure structural, seat, and anthropomorphic dummy response to vertical crash loads. The specimen had nominally zero pitch, roll and yaw at impact with a sink speed of 20 ft/sec. Results from this drop test and other drop tests of different transport sections will be used to prepare for a full-scale crash test of a B-720. S.L.

N84-12532# Aeronautical Research Labs., Melbourne (Australia).
A REVIEW OF AUSTRALIAN INVESTIGATIONS ON AERONAUTICAL FATIGUE DURING THE PERIOD APRIL 1981 TO MARCH 1983
G. S. Jost Mar. 1983 62 p refs
(AD-A130968; ARL-STRUC-TM-359) Avail: NTIS HC A04/MF A01 CSCL 11/4

This document was prepared for presentation to the 18th Conference of the International Committee on Aeronautical Fatigue scheduled to be held at Toulouse, France, on May 30 and 31, 1983. A summary is presented of Australian aircraft fatigue research and associated activities. The major topics discussed include the fatigue of both civil and military aircraft structures, fatigue damage repair and refurbishment and fatigue life monitoring and assessment. Author (GRA)

N84-12533# Weidlinger Associates, New York, N.Y.
YIELD SURFACE FOR BARS INCLUDING WARPING RESTRAINT
R. P. Daddazio, M. P. Bieniek, and F. D. DiMaggio 1 Feb. 1982 42 p refs
(Contract DNA001-81-C-0048)
(AD-A131393; DNA-TR-81-121) Avail: NTIS HC A03/MF A01 CSCL 11/4

A procedure is described for deriving yield surface equations for thin walled open cross sections for cases in which Saint Venant torsion is small compared to warping torsion. The yield surface equations are expressed in terms of an axial force, bending moments in two planes, and the warping moment or bimoment.

Equations are derived for the specific case of a z-section. These equations are shown to satisfy the uniqueness theorem of plastic analysis thereby furnishing the correct yield surface within the limits of validity of the assumptions made. The applicability and accuracy of the proposed equations are indicated. Author (GRA)

N84-12534# Weidlinger Associates, New York, N.Y.
SUBMERGED SHOCK RESPONSE OF A LINEARLY ELASTIC SHELL OF REVOLUTION CONTAINING INTERNAL STRUCTURE. USER'S MANUAL FOR THE ELSHOK CODE
R. Vasudevan and D. Ranlet 1 May 1982 144 p refs
(Contract DNA001-81-C-0048; DNA Proj. Y99-QAXS)
(AD-A131282; DNA-TR-81-184) Avail: NTIS HC A07/MF A01 CSCL 20/11

Presented herein is a user's manual for the ELSHOK computer code. This computer program calculates the transient response of a submerged ring-stiffened shell of revolution, with or without internal structure, to an underwater shock wave having an arbitrary direction of impingement. Linearly elastic structures are considered, and the surrounding fluid is treated as an infinite acoustic medium. Modal analysis is employed for the structure, while the analysis of the fluid is based upon the Doubly Asymptotic Approximation.
Author (GRA)

N84-12535# Army Materials and Mechanics Research Center, Watertown, Mass.
THE ANALYSIS OF CRACK GROWTH DATA WITH APPLICATION TO TRIP STEEL Final Report
Reinier Beeuwkes, Jr. Mar. 1983 63 p
(DA Proj. 1L1-61102-AH-42)
(AD-A132021; AMMRC-TR-83-14) Avail: NTIS HC A04/MF A01 CSCL 11/6

A procedure is advocated to replace the common practice of establishing a rate of crack growth law directly from increments of growth or from slopes of smooth curves drawn through crack length vs number of loading cycles data. In the advocated procedure, a postulated rate equation such as, for example, the power law da/dN approx (K)m, is integrated for the specimen geometry used and values of the integral corresponding to experimental crack lengths are plotted against cycles of loading to reach these lengths. Thus, where, and if, the rate equation is valid the plot will consist of one or more straight line segments for each of which constant parameters may be obtained, or confirmed if theoretical. Intersections of straight line segments will correspond to crack rate of growth discontinuities unobservable by the usual method. Using Trip Steel data supplied by Syracuse University as an example, it was found that all growth discontinuously at various amounts of growth law. This conclusion is not invalidated by a gradual decrease in loading during testing, or by the differences in analytical expressions for K found by different investigators. GRA

N84-12536# Princeton Univ., N. J. Dept. of Civil Engineering.
INTERACTION OF A DISLOCATION WITH A CRACK
A. Cemal Eringen Aug. 1983 42 p
(Contract N00014-76-C-0240; NR Proj. 064-410)
(AD-A131912; RR-83-SM-9; TR-59) Avail: NTIS HC A03/MF A01 CSCL 12/1

A solution is given of the field equations of nonlocal elasticity for a line crack interacting with a screw dislocation in an elastic plane under anti-plane shear loading. Displacement and stress fields are determined throughout the core region and beyond. In the case when the dislocation is absent, the circumferential stress is shown to vanish at the crack tip, increasing to a maximum along the crack line afterwards decreasing to its classical value at large distances from the crack tip. This is in contradiction with the classical elasticity solutions which predicts stress singularity at the crack tip and it is in accordance with the physical condition that the crack tip surface must be free of surface tractions. The presence of the dislocation alters the stress distribution considerably when it is close to the crack tip. The stress distributions, in the core region, are displayed. A fracture criterion based on the maximum stress is established and used to determine the theoretical strengths of pure crystals that contain a line crack. Results are in good agreement with those based on the atomic theories and experiments. Author (GRA)

N84-12537# Sandia Labs., Albuquerque, N. Mex.
A COMPARISON OF FINITE-ELEMENT PREDICTIONS AND EXPERIMENTAL DATA FOR THE FORCED RESPONSE OF THE DOE 100 kW VERTICAL-AXIS WIND TURBINE
D. W. Lobitz and W. N. Sullivan 1983 12 p refs Presented at the 6th Biennial Wind Energy Conf., Minneapolis, 1 Jun. 1983
(DE83-012624; SAND-82-2534C; CONF-830631-6) Avail: NTIS HC A02/MF A01

A specialized finite-element capability was developed to predict dynamic structural response of the vertical-axis wind turbine. Several types of experimental data taken from the DOE 100-kW rotor are compared with predictions. These data include parked rotor natural frequencies, very low wind centrifugal and gravitational load response, and vibratory response from wind loads covering the rotor operational spectrum. Generally, the agreement between theory and experiment is very satisfactory. It is concluded that the analysis package is suitable for engineering design. Shortcoming observed in modeling accuracy are believed to be due primarily to inadequacies in blade aerodynamic-load calculations.
DOE

N84-12538# Argonne National Lab., Ill.
ANALYTICAL RESPONSE OF CONCRETE STRUCTURES SUBJECTED TO HIGH TEMPERATURES
A. H. Marchertas and J. M. Kennedy 1983 11 p refs Presented at 7th Intern. Conf. on Structural Mech. in Reactor Technol., Chicago, 22 Aug. 1983
(DE83-009625; CONF-830805-9) Avail: NTIS HC A02/MF A01

Scenarios of nuclear reactor safety consider the possibility that structural concrete may be subjected to very high temperatures and thus raise the concern of containment integrity. The analytical models and numerical tools that were developed for the purpose of studying the high temperature behavior of concrete are discussed. A formulation for computing heat conduction and stress analysis is presented and incorporated into the computer code TEMP-STRESS. The code was used to simulate the high temperature concrete response of an existing experiment. Improvements to the analytical model, which represent current research efforts, are also presented. DOE

N84-12539# Du Pont de Nemours (E. I.) and Co., Aiken, S.C.
GRAIN-BOUNDARY CAVITATION AND WELD-UNDERBEAD CRACKING IN DOP-26 IRIDIUM ALLOY
W. Clanton Mosley, Jr. 1983 11 p refs Presented at the 17th Ann. Meeting of the Microbeam Analysis Society, Phoenix, Ariz., 8-12 Aug. 1983 Submitted for publication
(Contract DE-AC09-76SR-00001)
(DE83-015406; DP-MS-82-103; CONF-830815-9) Avail: NTIS HC A02/MF A01

Plutonium-238 oxide fuel pellets for the General Purpose Heat Source Radioisotopic thermoelectric generators to be used on the NASA Galileo Mission to Jupiter and the International Solar Polar Mission are produced and encapsulated in DOP-26 iridium alloy at the Savannah River Plant. DOP-26 iridium alloy was developed at the Oak Ridge National Laboratory and contains nominally 0.3 weight-percent tungsten, 60-ppM thorium and 50-ppM aluminum. Underbead cracks occasionally occur in the girth weld on the iridium alloy cladding in the area where the gas tungsten arc is quenched. A variety of electron beam techniques were used to determine the cause of cracking. Results are discussed. DOE

N84-12540# Oak Ridge National Lab., Tenn. Solid State Div.
ELECTRON-MICROSCOPE OBSERVATION OF CRACK PROPAGATION AND A DISLOCATION MODEL OF FRACTURE
S. M. Ohr 1983 10 p refs Presented at the Intern. Symp. on the Structure and Properties of Crystal Defects, Liblice (Czechoslovakia), 13 Jun. 1983
(Contract W-7405-eng-26)
(DE83-014623; CONF-830680-2) Avail: NTIS HC A02/MF A01

Electron microscope observations of the emission and distribution of dislocations at the crack tip during in-situ tensile deformation are discussed. The most interesting result was the direct observation of a dislocation-free zone (DFZ) between the crack tip and the plastic zone. In order to understand the origin of the DFZ, a dislocation theory of fracture was developed and the critical stress intensity factor K/sub g for the dislocation generation at the crack tip is proposed as the definition for the condition for crack tip deformation. DOE

N84-12541# Brookhaven National Lab., Upton, N. Y. Process Sciences Div.

THE EFFECT OF MOISTURE ON THE PHYSICAL AND DURABILITY PROPERTIES OF METHYL METHACRYLATE POLYMER CONCRETE

Jack J. Fontana and Walter Reams 1983 19 p refs Presented at the American Concrete Inst. 548th Symp. on Polymers and Concretes, Kansas City, Mo., 25-30 Sep. 1983

(Contract DE-AC02-76CH-00016)

(DE83-016733; BNL-33420; CONF-8309134-1) Avail: NTIS HC A02/MF A01

The compressive strength of methyl methacrylate PC composites which decays very rapidly as the moisture content of the coarse aggregate is increased from 0 to 1 wt % is discussed. The durability of the PC also shows evidence of decay. Addition of silane coupling agent, such as A-1120, to the monomer component of a PC composite increases the compressive strength of such composites made with moist coarse aggregates. The compressive strength of such PC composites are as high as a normal PCC used in highway applications. The durability of PC composites made with a silane additive seems to increase as the composite undergoes freeze thaw cycling which reinforces the justification that such materials can be used for PCC repairs without a sacrifice in use lifespans. DOE

N84-12542# Oak Ridge National Lab., Tenn. Metals and Ceramics Div.

CREEP AND TENSILE PROPERTIES OF ALLOY 800H-HASTELLOY X WELDMENTS

H. E. McCoy and J. F. King Aug. 1983 20 p refs

(Contract W-7405-eng-26)

(DE83-017067; ORNL/TM-8728) Avail: NTIS HC A02/MF A01

Hastelloy-X and alloy 800H were joined by the gas tungsten arc welding process with ERNiCr-3 filler and the shielded metal arc welding process with Inco weld-A filler. Test specimens were of two types: (1) made entirely of deposited Inco weld-A, and (2) machined transverse across the weldments to include Hastelloy-X, filler metal, and alloy 800H. They were aged 2000 and 10,000 h and subjected to short term tensile and creep tests. Inco weld-A and ERNiCr-3 are both suitable filler metals and result in welds that are stronger than the alloy 800H base metal. DOE

N84-12543# Sandia Labs., Albuquerque, N. Mex.

SINGLE SPECIMEN J-INTEGRAL TESTING

R. Salzbrenner, J. A. VanDenAvyle, and T. J. Lutz 1983 33 p refs Presented at the IMOG Meeting on Mech. Testing, Los Alamos, N. Mex., 1 Mar. 1983

(Contract DE-AC04-76DP-00789)

(DE83-016069; SAND-83-0142C; CONF-830385-1) Avail: NTIS HC A03/MF A01

Application of state of the art techniques for measurement of fracture toughness has enabled valid toughness measurements to be made on ductile cast irons. The measurement techniques were based on the elastic-plastic approach embodied in the J-integral. Although cast irons are generally perceived as being low in toughness, the value measured on ferritic, sheroidal graphite, ductile cast irons are quite high (K/sub IC/ = 80 to 106 MPa (INTEGRAL)m or 73 to 96 ksi (INTEGRAL)in from -80 to 250C. DOE

N84-12544# Sandia Labs., Albuquerque, N. Mex. Thermomechanical and Physical Div.

MECHANICS OF FRACTURE UNDER HIGH-RATE STRESS LOADING

Dennis Grady 1983 40 p refs Presented at the Intern. Union of Theoret. and Appl. Mech. Conf. on Geomater.: Rocks, Concretes, Soils, Evanston, Ill., 11 Sep. 1983

(Contract DE-AC04-76DP-00789)

(DE83-013770; SAND-83-1148C; CONF-830975-3) Avail: NTIS HC A03/MF A01

The fracture properties of brittle materials subjected to impulsive or high rate loading is considered. Fracture is viewed as a microstructural process through the activation, growth and coalescence of a system of interacting cracks. The loading rate dependence of fracture stress is explained in terms of inertia of isolated cracks. The number of cracks participating in the fracture process, and the number and size of fragments in the failed material are related to both the inherent flaw structure and the rate of energy application required to sustain the system of growing cracks. Differences in loading conditions leading to material failure can result in vastly different fragment size distributions. These differences are compared with physically based statistical laws and possible relations to the loading conditions are explored. Lastly, continuum modelling of dynamic fracture focused toward computational analyses of complex applied problems is covered. DOE

N84-12545# Brookhaven National Lab., Upton, N. Y.

UNIVERSALITY AND FRACTAL DIMENSION OF MODE LOCKING STRUCTURE IN SYSTEMS WITH COMPETING PERIODICITIES

Per Bak 1983 11 p refs Presented at the Workshop on Statics and Dyn. of Nonlinear Systems, Erice, Italy, 1 Jul. 1983

(Contract DE-AC02-76CH-00016)

(DE83-017352; BNL-33493; CONF-830796-1) Avail: NTIS HC A02/MF A01

The properties of physical systems with competing periodicities were investigated. Two very different situations are considered. In the first case the competition is between two periods in time, or two frequencies, in a system which is at the verge of entering into a chaotic state. In the second case the competition is between two periods in space. In both cases there is a nonlinear coupling which tend to lock the two periods together. For some values of the parameters the magnetic structure has a period of its own, not related to the periodicity of the underlying lattice. In other regimes of the phase diagram, where the effective coupling is stronger, the resulting structure is always commensurable with the lattice. A simple one dimensional Ising model with long range antiferromagnetic interactions is considered. DOE

N84-12546# Argonne National Lab., Ill. Components Technology Div.

ENDOCHRONIC THEORY OF DYNAMIC VISCOPLASTICITY

Hsuan-Chi Lin Jun. 1983 24 p refs

(Contract W-31-109-eng-38)

(DE83-017531; ANL-83-59) Avail: NTIS HC A02/MF A01

Engineering models in dynamic plasticity were studied. The concept of the endochronic theory of viscoplasticity and its subsequent improvement are discussed. Applications and extensions of the theory to various dynamic problems are presented. Thea strain rate effect in the improved endochronic theory and its application to wave propagation problems are discussed. It appears that endochronic theory provides a promising representation of realistic material behavior. DOE

N84-12547# Ames Lab., Iowa.

INFERENCE OF FATIGUE-CRACK CLOSURE STRESSES FROM ULTRASONIC-TRANSMISSION MEASUREMENTS

R. B. Thompson, C. J. Fiedler, and O. Buck 1983 10 p refs Presented at the Nondestructive Methods for Mater. Property Determination Conf., Hershey, Pa., 6-8 Apr. 1983

(Contract W-7405-eng-82)

(DE83-017684; IS-M-438; CONF-8304122-1) Avail: NTIS HC A02/MF A01

The two sides of the closed crack which are not in complete contact were examined. The interface is viewed as a planar array of alternating contacting and noncontacting regions. The stress

level controls the intimacy of contact, which is related to the spectra of ultrasonic waves reflected from, or transmitted through, the interface. The physical basis of the phenomenon is reviewed and preliminary results of its application to the problem of determining closure stresses in fatigue cracks are presented. DOE

N84-12548# Southampton Univ. (England). Inst. of Sound and Vibration Research.
PREDICTION OF DYNAMIC EFFECTS DUE TO VEHICLES CROSSING MILITARY BRIDGES
V. J. Virchis Jun. 1983 52 p refs Sponsored by UK Ministry of Defence, Military Vehicles and Engineering Establishment
(ISVR-TR-120) Avail: NTIS HC A04/MF A01

A computer model for the numerical analysis of the dynamic response of military bridges when traversed by tracked or wheeled vehicles was developed. The bridges may be of nonuniform depth and are represented as a single span, simply supported beam. The vehicles were represented as a multi-degree of freedom, linear spring-mass system with viscous damping. The model accounts for initial dynamic conditions, variable vehicle velocity, and the loss of vehicle wheel contact with the surface of the bridge. Predictions are presented for a Challenger type vehicle crossing UK BR 80 type bridges concerning bridge length, ramp slopes, vehicle velocity and initial conditions. Results show that impact factor remains below the design limit for vehicle speed up to 35 kph. The state of the vehicle at entry, and the slope of the bridge ramps has a very significant effect upon the dynamic response of the bridge during the passage of the vehicles.
Author (ESA)

N84-12549 Illinois Univ., Urbana-Champaign.
NUMERICAL ANALYSIS OF STABLE CRACK GROWTH IN ELASTIC-PLASTIC MATERIALS IN SMALL SCALE AND GENERAL YIELDING Ph.D. Thesis
Poh-Sang Lam 1983 135 p
Avail: Univ. Microfilms Order No. DA8309972

Stable crack growth problems in elastic-plastic materials are investigated with the aid of the finite element method. The formulation used for steady state crack growth under small scale yielding conditions has the feature that the finite element mesh convects along with the moving crack tip. Various models for plastic flow were used. In Mode 3, calculations were carried out for J(sub2) incremental theory and a modified J(sub2) deformation theory meant to introduce effects related to flow at a yield surface vertex. Dissert. Abstr.

N84-12550 Stanford Univ., Calif.
CUMULATIVE DAMAGE IN COMPONENTS OF STEEL STRUCTURES UNDER CYCLIC INELASTIC LOADING Ph.D. Thesis
Mahmud Zohrei 1983 257 p
Avail: Univ. Microfilms Order No. DA8307248

Damage accumulation and resistance deterioration due to local buckling in beam flanges and crack propagation at weldments were investigated. The experiments show that the response of components can be separated into a deterioration threshold phase and a deterioration phase. Cumulative damage models are developed for the deterioration threshold range as well as the deterioration range. Constant amplitude tests show that the number of cycles to failure for constant amplitude cycling can be described by Coffin-Manson fatigue model. Utilizing the linear damage accumulation hypothesis, suitable damage models are derived for arbitrary histories. As an alternative, plastic fracture mechanics concepts can be employed to predict crack propagation and fracture at weldments. A crack growth rate model together with an initial crack size are used for this purpose. Dissert. Abstr.

N84-12551 Purdue Univ., Lafayette, Ind.
EVALUATION OF THE CRACK GAGE AS AN ADVANCED INDIVIDUAL AIRCRAFT TRACKING CONCEPT Ph.D. Thesis
Alon DumanisModan 1982 358 p
Avail: Univ. Microfilms Order No. DA8310820

The results of an experimental and analytical investigation on the advanced approach for employing the crack gage as an aircraft fatigue monitoring device are discussed in the report. The crack gage is a simple device which provides a convenient means for determining the potential damage, that is crack growth, in a structure, since crack extension in the gage is a result of loads on the structure which cause the structural damage. Two models were examined to generate transfer functions relating gage and structure crack lengths. The Double Gage Model (DGM), which simultaneously employs two crack gages, was analyzed and evaluated to yield a load dependent transfer function. Analytical results are compared with available experimental data for constant amplitude loading as well as for various spectrum loadings.
Dissert. Abstr.

N84-12552 Stanford Univ., Calif.
ON THE DYNAMIC FRACTURE OF BARS, BEAMS AND PLATES Ph.D. Thesis
Cesar Levy 1983 187 p
Avail: Univ. Microfilms Order No. DA8307180

The investigation of the dynamic fracture of bars, beams, and plates under various loading conditions was undertaken in two distinct areas the numerical solution of crack propagation problems using a finite difference code and the analytical solution of some beam fracture problems using several one dimensional models. The motion of the crack tip, for the double cantilever beam (DCB) specimen, and for the single edge notch (SEN) specimen, was obtained for various loading conditions by means of recently proposed finite difference code. The numerical results for the DCB model were compared with experimental results and found to be in good numerical and qualitative agreement. Dissert. Abstr.

N84-12553 Lehigh Univ., Bethlehem, Pa.
ELASTIC-PLASTIC FRACTURE OF CYLINDRICAL SHELLS CONTAINING PART-THROUGH CIRCUMFERENTIAL CRACKS Ph.D. Thesis
Hesham Ahmed Ezzat 1983 235 p
Avail: Univ. Microfilms Order No. DA8306369

The problem of fatigue crack propagation and ductile fracture in a cylindrical shell containing a macroscopic circumferential flaw is considered. The main interest in the current investigation is in applications to line pipes under secondary axial stresses. The stress intensity factor for the part through crack used in analyzing and correlating the fatigue crack propagation rate is obtained by using a line spring model in conjunction with Reissner's shell theory. To analyze the ductile fracture instability and to correlate the experimental and theoretical results the crack mouth opening displacement is used as the parameter. The limited data on fatigue crack propagation give the expected results, namely that the crack propagation rate in pipes are predicted from the fatigue results obtained from simpler geometries provided the stress intensity factors in the pipes are calculated with sufficient accuracy. Dissert. Abstr.

N84-12205# SDRC Engineering Services Ltd., Herts (England).
CALCULATION OF FORCED RESPONSE TO BASE EXCITATION USING EXPERIMENTALLY DERIVED MODAL PARTICIPATION FACTORS
J. Cory, J. M. OKeefe, and K. L. Howard *In* ESA Spacecraft Vibration Testing using Multiaxis Hydraul. Vibration Systems Jul. 1983 p 119-122 (For primary document see N84-12197 03-14)
Avail: NTIS HC A09/MF A01

N84-12811# Office National d'Etudes et de Recherches Aerospatiales, Paris (France).
DEVELOPMENT OF THE BASIC METHODS NEEDED TO PREDICT THE AEROELASTIC BEHAVIOR OF HELICOPTERS
R. Dat *In its* La Rech. Aerospatiale, Bimonthly Bull. No. 1983-1/212, Jan.-Feb. 1983 (ESA-TT-814) Jul. 1983 p 37-54 refs Transl. into ENGLISH from La Rech. Aerospatiale, Bull. Bimensuel (Paris), no. 1983-1/212, Jan.-Feb. 1983 (For primary document see N84-12810 03-70)
Avail: NTIS HC A05/MF A01; HC in ENGLISH available at ONERA, Paris FF 60; original report in FRENCH available at ONERA, Paris FF 60

N84-12812# Office National d'Etudes et de Recherches Aerospatiales, Paris (France).
PRESENT TRENDS IN STRUCTURAL ANALYSIS AT ONERA
R. Valid *In its* La Rech. Aerospatiale, Bimonthly Bull. No. 1981-1/212, Jan.-Feb. 1983 (ESA-TT-814) Jul. 1983 p 55-77 refs Transl. into ENGLISH from La Rech. Aerospatiale, Bull. Bimensuel (Paris), no. 1983-1/212, Jan.-Feb. 1983 (For primary document see N84-12810 03-70)
Avail: NTIS HC A05/MF A01; HC in ENGLISH available at ONERA, Paris FF 60; original report in FRENCH available at ONERA, Paris FF 60

42 GEOSCIENCES (GENERAL)

No abstracts in this category.

43 EARTH RESOURCES

Includes remote sensing of earth resources by aircraft and spacecraft; photogrammetry; and aerial photography.

For instrumentation see *35 Instrumentation and Photography.*

N84-12554 Bayerische Akademie der Wissenschaften, Munich (West Germany).
INVESTIGATION OF MATHEMATICAL MODELS TO COMBINE A TERRESTRIAL NETWORK WITH A SATELLITE NETWORK Ph.D. Thesis [UNTERSUCHUNG DER MATHEMATISCHEN MODELLE ZUR KOMBINATION EINES TERRESTRISCHEN NETZES MIT EINEM SATELLITENNETZ]
Zhongmo Zhou 1983 97 p refs In GERMAN; ENGLISH summary
(Ser-C-274; ISBN-3-7696-9326-4; ISSN-0065-5325) Copyright. Avail: Issuing Activity

Transformation models were investigated in order to transform a terrestrial geodetic network into a geocentric reference system (satellite network) and vice versa. Besides the transformation parameters (translation, rotation) the models also determine systematic scale and orientation errors of the terrestrial network. The theoretical models are proven by numerical examples.
Author (ESA)

N84-12555*# EROS Data Center, Sioux Falls, S. Dak.
LANDSAT 4 INVESTIGATIONS OF THEMATIC MAPPER AND MULTISPECTRAL SCANNER APPLICATIONS Quarterly Report
Donald T. Lauer, Principal Investigator 30 Jun. 1983 2 p ERTS (NASA Order S-10757-C)
(E84-10006; NASA-CR-174521; NAS 1.26:174521) Avail: NTIS HC A02/MF A01 CSCL 08B

Progress in the investigation of the quality and performance of LANDSAT 4 TM data is reported. Average mean brightness values were computed for each band and a look-up table was designed to place the values at about 1.0 density on the straight line portion of the film's H and D curve. Manual interpretation of bands 5 and 7 indicated these data to be good sources for determining locations of dugouts and small ponds as water sources.
M.G.

N84-12556*# Utah Univ., Salt Lake City. Center for Remote Sensing and Cartography.
IDENTIFYING ENVIRONMENTAL FEATURES FOR LAND MANAGEMENT DECISIONS Annual Report
28 Oct. 1983 76 p refs ERTS
(Grant NAGw-95)
(E84-10016; NASA-CR-174543; NAS 1.26:174543) Avail: NTIS HC A04/MF A01 CSCL 04B

Pairs of HCMM day-night thermal infrared (IR) data were selected to examine patterns of surface temperature and thermal inertia (TI) of peninsular Florida. GOES and NOAA-6 thermal IR, as well as National Climatic Center temperatures and rainfall, were also used. The HCMM apparent thermal inertia (ATI) images closely correspond to the General Soil Map of Florida, based on soil drainage classes. Areas with low ATI overlay well-drained soils, such as deep sands and drained organic soils. Areas with high ATI overlay areas with wetlands and bodies of water. The HCMM ATI images also correspond well with GOES-detected winter nocturnal cold-prone areas. Use of HCMM data with Carlson's energy balance model shows both high moisture availability (MA) and high thermal inertia (TI) of wetland-type surfaces and low MA and low TI of upland, well-drained soils. Since soil areas with low TI develop higher temperatures during the day, then antecedent patterns of highest maximum daytime surface temperature can also be used to predict nocturnal cold-prone areas in Florida.
Author

N84-12557*# Texas A&M Univ., College Station. Dept. of Mathematics.
PROCEEDINGS OF THE NASA SYMPOSIUM ON MATHEMATICAL PATTERN RECOGNITION AND IMAGE ANALYSIS Final Report, 16 Jul. 1982 - 15 Jul. 1983
L. F. Guseman, Jr. 1983 608 p refs Symp. held in Houston, Tex., 1-3 Jun. 1983 Original contains imagery. Original photography may be purchased from the EROS Data Center, Sioux Falls, S.D. 57198 ERTS
(Contract NAS9-16664)
(E83-10032; NASA-CR-171696; NAS 1.26:171696) Avail: NTIS HC A99/MF A01 CSCL 05B

The application of mathematical and statistical analyses techniques to imagery obtained by remote sensors is described by Principal Investigators. Scene-to-map registration, geometric rectification, and image matching are among the pattern recognition aspects discussed. For individual titles, see N84-12558 through N84-12575.

N84-12558*# Virginia Polytechnic Inst. and State Univ., Blacksburg. Dept. of Electrical Engineering and Computer Science.
RELATIVE ELEVATION DETERMINATION FROM LANDSAT IMAGERY Final Report
R. M. Haralick and S. Wang *In* Texas A and M Univ. Proc. of the NASA Symp. on Math. Pattern Recognition and Image Analysis 1983 p 3-51 refs Original contains imagery. Original photography may be purchased from the EROS Data Center, Sioux Falls, S.D. 57198 ERTS (For primary document see N84-12557 03-43)
Avail: NTIS HC A99/MF A01 CSCL 05B

In LANDSAT imagery, spectral and spatial information can be used to detect the drainage network as well as the relative elevation model in mountainous terrain. To do this, the mixed information of material reflectance and topographic modulation in the original LANDSAT imagery must be first separated. From the material reflectance information, big visible rivers can be detected. From the topographic modulation information, ridges and valleys can be detected and assigned relative elevations. Finally, a relative elevation model can be generated by interpolating values for nonridge and nonvalley pixels.
Author

N84-12559*# National Aeronautics and Space Administration. Lyndon B. Johnson Space Center, Houston, Tex.
ESTIMATING LOCATION PARAMETERS IN A MIXTURE MODEL Final Report
Richard P. Heydorn and Rehka Basu *In* Texas A and M Univ. Proc. of the NASA Symp. on Math. Pattern Recognition and Image Analysis 1983 p 55-76 refs ERTS (For primary document see N84-12557 03-43)
Avail: NTIS HC A99/MF A01 CSCL 05B

Mixture models of the form h = sum to M terms, one for each positive integer from 1 to N lambda sub j f (j) sub theta sub j where theta sub j is a translation parameter are considered. An approach is discussed which makes use of a Caratheodory theorem

on the trigonometric moment problem to determine M and theta sub j j = 1,2,...,M. This theorem is also applied to show that translates of many common distributions lead to identifiable mixtures. Author

N84-12560*# Rice Univ., Houston, Tex.
MULTIVARIATE DENSITY ESTIMATION AND REMOTE SENSING Final Report
David W. Scott *In* Texas A and M Univ. Proc. of the NASA Symp. on Math. Pattern Recognition and Image Analysis 1983 p 77-92 refs Original contains imagery. Original photography may be purchased from the EROS Data Center, Sioux Falls, S.D. 57198 ERTS (For primary document see N84-12557 03-43)
Avail: NTIS HC A99/MF A01 CSCL 05B

Current efforts to develop methods and computer algorithms to effectively represent multivariate data commonly encountered in remote sensing applications are described. While this may involve scatter diagrams, multivariate representations of nonparametric probability density estimates are emphasized. The density function provides a useful graphical tool for looking at data and a useful theoretical tool for classification. This approach is called a thunderstorm data analysis. Author

N84-12561*# Jet Propulsion Lab., California Inst. of Tech., Pasadena.
AUTOREGRESSIVE MODELS FOR USE IN SCENE SEGMENTATION Final Report
M. Naraghi *In* Texas A and M Univ. Proc. of the NASA Symp. on Math. Pattern Recognition and Image Analysis 1983 p 93-122 refs ERTS (For primary document see N84-12557 03-43)
Avail: NTIS HC A99/MF A01 CSCL 05B

A scene segmentation approach is presented which is based on generating autoregressive field models for each scene component (class) from its a priori spatial statistics. A methodology is also described for using these models in achieving optimal segmentation of a scene. The derivations are presented for the case of single band imagery, however, the method is believed to be extendable to multispectral data. Author

N84-12562*# Houston Univ., Tex. Dept. of Mathematics.
MIXTURE MODELS FOR DEPENDENT OBSERVATIONS Final Report
Charles Peters *In* Texas A and M Univ. Proc. of the NASA Symp. on Math. Pattern Recognition and Image Analysis 1983 p 123-142 refs ERTS (For primary document see N84-12557 03-43)
Avail: NTIS HC A99/MF A01 CSCL 05B

Parametric mixture models appropriate for data presented in homogeneous blocks of varying sizes from several unidentified source populations are considered. For most applications, the data elements within each block are dependent. Models are proposed for multivariate normal data incorporating two types of dependence, exchangeability of elements within blocks, and a Markov structure for blocks. The consequences of assuming exchangeability, when in fact the Markov structure holds, are explored. Computational problems for each model are considered, and results of a simple test of the exchangeability hypothesis for LANDSAT data are presented. Author

N84-12563*# Texas Univ., Austin.
AN EMPIRICAL BAYES APPROACH TO SPATIAL ANALYSIS Final Report **c65**
C. N. Morris and H. Kostal *In its* Proc. of the NASA Symp. on Math. Pattern Recognition and Image Analysis 1983 p 143-166 refs ERTS (For primary document see N84-12557 03-43)
Avail: NTIS HC A99/MF A01 CSCL 12A

Multi-channel LANDSAT data are collected in several passes over agricultural areas during the growing season. How empirical Bayes modeling can be used to develop crop identification and discrimination techniques that account for spatial correlation in such data is considered. The approach models the unobservable parameters and the data separately, hoping to take advantage of the fact that the bulk of spatial correlation lies in the parameter process. The problem is then framed in terms of estimating posterior probabilities of crop types for each spatial area. Some empirical Bayes spatial estimation methods are used to estimate the logits of these probabilities. Author

N84-12564*# Texas A&M Univ., College Station. Center for Approximation Theory.
SPLINE CLASSIFICATION METHODS Final Report **c64**
L. F. Guseman, Jr. and L. L. Schumaker *In its* Proc. of the NASA Symp. on Math. Pattern Recognition and Image Analysis 1983 p 167-190 refs ERTS (For primary document see N84-12557 03-43)
Avail: NTIS HC A99/MF A01 CSCL 12A

The use of spline functions in the development of classification algorithms is discussed. A method is formulated for producing spline approximations to univariate density functions when each density function is described by a histogram of measurements. The resulting approximations are then incorporated into a Bayesian classification procedure for which the probability of misclassification can be readily computed. Some preliminary numerical results are presented to illustrate the method. Author

N84-12565*# Texas A&M Univ., College Station. Dept. of Statistics.
QUANTILE DATA ANALYSIS OF IMAGE DATA Final Report
Emanuel Parzen *In its* Proc. of the NASA Symp. on Math. Pattern Recognition and Image Analysis 1983 p 191-242 refs ERTS (For primary document see N84-12557 03-43)
Avail: NTIS HC A99/MF A01 CSCL 05B

Quantile data analysis and functional statistical inference methods are introduced and applied to provide representations of spectral data which may lead to simple statistical discriminators effective for the estimation of ground truth from satellite spectral measurements. To estimate the ground truth of a pixel, the probability of each possible ground truth is estimated, given observed (estimated) quantile theoretic statistical characteristics of the multispectral image data corresponding to the pixel and its neighboring pixels. A strategy for determining which statistical characteristics discriminate best is described. Results are reported of quantile data analysis of an extensive collection of training files of image data. Author

N84-12566*# Texas A&M Univ., College Station.
DISCRIMINATION RELATIVE TO MEASURES OF NONNORMALITY **c64**
W. B. Smith and E. P. Shine *In its* Proc. of the NASA Symp. on Math. Pattern Recognition and Image Analysis 1983 p 243-276 refs ERTS (For primary document see N84-12557 03-43)
Avail: NTIS HC A99/MF A01 CSCL 12A

The robustness of discriminant functions to nonnormality is investigated. The performance of procedures relative to measures of the difference between the actual distribution of the observations and the usual assumption of normal densities is assessed. For example, the two population, mixed distributions problem with equal costs of misclassification are considered. The parameters are estimated by maximum likelihood and recently proposed robust methods. Author

N84-12567*# Texas A&M Univ., College Station.
REPEATED-MEASURES ANALYSIS OF IMAGE DATA Final Report
H. J. Newton *In its* Proc. of the NASA Symp. on Math. Pattern Recognition and Image Analysis 1983 p 277-194 refs ERTS (For primary document see N84-12557 03-43)
Avail: NTIS HC A99/MF A01 CSCL 05B

It is suggested that using a modified analysis of variance procedure on data sampled systematically from a rectangular array of image data can provide a measure of homogeneity of means over that array in single directions and how variation in perpendicular directions interact. The modification of analysis of variance required to account for spatial correlation is described theoretically and numerically on simulated data. Author

N84-12568*# Jet Propulsion Lab., California Inst. of Tech., Pasadena.
SAR SPECKLE NOISE REDUCTION USING WIENER FILTER Final Report c33
Tae H. Joo and Daniel N. Held *In* Texas A and M Univ. Proc. of the NASA Symp. on Math. Pattern Recognition and Image Analysis 1983 p 295-310 refs Original contains imagery. Original photography may be purchased from the EROS Data Center, Sioux Falls, S.D. 57198 ERTS (For primary document see N84-12557 03-43)
Avail: NTIS HC A99/MF A01 CSCL 09C

Synthetic aperture radar (SAR) images are degraded by speckle. A multiplicative speckle noise model for SAR images is presented. Using this model, a Wiener filter is derived by minimizing the mean-squared error using the known speckle statistics. Implementation of the Wiener filter is discussed and experimental results are presented. Finally, possible improvements to this method are explored. M.G.

N84-12569*# Maryland Univ., College Park.
IMAGE MATCHING USING GENERALIZED HOUGH TRANSFORMS Final Report
Larry S. Davis, Fu-pei Hu, Vincent Hwang, and Les Kitchen *In* Texas A and M Univ. Proc. of the NASA Symp. on Math. Pattern Recognition and Image Analysis 1983 p 311-326 refs Original contains imagery. Original photography may be purchased from the EROS Data Center, Sioux Falls, S.D. 57198 ERTS (For primary document see N84-12557 03-43)
Avail: NTIS HC A99/MF A01 CSCL 05B

An image matching system specifically designed to match dissimilar images is described. A set of blobs and ribbons is first extracted from each image, and then generalized Hough transform techniques are used to match these sets and compute the transformation that best registers the image. An example of the application of the approach to one pair of remotely sensed images is presented. M.G.

N84-12570*# LNK Corp., Silver Spring, Md.
ANALYSIS OF SUBPIXEL REGISTRATION ACCURACY Final Report
David Lavine, Laveen N. Kanal, Carlos A. Berenstein, Eric Slud, and Charles Herman *In* Texas A and M Univ. Proc. of the NASA Symp. on Math. Pattern Recognition and Image Analysis 1983 p 327-412 refs ERTS (For primary document see N84-12557 03-43)
Avail: NTIS HC A99/MF A01 CSCL 05B

Geometric and probabilistic models for subpixel accuracy are developed. The geometric models bound the error in offset estimation using the pixels in an observed digital straight line. One probabilistic model bounds the estimate of error offset for continuous images. The other model bounds the error for discrete images given that one is in the correct pixel. Author

N84-12571*# Purdue Univ., Lafayette, Ind.
SIMULATION ASPECTS IN THE STUDY OF RECTIFICATION OF SATELLITE SCANNER DATA Final Report
Edward M. Mikhail and Fidel C. Paderes, Jr. *In* Texas A and M Univ. Proc. of the NASA Symp. on Math. Pattern Recognition and Image Analysis 1983 p 413-484 refs ERTS (For primary document see N84-12557 03-43)
Avail: NTIS HC A99/MF A01 CSCL 05B

Complete sensor/platform modelling is derived and used for the generation of synthetic data and for rectification studies of satellite scanner data. All satellite position and sensor attitude parameters are recovered. Rectification accuracy improves marginally when using more than 25 control points, and is highly sensitive to errors in image point identification. Author

N84-12572*# National Aeronautics and Space Administration. National Space Technology Labs., Bay Saint Louis, Miss.
PROGRESS IN THE SCENE-TO-MAP REGISTRATION INVESTIGATION Final Report
D. D. Dow *In* Texas A and M Univ. Proc. of the NASA Symp. on Math. Pattern Recognition and Image Analysis 1983 p 485-506 refs ERTS (For primary document see N84-12557 03-43)
Avail: NTIS HC A99/MF A01 CSCL 05B

The geometric accuracy of the scene-to-map registration process for P-format LANDSAT MSS data for scenes from Kansas and Louisiana/Mississippi is discussed. Large scale row and column bias values and row and column standard deviation values were measured for the P-format data sets indicating a poor georegistration accuracy for these geometrically corrected LANDSAT MSS scenes. Experimental work is underway with A-format LANDSAT MSS scenes from the same locations to examine the influence of the number of ground control points and the spatial distribution of ground control points on geometric registration accuracy. An early conclusion from this work is that the root mean square approach for assessing how well the ground control points fit the mapping equations measures a different aspect of georegistration accuracy than does the approach of evaluating the bias (offset) and standard deviation using independently chosen ground reference points. M.G.

N84-12573*# Hunter Coll., New York. Dept. of Geology and Geography.
RELATING SPATIAL PATTERNS IN IMAGE DATA TO SCENE CHARACTERISTICS Final Report
Alan H. Strahler and Curtis E. Woodcock *In* Texas A and M Univ. Proc. of the NASA Symp. on Math. Pattern Recognition and Image Analysis 1983 p 507-542 refs Presented at the 17th Intern. Symp. on Remote Sensing of the Environ., Ann Arbor, Mich., May 1983 Original contains imagery. Original photography may be purchased from the EROS Data Center, Sioux Falls, S.D. 57198 ERTS (For primary document see N84-12557 03-43)
(Contract NAS9-16664)
Avail: NTIS HC A99/MF A01 CSCL 05B

In remote sensing, the primary goal is accurate scene inference, in which characteristics of the scene are inferred from the image data. More effective inference of scene characteristics can be accomplished through the use of techniques that use explicit models of spatial pattern. Spatial patterns in image data are functionally related to the size and spacing of elements in the scene and to the spatial resolution of the image data. At resolutions where variance is high, scene inference techniques should rely heavily on data from the spatial domain. As variance decreases, effective scene inference will increasingly rely on spectral data. Author

N84-12574*# SRI International Corp., Menlo Park, Calif. Artificial Intelligence Center.
SHAPE FROM SHADING: AN ASSESSMENT Final Report
Grahame B. Smith *In* Texas A and M Univ. Proc. of the NASA Symp. on Math. Pattern Recognition and Image Analysis 1983 p 543-576 refs ERTS (For primary document see N84-12557 03-43)
(Contracts NAS9-16664; MDA903-83-C-0027)
Avail: NTIS HC A99/MF A01 CSCL 05B

Previous efforts to recover surface shape from image irradiance are reviewed in order to assess what can and cannot be accomplished. The informational requirements and restrictions of these approaches are considered. In dealing with the question of what surface parameters can be recovered locally from image shading, it is shown that, at most, shading determines relative surface curvature, i.e., the ratio of surface curvature measured in orthogonal image directions. The relationship between relative surface curvature and the second derivatives of image irradiance is independent of other scene parameters, but insufficient to determine surface shape. This result places in perspective the difficulty encountered in previous attempts to recover surface orientation from image shading. M.G.

N84-12575*# Kansas Univ. Center for Research, Inc., Lawrence. Telecommunications and Information Sciences Lab.
THE INFLUENCE OF SENSOR AND FLIGHT PARAMETERS ON TEXTURE IN RADAR IMAGES Final Report c32
V. S. Frost, K. S. Shanmugan, and J. C. Holtzman *In* Texas A

and M Univ. Proc. of the NASA Symp. on Math. Pattern Recognition and Image Analysis 1983 p 577-608 refs Original contains imagery. Original photography may be purchased from the EROS Data Center, Sioux Falls, S.D. ERTS (For primary document see N84-12557 03-43)
Avail: NTIS HC A99/MF A01 CSCL 17I

Texture is known to be important in the analysis of radar images for geologic applications. It was previously shown that texture features derived from the grey-level co-occurrence matrix (GLCM) can be used to separate large scale texture in radar images. The influence of sensor parameters, specifically the spatial and radiometric resolution and flight parameters, i.e., the orientation of the surface structure relative to the sensor, on the ability to classify texture based on the GLCM features is investigated. It was found that changing these sensor and flight parameters greatly affects the usefulness of the GLCM for classifying texture on radar images. M.G.

N84-12576*# National Aeronautics and Space Administration. Earth Resources Labs., Bay St. Louis, Miss.
EARTH RESOURCES LABORATORY RESEARCH AND TECHNOLOGY Annual Report, 1983
15 Nov. 1983 63 p Original contains color imagery. Original photography may be purchased from the EROS Data Center, Sioux Falls, S.D. 57198 ERTS
(E84-10033; NASA-TM-85476; NAS 1.15:85476) Avail: NTIS HC A04/MF A01 CSCL 05B

The accomplishments of the Earth Resources Laboratory's research and technology program are reported. Sensors and data systems, the AGRISTARS project, applied research and data analysis, joint research projects, test and evaluation studies, and space station support activities are addressed. M.G.

N84-12577# Geological Survey, Washington, D. C.
ANALYSIS OF THE WORLD DISTRIBUTION OF METAL-RICH SUBSEA MANGANESE NODULES
V. E. McKelvey, Nancy A. Wright, and Roger W. Bowen 1983 59 p refs
(USGS-Circ-886; LC-82-600335) Avail: NTIS HC A04/MF A01

The world average metal content of manganese modules, the average metal content of modules in each of the oceans, the world average metal content of modules in latitudinal zones, the relation of the metal content of modules to water depth, the relation of module concentration to water depth, metal-rich types of manganese modules, and genetic implantion of variations in composition of manganese modules are discussed. N.W.

N84-12578# Canada Inst. for Scientific and Technical Information, Ottawa (Ontario).
HANDBOOK ON THE DETERMINATION OF THE PHYSICAL, THERMAL AND MECHANICAL PROPERTIES OF FROZEN SOILS
R. M. Sarkisyan, A. Z. Nersesova, S. S. Vyalov, and A. G. Zatsarnaya 1983 207 p Transl. into ENGLISH of handbook of the Scientific Research Inst. of Foundations and Underground Structures of the State Committee of the Council of Ministers, USSR for Construction, Moscow, 1973
(NRC/CNR-TT-2064; ISSN-0077-5606) Avail: NTIS HC A10/MF A01

Moisture content, ice content, specific weight, salinity, heat capacity, thermal conductivity and thermal diffusivity, and freezing point depression of saline soils are discussed. Thermocouples, flat electric heaters, and thermometers are also discussed. Preparation of soil samples, compressibility of frozen and thawing soils, resistance of frozen soils to normal pressure, spherical stamp method of testing, long-term value cohesion of frozen soil, uniaxial compression under constantly changing pressure, resistance of frozen and thawed soils to shear, shear along the lateral surface of foundations, tangential heaving forces of soils, and viscosity of ice inclusions are discussed. N.W.

N84-12579# European Space Agency, Paris (France).
REMOTE SENSING APPLICATIONS FOR ENVIRONMENTAL STUDIES
N. Longdon, comp. and O. Melita, comp. Jul. 1983 303 p refs Partly in ENGLISH and FRENCH Proc. of EARSeL/ESA Symp., Brussels, 26-28 Apr. 1983 sponsored by the Commission of the European Communities and Parliamentary Assembly of the Council of Europe
(ESA-SP-188; ISSN-0379-6566) Avail: NTIS HC A14/MF A01

Land and marine applications of remote sensing by aircraft and satellites for environmental studies were discussed. Thematic mapping, pollution monitoring, coastal ecology, crop inventory, and marine biology applications were considered. For individual titles, see N84-12580 through N84-12617.

N84-12580# Technische Univ. Munich, Garching (West Germany). Inst. for General and Applied Geodesy.
USE OF REMOTE SENSING METHODS FOR THE ECOLOGICAL MAPPING PROJECT OF THE EUROPEAN COMMUNITY
J. Bodechtel and F. Jaskolla *In* ESA Remote Sensing Appl. for Environ. Studies Jul. 1983 p 3-7 (For primary document see N84-12579 03-43)
Avail: NTIS HC A14/MF A01

In order to examine the potential contribution of remote sensing to the collection of data for the ecological mapping of the European Community, environmental mapping requirements, and which indicators can be recorded or kept up-to-date by of remote sensing were studied. Test sites were investigated by aerial and satellite imagery. Based on LANDSAT-2 images and the LANDSAT-D, SPOT generation of satellites a significant impact on ecological mapping is predicted including the increased availability of data over the whole European territory in order to reduce the gap between the member states; ensured regular updating of data; and improved interregional and international comparability of data. Author (ESA)

N84-12581# Joint Research Centre of the European Communities, Ispra (Italy).
MONITORING OF RENEWABLE RESOURCES (A LAND INFORMATION SYSTEM FOR EUROPE)
G. Fraysse *In* ESA Remote Sensing Appl. for Environ. Studies Jul. 1983 p 9-12 refs (For primary document see N84-12579 03-43)
Avail: NTIS HC A14/MF A01

A combination of data collected by second generation Earth observation satellites and meteorological satellites with conventional data used as input to an agromet model is suggested for an agricultural information system for the European Community. Legislative, economic, and social benefits, parameters and required action are summarized. Accuracy requirements, sampling strategy, and system design are outlined. Author (ESA)

N84-12582# Freiburg Univ. (West Germany). Abt. Luftbildmessung und Fernerkundung.
CONSIDERATIONS ON A PERMANENT INVENTORY AND MONITORING SYSTEM FOR EUROPEAN FORESTS
G. Hildebrandt *In* ESA Remote Sensing Appl. for Environ. Studies Jul. 1983 p 13-18 refs (For primary document see N84-12579 03-43)
Avail: NTIS HC A14/MF A01

A forest inventory approach, in which short term monitoring of major forest area changes by satellite image interpretation is combined with a longterm multiphase sampling of forest resources and silvicultural conditions using IR aerial photographs and ground measurements, is introduced. The approach involves precise geometric correction of the satellite images; and overlay of boundaries (countries, inventory units) and north-south or east-west oriented gridlines of the geodetic reference system in 8 km distances. For each unit, determination of the area of forest lands and main forest types for the entire unit and each strip within the unit; calculation of the strip's forest area in percentage; and PPs-selection with random figures from 1 to 100 until a certain percentage of the unit's forest area is achieved. The selected strips are defined by their x/y coordinates and are used

for any following inventory as permanent sample strips. The approach was tested using the Black Forest. Author (ESA)

N84-12583# Centre National de la Recherche Scientifique, Verrieres-le-Buisson (France). Service d'Aeronomie.
REMOTE SENSING INSTRUMENTS FOR TRACE SPECIES MEASUREMENTS IN THE TROPOSPHERE AND STRATOSPHERE: A REVIEW
G. Megie *In* ESA Remote Sensing Appl. for Environ. Studies Jul. 1983 p 19-24 refs (For primary document see N84-12579 03-43)
Avail: NTIS HC A14/MF A01

Air and spaceborne passive sensors which use an external source such as the Sun, the Moon or a star to derive from the absorption properties of the atmosphere within a specific wavelength range the total content or altitude profile of a given species; and active sensors characterized by the existence of an internal source of light, either continuous or pulsed, are considered. The complementarity of these two types of sensors for atmospheric applications with respect to the various altitude regions to be sounded, and the importance of ground truth validation for global monitoring and trend analysis of atmospheric trace species, are emphasized. Author (ESA)

N84-12584# Ecole Normale Superieure, Paris (France).
CONTRIBUTION OF SATELLITE REMOTE SENSING TO KNOWLEDGE OF THE LITTORAL FROM THE MOUTH OF THE LOIRE TO THAT OF THE GIRONDE (FRANCE) [CONTRIBUTION DE LA TELEDETECTION SATELLITAIRE A LA CONNAISSANCE DU LITTORAL DE L'EMBOUCHURE DE LA LOIRE A CELLE DE LA GIRONDE]
Francois Cuo *In* ESA Remote Sensing Appl. for Environ. Studies Jul. 1983 p 27-29 refs In FRENCH (For primary document see N84-12579 03-43)
Avail: NTIS HC A14/MF A01

The contribution of LANDSAT, NOAA, Tiros N, SEASAT, Nimbus 7, HCMM, and METEOSAT data to the study of coastal water and geomorphology is outlined. Combined with numerical models, these data enable coastal dynamics to be explained. Temperature data offer insights into the kinematics of coastal water. Side-looking radar data are used to study the direction of surges, which explain coastal evolutions recorded by active and passive visible and near IR scanners. Perspectives for environmental effects and pollution monitoring are outlined. Author (ESA)

N84-12585# European Space Agency, Paris (France).
CONTRIBUTIONS OF REMOTE SENSING SATELLITE TRACKING TECHNIQUES TO MARINE ENVIRONMENT MONITORING AND MARINE APPLICATIONS
G. Duchossois *In its* Remote Sensing Appl. for Environ. Studies Jul. 1983 p 31-34 refs (For primary document see N84-12579 03-43)
Avail: NTIS HC A14/MF A01

The state-of-the-art of remote sensing satellite techniques for the monitoring of marine geophysical parameters such as waves, winds, sea surface temperature, and the current and potential utilization of satellite data for marine applications where knowledge and monitoring of sea-state conditions is essential (ship routing, off-shore activities, fisheries, oil pollution), are reviewed. Commercial possibilities are outlined. Results from oceanic missions show the feasibility of measuring marine geophysical parameters from space with adequate accuracy and in a continuous and reliable way. Author (ESA)

N84-12586# Joint Research Centre of the European Communities, Ispra (Italy).
MARINE REMOTE SENSING ACTIVITIES OF THE JOINT RESEARCH CENTER, ISPRA, ITALY
S. Camagni, S. GallideParatesi, R. Gillot, G. Maracci, W. Mehl, N. Omenetto, A. Pedrini, G. Rossi, P. Schlittenhardt, B. Sturm et al *In* ESA Remote Sensing Appl. for Environ. Studies Jul. 1983 p 35-49 refs (For primary document see N84-12579 03-43)
Avail: NTIS HC A14/MF A01

Remote sensing of the propagation of anthropogenic pollutants in estuarine and coastal areas; evaluation of chlorophyll concentrations for fishery application; optical diagnosis of oil pollution; and multisensor oil slick detection and assessment exercises in the Mediterranean and in the North Sea are described. The JRC programs are designed to confirm that aerospace data present many advantages over conventional measurement techniques for detection, monitoring and/or prediction of particular situations of fishery and marine pollution in the European Community and associated countries. Author (ESA)

N84-12587# Groupement pour le Developpement de la Teledetection Aerospatiale, Toulouse (France). SPOT Image.
SPOT POTENTIAL APPLICATIONS: AN OVERVIEW OF THE RESULTS OF THE SIMULATION CAMPAIGNS
J. P. leGorgeu and J. C. Rivereau *In* ESA Remote Sensing Appl. for Environ. Studies Jul. 1983 p 51-56 refs In FRENCH (For primary document see N84-12579 03-43)
Avail: NTIS HC A14/MF A01

The use of the SPOT satellite for rural, urban, and coastal zone studies was simulated. For agriculture and land use, SPOT's high resolution is well adapted to European parcelling conditions (2 ha). The 10 m resolution is adequate for urban planning requirements. In coastal zones, ocean dynamics, strands under shallow water, and marine vegetation can be studied. The SPOT images can replace medium and large scale aerial photographs for thematic mapping. Author (ESA)

N84-12588# Centre de Recherches en Physique de l'Environnement, Issy-les-Moulineaux (France).
RADAR INVESTIGATION OF SOILS AND SEA (ERASME): C BAND HELICOPTER-BORNE SCATTEROMETER. APPLICATION TO SOIL MOISTURE MEASUREMENT [ERASME: DIFFUSIOMETRE HELIPORTABLE EN BANDE C. APPLICATION A LA MESURE DE L'HUMIDITE DES SOLS]
R. Bernard and D. Vidal-Madjar *In* ESA Remote Sensing Appl. for Environ. Studies Jul. 1983 p 59-64 refs In FRENCH (For primary document see N84-12579 03-43)
Avail: NTIS HC A14/MF A01

A 5.35 GHz scatterometer used to simulate the ERS-1 (ESA satellite) and other spaceborne instruments is described. It can operate at several angles of incidence and polarization configurations. It was used for agronony, glaciology, and ocean surface wind measurements. The use of the scatterometer to study changes in surface water layers (down to 1 m) is outlined. Author (ESA)

N84-12589# Technische Univ. Munich, Garching (West Germany). Geowissenschaftliche Fernerkundung.
THE MODULAR OPTOELECTRONIC SCANNER (MOMS) ON STS-7, JUNE 83
Johann Bodechtel *In* ESA Remote Sensing Appl. for Environ. Studies Jul. 1983 p 65-68 (For primary document see N84-12579 03-43)
Avail: NTIS HC A14/MF A01

The Modular Optoelectronic Multispectral Scanner (MOMS) designed for regional and global optical remote sensing applications is presented. The SPAS STS-7 flight serves the technological space verification of the sensor and the demonstration of geoscientific and application-oriented experiments in worldwide distributed areas. The MOMS is a pushbroom, modular, sensor. It employs the dual lens principle for scan line extensions beyond one CCD array (up to six arrays per focal plane possible), and operates in the 0.5 to 2.3 micron range. Focal length is 237 mm; 6912 pixels per line; resolution = 20 x 20 m at 300 km altitude; total field of view = 26.2 deg (140 km); radiometric resolution = 128 gray levels (7 bit) Author (ESA)

N84-12590# Consiglio Nazionale delle Ricerche, Florence (Italy). Ist. di Ricerca sulle Onde Elettromagnetiche.
THE ISTITUTO DI RICERCA SULLE ONDE ELETTROMAGNETICHE (IROE)-LIDAR REMOTE SENSING OF THE ENVIRONMENT
V. Cappellini, F. Castagnoli, M. Morandi, L. Pantani, I. Pippi, B.

Radicati, L. Stefanutti, and C. Susini *In* ESA Remote Sensing Appl. for Environ. Studies Jul. 1983 p 69-78 refs (For primary document see N84-12579 03-43)
Avail: NTIS HC A14/MF A01

A method of measuring the extinction coefficient in heavy fog based on the extrapolation of the extinction coefficient from lidar signatures by operating the lidar with different receiver apertures was developed. Stratospheric aerosol measurements are carried out regularly and the evolution of the volcanic cloud produced by the Mexican volcano El Chichon is followed. The use of lidar systems in remote sensing of land and sea surface was investigated, especially the analysis of oil films on the surface of natural waters by fluorescence lidars. A fluorescence lidar simulator was developed. A technique for identification of natural targets by differential reflectance lidar was developed. Author (ESA)

N84-12591# Centre National pour l'Exploitation des Oceans, Brest (France). Centre Oceanologique de Bretagne.
APPLICATION OF HIGH RESOLUTION SATELLITE DATA TO COASTAL ZONES: SPOT SIMULATIONS DURING ECOLOGICAL SURVEY OF THE BRITANNY COAST [APPLICATION DES DONNEES SATELLITAIRES HAUTE RESOLUTION A L'OBSERVATION DU MILIEU LITTORAL LE CAS DES SIMULATIONS SPOT DANS LE CADRE DE LA VEILLE ECOLOGIQUE DES COTES BRETONNES]
L. Loubersac *In* ESA Remote Sensing Appl. for Environ. Studies Jul. 1983 p 79-85 refs In FRENCH; ENGLISH summary (For primary document see N84-12579 03-43)
Avail: NTIS HC A14/MF A01

Typical digital image processing methodologies based upon simulated SPOT data were developed in order to extract intertidal and infratidal zones from original images, to establish quantitative assessment of different features and to inventory resources to be exploited or protected. An example from a coastline study is presented. Author (ESA)

N84-12592# Canada Centre for Remote Sensing, Ottawa (Ontario).
REMOTE SENSING USING THE AIRBORNE MEIS 2 MULTIDETECTOR ELECTRO OPTICAL IMAGING SCANNER
S. M. Till, W. D. McColl, and R. A. Neville *In* ESA Remote Sensing Appl. for Environ. Studies Jul. 1983 p 87-92 refs (For primary document see N84-12579 03-43)
Avail: NTIS HC A14/MF A01

A pushbroom imaging scanner, MEIS 2, which uses charged coupled device linear array detectors, with spectral response covering the visible and near infrared regions was developed. It has a low noise-equivalent radiance and high spatial resolution, and combines flexibility of operation with real-time data processing. Flight trials demonstrate the capabilities of MEIS 2 for monitoring and mapping the environment. Applications include resource classification, vegetation stress analysis, and passive bathymetry, as well as digital cartography and terrain mapping. Author (ESA)

N84-12593# International Inst. for Aerial Survey and Earth Sciences, Enschede (Netherlands).
MAJOR WATER CONSERVATION AND RECLAMATION PROJECTS IN THE JIANGHAN PLAIN AND SURROUNDINGS, HUBEI PROVINCE, CHINA
I. Woldai *In* ESA Remote Sensing Appl. for Environ. Studies Jul. 1983 p 93-101 refs Sponsored by Netherlands Organization for the Advancement of Pure Research (ZWO) (For primary document see N84-12579 03-43)
Avail: NTIS HC A14/MF A01

Major water conservation and reclamation projects in the Jianghan Plain were analyzed using sequential images, false color composites and computer compatible tapes. Landforms and land use units were mapped. A dense network of canals and dikes and water retention basins was identified, mostly unrecorded in published maps. The diversional canals and dikes altered the pattern of flood devastation and siltation in the area. The reclamation of additional land around the low-lying lakes for cultivation was possible. Author (ESA)

N84-12594# Ghent Univ. (Belgium). Lab. for Regional Geography and Landscape Science.
INVENTORING AND MONITORING OF LANDSCAPE AS A NATURAL AND CULTURAL RESOURCE
M. Antrop *In* ESA Remote Sensing Appl. for Environ. Studies Jul. 1983 p 105-113 refs (For primary document see N84-12579 03-43)
Avail: NTIS HC A14/MF A01

The utility of remote sensing imagery for landscape studies is evaluated. Significant holistic and structural aspects of the landscape can be derived directly from image characteristics. Visual image interpretation, in particular photomorphic image classification, allows a fast and easy chorological and typological hierarchical landscape classification. Landscape units determined this way can be interpreted in ecological and geostructural perspective. Textural analysis is the most interesting quantitative interpretation technique for structural analysis of the landscape. The principal objectives for image interpretation for landscape studies are: updating of existing regional landscape classifications; hierarchical structurization of the landscape units and fitting of the microlevel units in the macrolevel ones, which are on a continental-European scale; detection of landscapes with high historical and cultural value; and detection and monitoring of zones with rapid changes and high intensity in land use. Author (ESA)

N84-12595# Universite Catholique de Louvain (Belgium). Lab. de Teledetection.
SAR 580: IMAGES FOR AGRICULTURAL AND FOREST SURVEY. FIRST RESULTS IN MIDDLE BELGIUM
Et. Bartholome and E. Barisano *In* ESA Remote Sensing Appl. for Environ. Studies Jul. 1983 p 115-121 refs (For primary document see N84-12579 03-43)
Avail: NTIS HC A14/MF A01

Some X and C band SAR 580 optical data acquired over Middle Belgium were analyzed for agricultural and forest inventory. On a mid range test site, visual classification gives mean agreement level of 78% compared with ground truth, while statistically classified spectral data derived from photos give 75%, and visual classification up to 99%. On a forest test site, six species can be classified on black and white air photos, while SAR discriminates four classes. Confusions do not appear between the same species on SAR data and multispectral data, underlining the interest of combination of both kinds of data. Author (ESA)

N84-12596# Ghent Univ. (Belgium). Lab. for Regional Geography and Landscape Studies.
MEASURING LANDSCAPE INFORMATION CONTENT AND DISTRIBUTION ON A SAR-580 IMAGE
Hugo Degroof *In* ESA Remote Sensing Appl. for Environ. Studies Jul. 1983 p 123-127 refs (For primary document see N84-12579 03-43)
Avail: NTIS HC A14/MF A01

An information theoretical approach to measure and evaluate the information content of an optically processed SAR-image is presented. The radar image is considered as a database for visual interpretation. It is shown that an interpretation key, elaborated according to the principles of conventional air photointerpretation and applied to the image, results in considerable loss of information. The elaboration of several interpretation keys, adapted for different subimages, gives a significant increase of information. The subimages were constructed relative to the system characteristics of SAR-580 and were oriented perpendicular to scan direction. The variation in information content shows a normal distribution across track. The subimages were evaluated according to their information content. Three classes were determined: low, moderate, and high information content zone. Author (ESA)

N84-12597# Ghent Univ. (Belgium). Lab. for Regional Geography and Landscape Studies.
INTERPRETABILITY OF WETLAND ON SEASAT-A IMAGERY IN THE POLDERLAND OF FLANDERS: A STRUCTURAL APPROACH
Hans Dufourmont *In* ESA Remote Sensing Appl. for Environ.

Studies Jul. 1983 p 129-132 refs (For primary document see N84-12579 03-43)
Avail: NTIS HC A14/MF A01

Visual interpretation of wetland in the polderland of Flanders was tested using SEASAT-A radar imagery. An approach based upon Gestalt-laws was chosen. This method results in a structural and hierarchical interpretation. The degree of detail increases gradually from high to low order hierarchical levels, so that previous interpretation steps offer a possibility of control for more detailed interpretation. Author (ESA)

N84-12598# Geological Survey of Greenland, Copenhagen (Denmark).
GLACIOLOGICAL APPLICATIONS OF LANDSAT IMAGES IN CONNECTION WITH HYDROPOWER INVESTIGATIONS IN WEST GREENLAND
Henrik Hoejmark Thomsen *In* ESA Remote Sensing Appl. for Environ. Studies Jul. 1983 p 133-136 refs (For primary document see N84-12579 03-43)
Avail: NTIS HC A14/MF A01

Digital image-processing of LANDSAT data (MSS) was started in connection with mapping of the hydroelectric potential of West Greenland. The Greenland ice sheet offers special problems in delineating individual ice streams. Geometrically corrected and contrast stretched LANDSAT images were used to detect flowline patterns, crevasse patterns and supraglacial streams, all of which can be related to ice and meltwater drainage. Mapping of the subglacial topography was attempted by studying shadow patterns on LANDSAT images taken under conditions of low Sun angle. Results show that digital image-processing of LANDSAT data is useful for mapping ice surface features. which can be used directly in glaciological-hydrological investigations and as a basis for planning of detailed investigations. Author (ESA)

N84-12599# Freiburg Univ. (West Germany). Abt. Luftbildmessung und Fernerkundung.
FIRST RESULTS OF THE EVALUATIONS OF THE EUROPEAN SAR 580 DATA FOR AGRICULTURAL AND FORESTRY PURPOSES IN TEST SITE D6, FREIBURG (WEST GERMANY)
R. Kessler, P. Reichert, and P. Loesche *In* ESA Remote Sensing Appl. for Environ. Studies Jul. 1983 p 137-145 refs (For primary document see N84-12579 03-43)
Avail: NTIS HC A14/MF A01

The separability of vegetation classes using X and C band HH polarized SAR 580 data was investigated. Results show that visual interpretation leads to better results than a standard maximum likelihood classification. However, the visual interpretation can be improved by analog or digital image enhancement techniques. The radar signal intensity allows a reliable distinction of the agricultural and forestry crops; pattern recognition technics have to be applied as well, especially for the classification of forest types. Use of the L-band and the crosspolarized data improve the separability of agricultural and forestry crops. Author (ESA)

N84-12600# Institut Geographique National, Brussels (Belgium).
REMOTE SENSING AND TOPOGRAPHIC MAPS
J. Loodts and J. Theatre *In* ESA Remote Sensing Appl. for Environ. Studies Jul. 1983 p 147-156 refs (For primary document see N84-12579 03-43)
Avail: NTIS HC A14/MF A01

A process which allows the combination of remote sensing data with small scale topographic maps is described. Every treatment is performed on raster systems. Two raster systems are used: one is dedicated to remote sensing data classification, the second is used for cartographic purposes (topographic and thematic maps). Conciliation of cartographic and remote sensing languages is discussed. The former deals with structure, the latter deals with classes in terms of multispectral distribution. Quantitatively they are not the same. One way to avoid this problem is to use the concept of geocode and structural stability models.
Author (ESA)

N84-12601# Eurosense B.V., The Hague (Netherlands). Remote Sensing Dept.
AN OPERATIONAL REMOTE SENSING METHODOLOGY FOR THE DETECTION, INVENTORY AND ENVIRONMENTAL MONITORING OF WASTE DISPOSAL SITES
J. L. vanGenderen, J. A. vandeGriend (Provincial Government of South Holland), and H. T. C. vanStokkom (Netherlands Remote Sensing Board) *In* ESA Remote Sensing Appl. of Environ. Studies Jul. 1983 p 149-156 refs (For primary document see N84-12579 03-43)
Avail: NTIS HC A14/MF A01

A classification of waste disposal sites was developed and used for the systematic interpretation of the remote sensing data of a 150 sq km test area. The devised methodology is described. The results of the ground truth confirm that using 1:10,000 color infrared aerial photography, it is possible to detect and locate all active waste disposal sites, and most former waste disposal sites. In most cases, remote sensing techniques cannot say whether the material being tipped in the waste disposal site is toxic or not. With active sites, it is only possible to determine the physical state of the waste disposal material. Whether this is detrimental to the environment or not can only be determined by indirect means (e.g., vegetation stress). With a few exceptions, it is impossible to say when the material was tipped. Accuracy tests show that the results are sufficiently reliable to enable remote sensing to be used in a cost-effective operational mode as part of regional environmental management activities. Author (ESA)

N84-12602# Sheffield Univ. (England). Dept. of Geography.
THE USE OF AIRBORNE THEMATIC MAPPER SIMULATION DATA FOR THE ESTIMATION AND MAPPING OF GREEN LEAF AREA INDEX (GLAI)
D. E. Williams (Natural Environment Research Council, Swindon, UK), P. Curran, and N. Wardley *In* ESA Remote Sensing Appl. for Environ. Studies Jul. 1983 p 157-160 refs (For primary document see N84-12579 03-43)
(Contract NERC-MSS-82)
Avail: NTIS HC A14/MF A01

An experiment to estimate and map the green leaf area index (GLAI), as part of simulation studies for the LANDSAT 4 thematic mapping mission, is described. Using an airborne channel scanner, the perpendicular vegetation index (PVI) was obtained from the ratio of the near infrared band, i.e., bands MSS 7 + 8, over the red bands (MSS 4 + 5). The GLAI was then predicted using the equation PVI = 16.59 (8.11 log GLAI). Due to a reduced number of sample points, four classes of GLAI were used. Results show that the accuracy of classification increases for higher GLAI. This is to be expected because the same error is a smaller percentage to the absolute PVI than for low GLAI. Woodland areas were included because with the high resolution data the texture and shading gives spurious results. Author (ESA)

N84-12603# Dundee Univ. (Scotland). Carneige Lab. of Physics.
SATELLITE REMOTE SENSING, ENVIRONMENTAL MONITORING AND THE OFFSHORE OIL AND GAS INDUSTRIES
A. P. Cracknell, K. Muirhead, R. D. Callison, and N. A. Campbell *In* ESA Remote Sensing Appl. for Environ. Studies Jul. 1983 p 163-171 refs Sponsored by UK Science and Engineering Research Council and Manpower Services Commission (For primary document see N84-12579 03-43)
Avail: NTIS HC A14/MF A01

Monitoring of oil slicks using meteorological satellites and LANDSAT is described. Results from the Gulf of Mexico are presented. The use of TIROS-N data for the monitoring of gas flares from production platforms in the North Sea is described. Slicks are manifested more clearly in the visible than in the infrared spectral channels; reasons for this, in terms of the temperature and emissivity of both oil and water were explored. Difficulties associated with spatial resolution, spectral resolution, the frequency of coverage governed by orbital considerations, the common presence of cloud cover and the need for real-time access to, and processing of satellite data are discussed. Gas flares can be

monitored successfully using the infrared band of the AVHRR on the TIROS-N satellites. With very few exceptions, it is possible to identify unambiguously the platform that is responsible for any given flare. Although it is possible to classify flares roughly into large, medium and small it is not possible to derive a reliable estimate, from the satellite data, for the quantity of gas being burned. Author (ESA)

N84-12604# European Space Agency, Paris (France).
TWO DIFFERENT ASPECTS OF PHYTOPLANKTON BLOOM SEEN BY SATELLITE (CZCS) IN THE WESTERN ENGLISH CHANNEL [DEUX ASPECTS DIFFERENTS DES FLORAISONS DE PHYTOPLANCTON VUS PAR SATELLITE (CZCS) EN MANCHE OCCIDENTALE]
C. Dupouy (ORSTOM, Bondy, France) *In* ESA Remote Sensing Appl. for Environ. Studies Jul. 1983 p 173-177 refs In FRENCH; ENGLISH summary Sponsored by CNRS, CNES and French Ministry of the Environment (For primary document see N84-12579 03-43)
Avail: NTIS HC A14/MF A01

Two images recorded during summer by the CZCS on NIMBUS 7 over the English Channel are presented. They provide a synpotic view of very large patterns of complex shape related differently in June and July to the thermal front. Spectral signatures measured during two oceanographic campaigns at the same time as the images allow the development of an algorithm for determination of chlorophyll concentration in the zone. Corresponding hydrologic and biological data prove that the two observed phytoplankton blooms have a different type (diatoms/dinoflagellates) and probably do not have the same implications on the marine food chain.
Author (ESA)

N84-12605# Bergen Univ. (Norway). Inst. of Geophysics.
APPLICATION OF REMOTE SENSING FOR STUDIES, MAPPING AND FORECASTING OF EDDIES ON THE NORWEGIAN CONTINENTAL SHELF
Ola M. Johannessen, Johnny A. Johannessen, and Brian A. Farrelly *In* ESA Remote Sensing Appl. for Environ. Studies Jul. 1983 p 179-187 refs (For primary document see N84-12579 03-43)
Avail: NTIS HC A14/MF A01

An integrated remote sensing/in situ observational study of the Norwegian continental shelf is recommended. A series of waves exists on this front, with a wavelength of 100 km and a wave width of 50 km. These waves develop into eddies which propagate northwards with a speed of 0.2 to 0.3 knots and with an orbital speed of more than 3 knots. The strong currents associated with these eddies interfere with oil drilling operations. Active sensors, similar to those of ERS-1 (ESA satellite) are advocated, for example the SIR-B SAR to be launched by a space shuttle in 1984. Land or platform based high frequency radar is also advocated.
Author (ESA)

N84-12606# Ministere de l'Environment et du Cadre de Vie, Neuilly (France).
ACTUAL STATE AND RECENT EVOLUTION OF THE FRENCH COAST OBSERVED BY REMOTE SENSING USING LANDSAT RECORDINGS [ETAT ACTUEL ET EVOLUTION RECENTE DE L'ENVIRONNEMENT DU LITTORAL FRANCAIS OBSERVE PAR TELEDETECTION A PARTIR DES ENREGISTREMENTS LANDSAT]
M. Lenco *In* ESA Remote Sensing Appl. for Environ. Studies Jul. 1983 p 189-195 In FRENCH (For primary document see N84-12579 03-43)
Avail: NTIS HC A14/MF A01

LANDSAT images of the French coast provided physical, cartographic, and numerical information for an environmental survey of a maritime zone 5 km wide, and a 20 km wide coastal strip. False color composites (1:100,000) from bands 4,5 and 7 were produced for the recent past and 5 years ago. Two map series were obtained: one showing biophysically homogeneous zones, nature of coastline, physical characteristics of ocean surface; and the other showing land use, The latter series has 40 catagories describing present situation and changes occuring in the past 5 years, with numerical results by administrative department and in strips parallel to the coast. Author (ESA)

N84-12607# Ministere de l'Environment et du Cadre de Vie, Neuilly (France). Direction de la Prevention des Pollutions.
REMOTE SENSING APPLIED TO MARINE POLLUTION CONTROL
J. M. Massin *In* ESA Remote Sensing Appl. for Environ. Studies Jul. 1983 p 197-202 (For primary document see N84-12579 03-43)
Avail: NTIS HC A14/MF A01

The requirements of a remote sensing sensing system to monitor marine pollution, particularly oil pollution, are outlined, and a study of the possibilities offered by remote sensing in setting up models to anticipate pollution movements at sea is proposed. Multisensor systems with real time display and interactive processing of data on board surveillance aircraft are advocated. Research and development of the sensor and its software should be undertaken simultaneously. Standardization of computer languages, data handling, and reporting is urged, to facilitate international cooperation. Author (ESA)

N84-12608# Technical Univ. of Denmark, Lyngby. Inst. of Electromagnetics.
INTRODUCTORY STUDIES OF NATURAL CONTAMINATION AND MANMADE POLLUTION IN DANISH WATERS
A. Nielsen (National Agency of Environmental Protection, Charlottenlund, Denmark), P. Hansen, A. Malmgren (Academy of Technical Sciences, Hoersholm, Denmark), and V. Hansen (Danish Inst. for Fisheries and Marine Research, Hirtsnals) *In* ESA Remote Sensing Appl. in Environ. Studies Jul. 1983 p 203-210 refs (For primary document see N84-12579 03-43)
Avail: NTIS HC A14/MF A01

A satellite-aircraft system for surveying oil spills and plankton blooms is outlined. Retrieval of chlorophyll concentration from airborne multispectral scanner measurements is described. A plankton bloom in the Baltic Sea observed by LANDSAT is discussed. Observation of plankton blooms requires frequent coverage with a medium resolution satellite sensor, such as the coastal zone color scanner or the multispectral scanner on MOS-1. Direct acquisition of data from satellites is preferred, but may be too expensive. Meteorological data and physical, chemical, and biological measurements can be obtained from existing sources. Aircraft-borne cameras and multispectral scanners can supplement satellite coverage in cloudy conditions. Author (ESA)

N84-12609# Technical Univ. of Denmark, Lyngby.
PASSIVE RADIOMETRY AND OTHER REMOTE SENSING DATA INTERPRETATION FOR OIL SLICK THICKNESS ASSESSMENT, IN AN EXPERIMENTAL CASE
N. Skou, F. Toselli (Joint Research Centre of the European Communities), and A. Wadsworth (Inst. Francais du Petrole, Rueil-Malmaison, France) *In* ESA Remote Sensing Appl. in Environ. Studies Jul. 1983 p 221-216 refs (For primary document see N84-12579 03-43)
Avail: NTIS HC A14/MF A01

Oil spills in the Mediterranean Sea were monitored by remote sensing. Three microwave radiometers (5, 17 and 34 GHz) with profiling and imaging modes were flown over 5 slicks spreading out from original surfaces of 20,000 sqm each. Infrared and sea truth measurements were also made. The slick thickness obtained by the radiometers indicates oil volumes in fair agreement with the quantities spilled. With the imaging mode, areal extent of the oil is directly depicted in just one pass. Oil thickness is measured with sufficient accuracy to assess the total oil volume in the slick. Aircraft navigation is straightforward due to a reasonable swath width of the imaging radiometer. In the low flying profiling mode, oil thickness is measured with great accuracy and resolution. Detailed thickness distributions within the oil slick can be measured. Navigation is delicate over limited sized slicks. The measured profiles must be superimposed semiautomatically on imagery of the oil slick taken simultaneously from the same aircraft
Author (ESA)

N84-12610# Dundee Univ. (Scotland). Carnegie Lab. of Physics.
NORMALIZATION OF WATER-LEAVING RADIANCE OBTAINED FROM THE COASTAL ZONE COLOUR SCANNER (CZCS) DATA
S. M. Singh *In* ESA Remote Sensing Appl. in Environ. Studies Jul. 1983 p 217-222 refs Sponsored by UK Science and Engineering Research Council (For primary document see N84-12579 03-43)
Avail: NTIS HC A14/MF A01

A method of normalizing the water-leaving radiances retrieved from the CZCS date, which shows that variations in the normalized water-leaving radiances are due to the variations in the water quality only, was developed. The method removes those variations in the water-leaving radiance which are caused by the variations in the global irradiance on the water-surface. When the log of chlorophyll-like pigment concentrations is plotted against the log of the water-leaving radiance ratio in two spectral channels, the slope of the regression line does not change after normalizing the radiances. However, the intercept of the regression line changes significantly. An expression for the normalized value of the intercept is derived. It is shown that another normalization procedure does not account for all factors which cause variations in the global irradiance. Author (ESA)

N84-12611# Centre d'Etudes Techniques de l'Equipment, Aix-en-Provence (France).
OPERATIONAL UTILIZATION OF REMOTE SENSING IN A STUDY OF THE IMPACT OF DISPOSAL OF URBAN WASTE AT SEA [UTILISATION OPERATIONNELLE DE LA TELEDETECTION DANS LE CADRE D'UNE ETUDE D'IMPACT D'UN REJET URBAIN EN MER]
Claudine Valerio *In* ESA Remote Sensing Appl. in Environ. Studies Jul. 1983 p 223-227 refs In FRENCH; ENGLISH summary (For primary document see N84-12579 03-43)
Avail: NTIS HC A14/MF A01

Airborne quantitative photographic remote sensing links with other means to collect data on the effects of sewage discharge into the sea are shown. Since there are two possible polluting sources for the beach (the river and the sewage) two different dye tracers were used simultaneously in the same marine zone to evaluate the individual influence of both sources. Results show that both sources contribute significantly to beach pollution, and illustrate the usefulness of remote sensing for studying the interactions. Author (ESA)

N84-12612# Institut Francais du Petrole, Rueil-Malmaison.
RADAR BATHYMETRY : A REVIEW
A. Wadsworth and P. Piau *In* ESA Remote Sensing Appl. for Environ. Studies Jul. 1983 p 229-238 refs (For primary document see N84-12579 03-43)
Avail: NTIS HC A14/MF A01

Use of imaging radar (SAR or SLAR) to provide information on sea bottom features, corresponding to morphology of the sea floor, in shallow waters, is described. It is shown how, with the same kind of imaging radar, valuable information can be extracted on significant bottom features, in the case of medium depths. The possibility of having a rough but almost real bathymetry, in the deepest seas, when using altimeter data, is depicted. An interpretation of the mechanism of the visualization of bathymetry by an imaging radar is discussed. Author (ESA)

N84-12613# Universidad Politecnica de Barcelona (Spain). Centre de Calcul.
MAPPING LAND USE IN CATALONIA (SPAIN) [UN ESSAI DE CARTOGRAPHIE DE L'UTILISATION DES SOLS EN CATALOGNE]
R. Arbiol, O. Vinas, and Joseph M. Camarasa (Generalitat de Catalunya, Barcelona) *In* ESA Remote Sensing Appl. for Environ. Studies Jul. 1983 p 241-247 refs In FRENCH; ENGLISH summary (For primary document see N84-12579 03-43)
Avail: NTIS HC A14/MF A01

A map of land use in a 32,000 sq km area of Spain was produced using LANDSAT imagery. A classification process which includes an unsupervised analysis of 87 scenes, 27 X 19 km, supervised analysis of small, homogeneous zones, and classification of all the pixels of each scene by the lowest distances was used. Agreement between the automatic classification and manual data from agronomical maps is excellent, in spite of snow cover of several zones. Author (ESA)

N84-12614# Belfotop P.v.b.a., Wemmel (Belgium).
INVENTORY OF FLEMISH FORESTS USING MEDIUM-SCALE COLOR INFRARED (CIR) PHOTOGRAPHY AND CIR ORTHOPHOTOPLANS AS BASE FOR A FOREST MANAGEMENT DATA BANK
P. R. Coppin, B.P. DeRoover, W. M. Dewispelaere (CEVA, Melle-Gontrode, Belgium), and R. E. Goossens (CEVA, Melle-Gontrode, Belgium) *In* ESA Remote Sensing Appl. in Environ. Studies Jul. 1983 p 249-255 (For primary document see N84-12579 03-43)
Avail: NTIS HC A14/MF A01

Remote sensing techniques were used for a complete assessment of the Flemish forest situation in order to develop an operational methodology for producing sequential forest inventories; to create a forest management data bank; and to produce base maps with high accuracy. Material consisted of CIR-transparencies and orthophotoplans. digitizer and microcomputer were used. The information resulting from interpretation, fieldwork and other sources was produced in numerical and analog (overlays, computer-maps) form. The data bank allows further extension of information at management level. Author (ESA)

N84-12615# Groupement pour le Developpement de la Teledetection Aerospatiale, Toulouse (France).
THE SPOT DISTRIBUTION SYSTEM
J. D. Dupuy *In* ESA Remote Sensing Appl. in Environ. Studies Jul. 1983 p 257-259 (For primary document see N84-12579 03-43)
Avail: NTIS HC A14/MF A01

The SPOT system consists of the French Space Agency (CNES) responsible for the program development and operator of the SPOT series; the SPOT IMAGE Company which markets and distributes SPOT products on a worldwide basis; and a network of foreign ground receiving stations under contract with SPOT IMAGE. The data acquisition-distribution system features on request data acquisition policy with an acquisition fee proportional to the amount of data acquired by the foreign ground stations; definition of marketing areas between SPOT IMAGE and the distribution centers; data distribution on a nondiscriminatory basis; and protection of SPOT data by a copyright. Author (ESA)

N84-12616# Catania Univ. (Italy). Inst. of Machinery.
REMOTE SENSING ANALYSIS OF OIL POLLUTION IN AUGUSTA BAY, SICILY
Alberto L. Geraci and Tommaso Caltabiano *In* ESA Remote Sensing Appl. in Environ. Studies Jul. 1983 p 261-271 refs (For primary document see N84-12579 03-43)
Avail: NTIS HC A14/MF A01

Simultaneous acquisition of data from infrared photography and thermal infrared imagery was used to study oil pollution in a Mediterranean bay. Conventional 35 mm cameras and an airborne thermovision system were used. Highly polluted areas and illegally discharging vessels are clearly discernible. Infrared photography and thermal infrared imagery must be used in conjunction with each other to provide accurate interpretation of the data. Author (ESA)

N84-12617# Eurosense Belfotop G.m.b.H., Huerth (West Germany).
THE SYNTHESIZED CLIMATIC FUNCTION MAP
Siegfried Haberl and Peter Stock (Hommunalverband Ruhrgebiet, Essen, West Germany) *In* ESA Remote Sensing Appl. in Environ. Studies Jul. 1983 p 273-281 refs (For primary document see N84-12579 03-43)
Avail: NTIS HC A14/MF A01

Aircraft and balloon-borne multispectral scanner data were

used for infrared thermography of an urban area in order to study the microclimate. The data were combined with ground truth data from weather stations to produce a climatic function map. Night and daytime thermal maps were compared, showing the heat loss relative to land use and type of material. Author (ESA)

N84-12618# Army Cold Regions Research and Engineering Lab., Hanover, N. H.
PREDICTING LAKE ICE DECAY Special Report
George D. Ashton Jun. 1983 8 p
(AD-A132012; CRREL-SR-83-19) Avail: NTIS HC A02/MF A01 CSCL 08/12

A nine-year record of the lake ice decay pattern of Post Pond in Lyme, New Hampshire, is analyzed using a simple algorithm. Quite good correlations between decay rates and thawing degree-days are obtained using heat transfer coefficients on the order of 15-20 W/sq. m./deg C. Author (GRA)

N84-12619# Army Cold Regions Research and Engineering Lab., Hanover, N. H.
MECHANICAL BEHAVIOR OF SEA ICE
Malcolm Mellor Jun. 1983 115 p
(AD-A131852; CRREL-MONO-83-1) Avail: NTIS HC A06/MF A01 CSCL 08/12

The first part of the report provides an introduction to the mechanics of deformable solids, covering the basic ideas of stress and strain, rheology, equilibrium equations, strain/displacement relations, constitutive equations, and failure criteria. Fracture mechanics and fracture toughness are also reviewed briefly. The second part summarizes available data on the mechanical properties of freshwater ice and saline ice, accounting for the influences of strain rate and loading rate, temperature, porosity, salinity, and grain size. Boundary value problems are not dealt with, but there is discussion of some miscellaneous topics, including thermal strains, behavior of brash ice, and pressure ridges. The report was written as a study text for a NATO Advanced Study Institute on Sea/Ice/Air Interactions, and was intended to be used in conjunction with companion texts on related topics. This report was written during the summer of 1981, and thus does not cover all results which appeared after the end of 1981. GRA

N84-12620# Texas Univ., Austin. Bureau of Economic Geology.
ESTIMATION OF UNCERTAINTY IN COAL RESOURCES Final Report
S. J. Tewalt, M. A. Bauer, D. Mathew, M. P. Roberts, W. B. Ayers, Jr., J. W. Barnes, W. R. Kaiser, N. Kim, E. D. Orr, and C. H. Wilson Jun. 1983 156 p refs Sponsored by EPRI
(EPRI Proj. 1367-1)
(DE83-902538; EPRI-EA-3133) Avail: NTIS HC A08/MF A01

A methodology was devised that provided coal resource estimates and quantified their associated uncertainty. The regional test area was the Wilcox Group outcrop in east-central Texas. Geostatistics did not yield a dependency structure for the entire area; therefore, alternate methods were used: (1) equal weighting over the entire area; (2) equal weighting within grid cells and (3) equal weighting within internally homogeneous blocks chosen by using statistical or geologic parameters. The methodology was successfully transferred to the Tongue River Member, Wyoming, and to the Allegheny Formation, Ohio. Tonnages calculated for Wyoming and Ohio exceeded official estimates because deep-basin, thick continuous coals were included. Depositional models were used to calculate resources for the entire Gulf Coast. Calculated resources indicate the magnitude of total resources, but do not quantitatively measure the associated uncertainty.

N84-12621# Mine Safety and Health Administration, Denver, Colo. Health and Safety Analysis Center.
USE OF AIRCRAFT IMAGERY IN EVALUATING GROUND STABILITY AT OPEN-PIT URANIUM MINES IN GAS HILLS, WYOMING
R. L. Stahl 1983 14 p refs
(DE83-903011; MSHA/IR-1131) Avail: NTIS HC A02/MF A01

Ground stability in open pit mining operations in the Gas Hills, Wyoming is evaluated. The approach uses aircraft imagery to identify geologic features, such as fractures and faults, that can affect ground stability in surface mines. Operators in the Gas Hills are using this technology as a mine planning and design tool to avoid or to minimizes the effects of fractures and faults on ground stability. This remote sensing tool is appealing because it is inexpensive, accurate, and one that permits rapid evaluation of a mining area on a local and regional scale. DOE

N84-12622# Midwest Research Inst., Golden, Colo. Renewable Resource Assessment and Instrumentation Branch.
REVIEW OF POTENTIAL SATELLITE TECHNIQUES FOR MESOSCALE MAPPING OF INSOLATION
C. J. Riordan and Roland L. Hulstrom Jun. 1983 30 p refs
(Contracts DE-AC02-77CH-00178; EG-77-C-01-4042)
(DE83-011998; SERI/TR-215-1824) Avail: NTIS HC A03/MF A01

Techniques to characterize mesoscale insolation variations using satellite derived data on cloud cover were reviewed. Representative statistical and physical models that incorporate satellite data are described. Reported accuracies of the models indicate the feasibility of using satellite techniques, but practicality has yet to be demonstrated. Issues to be resolved include cost and accessibility of high volume satellite data, cost accuracy of data preprocessing, and accuracy of models under various amounts of cloud cover. Use of a simple clear sky model with a satellite derived cloud cover modifier is recommended. DOE

N84-12623# Geological Survey, Alexandria, Va.
ALASKA'S MINERAL RESOURCES Annual Report for 1982
1982 67 p refs
(DE83-016599; USFS-CIRC-884) Avail: NTIS HC A04/MF A01

Federal and state publications, trade and professional journals, symposia proceedings, public meetings and hearings, press releases, and newspaper and magazine articles were sources of the information presented. Only onshore areas of Alaska are addressed, and information on minerals of interest in two broad categories: energy resources (oil and gas, uranium, coal and peat, and geothermal resources) and nonfuel, critical, and strategic minerals is provided. DOE

N84-12624# Environmental Protection Agency, Ada, Okla. Earth Sciences Div.
VELOCITY PLOTS AND CAPTURE ZONES OF PUMPING CENTERS FOR GROUND-WATER INVESTIGATIONS
J. F. Keely and C. F. Tsang Berkeley, Calif. California Univ., Lawrence Berkeley Lab. May 1983 41 p refs Presented at the 3rd Natl. Symp. on Aquifer Restoration and Groundwater Monitoring, Columbus, Ohio, 25-27 May 1983
(DE83-016618; LBL-16101; CONF-830561-3) Avail: NTIS HC A03/MF A01

Defining the geometry of the portion of the aquifer contributing water to the well (the capture zone) is outlined. Nonpumping monitoring wells are commonly installed and sampled to delineate the extent of a contaminant plume and its chemical character. Samples from municipal and private pumping wells are frequently collected during ground water contamination investigations. Pumping wells are also employed for remedial actions. Velocity distribution plots by manual and computerized methods are illustrated. DOE

N84-12625# Michigan Univ., Ann Arbor.
TO QUENCH OUR THIRST: THE PRESENT AND FUTURE STATUS OF FRESHWATER RESOURCES OF THE UNITED STATES, PART 3
David A. Francko and Robert G. Wetzel 1983 150 p refs
(Contract DE-AC02-76EV-01599)
(DE83-016791; DOE/EV-01599/235-Pt-3; COO-1599-235-Pt-3; COO-1599-233; LC-83-1071; ISBN-0-472-10032-7; ISBN-0-472-08037-7) Avail: NTIS HC A07/MF A01

The current situation in United States water resources, including an overview of the hydrologic cycle, supply and demand crises,

and reduction of consumption of water and the degradation of existing supplies, are included and maximize the effectiveness of natural processes which recharge surface and groundwater reserves. DOE

N84-12626# Duke Univ., Durham, N. C. Dept. of History.
DEVELOPMENT OF A DATA BASE FOR CARBON DIOXIDE RELEASES RESULTING FROM CONVERSION OF LAND TO AGRICULTURAL USES
J. F. Richards, Jerry S. Olson (ORNL), and Ralph M. Rotty (Oak Ridge Associated Univ.) Jul. 1983 145 p
(Contracts DE-AC05-76OR-00333; W-7405-eng-26)
(DE83-015728; ORAU/IEA-82-10(M); ORNL-TM-8801) Avail: NTIS HC A07/MF A01

Worldwide conversion of land to regular agricultural uses for the periods 1860 to 1920 and 1920 to 1978 was summarized. New estimates are made for nation by nation conversion of land into permanent cropland. Estimated carbon content was tabulated for each type of vegetation removed. The estimated increased releases of CO2 are presented by country or colony and by world region, and in a global summary for the two chronological periods. A global tabulation excluding Greenland and Antarctica, reveals that approximately 440 million hectares were converted to arable land between 1860 and 1920, increasing during 1920 to 1978 to 470 million hectares. Shrinkage of arable land within individual countries, which presumes reversion to woodland or lesser vegetation, totaled only 8.7 million hectares in the first period in contrast to 51 million hectares in the second period. Expansion of regularly cropped area resulted in releases of nearly 39 x 10(9) tons of carbon from the live plant mass during the 118 year period. Preliminary estimates of losses from oxidation of humus from the same area were smaller, amounting to about 23 x 10(9) tons of carbon. DOE

N84-12627# Michigan State Univ., Hickory Corners. Biological Station.
LIMNOLOGY, SECOND EDITION
Robert G. Wetzel Philadelphia Saunders College Publishing 1983 866 p refs Sponsored in part by NSF
(Contract DE-AC02-76EV-01599)
(DE83-016792; DOE/EV-01599-235-Pt-4; COO-1599-235-Pt-4; COO-1599-234; LC-81-53073; ISBN-0-03-057913-9) Avail: NTIS HC A99/MF A01

The book is intended as an updated resume of the field. The initial chapters cover water as a substance, geomorphology, water economy relations, light, thermal properties, and hydro- 1 dynamics. A brief discussion is included on productivity and ecosystem trophic relationships. The fundamental chemical dynamics are introduced with a continual integration of the biota. DOE

N84-12628# Technische Univ., Vienna (Austria). Inst. fuer Photogrammetrie.
RECTIFICATION OF MULTISPECTRAL SCANNER IMAGES Ph.D. Thesis [REKTIFIZIERUNG VON MULTISPEKTRAL-SCANNERAUFNAHMEN. ENTWICKLUNG UND ERPROBUNG EINES EDV-PROGRAMMES]
Josef Jansa May 1983 116 p refs In GERMAN; ENGLISH summary
(GEOWISS-MITT-24-1983) Avail: NTIS HC A06/MF A01

The main types of multispectral scanner (MSS) image distortion are discussed and illustrated by their influence on images of a regular grid. Techniques to rectify MSS imagery densities using the nonparametric solution with least squares interpolation are outlined. The rectification can be performed digitally of optically. The main steps of the process are reviewed along with the corresponding sections of the computer program (point selection and measurement, determining image distortions by least square interpolation, selecting pixel size, slit length, rectification itself, and mosaicing). Possibilities of error detection and of quality evaluation are considered. Author (ESA)

N84-12629# European Space Agency, Paris (France).
OBSERVATION OF THE EARTH IN THE MIDDLE INFRARED Final Report
M. Dinguirard, M. Grellier, and M. Laug Sep. 1983 30 p refs Transl. into ENGLISH of "Observation de la Terre dans l'Infrarouge moyen, Rapport Final", ONERA, Toulouse Report CERT-9/6026-DERO, Feb. 1977
(ESA-TT-790; CERT-9/6026-DERO) Avail: NTIS HC A03/MF A01

The optimal spectral bandwidth of the middle infrared windows around 1.65 and 2.30 microns, constituting a compromise between an adequate signal level and a low influence of spatial or seasonal variations in the concentration of water vapor in the atmosphere, was evaluated. The computer code LOWTRAN 3 for the computation of atmospheric transmission was simplified for an HP 9830 A computer. Results show that atmospheric effects can be ascertained and that there are advantages in sacrificing mean transmittance to obtain a larger signal (by using a wider window) up to a limit determined by instrument noise level. Author (ESA)

N84-12630# Research Inst. of National Defence, Linkoeping (Sweden). Dept. 3.
OBSERVATIONS AND CLASSIFICATIONS WITH A 35/94 GHz RADIOMETER OF TERRAIN NEAR MOTALA, SWEDEN, JULY 1982
Bengt Svensson Jun. 1983 33 p refs Original contains color illustrations
(FOA-C-30325-E1,E3; ISSN-0347-3708) Avail: NTIS HC A03/MF A01; Research Inst. of National Defence, Stockholm KR 50

Measurements with an imaging, dual-frequency radiometer system of the terrain around a TV tower are presented. The radiometers are of the Dicke-type with 60 and 30.5 cm parabolic Cassegrain antennas. The antennas were controlled by a desk-top computer, which also managed the data sampling and recording. Color-coded radiometric images were constructed from the processed data. Reflection of cold sky radiation from smooth surfaces (metals, plastics, roads) produces a contrast compared with the less reflective surroundings. The images were analyzed with respect to the characteristics of different objects and types of terrain. A classification diagram and image classifications are obtained. Author (ESA)

N84-12631# Federal Geodetic Control Committee, Rockville, Md. Instrument Subcommittee.
TEST AND DEMONSTRATION OF MACROMETER (TM) MODEL V-1000 INTERFEROMETRIC SURVEYOR
Larry D. Hothem and Charles J. Fronczek May 1983 41 p refs (PB83-239103; FGCC-IS-83-2; NOAA-83072201) Avail: NTIS HC A03/MF A01 CSCL 08E

An interferometric surveying system which uses radio signals from the satellites of the Global Positioning system (GPS) to determine three dimensional relative positions of survey stations without requiring interstation visibility was demonstrated. Macrometer model V-1000 receivers and the model P-1000 data processor were tested in order to assess the accuracies of Macrometer determinations of base line lengths, azimuths, and ellipsoidal height differences, the FGCC used terrestrial surveys as standards for comparison. The coordinates for the test network were obtained from a special adjustment of the U.S. Transcontinental Traverse. GRA

N84-12632# Woods Hole Oceanographic Institution, Mass.
SEDIMENT TRANSPORT IN A TIDAL INLET Technical Report, 15 Oct. 1980 - 14 Oct. 1982
David G. Aubrey and Paul E. Speer Jun. 1983 113 p refs Sponsored in part by NOAA
(Contract DAAG29-81-K-0004; Grants NA79AA-D-00102; NA80AA-D-00077)
(PB83-242271; WHOI-TR-83-20; NOAA-83080101) Avail: NTIS HC A06/MF A01 CSCL 08H

Various aspects of sediment transport in and around natural, unstructured tidal inlets were investigated, Concentrating on two tidal inlets and combining detailed field observations with numeri-

cal model studies of tidal flows in inlet/estuarine environments, several aspects of tidal inlet behavior were clarified. Primary scientific items addressed include: (1) Diagnostic numerical model of generation and propagation of tidal nonliniarities in shallow estuarine channels; (2) effects of flow curvature on tidal inlet sediment transport; (3) definition of mechanisms by which tidal inlets migrate in a direction; (4) hypothesis of a mechanism for rapid barrier spit growth in locations with low rates of littoral transport; (5) clarification of long term patterns of sea level rise to assess its role in tidal inlet/esturarine evolution; and (6) historical descriptions of massive inlet migration at two inlets as supporting evidence for the inlet modeling studies. GRA

N84-12633# Wyoming Univ., Laramie. Water Resources Research Inst.
SNOWY RANGE OBSERVATORY: CLIMATOLOGICAL AND STREAMFLOW DATA REPORT 1982
Greg L. Kerr and Thomas A. Wesche Jan. 1983 91 p ref
(Contract DI-14-34-0001-2154)
(PB83-243147; W83-03675; OWRT-A-030-WYO(1)) Avail: NTIS HC A05/MF A01 CSCL 08H

Data for climatologic and water year streamflow from the Snowy Range Water Resources Observatory are presented. Included in the Observatory are 21 recording precipitation gages, six recording hygrothermographs, five anemometers and seven streamflow gaging stations. GRA

44 ENERGY PRODUCTION AND CONVERSION

Includes specific energy conversion systems, e.g., fuel cells and batteries; global sources of energy; fossil fuels; geophysical conversion; hydroelectric power; and wind power.

For related information see also *07 Aircraft Propulsion and Power, 20 Spacecraft Propulsion and Power, 28 Propellants and Fuels,* and *85 Urban Technology and Transportation.*

N84-12634*# TRW Space Technology Labs., Redondo Beach, Calif. Power Sources Engineering Dept.
STUDY OF MULTI-KILOWATT SOLAR ARRAYS FOR EARTH ORBIT APPLICATIONS Final Report, 19 Nov. 1980 - 30 Jun. 1983
Robert E. Patterson 15 Oct. 1983 200 p refs
(Contract NAS8-34131)
(NASA-CR-170939; NAS 1.26:170939; Rept-38172-6001-UE-00) Avail: NTIS HC A09/MF A01 CSCL 10A

A miniaturized Cassegrainian concentrator (MCC) solar array concept is being developed with the objective of significantly reducing the recurring cost of multikilowatt solar arrays. The desired cost reduction is obtained as a result of using very small high efficiency solar cells in conjuction with low cost optics. The MCC single element concept incident slar radiation is reflected rom a primary parabolic reflector to a secondary hyperbolic reflector and finally to a 4 millimeter diameter solar cell. A light catcher cone is used to improve off axis performance. The solar cell is mounted to a heat fin. An element is approximately 13 millimeters thick which permits efficient launch stowage of the concentrator system panels without complex optical component deployments or retractions. The MCC elements are packed in bays within graphite epoxy frames and are electrically connected into appropriate series-parallel circuits. A MCC sngle element with a 21 sq cm entrance aperture and a 20 efficient, 0.25 sq cm gallium arsenide solar cell has the same power output as 30 sq cm of 11-percent efficiency (at 68 C) silicon solar cells. S.C.L.

N84-12635*# National Aeronautics and Space Administration. Pasadena Office, Calif.
FLUIDIZED BED GASIFICATION OF BIOMASS TO METHANE Patent Application
Shaik A. Qader, inventor (to NASA) (JPL, California Inst. of Tech., Pasadena) Filed 31 Oct. 1983 20 p
(Contract NAS7-100)
(NASA-Case-NPO-15903-1; US-Patent-Appl-SN-547171) Avail: NTIS HC A02/MF A01 CSCL 10A

Biomass particles are pelletized in pelletizer. The pellets form a fluidized bed of biomass in hot steam gas fed into the bottom inlet of a reactor. Catalyst particles shower downwardly through the reactor and are collected in an engager before recycle. The biomass particles are pyrolyzed to form char which is gasified by the steam to form CO and H2 gas. This gas reacts with the falling catalyst particles to form a methane gas product which is recovered after separation in separator. NASA

N84-12636# Air Force Systems Command, Wright-Patterson AFB, Ohio. Foreign Technology Div.
STORAGE OF ENERGY IN MAGNETIC FIELD OF SUPERCONDUCTIVE COILS
Nina Lipinska and Wojciech Lipinski 27 Jul. 1983 8 p Transl. into ENGLISH from Wiad. Elektrotechnizne (Poland), v. 42, no. 8, 1974 p 183-184
(AD-A131898; AD-F630058; FTD-ID(RS)T-1094-83) Copyright. Avail: NTIS HC A02/MF A01 CSCL 10/2

The storage of energy in the magnetic field of superconductive coils is discussed. The selection of superconducting materials is discussed, as is operational stability. R.J.F.

N84-12637# Air Force Systems Command, Wright-Patterson AFB, Ohio. Foreign Technology Div.
TRANSACTIONS OF THE CHINESE SOLAR ENERGY SOCIETY (SELECTED ARTICLES)
Zhonglin Sun, Shaozhen Xiong, Zongpan Wang, Xuesheng Jiang, and Wenli Yin 4 Aug. 1983 20 p Transl. into ENGLISH from Energiae Solaris Sinica (China), v. 3, no. 4, 1982 p 449-454; 457-459
(AD-A131870; AD-E850387; FTD-ID(RS)T-1067-83) Avail: NTIS HC A02/MF A01 CSCL 10/2

Topics of discussion include: the Ni/alpha-Si Schottky barrier solar cell, and the heterojunction SnO2/n-Si solar cells. B.G.

N84-12638# Hebrew Univ., Jerusalem (Israel).
FOURTH INTERNATIONAL CONFERENCE ON PHOTOCHEMICAL CONVERSION AND STORAGE OF SOLAR ENERGY
1982 351 p refs Proceedings of Conf. held in Jerusalem, 8-13 Aug. 1982 Sponsored in part by the Israel Ministry of Energy and Infrastructure and General Electric Co. of U.S.A. and the Israel Chemical Society
(Grant DE-FG02-81ER-10961)
(DE83-014760; DOE/ER-10961/1; CONF-8208106-Absts) Avail: NTIS HC A16/MF A01

Abstracts of 123 papers under the following topics are presented: conversion of sunlight into electrical power and photoassisted electrolysis at semiconductor electrodes; photosensitized reactions on surfaces; the role of porphyrins and chlorophylls in artificial photosynthesis; oxidation reduction photochemistry in homogeneous solutions; photoelectron transfer in organized assemblies; photogalvanic cells and effects; elementary processes in catalytic reactions at the interrace between colloidal microelectrodes and solutions; and luminescent solar collectors and concentrators. Author and subject indexes are included. DOE

N84-12639# Acurex Corp., Mountain View, Calif.
DEVELOPMENT OF MASS-PRODUCIBLE LINE-FOCUS TRACKING CONCENTRATING SOLAR COLLECTORS. CATEGORY 1: COLLECTORS Final Report
J. Reese, Jr., V. Wong, G. Sutton, and H. Gumbel Jul. 1983 114 p
(Contract DE-FC04-80CS-30264)
(DE83-015629; DOE/CS-30264/T1) Avail: NTIS HC A06/MF A01

The detailed design of a low cost, mass producible, line focusing parabolic trough solar colledtor was studied. The fabrica-

tion and test of a prototype drive string for this design, and the conceptual definition of a plant for its mass production are described. The design represents a significant advancement in the state of the art for cost effective, medium temperature (930 to 3150 C) solar thermal collectors. The improved collector performance, manufacturing costs, installation costs, and reliability to yield a major reduction in the cost of delivered thermal energy are outlined. DOE

N84-12640# Anradex Ltd., San Francisco, Calif.
TAILORING POLYMER FILMS FOR SOLAR-COLLECTION USE, PHASE 1 Final Report
John P. Fouser Sep. 1983 8 p
(Contract DE-AC03-82SF-11593)
(DE83-018117; DOE/SF-115393/T1) Avail: NTIS HC A02/MF A01

Several types of Polyacrylonitrile (PAN) polymers in film form that could meet the performance criteria with respect to thermal, ultraviolet, and tensile strength stability for use as exterior glazing in a low cost solar collector or for the internal heat exchange component were evaluated. Seven film specimens were tested. It is concluded that acrylonitrile homopolymer films when properly cast and processed have good mechanical properties, have long uv stability, and are usable for prolonged periods at 300 F. DOE

N84-12641# Midwest Research Inst., Golden, Colo. Materials Research Branch.
POLYMER DEGRADATION ON REFLECTING METAL FILMS: FOURIER TRANSFORM INFRARED (FTIR) REFLECTION-ABSORBANCE STUDIES
J. D. Webb, P. Schissel, T. M. Thomas, J. R. Pitts, and A. W. Czanderna Jul. 1983 9 p refs Presented at the 27th Ann. Intern. Tech. Symp. on High Speed Photography, Videography and Photonics, San Diego, Calif., 22-26 Aug. 1983
(Contracts DE-AC02-77CH-00178; EG-77-C-01-4042)
(DE83-012129; SERI/TP-255-2054; CONF-830874-16) Avail: NTIS HC A02/MF A01

The technique of Fourier transform infrared reflection-absorption (FTIR-RA) spectroscopy was successfully adapted to studying bulk and interfacially activated photodegradation of several types of polymers on various metallic substrates. The technique enables qualitative and quantitative study of photochemical reaction mechanisms and rates. A Controlled Environmental Exposure Chamber (CEEC), which permits collection of IR-RA spectra of the polymer/metal samples during their exposure to controlled spectral distributions of UV, temperatures, and gas mixtures, was built into the sample compartment of a Nicolet 7199 FTIR spectrophotometer. Surface analysis, gel permeation chromatography (GPC), UV spectroscopy, and UV spectroradiometry were used to complement the FTIR-RA results. DOE

N84-12642# Argonne National Lab., Ill. Chemical Technology Div.
RAGONE CHARACTERISTICS OF AQUEOUS MOBILE BATTERIES AND THEIR APPLICATION IN PROJECTING RANGES OF ELECTRIC VEHICLES
F. Hornstra, C. C. Christianson, D. Corp, D. Fredrickson, E. Gay, E. Hayes, C. Webster, and N. P. Yao 1983 3 p refs Presented at the Electrochemical Society Fall Meeting, Washington, D.C., 9 Oct. 1983
(Contract W-31-109-eng-38)
(DE83-014701; CONF-831086-3) Avail: NTIS HC A02/MF A01

A Ragone characteristic is defined as the specific energy available from a battery as a function of the specific power level at which it is discharged. Ragone plots obtained are given for the following electric vehicle propulsion batteries: NiZn, Ni/Fe, improved state of the art lead-acid, a lead-acid designed for hybrid vehicle application, and a standard golf cart battery. It is found that the ragone plots can be used to project the range of an electric vehicle with a particular battery. DOE

N84-12643# Pacific Northwest Lab., Richland, Wash.
INITIAL OPERATION OF THE COMPRESSED AIR EXPERIMENT AT PITTSFIELD, ILLINOIS
T. J. Doherty, R. P. Marshall, and L. D. Kannberg Apr. 1983 6 p refs Presented at the Intersoc. Energy Conversion Eng. Conf., Washington, D.C., 1 Aug. 1983
(Contract DE-AC06-76RL-01830)
(DE83-016930; PNL-SA-11132; CONF-8308102-1) Avail: NTIS HC A02/MF A01

The status of work on the compressed air energy storge experiment at Pittsfield, Illinois is briefly described. The objectives of the Pittsfield Aquifer Test are: to demonstrate the use of aquifers as compressed air storage reservoirs, to validate and modify stability criteria from earlier studies, and to correlate field data with predictions developed by numerical modeling and laboratory experiments. Field exploration confirmed the presence of a domal structure near Pittsfield. All construction activities, includng well field development, subsurface instrumentation, and all surface facilities are complete. Bubble development activities have been conducted. Well logging, acid treatments, and operation are discussed. DOE

N84-12644# Midwest Research Inst., Golden, Colo. Solar Energy Research Inst.
THERMOCHEMICAL ENERGY SYSTEMS RESEARCH
R. Gerald Nix Aug. 1983 7 p refs Presented at the Phys. and Chem. Energy Storage Ann. Contractors' Rev. Meeting, Arlington, Va., 12-14 Sep. 1983
(Contracts DE-AC02-77CH-00178; EG-77-C-01-4042)
(DE83-012132; SERI/TP-234-2060; CONF-830974-3) Avail: NTIS HC A02/MF A01

Research on Heat-pump thermochemical energy systems and thermochemical reduction of CO2 to CO for open-loop solar energy transport is described. Analysis of the NaOH-H2O heat-pumped system indicted cost effectiveness relative to hot oil solar system with parabolic trough receivers for production of 0.101 MPa saturated steam high-temperature heat-pumped systems are being defined. DOE

N84-12645# Rutgers Univ., New Brunswick, N. J. Dept. of Chemistry.
NEW MATERIALS FOR ORGANIC PHOTOVOLTAIC CELLS Final Report
George R. Bird, Joseph Potenza, Ronald R. Sauers, and Irwin Tobias 1983 40 p refs
(Contract DE-AC02-79ER-10463)
(DE83-016845; DOE/ER-10463/1) Avail: NTIS HC A03/MF A01

Activities of the reported program include: determination of the desirable properties of photovoltaic dyes; synthesis and selection of photovoltaic dyes; crystallographic studies of selected dyes; a model for describing the mobility of excitions in crystals of strong chromospheres; measurement of properties of dyes; and testing of cells. DOE

N84-12646# California Univ., Livermore. Lawrence Livermore Lab.
INITIAL ASSESSMENT OF THE MHD STABILITY OF TMX-U
W. E. Nexsen 4 Aug. 1983 10 p refs
(Contract W-7405-eng-48)
(DE83-016521; UCID-19832) Avail: NTIS HC A02/MF A01

In its operation to date TMX-U has reached values of beta which, for all except the hot electron beta, are close to the proposal values and has not encountered MHD stability problems. The hot electron beta values are presently limited by gyrotron output power and pulse length as well as ion confinement time. Further exploration of stability awaits full thermal barrier operation. DOE

N84-12647# Vitro Labs., Silver Spring, Md. Building Systems Research Branch.
RELIABILITY AND MAINTAINABILITY STUDY OF SELECT SOLAR-ENERGY-SYSTEM COMPONENTS IN THE NATIONAL SOLAR DATA NETWORK Final Report
Paul W. Kendall, Terry L. Logee, and Michael G. Raymond Jun. 1983 82 p refs
(Contracts DE-AC02-77CH-00178; EG-77-C-01-4042)

(DE83-011974; SERI/STR-254-1848) Avail: NTIS HC A05/MF A01

The reliability and maintainability of select solar energy system components evaluated in 16 solar heating and cooling systems over a one-year period is addressed. The systems evaluated were instrumented sites from the National Solar Data Network (NSDN). A complete description and system schematic for each site is provided. Quantitative R and M data (e.g., Failure Rate and Mean Time Between Failures) on pumps, motors and fans from the selected NSDN sites, along with conclusions and recommendations based on comparative data for other components are provided. In summary, pumps, valves, and heat exchangers in solar heating and cooling (SHAC) systems appear to be very reliable and show failure rates comparable to other mechanical system applications. Control systems typically used in SHAC systems appear to be the least reliable but still fall within the range of failures exhibited by other mechanical systems. Evidence suggests that piping leaks in SHAC systems occur at three times the rate of other mechanical systems. Recommendations are provided on other areas of research necessary to determine the useful life of SHAC system components. Actual failures encountered in the 16 systems evaluated are described. DOE

N84-12648# Energy Information Administration, Washington, D.C. Office of Energy Markets and End Use.

SHORT-TERM ENERGY OUTLOOK. VOLUME 2. METHODOLOGY

May 1983 90 p refs 2 Vol.

(DE83-016853; DOE/EIA-0202(83/2Q)-2) Avail: NTIS HC A05/MF A01

Recent changes in forecasting methodology for nonutility distillate fuel oil demand and for the near-term petroleum forecasts are discussed. The accuracy of previous short-term forecasts of most of the major energy sources published in the last 13 issues of the Outlook is evaluated. Macroeconomic and weather assumptions are included in this evaluation. Energy forecasts for 1983 are compared. Structural change in US petroleum consumption, the use of appropriate weather data in energy demand modeling, and petroleum inventories, imports, and refinery runs are discussed. DOE

N84-12649# Pacific Northwest Lab., Richland, Wash.

INNOVATIVE INDUSTRIAL-MATERIALS PROCESSES

G. J. Hane, S. G. Hauser, T. A. Williams, and R. Abarcar (Energetics Corp.) Aug. 1983 32 p refs Presented at the 18th Intersoc. Energy Conversion Engr. Conf., Orlando, Fla., 21-26 Aug. 1983 (Contract DE-AC06-76RL-01830)

(DE83-016784; PNL-SA-11354; CONF-830812-45) Avail: NTIS HC A03/MF A01

A preliminary identification of innovative industrial-materials processes that have the potential for significant energy conservation, yet require long-term research to achieve that potential is described. Potential alternative processes in eight major materials-processing industries are reviewed. These industries are chemical; iron and steel; aluminum; petroleum refining; paper and pulp; food and kindred products; stone, clay, and glass; and textiles. DOE

N84-12650# Midwest Research Inst., Golden, Colo. Building Systems Research Branch.

PASSIVE-SOLAR PERFORMANCE: SUMMARY OF 1981-1982 CLASS B RESULTS

Joel Swisher and Thomas Cowing Jun. 1983 262 p (Contract DE-AC02-77CH-00178)

(DE83-009407; SERI/SP-281-1847) Avail: NTIS HC A12/MF A01

The residential class-B passive solar performance monitoring program which is a low cost program that evaluates the thermal performance of selected residential buildings throughout the country is discussed. The program provides a consistent measure of the thermal performance of different types of passive buildings in different climates. Instrumentation is limited to that needed to calculate the monthly building energy balance, separating passive solar heating from the other building energy flows. Thermal storage and other individual components are not monitored, and no attempt is made to determine a buildings thermal processes in detail. Each of the 40 monitored buildings is summarized separately. Each summary includes a description of the building, its thermal characteristics, the measurements taken, and the building's thermal performance. DOE

N84-12651# Energieconsulting Heidelburg (West Germany).

HEATING WITH WIND ENERGY, PART B Final Report, Apr. 1981

Ullrich Kaier and Friedrich Czink Bonn Bundesministerium fuer Forschung und Technologie Jun. 1983 316 p refs In GERMAN; ENGLISH summary Sponsored by Bundesministerium fuer Forschung und Technologie

(BMFT-FB-T-83-131-Pt-B; ISSN-0340-7608) Avail: NTIS HC A14/MF A01; Fachinformationszentrum, Karlsruhe West Germany DM 48

Wind energy resources for heating are surveyed. Ten locations in the countryside and three locations along the coast of West Germany were investigated. Wind velocities between 3 and 15 m/sec were found to be suitable. An international marketing analysis on wind energy convertering systems up to 20 kW is summarized. Over 200 manufacturers in 22 countries were contacted and 52 delivery offers were obtained, 4 of which were chosen according to the following criteria: power output on the order of 10 kW for 10 m/sec wind velocity, type description, dimensions, speed rise, security devices and price. Insufficient matching between wind converters and generators is pointed out, but it is concluded that the four systems chosen represent a good starting point solution. Author (ESA)

N84-12652# Gesellschaft fuer Kohleverfluessigung m.b.H., Saarbruecken (West Germany).

PREPARATION OF A DESIGN STUDY FOR THE CONSTRUCTION OF A 2 MILLION TONS/ANNUM COMMERCIAL SCALE HYDROGENATION PLANT Final Report, Mar. 1982

Juergen Bernert, Anton Rudolf Ellinghaus, Winfried Hoffmann, Christian Warnstaedt, Hans Dohren, Guenter Holzapfel, Uwe Krieger, and Lothar Lauer Bonn Bundesministerium fuer Forschung und Technologie Jul. 1983 174 p In GERMAN; ENGLISH summary Sponsored by Bundesministerium fuer Forschung und Technologie

(BMFT-FB-T-83-135; ISSN-0340-7608) Avail: NTIS HC A08/MF A01; Fachinformationszentrum, Karlsruhe, West Germany DM 34

A project study for a coal hydrogenation complex with premium gasoline as main product is presented. The plant is designed to operate at 300 bar pressure. Preheating of the coal paste was improved by utilizing process effluent heat. Applying heat integration to maximum extent a calorific yield $>$ 66 % is achieved. Hydrogen demand is covered by pressured gasification of the hydrogenation residue and by fractionation of coke-oven-gas. The coal oil product is upgraded by hydrotreating, hydrocracking and reforming processes. The plant is found to be technically feasible. Feed stocks : (in million t p.a.) coal 1.9; coke-oven gas 0.26; blend components 0.17. Products : premium gasoline 0.9; liquified petroleum gas 0.1; synthetic natural gas 0.3. Author (ESA)

N84-12653# Istituto di Ricerca e Tecnologia per lo Studio del Plasma Nello Spazio, Frascati (Italy).

ORBITING WIRE AS A DYNAMO: AUXILIARY POWER POSSIBILITIES FOR SPACE PLATFORMS

G. Mastrantonio Mar. 1983 12 p refs Sponsored by CNR (IFSI-83-3) Avail: NTIS HC A02/MF A01

A technique to short circuit the electric field set up by the Earth's magnetic field in an orbiting metal wire, so that energy can be extracted is described. Useful powers of 3 kw for wire length 1 km, 4 mm in diameter and for external load equal to the wire resistance are predicted. By varying the wire length as well as its cross-section low-voltage, high current (and vice-versa) needs can be met. Author (ESA)

45 ENVIRONMENT POLLUTION

Includes air, noise, thermal and water pollution; environment monitoring; and contamination control.

N84-12654* National Aeronautics and Space Administration. National Space Technology Labs., Bay Saint Louis, Miss.
METHOD FOR TREATING WASTEWATER USING MICROORGANISMS AND VASCULAR AQUATIC PLANTS Patent
Billy C. Wolverton, inventor (to NASA) Issued 15 Nov. 1983 7 p Filed 28 Dec. 1981 Supersedes N82-25335 (20 - 16, p 2214)
(NASA-Case-NSTL-10; US-Patent-4,415,450;
US-Patent-Appl-SN-335036; US-Patent-Class-210-602;
US-Patent-Class-210-605; US-Patent-Class-210-617;
US-Patent-Class-210-151; US-Patent-Class-47-58) Avail: US Patent and Trademark Office CSCL 13B

A method for treating wastewater compresses subjecting the wastewater to an anaerobic setting step for at least 6 hours and passing the liquid effluent from the anaerobic settling step through a filter cell in an upflow manner. There the effluent is subjected first to the action of anaerobic and facultative microorganisms, and then to the action of aerobic microorganisms and the roots of at least one vascular aquatic plant.
Official Gazette of the U.S. Patent and Trademark Office

N84-12655# Pacific Northwest Lab., Richland, Wash.
DETECTING LONG-TERM ECOLOGICAL EFFECTS IN FORESTS AND FOOD CHAINS
W. T. Hinds Oct. 1982 3 p
(Contract DE-AC06-76RL-01830)
(DE83-003469; PNL-SA-10870) Avail: NTIS HC A02/MF A01

The fundamentals of cost effective long term monitoring were examined and methods appropriate for western ecosystems were developed. Optimized field measurements for two contrasting situations, old growth forests and terrestrial predation in shallow aquatic habitats were undertaken. The approach and methodology used in this fundamental research into long term effects detection is presented. DOE

N84-12656# Department of Energy, Bartlesville, Okla. Energy Technology Center.
VEHICLE-EMISSION CHARACTERISTICS USING MECHANICALLY EMULSIFIED ALCOHOL/DIESEL FUELS
J. R. Allsup, D. E. Seizinger, F. W. Cox, A. L. Brooks (Inhalation Toxicology Research Inst.), and R. O. McClellan (Inhalation Toxicology Research Inst.) Jul. 1983 12 p refs
(DE83-016012; DOE/BETC-RI-83/4) Avail: NTIS HC A02/MF A01

A light duty diesel vehicle fueled with an emulsified alcohol/diesel fuel was operated under cyclic mode. Emission and fuel economy measurements were taken during vehicle operation. It is shown that the volumetric fuel economy decreased slightly. Carbon monoxide emissions increased slightly, and oxides of nitrogen showed no significant change. Particulate emissions were reduced slightly, and the particulate extractables increased slightly. The environmental effect of these data cancel each other resulting in no significant changes in the total release of biological activity into the environment. DOE

N84-12657# Oak Ridge National Lab., Tenn. Carbon Dioxide Information Center.
INVENTORY OF NUMERIC DATA FOR CARBON DIOXIDE RESEARCH
Julia A. Watts and Linda J. Allison Jul. 1983 210 p refs
(Contract W-7405-eng-26)
(DE83-017571; ORNL/CDIC-1) Avail: NTIS HC A10/MF A01

The results of a survey to determine the status and availability of numerical data for application in carbon dioxide research and modeling studies are documented. The inventory focuses on the identification, status, and accessibility of data pertinent to the carbon cycle and climate research programs of the US Department of Energy Carbon Dioxide Research Division. The inventory process will continue to evolve as research programs proceed and new data are collected or identified as being needed for specific research efforts. This report is one mechanism of promoted contributor/user interaction. It is hoped that the report will give direction to secondary users of the data by identifying the primary collectors, the types of data collected and availability, and how the data have been applied and/or interpreted. It serves as a guide for the Carbon Dioxide Information Center (CDIC) in the acquisition, organization, documentation, and evaluation of data to meet research needs. DOE

46 GEOPHYSICS

Includes aeronomy; upper and lower atmosphere studies; ionospheric and magnetospheric physics; and geomagnetism.

For space radiation see *93 Space Radiation.*

N84-12658 Washington Univ., Seattle.
A STUDY OF COHERENT STRUCTURES IN THE NEAR-NEUTRAL MARINE ATMOSPHERIC BOUNDARY LAYER Ph.D. Thesis
William Jason Shaw 1982 213 p
Avail: Univ. Microfilms Order No. DA8304413

Aircraft from the JASIN Experiment were used to demonstrate the presence of vertically coherent structures in the near-neutral marine atmospheric boundary layer (ABL) and to examine their importance in the overall turbulent transfer. Conditional sampling, using the time varying dissipation rate as an indicator, was the technique for studying such structures. Their fractional area coverage, gamma, was shown to be quite sensitive in the surface layer to the height of measurement and to the surface roughness while being independent of heat flux. The surface stress field varies significantly over the extratropical ocean in response to sea surface temperature variations and that burst structure distributions are in equilibrium with the local stress field. Variations in the stress field may be partially responsible for the organization of mesoscale ABL secondary flow. Dissert. Abstr.

N84-12659 Georgia Inst. of Tech., Atlanta.
A CASE STUDY OF GRAVITY WAVE-CONVECTIVE STORM INTERACTIONS Ph.D. Thesis
James George Stobie 1982 133 p
Avail: Univ. Microfilms Order No. DA8310659

An analysis of a series of storms that struck the North Central U.S. on 9 May 1979 is presented. Using barograph traces from 30 stations and employing filtering and spectral analysis techniques. Evidence was found of gravity waves with periods of about 3 hours and wavelength of approximately 300 km propagating along a 200 km wide track parallel to the jet. It was also found that the precipitation patterns from the storms often followed the motion of the waves. Upper air soundings in the area indicate that vertical wind shear may be a source of gravity waves. An analytical model for such waves is presented and their horizontal and vertical structure discussed. Dissert. Abstr.

N84-12660 Purdue Univ., Lafayette, Ind.
NUMERICAL SIMULATION OF CONVECTIVE SCALING Ph.D. Thesis
Jeffry Rothermel 1982 268 p
Avail: Univ. Microfilms Order No. DA8310857

Convective scaling in the atmosphere using a two dimensional nonlinear spectral mode was studied, and the difference between the aspect rations for mesoscale cellular convection (MCC) and laboratory cells was investigated. To investigate this difference, one of two approaches was pursued. Firstly, physical processes such as latent heat release or eddy anisotropy may act to increase the aspect ratio of the convection from cumulus scale to mesoscale (i.e., MCC). The alternate approach, adopted here, suggests that there is a mesoscale organization of small scale convective elements into a system with a collectively broad horizontal scale,

consistent with radar observations of convective organization in clear air and data collected by aircraft within MCC. Such a process is likely attributable to the nonlinearly inherent in the shallow convection problem. Dissert. Abstr.

N84-12661 Bayerische Akademie der Wissenschaften, Munich (West Germany).
ACCURACY OF GRAVIMETRICALLY DETERMINED ABSOLUTE AND RELATIVE GEOID HEIGHTS [ZUR GENAUIGKEIT GRAVIMETRISCH BESTIMMTER ABSOLUTER UND RELATIVER GEOIDHOEHEN]
Bernhard Heck and Werner Grueninger 1983 35 p refs In GERMAN; ENGLISH summary
(Ser-A-97; ISBN-3-7696-8179-7; ISSN-0065-5309) Copyright. Avail: Issuing Activity

The sources of error affecting the accuracy of determination of geoid undulations and height anomalies obtained by combining a set of spherical harmonic coefficients and terrestrial gravity anomalies were investigated. Errors in absolute and relative undulations are estimated in detail, based on a modification of Stoke's integral formula. If a geopotential model such as GEM 10, GRIM 2 and mean gravity anomalies over surface elements of 2 to 10 km side length are used, absolute undulations have a global rms of + or - 1 to 3 dm. Relative undulations between points 10 km apart can be derived with an accuracy of a few mm. By using the modified Stokes functions instead of the original Stokes' formula the integration area can be strongly diminished. Author (ESA)

N84-12662*# National Aeronautics and Space Administration. Goddard Space Flight Center, Greenbelt, Md.
CRUSTAL DEFORMATION, THE EARTHQUAKE CYCLE, AND MODELS OF VISCOELASTIC FLOW IN THE ASTHENOSPHERE
Steven C. Cohen and Matthew J. Kramer Oct. 1983 39 p refs
(NASA-TM-85117; GSFC-921; NAS 1.15:85117) Avail: NTIS HC A03/MF A01 CSCL 08K

The crustal deformation patterns associated with the earthquake cycle can depend strongly on the rheological properties of subcrustal material. Substantial deviations from the simple patterns for a uniformly elastic earth are expected when viscoelastic flow of subcrustal material is considered. The detailed description of the deformation pattern and in particular the surface displacements, displacement rates, strains, and strain rates depend on the structure and geometry of the material near the seismogenic zone. The origin of some of these differences are resolved by analyzing several different linear viscoelastic models with a common finite element computational technique. The models involve strike-slip faulting and include a thin channel asthenosphere model, a model with a varying thickness lithosphere, and a model with a viscoelastic inclusion below the brittle slip plane. The calculations reveal that the surface deformation pattern is most sensitive to the rheology of the material that lies below the slip plane in a volume whose extent is a few times the fault depth. If this material is viscoelastic, the surface deformation pattern resembles that of an elastic layer lying over a viscoelastic half-space. When the thickness or breath of the viscoelastic material is less than a few times the fault depth, then the surface deformation pattern is altered and geodetic measurements are potentially useful for studying the details of subsurface geometry and structure. Distinguishing among the various models is best accomplished by making geodetic measurements not only near the fault but out to distances equal to several times the fault depth. This is where the model differences are greatest; these differences will be most readily detected shortly after an earthquake when viscoelastic effects are most pronounced. S.L.

N84-12663*# National Aeronautics and Space Administration. Goddard Space Flight Center, Greenbelt, Md.
SCALE LENGTHS IN QUASI-PARALLEL SHOCKS
J. D. Scudder, L. F. Burlaga, and E. W. Greenstadt (TRW, Redondo Beach, Calif.) Oct. 1983 15 p refs Submitted for publication
(NASA-TM-85109; NAS 1.15:85109) Avail: NTIS HC A02/MF A01 CSCL 03B

Examples of an interplanetary and the bow shock illustrate the small relative size of the electrostatic layer relative to the scale of the magnetic fluctuations in quasi-parallel shocks. While both examples are supercritical, the interplanetar example is marginally so, showing a thickness in absolute and convected ion larmor radii units that is thicker (approximately 13 U/omega sub ci) than at the bow shock (approximately omega sub ci). The fluid speed changes abruptly in the quasi-parallel shock on this shorter scale. The increase in electron and ion random energies also is clearly seen on this shorter scale. In the interplanetary example the scale of the electric layer is certainly less than 1/60th that of the up or downstreams magnetic fluctuations. The thickness of the earth's bow shock deceleration layer is dramatically narrower than any domain of upstream waves as controlled by reflected, intermediate, or diffuse ions. Author

N84-12664*# Illinois Univ., Urbana. Aeronomy Lab.
OBSERVATIONS OF THE UPPER TROPOSPHERE AND LOWER STRATOSPHERE USING THE URBANA COHERENT-SCATTER RADAR
L. D. Goss and S. A. Bowhill 1 Jul. 1983 117 p refs
(Grant NsG-7506)
(NASA-CR-174594; NAS 1.26:174594; ISSN-0568-0581; AR-111; UILU-ENG-83-2503) Avail: NTIS HC A06/MF A01 CSCL 04A

The Urbana coherent-scatter radar was used to observe the upper troposphere and lower stratosphere, and 134 hours of data were collected. Horizontal wind measurements show good agreement with balloon-measured winds. Gravity waves were frequently observed, and were enhanced during convective activity. Updrafts and downdrafts were observed within thunderstorms. Power returns are related to hydrostatic stability, and changes in echo specularity are shown. Author

N84-12665# Air Force Geophysics Lab., Hanscom AFB, Mass.
PROPERTIES OF THE NEUTRAL DENSITY AND COMPOSITION IN THE THERMOSPHERE
C. R. Philbrick, M. E. Gardner, and P. Lammerzahl 1983 5 p refs
(AF Proj. 6690)
(AD-A131557; AFGL-TR-83-0160) Avail: NTIS HC A02/MF A01

Measurements of the density and composition of the thermosphere between 150 and 500 km, which were obtained by the X3-1 satellite, were compared with the Jarchia and MSIS models. The measurements of the O, N2, N and Ar show some difference from the current models which should be considered during the preparation of the next CIRA model. The Ar measurements are particularly useful in examining the response of the neutral atmosphere to geomagnetic heating. These results are useful in establishing the appropiate lower boundary conditions for modeling of the thermosphere. Author

N84-12666# ENSCO, Inc., Springfield, Va. Signal Analysis Systems Div.
DESCRIPTION OF AN AUTOMATIC SEISMIC MEASUREMENTS PACKAGE: ANALYSIS AND DESIGN GOALS
Robert Sax 1 Sep. 1982 115 p
(Contract F08606-80-C-0021; ARPA Order 2551)
(AD-A132067; SAS-TR-81-03) Avail: NTIS HC A06/MF A01 CSCL 17/10

This is a system concept study of how the VSC seismic system could operate as a test bed for developing an optimum automated worldwide seismic network. Many problems are anticipated in developing such a network. These are discussed in a theoretical way and algorithms are suggested which could be tested by the VSC system. These would lead to more optimum performance of an automated seismic network. Author (GRA)

N84-12667# Air Force Geophysics Lab., Hanscom AFB, Mass. Meteorology Div.
VARIABILITY OF ATMOSPHERIC DENSITY IN THE MIDDLE ATMOSPHERE Interim Scientific Report
Arthur J. Kantor 17 Mar. 1983 25 p
(AF Proj. 6670)

(AD-A131985; AD-F000018; AFGL-TR-83-0079; AFGL-ERP-830) Avail: NTIS HC A02/MF A01 CSCL 04/1

An analysis of the time and space variability of density in the middle atmosphere has been developed in this report, affording a means to determine density changes that occur over distances out to 200 nmi and time periods of 1 to 72 hr. Spatial variations - The rms differences between densities at locations 50, 100, and 200 nmi apart are provided in Tables 4, 8 and 11 for low- and middle- latitude stations at altitudes from 20 through 60 km. These rms values are estimates of the day-to-day variability around the mean density gradients given in Table 5 for low latitudes and Tables 9 and 12 for middle latitudes. Time variations - The rms variability of density for time periods from 1 to 12 hr in tropical regions is given in Table 13 for altitudes up to 60 km. Estimates were derived using autocorrelation theory and an analysis of the diurnal variation of density, which is the dominant periodic cycle at low latitudes. Analyses of available density observations at several midlatitude locations for altitudes between 30 and 60 km provide reasonable estimates of the magnitude (and changes with season and latitude) of the variability of density with time for periods up to 72 hr. Variations of density at these latitudes are relatively small during summer and do not increase significantly with time. Rms variations remain between 1-1/2 and 4 percent for all periods up to 72 hr. GRA

N84-12668# Stanford Univ., Calif. Dept. of Geophysics.

EFFECTS OF MICROSTRUCTURE AND PORE FLUIDS ON THE ACOUSTIC PROPERTIES OF GRANULAR MATERIALS Final Report, Feb. 1982 - Jan. 1983

Amos Nur 8 Aug. 1983 133 p

(Contract N00014-77-C-0390)

(AD-A131983; AD-F000018) Avail: NTIS HC A07/MF A01 CSCL 08/7

The purpose of this paper is to explain the effects of granular microstructure and effective pressure on low frequency velocities in water saturated granular materials. Micromechanical models are developed for the dry frame moduli. Unambiguous predictions are stated explicity for Vp, Vs, and Vp/Vs as a function of grain characteristics, porosity, and effective pressure. The predictions of each step are systematically tested by laboratory measurements of Vp and Vs in glass beads and quartz sands. Signal velocities were measured by an ultrasonic pulse transmission technique at frequencies approx 200 kHz. All measurements were obtained in vacuum dry (<10 micrometers) samples. Although signal velocities are generally equivalent to group velocities in dissipative media, we are aware of no evidence for dispersion in vacuum dry samples of similar composition. Errors in the moduli are expected to be less than 5%. These moduli are in fact frequency-independent, dry frame moduli and as such are expected to apply across seismic, acoustic, and ultrasonic frequency ranges. GRA

N84-12669# Ohio State Univ., Columbus. Dept. of Geodetic Science and Surveying.

ACCURACY ESTIMATES OF GRAVITY POTENTIAL DIFFERENCES BETWEEN WESTERN EUROPE AND UNITED STATES THROUGH LAGEOS SATELLITE LASER RANGING NETWORK

D. P. Hajela Feb. 1983 76 p

(Contract F19628-82-K-0022; AF Proj. 2309)

(AD-A131838; OSU/DGSS-345; AFGL-TR-83-0132; SR-3) Avail: NTIS HC A05/MF A01 CSCL 08/5

The presently attainable accuracy of connecting the vertical datums of regions, which are separated by oceans, has been investigated. The vertical datum connections are established through geocentric positions of laser tracking stations by estimating the geopotential at these stations, and also utilizing the geopotential differences between stations in each region obtained through leveling. The Western Europe-USA vertical datum connection has been examined in detail. Accuracy estimates of a few other datum connections are also given. Four stations in Western Europe and 14 stations in USA were considered in the Lageos satellite laser ranging (SLR) network (January 1982). The currently available accuracy estimates (December 1981) of the potential coefficients describing the earth's gravity field to degree 180 were used, along with gravity anomalies in a small area around each SLR station. Various anomaly spacing, data cap size, anomaly accuracy were tried to determine the effect on the accuracy of the vertical datum connection. It was found that anomaly spacing need not be more dense than 10 prime. Different accuracy estimates for the SLR station positions, and any displacement of the SLR coordinate system origin from the geocenter, were considered. The corresponding values for the vertical connection, if anomalies were used in a data cap of 1 deg radius, were 50 and 52 kgal/cm. GRA

N84-12670# Southwest Research Inst., San Antonio, Tex.

MAGNETOSPHERIC PLASMA STUDIES USING DATA FROM THE DYNAMICS HIGH AND LOW ALTITUDE PLASMA INSTRUMENTS

J. N. Barfield Hanscom AFB, Mass. AFGL 15 May 1983 52 p

(Contract F19628-82-K-0024; AF Proj. 7661)

(AD-A131793; SR-1; AFGL-TR-83-0134) Avail: NTIS HC A04/MF A01 CSCL 04/1

Plasma data from the High and Low Altitude Plasma Instruments aboard the Dynamics 1 and 2 (DE-1 and DE-2) satellites have been analyzed to investigate high latitude plasma characteristics. DE-1 hot plasma observations in the mid-altitude polar cusp have shown evidence of a significant velocity filtering phenomenon which is consistent with a latitudinally narrow region of plasma injection located at a geocentric distance of about 8 earth radii (RE). This velocity filtering effect allows the measurement of much smaller flow velocities (about km/s) than have heretofore been possible with plasma measurements. Observations at altitudes of 2-3 RE indicate two distinct types of counterstreaming electron events. The type 1 event is characterized by two Maxwellian distribution functions, an isotropic high-temperature component and a field-aligned low temperature component. Type 1 events appear to involve wave-particle interactions while type 2 events imply direct acceleration by oppositely-directed electric fields pointing toward the satellite along magnetic field lines. The data indicate that cold ionospheric electrons, which carry the downward region-1 Birkeland currents on the morning side, are accelerated upward by potential drops of tens of eV at altitudes of several thousand kilometers. This acceleration process allows spacecraft above those altitudes to measure routinely the charge carriers of both downward and upward current systems. GRA

N84-12671# Pittsburgh Univ., Pa. Dept. of Physics and Astronomy.

OI 630.0 NM OPTICAL MEASUREMENTS OF NEUTRAL WINDS, TEMPERATURES AND AIRGLOW ENHANCEMENTS DURING THE BIME PROGRAM Final Report, 1 Dec. 1981 - 31 May 1983

Manfred A. Biondi 25 Jul. 1983 25 p

(Grants NSF ATM-81-21723; AF-AFOSR-0055-82; AF Proj. 2310)

(AD-A131695; AFOSR-83-0711TR) Avail: NTIS HC A02/MF A01 CSCL 04/1

A 100 mm aperture, field-widened Fabry-Perot interferometer was used in support of the B.I.M.E. F-region chemical release program to measure 630.0 nm night-glow line profiles and from this to determine the pattern of F-region thermospheric dynamics (neutral velocity vector vn and neutral temperature Tn versus time) from 24 August 1982 to 19 September 1982 at Natal Brazil. A 3-channel, sky-mapping filter photometer measured the temporal and spatial evolution of the 630.0 nm airglow enhancement produced by the first B.I.M.E. release (8 Sept. 1982). Clouds over our observing site obscured the second B.I.M.E. release (13 Sept. 1982). Author (GRA)

N84-12672# Los Alamos Scientific Lab., N. Mex.

MICROEARTHQUAKES INDUCED DURING HYDRAULIC FRACTURING AT THE FENTON HILL HDR SITE: THE 1982 EXPERIMENTS

Hans Keppler (Bundesanstalt fuer Geowissenschaften und Rohstoffe), Christopher F. Pearson, Robert M. Potter, and James N. Albright 1983 7 p refs Presented at the Geothermal Resources Council's Ann. Meeting, Portland, Oreg., 24-27 Oct. 1983

(Contract W-7405-eng-36)

(DE83-014191; LA-UR-83-1678; CONF-831041-2) Avail: NTIS HC A02/MF A01

The on-site real-time processing of microearthquake signals that occur during massive hydraulic fracturing provides a notion of the location and growth of the fracture system being created. This enables quick decisions to be made in regard to the ongoing operations. The analytical results and impact of the hypocenter mapping during the 1982 fracturing experiments in the Fenton Hill Phase II Hot Dry Rock geothermal reservoir are reported. DOE

N84-12673# Geological Survey, Denver, Colo.
COMPILATION OF SELECTED FAULTS AND LINEAMENTS THAT MAY BE RELEVANT TO A STUDY OF SEISMIC ACTIVITY IN SOUTHERN NEVADA AND PART OF ADJACENT CALIFORNIA
R. C. Buckham Feb. 1983 27 p refs
(Contracts DE-AI08-76DP-00474; AT(29-2)-474)
(DE83-017085; USGS-474-11) Avail: NTIS HC A03/MF A01

The enclosed preliminary map shows selected prominent faults and regional topographic lineaments that may be relevant to a study of known or potential seismic activity in the California-southern Nevada region surrounding the Nevada Test Site. DOE

N84-12674# Uppsala Ionospheric Observatory (Sweden).
[ACTIVITIES REPORT ON IONOSPHERIC OBSERVATION] Annual Report, 1982
1983 52 p refs Sponsored by Swedish Board for Space Activities and Swedish Natural Science Research Council
(UIO-AR-83-05; ISSN-0349-2702) Avail: NTIS HC A04/MF A01

Sounding rocket electrostatic wave investigations; experiments involving provoked ionospheric disturbances; noctilucent cloud research; and Viking satellite studies of ionosphere-magnetosphere coupling are summarized. Ionospheric modification by stimulated high frequency emissions; studies of auroras using International Magnetospheric Study and EISCAT radar data; and a bistatic coherent radar for subaural latitudes are described.
Author (ESA)

N84-12675# Istituto di Ricerca e Tecnologia per lo Studio del Plasma Nello Spazio, Frascati (Italy).
A COMPARISON BETWEEN GEOS 1 MAGNETIC FIELD MEASUREMENTS AND SOME MODELS OF THE GEOMAGNETIC FIELD
E. Amata, M. Candidi, R. Orfei, and C. Signorini Apr. 1983 29 p refs
(IFSI-82-5) Avail: NTIS HC A03/MF A01

Four magnetospheric field models in the range 4.4 to 7 RE on the dayside of the magnetosphere and for latitudes close to the xy GSM plane were compared with GEOS 1 data. The Olsen-Pfitzer 1976 (OP76) model, which includes all kinds of distributed currents in the magnetosphere and the tilt of Earth's magnetic dipole gives the best results: 2% to 3% difference from experimental data on field value and direction. The Mead-Fairfield (MF) model, derived by making least squares fits to magnetic measurements taken in the interval 6 to 8 RE and 13 to 15 RE performs well. Since near-Earth data indicate a scarcity of points near the magnetic equatorial plane, extrapolated values of the MF model were used. The OP76 model does not take into account the effects of the interplanetary magnetic field on the magnetosphere; this could be the reason of the residual differences with the GEOS 1 data. Author (ESA)

N84-12676# Istituto di Ricerca e Tecnologia per lo Studio del Plasma Nello Spazio, Frascati (Italy).
OBSERVATION OF MULTIPLE ION BEAMS IN THE MAGNETOTAIL LOW LATITUDE BOUNDARY LAYER. EVIDENCE FOR A DOUBLE H+ POPULATION
M. Candidi, S. Orsini, A. Ghielmetti (Bern Univ.), and H. Balsiger (Bern Univ.) Sep. 1982 18 p refs Sponsored by Swiss National Science Foundation Original contains color illustrations
(IFSI-82-10) Avail: NTIS HC A02/MF A01

The ISSE 2 plasma experiment detected the double peak population frequently found in the low latitude boundary layer of the magnetotail at times of enhanced geomagnetic activity. This population consists of ionospheric O+ and H+ mixed with solar wind plasma (typically H+ and He++). Analysis of the low energy peak indicates that it contains two clearly distinguishable proton populations. The energy ratios between the O+ and H+ beams indicate that one of the H+ populations is of ionospheric origin and flows tailward together with the ionospheric O+. The characteristics of the other H+ population suggest a higher altitude origin, and the presence of an H++ population with the same characteristics suggests that it is the solar wind H+ component.
Author (ESA)

N84-12677# CER Corp., Las Vegas, Nev.
GEOLOGIC STUDY OF THE WIND RIVER BASIN, FREMONT AND NATRONA COUNTIES, CENTRAL WYOMING Topical Report, Aug. 1981 - Jul. 1982
Perry J. Refolo Dec. 1982 123 p Sponsored by Gas Research Inst.
(PB83-254912; GRI-81/0025.7) Avail: NTIS HC A06/MF A01 CSCL 08G

A geologic overview of Wind River Basin stratigraphy is presented with special emphasis placed on gas-bearing units having low permeability. In addition, information is provided on the interrelation of technologic and economic factors governing development of the tight gas sands resource within the basin. The Wind River Basin contains numerous low permeability, gas bearing lenticular and blanket sands that are believed to represent significant resource potential. The geologic section from Late Cretaceous to Eocene is of primary interest here and includes rocks of the Frontier, Mesaverde, Meeteetse, Lance, Fort Union, and Muddy stratigraphic units. Depths of the formations vary from surface exposure on the west, south, and east fringes of the basin to 25,000 feet in the northern portion where the basin is structurally deeper. GRA

47 METEOROLOGY AND CLIMATOLOGY

Includes weather forecasting and modification.

N84-12678 Wyoming Univ., Laramie.
FIELD AND LABORATORY STUDIES OF ICE NUCLEATION IN WINTER OROGRAPHIC CLOUDS Ph.D. Thesis
David Clark Rogers 1982 176 p
Avail: Univ. Microfilms Order No. DA8310152

The present research was divided into two separate but related areas: Cloud microphysical data from instrumented aircraft flights through winter clouds over Elk Mountain were analyzed to assess the formation of ice crystals under natural conditions. The results indicated that for these supercooled clouds, most crystals form near the upwind edge of the cloud, where water vapor condenses on available cloud condensation nuclei(CCN). Two possible explanations were offered: the active nuclei are either very small contact ice nuclei, or they are a subset of the CCN known as "condensation-freezing ice nuclei". Furthermore, this formation was indicated as likely to be a primary nucleation process since there was a strong temperature dependence of crystal concentration; the ensemble of data showed typical concentrations of one per liter at -15 C and changed by a factor 10 for a 9 C temperature change. Dissert. Abstr.

N84-12679 Texas A&M Univ., College Station.
A NUMERICAL STUDY ON THE EVOLUTION OF TORNADOES Ph.D. Thesis
Fred Hayse Proctor 1982 283 p
Avail: Univ. Microfilms Order No. DA8309693

The evolution of the thermal and dynamic structure of tornadoes is studied via numerical simulation. The model, which is axisymmetric, includes prognostic equations governing motion, a diagnostic pressure equation, and prognostic equations for potential temperature, water vapor, and liquid water. Condensation processes are included so as to provide a physically realistic driving mechanism

for the tornado. Subgrid turbulence is parameterized by a deformation dependent eddy viscosity. The numerical domain is 1 km x 1 km with a grid resolution of 12.5 m. The lateral and top boundaries are open to mass flow. The equations are solved with the aid of quadratic conservative differences in space and Adams-Bashforth differences in time. Seven major experiments are performed of which the first six simulate tornado development in the presence of constant ambient circulations with differing surface roughness and vertical stability near the ground. In the last experiment the early stages of tornado demise are simulated by suddenly reducing the ambient circulation. Dissert. Abstr.

N84-12680 Princeton Univ., N. J.
MECHANISMS OF MONSOONAL CYCLOGENESIS Ph.D. Thesis
Prashant Dattatraya Sardeshmukh 1982 209 p
Avail: Univ. Microfilms Order No. DA305910

The relationship between synoptic scale disturbances of the Southwest Monsoon and the large scale circulation in which they are embedded is examined. Barotropic and baroclinic instability of the mean monsoonal flow is studied. A monsoon like disturbance simulated by a high resolution atmospheric general circulation model is analyzed. The model's July mean vorticity balance at 200 mb is studied in detail to assess the effect of transients of all scales on the large scale flow in the tropics. Some conclusions that may be drawn from this work are: (1) the zonally varying lower tropospheric monsoonal flow is barotropically unstable. Rapid localized growth can occur by this process in certain preferred geographical regions such as the Bay of Bengal; (2) the upper tropospheric tropical easterly jet is baroclinically as well as barotropically unstable. The characteristics of the most unstable modes compare favorably with those of observed waves in the easterlies. These modes are confined to the upper troposphere, but modes of slightly longer wavelength, with only slightly lower growth rates, penetrate to the ground with appreciable amplitude. Dissert. Abstr.

N84-12681# Florida State Univ., Tallahassee. Dept. of Oceanography.
ON THE WIND STRESS - SEA LEVEL POWER LAW
Gary T. Mitchum and Wilton Sturges Jun. 1983 21 p
(Contract N00014-75-C-0201; NR Proj. 083-231)
(AD-A132035; Rept-214) Avail: NTIS HC A02/MF A01 CSCL 08/3

The response of coastal sea level to local forcing by synpotic scale winds is usually assumed to be linear in wind stress. However, the response of sea level at St. Petersburg, Florida is found to be not linear, but to a power significantly less than one. The observed power-law exponent is 0.8 + or - 0.1. The deviation from linearity in the power law is shown to be consistent with the effect of the quadratic form of the instantaneous bottom drag law. Therefore, the non-linear response should be true, to varying degrees, on many continental shelves. Recognition of this non-linear sea level response to wind stress may allow significant improvement in the analysis of some sea-level problems. Author (GRA)

N84-12682# Air Force Geophysics Lab., Hanscom AFB, Mass.
WIND-SPEED EXTREMES IN THE NORTHERN HEMISPHERE, 30 THROUGH 60 km Environmental Research Papers
Arthur J. Kantor and Eugene A. Bertoni 2 Feb. 1983 110 p
(AF Proj. 6670)
(AD-A132019; AFGL-TR-83-0029; AFGL-ERP-823) Avail: NTIS HC A06/MF A01 CSCL 04/2

This report provides Northern Hemisphere maps of monthly 90-, 95-, and 99-percentile scalar speeds (10-, 5-, and 1-percent extremes) for altitudes 30 through 60 km. Observed meridional and zonal mean winds and their associated standard deviations were used to derive the magnitude of the mean monthly wind vectors and vector standard deviations. Extreme scalar speeds were then calculated from the magnitudes of the vector means and vector standard deviations, assuming a circular normal distribution. The data used to derive these values consist of wind measurements at and above 30 km from 8 years of data at 12 Meteorological Rocket Network (MRN) stations in the northern hemisphere. Also presented are tables of monthly and annual 10-, 5-, and 1-percent wind-speed extremes at each of the 12 MRN stations. Author (GRA)

N84-12683# Air Force Geophysics Lab., Hanscom AFB, Mass.
WINDS: CHAPTER 6, 1983 REVISION. HANDBOOK OF GEOPHYSICS AND SPACE ENVIRONMENTS Environmental Research Papers
Allen E. Cole, Donald D. Grantham, Irving I. Gringorten, Arthur J. Kantor, and Paul Tattelman 21 Mar. 1983 65 p
(AF Proj. 6670)
(AD-A132018; AFGL-TR-83-0080; AFGL-ERP-831) Avail: NTIS HC A04/MF A01 CSCL 04/2

This report is a revision of Chapter 4 of the 1965 Edition, Handbook of Geophysics and Space Environments. The need for geophysical and astrophysical information is critical to the design of aircraft, missiles, and satellites. The Handbook of Geophysics and Space Environments is an attempt by the U.S. Air Force to organize some of these data into one source. Winds, surface to 90 km, are discussed in this Chapter. Information on winds as a function of height, large scale wind structure, wind profiles, and design data on winds are included. Author (GRA)

N84-12684# Army Cold Regions Research and Engineering Lab., Hanover, N. H.
SNOW COVER AND METEOROLOGY AT ALLAGASH, MAINE, 1977 - 1980 Special Report
Roy E. Bates Jun. 1983 54 p
(AD-A132013; CRREL-SR-83-20) Avail: NTIS HC A04/MF A01 CSCL 04/2

A complete meteorological field station and a snow survey network were set up in the Allagash River Watershed to record baseline conditions prior to construction of the proposed Dickey-Lincoln Dam in the upper St. John River Basin in Allagash, Maine. Nearly three years of daily data (Oct 1977-May 1980) are summarized and compared to long-term climatic conditions for nearby National Weather Service stations. Air temperature values for Allagash are similar to those for the two nearest meteorological stations; water equivalent precipitation amounts and snowfall totals in the Allagash basin are inconsistent with those for nearby meteorological stations. Author (GRA)

N84-12685# Naval Ocean Systems Center, San Diego, Calif.
OPTICAL EXTINCTION COEFFICIENTS BENEATH MARINE STRATUS CLOUDS. COMPARISON OF COEFFICIENTS CALCULATED FROM OBSERVED AEROSOL SPECTRA WITH COEFFICIENTS SPECIFIED BY THE NAVY AEROSOL MODEL Analysis Report, Nov. 1982 - Feb. 1983
V. R. Noonkester 2 May 1983 32 p
(NOSC Proj. F59551)
(AD-A132011; NOSC/TD-587) Avail: NTIS HC A03/MF A01 CSCL 07/4

Vertical profiles of extinction coefficients for wavelengths of 0.53, 3.75, and 10.59 micro meters were calculated from observed profiles of the liquid water aerosol spectra in marine stratus layers. These profiles were obtained for air masses characterizing marine and continental air masses. A recently developed Navy aerosol model specifies optical extinction by aerosols at the surface as a function of wind speed, relative humidity (less than saturate), and air mass type. The capability of the model to duplicate the observed profiles below cloud base was determined. The surface model was applied to the above-surface conditions by assuming various vertical profiles of relative humidity below cloud base. Comparison of the observed and model profiles were made for various combinations of surface wind speed, humidity profiles, and air mass type. These comparisons indicated that the model could not reproduce the observed profiles of optical extinction by aerosols below marine stratus clouds. GRA

N84-12686# Air Force Geophysics Lab., Hanscom AFB, Mass. Meteorology Div.
EVALUATION OF AUTOMATED IMAGERY ANALYSIS ALGO-

RITHMS FOR USE IN THE THREE-DIMENSIONAL NEPHANALYSIS MODEL AT AFGWC (AIR FORCE GLOBAL WEATHER CENTRAL) Interim Scientific Report
Robert P. DEntremont, Rupert S. Hawkins, and James T. Bunting 28 Dec. 1982 41 p
(AF Proj. 6670)
(AD-A131986; AD-F000018; AFGL-TR-82-0397; AFGL-ERP-817) Avail: NTIS HC A03/MF A01 CSCL 17/5

Two different imagery analysis algorithms, one of which is currently in use by the 3DNEPH automated cloud analysis program at the Air Force Global Weather Central (AFGWC), and the other developed at AFGL, were evaluated and compared on a sample set of DMSP IR data (10.2 to 12.8 micrometers) with the aid of the AFGL Man-computer Interactive Data Access System. The 3DNEPH algorithm, MODAL, and the AFGL algorithm, CLUSTER, were designed to separate cloud layers in IR satellite imagery. Such information is used by the 3DNEPH to compute cloud analysis parameters as percent cloud (earth) coverage and cloud heights. Both algorithms were found to perform well under some meteorological circumstances. but not so well under others. In general, however, it was found that CLUSTER performs better. The CLUSTER algorithm found clear/cloud boundaries, numbers of cloud layers, and fractional cloud covers that are closer to estimates made by analysts looking at corresponding IR and visible images. The MODAL algorithm found more cloud layers than were observed, and tended to overanalyze the transition regions between cloud layers. The AFGWC has recognized the limitations of MODAL and the complications in its computer code. Subsequently, a substantially revised version of the 3DNEPH has been written, and is known as the Real-Time Nephanalysis (RTNEPH). GRA

N84-12687# Air Force Geophysics Lab., Hanscom AFB, Mass. Meteorology Div.
SNOW CHARACTERIZATION INSTRUMENTS Interim Scientific Report
Lawrence C. Gibbons, Anthony J. Matthews, Robert O. Berthel, and Vernon G. Plank 1 Mar. 1983 31 p
(AF Proj. 6670)
(AD-A131984; AD-F000018; AFGL-TR-83-0063; AFGL-IP-316) Avail: NTIS HC A03/MF A01 CSCL 04/2

This report details the design, fabrication, and operation of three new instruments that were developed at AFGL to define some of the physical characteristics of naturally falling snow. Two are devices for the measurement of fall velocity and high-resolution snow rate. The other was conceived for the documentation of the ice-crystal composition of the prevailing snow. Problems that surfaced during the first year of operation are discussed along with the plans to correct the deficiencies. Examples of the data supplied by these instruments are shown. Author (GRA)

N84-12688# Army Engineer Waterways Experiment Station, Vicksburg, Miss. Hydraulics Lab.
POSTSTORM RECONNAISSANCE OF TROPICAL STORM CHRIS Final Report
Thomas H. Flor Jul. 1983 20 p
(AD-A131948; WES/MP/HL-83-5) Avail: NTIS HC A02/MF A01 CSCL 04/2

This report presents the results of a poststorm reconnaissance to determine the extent of flooding caused in Tropical Storm Chris along the Texas-Louisiana coastline in September 1982. This survey covered the coastal area from Sabine Pass, Texas, to Cameron, Louisiana. Tropical Storm Chris made landfall 7 miles east of Sabine Pass at 0600 CDT 11 September 1982. The highest storm-generated surge, in the range of 8.5 to 9 ft, occurred at Peveto Beach, 8 miles east of the point of landfall. Storm-induced flooding west and east of the point of landfall is estimated to have reached 2.8 ft above perdicted tide level 17 miles to the west and 2.5 ft above predicted tide 19 miles to the east. The meteorological history of Tropical Storm Chris is included as an appendix to this report. Author (GRA)

N84-12689# Weather Wing (5th), Langley AFB, Va.
WORLD-WIDE SEA-SURFACE TEMPERATURES Final Report
Ransom R. Traxler and Gerald L. Wheeler Apr. 1983 254 p
(AD-A131892; AD-E850385; Rept-5WW-TN-83/001; Rept-5WW-TN-79/001) Avail: NTIS HC A12/MF A01 CSCL 04/2

This technical note contains sea-surface isotherm charts divided into geographical sections for the Atlantic, Pacific, and Indian Oceans as well as North American Lakes and Hudson Bay. Each section is further divided into 12 monthly sets of charts, each set containing a maximum, mean, and minimum temperature chart (except for the Canadian lakes and Hudson Bay section, which only has a mean value). Also included is a table on approximate survival times of humans immersed in the sea with ordinary clothes. GRA

N84-12690# Army Cold Regions Research and Engineering Lab., Hanover, N. H.
PROCEEDINGS OF 1ST INTERNATIONAL WORKSHOP ON ATMOSPHERIC ICING OF STRUCTURES
L. David Minsk Jun. 1983 378 p Workshop held at Hanover, N.H., 1-3 June 1982
(AD-A131869; AD-E850387; CRREL-SR-83-17) Avail: NTIS HC A17/MF A01 CSCL 08/12

The accumulation of ice in its various forms on structures has long been recognized as a significant and costly problem for both industry and government world-wide. The purpose of this First International Workshop on Atmospheric Icing of Structures was to bring together scientists, engineers and managers from industrial and military organizations from around the world that have an interest in the accretion of ice on structures. The presumption underlying the use of 'First' in the title of the workshop is that this meeting would demonstrate the need for continued exchange of ideas, of reports of work accomplished and of future plans, and further identification of research areas requiring particular attention. The 39 papers from 10 countries presented at the workshop were organized into four technical sessions representing the various aspects of structural ice accretion studies underway. Topics included: Basic research; Physics of ice accretion; Simulation and modeling; Design-oriented research; Meteorological measurements and damage observations; and Iceload measurements and design practices. GRA

N84-12691# Systems and Applied Sciences Corp., Hampton, Va.
MESOCYCLONE DETECTION AND CLASSIFICATION ALGORITHM
James G. Wieler and Ralph J. Donaldson, Jr. Jun. 1983 7 p
(Contract F19628-82-C-0023; AF Proj. 6670)
(AD-A131826; AFGL-TR-83-0166) Avail: NTIS HC A02/MF A01 CSCL 04/2

A proposed four dimensional algorithm for automated detection of mesocyclones employs resolution dependent thresholds of rotational velocity and shear. This algorithm incorporates complementary features of earlier techniques suggested by Hennington and Burgess and by Forsyth, Bjerkaas and Petrocchi. Classification of mesocyclones by calculation of total rotational kinetic energy is proposed as a possible means for early assessment of the destructive energy of the resultant tornado. Author (GRA)

N84-12692# Avco-Everett Research Lab., Mass.
TURBULENCE ENVIRONMENT CHARACTERIZATION Interim Technical Report, 15 Mar. - 30 Sep. 1977
Merlin G. Miller and P. L. Zieske Dec. 1977 37 p
(Contract F30602-76-C-0054; DARPA Order 2646; AF Proj. 2646) (AD-A131815) Avail: NTIS HC A03/MF A01 CSCL 04/2

This report presents discussions of a variety of activities and results relative to the characterization of atmospheric turbulence and its effects on optical propagation at the AMOS Observatory in Maui, Hawaii. The major emphasis is on experimental results obtained during the last 6 months. A brief discussion of the operational aspects and status of the instrumentation is also included. Data were obtained with the Seeing Monitor, State Sensor, microthermal probes and/or acoustic sounder on more than 20 occasions during the period. Much of this data were of a simultaneous nature. A detailed comparative analysis of the data

has not yet been completed. Twelve nights of Star Sensor data yielded valued of the log amplitude variance in the range from 3/10000 to 7.2/1000 with an average of 5.1/1000. This device is a new model of the original instrument built by NOAA which was installed at AMOS in June 1977. The much shorter data collection cycle has virtually eliminated the nonstationarity problems encountered previously. However, there are significant differences between the data obtained with the two devices. GRA

N84-12693# Pacific Northwest Lab., Richland, Wash.
ESTIMATING LONG-TERM MEAN WINDS FROM SHORT-TERM WIND DATA
W. R. Barchet and W. E. Davis Aug. 1983 31 p refs
(Contract DE-AC06-76RL-01830)
(DE83-017417; PNL-4785) Avail: NTIS HC A03/MF A01

The estimation of long term mean winds from short term data which is especially important in the area of wind energy is discussed. It is desirable to obtain reliable estimates of the long term wind speed from as short a period of on site measurements as possible. Seven different methods of estimating the long term average wind speed were studied and the performance of these techniques was compared. Three linear, three weather pattern, and one eigenvector methods were compared for measurement periods ranging from 3 months to 36 months. Average errors, both relative and absolute, and the rms errors in the techniques were determined. The best technique for less than 12 months of measurement was the eigenvector method using weekly mean wind speeds. This method however, was only slightly better than the linear adjusted method. When 12 or more months of data were used, the difference in errors between techniques was found to be slight. DOE

N84-12694# Pacific Northwest Lab., Richland, Wash.
A SUBSYNOPTIC ENVIRONMENT ASSOCIATED WITH TWO INTER-MOUNTAIN SEVERE THUNDERSTORM EVENTS
M. N. Schwartz and G. L. Andrews May 1983 5 p refs Presented at the American Meteorological Society Meeting, Tulsa, Okla., Oct. 1983
(Contract DE-AC06-76RL-01830)
(DE83-014498; PNL-SA-11188; CONF-8310115-1) Avail: NTIS HC A02/MF A01

Isentropic analysis provided the means for revealing a subsynoptic feature, the thermal line, that is virtually impossible to detect on a surface map. The initial convective activity occurred in the vicinity of this boundary rather than near the more salient surface features (e.g., thermal low and cold front). Isentropic analysis also showed that the location of the thermal line did coincide with a region of significant upward motion. Thus, in these cases, it appears the subsynoptic features (e.g., thermal line and it's associated environment) were catalysts for the initial convection while the synoptic conditions provided the favorable environment for severe thunderstorms. DOE

N84-12695# European Space Agency, Paris (France).
RADAR METEOROLOGY IN CLOUD PHYSICS AND RADIO WAVE PROPAGATION RESEARCH
Arno Schroth Sep. 1983 368 p refs Transl. into ENGLISH of "Radarmeteorol. in der Wolkenphys. u. Ausbreitungsforsch. mit Radiowellen" rept. DFVLR-Mitt-82-09 DFVLR, Oberpfaffenhofen, West Germany, Jun. 1982 Original report in GERMAN previously announced as N83-21717
(ESA-TT-808; DFVLR-Mitt-82-09) Avail: NTIS HC A16/MF A01; original German version available from DFVLR, Cologne DM 91,60

The task of a weather radar in meteorology and radio wave propagation research is discussed, and the most important development stages are presented, from the standard weather radar to the coherent polarization diversity radar. The basic design, measurement applications and the limitations of the individual devices are investigated. The theory on which the system design of a coherent polarization diversity radar is based is described, and used to interpret measured data. The main parameters and their effect on the design of such a device are outlined. A production proposal is made, and the values of the significant radar parameters are given. Author (ESA)

N84-12696# Aeronautical Research Inst. of Sweden, Stockholm. Structures Dept.
GUST STRUCTURE AND GUST STATISTICS. RESULTS FROM AN ANALYSIS OF ATMOSPHERIC TURBULENCE MEASUREMENTS BY USING CONDITIONAL SAMPLING TECHNIQUE
Magnus Linde Jun. 1983 57 p refs
(Contracts NE-5061-015; NE-5061-016)
(FFA-TN-1983-28) Avail: NTIS HC A04/MF A01

Gust structure and gust statistics of the atmospheric boundary layer were investigated, using turbulence measurements from two different places and at heights up to 135 m above ground, analyzed by conditional sampling. It is found that the atmospheric turbulence is not isotropic. Gusts with positive slope are more frequent when the turbulence intensity is high. The results indicate that the gust front line has a paraboia-like shape in the horizontal plane. The gust frequency varies exponentially with amplitude in a fixed point in space. Considerable difference in gust frequency and gust amplitude are found when comparing the results for different levels above ground. Author (ESA)

N84-12697# World Meteorological Organization, Geneva (Switzerland).
GUIDE TO AGRICULTURAL METEOROLOGICAL PRACTICES, SECOND EDITION
1981 234 p refs
(WMO-134; ISBN-92-63-12134-6) Avail: NTIS MF A01; print copy available at WMO, Geneva

World Meteorological Organization procedures concerning agricultural meteorological elements and their observations; agricultural meteorological data, their presentation and statistical analysis; weather forecasts for agriculture; agrometeorological forecasting; applications of meteorology to agriculture; and weather risk assessment for agricultural planning are presented. Plant injury from air pollution is discussed. International organizations of interest to agricultural meteorologists are listed. Author (ESA)

N84-12698# Royal Netherlands Meteorological Inst., De Bilt. Oceanografisch Onderzoek.
ON THE GROWTH OF GRAVITY-CAPILLARY WAVES BY WIND Master's Thesis - Utrecht Univ.
Klaartje vanGastel 1983 73 p refs
(KNMI-WR-83-10) Avail: NTIS HC A04/MF A01

For the case of 1 cm gravity-capillary waves the exact equations for the wave motion in air and water derived. Effects of viscosity and surface tension are included. A closed expression for the growth rate of the waves is found. The expression still contains an unknown perturbation stream function in air. This stream function is determined for the case of a linear wind profile (LWP). In this LWP model it is a linear combination of an exponential function and a weighted integral of the Airy function. By estimating the integral for a fairly small wave-number interval, there is good agreement with numerical results confirmed experimentally. Author (ESA)

N84-12699# National Weather Service, Salt Lake City, Utah.
CLIMATE OF PHOENIX, ARIZONA (REVISED)
Robert J. Schmidli Mar. 1983 92 p refs
(PB83-246801; NOAA-TM-NWS-WR-177-Rev) Avail: NTIS HC A05/MF A01 CSCL 04B

Comprehensive data on the climate of Phoenix is provided. Data includes a history of weather observations, temperature, pricipatation, thunderstorms, hail, tornadoes, sunshine, cloudiness, fog, wind, and pressure. S.C.L.

N84-12700# National Oceanic and Atmospheric Administration, Miami, Fla. Atlantic Oceanographic and Meteorological Labs.
OMEGA DROPWINDSONDE PROCESSING
James Franklin May 1983 39 p refs
(PB83-248773; NOAA-TM-ERL-AOML-54; NOAA-83081107) Avail:

NTIS HC A03/MF A01 CSCL 04B

During the Global Atmospheric Research Program's Alpine Experiment (ALPEX) of 1982, 187 atmospheric soundings were obtained with Omega dropwindsondes. These data were post-processed at the NOAA Atlantic Oceanographic and Meteorological Laboratory Hurricane Research Division to improve the quality of the data set. The errors common to Omega dropwindsonde data are described, and corrections of these problems through post-processing are illustrated using soundings from ALPEX and Hurricane Debby (1982). Author (GRA)

48 OCEANOGRAPHY

Includes biological, dynamic and physical oceanography; and marine resources.

N84-12701# Australian Oceanographic Data Centre, North Sydney.

AUSTRALIAN OCEANOGRAPHIC DATA CENTRE BULLETIN 16

May 1983 55 p

(AD-A132002) Avail: NTIS HC A04/MF A01 CSCL 08/10

Contents: AODC Data Management System; AODC Bathythermal Data Outputs; Southern Ocean Environmental Brief; The Marine Studies Centre; Monitoring of High Frequency Currents, on the Inner Continental Shelf on NSW; Ocean Sciences Institute Announced; Western Tasman Oceanographic Analysis - NAS NOWRA; Availability of Ran Ships for Oceanographic Data Collection. GRA

N84-12702 Princeton Univ., N. J.

ADJUSTMENT IN THE OCEANS: THE LONG-PERIOD TIDES AND COASTAL UPWELLING Ph.D. Thesis

James Alfred Carton 1983 214 p

Avail: Univ. Microfilms Order No. DA83-06607

Long-period tides in a bounded basin are discussed. As the period of the forcing incerease, a region of equilibrium spreads westward from the eastern boundary, so that for periods as short as a month the equilibrium tide may be appropriate. The resonse of the eastern ocean to wind forcing is discussed. The response of the coastal ocean may either be viewed as the response to a series of distinct wind events, or it may be viewed climatologically as the response to stochastic forcing. The response of the coastal ocean to an alongshore wind event which is confined in space and time depends on the ratio of the time scale of the storm to the distance to the equatorward edge of the storm, divided by the speed of the along shore waves. When this ratio is much greater than one the maximum along shore velocity and upwelling occur during the passage of the storm. When this ratio is much less than one the maximum velocity and upwelling occur after the passage of the storm. The response outside the region of forcing and for different stratifications and topography are explored.

Dissert. Abstr.

51 LIFE SCIENCES (GENERAL)

Includes genetics.

N84-12703# Naval Aerospace Medical Research Lab., Pensacola, Fla.

ERUPTION OF PERMANENT DENTITION IN RHESUS MONKEYS EXPOSED TO ELF (EXTREMELY LOW FREQUENCY) FIELDS Interim Report

Tony D. David, Gregory A. Harris, and John A. Bley, Jr. Apr. 1983 26 p

(NAMRL Proj. M0096PN)

(AD-A132065; NAMRL-1295) Avail: NTIS HC A03/MF A01 CSCL 06/18

In a study initiated to determine the biological effects of extremely low frequency ELF electric and magnetic fields associated with a submarine communications system ELF-exposed male rhesus monkeys gained weight at a slightly faster rate than control males. In order to obtain sufficient data on the physiological effects of electromagnetic fields, a second ELF study was initiated. Whereas the first study was initiated with wild-caught young adult animals, the second study utilized colony-bred animals beginning at 30 days of age. The emphasis of the second study was to substantiate previous findings and determine the underlying mechanisms involved. As in the first study, 30 primates (male and female) were exposed to the ELF electric and magnetic fields, and 30 control animals received the same care and treatment, but were not exposed. This report deals with the development of the permanent teeth relative to ELF exposure and sex. A consistent trend noted was that the teeth of female animals erupted at a slightly earlier age than males. However, no significant differences due to ELF exposure or sex were detected. Author (GRA)

N84-12704# Naval Aerospace Medical Research Lab., Pensacola, Fla.

EFFECTS OF PULSED MICROWAVES AT 1.28 AND 5.62 GHz ON RHESUS MONKEYS (MACACA MULATTA) PERFORMING AN EXERCISE TASK AT THREE LEVELS OF WORK Final Report

James Knepton, John DeLorge, and Toby Griner 10 Mar. 1983 35 p

(NAMRL Proj. F58524)

(AD-A132057; NAMRL-1293) Avail: NTIS HC A03/MF A01 CSCL 06/18

The present experiment studies both behavioral and physiological consequences of exposing exercising rhesus monkeys to microwave radiation. At 1.28 Ghz four of the monkeys were exposed to power densities of 25, 41, and 89 mW/sg cm. At the highest power density exercising animals consistently had a lower response rate, a higher heart rate, and a greater increase in colonic temperature. At lower power densities the effects were generally less evident and were idiosyncratic. At 5.62 GHz five monkeys were exposed to power densities of 25, 41, and 89 mW/sg cm. Differences from controls were found only at 43 mW/sq cm: (1) colonic temperature averaged +0.8 C higher (N=2), (2) response rate decreased (N=5) when the heaviest work load occurred during the terminal third of the session, and (3) heart rate (N=2) was higher. These experiments demonstrate the microwaves will produce cardiovascular effects in addition to those produced by exercise alone and that body temperature induced by microwave energy does not seem to be further accelerated by exercise. The results also illustrate that monkeys working a physically arduous task are more likely to stop working when exposed to microwave than when working a less arduous task.

GRA

N84-12705# Naval Aerospace Medical Research Lab., Pensacola, Fla.

A RESTRAINT CHAIR WITH ROWING-LIKE MOVEMENT FOR EXPOSING EXERCISING NONHUMAN PRIMATES TO MICROWAVE IRRADIATION

James Knepton, Clayton Ezell, and John DeLorge 20 Apr. 1983 21 p

(NAMRL Proj. F58524)

(AD-A132047; NAMRL-1298) Avail: NTIS HC A02/MF A01 CSCL 06/18

Design and construction of a Styrofoam exercise restraint chair is described for use with rhesus monkeys exposed to microwaves. Monkeys usually learn the rowing-like motion of the device within five 1-hour conditioning sessions. Radiation intensity measure of the chair and an example animal experiment demonstrated the chair's suitability for bioelectromagnetic studies. Results of a series of base-line behavioral sessions demonstrated concomitant exercise work load effects on colonic temperature heart rate, correct response rate, and post-reinforcement pause time. With additional instrumentation, detection of minute disturbances of integrated psychological and physiological mechanisms by unusual environmental factors may be possible. GRA

N84-12706# Naval Aerospace Medical Research Lab., Pensacola, Fla.
EFFECT OF PULSED 5.62 GHz MICROWAVES ON SQUIRREL MONKEYS (SAIMIRI SCIUREUS) PERFORMING A REPEATED ACQUISITION TASK Final Report
James Knepton and John DeLorge 28 Jan. 1983 21 p
(NAMRL Proj. F51524)
(AD-A132045; NAMRL-1291) Avail: NTIS HC A02/MF A01 CSCL 06/18

Navy personnel assigned to perform duties in the vicinity of microwave irradiating devices are subject to possible hazards if the irradiation is of adequate intensity and frequency. Data are of critical need to establish safety standards for human exposure to microwaves. In an effort to provide such information squirrel monkeys were trained on a task that required learning and were subsequently irradiated with microwaves while they performed the task. Four male squirrel monkeys trained to perform a repeated learning task demonstrated performance decay while being exposed to pulsed 5.62 GHz microwave radiation in the far-field situation at power densities of 38 and 46 mW/sq cm, but there was only slight learning impairment. There was little, if any, effect on learning or performance at 17 and 32 mW/sq cm. The performance effect became evident when the monkey's colonic temperature increased 1 C or more above the small increases that occurred during sham exposure. There was no evidence of either thermal or behavioral adaption, nor were there indications of lasting microwave effects. Specific absorption rate (SAR) values, obtained from saline and tissue-simulating models, coupled with the performance decay finding at 38 and 46 mW/sq cm indicate that special attention should be given to exposures of the head and extremities when establishing safety standards for human exposure. GRA

N84-12707# School of Aerospace Medicine, Brooks AFB, Tex.
COMBINED EFFECTS OF IONIZING RADIATION AND ANTICHOLINESTERASE EXPOSURE ON RODENT MOTOR PERFORMANCE Final Report, Oct. 1982 - Jan. 1983
Thomas G. Wheeler and Robert E. Cordts Jul. 1983 16 p
(AF Proj. 7757)
(AD-A131847; SAM-TR-83-30) Avail: NTIS HC A02/MF A01 CSCL 06/18

Ionizing radiation and anticholinesterase exposure produce a performance decrement. The objective of this study was to determine if combined exposure would produce a greater deficit than either insult present alone. Five behavioral measures were taken on four experimental test groups. The test groups consisted of: (1) sham controls, (2) radiation exposure only (7 Gy), (3) physostigmine exposure only (0.1 mg/kg), and (4) radiation-plus physostigimine exposure. The behavioral measures were: (1) ability to maintain balance on a rotating rod, and (2) four measures of general motor activity in an activity monitor--crossing rearings, groomings, and boli excreted. Animals were evaluated on the behavioral test battery three times postirradiation (45 min, 4 days, and 8 days). The radiation-only test group had a 30% performance deficit at 45 min postirradiation which decreased to a 60% deficit by Day 8. The physostigimine test group had a 40% deficit for each of the periods. The combined treatment groups showed a 60% performance deficit on each of the tests periods. All measures of performance indicated that the combined exposure to ionizing radiation and physostigmine was much greater than either insult alone. The extent of the performance deficit was task dependent and appears to be a nonlinear function. The underlying mechanisms are not yet known. GRA

N84-12708# Army Research Inst. of Environmental Medicine, Natick, Mass.
NALOXONE DOES NOT AFFECT VENTILATORY RESPONSES TO HYPOXIA AND HYPERCAPNIA IN RATS
Richard A. Steinbrook, Henry A. Feldman, Vladimir Fencl, Vincent A. Forte, Jr., and Ronald A. Gabel 11 Aug. 1983 10 p
(DA Proj. 3M1-61102-BS-10)
(AD-A131836; USARIEM-M-42/83) Avail: NTIS HC A02/MF A01 CSCL 06/15

Ventilatory responses (tidal volume, respiratory frequency, and minute ventilation) to steady-state hypoxia and steady-state hypercapnia were measured plethysmographically in awake unrestrained adult rats, before and after subcutaneous injection of placebo (saline) or naloxone in doses up to 5.0 mg/kg. Naloxone did not alter the ventilatory responses to hypoxia or hypercapnia. GRA

N84-12709# Argonne National Lab., Ill.
MEASUREMENTS, IN VIVO, OF PARAMETERS OF THE DOPAMINE SYSTEM
A. M. Friedman, O. T. DeJesus, R. Dinerstein, and J. Revenaugh 1983 30 p refs Presented at the Natl. Inst. of Health Workshop, Bethesda, Md., 22 Jun 1983 Prepared in cooperation with Chicago Univ., Ill.
(Contract W-31-109-eng-38)
(DE83-017964; CONF-8306122-1) Avail: NTIS HC A03/MF A01

Methods of measuring important parameters of the dopamine system in the living animal by use of PET techniques are discussed. Especially the density and binding affinity of postsynaptic neuroreceptors, the activity of neurons. In vivo, this is generally related to the turnover of neurotransmitter and can also be related to the uptake of precursor compounds by the neurons. If the transmitter and neuroleptic compound compete for the same binding sites these two effects are interwoven and are not easily isolated. It appears that the movement of neuroleptic drugs from the brain is slow enough to allow equilibrium to be maintained between ligand and receptor, especially after some time for the initial washout and translocation in the brain. To test the consequences of equilibrium binding and the possible use of the model for measurement of receptor densities by emission tomography Clark's equilibrium model of ligand binding was modified. The solutions of the equations and some comparisons of the predictions of the model with data, as well as its application to tomographic measurements are described. DOE

N84-12710# Wisconsin Univ., Madison.
PHYTOCHROME FROM GREEN PLANTS: ASSAY, PURIFICATION, AND CHARACTERIZATION
Peter H. Quail 1983 28 p refs
(Contract DE-AC02-81ER-10903)
(DE83-017447; DOE/ER-10903/4) Avail: NTIS HC A03/MF A01

Phytochrome from the chlorophyllous cells of light grown higher plants and green algae was isolated and characterized. Spectral and immunochemical analysis of phytochrome from green oat tissue indicates the presence of two distinct species of the molecule: a minority species that is recognized by antibodies directed against phytochrome from etiolated tissue and that has an apparent molecular mass of 124 kilodaltons (kD), the same as that of the native molecule from etiolated tissue; and a majority species that is not recognized by antietiolated tissue phytochrome Iq and has a Pr absorbance maximum some 14 nm shorter than its etiolated tissue counterpart. It is established that these different molecular species preexist in the green cell and are not the results of posthomogenization modifications. Monoclonal antibodies specific for antigenic sites distributed throughout the length of the etiolated tissue phytochrome polypeptide were identified. Axenic cultures of the alga Mesotaenium are established and phytochrome isolated from these cells is analyzed. DOE

N84-12711# Environmental Protection Agency, Research Triangle Park, N.C. Inhalation Toxicology Div.
PULMONARY DOSIMETRY OF NITROGEN DIOXIDE IN ANIMALS AND MAN
E. J. Miller, J. A. Graham, J. H. Overton (Northrop Services Inc.), and E. T. Myers (Northrop Services Inc.) 1983 15 p refs
(PB83-243394; EPA-600/D-83-091) Avail: NTIS HC A02/MF A01 CSCL 06T

Using a general mathematical model formulation for the transport of gases in the lungs, the regional pulmonary deposition of nitrogen dioxide (NO2) in man, rabbits, guinea pigs, and rats was studied. The model formulation utilizes lung morphometric data and includes parameters reflecting physiochemical properties

of NO2, ventilatory patterns, and chemical reactions of NO2 with components of the protective layer linings of the lungs. Sensitivity of model predicted doses to changes in some of the above parameters are discussed as well as qualitative comparisons between animals and man in the shape of the dose curves.
Author (GRA)

52 AEROSPACE MEDICINE

Includes physiological factors; biological effects of radiation; and weightlessness.

N84-12712* National Aeronautics and Space Administration, Washington, D. C.
AEROSPACE MEDICINE AND BIOLOGY: A CONTINUING BIBLIOGRAPHY WITH INDEXES (SUPPLEMENT 250)
Oct. 1983 78 p
(NASA-SP-7011(250); NAS 1.21:7011(250)) Avail: NTIS HC $7.00 CSCL 06E

This bibliography lists 265 reports, articles and other documents introduced into the NASA scientific and technical information system in September 1983. Author

N84-12713# Committee on Science and Technology (U. S. House).
BIOLOGICAL CLOCKS AND SHIFT WORK SCHEDULING
Washington GPO 1983 411 p refs Hearings before the Subcomm. on Invest. and Oversight of the Comm. on Sci. and Technol., 98th Congr., 1st Sess., no. 7, 23-24 Mar. 1983
(GPO-21-747) Avail: Subcommittee on Investigations and Oversight

A variety of problems which hold consequences for labor, management, and the general public result for shift work scheduling that is not based on research in circadian rhythm. Representatives of airline pilots, nurses, police, factory workers, and nuclear power plant operators delineate the physiological, psychological, and social effects of rotating shifts. Pilot fatigue and desynchronosis as factors in aircraft accidents is examined as well as management efforts to address problems of biological rhythms and shift work scheduling. A.R.H.

N84-12714# Army Aeromedical Research Lab., Fort Rucker, Ala.
EXTENT OF HEARING LOSS AMONG ARMY AVIATORS AT FORT RUCKER, ALABAMA
Leslie J. Peters and Helen Ford Aug. 1983 62 p
(DA Proj. 3E1-62777-A-878)
(AD-A132069; USAARL-83-12) Avail: NTIS HC A04/MF A01 CSCL 06/19

This study provided hearing threshold data for Army aviators stationed at Fort Rucker, Alabama, from February through August 1982. The mean pure tone thresholds were found to be improved when compared to data gathered by Walden and McCurdy in 1971. This improvement partially was attributed to redesign of the aviation helmet and increased awareness and compliance with hearing conservation measures. It is possible that tighter administrative controls also contributed to the reduced threshold values. This study further indicated that, for Fort Rucker aviators, there exist three threshold regions correlated with flight hours: 50-400 flight hours, 401-3000 flight hours, and 3001-6000 flight hours. Each region has a specific range of hearing loss measured by comparing 2000 and 4000 Hz thresholds for the left ear. Anyone falling outside the threshold range for her/his respective region could be identified for possible follow-up procedures.
Author (GRA)

N84-12715# Naval Aerospace Medical Research Lab., Pensacola, Fla.
FIGURAL AFTEREFFECTS: AN EXPLANATION IN TERMS OF MULTIPLE MECHANISMS IN THE HUMAN VISUAL SYSTEM
Micheline Y. Eraud, Frank M. Bagrash, and Gerald R. Stoffer 19 Apr. 1983 21 p
(AD-A132066; NAMRL-MONOGRAPH-30) Avail: NTIS HC A02/MF A01 CSCL 05/10

As an alternative to the classical explanation of figural aftereffects (FAE), it was hypothesized that FAE are due to changes in the relative activities of multiple mechanisms tuned to specific features of the stimulus pattern. Changes along the stimulus dimensions of size and orientation were studied. The rationale was that prolonged exposure to an inspection figure (IF) of a particular size or orientation would change the appearance of a test figure (TF) to the extent that these two figures stimulate the same mechanism. Following selective adaption to a particular IF, subjects were required to make size or orientation judgements with the size or orientation of the IF serving as the anchor for these judgments. Results indicated that there was a particular range of TF size or orientation over which a given IF would produce perceptual changes. The TFs outside this range were not affected. Findings were compared with the classical explanation and the role of multiple mechanisms as a basis of FAE was elaborated. Author (GRA)

N84-12716# Naval Aerospace Medical Research Lab., Pensacola, Fla.
AN AGE COMPARISON OF THE VESTIBULO-OCULAR COUNTERROLL REFLEX Interim Report
Jay G. Pollack and Charles Diamond 22 Feb. 1983 20 p
(NAMRL Proj. F58528)
(AD-A132064; NAMRL-1292) Avail: NTIS HC A02/MF A01 CSCL 06/16

This report examines the relationship between age and a measure considered to be related to static otolith function; vis., the amplitude of ocular counterroll under conditions of static whole body tilts. Amount of counterroll was measured for two groups of subjects (22 to 34 years, and 50 to 74 years) to whole body tilts to the right and left. It was found that the young group exhibited more counterroll to tilt than the older group, but this difference was small. In addition, head tilts to the right produced larger counterrolls than tilts to the left in both groups. It is concluded that, because of the considerable variability in the responses from subject to subject, the potential contribution of the static counterroll response to the establishment of agefree biomedical standards is limited. Author (GRA)

N84-12717# Naval Aerospace Medical Research Lab., Pensacola, Fla.
VESTIBULO-OCULAR REFLEX GAIN IN MAN DURING ACTIVE VERSUS PASSIVE OSCILLATION AND THE INFLUENCE OF VOLUNTARY GAZE-CONTROL TASKS Interim Report
Ralph M. Jell, C. W. Stockwell, G. T. Turnipseed, and F. E. Guedry, Jr. 13 Dec. 1982 15 p
(AD-A132006; NAMRL-1290) Avail: NTIS HC A02/MF A01 CSCL 06/19

This report compares passive and active oscillation and also examines effects of instruction sets on the vestibulo-oular reflex in order to establish procedural guidelines for simple procedures for testing visual and vestibular interaction in operational settings. Manual oscillation was feasible for generating passive whole-body oscillations up to 1.0 Hz. Below 1.0 Hz, VOR gain was virtually zero when subjects tracked a head-fixed target and -1.0 when they tracked an earth-fixed target. Below 1.0 Hz in darkness, VOR gain was intermediate between these two values, but it was markedly influenced by instructions: when subjects were instructed to track an imagined earth-fixed target, the gain was significantly higher than it was when they were instructed to track an imagined head-fixed target. At oscillation frequencies above 1.0 Hz, VOR gain converged at approximately -0.90, regardless of instructions or stimulus conditions. VOR gain was the same whether oscillation was active or passive, except under the condition imagined head-fixed target in darkness, where active oscillation yielded higher gains than passive oscillation. Author (GRA)

N84-12718# Army Command and General Staff Coll., Fort Leavenworth, Kansas.
PHYSICAL FITNESS AS A MODERATOR OF COGNITIVE DEGRADATION DURING SLEEP DEPRIVATION M.S. Thesis
Henry L. Thompson, III 3 Jun. 1983 164 p

(AD-A131962; AD-E750837) Avail: NTIS HC A08/MF A01 CSCL 06/14

There has been considerable speculation in the military as to the ability of physical fitness to moderate cognitive degradation resulting from sleep deprivation during continuous combat operations. The purpose of this investigation was to test the hypothesis that the level of physical fitness would moderate cognitive degradation such that individuals in a high fitness group would show less cognitive degradation during sleep deprivation than individuals in a low fitness group. To test the hypothesis, 16 male ROTC students participated in a 48 hours field training exercise without sleep. Cognitive performance measures made at regular intervals throughout the exercise revealed significant cognitive performance degradation beginning at 24 hours. Degradation continued throughout the exercise. Performance decrements appeared to have recovered to pre-deprivation levels after 24 hours of rest. Analyses did not reveal a significant main effect of physical fitness level. Although there were several interesting findings, the physical fitness hypothesis was not supported. GRA

N84-12719# Army Research Inst. of Environmental Medicine, Natick, Mass.

EFFECT OF ATROPINE ON THE EXERCISE-HEAT PERFORMANCE OF MAN

M. N. Sawka, L. Levine, M. A. Kolka, B. S. Appleton, and B. E. Joyce Jul. 1983 18 p

(DA Proj. 3M1-62734-A-875)

(AD-A131843; USARIEM-M41/83) Avail: NTIS HC A02/MF A01 CSCL 06/19

This paper summarizes the findings from two recent studies involving the physiological effects of atropine (0-4 mg, i.m.) on soldiers performing physical exercise in hot-dry environments. Study I determined the threshold of physiological effects and the gradation of these effects with increasing dosage of atropine. Study II examined the effects of exercise-heat acclimation on the reduced physical exercise performance that occurs following atropine administration. The following new observations were made: (1) a 0.5 mg dose of atropine elevates heart rate, rectal temperature and mean skin temperature; (2) atropine exerts its peak physiological effects approximately 70 minutes after intramuscular injection; (3) within the dosage levels tested, the magnitude of the elevated heart rate response is curvilinearly related to atropine dosage, whereas, the magnitude of the elevated rectal temperature response is linearly related atropine dosage; (4) repeated administration of atropine over a number of days does not alter thermoregulatory responses; (5) heat acclimation improves exercise-heat performance of individuals under the influence of atropine by enabling a reduced rectal temperature; and (6) heat acclimation increases the sweat output of individuals under the influence of atropine; however, the absolute reduction in sweat output from atropine is the same pre- and post-heat acclimation. GRA

N84-12720# Brookhaven National Lab., Upton, N. Y. Div. of Chemical Sciences.

USES OF SYNCHROTRON RADIATION

B. M. Gordon 1983 11 p refs Presented at the Workshop on Uses of Nucl. Anal. Methods in Metal Toxicology, Upton, N.Y., 11 Oct. 1982

(Contract DE-AC02-76CH-00016)

(DE83-014431; BNL-33143; CONF-8210106-5) Avail: NTIS HC A02/MF A01

X-ray fluorescence has long been used as a techniques for elemental analysis. X-ray fluorescence techniques have a number of features that make them attractive for application to biomedical samples. In the past few years synchrotron radiation X-ray sources have been developed and, because of their properties, their use can improve the sensitivity for trace element analysis by two to three orders of magnitude. Also, synchrotron radiation will make possible an X-ray microprobe with resulution in the micrometer range. The National Synchrotron Light Source (NSLS), a dedicated synchrotron radiation source recently built at Brookhaven National Laboratory, will have a facility for trace element analysis by X-ray fluorescence and will be available to all interested users. DOE

53 BEHAVIORAL SCIENCES

Includes psychological factors; individual and group behavior; crew training and evaluation; and psychiatric research.

N84-12721# Tennessee Univ., Knoxville. Dept. of Psychology.

EFFECT OF NOISE IN THE THREE-PARAMETER LOGISTIC MODEL

Fumiko Samejima 25 Dec. 1982 99 p

(Contract N00014-81-C-0569; DA Proj. RR04204)

(AD-A131867; AD-E850387; RR-82-2-ONR) Avail: NTIS HC A05/MF A01 CSCL 05/10

In the preceding research report, ONR/RR-82-1 (Information Loss Caused by Noise in Models for Dichotomous Items), observations were made on the effect of noise accommodated in different types of models on the dichotomous response level. In the present paper, focus is put upon the three-parameter logistic model, which is widely used among researchers. An emphasis is put upon the speed of convergence to the normality of the conditional distribution of the maximum likelihood estimate, given a specific ability level. Author (GRA)

N84-12722# Naval Postgraduate School, Monterey, Calif.

RACIAL BIAS AND PREDICTIVE VALIDITY IN TESTING FOR SELECTION

R. A. Weitzman Jul. 1983 43 p

(AD-A131830; NPS54-83-008) Avail: NTIS HC A03/MF A01 CSCL 05/10

In contrast to the Cleary-McNemar view affirmed by Cole in the October 1981 issue of the American Psychologist on testing, questions of bias are fundamentally question of validity, this report shows that freedom from statutory test bias, as interpreted by the courts, is different from predictive validity. Use of a score adjustment formula developed here to correct for statutory test bias shows in typical cases not only that the correction tends only negligibly to reduce predictive validity but also that the enhancement of predictive validity without regard to statutory test bias can add a sizable criterion-independent decrement selectively to the already low test scores of low scoring demographic groups. Author (GRA)

N84-12723# Los Alamos Scientific Lab., N. Mex.

VARIATIONS IN TASK AND THE IDEAL OBSERVER

Kenneth M. Hanson 1983 9 p refs Presented at the SPIE Conf. on Appl. of Opt. Instr. to Med. 11, Atlanta, 17-19 Apr. 1983 Submitted for publication

(Contract W-7405-eng-36)

(DE83-015394; LA-UR-83-2166; CONF-8304111-1) Avail: NTIS HC A02/MF A01

In most previous studies involving the ideal observer, the task considered was that of simple detection where it is assumed that there is complete a priori knowledge of the background and of the possible object's shape, amplitude, and position. It is shown that redefining the detection task to include the possibility of an unknown, slowly varying background reduces the importance of the low-frequency components in the image for the ideal observer. More complicated tasks than object detection are also considered, such as determination of an object's position and width and the resolution of two objects. These higher-order tasks further enhance the importance of the high-frequency information content of the image. DOE

N84-12724# Research Inst. of National Defence, Stockholm (Sweden). Dept. 5.

COHERENCE OF APPRAISAL AND COPING: PARACHUTE JUMP EFFECTIVENESS

Ben Shalit, Leif Carlstedt, Berit Staahlberg-Carlstedt, and Inga-Lill Taeljedalshalit Jul. 1983 25 p refs

(FOA-C-55058-H3; ISSN-0347-7665) Avail: NTIS HC A02/MF A01

A model describing the perceptual process, the sequential adjustment model (SAM), based on the interaction of three

phases (appraisal, mobilization, realization) with three modalities (cognitive, affective, instrumental) describing nine sequential (conditional probability) perceptual processing stages is proposed. Model sequentiality and predictive power is tested against the criterion of the performance of a first parachute jump. The sequentiality in each individual's appraisal was tested. The criterion for sequentiality was that all stages were cleared in terms of appraisal effectiveness. Results show that 85% of those who jumped well show sequentiality, while 53% of those who jumped poorly show sequentiality, and 10% of those who do not show sequentiality jumped well. Analysis of SAM's conjunctive character shows prediction effectiveness of 90% for the poor jump. Analysis based on a compensatory model gives a prediction effectiveness of 80% for the poor jump. A hypothesis that the sequentiality in the perceptual process is more important for good performance than the quality of the process' stages was generated.

Author (ESA)

54 MAN/SYSTEM TECHNOLOGY AND LIFE SUPPORT

Includes human engineering; biotechnology; and space suits and protective clothing.

N84-12725*# Whitmore Enterprises, San Antonio, Tex.
LOWER BODY GRADUATED NEGATIVE PRESSURE SYSTEM Final Report
[1983] 3 p
(Contract NAS9-16810)
(NASA-CR-171717; NAS 1.26:171717) Avail: NTIS HC A02/MF A01 CSCL 05H

The first task concerning the Lower Body Negative Pressure Suit was to determine the best type construction for a leg section with these goals in mind: good mobility, minimum amount of bulk, ease of storage, lightweight, rigid enough to withstand atmospheric pressure, and minimum amount of preparation before donning and donning time. After a study of three systems, wire hoops (rings) separated on inch apart in an airtight material furnished by NASA were chosen.

Author

N84-12726# Army Research Inst. of Environmental Medicine, Natick, Mass.
EFFECTIVENESS IN REDUCING HEAT STRESS OF THREE CONDITIONED-AIR COOLING VESTS WORN WITH AND WITHOUT COOLING AIR SUPPLIED TO A FACE PIECE
George F. Fonseca Mar. 1983 42 p
(DA Proj. 3E1-62777-A-878)
(AD-A131975; AD-F000018; USARIEM-T-1/83) Avail: NTIS HC A03/MF A01 CSCL 06/17

The auxiliary cooling provided by three different air-cooled vests and a ventilated XM-29 Face Piece was directly measured on a life-sized, heated, sectional manikin. These air-cooled systems were worn with a combat vehicle crewman (CVC) ensemble with a complete chemical protective (CW) suit. Cooling rates (watts) were determined for both dry (non-sweating) and completely wet (maximal sweating) skin conditions. At low ventilating air flow rates these air-cooled vests provided cooling primarily over the torso surface. Up to 95% of the cooling provided over the torso-arms-legs areas was over the torso. At higher air flows this percentage decreased to 55%. The design of an air-cooled vest can increase the efficiency of cooling of the ventilating air by maximizing the proportion of cooling air that diffuses over the surface of the body and minimizing the proportion of cooling air that exits an air-cooled vest directly through the clothing to the hot environment. Under the experimental conditions of this study the air-ventilated XM-29 Face Piece contributed about 20% to the total cooling.

Author (GRA)

N84-12040*# National Aeronautics and Space Administration. Langley Research Center, Hampton, Va.
PILOT RESPONSE WITH CONVENTIONAL DISPLAYS
James J. Adams *In its* Controls, Displays and Inform. Transfer for Gen. Aviation IFR Operations Oct. 1983 p 155-157 (For primary document see N84-12029 03-01)
Avail: NTIS HC A12/MF A01 CSCL 05H

N84-12041*# National Aeronautics and Space Administration. Langley Research Center, Hampton, Va.
SINGLE PILOT SCANNING BEHAVIOR IN SIMULATED INSTRUMENT FLIGHT
Jack E. Pennington *In its* Controls, Displays and Inform. Transfer for Gen. Aviation IFR Operations Oct. 1983 p 159-169 refs (For primary document see N84-12029 03-01)
Avail: NTIS HC A12/MF A01 CSCL 05H

N84-12043*# National Aeronautics and Space Administration. Langley Research Center, Hampton, Va.
DISPLAY RESEARCH: PILOT RESPONSE WITH THE "FOLLOW-ME" BOX DISPLAY
James J. Adams *In its* Controls, Displays and Inform. Transfer for Gen. Aviation IFR Operations Oct. 1983 p 181-188 (For primary document see N84-12029 03-01)
Avail: NTIS HC A12/MF A01 CSCL 05H

N84-12047*# National Aeronautics and Space Administration. Langley Research Center, Hampton, Va.
PROPOSED STUDY TO DETERMINE POTENTIAL FLIGHT APPLICATIONS AND HUMAN FACTORS DESIGN GUIDELINES OF VOICE RECOGNITION/SYNTHESIS SYSTEMS
Hugh P. Bergeron *In its* Controls, Displays and Inform. Transfer for Gen. Aviation IFR Operations Oct. 1983 p 225-227 (For primary document see N84-12029 03-01)
Avail: NTIS HC A12/MF A01 CSCL 05H

55 PLANETARY BIOLOGY

Includes exobiology; and extraterrestrial life.

No abstracts in this category.

59 MATHEMATICAL AND COMPUTER SCIENCES (GENERAL)

N84-12727*# Rensselaer Polytechnic Inst., Troy, N. Y. Dept. of Mathematical Sciences.
ADAPTIVE FINITE ELEMENT METHODS FOR PARABOLIC PARTIAL DIFFERENTIAL EQUATIONS Interim Report
Joseph E. Flaherty, J. Michael Coyle, Raymond Ludwig, and Stephen F. Davis May 1983 23 p
(Contracts NAS1-17070; DAAG29-82-K-0197; AF Proj. 9749)
(NASA-CR-174490; AD-A131824; AFOSR-83-0689TR) Avail: NTIS HC A02/MF A01 CSCL 12/1

The authors discuss a finite element method for solving initial boundary value problems for vector systems of partial differential equations in one space dimension and time. The method automatically adjusts the computational mesh as the solution evolves in time so as to approximately minimize the local discretization error. They are thus able to calculate accurate solutions with fewer elements than would be necessary with a uniform mesh. This overall method contains two distinct steps: a solution step and a mesh selection step. They solve the partial differential equations using a finite element Galerkin method on trapezoidal space time elements with either piecewise linear or cubic Hermits polynomial approximations. A variety of mesh selection strategies are discussed and analyzed. Results are presented for several computational examples.

GRA

N84-12728# Northwestern Univ., Evanston, Ill. Dept. of Engineering Science and Applied Mathematics.
FIRST PASSAGE TIMES IN STOCHASTIC DIFFERENTIAL EQUATIONS OF MATHEMATICAL PHYSICS AND ENGINEERING Final Report
Bernard J. Matkowsky May 1983 9 p
(Grant AF-AFOSR-3602-78; AF Proj. 2304)
(AD-A131705; AFOSR-83-0693TR) Avail: NTIS HC A02/MF A01 CSCL 12/1

The effects of random (stochastic) perturbations on deterministic dynamical system were considered including the effects of noise on deterministic dynamics (such noise exists in all physical systems), and specific physical effects, the details of which are very complicated, and are modeled as stochastic terms. GRA

60 COMPUTER OPERATIONS AND HARDWARE

Includes computer graphics and data processing.

For components see *33 Electronics and Electrical Engineering.*

N84-12729 Royal Signals and Radar Establishment, Malvern (England).
AN INTRODUCTION TO THE AXIS TEST BOX
A. L. Simcock Apr. 1983 11 p refs
(RSRE-3583; BR89151) Copyright. Avail: Issuing Activity

The AXIS project and the need for a test box are described. The AXIS switch consists of a central processor which controls a switching matrix and a number of group terminating units (GTU). Each GTU serves a line carrying a traffic group, which is a set of subscriber channels multiplexed together, derived either from a local multiplexer or over a trunk link connected to another switch. The switching matrix is able to connect together individual subscriber channels from the same or different groups. Both GTU and matrix present the same type of electrical interface to the controlling CPU. The test box offers a single interface identical to the control interface of the CPU, and permits its user to inject signals into a peripheral and monitors its responses freely. A test box was built entirely in hardware, but had operational limitations so a microprocessor controlled test box was developed.
Author (ESA)

N84-12730*# National Aeronautics and Space Administration. Lewis Research Center, Cleveland, Ohio.
A GRAPHICS SUBSYSTEM RETROFIT DESIGN FOR THE BLADED-DISK DATA ACQUISITION SYSTEM M.S. Thesis
Ronald R. Carney Jan. 1983 74 p refs
(NASA-TM-83510; E-1760; NAS 1.15:83510) Avail: NTIS HC A04/MF A01 CSCL 09B

A graphics subsystem retrofit design for the turbojet blade vibration data acquisition system is presented. The graphics subsystem will operate in two modes permitting the system operator to view blade vibrations on an oscilloscope type of display. The first mode is a real-time mode that displays only gross blade characteristics, such as maximum deflections and standing waves. This mode is used to aid the operator in determining when to collect detailed blade vibration data. The second mode of operation is a post-processing mode that will animate the actual blade vibrations using the detailed data collected on an earlier data collection run. The operator can vary the rate of payback to view differing characteristics of blade vibrations. The heart of the graphics subsystem is a modified version of AMD's "super sixteen" computer, called the graphics preprocessor computer (GPC). This computer is based on AMD's 2900 series of bit-slice components.
Author

N84-12731# Ballistic Research Labs., Aberdeen Proving Ground, Md.
PROCEDURES FOR THE TRANSFER OF DATA FILES BETWEEN THE BRL CYBER COMPUTER SYSTEM AND THE IBD HEWLETT-PACKARD MINICOMPUTER NETWORK Final Report
Caledonia L. Henry Aug. 1983 64 p
(DA Proj. 1L1-62618-AH-80)
(AD-A132063; ARBRL-MR-03298) Avail: NTIS HC A04/MF A01 CSCL 09/2

Frequently, files stored on one computer must be transferred to another computer. This need has become more prevalent in the last few years with the advent of satellite minicomputer networks within the Ballistic Research Laboratory (BRL). In particular, the Interior Ballistics Division (IBD) of the BRL has established a minicomputer network with a HEWLETT-PACKARD (HP) 1000-F minicomputer at the hub. Experimental date recorded on analog tape are converted to digital form and stored on digital tape and/or disk for further processing. This conversion is accomplished using an HP analog to digital converter. These data may be transferred from the HP1000 to one of the several HP9845 microcomputers within the IBD for intermediate or final analysis. If analysis is desired on a larger machine, the data may be transferred to the BRL's Control Data Corp (CDC) computer mainframe system. This system is composed of a CDC CYBER 173 (MFA), a CDC CYBER 825 (MFB) and a CDC CYBER 7600 (MFZ). MFA is the common link to MFB and MFZ, and, therefore, is the transfer point for the CDC system. After the data analysis is finished on the CDC system, output data files are sent to the minicomputer or microcomputer site for such things as interactive computer graphics processing or additional analysis using existing software. So, the transfer from MFA to the HP9845 is also required. The method herein discussed has proven to be a convenient means of transferring files (primarily data files) between an HP9845 and MFA. GRA

N84-12732*# Carnegie-Mellon Univ., Pittsburgh, Pa. Dept. of Computer Science.
SOFTWARE VOTING IN ASYNCHRONOUS NMR (N-MODULAR REDUNDANCY) COMPUTER STRUCTURES Interim Report
Gary York, Daniel Siewiorek, and Zary Segall 6 May 1983 36 p
(Grant NAG1-198; Contracts DASG60-80-C-0057; Grant NSF ECS-81-2070)
(NASA-CR-174488; NAS 1.26:174488; AD-A131900; AD-F630058; CMU-CS-83-128) Avail: NTIS HC A03/MF A01 CSCL 09/2

This paper has explored some of the attributes of NMR computer systems. Many features of software voters have been explored both experimentally and theoretically. Section 2 has presented some software voting concepts. N-modular redundancy has been described and the software concepts of time skew and space redundancy have been explained. Various synchronization issues have been presented, including time-outs, points of synchronization, and asynchronous versus synchronous systems. The frequency of voting and the data granularity were shown to be important factors in determining the reliability of NMR systems. Finally, a technique was described to allow easy bit-by-bit voting on words of data. In Section 4, some experiments were presented to help measure the overhead involved in software voting. The type of voter, the voting frequency, and the average instruction execution time were incorporated into a model of voting overhead. Section 5 shows a number of synchronization experiments. The amount of variation in process execution speed that can be tolerated was determined for three different types of variation.
GRA

N84-12733# General Atomic Co., San Diego, Calif.
HARDWARE AND SOFTWARE CONFIGURATION OF THE DOUBLET 3 DIAGNOSTIC-DATA-ACQUISITION COMPUTER SYSTEM
B. B. McHarg, Jr. May 1983 84 p refs
(Contract DE-AC02-76ET-51001)
(DE83-013427; GA-A-17031) Avail: NTIS HC A05/MF A01

The Doublet 3 data acquisition computer system acquires, archives, and processes over 3 megabytes (mb) of data from each shot of the experiment. A shot lasts 1 to 2 s and occurs every 5 to 6 min with 50 to 100 shots/day. The data acquisition system was configured to efficiently handle the increasing quantity of data as new diagnostics are added (5 mb within a year) and to

provide interactive capability during operations. The computer tasks that accomplish this acquisition begin execution immediately on reboot of the computer system and continue throughout the preacquisition stage before a shot, the actual acquisition stage when the shot is fired, and the postacquisition, or analysis, stage. The hardware and software configuration of the Doublet 3 data-acquisition system, and the interaction of the computer tasks with each other as well as with database files, data files, and global tables are described. Detailed descriptions of these files and tables are given. DOE

N84-12734# Monsanto Research Corp., Miamisburg, Ohio.
CALORIMETER OPERATING SYSTEM IMPLEMENTED ON A Z-80 MICROCOMPUTER IN READ ONLY MEMORY
Jerry R. Wetzel 29 Jul. 1983 94 p refs
(Contract DE-AC04-76DP-00053)
(DE83-016647; MLM-3085) Avail: NTIS HC A05/MF A01

The operations necessary for nondestructive, calorimetric determination the power in watts of a radioactive sample were implemented on a Z-80 based of microprocessor. The resulting system reduces the size of the analyzer electronics and determines the sample value independent of operator calculations. The time required for analysis is reduced approximately 40% using the prediction of equilibration technique. The system is capable of running in stand-alone mode or in the remote in communication with a minicomputer. All running operations can be controlled remotely from the minicomputer over an RS-232 serial communications link. This package reduces the cost of the electronics by some $7000 to $10,000 while maintaining a 0.5 (SIGMA) V out of 1.0 V resolution. This report describes the Z-80 microprocessor and associated equipment used. DOE

N84-12735# Sandia Labs., Albuquerque, N. Mex.
PLT: A MULTIPURPOSE PLOTTING PACKAGE
Colin B. Selleck and Mark P. Sears Aug. 1983 116 p refs
(Contract DE-AC04-76DP-00789)
(DE83-018261; SAND-83-0637) Avail: NTIS HC A06/MF A01

The PLT is a device independent plotting package developed under the ARIES project. It is built on top of the Sandia Virtual Device Interface (VDI) and therefore supports many different devices. The capabilities of the package include basic plotting primitives, clipping subroutines, color, element plotting routines, software and hardware text, two dimensional graph plotting, mapping subroutines and routines to set various PLT parameters. The PLT is coded in RATFOR, a FORTRAN preprocessor and is currently supported on VAX/VMS. DOE

N84-12736# Los Alamos Scientific Lab., N. Mex.
LINKED STATE MACHINES
Harold K. Knudsen Jul. 1983 86 p refs
(Contract W-7405-eng-36)
(DE83-4000123; LA-9770-MS) Avail: NTIS HC A05/MF A01

Procedures for the analysis and design of linked state machines are developed. These procedures are for the study of the finite state nondeterministic, and possibly cncurrent, processes that arise in models of communication protocols, digital hardware, and computer programs. Linked state machines (LSMs) are currently used for description (for example, specification) of protocols and hardware but are not widely used for analysis and design. This study develops tools for analysis and design by formulating mathematical descriptions of LSMs, developing methods for generating different representations of LSMs, and developing a method of reduction that allows the behavior of a selected part of an LSM to be modeled. The relationship between LSMs and Petri nets is also studied. In addition, conditions that allow the synthesis of speed independent LSMs are stated and proved. The procedures developed for the analysis and design of LSMs are mostly algorithmic and can be applied to the (hand) analysis of (some) systems with several hundred states. These procedures also will serve as a basis for computer-aided analysis and design of LSMs. DOE

N84-12737# Los Alamos Scientific Lab., N. Mex. Computer Graphics Group.
REVIEW OF THE ANSI METAFILE AND VIRTUAL DEVICE INTERFACE STANDARDIZATION ACTIVITIES
Theodore N. Reed 1983 9 p refs Presented at the Computer Graphics Intern. Conf. and Exhibition, London, 18-20 Oct. 1983
(Contract W-7405-eng-36)
(DE83-015925; LA-UR-83-2257; CONF-8310130-1) Avail: NTIS HC A02/MF A01

The American National Standards Institute (ANSI) is developing several graphics standards. Two of these standards, the Virtual Device Metafile and the Virtual Device Interface, are reviewed. The purpose, basic concepts, and philosophy of these standards are discussed and contrasted with current practice and the proposed Graphical Kernel System Standard. The proposed Virtual Device Metafile has been accepted by the International Standards Organization as a new WG2 work item. DOE

N84-12738# California Univ., Berkeley. Lawrence Berkeley Lab.
EXPERIMENTAL STUDIES RELATING ENVIRONMENTAL LIGHTING AND FLICKER TO VISUAL FATIGUE IN VDT OPERATORS
Samuel M. Berman, Daniel S. Greenhouse, Ian L. Bailey, and Arthur Bradley Jun. 1983 7 p refs Presented at the 20th Session of the Comm. Intern. de l'Eclairage, Amsterdam, 31 Aug. - 8 Sep. 1983
(Contract DE-AC03-76SF-00098)
(DE83-016316; LBL-16299; CONF-8308104-1; EEB-L-83-05; L-75) Avail: NTIS HC A07/MF A01

An operator of a visual display terminal (VDT) typically is confronted with two flickering light sources: VDT phosphor with its inherent refresh rate, and the ambient fluorescent illumination reflected from the screen. Due to differences in frequency, the two sources of flicker can produce low-frequency beats in the net light intensity presented to the VDT operator. These low frequencies, on the order of a few hertz, can lead to adaptation of visual sensory mechanism. An experiment was constructed in which a stable, high-amplitude beat is produced, with frequency chosen to enhance the possibility of detecting a visual system response. By adjusting the environmental lightning to produce a sinusoidal flicker at 69 Hz, and employing a VDT with a 61-Hz refresh rate, an 8-Hz beat frequency in the light emanating from the VDT screen was produced. By measuring temporal contract sensitivity at 8 Hz as a test of sensory visual system response, it was found that two of these subjects showed a reduced sensitivity when exposed to this stimulus, as compared with three sets of control conditions in which the 8-Hz beat was not present. Possible relations between this sensory adaptation and the factors of subjective visual fatigue and reduced levels of task performance are discussed. DOE

61 COMPUTER PROGRAMMING AND SOFTWARE

Includes computer programs, routines, and algorithms.

N84-12739 National Physical Lab., Teddington (England). Div. of Information Technology and Computing.
ADA-EUROPE GUIDELINES FOR THE PORTABILITY OF ADA PROGRAMS, SECOND EDITION
John C. D. Nissen, Peter Wallis, Brian A. Wichmann, John Barnes, Jim Briggs, Ted Dowling, Stephen Goldsack, Hans Jeanrond, Carlo Montanegro, Alan Montgomery et al Jul. 1983 43 p refs
(NPL-DITC-27/83; ISSN-0262-5369) Copyright. Avail: Issuing Activity

A users guide for designing and coding portable Ada programs is supplied. Layout and numbering follow the Ada language reference manual. Tasks, program structure, compilation issues, exceptions, generic program units, representation specifications, implementation dependent features, input/output routines, lexical elements, declarations, types, names, expressions, statements, subprograms, packages, and visibility rules are covered. Guidelines

are classified as mandatory, recommended, or suggested.
Author (ESA)

N84-12740 National Physical Lab., Teddington (England). Div. of Information Technology and Computing.
GUIDELINES FOR THE DESIGN OF LARGE MODULAR SCIENTIFIC LIBRARIES IN ADA Interim Report
G. T. Symm, B. A. Wichmann, J. Kok (Stichting Mathematisch Centrum), and D. T. Winter (Stichting Mathematisch Centrum) Jul. 1983 95 p refs
(NPL-DITC-28/83; ISSN-0262-5369; IR-2) Copyright. Avail: Issuing Activity

Guidelines for constructing numerical analysis packages for basic computations, and applications packages, using Ada are presented. Problems related to precision, composite data types, information passing, error handling, working space organization, and real time environment are discussed. Author (ESA)

N84-12741 Royal Signals and Radar Establishment, Malvern (England).
THE AXIS TEST BOX SOFTWARE REPORT
A. L. Simcock Apr. 1983 59 p refs
(RSRE-3585; BR89152) Copyright. Avail: Issuing Activity

The software program which the M6809 microprocessor obeys to perform the functions of the AXIS test box is presented. The Test Box offers a single interface identical to the control interface of the CPU, and permits its user to inject signals into a peripheral and monitors its responses freely. Author (ESA)

N84-12742*# National Aeronautics and Space Administration. Langley Research Center, Hampton, Va.
A MODEL FOR THE DISTRIBUTED STORAGE AND PROCESSING OF LARGE ARRAYS Final Report
Piyush Mehrota and Terrence W. Pratt (Virginia Univ.) Oct. 1983 52 p refs
(Contracts NAS1-17070; NAS1-17130; Grant NSF MCS-78-00763) (NASA-CR-172252; ICASE-83-59; NAS 1.26:172252) Avail: NTIS HC A03/MF A01 CSCL 09B

A conceptual model for parallel computations on large arrays is developed. The model provides a set of language concepts appropriate for processing arrays which are generally too large to fit in the primary memories of a multiprocessor system. The semantic model is used to represent arrays on a concurrent architecture in such a way that the performance realities inherent in the distributed storage and processing can be adequately represented. An implementation of the large array concept as an Ada package is also described. Author

N84-12743# Air Force Systems Command, Wright-Patterson AFB, Ohio. Foreign Technology Div.
PROCESSING ELEMENTS
Waclaw Piwonski 28 Jun. 1983 10 p Transl. into ENGLISH from Wiadomosci Telekomun. (Poland), v. 21, no. 7-8, Jul. - Aug. 1981 p 191-193
(AD-A131068; FTD-ID(RS)T-0716-83) Avail: NTIS HC A02/MF A01 CSCL 09/2

Domestic hardware, multiple-access software methods, the basic telecommunication access method (BTAM), the telecommunication access method, conversational remote job processing, and the time-sharing subsystems are discussed. N.W.

N84-12744# Ballistic Research Labs., Aberdeen Proving Ground, Md.
A COMPUTER SUBROUTINE FOR EVALUATING POLYGAMMA FUNCTIONS FOR COMPLEX ARGUMENTS Final Report
James N. Walbert Jul. 1983 23 p
(DA Proj. 1L1-62618-AH-80)
(AD-A131936; AD-F300298; ARBRL-TR-02510) Avail: NTIS HC A02/MF A01 CSCL 09/2

The series and formulas used to evaluate polygamma functions are discussed in sufficient detail to enable the user to correctly implement the computer code. Estimates of precision are given, and a listing of the code appears in the appendix. GRA

N84-12745# Texas Univ., Austin. Inst. for Computing Science and Computer Applications.
THE USE OF A FORMAL SIMULATOR TO VERIFY A SIMPLE REAL TIME CONTROL PROGRAM
Robert S. Boyer, Milton W. Green (SRI International, Menlo Park, Calif.), and J. Strother Moore Jul. 1982 20 p
(Contract N00014-81-K-0634; Grant NSF MCS-82-02943)
(AD-A131732; ICSCA-CMP-29) Avail: NTIS HC A02/MF A01 CSCL 09/2

The authors present an initial and elementary investigation of the formal specification and mechanical verification of programs that interact with environments. They describe a mechanical proof that a simple, real time control program keeps a vehicle on a straightline course in a variable crosswind. To formalize the specification they define a mathematical function which models the interaction of the program and its environment. They then state and proved two theorems about this function: the simulated vehicle never gets farther than three units away from the intended course, and it homes to the course if the wind ever remains steady for at least four sampling units. GRA

N84-12746# Weizmann Inst. of Science, Rehovoth (Israel). Dept. of Applied Mathematics.
GRIDPACK: TOWARD UNIFICATION OF GENERAL GRID PROGRAMMING Final Technical Report
Achi Brandt and Dan Ophir Jun. 1983 40 p
(Contract DAJA37-79-C-0504; DA Proj. 1T1-61102-BH-57)
(AD-A131692) Avail: NTIS HC A03/MF A01 CSCL 09/2

GRIDPACK is a fully portable FORTRAN extension, including economic data structures, routines and macro-statements, for simplifying and unifying the programming of grid operations in general two-dimensional domains. These operations include the introduction and modification of grids, boundaries, inner and outer subgrids, grid functions, boundary functions and finite-difference operators, including operators near and on boundaries; interpolation between grids; sweeping conveniently and with full efficiency over grids; displaying grids, grid functions, boundary functions and boundary shapes; etc. The software will facilitate and modularize multigrid programming, permitting writing many processes once for all,, including combinations of fast solvers with flexible local grid adaptations. Author (GRA)

N84-12747# Naval Postgraduate School, Monterey, Calif.
COMPUTER SYSTEM DESIGN ENVIRONMENT SOFTWARE DEVELOPMENT PLAN
Alan A. Ross and Jeanne Bowers 29 Jul. 1983 25 p
(AD-A131651; NPS52-83-009) Avail: NTIS HC A02/MF A01 CSCL 09/2

The Computer Systems Design Environment (CSDE) project is an attempt at automated design of computer systems. The project develops a system which will accept functional statements of requirements from the designer (utilizing a user friendly dialogue); translate those requirements into software and hardware primitives; evaluate those primitives and develop a proposed system using a Library of Realization Volumes. The CSDE will also verify that timing requirements have been met by the proposed hardware and software; and present the system design to the designer (in a user friendly format). The CSDE will be a prototype based on an existing feasibility demonstration version which has verified the concept. The prototype version will explore issues of adaptability, user friendliness and design system performance. This paper is a plan for the development of the CSDE. Author (GRA)

N84-12748# Oak Ridge National Lab., Tenn.
COMMENTS ON ISO/TC 97/SC 18/WG3 N120
James David Mason 1983 3 p Presented at the Assoc. Franc. de Normalisation (AFNOR) Meeting, Paris, 12 Apr. 1983
(Contract W-7405-eng-26)
(DE83-011391; CONF-830492-1) Avail: NTIS HC A02/MF A01

The structure of documents that office systems must deal with is considered in comments on a draft international standard for computer languages for processing text. DOE

N84-12749# California Univ., Berkeley. Engineering and Technical Services Div.
ENVIRONMENTS AND SEARCH PATHS FOR THE SOFTWARE TOOLS
T. Breckon Aug. 1983 7 p refs Presented at the USENIX/ Software Tools Joint Conf., Toronto, 11-15 Jul. 1983
(Contract DE-AC03-76SF-00098)
(DE83-016607; LBL-16445; CONF-830792-1) Avail: NTIS HC A02/MF A01

In order to maximize on the efficiency and minimize on the cost of environments, the following criteria was followed in developing a model for the Software Tools: (1) Keep the set of environment routines to a minimum. Try to avoid changes to existing software; (2) use existing Tools software whenever possible; (3) design a model that can be portably implemented, but don't restrict the design to a single implementation. Using the above design criteria, the environment model described in this paper is based on the concept of a symbol table. In other words, an environment is simply a set of names (or symbols) and their values. This concept allows environments to be portably implemented using existing symbol table routines. The model consists of a very small set of routines because it is based on such a simple concept. This concept is general enough to not restrict environments to a single implementation. DOE

N84-12750# California Univ., Livermore. Lawrence Livermore Lab.
PRAXIS LANGUAGE ENVIRONMENT: DISTRIBUTION-PACKAGE DESCRIPTION
James M. Duffy and Anthony J. DeGroot 5 Aug. 1983 27 p
(Contract W-7405-eng-48)
(DE83-017546; UCID-30196) Avail: NTIS HC A03/MF A01

This document describes the organization, generation, distribution and archival of the complete Praxis Language System. Included are three compilers and support packages, as well as, the sources to generate these images. Most users want and will only need the binaries and synopses files and need not worry about the source files, and generating a compiler from scratch. DOE

N84-12751# Stanford Univ., Calif. Systems Optimization Lab.
USER'S GUIDE FOR SOL/NPSOL: A FORTRAN PACKAGE FOR NONLINEAR PROGRAMMING
Philip E. Gill, Walter Murray, Michael A. Saunders, and Margaret H. Wright Jul. 1983 42 p refs
(Contracts DE-AT03-76ER-72018; DE-AM03-76SF-00326; N00014-75-C-0267; DAAG29-81-K-156; Grants NSF MCS-79-26009; NSF ECS-80-12974)
(DE83-016903; SOL-83-12) Avail: NTIS HC A03/MF A01

The user's guide is provided for Version 1.1 of SOL/NPSOL, a set of FORTRAN subroutines designed to minimize an abritary smooth function subject to constraints, which may include simple bounds on the variables, linear constraints and smooth nonlinear constraints. (NPSOL may also be used for unconstrained, bound-constrained and linearly constrained optimization.) The user must provide subroutines that define the objective and constraint functions and their gradients. All matrices are treated as dense, and hence NPSOL is not intended for large sparse problems. The NPSOL program uses a sequential quadratic programming (SQP) algorithm, in which the search direction is the solution of a quadratic programming (QP) subproblems. The algorithm treats bounds, linear constraints and nonlinear constraints separately. The Hessian of each QP subproblem is a positive-definite quasi-Newton approximation to the Hessian of an augmented Lagrangian function. The steplength at each iteration is required to produce a sufficient decrease in an augmented Lagrangian merit function. Each QP subproblem is solved using a quadratic programming package with several features that improve the efficiency of an SQP algorithm. DOE

N84-12752# Stanford Univ., Calif. Systems Optimization Lab.
USER'S GUIDE FOR SOL/QPSOL: A FORTRAN PACKAGE FOR QUADRATIC PROGRAMMING
Philip E. Gill, Walter Murray, Michael A. Saunders, and Margaret H. Wright Jul. 1983 41 p refs
(Contracts DE-AT03-76ER-72018; DE-AC03-76SF-00326; DAAG29-79-C-0110; N00014-75-C-0267; Grants NSF MS-79-26009; NSF ECS-80-12974)
(DE83-016990; SOL-83-7) Avail: NTIS HC A03/MF A01

The user's guide is provided for Version 3.1 of SOL/QPSOL, a set of FORTRAN subroutines designed to locate the minimum value of an arbitrary quadratic function subject to linear constraints and simple upper and lower bounds. If the quadratic function is convex, a global minimum is found; otherwise, a local minimum is found. The method used is most efficient when many constraints or bounds are active at the solution. The QPSOL treats the Hessian and general constraints as dense matrices, and hence is not intended for large sparse problems. DOE

N84-12753# Sandia Labs., Albuquerque, N. Mex.
DRAMIN: TRANSFERRING DATA FROM THE APPLICON GRAPHIC SYSTEM TO A DRAM INPUT FILE USER GUIDE
W. Brien Bopp and Paul A. Erickson 29 Jun. 1983 16 p refs
(Contract DE-AC04-76DP-00789)
(DE83-018235; SAND-83-1265) Avail: NTIS HC A02/MF A01

The procedure for linking a CAD graphics file to a mechanism program through a software translator is defined. Included are instructions for appending data to an Applicon AGS 880 graphics file which can be processed through DRAMIN to produce an output file suitable for engineering analysis using DRAM. DOE

N84-12754# Brookhaven National Lab., Upton, N. Y.
HIGH-LEVEL CONTROL PROGRAMS AT NSLS
Eva S. Bozoki 1983 5 p refs Presented at the EPS Conf. on Computing in Accelerator Design and Operation, Berlin, 20-23 Sep. 1983
(Contract DE-AC02-76CH-00016)
(DE83-010935; BNL-33652; CONF-8309144-1) Avail: NTIS HC A02/MF A01

The mathematical model of an accelerator can be used to control its operation and also to simulate its behavior. Through the use of such modeling programs it is possible to control a few important machine parameters rather than the many individual magnets. Such programs have been implemented for the current generation of accelerators. At the NSLS, two control program systems have been developed; TRANCO for the transport lines and RING for the accelerator/storage rings. These systems are modular, can be used independently or in conjunction with each other, can communicate with each other via sequential and random access data files and has a common data base. DOE

N84-12755# Oak Ridge National Lab., Tenn.
USING PAFEC AS A PREPROCESSOR FOR COSMIC/ NASTRAN
W. H. Gray and T. V. Baudry (PAFEC Engineering Consultants, Knoxville, Tenn.) 1983 12 p refs Presented at the 11th NASTRAN User's Colloq., San Francisco, 2 May 1983
(Contract W-7405-eng-26)
(DE83-017179; CONF-8305128-1) Avail: NTIS HC A02/MF A01

A software interface that permits PAFEC to be used as a preprocessor for COSMIC/NASTRAN is described. This user-friendly software, called PAFCOS, frees the stress analyst from the laborious and error prone procedure of creating and debugging a finite-element model with PAFEC, thus taking full advantage of the free-format engineering-keyword-oriented data structure of PAFEC, the amount of time spent during model generation can be drastically reduced. The PAFCOS software will automatically convert a PAFEC data structure into a SOSMIC/NASTRAN bulk data deck. The capabilities and limitations of the PAFCOS software are fully discussed. DOE

N84-12756# Deutsche Forschungs- und Versuchsanstalt fuer Luft- und Raumfahrt, Oberpfaffenhofen (West Germany). Abt. Regelung.
MONTE CARLO COMPUTER SIMULATION PROGRAM (MCHP) SUPPORTING A COVARIANCE ANALYSIS USING THE STANHP PROGRAM

Rainer Froriep Mar. 1983 49 p refs In GERMAN; ENGLISH summary
(DFVLR-Mitt-83-06) Avail: NTIS HC A03/MF A01; DFVLR, Cologne DM 17,50

A Monte Carlo simulation FORTRAN program MCHP is described. Nonlinear stochastically disturbed missile guidance loops can be investigated using covariance analysis with the STANHP program. A comparative Monte Carlo simulation is performed in order to investigate whether STANHP achieves a shorter computation time compared to a Monte Carlo simulation of whether the linearization assumptions are valid. The application of MCHP is demonstrated step by step. Author (ESA)

N84-12757# National Weather Service, Kansas City, Mo.
ASSEMBLY LANGUAGE GRAPHICS LIBRARY (EGR1.LB) WITH FORTRAN INTERFACING
Thomas J. Egger Jul. 1983 96 p
(PB83-239624; NOAA-NWS-CRCP-9; NOAA-83072601) Avail: NTIS HC A05/MF A01 CSCL 09B

The Assembly Language Graphics Library, EGR1.LB, is a series of subroutines that enables the programmer to generate graphic products using assembly language or FORTRAN. The library was designed to: (1) have faster routines than existing routines; (2) lessen core requirements; and (3) reduce disk space requirements. GRA

N84-12758# Federal Compiler Testing Center, Falls Church, Va. Federal Software Testing Center.
NORTHERN TELECOM, INCORPORATED NTI-585 ACOBOL/3 RELEASE 3 (COBOL TECHNICAL REPORT)
6 May 1983 13 p
(PB83-241521; OSD/FSTC-83/186) Avail: NTIS HC A02/MF A01 CSCL 09B

This FSTC Technical Report for the Northern Telecom, Inc., ACOBOL/3 Release 3 running under the OMNITASK 4.1 Release A10 provides a consolidated summary of the results obtained from the evaluation of the subject compiler against the Indexed I-O, Level 1 of the 1974 COBOL Standard (X3.23-1974/FIPS PUB 21-1). This technical report is made up of several sections showing all the discrepancies found - if any. A companion report Validation Summary Report OSD/FSTC-83/185 provides information regarding the validation of the compiler as the Low-Intermediate level of Federal Standard COBOL (FIPS PUB 21-1). GRA

N84-12759# Federal Compiler Testing Center, Falls Church, Va. Federal Software Testing Center.
NORTHERN TELECOM INCORPORATED NTI-585 XCOBOL, RELEASE 3 Validation Summary Report
6 May 1983 60 p
(PB83-241539; OSD/FSTC-83/187) Avail: NTIS HC A04/MF A01 CSCL 09B

This Validation Summary Report (VSR) for the Northern Telecom, Inc., IBM 3033 MVS Release 5 running under the NTI-585, OMNITASK 4.1 Release A10 provides a consolidated summary of the results obtained from the validation of the subject compiler aginst The 1974 COBOL Standard (X3.23-1974/FIPS PUB 21-1). The compiler was validated against the Low-Intermediate level of FIPS PUB 21.1. The VSR is made up of several sections showing all the discrepancies found - if any. These include an overview of the validation which lists all categories of discrepancies by level/module within X3.23-1974, a section relating the categories of discrepancies to each of the Federal Levels of the language, and a detailed listing of discrepancies together with the test which failed. GRA

N84-12760# Federal Compiler Testing Center, Falls Church, Va. Federal Software Testing Center.
NORTHERN TELECOM, INCORPORATED NTI-585 XCOBOL, RELEASE 3 (COBOL TECHNICAL REPORT)
6 May 1983 13 p
(PB83-241547; OSD/FSTC-83/188) Avail: NTIS HC A02/MF A01 CSCL 09B

This FSTC Technical Report for the Northern Telecom, Inc., IBM 3033 MVS Release 5 running under the NTI - 585, OMNITASK 4.1 Release A10 provides a consolidated summary of the results obtained from the evaluation of the subject compiler against the Indexed I-0, Level 1 of the 1974 COBOL Standard (X3.23-1974/FIPS PUB 21-1). This technical report is made up of several sections showing all the discrepancies found - if any. A companion report Validation Summary Report OSD/FSTC-83/185 provides information regarding the validation of the compiler as the Low-Intermediate level of Federal Standard COBOL (FIPS PUB 21-1). GRA

N84-12761# Federal Compiler Testing Center, Falls Church, Va. Federal Software Testing Center.
DIGITAL EQUIPMENT CORPORATION VAX 11/750, VAL-11 COBOL VERSION 2.2 Validation Summary Report
10 May 1983 58 p
(PB83-241588; OSD/FSTC-83/200) Avail: NTIS HC A04/MF A01 CSCL 09B

This Validation Summary Report (VSR) for the Digital Equipment Corp., VAX-11 COBOL Version 2.2 running under the VAX/VMS Version 3.2 provides a consolidated summary of the results obtained from the validation of the subject compiler against the 1974 COBOL Standard (X3.23-1974/FIPS PUB 21-1). The compiler was validated against the Low-Intermediate level of FIPS PUB 21-1. The VSR is made up of several sections showing all the discrepancies found - if any. These include an overview of the validation which lists all categories of discrepancies by level/module within X3.23-1974, a section relating the categories of discrepancies to each of the Federal Levels of the language, and a detailed listing of discrepancies together with the tests which failed. GRA

N84-12762# Federal Compiler Testing Center, Falls Church, Va. Federal Software Testing Center.
NCR CORPORATION NCR 9300 ITX-BASIC RELEASE 1.1
18 May 1983 15 p
(PB83-243410; OSD/FSTC-83/176) Avail: NTIS HC A02/MF A01 CSCL 09B

This Validation Summary Report (VSR) for the NCR Corporation, NCR ITX-BASIC, Release 1.1 running under the NCR ITX Release 1.0 provides a consolidated summary of the results obtained from the validation of the subject compiler against the 1978 BASIC Standard (X3.60-1978/FIPS PUB 68). The compiler was validated against the Minimal BASIC level of FIPS PUB 68. The VSR is made up of several sections showing all the discrepancies found - if any. These include an overview of the validation which lists all categories of discrepancies within X3.60-1978 and a detailed listing of discrepancies together with the tests which failed. GRA

N84-12763# Federal Compiler Testing Center, Falls Church, Va. Federal Software Testing Center.
COMPUTER SCIENCES CORPORATION UNIVAC 1100/80 CSTS FORTRAN, RELEASE FTN148
25 Apr. 1983 13 p
(PB83-243428; OSD/FSTC-83/180) Avail: NTIS HC A02/MF A01 CSCL 09B

This Validation Summary Report (VSR) for the Computer Sciences Corporation, CSTS FORTRAN Release FTN148 running under the CSTS II Release 2 provides a consolidated summary of the results obtained from the validation of the subject compiler against the 1978 FORTRAN Standard (X3.9-1978/FIPS PUB 69). The compiler was validated against the April 25, 1983 level of FIPS PUB 69. The VSR is made up of several sections showing all the discrepancies found - if any. These include an overview of the validation which lists all categories of discrepancies within X3.9-9-1978, and a detailed listing of discrepancies together with the tests which failed. GRA

N84-12764# Federal Compiler Testing Center, Falls Church, Va. Federal Software Testing Center.
DIGITAL EQUIPMENT CORPORATION, PDP-11/44 COBOL-81 VERSION 2.0

10 May 1983 51 p
(PB83-247734; OSD/FSTC-83/202) Avail: NTIS HC A04/MF A01 CSCL 09B

This Validation Summary Report (VSR) for the Digital Equipment Corp., COBOL-81 Version 2.0 runnning under the RSTS/E Version 8.0 provides a consolidated summary of the results obtained from the validation of the subject compiler against the 1974 COBOL Standard (X3.23-1974/FIPS PUB 21-1). The compiler was validated against the Low-Intermediate level of FIPS PUB 21-1. The VSR is made up of several sections showing all the discrepancies found - if any. These include an overview of the validation which lists all categories of discrepancies by level/module within X3.23-1974, a section relating the categories of discrepancies to each of the Federal Levels of the language, and a detailed listing of discrepancies together with the tests which failed. GRA

N84-12765# Federal Compiler Testing Center, Falls Church, Va. Federal Software Testing Center.
DIGITAL EQUIPMENT CORPORATION COBOL-81 VERSION 2.0 (COBOL TECHNICAL REPORT)
10 May 1983 20 p
(PB83-247742; OSD/FSTC-83/203) Avail: NTIS HC A02/MF A01 CSCL 09B

This FSTC Technical Report for the Digital Equipment Corp., COBOL-81 Version 2.0 running under the RSTS/E Version 8.0 provides a consolidated summary of the results obtained from the evaluation of the subject compiler against the Indexed I-0, Levels 1 and 2 Sort/Merge, Levels 1 and 2 Relative I-=0, Level 2 of the 1974 COBOL Standard (X3.23-1974/FIPS PUB 21-1). This technical report is made up of several sections showing all the discrepancies found - if any. A companion report Validation Summary Report OSD/FSTC-81/202 provides information regarding the validation of the compiler as the Low-Intermediate level of Federal Standard COBOL (FIPS PUB 21-1). GRA

N84-12766# Office of Software Development, Falls Church, Va. Federal Software Testing Center.
PERKIN-ELMER, PERKIN-ELMER 3230 COBOL R07 (PRE-RELEASE) Validation Summary Report
7 Jun. 1983 52 p refs
(PB83-238600; OSD/FSTC-83/205) Avail: NTIS HC A04/MF A01 CSCL 09B

This Validation Summary Report (VSR) for the Perkin-Elmer, COBOL R07 (Pre-Release) running under the OS/32 Release RO6-01 provides a consolidated summary of the results obtained from the validation of the subject compiler against the 1974 COBOL Standard (X3.23-1974/FIPS PUB 21-1). The compiler was validated against the Low-Intermediate level of FIPS PUB 21-1. The VSR is made up of several sections showing all the discrepancies found - if any. These include an overview of the validation which lists all categories of discrepancies by level/module within X3.23-1974, a section relating the categories of discrepancies to each of the Federal Levels of the language, and a detailed listing of discrepancies together with the tests which failed. GRA

62 COMPUTER SYSTEMS

Includes computer networks.

N84-12767# Rockwell International Corp., Golden, Colo. Energy Systems Group.
DEVELOPMENT OF A UNIQUE PHYSICAL METROLOGY LABORATORY RECALL SYSTEM
Cynthia Y. Cannon, M. J. Chambers, ed., and G. Shekell 1 Aug. 1983 51 p
(Contract DE-AC04-76DP-03533)
(DE83-017415; RFP-3500) Avail: NTIS HC A04/MF A01

The Rocky Flats Standards Laboratory is required to maintain a calibration recall program. The Standards Laboratory has three distinct and separate recall systems. Each of these recall systems currently has new needs and requirements that cannot be provided by the present system in a reasonable length of time or at a reasonable cost. The Physical Metrology Laboratory (PML) of the Rocky Flats Standards Laboratory was the first of the three recall programs to be changed. This new PML recall incorporates a data base management concept which is a departure from the old PML recall on the Rocky Flats mainframe computer system. This new in-house system organizes the data in a manner that provides the current recall information as-well-as statistical and trend information and is designed with enough flexibility to encompass future needs and requirements. This report discusses the new PML recall which utilizes the HP System 45 Data Base Management program. DOE

63 CYBERNETICS

Includes feedback and control theory.

For related information see also *54 Man/System Technology and Life Support.*

N84-12768# Naval Ship Research and Development Center, Bethesda, Md. Computation Mathematics/Logistics Dept.
ROBOTICS: AN INTRODUCTION TO TODAY'S ROBOT AND FUTURE TRENDS Final Report
Kevin R. Scully Jul. 1983 41 p
(AD-A132070; DTNSRDC/CMLD-83-20) Avail: NTIS HC A03/MF A01 CSCL 06/4

A robot consists basically of three components: the power supply, the mechanical unit, and the controller a microprocessor or minicomputer. The complexity of the control center determines the capabilities of the robot, which vary from material handling, painting, welding, and nondestructive testing, to identifying a given object in a random collection of objects and assembling it with other parts into a complex device. As features such as vision, tactile sensing, mobility, and CAD/CAM move from the research laboratory to the factory floor, robot capabilities will become virtually unlimited. There are three programming techniques available with today's robot: (1) manual lead through programming; (2) teach pendant programming; and (3) textual language programming. Textual language programming may be done off-line, whereas the other two programming methods are done on-line. GRA

N84-12769# Massachusetts Inst. of Tech., Cambridge. Artificial Intelligence Lab.
USING STRUCTURAL AND FUNCTIONAL INFORMATION IN DIAGNOSTIC DESIGN
Walter Hamscher Jun. 1983 70 p
(Contract N00014-80-C-0505)
(AD-A131859; AI-TR-707) Avail: NTIS HC A04/MF A01 CSCL 09/2

We wish to design a diagnostic for a device from knowledge of its structure and function. The diagnostic should achieve both coverage of the faults that can occur in the device, and should strive to achieve specificity in its diagnosis when it detects a fault. A system is described that uses a simple model of hardware structure and function, representing the device in terms of its intenral primitive functions and connections. The system designs a diagnostic in three steps. First, an extension of path sensitization is used to design a test for each of the connections in the device. Next, the resulting tests are improved by increasing their specificity. Finally the tests are ordered so that each relies on the fewest possible connections. We describe an implementation of this system and show examples of the results for some simple devices. GRA

N84-12770# Stanford Univ., Calif. Dept. of Computer Science.
ARTIFICIAL INTELLIGENCE: COGNITION AS COMPUTATION
Avron Barr Aug. 1982 32 p
(Contract N00014-79-C-0302)
(AD-A131804; SU-STAN-CS-82-956; SU-STAN-HPP-82-20) Avail: NTIS HC A03/MF A01 CSCL 09/2

The ability and compulsion to know are as characteristic of our human nature as are our physical posture and our languages. Knowledge and intelligence, as scientific concepts, are used to describe how an organism's experience appears to mediate its behavior. This report discusses the relation between artificial intelligence (AI) research in computer science and the approaches of other disciplines that study the nature of intelligence, cognition, and mind. The state of AI after 25 years of work in the field is reviewed, as are the views of its practitioners about its relation to cognate disciplines. The report concludes with a discussion of some possible effects on our scientific work of emerging commercial applications of AI technology, that is, machines that can know and can take part in human cognitive activities. GRA

N84-12771# Delaware Univ., Newark. Dept. of Computer and Information Sciences.
PREREQUISITES FOR DERIVING FORMAL SPECIFICATIONS FROM NATURAL LANGUAGE REQUIREMENTS Final Report, 1 Sep. 1981 - 28 Feb. 1983
Ralph M. Weischedel Apr. 1983 13 p
(Contract F49620-79-C-0131; Grant AF-AFOSR-0190-80; AF Proj. 2304)
(AD-A131722; AFOSR-83-0687TR) Avail: NTIS HC A02/MF A01 CSCL 09/2

Since English specifications and formal specifications of modules are complementary and since formal specifications require so much effort to write, our work has investigated application of artificial intelligence techniques to aid in the software specification process. The effort for this year concentrated on constructing a small prototype of a system that transforms English descriptions to formal specifications under significant user assistance. GRA

N84-12772# Massachusetts Inst. of Tech., Cambridge. Artificial Intelligence Lab.
REPRESENTATIONS FOR REASONING ABOUT CHANGE
Reid G. Simmons and Randall Davis Apr. 1983 55 p
(Contract N00014-80-C-0505)
(AD-A131649; AI-Memo-702) Avail: NTIS HC A04/MF A01 CSCL 06/4

This paper explores representations used to reason about objects which change over time, and the processes which cause changes. Specifically, we are interested in solving a problem known as geologic interpretation. To help solve this problem, we have developed a simulation technique, which we call imaging. Imaging takes a sequence of events and simulates them by drawing diagrams. In order to do this imaging, we have developed two representations of objects, one involving histories and the other involving diagrams, and two corresponding representations of physical processes, each suited to reasoning about one of the object representations. These representations facilitate both spatial and temporal reasoning. Author (GRA)

N84-12773# Stanford Univ., Calif. Center for Research on Organizational Efficiency.
SEARCH AMONG QUEUES
Amihai Glazer and Rafael Hassin Jun. 1983 22 p
(Contract N00014-79-C-0685)
(AD-A131639; SU-TR-406) Avail: NTIS HC A02/MF A01 CSCL 12/1

Customers must often wait to obtain some service or goods, the wait usually being longer the greater the total number of persons who have yet to be served. This phenomenon is especially common in transportation markets, such as the trucking, household moving, and bus industries. Nor is it unknown for customers to have to wait for the services of accountants, lawyers, dentists, physicians, and, most importantly, plumbers. When for some reason shortages occur, rationing is often accomplished by queuing; new models of automobiles and computers have lately been subject to such shortages. Recent research has shown that explanations of market behavior should incorporate customer's aversion to such waiting. The fundamental idea is that a customer who arrives at some facility and finds a long queue may find it worthwhile to balk, incur some search cost, and find a shorter queue at some other facility. This in turn means that excess capacity may result not from oligopoly of inefficiencies, but from a socially beneficial effort to reduce consumers' waiting costs. GRA

N84-12774# Argonne National Lab., Idaho Falls, Idaho. Mathematics and Computer Science Div.
AUTOMATED REASONING IN MAN-MACHINE CONTROL SYSTEMS
Rex C. Stratton and Ewing L. Lusk 1983 16 p refs Presented at the Am. Nucl. Soc. Winter Meeting, San Francisco, 30 Oct. - 3 Nov. 1983
(Contract W-31-109-eng-38)
(DE83-014307; CONF-831047-7) Avail: NTIS HC A02/MF A01

A project being undertaken at Argonne National Laboratory to demonstrate the usefulness of automated reasoning techniques in the implementation of a man-machine control system being designed at the EBR-2 nuclear power plant is described. It is shown how automated reasoning influences the choice of optimal roles for both man and machine in the system control process, both for normal and off-normal operation. In addition, the requirements imposed by such a system for a rigorously formal specification of operating states, subsystem states, and transition procedures have a useful impact on the analysis phase. The definitions and rules are discussed for a prototype system which is physically simple yet illustrates some of the complexities inherent in real systems. DOE

64 NUMERICAL ANALYSIS

Includes iteration, difference equations, and numerical approximation.

N84-12775 California Univ., Berkeley.
SECOND ORDER PARTIAL DIFFERENTIAL EQUATIONS OF MIXED TYPE Ph.D. Thesis
Massoud Agahi 1982 197 p
Avail: Univ. Microfilms Order No. DA8312738

The study of equations of mixed type originated in the pioneering work of tricomi. The existence and uniqueness of a boundary value problem - known as the tricomi problem - was established for the equation yu(subxy) + u(subyx) = 0. Interesh in equations of mixed type rose sharply when Frankl' showed that the equation models transonic flow. Dissert. Abstr.

N84-12776 Max-Planck-Institut fuer Plasmaphysik, Garching (West Germany).
CRANK-NICHOLSON DIFFERENCE SCHEMES FOR SOLVING COUPLED SYSTEMS OF NONLINEAR DIFFUSION EQUATIONS
K. vonFinckenstein (Technische Hochschule, Darmstadt, West Germany), D. Duechs, and O. DeBarbieri Apr. 1983 21 p refs Sponsored by Euratom
(IPP-6/223) Copyright. Avail: Issuing Activity

It is shown how the set of nonlinear equations resulting from a Crank-Nicholson discretization of a system of nonlinear diffusion equations can be solved by Newton's iterative method. It is proved that the first step of this method only requires solving a linearized (Crank-Nicholson) form of the diffusion equations, and that, under rather mild conditions, the matrices involved at each iteration are not singular. Author (ESA)

N84-12777*# National Aeronautics and Space Administration. Langley Research Center, Hampton, Va.
DESIGN, DEVELOPMENT AND USE OF THE FINITE ELEMENT MACHINE Final Report
Loyce M. Adams and Robert C. Voigt Oct. 1983 19 p refs
(Contracts NAS1-17070; NAS1-17130)
(NASA-CR-172250; ICASE-83-56; NAS 1.26:172250) Avail: NTIS HC A03/MF A01 CSCL 12A

Some of the considerations that went into the design of the Finite Element Machine, a research asynchronous parallel computer are described. The present status of the system is also discussed

along with some indication of the type of results that were obtained. M.G.

N84-12778*# Technische Hogeschool, Delft (Netherlands).
MULTIDIMENSIONAL EXPLICIT DIFFERENCE SCHEMES FOR HYPERBOLIC CONSERVATION LAWS Final Report
Bram vanLeer Nov. 1983 8 p refs
(Contract NAS1-15810)
(NASA-CR-172254; ICASE-83-61; NAS 1.26:172254) Avail: NTIS HC A02/MF A01 CSCL 12A

First and second order explicit difference schemes are derived for a three dimensional hyperbolic system of conservation laws, without recourse to dimensional factorization. All schemes are upwind (backward) biased and optimally stable. GRA

N84-12779# Loughborough Univ. of Technology (England). Dept. of Transport Technology.
A THIN-WALLED BEAM FINITE ELEMENT
A. M. S. Al-Sheikh and P. W. Sharman Apr. 1983 30 p refs
(TT-8302) Avail: NTIS HC A03/MF A01

A stiffness matrix for a thin walled open section beam is presented, using the Euler-Bernoulli assumptions of plane sections remaning plane and Vlasov's assumption of a non-deforming cross section. The torsion warping theory is presented in detail and the use of an arbitrary reference axis enables the element to be utilized in a general structural analysis program. Some examples are analyzed by continuum and finite element theory to support the work. M.G.

N84-12780# Aeronautical Research Labs., Melbourne (Australia).
MAXIMUM LIKELIHOOD ESTIMATION OF LINEAR DYNAMIC SYSTEM PARAMETERS
T. G. Ryall Jan. 1983 17 p refs
(AR-002-934; ARL-Struc-395) Avail: NTIS HC A02/MF A01

The maximum likelihood method is used to estimate dynamic system parameters when a linear system is excited by random or deterministic inputs. Author

N84-12781# Tata Inst. of Fundamental Research, Bombay (India).
ON WARING'S PROBLEM g (4) < OR = 20
R. Balasubramanian [1979] 32 p refs
Avail: NTIS HC A03/MF A01

A refinement to the proof that every integer is a sum of at most 21 biguadrates, namely, that every positive integer is a sum of not move than twenty biguadrates is attempted. N.W.

N84-12782# North Carolina Univ., Chapel Hill. Center for Stochastic Processes.
WEAK AND STRONG LAW RESULTS FOR A FUNCTION OF THE SPACINGS
William P. McCormick May 1983 16 p refs
(Contract F49620-82-C-0009; Grant NSF MCS-82-02259)
(AD-A130705; AFOSR-83-0627TR; TR-30) Avail: NTIS HC A02/MF A01 CSCL 12/1

Let [U sub n > or = 1] be i.i.d. uniform on (0.1) random variables and define S sub i, n = U sub i, n-1 - U sub i-1, u-1, i=1..., n where the U i, n-1 are the order statistics from a sample of size u-1 and U sub 0, n-1 = 0 and U sub n, n-1 = 1. The S sub i, n are called the spacings divided by U sub 1, ..., U sub n-1. For a fixed integer l, set M sub l, n=max (1 < or = i < or = n - l) max(i < or = j < or = i + l) S sub j,n. Exact and weak limit results are obtained for the M sub l,n. N.W.

N84-12783# Arnold Engineering Development Center, Arnold Air Force Station, Tenn.
NUMERICAL SOLUTION OF THE THREE-DIMENSIONAL UNSTEADY EULER EQUATIONS Final Report, 1 Jan. 1982 - 31 Dec. 1982
K. Koenig and J. M. Barton Aug. 1983 43 p
(AD-A132034; AEDC-TR-83-22) Avail: NTIS HC A03/MF A01 CSCL 12/1

A user's guide is presented for the three-dimensional, time-dependent Euler code, ARO-1. The guide provides a brief theoretical background for the explicit MacCormack algorithm and its application to the Euler equations. The main routines of the program are described and the calling order examined for a sample computational step. The primary code variables are defined, along with the nondimensionalization employed. Specification of the initial and boundary conditions is discussed from a theoretical and practical perspective. The required input data are presented for a sample case. This report serves two purposes: to introduce the principles of computational fluid dynamics to engineers and scientists unfamiliar with this subject and to provide detailed instructions on the use of this particular computer solution of the Euler equations. GRA

N84-12784# Carnegie-Mellon Univ., Pittsburgh, Pa. Management Sciences Research Group.
DISJUNCTIVE PROGRAMMING AND A HIERARCHY OF RELAXATIONS FOR DISCRETE OPTIMIZATION PROBLEMS
Egon Balas Jun. 1983 43 p
(Contract N00014-82-K-0329; NR Proj. 047-607)
(AD-A132004; MSRR-492; WP-69-82-83) Avail: NTIS HC A03/MF A01 CSCL 12/1

The author discusses a new conceptual framework for the convexification of discrete optimization problems, and a general technique for obtaining approximations to the convex hull of the feasible set. The concepts come from disjunctive programming and the key tool is a description of the convex hull of a union of polyhedra in terms of a higher dimensional polyhedron. Although this description was known for several years, only recently was it shown by Jeroslow and Lowe to yield improved representations of discrete optimization problem as the intersection (conjunction) of unions of polyhedra, and define an operation that takes one such expression into another, equivalent one, with fewer conjuncts. Then introduced is a class of relaxations based on replacing each conjunct (union of polyhdera) by its convex hull. The strength of the relaxation increases as the number of conjuncts decreases, and the class of relaxations forms a hierarchy that spans the spectrum between the common linear programming relaxation, and the convex hull of the feasible set itself. Instances where this approach presents advantages include critical path problems in disjunctive graphs, network synthesis problems, certain fixed charge network flow problems, etc. The author illustrates the approach on the first of these problems, which is a model for machine sequencing. Author (GRA)

N84-12785# Analytic Sciences Corp., Reading, Mass.
THE EFFECT OF COORDINATE SYSTEM ROTATION ON SPHERICAL HARMONIC EXPANSIONS: A NUMERICAL METHOD
Jacob D. Goldstein 1 Apr. 1983 31 p
(Contract F19628-83-C-0053; AF Proj. 3201)
(AD-A131974; AFGL-TR-83-0008; SR-1) Avail: NTIS HC A03/MF A01 CSCL 08/5

A numerical method is presented for effecting the transformation of a spherical harmonic expansion under an arbitrary rotation of the coordinate system. Included are results of numerical tests with expansions to degree and order 180. These results demonstrate the high accuracy of the algorithm. Author (GRA)

N84-12786# Princeton Univ., N. J. Dept. of Civil Engineering.
ON DIFFERENTIAL EQUATIONS OF NONLOCAL ELASTICITY AND SOLUTIONS OF SCREW DISLOCATION AND SURFACE WAVES
A. Cemal Eringen Aug. 1983 43 p
(Contract N00014-76-C-0240; NR Proj. 064-410)
(AD-A131911; RR-83-SM-10; TR-58) Avail: NTIS HC A03/MF A01 CSCL 12/1

Integro-partial differential equations of the liner theory of nonlocal elasticity are reduced to singular partial differential equations for a special class of physically admissible kernels. Solutions are obtained for the screw dislocation and surface waves. Experimental observations and atomic lattice dynamics appear to support the theoretical results very nicely. Author (GRA)

N84-12787# Pittsburgh Univ., Pa. Center for Multivariate Analysis.
LIMIT THEOREMS FOR THE EIGENVALUES OF PRODUCT OF TWO RANDOM MATRICES
Y. Q. Yin and P. R. Krishnaiah Dec. 1982 29 p
(Contract F49620-82-K-0001)
(AD-A131682; TR-82-39; AFOSR-83-0697TR) Avail: NTIS HC A03/MF A01 CSCL 12/1

In this paper, the authors showed that the spectral distributions of a sequence of the products of random matrices will tend to a distribution function in the limit as the number of variables tend to infinity. GRA

N84-12788# Argonne National Lab., Ill. Mathematics and Computer Science Div.
APPLIED MATHEMATICAL SCIENCES RESEARCH AT ARGONNE Progress Report, 1 Apr. 1982 - 31 Mar. 1983
Gail W. Pieper, ed. 1983 43 p
(Contract W-31-109-eng-38)
(DE83-3014268; ANL-83-31) Avail: NTIS HC A03/MF A01

Various projects carried out in three major areas of research (applied analysis, computational mathematics, and software engineering) are discussed. Information on section staff, visitors, workshops, and seminars is found in the appendices. DOE

N84-12789# California Univ., Livermore. Lawrence Livermore Lab.
LECTURE NOTES FOR CONTACT-IMPACT ALGORITHMS FOR LARGE-DEFORMATION FINITE-ELEMENT ANALYSIS
J. O. Hallquist 6 May 1983 36 p refs Presented at Struct. Dyn. Meeting, Ispra, Italy, 16 May 1983
(Contract W-7405-eng-48)
(DE83-013039; UCRL-89157; CONF-830582-4) Avail: NTIS HC A03/MF A01

Finite element codes with contact-impact capability are applicable to a class of structural problems where adjacent components may independently slide, separate, and impact along interfaces. Problems of this sort are common in the defense community for analyzing axisymmetric gun fired projectiles, laydown bombs, and a variety of shape charge designs of either the jet or fragment type. The nuclear industry has interest in analyzing the impact of shipping casks containing radioactive materials, pipe to pipe impact, as well as soil-structure interaction problems. Three dimensional algorithms are considered in this paper. Similar techniques are employed in two dimensions. Several example applications are shown. DOE

N84-12790# Michigan Univ., Ann Arbor. Dept. of Mathematics.
RELATIVE SYMMETRIES OF DIFFERENTIAL EQUATIONS
Boris A. Kupershmidt N. Mex. Los Alamos Scientific Lab. 1983 6 p refs Presented at the 2nd Intern. Conf. on Differential Equations, Birmingham, Ala., Mar. 1983
(Contract W-7405-eng-36)
(DE83-015231; LA-UR-83-2045; CONF-830378-1) Avail: NTIS HC A02/MF A01

Let delta:J(infinity)nu approaches J(infinity)pi be a differential operator where J(infinity)nu is the infinite-jet bundle of the bundle nu:F approaches M(resp. pi:E approaches M). Let I(1) sub nu be the Cartan submodule of the module lambda(1) (K sub nu) of 1-forms over the ring K sub nu = C(infinity)(J(infinity)nu). Among all derivations of K sub pi into K sub nu along delta*, those which map I(1)pi into I(1)nu are classified. They turn out to be quasi-evolution equations. M.G.

N84-12791# Fermi National Accelerator Lab., Batavia, Ill.
NEW SOLUBLE APPROXIMATION TO FOKKER-PLANCK EQUATIONS
Jonathan F. Schonfeld May 1983 9 p refs Presented at the 49th Semi-Ann. Statist. Mech. Meeting, New Brunswick, N.J., 12-13 May 1983
(Contract DE-AC02-76CH-03000)
(DE83-016210; FERMILAB-CONF-83/45-THY; CONF-8305125-1) Avail: NTIS HC A02/MF A01

The new results described, in the present one-dimensional context, constitute a necessary prerequisite for more realistic studies. The analysis described concerns the semiclassical approximation to the solution of the Fokker-Planck equation. DOE

N84-12792# Chalmers Univ. of Technology, Goteborg (Sweden). Dept. of Mathematics.
BRANCHING PROCESSES IN PERIODICALLY VARYING ENVIRONMENT
Peter Jagers and Olle Nerman 1983 27 p refs Submitted for publication
(CTH-Math-1983-12-Preprint; ISSN-0347-2809) Avail: NTIS HC A03/MF A01

In order to model the diurnal variation of cell populations, general one-type branching processes whose individuals reproduce in a manner that is influenced by time in a periodic fashion are studied. A Malthusian growth rate is established as well as a periodically varying asymptotic composition, for example over ages. Author (ESA)

N84-12793# Chalmers Univ. of Technology, Goteborg (Sweden). Dept. of Mathematics.
ON SPACE-TIME MEANS AND EVERYWHERE DEFINED SCATTERING OPERATORS FOR NONLINEAR KLEIN-GORDON EQUATIONS
Philip Brenner 1983 20 p refs Submitted for publication
(CTH-Math-1983-13-Preprint; ISSN-0347-2809) Avail: NTIS HC A02/MF A01

Space-time estimates for the linear Klein-Gordon equation are derived, and are applied together with previous results to prove similar estimates for the nonlinear Klein-Gordon equation. Applying an argument based on the small data case, these estimates, are used to prove the existence of everywhere defined scattering operators in the case of nonlinearities of the from f (u) = determinant of matrix u to the inverse of rho for $1 + 4/n <$ rho $<$ or $= 1 + 4/(n-1)$ for $n=3$ and 4, and with a slightly smaller upper bound, also for $m=5$ and 6. Author (ESA)

N84-12794# Fondazione Ugo Bordoni, Rome (Italy).
REDUCTION OF STRUCTURAL COMPLEXITY IN EVALUATING CONVOLUTIONS BY POLYNOMIAL TRANSFORMS
Giuseppe Hartinelli (Rome Univ.) Dec. 1981 9 p refs
(FUB-59-1981) Avail: NTIS HC A02/MF A01

A method for computing by polynomial transforms the polynomial products modulo z to the Mth power, M = Z to the t power, is proposed. The resulting procedure simplifies the structural complexity of the elaboration process of a two-dimensional convolution based on polynomial transforms. Author (ESA)

N84-12795# Sheffield Univ. (England). Dept. of Control Engineering.
ON SENSITIVITY, COMPENSATION AND THE APPROACH TO THE ASYMPTOTES IN MULTIVARIABLE ROOT-LOCI
D. H. Owens and G. S. Virk Oct. 1982 37 p refs
(Grant SRC-GR/B/79455)
(RR-222) Avail: NTIS HC A03/MF A01

Dynamic transformation techniques are used to characterize the rate of approach of multivariable root-loci to the asymptotes by calculation of the third term in the Puiseux series using the system Markov parameter matrices. The design of compensators to eliminate the sensitivity of the pivots to control data is suggested by maximizing the rate of approach to the asymptotes.
Author (ESA)

N84-12796 Maryland Univ., College Park.
PYRAMID METHODS IN IMAGE ANALYSIS Ph.D. Thesis
Tsai-Hong Hong 1982 215 p
Avail: Univ. Microfilms Order No. DA8308741

The properties of multi-resolution versions of images, and developing methods of solving problems in image analysis using multi-resolution data structures are investigated. Features of these structures are investigated, such as their ability to make global features become local, their potential for cooperation between

different resolutions, and the use of relations within levels. Several hierarchical data structures, such as grey-level linked, edge, surroundedness, multi-feature, line, and curve pyramids are introduced. The grey-level linked pyramid creates linked subtrees in a pyramid. Each subtree defines a region with more or less homogeneous properties. Two approaches are taken to make use of reduced-resolution versions of the image. The first is to use a parallel, iterative, forced choices approach to update link strengths between pairs of nodes at successive levels of the pyramid, based on similarity. The second approach does not require immediate forced choices. Link strengths is defined, based on proximity and similarity, and iteratively recomputes the pixel values and adjusts the link strengths. Dissert. Abstr.

N84-12797 Tennessee Univ., Knoxville.
RANK MODIFICATION METHOD FOR CERTAIN SINGULAR SYSTEMS OF LINEAR EQUATIONS Ph.D. Thesis
William Joseph Harrod 1982 185 p
Avail: Univ. Microfilms Order No. DA8313300

This dissertation is mainly concerned with a general purpose algorithm for computing a solution to the consistent system of linear equations Aw = f where A is a real matrix of order n, with rank n - 1, and f is a real n-dimensional vector. The algorithm, called the Rank Modification Method, is based upon the transformation of A into a nonsingular matrix by a rank one modification, followed by the solution of an associated nonsingular system of linear equations. The primary application is the computation of a solution w to the homogeneous system of linear equations Aw = O, where A is a singular irreducible M-matrix. This vector w is unique up to scalar multiples and it is important in many areas of the mathematical sciences, including queueing networks, input-output economic models, and in compartmental analysis tracer models. Dissert. Abstr.

N84-12564*# Texas A&M Univ., College Station. Center for Approximation Theory.
SPLINE CLASSIFICATION METHODS Final Report
L. F. Guseman, Jr. and L. L. Schumaker *In its* Proc. of the NASA Symp. on Math. Pattern Recognition and Image Analysis 1983 p 167-190 refs ERTS (For primary document see N84-12557 03-43)
Avail: NTIS HC A99/MF A01 CSCL 12A

N84-12566*# Texas A&M Univ., College Station.
DISCRIMINATION RELATIVE TO MEASURES OF NON-NORMALITY
W. B. Smith and E. P. Shine *In its* Proc. of the NASA Symp. on Math. Pattern Recognition and Image Analysis 1983 p 243-276 refs ERTS (For primary document see N84-12557 03-43)
Avail: NTIS HC A99/MF A01 CSCL 12A

65 STATISTICS AND PROBABILITY

Includes data sampling and smoothing; Monte Carlo method; and stochastic processes.

N84-12798# North Carolina Univ., Chapel Hill. Dept. of Statistics.
AN ITERATED LOGARITHM LAW RESULT FOR EXTREME VALUES FROM GAUSSIAN SEQUENCES
William P. McCormick Mar. 1983 19 p refs
(Contract F49620-82-C-0009; AF Proj. 2304)
(AD-A129559; TR-29; AFOSR-83-0510TR) Avail: NTIS HC A02/MF A01 CSCL 12/1

Let [X sub n, n > or = 1] be a stationary Gaussian sequence with EX sub 1 = 0, EX(2) sub 1 = 1, and r sub n = EX sub 1 X sub n+1. Let Z(i) sub n denote the ith maximum of X sub 1,...,X sub n and a sub n=(lnlnn) (2lnn) to the -1/2 power, b sub n = (2lnn) to the 1/2 power -(ln(4pi lnn))/(2(2lnn) to the 1/2 power). The set of almost sure limit points of the vectors ((Z(1) sub n b sub n) A(-1) sub n, (Z(2) sub n - b sub n)a(-1) sub n,...(Z(l) sub n - b sub n)a(-1) sub n) is determined. The number of components l=l(n) approaches infinity as n approaches infinity. M.G.

N84-12799# North Carolina Univ., Chapel Hill. Dept. of Statistics.
ASYMPTOTIC MAXIMAL DEVIATION OF m-SMOOTHERS
Wolfgang Haerdle Apr. 1983 21 p
(Contract F49620-82-C-0009; AF Proj. 2304)
(AD-A131906; MMS-1523; AFOSR-83-0688TR) Avail: NTIS HC A02/MF A01 CSCL 12/1

Probabilities of maximal deviation are computed in a similar way as in Bickel and Rosenblatt (1973) for density estimation and in Johnston (1982) for nonparametric regression function estimation. GRA

N84-12800# North Carolina Univ., Chapel Hill. Operations Research and Systems Analysis.
AN ALTERNATIVE TO THE MONTE CARLO ESTIMATION OF NETWORK RELIABILITY
George S. Fishman Aug. 1983 24 p
(Contract N00014-76-C-0302)
(AD-A131849; UNC/ORSA/TR-83/2) Avail: NTIS HC A02/MF A01 CSCL 12/1

This paper describes a numerical method based on quasi-random points for estimating the probability g(s,t) that vertices s and t are connected in an undirected network G=(V,M) with V perfect vertices and M randomly and independently failing edges. GRA

N84-12801# Stanford Univ., Calif. Dept. of Statistics.
KINGMAN'S SUBADDITIVE ERGODIC THEOREM
J. Michael Steele 3 Sep. 1982 11 p
(Contract N00014-76-C-0475)
(AD-A131795; SU-TR-324) Avail: NTIS HC A02/MF A01 CSCL 12/1

The objective of this note is to give a proof of Kingman's subadditive ergodic theorem which is perhaps simpler and more direct than those previously given. GRA

N84-12802# Oak Ridge National Lab., Tenn. Dept. of Computer Sciences.
WHY DIDN'T BOX-JENKINS WIN (AGAIN)?
David J. Pack and Darryl J. Downing 1983 28 p refs Presented at the 3rd Intern. Symp. on Forecasting, Philadelphia, 5 Jun. 1983
(Contract W-7405-eng-26)
(DE83-014043; CONF-830682-2) Avail: NTIS HC A03/MF A01

This paper focuses on the forecasting performance of the Box-Jenkins methodology applied to the 111 time series of the Makridakis competition. It considers the influence of the following factors: (1) time series length, (2) time series information (autocorrelation) content, (3) time series outliers or structural changes, (4) averaging results over time series, and (5) forecast time origin choice. It is found that the 111 time series contain substantial numbers of very short series, series with obvious structural change, and series whose histories are relatively uninformative. If these series are typical of those that one must face in practice, the real message of the competition is that univariate time series extrapolations will frequently fail regardless of the methodology employed to produce them. DOE

N84-12803# Pacific Northwest Lab., Richland, Wash.
TRAN-STAT (STATISTICS FOR ENVIRONMENTAL STUDIES). ISSUE NO. 24: FIELD SAMPLING DESIGNS, SIMPLE RANDOM AND STRATIFIED RANDOM SAMPLING
Richard O. Gilbert Aug. 1983 38 p refs
(Contract DE-AC06-76RL-01830)
(DE83-016826; PNL-SA-11551) Avail: NTIS HC A03/MF A01

Several methods are discussed by which sampling locations and times for environmental studies may be selected including haphazard, judgment, probability, and systematic methods. In practice, a given sampling plan may be a composite of several methods (excluding haphazard sampling which should always be avoided). The probability methods such as simple and stratified

random sampling have the nice statistical property of being statistically unbiased, but systematic sampling may give a more accurate estimate of means and totals. Judgment must be used in defining the target population of units to be sampled, and the patterns of variation over time and space that should be considered when designing the study. But biased estimates of parameters can result if an individual chooses subjectively the exact location and times a sample or measurement is taken. The allocation of samples to different regions or strata (in time or space) can be determined using formulas presented here if there is advance information available on costs of sampling and the variances for each strata. Some suggestions are made for how to treat less-than and negative data when computing means and variances. DOE

N84-12804# Pacific Northwest Lab., Richland, Wash.
WEIGHTED NONPARAMETRIC TAIL ESTIMATION PROCEDURES
D. B. Carr and H. D. Tolley Sep. 1983 47 p refs
(Contract DE-AC06-76RL-01830)
(DE83-017870; PNL-SA-11167) Avail: NTIS HC A03/MF A01

Procedures for univariate nonparametric estimation of tail probabilities are investigated. Extrapolated values for tail probabilities beyond the data are also obtained based on the shape of the density in the tail. Several estimators which use exponential weighting are described. These are compared in a Monte Carlo study to nonweighted estimators, to the empirical cdf, to an integrated kernel, to a Fourier series estimate, to a penalized likelihood estimate and a maximum likelihood estimate. Selected weighted estimators are shown to compare favorably to many of these standard estimators for the sampling distributions investigated. DOE

N84-12805# Argonne National Lab., Ill. Div. of Biological and Medical Research.
ESTIMATION OF THE RIDGE CONSTANT: AN APPROACH BASED ON THE CONDITION INDEX
B. A. Carnes, M. E. Ginevan, and D. M. Eychner 1983 18 p refs Presented at the Ann. Meeting of Am. Statist. Assoc. and other Statist. Groups, Toronto, Canada, 15 Aug. 1983
(Contract W-31-109-eng-38)
(DE83-017955; CONF-830899-3) Avail: NTIS HC A02/MF A01

A Monte Carlo simulation was conducted to evaluate the response of ridge regression solutions to increasing collinearity. Specifically, the magnitude of the ridge constant was sensitive to variability in the response vector while appearing insensitive to collinearity. The insensitivity to collinearity was especially apparent when the response vector was oriented toward a minor dimension in the structure of the predictor variables. Limit arguments indicated that, in the minor dimension case, the increasing magnitude of the inner product of the least squares coefficient vector in the denominator of the optimum estimate for the ridge constant was responsible for the insensitivity to collinearity. Since ridge regression was proposed to deal with collinearity, this behavior suggests a defect in the generally used estimate for the optimum ridge constant. To solve this problem, we propose a condition index estimate for the ridge constant based on the eigenvalues of the augmented X'X matrix; this approach ensures sensitivity to collinearity and insensitivity to the behavior of the response vector. DOE

N84-12806 Adelphi Univ., Garden City, N. Y.
DETERMINISTIC MODELS IN MATHEMATICAL DEMOGRAPHY: AN INVESTIGATION OF STABLE POPULATION THEORY INCLUDING AN ANALYSIS OF THE POPULATION STATISTICS OF DENMARK Ph.D. Thesis
John Impagliazzo 1982 330 p
Avail: Univ. Microfilms Order No. DA8311096

A consolidation of the many fragments of literature on stable population theory into a single, unified entity formally presented as a mathematical work was offered. Historical and mathematical developments are first illustrated as well as the construction of various life tables. Mortality and fertility are investigated using models such as those developed by Gompertz, Makeham, and Malthus and Verhulst. The Lexis grid is employed wherever appropriate, and use of this grid illustrates the development of a birth cohort. Deterministic models of stable population theory are rigorously shown. The discrete time recurrence model is generated by population age structures illustrated by population pyramids; the population renewal equation which results from this model is then used to demonstrate the ergodic property of stable population theory. The continuous time models of Lotka and Feller are also discussed. Author

N84-12563*# Texas Univ., Austin.
AN EMPIRICAL BAYES APPROACH TO SPATIAL ANALYSIS Final Report
C. N. Morris and H. Kostal *In its* Proc. of the NASA Symp. on Math. Pattern Recognition and Image Analysis 1983 p 143-166 refs ERTS (For primary document see N84-12557 03-43)
Avail: NTIS HC A99/MF A01 CSCL 12A

66 SYSTEMS ANALYSIS

Includes mathematical modeling; network analysis; and operations research.

N84-12807# Desmatics, Inc., State College, Pa.
ON THE PERFORMANCE OF TWO-STAGE GROUP SCREENING EXPERIMENTS
Carl A. Mauro Aug. 1983 25 p
(Contract N00014-79-C-0650; NR Proj. 042-467)
(AD-A131970; TR-113-9) Avail: NTIS HC A02/MF A01 CSCL 12/1

Many experimental situations require consideration of a large number of factors. For example, computer simulation studies frequently characterized by the inclusion of an exceptionally large number of input variables. Because of resource limitations, there is often a need in such situations for an efficient method of factor screening. One possible screening strategy is two-stage group screening. This report attempts to examine the performance characteristics of two-stage group screening experiments as a function of a constant signal-to-noise ratio for all important factors. The effect of group-factor cancellation on performance is also investigated. Author (GRA)

N84-12808# Massachusetts Inst. of Tech., Cambridge. Lab. for Information and Decision.
THE EFFECTS OF SMALL NOISE ON IMPLICITLY DEFINED NON-LINEAR DYNAMICAL SYSTEMS
Shankar Sastry Sep. 1982 50 p
(Grant AF-AFOSR-0258-82; AF Proj. 2304)
(AD-A131632; LIDS-P-1249; AFOSR-83-0666TR) Avail: NTIS HC A03/MF A01 CSCL 09/4

The dynamics of a large class of nonlinear systems are described implicitly, i.e., as a combination of algebraic and differential equations. These dynamics admit of jump behavior. We extend the deterministic theory to a stochastic theory since: (1) the deterministic theory is restrictive; (2) the macroscopic deterministic description of dynamics frequently arises from an aggregation of microscopically fluctuating dynamics; and (3) to robustify the deterministic one in the limit that the intensity of the additive white noise tends to zero. We study the modelling issues involved in applying this stochastic theory to the study of the noise behavior of a multivibrator circuit, discuss the limitations of our methodology for certain classes of systems and present a modified approach for the analysis of sample functions of noisy nonlinear circuits. GRA

67 THEORETICAL MATHEMATICS

Includes topology and number theory.

No abstracts in this category.

70 PHYSICS (GENERAL)

For geophysics see *46 Geophysics*. For astrophysics see *90 Astrophysics*. For solar physics see *92 Solar physics*.

N84-12809*# National Aeronautics and Space Administration. Ames Research Center, Moffett Field, Calif.

THERMAL CONDUCTANCE MEASUREMENTS OF PRESSED OFHC COPPER CONTACTS AT LIQUID HELIUM TEMPERATURES

Louis J. Salerno, P. Kittel, and A. L. Spivak (Trans-Bay Electronics, Richmond, Calif.) Nov. 1983 14 p refs

(NASA-TM-85861; A-9542; NAS 1.15:85861) Avail: NTIS HC A02/MF A01 CSCL 20M

The thermal conductance of oxygen-free high conductivity (OFHC) copper sample pairs with surface finishes ranging from 0.1 to 1.6-micrometers rms roughness was investigated over the range of 1.6 to 6.0-K under applied contact forces up to 670 N. The thermal conductance increases with increasing contact force; however, no correlation can be drawn with respect to surface finish. Author

N84-12810# Office National d'Etudes et de Recherches Aerospatiales, Paris (France).

LA RECHERCHE AEROSPATIALE, BIMONTHLY BULLETIN, NO. 1983-1/212, JANUARY-FEBRUARY 1983

Claude Sevestre, ed. Paris ESA Jul. 1983 80 p refs Transl. into ENGLISH of La Rech. Aerospatiale, Bull. Bimensuel (Paris), no. 1983-1/212, Jan.-Feb 1983 Individual titles previously announced as A83-45973 through A83-45975

(ESA-TT-814) Avail: NTIS HC A05/MF A01; HC in ENGLISH available at ONERA, Paris FF 60; original report in FRENCH available at ONERA, Paris FF 60

Signal representation in the time-frequency plane; VHF radar transmission; vacuum chamber trajectory measurement by high speed cinematography; methods to predict the aeroelastic behavior of helicopters; trends in aerodynamic structural analysis; and random eddies in wakes and mixing layers are treated. For individual titles, see N84-12811 through N84-12813.

N84-12811# Office National d'Etudes et de Recherches Aerospatiales, Paris (France).

DEVELOPMENT OF THE BASIC METHODS NEEDED TO PREDICT THE AEROELASTIC BEHAVIOR OF HELICOPTERS c39

R. Dat *In its* La Rech. Aerospatiale, Bimonthly Bull. No. 1983-1/212, Jan.-Feb. 1983 (ESA-TT-814) Jul. 1983 p 37-54 refs Transl. into ENGLISH from La Rech. Aerospatiale, Bull. Bimensuel (Paris), no. 1983-1/212, Jan.-Feb. 1983 (For primary document see N84-12810 03-70)

Avail: NTIS HC A05/MF A01; HC in ENGLISH available at ONERA, Paris FF 60; original report in FRENCH available at ONERA, Paris FF 60

Helicopter performance prediction by linear and nonlinear techniques is discussed. Finite element structural analysis methods, methods for calculating coupled unsteady aerodynamic forces, ground and flight vibration test methods, and techniques for constructing aeroelastically similar models and testing them in wind tunnels are considered. Problems formulated for fixed wing aircraft are not directly applicable to helicopters because of the presence of periodic coefficients in the Lagrange equations, structural and aerodynamic nonlinearities due to the large amplitude of the blade deflections in flapping and in pitch, and the presence of shock waves on the advancing blade along with unsteady stall on the retreating blade. However, linear methods can be used if they employ an appropriate strategy in iterative algorithms, or if they are coupled with simplified nonlinear models. Author (ESA)

N84-12812# Office National d'Etudes et de Recherches Aerospatiales, Paris (France).

PRESENT TRENDS IN STRUCTURAL ANALYSIS AT ONERA c39

R. Valid *In its* La Rech. Aerospatiale, Bimonthly Bull. No. 1981-1/212, Jan.-Feb. 1983 (ESA-TT-814) Jul. 1983 p 55-77 refs Transl. into ENGLISH from La Rech. Aerospatiale, Bull. Bimensuel (Paris), no. 1983-1/212, Jan.-Feb. 1983 (For primary document see N84-12810 03-70)

Avail: NTIS HC A05/MF A01; HC in ENGLISH available at ONERA, Paris FF 60; original report in FRENCH available at ONERA, Paris FF 60

Coupling of variational principles; a posteriori error estimates; homogenization methods; finite set analysis of free vibration of structures with cyclic symmetries; and nonlinear problems are reviewed. Structures in composite materials, and fluid-structure interaction are discussed. When calculating the eigenvibrations of a coupled fluid-structure system for a fluid flow through an opening in the chamber, the vibratory problem reduces to a problem linearized from a nonlinear steady state problem giving a prestressed state. The use of Euler-Lagrange type methods and their variants is appropriate. Author (ESA)

N84-12813# Office National d'Etudes et de Recherches Aerospatiales, Paris (France).

RANDOM EDDIES IN WAKES AND MIXING LAYERS c02

R. Legendre *In its* La Rech, Aerospatiale, Bimonthly Bull. No. 1983-1/212, Jan.-Feb. 1983 (ESA-TT-814) Jul. 1983 p 77-78 Transl. into ENGLISH from La Rech. Aerospatiale, Bull. Bimensuel (Paris), no. 1983-1/212, Jan.-Feb. 1983 (For primary document see N84-12810 03-70)

Avail: NTIS HC A05/MF A01; HC in ENGLISH available at ONERA, Paris FF 60; original report in FRENCH available at ONERA, Paris FF 60

The design of experiments to study large eddies inside shear flows at high Reynolds numbers is discussed. Following the movement of a perturbation and evaluating rate of creation or dissipation by correlating two measurements at a short distance from the same fluid mass is advocated. Correlating measurements at medium distance points should be avoided, for example in a jet and at a few diameters from the jet. When studying long distance noise, the mixing of data from throughout the turbulent domain must be accepted unless the parabolic mirror is used, with the mirror having a wide diameter in comparison with the wavelength studied. The long distance noise spectrum does not depend only on the coil frequency of the large or smaller vortices (the very small ones emit practically nothing), but also on the lifetimes of the vortices from their formation until their dissipation. These lifetimes constitute additional mean pseudoperiods. Author (ESA)

N84-12814# Air Force Systems Command, Wright-Patterson AFB, Ohio. Foreign Technology Div.

UKRAINIAN PHYSICS JOURNAL (SELECTED ARTICLES)

V. A. Kochelap and S. I. Pekar 5 Jul. 1983 34 p refs Transl. into ENGLISH from Ukr. Fiz. Zh. (USSR), v. 15, no. 7, Jul. 1970 p 1057-1067 and 1213-1216

(AD-A131087; FTD-ID(RS)T-0507-83) Avail: NTIS HC A03/MF A01 CSCL 20/5

Topics discussed included: geographic transliteration, kinetic lasers based on light enduced chemical reactions in stationary regime, and heat pumping of photo induced chemical reactions. N.I.S.

N84-12815# General Atomic Co., San Diego, Calif.

COMPARATIVE EVALUATION OF EXISTING CONCEPTS FOR A 10-TESLA FED TOROIDAL FIELD COIL

W. Y. Chen, J. S. Alcorn, and J. Purcell Dec. 1982 8 p refs Presented at the Applied Superconductivity Conf., Knoxville, Tenn., 30 Nov. - 3 Dec. 1982

(Contract DE-AT03-76ET-51011; GA Proj. 3235)
(DE83-012817; GA-A-16923; CONF-821108-30) Avail: NTIS HC A02/MF A01

The existing design concept options for FED toroidal field coils were studied. The various design concepts are: (1) forced flow cooled NbTi cabled conductor; (2) He-II bath cooled NbTi cabled conductor; and (3) He-I bath cooled Nb3Sn-NbTi hybrid with cabled conductor. These design concepts are valuated based upon their relative merits, including technological maturity, operational reliability, overall reactor compatability, maintainability, and cost. The normalization of each design concept to meet similar operational requirements was investigated. The critical issues in the TF coil design, including the structural role of the helium vessel, quench protection, accommodation of neutronic and eddy current heating, credible fault criteria, and the possibility of prototype coil demonstration are discussed. The consequences and implications of extending the peak field in the range from 8 to 10 tesla was also studied. DOE

N84-12816# California Univ., Livermore. Lawrence Livermore Lab.
THEORETICAL AND EXPERIMENTAL STUDIES OF SHOCK-COMPRESSED BENZENE AND POLYBUTENE
F. H. Ree, W. J. Wellis, R. J. Trainor, A. C. Mitchell, and M. Boslough 13 Jul. 1983 5 p refs Presented at Am. Phys. Soc. Meeting on Shock Waves in Condensed Media, Santa Fe, N. Mex., 18 Jul. 1983
(Contract W-7405-eng-48)
(DE83-015884; UCRL-88800; CONF-830719-23) Avail: NTIS HC A02/MF A01

Experimental and theoretical studies are reported on shock pressure, volume, and temperature of liquid polybutene and benzene over the pressure ranges 19 to 210 GPa and 39 to 70 GPa, respectively. Analysis of the (P-V) Hugoniot data is consistent with a model which assumes hydrocarbons to be decomposed into a dense diamond-like phase and hydrogen in the molecular phase. Observed deviations between the experimental and the theoretical temperature data may be due to large heat capacities associated with few heavy hydrocarbon species which are neglected in the above hydrocarbon model. DOE

N84-12817# Massachusetts Inst. of Tech., Cambridge. Magnetics Group.
THE 12-T SOLENOID-DESIGN OPTIONS FOR THE MFTF-B UPGRADE
Joel H. Schultz and Nikolai Kiatchenko 29 Jul. 1983 62 p refs
(Contract DE-AC02-78ET-51013)
(DE83-016646; DOE/ET-51013/91; PFC/RR-83-20) Avail: NTIS HC A04/MF A01

The major options fo the 12 T magnets examined are the selection of normal, superconducting or hybrid normal/superconducting magnet systems. The tradeoffs are those between the higher initial cost of superconducting magnet system, the need for thick shielding of superconducting magnets, higher recirculating power in the normal magnets and poorly characterized reliability of lightly shielded normal magnets. The size and shielding tradeoffs among these options are illustrated. The design concepts presented here are evaluated only for the first design iteration of MFTF-B + T, mentioned above. In particular, all concepts now considered have made topological improvements in the center cell, so that neutral beam power is no longer a strong function of choke coil size. This function was strongly favorable to the use of normal magnets over superconducting magnets and its absence is discussed qualitatively in the cost comparisons. DOE

71 ACOUSTICS

Includes sound generation, transmission and attenuation. For noise pollution see *45 Environment Pollution.*

N84-12818 Admiralty Underwater Weapons Establishment, Portland (England).
TURN-AROUND LOSS FOR OCEANIC SOUND ON A BOTTOM SLOPE
D. E. Weston Apr. 1983 14 p refs
(AUWE-TN-705/83; ACC-67227; BR88862) Copyright. Avail: Issuing Activity

Formulas for turnaround loss for oceanic sound reflected from a region of bottom slope are derived, and the effects of the slope being finite are discussed. With finite slope an outgoing ray after its last bottom bounce may be either upgoing or downgoing, bottom slope is not small in comparison with the ray angles, and the concepts of ray invariance or characteristic time cannot be applied indiscriminately. Since there is a finite number of reflections, an integral may not give a good approximation for the summed bottom losses. After turn around there may be an error in the final or deep-water value of the magnitude of the ordinary grazing angle. Author (ESA)

N84-12819 Admiralty Marine Technology Establishment, Teddington (England).
SHORT-RANGE ACOUSTIC INTENSITY VECTORS OF THE PEKERIS SHALLOW WATER MODEL
E. A. Skelton Aug. 1983 34 p refs
(AMTE(N)-TM-83065) Copyright. Avail: Issuing Activity

Intensity vectors of the Pekeris model are calculated from values of acoustic pressure and particle velocity obtained by numerical integration. Plots of the vectors, for the cases of no-seabed, a rigid seabed and fast and slow seabeds, illustrate the usefulness of the intensity vector approach as an aid to understanding the physics of underwater sound propagation. The way in which both the magnitude and direction of the energy flow in the sea can be controlled by the properties of the seabed, especially when these properties are such as to allow the propagation of normal modes is illustrated. Complex interference patterns and circulatory energy flows are highlighted. Author (ESA)

N84-12820# Naval Underwater Systems Center, New London, Conn. Surface Ship Sonar Dept.
THE EFFECT OF NOISY REFLECTION DATA ON AN INVERSE METHOD FOR DETERMINING THE STRUCTURE OF A LAYERED OCEAN BOTTOM
David J. Thomson (Defence Research Estab. Pacific) and Peter D. Herstein 18 Jul. 1983 20 p Presented at the 105th Meeting of the Acoustic Soc. of Am., Cincinnati, 11 May 1983
(NUSC Proj. A65000)
(AD-A131976; AD-F000018; NUSC-TD-6947) Avail: NTIS HC A02/MF A01 CSCL 20/1

A basic inverse problem in underwater acoustics is the determination of the structure of the sea bed from a limited knowledge of its reflection coefficient. For many applications, an adequate model for studying the acoustic interaction is provided by the scattering of plane waves by a layered liquid medium. In contrast to formally exact solutions to this inverse scattering problem, Candel, et al., (J. Sound Vib. 68, 571-595 (1980)) developed an approximate scheme which is readily implemented numerically. Under the assumption of nonabsorptive media, the reconstruction of both sediment density and sound-speed profiles is effected by the numerical integration of a system of four first-order differential equations requiring impulse response data for two distinct grazing angles. In this paper, the effect of additive noise on the inversion algorithm is examined for synthetic reflection data generated for a geoacoustic model of deep-sea sediments representative of the Hatteras Abyssal Plain. Author (GRA)

N84-12821# Naval Research Lab., Washington, D. C.
TRANSVERSE HORIZONTAL COHERENCE AND LOW-FREQUENCY ARRAY GAIN LIMITS IN THE DEEP OCEAN Interim Report
L. Bruce Palmer (Planning Systems, Inc., McLean, Va.), Dennis M. Dundore, Budd B. Adams, and John J. McCoy 9 Aug. 1983 42 p

(RR01108)
(AD-A131916; NRL-8695) Avail: NTIS HC A03/MF A01 CSCL 20/1

This report is a major output of a program in spatial properties of low-frequency acoustic fields in the deep ocean. This project was instituted at the Naval Research Laboratory in 1974 to provide a priori estimates of the capabilities and limitations of large-array performance due to coherence degradation from environmental causes. The project work has emphasized stochastic propagation measures of irregularities in the ocean. This approach has been followed to provide probabilistic predictions of the expected environmental limits to aperture designs. Only volume effects are treated in the present work to provide the outside practical limit on resolution, and hence size, of low-frequency arrays that our present knowledge of the internal structure of the deep ocean will permit. The special objective of this report is the presentation of an algorithm, the supporting theory of which has previously been published, which has subsequently been supported with a series of experimental investigation of the transverse horizontal coherence properties of the acoustic field following long-range propagation in the deep ocean. From this algorithm the gain of an array can be calculated provided it is restricted to those instances where bottom and surface interaction play a minor part in the overall intensity of the received field. Author (GRA)

N84-12822# Pennsylvania State Univ., University Park. Applied Research Lab.
ACOUSTIC PULSE SCATTERING FROM IMPEDANCE COVERED CYLINDERS Ph.D. Thesis
Abbas Khavaran Aug. 1983 136 p
(Contract N00024-79-C-6043)
(AD-A131653; ARL/PSU/TM-83-100) Avail: NTIS HC A07/MF A01 CSCL 20/1

An expression for the acoustic scattered pressure from an impedance covered cylinder due to an incident plane pulse is obtained analytically. The application of Fourier transform on time and subsequent Sommerfield-Watson transformation results in separate expressions for geometrically reflected pressure and for creeping (or circumferential) waves. Using Cauchy contour integration theorem and saddle point methods, the inverse Fourier transform is evaluated. The impulse response and convolution theorem have been utilized to obtain an expression for the scattered pressure for incident harmonic pulse train and FM pulses. The first arrival of acoustic wave at an observer point in the far field is shown to be due to the geometrically reflected pressure. After the first arrival, creeping waves are shown to circumnavigate the cylinder surface for an indefinite number of times and radiate off tangentially at any angle. These waves create the multiple echoes that return in the scattering of a single pulse. The circumferential waves are shown to decay exponentially as they encircle the cylinder surface. Author (GRA)

N84-12823# Sandia Labs., Albuquerque, N. Mex. Fluid Mechanics and Heat Transfer Div.
DOUBLE POROSITY MODEL FOR ACOUSTIC WAVE PROPAGATION IN FRACTURED-POROUS ROCK
R. K. Wilson 1983 9 p refs Presented at the Workshop on Media with Microstructure and Wave Propagation, Houghton, Mich., 24 Jan. 1983
(Contract DE-AC04-76DP-00789)
(DE83-017823; SAND-83-1902C; CONF-830141-4) Avail: NTIS HC A02/MF A01

The propagation of acoustic waves in a fluid-saturated porous medium containing a continuously distributed system of fractures is modeled analytically. The porous medium is assumed to consist of two degrees of porosity and the resulting model thus yields three types of longitudinal waves, one associated with the elastic properties of the matrix material and one each for the fluids in the pore space and the fracture space. Two approaches are taken into develop the equations; one based on Biot's approach utilizing the viscodynamic operator and one based on the continuum theory of mixtures. DOE

N84-12824# Ames Lab., Iowa.
COMPUTATIONAL TOOL FOR THE DESIGN OF ULTRASONIC SYSTEMS
S. J. Wormley, D. O. Thompson, and K. M. Lakin 1983 7 p refs Presented at the Conf. on Quantitative NDE, Santa Cruz, Calif., 7-12 Aug. 1983
(Contract W-7405-eng-82)
(DE83-018092; IS-M-460; CONF-830811-14) Avail: NTIS HC A02/MF A01

Advances in elastic wave scattering and inversion techniques have shown that advances in transducer technology are needed in order to fully exploit them. This is particularly true in the case of flaw sizing algorithms in which it has been demonstrated that a need exists for transducers with specified bandwidth characteristics. As a part of an effort to develop a composite, multiviewing ultrasonic transducer for flaw characterization, a computational tool has been developed which provides a convenient way to select driver pulse shapes and transducer characteristics which optimize this property. This computational tool is discussed. DOE

N84-12825# Ames Lab., Iowa.
ANALYTIC DIFFRACTION CORRECTIONS TO ULTRASONIC SCATTERING MEASUREMENTS
R. B. Thompson and T. A. Gray 1983 20 p refs Presented at the Conf. on Quantitative NDE, Santa Cruz, Calif., 7-12 Aug. 1983 Sponsored in part by AFWAL
(Contract W-7405-eng-82)
(DE83-018080; IS-M-446; CONF-830811-10) Avail: NTIS HC A02/MF A01

Ultrasonic theories generally predict a scattering amplitude which relates a spherically spreading, far-field scattered wave to an incident plane wave. In ultrasonic immersion measurements, the frequency and angular dependences of the scattering amplitude are convolved with those of the transmitting and receiving transducers and the propagation through the liquid-solid and solid-liquid interfaces. A set of approximate corrections for these effects for the cases of angle beam inspection through planar, spherically curved or cylindrically curved surfaces is presented. The primary parameters in the correction are the function D, which corrects for the diffraction effects occurring during a transducer calibration experiment, and the function C, which describes the on-axis pressure variation of the beam. The extension of those results to the aforementioned two media problems in which mode conversion, refraction, diffraction, and focussing all play interrelated roles is discussed. DOE

N84-12826# Brookhaven National Lab., Upton, N. Y.
HELIUM-FLOW MEASUREMENT USING ULTRASONIC TECHNIQUE
John H. Sondericker 1983 8 p refs Presented at the Cryog. Eng. Conf. and Intern. Cryog. Mater. Conf., Colorado Springs, 15-19 Aug. 1983
(Contract DE-AC02-76CH-00016)
(DE83-017765; BNL-33591; CONF-830841-16) Avail: NTIS HC A02/MF A01

The ideal cryogenic instrumentation for the colliding beam accelerator helium distribution system does not add pressure drop to the system, functions over the entire temperature range, has high resolution, and delivers accurate mass flow measurement data. The design and testing of an ultrasonic flowmeter which measures helium flow under different temperatures are described. A.R.H.

N84-12827# Ames Lab., Iowa.
MEASUREMENTS OF ULTRASONIC SCATTERING FROM NEAR-SURFACE FLAWS
D. K. Hsu (Colorado State Univ.), T. A. Gray, and R. B. Thompson 1983 19 p refs Presented at the Conf. on Quantitative NDE, Santa Cruz, Calif., 7 Aug. 1983
(Contract W-7405-eng-82)
(DE83-017693; IS-M-447; CONF-830811-2) Avail: NTIS HC A02/MF A01

In ultrasonic NDE measurements the detection of subsurface

flaws is of practical importance, especially flaws too far from the surface to be detected by eddy-current methods and yet close enough to the surface for the flaw-surface interaction to be important. Experimental results of ultrasonic scattering measurements of subsurface flaws in the presence of a fluid-solid interface are reported and these results are compared with theoretical calculations of subsurface flaw scattering. Comparison of the absolute value of the scattering amplitude in terms of frequency, flaw-to-surface distance, ultrasonic mode and scattering angle are made for an oblate spheroidal void in the interior of bulk titanium and for a spherical inclusion near the surface of a thermoplastic sample. Results of applying the one dimensional inverse Born algorithm to the sizing of near-surface flaws are also reported.
DOE

72 ATOMIC AND MOLECULAR PHYSICS

Includes atomic structure and molecular spectra.

N84-12828# Toronto Univ., Downsview (Ontario). Inst. for Aerospace Studies.
TRANSITION FLOW ION TRANSPORT VIA INTEGRAL BOLTZMANN EQUATION
Thomas Edward Darcie Oct. 1983 257 p refs
(UTIAS-269; ISSN-0082-5255) Avail: NTIS HC A12/MF A01

An approach is developed to solve the integral Boltzmann equation for the evolving velocity distribution of a source of ions, undergoing electrostatic acceleration through a neutral gas target. The theory is applicable to arbitrarily strong electric fields, any ion/neutral mass ratio greater than unity, and is not limited to spatially isotropic gas targets. A hard sphere collision model is used, with a provision for inelasticity. Both axial and radial velocity distributions are calculated for applications where precollision radial velocities are negligible, as is the case for ion beam extraction from high pressure sources. Theoretical predictions are tested through an experiment in which an atmospheric pressure ion source is coupled to a high vacuum energy analyzer. Excellent agreement results for configurations in which the radial velocity remains small. Velocity distributions are applied to predicting the efficiency of coupling an atmospheric pressure ion source to a quadrupole mass spectrometer and results clearly indicate the most desirable extracting configuration. A method is devised to calculate ion-molecule hard sphere collision cross sections for easily fragmented organic ions. M.G.

N84-12829# Naval Research Lab., Washington, D. C. Plasma Theory Branch.
DYNASTY 2: A NONLINEAR IMPLICIT CODE FOR RELATIVISTIC ELECTRON BEAM TRACKING STUDIES
B. Hui and M. Lampe 27 Jul. 1983 23 p refs
(Contract N60921-83-WR-W0088; DARPA Order 4395)
(AD-A131592; NRL-MR-5138) Avail: NTIS HC A02/MF A01 CSCL 12/1

The formulation of an implicit code Dynasty 2 is described. The code solves the EMPULSE equations without linearization. This code is applied to the study of beam tracking. Some applications are suggested. Author (GRA)

N84-12830# Air Force Geophysics Lab., Hanscom AFB, Mass.
ABSOLUTE COLLISIONAL EXCITATION CROSS SECTION MEASUREMENTS USING CROSSED MOLECULAR BEAMS Environmental Research Papers
Andrew Freedman, Alfred Rahbee, Joel A. Silver, and Alan C. Stanton 17 Mar. 1983 34 p
(AF Proj. 2303)
(AD-A132038; AFGL-TR-83-0078; AFGL-ERP-829) Avail: NTIS HC A03/MF A01 CSCL 07/4

The measurement of absolute excitation cross-sections of the asymmetric stretch mode (001) of H2O and CO2 for collisions with atomic oxygen is important in understanding the signatures of high-altitude rocket plumes. Experiments are performed in a crossed molecular beam apparatus in which a CVF detector measures the collisionally-induced infrared fluorescent signal. Calibration and testing of the atomic oxygen source was completed. It was installed into the crossed beam apparatus and vacuum tested in preparation for performing the excitation cross-section measurements. Upper limits have been established for the excitation cross sections for the systems 0 + CO2 and Ar + CO2. The values determined are 0.03A squared for 0 + CO2 at 3.85 km/sec and 0.003 A squared for Ar + CO2 at 2.27 km/sec. Monte Carlo trajectory analysis of the data provides accurate correction factors to the raw data that account for kinematic and experimental constraints inherent in these measurements. It further shows that measurements near threshold cannot be used to determine the functional energy dependence of the cross section. Further modifications and improvements in the experimental approaches to improve sensitivity will be discussed. Author (GRA)

N84-12831# Air Force Geophysics Lab., Hanscom AFB, Mass. Space Physics Div.
ELECTRON BEAM TRAJECTORY IN A PHOTOMETER FIELD OF VIEW Interim Scientific Report
Shu T. Lai and H. A. Cohen 16 Feb. 1983 19 p
(AF Proj. 7661)
(AD-A131949; AFGL-TR-83-0045; AFGL-ERP-824) Avail: NTIS HC A02/MF A01 CSCL 12/1

Theoretical calculations on the trajectory of an electron beam of kilovolt energy range in an ionospheric environment have been performed. By means of a succession of orthogonal transformations, the trajectory and luminosity as observed at a photometer with a given angular field of view are obtained. For the purpose of applications on rocket beam experiments, cases of various magnetic field orientations and beam energies have been examined. Singularities of luminosity exist in this model when the magnetic field is perpendicular to the electron velocity resulting in a non-propagation mode. Author (GRA)

N84-12832*# Iowa Univ., Iowa City. Dept. of Physics and Astronomy.
A MODEL FOR CHORUS ASSOCIATED ELECTROSTATIC BURSTS Progress Report
Crockett L. Grabbe 30 Jun. 1983 31 p
(Contracts NAS5-26819; N00014-76-C-0016)
(NASA-CR-174489; NAS 1.26:174489; AD-A131868; AD-E850387; U-OF-IOWA-83-23) Avail: NTIS HC A03/MF A01 CSCL 20H

The linear theory of the generation of electrostatic bursts of noise by electrons trapped in chorus wave packets is developed for a finite temperature electron beam and a Maxwellian electron and ion background. The growth rates determined qualitatively in good agreement with those obtained by previous authors from a more idealized model. Two connected instability mechanisms seem to be occurring: a beam plasma (electron-ion two-stream) instability commonly associated with intensification of the chorus power levels, and a transitional or borderline resistive medium instability commonly associated with chorus hooks. The physical reasons for the two mechanisms is discussed. In the second case electron beams are difficult to identify in the particle data. An expression is obtained for the maximum growth rate in terms of the ratios of the beam and electron thermal velocities to the beam velocity, and of the beam density to plasma density. It is anticipated that this may allow the observed peak in the electrostatic noise spectrum to be used as a diagnostic for the beam characteristics.
Author (GRA)

N84-12833# Washington Univ., Seattle. Dept. of Chemistry.
STUDY OF VIBRATIONAL ENERGY TRANSFER AT A SURFACE BY A TIME-OF-FLIGHT METHOD
Wei Yuan and B. S. Rabinovitch 31 Jul. 1983 28 p
(Contract N00014-75-C-0690; NR Proj. 092-549)
(AD-A131798; NR092-549-TR27) Avail: NTIS HC A03/MF A01 CSCL 07/3

A single collision, time-of-flight extension of the VEM method for the study of molecule-surface vibrational energy transfer is introduced. This refined technique helps election between possible

alternative trial analytic forms of the collisional transition probability function. A gaussian form is preferred over a boltzmann-exponential form for cyclobutene isomerization to 1,3-butadiene energized by collisions at a seasoned silica surface at 800 K. The study illustrates the difference between conventional accommodation coefficient measurements, which examine average energy changes, and the present studies which explore the energy transport at high levels corresponding to chemical reaction thresholds. GRA

N84-12834# National Science Foundation, Washington, D.C. Div. of Material Sciences.
INTERNATIONAL CONFERENCE ON VIBRATIONS AT SURFACES (3RD)
Hans Morawitz 4 Sep. 1982 124 p Conf. held at Asilomar, Calif., 1-4 Sep. 1982
(Grant AFOSR-ISSA-82-00029)
(AD-A131794; AFOSR-83-0647TR) Avail: NTIS HC A06/MF A01 CSCL 05/2

Topics related to vibration phenomena at surfaces are addressed including vibrational frequency shifts and widths, dynamical processes, electron loss spectroscopy, Raman scattering, infrared adsorption and reflection spectroscopy, beam surface scattering, and electron tunnelling spectroscopy. M.G.

N84-12835# New York Univ., New York. Dept. of Physics.
NEW RESULTS FOR TRANSITION PROBABILITIES IN TWO-LEVEL SYSTEMS: THE LARGE DETUNING REGIME
E. J. Robinson and P. R. Berman 7 Dec. 1982 27 p
(Contract N00014-77-C-0553; RR01107)
(AD-A131783) Avail: NTIS HC A03/MF A01 CSCL 20/10

The problem of calculating transition probabilities in two-level systems is studied in the limit where the detuning is large compared to the inverse duration of the interaction. Within each family, transition probabilities may be calculated from formulae that differ only in the numerical value of a scaling parameter. In cases where the coupling function has a pole in the complex time plane, the families are identified with the order of this singularity. In particular, for poles of first order, a connection with the Rosen-Zenet solution can be made. The analysis is performed via high-order perturbation expansions, which are shown to always converge for two-level systems driven by coupling potentials of finite pulse area. GRA

N84-12836# Washington Univ., Seattle. Dept. of Chemistry.
HIGH TEMPERATURE GAS ENERGY TRANSFER Annual Summary Report, 1 Aug. 1982 - 31 Jul. 1983
B. S. Rabinovitch 15 Aug. 1982 26 p
(Contract N00014-75-C-0690; NR Proj. 092-549)
(AD-A131782) Avail: NTIS HC A03/MF A01 CSCL 07/4

In the period of this report, vibrational energy transfer studies have been carried out with three types of molecules that fall into the energetic category: these are nitromethane, azomethane and methyl nitrite. Apart from a propensity for more complex reaction mechanisms and catalytic behavior, the energy transfer properties of energetic materials at a surface seem to follow just the behavior expected from the intermolecular potential and not that of the intramolecular or reaction potential. More stable molecules can thus suffice to delineate the energy transfer properties expected for energetic materials. The study of gas/surface energy transfer has been extended to metals, i.e. to various gold surfaces, which appear to be stronger energy transfer media than fused quartz. The behavior for cyclobutene on gold was studied up to 1250 K and strong collision behavior was found below 600 K. Extension to other metals is readily possible. The examination of liquid metal surfaces as energy transfer agents is being investigated. Tin metal is being studied. Extension to other liquids will be made. A theoretical model has been applied to the calculation of energy transfer amounts between molecules as a function of molecular size, energy level and ambient temperature. GRA

N84-12837# Massachusetts Inst. of Tech., Cambridge. Research Lab. of Electronics.
STUDY OF EXCITED STATE ENERGY TRANSFER PROCESSES Final Report, 1 Jan. 1981 - 31 Dec. 1982
J. R. Barthel, R. E. Duff, and W. J. Proffer 11 May 1983 3 p
(Grant AF-AFOSR-0067-81; AF Proj. 2301)
(AD-A131777; AFOSR-83-0619TR) Avail: NTIS HC A02/MF A01 CSCL 07/4

Several scaling and fitting laws for Rotationally Inelastic (RI) collisions have been developed and applied. These laws will provide a compact description of collisional processes for use in technological applications. GRA

N84-12838# Michigan State Univ., East Lansing. Dept. of Chemistry.
STUDIES OF THE CORRELATION OF ELECTRODE KINETICS WITH MOLECULAR STRUCTURE Final Scientific Report, Oct. 1980 - Jan. 1983
Michael J. Weaver Jun. 1983 15 p
(Grant AF-AFOSR-0271-80; AF Proj. 2303)
(AD-A131704; AFOSR-83-0720TR) Avail: NTIS HC A02/MF A01 CSCL 07/4

The overall objective is to develop our understanding of the connections between the kinetics and mechanisms of heterogeneous electron-transfer reactions at metal-electrolyte interfaces and the molecular structure of the reactant and the interfacial region. We have chiefly focussed attention on transition-metal redox couples, especially Co(III)/(II), Cr(III)/(II), and Ru(III)/(II) containing adsorbing inorganic and organic ligands at a number of electrocatalytic solid surfaces, especially silver, platinum, and gold, as well as at mercury electrodes. By combining electrochemical kinetic and reactant adsorption thermodynamic measurements, along with in situ vibrational spectroscopic studies using Surface-Enhanced Raman Scattering (SERS), the various catalytic influences exerted by the metal interface upon the energetics of electrode reactions have been probed in detail. GRA

N84-12839# Argonne National Lab., Ill. Materials Science and Technology Div.
NOVEL INTERACTIONS OF THE CHARGE-BALANCING CATIONS WITH FRAMEWORK DEFECTS AND TRAPPED HYDROGEN ATOMS IN HOLMIUM-EXCHANGED Y ZEOLITES
L. E. Iton Apr. 1983 4 p refs Presented at the 6th Intern. Zeolite Conf., Reno, Nev., 10-15 Jul. 1983
(Contract W-31-109-eng-38)
(DE83-014204; CONF-830756-6) Avail: NTIS HC A02/MF A01

The indirect superhyperfine interaction (TSHFI) between impurity electrons and host nuclei in Van Vleck paramagnets is induced by the large magnetic polarizability of the ground singlet electronic state of the Van Vleck cation. ISHFI effects were observed on neutral, spin S = 1/2 impurities for the first time. The ISHFI appear in the EPR spectrum of Na-Y zeolite, partially (BETA)-irradiated. DOE

N84-12840# Stanford Linear Accelerator Center, Calif.
MONITORING OF THE STANFORD LINAC MICROBUNCHES' POSITION
J. C. Denard, G. Oxoby, J. L. Pellegrin, and S. Williams 1983 4 p refs Presented at Particle Accelerator Conf., Santa Fe, N. Mex., 21 Mar. 1983
(Contract DE-AC03-76SF-00515)
(DE83-012712; SU-SLAC-Pub-3058; CONF-830311-143) Avail: NTIS HC A02/MF A01

A new hardware was developed to measure the trajectory of microbunches along the Stanford Linac. To be suitable for the operation of the SLAC Single Pass Collider, the bunches absolute position must be kept within + or - microns of the accelerator center, and the acquisition of this measurement must be made along the machine in a snapshot fashion. Typically, the position of three bunches will be monitored during subsequent shots; we expect a minimum charge of 10(9) particles per bunch and a time spacing between bunches of 50 nanoseconds. The mechanics of the position detectors is described as well as the general system organization and the calibration of various components. DOE

N84-12841# California Univ., Livermore. Lawrence Livermore Lab.
MAGNETIC SWITCHING
Daniel L. Birx, E. Cook, S. Hawkins, S. Poor, L. Reginato, J. Schmidt, and Martin Smith 1983 8 p refs Presented at the IEEE Power Electron. Spec. Conf., Albuquerque, N. Mex., 6 Jun. 1983
(Contract W-7405-eng-48)
(DE83-012952; UCRL-88647; CONF-830621-10) Avail: NTIS HC A02/MF A01

The development program in magnetic switching which was aimed at solving the rep-rate and reliability limitations of the ATA spark gaps is discussed. The end result was a prototype physically very similar to the present Advanced Test Accelerator (ATA) pulse power unit but vastly superior in performance. This prototype, which is easily adaptable to the existing systems, has achieved a burst rep-rate of 20 kHz and an output voltage of 500 kV. A one-on-one substitution of the existing pulse power module would result in a 100 MeV accelerator. Furthermore, the high efficiency of the magnetic pulse compression stages allowed CW operation of the prototype at one kilohertz opening up of the applications for the pulse power. Performance and design details are described. DOE

N84-12842# Stanford Linear Accelerator Center, Calif.
FROM ACCELERATORS TO STORAGE RINGS TO ?
W. K. H. Panofsky Feb. 1983 5 p Presented at the Particle Accelerator Conf., Santa Fe, N. Mex., 21 Mar. 1983
(Contract DE-AC03-76SF-00515)
(DE83-011849; SU-SLAC-Pub-3062; CONF-830311-153) Avail: NTIS HC A02/MF A01

A general but highly subjective overview of the expectation for accelerators and colliders for high energy physics are given, but not extended developments of accelerators and storage rings for application to nuclear structure physics, synchrotron radiation, medical applications or industrial use. DOE

N84-12843# Los Alamos Scientific Lab., N. Mex.
VECTORIZED MONTE CARLO PHOTON TRANSPORT
F. W. Bobrowicz, J. E. Lynch, K. J. Fisher, and J. E. Tabor May 1983 19 p refs
(Contract W-7405-eng-36)
(DE83-014807; LA-9752-MS) Avail: NTIS HC A02/MF A01

The results of current research in the development of a CRAY algorithm for time dependent Monte Carlo photon radiation transport is presented. The method that was developed is a fully vectorized particle-vector scheme. This technique tracks groups of particles simultaneously using a vector-stack formalism based upon particle events. Timing comparisons between this algorithm and the traditional single-particle approach are presented. DOE

N84-12844# Virginia Univ., Charlottesville. Dept. of Physics.
EXPERIMENTS ON THE NUCLEAR INTERACTIONS OF PIONS Progress Report
K. O. H. Ziock and R. C. Minehart Jul. 1983 13 p
(Contract DE-AS05-76ER-04043)
(DE83-016285; DOE/ER-0403/43) Avail: NTIS HC A02/MF A01

Progress in a variety of experiments during the preceding year were reported. These include quasi-free-scattering of pions from light nuclei, pion absorption and elastic scattering. Experiments on pion decay to search for massive neutrinos were conducted. The results of a search for free quarks was reported. Most of these efforts will continue into the future and proposed research in these various activities as well as new ones in the field of pionium and a study of the (1C OMEGA)(*), (1C OMEGA)0 mass difference are discussed. DOE

N84-12845# Los Alamos Scientific Lab., N. Mex. Theoretical Div.
HADRONIC MULTIPLICITY DISTRIBUTIONS: EXAMPLE OF A UNIVERSAL STOCHASTIC MECHANISM
P. Carruthers 1983 10 p refs Presented at the 14th Inter. Symp. on Multiparticle Dyn., Lake Tahoe, Nev., 1 Jun. 1983
(Contract W-7405-eng-36)
(DE83-015232; LA-UR-83-2041; CONF-830689-1) Avail: NTIS HC A02/MF A01

The existence of approximate scaling of hadronic charged multiplicity distributions when plotted in KNO form (i.e., anti n P/sub n/ vs. n/anti n) continues to attract interest. Both the existence of the phenomenon, and the shape of the scaling cure psi (n/anti n) = anti n P/sub n/ (large n, anti n) was explained from many geometrical-dynamical points of view. These results depend on a generic framework independent of dynamical details, which context moreover occurs in many areas of science. This view imposes global constraints on any modelistic view which is respected as are the symmetries of a theory. What one learns from the existence of scaling and the form of psi is indeed interesting but different from traditional views. DOE

N84-12846# Washington Univ., Seattle. Lab. of Nuclear Physics.
UNIVERSITY OF WASHINGTON SUPERCONDUCTING-BOOSTER PROJECT
J. G. Cramer, D. W. Storm, and R. Vandenbosch 1983 16 p refs Presented at the 6th Intern. Tandem Conf., Chester, United Kingdom, 16 Apr. 1983
(Contract DE-AC06-81ER-40048)
(DE83-015689; DOE/ER-40048/62-L3; CONF-8304105-4) Avail: NTIS HC A02/MF A01

The University of Washington Nuclear Physics Laboratory has designed a superconducting linac booster with an equivalent dc accelerating voltage of 24.35 MV, which will be injected by the existing FN Tandem Van de Graaff accelerator. The design is based on the lead-plated copper quarter-wave resonator units developed by the Stoney Brook/Weizmann group. The UW booster, unlike previous designs, will accelerate p, d, t, (3)He, and (4)He as well as light heavy ions (A < 56). Design studies of system performance give proton energies of almost 38 MeV and energies for light-heavy ions of over 15 MeV/AMU, diminishing with A to about 7 MeV/AMU for (56)Fe (assuming most probable charge). Beam dynamics studies show that debunching gives (RADICAL)E/E approx. = 10(+4) or about 5 keV for protons and bunching gives a time resolution on target of about 40 to 60 ps. The UW Booster Project has been recommended by NSAC and is to be funded in the FY'84 and FY'85 budgets of the US Department of Energy at a cost of about $8 million. Final planning and development are now in progress. Construction is to begin in late 1983. DOE

N84-12847# California Univ., Berkeley. Lawrence Berkeley Lab. Nuclear Science Div.
STATISTICAL CALCULATION OF COMPLETE EVENTS IN MEDIUM-ENERGY NUCLEAR COLLISIONS
Joergen Randrup 1983 17 p refs Presented at the Nordic Winter School on Nucl. Phys., Hemsedal, Norway, 10-20 Apr. 1983
(Contract DE-AC03-76SF-00098)
(DE83-015951; LBL-15877; CONF-8304104-2) Avail: NTIS HC A02/MF A01

The essential tools for formulating a statistical model for the nuclear disassembly process are presented. The quick disassembly (explosion) of a hot nuclear system, a so called source, into multifragment final states, which compete according to their statistical weight is considered. First some useful notation is introduced. The expressions for exclusive and inclusive distributions are given and the factorization of an exclusive distribution into inclusive ones is carried out. In turn, the grand canonical approximation for one fragment inclusive distributions is introduced. Finally, it is outlined how to generate a statistical sample of complete final states. On this basis, a model for statistical simulation of complete events in medium energy nuclear collisions was developed. DOE

N84-12848# California Univ., Livermore. Lawrence Livermore Lab.
MEASUREMENTS OF THE EMITTANCE AND CURRENT DENSITY PROFILE OF THE BEAM PRODUCED BY THE ATA INJECTOR

Thomas J. Fessenden 27 Jun. 1983 18 p refs
(Contract W-7405-eng-48)
(DE83-016522; UCID-19839) Avail: NTIS HC A02/MF A01

Measurements of the normalized emittance of the beam produced by the advanced test accelerator injector yielded values near 0.4 radian-centimeters at currents up to 10 kAmps. The instrument was also used to obtain beam-current-density profiles in two dimensions at the entrance mask of the instrument. DOE

N84-12849# Stanford Linear Accelerator Center, Calif.
MINIMAL UNITARY (COVARIANT) SCATTERING THEORY
J. V. Lindesay and A. Markevich Jun. 1983 3 p refs Presented at the 10th Intern. Conf. on Few-Body Probl. in Phys. Karlsruhe, West Germany, 21-17 Aug. 1983
(Contract DE-AC03-76SF-00515)
(DE83-014896; SU-SLAC-Pub-3147; CONF-830862-3) Avail: NTIS HC A02/MF A01

In the minimal three particle equations developed by Lindesay the two body input amplitude was an on shell relativistic generalization of the nonrelativistic scattering model characterized by a single mass parameter (SIGMA) which in the two body (m + m) system looks like an s-channel bound state ((SIGMA) < 2m) or virtual state ((SIGMA) > 2m). Using this driving term in covariant Faddeev equations generates a rich covariant and unitary three particle dynamics. However, the simplest way of writing the relativistic generalization of the Faddeev equations can take the on shell Mandelstam parameter s = 4(g(2) + m(2)), in terms of which the two particle input is expressed, to negative values in the range of integration required by the dynamics. This problem was met in the original treatment by multiplying the two particle input amplitude by THETA (s). DOE

N84-12850# Stanford Linear Accelerator Center, Calif.
COVARIANT THEORY WITH A CONFINED QUANTUM
H. Pierre Noyes and G. Pastrana Jun. 1983 3 p refs Presented at the 10th Intern. Conf. on Few-Body Probl. in Phys., Karlsruhe, West Germany, 21-27 Aug. 1983
(Contract DE-AC03-76SF-00515)
(DE83-014897; SU-SLAC-Pub-3146; CONF-830862-2) Avail: NTIS HC A02/MF A01

Lindesay, Noyes and Lindesay, and by Lindesay and Markevich have shown that by usng a simple unitary two particle driving term in convariant Faddeev equations a rich covariant and unitary three particle dynamics is generated, including single quantum exchange and production. The basic observation is that if the two particle input amplitudes used as driving terms in a three particle Faddeev equation are assumed to be simply bound state poles with no elastic scattering cut, they generate rearrangement collisions, but breakup is impossible. DOE

N84-12851# Oak Ridge National Lab., Tenn.
IMPLICATIONS OF HEAVY-ION-INDUCED SATELLITE X-RAY EMISSION. 1: INTRODUCTION
S. Raman and C. R. Vane 1983 23 p refs Presented at the 3rd Intern. Conf. on Particle-Induced X-ray Emission (PIXE) and its Analytical Applications, Heidelberg, 18 Jul. 1983
(Contract W-7405-eng-26)
(DE83-015682; CONF-830772-2) Avail: NTIS HC A02/MF A01

Regardless of how induced, X-ray spectra are sensitive to the chemical environment of the emitting atom and yield information on the atomic and electronic structure of host materials. Those spectra resulting from light ion and heavy ion excitations are the main topics covered. Highly energetic ions are capable of producing multiple innershell ionization. The resulting spectrum of X-rays from a particular target atom is composed of a complex series of satellite lines. Environmental effects give rise to the redistribution of intensity from one satellite group to another. These changes are correlated with bulk chemical properties (valence electron densities, effective charges, covalencies, etc.). The possibility of obtaining new chemical information (for example, in implanted materials and in metal alloys) exists but requires greater experimental and theoretical understanding of both parametric variations and the fine structure of satellite lines. DOE

N84-12852# Michigan Univ., Ann Arbor. Dept. of Physics.
THE 83-INCH CYCLOTRON RESEARCH PROGRAM Final Report
W. C. Parkinson Jul. 1983 58 p
(Contract DE-AC02-76ER-02167)
(DE83-015827; DOE/ER-02167/T1) Avail: NTIS HC A04/MF A01

The construction of a modern variable energy cyclotron facility at The University of Michigan to be used for research in nuclear spectroscopy was authorized. The legislature of the State of Michigan made available funds for construction of a building to house the 83 inch cyclotron and auxiliary equipment as well as the University's remodeled 42 inch cyclotron. The research program centered around the 83 inch cyclotron was funded by the AEC and its successors, the Energy Research and Development Administration (ERDA) and the Department of Energy (DOE), from September 1964 through March 1977. The program represented a continuation of the research effort using the 42 inch cyclotron facility which was supported continuously by the AEC since February 1950. This final report to DOE briefly describes the research facility, the research program, and highlights the principal accomplishments of the effort. A historical note to place this effort within the context of nuclear physics research in the Department of Physics of the University of Michigan is included. DOE

N84-12853# Los Alamos Scientific Lab., N. Mex. Center for Nonlinear Studies and Theoretical Div.
SOLITONS AND POLARONS IN QUASI-ONE DIMENSIONAL CONDUCTING POLYMERS AND RELATED MATERIALS
David K. Campbell 1983 33 p refs Presented at the 2nd Intern. Conf. on Molecular Electronic Devices, Washington, 13 Apr. 1983
(Contract W-7405-eng-36)
(DE83-015233; LA-UR-83-2039; CONF-830109-1) Avail: NTIS HC A03/MF A01

In recent years it has become increasingly appreciated that fundamentally nonlinear excitations, solitons, play an essential role in an incredible variety of natural systems. These solitons, which frequently exhibit remarkable stability under interactions and perturbations, often dominate the transport, response, or structural properties of the systems in which they occur. An introduction to the solitons that occur in quasi-one dimensional conducting polymers (synmetals) and related systems are presented. The relevance of this subject to molecular electronic devices is twofold. First, many of these materials have molecular structures similar to possible prototype molecular switches. Second, to understand in detail how a molecular electronic device could work, it is essential to have a broad perspective on the nature of possible excitations in a variety of natural and synthetic molecular materials. DOE

N84-12854# Stanford Linear Accelerator Center, Calif.
BARYON-ANTIBARYON ANGULAR CORRELATIONS IN QUARK JETS
Alfred Bartl (Wien Univ.) Jul. 1983 6 p refs Presented at the 14th Intern. Symp. on Multiparticle Dynamics, Lake Tahoe, Calif., 22-27 Jun. 1983 Sponsored in part by Fonds zur Foerderung der Wissenschaftlichen Forschung in Oesterreich
(Contract DE-AC03-76SF-00515)
(DE83-015923; SLAC-PUB-3163; CONF-830689-2) Avail: NTIS HC A02/MF A01

The azimuthal angular distribution of baryon-antibaryon pairs in a quark jet is calculated and compared with experimental data in e(+)e(-) annihilation. DOE

N84-12855# Fermi National Accelerator Lab., Batavia, Ill.
A THOUSAND TeV IN THE CENTER OF MASS: INTRODUCTION TO HIGH-ENERGY STORAGE RINGS
J. D. Bjorken 1982 39 p refs Presented at the 1982 NATO Adv. Study Inst., Lake George, N.Y., Jun. 1982
(Contract DE-AC02-76CH-03000)
(DE83-015649; FERMILAB-Conf-82/55-THY; CONF-8206212-1) Avail: NTIS HC A03/MF A01

A hypothetical 500 TeV proton storage ring accelerator is discussed. Machine parameters are given, linear optics and betatron motions are discussed, questions of errors, tolerances and nonlinear resonances are surveyed and some of the demands on the detection apparatus, especially the apparent inevitability of multiple interactions per bunch crossing are discussed. DOE

N84-12856# Ohio State Univ., Columbus. Dept. of Chemistry.
KINETICS OF GROWTH AND DECAY OF EXCITED RARE-GAS ATOMS AND MOLECULES IN THE PULSE RADIOLYSIS OF PURE RARE GASES AND OF MIXTURES OF RARE GASES WITH MOLECULAR QUENCHING AGENTS Technical Progress Report
Richard F. Firestone 15 Jul. 1983 19 p refs
(Contract DE-AC02-76ER-01116)
(DE83-017016; DOE/ER-01116/36) Avail: NTIS HC A02/MF A01

The temporal behavior of vibrationally relaxed first triplet Kr2 in the presence of N2 was examined, and the rate constant for destructive quenching by N2 was evaluated at 298K. Its value is of the same order of magnitude as that for quenching of first triplet Ar2, but is somewhat smaller. This suggests that the krypton and argon excimers excite different electronic states of N2, the former leading to N2(A) and N2(B) and the latter principally to N2(C), in accord with the general rule that near-resonant energy transfer tends to be favored over vents which form products bearing significant translational energy. A new value for the spontaneous radiative decay constant of vibrationally relaxed first triplet Kr2 was determined. A generalized mechanism for decay of Paschen(ls) atoms and for concomitant growth and decay of bound-state excimer molecules was developed. DOE

N84-12857# Sandia Labs., Albuquerque, N. Mex.
USING INNER-SHELL X-RAYS AS AN ION-BEAM DIAGNOSTIC
G. R. Montry, E. J. McGuire, and E. J. T. Burns 1983 4 p refs Presented at the 5th Intern. Conf. on High Power Particle Beams, San Francisco, 12 Sep. 1983
(Contract DE-AC04-76DP-00789)
(DE83-017784; SAND-83-0617C; CONF-830911-12) Avail: NTIS HC A02/MF A01

A beam of protons impinging on a metal foil ionizes inner shell electrons, leaving an atom in an excited state. The atom then decays via a cascade of Auger or radiative transitions. The various radiative transitions resulting from the ionization of M-shell electrons in gold foils were analyzed and the results were combined with a 1-D hydrodynamic code in order to predict the time dependent X-ray signals emitted from a target irradiated by proton beams. A comparison of the theoretical and measured signals shows that inner shell X-rays can be used as a viable ion beam diagnostic. In particular, gold M-shell radiation was used to infer the proton current as a function of time with the applied B ion diode on the PROTO 1 accelerator. DOE

N84-12858# Sandia Labs., Albuquerque, N. Mex.
BEAM-TARGET INTERACTION OF INTENSE ION BEAMS: THEORY AND EXPERIMENT
T. A. Mehlhorn, J. M. Peek, J. N. Olsen, E. J. McGuire, A. V. Farnsworth, Jr., and F. C. Young (NRL, Washington, D.C.) 1983 7 p refs Presented at the 5th Intern. Conf. on High Power Particle Beams, San Francisco, 12 Sep. 1983
(Contract DE-AC04-76DP-00789)
(DE83-018264; SAND-83-1316C; CONF-830911-11) Avail: NTIS HC A02/MF A01

Work continued toward the goal of developing and experimentally verifying a numerical model that can accurately predict the stopping power of any ion in any target material at any density, temperature, and degree of ionization. Theoretical work to compute the stopping power of low Z ions in partially ionized material is described. Attempts to develop an accurate description of the atomic electron contribution to the stopping power, especially around the maximum of the curve are also examined. The atomic electron stopping power models (e.g., the local oscillator model, the generalized oscillator strength model, etc.) use realistic descriptions of atomic and solid state charge densities and energy levels. DOE

N84-12859# Argonne National Lab., Ill. Physics Dept.
THE 100% ALIGNMENT OF HYDROGEN EXCITED STATES IN BEAM-FOIL SPECTROSCOPY
H. G. Berry, D. Neek, L. P. Somerville, and J. Hardis 1983 2 p Presented at the Symp. on Atomic Spectry. (SAS-83), Berkeley, Calif., 12 Sep. 1983
(Contract W-31-109-eng-38)
(DE83-017963; CONF-830936-2) Avail: NTIS HC A02/MF A01

The relative population production of high n-states in hydrogen following electron capture by fast protons of 50 to 100 keV energy in beam-foil collisions was measured. The photon-emission from high n-states of the Balmer series (up to n = 15) was observed. DOE

N84-12860# Argonne National Lab., Ill.
NUCLEON-NUCLEON INTERACTIONS AND POLARIZED-BEAM (BOTH PROTON AND ANTIPROTON) FACILITIES AT LAMPF 2
Akihiko Yokosawa 1983 13 p refs Presented at the 3rd LAMPF 2 Workshop, Los Alamos, N. Mex., 18 Jul. 1983
(Contract W-31-109-eng-38)
(DE83-017215; CONF-830798-1) Avail: NTIS HC A02/MF A01

Experimental results of nucleon-nucleon interactions mainly up to 12 GeV/c are reviewed and polarized beam (both proton and antiproton) facilities at LAMPF 2 are proposed. DOE

N84-12861# California Univ., Berkeley. Lawrence Berkeley Lab. Nuclear Science Div.
QUARK-GLUON PLASMA FORMATION
M. Gyulassy 1983 11 p refs Presented at the 6th Intern. Balaton Topical Conf. on High Energy Nucl. Phys., Balatonfured, Hungary, 6-11 Jun. 1983
(Contract DE-AC03-76SF-00098)
(DE83-017742; LBL-16295; CONF-830674-4) Avail: NTIS HC A02/MF A01

The production of high baryon density plasmas at 10 GeV/A and low baryon density plasmas at 1 TeV/A via nuclear collisions is discussed. DOE

N84-12862# Brookhaven National Lab., Upton, N. Y. Physics Dept.
PROGRESS IN LATTICE GAUGE THEORY
Michael Creutz 1983 20 p refs Presented at the 4th Adriatic Meeting on Particle Phys., Dubrovnik, Yugoslavia
(Contract DE-AC02-76CH-00016)
(DE83-014055; BNL-33649; CONF-8306125-1) Avail: NTIS HC A02/MF A01

An overview of the current status of lattice gauge theory calculations is provided. Some technical points on group integration, gauge fixing, and order parameters are reviewed. Various Monte Carlo algorithms are discussed. Finally, alternatives to the Wilson action are considered in the context of universality for the continuum limit. DOE

N84-12863# Oak Ridge National Lab., Tenn. Atomic, Molecular and High Voltage Physics Group.
ELECTRON-MOLECULE INTERACTIONS IN GASES AND LIQUIDS: THE ELECTRON-ATTACHMENT PROCESS IN GASES AND NONPOLAR LIQUIDS
L. G. Christophorou (Tennessee Univ., Knoxville) and K. Siomos 1983 13 p refs Presented at the 3rd Intern. Swarm Seminar, Innsbruck, 3 Aug. 1983
(Contract W-7405-eng-26)
(DE83-017205; CONF-8308112-2) Avail: NTIS HC A02/MF A01

Efforts were made to relate knowledge on electron-molecule interactions in gases to that on similar processes in liquids. In addition, interphase studies of electron-molecule interactions were initiated to study the effects of density and nature of a medium on the isolated-molecule properties and interactions in the intermediate density range between a low-pressure gas and the condensed phase. The nature of electron attachment processes

in nonpolar liquids, the effect of the attaching gas molecule itself and the electron state on the attachment rate constant, and the relation of electron attachment processes in nonpolar liquids to those in gases are discussed. DOE

N84-12864# Ames Lab., Iowa.
NEW DEVELOPMENTS AND OPPORTUNITIES FOR NMR IN METAL-HYDROGEN SYSTEMS
R. G. Barnes 1983 3 p Presented at the Hydrogen in Metals Intern. Meeting, Wroclaw, 20-23 Sep. 1983
(Contract W-7405-eng-82)
(DE83-017696; IS-M-435; CONF-8309136-1) Avail: NTIS HC A02/MF A01

Nuclear magnetic resonance (NMR) methods continue to make strong contributions to understand crystal structure and atom locations and electronic structure in metal-hydrogen systems, as well as the changes that occur in these properties at structural and electronic phase transitions. NMR methods also afford an almost uniquely powerful approach to the study of hydrogen motion (diffusion). In this brief survey some recent developments in experimental methods and in types of systems studied are reviewed, and the consequences and opportunities for further investigation which these developments afford are outlined. DOE

N84-12865# Brookhaven National Lab., Upton, N. Y.
HADRON-HADRON COLLIDER GROUP
R. Palmer, J. Peoples, C. Ankenbrandt, C. Baltay, R. Diebold, E. Eichten, H. Gordon, P. Grannis, R. Lanou, and J. Leveille 1982 8 p refs Presented at the Elementary Particle Phys. and Future Facilities Summer Study, Snowmass, Colo., 28 Jun. 1982 Prepared in cooperation with Fermi National Accelerator Lab., Batavia, Ill., ANL, Ill., State Univ. of New York, Stony Brook, Brown Univ., Providence, R.I., Michigan Univ., Ann Arbor, Rockefeller Univ., N.Y., Pennsylvania Univ., Philadelphia and Columbia Univ., N.Y.
(Contract W-31-109-eng-38)
(DE83-010704; ANL-HEP-CP-83-22; CONF-8206120-9) Avail: NTIS HC A02/MF A01

A rough assessment of the characteristics of a hadron-hadron collider which could study the 1 TeV mass scale was made. Since there is very little theoretical guidance for the type of experimental measurements which could illuminate this mass scale, the types of experiments which were done at the ISR, and which are in progress at the SPS collider to these higher energies were extended. Experiment proposals are described including high transverse momentum jets, high transverse momentum (LC OMEGA)0 prime, direct single photons, Drell-Yan muon pair production, heavy Z0's decaying to (SIGMA)(-) (SIGMA) (+). technieta production eta/sub T/, and gluino production. Detector requirements are reviewed. DOE

N84-12866# Sandia Labs., Albuquerque, N. Mex.
MAGNETIC TRAPPING OF INTENSE ION BEAMS
Thomas P. Wright, Wendland Beezhold, Thomas A. Melhorn, and Thomas W. L. Sandford 1983 8 p refs Presented at the 5th Intern. Conf. on High Power Particle Beams, San Francisco, 12 Sep. 1983
(Contract DE-AC04-76DP-00789)
(DE83-017356; SAND-83-0115C; CONF-830911-2) Avail: NTIS HC A02/MF A01

Intense light ion beam sources are being developed for the inertial confinement fusion program. The possibility of trapping converging ion beams from such sources by imposition of a strong local mirror magnetic field in the target region and by using a thin stripping foil to suddenly increase the ionic charge is investigated. Applications of this concept include generation of compact hot ion rings for MFE studies, generation of intense K-shell radiation sources and heating thin foils to drive ICF targets. In the last application, the trapped ions reflex through the foil several times, leading to enhanced deposition and heating. The stripping, trapping and energy deposition of a 5.0 MeV Lithium beam is discussed. It is assumed that the Lithium ions are initially singly ionized and that they are ballistically focused onto the target foil. DOE

N84-12867# Oak Ridge National Lab., Tenn. Physics Div.
ELECTRON-ION COLLISIONS
D. H. Crandall 1982 75 p refs Presented at the NATO Adv. Study Inst. on the Atomic Phy. of Highly Ionized Atoms, Cargese, France, 7-18 Jun. 1982
(Contract W-7405-eng-26)
(DE83-017211; CONF-8206219-1-Draft) Avail: NTIS HC A04/MF A01

Basic physics aspects of inelastic processes of excitation, ionization, and recombination that occur during electron-ion collisions are discussed. Except for cases of illustration along isoelectronic sequences, only multicharged (at least +2) ions are specifically discussed with some emphasis on aspects associated with ionic charge. The viewpoint is primarily experimental with most attention to electron-ion interacting beams experiments. DOE

N84-12868# Stanford Linear Accelerator Center, Calif.
JET PRODUCTION AND HIGH p/SUB T/ PHENOMENA IN PHOTON-PHOTON REACTIONS
Norbert Wermes May 1983 21 p refs Presented at the 5th Intern. Workshop on Photon-Photon Collisions, Aachen, 13-16 Apr. 1983
(Contract DE-AC03-76SF-00515)
(DE83-016397; SU-SLAC-Pub-3121; CONF-8304110-3) Avail: NTIS HC A02/MF A01

The status of experimental investigations of high p sub T phenomena and jet production in photon-photon collisions is reviewed. Taking the challenging questions on hard scattering processes in gamma-gamma reactions as a guide, the experimental approach to these questions is summarized. Results from the PETRA experiments CELLO, JADE, PLUTO, and TASSO are presented including preliminary results on the Q(2)-dependence of jet cross sections. Experimental limitations and background problems are discussed. DOE

73 NUCLEAR AND HIGH-ENERGY PHYSICS

Includes elementary and nuclear particles; and reactor theory.

For space radiation see *93 Space Radiation.*

N84-12869# Los Alamos Scientific Lab., N. Mex.
SPACE NUCLEAR SAFETY PROGRAM Progress Report
S. E. Bronisz, comp. Jun. 1983 5 p ref
(Contract W-7405-eng-36)
(DE83-014070; LA-9794-PR) Avail: NTIS HC A02/MF A01

This technical monthly report covers studies related to the use of (238)PuO2 in radioisotope power systems carried out for the Office of Special Nuclear Projects of the US Department of Energy by Los Alamos National Laboratory. Most of the studies discussed here are ongoing. Results and conclusions described may change as the work continues. DOE

N84-12870# Los Alamos Scientific Lab., N. Mex.
SPACE REACTORS: PAST, PRESENT AND FUTURE
David Buden and Joseph A. Angelo (Florida Inst. of Technology) 1983 9 p Presented at the 18th Intersoc. Energy Conversion Eng. Conf., Orlando, Fla., 21 Aug. 1983
(Contract W-7405-eng-36)
(DE83-011177; LA-UR-83-1210; CONF-830812-4) Avail: NTIS HC A02/MF A01

In the 1990s and beyond, advanced-design nuclear reactors could represent the prime source of both space power and propulsion. Many sophisticated military and civilian space missions of the future will require first kilowatt and then megawatt levels of power. Key technology developments that accompanied past US space nuclear power development efforts, on-going programs, and reactor technologies that will satisfy megawatt power level needs and beyond are discussed. DOE

N84-12871# Oregon Univ., Eugene.
THEORY OF ELEMENTARY PARTICLES Annual Report
N. Deshpande 1 Dec. 1982 7 p refs
(Contract DE-AT06-76ER-70004)
(DE83-015904; DOE/ER-70004/351) Avail: NTIS HC A02/MF A01

High energy physics research is summarized. Topics include polarization experiments in particle physics, quark systems, electron-positron annihilation, the Dreil-Yan process, the Valon model for hadron structure, and X-ray optics and accelerators. DOE

N84-12872# Northwestern Univ., Evanston, Ill. Dept. of Physics and Astronomy.
THEORY OF HYPERFINE ANOMALIES IN MUONIC ATOMS
A. J. Freeman, J. V. Mallow (Loyola Univ., Chicago), J. P. Desclaux (BNL), and M. Weinert 1983 12 p refs Presented at the Yamada Conf. on Muon Spin Rotation and Assoc. Probl., Shimoda, Japan, 18 Apr. 1983
(Contract DE-AC02-76CH-00016)
(DE83-015392; BNL-33379; CONF-830455-8) Avail: NTIS HC A02/MF A01

Negative muon spin precession experiments by Yamazaki, et al. have found giant hyperfine anomalies in muonic atoms ranging from a few percent up to 36%. In order to understand their results, Breit interaction calculations based on atomic self consistent unrestricted Dirac-Fock solutions which explicitly include air electrons and the negative muon are presented. The Breit interaction results (including the relativistic correction for the bound muon g-factor), vary from near zero for (SIGMA)(*) C/N to -5% for (SIGMA)(+)Pd/Bh; this latter is much larger than the calculated muonic or nuclear Bohr-Weisskopf anomalies and much smaller than the 36% measured value. For (SIGMA)(+)Ni/Co a calculated range of results (depending on assumed electronic configurations) of -2.3 to -2.7% were found in excellent agreement with recent measurements of the Yamazaki group. This excellent agreement in (SIGMA)(+)Ni/Co provides strong support for the earlier suggestions that the discrepancy in the case of (SIGMA)(+) Pd/Rh is due to experimental factors. DOE

N84-12873# Idaho National Engineering Lab., Idaho Falls. Diagnostic Measurements Branch.
REAL-TIME ATTENUATION OF HEATED OPTICAL FIBERS IN A NUCLEAR REACTOR
Judy K. Partin, Jon O. Bolstad, and David R. Collins 1983 9 p refs Presented at the PHOTON: Intern. Conf. on Exhibition on Opt. Fibers and their Applicances, Paris, 16 May 1983
(Contract DE-AC07-76ID-01570)
(DE83-015141; EGG-M-06683; CONF-830580-2) Avail: NTIS HC A02/MF A01

Fiber-optic attenuation induced by gamma and neutron radiation in a reactor was characterized. In-situ attenuation measurements were made of promising waveguide materials during radiation exposure at elevated temperatures characteristic of reactor environments. Testing was done in a swimming pool type reactor generating about one kilowatt thermal power and producing dose rates of about ten billion n/sq cm/sec fast neutrons (> 1 MeV), ten billion n/sq/cm (2)/sec thermal neutrons, and six billion rad/h gamma radiation. Samples of state of the art radiation resistant waveguides were received from five manufacturers and tested simultaneously. One set of waveguides was held at 1800 C temperature and the other set remained at 200 C. Attenuation was monitored continuously in several spectral bands in the 600 to 1050 nanometer region. Test results are presented. DOE

N84-12874# Brookhaven National Lab., Upton, N. Y. Dept. of Nuclear Energy.
ASSESSMENT OF TRAC-PF1 AND RELAP5/MOD1 CODES WITH GE LARGE-VESSEL BLOWDOWN TEST
J. H. Jo Jun. 1983 7 p refs Presented at the Am. Nucl. Soc. Winter Meeting, San Francisco, 30 Oct. 1983
(Contract DE-AC02-76CH-00016)
(DE83-015384; BNL-NUREG-33352; CONF-831476-6) Avail: NTIS HC A02/MF A01

The large vessel blowdown Test No. 5801-15 was simulated with the TRAC-PF1 (Version 7.0) and RELAP5/MOD1 (Cycle 14) codes. The test facility consisted of a pressure vessel, 49 in. in diameter by 14 ft long, a 2.5 in. diameter converging-diverging nozzle and a blowdown line connected to the center of the upper part of the vessel (elevation from the bottom of the vessel 10.5 ft). The vessel was filled with saturated water up to 5.5 ft at 1060 psia. The test was initiated by rupturing a disc attached at the end of the nozzle. Blowdown phenomena such as critical blowdown flow and the level swell during blowdown from a partially water filled vessel was studied. Understanding of these phenomena is essential for the analysis of Loss-of-Coolant and steam generator steam line break accidents. DOE

N84-12875# Oak Ridge National Lab., Tenn.
THEORETICAL ASPECTS OF THROAT-LAUNCH MICROWAVE HEATING IN EBT-S
D. B. Batchelor, R. C. Goldfinger, D. A. Rasmussen, and D. W. Swain 1983 15 p refs Presented at the Workshop on Advanced Bumpy Torus Concepts, Rancho Santa Fe, Calif., 11 Jul. 1983
(Contract W-7405-eng-26)
(DE83-015762; CONF-830758-1) Avail: NTIS HC A02/MF A01

A simple radiation power balance model is used to gain insight into the role of antenna directivity and polarization control when throat launch is used to improve core heating efficiency and to separate ring heating from core heating. Ray tracing calculations are used to illustrate energy flow and absorption behavior for various throat launch positions and angles. DOE

N84-12876# Department of Energy, Washington, D. C. Office of Energy Research.
NEW FACILITIES FOR THE US HIGH-ENERGY PHYSICS PROGRAM
Jul. 1983 75 p
(DE83-016589; DOE/ER-0169) Avail: NTIS HC A04/MF A01

The 1983 Subpanel on New Facilities of the High Energy Physics Advisory Panel made the following recommendations: (1) the Subpanel unanimously recommends the immediate initiation of a multi-TeV high-luminosity proton-proton collider project with the goal of physics experiments at this facility at the earliest possible data; (2) the Subpanel recommends the rapid completion of current construction projects, Tevatron and the SLAC Linear Collider (SLC), the upgrading of the Cornell Electron Storage Ring (CESR) and associated detectors, and the thorough utilization of all existing facilities; (3) the Subpanel recommends that Fermilab not proceed at this time with the Dedicated Collider (DC); (4) by a majority vote, the Subpanel recommends that the Colliding Beam Accelerator (CBA) project at Brookhaven not be approved; (5) the Subpanel recommends that technology research and development, particularly advanced accelerator research and development, be strongly supported. DOE

N84-12877# Colorado Univ., Boulder. Lab. for Nuclear Physics.
LOW ENERGY NUCLEAR PHYSICS AND ACCELERATOR DEVELOPMENT Final Report, 1 Feb. 1981 - 31 Mar. 1983
31 Mar. 1983 86 p refs
(Contract DE-AC02-81ER-40014)
(DE83-013384; DOE/ER-40014/T1) Avail: NTIS HC A05/MF A01

The nuclear physics experimental program is described in detail. Transfer reactions, charge exchange reactions, elastic and inelastic scattering, total neutron cross sections ((3)He, xn), reactions on heavy targets, (3)He-induced fission of nuclei $159 < A < 232$, and the (28)Si(D, pn) reaction were studied. Energy level studies by gamma spectroscopy are described. The operations and facility development of the 52-inch variable energy AVF cyclotron are detailed. Publications are listed. DOE

N84-12878# Stanford Linear Accelerator Center, Calif.
PHYSICS AT VERY HIGH ENERGIES
Anne Mosher 1983 681 p refs Proc. of the Summer Inst. on Particle Phys., 16-27 Aug. 1982

(Contract DE-AC03-76SF-00515)
(DE83-012854; SLAC-259; CONF-820897) Avail: NTIS HC A99/MF A01

Separate abstracts were prepared for the 26 papers from the SLAC Summer Institute on Particle Physics. DOE

N84-12879# Stanford Linear Accelerator Center, Calif.
TAU AND B LIFETIME MEASUREMENTS FROM THE MARK 2
Gail G. Hanson 20 Jul. 1983 3 p refs Presented at the Intern. Europhys. Conf. on High Energy Phy., Brighton, England, 20-27 Jul. 1983
(Contract DE-AC03-76SF-00515)
(DE83-018219; SU-SLAC-Pub-3187; CONF-830718-6) Avail: NTIS HC A02/MF A01

Measurement of the tau lifetime checks whether the tau couples to the charged weak current with the same universal coupling strength as the e and (SIGMA). The lifetime of bottom hadrons measures the weak coupling between the bottom quark and the charm and up quarks. Measurements of these lifetimes were made with the MARK II detector at the e(+) e(-) storage ring PEP at 29.0 GeV center-of-mass energy. DOE

N84-12880# Los Alamos Scientific Lab., N. Mex.
DEVELOPING A 500-eV PROTON BEAM
Edwin P. Chamberlin, John F. Benage, Jr., and Harry E. Williams 1983 13 p refs Presented at the Polarized Ion Workshop, Vancouver, 23 May 1983
(Contract W-7405-eng-36)
(DE83-012781; LA-UR-83-1466; CONF-830591-1) Avail: NTIS HC A02/MF A01

Tests have been carried out which indicate that H intensity limitations in lamb shift polarized ion sources result from large divergence in the 500 eV H+ ion beam. Intensity limitations due to other effects are not yet measurable. DOE

N84-12881# Oak Ridge National Lab., Tenn.
PATRAM '83: 7TH INTERNATIONAL SYMPOSIUM ON PACKAGING AND TRANSPORTATION OF RADIOACTIVE MATERIALS, SUMMARIES
1983 483 p refs Symp. held in New Orleans, 15-20 May 1983
(Contract W-7405-eng-26)
(DE83-012390; CONF-830528-Summ.) Avail: NTIS HC A21/MF A01

Papers were presented at the following sessions: international regulations; materials, fracture toughness of ferritic steels; risk analysis techniques; storage in packagings; packaging design considerations; monolithic cast iron casks; risk analysis; facility/transportation system interface; research and development programs; UF6 packagings; national regulations; transportation operations and traffic; containment, seals, and leakage; radiation risk experience; emergency response; structural modeling and testing; transportation system planning; institutional issues and public response; packaging systems; thermal analysis and testing; systems analysis; structural analyses; quality assurance; packaging and transportation systems; physical protection; criticality and shielding; transportation operations and experience; standards; shock absorber technology; and information and training for regulatory compliance. Individual summaries are title listed. DOE

N84-12882# Los Alamos Scientific Lab., N. Mex.
EFFECT OF RF STRUCTURE ON CUMULATIVE BEAM BREAKUP
R. L. Gluckstern (Maryland Univ.), R. K. Cooper, and P. J. Channell 1983 5 p refs Presented at the 12th Intern. Conf. on High Energy Accelerators, Batavia, Ill., 11-16 Aug. 1983
(Contract W-7405-eng-36)
(DE83-017302; LA-UR-83-2317; CONF-830822-5) Avail: NTIS HC A02/MF A01

The effect of RF structure of a linac beam on cumulative beam breakup in the presence of external focusing is examined. Starting with the difference equations of Helm and Loew, two forms of an exact analytic solution for coasting beams are derived: as a sum of products of Gegenbauer polynomials involving external focusing and RF structure, and as an integral involving these same parameters. The continuous-beam limit of Neil, Hall, and Cooper is obtained as the bunch separation goes to zero. An explicit solution is presented for the steady state, including modulation of the incoming displacement, showing both stable and unstable behavior with distance. Asymptotic amplitude expressions are derived for the transient solution, which leads to even larger beam displacements. Approximate solutions also are obtained for accelerated and decelerated beams. Comparison with numerical simulations are presented. DOE

N84-12883# California Univ., Livermore. Lawrence Livermore Lab.
HAZARDS CONTROL DEPARTMENT ANNUAL TECHNOLOGY REVIEW, 1982
R. V. Griffith, ed. 15 Jun. 1983 72 p refs
(Contract W-7405-eng-48)
(DE83-015598; UCRL-50007-82) Avail: NTIS HC A04/MF A01

The period from October 1981 to September 1982, is covered by three major sections. The first section, progress reports, includes studies in areas of industrial hygiene, instrument development, environmental protection, radiation protection and fire safety. The second section, technical notes, contains reports on interesting activities of a more limited scope. The third section lists recent publications. DOE

N84-12884# California Univ., Davis.
TRANSMISSION OF FAST NEUTRONS FROM THE Li(d,xn) REACTION THROUGH THICK IRON
D. L. Johnson, F. M. Mann, L. L. Carter, G. L. Woodruff (Washington Univ.), F. P. Brady, J. L. Romero, J. L. Ullmann, M. L. Johnson, and C. M. Castaneda May 1983 12 p refs Presented at the 6th Intern. Conf. on Radiation Shielding, Tokyo, 16-20 May 1983 Prepared in cooperation with Westinghouse Hanford Co., Richland, Wash.
(Contract DE-AC06-76FF-02170)
(DE83-015975; HEDL-SA-2723-FP; CONF-830538-17) Avail: NTIS HC A02/MF A01

Measurements of the spectra of neutrons that leaked through about 30 cm of iron were performed. The neutron source was produced by a beam of 35 MeV deuterons which was stopped in a target of lithium as in the Fusion Materials Irradiation Test (FMIT) facility. The source spectrum peaks near 14 MeV in the forward direction, but is broad and has a small tail that extends to 50 MeV. The leakage spectra were observed from about 10 keV to 20 MeV using proton recoil proportional counters and an NE213 liquid scintillator. Measurements were also obtained of the energy deposited by neutron and gamma radiation within the iron using thermoluminescent detectors (TLDs) and also of the flux-spectra of gamma rays emitted from the iron using the NE213 detector. Monte Carlo calculations were performed using ENDF/B-5 and other cross sections for direct comparison to experimental results. The results of the comparison are discussed. DOE

N84-12885# California Univ., Berkeley. Lawrence Berkeley Lab. Nuclear Science Div.
NEW STATISTICAL AND NON-STATISTICAL EFFECTS IN DEEP INELASTIC HEAVY-ION COLLISIONS
L. g. Moretto Mar. 1983 19 p refs Presented at the Intern. Symp. on Nucl. Phys. at Large Tandem Accelerators, Legnaro-Padova, Italy, 15-17 Mar. 1983
(Contract DE-AC03-76SF-00098)
(DE83-015732; LBL-16371; CONF-830384-1) Avail: NTIS HC A02/MF A01

The physics of deep inelastic heavy ion collisions is reviewed. Three aspects are selected for illustration. The first is the problem posed by the angular distributions. The role of quantal fluctuations (diffraction) and of dynamical fluctuations is discussed. The possibility of extracting angular momentum fluctuations from the angular distribution width is pointed out. The likely sources of angular momentum fluctuations are discussed. The second problem is that of energy dissipation and partition. The experimental evidence from thermal equilibrium is reviewed and experiments to

test thermal equilibrium through the measurement of the variance in the energy distribution are suggested. The correlation between energy loss and the mass variance is reviewed in terms of the mass transfer mechanism. Possible ways to determine the mass of the transferred particle are illustrated. The third problem considered is the experimental lack of mass drift in the mass distributions vs Z-value when it is expected on the basis of potential energy considerations. Author

N84-12886# California Univ., Berkeley. Lawrence Berkeley Lab. Accelerator and Fusion Research Div.
EFFICIENT RADIATION-HARDENED, 400- AND 800-keV NEUTRAL-BEAM INJECTION SYSTEMS
O. A. Anderson, W. S. Cooper, J. A. Fink, D. A. Goldberg, L. Ruby, L. Soroka, and J. Tanabe Apr. 1983 9 p refs Presented at the 5th Topical Meeting on Technol. of Fusion Energy, Knoxville, Tenn., 26-28 Apr. 1983
(Contract DE-AC03-76SF-00098)
(DE83-015691; LBL-15066; CONF-830406-94) Avail: NTIS HC A02/MF A01

Designs are presented for two negative-ion based neutral beam lines with reactor-level power output. Both beam lines make use of such technologically advanced features as high-current-density surface-conversion ion sources; transverse-field-focussing acceleration and transport; and laser photodetachment. Beam and vacuum calculations are given for one design and a proof-of-principle test system currently under development is described. DOE

N84-12887# Oak Ridge National Lab., Tenn.
GENERATION OF MONOENERGETIC POSITRONS
L. D. Hulett, Jr., J. M. Dale, P. D. Miller, Jr., C. D. Moak, S. Pendyala (State Univ. of New York), W. Triftshaeuser (Hochschule der Bundeswehr), R. H. Howell, and R. A. Alvarez 1983 7 p refs Presented at the NATO Advanced Res. Workshop on Positron Scattering in Gases, London, 19 Jul. 1983 Prepared in cooperation with LLNL, Calif.
(Contract W-7405-eng-26)
(DE83-015535; CONF-830770-2) Avail: NTIS HC A02/MF A01

Many experiments were performed in the generation and application of monoenergetic positron beams using annealed tungsten moderators and fast sources of Co(58), Na(22), C(11), and LINAC bremsstrahlung. The degrees of success from various approaches are compared. Moderators made from both single crystal and polycrystal tungsten were tried. Efforts to grow thin films of tungsten to be used as transmission moderators and brightness enhancement devices are in progress. DOE

N84-12888# Los Alamos Scientific Lab., N. Mex.
LONGITUDINAL SPACE-CHARGE EFFECTS IN BUNCHED BEAMS
Paul J. Channell 1983 8 p refs Presented at the 12th Intern. Conf. on High Energy Accelerators, Batavia, Ill., 11-16 Aug. 1983
(Contract W-7405-eng-36)
(DE83-017305; LA-UR-83-2339; CONF-830822-6) Avail: NTIS HC A02/MF A01

The theory of the longitudinal stability of a single bunch is reviewed. Many stability analyses are inconsistent because of the neglect of nonlinear effects. The stability problem to be able to include nonlinear phenomena and derive the usual coupled-mode instabilities. The effect of nonlinearities are examined and induction of a bunched beam to look like an unbunched beam with the peak current; in other words, the Boussard criterion must be used. DOE

74 OPTICS

Includes light phenomena.

N84-12889*# National Aeronautics and Space Administration. Goddard Space Flight Center, Greenbelt, Md.
LUMINOSITY ENHANCEMENT IN RELATIVISTIC JETS AND ALTERED LUMINOSITY FUNCTIONS FOR BEAMED OBJECTS
C. Megan Urry and R. A. Shafer Aug. 1983 23 p refs Submitted for publication
(NASA-TM-85053; NAS 1.15:85053) Avail: NTIS HC A02/MF A01 CSCL 20F

Due to relativistic effects, the observed emission from relativistic jets is quite different from the rest frame emission. Systematic differences between the observed and intrinsic intensities of sources in which jet phenomena are occurring are discussed. Assuming that jets have a power law luminosity function of a slope B, the observed luminosity distribution as a function of the velocity of the jet, the spectral index of the rest frame emission, and the range of angles of the jets relative to our line of sight are calculated. The results is well-approximated by two power laws, the higher luminosity end having the original power law index X and the lower luminosity end having a flattened exponent independent of B and only slightly greater than 1. A model consisting of beamed emission from a jet and unbeamed emission from a stationary central component is investigated. The luminosity functions for these two-component sources are calculated for two ranges of angles. For sources in which beaming is important, the luminosity function is much flatter. Because of this, the relative numbers of "beamed" and "unbeamed" sources detected on the sky depend strongly on the luminosity at which the comparison is made. Author

N84-12890# Air Force Systems Command, Wright-Patterson AFB, Ohio. Foreign Technology Div.
THE POSSIBILITY OF AMPLIFYING INFRARED RADIATION BY HIGH-PRESSURE REACTING GAS
V. A. Kochelan and Yu. A. Kubibnyy 22 Jun. 1983 11 p refs Transl. into ENGLISH from Ukr. Fiz. Zh. (USSR), v. 17, no. 1, Jan. 1972 p 149-151
(AD-A131086; FTD-ID(RS)T-0569-83) Avail: NTIS HC A02/MF A01 CSCL 17/5

The process of stimulated light emission which is preceded by a chemical reaction, from which populated molecules are formed is being investigated. Author

N84-12891# ITT Electro-Optical Products Div., Roanoke, Va.
ULTRA LOW LOSS OPTICAL FIBER CABLE ASSEMBLIES, VOLUME 2 Final Technical Report, Dec. 1978 - Dec. 1982
C. Hand 7 Jun. 1983 285 p 2 Vol.
(Contract DAAB07-78-C-2922)
(AD-A132008; ITT-80-22-07-Vol-2;
CECOM/DRSEL-TR-78-2922F-2) Avail: NTIS HC A13/MF A01 CSCL 17/2

This final report describes the development of tactical fiber optic cable assemblies. The effort was to develop a tactically deployable cable capable of a transmission rate of 20 Mb/s over 8 km repeaterless lengths. The optical performance required to meet the requirements is a dispersion of less than 2 ns/km and an attenuation of less than 5 dB/km at 0.85 micrometer combined with connector interface losses of less than 1 dB (1.5 dB at bulkhead receptacle). Experimental results of fiber, cable, and cable assembly testing are reported. GRA

N84-12892# ITT Electro-Optical Products Div., Roanoke, Va.
ULTRA LOW LOSS OPTICAL FIBER CABLE ASSEMBLIES, VOLUME 1 Final Technical Report, Dec. 1978 - Dec. 1982
C. Hand 7 Jun. 1983 135 p 2 Vol.
(Contract DAAB07-78-C-2922)
(AD-A132007; ITT-80-22-07-Vol-1;
CECOM/DRSEL-TR-78-2922F-1) Avail: NTIS HC A07/MF A01 CSCL 17/2

This final report describes the development of tactical fiber optic cable assemblies. The effort was to develop a tactically deployable cable capable of a transmission rate of 20 Mb/s over 8 km repeaterless lengths. The optical performance required to meet the requirements is a dispersion of less than 2 ns/km and an attentuation of less than 5 dB/km at 0.85 micrometers combined with connector interface losses of less than 3 dB (1.5 dB at bulkhead receptacle). Experimental results of fiber, cable, and cable assembly testing are reported. GRA

N84-12893# Galileo Electro-Optics Corp., Sturbridge, Mass.
EVALUATION OF MULTICOMPONENT FLUORIDE GLASS CANDIDATES FOR DOUBLE CRUCIBLE DRAWN OPTICAL FIBER Final Technical Report, 15 Jan. 1981 - 15 Jan. 1983
James L. Mansfield Hanscom AFB, Mass. RADC Jun. 1983 64 p
(Contract F19628-81-C-0073)
(AD-A131932; RADC-TR-83-131) Avail: NTIS HC A04/MF A01 CSCL 11/2

Fluorozirconate and fluorohafnate glass compositions have been investigated as potential candidates for mid-IR transmitting optical communication fiber. Suitable candidates have been identified, and multi-meter lengths of low strength, Teflon clad fiber have been drawn. The preform draw method has been found more suitable than the single crucible draw method. Various bulk fabrication methods have been developed, and small quantities of optical quality glass have been cast. These glasses have been well characterized in terms of physical properties. Author (GRA)

N84-12894# Colorado State Univ., Fort Collins. Dept. of Physics.
NOVEL TECHNIQUES FOR ENHANCED REFLECTIVITY INFRARED MIRRORS Final Report
James R. Sites Kirtland AFB, N. Mex. AFWL Jul. 1983 42 p
(Contract F29601-82-K-0009; AF Proj. 317J)
(AD-A131924; AFWL-TR-83-13) Avail: NTIS HC A03/MF A01 CSCL 07/4

Three types of thin films for high reflectivity mirror applications have been deposited and characterized. High and low refractive index oxide films deposited by ion beam sputtering have low optical absorption and sound mechanical properties. Refractory metal films produced by laser photodissociation display good reflectivity. Chemical vapor deposition of ZnSe layers has been used to explore the crystalline structures possible with different substrates and growth parameters. Author (GRA)

N84-12895# California Univ., Berkeley. Lawrence Berkeley Lab. Applied Physics and Laser Spectroscopy Group.
NOVEL METHOD FOR THE STUDY OF OPTICAL PROPERTIES OF SURFACES
Nabil M. Amer and Marjorie A. Olmstead Nov. 1982 15 p refs Presented at the 2nd IUPAP Semiconductor Symp. on Surfaces and Interfaces, Trieste, Italy, 30 Aug. - 3 Sep. 1982
(Contract DE-AC03-76SF-00098; DARPA Order 3343)
(DE83-012899; LBL-15743; CONF-8208146-1) Avail: NTIS HC A02/MF A01

A new technique, photothermal displacement spectroscopy, for probing the optical properties of surfaces is presented. Optical spectra are obtained directly, and surface and bulk contributions are easily and unambiguously differentiated. The technique is well suited for in situ ultrahigh vacuum experiments. DOE

N84-12896# Brookhaven National Lab., Upton, N. Y.
OPERATION OF THE BROOKHAVEN MPS FACILITY
A. Etkin, K. J. Foley, R. S. Longacre, W. A. Love, T. W. Morris, E. D. Platner, V. A. Polychronakos, A. C. Saulys, C. D. Wheeler, M. A. Kramer (City Coll. of N.Y.) et al 1983 8 p refs Presented at the Intern. Europhys. Conf. on High Energy Phys. Brighton, United Kingdom, 20-27 Jul. 1983
(Contract DE-AC02-76CH-00016)
(DE83-015383; BNL-33326; CONF-830718-1) Avail: NTIS HC A02/MF A01

The multiparticle spectrometer was recently equipped with a set of narrow cell drift chambers employing a compact, inexpensive, readout scheme. This has given an order of magnitude improvement in beam rate as well as better spatial resolution. Two experiments were completed in the first year of operation, a good test of the system. This type of a drift chamber arrangement is ideal for use at high luminosity hadron colliders. Doe

N84-12897# Cornell Univ., Ithaca, N.Y. High Energy Synchrotron Source.
DESIGN OF DOUBLY FOCUSING, TUNABLE (5 - 30 keV), WIDE-BANDPASS OPTICS MADE FROM LAYERED SYNTHETIC MICROSTRUCTURES
D. H. Bilderback, B. M. Lairson, T. W. Barbee, Jr. (Stanford Univ.), G. E. Ice (ORNL), and C. J. Sparks, Jr. (ORNL) 1982 34 p refs Presented at the Intern. Conf. on X-Ray and VUV Synchrotron Radiation Instr., Hamburg, 9 Aug. 1982
(Contract W-7405-eng-26)
(DE83-015492; CONF-820839-9) Avail: NTIS HC A03/MF A01

Layered Synthetic Microstructures (LSMs) show great promise as focusing, high-throughput, hard X ray monochromators. Experimental reflectivity vs. energy curves were obtained on carbon-tungsten and carbon-molybdenum LSMs of up to 260 layers in thickness. Reflectivities for three flat LSMs with different bandpasses were 70% with (RADICAL)E/E = 5.4%, 66% with (RADICAL)E/E = 1.4%, AND 19% with (RADICAL)E/E = 0.6%. A new generation of variable bandwidth optics using two successive LSMs is proposed. The first element is an LSM deposited on a substrate that is water cooled as it intercepts direct radiation from a storage ring. The bandpass is adjusted by choosing interchangeable first elements from an assortment of LSM's with different bandpasses (for example, (RADICAL)E/E = 0.005, 0.01, 0.02, 0.05, 0.1). The second LSM consists of a multilayered structure with a 10% bandpass built onto a flexible substrate that is bent for sagittal focusing. The result doubles focusing optics with an adjustable energy bandpass that are tunable from 5 to 30 keV. DOE

N84-12898# University of Southern California, Marina del Rey. Inst. for Physics and Imaging Science.
LARGE-AREA MERCURIC IODIDE PHOTODECTORS
J. Markakis, C. Ortale, W. Schnepple, J. Iwanczyk, and A. Dabrowski 1983 8 p Presented at the Nucl. Sci. Symp., San Francisco, 19 Oct. 1983 Prepared in cooperation with Edgerton, Germeshausen and Grier, Inc., Goleta, Calif.
(Contract DE-AC08-83NV-10282)
(DE83-013035; CONF-831015-2) Avail: NTIS HC A02/MF A01

The limits of the active area of mercuric iodide photodetectors imposed by the size of available crystals, electronic noise, and the uniformity of charge carrier collection are discussed. Theoretical calculations of the photodetector electronic noise are compared with the experimental results. Different entrance contacts were studied including semitransparent palladium films and conductive liquids. HgI2 photodetectors with active area up to 4 sq cm are matched with NaI(Tl) and CsI(Tl) scintillation crystals and are evaluated as gamma radiation spectrometers. DOE

N84-12899# California Univ., Livermore. Lawrence Livermore Lab. Environmental Sciences Div.
PROCESS, PRODUCT, AND WASTE-STREAM MONITORING WITH FIBER OPTICS
Fred P. Milanovich and Tomas Hirschfeld Jul. 1983 13 p refs Presented at the Instrument Soc. of Am. Conf. and Exhibit, Houston, 11-14 Oct. 1983
(Contract W-7405-eng-48)
(DE83-011102; UCRL-89026; CONF-8310102-1) Avail: NTIS HC A02/MF A01

Fiber optic technology, motivated by communications and defense applications, has advanced significantly the past ten years. In particular, advances were made in visible radiation transmission efficiency with concurrent reductions in fiber size, weight, and cost. These advances in fiber optic technology were coupled with analytical fluorescence analysis to establish a new technology - remote fiber fluorimetry (RFF). Laser-based RFF offers the potential to measure and monitor from one central and remote laboratory, on-line, and in near real time, trace (ppM) to substantial (g/L) concentrations of selected chemical species in typical process, product, and waste streams. The fluorimeter consists of a fluorescence or Raman spectrometer; unique coupling optics that separates input excitation (laser) radiation from return (fluorescence) radiation; a fiber optic cable; and an optrode - a terminal that interfaces the fiber to the measurement point, which is designed to respond quantitatively to a particular chemical species. At LLNL, research is underway into optrodes that measure pressure,

temperature, and pH and those that detect and quantify various actinides, sulfates, inorganic chloride, hydrogen sulfide, aldehydes, and alcohols. DOE

N84-12900# California Univ., Livermore. Lawrence Livermore Lab. Materials Fabrication Div.

FABRICATION OF MACHINED OPTICS FOR PRECISION APPLICATIONS

Norman J. Brown, Robert R. Donaldson, and Daniel C. Thompson 2 Aug. 1983 17 p refs Presented at the SPIE Symp. on Optical Surface Technol., Garmisch-Partenkirchen, West Germany, 12-14 Apr. 1983

(Contract W-7405-eng-48)

(DE83-015720; UCRL-89674; CONF-8304117-1) Avail: NTIS HC A02/MF A01

Precision machining is today an important increment to the optical fabrication repertoire; adding much, replacing little. Through a historical survey and a discussion of machine design, a feel to the pace of development and the degree to which further developments are anticipated are given. Metrology, for example, has advanced to the level of a few atom layers. Further dramatic increases in capability from metrology precision are unlikely, but developments from more sophisticated uses of metrology and servo-technology are surely possible. Machine design, environmental control, and numerical control are being applied with increasing understanding and sophistication. Tooling and machinability studies are in their infancy, in many cases waiting for third generation machines for sufficient control to sort out effects. Polishing techniques are in a similarly primitive state. Finally, precision machining does not stand alone as a fabrication process, that successful applications will stem from the cooperative planning of optical designers, machine technologists, and optical finishers. DOE

N84-12901# Sandia Labs., Albuquerque, N. Mex.

DEVELOPMENT OF A PORTABLE SPECULAR REFLECTOMETER FOR MONITORING SOLAR-MIRROR MATERIALS

R. B. Pettit, J. M. Freese, and A. R. Mahoney 1983 29 p refs Presented at the 27th Ann. Intern. Tech. Symp. on High Speed Phot., Videography and Photonics, San Diego, Calif., 21 Aug. 1983

(Contract DE-AC04-76DP-00789)

(DE83-016065; SAND-83-0912C; CONF-830874-17) Avail: NTIS HC A03/MF A01

The general design requirements of a portable reflectometer which can determine the specular reflectance properties of solar mirror materials are presented. Based on these considerations, a prototype instrument was developed. The operation and performance of this instrument are discussed, including the accuracy, stability, reproducibility, temperature response, and outdoor performance. Instrument limitations and future developments in this area are discussed. DOE

N84-12902# Chicago Univ., Ill.

FUNDAMENTALS AND TECHNIQUES OF NONIMAGING OPTICS, VOLUME 2 Technical Progress Report

Roland Winston and Joseph J. OGallagher 15 Jun. 1983 108 p refs 2 Vol.

(Contract DE-AC02-80ER-10575)

(DE83-015447; DOE/ER-10575/T1) Avail: NTIS HC A06/MF A01

The formalism describing the operation is being defined, nonimaging concentrators and are being designed, and experiments and analytical studies are being conducted to evaluate the performance of new designs. In addition, components and materials particularly suited for use with these techniques were studied, and applications with an emphasis on solar energy concentration were explored. The motivation for the basic principles of nonimaging optics as they developed before 1978 are surveyed. The present status of the subdiscipline of nonimaging optics is summarized and an overview of the potential for future developments which is just beginning to emerge is presented. DOE

N84-12903# Ames Lab., Iowa.

ULTRASENSITIVE OPTICAL ROTATION AND REFRACTIVE-INDEX MEASUREMENTS

Edward S. Yeung 1983 8 p refs Presented at the 27 Ann. Intern. Tech. Symp. on High Speed Phot., Videography and Photonics, San Diego, Calif., 21-25 Aug. 1983

(Contract W-7405-eng-82)

(DE83-018078; IS-M-452; CONF-830874-25) Avail: NTIS HC A02/MF A01

Among the many techniques that benefited from the development of laser technology, two examples are the improved detectability in optical rotation and in refractive index measurements. In conjunction with liquid chromotography, one takes advantage of the improved detectability to study molecules that are present in small quantities in fairly complex samples, such as biological fluids and fossil fuels. The high degree of collimation of the laser allows better levels of extinction to be achieved between crossed polarizers. The amount of scattered light, and thus the amount of depolarization, is greatly reduced. This then allows small rotations of the polarization axis of light to be detected. A detectability of 1.5 x 10 to the 5th power degrees is achieved. The high monochromaticity of the laser brings about new applications of Fabry-Perot interferometry. The interference fringes are used to monitor refractive index changes inside the interferometer. In conjunction with a flow cell interfaced to a liquid chromatograph, a detectability of 4 x 10 to the 9th power RI units is possible. DOE

N84-12904# Los Alamos Scientific Lab., N. Mex. Nondestructive Testing Unit.

SURVEY OF FLASH X-RAY TECHNIQUES AND APPLICATIONS

Lawrence E. Bryant, Jr. and Jake P. Lucero 1983 7 p Presented at the 27th Ann. Intern. Tech. Symp. on High Speed Phot., Videography and Photonics, San Diego, Calif., 21-16 Aug. 1983

(Contract W-7405-eng-36)

(DE83-017234; LA-UR-83-2400; CONF-830874-20) Avail: NTIS HC A02/MF A01

Flash X-ray diagnostics of high speed dynamic tests need to be reliable as testing is quite expensive and time consuming. Preparation for a first time test involves many partial or preliminary tests to verify adequacy of X-ray energy, X-ray exposure, film/screen combination, film holder protection, flash X-ray generator protection, triggering, and timing techniques. Once these preparations are successfully completed, very informative results are attainable for a variety of tests including jetting, welding, and casting. DOE

N84-12905# Los Alamos Scientific Lab., N. Mex. Nondestructive Testing Unit.

HIGH-SPEED VIDEOGRAPHY COMBINED WITH AN X-RAY IMAGE INTENSIFIER FOR DYNAMIC RADIOGRAPHY

Lawrence E. Bryant, Jr. 1983 5 p Presented at the 27th Ann. Intern. Tech. Symp. on High Speed Phot., Videography and Photonics, San Diego, Calif., 21-26 Aug. 1983

(Contract W-7405-eng-36)

(DE83-017233; LA-UR-83-2399; CONF-830874-21) Avail: NTIS HC A02/MF A01

The Spin Physics SP-2000 high speed video system is combined with an X ray source, a dynamic event having internal (not directly visible) movement and an X-ray image intensifier to perform dynamic radiography. The cesium iodide input fluor and P-20 output fluor of the image intensifier rapidly decays to allow X-ray imaging up to 12,000 pictures per second. Applications of this technique include internal functioning of a compressor, turbulent-water action, and other mechanical actions. DOE

N84-12906# Deutsche Bundespost, Darmstadt (West Germany). Forschungsinst.

ATTENUATION MEASUREMENTS BETWEEN 840 AND 1620 NM ON AN OPTICAL CABLE IN BERLIN [DAEMPFUNGSMESSUNGEN ZWISCHEN 840 NM UND 1620 NM AN EINER OPTISCHEN KABELSTRECKE IN BERLIN]

Walter Heitmann Apr. 1983 19 p refs In GERMAN; ENGLISH summary
(FI-465-TBr-22) Avail: NTIS HC A02/MF A01

Spectral attenuation measurements between 840 nm and 1620 nm were performed on an optical cable of 3.6 km length with 13 gradient index fibres. A grating monochromator as optical source and a cooled lead sulfide photoresistor as detector were used. The upper limit of the dynamic range of the measuring system is between 35 dB and 40 dB. Attenuation values from 2.8 dB/km to 3.3 dB/km are found at 850 nm which are clearly below those reported by the company. The region around 1300 nm is characterized by a narrow-band minimum between two OH-absorption bands. Losses at 1300 nm range from 2.0 dB/km to 2.8 dB/km. The optical cable can therefore be used within certain limitations for this spectral region. Values between 1.9 dB/km and 2.8 dB/km are measured at 1550 nm. Author (ESA)

N84-12907# European Space Agency, Paris (France).
RETROREFLECTOR YO3: STUDY OF THE OPTICAL PROPERTIES OF PROTECTED MIRRORS
M. Dinguirard Sep. 1983 30 p refs Transl. into ENGLISH of "Retroreflecteur Y03: Etude des Proprietes Opt. des Miroirs Proteges" rept. CERT-5/6026-DERO ONERA, Toulouse, Oct. 1976
(ESA-TT-789; CERT-5/6026-DERO) Avail: NTIS HC A03/MF A01

The influence of a dielectric deposit (silica or alumina) on the reflective power of the mirrors which make up a trihedron was analyzed. This deposit, between 2 and 6 microns thick, ensures thermal protection of the retroreflector in the lunar environment. A reflective power of 85% per mirror is specified for an aluminum reflective coating. The analysis shows that deposit thickness must be controlled to within limits which ensure that the interferences do not lead to losses of more than 5%. If feasibility tests result in reflective powers < 85%, interferential layers can be used to raise the reflection of the aluminum from 90% to 96%. The thick silica deposit intended for thermal protection is applied on top of this treatment. However, this solution makes the mirror very selective, and could prejudice thermal qualities. Author (ESA)

N84-12908# Fondazione Ugo Bordoni, Rome (Italy).
ECONOMIC STUDY OF LONG DISTANCE OPTICAL FIBRE LINKS
G. Bonaventura (ASST, Rome), 0. Cottatellucci (Ist. Superiore delle Poste e delle Telecomunicazioni, Rome), B. Daino, G. Demarchis, U. Mocci, and G. Ravaioli Jun. 1982 8 p
(FUB-38-1982; C-11) Avail: NTIS HC A02/MF A01

Economic comparison of configurations using different types of fibers, cables, laying conditions and transmission systems to be used for long distance optical communication is summarized. Multimode graded-index fibers with a bandwidth of 800 MHz (at 1300 mm) give more economical plants than fibers with 1000 MHz/Km. With fast increase of services the laying of cables in ducts is more convenient than laying in trench. Cable capacities of 12 to 24 optical fibers are preferred. Adopting this rather low capacity for the cables leaves the possibility of laying another cable with monomode fibers after a few years. Author (ESA)

75 PLASMA PHYSICS

Includes magnetohydrodynamics and plasma fusion.

For ionospheric plasmas see *46 Geophysics*. For space plasmas see *90 Astrophysics*.

N84-12909# Nagoya Univ. (Japan). Inst. of Plasma Physics.
MAGNETOHYDRODYNAMIC EQUILIBRIUM AND STABILITY OF SPHEROMAK PLASMA IN FLUX CONSERVER
Shobu Kaneko (Tokyo Univ., Japan) and Akio Takimoto (Tokyo Univ., Japan) Aug. 1983 33 p refs
(IPPJ-642) Avail: NTIS HC A03/MF A01

The Green-function method is applied to the Grad-Shafranov equation for the plasma in a flux conserver with a rectangular cross section. The linear and the nonlinear MHD equilibrium configurations for various strengths of the toroidal magnetic field B are determined by this method. The average beta value < B > and the safety factor are also evaluated. When B is increased from zero, < B > decreases and vanishes at a force-free configuration. The safety factor takes a maximum value on the magnetic axis. A sufficient condition for stability to symmetric perturbations is derived by use of Edenstraser's condition. This sufficient condition holds for the flux conserver of any shape. As an example, the region, in which this sufficient condition is fulfilled, is shown graphically for the flux conserver with rectangular cross section. Author

N84-12910# Nagoya Univ. (Japan). Inst. of Plasma Physics.
A STEADY-STATE AXISYMMETRIC TOROIDAL SYSTEM
K. Hirano Aug. 1983 67 p refs
(IPPJ-643) Avail: NTIS HC A04/MF A01

Conditions for achieving a steady state in an axisymmetric toroidal system were studied with emphasis on a very high beta field reversed configuration. Analysis made for the electromotive force produced by the Ohkawa current induced by a neutral beam injection shows that since the perpendicular component of the current to the magnetic field can be generated automatically by diamagnetic effect only the parallel component must be driven by the electromotive force. The drive of the parallel component generates the shear in the field line, so that the pure toroidal field on the magnetic axis is rotated towards the plasma boundary and is matched to the external field lines. This matching condition determines the necessary amount of injection beam current and power. It is demonstrated that a very high beta field reversed configuration requires only small amount of the current driving beam power because almost all the toroidal current except that close to the magnetic axis is carried by diamagnetic current due to high beta. A low beta tokamak needs very high current driving power since most of the toroidal current is composed of the parallel component which must be driven by the beam. Author

N84-12911# Nagoya Univ. (Japan). Inst. of Plasma Physics.
ATOMIC PROCESSES IN HOT DENSE PLASMA
T. Kagawa (Nara Women's Univ.), T. Kato, T. Watanabe (Inst. of Physical and Chemical Research), and S. Karashima Aug. 1983 45 p refs Submitted for publication
(IPPJ-AM-31) Avail: NTIS HC A03/MF A01

Central field models and the theoretical analyses for some atomic processes in hot, dense, plasmas are reviewed. The qualitative trends of the density- and temperature-dependent properties of plasma particles, which could be used for plasma diagnostics, are described. Author

N84-12912# Nagoya Univ. (Japan). Inst. of Plasma Physics.
CROSS SECTIONS FOR CHARGE TRANSFERS OF HIGHLY IONIZED IONS IN HYDROGEN ATOMS
H. Tawara, T. Kato, and Y. Nakai (Japan Atomic Energy Inst.) Aug. 1983 114 p refs Revised Submitted for publication
(IPPJ-AM-30) Avail: NTIS HC A03/MF A01

Experimental data through mid 1983 are compiled on the total cross sections for the electron capture processes of highly ionized ions in collisions with hydrogen atoms. The results are shown in figures as a function of the collision energy. The cross sections for some related processes including electron detachment (or stripping) and excitation are also shown. This is the first up-dated version of IPPJ-AM-15. Author

N84-12913# Nagoya Univ. (Japan). Inst. of Plasma Physics.
BIBLIOGRAPHY ON ATOMIC PROCESSES IN HOT DENSE PLASMAS
T. Kato (Osaka Univ.), T. Kagawa (Nara Women's Univ.), S. Karashima (Science Univ. of Tokyo), N. Miyanaga (Osaka Univ.), H. Tawara (Tsukuba Univ.), N. Yamaguchi (Hiroshima Univ.), K. Yamamoto (Okayama Univ.), and K. Yonei Aug. 1983 48 p Submitted for publication
(IPPJ-AM-29) Avail: NTIS HC A03/MF A01

Information on atomic processes in hot dense plasmas which are connected with inertial confinement fusion and astrophysics was compiled from 114 records stored in the HIDENS data base. Energy level, f or A value, bound free transition, free-free transition, collision, and stopping power are listed along with the bibliographic citations fo each report. A.R.H.

N84-12914# Nagoya Univ. (Japan). Inst. of Plasma Physics.
ELECTRON CAPTURE AND LOSS CROSS SECTIONS FOR COLLISIONS BETWEEN HEAVY IONS AND HYDROGEN MOLECULES, REVISED
Hiroyuki Tawara, Takako Kato, and Yohta Nakai (Japan Atomic Energy Research Inst.) Jun. 1983 198 p refs Revised Submitted for publication
(IPPJ-AM-28) Avail: NTIS HC A09/MF A01

Experimental data on the cross sections for electron-capture and loss collisions between heavy ions (Z > or = Li) and hydrogen molecules are updated. The results are shown in graphs as a function of the incident energy of the ions. Author

N84-12915# Nagoya Univ. (Japan). Inst. of Plasma Physics.
CONSIDERATIONS OF THE THREE-WAVE INTERACTIONS
Tsutomu Kawata (Tokayama Univ., Japan) Aug. 1983 59 p refs
(IPPJ-641) Avail: NTIS HC A04/MF A01

As a typical case of higher-order matrix in two dimensions, the third-order eigenvalue problem developed for the inverse spectral transform solving the equations of three-wave interactions is discussed. The third-order matrix equation is reformulated by the mathematical concept, 'Riemann-Hilbert problem', which gives a simpler way to construct the soliton solution. The Green function for the associated eigenvalue problem is defined and the completeness relation of Jost functions is obtained. Through variational computations, squared Jost vectors are naturally introduced and the corresponding completeness is also obtained. According to the classical Green formula, another type of Green function for the linearized partial differential equation of the three-wave interactions is defined. This type of Green function is used to solve the non-homogeneous linear differential equation, which appears in perturbations of the three-wave interactions. Author

N84-12916# Metropolitan Coll. of Technology, Tokyo (Japan).
ROTATING AND PROPAGATING LIB STABILIZED BY SELF-INDUCED MAGNETIC FIELD
Hiroyuki Murakami, Takayuki Aoki (Tokyo Inst. of Tech.), Shigeo Kawata (Tokyo Inst. of Tech.), and Keishiro Niu (Tokyo Inst. of Tech.) Nagoya, Japan Nagoya Univ. Aug. 1983 29 p refs Sponsored in par. by Ministry of Education, Science and Culture, Japan Prepared in cooperation with Nagoya Univ.
(IPPJ-640) Avail: NTIS HC A03/MF A01

Rotating motions of propagating LIB are analyzed in order to suppress the instability of mixed mode of the Kelvin-Helmholtz, tearing and sausage types by the action of a self-induced magnetic field in the axial direction. The beams are assumed to be charge-neutralized but not current-neutralized. The steady-state solutions of propagating LIB with rotations are numerically obtained first. Through the dispersion relation with respect to the ikonal type of perturbations which are added to the steady-state solutions, the growth rates of instabilities appearing in LIB are obtained. It is concluded that if the mean rotating velocity of LIB is comparable to the propagation velocity, in other words, if the induced magnetic field intensity in the axial direction is comparable to the magnetic field intensity in the azimuthal direction, the macro-instability disappears in the propagating ion beam. Author

N84-12917# Massachusetts Inst. of Tech., Cambridge. Center for Space Research.
BEAM PLASMA TURBULENCE STUDY Final Report, 1 Aug. 1979 - 30 Sep. 1982
Tom Chang and Bruno Coppi 1 May 1983 83 p
(Contract F19628-79-C-0152; AF Proj. 7601)
(AD-A131946; AFGL-TR-83-0125) Avail: NTIS HC A05/MF A01 CSCL 20/9

We are concerned with the plasma wave radiations and turbulence, generated by natural or artificially produced charged beams and currents or plasma anisotropy, in the Earth's ionosphere and magnetosphere - particularly in the topside ionosphere and the suprauroral region. Specific problems studied during the three-year contract period include: ion conics and beams, lower hybrid waves and hybrid whistlers, nonlinear electrostatic ion cyclotron waves and cavitations, the beam-plasma-discharge phenomenon, strong plasma turbulence, electrostatic shocks across auroral field lines, particle-acceleration mechanisms, collisional effects, and anisotropy-driven magnetic reconnection processes. Major research contributions are described in detail in theis report. Complete lists of the titles of scientific publications and technical professional and technical presentations sponsored by this contract are also given, and important related professional activities are outlined. GRA

N84-12918# Boston Coll., Chestnut Hill, Mass.
STRONG COUPLING EFFECTS ON BOUND STATES IN PLASMAS Interim Progress Report, 1 Feb. 1982 - 31 Jan. 1983
Gabor J. Kalman Mar. 1983 11 p
(Grant AF-AFOSR-0091-81; AF Proj. 2301)
(AD-A131661; AFOSR-83-0637TR; ; IPR-2) Avail: NTIS HC A02/MF A01 CSCL 20/9

Further progress in the areas of: (1) kinetics and response of strongly coupled multicomponent plasmas; (2) study of plasma phase transition and determination of the degree of ionization of a dense plasma; and (3) generalization of the Thomas-Fermi-Debye-Huckel scheme for strongly coupled plasmas with atoms and ions, is reported. A multispecies formalism has been worked out. Details of the phase transition and of the critical curve have been found. Relationship to other works has been studied.
Author (GRA)

N84-12919# Harry Diamond Labs., Adelphi, Md.
NONLINEAR FORCE ON AN UNPOLARIZED RELATIVISTIC TEST PARTICLE TO SECOND ORDER IN THE TOTAL FIELD IN A NONEQUILIBRIUM BEAM-PLASMA SYSTEM
Howard E. Brandt Aug. 1983 24 p
(DA Proj. 1L1-161101-A-91-A)
(AD-A131631; HDL-TR-1995) Avail: NTIS HC A02/MF A01 CSCL 20/8

In the theory of electromagnetic radiation processes in nonequilibrium relativistic beam plasma systems, an important role is played by the time average nonlinear force acting on a relativistic test particle due to the total electromagnetic field. A major nonlinearity in the field arises from the dependence of the Lorentz force on the particle trajectory, which, in turn, depends on the field. Thereby the force has effectively a nonlinear dependence on the total electromagnetic field. In this document, the time average of this nonlinear force is derived to second order in the total field for the case of unpolarized and slightly perturbed relativistic particle trajectories. The latter condition is that of applicability of the classical Born approximation for a plasma, namely, that the relativistic particle momentum be much greater than the electromagnetic impulse received by the particle in a time interval given by the inverse plasma frequency. Possible important screening effects arising from test particle polarization are ignored here but will be fully addressed in another report. The result of the present calculation agrees with that of Akopyan and Tsytovich. It is important in calculations of collective radiation and conditions for the occurrence of radiative instability in beam plasma systems. GRA

N84-12920# Cambridge Hydrodynamics, Inc., Mass.
BOUNDARY-INTEGRAL SIMULATIONS OF RAYLEIGH-TAYLOR INSTABILITY IN IDEAL MAGNETOHYDRODYNAMICS Final Report
Gregory R. Baker, Robert L. McCrory, and Steven A. Orszag Kirtland AFB, N. Mex. AFWL Aug. 1983 36 p
(Contract F29601-82-C-0036; AF Proj. 8809)
(AD-A131667; AFWL-TR-83-12) Avail: NTIS HC A03/MF A01 CSCL 20/9

Rayleigh-Taylor fluid instabilities are studied in the ideal magnetohydrodynamic (MHD) limit by applying boundary integral mathematical formulations to solve Laplace's equation with Dirichlet conditions on complicated boundaries. Instabilities in both the flute and sausage modes are studied for an accelerating thin cylindrical plasma, and calculations demonstrate the basic nonlinear dynamics of the z-pinch geometry. The dynamics and mathematics of plane thin shells and thin shells in cylindrical geometries with axisymmetric flow are discussed. Author (GRA)

N84-12921# Sandia Labs., Albuquerque, N. Mex.
INSTABILITIES IN CYLINDRICAL PLASMA LINERS IMPLODED BY HIGH MAGNETIC FIELDS
Thomas W. Hussey 1983 15 p refs Presented at the 3rd Intern. Conf. on Magagauss Magnetic Field Generation and Related Topics, Novosibirsk, USSR, 13 Jun. 1983
(Contract DE-AC04-76DP-00789)
(DE83-013640; SAND-83-1341C; CONF-830606-10) Avail: NTIS HC A02/MF A01

The hydromagnetic Rayleigh-Taylor instability is present in some devices in which plasma cylinders are imploded by high current. This instability is less damaging for implosions of cylindrical gas puffs than for implosions of cylindrical foils. This instability is different for foils, which correspond to thin shells of high aspect ratio, than it is for gas puffs, which have a very low aspect ratio. Recent work in which the effects of the Rayleigh-Taylor instability in thin foils are related to load design parameters was examined. The improved stability of gas puffs allow larger radius implosions with higher implosion velocities. Finally, a hybrid system with a uniform density gas inside a cylindrical foil offers much of the stability of gas puffs together with the uniformity and low inductance of a foil system. DOE

N84-12922# Georgia Inst. of Tech., Atlanta. School of Nuclear Engineering and Health Physics.
RIPPLE-REDUCTION POLOIDAL-FIELD COILS FOR TOKAMAK REACTORS
Glenn Bateman Feb. 1983 26 p refs
(Contract DE-AS05-78ET-52025)
(DE83-009532; GTFR-37) Avail: NTIS HC A03/MF A01

A conceptual design is presented using a combination of superconducting Ripple Reduction Poloidal Field (RRPF) coils together with normal saddle coils in an INTOR sized Tokamak reactor consisting of 8 toroidal field (TF) coils with 7.0 m by 9.4 m active coil bore. The RRPF coils consist of dipole magnetic coils placed between the TF coils and the neutron shielding to produce part of the shaping field needed for a D shaped plasma equilibrium and to reduce magnetic ripple near the top and bottom of the plasma. They are designed to share the TF coil cryostat and support structure, without obstructing access to the shielding, blanket or first wall. The normal (e.g., water cooled copper) saddle coils are imbedded in the shielding one meter away from the first wall. They carry less than 0.6 MA turns of current and consume less than 16 MW power to reduce magnetic ripple primarily near the midplane of the plasma. DOE

N84-12923# Oak Ridge National Lab., Tenn.
DESIGN OF THE ADVANCED TOROIDAL FACILITY (ATF-1)
R. L. Johnson, O. B. Adams, T. C. Jernigan, B. E. Nelson, J. F. Lyon, and P. B. Thompson 1983 17 p refs Presented at the 5th Topical Meeting on Technol. of Fusion Energy, Knoxville, Tenn., 26 Apr. 1983
(Contract W-7405-eng-26)
(DE83-012641; CONF-830406-63) Avail: NTIS HC A02/MF A01

The Advanced Toroidal Facility-1 (ATF-1) is a torsatron being designed at ORNL as a replacement for the ISX-B Tokamak. The concept for the device includes two continuous helical field coils which are segmented by way of demountable joints, two pair of vertical field coils and a set of twelve toroidal field coils. The vacuum vessel is placed inside the helical field coils and an external toroidal shell support structure is provided to react all coil and vacuum vessel loads. The present design status for all systems is discussed. DOE

N84-12924# JAYCOR, San Diego, Calif.
THEORETICAL STUDIES OF FUSION PHYSICS. VOLUME 1: SUMMARY Final Report
31 Mar. 1983 41 p refs
(Contract DE-AC03-80ER-53092)
(DE83-010378; DOE/ER-53092/T6-Vol-1-Summ) Avail: NTIS HC A03/MF A01

Theoretical studies were performed on each of the following topics: (1) absorption of waves near the cyclotron frequency by relativistic electrons in EBT; (2) power balance in a stable, adiabatic hot electron annulus; (3) whistler instability in a relativistic electron annulus; (4) adiabatic limits on electron temperature in the EBT annulus; and (5) summary of a model of the EBT ring heating/loss process. DOE

N84-12925# JAYCOR, San Diego, Calif.
THEORETICAL STUDIES OF FUSION PHYSICS. VOLUME 2: APPENDICES Final Report
31 Mar. 1983 182 p refs
(Contract DE-AC03-80ER-53092)
(DE83-010371; DOE/ER-53092/T6-Vol-2-App) Avail: NTIS HC A09/MF A01

The following appendices are given: (1) absorption of waves near the cyclotron frequency by relativistic electrons in EBT, (2) power balance in a stable, adiabatic hot electron annulus, (3) whistler instability in a relativistic electron annulus, and (4) adiabatic limit on electron temperature in the EBT annulus. DOE

N84-12926# Pacific Northwest Lab., Richland, Wash.
DEVELOPMENT OF MATERIALS FOR OPEN-CYCLE MHD Quarterly Report, period ending Mar. 1983
D. D. Marchant and J. L. Bates Jul. 1983 15 p refs
(Contract DE-AC06-76RL-01830)
(DE83-016334; PNL-4001-3) Avail: NTIS HC A02/MF A01

Channel components for open-cycle, coal-fired magnetohydrodynamic generators are being studied. Electrodes and insulators are being developed. The electrical conductivity was measured on several compositions based on hafnium oxide, rare earth oxides, and indium oxide. Indium oxide appears to be the main constituent required for high conductivity. As part of the development, materials are being corrosion tested in both Montana Rosebud coal slag and potassium sulfate (K2SO4). The results from three coal slag tests and one K2SO4 test are discussed. DOE

N84-12927# General Atomic Co., San Diego, Calif.
REAL-TIME DIAGNOSTIC-DATA-ACQUISITION SYSTEM FOR THE DOUBLET 3 TOKAMAK FUSION EXPERIMENT
Bill B. McHarg, Jr. May 1983 8 p refs Presented at the Conf. on Real-Time Computer Appl. in Particle and Nucl. Phys., Berkeley, Calif., 16-19 May 1983 Submitted for publication
(Contract DE-AT03-76ET-51011; GA Proj. 3344)
(DE83-015871; GA-A-17059) Avail: NTIS HC A02/MF A01

The Doublet III data acquisition computer system acquires, archives, and processes over three megabytes of data from each shot of the experiment. A shot lasts 1 to 2 seconds and occurs every 5 to 6 minutes with 50 to 100 shots/day. The data acquisition system was configured to efficiently handle the increasing quantity of data as new plasma instruments are added (five megabytes within a year) and to provide interactive capability during operations. The configuration is a dual CPU system with a dual port disk and bulk core memory. One CPU is devoted to acquisition and archiving while the other CPU is for analysis and interactive use. This system has enabled improved shot-to-shot processing or plasma data thus proving guidance to the physics operations team. A planned upgrade of Doublet III will require data handling of over 20 megabytes/shot. DOE

N84-12928# Los Alamos Scientific Lab., N. Mex. Center for Nonlinear Studies.
COMPUTATIONAL SYNERGETICS AND INNOVATION IN WAVE, VORTEX, AND PLASMA CLOUD DYNAMICS
Norman J. Zabusky (Pittsburgh Univ.) 1983 22 p refs Presented at the Fronts, Interfaces and Patterns Conf., Los Alamos, N. Mex.,

2-6 May 1983 Sponsored in part by the Office of Naval Research and Army Research Office
(Contract W-7405-eng-36)
(DE83-015252; LA-UR-83-1991; CONF-8305110-1) Avail: NTIS HC A02/MF A01

The computer, used in a heuristic mode, has greatly augmented the understanding of the mathematics of nonlinear dynamical processes. Examples are given of recent work in soliton mathematics (waves) and contour dynamics: a boundary integral evolutionary method that is applicable to a wide class of 2D flows. The role of good graphics in enhancing the discovery, retention, and communication of new mathematical properties of equations is illustrated. DOE

N84-12929# California Univ., Berkeley. Lawrence Berkeley Lab.
A 2-D SKIN-CURRENT TOROIDAL-MHD-EQUILIBRIUM CODE
B. Feinberg, R. A. Niland (Princeton Univ., N.J.), J. Coonrod (Princeton Univ., N.J.), and M. A. Levine Sep. 1982 54 p refs
(Contract DE-AC03-76SF-00098)
(DE83-016916; LBL-10070) Avail: NTIS MF A01

A two dimensional, toroidal, ideal MHD skin current equilibrium computer code is described. The code is suitable for interactive implementation on a minicomputer. Some examples of the use of the code for design and interpretation of toroidal cusp experiments are presented. DOE

N84-12930# Los Alamos Scientific Lab., N. Mex.
RECENT RESULTS IN THE LOS ALAMOS COMPACT TORUS PROGRAM
M. Tuszewski, W. T. Armstrong, Cris W. Barnes, D. C. Barnes, R. R. Bartsch, R. E. Chrien, J. C. Cochrane, D. S. Harned, I. Henins, D. W. Hewett et al 1983 6 p refs Presented at the 11th European Conf. on Controlled Fusion and Plasma Phys., Aachen, 5-9 Sep. 1983 Prepared in cooperation with Jaycor, Inc., Del Mar, Calif. and LLNL
(Contract W-7405-eng-36)
(DE83-014147; LA-UR-83-1898; CONF-830908-2) Avail: NTIS HC A02/MF A01

A compact toroid is a toroidal magnetic-plasma-containment geometry in which no conductors or vacuum-chamber walls pass through the hole in the torus. Two types of compact toroids are studied experimentally and theoretically at Los Alamos: spheromaks that are oblate in shape and contain both toroidal and poloidal magnetic fields, and field-reversed configurations (FRC) that are very prolate and contain poloidal field only. Progress in the development of the technologies is reported. DOE

N84-12931# Argonne National Lab., Ill.
STRUCTURE OF CONVECTIVE SURFACE DEPOSITS AND EFFECT ON MHD STEAM-PLANT DESIGN
T. R. Johnson, L. S. H. Chow, and E. B. Smyk 1983 8 p refs Presented at the 8th Intern. Conf. on MHD Elec. Power Generation, Moscow, 12 Sep. 1983
(Contract W-31-109-eng-38)
(DE83-010757; CONF-830906-1) Avail: NTIS HC A02/MF A01

Experimental and analytical investigations are being made of the seed-ash deposits that will form on convective-heat-transfer surfaces in the MHD steam-bottoming plant. The results show that, although fouling of the steam and air heaters will be severe, the fouling problems can be solved by proper specification of tube bank arrangements, gas velocities, soot-blower placement, and soot-blowing schedule, which will vary depending on the gas temperature. At gas temperatures below the seed melting point, weak, non-adherent deposits are formed and can be easily controlled by conventional soot blowers. At gas temperatures well above the seed melting point, it appears practical to operate steam and air heaters without soot blowing, because the deposit thickness will be limited by the formation of a freely flowing, molten surface. The intermediate-temperature range (1300 to 16000K) is the most troublesome because the deposits can become very strong and adherent. This section of the steam heaters must be designed to limit heat fluxes and must be operated with frequent soot blowing. DOE

N84-12932# California Univ., Livermore. Lawrence Livermore Lab.
FOKKER-PLANCK EQUATION IN MIRROR RESEARCH
Richard F. Post 11 Aug. 1983 37 p refs Presented at the Course and Workshop on Mirror-based and Field-reversed Approaches to Magnetic Fusion, Varenna, Italy, 7-17 Sep. 1983
(Contract W-7405-eng-48)
(DE83-016568; UCRL-89200; CONF-830909-2) Avail: NTIS HC A03/MF A01

Open confinement systems based on the magnetic mirror principle depend on the maintenance of particle distributions that may deviate substantially from Maxwellian distributions. Mirror research has therefore from the beginning relied on theoretical predictions of non-equilibrium rate processes obtained form solutions to the Fokker-Planck equation. The F-P equation plays three roles: design of the experiments, creation of classical stanars against which to compare experiments, and predictions concerning mirror based fusion power systems. Analytical and computational approaches to solving the F-P equation for mirror systems are reviewed, together with results and examples that apply to specific mirror systems, such as the tandem mirror. DOE

N84-12933# California Univ., Livermore. Lawrence Livermore Lab.
TIME-RESOLVED SPECTRAL MEASUREMENTS ABOVE 80 A
R. L. Kauffman, N. Ceglio, and H. Medecki 1 Jul. 1983 5 p refs Presented at the 27th Ann. Intern. Tech. Symp. of the Soc. of Photo-Opt. Instr. Engr., San Diego, Calif., 21-24 Aug. 1983
(Contract W-7405-eng-48)
(DE83-015616; UCRL-89538; CONF-830874-8) Avail: NTIS HC A02/MF A01

Time-resolved spectral measurements above 80 A from laser-produced plasmas were made. A transmission grating spectrograph whose primary components are a cylindrically-curved X-ray mirror for light collection, a transmission grating for spectral dispersions, and an X-ray streak camera for temporal resolution was used. A description of the instrument and an example of the data are given. DOE

N84-12934# Brookhaven National Lab., Upton, N. Y. Accelerator Dept.
INERTIAL FUSION WITH LOW-ENERGY HEAVY IONS
A. W. Maschke 1983 3 p refs Presented at the Particle Accelerator Conf., Santa Fe, N. Mex., 21-23 Mar. 1983
(Contract DE-AC02-76CH-00016)
(DE83-016709; BNL-32775; CONF-830311-187) Avail: NTIS HC A02/MF A01

High energy heavy ions are under study for inertial fusion applications. It may be possible to utilize heavy ions with energies less than 1 MeV, compared with the usual HIF approach using multi-GeV beams. DOE

N84-12935# Hanford Engineering Development Lab., Richland, Wash.
CONCEPTUAL DESIGN OF THE HIGH-FLUX VTA-2 TEST ASSEMBLY FOR FMIT
M. A. Vogel Aug. 1983 30 p refs
(Contract DE-AC06-76FF-02170)
(DE83-017022; HEDL-TME-83-19) Avail: NTIS HC A03/MF A01

The conceptual design of the test module for the high neutron flux vertical test assembly (VTA-2) is considered with emphasis on the thermal control systems available for monitoring test specimen temperatures at any desired temperature within the range of 100 to 6500 C. DOE

N84-12936# Argonne National Lab., Ill. Office of Fusion Power Program.
TOKAMAK FUSION REACTORS WITH LESS THAN FULL TRITIUM BREEDING
K. Evans, Jr., J. G. Gilligan, and J. Jung May 1983 46 p refs
(Contract W-31-109-eng-38)
(DE83-016711; ANL/FPP/TM-169) Avail: NTIS HC A03/MF A01

A study of commerical, Tokamak fusion reactors with tritium concentrations and tritium breeding ratios ranging from full deuterium-tritium operation to operation with no tritium breeding is presented. The design basis for these reactors is similar to those of STARFIRE and WILDCAT. Optimum operating temperatures, sizes, toroidal field strengths, and blanket/shield configurations are determined for a sequence of reactor designs spanning the range of tritium breeding, each having the same values of beta, thermal power, and first-wall heat load. Additional reactor parameters, tritium inventories and throughputs, and detailed costs are calculated for each reactor design. The disadvantages, advantages, implications, and ramifications of tritium-depleted operation are presented and discussed. DOE

N84-12937# Massachusetts Inst. of Tech., Cambridge. Plasma Fusion Center.
A MODEL FOR STRESSES IN CIRCULAR MAGNETS FOR TOROIDAL FUSION DEVICES
J. M. Noterdaeme Jun. 1983 26 p refs
(Contract DE-AC02-78ET-51013)
(DE83-016535; DOE/ET-51013/70; PFC/RR-83-7) Avail: NTIS HC A03/MF A01

Circular coils in toroidal fusion devices are subjected to in plane bending moments resulting from the interaction of the current with the inhomogeneous magnetic field. To take into account the support of the coils both externally through the in plane structure (a central cylinder), and internally through the out of plane structure (the coil forms a toroidal assembly which can take up the net inward force by a reaction in the toroidal direction) the coil is modelled as a circular beam on the elastic foundation. From the solutions for a single force acting on such a beam, the formulas for an arbitrary cos n theta variation of a distributed force was derived. The general system is solved by Fourier expansion of the the in plane loads and external reaction forces. The fraction of the net inward force reacted by the central cylinder and by the intercoil structure is varied continously, and a minimum for the ending moments is found for a particular value of this fraction (depending on the aspect ratio, the stiffness of the coil, and the intercoil structure). DOE

N84-12938# Texas Univ., Austin. Fusion Research Center.
OBSERVATIONS OF SOFT X-RAY FLUCTUATIONS WITH AN IMAGING ARRAY ON TEXT
J. A. Snipes, T. P. Kochanski, and S. B. Kim Aug. 1983 43 p refs
(Contract DE-AC05-78ET-53043)
(DE83-018118; DOE/ET-53043/6) Avail: NTIS HC A03/MF A01

Soft X-ray emissions from TEXT, a medium sized ohmically heated Tokamak, were measured using an array of 40 surface barrier diodes viewing the plasma through a narrow slit aperture. The level of soft X-ray emissions is found to correlate with electron temperature and density, plasma current, and Z effective. The time evolution of the soft X-ray signals is similar to that of the radiation from highly ionized heavy impurities, e.g., titanium and scandium. Typical signals rise with the increasing electron temperature as the current rises. The signals often exhibit sinusoidal oscillations simultaneously with the large MHD activity observed on the Mirnov coils. Sawtooth activity typically accompanies the quiescent phase of the discharge as MHD activity ceases and the plasma parameters become constant. Radial intensity profiles during normal sawtoothing are compared with those observed during the laser driven ablation injections of scandium. DOE

N84-12939# California Univ., Livermore. Lawrence Livermore Lab.
SUMMARY OF THE MARS TANDEM-MIRROR REACTOR DESIGN
B. Grant Logan 1 Sep. 1983 27 p refs Presented at the Course and Workshop on Mirror-Based and Field-Reversed Approaches to Magnetic Fusion, Varenna, Italy, 7-17 Sep. 1983
(Contract W-7405-eng-48)
(DE83-017293; UCRL-89296; CONF-830909-8) Avail: NTIS HC A03/MF A01

A two-year study of a commercial tandem-mirror reactor design (Mirror Advanced Reactor Study (MARS) is briefly reviewed. The end plugs are designed for trapped-particle stability, MHD ballooning, balanced geodesic curvature, and small radial electric fields in the central cell. New technologies such as lithium-lead blankets, 24 T hybrid coils, gridless direct converters and plasma halo vacuum pumps are highlighted. General characteristics of the MARS tandem mirror and STARFIRE Tokamak reactor design are compared. A design of an upgrade of MFTF-B incorporating many of the MARS features is discussed. DOE

N84-12940# California Univ., Livermore. Lawrence Livermore Lab.
THREE-DIMENSIONAL EQUILIBRIUM IN QUADRUPOLE SYMMETRIC TANDEM MIRRORS IN THE PARAXIAL LIMIT (REDUCED MHD)
L. Donald Pearlstein 29 Aug. 1983 19 p refs Presented at the Course and Workshop on Mirror-Based and Field-Reversed Approaches to Magnetic Fusion, Varenna, Italy, 7-17 Sep. 1983
(Contract W-7405-eng-48)
(DE83-017840; UCRL-89767; CONF-830909-7) Avail: NTIS HC A02/MF A01

Equilibrium in quadrupole symmetric mirrors is fully three dimensional: however, because axial scale lengths are long compared with radial scale lengths (equivalently weak curvature) it is possible to reduce the complexity of the equations by expanding in the appropriate smallness parameter. Such a procedure leads to set of reduced MHD equations. The general theory is presented, numerical results discussed, modifications due to finite Larmor radius are added, and an analytic solution for sharp boundary pressure models is developed. DOE

N84-12941# Sandia Labs., Albuquerque, N. Mex.
ION STOPPING IN HEATED TARGETS
J. N. Olsen, T. A. Mehlhorn, D. J. Johnson, and P. L. Dreike 1983 5 p refs Presented at the 5th Intern. Conf. on High Power Particle Beams, San Francisco, 12 Sep. 1983
(Contract DE-AC04-76DP-00789)
(DE83-017800; SAND-83-0620C; CONF-830911-10) Avail: NTIS HC A03/MF A01

Ion stopping departs from classical, cold material values as the target material heats to appreciable ionization levels. This phenomenon was investigated experimentally on the Proto I accelerator with a radial, applied-B field ion diode. When the beam is focused to 0.5 TW/cm(2) on thin aluminum film targets the time-resolved departure from cold stopping is clear. The observations and early interpretations are presented. DOE

N84-12942# Sandia Labs., Albuquerque, N. Mex.
APPLIED-B ION DIODE EXPERIMENTS ON PBFA 1
P. L. Dreike, E. J. T. Burns, D. J. Johnson, S. A. Slutz, J. T. Crow, R. J. Leeper, L. P. Mix, F. C. Perry, and D. B. Seidel 1983 5 p refs Presented at the 5th Intern. Conf. on High Power Particle Beams, San Francisco, 12 Sep. 1983
(Contract DE-AC04-76DP-00789)
(DE83-017792; SAND-83-0611C; CONF-830911-7) Avail: NTIS HC A02/MF A01

The Applied-B diode has produced the highest brightness proton beam of any diode at the 1 TW and 3 TW power levels on the Proto-I and Proto-II accelerators. An experiment on PBFA I to study the diode's electrical coupling to the accelerator, ion conversion efficiency, and focusability of the proton component of the beam is discussed. The particular diode is a slightly larger version of a diode used successfully on Proto II. The diode radius was increased from 14 to 15 cm, and the height from 5 cm to 6 cm, increasing the diode area from 440 cm(2) to 560 cm(2) to accommodate PBFA-I's lower output impedance. Current neutralized beam propagation is provided by injecting the beam into a gas cell with a 2 m mylar window a few mm from the AK gap, typically filled with 5 Torr argon. DOE

N84-12943# Sandia Labs., Albuquerque, N. Mex.
DIAGNOSING THE ION BEAM ON THE APPLIED-B DIODE

E. J. T. Burns, J. T. Crow, P. L. Dreike, D. J. Johnson, R. J. Leeper, L. P. Mix, F. C. Perry, S. A. Slutz, W. A. Stygar, and J. Chang 1983 5 p refs Presented at the 5th Intern. Conf. on High Power Particle Beams, San Francisco, 12 Sep. 1983
(Contract DE-AC04-76DP-00789)
(DE83-017822; SAND-83-0612C; CONF-830911-5) Avail: NTIS HC A02/MF A01

A variety of diagnostics measure the ion beam parameters from the Applied-B diode on the PBFA-1 accelerator. New hanger dB/dt monitors measure the voltage in the diode feeds. The total proton charge is measured by Li/Cu activation. A Rutherford-scatterer, Thomson parabola particle analyzer measures approximately 50% of the ion current as carbon and oxygen ions from the epoxy-filled grooved anodes. The microscopic divergence of the proton beam is 15 and 25 milliradians HWHM in the horizontal and vertical directions, respectively, as measured by a Rutherford-scattering camera. DOE

N84-12944# Sandia Labs., Albuquerque, N. Mex.
LIGHT-ION-BEAM FUSION
J. Pace VanDevender 1983 7 p refs Presented at the 5th Intern. Conf. on High Power Particle Beams, San Francisco, 12 Sep. 1983
(Contract DE-AC04-76DP-00789)
(DE83-018263; SAND-83-1992C; CONF-830911-8) Avail: NTIS HC A02/MF A01

The inertial confinement fusion program with light ion drivers is developing high-intensity ion-beam-driver technology on PBFA 1. That technology is to be used to study implosion hydrodynamics of small fuel masses on PBFA 2. Power concentration is the key issue. The research on beam production and focusing is interpreted to given guidelines for future research in the ICF Program. Progress is reviewed and the impact of problems of ion impurities and beam energy spread are discussed. The lithium-ion option for PBFA 2 was chosen, and the rationale for that decision is summarized. DOE

N84-12945# Sandia Labs., Albuquerque, N. Mex.
AMPFION HYBRID DIODES ON HYDRAMITE AND PBFA-1
C. W. Mendel, Jr., J. P. Quintenz, P. A. Miller, R. J. Anderson, J. T. Crow, S. E. Rosenthal, M. M. Widner, and J. P. VanDevender 1983 6 p refs Presented at the 5th Intern. Conf. on High Power Particle Beams, San Francisco, 12 Sep. 1983
(Contract DE-AC04-76DP-00789)
(DE83-017824; SAND-83-0575C; CONF-830911-9) Avail: NTIS HC A02/MF A01

Three diodes are discussed; a 20 cm focal length equatorial-feed or extraction diode for the 0.8 TW Hydramite pulser and 25 and 15 cm focal length polar-feed diodes for the PBFA-I pulser (approx. 10 TW at the diode terminals). Progress toward the ultimate goals of high efficiency and small focus is described. More importantly, data is presented which leads one to conclude that the diode is reasonably well understood. This includes data on the uniformity of the diode output, data showing the interaction of the relativistic electron cloud with the field coil, data showing the accuracy of focusing predictions, and other comparisons between data and theoretical modeling. One critical and poorly understood part of the dode is the anode. Anode turn-on delay is discussed, along with the limitations it implies for the present technology. DOE

N84-12946# California Univ., Livermore. Lawrence Livermore Lab. Magnetic Fusion Energy Program.
VACUUM MEASUREMENTS ON THE TANDEM MIRROR EXPERIMENT UPGRADE (TMX-U) FUSION EXPERIMENT
M. O. Calderon, A. L. Hunt, D. D. Lang, W. E. Nexsen, W. L. Pickles, and W. C. Turner 1983 29 p refs Presented at the 9th Intern. Vacuum Congr. and 5th Intern. Conf. on Solid Surfaces, Madrid, 26 Sep. 1983
(Contract W-7405-eng-48)
(DE83-017836; UCRL-88916; CONF-8309103-7) Avail: NTIS HC A03/MF A01

The gas inventory of the Tandem Mirror Experiment Upgrade (TMX-U) must be carefully controlled, if it is to successfully create various plasma configurations for thermal-barrier experiments designed to provide an improved performance for tandem-mirror experiments. Progress on the calibration methods and pressure measurements of machine conditions derived from improved neutral-beam gas control, and changes to the internal baffling geometry and the gettering system is reported. DOE

N84-12947# Illinois Univ., Urbana. Nuclear Engineering Lab.
TFTR ALPHA EXTRACTION AND MEASUREMENT PROJECT Technical Progress Report
G. A. Gerdin and B. W. Wehring 1 Sep. 1983 46 p refs
(Contract DE-AC02-83ER-53147)
(DE83-018120; DOE/ER-53147/1) Avail: NTIS HC A03/MF A01

A passive approach to the extraction and measurement of alpha particles from Tokamak fusion reactors is analyzed and the construction and preliminary results of a fast data-acquisition system are described. The passive approach is the converter foil concept whereby alphas leaving the plasma on large banana orbits strike carbon foils which slow down to around 0.5 MeV. At this energy a sizeable fraction of the alphas are neutral and hence can be analyzed by methods similar to those used in charge-exchange neutral detectors. Alpha loss orbits in TFTR, the thermal and particle flux to the foil on the TFTR edge, and the limitations in detector location caused by radiation are analyzed. The fast data-acquisition system, which operates in the pulse-height-analysis (PHA) mode to discriminate against low-energy background radiation, consists of an alpha detector, a commercial preamplifier, a fast PHA module (built-in house) and an inexpensive microcomputer. DOE

N84-12948# California Univ., Livermore. Lawrence Livermore Lab. TMX-U Group.
STATUS OF TANDEM-MIRROR CONFINEMENT
D. E. Baldwin 30 Aug. 1983 12 p refs Presented at the 11th European Conf. on Controlled Fusion and Plasma Phys., Aachen, 5-9 Sep. 1983
(Contract W-7405-eng-48)
(DE83-017369; UCRL-89771; CONF-830908-5) Avail: NTIS HC A02/MF A01

Recent end-stopping experiments in TMX-Upgrade show strong plugging of the central cell by lower-density plugs, requiring both electron-cyclotron heating (ECRH) and 470 neutral-beam injection, consistent with the thermal-barrier concept. These experiments have low density (n < 10 to the 12th power/cu cm) due to inefficient ECRH power coupling. Hot-ion and hot-electron buildup are consistent with Fokker-Planck calculations. No ion-cyclotron activity is observed in the plugs; occasional electron-cyclotron activity is observed. With plugging, axial lifetimes (tau/sub parallel/> 40 ms) are larger than radial (tau/sub perpendicular/ = 5 to 10 ms) due to observed non-ambipolar ion transport. Recent tandem-mirror theoretical activities are also surveyed. DOE

N84-12949# General Atomic Co., San Diego, Calif.
NUCLEAR DESIGN OF A VERY-LOW-ACTIVATION FUSION REACTOR
E. T. Cheng and G. R. Hopkins Jun. 1983 7 p refs Presented at the 5th Topical Meeting on Technol. of Fusion Energy, Knoxville, Tenn., 26-28 Apr. 1983
(Contract DE-AT03-76ET-51011; GA Proj. 3235)
(DE83-017470; GA-A-17012; CONF-830406-109) Avail: NTIS HC A02/MF A01

The nuclear design aspects of using very-low-activation materials, such as SiC, MgO, and aluminum for fusion-reactor first wall, blanket, and shield applications were investigated. In addition to the advantage of very-low radioactive inventory, it was found that the very-low-activation fusion reactor can also offer an adequate tritium-breeding ratio and substantial amount of blanket nuclear heating as a conventional-material-structured reactor does. The most-stringent design constraint found in a very-low-activation fusion reactor is the limited space available in the inboard region of a Tokamak concept for shielding to protect the superconducting toroidal field coil. A reference design was developed which

mitigates the constraint by adopting a removable tungsten shield design that retains the inboard dimensions and gives the same shield performance as the reference STARFIRE Tokamak reactor design. DOE

N84-12950# Massachusetts Inst. of Tech., Cambridge. Dept. of Nuclear Engineering.
CONSTRAINTS ON THE SCALE OF TOROIDAL-FUSION EXPERIMENTS WITH APPLICATION TO THE DESIGN OF A HELICAL-AXIS STELLARATOR Ph.D. Thesis
Jean-Marie Noterdaeme May 1983 313 p refs
(Contract DE-AC02-78ET-51013)
(DE83-016812; DOE/ET-51013/88; PFC/RR-83-19) Avail: NTIS HC A14/MF A01

Applying the constaints to he design of a helical axis stellarator, a limit on the combination of toroidal field, current density and major radius is found. Another major constraint for this concept is the ability to obtain the plasma physics parameters dictated by similarity considerations. This depends on the heating method used. A minimum scale experiment with 2 periods and no linkage of the toroidal and poloidal coils, would have a major radius of 1.2m, a toroidal field of 3.5T and 2MW of ECRH power (for beta = 1% nu = 10). DOE

N84-12951# Wisconsin Univ., Madison.
DRIFT WAVE STUDIES IN A LINEAR MULTIPLE MIRROR Ph.D. Thesis
Michael Anthony Makowski Jun. 1983 109 p
(Contract DE-AC02-76ET-53051)
(DE83-016881; DOE/ET-53051/57) Avail: NTIS HC A06/MF A01

The drift wave is modeled by a linear kinetic theory which treats finite ion gyroradius, collisions, an electron temperature gradient, and trapped electrons. The theory predicts three unstable modes, only one of which is consistent with all of the above measurements. This instability is a Doppler shifted drift cyclotron instability modified by trapped particle effects. DOE

N84-12952# Oak Ridge National Lab., Tenn. Fusion Energy Div.
DETAILED MODELING OF MICROWAVE ENERGY DEPOSITION IN EBT DEVICES
D. B. Batchelor, D. A. Rasmussen, and R. C. Goldfinger Aug. 1983 35 p refs
(Contract W-7405-eng-26)
(DE83-017496; ORNL/TM-8770) Avail: NTIS HC A03/MF A01

Ray-tracing studies were combined with a simple wave power balance model to provide a complete, albeit approximate, description of microwave power deposition in the ELMO Bumpy Torus (EBT-I), EBT-Scale (EBT-S), and EBT Proof-of-Principle (EBT-P) devices. Electron cyclotron absorption of ordinary and extraordinary waves by the combined core plasma and relativistic annuli is calculated using a fully relativistic damping package developed for the RAYS geometrical optics code. The rays are traced in finite-beta bumpy cylinder plasma equilibria that are obtained from a two-dimensional (2-D) equilibrium code. These results for direct, single-pass absorption are combined with results from a statistical model for the deposition of multiply reflected and mode-converted waves to obtain estimates of the power deposited in the core, surface, and annulus plasma components. Experimental measurements of wave power flux on the cavity wall in EBT-S made with a simple microwave calorimeter are in good agreement with predictions of the model for a variety of operating configurations. DOE

N84-12953# Science Applications, Inc., La Jolla, Calif. Applied Plasma Physics and Technology Div.
REVERSED-FIELD PINCH LARGE ASPECT RATIO EQUILIBRIUM
D. Dobrott and D. D. Schnack Jul. 1983 19 p refs
(Contract DE-AC03-81ER-53113)
(DE83-016771; SAI-02383-468LJ; APS-89) Avail: NTIS HC A02/MF A01

A large aspect ratio, finite beta solution of the Grad-Shafranov is obtained for the reversed-field pinch. The resulting model exhibits toroidal magnetic-field reversal, while maintaining unidirectional toroidal current density. In the limit of zero beta and infinite aspect ratio, the familiar force-free, Bessel function model is recovered. By suitable re-ordering processes, tokamak results are recovered. The reversed-field pinch and the tokamak results are compared with respect to safety factor, shear, toroidal and poloidal beta, V'' and toroidal magnetic shift. DOE

N84-12954# California Univ., Livermore. Lawrence Livermore Lab.
THERMAL BARRIERS: THEIR PURPOSE AND FUNCTIONING
D. E. Baldwin 29 Aug. 1983 23 p refs Presented at the Course and Workshop on Mirror-Based and Field-Reversed Approaches to Magnetic Fusion, Varenna, Italy, 7 Sep. 1983
(Contract W-7405-eng-48)
(DE83-017365; UCRL-89769; CONF-830909-5) Avail: NTIS HC A02/MF A01

Thermal barrier formation, ion pumping, high-field throttle coil, and microstability are discussed. DOE

N84-12955# California Univ., Livermore. Lawrence Livermore Lab.
TMX-U EXPERIMENTAL RESULTS
T. C. Simonen, S. L. Allen, T. A. Casper, J. F. Clauser, C. A. Clower, F. H. Coensgen, D. L. Correll, W. F. Cummins, C. C. Damm, B. H. Failor et al 31 Aug. 1983 24 p refs Presented at the Course and Workshop on Mirror-Based and Field-reversed Approaches to Magnetic Fusion, Varenna, Italy, 7 Sep. 1983
(DE83-016790; UCRL-89286; CONF-830909-4) Avail: NTIS HC A02/MF A01

Mirror-confined electrons with 30 to 70 keV mean energy densities of 0.5 to 2.0 x 10 to the 12th power/cu cm and average betas of 3 to 5% are produced using electron-cyclotron resonant heatng (ECRH). These results are consistent with an electron Fokker-Planck code. Improved ion-cyclotron microstability is observed using neutral beam injection at 470 to the magnetic axis, rather than at 900 as in the previous experiment, TMX. Strong end plugging was produced using a combination of ECRH gyrotrons with sloshing-ion beam injection. In\these low-density central cell experiments (3 x 10 to the 11th power/cu cm the axial losses (tau-sub parallel/ = 20 to 80 ms) are smaller than the nonambipolar radial losses (tau/sub perpendicular/ = 4 to 8 ms). Plugging achieved with a central cell density double that of the end plugs. Although no direct measurements are yet available to determine if a thermal barrier potential dip is generated, these experiments support many theoretical features of the thermal barrier concept. DOE

N84-12956# Oak Ridge National Lab., Tenn. Engineering Physics Div.
MONTE CARLO CALCULATIONS OF NEUTRON AND GAMMA-RAY ENERGY SPECTRA FOR FUSION-REACTOR SHIELD DESIGN: COMPARISON WITH EXPERIMENT
R. T. Santoro and J. M. Barnes Aug. 1983 26 p refs
(Contract W-7405-eng-26)
(DE83-016932; ORNL/TM-8707) Avail: NTIS HC A03/MF A01

Neutron and gamma-ray spectra resulting from the interactions of approx. 14-MeV neutrons in laminated slabs of stainless steel type-304 and borated polyethylene were calculated using the Monte Carlo code MCNP. The calculated spectra are compared with measured data as a function of slab thickness and material composition and as a function of detector location behind the slabs. Comparisons of the differential energy spectra are made for neutrons with energies above 850 keV and for gamma rays with energies above 750 keV. The measured neutron spectra and those calculated using Monte Carlo methods agree within 5% to 50% depending on the slab thickness and composition and neutron energy. The agreement between the measured and calculated gamma-ray energy spectra is also within this range. The MCNP data are also in favorable agreement with attenuated

data calculated previously by discrete ordinates transport methods and the Monte Carlo code SAM-CE. DOE

N84-12957# General Atomic Co., San Diego, Calif.
VARIATIONAL-MOMENT METHOD FOR COMPUTING MAGNETOHYDRODYNAMIC EQUILIBRIA
L. L. Lao Aug. 1983 46 p refs Presented at the 2nd European Workshop on Computational Problems in the Calculation of MHD Equilibria, Wildhaus (Switzerland), 12-14 Sep. 1983
(Contract DE-AT03-76ET-51011)
(DE83-017477; GA-A-17188; CONF-8309137-1) Avail: NTIS HC A03/MF A01

A fast yet accurate method to compute magnetohydrodynamic equilibria is provided by the variational-moment method, which is similar to the classical Rayleigh-Ritz-Galerkin approximation. The equilibrium solution sought is decomposed into a spectral representation. The partial differential equations describing the equilibrium are then recast into their equivalent variational form and systematically reduced to an optimum finite set of coupled ordinary differential equations. An appropriate spectral decomposition can make the series representing the solution coverge rapidly and hence substantially reduces the amount of computational time involved. The moment method was developed first to compute fixed-boundary inverse equilibria in axisymmetric toroidal geometry, and was demonstrated to be both efficient and accurate. The method since was generalized to calculate free-boundary axisymmetric equilibria, to include toroidal plasma rotation and pressure anisotropy, and to treat three-dimensional toroidal geometry. In all these formulations, the flux surfaces are assumed to be smooth and nested so that the solutions can be decomposed in Fourier series in inverse coordinates. These developments and the advantages and limitations of the moment method are reviewed. The use of alternate coordinates for decomposition is discussed. DOE

N84-12958# Oak Ridge National Lab., Tenn. Fusion Energy Div.
ELECTRON-CYCLOTRON-HEATING EXPERIMENTS IN TOKAMAKS AND STELLARATORS
A. C. England 1983 54 p refs Presented at the IEEE Intern. Conf. on Plasma Sci., San Diego, Calif., 22 May 1983
(Contract W-7405-eng-26)
(DE83-017210; CONF-830590-2) Avail: NTIS HC A04/MF A01

The application of high-frequency microwave radiation to plasma heating near the electron-cyclotron frequency in Tokamaks and stellarators is reviewed. Successful plasma heating by microwave power was demonstrated in numerous experiments. Predicted future technological developments and current theoretical understanding suggest that a vigorous program in plasma heating will continue to yield promising results. DOE

N84-12959# Oak Ridge National Lab., Tenn.
PROPAGATION AND ABSORPTION OF ELECTROMAGNETIC WAVES IN FULLY RELATIVISTIC PLASMAS
D. B. Batchelor, R. C. Goldfinger, and H. Weitzner (New York Univ., N.Y.) 1983 6 p refs Presented at the 5th Topical Conf. on Radio Frequency Plasma Heating, Madison, Wisc., 21 Feb. 1983
(Contract W-7405-eng-26)
(DE83-017246; CONF-830210-20) Avail: NTIS HC A02/MF A01

Electron cyclotron heating calculations were made for plasmas with electron temperatures above 10 keV. It was assumed that n/sub parallel/ = 0 so that Doppler broadening is not present and relativistic effects are maximum. The plasma distribution function is assumed to be an isotropic relativistic Maxwellian. Author

N84-12960# California Univ., Livermore. Lawrence Livermore Lab.
MULTIDIPOLE MAGNETIC FIELDS FOR PLASMA CONFINEMENT
Ta-Ming Fang (Boston Univ., Mass.) Jul. 1983 22 p refs
(Contract W-7405-eng-48)
(DE83-016014; UCID-19852) Avail: NTIS HC A02/MF A01

Plasma confinement by permanent magnets was studied and an analytic formula for the field of a single bar magnet was obtained. Generalization to various configurations of multidipole fields was also found. Any two-dimensional field may now be completely described by a simple function of complex variables in closed form. Vector potential was also obtained by integrating over a prescribed Riemann surface. The confinement of plasma by multidipole fields then becomes obvious through conservation principles. DOE

N84-12961# Oak Ridge National Lab., Tenn. Fusion Energy Div.
EFFECT OF MAGNETIC BENDING ON THE HIGH-FREQUENCY STABILITY OF THE ELMO BUMPY TORUS
Adel M. ElNadi, J. C. Whitson, H. A. Kirolous (Cairo Univ., Giza, Egypt), and H. F. Hassan (Cairo Univ., Giza, Egypt) 1983 7 p refs Presented at the Spring Coll. on Radiation in Plasmas., Trieste, Italy
(Contract W-7405-eng-26)
(DE83-017177; CONF-8305127-1) Avail: NTIS HC A02/MF A01

The high frequency stability of the ELMO Bumpy Torus (EBT) device when the wave vector has a finite component along the magnetic field lines was investigated. Author

N84-12962# Sandia Labs., Albuquerque, N. Mex.
CHEMICAL EROSION OF FIRST-WALL MATERIALS BY ATOMIC HYDROGEN AT HIGH TEMPERATURES
C. I. H. Ashby 1983 15 p refs Presented at the 3rd Topical Meeting on Fusion Reactor Mater., Albuquerque, N. Mex.
(Contract DE-AC04-76DP-00789)
(DE83-017161; SAND-83-0941C; CONF-830942-2) Avail: NTIS HC A02/MF A01

The chemical erosion of C, TiB2, and TiC by reaction with H was studied from 420 to 1540 K using H pressures characteristic of fusion devices. For graphite, erosion yields range from 2.0 to 7.4 C/H over this temperature range. A change in the gas phase product distribution is observed as a function of temperature and reaction time. Methane is most abundant at low temperatures and short reaction times, while C2 and C3 species increase in abundance at higher temperatures and after extended reaction times. For C-rich TiC, initial behavior is similar to graphite, but the time evolution of gas phase products differs. TiB2 shows no evidence of reaction below 1300 K and lower erosion yields than graphite at higher temperatures. The superior erosion resistance of TiB2 suggests that it may be a better candidate material than graphite for fusion applications requiring refractory low-Z materials. DOE

N84-12963# Centre National de la Recherche Scientifique, Orleans (France). Lab. de Physique et Chimie de l'Environnement.
[ACTIVITIES REPORT OF THE LABORATORY OF ENVIRONMENTAL PHYSICS AND CHEMISTRY] Annual Report, 1 Apr. 1982 - 1 Jul. 1983 [RAPPORT D'ACTIVITE, 1 APR. 1982 AU 1 JUL. 1983]
1983 84 p refs In FRENCH
Avail: NTIS HC A05/MF A01

The physics of ionized media and the physiochemistry of Earth and planetary atmospheres were studied. Hot plasma dynamics; signal processing; plasma diagnostics; ion-molecule reactions in low temperature plasmas; and volcanic influence on the lower atmosphere are discussed. Author (ESA)

N84-12964# Fom-Instituut voor Plasmafysica, Jutphaas (Netherlands).
A NUMERICAL MODEL FOR DIFFUSION OF HELIUM IN A HYDROGEN PLASMA
J. H. H. M. Potters Jul. 1983 46 p refs Sponsored by Euratom and Nederlandse Organisatie voor Zuiver Wetenschappelijk Onderzoek (ZWO)
(Rept-83-147) Avail: NTIS HC A03/MF A01

A quasicylindrical steady state numerical model for the

diffusion of helium in a hydrogen plasma, adopting collisional, plus anomalous transport for the charged species is presented. The coupled momentum and conservation equations for H+, He+ and He++ are solved to obtain radial profiles of their densities, consistent with those of the neutral species. For the neutrals, a diffusion equation is used for the transport of H, whereas He is assumed to enter the plasma with an energy equal to the temperature of the plasma immediately in front of the wall. A stable numerical scheme for the solution of the coupled ion and electron energy balances is discussed. For the JET Tokamak, collisional effects are shown to enhance alpha particle density 10 cm in front of the wall. The neutral helium density that accumulates in the outer plasma is too low to allow for pumping helium from a cool plasma/gas blanket. Author (ESA)

N84-12965# Istituto di Ricerca e Tecnologia per lo Studio del Plasma Nello Spazio, Frascati (Italy).
DISSIPATIVE INSTABILITIES OF MAGNETIC NEUTRAL LAYERS WITH VELOCITY SHEAR
M. Dobrowolny, P. Veltri (Calabria Univ., Cosenza, Italy), and A. Mangeney (Observatoire de Meudon, France) Nov. 1982 36 p refs
(IFSI-82-13) Avail: NTIS HC A03/MF A01

The general problem of instability of magnetic neutral sheets in the presence of velocity shear is considered in the framework of dissipative MHD. Resistivity and viscosity are included in the treatment. The scalings for ordinary tearing modes, and the parity and reality properties of the corresponding eigenmodes, are shown to constitute a singular case which is not recovered when either viscosity and/or velocity shear are present in a sufficient amount. Orderings for growth rates are discussed and an example containing the effect of velocity shear is treated. Author (ESA)

76 SOLID-STATE PHYSICS

includes superconductivity.

For related information, see also *33 Electronics and Electrical Engineering* and *36 Lasers and Masers.*

N84-12966# Polish Academy of Sciences, Warsaw. Dept. of the Theory of the Continuous Media.
HAMILTONIAN FOR ANTISOTROPIC BODIES WITH DEFECTS
Rmuald K. Kotowski and Vladimir I. Alshite (Academy of Sciences, USSR) 1983 24 p refs
(ISSN-0208-5658) Avail: Issuing activity

The Hamiltonian obtained by Bross for the isotropic case is generalized for the crystal with an arbitrary anisotropy. A continuous description of a body is used which is valid only at low temperatures when long wave phonons predominate in the phonon spectrum. The obtained Hamiltonian describes the interaction of defects with the acoustic branch of phonons. A.R.H.

N84-12967# Instituto de Pesquisas Espaciais, Sao Jose dos Campos (Brazil).
SINGLE Pb (1-X)Sn(X) Te CRYSTAL GROWTH BY VAPOR PHASE TRANSPORT, WITH FORMATION OF A LIQUID/SOLID INTERFACE [CRESIMENTO DE MONOCRISTAIS DE PB 1-X SN-XTE POR TRANSPORTE DE FASE VAPOR, COM FORMACAO DE UMA INTERFASE DE CRESCIMENTO LIQUIDO/SOLIDO]
Chen Ying An and I. N. Bandeira Jul. 1983 8 p refs In PORTUGUESE; ENGLISH summary Presented at the 35th Ann. Meeting of SBPC, Belem, Brazil, 6-13 Jul. 1983
(INPE-2811-PRE/369) Avail: NTIS HC A02/MF A01

Due to segregation effects, single-crystals of Pb(1-x)Sn(x)-Te growth by Bridgman techniques have an inhomogeneous composition profile. A vapor phase transport growth process was developed in order to reduce convective flows. This is due to the very thin melt layer in front of the crystal, that makes convective flows small and solute mixing in the melt very low. By this process single-crystals with 50 mm length by 15 diameter and a high degree of homogeneity were grown. Author

N84-12968*# National Aeronautics and Space Administration. Pasadena Office, Calif.
METHOD AND APPARATUS FOR MINIMIZING CONVECTION DURING CRYSTAL GROWTH FROM SOLUTION Patent Application
Paul J. Shlichta, inventor (to NASA) (JPL, California Inst. of Tech., Pasadena) Filed 31 Oct. 1983 23 p
(Contract NAS7-100)
(NASA-Case-NPO-15811-1; US-Patent-Appl-SN-547175) Avail: NTIS HC A02/MF A01 CSCL 20B

A method and apparatus are disclosed for growing in a gravitational field a microscopic crystal from a solution. The solution is held in a vertical chamber which is relatively thin, the thin being generally perpendicular to the vertical. There is a substrate crystal disposed at either the upper or lower end of the chamber and the crystal grows from this substrate crystal in one direction. The temperature conditions of the solution are controlled so that, as the crystal forms, the effects of buoyant convection within the solution are minimized. This is accomplished in two different ways depending upon whether the crystal is grown from the upper or lower end of the chamber. When grown from the upper end of the chamber, the temperature of the solution is controlled so that it remains essentially isothermal so that there is essentially no heat loss from the solution. When the crystal is grown from the lower end of the chamber, the temperature of the solution is controlled so that there is a differential in temperature throughout the solution which provides a positive thermal gradient within the chamber. NASA

N84-12969# Stanford Univ., Calif. Dept. of Materials Science and Engineering.
FABRICATION AND PROPERTIES OF MULTILAYER STRUCTURES Final Report, 1 Sep. 1979 - 31 Dec. 1981
William A. Tiller, Troy W. Barbee, Jr., Y. T. Thathachar, Lynn Nagel, and W. Dibble Aug. 1983 118 p
(Contract MDA903-81-C-0484; ARPA Order 3706)
(AD-A131934; AD-E850386; SU-DMS-83-R-4) Avail: NTIS HC A06/MF A01 CSCL 13/8

The purpose of the work presented in this paper was to develop the reactive sputtering synthesis process so that continuous layers of controllable structure and composition could be formed in a reproduceable and routine manner. Refractory oxides were chosen as the class of materials to be studied. In this paper we report the results of our studies on the reactive deposition of the oxides of silicon (SiOX). Films of SiOX ($0 < x < 2$) were synthesized at high rates onto substrates held at room temperature. A systematic investigation of the structure-composition-synthesis process variables was conducted for this system and it was clearly demonstrated that films of controllable stoichiometry, varying over the range SiO.1 to SiO2, (Ts approx $<$ 65 deg C). The low temperature nature of this process is a unique feature of high industrial potential as it provides a method for forming SiOX passivating films that does not include time-temperature cycling that could degrade existing device structures. GRA

N84-12970# California Univ., San Diego, La Jolla. Dept. of Electrical Engineering and Computer Sciences.
SURFACE AND INTERFACIAL PROPERTIES OF Ga(0.47) In(0.53) As ALLOYS Final Report, 1 Apr. 1982 - 31 Mar. 1983
H. H. Wieder 26 Jul. 1983 45 p
(Contract N00019-82-C-0204)
(AD-A131925) Avail: NTIS HC A03/MF A01 CSCL 20/12

High frequency C-V measurements and quasi-static gate-controlled galvanomagnetic measurements have confirmed theoretical predictions that the surface Fermi level of Ga0.47In0.53As is pinned by lattice defect-related surface states at approximately 0.55 eV above the valence band edge. The total density of the donor and acceptor centers, related to these defects, is two to three orders smaller than those of InP and the respective barrier heights of n and p-type Ga0.47In0.53As-metal contacts are

consistent with the equilibrium surface Fermi level of Al203 as well as other dielectric-Ga0.47In0.53As interfaces. Author (GRA)

N84-12971# Air Force Systems Command, Wright-Patterson AFB, Ohio. Foreign Technology Div.
THE GROWTH AND MEASUREMENT OF SINGLE-CRYSTAL DOPED GGG (Gd3-xCaxGa5-xZrx012)
Zhang Luohui, Bai Naizhi, Zhao Yuzhen, Lin Chengtian, and Liu Hairun 10 Aug. 1983 14 p Transl. into ENGLISH from Guisuanyan Xuebao (China), v. 10, no. 3, Sep. 1982 p 332-337
(AD-A131875; FTD-ID(RS)T-1090-83) Avail: NTIS HC A02/MF A01 CSCL 20/2

By chemical analysis and X ray lattice parameter determination of the crystals, the segregation coefficients of CaO and ZrO2 from the melt and the influences of CaO and ZrO2 contents on the lattice parameter of the crystal were determined. The similarities and difference and differences in the growth and some of the properties of the single crystals of pure and doped GGG were examined. Experimental results not only show that, during the growth, the control of perfection of GGG (Ca,Zr) single crystals is more difficult, but also indicate that doped GGG (Ca,Zr) are liable to produced color center after irradiation. Author

N84-12972# Air Force Wright Aeronautical Labs., Wright-Patterson AFB, Ohio.
THE STUDY OF THIN FILMS ON SEMI-INSULATING GALLIUM ARSENIDE BY ELLIPSOMETRY Final Report, Jan. - Dec. 1982
Neil T. McDevitt and William L. Baun Jun. 1983 35 p
(AF Proj. 2303)
(AD-A131844; AFWAL-TR-83-4034) Avail: NTIS HC A03/MF A01 CSCL 14/2

A computer-grid procedure is discussed where delta and psi values obtained from a thin filmed surface are used to estimate the optical constants of the film-free surface. Thin films can be measured with reasonable accuracy on gallium arsenide; however, the optical constants of these films cannot be obtained. Author (GRA)

N84-12973# Colorado State Univ., Fort Collins. Dept. of Electrical Engineering.
GROWTH AND CHARACTERIZATION OF InP AND InGaAs FILMS USING THE HYDRIDE VPE TECHNIQUE Final Report, 22 Oct. 1981 - 22 Oct. 1982
21 Oct. 1982 76 p
(Contract N00019-81-C-0425)
(AD-A131841) Avail: NTIS HC A05/MF A01 CSCL 20/12

The advantages of the hydride growth technique are that the control is good because the anion and cation concentrations are separately controlled, and it can be easily scaled up. The disadvantages are that the films tend to have a higher background carrier concentration and a rougher morphology. The focus of this research was to find ways to mitigate or possibly eliminate these disadvantages. An in-depth theoretical comparison between the chloride and hydride growth techniques showed that hydride growth is thermodynamically similar to steady state chloride growth when the HCl:PH3 ratio is 3:1. If chloride systems are inherently cleaner than hydride systems it is possibly due to the cleaning reaction of the phosphorus with the liquid indium to form InP with a subsequent attack of the InP by HCl. However, it seems more likely that the source of the higher carrier concentration is due to the less pure HCl used. We showed this by growing lower carrier concentration InP films when we used HCl generated from ultrapure PCl3. GRA

N84-12974# Washington Univ., Seattle. Semiconductor Research Lab.
CLUSTERING AND ORDERING IN 3-5 ALLOYS Annual Scientific Report, 1 Jun. 1982 - 31 May 1983
C. M. Wolfe, M. W. Muller, G. A. Davis, S. Julie Hsieh, and K. A. Salzman 31 Jul. 1983 57 p
(Grant AF-AFOSR-0231-82; AF Proj. 2306)
(AD-A131785; WU/SRL-59583-1; AFOSR-83-0715TR) Avail: NTIS HC A04/MF A01 CSCL 20/2

The III-V semiconducting alloys are typically grown by epitaxial techniques at temperatures where, in the absence of substrate effects, they are thermodynamically unstable. This can result in problems associated with clustering of like atoms or ordering of unlike atoms. Long-range ordering could yield interesting III-V ternary compounds. Several concepts are discussed which could reduce clustering and promote long-range ordering in III-V alloys. Recent results indicate that the local atomic structure in GaxIn1-xAs is chalcopyrite-like and that long-range ordering may be thermodynamically feasible. Kinetically, it is suggested that growth on substrates could promote long-range order. GRA

N84-12975# California Univ., San Diego. Office of Contract and Grant Administration.
SILICIDE FORMATION AND SCHOTTKY BARRIER OF RARE-EARTH METALS ON SI Final Technical Report, 1 Jun. 1981 - 30 Sep. 1983
S. S. Lau 30 Sep. 1983 161 p
(Contract MDA903-81-C-0348; ARPA Order 3011)
(AD-A131750) Avail: NTIS HC A08/MF A01 CSCL 20/12

The objectives of this program are to investigate the electrical properties and growth characteristics of rare-earth silicides that potentially form low energy barriers on n-type Si. A more general objective is to set up Rutherford backscattering spectrometry at UCSD. For the investigation of rare-earth silicides, we concentrate working on ErSi2 (all rare-earth silicides are similar in characteristics and properties, Er is slightly less reactive with oxygen). More recently GdSi2 has also been investigated. We report here the results of our investigation. Generally speaking, we believe that the major problems of rare-earth silicides have been solved. Rutherford backscattering spectrometry is now on-line at UCSD. Author (GRA)

N84-12976# California Univ., San Diego. Office of Contract and Grant Administration.
SILICIDE FORMATION AND SCHOTTKY BARRIER OF RARE-EARTH METALS ON SI Semiannual Technical Report, 1 Jul. - 31 Dec. 1982
S. S. Lau 30 Sep. 1983 53 p
(Contract MDA903-81-C-0348; ARPA Order 3011)
(AD-A131749) Avail: NTIS HC A04/MF A01 CSCL 20/12

Activities included the arrival of the General Ionex Tandetron accelerator. This machine is being set up for backscattering experiments. It is expected to be on-line in a few months. Perfecting of the technique of fabricating pit-free ErSi2 diodes is planned. Measurement barrier heights of Er and ErSi2 on p and n type Si was done. For p-type Si, the measurements were done at room temperature. For n-type Si, the measurements were done at 77 degrees K. R.J.F.

N84-12977# California Univ., San Diego. Office of Contract and Grant Administration.
SILICIDE FORMATION AND SCHOTTKY BARRIER OF RARE-EARTH METALS ON SI Semiannual Technical Report, 1 Jan. - 30 Jun. 1982
S. S. Lau 30 Sep. 1983 25 p
(Contract MDA903-81-C-0348; ARPA Order 3011)
(AD-A131748) Avail: NTIS HC A02/MF A01 CSCL 20/12

Activities included following the design and construction of mechanical masks for Er (and other thin film) depositions and the completion of the construction of a vacuum annealing furnace. The vacuum chamber is pumped by a turbo-molecular pump and is capable of annealing 88 different samples sequentially in one pump-down. The normal operating pressures is $< 2 \times 1$- to the -7 torr and the chamber is relatively free from carbon and oxygen contamination. Investigation of annealing Er layers deposited on Si in our new vacuum furnace was done. The electronic properties of ErSi2 diodes using mechanical masks were investigated by Applied Physics Letters of our paper entitled Surface Morphology of Erbium Silicides (See Appendix A). R.J.F.

N84-12978# Carnegie-Mellon Univ., Pittsburgh, Pa.
A PROGRAM OF RESEARCH ON MICROFABRICATION TECHNIQUES FOR VLSI MAGNETIC DEVICES Interim Progress

Report, 30 Sep. 1981 - 29 Sep. 1982
M. H. Kryder, C. L. Bauer, J. A. Rayne, and A. Guzman 1 Oct. 1982 264 p
(Grant AF-AFOSR-0284-80; AF Proj. 2305)
(AD-A131706; AFOSR-83-0685TR) Avail: NTIS HC A12/MF A01 CSCL 20/12

Means of fabricating, selectively modifying, and characterizing single crystal epitaxial garnet and amorphous magnetic thin films are being investigated with the intention of developing new materials and processes for magnetic devices including bubble, recording, magneto-optic, and micro-wave devices. Submicron ion unimplantable garnets have been developed for ion-implanted contiguous disk devices. A wideband ferromagnetic resonance spectrometer and a high resolution magneto-optic photometer were developed and used to measure the magneto-striction and crystalline anisotropy constants of these materials. It was found that ion implantation dramatically reduces the crystalline anisotropy field and that a large portion of the change in uniaxial anisotropy of garnets is produced by non-stress related mechanisms which became more important as bubble size is reduced. Transmission electron microscopy investigations of ion implanted garnets have revealed clearly observable changes in stress and structure produced by implantation. Amorphous magnetic materials have been developed which support submicrometer sized domains for bubble and magneto-optic device applications. A number of high density bubble devices have been designed and fabricated: 2-4 micrometers period ion-implanted contiguous disk devices, 4-8 micrometer period current-accessed devices, and 2-6 micrometer period current-accessed ion implanted devices with 4 to 16 times lower power dissipation than earlier current-accessed devices. Author (GRA)

N84-12979# Los Alamos Scientific Lab., N. Mex.
MUON SPIN RELAXATION IN FERROMAGNETIC PdMn
S. A. Dodds, G. A. Gist, R. H. Heffner, M. Leon, D. E. McLaughlin, J. A. Mydosh, G. J. Nieuwenhuys, and M. E. Schillaci 1983 10 p refs Presented at the Yamada Conf. on Muon Spin Rotation and Assoc. Probl., Shimoda, Japan, 18 Apr. 1983
(Contract W-7405-eng-36)
(DE83-012659; LA-UR-83-1405; CONF-830455-6) Avail: NTIS HC A02/MF A01

Positive muon ((SIGMA)()) spin relaxation experiments were carried out in the dilute ferromagnetic alloy Pd + 2 at % Mn (T/sub c/ = 5.80K). In the paramagnetic state the inhomogeneous (SIGMA)() linewidth is proportional to the bulk magnetization. Below T/sub c/ the (SIGMA)() linewidth and the width of the (SIGMA)() local field distribution in zero applied field are both in qualitative accord with the Sherrington-Kirkpatrick theory of disordered magnets. DOE

N84-12980# Sandia Labs., Albuquerque, N. Mex.
RADIATION-INDUCED TRANSIENT ACOUSTIC LOSS IN QUARTZ CRYSTALS
D. R. Koehler and J. J. Martin 1982 19 p refs Presented at the 37th Ann. Frequency Control Symp., Philadelphia, 31 May 1982
(Contract DE-AC04-76DP-00789)
(DE83-012626; SAND-82-2983C; CONF-8205188-1) Avail: NTIS HC A02/MF A01

The radiation induced transient acoustic loss was measured over the 280 K to 400 K temperature range for a set of unswept, Li-swept, Na-swept and H-swept synthetic crystals all fabricated from the same original bar of quartz. Similar measurements were made on a pair of natural quartz crystals. No transient acoustic loss increase was observed in the H-swept sample. At the lower temperatures the radiation induced loss decayed approximately as t/sup -1/2/a while at the higher temperatures a faster decay was more evident. The unswept showed a peak in the transient loss around 360 K while the alkali swept crystals had a peak near 390 K. The transient loss increased in the natural quartz samples for temperature up to 400 K, suggesting a peak at higher temperatures. Additional IR, ESR and annealing experimentation is suggested to further characterize this defect and such work is now being planned. DOE

N84-12981# Oak Ridge National Lab., Tenn. Solid State Div.
HYDROGEN IN MgO CRYSTALS THERMOCHEMICALLY REDUCED AT VERY HIGH TEMPERATURES
Y. Chen Aug. 1982 19 p refs Presented at the US/Japan Seminar on Recombination Induced Defect Formation in Crystals, Urbana, Ill., 2 Jun. 1982
(Contract W-7405-eng-26)
(DE83-014058; CONF-8206201-Draft) Avail: NTIS HC A02/MF A01

Evidence is presented that positve H ions are the main electron traps responsible for the long lived luminescence of the F centers observed at 2.3 eV in thermochemically reduced MgO crystals. DOE

N84-12982# Oak Ridge National Lab., Tenn.
IMPLICATIONS OF HEAVY-ION-INDUCED SATELLITE X-RAY EMISSION. PART 2: PRODUCTION OF K AND L X-RAYS BY 0.9 TO 2.6 MeV/u Ar IONS IN THICK TARGETS OF V, Cu, Nb, Ta, AND Pt
G. D. OKelley, R. L. Auble, L. D. Hulett, Jr., H. J. Kim, W. T. Milner, S. Raman, O. Shaha (Nuclear Research Centre-Negev), C. R. Vane, J. P. Young, and G. Lapicki (East Carolina Univ.) 1983 37 p refs Presented at the 3rd Intern. Conf. on Particle-Induced X-ray Emission (PIXE) and its Analytical Applications, Heidelberg, 18 Jul. 1983
(Contract W-7405-eng-26)
(DE83-015681; CONF-830772-4) Avail: NTIS HC A03/MF A01

Cross sections are reported for X-ray production in targets of (23)V, (29)Cu, (41)Nb, (73)Ta, and (78)Pt by (4)OAr ions of 36.0, 56.4, 76.6, and 103 MeV. Because the targets were relatively thick, approx. 1 mg/cm(2), the data were corrected, using a novel approach, for projectile energy loss and X-ray attenuation in the targets. The cross sections so analyzed are compared with the predictions of the first Born approximation as well as with those of a more extensive treatment which includes energy loss, Coulomb deflection, perturbed stationary state, and relativistic effects. The significant discrepancies between the data and this letter theory are attributed primarily to the influence of multiple ionization on the X-ray emission probabilities. DOE

N84-12983# California Univ., Livermore. Lawrence Livermore Lab.
REVIEW OF SOME RECENT THEORETICAL CALCULATIONS OF PHASE TRANSITIONS AND COMPARISONS WITH EXPERIMENTAL RESULTS
Marvin Ross 11 Jul. 1983 10 p refs Presented at the Am. Phys. Soc. Meeting on Shock Waves in Condensed Media, Santa Fe, N. Mex., 18-21 Jul. 1983
(Contract W-7405-eng-48)
(DE83-015863; UCRL-89549; CONF-830719-26) Avail: NTIS HC A02/MF A01

Recent studies on structural phase transitions, metallization and melting were reviewed. Theoretical methods were increasingly successful in predicting these properties. A major difficulty remains in the determination of effective metal pair-potentials for finite temperature calculations in non-simple metals. DOE

N84-12984# Oak Ridge National Lab., Tenn. Fusion Energy Div.
TRANSIENT HEAT TRANSFER IN SUPERFLUID HELIUM, PART 2
Lawrence Dresner 1983 11 p refs Presented at the MIT Short Course on Large-Scale Appl. of Superconductivity, Cambridge, Mass., 19 Jul. 1983
(Contract W-7405-eng-26)
(DE83-015767; CONF-830776-1-Pt-2) Avail: NTIS HC A02/MF A01

Three classical problems associated with the ordinary diffusion equation concern the temperature in: (1) a half-space with clamped heat flux at the free face; (2) a half-space with clamped temperature

at the free face; and (3) an infinite medium with a pulsed plane heat source. These problems are also important for the nonlinear diffusion equation based on the Gorter-Mellink relation, which describes heat transport in superfluid helium. A similarity solution to problem (1), the clamped-flux problem, was found and compared, with good agreement, with experimental data of van Sciver. (A similarity solution is one in which the profiles of temperataure rise (RADICAL)T versus distance Z at different times t can be obtained from one another by suitable (different) stretching of the temperature and distance axes.) Similarity solutions are given in analytic form to problems (2) and (3), the clamped-temperature and pulsed-source problems. DOE

N84-12985# California Univ., Livermore. Lawrence Livermore Lab.
CHARACTERIZATION BY X-RAY TOPOGRAPHY OF LASER-INDUCED DAMAGE IN POTASSIUM DIHYDROGEN PHOSPHATE CRYSTALS
H. Newkirk, J. Swain, S. Stokowski, D. Milam, D. Smith (Pennsylvania State Univ., State College), and H. Klapper (Technischen Hochschule, Aachen) 1983 16 p refs Presented at the 7th Intern. Conf. on Crystal Growth, Stuttgart, 12 Sep. 1983
(Contract W-7405-eng-48)
(DE83-012045; UCRL-88824-Rev-1; CONF-830927-1-Rev-1) Avail: NTIS HC A02/MF A01

X-ray topography was used to characterize crystals of potassium dihydrogen phosphate and volumes in these crystals that were damaged by 1-ns, 1064-nm laser pulses. The crystals exhibited a nonuniform distribution of defects: linear dislocation networks, cracks, transition or growth layers, sectors and inclusions at which dislocation networks were initiated. The damaged volumes contained individual domains each composed of a central core of highly disturbed material surrounded by a spherically symmetric radial strain field. There was not an unambiguous correlation between the preexisting X-ray topography microstructure of a test volume and its laser damage threshold. In some crystals, thresholds were least in test volumes with a high density of line defect networks. In other crystals, volumes free of defects had the least thresholds. Therefore, some entity not resolvable by X-ray topography, possibly a point defect impurity cluster, was the limiting cause of damage. DOE

N84-12986# Sandia Labs., Albuquerque, N. Mex.
HOLE TRAPPING, RECOMBINATION, AND SPACE CHARGE IN IRRADIATED SANDIA OXIDES
R. C. Hughes and C. H. Seager 1983 23 p refs Presented at the 20th IEEE Ann. Conf. on Nucl. and Space Radiation Effects, Gatlinburg, Tenn., 18 Jul. 1983
(Contract DE-AC04-76DP-00789)
(DE83-015212; SAND-83-0576C; CONF-830714-12) Avail: NTIS HC A02/MF A01

A computer model for calculating radiation effects in MOS oxides is presented. Good agreement is obtained between theory and photoconductivity experiments (photocurrent and flat band shift as a function of total dose) on radiation hard oxides. It is also shown that doses above 10 to the 8th power rads (delivered by a focused electron beam) are required to produce a significant number of new defect traps. DOE

N84-12987# Brookhaven National Lab., Upton, N. Y. Physics Dept.
COMMENSURABILITY, CHAOS, AND THE DEVIL'S STAIRCASE
Per Bak and M. Hoegh Jensen (Copenhagen Univ.) 1982 28 p refs
(Contract DE-AC02-76CH-00016)
(DE83-013280; BNL-33117) Avail: NTIS HC A03/MF A01

These lectures deal with the effects of the discrete lattice on modulated structures in solid state physics. The modulated structure could be a periodic lattice distortion, a sinusoidal or helical magnetic structure, staging of alkali metals in graphite intercalation compounds, polytypism in crystal formation, or some other periodic arrangement. Models discussed include the 1d Ising model with long range antiferromagnetic interactions in a magnetic field, the 3d Ising model with competing interactions, and the discrete phi(4) model. DOE

N84-12988# California Univ., Livermore. Lawrence Livermore Lab.
THERMAL PERFORMANCE OF THE MFTF MAGNETS
J. H. VanSant 1983 11 p refs Presented at the Cryogenic Eng. Conf., Colorado Springs, 15 Aug. 1983
(Contract W-47505-eng-48)
(DE83-016275; CONF-830841-3; UCRL-88696) Avail: NTIS HC A02/MF A01

A yin-yang pair of liquid-helium (LHe) cooled, superconducting magnets were tested as part of a series of tests with the mirror fusion test facility. These tests were performed to determine the success of engineering design used in major systems of the MFTF and to provide a technical base for rescoping from a single-mirror facility (MFTF) to the large tandem-mirror configuration (MFTF-B) now under construction. The magnets were cooled, operated at their design current and magnetic field, and warmed to atmospheric temperature. Their thermal behavior during these tests is described. DOE

N84-12989# Brookhaven National Lab., Upton, N. Y.
TEMPERATURE DEPENDENCE OF THE ELECTRIC-FIELD GRADIENT IN Er METAL
M. H. Rafailovich, O. C. Kistner, E. Dafni (Weizmann Inst.), A. W. Sunyar, M. Mohsen, S. Vajda (State Univ. of N.Y.), and G. D. Sprouse (State Univ. of N.Y.) 1983 6 p refs Presented at the 6th Intern. Conf. on Hyperfine Interactions, Groningen, Netherlands, 4 Jul. 1983
(Contract DE-AC02-76CH-00016)
(DE83-015564; BNL-33376; CONF-830779-1) Avail: NTIS HC A02/MF A01

The method of perturbed angular distributions was used to measure the temperature dependence of the electric-field gradient in Er single crystal for 98 K less than or equal to T less than or equal to 456 K. The I/sup pi/ = 11(-) isomer in (154)Er was used as a probe. DOE

N84-12990# Oak Ridge National Lab., Tenn.
SUPERCONDUCTOR STABILITY, 1983: A REVIEW
Lawrence Dresner 1983 30 p refs Presented at the MIT Short Course on Large-Scale Appl. of Superconductivity, Cambridge, Mass., 19 Jul. 1983
(Contract W-7405-eng-26)
(DE83-015506; CONF-830776-2) Avail: NTIS HC A03/MF A01

Three main topics were discussed, namely, internally cooled superconductors, cooling by superfluid helium, and metastable magnets. The discussion of each has centered around a dominant idea, and it is fitting to highlight these ideas by way of conclusion. With regard to internally cooled superconductors, most of what was learned in the last few years centers n the strong motion caused by the thermal expansion of helium. How naive were early calculations that treated the helium as though it were incompressible. Discussion of He-II was organized around the Gorter-Mellink relation and the solutions of the nonlinear diffusion equation to which it gives rise. And discussion of metastable magnets revolved around the fruitful concept of the MPZ. These three ideas are sturdy trunks that support much of the thought about superconductor stability that has flowered in the past several years. DOE

N84-12991# California Univ., Livermore. Lawrence Livermore Lab.
METHODS FOR DECONVOLUTING AND INTERPRETING COMPLEX GAMMA AND X-RAY SPECTRAL REGIONS
Ray Gunnink Jun. 1983 6 p ref Presented at the Am. Nucl. Soc. Winter Meeting, San Francisco, 30 Oct. 1983
(Contract W-7405-eng-48)
(DE83-013585; UCRL-89364; CONF-831047-1) Avail: NTIS HC A02/MF A01

Germanium and silicon detectors are now widely used for the

detection and measurement of X and gamma radiation. However, some analysis situations and spectral regions were heretofore too complex to deconvolute and interpret by techniques in general use. One example is the L X ray spectrum of an element taken with a Ge or Si detector. New tools and methods that were developed to analyze complex spectral regions are described, and illustrated with examples. DOE

N84-12992# Columbia Univ., New York.
DEFECT INTERACTIONS AT HIGH CONCENTRATIONS IN SOLID OXIDE ELECTROLYTES Progress Report, 1 Aug. 1982 - 31 Jul. 1983
A. S. Nowick 1983 13 p refs
(Contract DE-AC02-78ER-04693)
(DE83-016849; DOE/ER-04693/T4) Avail: NTIS HC A02/MF A01

Progress was made in the study of M(+) doped ceria (CeO2), where ionic radii were studied. A striking dependence of conductivity (and the controlling parameter, H/sub A/, the association enthalpy of a M(+3)-V/sub O/pair) on dopant radius was found. Subsequent work on computer simulation calculations in the laboratory shows remarkable agreement with these experiments. Particularly striking was the high H/sub A/-value, of 0.67 eV, for Sc-V/sub O/pairs, Sc(+3) being the smallest dopant ion studied. DOE

N84-12993# California Univ., Berkeley. Lawrence Berkeley Lab. Applied Physics and Laser Spectroscopy Group.
OPTICAL PROPERTIES AND CORRELATION ENERGY OF DEFECTS IN a-Ge:H
Andrew Skumanich and Nabil M. Amer Jul. 1983 6 p refs Presented at the 10th Intern. Conf. on Amorphous and Liquid Semiconductors, Tokyo, 22-26 Aug. 1983
(Contract DE-AC03-76SF-00098)
(DE83-016697; LBL-16454; CONF-830895-4) Avail: NTIS HC A02/MF A01

Gap-state optical absorption of undoped and doped a-Ge:H was measured using photothermal deflection spectroscopy. It is shown that the absorption is due to Ge dangling bond defects whose energy lies approx. 0.5 eV below the conduction band. The correlation energy of the defect is determined to be approx. 0.1 eV. Unlike a-Si:H, gap-state absorption of a-Ge:H shows little or no change after intense illumination. DOE

N84-12994# Sandia Labs., Albuquerque, N. Mex. Div. 1111.
PROCEEDINGS OF THE WORKSHOP ON ION MIXING AND SURFACE LAYER ALLOYING
M. A. Nicolet (California Inst. of Technology) and Samuel T. Picraux May 1983 179 p refs Workshop held in Pasadena, Calif., 15-16 Apr. 1983
(Contract DE-AC04-76DP-00789; Grant N00014-83-G-0057)
(DE83-015354; SAND-83-1230; CONF-830468) Avail: NTIS HC A09/MF A01

The basic mechanisms of ion mixing, its relation to high-dose implantation, and areas of potential applications were covered. In addition, the major conclusions of the workshop were outlined and a tentative scheme of nomenclature for the mechanisms of ion mixing was given. Separate abstracts were prepared for 14 of the summaries; the remaining two pages previously were abstracted. DOE

N84-12995# Oak Ridge National Lab., Tenn.
SUPERCONDUCTING STABILITY, 1983: A REVIEW
Lawrence Dresner 1983 28 p refs Presented at the Cryogenic Eng. Conf. and Intern. Cryogenic Mater. Conf., Colorado Springs, 15 Aug. 1983
(Contract W-7405-eng-26)
(DE83-017262; CONF-830841-4) Avail: NTIS HC A03/MF A01

Internally cooled superconductors, cooling by superfluid helium, and metastable magnets were discussed. With regard to internally cooled superconductors, most of what was learned in the last few years centers on he strong motion caused by the thermal expansion of helium. Discussion of He-II was organized around the Gorter-Mellink relation and the solutions of the nonlinear diffusion equation it gives rise to. And our discussion of metastable magnets revolved around the fruitful concept of the minimum propagating zone (MPZ). These three ideas support much of the though about superconductor stability that has flowered in the past several years. DOE

N84-12996# California Univ., Berkeley. Lawrence Berkeley Lab.
PHONON-INDUCED ENHANCEMENTS OF THE ENERGY GAP AND CRITICAL CURRENT IN SUPERCONDUCTING ALUMINUM Ph.D. Thesis
Daniel Seligson May 1983 166 p refs
(Contract DE-AC03-76SF-00098)
(DE83-015210; LBL-16290) Avail: NTIS HC A08/MF A01

The 8 to 10 GHz phonons were generated by piezoelectric transduction of a microwave and by means of a quartz delay line, were allowed to enter the aluminum only after the microwaves had long since disappeared. The maximum enhancements detected were [deltaT/T/sub c/] = -0.07, for i/sub c/ and [deltaT/T/sub c/] = -0.03 for (RADICAL). The power- and temperature-dependence (0.82 less than or equal to T/T/sub c/ less than or equal to 0.994) of the enhancements were compared with the prediction of a theory. The gap-enhancement was in good agreement with the theory only for low input lower. The critical current measurements are predicted to be in rough agreement with the (RADICAL) measurements but this was not observed. The magnitude of the critical current enhancements was typically more than twice the observed gap enhancements. The measured critical current enhancement was elatively independent of temperature whereas the gap enhancement decreased rapidly as the temperature was lowered. DOE

N84-12997# Ames Lab., Iowa.
SPUTTERED C-AXIS INCLINED PIEZOELECTRIC FILMS AND SHEAR-WAVE RESONATORS
J. S. Wang, K. M. Lakin, and A. R. Landin 1983 8 p refs Presented at the 37th Frequency Control Symp., Philadelphia, 1-3 Jun. 1983 Sponsored in part by AFOSR
(Contract W-7405-eng-82)
(DE83-017253; IS-M-428; CONF-8306120-1) Avail: NTIS HC A02/MF A01

Well oriented ZnO and AlN films with C-axis inclined from the film normal were grown in a reactive dc planar magnetron sputtering system having an auxiliary anode structure. The columnar structure of the C-axis crystallites, included from the Si substrate normal, was clearly visible in SEM. Films having C-axis inclination angles up to 450 and thicknesses up to 10 microns were obtained. Composite resonators were fabricated by sputtering ZnO or AlN films onto the p(+) Si membrane. Typically, these resonators exhibited Q s of about 5000 in 200 MHz to 500 MHz fundamental resonance range. Of particular interest is the temperature compensation of resonant frequency. Resonators having an absolute temperature coefficient of series resonant frequency of less than 1 ppM/C0 around room temperature were made for both ZnO/Si and AlN/Si composite structures. The temperature coefficient of the ZnO and AlN plate resonators was also measured to be -36.2 ppM/C and -25 ppM/C which suggested the temperature coefficient of the p(+) Si membrane to be about +9 ppM/C in the shear mode. DOE

N84-12998# Sandia Labs., Albuquerque, N. Mex.
PHYSICS OF ION IMPLANTATION: ION-CASCADE PROCESSES AND PHYSICAL STATE OF THE IMPLANTED SOLID
S. T. Picraux 1983 40 p refs Presented at the NATO Advanced Study Inst. on Surface Engr., Les Arcs, France, 3 Jul. 1983
(Contract DE-AC04-76DP-00789)
(DE83-017152; SAND-83-1046C; CONF-830787-2) Avail: NTIS HC A03/MF A01

During ion implantation into solids a number of important processes take place which alter the physical state of the near-surface region. A clear understanding of these processes and the resulting microstructural modifications is invaluable in utilizing ion implantation to engineer surfaces through the controlled modification of surface properties. This lecture summarizes current

theoretical and experimental understanding in these areas. Basic ion implantation processes discussed include implantation fluence, stopping powers, ion range, damage energy, enhanced diffusion, ion mixing, and sputtering. The physical state of the implanted solid is then considered. Equilibrium and metastable implanted alloy formation is reviewed and the resulting structures are discussed. DOE

N84-12999# Fermi National Accelerator Lab., Batavia, Ill.
OPERATIONAL STUDIES AND EXPECTED PERFORMANCE OF SUPERCONDUCTING QUADRUPOLE MAGNETS IN THE FIRST STAGES OF SECONDARY BEAMS
P. H. Garbincius, P.O. Mazur, R. P. Stanek, R. P. Smith (Argonne National Lab., Ill.), S. H. Kim (Argonne National Lab., Ill.), C. I. Krieger (Argonne National Lab., Ill.), J. D. Gonczy (Argonne National Lab., Ill.), A. L. Kelly (Argonne National Lab., Ill.), D. C. Underwood (Argonne National Lab., Ill.), E. J. Wallace (Argonne National Lab., Ill.) et al Aug. 1983 4 p refs Presented at the 12th Intern. Conf. on High Energy Accelerators, Batavia, Ill., 11 Aug. 1983
(Contract DE-AC02-76CH-03000)
(DE83-016734; FERMILAB/TM-1202; CONF-830822-15) Avail: NTIS HC A02/MF A01

A low current, large bore, epoxy impregnated superconducting quadrupole magnet was constructed as a possible prototype for secondary beam use. Beam quenching tests were performed by targetting a primary proton beam directly onto the quadrupole coil and by using the quadrupole in its anticipated role as part of the first stage flux collection triplet for a zero degree anti-proton secondary beam formed from the decays of neutral Lambda particles. Comparing the results with similar tests performed using forced flow energy saver dipoles shows that the epoxy impregnated quadrupoles have a much greater sensitivity to beam induced quenching at a similar fraction of the conductor short sample limit. Calculations using the CASIM program indicate that such epoxy impregnated coils would not be viable as first stage flux collection elements without appreciable collimation and subsequent loss of secondary beam acceptance. Quadrupoles based on energy saver technology appear capable of tolerating acceptable primary beam intensities. The momentum dispersing bends require even larger aperture superconducting dipoles or neutral beam dump within the bend string. DOE

N84-13000# Deutsche Bundespost, Darmstadt (West Germany). Forschungsinst.
LIQUID PHASE EPITAXY OF InP/In1-xGaxAsyP1-y HETERO-STRUCTURES. PART 3: PHASE DIAGRAMS
Eckart Kuphal Feb. 1983 43 p refs In GERMAN; ENGLISH summary
(FI-65-TBr-20-Pt-3) Avail: NTIS HC A03/MF A01

The semiconductor material system In sub 1-x Ga sub x As sub y P sub 1-y lattice-matched to (100) InP was studied. Layers of this system covering the full wavelength range from 0.92 to 1.65 micron were grown by liquid phase epitaxy. The solid-liquid phase diagram of this system was experimentally determined at 630 C using the two-phase-solution technique and at 600 C using the supercooling technique. The phase diagrams of the limiting cases of this system, InP and In0.53Ga0.47As, were measured. By fitting suitable functions to the data, an empirical phase diagram of the system in the temperature range between 570 and 660 C was established. The functions also fit the phase diagrams of the limiting cases of this system. An empirical formula for the energy of the band gap as a function of x and y is given. The phase diagram of In1-xGaxAs is treated, to make predictions about the miscibility gap and the lattice mismatch as a function of supersaturation in In1-xGaxAs. Author (ESA)

N84-13001# Valvo G.m.b.H., Hamburg (West Germany). Entwicklung Professionelle Roehren und Baugruppen.
PREDEVELOPMENT OF IR-CCD COMPONENTS Final Report, Dec. 1981
Juergen Siebeneck, Lutz Gablor, and Uwe Suckow Bonn Bundesministerium fuer Forschung und Technologie Jul. 1983 71 p In GERMAN; ENGLISH summary Sponsored by Bundesministerium fuer Forschung und Technologie
(BMFT-FB-T-83-133; ISSN-0340-7608) Avail: NTIS HC A04/MF A01; Fachinformationszentrum, Karlsruhe, West Germany DM 15

Infrared charge coupled devices (IR-CCD) from extrinsic silicon are described. A 150 picture element monolithic line sensor was developed. Indium doped silicon substrates of < 100 > orientation, 1 to 2 x 10 to the 17th power/cucm concentration and 500 micron thickness were used. The measured black body responsitivity of the detectors lies in the 100 A/W range (50 K, 1000 V/cm) and the corresponding detectivity at 10 to the 11th power cm/sq root s/W. To optimize the system the electrical properties of surface, bulk and profile CCD's were tested as a function of temperature. At 50 K, the operating temperature of In doped Si, BCCD's is the best solution. The picture element size of the line sensor was 15 micron x 30 micron. The pitch was 60 micron. The transfer structure to inject the photocharge from the detector into the CCD register can do antiblooming and skimming. The homogeneity of the responsivity of the line sensor is 5%. Author (ESA)

N84-13002# AEG-Telefunken, Ulm (West Germany). Forschungsinst.
APPLICATIONS OF ANALOG CHANGE COUPLED DEVICES (CCD'S) Final Report, Apr. 1981
Peter Christiansen, Paul Gebhardt, Gerhard Kohlbacher, Helmuth Schinagel, Anton Stuermer, and Winfrid Wolf Bonn Bundesministerium fuer Forschung und Technologie Jul. 1983 143 p refs In GERMAN; ENGLISH summary Sponsored by Bundesministerium fuer Forschung und Technologie
(BMFT-FB-T-83-141; ISSN-0340-7608) Avail: NTIS HC A07/MF A01; Fachinformationszentrum, Karlsruhe, West Germany DM 30

Applications of analog CCD structures, and problems of peripheral circuits were studied, yielding insight into linear metal oxide semiconductor circuit design including the possibilities of computer aided design. Besides CCD filters, applications in consumer electronics were investigated. A concept for a CCD-PAL decoder in color television receivers was developed. Filters with switched capacitors were designed. The main results of the system studies were experimentally verified by test chips. Author (ESA)

77 THERMODYNAMICS AND STATISTICAL PHYSICS

Includes quantum mechanics; and Bose and Fermi statistics.

For related information see also *25 Inorganic and Physical Chemistry* and *34 Fluid Mechanics and Heat Transfer.*

N84-13003# California Univ., Berkeley. Lawrence Berkeley Lab. Materials and Molecular Research Div.
APPLICATIONS OF MOLECULAR QUANTUM MECHANICS TO PROBLEMS IN CHEMISTRY
Henry F. Schaefer, III Mar. 1983 10 p refs Presented at Intern. Congr. of Pure and Appl. Chem., Cologne, West Germany, 5-10 Jun. 1983
(Contract DE-AC03-76SF-00098)
(DE83-015943; LBL-15762; CONF-830694-1) Avail: NTIS HC A02/MF A01

The past decade has witnessed remarkable progress in the development of rigorous quantum mechanical methods for the study of molecular electronic structure. Key developments include the emergence of large scale configuration interaction methods (including more than one million variational parameters) and of analytic first and second energy derivative techniques. These advances have greatly increased the scope of current applications of quantum mechanics to chemistry. Present and anticipated future developments with respect to the fields of physical, organic, and inorganic chemistry are surveyed. DOE

N84-13004# North Carolina Univ., Chapel Hill. Dept. of Physics and Astronomy.
RESEARCH IN THEORETICAL PHYSICS
H. vanDam 1983 14 p refs
(Contract DE-AS05-79ER-10448)
(DE83-0166222; DOE/ER-10448/1) Avail: NTIS HC A02/MF A01

Topics include massive neutrinos, the invisible axion, global supersymmetry in grand unification, Kaluza-Klein anomalies, theory of gravity, quarkonium hyperfine splittings and the QCD scale parameter, a supersymmetric preon model, quantum mechanics of an extended object, E(6) theory without domain walls, and tensor methods for E(6). DOE

N84-13005# California Univ., San Diego, La Jolla. Energy Center.
EMPIRICAL VALIDATION OF COMPUTER MODELS FOR PASSIVE-SOLAR RESIDENCES Final Report
Anthony V. Sebald 1 Jun. 1983 114 p refs
(Contract DE-AC02-80CS-30260)
(DE83-016887; DOE/CS-30260/1) Avail: NTIS HC A06/MF A01

The theoretical underpinnings for experimental validation of thermodynamic models of passive solar buildings are given. Computer algorithms for such validation are discussed. Models for passive solar buildings are essentially incapable of validation in the classical sense. This is principally due to the fact that buildings are exposed to excitations which have insufficient frequency content to permit estimation of the coefficients in all but the most rudimentary models. One can, however, generate a set of possible models which explain the measured data. Unfortunately, while all models in the set may equally well track the measured data, the coefficients may vary significantly within the set. When used to estimate auxiliary energy consumption by simulation, models within the set may predict substantially different consumptions. DOE

N84-13006# Los Alamos Scientific Lab., N. Mex.
DENSE MOLECULAR THERMODYNAMICS
J. D. Johnson, M. S. Shaw, and B. L. Holian 1983 5 p refs Presented at the Am. Phys. Soc. Meeting on Shock Waves in Condensed Media, Santa Fe, N. Mex., 18-21 Jul. 1983
(Contract W-7405-eng-36)
(DE83-015216; LA-UR-83-2232; CONF-830719-16) Avail: NTIS HC A02/MF A01

The thermodynamics of dense molecular fluids from the theoretical view were examined. Interests range from modeling single-species, spherically symmetric, atomic systems, through adding the complication of nonspherical molecular potentials, to mixing various molecular species with the inclusion of chemistry. Accomplishments and directional evaluation to be taken in attacking the unsolved problems was discussed. The various theoretical approaches, both analytic and numerical, are presented. A discussion of the recent advance in treating nonspherical molecular potentials with effective spherical potentials in the calculation of thermodynamics is described. DOE

N84-13007# Hubschrauberflugplaz der US-Army, Frankfurt am Main (West Germany).
NOISE EMISSION BY HELICOPTERS [LAERMIMISSION DURCH HURBSCHRAUBERBETRIEB]
Rickmann and Schilling 24 Aug. 1982 43 p In GERMAN
Avail: NTIS HC A03/MF A01

Noise level measurements were performed in urban areas subject to noise from small and large helicopters flying at between 140 and 200 m altitude. During the day the equivalent continuous noise level is 48dB(A) which is 2dB(A) below the allowed maximum. During the night the level is 55dB(A) which is 20dB(A) above the maximum. These results are only valid during the summer.
Author (ESA)

N84-13008# Rice Univ., Houston, Tex. Dept. of Chemical Engineering.
NEW CONFORMAL SOLUTION THEORY Final Report, 1979 - 1982
T. W. Leland, Y. P. Chen, T. Hang, P. Angelo, and K.-H. Naumann Jul. 1983 115 p refs Sponsored by Gas Research Inst.
(PB83-249441; GRI-81/0051) Avail: NTIS HC 06/MF A01 CSCL 07D

A new theory for computing thermodynamic properties of liquid and vapor mixtures and equilibrium K-valves was developed and demonstrated. A new procedure for computer calculation of thermodynamic properties of liquid and vapor mixtures long with their equilibrium K-valve was demonstrated theoretically and practically. The procedure is basically designed for use with computers. The mixture properties obtained are compressibility factors enthalpy, entropy, and densities of liquids and vapors at both high and low pressures from cryogenic temperatures to reservoir conditions. Equilibrium K-valves are predicted simultaneously. These properties are essential for: design of heat exchangers, compressors, turbo-expanders, separation processes for gases and liquids, dew point and bubble point calculations, and reservoir operations. GRA

80 SOCIAL SCIENCES (GENERAL)

Includes educational matters.

N84-13009# Southeastern Center for Electrical Engineering Education, Inc., St. Cloud, Fla.
USAF/SCEEE SUMMARY FACULTY RESEARCH PROGRAM (1982) RESEARCH REPORTS, VOLUME 2 Final Report
Warren D. Peele and Earl I. Steele Oct. 1982 780 p refs 2 Vol.
(Contract F49620-82-C-0035; AF Proj. 2301)
(AD-A130770; AFOSR-83-0614TR) Avail: NTIS HC A99/MF A01 CSCL 05/1

Scientists who competed for a ten-week assignment to perform research at Air Force laboratories and centers are listed and results of their investigations in electrical engineering are summarized.
A.R.H.

81 ADMINISTRATION AND MANAGEMENT

Includes management planning and research.

N84-13010# Information Spectrum, Inc., Arlington, Va.
RIS ASSESSMENT TECHNIQUES: A HANDBOOK FOR PROGRAM MANAGEMENT PERSONNEL
Jul. 1983 255 p refs
(Grant MDA903-82-G-0055)
(AD-A131596; ISI-V-3836-05) Avail: NTIS HC A12/MF A01 CSCL 05/1

The primary objectives of this handbook are to make the reader aware of the risk assessment techniques being used by Department of Defense organizations, to alert the reader to the advantages and disadvantages of these techniques, and to assist him in applying risk assessment to his acquisition program. The handbook is intended to be a practical guide and reference for program management personnel - not a textbook dealing with the theories supporting risk analysis, nor a user's manual for applying any particular techniques. Thus, the handbook is organized to address, in summary, the most important questions to program management personnel, i.e., Why do a risk assessment? What techniques are available? How do I select and implement a technique? These questions are answered in the first six chapters. This summary-level material is supported by a series of Appendices that provide detailed discussions of the techniques in use, the service regulations pertaining to risk assessments, a glossary of terms, and a structured bibliography. GRA

N84-13011# McDonnell-Douglas Astronautics Co., St. Louis, Mo.
MODELS OF MAINTENANCE RESOURCES INTERACTION: PEACETIME OPERATIONS Final Report
Carl F. Asiala, Susan L. Loy, Ralph Hameister, William J. Cody, and Frank A. Maher Brooks AFB, Tex. Air Force Human Resources Lab. Jul. 1983 62 p refs
(Contract F33615-77-C-0074; AF Proj. 1710)
(AD-A131379; AFHRL-TR-82-19) Avail: NTIS HC A04/MF A01 CSCL 15/5

The primary objective of this study was to provide the Air Force with models of the interactive effects of manpower, spares, and support equipment for a current operational system. Initial tasks established the peacetime data requirements of a current operational fighter, the available sources of data, and the critical variables for the Logistics Composite Model (LCOM) simulations. The simulated environments relate directly to the Air Force base level data, e.g., flying profiles, mission, and resource allocation levels. The majority of the data for this study were obtained from the following sources: Air Force and contractor publications, Maintenance Data Collection (MDC) system, and structured interviews with operations and maintenance personnel. Regression models were developed for significant LCOM variables. The LCOM and the regression models of interaction developed in this study have applicability to design and management issues.
Author (GRA)

N84-13012# Young (Arthur) and Co., Washington, D. C.
OFFICE AUTOMATION MANAGEMENT GUIDE Final Report, Apr. - May 1983
May 1983 49 p
(Contract MDA903-79-C-0690)
(AD-A131770) Avail: NTIS HC A03/MF A01 CSCL 05/2

The Guide outlines planning, acquisition, implementation and post implementation evaluation considerations for information managers who are responsible for establishing office automation programs. This Guide was developed by Arthur Young & Company for the Information Resources Management Directorate, OASD(C). The Guide is intended to assist the Department in realizing the opportunities to increase the productivity and effectiveness of professional, administrative, and clerical personnel that are presented by office automation technologies. Author (GRA)

N84-13013# California Univ., Livermore. Lawrence Livermore Lab.
REVITALIZATION: AN ORGANIZATIONAL PROGRAM FOR THE INDIVIDUAL
Jack M. Brewer Jul. 1983 6 p Presented at the Organizational Develop. Conf., Pasadena, Calif., 11 Oct. 1983
(Contract W-7405-eng-48)
(DE83-014949; UCRL-89432; CONF-831096-1) Avail: NTIS HC A02/MF A01

Progressive devitalization is a malady that afflicts many workers resulting in tremendous costs to organizations. This malady has long been recognized by management but little has been done to treat it. A new approach to the problem has been instituted at Lawrence Livermore National Laboratory, in the form of a group program called Revitalization. Early results have been very encouraging. The program will continue to be designed and improved in the hope of bringing more productivity to the organization and self-esteem to the individual. DOE

N84-13014# Pacific Northwest Lab., Richland, Wash.
MANAGEMENT OF QA IN AN R AND D ORGANIZATION
Dennis E. Ryder Jun. 1983 7 p refs Presented at the 37th Ann. Am. Soc. for Quality Control Congr., Boston, 24-26 May 1983
(Contract DE-AC06-76RL-01830)
(DE83-016924; PNL-SA-10382; CONF-830535-3) Avail: NTIS HC A02/MF A01

Application of more formal QA-system principles and practices are slowly but surely becoming a fact of life for many of the nation's R and D organizations. As an example, the US Department of Energy (DOE) in 1981 issued an order to its field offices that involved requirements for the assurance of quality achievement in DOE programs. This paper will provide useful information based upon actual experience in the development and implementation of an R and D QA Program at a national laboratory. It will include a discussion of the R and D product (data), primary QA concerns, management of the QA program and QA organization, QA planning, and contributions that QA personnel can make to the R and D effort. DOE

N84-13015# Max-Planck-Gesellschaft zuer Foerderung der Wissenschaft e.V., Garching (West Germany).
PORTRAIT OF THE MAX-PLANCK RESEARCH ORGANIZATION AND ITS INSTITUTES [MPG: DIE MAX-PLANCK-GESELLSCHAFT UND IHRW INSTITUTE. PORTRAET EINER FORSCHUNGSORGANISATION]
Robert Gerwin, ed. and Barbara Holtz, ed. 1 May 1983 147 p In GERMAN
Avail: NTIS HC A07/MF A01

Size and distribution of the institutes, legal form and financing, basis of the scientific policy, organization structure, research-organizational field, scientific cooperation, and reports of the Max-Planck organisation are explained. Biological-medical, chemical-physical-technical and human research sections are presented. Author (ESA)

N84-13016# Arizona State Office of Economic Planning and Development, Phoenix.
ARIZONA STATE SCIENCE, ENGINEERING AND TECHNOLOGY PROCESS Final Report
15 Mar. 1983 264 p
(Grant NSF ISP-80-19800)
(PB83-237107; NSF-ISP-83004) Avail: NTIS HC A12/MF A01 CSCL 05A

The progress of the Arizona State Science, Engineering and Technology Program (SSET) is summarized. The development of a work plan is described and state priority policy issues are identified. SSET advisory council meetings, coordination efforts, and response to a request from the director of the Department of Human Services are discussed. Two areas deemed crucial for program effectiveness are considered: (1) the development of an on-going mechanism to access the universities and other technical communities; and (2) the identification of end-user needs. Transportation options for rural Arizona are considered and criteria for developing urban lands in Arizona are explored. The need for Arizona to provide a policy to take advantage of telecommunications technology is expressed. GRA

82 DOCUMENTATION AND INFORMATION SCIENCE

Includes information storage and retrieval technology; micrography; and library science.

For computer documentation see *61 Computer Programming and Software.*

N84-13017* National Aeronautics and Space Administration, Washington, D. C.
NASA PATENT ABSTRACTS BIBLIOGRAPHY. SECTION 1: ABSTRACTS. A CONTINUING BIBLIOGRAPHY
Jul. 1983 56 p
(NASA-SP-7039(23); NAS 1.21:7039(23)) Avail: NTIS HC A04 CSCL 05B

Abstracts are cited for 129 patents and patent applications introduced into the NASA scientific and technical information system during the period January 1983 through June 1983. Each entry consists of a citation, an abstract, and in most cases, a key illustration selected from the patent or patent application. S.L.

N84-13018* National Aeronautics and Space Administration, Washington, D. C.
NASA PATENT ABSTRACTS BIBLIOGRAPHY. SECTION 2:

INDEXES. A CONTINUING BIBLIOGRAPHY (SUPPLEMENT 23)
Jul. 1983 373 p
(NASA-SP-7039(23); NAS 1.21:7039(23)) Avail: NTIS HC A16 CSCL 05B

Entries for 4000 patent and patent applications citations for the period May 1969 through June 1983 are listed. Subject, invention, source, number, and accession number indexes are included. S.L.

N84-13019# Boeing Aerospace Co., Seattle, Wash.
INTEGRATED CUING REQUIREMENTS (ICR) STUDY: DEMONSTRATION DATA BASE AND USERS GUIDE Final Report
Richard Farrell and Richard Barker Brooks AFB, Tex. Air Force Human Resources Lab. Jul. 1983 142 p
(Contract F33615-79-C-0014; AF Proj. 6114)
(AD-A131119; AFHRL-TP-82-25(2)) Avail: NTIS HC A07/MF A01 CSCL 05/2

The goal of the Integrated Cuing Requirements (ICR) Study was to consolidate and synthesize existing human sensory/perceptual data, principles and models in a manner which would make this information readily accessible and useful to the community of aircrew training device (ATD) design engineers. The goal of the ICR study was to extract and consolidate the relevant data into an accessible format and to provide, where feasible, a synthesis of the literature which included recommendations relevant to equipment design. The intended output of this activity was and ICR Data Base containing the available sensory/perceptual data in a form useful for specification and design purposes, and an ICR Users Guide to facilitate access to the data by the ATD engineer. Volume I of this technical paper presents the results of an Independent Feasibility Analysis and a subsequent Demonstration Study Evaluation, the purpose of which was to develop, test, and refine an approach to the ICR Study objectives discussed above. These activities constituted Phase I of the effort. The project was structured such that no decisions on full-scale implementation of the approach (Phase II) would be made until an evaluation of Phase I had been completed. Volume II of this technical paper contains the Phase I Demonstration Data Base and Users Guide. GRA

N84-13020# Army Research Inst. for the Behavioral and Social Sciences, Arlington, Va.
AN INVESTIGATION OF GEOMETRIC RADAR SHAPES FOR STEREOTYPING
Richard J. Carter Aug. 1981 26 p refs
(DA Proj. 2Q7-62722-A-765)
(AD-A131120; ARI-TR-570) Avail: NTIS HC A03/MF A01 CSCL 06/16

This investigation sought to determine whether any of the symbols which are currently being used or are proposed for usage in future air defense systems are stereotyped with the meanings hostile, friendly, and unknown. Each of the 100 male service members sorted 60 shapes into four categories, namely friend, hostile, unknown, and other depending upon what each shape control. The personnel also rank ordered the shapes which had been sorted into the first three categories. Chi square statistics were used to analyze the data. Shapes were identified which are stereotyped with the three meanings. The 5-Pointed Star, Heart, and Flag were associated with the friend meaning. The Swastika and Question Mark were associated with the hostile and unknown meanings respectively. The results of this experiment will be utilized in future research which will be aimed at deriving a standard symbology for application to radar assisted air defense systems. Author (GRA)

N84-13021# Naval Submarine Medical Research Lab., Groton, Conn.
THE COMPUTERIZATION OF MATERIAL SAFETY DATA SHEET INFORMATION Interim Report
Michael L. Shea, Christopher J. Eident, Thomas P. Santoro, Elizabeth L. Megos, and Dieter Boessmann 20 Jul. 1983 49 p
(M0100PN; F58524)
(AD-A131992; NSMRL-MR-83-4) Avail: NTIS HC A03/MF A01 CSCL 09/2

FORTRAN computer programs were written in order to store and retrieve material safety data sheet (MSDS) information. The first program is used to add individual MSDS information to the master file whereas the second program allows the master file to be printed. The third and fourth programs allows for manipulation of the data in the master file such as searching and matching for specific information within the different information categories. Under development are programs used to extract certain data from the hazardous materials information system (HMIS) and incorporate them into the MSDS system. When completed, the on-line hazardous compound records will number approximately 16,000. Author (GRA)

N84-13022# Syracuse Univ., Utica, N. Y.
INFORMATION RETRIEVAL RESEARCH SUPPORT Final Technical Report
Joseph J. Arlotto May 1983 47 p
(Contract F30602-79-C-0195; AF Proj. 5581)
(AD-A131990; RADC-TR-83-120) Avail: NTIS HC A03/MF A01 CSCL 09/2

This report describes work performed by Utica College students of various academic disciplines to undertake study efforts and provide products in the Information Sciences. The report provides a synopsis of the individual investigation study efforts in such areas as information handling information processing, data extraction and data management. When appropriate, individual data gathering efforts were published as separate technical reports under this contract. Author (GRA)

N84-13023# Federal Aviation Administration, Washington, D.C. Office of Management Systems.
INFORMATION RESOURCES MANAGEMENT PLAN
Aug. 1983 208 p
(AD-A131964) Avail: NTIS HC A10/MF A01 CSCL 05/1

This Plan documents the Federal Aviation Administration's long-term plan for applying systems analysis and automated data processing technology to its information needs. As a long-range Plan, it provides a sound basis for both the Executive and Legislative Branches to properly appraise funding needs. It retains the flexibility needed to accommodate future technology as it becomes applicable to individual subsystems and it becomes evident that the new technology will improve our return on investment. The Plan begins institutionalizing a process of regular and comprehensive assessments of FAA's information posture and needs. This Plan is the framework for the development, operation, and management of agency information resources and for the regular review of performance as well as resource and priority decisions. The FAA will follow through on this planning effort with the detailed requirements documentation, system specifications, cost benefit analyses, and the other actions sound system management requires. GRA

N84-13024# Defense Technical Information Center, Alexandria, Va.
SOURCE HEADER LIST, SUPPLEMENT 1 Report, period ending 14 Jun. 1983
James P. Burrell Jul. 1983 227 p
(AD-A131800; DTIC/TR/83/3-Suppl-1) Avail: NTIS HC A11/MF A01 CSCL 05/2

This publication is a one volume, alphabetically arranged, compilation of corporate author names used by the Defense Technical Information Center since April 1982. It is a supplement to the two volume Source Header List (AD-A115 000, AD-A115 001). Taken together these three volumes contain all corporate source names in the DTIC data base system. Each source name is assigned a 6-digit numeric code for computer input and retrieval purposes plus a 4-digit alphanumeric geopolitical code and an alphanumeric type code. Source names displayed are included as data elements in the Technical Report, Work Unit Information System, Research and Development Program Planning, and Independent Research and Development data bases maintained by DTIC. GRA

N84-13025# Technische Univ., Graz (Austria). Inst. fuer Digital Bildverarbeitung und Graphik.
[ACTITITIES REPORT ON THE PROJET DESBOD] Annual Report, 1981-82 [DESBOD: JAHRSBEREICHT]
W. Kainz and M. Rainzinger 30 Apr. 1982 87 p refs In GERMAN Sponsored by Bundesministerium fuer Wissenschaft und Forschung
(Rept-5) Avail: NTIS HC A05/MF A01

The status of project DESBOD, a system for digital acquisition, storage and processing of local geographical and land data, is reported. Geographical data structures used in geographical information systems are reviewed. The data acquisition method is explained. The interactive manual digitizing system is described. Results of automatic acquisition of topographic data by means of a raster scanner are presented. Author (ESA)

N84-13026# Woods (James E.), Ames, Iowa.
NBS (NATIONAL BUREAU OF STANDARDS) WORKSHOP: ENVIRONMENTAL CONTROL FOR ARCHIVAL RECORDS STORAGE Final Report
Warren B. Johnson, William P. Lull, Charles A. Madson, Amos Turk, Karl L. Westlin, James E. Woods, and Paul N. Banks Aug. 1983 54 p refs Workshop held in Washington, D.C., 19-20 Jan. 1983 Sponsored in cooperation with NBS, GSA, and National Archives and Records Service
(PB83-242230; NBS-GCR-83-438) Avail: NTIS HC A04/MF A01 CSCL 05B

The control of environmental conditions in spaces used for storage of paper-based archival records is considered. The rationale for establishing levels of air quality for archival storage was explored and equipment technology was reviewed regarding its capability to provide optimum environmental conditions for archival storage facilities. Methods of thermal and air quality control are discussed and recommendations made for performance evaluation of environmental conditioning systems. Monitoring and assessment procedures to evaluate performance of environmental conditioning systems and components are addressed. GRA

N84-13027# National Library of Medicine, Bethesda, Md.
PERMUTED MEDICAL SUBJECT HEADINGS, 1984
1983 379 p
(PB83-234781; NLM-MED-83-04) Avail: NTIS HC A17/MF A01 CSCL 05B

The document is a computer-generated display of all terms, i.e., descriptors and cross references, in the alphabetic list of the National Library of Medicine's Medical Subject Headings (MeSH) for 1984, as well as all citation type, check tag, and geographic descriptors in the Annotated Alphabetic MeSH, 1984. The Permuted MeSH term and then lists all the MeSH terms in which that word appears. GRA

N84-13028# National Library of Medicine, Bethesda, Md.
MEDICAL SUBJECT HEADINGS, TREE STRUCTURES, 1984
1983 458 p
(PB83-223164; NLM-MED-83-03) Avail: NTIS HC A20/MF A01 CSCL 05B

All medical subject headings currently in use by the National Library of Medicine's indexers, catalogers, and searchers are arranged in a hierarchical manner showing relationships between broader and narrower terms. Minor and geographic descriptors are included. GRA

N84-13029# National Library of Medicine, Bethesda, Md.
MEDICAL SUBJECT HEADINGS, ANNOTATED ALPHABETIC LIST, 1984
1983 849 p Revised
(PB83-223156; NLM-MED-83-02-Rev) Avail: NTIS HC A99/MF A01 CSCL 05B

Alphabetic lists of all subject descriptors used by indexers and catalogers at the National Library of Medicine are presented. These include subject headings cross references; geographic headings; nonMeSH terms; check tags; tree numbers; and notes for indexes, catalogers, and online searchers. GRA

N84-13030 Rutgers - The State Univ., New Brunswick, N. J.
A STUDY OF CRITICAL FACTORS AFFECTING THE DEVELOPMENT OF PERFORMANCE MEASURES IN EVALUATING BIBLIOGRAPHIC INFORMATION RETRIEVAL SYSTEMS Ph.D. Thesis
John James Regazzi, III 1983 269 p
Avail: Univ. Microfilms Order No. DA8308449

This study is an investigation into critical factors which would constitute reliable performance measures for bibliographic information retrieval systems. Thirty-two (32) judges, grouped by type of judge (researcher or student), level (senior or junior), speciality (biomedicine or social science), and evaluation context (relevance or utility), were asked to rate sixteen (16) documents on alcohol studies which included four (4) different search topics and four (4) document citations and abstracts for each search topic. Half of the judges were asked to rate the documents on how relevant the documents on the basis of the document's percieved utility for the individual judge. After rating the documents, judges were also asked to rate the importance of five (5) document attributes (author, title, abstract, source of publication, and date of publication) and six (6) information attributes (accuracy, completness, subject, suggestiveness, timeliness, and treatment). The findings of the experiment indicate no significant difference in document rating, document attributes, or information attributes due to the evaluation context. Dissert. Abstr.

83 ECONOMICS AND COST ANALYSIS

Includes cost effectiveness studies.

N84-13031# Oak Ridge National Lab., Tenn. Engery Div.
TWO TYPES OF VALUES AND THEIR ASSESSMENT BY THE COLLECTIVE INTEREST
Paul R. Intemann 1982 26 p refs
(Contract W-7405-eng-26)
(DE83-012064; DOE/NBM-3012064) Avail: NTIS HC A03/MF A01

To better understand the meaning of value, it can be helpful to categorize values into different types. One such categorization is to divide them into functional values and perceptual values. Functional value is assigned on the basis of how much something contributes to or takes from the proper operation of a system. Perceptual value is assigned on the basis of how much something pleases or displeases an individual. In a mixed economy the responsibility of government in influencing the assessment of value is different for the two different types. For functional values, evaluation and resulting action by the government as a representative of the collective interest are based on maintenance or improvement of the system. This corresponds to Hardin's notion of averting the tragedy of the commons. For perceptual values, evaluation by the government is based on widening the choice available to individuals. This corresponds to Davidoff's and Reiner's theory of planning. The significance of this difference is explored using wilderness preservation policy as an example. DOE

84 LAW AND POLITICAL SCIENCE

Includes space law; international law; international cooperation; and patent policy.

N84-13032# Committee on Science and Technology (U. S. House).
NATIONAL AERONAUTICS AND SPACE ACT OF 1958, AS AMENDED AND RELATED LEGISLATION
S. Neil Hosenball, John E. OBrien, Elizabeth N. Siegel, and Cathy P. Runde Washington GPO 1983 220 p Presented to the Comm. on Sci. and Technol., 98th Congr., 1st Sess., Oct. 1983 Prepared by General Counsel's Office of NASA
(GPO-24-491) Avail: Committee on Science and Technology

The National Aeronautics and Space Act of 1958 is provided. Related legislation concerning authorization and appropriation

requirements, employees, procurement, administrative claims and litigation. The Tracking and Data Relay Satellite System, technology applications, relationships with other agencies, energy, and climate and applications is appended. N.W.

85 URBAN TECHNOLOGY AND TRANSPORTATION

Includes applications of space technology to urban problems; technology transfer; technology assessment; and surface and mass transportation.

For related information see *03 Air Transportation and Safety, 16 Space Transportation,* and *44 Energy Production and Conversion.*

N84-13033*# National Aeronautics and Space Administration, Washington, D. C.
SPINOFF, 1983
James J. Haggerty May 1983 145 p Original contains color illustrations
(NASA-TM-85475; NAS 1.15:85475) Avail: NTIS MF A01; avail: SOD HC CSCL 05A

A 25th anniversary pictorial resume that underlines the challenging nature of NASA programs and their extraordinary demands for technological input, NASA's current mainline programs, which require development of new technology and therefore expand the bank of technology available for transfer in future years. A representative sampling of spinoff products and processes resulting from technology utilization, or secondary application, and the mechanisms NASA employs to stimulate technology utilization are provided. Contact sources for further information about the Technology utilization Program are also provided. N.W.

N84-13034# Argonne National Lab., Ill. Center for Transportation Research.
ENERGY USE AND RANGE OF ELECTRIC VEHICLES IN SELECTED US DEPARTMENT OF ENERGY SITES
Sarah LaBelle Jul. 1983 8 p refs Presented at the Elect. Vehicle Council Symp. and EXPO, Dearborn, Mich., 4-6 Oct. 1983
(Contract W-31-109-eng-38)
(DE83-015719; CONF-831020-1) Avail: NTIS HC A02/MF A01

The experience of selected private- and public-sector operators of electric vehicles is summarized, particularly with respect to energy use (kWh/mi) and range under various conditions. Comparisons are made with US Postal Service experience, and with manufacturer's expectations of vehicle performance. Analyses of the effect of vehicle characteristics and driver behavior on average energy use and range are presented, indicating the extent to which each of these factors influences performance and how these factors might be altered. DOE

88 SPACE SCIENCES (GENERAL)

No abstracts in this category.

89 ASTRONOMY

Includes radio and gamma-ray astronomy; celestial mechanics; and astrometry.

N84-13035 Max-Planck-Institut fuer Physik und Astrophysik, Garching (West Germany). Inst. fuer Extraterrestrische Physik.
INFORMATION PROCESSING FOR THE INFRARED BALLOON TELESCOPE GOLDENER DRACHE [INFORMATIONSVERARBEITUNG AM INFRAROT-BALLON-TELESKOP GOLDENER DRACHE]
Leo Haser Feb. 1983 63 p refs In GERMAN
(MPE-38; ISSN-0340-8922) Copyright. Avail: Issuing Activity

The information processing system of the ground station and balloon carrying an infrared telescope is described. The ground-balloon link is achieved by telemetry and the control by a computer. The operation scheme contains programs for planning, observations, decision aids during the flight, remote control, telemetry interpretation, and data registration. The real time data are presented partly via computer and partly via direct signal coding. All data can be stored on magnetic tape. Author (ESA)

N84-13036*# National Aeronautics and Space Administration, Washington, D. C.
NASA FACTS: IRAS - MAPPING THE INFRARED SKY
[1982] 8 p
(NASA-Facts-139; NAS 1.20:139) Avail: NTIS MF A01; HC SOD CSCL 03A

The infrared spectrum, the IRAS project, surveying the infrared sky, and IRAS and infrared astronomy are summarized. N.W.

N84-13037# Air Force Geophysics Lab., Hanscom AFB, Mass.
THE FAR INFRARED SKY SURVEY EXPERIMENT Final Report
Stephan D. Price, Thomas L. Murdock, and Kandiah Shivanandan 18 Feb. 1983 52 p
(DA Proj. 7670)
(AD-A131966; AFGL-TR-83-0055; AFGL-ERP-826) Avail: NTIS HC A04/MF A01 CSCL 17/5

Approximately 9000 square degrees of the celestial sphere was surveyed in four infrared bands with a rocket-probe-borne telescope. This Far Infrared Sky Survey Experiment (FIRSSE) covered the galactic plane between 120 degrees and 255 degrees longitude and the Orion and Taurus Molecular Clouds. A list of almost 300 bright 90 micrometer sources is presented along with associated measurements at 20, 27 and 40 micrometers. A description is given of the conduct of the experiment, the first space-borne use of super-fluid helium under active thermal loading. Author (GRA)

N84-13038# Washington Univ., Seattle. Lab. of Nuclear Physics.
CROSS SECTIONS RELEVANT TO GAMMA-RAY ASTRONOMY: ALPHA-PARTICLE-INDUCED REACTIONS
Alan G. Seamster, Eric B. Norman, Donald D. Leach, P. Dyer, and D. Bodansky 1983 35 p refs
(Contract DE-AC06-81ER-40048)
(DE83-015533; DOE/ER-40048/61) Avail: NTIS HC A03/MF A01

Gamma ray production cross sections were measured for the gamma ray lines most strongly excited in the alpha particle bombardments of (20)Ne, (24)Mg, (27)Al, (28)Si, and (56)Fe for alpha particle energies from threshold to approximately 27 MeV. Tabulations of cross sections averaged over alpha particle energy bins of 1 MeV are provided for calculations relevant to gamma ray line astronomy. Examples are given of astrophysical information which might be extracted from spectra acquired with gamma ray spectrometers in space using these cross sections. DOE

N84-13039*# National Aeronautics and Space Administration. Goddard Space Flight Center, Greenbelt, Md.
DEVELOPMENT OF A SEGMENTED n-TYPE GERMANIUM DETECTOR, AND ITS APPLICATION TO ASTRONOMICAL GAMMA-RAY SPECTROSCOPY
N. Gehrels, T. L. Cline, B. J. Teegarden, J. Tueller, M. Leventhal (Bell Telephone Labs.), C. J. MacCallum (SNL), and P. Ryge (Princeton Gamma-Tech, Inc.) 1983 7 p Presented at the Nucl. Sci. Symp., San Francisco, 19 Oct. 1983
(Contract DE-AC04-76DP-000789)
(NASA-TM-85435; NAS 1.15:85435; DE83-011315; SAND-83-1065C; CONF-831015-1) Avail: NTIS HC A02/MF A01 CSCL 17E

Extensive calculations and simulations have shown that the instrumental background in a coaxial germanium photon detector flown at balloon altitudes or in space, can be substantially reduced by segmenting the outer contact. The contact is divided into horizontal strips around the side of the detector, giving it many characteristics similar to that of a stack of planar detectors. By choosing different segment coincidence requirements in different energy ranges, one can obtain a factor of approx. 2 increase in sensitivity to spectral lines between 40 keV and 1 MeV, compared with an unsegmented detector. The reverse electrode configuration (using n-type germanium), with the p contact outside, is preferred for this application due to its thin dead layer and resistance to radiation damage in space. A small two segment n type detector is being developed to serve as a prototype for larger multisegment devices. Results of this development effort and of detector tests are presented. DOE

N84-13040 Massachusetts Univ., Amherst.
A SEARCH FOR RADIO PULSARS IN THE NORTHERN SKY: DISCOVERY OF A PULSAR IN A UNIQUE BINARY SYSTEM Ph.D. Thesis
Marc Damashek 1983 88 p
Avail: Univ. Microfilms Order No. DA8310278

A sensitive search for pulsars was conducted using the 92 meter transit telescope of the National Radio Astronomy Observatory. Nearly 50% of the sky north of -20 deg declination was searched, using an on-line computer to process all search data in real time. The search program was sensitive to pulsars in the period range 0.0333 to 3.9 seconds, with dispersion measures between 0 and 130 cm (3) pc. The limiting flux density reached was approximately 10 mJy at 390 MHz. Twenty-three previously unknown pulsars were discovered in the course of the search, and three of these are noteworthy. The PSR 0320 + 39, 28 with a pulse period of 3.0321 seconds, was found to exhibit subpulses which drift exclusively from the leading to the trailing edge of the pulse profile. The position and dispersion measure of PSR 0458 + 46 are consistent with a physical association between that pulsar and the supernova remnant HB 9. The PSR 0655 + 64 was found to be a member of a binary system. The pulsar parameters and orbital elements of the PSR 0655 + 64 system were determined through an extensive series of pulse timing observations at the NRAO 43 meter telescope. Dissert. Abstr.

90 ASTROPHYSICS

Includes cosmology; and interstellar and interplanetary gases and dust.

N84-13041 Massachusetts Univ., Amherst.
THE EXCITATION OF SiO IN CIRCUMSTELLAR ENVELOPES Ph.D. Thesis
Steven Emery Robinson 1983 114 p
Avail: Univ. Microfilms Order No. DA8310327

The envelopes of Mira variables and VY CMa are modeled as time independent, spherically symmetric, outflowing gas. The excitation of SiO in this environment is studied as it pertains to inversion mechanisms, using the Sobolev formalism. A new mechanism, anisotropic escape, is presented for generating ground state SiO masers, and is shown to produce luminosities comparable to those observed for $v > 0$ masers. A search for ground state maser emission produced only upper limits of $T(A) < 1K$ for 41 late type giant stars. This may indicate that there is a lower limit on mass loss rates for maser stars. In the models, excited vibrational state masers are found to have low luminosities. It is shown that suppression of the anisotropic escape mechanism by judicious choice of velocity law can increase the efficiency of the Kwan and Scoville radiative trapping process, and yield maser fluxes comparable to those observed. This may indicate large regions of moderate acceleration in maser star envelopes. Smoothly distributed dust shells are found to make no qualitative changes in earlier models. They do, however, suppress the anisotropic escape process within the shell cavity, resulting in increased photon fluxes from $v > 0$ masers, and decreased fluxes from $v = 0$ masers. Dissert. Abstr.

N84-13042 Colorado Univ., Boulder.
A STUDY OF DEPLETION IN LOW-VELOCITY DIFFUSE INTERSTELLAR GAS Ph.D. Thesis
Karie Ann Meyers 1982 112 p
Avail: Univ. Microfilms Order No. DA8309859

The diffuse gas in the Scorpius-Ophiuchi region of the sky was studied in order to determine the effect of a weak shock on interstellar abundances. Using high-resolution spectra from the Copernicus satellite, column densities were derived from atomic species in five lines of sight. Each line-of-sight contains two or more velocity components and depletions were calculated for the separate components. In addition, optical observations of two molecular species, CH and CH+, were made for four lines-of-sight. The presence of CH+ was used as a shock signature and the CH/CH+ velocity separation was used to determine the velocity of the observed shock. Dissert. Abstr.

N84-13043 Texas Univ., Austin.
DYNAMICAL EVOLUTION OF SUBSTUCTURE IN MOLECULAR CLOUDS Ph.D. Thesis
David Loren Gilden 1982 534 p
Avail: Univ. Microfilms Order No. DA8309149

There is abundant and diverse evidence that clumping is a common feature of molecular clouds. These observations have motivated a dynamical model of molecular clouds which views them as an ensemble of interacting clumps of gas. The primitive forms of clump interaction were studied through the technique of hydrodynamical simulation. The simplest interaction is that of a single clump plowing through an ambient medium. Plowing clumps in both subsonic and supersonic regimes were studied with particular emphasis on the physics of shock compression and rarefaction, vorticity, and drag. The infrared emission spectra of the shock-heated gas associated with supersonic clumps was also calculated. It is found that an ensemble of clumps will emit radiation, primarily in clump wake, sufficient to be observable. The observation of this infrared radiation is proposed as a consistency test of clumpy models of molecular clouds. Gravitational instability and clump coalescence were studied in simulations of clump collisions. The thermal stability of molecular gas was also studied, and unstable condensation modes in secularly cooling gas were found. These modes damp before reaching nonlinearity, but provide a continual source of acoustic perturbation. Dissert. Abstr.

N84-13044*# National Aeronautics and Space Administration. Goddard Space Flight Center, Greenbelt, Md.
SPECTRAL ANALYSIS OF MAGNETOHYDRODYNAMIC FLUCTUATIONS NEAR INTERPLANETARY SCHOCKS
Adolfo F. Vinas, Melvin L. Goldstein, and Mario H. Acuna Nov. 1983 43 p refs
(NASA-TM-85119; NAS 1.15:85119) Avail: NTIS HC A03/MF A01 CSCL 03B

Evidence for two types of relatively large amplitude MHD waves upstream and downstream of quasi-parallel forward and reverse interplanetary shocks is presented. The first mode is an Alfven wave with frequencies (in the spacecraft frame) in the range of 0.025 to 0.07 Hz. This is a left-hand polarized mode and propagates within a few degrees of the ambient magnetic field. The second is a fast MHD mode with frequencies in the range of 0.025 to 0.17 Hz, right-hand polarization and propagating along the magnetic field. These waves are detected principally in association with quasi-parallel shock. The Alfven waves are found to have plasma rest frame frequencies in the range of 1.1 to 6.3 mHz with wavelengths in the order of 4.8 x 10 to the 8th power to 2.7 x 10 to the 9th power cm. Similarly, the fast MHD modes have rest frame frequencies in the range 1.6 to 26 mHz with typical wavelengths about 2.19 x 10 to the 8th power cm. The magnetic field power spectrum in the vicinity of these interplanetary shocks is much steeper than f to the -s/3 at high frequencies. The observed

spectra have a high frequency dependence of f to the -2/5 to f to the -4. Author

N84-13045*# National Aeronautics and Space Administration. Goddard Space Flight Center, Greenbelt, Md.
RADIAL VARIATIONS OF LARGE-SCALE MAGNETOHYDRODYNAMIC FLUCTUATIONS IN THE SOLAR WIND
L. F. Burlaga and M. L. Goldstein Nov. 1983 19 p refs Submitted for publication
(NASA-TM-85116; NAS 1.15:85116) Avail: NTIS HC A02/MF A01 CSCL 03B

Two time periods are studied for which comprehensive data coverage is available at both 1 AU using IMP-8 and ISEE-3 and beyond using Voyager 1. One of these periods is characterized by the predominance of corotating stream interactions. Relatively small scale transient flows characterize the second period. The evolution of these flows with heliocentric distance is studied using power spectral techniques. The evolution of the transient dominated period is consistent with the hypothesis of turbulent evolution including an inverse cascade of large scales. The evolution of the corotating period is consistent with the entrainment of slow streams by faster streams in a deterministic model. Author

N84-13046*# National Aeronautics and Space Administration. Goddard Space Flight Center, Greenbelt, Md.
BOUNDARY LAYERS IN CATACLYSMIC VARIABLES: THE HEAO-1 X-RAY CONSTRAINTS
Kenneth A. Jensen Oct. 1983 41 p refs Submitted for publication
(NASA-TM-85112; NAS 1.15:85112) Avail: NTIS HC A03/MF A01 CSCL 03B

The predictions of the boundary layer model for the X-ray emission from novae are summarized. A discrepancy between observations and theory in the X-ray observations is found. Constraints on the nature of the boundary layers in novae, based on the lack of detections of novae in the HEAO-1 soft X-ray survey are provided. Temperature and column densities for optically thick boundary layers in novae are estimated. N.W.

N84-13047# Arizona State Univ., Tempe. Dept. of Physics.
HYDRODYNAMIC SIMULATIONS OF A COMBINED HYDROGEN, HELIUM THERMONUCLEAR RUNAWAY ON A 10 KM NEUTRON STAR
S. Starrfield, S. Kenyon (Illinois Univ., Urbana), J. W. Truran (Illinois Univ., Urbana), and W. M. Sparks 1983 6 p refs Presented at the Workshop on Cataclysmic Variables and Low-Mass X-Ray Binaries, Boston, 12-14 Jan. 1983 Submitted for publication
(Contract W-7405-eng-36)
(DE83-012658; LA-UR-83-1406; CONF-830135-3) Avail: NTIS HC A02/MF A01

A Lagrangian, hydrodynamic stellar evolution computer code was used to evolve a thermonuclear runaway in the accreted hydrogen rich envelope of a 1.0 solar mass, 10 km neutron star. The simulation produced an outburst which lasted about 2000 sec and peak effective temperature was 3 keV. The peak luminosity exceeded 2 x 10 to the 5th power solar L. A shock wave caused a precursor in the light curve which lasted 10 to the 5th power sec. DOE

N84-13048# Wuerzburg Univ. (West Germany). Lehrstuhl Astronomie.
[ACTIVITIES REPORT OF THE INSTITUTE OF ASTRONOMY AND ASTROPHYSICS] Annual Report, 1982 [JAHRESBERICHT (1982)]
1982 6 p refs In GERMAN
Avail: NTIS HC A02/MF A01

Solar physics (dynamics of photospherical layers, global solar characteristics, seismology of sunlike main sequence stars) is discussed. Stellar atmospheres and stellar structures (sound generation in stars, convection zones) are considered. Galactic and extragalactic astronomy (Wolf-Rayet stars, galaxies) are treated. Author (ESA)

N84-13049*# National Aeronautics and Space Administration. Goddard Space Flight Center, Greenbelt, Md.
THE STRUCTURE OF THE PLASMA SHEET-LOBE BOUNDARY IN THE EARTH'S MAGNETOTAIL
S. Orsini, M. Candidi, V. Formisano, H. Balsiger (Bern Univ.), A. Ghielmetti (Bern Univ.), and K. W. Ogilvie Sep. 1982 33 p refs Prepared in cooperation with Ist. di Ricerca e Tecnologia per lo Studio del Plasma Nello Spazio Original contains color illustrations
(NASA-TM-85434; NAS 1.15:85434; IFSI-82-9) Avail: NTIS HC A03/MF A01 CSCL 03B

The structure of the magnetotail plasma sheet-plasma lobe boundary was studied by observing the properties of tailward flowing O+ ion beams, detected by the ISEE 2 plasma experiment inside the boundary during three time periods. The computed value of the north-south electric field component as well as the O+ parameters are shown to change at the boundary. The results are related to other observations made in this region. The O+ parameters and the Ez component behavior are shown to be consistent with that expected from the topology of the electric field lines in the tail as mapped from the ionosphere.Author (ESA)

N84-13050# Istituto di Ricerca e Tecnologia per lo Studio del Plasma Nello Spazio, Frascati (Italy).
INTERPLANETARY ALFVENIC FLUCTUATIONS: A STATISTICAL STUDY OF THE DIRECTIONAL VARIATIONS OF THE MAGNETIC FIELD
B. Bavassano and F. Mariani Nov. 1982 21 p refs
(IFSI-82-14) Avail: NTIS HC A02/MF A01

Magnetic field data from Helios 1 and 2 were used to test a stochastic model for interplanetary Alfvenic fluctuations. A statistical analysis of the directional variations of the interplanetary field was performed for Alfvenic regions of the solar wind. The experimental distributions agree reasonably well with those predicted by theory. A rough estimate for the correlation length of the observed fluctuations was inferred. Findings in the near Earth region agree with previous determinations. A decrease of the correlation length approaching the Sun is found, essentially related to the observed enhancement in the angular variability of the magnetic field near the Sun. Author (ESA)

N84-13051 Washington Univ., Seattle.
PROBLEMS OF STELLAR EVOLUTION IN STAR CLUSTERS OF THE MAGELLANIC CLOUDS Ph.D. Thesis
Edward William Olszewski 1983 202 p
Avail: Univ. Microfilms Order No. DA8308634

Three facets of the stellar and cluster content of the Magellanic clouds are presented. Spectra and photometry of superluminous giants, stars which are much brighter than predicted by stellar evolution theory, are studied to attempt to constrain models of the evolutionary state of these stars. Color-magnitude diagrams are constructed of three clusters, NGC 1711, NGC 1755, and NGC 2041, which may be the youngest clusters capable of making superluminous stars. A preliminary color-magnitude diagram of Kron 34, an SMC cluster which may contain a planetary nebula, is discussed. The second topic concerns the age and size distribution of the open clusters in the field of the cluster NGC 1978. This work is compared to previous studies, and shows that the region just north of Constellation 3 has undergone vigorous recent (less than 108 years ago) star formation. The lack of old (older than 109 years) clusters in this field is discussed. A new type of nebulous object, called wisps, is briefly examined. Finally, a color-magnitude diagram of NGC 1978 is presented. The age and metal abundance of NGC 1978 is derived, and compared to previous investigations. Dissert. Abstr.

N84-13052 Cornell Univ., Ithaca, N.Y.
SPHERICAL SIMULATIONS OF LARGE SCALE STRUCTURE IN THE UNIVERSE Ph.D. Thesis
Glenn Lyle Hoffman, Jr. 1983 209 p
Avail: Univ. Microfilms Order No. DA8309492

Spherical simulations of rich clusters, holes and 'honeycombs' in the large scale distribution of galaxies in the universe are

presented. We assume spherical symmetry, dissipationless dust and a Friedmann background universe with zero cosmological constant, and allow for some redirection of radial motion into transverse motion in the cores of the rich clusters. Cluster models with a wide range of cosmological density parameters, 0.02 < or = to omega < or 1.0, are fit to observations of the velocity dispersion in cones around Virgo. All models within that range of omega can be fit equally well, if the ratio of mass to luminosity density is allowed to vary with radius from the cluster core. The mass of the cluster core is thus determined accurately, independent of omega: M sub 60 is approximately 10 to the 14th power .1h M sub sun and (M/L) sub 60 is approximately 450 h M sub sun/L sub sun. Dissert. Abstr.

N84-13053 Princeton Univ., N. J.
FAINT GALAXIES IN THE COMA CLUSTER: LUMINOSITY FUNCTION AND SPATIAL DISTRIBUTION Ph.D. Thesis
Brian C. Beckman 1983 149 p
Avail: Univ. Microfilms Order No. DA8309606

Two-band photometry of 4-m plates of the core of the Coma cluster, done through methods of digital image processing is reported. A catalog of galaxies in the inner 22' of the cluster field was compiled and analyzed. The existence of a feature in the luminosity function at absolute magnitude M(a) = -18.2(Ho = 50 km/sec-Mpc, distance modulus = 35.7), first seen by Abell, is confirmed. The counts of galaxies in the cluster turn up sharply at this feature. The luminosity function faintward of the feature represents a population of dwarf ellipticals in the cluster between M(a) and M(lim) = -12.1, which contributes about 12% of the total cluster light. The counts in the dwarf population turn over at M (dagger) = -14.7. The turnover is analogous to the classical turnover in field and cluster luminosity functions, which is well established at M# = -20.7. Faintward of M (dagger), the counts eventually meet the background by by M(lim) Therefore, most, if not all, cluster galaxies in the core region are seen in this survey. The limit of the survey is J(lim) = 23.6. The number of cluster galaxies in the 0.41 deg(2) field down to the faint limit is 2,385 + or - 382. There is strong evidence for luminosity (mass) segregation of the dwarf population. The luminosity function of the population brightward of M (dagger) is a power law of index alpha approx. = -1.65. Dissert. Abstr.

N84-13054 Yale Univ., New Haven, Conn.
SIMULATIONS OF GALAXY MERGERS Ph.D. Thesis
Jens Verner Villumsen 1982 145 p
Avail: Univ. Microfilms Order No. DA8310527

A theoretical investigation of the mechanisms and results of mergers of elliptical galaxies is discussed. An N-body code is developed to simulate the dynamics of centrally concentrated collisionless systems. It is used for N-body simulations of the mergers of galaxies with mass ratios of 1:1, 2:1, and 3:1 with a total of 1200 or 2400 particles. The initial galaxies are spherical and non-rotating with Hubble type profiles and isotropic velocity distributions. The remnants are flattened (up to E4) and are oblate, triaxial or prolate depending on the impact parameter. Equal mass mergers are more flattened than unequal mass mergers and have significant velocity anisotropies. The remnants have Hubble type profiles with decreased central surface brightness and increased core radii and tidal radii. In some unequal mass mergers 'isothermal' haloes tend to form. The density profiles are inconsistent with De Vaucouleurs profiles even though the initial profiles were not. The central velocity dispersion increases in 1:1 and 2:1 mass mergers but decreases in 3:1 mass mergers. Near head-on mergers lead to prolate systems with little rotation while high angular momentum mergers lead to oblate systems with strong rotation.Dissert. Abstr.

91 LUNAR AND PLANETARY EXPLORATION

Includes planetology; and manned and unmanned flights. For spacecraft design see *18 Spacecraft Design Testing, and Performance*. For space stations see *15 Launch Vehicles and Space Vehicles*.

N84-13055 Texas Univ., Austin.
THE CHEMICAL EVOLUTION OF THE COMA OF COMET P/STEPHAN-OTERMA Ph.D. Thesis
Anita Light Cochran 1982 241 p
Avail: Univ. Microfilms Order No. DA8309129

Observations of comet P/Stephan-Oterma were made with an intensified dissector scanner spectrograph on the McDonald Observatory 2.7m telescope. These spectra covered a range of heliocentric distances from 2.3 au pre-perihelion to 1.8 au post-perihelion. A study of the spatial distribution of the gases in the coma was conducted. Column densities of the observed cometary emissions (CN, C3, CH, and C2) were calculated. It was shown that Stephan-Oterma was very nearly spherically symmetric. A computer code to calculate the time dependent non-equilibrium chemistry taking place within the coma was developed. Models were calculated to pure gas-phase chemistry and for gas phase chemistry plus grain photolysis. It was shown that: (1) HCN is the parent for CN;(2) C2H2 is a parent for C2;(3) pure gas-phase chemistry cannot adequately reproduce the observed C3 but a single-step process such as grain photolysis can; (4) there must be much more CH4 in this comet than had previously been envisioned for any comet; and (5) at least prior to perihelion, the vaporization rate seems to have been controlled by water vaporization. The model of Haser (1957) is discussed and it is shown that a family of solutions for this model exist which can reproduce the observed CN gas distribution. Dissert. Abstr.

N84-13056*# Aerospace Corp., El Segundo, Calif.
THE MIMAS GHOST REVISITED: AN ANALYSIS OF THE ELECTRON FLUX AND ELECTRON MICROSIGNATURES OBSERVED IN THE VICINITY OF MIMAS AT SATURN
D. L. Chenette and E. C. Stone (California Inst. of Tech.) 8 Jun. 1983 42 p refs
(Grant NGR-05-002-160)
(NASA-CR-174596; NAS 1.26:174596; ATR-83(9990)-3) Avail: NTIS HC A03/MF A01 CSCL 03B

An analysis of the electron absorption signature observed by the Cosmic Ray System (CRS) on Voyage 2 near the orbit of Mimas is presented. We find that these observations cannot be explained as the absorption signature of Mimas. Combing Pioneer 11 and Voyager 2 measurements of the electron flux at Mimas's orbit (L=3.1), we find an electron spectrum where most of the flux above approx 100 keV is concentrated near 1 to 3 MeV. The expected Mimas absorption signature is calculated from this spectrum neglecting radial diffusion. A lower limit on the diffusion coefficient for MeV electrons is obtained. With a diffusion coefficient this large, both the Voyager 2 and the Pioneer 11 small-scale electron absorption signature observations in Mimas's orbit are enigmatic. Thus we refer to the mechanism for producing these signatures as the Mimas ghost. A cloud of material in orbit with Mimas may account for the observed electron signature if the cloud is at least 1% opaque to electrons across a region extending over a few hundred kilometers. Author

N84-13057*# Arizona State Univ., Tempe. Dept. of Geology.
GALILEAN SATELLITE GEOMORPHOLOGY Final Report
Michael C. Malin 21 Sep. 1983 5 p refs
(Grant NAGw-139)
(NASA-CR-174574; NAS 1.26:174574) Avail: NTIS HC A02/MF A01 CSCL 03B

Research on this task consisted of the development and initial application of photometric and photoclinometric models using interactive computer image processing and graphics. New programs were developed to compute viewing and illumination angles for

every picture element in a Voyager image using C-matrices and final Voyager ephemerides. These values were then used to transform each pixel to an illumination-oriented coordinate system. An iterative integration routine permits slope displacements to be computed from brightness variations, and correlated in the cross-sun direction, resulting in two dimensional topographic data. Figure 1 shows a 'wire-mesh' view of an impact crater on Ganymede, shown with a 10-fold vertical exaggeration. The crater, about 20 km in diameter, has a central mound and raised interior floor suggestive of viscous relaxation and rebound of the crater's topography. In addition to photoclinometry, the computer models that have been developed permit an examination on non-topographically-derived variations in surface brightness. B.W.

N84-13058*# Iowa Univ., Iowa City. Dept. of Physics and Astronomy.
JUPITER DATA ANALYSIS PROGRAM: ANALYSIS OF VOYAGER WIDEBAND PLASMA WAVE OBSERVATIONS Semiannual Technical Progress Report, 15 Apr. - 14 Oct. 1983
W. S. Kurth 28 Oct. 1983 18 p
(Contract NAGw-337)
(NASA-CR-174575; NAS 1.26:174575) Avail: NTIS HC A02/MF A01 CSCL 03B

Voyager plasma wave wideband frames from the Jovian encounters are analyzed. The 511 frames which were analyzed were chosen on the basis of low-rate spectrum analyzer data from the plasma wave receiver. These frames were obtained in regions and during times of various types of plasma or radio wave activity as determined by the low-rate, low-resolution data and were processed in order to provide high resolution measurements of the plasma wave spectrum for use in the study of a number of outstanding problems. Chorus emissions at Jupiter were analyzed. The detailed temporal and spectral form of the very complex chorus emissions near L = 8 on the Voyager 1 inbound passage was compared to both terrestrial chorus emissions as well as to the theory which was developed to explain the terrestrial waves. N.W.

N84-13059*# Lunar and Planetary Inst., Houston, Tex.
WORKSHOP ON PRISTINE HIGHLANDS ROCKS AND THE EARLY HISTORY OF THE MOON
John Longhi, ed. and Graham Ryder, ed. 1983 94 p refs Workshop held in New Orleans, 15-17 Oct. 1982
(NASA-CR-174584; NAS 1.26:174584; LPI-TR-83-02) Avail: NTIS HC A05/MF A01 CSCL 03B

Oxide composition of the Moon, evidence for an initially totally molten Moon, geophysical contraints on lunar composition, random sampling of a layered intrusion, lunar highland rocks, early evolution of the Moon, mineralogy and petrology of the pristine rocks, relationship of the pristine nonmore rocks to the highlands soils and breccias, ferroan anorthositic norite, early lunar igneous history, compositional variation in ferroan anosthosites, a lunar magma ocean, deposits of lunar pristine rocks, lunar and planetary compositions and early fractionation in the solar nebula, Moon composition models, petrogenesis in a Moon with a chondritic refractory lithophile pattern, a terrestrial analog of lunar ilmenite bearing camulates, and the lunar magma ocean are summarized. N.W.

N84-13060*# Lunar and Planetary Inst., Houston, Tex.
WORKSHOP ON PRISTINE HIGHLANDS ROCKS AND THE EARLY HISTORY OF THE MOON
John Longhi, ed. and Graham Ryder, ed. 17 Oct. 1983 97 p refs Workshop held at New Orleans, 15-17 Oct. 1982
(Contract NASw-3389)
(NASA-CR-174600; NAS 1.26:174600; LPI-TR-83-02) Avail: NTIS HC A05/MF A01 CSCL 03B

An estimate of the bulk, major oxide composition of the Moon, selenologic and seismologic evidence of an initially totally molten moon, geophysical constraints on lunar composition, random sampling of a layered intrusion, chronologic and isotopic systematics of lunar highland rocks, the early evolution of the Moon as inferred from mare basaltic liquids mineralogy and petrology of the pristine rocks, compositional relationship of the pristine nonmare rocks to the highland soils and breccias, ferroan anosthositic norite, early lunar igneous history, compositional variation in ferroan anosthsites, macro and microsegregation in a solidifying lunar magma ocean, nickel in olivines and parent magmas of lunar pristine rocks, identification of regional deposits of lunar pristine rocks from orbital geochemical data, lunar and planetary compositions and early fractionation in the solar nebula, models of bulk moon composition, petrogenesis in a moon with a chondritic refractory lithophile pattern, a terrestrial analog of lunar ilmenite bearing cumulates, and the lunar magma ocean 13 years after Apollo 11 are abstracted. N.W.

N84-13061*# Lunar and Planetary Inst., Houston, Tex.
CONFERENCE ON PLANETARY VOLATILES
Robert O. Pepin, comp. and Richard OConnell, comp. 1983 213 p refs Proc. of a Conf. held in Alexandria, Minn., 9-12 Oct. 1982
(NASA-CR-174583; NAS 1.26:174583; LPI-TR-83-01) Avail: NTIS HC A10/MF A01 CSCL 03B

Present volatile inventories, volatiles in Earth's interior, the sources of planetary volatiles, the origin of planetary atmospheres, near-surface volatile reservoirs, planetary evolution and degassing, loss of gases to space, thermal evolution, and oxygen in atmospheres are addressed. N.W.

N84-13062# Istituto di Ricerca e Tecnologia per lo Studio del Plasma Nello Spazio, Frascati (Italy).
COMMENT ON THE OBSERVED PLASMA DENSITIES IN JUPITER'S DISTANT MAGNETOTAIL (WAKE); A POSSIBLE EXPLANATION
S. Grzedzielski (Polish Academy of Sciences, Warsaw) and W. Macek Jan. 1983 8 p refs Submitted for publication
(IFSI-83-2) Avail: NTIS HC A02/MF A01

The averaged plasma density observed by Voyager 2 inside the distant Jovian magnetotail is discussed. The relatively high tail plasma density indicates that the tail cavity is continuously supplied by solar wind leaking through the tail boundary. It is shown that this can explain the observed density in the tail cavity if the tail boundary is a rotational discontinuity. Plasma transport through a lateral element of tail boundary is determined by the local Alfven velocity corresponding to the interconnecting normal component of the interplanetary magnetic field and by the local solar wind density. Author (ESA)

N84-13063 Princeton Univ., N. J.
GEOMORPHIC STUDIES OF MARS Ph.D. Thesis
Lisa Ann Rossbacher 1983 262 p
Avail: Univ. Microfilms Order No. DA8309618

The photographs from the Viking mission provide evidence for geomorphic activity on Mars. Geomorphic activity is mostly limited to aeolian processes and mass movements. However, the surficial features attest to a history that includes an early cratering episode of meteorite bombardment, subsequent fluvial and aeolian activity, and more recent volcanism. The shifts in dominant processes in part reflect changes in the sources of geomorphic energy at Mars' surface. Overall, several lines of evidence suggest that water, as a liquid or solid, has played a more significant role in martian geomorphology than previously believed. Detailed study of the Viking photographs, including morphometric measurements and regional detailed geomorphic mapping, also reveals a group of landforms that are not easily explained by any of these major processes. These features, which are found in both hemispheres and the equatorial region of Mars, include rimless depressions, lobate debris flows, polygonally fractured ground, and curvilinear features. Dissert. Abstr.

92 SOLAR PHYSICS

Includes solar activity, solar flares, solar radiation and sunspots.

N84-13064*# California Inst. of Tech., Pasadena.
THE RELATIVE ABUNDANCES OF Sn, Te, Xe, Ba AND Ce

Ph.D. Thesis
Keith E. Krombel 1983 155 p refs
(Grant NGR-05-002-160)
(NASA-CR-174599; NAS 1.26:174599; SRL-83-12) Avail: NTIS HC A08/MF A01 CSCL 03B

Elements with even atomic number (Z) in the interval 50 < or = Z < or = 58 were resolved in the cosmic radiation using the Heavy Nuclei Experiment on the HEAO-3 satellite. Their relative abundances were compared with the results expected from pure r-process material, pure s-process material, and solar system material, both with and without a modification due to possible first ionization potential effects. Such effects may be the result of the preferential acceleration, and hence enhancement in the cosmic rays, of those elements having low first ionization potentials. Measurements were found to be inconsistent with pure r-process material at the greater than 98% confidence level whether or not the first ionization potential adjustments are made. Author

N84-13065*# National Aeronautics and Space Administration. Goddard Space Flight Center, Greenbelt, Md.
INTERPRETATION OF 3He VARIATIONS IN THE SOLAR WIND
M. A. Coplan (Maryland Univ., College Park), K. W. Ogilvie, J. Geiss (Bern Univ.), and P. Bochsler Jun. 1983 45 p refs
(NASA-TM-85049; NAS 1.15:85049) Avail: NTIS HC A03/MF A01 CSCL 03B

The ion composition instrument (ICI) on ISEE-3 observed the isotopes of helium of mass 3 and 4 in the solar wind almost continuously between August 1978 and July 1982. This period included the increase towards the maximum of solar activity cycle 21, the maximum period, and the beginning of the descent towards solar minimum. Observations were made when the solar wind speed was between 300 and 620 km/s. For part of the period evidence for regular interplanetary magnetic sector structure was clear and a number of 3He flares occurred during this time. Author

N84-13066*# Alabama Univ., Huntsville.
PRELIMINARY STUDIES OF SOLAR ADVANCE OBSERVATORY AND SOLAR BEACON FACILITY Final Report
S. T. Wu Aug. 1983 61 p refs
(Contract NAS8-34573)
(NASA-CR-170937; NAS 1.26:170937) Avail: NTIS HC A04/MF A01 CSCL 03B

The Advance Solar Observatory, the Solar Beacon Facility, and measurement of the solar diameter using the solar beacon are discussed. N.W.

N84-13067*# Jet Propulsion Lab., California Inst. of Tech., Pasadena.
SOLAR WIND FIVE
Marcia Neugebauer, ed. Washington Nov. 1983 688 p refs Conf. held in Woodstock, Vt., 1-5 Nov. 1982
(NASA-CP-2280; NAS 1.55:2280) Avail: NTIS HC A99/MF A01 CSCL 03B

Topics of discussion were: solar corona, MHD waves and turbulence, acceleration of the solar wind, stellar coronae and winds, long term variations, energetic particles, plasma distribution functions and waves, spatial dependences, and minor ions. For individual titles, see N84-13068 through N84-13126.

N84-13068*# New Hampshire Univ., Durham. Space Science Center.
CORONAL HEATING BY WAVES
Joseph V. Hollweg *In* JPL Solar Wind Five Nov. 1983 p 5-22 refs (For primary document see N84-13067 03-92)
(Grant NAGw-76)
Avail: NTIS HC A99/MF A01 CSCL 03B

Alfven waves or Alfvenic surface waves carry enough energy into the corona to provide the coronal energy requirements. Coronal loop resonances are an appealing means by which large energy fluxes enter active region loops. The wave dissipation mechanism still needs to be elucidated, but a Kolmogoroff turbulent cascade is fully consistent with the heating requirements in coronal holes and active region loops. Author

N84-13069*# Chicago Univ., Ill. Dept. of Physics.
DIRECT CORONAL HEATING FROM DISSIPATION OF MAGNETIC FIELD
E. N. Parker *In* JPL Solar Wind Five Nov. 1983 p 23-32 refs (For primary document see N84-13067 03-92)
(Grant NGL-14-001-001)
Avail: NTIS HC A99/MF A01 CSCL 03B

The visible corona of the Sun appears to be heated by direct dissipation of magnetic fields. The magnetic fields in the visible corona are tied at both ends to the photosphere where the active convection continually rotates and shuffles the footpoints in a random pattern. The twisting and wrapping of flux tubes about each other produce magnetic neutral sheets in a state of dynamical nonequilibrium such that the current sheets become increasingly concentrated with the passage of time. Dissipation of the high current densities takes place regardless of the high electrical conductivity of the fluid. The convection on the feet of the lines of force at the surface of the Sun goes directly (within a matter of 10 to 20 hours) into heat in the corona. The rate of doing work seems adequate to supply the necessary 10 to the 7th power ergs/square cm. sec for the active corona. Author

N84-13070*# Hulburt (E. O.) Center for Space Research, Washington, D.C.
HRTS OBSERVATIONS OF THE FINE STRUCTURE AND DYNAMICS OF THE SOLAR CHROMOSPHERE AND TRANSITION ZONE
Kenneth P. Dere *In* JPL Solar Wind Five Nov. 1983 p 33-44 refs (For primary document see N84-13067 03-92)
Avail: NTIS HC A99/MF A01 CSCL 03B

Arc-second UV observations of the Sun by the NRL High Resolution Telescope and Spectrograph (HRTS) have led to the discovery of dynamic fine structures such as 400 km/s coronal jets and chromospheric jets (spicules) and have provided new information about the structure and dynamics of the transition zone. These observations are reviewed and their relevance to the origin of the solar wind is discussed. Author

N84-13071*# Harvard-Smithsonian Center for Astrophysics, Cambridge, Mass.
SPECTROSCOPIC MEASUREMENTS OF SOLAR WIND GENERATION
John L. Kohl, George L. Withbroe, Carlos A. Zapata, and Giancarlo Noci (Padua Univ., Italy) *In* JPL Solar Wind Five Nov. 1983 p 47-60 refs (For primary document see N84-13067 03-92)
(Grant NAG5-613)
Avail: NTIS HC A99/MF A01 CSCL 03B

Spectroscopically observable quantities are described which are sensitive to the primary plasma parameters of the solar wind's source region. The method is discussed in which those observable quantities are used as constraints in the construction of empirical models of various coronal structures. Simulated observations are used to examine the fractional contributions to observed spectral intensities from coronal structures of interest which co-exist with other coronal structures along simulated lines-of-sight. The sensitivity of spectroscopic observables to the physical parameters within each of those structures is discussed. Author

N84-13072*# Sacramento Peak Observatory, Sunspot, N. Mex.
CORONAL TRANSIENTS IN FE XIV 5303A: FIRST TWO-DIMENSIONAL PHOTOELECTRIC GROUND-BASED OBSERVATIONS
Richard C. Altrock and Howard L. DeMastus *In* JPL Solar Wind Five Nov. 1983 p 63-67 refs (For primary document see N84-13067 03-92)
Avail: NTIS HC A99/MF A01 CSCL 03B

An observational program was undertaken at Sacramento Peak Observatory to photoelectrically detect coronal transients. Continuous observations are made in the Fe XIV 5303A green line,

utilizing the 40 cm coronagraph and the Photoelectric Coronal Photometer. Scans at three heights above the limb are combined to form a low resolution picture of the greenline corona every 20 to 30 minutes. Difference pictures, relative to an initial scan, are generated to search for sudden changes in the corona. The first few days of operation of this program have yielded three low-lying events (< 1.55 solar radii) following minor chromospheric activity (a surge and eruptive prominences), which propagated up through the corona with velocities on the order of 100 km/s. Author

N84-13073*# National Aeronautics and Space Administration. Goddard Space Flight Center, Greenbelt, Md.
MAGNETOHYDRODYNAMIC TURBULENCE IN THE SOLAR WIND
William H. Matthaeus and Melvyn L. Goldstein *In* JPL Solar Wind Five Nov. 1983 p 73-80 refs (For primary document see N84-13067 03-92)
Avail: NTIS HC A99/MF A01 CSCL 03B

Recent work in describing the solar wind as an MHD turbulent fluid has shown that the magnetic fluctuations are adequately described as time stationary and to some extent as spatially homogeneous. Spectra of the three rugged invariants of incompressible MHD are the principal quantities used to characterize the velocity and magnetic field fluctuations. Unresolved issues concerning the existence of actively developing turbulence are discussed. Author

N84-13074*# Technische Univ., Brunswick (West Germany). Inst. fuer Geophysik und Meteorologie.
OBSERVATIONS OF HYDROMAGNETIC TURBULENCE IN THE SOLAR WIND
K. U. Denskat and F. M. Neubauer (Cologne Univ., West Germany) *In* JPL Solar Wind Five Nov. 1983 p 81-92 refs (For primary document see N84-13067 03-92)
Avail: NTIS HC A99/MF A01 CSCL 03B

MHD turbulence is studied by anayzing magnetic field and plasma observations from Helios-1 and -2 at minimum solar activity. The steady conditions in the plasma flows and the magnetic field sector structure in 1975/1976 facilitate an investigation of the radial evolution of the turbulence from 0.29 to 1AU. In high speed streams the fluctuations in the solar wind velocity v and the magnetic field b are highly correlated (the correction coefficient almost being one), which indicates that the turbulence is mainly Alfvenic in high speed plasma. While some general fluctuation properties remain essentially unchanged from 0.29 to 1AU, power spectral analysis reveals a different frequency composition of the Alfvenic turbulence at different heliocentric distances. At 0.3AU much more 'high' frequency fluctuations contribute to the total power in the magnetic field and velocity fluctuations than at 1AU. The contributions of field magnitude fluctuations are found to be distance and frequency dependent. Magnetic field spectra with an extended frequency range up to 470Hz show certain frequency bands, where the steepness of the spectra is independent of the helicocentric distance. Author

N84-13075*# Queen Mary Coll., London (England). Dept. of Applied Mathematics.
ALFVEN SOLITONS IN THE SOLAR WIND
Chris Ovenden and Steven J. Schwartz *In* JPL Solar Wind Five Nov. 1983 p 93-98 refs (For primary document see N84-13067 03-92)
Avail: NTIS HC A99/MF A01 CSCL 03B

A nonlinear Alfven soliton solution of the MHD equations is presented. This solution represents the final state of modulationally unstable Alfven waves. A model of the expected turbulent spectrum due to a collection of such solitons is briefly described. Author

N84-13076*# Consiglio Nazionale delle Ricerche, Frascati (Italy). Ist. di Fisica dello Spazio Interplanetario.
INTERPLANETARY ALFVENIC FLUCTUATIONS: A STATISTICAL STUDY OF THE DIRECTIONAL VARIATIONS OF THE MAGNETIC FIELD
B. Bavassano and F. Mariani (Rome Univ.) *In* JPL Solar Wind Five Nov. 1983 p 99-104 refs (For primary document see N84-13067 03-92)
Avail: NTIS HC A99/MF A01 CSCL 03B

Magnetic field data from HELIOS 1 and 2 are used to test a stochastic model for Alfvenic fluctuations recently proposed. A reasonable matching between observations and predictions is found. A rough estimate of the correlation length of the observed fluctuations is inferred. Author

N84-13077*# College of William and Mary, Williamsburg, Va.
THEORY OF HYDROMAGNETIC TURBULENCE
David Montgomery *In* JPL Solar Wind Five Nov. 1983 p 107-130 refs (For primary document see N84-13067 03-92)
(Grant NsG-7416)
Avail: NTIS HC A99/MF A01 CSCL 03B

The present state of MHD turbulence theory as a possible solar wind research tool is surveyed. The theory is statistical, and does not make statements about individual events. The ensembles considered typically have individual realizations which differ qualitatively, unlike equilibrium statistical mechanics. Most of the theory deals with highly symmetric situations; most of these symmetries have yet to be tested in the solar wind. The applicability of MHD itself to solar wind parameters is highly questionable; yet it has no competitors, as a potentially comprehensive dynamical description. The purpose of solar wind research require sharper articulation. If they are to understand radial turbulent plasma flows from spheres, laboratory experiments and numerical solution of equations of motion may be cheap alternative to spacecraft. If 'real life' information is demanded, multiple spacecraft with variable separation may be necessary to go further. The principal emphasis in the theory so far has been on spectral behavior for spatial covariances in wave number space. There is no respectable theory of these for highly anisotropic situations. A rather slow development of theory acts as a brake on justifiable measurement, at this point. Author

N84-13078*# Jet Propulsion Lab., California Inst. of Tech., Pasadena.
OBSERVATIONAL CONSTRAINTS ON SOLAR WIND ACCELERATION MECHANISMS
Marcia Neugebauer *In its* Solar Wind Five Nov. 1983 p 135-146 refs (For primary document see N84-13067 03-92)
(Contract NAS7-100)
Avail: NTIS HC A99/MF A01 CSCL 03B

A complete theoretical understanding of the acceleration of the solar wind must account for at least three types of solar wind flow: high-speed streams associated with coronal holes, low-speed boundary layer flows associated with sector boundaries, and both high- and low-speed flows associated with impulsive ejections from the Sun. The properties of each type of flow are summarized. Author

N84-13079*# Massachusetts Inst. of Tech., Cambridge. Center for Space Research.
ROLE OF THERMAL CONDUCTION IN THE ACCELERATION OF THE SOLAR WIND
Stanislaw Olbert *In* JPL Solar Wind Five Nov. 1983 p 149-162 (For primary document see N84-13067 03-92)
Avail: NTIS HC A99/MF A01 CSCL 03B

The thermal and suprathermal processes involving solar wind electrons are discussed from a theoretical point of view. A model for the electron distribution function, f(e), based on the solutions of the Boltzmann equation in Krook's approximation is outlined: the angular and energy dependences of for various distances from the Sun between the coronal base and the Earth are presented with the express purpose of obtaining the radial profile of the heat flux generated by the suprathermals. The basic fluid-dynamical equations for the solar wind plasma as a whole along any given magnetic field line are solved. Results are in good agreement with observations. The predicted density and temperature profiles for positive ions exhibit the characteristics of recent measurements, both in the corona (above the coronal holes) and

between 0.3 and 1 A.U. (the Helios region). It is concluded that the suprathermal electrons play an important role in the formation and the dynamics of the solar wind. A.R.H.

N84-13080*# National Aeronautics and Space Administration. Goddard Space Flight Center, Greenbelt, Md.
THE COLLAPSE OF THE LOCAL, SPITZER-HAERM FORMULATION AND A GLOBAL-LOCAL GENERALIZATION FOR HEAT FLOW IN AN INHOMOGENEOUS, FULLY IONIZED PLASMA
Jack D. Scudder and Stanislaw Olbert (MIT, Cambridge) *In* JPL Solar Wind Five Nov. 1983 p 163-182 refs (For primary document see N84-13067 03-92)
Avail: NTIS HC A99/MF A01 CSCL 03B

The breakdown of the classical (CBES) field aligned transport relations for electrons in an inhomogeneous, fully ionized plasma as a mathematical issue of radius of convergence is addressed, the finite Knudsen number conditions when CBES results are accurate is presented and a global-local (GL) way to describe the results of Coulomb physics moderated conduction that is more nearly appropriate for astrophysical plasmas are defined. This paper shows the relationship to and points of departure of the present work from the CBES approach. The CBES heat law in current use is shown to be an especially restrictive special case of the new, more general GL result. A preliminary evaluation of the dimensionless heat function, using analytic formulas, shows that the dimensionless heat function profiles versus density of the type necessary for a conduction supported high speed solar wind appear possible. A.R.H.

N84-13081*# National Oceanic and Atmospheric Administration, Boulder, Colo. Space Environment Lab.
MAGNETOHYDRODYNAMIC MODELING OF CORONAL STRUCTURE AND EXPANSION
S. T. Suess *In* JPL Solar Wind Five Nov. 1983 p 183-198 refs (For primary document see N84-13067 03-92)
Avail: NTIS HC A99/MF A01 CSCL 03B

The presence of a magnetic field in the corona adds structure to the solar wind and almost certainly plays an important role in the energetics of the flow. Analytical and numerical modeling of gas-magnetic field interactions as used to compute steady, global flow are discussed. The approach used in, and results from a recent global model (Steinolfson, Suess and Wu, 1982) are discussed. Ideas on the most effective ways to improve the physical content and numerical efficiency of these models are outlined. Solutions of the MHD equations are discussed only in order to find steady-state flows, even though this often entails solving time-dependent equations. A.R.H.

N84-13082*# Colorado Univ., Boulder. Lab. for Atmospheric and Space Physics.
OBSERVATIONAL EVIDENCE FOR SOLAR WIND ACCELERATION AT THE BASE OF CORONAL HOLES
G. J. Rottman and F. Q. Orrall (Hawaii Univ., Honolulu) *In* JPL Solar Wind Five Nov. 1983 p 199-210 refs (For primary document see N84-13067 03-92)
(Grants NsG-5178; NGR-12-001-011)
Avail: NTIS HC A99/MF A01 CSCL 03B

An EUV spectrometer with a microchannel plate detector was developed to measure Doppler shifts of coronal and transition region lines. The results of three sounding rocket fights of this instrument indicate that EUV resonance emission lines are systematically shifted toward shorter wavelength within coronal holes. This 'blue-shift' signature, first identified within compact low latitude holes, was also observed in a well developed polar coronal hole. The maximum measured shift within these coronal holes corresponds to a velocity relative to the remaining solar disc of 12 km/s in lambda 625 Mg X T to the approximately 10 to the 6.15 K power and 7 km /s/ in lambda 629 OV (T to the approximately 10 to the 5.4 K power). The existing data indicate that these blue-shifts are a common (and possibly universal) signature of coronal holes. These data provide important information on the acceleration of coronal plasma in open magnetic field regions, although the interpretation of observed Doppler shifts to derive a systematic mass flux is to some extent model dependent. A straightforward hypothesis is that the blueshift signature is a direct manifestation of the high speed solar wind deep within the transition region and inner corona. Author

N84-13083*# Harvard-Smithsonian Center for Astrophysics, Cambridge, Mass.
MULTIPLE TRANSONIC SOLUTIONS AND A NEW CLASS OF SHOCK TRANSITIONS IN SOLAR AND STELLAR WINDS
Shadia R. Habbal, Kanaris Tsinganos, and Robert Rosner *In* JPL Solar Wind Five Nov. 1983 p 213-219 refs (For primary document see N84-13067 03-92)
(Grants NAGw-249; NAGw-79)
Avail: NTIS HC A99/MF A01 CSCL 03B

The steady isothermal solar wind equations are shown to admit, under certain circumstances, mutliple transonic solutions when, for example, momemtum deposition gives rise to multiple critical points in the flow. These multiple solutions consist of a continuous solution and solutions which involve shock transitions between critical solutions. The ambiguity arising from the multiplicity of the solutions can be resolved by following the time evolution of a wind profile with one critical point. Results of the numerical integration of the time-dependent equations with momentum addition show that each of these multiple solutions is physically accessible and depends on the rate of change of momentum deposition. These results suggest that standing shocks are likely to be present in the inner solar wind flow. Author

N84-13084*# Harvard-Smithsonian Center for Astrophysics, Cambridge, Mass. Geophysical Inst.
OBSERVATION OF WINDS IN COOL STARS
A. K. Dupree *In* JPL Solar Wind Five Nov. 1983 p 229-240 refs (For primary document see N84-13067 03-92)
(Grant NAG5-87)
Avail: NTIS HC A99/MF A01 CSCL 03B

Sufficient observational material - ultraviolet spectroscopic measures, quantitative optical spectroscopy, and X-ray photometry exists to enable discernment of the presence and character of mass loss in cool stars and to establish meaningful constraints on theoretical models. Two determinants of atmospheric wind structure - temperature and gravity - may suffice in a most superficial way to define the wind and atmospheric structure in a star; however more extensive observations demonstrate the importance of magnetic surface activity and its particular geometrical configuration. Successive observations of an active binary system and a supergiant star reveal that magnetic activity and perhaps mass loss occur on restricted regions of a stellar surface and that long lived structures are present in a wind. Author

N84-13085*# National Center for Atmospheric Research, Boulder, Colo. High Altitude Observatory.
THEORY OF WINDS IN LATE-TYPE EVOLVED AND PRE-MAIN-SEQUENCE STARS
K. B. MacGregor *In* JPL Solar Wind Five Nov. 1983 p 241-262 refs Sponsored by NSF (For primary document see N84-13067 03-92)
Avail: NTIS HC A99/MF A01 CSCL 03B

Recent observational results confirm that many of the physical processes which are known to occur in the Sun also occur among late-type stars in general. One such process is the continuous loss of mass from a star in the form of a wind. There now exists an abundance of either direct or circumstantial evidence which suggests that most (if not all) stars in the cool portion of the HR diagram possess winds. An attempt is made to assess the current state of theoretical understanding of mass loss from two distinctly different classes of late-type stars: the post-main-sequence giant/supergiant stars and the pre-main-sequence T Tauri stars. Toward this end, the observationally inferred properties of the wind associated with each of the two stellar classes under consideration are summarized and compared against the predictions of existing theoretical models. Although considerable progress has been made in attempting to identify the mechanisms re-

sponsible for mass loss from cool stars, many fundamental problems remain to be solved. Author

N84-13086*# Wisconsin Univ., Madison. Dept. of Astronomy.
THE WINDS AND CORONAE OF EARLY-TYPE STARS
J. P. Cassinelli *In* JPL Solar Wind Five Nov. 1983 p 263-278 refs (For primary document see N84-13067 03-92)
Avail: NTIS HC A99/MF A01 CSCL 03B

The properties of the winds of hot stars as derived from radio, ultraviolet and X-ray observations is presented. Special focus is given to observations that test line driven wind theory. In this theory the wind properties are determined by the stellar effective temperature and surface gravity, but not parameters that specify the mechanical or wave fluxes from the star. Alternate explanations of the X-ray emission from the early-type stars are discussed. Evidence is given for the presence of coronal zones at the base of the stellar winds. Author

N84-13087*# National Center for Atmospheric Research, Boulder, Colo. High Altitude Observatory.
STELLAR WINDS DRIVEN BY MULTI-LINE SCATTERING
David B. Friend *In* JPL Solar Wind Five Nov. 1983 p 281-287 refs (For primary document see N84-13067 03-92)
(Grant NSF AST-80-19874)
Avail: NTIS HC A99/MF A01 CSCL 03B

This paper presents a model of a radiation-driven stellar wind with overlapping spectral lines. It is based on the Castor, Abbott, and Klein (CAK) theory. The presence of overlapping lines allows a photon to be scattered many times in different lines. The properties of the wind at any point depend on the wavelength-averaged intensity, which in turn depends on the structure of the wind. A self-consistent wind model is found. The mass loss rate does not saturate as line overlap becomes more pronounced, but continues to increase. The terminal velocity is much larger than in the CAK model, while the velocity law is shallower. This model might help explain the massive winds from Wolf-Rayet stars. B.W.

N84-13088*# Harvard-Smithsonian Center for Astrophysics, Cambridge, Mass.
FORMATION OF STANDING SHOCKS IN STELLAR WINDS AND RELATED ASTROPHYSICAL FLOWS
K. Tsinganos, S. R. Habbal, and R. Rosner *In* JPL Solar Wind Five Nov. 1983 p 289-293 refs (For primary document see N84-13067 03-92)
(Grants NAGw-249; NAGw-79)
Avail: NTIS HC A99/MF A01 CSCL 03B

Stellar winds and other analogous astrophysical flows can be described, to lowest order, by the familiar one dimensional hydrodynamic equations which, being nonlinear, admit in some instances discontinuous as well as continuous transonic solutions for identical inner boundary conditions. The characteristics of the time dependent differential equations of motion are described to show how a perturbation changes profile in time and, under well defined conditions, develops into a stationary shock discontinuity. The formation of standing shocks in wind type astrophysical flows depends on the fulfillment of appropriate necessary conditions, which are determined by the conservation of mass, momentum and energy across the discontinuity, and certain sufficient conditions, which are determined by the flow's history. B.W.

N84-13089*# California Univ., Los Angeles. Dept. of Atmospheric Sciences.
SOLAR CYCLE VARIATIONS OF THE SOLAR WIND
N. U. Crooker *In* JPL Solar Wind Five Nov. 1983 p 303-314 refs (For primary document see N84-13067 03-92)
(Grant NSF ATM-81-20455)
Avail: NTIS HC A99/MF A01 CSCL 03B

Throughout the course of the past one and a half solar cycles, solar wind parameters measured near the ecliptic plane at 1 AU varied in the following way: speed and proton temperature have maxima during the declining phase and minima at solar minimum and are approximately anti-correlated with number density and electron temperature, while magnetic field magnitude and relative abundance of helium roughly follow the sunspot cycle. These variations are described in terms of the solar cycle variations of coronal holes, streamers, and transients. The solar wind signatures of the three features are discussed in turn, with special emphasis on the signature of transients, which is still in the process of being defined. It is proposed that magnetic clouds be identified with helium abundance enhancements and that they form the head of a transient surrounded by streamer like plasma, with an optional shock front. It is stressed that relative values of a parameter through a solar cycle should be compared beginning with the declining phase, especially in the case of magnetic field magnitude. Author

N84-13090*# California Univ., San Diego, La Jolla. Dept. of Electrical Engineering and Computer Sciences.
SOLAR CYCLE EVOLUTION OF THE SOLAR WIND IN THREE DIMENSIONS
B. J. Rickett and W. A. Coles *In* JPL Solar Wind Five Nov. 1983 p 315-322 refs (For primary document see N84-13067 03-92)
(Contract F19628-82-K-0015; Grant NSF ATM-82-09603)
Avail: NTIS HC A99/MF A01 CSCL 03B

Measurements of the solar wind speed both in and out of the ecliptic are presented for 1971-82. The speed estimates, which were made with the interplanetary scintillation system at UC San Diego, have been compared to in situ for large, slowly evolving structures, and thus such structures can be studied up to 60 degrees north and south heliographic latitude. Annual average wind speeds are presented versus latitude for an entire solar cycle. Fast wind streams from the poles persisted through declining and low solar activity, but were closed off during four years of high activity. This evolution follows that of the polar coronal holes, as displayed by comparing averaged speed and coronal density over latitude and longitude. The most recent data (1982) show the reestablishment of large tilted polar holes and associated fast streams. Coronal magnetic field data show that the neutral sheet is confined to low latitudes at solar minimum and extends to high latitudes at solar maximum; thus the slow solar wind comes from the same latitude range as that of the neutral sheet. Author

N84-13091*# Jet Propulsion Lab., California Inst. of Tech., Pasadena.
SOLAR CYCLE VARIATIONS IN THE INTERPLANETARY MAGNETIC FIELD
J. A. Slavin and E. J. Smith *In its* Solar Wind Five Nov. 1983 p 323-331 refs (For primary document see N84-13067 03-92)
Avail: NTIS HC A99/MF A01 CSCL 03B

ISEE 3 interplanetary magnetic field measurements have been used to extend the NSSDC hourly averaged IMF composite data set through mid-1982. Most of sunspot cycle 20 (start:1964) and the first half of cycle 21 (start:1976) are now covered. The average magnitude of the field was relatively constant over cycle 20 with approx. 5-10% decreases in 1969 and 1971, when the Sun's polar regions changed polarity, and a 20% decrease in 1975-6 around solar minimum. Since the start of the new cycle, the total field strength has risen with the mean for the first third of 1982 being about 40% greater than the cycle 20 average. As during the previous cycle, an approx. 10% drop in IMF magnitude accompanied the 1980 reversal of the solar magnetic field. While the interplanetary magnetic field is clearly stronger during the present solar cycle, another 5-7 years of observations will be needed to determine if cycle 21 exhibits the same modest variations as the last cycle. Accordingly, it appears at this time that intercycle changes in IMF magnitude may be much larger than the intracycle variations. B.W.

N84-13092*# Boston Coll., Chestnut Hill, Mass. Dept. of Physics.
SOLAR WIND VARIATIONS IN THE 60-100 YEAR PERIOD RANGE: A REVIEW
J. Feynman *In* JPL Solar Wind Five Nov. 1983 p 333-345 refs (For primary document see N84-13067 03-92)
(Grant NSF ATM-81-1753)

Avail: NTIS HC A99/MF A01 CSCL 03B

The evidence for and against the reality of a solar wind variation in the period range of 60-100 years is reexamined. Six data sets are reviewed; sunspot numbers, geomagnetic variations, two auroral data sets and two (14)C data sets. These data are proxies for several different aspects of the solar wind and the presence or absence of 60-100 year cyclic behavior in a particular data set does not necessarily imply the presence or absence of this variation in other sets. It was concluded that two different analyses of proxy data for a particular characteristic of the heliospheric solar wind yielded conflicting results. This conflict can be resolved only by future research. It is also definitely confirmed that proxy data for the solar wind in the ecliptic at 1 A.U. undergo a periodic variation with a period of approximately 87 years. The average amplitude and phase of this variation as seen in eleven cycles of proxy data are presented. B.W.

N84-13093*# Chinese Academy of Sciences, Peking. Inst. of the History of Natural Science.

PERIODICITIES IN THE OCCURRENCE OF AURORA AS INDICATORS OF SOLAR VARIABILITY

Dai Nian-zu, Chen Mei-dong, Zhang Zhen-jin (Central China Teacher's Coll., Wuhan), and Michael Mendillo (Boston Univ.) *In* JPL Solar Wind Five Nov. 1983 p 349-352 refs (For primary document see N84-13067 03-92)

(Contract F19628-81-K-0051)

Avail: NTIS HC A99/MF A01 CSCL 03B

A compilation of records of the aurora observed in China from the Time of the Legends (2000 - 3000 B.C.) to the mid-18th century has been used to infer the frequencies and strengths of solar activity prior to modern times. A merging of this analysis with auroral and solar activity patterns during the last 200 years provides basically continuous information about solar activity during the last 2000 years. The results show periodicities in solar activity that contain average components with a long period (approx. 412 years), three middle periods (approx. 38 years, approx. 77 years, and approx. 130 years), and the well known short period (approx. 11 years). Author

N84-13094*# Max-Planck-Institut fuer Aeronomie, Katlenburg-Lindau (West Germany).

RADIAL EVOLUTION OF ION DISTRIBUTION FUNCTIONS

Eckart Marsch *In* JPL Solar Wind Five Nov. 1983 p 355-367 refs (For primary document see N84-13067 03-92)

Avail: NTIS HC A99/MF A01 CSCL 03B

A survey of solar wind ion velocity distributions and derived parameters (temperature, ion differential speed, heat flux, adiabatic invariants) is presented with emphasis on the heliocentric distance range between 0.3 and 1 AU traversed by the Helios solar probe. The radial evolution of nonthermal features are discussed which are observed to be most pronounced at perihelion. Within the framework of quasilinear plasma theory, wave particle interactions that may shape the ion distributions are considered. Some results of a self consistent model calculation are presented accounting for ion acceleration and heating by resonant momentum and energy exchange with ion cyclotron and magnetosonic waves propagating away from the Sun along the interplanetary magnetic field. Another tentative explanation for the occurrence of large perpendicular proton temperatures is offered in terms of heating by Landau damping of lower hybrid waves. B.W.

N84-13095*# Max-Planck-Institut fuer Physik und Astrophysik, Garching (West Germany). Inst. fuer Extraterrestrische Physik.

ELECTROSTATIC WAVES AND ANOMALOUS TRANSPORT IN THE SOLAR WIND

C. T. Dum *In* JPL Solar Wind Five Nov. 1983 p 369-376 refs (For primary document see N84-13067 03-92)

Avail: NTIS HC A99/MF A01 CSCL 03B

In situ measurements of fluctuation spectra and particle distribution functions have now been carried out throughout interplanetary space. The link between these observations is established by theories of wave particle interaction. Linear instability analysis for the actual nonMaxwellian particle distribution functions and an examination of the velocity dependence of microscopic diffusion coefficients form the basis of such an investigation. It is described in more detail for the short wavelength, ion acoustic like turbulence which is found by linear instability analysis to correspond to the observed electrostatic fluctuations. Of the transport processes associated with these fluctuations, electron heat conduction and electron ion energy transfer are of particular importance for macroscopic solar wind expansion. These effects are studied with the aid of an anomalous transport theory. This theory (Dum, 1978 a,b) is based on the dominance of elastic scattering of electrons by fluctuations, similar to (enhanced) electron ion collisions. It has a much wider range of applicability than classical transport theory, which assumes dominance of Coulomb collisions for elastic and inelastic scattering. B.W.

N84-13096*# Observatoire de Paris-Meudon (France). Dept. de Recherche Spatiale.

MEASUREMENT OF MACROSCOPIC PLASMA PARAMETERS WITH A RADIO EXPERIMENT: INTERPRETATION OF THE QUASI-THERMAL NOISE SPECTRUM OBSERVED IN THE SOLAR WIND

P. Couturier, S. Hoang, N. Meyer-Vernet, and J. L. Steinberg *In* JPL Solar Wind Five Nov. 1983 p 377-383 refs (For primary document see N84-13067 03-92)

Avail: NTIS HC A99/MF A01 CSCL 03B

The ISEE-3 SBH radio receiver has provided the first systematic observations of the quasi-thermal (plasma waves) noise in the solar wind plasma. The theoretical interpretation of that noise involves the particle distribution function so that electric noise measurements with long antennas provide a fast and independent method of measuring plasma parameters: densities and temperatures of a two component (core and halo) electron distribution function have been obtained in that way. The polarization of that noise is frequency dependent and sensitive to the drift velocity of the electron population. Below the plasma frequency, there is evidence of a weak noise spectrum with spectral index -1 which is not yet accounted for by the theory. The theoretical treatment of the noise associated with the low energy (thermal) proton population shows that the moving electrical antenna radiates in the surrounding plasma by Carenkov emission which becomes predominant at the low frequencies, below about 0.1 F sub P. Author

N84-13097*# California Univ., Los Angeles. Inst. of Geophysics and Planetary Physics.

MULTIPLE SPACECRAFT OBSERVATIONS OF INTERPLANETARY SHOCKS: CHARACTERISTICS OF THE UPSTREAM ULF TURBULENCE

C. T. Russell, E. J. Smith (JPL, California Inst. of Tech., Pasadena), B. T. Tsurutani (JPL, California Inst. of Tech., Pasadena), J. T. Gosling (LASL), and S. J. Bame (LASL) *In* JPL Solar Wind Five Nov. 1983 p 385-400 refs (For primary document see N84-13067 03-92)

(Contracts NAS5-27752; NAS7-100; NASA Order S-50864-A)

Avail: NTIS HC A99/MF A01 CSCL 03B

All interplanetary shocks observed by ISEE-3 and either ISEE-1 or ISEE-2 or both in 1978 and 1979 are examined for evidence of upstream waves. In order to characterize the properties of these shocks it is necessary to determine accurate shock normals. An overdetermined set of equations were inverted to obtain shock normals, velocities and error estimates for all these shocks. Tests of the method indicate it is quite reliable. Using these normals the Mach number and angle were between the interplanetary magnetic field and the shock normal for each shock. The upstream waves were separated into two classes: whistler mode precursors which occur at low Mach numbers and upstream turbulence whose amplitude at Mach numbers greater than 1.5 is controlled by the angle of the field to the shock normal. The former waves are right hand circularly polarized and quite monochromatic. The latter waves are more linearly polarized and have a broadband featureless spectrum. B.W.

N84-13098*# Los Alamos Scientific Lab., N. Mex.
ELECTRON HEATING AT INTERPLANETARY SHOCKS
W. C. Feldman, J. R. Asbridge, S. J. Bame, J. T. Gosling, and R. D. Zwickl *In* JPL Solar Wind Five Nov. 1983 p 403-411 refs (For primary document see N84-13067 03-92)
Avail: NTIS HC A99/MF A01 CSCL 03B

Data for 41 forward interplanetary shocks show that the ratio of downstream to upstream electron temperatures. T sub e (d/u) is variable in the range between 1.0 (isothermal) and 3.0. On average, (T sub e (d/u) = 1.5 with a standard deviation, sigma e = 0.5. This ratio is less than the average ratio of proton temperatures across the same shocks, (T sub p (d/u)) = 3.3 with sigma p = 2.5 as well as the average ratio of electron temperatures across the Earth's bow shock. Individual samples of T sub e (d/u) and T sub p (d/u) appear to be weakly correlated with the number density ratio. However the amounts of electron and proton heating are well correlated with each other as well as with the bulk velocity difference across each shock. The stronger shocks appear to heat the protons more efficiently than they heat the electrons. Author

N84-13099*# California Inst. of Tech., Pasadena.
TEMPORAL VARIATIONS OF THE ANOMALOUS OXYGEN COMPONENT
A. C. Cummings and W. R. Webber (New Hampshire Univ.) *In* JPL Solar Wind Five Nov. 1983 p 427-434 refs (For primary document see N84-13067 03-92)
(Contract NAS7-918; Grants NAGw-200; NGR-05-002-160)
Avail: NTIS HC A99/MF A01 CSCL 03B

Data from the cosmic ray experiment on Voyagers 1 and 2 was used to examine anomalous oxygen in the time period from launch in 1977 to the end of 1981. Several time periods were found where large periodic (typically 26 day) temporal variations of the oxygen intensity between approximately 5 - 15 MeV/nuc are present. Variations in intensity by up to a factor of 10 are observed during these periods. Several characteristics of these variations indicate that they are not higher energy extensions of the low energy particle (approximately 1 MeV/nuc) increases found in many corotating interaction regions (CIR's). Many of these periodic temporal variations are correlated with similar, but much smaller, recurrent variations in the > 75 MeV proton rate. Voyager 1 and Voyager 2 counting rates were compared to estimate the local radial gradient for both the protons and the oxygen. The proton gradients during periods of both maximum and minumum fluxes are consistent with the overall positive radial gradients reported by others from Pioneer and near-Earth observations, supporting the view that these variations are due to local modulation of a source outside the radial range of project measurements. In contrast, the oxygen gradients during periods of maximum proton flux differ in sign from those during minimum proton fluxes, suggesting that the origin of the oxygen variations is different from that of the protons. R.J.F.

N84-13100*# California Inst. of Tech., Pasadena.
VOYAGER MEASUREMENTS OF THE ENERGY SPECTRUM, CHARGE COMPOSITION, AND LONG TERM TEMPORAL VARIATIONS OF THE ANOMALOUS COMPONENTS IN 1977-1982
W. R. Webber (New Hampshire Univ.) and A. C. Cummings *In* JPL Solar Wind Five Nov. 1983 p 435-440 refs (For primary document see N84-13067 03-92)
(Contract NAS7-918; Grants NAGw-200; NGR-05-002-016)
Avail: NTIS HC A99/MF A01 CSCL 03B

The large collecting area and wide energy range of the cosmic ray experiment on Voyager 1 and 2 was used to examine the energy spectra, charge composition, and long term temporal variations of the anomalous components in 1977-1982. Individual energy spectra are obtained for 17 separate quiet time periods during the time interval. The composite spectra of anomalous He, N, O, and Ne are obtained to a new level of precision. This includes the spectral shape and the relative abundance. Essentially, the spectral shape of N, O, and Ne appear to be similar. The ratios of anomalous N and Ne to O are found to be different from both the solar cosmic ray and galactic cosmic ray source composition. Some evidence is found for the enhancement of Ar as well. In the case of elements such as C, Mg, S, and Fe it is difficult to separate a possible lower intensity anomalous component from a quasi-steady interplanetary component that appears to be present at the lowest energies. The long term temporal variations of the anomalous He and O components were studied from 1977-82, a period from minimum to maximum in the modulation cycle. The tracking between these anomalous component intensities and the integral intensity of > 75 MeV protons is striking; however, the intensity decrease of the anomalous components is much greater. R.J.F.

N84-13101*# Jet Propulsion Lab., California Inst. of Tech., Pasadena.
THE EFFECT OF THE SOLAR FIELD REVERSAL ON THE MODULATION OF GALACTIC COSMIC RAYS
B. T. Thomas and B. E. Goldstein *In its* Solar Wind Five Nov. 1983 p 441-448 refs (For primary document see N84-13067 03-92)
(Contract NAS7-100)
Avail: NTIS HC A99/MF A01 CSCL 03B

There is now a growing awareness that solar cycle related changes in the large-scale structure of the interplanetary magnetic field (IMF) may play an important role in the modulation of galactic cosmic rays. To date, attention focussed on two aspects of the magnetic field structure: large scale compression regions produced by fast solar wind streams and solar flares, both of which are known to vary in intensity and number over the solar cycle, and the variable warp of the heliospheric current sheet. It is suggested that another feature of the solar cycle is worthy of consideration: the field reversal itself. If the Sun reverses its polarity by simply overturning the heliospheric current sheet (northern fields migrating southward and vice-versa) then there may well be an effect on cosmic ray intensity. However, such a simple picture of solar reversal seems improbable. Observations of the solar corona suggest the existence of not one but several current sheets in the heliosphere at solar maximum. The results of a simple calculation to demonstrate that the variation in cosmic ray intensities that will result can be as large as is actually observed over the solar cycle are given. R.J.F.

N84-13102*# National Center for Atmospheric Research, Boulder, Colo. High Altitude Observatory.
INTERPLANETARY SCINTILLATION OBSERVATIONS OF THE SOLAR WIND CLOSE TO THE SUN AND OUT OF THE ECLIPTIC
D. G. Sime *In* JPL Solar Wind Five Nov. 1983 p 453-468 refs Sponsored in part by NSF (For primary document see N84-13067 03-92)
Avail: NTIS HC A99/MF A01 CSCL 03B

A brief review is given of recent developments in the observation of the solar wind by the method of interplanetary scintillation. The emphasis is on observations of the velocity structure, the electron density and the effect of propagating disturbances in the interplanetary medium as detected principally by intensity and phase scintillation and by spectral broadening. Author

N84-13103*# National Aeronautics and Space Administration. Goddard Space Flight Center, Greenbelt, Md.
RADIO EVIDENCE FOR INTERPLANETARY STREAMERS IN THE RANGE 10-170 SOLAR RADII
J. Fainberg, J.-L. Bougeret (CNRS), and R. G. Stone *In* JPL Solar Wind Five Nov. 1983 p 469-474 refs (For primary document see N84-13067 03-92)
Avail: NTIS HC A99/MF A01 CSCL 03B

Type III radio storms are observed by the radio experiment on board the International Sun Earth Explorer 3 out to 0.5-0.8 AU from the Sun, at a rate of 2 to 3 storms per solar rotation near solar maximum. They correlate with the type I and type III radio storms observed at higher frequencies, originating closer to the Sun. They are associated with an almost continuous injection of suprathermal electrons into the interplanetary medium. Some of

the properties of the regions where the particles propagate are discussed, using the radio emission as a tracer. Author

N84-13104*# Alaska Univ., Fairbanks. Inst. for Geophysics.
SOLAR WIND DISTURBANCES IN THE OUTER HELIOSPHERE CAUSED BY SUCCESSIVE SOLAR FLARES FROM THE SAME ACTIVE REGION
S.-I. Akasofu and K. Hakamada (Chubu Inst. of Technology) *In* JPL Solar Wind Five Nov. 1983 p 475-480 refs (For primary document see N84-13067 03-92)
(Contract F19628-81-K-0024)
Avail: NTIS HC A99/MF A01 CSCL 03B

Solar wind disturbances caused by successive flares from the same active region are traced to about 20 AU, using the modeling method developed by Hakamada and Akasofu (1982). It is shown that the flare-generated shock waves coalesce with the co-rotating interaction region of the interplanetary magnetic field, resulting in a large-scale magnetic field structure in the outer heliosphere. Such a structure may have considerable effects on the propagation of galactic cosmic rays. Author

N84-13105*# Max-Planck-Institut fuer Aeronomie, Katlenburg-Lindau (West Germany).
THE AVERAGE SOLAR WIND IN THE INNER HELIOSPHERE: STRUCTURES AND SLOW VARIATIONS
Rainer Schwenn *In* JPL Solar Wind Five Nov. 1983 p 489-507 refs (For primary document see N84-13067 03-92)
Avail: NTIS HC A99/MF A01 CSCL 03B

Measurements from the HELIOS solar probes indicated that apart from solar activity related disturbances there exist two states of the solar wind which might result from basic differences in the acceleration process: the fast solar wind ($v > 600$ kms(-)1) emanating from magnetically open regions in the solar corona and the 'slow' solar wind ($v > 400$ kms(-)1) correlated with the more active regions and its mainly closed magnetic structures. In a comprehensive study using all HELIOS data taken between 1974 and 1982 the average behavior of the basic plasma parameters were analyzed as functions of the solar wind speed. The long term variations of the solar wind parameters along the solar cycle were also determined and numerical estimates given. These modulations appear to be distinct though only minor. In agreement with earlier studies it was concluded that the major modulations are in the number and size of high speed streams and in the number of interplanetary shock waves caused by coronal transients. The latter ones usually cause huge deviations from the averages of all parameters. Author

N84-13106*# Massachusetts Inst. of Tech., Cambridge. Center for Space Research.
THE RADIAL EVOLUTION OF THE SOLAR WIND, 1-10 AU
P. R. Gazis and A. J. Lazarus *In* JPL Solar Wind Five Nov. 1983 p 509-519 refs (For primary document see N84-13067 03-92)
Avail: NTIS HC A99/MF A01 CSCL 03B

The interplanetary plasma and magnetic field observations from 1 to 10 AU are reviewed. Over this distance no clear reduction in average speed is seen. The range of wind speeds becomes smaller though high speed streams are still observed. The density, temperature and magnetic field profiles become dominated by the large values seen in the co-rotating interaction regions. The temperature falls more slowly than would be expected from a simple, adiabatic model. Co-rotating shocks appear beyond approximately 3 AU in Voyager data as opposed to beyond approximately 1.5 AU in the Pioneer data. Reverse shocks appear later than forward shocks; reverse shocks do not begin to appear until approximately 4 AU; reverse shocks appear to decay more rapidly than forward shocks. No clear effect due to interaction with the interstellar medium was seen in this radial range. R.J.F.

N84-13107*# National Aeronautics and Space Administration. Ames Research Center, Moffett Field, Calif.
SPATIAL DEPENDENCES IN THE DISTANT SOLAR WIND: PIONEERS 10 AND 11
Edward J. Smith (JPL) and Aaron Barnes *In* JPL Solar Wind Five Nov. 1983 p 521-535 refs (For primary document see N84-13067 03-92)
(Contract NAS7-100)
Avail: NTIS HC A99/MF A01 CSCL 03B

Pioneer 10, 11 observations of the solar wind and magnetic field between 1 and 20 AU are reviewed. Spatial dependences, which are emphasized, must be inferred in the presence of large temporal variations including solar cycle effects. The separation of spatial and temporal dependences is achieved principally through the use of multipoint observations including baseline measurements at 1 AU. Measurements of the solar wind parameters (radial speed, flux, proton temperature) and of the magnetic field magnitude and components are compared with two theories, the Parker theory which assumes radial, azimuthally symmetric flow and the Goldstein-Jokipii theory which includes effects associated with stream-stream interactions. The observed radial gradients in the proton density and velocity and the magnetic field are consistent with the Parker model. A qualitative dependence of field magnitude on heliomagnetic latitude, i.e., referred to the observed location of the heliospheric current sheet, was derived. The field strength was found to decrease with distance from the current sheet. R.J.F.

N84-13108*# Bonn Univ. (West Germany). Inst. fuer Astrophysik und Extraterrestrische Forschung.
THEORY OF INTERSTELLAR MEDIUM DIAGNOSTICS
H. J. Fahr *In* JPL Solar Wind Five Nov. 1983 p 541-551 refs (For primary document see N84-13067 03-92)
Avail: NTIS HC A99/MF A01 CSCL 03B

The theoretical interpretation of observed interplanetary resonance luminescence patterns is used as one of the most promising methods to determine the state of the local interstellar medium (LISM). However, these methods lead to discrepant results that would be hard to understand in the framework of any physical LISM scenario. Assuming that the observational data are reliable, two possibilities which could help to resolve these discrepancies are discussed: (1) the current modeling of resonance luminescence patterns is unsatisfactory and has to be improved, and (2) the extrapolated interstellar parameters are not indicative of the unperturbed LISM state, but rather designate an intermediate state attained in the outer regions of the solar system. It is shown that a quantitative treatment of the neutral gas-plasma interaction effects in the interface between the heliospheric and the interstellar plasmas is of major importance for the correct understanding of the whole complex. M.G.

N84-13109*# University of Southern California, Los Angeles.
THE INTERPLANETARY HYDROGEN AND HELIUM GLOW AND THE INFERRED INTERSTELLAR GAS PROPERTIES
Darrell L. Judge *In* JPL Solar Wind Five Nov. 1983 p 557-563 refs (For primary document see N84-13067 03-92)
Avail: NTIS HC A99/MF A01 CSCL 03B

Observations of the interplanetary hydrogen and helium glow have been obtained by a number of spacecraft and rocket experiments during the past fifteen years. Important results have been established on the temperature, density, velocity, spatial dependence, and hydrogen to helium ratio. However, only four spacecraft launched to date are investigating the outer solar system and of these four the Pioneer 10 spacecraft is the farthest out at 28 A.U. Observations from this spacecraft at great distances have permitted an improved analysis of the effects which are only evident at large distances from the Sun. Perhaps the most significant result in this regard is the clear evidence of the importance of multiple scattering of solar Ly-alpha; an effect which has not been observed in earlier work. Ignoring this effect can lead to a gross overestimate of the local galactic glow. Current best estimates of the galactic glow and the local interstellar wind parameters obtained by the Pioneer 10 photometer at great distances are presented, in addition to complementary experimental observations of particular interest. Author

N84-13110*# Los Alamos Scientific Lab., N. Mex.
SOLAR WIND MINOR IONS: RECENT OBSERVATIONS
S. J. Bame *In* JPL Solar Wind Five Nov. 1983 p 573-589 refs (For primary document see N84-13067 03-92)
Avail: NTIS HC A99/MF A01 CSCL 03B

Systematic studies show that the minor ions generally travel with a common bulk speed and have temperatures roughly proportional to their masses. It was determined that (3)He(++) content varies greatly; (3)He(++)/(4)He(++) ranges from as high as 10(-12) values to below 2 x 10(-4). In some solar wind flows which can be related to energetic coronal events, the minor ions are found in unusual ionization states containing Fe(16+) as a prominent ion, showing that the states were formed at unusually high temperatures. Unexpectedly, in a few flows substantial quantities of (4)He(+) were detected, sometimes with ions identifiable as O(2+) and O(3+). Surprisingly, in some of these examples the ionization state is mixed showing that part of the plasma escaped the corona without attaining the usual million-degree temperatures while other parts were heated more nearly in the normal manner. Additionally, detailed studies of the minor ions increased our understanding of the coronal expansion. For example, such studies contributed to identifying near equatorial coronal streamers as the source of solar wind flows between high speed streams. M.G.

N84-13111*# National Aeronautics and Space Administration. Goddard Space Flight Center, Greenbelt, Md.
THE RELATIVE ABUNDANCE OF 3He(++) IN THE SOLAR WIND
M. A. Coplan (Maryland Univ.), K. W. Ogilvie, P. Bochsler (Bern Univ.), and J. Geiss (Bern Univ.) *In* JPL Solar Wind Five Nov. 1983 p 591-596 refs (For primary document see N84-13067 03-92)
(Contract NAS2-5472)
Avail: NTIS HC A99/MF A01 OSCL 03B

Continuous measurements of solar wind 3He(++) and 4He(++) were made covering a full range of solar wind conditions. The average flux ratio derived from these data is 2310 + or - 50, in excellent agreement with the Apollo foil measurements. A probable correlation between average flux ratio and solar activity was found; however, an examination of the data during periods of 3He(++)-rich solar flares shows no detectable increase in 3He(++) in the solar wind. M.G.

N84-13112*# Maryland Univ., College Park. Dept. of Physics and Astronomy.
IRON CHARGE STATES OBSERVED IN THE SOLAR WIND
F. M. Ipavich, A. B. Galvin, G. Gloeckler, D. Hovestadt, B. Klecker, and M. Scholer *In* JPL Solar Wind Five Nov. 1983 p 597-604 refs Prepared in cooperation with Max-Planck-Institute fuer Physik und Astrophysik, Garching (West Germany) (For primary document see N84-13067 03-92)
(Contracts NAS5-26739; BMFT-RV14-B8/74)
Avail: NTIS HC A99/MF A01 CSCL 03B

Solar wind measurements from the ULECA sensor of the Max-Planck-Institut/University of Maryland experiment on ISEE-3 are reported. The low energy section of approx the ULECA sensor selects particles by their energy per charge (over the range 3.6 keV/Q to 30 keV/Q) and simultaneously measures their total energy with two low-noise solid state detectors. Solar wind Fe charge state measurements from three time periods of high speed solar wind occurring during a post-shock flow and a coronal hole-associated high speed stream are presented. Analysis of the post-shock flow solar wind indicates the charge state distributions for Fe were peaked at approx +16, indicative of an unusually high coronal temperature (3,000,000 K). In contrast, the Fe charge state distribution observed in a coronal hole-associated high speed stream peaks at approx -9, indicating a much lower coronal temperature (1,400,000 K). This constitutes the first reported measurements of iron charge states in a coronal hole-associated high speed stream. M.G.

N84-13113*# Applied Physics Lab., Johns Hopkins Univ., Laurel, Md.
SPATIAL VARIATION OF IRON ABUNDANCE IN THE HIGH SPEED SOLAR WIND, 1972 TO 1976
D. G. Mitchell, E. C. Roelof, and S. J. Bame (LASL) *In* JPL Solar Wind Five Nov. 1983 p 605-612 refs (For primary document see N84-13067 03-92)
(Grant NAGw-264; Contract N00024-83-C-5301)
Avail: NTIS HC A99/MF A01 CSCL 03B

The Fe/H ratios in the peaks of high speed streams (HSS) during the decline of Solar Cycle 20 and the following minimum (October 1972-December 1976) were analyzed. The response of the 50-200 keV ion channel of the APL/JHU energetic particle experiment (EPE) on IMP-7 and 8 to solar wind iron ions at high solar wind speeds and Fe measurements were compared with solar wind H and He parameters from the Los Alamos National Laboratory (LANL) instrments on the same spacecraft. In general, the Fe distribution parameters (bulk velocity, flow direction, temperature) are found to be similar to the LANL He parameters. Although the average Fe/H ratio in many steady HSS peaks agrees within observational uncertainties with the nominal coronal ratio of 4.7 x 10(-5), abundance variations of a factor of up to 6 are obtained across a given coronal-hole associated HSS. Over the period 1973-1976, a steady decrease in the average quiet-time Fe/H ratio by a factor of about 4 is measured on both IMP-7 and 8. M.G.

N84-13114*# Bern Univ. (Switzerland). Inst. fuer Physilalisches.
MIXED SOLAR WIND ORIGINATING FROM CORONAL REGIONS OF DIFFERENT TEMPERATURES
P. Bochsler *In* JPL Solar Wind Five Nov. 1983 p 613-622 refs Sponsored in part by the Swiss National Science Foundation (For primary document see N84-13067 03-92)
Avail: NTIS HC A99/MF A01 CSCL 03B

Ionization states of elements in the solar wind are often used to determine thermal gradients in the lower corona. This method is based on the assumption, that in the beginning, solar wind material has a homogeneous temperature determining the original charge state of elements. Features in M/Q-spectra which might appear if the above assumption is violated are investigated and compared with observational evidence. M.G.

N84-13115*# Harvard-Smithsonian Center for Astrophysics, Cambridge, Mass.
INTERPRETING THE SOLAR WIND IONIZATION STATE
Stanley P. Owocki *In* JPL Solar Wind Five Nov. 1983 p 623-641 refs (For primary document see N84-13067 03-92)
(Grant NAGw-249)
Avail: NTIS HC A99/MF A01 CSCL 03B

The ionization state of the solar coronal expansion is frozen within a few solar radii of the solar photosphere, and spacecraft measurements of the solar wind heavy ion charge state can therefore yield information about coronal conditions (e.g., electron temperature). Previous interpretations of the frozen-in ionization state have always assumed that in the coronal freezing-in region, (1) all heavy ions flow at the same bulk speed as protons, (2) the electron velocity distribution function is Maxwellian, and (3) conditions vary in space but not in time. The consequences of relaxing these assumptions for the interpretation of solar wind charge state measurements are examined. It is found that: (1) the temperature inferred by traditional interpretation of the interplanetary ionization state overestimates (underestimate) the actual coronal electron temperature if higher ion charge stages flow systematically faster (slower) than lower stages at the coronal freezing radius; (2) temperatures inferred from relative abundance measurements of ion-charge-stages with high ionization potentials moderately overestimate the actual coronal electron temperature if the high-energy tail of the coronal electron velocity distribution is enhanced relative to a Maxwellian distribution; (3) the propagation of a disturbance, e.g., a shock wave, through the corona can strongly affect the frozen-in charge state, but only over a time (a

few times ten minutes) corresponding to the coronal transit time for the disturbance. M.G.

N84-13116*# Bonn Univ. (West Germany). Inst. fuer Astrophysik und Extraterrestrische Forschung.
MINOR CONSTITUENTS IN THE SOLAR WIND ORIGINATING FROM PLASMA-DUST INTERACTIONS
Hartmut W. Ripken *In* JPL Solar Wind Five Nov. 1983 p 643-645 refs (For primary document see N84-13067 03-92)
Avail: NTIS HC A99/MF A01 CSCL 03B

Atoms, molecules, and atomic and molecular ions generated by solar wind interactions with dust grains of the zodiacal cloud are discussed. The main processes leading to the generation of these particles are described and relevant methods of observation are examined. M.G.

N84-13117*# Max-Planck-Institut fuer Physik und Astrophysik, Garching (West Germany). Inst. fuer Extraterrestrische Physik.
SURVEY OF He(+)/He(2+) ABUNDANCE RATIOS IN ENERGETIC PARTICLE EVENTS
D. Hovestadt, B. Klecker (Maryland Univ.), and G. Gloeckler *In* JPL Solar Wind Five Nov. 1983 p 647-652 refs (For primary document see N84-13067 03-92)
(Contracts NAS5-20062; BMFT-RV-14-B8/74)
Avail: NTIS HC A99/MF A01 CSCL 03B

The helium charge distribution in the energy range 0.4 to 0.62 MeV/nucleon in energetic particle events was studied. An average He+/He2+ ratio of 0.12 + or - 0.04 with ratios exceeding 0.3 for 41 out of 420 days events richest in He+ and no significant differences of the proton energy spectra, and the abundance of helium relative to protons and heavy ions for He+ rich events (He+/He2+ $>$ 0.3) and for events with He+/He2+ $<$ 0.3, respectively. It is also found that He+ rich events are predominantly low in energetic particle intensity. E.A.K.

N84-13118*# New Hampshire Univ., Durham. Center for Space Science.
ACCELERATION OF HEAVY IONS IN THE SOLAR WIND
Philip A. Isenberg *In* JPL Solar Wind Five Nov. 1983 p 655-661 refs (For primary document see N84-13067 03-92)
(Grants NAG5-130; NAGw-76)
Avail: NTIS HC A99/MF A01 CSCL 03B

The preferential acceleration and heating of solar wind heavy ions by the resonant cyclotron interaction were studied. It is concluded that this interaction is incapable of producing the observed differential speeds for reasonable solar wind parameters. E.A.K.

N84-13119*# California Univ., Irvine. Dept. of Physics.
MODELING OF TRANSIENT DISTURBANCES IN CORONAL-STREAMER CONFIGURATIONS
R. S. Steinolfson *In* JPL Solar Wind Five Nov. 1983 p 667-673 refs (For primary document see N84-13067 03-92)
Avail: NTIS HC A99/MF A01 CSCL 03B

Numerical simulations of the formation and propagation of mass ejection, loop transients in coronal streamers are discussed. The simulations are accomplished with numerical solutions of the single fluid, ideal MHD equations of motion in the meridional plane. The streamer is produced by simulating the relaxation of an initially radial hydrodynamic flow coupled with a dipole magnetic field. The simulated transient then results from an energy release at the base of the streamer. The legs of the loop transient produced remain essentially stationary while the loop expands mainly in the radial direction with velocities of 400 to 750 km s-1. Once the leading edge of the transient has passed out of the lower corona, the initial streamer configuration is restored after 15 to 24 hours. A second energy release 2 hours later than, and with an energy release identical to, the first does not produce a significant coronal disturbance. E.A.K.

N84-13120*# National Center for Atmospheric Research, Boulder, Colo. High Altitude Observatory.
QUASI-STEADY SOLAR WIND DYNAMICS
V. J. Pizzo *In* JPL Solar Wind Five Nov. 1983 p 675-691 refs Sponsored in part by NSF (For primary document see N84-13067 03-92)
Avail: NTIS HC A99/MF A01 CSCL 03B

Progress in understanding the large scale dynamics of quasi-steady, corotating solar wind structure was reviewed. The nature of the solar wind at large heliocentric distances preliminary calculations from a 2-D MHD model are used to demonstrate theoretical expectations of corotating structure out to 30 AU. It is found that the forward and reverse shocks from adjacent CIR's begin to interact at about 10 AU, producing new shock pairs flanking secondary CIR's. These sawtooth secondary CIR's interact again at about 20 AU and survive as visible entities to 30 AU. The model predicts the velocity jumps at the leading edge of the secondary CIR's at 30 AU should be very small but there should still be sizable variations in the thermodynamic and magnetic parameters. The driving dynamic mechanism in the distant solar wind is the relaxation of pressure gradients. The second topic is the influence of weak, nonimpulsive time dependence in quasi-steady dynamics. It is suggested that modest large scale variations in the coronal flow speed on periods of several hours to a day may be responsible for many of the remaining discrepancies between theory and observation. Effects offer a ready explanation for the apparent rounding of stream fronts between 0.3 and 1.0 AU discovered by Helios. E.A.K.

N84-13121*# Naval Research Lab., Washington, D. C. Center for Space Research.
ASSOCIATIONS BETWEEN CORONAL MASS EJECTIONS AND INTERPLANETARY SHOCKS
N. R. Sheeley, Jr., R. A. Howard, M. J. Koomen, D. J. Michels, R. Schwenn, K. H. Muhlhauser, and H. Rosenbauer *In* JPL Solar Wind Five Nov. 1983 p 693-702 refs Prepared in cooperation with Max-Planck-Inst. for Aeronomie, Katlenburg-Lindau (West Germany) (For primary document see N84-13067 03-92)
Avail: NTIS HC A99/MF A01 CSCL 03B

Nearly continuous complementary coronal observations and interplanetary plasma measurements for the years 1979-1982 are compared. It is shown that almost all low latitude high speed coronal mass ejections (CME's) were associated with shocks at HELIOS 1. Some suitably directed low speed CME's were clearly associated with shocks while others may have been associated with disturbed plasma (such as NCDE's) without shocks. A few opposite hemisphere CME's associated with great flares seem to be associated with shocks at HELIOS. E.A.K.

N84-13122*# National Aeronautics and Space Administration. Goddard Space Flight Center, Greenbelt, Md.
VELOCITY PROFILES OF INTERPLANETARY SHOCKS
H. V. Cane *In* JPL Solar Wind Five Nov. 1983 p 703-709 refs (For primary document see N84-13067 03-92)
Avail: NTIS HC A99/MF A01 CSCL 03B

The type 2 radio burst was identified as a shock propagating through solar corona. Radio emission from shocks travelling through the interplanetary (IP) medium was observed. Using the drift rates of IP type II bursts the velocity characteristics of eleven shocks were investigated. It is indicated that shocks in the IP medium undergo acceleration before decelerating and that the slower shocks take longer to attain their maximum velocity. E.A.K.

N84-13123*# Los Alamos Scientific Lab., N. Mex.
PLASMA PROPERTIES OF DRIVER GAS FOLLOWING INTERPLANETARY SHOCKS OBSERVED BY ISEE-3
R. D. Zwickl, J. R. Asbridge, S. J. Bame, W. C. Feldman, J. T. Gosling, and E. J. Smith (JPL) *In* JPL Solar Wind Five Nov. 1983 p 711-717 refs (For primary document see N84-13067 03-92)
(Contract NAS7-100)
Avail: NTIS HC A99/MF A01 CSCL 03B

Plasma fluid parameters calculated from solar wind and magnetic field data to determine the characteristic properties of driver gas following a select subset of interplanetary shocks were studied. Of 54 shocks observed from August 1978 to February

1980, 9 contained a well defined driver gas that was clearly identifiable by a discontinuous decrease in the average proton temperature. While helium enhancements were present downstream of the shock in all 9 of these events, only about half of them contained simultaneous changes in the two quantities. Simultaneous with the drop in proton temperature the helium and electron temperature decreased abruptly. In some cases the proton temperature depression was accompanied by a moderate increase in magnetic field magnitude with an unusually low variance, by a small decrease in the variance of the bulk velocity, and by an increase in the ratio of parallel to perpendicular temperature. The cold driver gas usually displayed a bidirectional flow of suprathermal solar wind electrons at higher energies. E.A.K.

N84-13124*# Catholic Univ. of America, Washington, D.C. Dept. of Mechanical Engineering.

COROTATING SHOCKS IN INNER HELIOSPHERE

Y. C. Whang *In* JPL Solar Wind Five Nov. 1983 p 719-727 refs (For primary document see N84-13067 03-92)
(Grants NsG-7422; NSF ATM-81-19302)
Avail: NTIS HC A99/MF A01 CSCL 03B

Two possible corotating shocks in the inner heliosphere where the solar wind is composed of low 8 plasma are reported. In the region where the solar wind is slightly super Alfvenic, reverse corotating fast MHD shocks can form at the leading edge of a high speed stream. These shocks possess a switch on mechanism for amplification of tangential small scale fluctuations. The second one is the coronal slow shocks which may be imbedded in large coronal holes at low altitide in the sub Alfvenic region. E.A.K.

N84-13125*# Max-Planck-Institut fuer Aeronomie, Katlenburg-Lindau (West Germany).

ON THE FIELD CONFIGURATION IN MAGNETIC CLOUDS

H. Goldstein *In* JPL Solar Wind Five Nov. 1983 p 731-733 refs (For primary document see N84-13067 03-92)
Avail: NTIS HC A99/MF A01 CSCL 03B

Interplanetary magnetic clouds are represented by cylindrically symmetric equilibrium solutions of the MHD equations. The radial magnetic pressure gradient of the force free field is balanced by the curvature stress. The field inside is essentially parallel to the cylinder axis, far outside it is oriented in azimuthal direction. These configurations therefore differ from the nonselfconsistent model where the field lines are tightly wound even near the axis. E.A.K.

N84-13126*# National Aeronautics and Space Administration. Goddard Space Flight Center, Greenbelt, Md.

INTERACTION OF THE PLASMA TAIL OF COMET BRADFIELD 1979L ON 1980 FEBRUARY 6 WITH A POSSIBLY FLARE-GENERATED SOLAR-WIND DISTURBANCE

Malcolm B. Niedner, Jr., John C. Brandt, R. D. Zwickl, and S. J. Bame *In* JPL Solar Wind Five Nov. 1983 p 737-742 refs Prepared in cooperation with LASL, Los Alamos, N.Mex. (For primary document see N84-13067 03-92)
Avail: NTIS HC A99/MF A01 CSCL 03B

Solar wind plasma data from the ISEE-3 and Helios 2 spacecraft were examined to explain a uniquely rapid 10 deg turning of the plasma tail of comet Bradfield 1979L on 1980 February 6. It was suggested that the tail position angle change occurred in response to a solar wind velocity shear across which the polar component changed by approx. 50 km s-1. The present activity was caused by noncorotating, disturbed plasma flows probably associated with an Importance 1B solar flare. E.A.K.

N84-13127# Midwest Research Inst., Golden, Colo. Buildings Systems Research Branch.

MODEL FOR ILLUMINANCE ON HORIZONTAL AND VERTICAL SURFACES

Claude L. Robbins and Kerri C. Hunter May 1983 46 p refs
(Contracts DE-AC02-77CH-00178; EG-C-01-4042)
(DE83-011973; SERI/TR-254-1703) Avail: NTIS HC A03/MF A01

The Robbins-Hunter model for determining illuminance on horizontal and vertical surfaces is presented. It is compared with a wide range of other models designed for the same purpose, and all the models are compared with measurements made at the daylighting laboratory. The model uses simple algebraic expressions, and the inputs to the model are from Typical Meteorological Year (TMY) and Estimated Typical Meteorological Year (ETMY) weather data. This enables the model to be applied to all 247 cities in the TMY and ETMY weather station network. All of the models provide results that vary with measured data. Models that consider atmospheric moisture (turbidity) seem to be more accurate than those that do not. The Robbins-Hunter model agrees most closely with measured illuminance under all conditions of turbidity and cloud cover. DOE

N84-13128# Midwest Research Inst., Golden, Colo. Solar Energy Research Inst.

GRAPHICAL METHOD FOR DETERMINING INTERFLECTED DAYLIGHT IN CLEAR CLIMATES

Claude L. Robbins and Kerri C. Hunter Jul. 1983 7 p refs Presented at the 8th Natl. Passive Solar Conf., Santa Fe, N.Mex., 7-9 Sep. 1983
(Contracts DE-AC02-77CH-00178; EG-77-C-01-4042)
(DE83-011989; SERI/TP-254-2027; CONF-830929-5) Avail: NTIS HC A02/MF A01

An extension of the daylight factor method of analysis that includes a graphical method for determining interflected light in clear climates is presented. The interflected component of daylight, called the internal reflectance component (IRC), was determined for overcast skies in research performed in the United Kingdom. The technique developed by the Building Research Establishment in the United Kingdom is based on determining an average IRC for a given room or space. Using a daylight availability model developed at SERI, a similar average IRC analysis technique is established for clear skies. The results of applying the SERI daylight availability model suggest that a critical element in determining the IRC under clear sky conditions is the ratio of global to diffuse (G/d) illuminance on a horizontal surface. This graphical technique for determining clear sky IRC values is expected to enhance the accuracy of daylighting system design by simplifying the format used in clear sky computation. DOE

N84-13129# Istituto di Ricerca e Tecnologia per lo Studio del Plasma Nello Spazio, Frascati (Italy).

INTERPLANETARY PERTURBATIONS ASSOCIATED WITH TYPE 4 SOLAR FLARES

N. Iucci (Rome Univ.), M. Parisi, M. Storini, and G. Villoresi May 1982 23 p refs Presented at 5th Intern. Symp. on Solar Terrestrial Phys., Ottawa, May 1982 Sponsored by CNR
(IFSI-82-6) Avail: NTIS HC A03/MF A01

Interplanetary perturbations associated with Forbush decreases from 1965 to 1974 are studied. The systematic appearance of the results confirms that type 4 solar flares are the origin of these perturbations. The perturbation front is a wide (100 deg in longitude) driven shock followed by a magnetic blob and high speed plasma cloud of 0.5 AU average radial dimension at the Earth orbit, emitted in a short time interval (10 hr average) immediately following the type 4 solar flare. The Forbush decrease amplitude is correlated with an empirical parameter which caters for the importance of the shock and magnetic blob at the perturbation front. In the interplanetary regions in which the galactic cosmic ray intensity is depressed, low energy cosmic ray fluxes are observed. Author (ESA)

N84-13130# Istituto di Ricerca e Tecnologia per lo Studio del Plasma Nello Spazio, Frascati (Italy).

THE BEHAVIOR OF THE COSMIC RAY EQUATORIAL ANISOTROPY INSIDE FAST SOLAR WIND STREAMS EJECTED BY CORONAL HOLES

N. Iucci (Rome Univ.), M. Parisi, M. Storini, and G. Villoresi Dec. 1983 27 p refs Sponsored by CNR
(IFSI-82-16) Avail: NTIS HC A03/MF A01

The cosmic ray equatorial anisotropy inside broad high-speed solar wind streams ejected by coronal holes, i.e, in quasistationary condition, was analyzed. From the beginning to the end of

the stream the amplitude of the first and second harmonics of the anisotropy are found to decrease remarkably, by factors of 2.5 and 2.0 respectively, while the phases do not show systematic variations. The development of the stream structure in interplanetary space together with the Parker theory on the diurnal anisotropy in stationary condition explains the large variation observed in the first harmonic of the anisotropy. The behavior of the second harmonic is discussed. Author (ESA)

93 SPACE RADIATION

Includes cosmic radiation; and inner and outer Earth's radiation belts.

For biological effects of radiation see *52 Aerospace Medicine*. For theory see *73 Nuclear and High-Energy Physics*.

N84-13131 Colorado Univ., Boulder.
ULTRAVIOLET EXTINCTION PROPERTIES OF GRAINS IN THE INTERSTELLAR MEDIUM Ph.D. Thesis
Charles Gregory Seab 1982 195 p
Avail: Univ. Microfilms Order No. DA8309866

The IUE satellite was used to derive UV extinction curves for 58 stars, ranging in spectral type from O6 to A5, and with E(B-V) reddenings from 0.09 to 1.59 mag. Anomalous extinction curves were particularly sought in the project. The most striking discovery was the near absence of the 2175 A extinction feature from the line of sight towards HD 29647 in the Taurus dark cloud. The collection of data was analyzed in several ways. Patterns are sought in the collection as a whole, in homogeneous subsets of the data, and in relation to diffuse band strengths. A search for diffuse bands in the UV was done by stacking 48 of the extinction curves to reduce the noise. The stacked curve showed no evidence of new diffuse bands. To help interpret the anomalous extinction curves, a theoretical simulation of grain processing in interstellar shocks was undertaken. Shock processing was found to cause strong 2175 A bumps and high far UV extinction. Comparison to extinction curves associated with supernova remnants confirms the predictions of strong 2175 A bumps, and partially confirms the prediction of high far UV extinction. Dissert. Abstr.

N84-13132# Fermi National Accelerator Lab., Batavia, Ill.
EVOLUTION OF THE ULTRA HIGH ENERGY COSMIC RAY SPECTRON BY TRANSPORT EQUATION
C. T. Hill and D. N. Schramm Apr. 1983 4 p refs Presented at the 18th Intern. Cosmic Ray Conf., Bangalore, India, 22 Aug. 1983
(Contract DE-AC02-76CH-03000)
(DE83-013711; Fermilab-CONF-83/32-THY; CONF-830830-4) Avail: NTIS HC A02/MF A01

Ultra-high energy proton primaries interacting with the 3 K photon background are treated as a transport phenomenon. Baryon number is explicity conserved and the evolved spectrum develops a bump at a scale of order 5x10 to the 19 power eV, below the cutoff, due to the pile up of energy degraded protons. This may correspond in part to the observed ankle structure in the CR spectrum. DOE

N84-13133# Los Alamos Scientific Lab., N. Mex.
PHOTON DAMPING IN COSMIC-RAY ACCELERATION IN ACTIVE GALACTIC NUCLEI
Stirling A. Colgate 7 Apr. 1983 5 p refs Presented at the 18th Intern. Cosmic Ray Conf., Bangalore, India, 22 Aug. - 3 Sep. 1983
(Contract W-7405-eng-36)
(DE83-011320; LA-UR-83-1048; CONF-830830-2) Avail: NTIS HC A02/MF A01

The usual assumption of the acceleration of ultra high energy cosmic rays, greater than or equal to 10(18) eV in quasars, Seyfert galaxies and other active galactic nuclei is challenged on the basis of the photon interactions with the accelerated nucleons. This is similar to the effect of the black body radiation on particles < 10(20) eV for times of the age of the universe except that the photon spectrum is harder and the energy density greater by approx. = 10(15). Hence, a single traversal, radial or circumferential, of radiation whose energy density is no greater than the emitted flux will damp an ultra high energy. Hence, it is unlikely that any reasonable configuration of acceleration can void disastrous photon energy loss. A different site for ultra high energy cosmic ray acceleration must be found. DOE

N84-13134# Washington Univ., Seattle. Dept. of Physics.
ULTRA-RELATIVISTIC HEAVY IONS AND COSMIC RAYS
Lawrence McLerran May 1983 30 p refs Presented at the Bartol Inst. Conf., Newark, Del., 1 May 1983
(Contract DE-AC06-81ER-40048)
(DE83-015881; CONF-8305123-1) Avail: NTIS HC A03/MF A01

The collisions of ultra-relativistic heavy ions, E/sub /N/ greater than or equal to 1 TeV/nucleon are most interesting, since, at these energies, matter is produced at a sufficiently high energy density that a quark-gluon plasma has a good chance to form. Very heavy ions are also most interesting since the matter forms in a larger volume than for light ions, and the matter is at a somewhat higher density. At very high energies with very heavy ions there is great flexibility in the experimental signals which might be studied, as well as the nature of the matter which is produced. The fragmentation region and central region provide different environments where a plasma might form. The former is baryon rich while the central region is high temperature with low baryon number density and is not accessible except at very high energies. DOE

99 GENERAL

N84-13135# Air Force Systems Command, Wright-Patterson AFB, Ohio. Foreign Technology Div.
HORIZONS OF TECHNOLOGY (SELECTED ARTICLES)
Zdzislaw Perkowski 21 Jul. 1983 19 p Transl. into ENGLISH from Horyzonty Tech. (Poland), v. 32, no. 11, 1979 p 3, 18-10 and 26
(AD-A131897; AD-F630058; FTD-ID(RS)T-0817-83) Avail: NTIS HC A02/MF A01 CSCL 17/2

The theory and design of acyclic electric machines, movable electric contacts, and electromagnetic fields in acyclic machines are discussed in general terms. R.J.F.

Typical Subject Index Listing

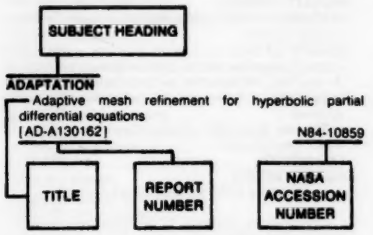

The subject heading is the key to the subject content of the document. Titles, report numbers, and accession numbers of pertinent documents are provided under each subject heading. When the title is insufficiently descriptive of the document content, a title extension has been added, separated from the title by three hyphens. The report number helps to indicate the type of document cited (e.g., NASA report, NASA translation, NASA contractor report). The NASA accession number is the number by which the document abstracts are arranged in this journal and by which the document is sold or requested. The titles, with title extensions if present, are arranged under each subject heading in ascending accession number order. The subject headings have been selected from the latest revision of the *NASA Thesaurus* (NASA SP-7051).

A

ABLATION
Inertial effects in laser-driven ablation
[DE83-016941] N84-12478
ABSORPTION SPECTRA
Advanced diagnostics and instrumentation for chemically reactive flow systems
[AD-A131814] N84-12251
Infrared characteristics of gas plumes
[AD-A131796] N84-12269
Infrared-laser spectroscopy using a long-pathlength absorption cell
[DE83-014197] N84-12480
Optical properties and correlation energy of defects in a-Ge:H
[DE83-016697] N84-12993
ABSORPTION SPECTROSCOPY
Polymer degradation on reflecting metal films: Fourier transform infrared (FTIR) reflection-absorbance studies
[DE83-012129] N84-12641
ABSTRACTS
Center for electronics and electrical engineering technical progress bulletin covering signals and systems program, April 1982 - September 1982
[PB83-241158] N84-12405
ACCELERATED LIFE TESTS
Long term evaluation of the effects of shale oil produced JP-4 on aircraft construction materials
[AD-A131665] N84-12161
ACCELERATION
Inertial effects in laser-driven ablation
[DE83-016941] N84-12478
ACCELERATION (PHYSICS)
High-sensitivity mass spectrometry with a tandem accelerator
[DE83-017914] N84-12274
ACCESSORIES
All-electric accessory drive systems: Implications on engine design and performance N84-12184
ACCIDENT INVESTIGATION
Controls, Displays, and Information Transfer for General Aviation IFR Operations
[NASA-CP-2279] N84-12029
ACCIDENTS
Bibliography of coefficient of friction literature relating to slip type accidents --- slipping accidents
[PB83-243626] N84-12334
Assessment of TRAC-PF1 and RELAP5/MOD1 codes with GE large-vessel blowdown test
[DE83-015384] N84-12874
ACCOMMODATION
Visual accommodation trainer-tester
[NASA-CASE-ARC-11426-1] N84-12193
ACCUMULATORS
A multistage spent particle collector and a method for making same
[NASA-LEW-13914-1] N84-12447
Development of mass-producible line-focus tracking concentrating solar collectors. Category 1: Collectors
[DE83-015629] N84-12639
ACCURACY
Theoretical modelling of three-dimensional vortex flows in aerodynamics N84-12116
Transient temperature response of strain gages, revision 1
[DE83-017514] N84-12459
Analysis of subpixel registration accuracy N84-12570
Progress in the scene-to-map registration investigation N84-12572
ACOUSTIC PROPAGATION
Short-range acoustic intensity vectors of the Pekeris shallow water model
[AMTE(N)-TM-83065] N84-12619
ACOUSTIC PROPERTIES
Effects of microstructure and pore fluids on the acoustic properties of granular materials
[AD-A131983] N84-12668
ACOUSTIC SCATTERING
Transverse horizontal coherence and low-frequency array gain limits in the deep ocean
[AD-A131916] N84-12621
Acoustic pulse scattering from impedance covered cylinders
[AD-A131653] N84-12622
ACOUSTIC SOUNDING
Turbulence environment characterization
[AD-A131815] N84-12692
ACOUSTIC VELOCITY
The effect of noisy reflection data on an inverse method for determining the structure of a layered ocean bottom
[AD-A131976] N84-12620
ACRYLONITRILES
Tailoring polymer films for solar-collection use, phase 1
[DE83-018117] N84-12640
ACTIVE CONTROL
Control of multiaxis vibration systems N84-12203
ACTUATORS
Hydraulic actuators and associated components suited for multiaxis vibration systems --- spacecraft testing N84-12201
Simulation of electro-servo-hydraulic actuator for high quality testing --- of spacecraft N84-12206
IPACS guidance navigation and control system considerations and test activities N84-12245
ADA (PROGRAMMING LANGUAGE)
Ada-Europe guidelines for the portability of Ada programs, second edition
[NPL-DITC-27/83] N84-12739
Guidelines for the design of large modular scientific libraries in Ada
[NPL-DITC-28/83] N84-12740
ADAPTIVE FILTERS
Evaluation of a total energy-rate sensor on a transport airplane
[NASA-TP-2212] N84-12164
ADDITIVES
Hydrogen-air detonations
[DE83-009289] N84-12278
The effect of moisture on the physical and durability properties of methyl methacrylate polymer concrete
[DE83-016733] N84-12541
ADHESIVES
Long term evaluation of the effects of shale oil produced JP-4 on aircraft construction materials
[AD-A131665] N84-12161
ADSORPTION
Research and development for investigations of metallic adsorptions on metal surfaces by optical techniques complemented by dc resistivity and auger spectroscopy
[AD-A131739] N84-12351
International Conference on Vibrations at Surfaces (3rd)
[AD-A131794] N84-12834
AERIAL PHOTOGRAPHY
The synthesized climatic function map N84-12617
AERODYNAMIC CHARACTERISTICS
Aerodynamic design for overall vehicle performance N84-12077
Predicting aerodynamic characteristics of vortical flows on three-dimensional configurations using a surface-singularity panel method N84-12112
The Tracked Wing In Ground-Effect (TWIG) N84-12155
AERODYNAMIC COEFFICIENTS
Dynamic-stall regulation of the Darrieus turbine
[DE83-017994] N84-12097
Vortex flow simulations past wings using the Euler-equations N84-12118
AERODYNAMIC CONFIGURATIONS
Computational methods for subsonic and transonic aerodynamic design N84-12074
Aerodynamic design for overall vehicle performance N84-12077
Transonic empirical configuration design process N84-12079
Transonic configuration design N84-12081
AERODYNAMIC DRAG
Dynamic-stall regulation of the Darrieus turbine
[DE83-017994] N84-12097
AERODYNAMIC HEAT TRANSFER
Space Shuttle external interference heating test
[AD-A131688] N84-12215
Determination of the uncertainty of experimental heat-flux calibrations
[AD-A131918] N84-12450
AERODYNAMIC INTERFERENCE
Special Course on Subsonic/Transonic Aerodynamic Interference for Aircraft
[AGARD-R-712] N84-12072
Subsonic/Transonic Aerodynamic Interference for Aircraft: Introductory remarks N84-12073
Computational methods for subsonic and transonic aerodynamic design N84-12074
Subsonic/transonic viscous interactions N84-12075
Aerodynamic design for overall vehicle performance N84-12077
Application of computational procedures in aerodynamic design N84-12078
Transonic empirical configuration design process N84-12079
Aerodynamic interference: A general overview N84-12080
Transonic configuration design (fighter) N84-12082
External stores interference N84-12083
Interference problems in aircraft design N84-12084
Engine/airframe interference N84-12085
Engine-airframe interference effects N84-12086
A study of wing-body aerodynamic interference of a light twin aircraft utilizing a panel method potential flow program N84-12134
AERODYNAMIC LOADS
Study of an asymptotic method for helicopter rotor blade aerodynamic loads N84-12135
AERODYNAMIC STALLING
Application of the small body pressure transducer
[AD-A131733] N84-12454
AERODYNAMICS
Aeronautical Engineering: A continuing bibliography with indexes (supplement 166)
[NASA-SP-7037(166)] N84-12027

AFWAL FY82 technical accomplishments
[AD-A131839] N84-12054
Acta Aeronautica et Astronautica Sinica
[AD-A131828] N84-12055
Vortical flow management for improved configuration aerodynamics: Recent experiences N84-12129

AEROELASTICITY
Acta Aeronautica et Astronautica Sinica
[AD-A131828] N84-12055
Aeroelastic analysis for propellers - mathematical formulations and program user's manual
[NASA-CR-3729] N84-12530
Development of the basic methods needed to predict the aeroelastic behavior of helicopters N84-12811

AERONAUTICAL ENGINEERING
Aeronautical Engineering: A continuing bibliography with indexes (supplement 166)
[NASA-SP-7037(166)] N84-12027
AFWAL FY82 technical accomplishments
[AD-A131839] N84-12054

AEROSOLS
The Istituto di Ricerca sulle Onde Elettromagnetiche (IROE)-lidar remote sensing of the environment N84-12590
Optical extinction coefficients beneath marine stratus clouds. Comparison of coefficients calculated from observed aerosol spectra with coefficients specified by the Navy aerosol model
[AD-A132011] N84-12685

AEROSPACE ENGINEERING
Activities report of the aerospace industry in West Germany N84-12140
Practical experience during installation of the large multiaxes vibration test facility SAMSON N84-12199
Hydraulic actuators and associated components suited for multiaxis vibration systems --- spacecraft testing N84-12201

AEROSPACE ENVIRONMENTS
The hydraulic multiaxes vibrator: Its capabilities to simulate real mechanical environments and to verify aerospace structures N84-12198
Winds: Chapter 6, 1983 revision. Handbook of Geophysics and Space Environments
[AD-A132018] N84-12683

AEROSPACE MEDICINE
Aerospace Medicine and Biology: A continuing bibliography with indexes (supplement 250)
[NASA-SP-7011(250)] N84-12712

AEROSPACE SYSTEMS
Engineering services in support of the AFGL sounding rocket program
[AD-A131929] N84-12211

AEROTHERMOCHEMISTRY
Executive summary, aerothermal modeling program, phase 1
[NASA-CR-174602] N84-12263
Aerothermal modeling program, phase 1
[NASA-CR-168243-VOL-1] N84-12264
Aerothermal modeling program, phase 1
[NASA-CR-168243-VOL-2] N84-12265

AEROTHERMODYNAMICS
Analytical prediction of aerothermal environment in a wing-elevon cove --- space shuttle orbiter
[NASA-TM-85711] N84-12412

AFTERGLOWS
Atmospheric-pressure argon afterglows as a detector for gas chromatography
[DE83-017695] N84-12282

AGE FACTOR
An age comparison of the vestibulo-ocular counterroll reflex
[AD-A132064] N84-12716

AGING (BIOLOGY)
An age comparison of the vestibulo-ocular counterroll reflex
[AD-A132064] N84-12716

AGRICULTURE
Remote Sensing Applications for Environmental Studies --- conferences
[ESA-SP-188] N84-12579
SPOT potential applications: An overview of the results of the simulation campaigns N84-12587
Development of a data base for carbon dioxide releases resulting from conversion of land to agricultural uses
[DE83-015728] N84-12626

AGROMETEOROLOGY
Guide to agricultural meteorological practices, second edition
[WMO-134] N84-12697

AIR
Hydrogen-air detonations
[DE83-009289] N84-12278
Ion-ion recombination rate in the EMP source region
[AD-A131148] N84-12339

AIR COOLING
Effectiveness in reducing heat stress of three conditioned-air cooling vests worn with and without cooling air supplied to a face piece
[AD-A131975] N84-12726

AIR DEFENSE
An investigation of geometric radar shapes for stereotyping
[AD-A131120] N84-13020

AIR FLOW
Evaluation of a total energy-rate sensor on a transport airplane
[NASA-TP-2212] N84-12164

AIR JETS
Numerical simulations of fuel droplet flows using a Lagrangian triangular mesh
[NASA-CR-168263] N84-12411

AIR LAND INTERACTIONS
Numerical modeling techniques for half-space (ground) problems N84-12374

AIR LAUNCHING
A balloon design for 9000 pounds at 90,000 feet: Recommendations based on heavy-load balloon history
[AD-A131987] N84-12093

AIR MASSES
Optical extinction coefficients beneath marine stratus clouds. Comparison of coefficients calculated from observed aerosol spectra with coefficients specified by the Navy aerosol model
[AD-A132011] N84-12685

AIR POLLUTION
Soot formation from polycyclic aromatics
[DE83-009750] N84-12271
Detecting long-term ecological effects in forests and food chains
[DE83-003469] N84-12655

AIR TO SURFACE MISSILES
Hypervelocity missile: Based on the concept of aircraft/missile integration for maximum firepower N84-12058
F-16 Penguin anti-ship missile integration N84-12059

AIR TRAFFIC CONTROL
Study to determine the IFR operational profile and problems to the general aviation pilot N84-12032
A flight investigation of simulated data link communications during single-pilot IFR flight N84-12046
Airport and air traffic control system
[OTA-STI-175] N84-12143
Airport and air traffic control system. Executive summary N84-12144
Airport and air traffic control system. Introduction and overview N84-12145
The National Airspace System N84-12146
Aviation growth scenarios N84-12147
Technology and the future evolution of the ATC system N84-12148
Airport capacity alternatives N84-12149
Policy implications N84-12150

AIR TRANSPORTATION
Domestic scheduled air transport for the year 2000. Financial and capacity related effects of supply alternatives, considering, also, the cooperation with high speed rail transport services --- West Germany
[DFVLR-FB-83-03] N84-12141

AIR WATER INTERACTIONS
The dependence of the radar modulation transfer function on environmental conditions and wave parameters
[AD-A131858] N84-12348
On the growth of gravity-capillary waves by wind
[KNMI-WR-83-10] N84-12698

AIRBORNE EQUIPMENT
Remote sensing using the airborne MEIS 2 multidetector electro optical imaging scanner N84-12592
Passive radiometry and other remote sensing data interpretation for oil slick thickness assessment, in an experimental case N84-12609

AIRBORNE SURVEILLANCE RADAR
Tracking theory for airborne surveillance radars
[AD-A131792] N84-12350

AIRBORNE/SPACEBORNE COMPUTERS
Effects of integrated maintenance on the definitions of onboard equipments --- Mirage 2000 aircraft N84-12068

AIRCRAFT ACCIDENTS
Controls, Displays, and Information Transfer for General Aviation IFR Operations
[NASA-CP-2279] N84-12029
Single pilot IFR accident data analysis N84-12031
A summary and integration of research concerning single pilot IFR operational problems N84-12034
Lessons learned from FY82 US Army aviation mishaps
[AD-A131725] N84-12137

AIRCRAFT ANTENNAS
Numerical modelling methods for predicting antenna performance on aircraft N84-12375

AIRCRAFT COMMUNICATION
Weather data communication and utilization N84-12045

AIRCRAFT CONSTRUCTION MATERIALS
Long term evaluation of the effects of shale oil produced JP-4 on aircraft construction materials
[AD-A131665] N84-12161

AIRCRAFT CONTROL
Integration of Fire Control, Flight Control and Propulsion Control Systems
[AGARD-CP-349] N84-12056
Integration of fire, flight and propulsion control systems: An overview, retrospective and prospective N84-12057
Application of flight controls technology to engine control systems N84-12061
The use of a formal simulator to verify a simple real time control program
[AD-A131732] N84-12745

AIRCRAFT DESIGN
An integrated AFCS for the "PROFILE"-mode N84-12069
Computational methods for subsonic and transonic aerodynamic design N84-12074
Aerodynamic interference: A general overview N84-12080
Transonic configuration design N84-12081
Transonic configuration design (fighter) N84-12082
External stores interference N84-12083
Interference problems in aircraft design N84-12084
Engine/airframe interference N84-12085
Engine-airframe interference effects N84-12086
Geometries for roughness shapes in laminar flow
[NASA-CASE-LAR-13255-1] N84-12092
Recent studies at NASA-Langley of vortical flows interacting with neighboring surfaces N84-12109
Design considerations for bearingless rotor hubs
[AD-A131660] N84-12162
Ground and inflight operational effects of APU's N84-12182

AIRCRAFT ENGINES
The relations between the numerical control of the engine and other aircraft functions N84-12062
Engine/airframe interference N84-12085
Engine-airframe interference effects N84-12086
Auxiliary power systems with gas turbines N84-12170
Hot gas APU starter for advanced aircraft applications N84-12178
A jet fuel starter for lowest system life cycle cost N84-12179
Cost efficient on board power for airline operation N84-12180
APU operational efficiency N84-12181
Ground and inflight operational effects of APU's N84-12182
Super integrated power unit for fighter aircraft N84-12183
Implementing microprocessor technology in aircraft electrical power generating system control N84-12185
150 hour engine test of corrosion inhibited MIL-L-23699C oil
[AD-A131633] N84-12317

AIRCRAFT EQUIPMENT
Effects of integrated maintenance on the definitions of onboard equipments --- Mirage 2000 aircraft N84-12068
Auxiliary Power Systems
[AGARD-CP-352] N84-12168
Secondary power systems for fighter aircraft experiences today and requirements for a next generation N84-12171
Small auxiliary power unit design constraints N84-12172
APU in commercial airline operation N84-12173
Auxiliary power units for wide-body aircraft N84-12174
Secondary power supplies for a small single engine combat aircraft N84-12175
Optimization of engine power offtake by secondary power system design N84-12177

AIRCRAFT HAZARDS
Analysis of general aviation single-pilot IFR incident data obtained from the NASA Aviation Safety Reporting System N84-12033
Correlation of laboratory-scale fire test methods for seat blocking layer materials with large-scale test results
[AD-A131666] N84-12138

AIRCRAFT INDUSTRY
Develop a normative or descriptive model of the international/domestic civil aviation industry, volume 3
[AD-A131878] N84-12051

Develop a normative or descriptive model of the international/domestic civil aviation industry, volume 2 [AD-A131877] N84-12052
Develop a normative or descriptive model of the international/domestic civil aviation industry. Volume 1: Executive summary [AD-A131876] N84-12053
Application of computational procedures in aerodynamic design N84-12078

AIRCRAFT INSTRUMENTS
Pilot response with conventional displays N84-12040

AIRCRAFT LANDING
Simulator study of flight characteristics of a large twin-fuselage cargo transport airplane during approach and landing [NASA-TP-2183] N84-12190

AIRCRAFT MAINTENANCE
Models of maintenance resources interaction: Peacetime operations [AD-A131379] N84-13011

AIRCRAFT NOISE
Noise emission by helicopters N84-13007

AIRCRAFT PERFORMANCE
Integration of Fire Control, Flight Control and Propulsion Control Systems [AGARD-CP-349] N84-12056
Auxiliary power requirements: Their role in aircraft performance N84-12169

AIRCRAFT PILOTS
An overview of the demonstration advanced avionics system guest pilot evaluation conducted at Ames Research Center N84-12049
Extent of hearing loss among Army aviators at Fort Rucker, Alabama [AD-A132069] N84-12714

AIRCRAFT SAFETY
Lessons learned from FY82 US Army aviation mishaps [AD-A131725] N84-12137

AIRCRAFT STRUCTURES
Aircraft transparency testing methodology and evaluation criteria. Part 2: Methodology development for improved durability [AD-A131928] N84-12157
Aircraft transparency testing methodology and evaluation criteria. Part 1: Test methods and information analysis [AD-A131927] N84-12158
Flightline thermal environment testing of F-111 transparencies [AD-A131642] N84-12163
Vibration response of geometrically nonlinear elastic beams to pulse and impact loading [NASA-CR-174495] N84-12527
Evaluation of the crack gage as an advanced individual aircraft tracking concept N84-12551

AIRCRAFT WAKES
The effect of wing tip devices on the far-field wake of a Paris Aircraft N84-12131

AIRFOILS
Acta Aeronautica et Astronautica Sinica [AD-A131828] N84-12055
Subsonic/transonic viscous interactions N84-12075
Aerodynamic design for overall vehicle performance N84-12077
Application of computational procedures in aerodynamic design N84-12078
Dynamic-stall regulation of the Darrieus turbine [DE83-017994] N84-12097
Steady and unsteady flow models for airfoils with spoiler N84-12136

AIRFRAMES
Engine/airframe interference N84-12085
Engine-airframe interference effects N84-12086
Influence of the airframe on the performance of antennas for avionics N84-12372
A review of Australian investigations on aeronautical fatigue during the period April 1981 to March 1983 [AD-A130968] N84-12532

AIRGLOW
Oi 630.0 nm optical measurements of neutral winds, temperatures and airglow enhancements during the BIME program [AD-A131695] N84-12671

AIRLINE OPERATIONS
Activities report of the aerospace industry in West Germany N84-12139
Activities report of the aerospace industry in West Germany N84-12140
Airport capacity alternatives N84-12149

AIRPORTS
Airport and air traffic control system [OTA-STI-175] N84-12143
Airport and air traffic control system. Executive summary N84-12144
Airport and air traffic control system. Introduction and overview N84-12145
Policy implications N84-12150

AIRSHIPS
Some trends in airship technology developments [AGARD-R-717] N84-12050

AIRSPACE
General aviation single pilot IFR autopilot study N84-12035

ALASKA
Alaska's mineral resources [DE83-016599] N84-12623

ALGAE
Phytochrome from green plants: Assay, purification, and characterization [DE83-017447] N84-12710

ALGEBRA
The effects of small noise on implicitly defined non-linear dynamical systems [AD-A131632] N84-12808

ALGORITHMS
Application of computational procedures in aerodynamic design N84-12078
Progress on ultrasonic flaw sizing in turbine-engine rotor components: Bore and web geometries [DE83-018081] N84-12167
Preliminary data processing plan for the thermal plasma experiment on the HILAT satellite [AD-A132017] N84-12209
Tracking theory for airborne surveillance radars [AD-A131792] N84-12350
Optimum reception in non-Gaussian electromagnetic interference environments. Part 2: Optimum and suboptimum threshold signal detection in class A and B noise [PB83-241141] N84-12364
Inverse born approximation: Exact determination of shape of convex voids [DE83-017685] N84-12512
Spline classification methods N84-12564
Description of an automatic seismic measurements package: Analysis and design goals [AD-A132067] N84-12666
Evaluation of automated imagery analysis algorithms for use in the three-dimensional nephanalysis model at AFGWC (Air Force Global Weather Central) [AD-A131986] N84-12686
Mesocyclone detection and classification algorithm [AD-A131826] N84-12691
Numerical solution of the three-dimensional unsteady Euler equations [AD-A132034] N84-12783
The effect of coordinate system rotation on spherical harmonic expansions: A numerical method [AD-A131974] N84-12785
Lecture notes for contact-impact algorithms for large-deformation finite-element analysis [DE83-013039] N84-12789
Rank modification method for certain singular systems of linear equations N84-12797
An alternative to the Monte Carlo estimation of network reliability [AD-A131849] N84-12800
On the performance of two-stage group screening experiments [AD-A131970] N84-12807
The effect of noisy reflection data on an inverse method for determining the structure of a layered ocean bottom [AD-A131976] N84-12820
Methods for deconvoluting and interpreting complex gammaand X-ray spectral regions [DE83-013585] N84-12991

ALIGNMENT
Using an X-ray-sensitive vidicon and remote-control stage mechanism to obtain critical radiographic alignment of small explosive devices [DE83-012846] N84-12326

ALKALI METALS
Equations of state for the alkali metals, with generalizations to NaCl [DE83-018075] N84-12280

ALLOYS
Miniature charpy-impact test results for the irradiated ferritic alloys HT-9 and modified 9Cr-1Mo [DE83-016935] N84-12300
Clustering and ordering in 3-5 alloys [AD-A131785] N84-12974

ALPHA PARTICLES
TFTR alpha extraction and measurement project [DE83-018120] N84-12947
Cross sections relevant to gamma-ray astronomy: Alpha-particle-induced reactions [DE83-015533] N84-13038

ALPINE METEOROLOGY
Omega Dropwindsonde processing [PB83-248773] N84-12700

ALTIMETERS
Test operations procedure: Absolute altimeters [AD-A131746] N84-12185

ALTITUDE
Variability of atmospheric density in the middle atmosphere [AD-A131985] N84-12667

ALTITUDE CONTROL
Flight test validation of a design procedure for digital autopilots N84-12036

ALUMINUM
Phonon-induced enhancements of the energy gap and critical current in superconducting aluminum [DE83-015210] N84-12996

ALUMINUM ALLOYS
Solidification of aluminum and aluminum alloys at high levels of undercooling N84-12286
Mechanical property evaluation of P/M (Powder-Metallurgy) aluminum 7090-T7E71 plate [AD-A132058] N84-12290

AMMONIA
Isotope dependence of the breakdown strength of gases [DE83-017272] N84-12430

AMORPHOUS SEMICONDUCTORS
Amorphous silicon-carbon films [DE83-018077] N84-12259
Optical properties and correlation energy of defects in a-Ge:H [DE83-016697] N84-12993

AMPLIFICATION
Evaluation of the Beijing Instrument Factory GDB-44F photomultiplier [DE84-000849] N84-12398

AMPLIFIERS
Creation of ultra-high-pressure shocks by the collision of laser-accelerated disks: Experiment and theory [DE83-017366] N84-12486

AMPLITUDE DISTRIBUTION ANALYSIS
Effect of frequency-averaging on estimation of clutter statistics used in setting CFAR detection thresholds [AD-A131947] N84-12343

AMPLITUDES
Progress on ultrasonic flaw sizing in turbine-engine rotor components: Bore and web geometries [DE83-018081] N84-12167
Minimal unitary (covariant) scattering theory [DE83-014896] N84-12849

ANALOG CIRCUITS
Applications of analog Change Coupled Devices (CCD's) [BMFT-FB-T-83-141] N84-13002

ANALOG TO DIGITAL CONVERTERS
GSE for balloon-borne I.M.S.: Decommutator and D/A units [AD-A131845] N84-12452

ANALYSIS (MATHEMATICS)
Three-dimensional analysis of composite plates with material nonlinearity [AD-A131884] N84-12258
Applied mathematical sciences research at Argonne [DE83-3014268] N84-12788

ANALYSIS OF VARIANCE
Repeated-measures analysis of image data N84-12567
An alternative to the Monte Carlo estimation of network reliability [AD-A131849] N84-12800
On the performance of two-stage group screening experiments [AD-A131970] N84-12807

ANGLE OF ATTACK
On the generation of vortical flow at hypersonic speeds over elliptical cones N84-12114
Computational vortex flow aerodynamics N84-12117

ANGLES (GEOMETRY)
Investigation of the Rayleigh critical angle phenomenon for the characterization of surface properties [AD-A131530] N84-12340

ANGULAR CORRELATION
Baryon-antibaryon angular correlations in quark jets [DE83-015923] N84-12854

ANGULAR DISTRIBUTION
New statistical and non-statistical effects in deep inelastic heavy-ion collisions [DE83-015732] N84-12885
Temperature dependence of the electric-field gradient in Er metal [DE83-015564] N84-12989
Stellar winds driven by multi-line scattering N84-13087

ANGULAR MOMENTUM
A numerical study on the evolution of tornadoes N84-12679

New statistical and non-statistical effects in deep inelastic heavy-ion collisions
[DE83-015732] N84-12885
ANISOTROPIC MEDIA
Hamiltonian for antisotropic bodies with defects
[ISSN-0208-5658] N84-12966
ANISOTROPIC PLATES
An interactive computer program for analysis of ultrasonic modulus data on anistropic materials
[NPL-DMA(A)68] N84-12526
ANISOTROPY
Anisotropy and microstructure of Sm2(Co, Fe, Cu, Zr)17 magnetic materials
[AD-A131961] N84-12291
Beam plasma turbulence study
[AD-A131946] N84-12917
The behavior of the cosmic ray equatorial anisotropy inside fast solar wind streams ejected by coronal holes
[IFSI-82-16] N84-13130
ANNEALING
Semiconductor processing with excimer lasers
[DE83-007509] N84-12477
ANNUAL VARIATIONS
Predicting lake ice decay
[AD-A132012] N84-12618
Estimating long-term mean winds from short-term wind data
[DE83-017417] N84-12693
ANNULAR FLOW
Annular Momentum Control Device (AMCD)
N84-12241
ANODIC COATINGS
HgCdTe surface study program
[AD-A132071] N84-12266
ANOMALIES
Theory of hyperfine anomalies in muonic atoms
[DE83-015392] N84-12872
ANTARCTIC REGIONS
L band satellite communication experiment in the Antartic
[ESA-TT-805] N84-12356
ANTENNA ARRAYS
Performance analysis of a three-dimensional microwave lens in a cylindrical array scanning application
[AD-A131891] N84-12345
Simultaneous nulling in the sum and difference patterns of a monopulse antenna
[AD-A131865] N84-12347
ANTENNA DESIGN
The Performance of Antennas in Their Operational Environment
[AGARD-LS-131] N84-12367
Scale modelling and full scale measurement techniques with particular reference to antennas in their operational environments N84-12368
Interaction of antennas with masts under special consideration of the sensitivity and nonlinear effects in ship borne receiving systems N84-12371
Influence of the airframe on the performance of antennas for avionics N84-12372
Numerical modeling techniques for half-space (ground) problems N84-12374
Numerical modelling methods for predicting antenna performance on aircraft N84-12375
Effects of nonlinear loads on antennas and scatterers N84-12376
ANTENNA RADIATION PATTERNS
Simultaneous nulling in the sum and difference patterns of a monopulse antenna
[AD-A131865] N84-12347
ANTENNAS
Calculation of ground wave attenuation over irregular, inhomogeneous, layered media using PROGRAM WAGNER N84-12369
Numerical modeling techniques for antennas N84-12373
ANTIFERROMAGNETISM
Commensurability, chaos, and the devil's staircase
[DE83-013280] N84-12987
ANTIMONY
Effect of antimony on lead-acid battery negative electrode
[DE83-014680] N84-12404
ANTIOXIDANTS
Replacement of PBNA in HB and HC polymers used in SRM propellant and liner
[NASA-CR-170936] N84-12311
ANTIPARTICLES
Baryon-antibaryon angular correlations in quark jets
[DE83-015923] N84-12854
ANTIPROTONS
Nucleon-nucleon interactions and polarized-beam (both proton and antiproton) facilities at LAMPF 2
[DE83-017215] N84-12860
ANTISHIP MISSILES
F-16 Penguin anti-ship missile integration N84-12059
APPLICATIONS OF MATHEMATICS
Proceedings of the NASA Symposium on Mathematical Pattern Recognition and Image Analysis
[E83-10032] N84-12557
Applied mathematical sciences research at Argonne
[DE83-3014268] N84-12788
APPROACH
Simulator study of flight characteristics of a large twin-fuselage cargo transport airplane during approach and landing
[NASA-TP-2183] N84-12190
APPROACH CONTROL
General aviation single pilot IFR autopilot study
N84-12035
A simulator evaluation of an automatic terminal approach system N84-12037
Advanced symbology for general aviation approach to landing displays N84-12039
APPROACH INDICATORS
Advanced symbology for general aviation approach to landing displays N84-12039
APPROXIMATION
Progress on ultrasonic flaw sizing in turbine-engine rotor components: Bore and web geometries
[DE83-018081] N84-12167
Techniques for locating a remote HF transmitter from single-site measurements
[AD-A132014] N84-12342
Numerical calculations of turbulent recirculating heat transfer beyond two-dimensional back-steps and sudden pipe expansions N84-12439
Inverse born approximation: Exact determination of shape of convex voids
[DE83-017685] N84-12512
Bending of transversally loaded orthotropic rectangular and sector plates N84-12520
Disjunctive programming and a hierarchy of relaxations for discrete optimization problems
[AD-A132004] N84-12784
New soluble approximation to Fokker-Planck equations
[DE83-016210] N84-12791
APTITUDE
Racial bias and predictive validity in testing for selection
[AD-A131830] N84-12722
AQUATIC PLANTS
Method for treating wastewater using microorganisms and vascular aquatic plants
[NASA-CASE-NSTL-10] N84-12654
AQUICULTURE
Detecting long-term ecological effects in forests and food chains
[DE83-003469] N84-12655
AQUIFERS
Velocity plots and capture zones of pumping centers for ground-water investigations
[DE83-016618] N84-12624
Initial operation of the compressed air experiment at Pittsfield, Illinois
[DE83-016930] N84-12643
ARCHITECTURE (COMPUTERS)
Integrated powerplant control systems and potential performance benefits N84-12063
High dynamic global positioning system receiver
[NASA-CASE-NPO-16171-1-CU] N84-12151
Software voting in asynchronous NMR (N-Modular Redundancy) computer structures
[NASA-CR-174488] N84-12732
Computer system design environment software development plan
[AD-A131651] N84-12747
ARGON
Atmospheric-pressure argon afterglows as a detector for gas chromatography
[DE83-017695] N84-12282
ARIANE LAUNCH VEHICLE
Development of an ultrasonic testing procedure for electron beam welded parts for aerospace applications
[BMFT-FB-W-72-011] N84-12515
ARIZONA
Arizona State science, engineering and technology process
[PB83-237107] N84-13016
ARMED FORCES (UNITED STATES)
Evaluation of automated imagery analysis algorithms for use in the three-dimensional nephanalysis model at AFGWC (Air Force Global Weather Central)
[AD-A131986] N84-12686
ARRAYS
Use of superposition in calculating cooling requirements for circuit cards containing arrays of electronic components
[DE83-016091] N84-12428
Turbulent tube-flow heat transfer coefficients in the presence of flow imbalance in the tubes of a parallel array N84-12437
A model for the distributed storage and processing of large arrays
[NASA-CR-172252] N84-12742
ARTIFICIAL INTELLIGENCE
Robotics: An introduction to today's robot and future trends
[AD-A132070] N84-12768
Using structural and functional information in diagnostic design
[AD-A131859] N84-12769
Artificial intelligence: Cognition as computation
[AD-A131804] N84-12770
Prerequisites for deriving formal specifications from natural language requirements
[AD-A131722] N84-12771
Representations for reasoning about change
[AD-A131649] N84-12772
Automated reasoning in man-machine control systems
[DE83-014307] N84-12774
ARTIFICIAL SATELLITES
Acquisition, image and data compression
[AD-A131923] N84-12344
ASPECT RATIO
Reversed-field pinch large aspect ratio equilibrium
[DE83-016771] N84-12953
ASSEMBLIES
Ultra low loss optical fiber cable assemblies, volume 2
[AD-A132008] N84-12891
Ultra low loss optical fiber cable assemblies, volume 1
[AD-A132007] N84-12892
ASSEMBLY LANGUAGE
Assembly language graphics library (EGR1.LB) with Fortran interfacing
[PB83-239624] N84-12757
ASTRONOMICAL SPECTROSCOPY
Development of a segmented n-type germanium detector, and its application to astronomical gamma-ray spectroscopy
[NASA-TM-85435] N84-13039
Observation of winds in cool stars N84-13084
ASTRONOMICAL TELESCOPES
High Resolution Imager (HRI) for the Roentgen Satellite (ROSAT) definition study
[NASA-CR-174598] N84-12223
ASTROPHYSICS
Formation of standing shocks in stellar winds and related astrophysical flows N84-13088
ASYMPTOTES
On sensitivity, compensation and the approach to the asymptotes in multivariable root-loci
[RR-222] N84-12795
ASYMPTOTIC METHODS
Study of an asymptotic method for helicopter rotor blade aerodynamic loads N84-12135
ASYMPTOTIC SERIES
Weak and strong law results for a function of the spacings
[AD-A130705] N84-12782
ATMOSPHERIC BOUNDARY LAYER
A study of coherent structures in the near-neutral marine atmospheric boundary layer N84-12658
Gust structure and gust statistics. Results from an analysis of atmospheric turbulence measurements by using conditional sampling technique
[FFA-TN-1983-28] N84-12696
ATMOSPHERIC CHEMISTRY
Remote sensing instruments for trace species measurements in the troposphere and stratosphere: A review N84-12583
Activities report of the Laboratory of Environmental Physics and Chemistry N84-12963
ATMOSPHERIC CIRCULATION
Mechanisms of monsoonal cyclogenesis N84-12680
Winds: Chapter 6, 1983 revision. Handbook of Geophysics and Space Environments
[AD-A132018] N84-12683
Turbulence environment characterization
[AD-A131815] N84-12692
ATMOSPHERIC COMPOSITION
Properties of the neutral density and composition in the thermosphere
[AD-A131557] N84-12665
ATMOSPHERIC DENSITY
Properties of the neutral density and composition in the thermosphere
[AD-A131557] N84-12665
Variability of atmospheric density in the middle atmosphere
[AD-A131985] N84-12667
ATMOSPHERIC EFFECTS
The Istituto di Ricerca sulle Onde Elettromagnetiche (IROE)-lidar remote sensing of the environment
N84-12590

ATMOSPHERIC MODELS
Numerical simulation of convective scaling N84-12660
ATMOSPHERIC PHYSICS
Proceedings of 1st International Workshop on Atmospheric Icing of Structures [AD-A131869] N84-12690
Activities report of the Laboratory of Environmental Physics and Chemistry N84-12963
ATMOSPHERIC PRESSURE
Atmospheric-pressure argon afterglows as a detector for gas chromatography [DE83-017695] N84-12282
ATMOSPHERIC SOUNDING
Omega Dropwindsonde processing [PB83-248773] N84-12700
ATMOSPHERIC TEMPERATURE
Climate of Phoenix, Arizona (revised) [PB83-246801] N84-12699
ATMOSPHERIC TURBULENCE
Gust structure and gust statistics. Results from an analysis of atmospheric turbulence measurements by using conditional sampling technique [FFA-TN-1983-28] N84-12696
ATOMIC COLLISIONS
Hadron-hadron collider group [DE83-010704] N84-12865
Cross sections for charge transfers of highly ionized ions in hydrogen atoms [IPPJ-AM-30] N84-12912
Physics of ion implantation: Ion-cascade processes and physical state of the implanted solid [DE83-017152] N84-12998
ATOMIC ENERGY LEVELS
Kinetics of growth and decay of excited rare-gas atoms and molecules in the pulse radiolysis of pure rare gases and of mixtures of rare gases with molecular quenching agents [DE83-017016] N84-12856
ATOMIC EXCITATIONS
The 100% alignment of hydrogen excited states in beam-foil spectroscopy [DE83-017963] N84-12859
ATOMIC PHYSICS
Atomic processes in hot dense plasma [IPPJ-AM-31] N84-12911
Bibliography on atomic processes in hot dense plasmas [IPPJ-AM-29] N84-12913
ATOMIC STRUCTURE
Implications of heavy-ion-induced satellite X-ray emission. 1: Introduction [DE83-015682] N84-12851
Dense molecular thermodynamics [DE83-015216] N84-13006
ATOMIZERS
Constant-output atomizer --- Inhalation therapy and aerosol research [NASA-CASE-MFS-25631-1] N84-12406
ATROPINE
Effect of atropine on the exercise-heat performance of man [AD-A131843] N84-12719
ATTACK AIRCRAFT
Hypervelocity missile: Based on the concept of aircraft/missile integration for maximum firepower N84-12058
A nonlinear control law for piloting aircraft in the air-to-ground attack phase N84-12071
Secondary power supplies for a small single engine combat aircraft N84-12175
ATTITUDE (INCLINATION)
V/STOL (Vertical/Short Takeoff and Landing) low speed and transition equivalent systems analysis [AD-A131955] N84-12156
ATTITUDE CONTROL
Control of flexible spacecraft by optimal model following N84-12222
Integrated Flywheel Technology, 1983 [NASA-CP-2290] N84-12228
Integrated Power/Attitude Control System (IPACS) N84-12229
GSFC flywheel status N84-12230
Space station control requirements and flywheel system weights for combined momentum and energy storage N84-12236
Combined attitude control and energy storage N84-12237
IPACS attitude control technology considerations N84-12238
Flywheel electronics N84-12239
IPACS electronics: Comments on the original design and current efforts at Langley Research Center N84-12240
Annular Momentum Control Device (AMCD) N84-12241
Advanced Control and Power System (ACAPS) technology program N84-12243
Power system considerations and test activities N84-12244
IPACS guidance navigation and control system considerations and test activities N84-12245
AUDITORY DEFECTS
Extent of hearing loss among Army aviators at Fort Rucker, Alabama [AD-A132069] N84-12714
AURORAS
Solar wind variations in the 60-100 year period range: A review N84-13092
Periodicities in the occurrence of aurora as indicators of solar variability N84-13093
AUSTENITIC STAINLESS STEELS
Helium damage in austenitic stainless steels [DE83-017494] N84-12309
AUSTRALIA
Australian Oceanographic Data Centre bulletin 16 [AD-A132002] N84-12701
AUTOMATIC CONTROL
Robotics: An introduction to today's robot and future trends [AD-A132070] N84-12768
AUTOMATIC FLIGHT CONTROL
An integrated AFCS for the "PROFILE"-mode N84-12069
The use of a formal simulator to verify a simple real time control program [AD-A131732] N84-12745
AUTOMATIC PILOTS
Single pilot IFR program overview and status N84-12030
General aviation single pilot IFR autopilot study N84-12035
Flight test validation of a design procedure for digital autopilots N84-12036
A simulator evaluation of an automatic terminal approach system N84-12037
Control/display trade-off study for single-pilot instrument flight rule operations N84-12044
The use of a formal simulator to verify a simple real time control program [AD-A131732] N84-12745
AUTOMATION
Description of an automatic seismic measurements package: Analysis and design goals [AD-A132067] N84-12666
AUTOMOBILE ENGINES
Controlled combustion engine evaluation [DE83-011245] N84-12499
Optimum engine for methanol utilization [PB83-239459] N84-12507
AUTOMOBILE FUELS
Evaluation of unthrottled combustion system options for light duty applications with future syncrude derived fuels [DE83-017047] N84-12327
AUTOMOBILES
A study of the relationship between exhaust emissions and fuel economy [PB83-235564] N84-12506
Energy use and range of electric vehicles in selected US Department of Energy sites [DE83-015719] N84-13034
AUTOREGRESSIVE PROCESSES
Autoregressive models for use in scene segmentation N84-12561
AUXILIARY POWER SOURCES
Auxiliary Power Systems [AGARD-CP-352] N84-12168
Auxiliary power requirements: Their role in aircraft performance N84-12169
Auxilliary power systems with gas turbines N84-12170
Secondary power systems for fighter aircraft experiences today and requirements for a next generation N84-12171
Small auxiliary power unit design constraints N84-12172
APU in commercial airline operation N84-12173
Auxiliary power units for wide-body aircraft N84-12174
Secondary power supplies for a small single engine combat aircraft N84-12175
Hydraulic generation of auxilliary power for the Mirage 2000 aircraft N84-12176
Optimization of engine power offtake by secondary power system design N84-12177
Hot gas APU starter for advanced aircraft applications N84-12178
Cost efficient on board power for airline operation N84-12180
APU operational efficiency N84-12181
Ground and inflight operational effects of APU's N84-12182
All-electric accessory drive systems: Implications on engine design and performance N84-12184
The 400 Hz generators evolution, effects on installation arrangements N84-12186
Orbiting wire as a dynamo: Auxiliary power possibilites for space platforms [IFSI-83-3] N84-12853
AVIONICS
A simulator evaluation of an automatic terminal approach system N84-12037
NASA Demonstration Advanced Avionics System (DAAS) N84-12048
An overview of the demonstration advanced avionics system guest pilot evaluation conducted at Ames Research Center N84-12049
AFWAL FY82 technical accomplishments [AD-A131839] N84-12054
Some aspects of flight trajectory control in future avionic systems for combat aircraft N84-12066
Influence of the airframe on the performance of antennas for avionics N84-12372
From launching carrier rockets towards the Pacific on the accomplishments and problems of electronic technologies in our country [AD-A131088] N84-12380
AXIAL FLOW
On the structure of the turbulent vortex N84-12102
AXISYMMETRIC FLOW
The AGCE related studies of baroclinic flows in spherical geometry [NASA-CR-170934] N84-12415
Boundary-integral simulations of rayleigh-taylor instability in ideal magnetohydrodynamics [AD-A131667] N84-12920
AZIMUTH
Interaction of the plasma tail of comet Bradfield 1979L on 1980 February 6 with a possibly flare-generated solar-wind disturbance N84-13126

B

BACKGROUND NOISE
Technique for producing a coherent sum of the data from P78-1, F2, and F4 satellites [AD-A131965] N84-12210
Development of a segmented n-type germanium detector, and its application to astronomical gamma-ray spectroscopy [NASA-TM-85435] N84-13039
BACKGROUND RADIATION
Correlation between two spacecraft in the Doppler detection of a gravitational background radiation [IFSI-83-7] N84-12362
BACKSCATTERING
Speed-dependent collision effects on radar back-scattering from the ionosphere --- incoherent scatter radar [NASA-CR-173077] N84-12336
BACKWARD DIFFERENCING
Multidimensional explicit difference schemes for hyperbolic conservation laws [NASA-CR-172254] N84-12778
BACKWARD FACING STEPS
Computation of turbulent flows over backward-facing step [NASA-TM-85851] N84-12414
BACTERIA
Time-resolved laser studies on the energy transfer and the configurational changes in bacteriohodopsin [DE83-015708] N84-12487
BALANCE
Turbulent tube-flow heat transfer coefficients in the presence of flow imbalance in the tubes of a parallel array N84-12437
BALLOON-BORNE INSTRUMENTS
GSE for balloon-borne I.M.S.: Decommutator and D/A units [AD-A131845] N84-12452
Information processing for the infrared balloon telescope Goldener Drache [MPE-38] N84-13035
BALLOONS
A balloon design for 9000 pounds at 90,000 feet: Recommendations based on heavy-load balloon history [AD-A131987] N84-12093
BALMER SERIES
The 100% alignment of hydrogen excited states in beam-foil spectroscopy [DE83-017963] N84-12859
BALTIC SEA
Introductory studies of natural contamination and manmade pollution in Danish waters N84-12608
BANDWIDTH
IPACS attitude control technology considerations N84-12238

Computational tool for the design of ultrasonic systems
[DE83-018092] N84-12824

BARIUM
The relative abundances of Sn, Te, Xe, Ba and Ce
[NASA-CR-174599] N84-13064

BAROCLINIC INSTABILITY
Mechanisms of monsoonal cyclogenesis N84-12680

BAROMETERS
A case study of gravity wave-convective storm interactions N84-12659

BARS
On the dynamic fracture of bars, beams and plates N84-12552

BARYONS
Baryon-antibaryon angular correlations in quark jets
[DE83-015923] N84-12854

BASIC (PROGRAMMING LANGUAGE)
NCR Corporation NCR 9300 ITX-BASIC release 1.1
[PB83-243410] N84-12762

BATTERY CHARGERS
Charge characteristics of Ni/Fe traction cells
[DE83-014205] N84-12389

BAYES THEOREM
An empirical Bayes approach to spatial analysis N84-12563
Spline classification methods N84-12564

BAYS (TOPOGRAPHIC FEATURES)
Remote sensing analysis of oil pollution in Augusta Bay, Sicily N84-12616

BEACONS
Preliminary studies of Solar Advance Observatory and Solar Beacon Facility
[NASA-CR-170937] N84-13066

BEADS
Solid impingement erosion mechanisms and characterization of erosion resistance of ductile metals
[NASA-TM-83492] N84-12287

BEAM CURRENTS
The Los Alamos free-electron-laser oscillator experiment: Plans and present status
[DE83-017290] N84-12485
Measurements of the emittance and current density profile of the beam produced by the ATA injector
[DE83-016522] N84-12848
The 83-inch cyclotron research program
[DE83-015827] N84-12852
Developing a 500-eV proton beam
[DE83-012781] N84-12880
A steady-state axisymmetric toroidal system
[IPPJ-843] N84-12910
Rotating and propagating LIB stabilized by self-induced magnetic field
[IPPJ-840] N84-12916
Light-ion-beam fusion
[DE83-018263] N84-12944

BEAM INJECTION
Efficient radiation-hardened, 400- and 800-keV neutral-beam injection systems
[DE83-015691] N84-12886

BEAM INTERACTIONS
Electron-ion collisions
[DE83-017211] N84-12867
Effect of RF structure on cumulative beam breakup
[DE83-017302] N84-12882

BEAM NEUTRALIZATION
Windows and mirrors needed for a laser-driven photoneutralizer
[DE83-013562] N84-12473

BEAMS (SUPPORTS)
Design considerations for bearingless rotor hubs
[AD-A131660] N84-12162
Calculation of forced response to base excitation using experimentally derived modal participation factors N84-12205
On the dynamic fracture of bars, beams and plates N84-12552
A thin-walled beam finite element
[TT-8302] N84-12779

BEARINGLESS ROTORS
Design considerations for bearingless rotor hubs
[AD-A131660] N84-12162

BEARINGS
Unidirectional flexural pivot
[NASA-CASE-GSC-12622-1] N84-12492

BELGIUM
SAR 580: Images for agricultural and forest survey. First results in middle Belgium N84-12595
Interpretability of wetland on SEASAT-A imagery in the polderland of Flanders: A structural approach N84-12597
Remote sensing and topographic maps --- belgium N84-12600
Inventory of Flemish forests using medium-scale Color Infrared (CIR) photography and CIR orthophotoplans as base for a forest management data bank N84-12614

BENDING
Bending of transversally loaded orthotropic rectangular and sector plates N84-12520

BENTONITE
Formation of free hydrogen during radiolysis in a bed of clay
[DE83-017724] N84-12275

BENZENE
Polymers of phosphonylmethyl-2,4- and -2,6-diamino benzenes and the like
[NASA-ARC-11506-1] N84-12313
Development of a continuous monitor for detection of toxic organic compounds
[PB83-234922] N84-12461
Theoretical and experimental studies of shock-compressed benzene and polybutene
[DE83-015884] N84-12816

BETA FACTOR
Initial assessment of the MHD stability of TMX-U
[DE83-016521] N84-12646
A steady-state axisymmetric toroidal system
[IPPJ-643] N84-12910

BIAS
Racial bias and predictive validity in testing for selection
[AD-A131830] N84-12722

BIBLIOGRAPHIES
Aeronautical Engineering: A continuing bibliography with indexes (supplement 166)
[NASA-SP-7037(166)] N84-12027
Bibliography of coefficient of friction literature relating to slip type accidents --- slipping accidents
[PB83-243626] N84-12334
Topically classified bibliography on shapes of falling drops, drops in electric fields and related topics
[AD-A131134] N84-12417
Rising bubbles
[AD-A131572] N84-12418
Pulsed power bibliography. Volume 2: Annotated bibliography
[AD-A131753] N84-12468
Pulsed power bibliography. Volume 1: Indices
[AD-A131752] N84-12469
Nondestructive evaluation publications, 1981
[PB83-239574] N84-12517
Aerospace Medicine and Biology: A continuing bibliography with indexes (supplement 250)
[NASA-SP-7011(250)] N84-12712
Bibliography on atomic processes in hot dense plasmas
[IPPJ-AM-29] N84-12913
NASA patent abstracts bibiliography. Section 1: Abstracts. A continuing bibliography
[NASA-SP-7039(23)] N84-13017
NASA Patent Abstracts Bibliography. Section 2: Indexes. A continuing bibliography (supplement 23)
[NASA-SP-7039(23)] N84-13018

BINARY FLUIDS
The shock wave structure in one-component gas and in binary gas mixture
[ISSN-0208-5658] N84-12407

BINARY STARS
A search for radio pulsars in the Northern sky: Discovery of a pulsar in a unique binary system N84-13040
Observation of winds in cool stars N84-13084

BINARY SYSTEMS (MATERIALS)
Solidification of aluminum and aluminum alloys at high levels of undercooling N84-12286
New developments and oppotunities for NMR in metal-hydrogen systems
[DE83-017696] N84-12664
Muon spin relaxation in ferromagnetic PdMn
[DE83-012659] N84-12979

BIOASSAY
Phytochrome from green plants: Assay, purification, and characterization
[DE83-017447] N84-12710

BIODEGRADATION
Method for treating wastewater using microorganisms and vascular aquatic plants
[NASA-CASE-NSTL-10] N84-12654

BIOLOGICAL EFFECTS
Eruption of permanent dentition in rhesus monkeys exposed to ELF (Extremely low frequency) fields
[AD-A132065] N84-12703
Aerospace Medicine and Biology: A continuing bibliography with indexes (supplement 250)
[NASA-SP-7011(250)] N84-12712

BIOLOGICAL MODELS (MATHEMATICS)
Branching processes in periodically varying environment
[CTH-MATH-1983-12-PREPRINT] N84-12792

BIOMASS ENERGY PRODUCTION
Fluidized bed gasification of biomass to methane
[NASA-CASE-NPO-15903-1] N84-12635

BIOMEDICAL DATA
Uses of synchrotron radiation
[DE83-014431] N84-12720

BIOT METHOD
The treatment of convected vortices in compressible potential flow N84-12121

BIRD-AIRCRAFT COLLISIONS
Alternate T-38 transparency development. Part 4: Parametric studies
[AD-A131904] N84-12159
Flightline thermal environment testing of F-111 transparencies
[AD-A131642] N84-12163

BLADE TIPS
Helicopter rotor wake geometry and its influence in forward flight. Volume 2: Wake geometry charts
[NASA-CR-3727] N84-12091

BLANKETS
Feasibility of a laser or charged-particle-beam fusion-reactor concept with direct electric generation by magnetic-flux compression
[DE83-015735] N84-12482

BLOCKING
Correlation of laboratory-scale fire test methods for seat blocking layer materials with large-scale test results
[AD-A131666] N84-12138

BOEING 707 AIRCRAFT
Vertical drop test of a transport fuselage center section including the wheel wells
[NASA-TM-85706] N84-12531

BOILERS
Assessment of TRAC-PF1 and RELAP5/MOD1 codes with GE large-vessel blowdown test
[DE83-015384] N84-12874

BOLTZMANN TRANSPORT EQUATION
The shock wave structure in one-component gas and in binary gas mixture
[ISSN-0208-5658] N84-12407
Transition flow ion transport via integral Boltzmann equation
[UTIAS-269] N84-12828

BOOSTER ROCKET ENGINES
Test report for MSFC test 83-2. Pressure scaled water impact test of a 12.5 inch diameter model of the Space Shuttle Solid Rocket booster filament wound case and external TVC pod
[NASA-CR-174601] N84-12217

BORN APPROXIMATION
Elastic-wave inverse scattering in non-destructive evaluation
[DE83-017683] N84-12513

BORON
Chemiluminescence and laser induced fluorescence of boron atom reactions
[AD-A131709] N84-12471

BOUNDARY LAYER EQUATIONS
Subsonic/transonic viscous interactions N84-12075

BOUNDARY LAYER FLOW
Transonic empirical configuration design process N84-12079
Unsteady compressible laminar boundary-layer flow within an expansion wave
[AD-A131889] N84-12420
Experimental mixed-convection heat transfer from a large, vertical surface in a horizontal flow
[DE83-016419] N84-12429

BOUNDARY LAYER SEPARATION
Aerodynamics of Vortical Type Flows in Three Dimensions
[AGARD-CP-342] N84-12099
Boundary layer segmentation on sharp highly swept leading edges and its effects on secondary vortices N84-12132

BOUNDARY LAYERS
Dynamic-stall regulation of the Darrieus turbine
[DE83-017994] N84-12097
A gas-flow tracing technique applicable to rotating systems boundary layer on a rotating disk
[DE83-012761] N84-12425
Optical extinction coefficients beneath marine stratus clouds. Comparison of coefficients calculated from observed aerosol spectra with coefficients specified by the Navy aerosol model
[AD-A132011] N84-12685
Boundary layers in cataclysmic variables: The HEAO-1 X-ray constraints
[NASA-TM-85112] N84-13046

BOUNDARY VALUE PROBLEMS
Computational methods for subsonic and transonic aerodynamic design N84-12074
Improved wave drag predictions using modified linear theory
[NASA-CR-174494] N84-12096
Acta Mechanica Sinica (selected articles)
[AD-A131871] N84-12422

Zero-dimensional model of compressible gas flow in networks of pressure vessels: Program TRIC
[DE83-017121] N84-12431
Buckled plate vibrations, large amplitude vibrations and nonlinear flutter of elastic plates using high-order triangular finite elements N84-12523
Adaptive finite element methods for parabolic partial differential equations
[NASA-CR-174490] N84-12727
GRIDPACK: Toward unification of general grid programming
[AD-A131692] N84-12746
Multidimensional explicit difference schemes for hyperbolic conservation laws
[NASA-CR-172254] N84-12778
Boundary-integral simulations of rayleigh-taylor instability in ideal magnetohydrodynamics
[AD-A131667] N84-12920

BOUSSINESQ APPROXIMATION
The AGCE related studies of baroclinic flows in spherical geometry
[NASA-CR-170934] N84-12415

BOW WAVES
Scale lengths in quasi-parallel shocks
[NASA-TM-85109] N84-12663

BRANCHING (MATHEMATICS)
Branching processes in periodically varying environment
[CTH-MATH-1983-12-PREPRINT] N84-12792

BRASSES
Life prediction under stress corrosion conditions below K sub ISCC
[DE83-018074] N84-12307

BREADBOARD MODELS
IPACS electronics: Comments on the original design and current efforts at Langley Research Center N84-12240

BREAKDOWN
Isotope dependence of the breakdown strength of gases
[DE83-017272] N84-12430

BREMSSTRAHLUNG
Generation of monoenergetic positrons
[DE83-015535] N84-12887
Nonlinear force on an unpolarized relativistic test particle to second order in the total field in a nonequilibrium beam-plasma system
[AD-A131631] N84-12919

BRIDGES (STRUCTURES)
Prediction of dynamic effects due to vehicles crossing military bridges
[ISVR-TR-120] N84-12548

BRIGHTNESS
Relative elevation determination from LANDSAT imagery N84-12558

BRITTLENESS
Strain rate effects on ductile/brittle transitions in steels
[DE83-016906] N84-12308

BROKEN SYMMETRY
Research in theoretical physics
[DE83-0166222] N84-13004

BUBBLE CHAMBERS
Operation of the Brookhaven MPS Facility
[DE83-015383] N84-12896

BUBBLE MEMORY DEVICES
A program of research on microfabrication techniques for VLSI magnetic devices
[AD-A131706] N84-12978

BUCKLING
Buckled plate vibrations, large amplitude vibrations and nonlinear flutter of elastic plates using high-order triangular finite elements N84-12523

BUDGETING
Activities report of the aerospace industry in West Germany N84-12139
Activities report of the aerospace industry in West Germany N84-12140

BUMPY TORUSES
Theoretical aspects of throat-launch microwave heating in EBT-S
[DE83-015762] N84-12875
Theoretical studies of fusion physics. Volume 1: Summary
[DE83-010378] N84-12924
Theoretical studies of fusion physics. Volume 2: Appendices
[DE83-010371] N84-12925
Detailed modeling of microwave energy deposition in EBT devices
[DE83-017496] N84-12952
Effect of magnetic bending on the high-frequency stability of the ELMO Bumpy Torus
[DE83-017177] N84-12961

BUNCHING
Subharmonic buncher for the Los Alamos free-electron laser oscillator experiment
[DE83-015220] N84-12474

BURNING RATE
Correlation of laboratory-scale fire test methods for seat blocking layer materials with large-scale test results
[AD-A131666] N84-12138
Combustion modeling of composite solid propellants N84-12285

BURSTS
A study of coherent structures in the near-neutral marine atmospheric boundary layer N84-12658
A model for chorus associated electrostatic bursts
[NASA-CR-174489] N84-12832

BUTENES
Theoretical and experimental studies of shock-compressed benzene and polybutene
[DE83-015884] N84-12816

C

CALCULUS OF VARIATIONS
Variational-moment method for computing magnetohydrodynamic equilibria
[DE83-017477] N84-12957

CALIBRATING
Preliminary data processing plan for the thermal plasma experiment on the HILAT satellite
[AD-A132017] N84-12209
Technique for producing a coherent sum of the data from P78-1, F2, and F4 satellites
[AD-A131965] N84-12210
Determination of the uncertainty of experimental heat-flux calibrations
[AD-A131918] N84-12450
Development of a unique Physical Metrology Laboratory Recall System
[DE83-017415] N84-12767

CALIFORNIA
Compilation of selected faults and lineaments that may be relevant to a study of seismic activity in southern Nevada and part of adjacent California
[DE83-017085] N84-12673

CALORIMETERS
Calorimeter operating system implemented on a Z-80 microcomputer in read only memory
[DE83-016647] N84-12734

CAMERAS
Using an X-ray-sensitive vidicon and remote-control stage mechanism to obtain critical radiographic alignment of small explosive devices
[DE83-012846] N84-12326

CANOPIES
Aircraft transparency testing methodology and evaluation criteria. Part 2: Methodology development for improved durability
[AD-A131928] N84-12157
Aircraft transparency testing methodology and evaluation criteria. Part 1: Test methods and information analysis
[AD-A131927] N84-12158
Flightline thermal environment testing of F-111 transparencies
[AD-A131642] N84-12163

CANOPIES (VEGETATION)
The use of airborne thematic mapper simulation data for the estimation and mapping of Green Leaf Area Index (GLAI) N84-12602

CAPACITANCE
Development of instrumentation for monitoring carbon fiber emission
[PB83-233726] N84-12460

CAPACITORS
The performance of the perfluorocarbon liquid/plastic-film capacitor technology in pulse-power service. A current status report
[DE83-014606] N84-12402

CAPACITY
Ragone characteristics of aqueous mobile batteries and their application in projecting ranges of electric vehicles
[DE83-014701] N84-12642

CAPILLARY WAVES
On the growth of gravity-capillary waves by wind
[KNMI-WR-83-10] N84-12698

CARBIDES
Phonon dispersion of transverse basal-plane modes in alkali-graphite compounds
[DE83-003910] N84-12273

CARBON
Influence of heat-treatment and physicochemical properties on the electrochemical oxidation of carbon blacks in phosphoric acid
[DE83-017744] N84-12276
Creation of ultra-high-pressure shocks by the collision of laser-accelerated disks: Experiment and theory
[DE83-017366] N84-12486

CARBON DIOXIDE
Advanced technologies for the recovery, disposal, and reuse of carbon dioxide for atmospheric control
[DE83-016371] N84-12256
Development of a data base for carbon dioxide releases resulting from conversion of land to agricultural uses
[DE83-015728] N84-12626
Inventory of numeric data for carbon dioxide research
[DE83-017571] N84-12657

CARBON FIBER REINFORCED PLASTICS
An X-ray radiography study of delamination growth in notched carbon/epoxy laminates
[FFA-TN-1983-29] N84-12516
An interactive computer program for analysis of ultrasonic modulus data on anistropic materials
[NPL-DMA(A)68] N84-12526

CARBON FIBERS
Some trends in airship technology developments
[AGARD-R-717] N84-12050
Development of instrumentation for monitoring carbon fiber emission
[PB83-233726] N84-12460

CARGO AIRCRAFT
Simulator study of flight characteristics of a large twin-fuselage cargo transport airplane during approach and landing
[NASA-TP-2183] N84-12190

CARNOT CYCLE
Revised isothermal analysis program for Stirling engines
[DE83-017276] N84-12504

CARTESIAN COORDINATES
Numerical solution of the three-dimensional unsteady Euler equations
[AD-A132034] N84-12783

CASSEGRAIN ANTENNAS
Phase A study for a test satellite for propagation and transmission experiments in the 20/30 GHz frequency band
[BMFT-FB-W-83-009] N84-12355

CASSEGRAIN OPTICS
Study of multi-kilowatt solar arrays for Earth orbit applications
[NASA-CR-170939] N84-12634
HRTS observations of the fine structure and dynamics of the solar chromosphere and transition zone N84-13070

CAST ALLOYS
Single specimen J-integral testing
[DE83-016089] N84-12543

CATALOGS (PUBLICATIONS)
Source header list, supplement 1
[AD-A131800] N84-13024

CATALYSIS
Thermolysis of 4-methyl-4-phenyl malonyl peroxide: A new oxygen dependent chemiluminescent reaction
[AD-A131863] N84-12268
Chemical properties of metallic glasses
[DE83-017353] N84-12322

CATALYSTS
New approach to the generation of metal-bearing, medium-pore, shape-selective zeolites for Fischer-Tropsch catalysis: Spectroscopic studies of zeolites
[DE83-014344] N84-12254
Photoelectrochemical electrodes
[NASA-CASE-NPO-15458-1] N84-12262
Structural characterization of dispersed metal catalysts
[DE83-017145] N84-12305

CAVITATION CORROSION
Grain-boundary cavitation and weld-underbead cracking in DOP-26 iridium alloy
[DE83-015406] N84-12539

CAVITIES
Test report for MSFC test 83-2. Pressure scaled water impact test of a 12.5 inch diameter model of the Space Shuttle Solid Rocket booster filament wound case and external TVC pod
[NASA-CR-174601] N84-12217
Detection of cavities under concrete pavement
[AD-A131851] N84-12331
Steady laminar natural convection in open rectangular cavities N84-12441

CAVITY RESONATORS
Dielectric loss measurement at millimetre wave frequencies using an untuned cavity
[RSRE-3597] N84-12379

CELESTIAL GEODESY
The far infrared sky survey experiment
[AD-A131966] N84-13037

CELL DIVISION
Branching processes in periodically varying environment
[CTH-MATH-1983-12-PREPRINT] N84-12792

CENTRIFUGES
Practical computation of multidimensional thermal flows in a gas centrifuge
[DE83-005697] N84-12426
CERAMIC COATINGS
Development of strain tolerant thermal barrier coating systems, tasks 1 - 3
[NASA-CR-168251] N84-12312
CERAMICS
Investigation of inhomogeneity in ceramic reactor materials using laser-localized emission spectroscopy
[JUEL-1834] N84-12323
Elastic-wave inverse scattering in non-destructive evaluation
[DE83-017863] N84-12513
CERIUM
The relative abundances of Sn, Te, Xe, Ba and Ce
[NASA-CR-174599] N84-13064
CERIUM OXIDES
Defect interactions at high concentrations in solid oxide electrolytes
[DE83-016849] N84-12992
CHANGE DETECTION
Actual state and recent evolution of the French coast observed by remote sensing using LANDSAT recordings N84-12606
CHANNEL FLOW
Calculation of unsteady flow in tubes of combustion engines with special regard to multiple branching
[REPT-82.8] N84-12410
CHANNELS (DATA TRANSMISSION)
The relations between the numerical control of the engine and other aircraft functions N84-12062
Effects of integrated maintenance on the definitions of onboard equipments — Mirage 2000 aircraft N84-12068
CHAPMAN-ENSKOG THEORY
The collapse of the local, Spitzer-Haerm formulation and a global-local generalization for heat flow in an inhomogeneous, fully ionized plasma N84-13080
CHARGE CARRIERS
Large-area mercuric iodide photodectors
[DE83-013035] N84-12898
CHARGE COUPLED DEVICES
Predevelopment of IR-CCD components
[BMFT-FB-T-83-133] N84-13001
Applications of analog Change Coupled Devices (CCD's)
[BMFT-FB-T-83-141] N84-13002
CHARGE DISTRIBUTION
Survey of He(+)/He(2+) abundance ratios in energetic particle events N84-13117
CHARGE EFFICIENCY
Effect of antimony on lead-acid battery negative electrode
[DE83-014680] N84-12404
CHARGE EXCHANGE
Low energy nuclear physics and accelerator development
[DE83-013384] N84-12877
Cross sections for charge transfers of highly ionized ions in hydrogen atoms
[IPPJ-AM-30] N84-12912
CHARGE TRANSFER
Novel interactions of the charge-balancing cations with framework defects and trapped hydrogen atoms in holmium-exchanged Y zeolites
[DE83-014204] N84-12839
Large-area mercuric iodide photodectors
[DE83-013035] N84-12898
CHARGED PARTICLES
Feasibility of a laser or charged-particle-beam fusion-reactor concept with direct electric generation by magnetic-flux compression
[DE83-015735] N84-12482
Nonlinear force on an unpolarized relativistic test particle to second order in the total field in a nonequilibrium beam-plasma system
[AD-A131631] N84-12919
CHECKOUT
An introduction to the AXIS test box
[RSRE-3583] N84-12729
CHEMICAL ANALYSIS
Multi-detector gel permeation chromatography and its application to the analysis of industrial samples
[MQAD-808] N84-12283
Process, product, and waste-stream monitoring with fiber optics
[DE83-01102] N84-12899
CHEMICAL ATTACK
Novel composite membranes
[PB83-243170] N84-12284
Chemical erosion of first-wall materials by atomic hydrogen at high temperatures
[DE83-017161] N84-12962
CHEMICAL BONDS
Measurements, in vivo, of parameters of the dopamine system
[DE83-017964] N84-12709
Solitons and polarons in quasi-one dimensional conducting polymers and related materials
[DE83-015233] N84-12853
CHEMICAL COMPOSITION
Multi-detector gel permeation chromatography and its application to the analysis of industrial samples
[MQAD-808] N84-12283
CHEMICAL ENERGY
New materials for organic photovoltaic cells
[DE83-016845] N84-12645
CHEMICAL LASERS
Ukrainian Physics Journal (selected articles)
[AD-A131087] N84-12814
The possibility of amplifying infrared radiation by high-pressure reacting gas
[AD-A131086] N84-12890
CHEMICAL PROPERTIES
Chemical properties of metallic glasses
[DE83-017353] N84-12322
CHEMICAL REACTIONS
OI 630.0 nm optical measurements of neutral winds, temperatures and airglow enhancements during the BIME program
[AD-A131695] N84-12671
CHEMILUMINESCENCE
Thermolysis of 4-methyl-4-phenyl malonyl peroxide: A new oxygen dependent chemiluminescent reaction
[AD-A131863] N84-12268
Chemiluminescence and laser induced fluorescence of boron atom reactions
[AD-A131709] N84-12471
CHINA
From launching carrier rockets towards the Pacific on the accomplishments and problems of electronic technologies in our country
[AD-A131088] N84-12380
Major water conservation and reclamation projects in the Jianghan Plain and surroundings, Hubei Province, China — Landsat imagery N84-12593
CHLORINE
Novel composite membranes
[PB83-243170] N84-12284
CHLOROPHYLLS
Marine remote sensing activities of the Joint Research Center, Ispra, Italy N84-12586
Two different aspects of phytoplankton bloom seen by satellite (CZCS) in the western English Channel — coastal zone color scanner (CZCS) N84-12604
Introductory studies of natural contamination and manmade pollution in Danish waters N84-12608
Normalization of water-leaving radiance obtained from the Coastal Zone Colour Scanner (CZCS) data N84-12610
CHOLINESTERASE
Combined effects of ionizing radiation and anticholinesterase exposure on rodent motor performance
[AD-A131847] N84-12707
CHROMATOGRAPHY
Phytochrome from green plants: Assay, purification, and characterization
[DE83-017447] N84-12710
CHROMIUM
Study of chromium-free and chromium-reduced steels
[DE83-016717] N84-12294
CHROMIUM ALLOYS
Corrosion behavior of Fe-Cr-Ni-Zr alloys in aggressive environments at high temperatures
[DE83-014735] N84-12297
CHROMIUM STEELS
Miniature charpy-impact test results for the irradiated ferritic alloys HT-9 and modified 9Cr-1Mo
[DE83-016935] N84-12300
CHROMOSPHERE
HRTS observations of the fine structure and dynamics of the solar chromosphere and transition zone N84-13070
CIRCADIAN RHYTHMS
Biological clocks and shift work scheduling
[GPO-21-747] N84-12713
CIRCULAR CYLINDERS
Stability of a pair of stationary vortices in the leeward side of a cylinder in a potential flowfield
[AD-A131917] N84-12095
CIRCULAR PLATES
Bending of transversally loaded orthotropic rectangular and sector plates N84-12520
CIRCULATION
Microprocessor-based control system for flowing-electrolyte zinc-bromine battery systems
[DE83-012506] N84-12403
CITIES
The synthesized climatic function map N84-12617
Arizona State science, engineering and technology process
[PB83-237107] N84-13016
CIVIL AVIATION
Develop a normative or descriptive model of the international/domestic civil aviation industry, volume 3
[AD-A131878] N84-12051
Develop a normative or descriptive model of the international/domestic civil aviation industry, volume 2
[AD-A131877] N84-12052
Develop a normative or descriptive model of the international/domestic civil aviation industry. Volume 1: Executive summary
[AD-A131876] N84-12053
Domestic scheduled air transport for the year 2000. Financial and capacity related effects of supply alternatives, considering, also, the cooperation with high speed rail transport services — West Germany
[DFVLR-FB-83-03] N84-12141
Information resources management plan
[AD-A131964] N84-13023
CLASSIFICATIONS
Autoregressive models for use in scene segmentation N84-12561
Spline classification methods N84-12564
Mesocyclone detection and classification algorithm
[AD-A131826] N84-12691
CLIMATE
Review of potential satellite techniques for mesoscale mapping of insolation
[DE83-011998] N84-12622
Inventory of numeric data for carbon dioxide research
[DE83-017571] N84-12657
Climate of Phoenix, Arizona (revised)
[PB83-246801] N84-12699
CLIMATOLOGY
Snowy Range Observatory: Climatological and streamflow data report 1982
[PB83-243147] N84-12633
CLOUD COVER
Review of potential satellite techniques for mesoscale mapping of insolation
[DE83-011998] N84-12622
Model for illuminance on horizontal and vertical surfaces
[DE83-011973] N84-13127
Graphical method for determining interflected daylight in clear climates
[DE83-011989] N84-13128
CLOUD HEIGHT INDICATORS
Evaluation of automated imagery analysis algorithms for use in the three-dimensional nephanalysis model at AFGWC (Air Force Global Weather Central)
[AD-A131986] N84-12686
CLOUD PHYSICS
Field and laboratory studies of ice nucleation in winter orographic clouds N84-12678
Radar meteorology in cloud physics and radio wave propagation research
[ESA-TT-808] N84-12695
CLOUDS
Evaluation of automated imagery analysis algorithms for use in the three-dimensional nephanalysis model at AFGWC (Air Force Global Weather Central)
[AD-A131986] N84-12686
CLUMPS
Dynamical evolution of substucture in molecular clouds N84-13043
CLUTTER
Technique for producing a coherent sum of the data from P78-1, F2, and F4 satellites
[AD-A131965] N84-12210
Effect of frequency-averaging on estimation of clutter statistics used in setting CFAR detection thresholds
[AD-A131947] N84-12343
COAL
Estimation of uncertainty in coal resources
[DE83-902538] N84-12620
Alaska's mineral resources
[DE83-016599] N84-12623
COAL DERIVED LIQUIDS
Preparation of a design study for the construction of a 2 million tons/annum commercial scale hydrogenation plant
[BMFT-FB-T-83-135] N84-12652
COAL GASIFICATION
Preparation of a design study for the construction of a 2 million tons/annum commercial scale hydrogenation plant
[BMFT-FB-T-83-135] N84-12652

COAL LIQUEFACTION
Combustion of EDS mid-distillate and refined shale-oil residual fuel in a gas turbine with large single-combustion chamber
[DE83-017700] N84-12281
COAL UTILIZATION
Development of materials for open-cycle MHD
[DE83-016334] N84-12926
COASTAL CURRENTS
Application of remote sensing for studies, mapping and forecasting of eddies on the Norwegian continental shelf N84-12605
COASTAL ECOLOGY
Contribution of satellite remote sensing to knowledge of the littoral from the mouth of the Loire to that of the Gironde (France) N84-12584
Application of high resolution satellite data to coastal zones: SPOT simulations during ecological survey of the Britanny coast N84-12591
COASTAL WATER
Contribution of satellite remote sensing to knowledge of the littoral from the mouth of the Loire to that of the Gironde (France) N84-12584
Marine remote sensing activities of the Joint Research Center, Ispra, Italy N84-12586
SPOT potential applications: An overview of the results of the simulation campaigns N84-12587
Two different aspects of phytoplankton bloom seen by satellite (CZCS) in the western English Channel --- coastal zone color scanner (CZCS) N84-12604
Actual state and recent evolution of the French coast observed by remote sensing using LANDSAT recordings N84-12606
Remote sensing analysis of oil pollution in Augusta Bay, Sicily N84-12616
Adjustment in the oceans: The long-period tides and coastal upwelling N84-12702
COASTAL ZONE COLOR SCANNER
Normalization of water-leaving radiance obtained from the Coastal Zone Colour Scanner (CZCS) data N84-12610
COASTS
Application of high resolution satellite data to coastal zones: SPOT simulations during ecological survey of the Britanny coast N84-12591
Actual state and recent evolution of the French coast observed by remote sensing using LANDSAT recordings N84-12606
COATING
Development of strain tolerant thermal barrier coating systems, tasks 1 - 3
[NASA-CR-168251] N84-12312
COATINGS
Novel techniques for enhanced reflectivity infrared mirrors
[AD-A131924] N84-12894
Sputtered C-axis inclined piezoelectric films and shear-wave resonators
[DE83-017253] N84-12997
COAXIAL CABLES
Prototype fiber optic system to remote TRACALS radar
[AD-A132073] N84-12341
COBOL
Northern Telecom, Incorporated NTI-585 ACOBOL/3 release 3 (COBOL technical report)
[PB83-241521] N84-12758
Northern Telecom Incorporated NTI-585 XCOBOL, release 3
[PB83-241539] N84-12759
Northern Telecom, Incorporated NTI-585 XCOBOL, release 3 (COBOL technical report)
[PB83-241547] N84-12760
Digital Equipment Corporation VAX 11/750, VAL-11 COBOL version 2.2
[PB83-241588] N84-12761
Digital Equipment Corporation, PDP-11/44 COBOL-81 version 2.0
[PB83-247734] N84-12764
Digital Equipment Corporation COBOL-81 version 2.0 (COBOL technical report)
[PB83-247742] N84-12765
Perkin-Elmer, Perkin-Elmer 3230 COBOL R07 (pre-release)
[PB83-238600] N84-12766
COCKPIT SIMULATORS
A comparison of manual and vocal response modes for the control of aircraft subsystems
[AD-A132048] N84-12152
COCKPITS
Study to determine the IFR operational profile and problems to the general aviation pilot N84-12032
COEFFICIENT OF FRICTION
Bibliography of coefficient of friction literature relating to slip type accidents --- slipping accidents
[PB83-243626] N84-12334
COGNITION
Effect of noise in the three-parameter logistic model
[AD-A131867] N84-12721
Artificial intelligence: Cognition as computation
[AD-A131804] N84-12770
Representations for reasoning about change
[AD-A131649] N84-12772
COHERENT RADIATION
Studies of collisional and nonlinear radiative processes for development of coherent UV and XUV sources
[AD-A131837] N84-12467
COHERENT SCATTERING
Observations of the upper troposphere and lower stratosphere using the urbana coherent-scatter radar
[NASA-CR-174594] N84-12664
COLD WORKING
Cold sintering: A new powder consolidation process
[AD-A131687] N84-12292
Evaluation of several high-strength copper sheet alloys
[DE83-015612] N84-12298
COLLAPSE
Test report for MSFC test 83-2. Pressure scaled water impact test of a 12.5 inch diameter model of the Space Shuttle Solid Rocket booster filament wound case and external TVC pod
[NASA-CR-174601] N84-12217
COLLINEARITY
Estimation of the ridge constant: An approach based on the condition index
[DE83-017955] N84-12805
COLLISION AVOIDANCE
Airport capacity alternatives N84-12149
COLLISIONLESS PLASMAS
Scale lengths in quasi-parallel shocks
[NASA-TM-85109] N84-12663
COLLISIONS
Studies of collisional and nonlinear radiative processes for development of coherent UV and XUV sources
[AD-A131837] N84-12467
COLOR INFRARED PHOTOGRAPHY
An operational remote sensing methodology for the detection, inventory and environmental monitoring of waste disposal sites N84-12601
Inventory of Flemish forests using medium-scale Color Infrared (CIR) photography and CIR orthophotoplans as base for a forest management data bank N84-12614
COMBINATORIAL ANALYSIS
Research in net management techniques for tactical data networks
[AD-A131674] N84-12352
COMBUSTION
Combustion jet ignition N84-12188
Soot formation from polycyclic aromatics
[DE83-009750] N84-12271
COMBUSTION CHAMBERS
Analytical design of a liquid hydrogen fueled turbofan-ramjet engine for flight Mach numbers zero to five N84-12187
Executive summary, aerothermal modeling program, phase 1
[NASA-CR-174602] N84-12263
Aerothermal modeling program, phase 1
[NASA-CR-168243-VOL-1] N84-12264
Aerothermal modeling program, phase 1
[NASA-CR-168243-VOL-2] N84-12265
Erosive particle kinematics in the turbulent combustion boundary layer contacting a solid wall
[DE83-010594] N84-12272
Optimum engine for methanol utilization
[PB83-239459] N84-12507
COMBUSTION CONTROL
Controlled combustion engine evaluation
[DE83-011245] N84-12499
COMBUSTION PHYSICS
Materials processing in space program tasks-supplement
[NASA-TM-82548] N84-12196
Laser spectroscopy of propellant-like flames
[AD-A132042] N84-12267
COMET HEADS
The chemical evolution of the coma of comet P/Stephan-Oterma N84-13055
COMET TAILS
Interaction of the plasma tail of comet Bradfield 1979L on 1980 February 6 with a possibly flare-generated solar-wind disturbance N84-13126
COMETARY ATMOSPHERES
The chemical evolution of the coma of comet P/Stephan-Oterma N84-13055
COMETS
The chemical evolution of the coma of comet P/Stephan-Oterma N84-13055
Interaction of the plasma tail of comet Bradfield 1979L on 1980 February 6 with a possibly flare-generated solar-wind disturbance N84-13126
COMFORT
Ride quality meter
[NASA-CASE-LAR-12882-1] N84-12445
COMMERCIAL AIRCRAFT
APU in commercial airline operation N84-12173
COMMUNICATION CABLES
Economic study of long distance optical fibre links
[FUB-38-1982] N84-12908
COMMUNICATION NETWORKS
Trends in the development of teleinformatics
[AD-A131067] N84-12338
Telecommunications (selected articles)
[AD-A131872] N84-12346
Network design tool for EHF satellite communications networks
[AD-A131812] N84-12349
Research in net management techniques for tactical data networks
[AD-A131674] N84-12352
COMMUNICATION SATELLITES
Satellite communication, part 1
[INPE-2893-PRE/417] N84-12337
Network design tool for EHF satellite communications networks
[AD-A131812] N84-12349
COMPARISON
Why didn't Box-Jenkins win (again)?
[DE83-014043] N84-12802
COMPILERS
Northern Telecom, Incorporated NTI-585 ACOBOL/3 release 3 (COBOL technical report)
[PB83-241521] N84-12758
Northern Telecom Incorporated NTI-585 XCOBOL, release 3
[PB83-241539] N84-12759
Northern Telecom, Incorporated NTI-585 XCOBOL, release 3 (COBOL technical report)
[PB83-241547] N84-12760
Digital Equipment Corporation VAX 11/750, VAL-11 COBOL version 2.2
[PB83-241588] N84-12761
NCR Corporation NCR 9300 ITX-BASIC, release 1.1
[PB83-243410] N84-12762
Computer Sciences Corporation UNIVAC 1100/80 CSTS FORTRAN, release FTN148
[PB83-243428] N84-12763
Digital Equipment Corporation, PDP-11/44 COBOL-81 version 2.0
[PB83-247734] N84-12764
Digital Equipment Corporation COBOL-81 version 2.0 (COBOL technical report)
[PB83-247742] N84-12765
Perkin-Elmer, Perkin-Elmer 3230 COBOL R07 (pre-release)
[PB83-238600] N84-12766
COMPOSITE MATERIALS
Some trends in airship technology developments
[AGARD-R-717] N84-12050
Enthalpy - improved dielectric insulation for superconducting wires
[AD-A131857] N84-12316
New developments in composite-flywheel containment
[DE83-012583] N84-12497
COMPOSITE PROPELLANTS
Combustion modeling of composite solid propellants N84-12285
COMPRESSIBILITY EFFECTS
Laser velocimetry study of compressibility effects on the flow field of a delta wing N84-12108
COMPRESSIBLE BOUNDARY LAYER
Unsteady compressible laminar boundary-layer flow within an expansion wave
[AD-A131889] N84-12420
COMPRESSIBLE FLOW
Unsteady compressible laminar boundary-layer flow within an expansion wave
[AD-A131889] N84-12420
COMPRESSION LOADS
The effect of moisture on the physical and durability properties of methyl methacrylate polymer concrete
[DE83-016733] N84-12541
Theoretical and experimental studies of shock-compressed benzene and polybutene
[DE83-015884] N84-12816
COMPRESSORS
Satellite refrigerator compressors with the oil and moisture removal systems
[DE83-016079] N84-12502
COMPUTATION
Computational vortex flow aerodynamics N84-12117
Computation of three-dimensional unsteady flow in rigid and deformable curved tubes N84-12440
Design, development and use of the finite element machine
[NASA-CR-172250] N84-12777

Applied mathematical sciences research at Argonne [DE83-3014268] N84-12788

COMPUTATIONAL FLUID DYNAMICS

Transonic configuration design (fighter) N84-12082

Simulation of turbulent flows with a point vortex method N84-12119

Numerical solutions of the Euler equations simulating vortex flows around wings N84-12120

The treatment of convected vortices in compressible potential flow N84-12121

A contribution to the problem of vortex breakdown N84-12125

Aspects of second- and third-order panel methods demonstrated for the two-dimensional flat plate problem [NLR-TR-81074-U] N84-12433

Results of a new version of the LTRAN2-NLR (LTRANV) for unsteady viscous transonic flow computations [NLR-TR-81078-U] N84-12434

Turbulence modelling: A state-of-the-art review [CFD/83/3] N84-12435

A revised two-equation model of turbulence [CFD/83/5] N84-12436

Numerical solution of the three-dimensional unsteady Euler equations [AD-A132034] N84-12783

New conformal solution theory [PB83-249441] N84-13008

COMPUTER AIDED DESIGN

Computer system design environment software development plan [AD-A131651] N84-12747

Robotics: An introduction to today's robot and future trends [AD-A132070] N84-12768

Computational tool for the design of ultrasonic systems [DE83-016092] N84-12824

COMPUTER AIDED MAPPING

Remote sensing and topographic maps --- belgium N84-12600

Mapping land use in Catalonia (Spain) --- using LANDSAT imagery N84-12613

COMPUTER DESIGN

Application of computational procedures in aerodynamic design N84-12078

Ada-Europe guidelines for the portability of Ada programs, second edition [NPL-DITC-27/83] N84-12739

COMPUTER GRAPHICS

Multivariate density estimation and remote sensing N84-12560

Measurements, in vivo, of parameters of the dopamine system [DE83-017964] N84-12709

DRAMIN: Transferring data from the Applicon graphic system to A DRAM input file user guide [DE83-018235] N84-12753

Assembly language graphics library (EGR1.LB) with Fortran interfacing [PB83-239624] N84-12757

Galilean satellite geomorphology [NASA-CR-174574] N84-13057

COMPUTER NETWORKS

A fault-tolerant distributed computer network design and analysis for an integrated flight control system N84-12189

Trends in the development of teleinformatics [AD-A131067] N84-12338

Alternative transmission media for third-generation interface standards [PB83-238345] N84-12365

Procedures for the transfer of data files between the BRL CYBER computer system and the IBD Hewlett-Packard minicomputer network [AD-A132063] N84-12731

Linked state machines [DE83-4000123] N84-12736

COMPUTER PROGRAMMING

Ada-Europe guidelines for the portability of Ada programs, second edition [NPL-DITC-27/83] N84-12739

Processing elements [AD-A131068] N84-12743

GRIDPACK: Toward unification of general grid programming [AD-A131692] N84-12746

Prerequisites for deriving formal specifications from natural language requirements [AD-A131722] N84-12771

Applied mathematical sciences research at Argonne [DE83-3014268] N84-12788

Why didn't Box-Jenkins win (again)? [DE83-014043] N84-12802

COMPUTER PROGRAMS

Flight test validation of a design procedure for digital autopilots N84-12036

Application of computational procedures in aerodynamic design N84-12078

A study of wing-body aerodynamic interference of a light twin aircraft utilizing a panel method potential flow program N84-12134

A generalized computer code for developing dynamic gas turbine engine models (DIGTEM) [NASA-TM-83508] N84-12166

Control of flexible spacecraft by optimal model following N84-12222

Use of superposition in calculating cooling requirements for circuit cards containing arrays of electronic components [DE83-016091] N84-12428

Design and implementation of a preprocessing system for a sodium lidar [NASA-CR-174593] N84-12462

Evaluation of automated imagery analysis algorithms for use in the three-dimensional nephanalysis model at AFGWC (Air Force Global Weather Central) [AD-A131986] N84-12686

PLT: A multipurpose plotting package [DE83-018261] N84-12735

Computer system design environment software development plan [AD-A131651] N84-12747

Environments and search paths for the software tools [DE83-016607] N84-12749

Perkin-Elmer, Perkin-Elmer 3230 COBOL R07 (pre-release) [PB83-238600] N84-12766

Prerequisites for deriving formal specifications from natural language requirements [AD-A131722] N84-12771

Numerical solution of the three-dimensional unsteady Euler equations [AD-A132034] N84-12783

Dynasty 2: A nonlinear implicit code for relativistic electron beam tracking studies [AD-A131592] N84-12829

A 2-D skin-current toroidal-MHD-equilibrium code [DE83-016916] N84-12929

The computerization of material safety data sheet information [AD-A131992] N84-13021

Information retrieval research support [AD-A131990] N84-13022

Galilean satellite geomorphology [NASA-CR-174574] N84-13057

COMPUTER SYSTEMS DESIGN

An introduction to the AXIS test box [RSRE-3583] N84-12729

Linked state machines [DE83-4000123] N84-12736

Design, development and use of the finite element machine [NASA-CR-172250] N84-12777

COMPUTER SYSTEMS PERFORMANCE

An introduction to the AXIS test box [RSRE-3583] N84-12729

COMPUTER SYSTEMS PROGRAMS

Results of a new version of the LTRAN2-NLR (LTRANV) for unsteady viscous transonic flow computations [NLR-TR-81078-U] N84-12434

Software voting in asynchronous NMR (N-Modular Redundancy) computer structures [NASA-CR-174488] N84-12732

Ada-Europe guidelines for the portability of Ada programs, second edition [NPL-DITC-27/83] N84-12739

The AXIS test box software report [RSRE-3585] N84-12741

Monte Carlo computer simulation program (MCHP) supporting a covariance analysis using the STANHP program [DFVLR-MITT-83-06] N84-12756

COMPUTER TECHNIQUES

Technology and the future evolution of the ATC system N84-12148

Control of multiaxis vibration systems N84-12203

Numerical modeling techniques for antennas N84-12373

Structure and vibrational spectra of a model of a-Si:H with periodic boundary conditions [DE83-015245] N84-12390

Zero-dimensional model of compressible gas flow in networks of pressure vessels: Program TRIC [DE83-017121] N84-12431

Revised isothermal analysis program for Stirling engines [DE83-017276] N84-12504

Proceedings of the NASA Symposium on Mathematical Pattern Recognition and Image Analysis [E83-10032] N84-12557

Effect of noise in the three-parameter logistic model [AD-A131867] N84-12721

Hardware and software configuration of the Doublet 3 diagnostic-data-acquisition computer system [DE83-013427] N84-12733

Using structural and functional information in diagnostic design [AD-A131859] N84-12769

Representations for reasoning about change [AD-A131649] N84-12772

On the performance of two-stage group screening experiments [AD-A131970] N84-12807

Experiments on the nuclear interactions of pions [DE83-016285] N84-12844

Computational synergetics and innovation in wave, vortex, and plasma cloud dynamics [DE83-015252] N84-12928

COMPUTERIZED SIMULATION

General aviation single pilot IFR autopilot study N84-12035

Combustion jet ignition N84-12188

Simulation of electro-servo-hydraulic actuator for high quality testing --- of spacecraft N84-12206

Simulation of mechanical cross coupling of multiaxes vibration facilities N84-12207

Performance of add-on-type heat pump water heaters using two different test methods [PB83-222703] N84-12332

Aeroelastic analysis for propellers - mathematical formulations and program user's manual [NASA-CR-3729] N84-12530

Prediction of dynamic effects due to vehicles crossing military bridges [ISVR-TR-120] N84-12548

A numerical study on the evolution of tornadoes N84-12679

The use of a formal simulator to verify a simple real time control program [AD-A131732] N84-12745

High-level control programs at NSLS [DE83-010935] N84-12754

Monte Carlo computer simulation program (MCHP) supporting a covariance analysis using the STANHP program [DFVLR-MITT-83-06] N84-12756

On the performance of two-stage group screening experiments [AD-A131970] N84-12807

Hydrodynamic simulations of a combined hydrogen, helium thermonuclear runaway on a 10 km neutron star [DE83-012658] N84-13047

Simulations of galaxy mergers N84-13054

COMPUTERS

Hardware and software configuration of the Doublet 3 diagnostic-data-acquisition computer system [DE83-013427] N84-12733

Development of a unique Physical Metrology Laboratory Recall System [DE83-017415] N84-12767

CONCENTRATION (COMPOSITION)

Process, product, and waste-stream monitoring with fiber optics [DE83-01102] N84-12899

CONCENTRATORS

Fundamentals and techniques of nonimaging optics, volume 2 [DE83-015447] N84-12902

CONCRETE STRUCTURES

Analytical response of concrete structures subjected to high temperatures [DE83-009625] N84-12538

CONCRETES

Rapid runway repair program subtask 1.07 - rapid concrete cutting [AD-A131771] N84-12195

Detection of cavities under concrete pavement [AD-A131851] N84-12331

Non-destructive testing of non-metallic materials using microwaves [DRIC-T-6974] N84-12508

Analytical response of concrete structures subjected to high temperatures [DE83-009625] N84-12538

The effect of moisture on the physical and durability properties of methyl methacrylate polymer concrete [DE83-016733] N84-12541

CONDUCTIVE HEAT TRANSFER

Thermal conductance measurements of pressed OFHC copper contacts at liquid helium temperatures [NASA-TM-85861] N84-12809

CONES

On the generation of vortical flow at hypersonic speeds over elliptical cones N84-12114

CONFERENCES

Controls, Displays, and Information Transfer for General Aviation IFR Operations [NASA-CP-2279] N84-12029

Aerodynamics of Vortical Type Flows in Three Dimensions
[AGARD-CP-342] N84-12099
Auxiliary Power Systems
[AGARD-CP-352] N84-12168
Spacecraft Vibration Testing Using Multi-Axis Hydraulic Vibration Systems --- conferences
[ESA-SP-197] N84-12197
Integrated Flywheel Technology, 1983
[NASA-CP-2290] N84-12228
International Telecommunication Standards: Issues and Implications for the '80's
[PB83-241471] N84-12366
The Performance of Antennas in Their Operational Environment
[AGARD-LS-131] N84-12367
Proceedings of the 16th LAMPF Users-Group Meeting
[DE83-013215] N84-12488
Proceedings of the NASA Symposium on Mathematical Pattern Recognition and Image Analysis
[E83-10032] N84-12557
Remote Sensing Applications for Environmental Studies --- conferences
[ESA-SP-188] N84-12579
Fourth International Conference on Photochemical Conversion and Storage of Solar Energy
[DE83-014760] N84-12638
Proceedings of 1st International Workshop on Atmospheric Icing of Structures
[AD-A131869] N84-12690
Physics at very high energies
[DE83-012854] N84-12878
PATRAM '83: 7th International Symposium on Packaging and Transportation of Radioactive Materials, summaries
[DE83-012390] N84-12881
Proceedings of the Workshop on Ion Mixing and Surface Layer Alloying
[DE83-015354] N84-12994
NBS (National Bureau of Standards) Workshop: Environmental Control for Archival Records Storage
[PB83-242230] N84-13026
Workshop on Pristine Highlands Rocks and the early History of the Moon
[NASA-CR-174584] N84-13059
Workshop on Pristine Highlands Rocks and the Early History of the Moon
[NASA-CR-174600] N84-13060
Conference on Planetary Volatiles
[NASA-CR-174583] N84-13061
Solar Wind Five
[NASA-CP-2280] N84-13067

CONFIDENCE
Estimation of uncertainty in coal resources
[DE83-902538] N84-12620

CONFIDENCE LIMITS
Improving NDE (Non-destructive evaluation) capability through multiple inspection with application to gas turbine engine disks
[AD-A131762] N84-12509

CONFIGURATION INTERACTION
Applications of molecular quantum mechanics to problems in chemistry
[DE83-015943] N84-13003

CONGRESSIONAL REPORTS
US weather satellites and services
[GPO-25-753] N84-12208
Biological clocks and shift work scheduling
[GPO-21-747] N84-12713
National Aeronautics and Space Act of 1958, as amended and related legislation
[GPO-24-491] N84-13032

CONICAL BODIES
Theoretical modelling of three-dimensional vortex flows in aerodynamics N84-12116

CONNECTORS
Hermetically sealed microminiature multisocket connector
[DE83-017484] N84-12503
Ultra low loss optical fiber cable assemblies, volume 2
[AD-A132008] N84-12891
Ultra low loss optical fiber cable assemblies, volume 1
[AD-A132007] N84-12892

CONSERVATION EQUATIONS
Multidimensional explicit difference schemes for hyperbolic conservation laws
[NASA-CR-172254] N84-12778

CONSERVATION LAWS
Multidimensional explicit difference schemes for hyperbolic conservation laws
[NASA-CR-172254] N84-12778

CONSISTENCY
Constant-output atomizer --- Inhalation therapy and aerosol research
[NASA-CASE-MFS-25631-1] N84-12406

CONSTRAINTS
Small auxiliary power unit design constraints N84-12172
Constraints on the scale of toroidal-fusion experiments with application to the design of a helical-axis stellarator
[DE83-016812] N84-12950

CONSTRUCTION
Ground coupled heat-pump-system experimental results
[DE83-014011] N84-12427
Development of a continuous monitor for detection of toxic organic compounds
[PB83-234922] N84-12461
Initial operation of the compressed air experiment at Pittsfield, Illinois
[DE83-016930] N84-12643

CONSUMERS
Search among queues
[AD-A131639] N84-12773

CONTAINERLESS MELTS
Materials processing in space program tasks-supplement
[NASA-TM-82548] N84-12196
Containerless electromagnetic levitation melting of Cu-Fe and Ag-Ni alloys
[NASA-TM-82553] N84-12288

CONTAINMENT
New developments in composite-flywheel containment
[DE83-012583] N84-12497

CONTAMINANTS
Shuttle measured contaminant environment and modeling for payloads. Preliminary assessment of the space telescope environment in the shuttle bay
[NASA-TM-85111] N84-12216
Vehicle-emission characteristics using mechanically emulsified alcohol/diesel fuels
[DE83-016012] N84-12656

CONTINENTAL SHELVES
Application of remote sensing for studies, mapping and forecasting of eddies on the Norwegian continental shelf N84-12605

CONTINUOUS WAVE LASERS
Selective laser ionization for mass-spectral isotopic analysis
[DE83-017303] N84-12483

CONTINUOUS WAVE RADAR
Pulse signals in heterodyne and homodyne detection
[ESA-TT-809] N84-12357

CONTROL
Implementing microprocessor technology in aircraft electrical power generating system control N84-12185

CONTROL CONFIGURED VEHICLES
A nonlinear control law for piloting aircraft in the air-to-ground attack phase N84-12071

CONTROL THEORY
Controls, Displays, and Information Transfer for General Aviation IFR Operations
[NASA-CP-2279] N84-12029
Analysis of general aviation single-pilot IFR incident data obtained from the NASA Aviation Safety Reporting System N84-12033
Control of flexible spacecraft by optimal model following N84-12222
IPACS attitude control technology considerations N84-12238
Power system considerations and test activities N84-12244
Nonlinear dynamics and control of a vibrating rectangular plate
[NASA-CR-172215] N84-12528

CONTROLLED FUSION
Recent results in the Los Alamos compact torus program
[DE83-014147] N84-12930
Constraints on the scale of toroidal-fusion experiments with application to the design of a helical-axis stellarator
[DE83-016812] N84-12950

CONVECTION
Convection in horizontal porous media with different end temperatures N84-12438
Numerical simulation of convective scaling N84-12660
A subsynoptic environment associated with two inter-mountain severe thunderstorm events
[DE83-014498] N84-12694
Method and apparatus for minimizing convection during crystal growth from solution
[NASA-CASE-NPO-15811-1] N84-12968

CONVECTION CURRENTS
A case study of gravity wave-convective storm interactions N84-12659

CONVECTIVE FLOW
Steady laminar natural convection in open rectangular cavities N84-12441

CONVECTIVE HEAT TRANSFER
Experimental mixed-convection heat transfer from a large, vertical surface in a horizontal flow
[DE83-016419] N84-12429
Direct coronal heating from dissipation of magnetic field N84-13069

CONVOLUTION INTEGRALS
Reduction of structural complexity in evaluating convolutions by polynomial transforms
[FUB-59-1981] N84-12794

COOLANTS
Assessment of TRAC-PF1 and RELAP5/MOD1 codes with GE large-vessel blowdown test
[DE83-015384] N84-12874
Superconductor stability, 1983: A review
[DE83-015506] N84-12990

COOLING
Stress production and relief in the gold/silicon eutectic die-attach process
[DE83-015230] N84-12400
Use of superposition in calculating cooling requirements for circuit cards containing arrays of electronic components
[DE83-016091] N84-12428

COOLING SYSTEMS
Deposit formation and heat transfer in hydrocarbon rocket fuels
[NASA-CR-168277] N84-12225
Solidification of aluminum and aluminum alloys at high levels of undercooling N84-12286
A laboratory comparison of portable cooling systems for workers exposed to two levels of heat stress
[AD-A131848] N84-12423

COORDINATES
Vortex flow simulations past wings using the Euler-equations N84-12118
The effect of coordinate system rotation on spherical harmonic expansions: A numerical method
[AD-A131974] N84-12785

COPLANARITY
Multiple spacecraft observations of interplanetary shocks: Characteristics of the upstream ULF turbulence N84-13097

COPOLYMERIZATION
Radiolysis of resist polymers. 1: Poly(methyl-alpha-haloacrylates) and copolymers with methylmethacrylate
[AD-A131864] N84-12315

COPOLYMERS
Radiolysis of resist polymers. 1: Poly(methyl-alpha-haloacrylates) and copolymers with methylmethacrylate
[AD-A131864] N84-12315

COPPER
Solid state copper vapor laser modulator
[DE83-015837] N84-12475
Thermal conductance measurements of pressed OFHC copper contacts at liquid helium temperatures
[NASA-TM-85861] N84-12809

COPPER ALLOYS
Evaluation of several high-strength copper sheet alloys
[DE83-015812] N84-12298

CORE FLOW
Waves on vortex cores and their relation to vortex breakdown N84-12128

CORONAL HOLES
Observational evidence for solar wind acceleration at the base of coronal holes N84-13082

CORONAL LOOPS
Modeling of transient disturbances in coronal-streamer configurations N84-13119
The behavior of the cosmic ray equatorial anisotropy inside fast solar wind streams ejected by coronal holes
[IFSI-82-16] N84-13130

CORONAS
Associations between coronal mass ejections and interplanetary shocks N84-13121

CORRELATION
Effects of pressure-drop correlations on Stirling-engine predicted performance
[DE83-017279] N84-12501

CORROSION
Accelerated compatibility testing using corrosion fatigue techniques
[DE83-015104] N84-12296
Breakaway corrosion in mixed-gas environments
[DE83-014704] N84-12299

CORROSION PREVENTION
150 hour engine test of corrosion inhibited MIL-L-23699C oil
[AD-A131633] N84-12317

CORROSION RESISTANCE
Corrosion resistant coating
[NASA-NPO-15928-1] N84-12289

Corrosion behavior of Fe-Cr-Ni-Zr alloys in aggressive environments at high temperatures
[DE83-014735] N84-12297
Chemical properties of metallic glasses
[DE83-017353] N84-12322

CORROSION TESTS
Development of materials for open-cycle MHD
[DE83-016334] N84-12926

COSMIC PLASMA
The structure of the plasma sheet-lobe boundary in the Earth's magnetotail
[NASA-TM-85434] N84-13049

COSMIC RAYS
The relative abundances of Sn, Te, Xe, Ba and Ce
[NASA-CR-174599] N84-13064
Temporal variations of the anomalous oxygen component N84-13069
Voyager measurements of the energy spectrum, charge composition, and long term temporal variations of the anomalous components in 1977-1982 N84-13100
The effect of the solar field reversal on the modulation of galactic cosmic rays N84-13101
Photon damping in cosmic-ray acceleration in active galactic nuclei
[DE83-011320] N84-13133
Ultra-relativistic heavy ions and cosmic rays
[DE83-015881] N84-13134

COST ANALYSIS
Develop a normative or descriptive model of the international/domestic civil aviation industry, volume 3
[AD-A131878] N84-12051
Domestic scheduled air transport for the year 2000. Financial and capacity related effects of supply alternatives, considering, also, the cooperation with high speed rail transport services --- West Germany
[DFVLR-FB-83-03] N84-12141
Overview of state-of-the-art flywheel technology N84-12231
Electrical power trade-offs N84-12232

COST EFFECTIVENESS
Technology and the future evolution of the ATC system N84-12148
Cost efficient on board power for airline operation N84-12180
Advanced Control and Power System (ACAPS) technology program N84-12243

COSTS
Detecting long-term ecological effects in forests and food chains
[DE83-003469] N84-12655

COULOMB COLLISIONS
Electrostatic waves and anomalous transport in the solar wind N84-13095

COUPLED MODES
Universality and fractal dimension of mode locking structure in systems with competing periodicities
[DE83-017352] N84-12545

COUPLING
Tau and B lifetime measurements from the MARK 2
[DE83-018219] N84-12879
Strong coupling effects on bound states in plasmas
[AD-A131661] N84-12918

COVARIANCE
Mixture models for dependent observations N84-12562
Discrimination relative to measures of non-normality N84-12566
Covariant theory with a confined quantum
[DE83-014897] N84-12850

CRACK GEOMETRY
The analysis of crack growth data with application to trip steel
[AD-A132021] N84-12535

CRACK PROPAGATION
Accelerated compatibility testing using corrosion fatigue techniques
[DE83-015104] N84-12296
Life prediction under stress corrosion conditions below K sub ISCC
[DE83-018074] N84-12307
Helium damage in austenitic stainless steels
[DE83-017494] N84-12309
The Dugdale model for the compact specimen
[NASA-TM-85714] N84-12529
The analysis of crack growth data with application to trip steel
[AD-A132021] N84-12535
Electron-microscope observation of crack propagation and a dislocation model of fracture
[DE83-014623] N84-12540
Single specimen J-integral testing
[DE83-016069] N84-12543
Mechanics of fracture under high-rate stress loading
[DE83-013770] N84-12544
Numerical analysis of stable crack growth in elastic-plastic materials in small scale and general yielding N84-12549
Evaluation of the crack gage as an advanced individual aircraft tracking concept N84-12551
Elastic-plastic fracture of cylindrical shells containing part-through circumferential cracks N84-12553

CRACKING (FRACTURING)
Grain-boundary cavitation and weld-underbead cracking in DOP-26 iridium alloy
[DE83-015406] N84-12539

CRACKS
Interaction of a dislocation with a crack
[AD-A131912] N84-12536
Inference of fatigue-crack closure stresses from ultrasonic-transmission measurements
[DE83-017684] N84-12547

CRASH INJURIES
Safety report: General aviation crashworthiness project, phase 1
[PB83-917004] N84-12142

CRASHES
Vertical drop test of a transport fuselage center section including the wheel wells
[NASA-TM-85706] N84-12531

CRASHWORTHINESS
Safety report: General aviation crashworthiness project, phase 1
[PB83-917004] N84-12142
Review of aircraft crash structural response research
[AD-A131696] N84-12160

CREEP PROPERTIES
Evaluation of the kinematic variable (back stress) response of metals
[DE83-008381] N84-12293

CRITICAL FLOW
Vortex stability and breakdown N84-12122
Phonon-induced enhancements of the energy gap and critical current in superconductng aluminum
[DE83-015210] N84-12996

CROP IDENTIFICATION
An empirical Bayes approach to spatial analysis N84-12563
First results of the evaluations of the European SAR 580 data for agricultural and forestry purposes in test site D6, Freiburg (West Germany) N84-12599

CROP INVENTORIES
Mixture models for dependent observations N84-12562
Quantile data analysis of image data N84-12565
Monitoring of renewable resources (a land information system for Europe) --- remote sensing N84-12581
SAR 580: Images for agricultural and forest survey. First results in middle Belgium N84-12595

CROPS
Development of a data base for carbon dioxide releases resulting from conversion of land to agricultural uses
[DE83-015728] N84-12626

CROSS COUPLING
Simulation of mechanical cross coupling of multiaxes vibration facilities N84-12207

CROSS SECTIONS
Cross sections relevant to gamma-ray astronomy: Alpha-particle-induced reactions
[DE83-015533] N84-13038

CRUCIFORM WINGS
Solar powered aircraft
[NASA-CASE-LAR-12615-1] N84-12154

CRUDE OIL
Short-term energy outlook. Volume 2. Methodology
[DE83-016853] N84-12648

CRUISING FLIGHT
Engine/airframe interference drag at cruise conditions, using propulsion simulation
[NLR-TR-82012-U] N84-12098

CRYOGENIC EQUIPMENT
Helium-flow measurement using ultrasonic technique
[DE83-017765] N84-12826

CRYOGENIC MAGNETS
Thermal performance of the MFTF magnets
[DE83-016275] N84-12988

CRYOGENICS
Comparative evaluation of existing concepts for a 10-tesla FED toroidal field coil
[DE83-012817] N84-12815

CRYSTAL DEFECTS
Hamiltonian for antisotropic bodies with defects
[ISSN-0208-5658] N84-12966
Characterization by X-ray topography of laser-induced damage in potassium dihydrogen phosphate crystals
[DE83-012045] N84-12985
Defect interactions at high concentrations in solid oxide electrolytes
[DE83-016849] N84-12992
Optical properties and correlation energy of defects in a-Ge:H
[DE83-016697] N84-12993

CRYSTAL DISLOCATIONS
Interaction of a dislocation with a crack
[AD-A131912] N84-12536

CRYSTAL GROWTH
Materials processing in space program tasks-supplement
[NASA-TM-82548] N84-12196
Large-area mercuric iodide photodectors
[DE83-013035] N84-12898
Single Pb (1-x)Sn(x) Te crystal growth by vapor phase transport, with formation of a liquid/solid interface
[INPE-2811-PRE/369] N84-12967
Method and apparatus for minimizing convection during crystal growth from solution
[NASA-CASE-NPO-15811-1] N84-12968
The growth and measurement of single-crystal doped GGG (Gd3-xCaxGa5-xZrx012)
[AD-A131875] N84-12971
Growth and characterization of InP and InGaAs films using the hydride VPE technique
[AD-A131841] N84-12973
A program of research on microfabrication techniques for VLSI magnetic devices
[AD-A131706] N84-12978

CRYSTAL LATTICES
Investigation of the statistical mechanics of linear polymers for various physical conditions
[JUEL-1832] N84-12324
Microstructural origins of hot spots in RDX explosive and several reference inert materials
[AD-A132056] N84-12325
Clustering and ordering in 3-5 alloys
[AD-A131785] N84-12974
Commensurability, chaos, and the devil's staircase
[DE83-013280] N84-12987

CRYSTAL STRUCTURE
Influence of heat-treatment and physicochemical properties on the electrochemical oxidation of carbon blacks in phosphoric acid
[DE83-017744] N84-12276
Snow characterization instruments
[AD-A131984] N84-12687
New developments and oppotunities for NMR in metal-hydrogen systems
[DE83-017696] N84-12864
Review of some recent theoretical calculations of phase transitions and comparisons with experimental results
[DE83-015863] N84-12983

CRYSTALLOGRAPHY
New materials for organic photovoltaic cells
[DE83-016845] N84-12645

CUES
Integrated Cuing Requirements (ICR) study: Demonstration data base and users guide
[AD-A131119] N84-13019

CURRENT DENSITY
Measurements of the emittance and current density profile of the beam produced by the ATA injector
[DE83-016522] N84-12648
Diagnosing the ion beam on the applied-B diode
[DE83-017822] N84-12943

CURRENT DISTRIBUTION
Numerical modeling techniques for half-space (ground) problems N84-12374

CUSHIONS
Correlation of laboratory-scale fire test methods for seat blocking layer materials with large-scale test results
[AD-A131666] N84-12138

CUTTERS
Rapid runway repair program subtask 1.07 - rapid concrete cutting
[AD-A131771] N84-12195

CUTTING
Rapid runway repair program subtask 1.07 - rapid concrete cutting
[AD-A131771] N84-12195

CYCLIC LOADS
Cumulative damage in components of steel structures under cyclic inelastic loading N84-12550

CYCLOTRON RESONANCE
Acceleration of heavy ions in the solar wind N84-13118

CYCLOTRONS
The 83-inch cyclotron reseach program
[DE83-015827] N84-12852
Acceleration of heavy ions in the solar wind N84-13118

CYLINDRICAL BODIES
Water entry impact shock on flat faced cylindrical missiles
[AD-A131937] N84-12419

Acoustic pulse scattering from impedance covered cylinders
[AD-A131653] N84-12822
CYLINDRICAL SHELLS
Elastic-plastic fracture of cylindrical shells containing part-through circumferential cracks N84-12553

D

DAMAGE ASSESSMENT
Cumulative damage in components of steel structures under cyclic inelastic loading N84-12550
DAMPING
Measurement of macroscopic plasma parameters with a radio experiment: Interpretation of the quasi-thermal noise spectrum observed in the solar wind N84-13096
Photon damping in cosmic-ray acceleration in active galactic nuclei
[DE83-011320] N84-13133
DATA ACQUISITION
Space Shuttle external interference heating test
[AD-A131688] N84-12215
Ground coupled heat-pump-system experimental results
[DE83-014011] N84-12427
Design and implementation of a preprocessing system for a sodium lidar
[NASA-CR-174593] N84-12462
Review of potential satellite techniques for mesoscale mapping of insolation
[DE83-011998] N84-12622
Variability of atmospheric density in the middle atmosphere
[AD-A131985] N84-12667
Field and laboratory studies of ice nucleation in winter orographic clouds N84-12678
Snow characterization instruments
[AD-A131984] N84-12687
Australian Oceanographic Data Centre bulletin 16
[AD-A132002] N84-12701
Hardware and software configuration of the Doublet 3 diagnostic-data-acquisition computer system
[DE83-013427] N84-12733
Experiments on the nuclear interactions of pions
[DE83-016285] N84-12844
Real-time diagnostic-data-acquisition system for the Doublet 3 Tokamak fusion experiment
[DE83-015871] N84-12927
Information retrieval research support
[AD-A131990] N84-13022
Stellar winds driven by multi-line scattering N84-13087
Solar wind variations in the 60-100 year period range: A review N84-13092
Periodicities in the occurrence of aurora as indicators of solar variability N84-13093
DATA BASE MANAGEMENT SYSTEMS
Using PAFEC as a preprocessor for COSMIC/NASTRAN
[DE83-017179] N84-12755
Development of a unique Physical Metrology Laboratory Recall System
[DE83-017415] N84-12767
Real-time diagnostic-data-acquisition system for the Doublet 3 Tokamak fusion experiment
[DE83-015871] N84-12927
The computerization of material safety data sheet information
[AD-A131992] N84-13021
Information retrieval research support
[AD-A131990] N84-13022
DATA BASES
Electrical power trade-offs N84-12232
Integrated Cuing Requirements (ICR) study: Demonstration data base and users guide
[AD-A131119] N84-13019
Source header list, supplement 1
[AD-A131800] N84-13024
DATA LINKS
A flight investigation of simulated data link communications during single-pilot IFR flight N84-12046
Satellite communication, part 1
[INPE-2893-PRE/417] N84-12337
DATA MANAGEMENT
Utility of the cortical evoked response as a measure of photographic image quality
[AD-A131679] N84-12455
Australian Oceanographic Data Centre bulletin 16
[AD-A132002] N84-12701
Office automation management guide
[AD-A131770] N84-13012
DATA PROCESSING
Integration of fire, flight and propulsion control systems: An overview, retrospective and prospective N84-12057
Automated data reduction for optical interferometric data
[DE83-012075] N84-12457
Information resources management plan
[AD-A131964] N84-13023
Information processing for the infrared balloon telescope Goldener Drache
[MPE-38] N84-13035
DATA PROCESSING EQUIPMENT
Design and implementation of a preprocessing system for a sodium lidar
[NASA-CR-174593] N84-12462
Test and demonstration of Macrometer (TM) model V-1000 interferometric surveyor
[PB83-239103] N84-12631
DATA REDUCTION
Quantile data analysis of image data N84-12565
DATA SAMPLING
Gust structure and gust statistics. Results from an analysis of atmospheric turbulence measurements by using conditional sampling technique
[FFA-TN-1983-28] N84-12696
DATA SIMULATION
Simulation aspects in the study of rectification of satellite scanner data N84-12571
DATA STORAGE
Procedures for the transfer of data files between the BRL CYBER computer system and the IBD Hewlett-Packard minicomputer network
[AD-A132063] N84-12731
Development of a unique Physical Metrology Laboratory Recall System
[DE83-017415] N84-12767
The computerization of material safety data sheet information
[AD-A131992] N84-13021
DECAY
Predicting lake ice decay
[AD-A132012] N84-12618
DECISION MAKING
Search among queues
[AD-A131639] N84-12773
TRAN-STAT (statistics for environmental studies). Issue no. 24: Field sampling designs, simple random and stratified random sampling
[DE83-016826] N84-12803
Information resources management plan
[AD-A131964] N84-13023
DECOMMUTATORS
GSE for balloon-borne I.M.S.: Decommutator and D/A units
[AD-A131845] N84-12452
DECOMPOSITION
Theoretical and experimental studies of shock-compressed benzene and polybutene
[DE83-015884] N84-12816
DEFECTS
Progress on ultrasonic flaw sizing in turbine-engine rotor components: Bore and web geometries
[DE83-018081] N84-12167
Improving NDE (Non-destructive evaluation) capability through multiple inspection with application to gas turbine engine disks
[AD-A131762] N84-12509
Elastic-wave inverse scattering in non-destructive evaluation
[DE83-017683] N84-12513
DEFLECTION
Load deflection characteristics of inflated structures
[NASA-CR-174585] N84-12028
Bending of transversally loaded orthotropic rectangular and sector plates N84-12520
DEFORMATION
Computation of three-dimensional unsteady flow in rigid and deformable curved tubes N84-12440
Vibration response of geometrically nonlinear elastic beams to pulse and impact loading
[NASA-CR-174495] N84-12527
Endochronic theory of dynamic viscoplasticity
[DE83-017531] N84-12546
Crustal deformation, the earthquake cycle, and models of viscoelastic flow in the asthenosphere
[NASA-TM-85117] N84-12662
Lecture notes for contact-impact algorithms for large-deformation finite-element analysis
[DE83-013039] N84-12789
DEGRADATION
Radiolysis of resist polymers. 1: Poly(methyl-alpha-haloacrylates) and copolymers with methylmethacrylate
[AD-A131864] N84-12315
Physical fitness as a moderator of cognitive degradation during sleep deprivation
[AD-A131962] N84-12718
DELAMINATING
An X-ray radiography study of delamination growth in notched carbon/epoxy laminates
[FFA-TN-1983-29] N84-12516
DELTA WINGS
An experimental investigation of the vortex flow over delta and double-delta wings at low speed N84-12108
Laser velocimetry study of compressibility effects on the flow field of a delta wing N84-12108
On the generation of vortical flow at hypersonic speeds over elliptical cones N84-12114
Vortex flow simulations past wings using the Euler-equations N84-12118
DEMAND (ECONOMICS)
Short-term energy outlook. Volume 2. Methodology
[DE83-016853] N84-12648
DEMOGRAPHY
Develop a normative or descriptive model of the international/domestic civil aviation industry, volume 2
[AD-A131677] N84-12052
Deterministic models in mathematical demography: An investigation of stable population theory including an analysis of the population statistics of Denmark N84-12806
DENMARK
Deterministic models in mathematical demography: An investigation of stable population theory including an analysis of the population statistics of Denmark N84-12806
DENSE PLASMAS
Atomic processes in hot dense plasma
[IPPJ-AM-31] N84-12911
Bibliography on atomic processes in hot dense plasmas
[IPPJ-AM-29] N84-12913
Strong coupling effects on bound states in plasmas
[AD-A131661] N84-12918
DENSITY (MASS/VOLUME)
Method and apparatus for minimizing convection during crystal growth from solution
[NASA-CASE-NPO-15811-1] N84-12968
DENSITY MEASUREMENT
Properties of the neutral density and composition in the thermosphere
[AD-A131557] N84-12665
DEPLETION
A study of depletion in low-velocity diffuse interstellar gas N84-13042
DEPOSITION
Fabrication and properties of multilayer structures
[AD-A131934] N84-12969
DEPOSITS
Deposit formation and heat transfer in hydrocarbon rocket fuels
[NASA-CR-168277] N84-12225
Structure of convective surface deposits and effect on MHD steam-plant design
[DE83-010757] N84-12931
DESALINIZATION
Novel composite membranes
[PB83-243170] N84-12284
DESIGN
Hermetically sealed microminiature multisocket connector
[DE83-017484] N84-12503
DESIGN ANALYSIS
Safety report: General aviation crashworthiness project, phase 1
[PB83-917004] N84-12142
Optimization of engine power offtake by secondary power system design N84-12177
Analytical design of a liquid hydrogen fueled turbofan-ramjet engine for flight Mach numbers zero to five N84-12187
Development of mass-producible line-focus tracking concentrating solar collectors. Category 1: Collectors
[DE83-015629] N84-12639
Linked state machines
[DE83-4000123] N84-12736
Environments and search paths for the software tools
[DE83-016607] N84-12749
Using structural and functional information in diagnostic design
[AD-A131859] N84-12769
University of Washington superconducting-booster project
[DE83-015689] N84-12846
DESYNCHRONIZATION (BIOLOGY)
Biological clocks and shift work scheduling
[GPO-21-747] N84-12713
DETECTION
Detection of cavities under concrete pavement
[AD-A131851] N84-12331
Development of a continuous monitor for detection of toxic organic compounds
[PB83-234922] N84-12461

Variations in task and the ideal observer
[DE83-015394] N84-12723
DETERIORATION
Long term evaluation of the effects of shale oil produced JP-4 on aircraft construction materials
[AD-A131665] N84-12161
Cumulative damage in components of steel structures under cyclic inelastic loading N84-12550
DETONABLE GAS MIXTURES
Hydrogen-air detonations
[DE83-009289] N84-12278
DEUTERIUM
Isotope dependence of the breakdown strength of gases
[DE83-017272] N84-12430
Tokamak fusion reactors with less than full tritium breeding
[DE83-016711] N84-12936
DIAGNOSIS
Using structural and functional information in diagnostic design
[AD-A131859] N84-12769
DIAMONDS
Investigation of the statistical mechanics of linear polymers for various physical conditions
[JUEL-1832] N84-12324
DICKE RADIOMETERS
Observations and classifications with a 35/94 GHz radiometer of terrain near Motala, Sweden, July 1982
[FOA-C-30325-E1,E3] N84-12630
DIELECTRIC PROPERTIES
Enthalpy - improved dielectric insulation for superconducting wires
[AD-A131857] N84-12316
DIELECTRICS
Dielectric loss measurement at millimetre wave frequencies using an untuned cavity
[RSRE-3597] N84-12379
The performance of the perfluorocarbon liquid/plastic-film capacitor technology in pulse-power service. A current status report
[DE83-014606] N84-12402
DIES
Holding fixture for a hot stamping press
[NASA-CASE-GSC-12619-1] N84-12491
DIESEL ENGINES
Evaluation of unthrottled combustion system options for light duty applications with future syncrude derived fuels
[DE83-017047] N84-12327
Vehicle-emission characteristics using mechanically emulsified alcohol/diesel fuels
[DE83-016012] N84-12656
DIESEL FUELS
Vehicle-emission characteristics using mechanically emulsified alcohol/diesel fuels
[DE83-016012] N84-12656
DIFFERENCE EQUATIONS
Crank-Nicholson difference schemes for solving coupled systems of nonlinear diffusion equations
[IPP-6/223] N84-12776
DIFFERENCES
Speed-dependent collision effects on radar back-scattering from the ionosphere --- incoherent scatter radar
[NASA-CR-173077] N84-12336
DIFFERENTIAL EQUATIONS
Relative symmetries of differential equations
[DE83-015231] N84-12790
The effects of small noise on implicitly defined non-linear dynamical systems
[AD-A131632] N84-12808
Evolution of the ultra high energy cosmic ray spectron by transport equation
[DE83-013711] N84-13132
DIFFRACTION
Analytic diffraction corrections to ultrasonic scattering measurements
[DE83-016060] N84-12825
DIFFUSE RADIATION
A study of depletion in low-velocity diffuse interstellar gas N84-13042
DIFFUSION
Diffusion mass transfer of KOH through Ni/Zn battery membrane separators
[DE83-014551] N84-12387
Crank-Nicholson difference schemes for solving coupled systems of nonlinear diffusion equations
[IPP-6/223] N84-12776
DIFFUSION COEFFICIENT
Transport and relaxation processes in supercritical fluids
[DE83-015966] N84-12432
DIGITAL COMPUTERS
Full authority digital electronic engine controls and their integration with flight control systems in VSTOL aircraft N84-12064
DIGITAL DATA
Information retrieval research support
[AD-A131990] N84-13022
DIGITAL SIMULATION
Application of high resolution satellite data to coastal zones: SPOT simulations during ecological survey of the Britanny coast N84-12591
DIGITAL SYSTEMS
Integration of fire, flight and propulsion control systems: An overview, retrospective and prospective N84-12057
Alternative transmission media for third-generation interface standards
[PB83-238345] N84-12365
DIGITAL TECHNIQUES
Flight test validation of a design procedure for digital autopilots N84-12036
DIMERS
RF conditioned dc discharges for excitation of rare gas halide lasers
[DE83-016537] N84-12479
DIODES
Infrared-laser spectroscopy using a long-pathlength absorption cell
[DE83-014197] N84-12480
Applied-B ion diode experiments on PBFA 1
[DE83-017792] N84-12942
Diagnosing the ion beam on the applied-B diode
[DE83-017822] N84-12943
Ampfion hybrid diodes on hydramite and PBFA-1
[DE83-017824] N84-12945
DIPOLE ANTENNAS
Performance of antennas in plasma N84-12377
DIRECTIVITY
Theoretical aspects of throat-launch microwave heating in EBT-S
[DE83-015762] N84-12875
DISCRIMINANT ANALYSIS (STATISTICS)
Discrimination relative to measures of non-normality N84-12566
DISLOCATIONS (MATERIALS)
Electron-microscope observation of crack propagation and a dislocation model of fracture
[DE83-014623] N84-12540
DISPERSION
Phonon dispersion of transverse basal-plane modes in alkali-graphite compounds
[DE83-003910] N84-12273
DISPLACEMENT
Subsonic/Transonic Aerodynamic Interference for Aircraft: Introductory remarks N84-12073
Three-dimensional analysis of composite plates with material nonlinearity
[AD-A131884] N84-12258
DISPLACEMENT MEASUREMENT
Gauge block lasometer development
[DE83-018288] N84-12458
DISPLAY DEVICES
Controls, Displays, and Information Transfer for General Aviation IFR Operations
[NASA-CP-2279] N84-12029
A simulator evaluation of an automatic terminal approach system N84-12037
Pilot controls and SPIRF flight N84-12038
Pilot response with conventional displays N84-12040
A simulator evaluation of a rate-enhanced instrument landing system display N84-12042
Display research: Pilot response with the "follow-me" box display N84-12043
Control/display trade-off study for single-pilot instrument flight rule operations N84-12044
Experimental studies relating environmental lighting and flicker to visual fatigue in VDT operators
[DE83-016316] N84-12738
DISSIPATION
Effects of dissipation in one-dimensional inverse problems
[DE83-017692] N84-12353
Effects of microstructure and pore fluids on the acoustic properties of granular materials
[AD-A131983] N84-12668
DISTRIBUTED PARAMETER SYSTEMS
A fault-tolerant distributed computer network design and analysis for an integrated flight control system N84-12189
DISTRIBUTED PROCESSING
A model for the distributed storage and processing of large arrays
[NASA-CR-172252] N84-12742
DISTRIBUTION FUNCTIONS
Weak and strong law results for a function of the spacings
[AD-A130705] N84-12782
DISTURBANCES
Universality and fractal dimension of mode locking structure in systems with competing periodicities
[DE83-017352] N84-12545
DIURNAL VARIATIONS
Variability of atmospheric density in the middle atmosphere
[AD-A131985] N84-12667
Branching processes in periodically varying environment
[CTH-MATH-1983-12-PREPRINT] N84-12792
DOCUMENT STORAGE
NBS (National Bureau of Standards) Workshop: Environmental Control for Archival Records Storage
[PB83-242230] N84-13026
DOCUMENTATION
Praxis language environment: Distribution-package description
[DE83-017546] N84-12750
A study of critical factors affecting the development of performance measures in evaluating bibliographic information retrieval systems N84-13030
DOCUMENTS
Comments on ISO/TC 97/SC 18/WG3 N120
[DE83-011391] N84-12748
DOPED CRYSTALS
The growth and measurement of single-crystal doped GGG (Gd3-xCaxGa5-xZrx012)
[AD-A131875] N84-12971
Defect interactions at high concentrations in solid oxide electrolytes
[DE83-016849] N84-12992
Optical properties and correlation energy of defects in a-Ge:H
[DE83-016697] N84-12993
DOPPLER EFFECT
Correlation between two spacecraft in the Doppler detection of a gravitational background radiation
[IFSI-83-7] N84-12362
Observational evidence for solar wind acceleration at the base of coronal holes N84-13082
DOSIMETERS
Pulmonary dosimetry of nitrogen dioxide in animals and man
[PB83-243394] N84-12711
DRAG REDUCTION
Transonic configuration design N84-12081
The effects of wing tip devices on the performance of the BAe Jetstream N84-12130
DRAINAGE
Glaciological applications of LANDSAT images in connection with hydropower investigations in West Greenland N84-12598
DRAINAGE PATTERNS
Relative elevation determination from LANDSAT imagery N84-12558
DRIFT RATE
Evaluation of the stochastic drift of rate integrating gyros as preparation for the analysis of laser gyro drift measurements
[DFVLR-MITT-83-04] N84-12449
DRIVES
All-electric accessory drive systems: Implications on engine design and performance N84-12184
DROPS (LIQUIDS)
Numerical simulations of fuel droplet flows using a Lagrangian triangular mesh
[NASA-CR-168263] N84-12411
Topically classified bibliography on shapes of falling drops, drops in electric fields and related topics
[AD-A131134] N84-12417
Design and operation of a light-scattering device for sizing and velocimetry of large droplets
[DE83-902641] N84-12456
DUCTILITY
Solid impingement erosion mechanisms and characterization of erosion resistance of ductile metals
[NASA-TM-83492] N84-12287
Strain rate effects on ductile/brittle transitions in steels
[DE83-016906] N84-12308
DURABILITY
Assessment of potential for batteries in space applications N84-12246
Some comments on longevity by a technologist N84-12247
DYES
New materials for organic photovoltaic cells
[DE83-016845] N84-12645
DYNAMIC CHARACTERISTICS
Hydrogen-air detonations
[DE83-009289] N84-12278
Maximum likelihood estimation of linear dynamic system parameters
[AR-002-934] N84-12780
Quasi-steady solar wind dynamics N84-13120
DYNAMIC LOADS
Mechanics of fracture under high-rate stress loading
[DE83-013770] N84-12544

DYNAMIC MODELS
The vortex skeleton model for three-dimensional steady flows N84-12101
Dynamical evolution of substucture in molecular clouds N84-13043
Theory of hydromagnetic turbulence N84-13077
DYNAMIC PRESSURE
Application of the small body pressure transducer [AD-A131733] N84-12454
DYNAMIC RESPONSE
Alternate T-38 transparency development. Part 4: Parametric studies
[AD-A131904] N84-12159
Calculation of forced response to base excitation using experimentally derived modal participation factors N84-12205
System identification of structures with joint rotation N84-12330
A pressure-shear experiment for studying the dynamic plastic responses of metals at shear strain rates of 10 to the 5th power s(-1) N84-12519
Nonlinear dynamics and control of a vibrating rectangular plate
[NASA-CR-172215] N84-12528
DYNAMIC STRUCTURAL ANALYSIS
Review of aircraft crash structural response research [AD-A131696] N84-12160
Calculation of forced response to base excitation using experimentally derived modal participation factors N84-12205
System identification of structures with joint rotation N84-12330
Vertical drop test of a transport fuselage center section including the wheel wells
[NASA-TM-85706] N84-12531
A comparison of finite-element predictions and experimental data for the forced response of the DOE 100 kW vertical-axis wind turbine
[DE83-012624] N84-12537
Prediction of dynamic effects due to vehicles crossing military bridges
[ISVR-TR-120] N84-12548
First passage times in stochastic differential equations of mathematical physics and engineering
[AD-A131705] N84-12728
La Recherche Aerospatiale, Bimonthly Bulletin, no. 1983-1/212, January-February 1983
[ESA-TT-814] N84-12810
Development of the basic methods needed to predict the aeroelastic behavior of helicopters N84-12811
Present trends in structural analysis at ONERA N84-12812
DYNAMICS
Dynamic analysis of the fluidyne
[DE83-017283] N84-12500

E

EAR
An age comparison of the vestibulo-ocular counterroll reflex
[AD-A132064] N84-12718
EARLY STARS
The winds and coronae of early-type stars N84-13086
EARTH CRUST
Crustal deformation, the earthquake cycle, and models of viscoelastic flow in the asthenosphere
[NASA-TM-85117] N84-12662
EARTH RESOURCES
Observation of the Earth in the middle infrared
[ESA-TT-790] N84-12629
EARTHQUAKE RESISTANCE
System identification of structures with joint rotation N84-12330
EARTHQUAKES
Crustal deformation, the earthquake cycle, and models of viscoelastic flow in the asthenosphere
[NASA-TM-85117] N84-12662
Microearthquakes induced during hydraulic fracturing at the Fenton Hill HDR site: The 1982 experiments
[DE83-014191] N84-12672
ECLIPTIC
Solar cycle evolution of the solar wind in three dimensions N84-13090
Solar wind variations in the 60-100 year period range: A review N84-13092
ECOLOGY
Use of remote sensing methods for the ecological mapping project of the European community N84-12580
Development of a data base for carbon dioxide releases resulting from conversion of land to agricultural uses
[DE83-015728] N84-12626
ECONOMIC ANALYSIS
Domestic scheduled air transport for the year 2000. Financial and capacity related effects of supply alternatives, considering, also, the cooperation with high speed rail transport services — West Germany
[DFVLR-FB-83-03] N84-12141
The Tracked Wing In Ground-Effect (TWIG) N84-12155
Economic study of long distance optical fibre links
[FUB-38-1982] N84-12908
ECONOMIC FACTORS
US weather satellites and services
[GPO-25-753] N84-12208
To quench our thirst: The present and future status of freshwater resources of the United States, part 3
[DE83-016791] N84-12625
ECONOMICS
Two types of values and their assessment by the collective interest
[DE83-012084] N84-13031
ECOSYSTEMS
Limnology, second edition
[DE83-016792] N84-12627
Detecting long-term ecological effects in forests and food chains
[DE83-003469] N84-12655
EFFECTS
Strong coupling effects on bound states in plasmas [AD-A131661] N84-12918
EFFICIENCY
Assessment of energy-efficiency improvements for paint spray booths
[DE83-016680] N84-12320
Charge characteristics of Ni/Fe traction cells
[DE83-014205] N84-12389
Self-correction coil: Operation mechanism of self-correction coil
[DE83-016324] N84-12392
Solid-oxide fuel-cell performance
[DE83-017926] N84-12396
EIGENVALUES
Estimating location parameters in a mixture model N84-12559
Limit theorems for the eigenvalues of product of two random matrices
[AD-A131682] N84-12787
Considerations of the three-wave interactions
[IPPJ-841] N84-12915
EIGENVECTORS
Estimating location parameters in a mixture model N84-12559
Dissipative instabilities of magnetic neutral layers with velocity shear
[IFSI-82-13] N84-12965
ELASTIC ANISOTROPY
Investigation of the Rayleigh critical angle phenomenon for the characterization of surface properties
[AD-A131530] N84-12340
ELASTIC BENDING
Plastic deformations of a portable frame under short pulse loading on one column by an approximate method including effects of elasticity and plastic rate sensitivity N84-12521
ELASTIC BODIES
Vibration response of geometrically nonlinear elastic beams to pulse and impact loading
[NASA-CR-174495] N84-12527
ELASTIC CYLINDERS
Yield surface for bars including warping restraint
[AD-A131393] N84-12533
ELASTIC DEFORMATION
Mechanical behavior of sea ice
[AD-A131852] N84-12619
ELASTIC PLATES
Three-dimensional analysis of composite plates with material nonlinearity
[AD-A131884] N84-12258
ELASTIC PROPERTIES
Load deflection characteristics of inflated structures
[NASA-CR-174585] N84-12028
Buckled plate vibrations, large amplitude vibrations and nonlinear flutter of elastic plates using high-order triangular finite elements N84-12523
Numerical analysis of stable crack growth in elastic-plastic materials in small scale and general yielding N84-12549
On differential equations of nonlocal elasticity and solutions of screw dislocation and surface waves
[AD-A131911] N84-12786
ELASTODYNAMICS
Interaction of stress waves and cracks using a second order accurate finite difference method N84-12522
ELASTOMERS
Failure processes in elastomers at or near a rigid spherical inclusion
[AD-A132060] N84-12314
In-situ permeation tests of elastomeric O-ring seals
[DE83-015822] N84-12318
ELASTOPLASTICITY
Elastic-plastic fracture of cylindrical shells containing part-through circumferential cracks N84-12553
ELASTOSTATICS
Some bifurcation topics in non-linear elastostatics N84-12524
ELECTRIC AUTOMOBILES
Ragone characteristics of aqueous mobile batteries and their application in projecting ranges of electric vehicles
[DE83-014701] N84-12642
ELECTRIC BATTERIES
Charge characteristics of Ni/Fe traction cells
[DE83-014205] N84-12389
Comparative response of lead-acid and nickel-iron batteries to pulsed and constant-current loads
[DE83-017939] N84-12395
ELECTRIC CHARGE
Hadronic multiplicity distributions: Example of a universal stochastic mechanism
[DE83-015232] N84-12845
ELECTRIC COILS
Storage of energy in magnetic field of superconductive coils
[AD-A131898] N84-12636
ELECTRIC CONTACTS
Containerless electromagnetic levitation melting of Cu-Fe and Ag-Ni alloys
[NASA-TM-82553] N84-12288
Scientific-Technical Conference on Acyclic Electric Machines
[AD-A131880] N84-12381
Thermal conductance measurements of pressed OFHC copper contacts at liquid helium temperatures
[NASA-TM-85861] N84-12809
Horizons of technology (selected articles)
[AD-A131897] N84-13135
ELECTRIC CURRENT
Power-loading effects in gas-discharge models
[DE83-016504] N84-12393
Evaluation of the Beijing Instrument Factory GDB-44F photomultiplier
[DE84-000849] N84-12398
Phonon-induced enhancements of the energy gap and critical current in superconducting aluminum
[DE83-015210] N84-12996
ELECTRIC EQUIPMENT
Unipolar machine with superconductive excitation winding
[AD-A131820] N84-12383
ELECTRIC FIELDS
The effects of channel tortuosity on electromagnetic radiations from lightning return strokes N84-12335
Scale lengths in quasi-parallel shocks
[NASA-TM-85109] N84-12663
Eruption of permanent dentition in rhesus monkeys exposed to ELF (Extremely low frequency) fields
[AD-A132065] N84-12703
Temperature dependence of the electric-field gradient in Er metal
[DE83-015564] N84-12989
ELECTRIC GENERATORS
Super integrated power unit for fighter aircraft N84-12183
Implementing microprocessor technology in aircraft electrical power generating system control N84-12185
Synchronous generators with superconductive excitation windings
[AD-A131832] N84-12382
Steam turbine as unipolar generator
[AD-A131142] N84-12498
ELECTRIC MOTOR VEHICLES
Energy use and range of electric vehicles in selected US Department of Energy sites
[DE83-015719] N84-13034
ELECTRIC POWER
Implementing microprocessor technology in aircraft electrical power generating system control N84-12185
The 400 Hz generators evolution, effects on installation arrangements N84-12186
ELECTRIC POWER SUPPLIES
Auxiliary Power Systems
[AGARD-CP-352] N84-12168
Auxilliary power systems with gas turbines N84-12170
Hydraulic generation of auxilliary power for the Mirage 2000 aircraft N84-12176
ELECTRIC PROPULSION
All-electric accessory drive systems: Implications on engine design and performance N84-12184
Investigation of a pulsed electrothermal thruster
[NASA-CR-168266] N84-12227

ELECTRIC WIRE
Enthalpy - improved dielectric insulation for superconducting wires
[AD-A131857] N84-12316
Orbiting wire as a dynamo: Auxiliary power possibilities for space platforms
[IFSI-83-3] N84-12653
Ultra low loss optical fiber cable assemblies, volume 2
[AD-A132008] N84-12891
Ultra low loss optical fiber cable assemblies, volume 1
[AD-A132007] N84-12892
ELECTRICAL ENGINEERING
Center for electronics and electrical engineering technical progress bulletin covering signals and systems program, April 1982 - September 1982
[PB83-241158] N84-12405
USAF/SCEEE summary faculty research program (1982) research reports, volume 2
[AD-A130770] N84-13009
ELECTRICAL INSULATION
Enthalpy - improved dielectric insulation for superconducting wires
[AD-A131857] N84-12316
High-average-power rep rate systems
[DE83-013769] N84-12385
ELECTRICAL PROPERTIES
Silicide formation and Schottky barrier of rare-earth metals on Si
[AD-A131750] N84-12975
Silicide formation and Schottky barrier of rare-earth metals on Si
[AD-A131749] N84-12976
ELECTRICAL RESISTIVITY
Ionic conductivity in lithium hexaoxometallate solid solutions
[AD-A131842] N84-12250
Development of materials for open-cycle MHD
[DE83-016334] N84-12926
Direct coronal heating from dissipation of magnetic field N84-13069
ELECTRO-OPTICS
The modular optoelectronic scanner (MOMS) on STS-7, June 83 N84-12589
ELECTROCHEMICAL CELLS
Comparative response of lead-acid and nickel-iron batteries to pulsed and constant-current loads
[DE83-017939] N84-12395
ELECTROCHEMISTRY
Assessment of potential for batteries in space applications N84-12246
Mechanisms and kinetics of diphthalocyanine electrode processes
[AD-A131726] N84-12270
Reduction of CO2 to methanol and methane by photo and dark reactions on semiconductor electrodes
[PB83-249490] N84-12329
Studies of the correlation of electrode kinetics with molecular structure
[AD-A131704] N84-12838
ELECTRODES
Photoelectrochemical electrodes
[NASA-CASE-NPO-15458-1] N84-12262
Mechanisms and kinetics of diphthalocyanine electrode processes
[AD-A131726] N84-12270
Effect of antimony on lead-acid battery negative electrode
[DE83-014660] N84-12404
A multistage spent particle collector and a method for making same
[NASA-LEW-13914-1] N84-12447
Studies of the correlation of electrode kinetics with molecular structure
[AD-A131704] N84-12838
Development of materials for open-cycle MHD
[DE83-016334] N84-12926
ELECTROLYSIS
Fourth International Conference on Photochemical Conversion and Storage of Solar Energy
[DE83-014760] N84-12638
ELECTROMAGNETIC ABSORPTION
Propagation and absorption of electromagnetic waves in fully relativistic plasmas
[DE83-017246] N84-12959
ELECTROMAGNETIC FIELDS
Research and development for investigations of metallic adsorptions on metal surfaces by optical techniques complemented by dc resistivity and auger spectroscopy
[AD-A131739] N84-12351
Scientific-Technical Conference on Acyclic Electric Machines
[AD-A131880] N84-12381
Horizons of technology (selected articles)
[AD-A131897] N84-13135
ELECTROMAGNETIC INTERFERENCE
Optimum reception in non-Gaussian electromagnetic interference environments. Part 2: Optimum and suboptimum threshold signal detection in class A and B noise
[PB83-241141] N84-12364
ELECTROMAGNETIC PULSES
Ion-ion recombination rate in the EMP source region
[AD-A131148] N84-12339
ELECTROMAGNETIC RADIATION
The effects of channel tortuosity on electromagnetic radiations from lightning return strokes N84-12335
Effects of dissipation in one-dimensional inverse problems
[DE83-017692] N84-12353
The Performance of Antennas in Their Operational Environment
[AGARD-LS-131] N84-12367
Calculation of ground wave attenuation over irregular, inhomogeneous, layered media using PROGRAM WAGNER N84-12369
Numerical modeling techniques for antennas N84-12373
Interaction of the plasma tail of comet Bradfield 1979L on 1980 February 6 with a possibly flare-generated solar-wind disturbance N84-13126
ELECTROMAGNETIC SPECTRA
Evolution of the ultra high energy cosmic ray spectron by transport equation
[DE83-013711] N84-13132
ELECTROMAGNETIC WAVE TRANSMISSION
Propagation and absorption of electromagnetic waves in fully relativistic plasmas
[DE83-017246] N84-12959
ELECTROMECHANICAL DEVICES
Scientific-Technical Conference on Acyclic Electric Machines
[AD-A131880] N84-12381
Horizons of technology (selected articles)
[AD-A131897] N84-13135
ELECTROMECHANICS
The 400 Hz generators evolution, effects on installation arrangements N84-12186
ELECTRON ATTACHMENT
Electron-molecule interactions in gases and liquids: The electron-attachment process in gases and nonpolar liquids
[DE83-017205] N84-12863
ELECTRON BEAMS
Low energy electron magnetometer using a monoenergetic electron beam
[NASA-CASE-LAR-12706-1] N84-12444
Electron-beam diagnostics for the Los Alamos free-electron oscillator experiment
[DE83-017230] N84-12481
The Los Alamos free-electron-laser oscillator experiment: Plans and present status
[DE83-017290] N84-12485
Free-electron-laser research
[DE83-016957] N84-12489
Development of an ultrasonic testing procedure for electron beam welded parts for aerospace applications
[BMFT-FB-W-72-011] N84-12515
Electron beam trajectory in a photometer field of view
[AD-A131949] N84-12831
A model for chorus associated electrostatic bursts
[NASA-CR-174489] N84-12832
Nonlinear force on an unpolarized relativistic test particle to second order in the total field in a nonequilibrium beam-plasma system
[AD-A131631] N84-12919
ELECTRON BUNCHING
Electron-beam diagnostics for the Los Alamos free-electron oscillator experiment
[DE83-017230] N84-12481
Montoring of the Stanford Linac microbunches' position
[DE83-012712] N84-12840
Longitudinal space-charge effects in bunched beams
[DE83-017305] N84-12888
ELECTRON CAPTURE
The 100% alignment of hydrogen excited states in beam-foil spectroscopy
[DE83-017963] N84-12859
Cross sections for charge transfers of highly ionized ions in hydrogen atoms
[IPPJ-AM-30] N84-12912
Electron capture and loss cross sections for collisions between heavy ions and hydrogen molecules, revised
[IPPJ-AM-28] N84-12914
ELECTRON CYCLOTRON HEATING
Theoretical studies of fusion physics. Volume 1: Summary
[DE83-010376] N84-12924
Status of tandem-mirror confinement
[DE83-017369] N84-12948
Electron-cyclotron-heating experiments in Tokamaks and stellarators
[DE83-017210] N84-12958
ELECTRON DENSITY (CONCENTRATION)
Implications of heavy-ion-induced satellite X-ray emission. 1: Introduction
[DE83-015682] N84-12851
Design of doubly focusing, tunable (5 - 30 keV), wide-bandpass optics made from layered synthetic microstructures
[DE83-015492] N84-12897
Observations of soft X-ray fluctuations with an imaging array on TEXT
[DE83-018118] N84-12938
ELECTRON DISTRIBUTION
Role of thermal conduction in the acceleration of the solar wind N84-13079
ELECTRON EMISSION
Measurements of the emittance and current density profile of the beam produced by the ATA injector
[DE83-016522] N84-12848
ELECTRON ENERGY
Low energy electron magnetometer using a monoenergetic electron beam
[NASA-CASE-LAR-12706-1] N84-12444
Initial assessment of the MHD stability of TMX-U
[DE83-016521] N84-12646
Theoretical studies of fusion physics. Volume 1: Summary
[DE83-010376] N84-12924
Theoretical studies of fusion physics. Volume 2: Appendices
[DE83-010371] N84-12925
Tokamak fusion reactors with less than full tritium breeding
[DE83-016711] N84-12936
Observations of soft X-ray fluctuations with an imaging array on TEXT
[DE83-018118] N84-12938
Drift wave studies in a linear multiple mirror
[DE83-016881] N84-12951
Thermal barriers: Their purpose and functioning
[DE83-017365] N84-12954
ELECTRON GUNS
Measurements of the emittance and current density profile of the beam produced by the ATA injector
[DE83-016522] N84-12848
ELECTRON MICROSCOPES
Structural characterization of dispersed metal catalysts
[DE83-017145] N84-12305
ELECTRON MICROSCOPY
Electron-microscope observation of crack propagation and a dislocation model of fracture
[DE83-014623] N84-12540
ELECTRON MOBILITY
The collapse of the local, Spitzer-Haerm formulation and a global-local generalization for heat flow in an inhomogeneous, fully ionized plasma N84-13080
ELECTRON PARAMAGNETIC RESONANCE
Novel interactions of the charge-balancing cations with framework defects and trapped hydrogen atoms in holmium-exchanged Y zeolites
[DE83-014204] N84-12839
ELECTRON PLASMA
Electron heating at interplanetary shocks N84-13098
ELECTRON RECOMBINATION
Hole trapping, recombination, and space charge in irradiated Sandia oxides
[DE83-015212] N84-12986
ELECTRON SCATTERING
Electron-ion collisions
[DE83-017211] N84-12867
ELECTRON TRANSFER
Thermolysis of 4-methyl-4-phenyl malonyl peroxide: A new oxygen dependent chemiluminescent reaction
[AD-A131863] N84-12268
Studies of the correlation of electrode kinetics with molecular structure
[AD-A131704] N84-12838
ELECTRON TUNNELING
Laser activated MTOS microwave device
[NASA-NPO-16112-1] N84-12463
ELECTRONIC EQUIPMENT
From launching carrier rockets towards the Pacific on the accomplishments and problems of electronic technologies in our country
[AD-A131088] N84-12380
Use of superposition in calculating cooling requirements for circuit cards containing arrays of electronic components
[DE83-016091] N84-12428
ELECTRONICS
Flywheel electronics N84-12239
IPACS electronics: Comments on the original design and current efforts at Langley Research Center N84-12240

ELECTRONS
A multistage spent particle collector and a method for making same
[NASA-LEW-13914-1] N84-12447
The Mimas ghost revisited: An analysis of the electron flux and electron microsignatures observed in the vicinity of Mimas at Saturn
[NASA-CR-174596] N84-13056
ELECTROSTATIC WAVES
Scale lengths in quasi-parallel shocks
[NASA-TM-85109] N84-12663
Electrostatic waves and anomalous transport in the solar wind N84-13095
ELECTROSTATICS
High-sensitivity mass spectrometry with a tandem accelerator
[DE83-017914] N84-12274
A model for chorus associated electrostatic bursts
[NASA-CR-174489] N84-12832
ELECTROTHERMAL ENGINES
Investigation of a pulsed electrothermal thruster
[NASA-CR-168266] N84-12227
ELEMENTARY PARTICLE INTERACTIONS
Proceedings of the 16th LAMPF Users-Group Meeting
[DE83-013215] N84-12488
Operation of the Brookhaven MPS Facility
[DE83-015383] N84-12896
ELEMENTARY PARTICLES
Theory of elementary particles
[DE83-015904] N84-12871
ELEVATION
Relative elevation determination from LANDSAT imagery N84-12558
ELEVONS
Analytical prediction of aerothermal environment in a wing-elevon cove --- space shuttle orbiter
[NASA-TM-85711] N84-12412
ELIMINATION
Experimental and computational modeling of rarefaction wave eliminators suitable for the BRL 2.44 m shock tube
[AD-A131894] N84-12194
ELLIPSOMETERS
The study of thin films on semi-insulating gallium arsenide by ellipsometry
[AD-A131844] N84-12972
ELLIPTICAL CYLINDERS
On the generation of vortical flow at hypersonic speeds over elliptical cones N84-12114
ELLIPTICAL GALAXIES
Simulations of galaxy mergers N84-13054
EMBRITTLEMENT
Helium damage in austenitic stainless steels
[DE83-017494] N84-12309
EMISSION
Development of instrumentation for monitoring carbon fiber emission
[PB83-233726] N84-12460
EMISSION SPECTRA
Infrared characteristics of gas plumes
[AD-A131796] N84-12269
Laser interaction with metallic surfaces
[AD-A126269] N84-12464
Time-resolved spectral measurements above 80 A
[DE83-015616] N84-12933
Implications of heavy-ion-induced satellite X-ray emission. Part 2: Production of K and L X-rays by 0.9 to 2.6 MeV/u Ar ions in thick targets of V, Cu, Nb, Ta, and Pt
[DE83-015681] N84-12982
Observational evidence for solar wind acceleration at the base of coronal holes N84-13082
Theory of winds in late-type evolved and pre-main-sequence stars N84-13085
The winds and coronae of early-type stars N84-13086
EMITTANCE
Measurements of the emittance and current density profile of the beam produced by the ATA injector
[DE83-016522] N84-12848
EMULSIONS
Vehicle-emission characteristics using mechanically emulsified alcohol/diesel fuels
[DE83-016012] N84-12656
ENERGETIC PARTICLES
Solar Wind Five
[NASA-CP-2280] N84-13067
Survey of He(+)/He(2+) abundance ratios in energetic particle events N84-13117
ENERGY ABSORPTION
Solid impingement erosion mechanisms and characterization of erosion resistance of ductile metals
[NASA-TM-83492] N84-12287
Detailed modeling of microwave energy deposition in EBT devices
[DE83-017496] N84-12952
ENERGY CONSERVATION
Assessment of energy-efficiency improvements for paint spray booths
[DE83-016680] N84-12320
Performance of add-on-type heat pump water heaters using two different test methods
[PB83-222703] N84-12332
Comparison of technologies for new energy-efficient lamps
[DE83-015949] N84-12401
Ground coupled heat-pump-system experimental results
[DE83-014011] N84-12427
A study of the relationship between exhaust emissions and fuel economy
[PB83-235564] N84-12506
Innovative industrial-materials processes --- potential for energy conservation
[DE83-016784] N84-12649
Arizona State science, engineering and technology process
[PB83-237107] N84-13016
ENERGY CONSUMPTION
Short-term energy outlook. Volume 2. Methodology
[DE83-016853] N84-12648
Energy use and range of electric vehicles in selescted US Department of Energy sites
[DE83-015719] N84-13034
ENERGY CONVERSION EFFICIENCY
Space station energy sizing N84-12233
ENERGY DISSIPATION
Radiation-induced transient acoustic loss in quartz crystals
[DE83-012626] N84-12980
ENERGY GAPS (SOLID STATE)
Phonon-induced enhancements of the energy gap and critical current in superconducting aluminum
[DE83-015210] N84-12996
ENERGY LEVELS
Low energy electron magnetometer using a monoenergetic electron beam
[NASA-CASE-LAR-12706-1] N84-12444
Study of excited state energy transfer processes
[AD-A131777] N84-12837
Inertial fusion with low-energy heavy ions
[DE83-016709] N84-12934
ENERGY POLICY
Optimum engine for methanol utilization
[PB83-239459] N84-12507
Heating with wind energy, part B
[BMFT-FB-T-83-131-PT-B] N84-12651
ENERGY REQUIREMENTS
Evaluation of a total energy-rate sensor on a transport airplane
[NASA-TP-2212] N84-12164
Coronal heating by waves N84-13068
ENERGY SPECTRA
Uses of synchrotron radiation
[DE83-014431] N84-12720
Monte Carlo calculations of neutron and gamma-ray energy spectra for fusion-reactor shield design: Comparison with experiment
[DE83-016932] N84-12956
Voyager measurements of the energy spectrum, charge composition, and long term temporal variations of the anomalous components in 1977-1982 N84-13100
Evolution of the ultra high energy cosmic ray spectron by transport equation
[DE83-013711] N84-13132
ENERGY STORAGE
GSFC flywheel status N84-12230
Electrical power trade-offs N84-12232
Space station control requirements and flywheel system weights for combined momentum and energy storage N84-12236
Combined attitude control and energy storage N84-12237
Flywheel electronics N84-12239
Annular Momentum Control Device (AMCD) N84-12241
Magnetic bearings for inertial energy storage N84-12242
Advanced Control and Power System (ACAPS) technology program N84-12243
Power system considerations and test activities N84-12244
Assessment of potential for batteries in space applications N84-12246
Some comments on longevity by a technologist N84-12247
Alternate propulsion energy sources
[AD-A131939] N84-12249
Progress in developing repetitive pulse systems utilizing inductive energy storage
[DE83-015167] N84-12388
Storage of energy in magnetic field of superconductive coils
[AD-A131898] N84-12636
Fourth International Conference on Photochemical Conversion and Storage of Solar Energy
[DE83-014760] N84-12638
Initial operation of the compressed air experiment at Pittsfield, Illinois
[DE83-016930] N84-12643
Thermochemical energy systems research
[DE83-012132] N84-12644
ENERGY TECHNOLOGY
Assessment of potential for batteries in space applications N84-12246
ENERGY TRANSFER
Time-resolved laser studies on the energy transfer and the configurational changes in bacteriohodopsin
[DE83-015708] N84-12487
Thermochemical energy systems research
[DE83-012132] N84-12644
Study of vibrational energy transfer at a surface by a time-of-flight method
[AD-A131798] N84-12833
High temperature gas energy transfer
[AD-A131782] N84-12836
Study of excited state energy transfer processes
[AD-A131777] N84-12837
Modeling of transient disturbances in coronal-streamer configurations N84-13119
ENGINE AIRFRAME INTEGRATION
Engine/airframe interference N84-12085
Engine-airframe interference effects N84-12086
Engine/airframe interference drag at cruise conditions, using propulsion simulation
[NLR-TR-82012-U] N84-12098
ENGINE CONTROL
Integration of Fire Control, Flight Control and Propulsion Control Systems
[AGARD-CP-349] N84-12056
Integration of fire, flight and propulsion control systems: An overview, retrospective and prospective N84-12057
Application of flight controls technology to engine control systems N84-12061
The relations between the numerical control of the engine and other aircraft functions N84-12062
Full authority digital electronic engine controls and their integration with flight control systems in VSTOL aircraft N84-12064
The integration of flight and engine control for VSTOL aircraft N84-12070
ENGINE DESIGN
APU operational efficiency N84-12181
All-electric accessory drive systems: Implications on engine design and performance N84-12184
Analytical design of a liquid hydrogen fueled turbofan-ramjet engine for flight Mach numbers zero to five N84-12187
Executive summary, aerothermal modeling program, phase 1
[NASA-CR-174602] N84-12263
Aerothermal modeling program, phase 1
[NASA-CR-168243-VOL-1] N84-12264
Aerothermal modeling program, phase 1
[NASA-CR-168243-VOL-2] N84-12265
Optimum engine for methanol utilization
[PB83-239459] N84-12507
ENGINE PARTS
Development of strain tolerant thermal barrier coating systems, tasks 1 - 3
[NASA-CR-168251] N84-12312
ENGINE STARTERS
Hot gas APU starter for advanced aircraft applications N84-12178
A jet fuel starter for lowest system life cycle cost N84-12179
Cost efficient on board power for airline operation N84-12180
ENGINE TESTS
150 hour engine test of corrosion inhibited MIL-L-23699C oil
[AD-A131633] N84-12317
ENGINEERING MANAGEMENT
DRAMIN: Transferring data from the Applicon graphic system to A DRAM input file user guide
[DE83-018235] N84-12753
ENGLISH CHANNEL
Two different aspects of phytoplankton bloom seen by satellite (CZCS) in the western English Channel --- coastal zone color scanner (CZCS) N84-12804
ENTHALPY
Enthalpy - improved dielectric insulation for superconducting wires
[AD-A131857] N84-12316
ENVIRONMENT EFFECTS
Ground and inflight operational effects of APU's N84-12182

Scale modelling and full scale measurement techniques with particular reference to antennas in their operational environments N84-12368
Operational utilization of remote sensing in a study of the impact of disposal of urban waste at sea N84-12611
Development of a data base for carbon dioxide releases resulting from conversion of land to agricultural uses [DE83-015728] N84-12626
Activities report of the Laboratory of Environmental Physics and Chemistry N84-12963

ENVIRONMENT POLLUTION
Advanced technologies for the recovery, disposal, and reuse of carbon dioxide for atmospheric control [DE83-016371] N84-12256

ENVIRONMENT PROTECTION
Two types of values and their assessment by the collective interest [DE83-012064] N84-13031

ENVIRONMENT SIMULATION
The hydraulic multiaxes vibrator: Its capabilities to simulate real mechanical environments and to verify aerospace structures N84-12198

ENVIRONMENTAL CONTROL
To quench our thirst: The present and future status of freshwater resources of the United States, part 3 [DE83-016791] N84-12625
NBS (National Bureau of Standards) Workshop: Environmental Control for Archival Records Storage [PB83-242230] N84-13026

ENVIRONMENTAL MONITORING
Development of instrumentation for monitoring carbon fiber emission [PB83-233726] N84-12460
Remote Sensing Applications for Environmental Studies — conferences [ESA-SP-168] N84-12579
Use of remote sensing methods for the ecological mapping project of the European community N84-12580
Application of high resolution satellite data to coastal zones: SPOT simulations during ecological survey of the Britanny coast N84-12591
Inventoring and monitoring of landscape as a natural and cultural resource N84-12594
An operational remote sensing methodology for the detection, inventory and environmental monitoring of waste disposal sites N84-12601
Satellite remote sensing, environmental monitoring and the offshore oil and gas industries N84-12603
TRAN-STAT (statistics for environmental studies). Issue no. 24: Field sampling designs, simple random and stratified random sampling [DE83-016826] N84-12803

ENVIRONMENTAL TESTS
Aircraft transparency testing methodology and evaluation criteria. Part 2: Methodology development for improved durability [AD-A131928] N84-12157
Aircraft transparency testing methodology and evaluation criteria. Part 1: Test methods and information analysis [AD-A131927] N84-12158

EPITAXY
Clustering and ordering in 3-5 alloys [AD-A131785] N84-12974

EPOXY COMPOUNDS
Polymers of phosphonylmethyl-2,4- and -2,6-diamino benzenes and the like [NASA-ARC-11506-1] N84-12313

EPOXY MATRIX COMPOSITES
An X-ray radiography study of delamination growth in notched carbon/epoxy laminates [FFA-TN-1983-29] N84-12516

EQUATIONS OF MOTION
Dynamic analysis of the fluidyne [DE83-017283] N84-12500
Numerical solution of the three-dimensional unsteady Euler equations [AD-A132034] N84-12783

EQUATIONS OF STATE
Piston-displacement equations of state for sodium, potassium, and rubidium metals to 20 kbar from 300 K to 4 K [DE83-016079] N84-12252
Lithium equation-of-state [DE83-017988] N84-12253
Equations of state for the alkali metals, with generalizations to NaCl [DE83-018075] N84-12260
Zero-dimensional model of compressible gas flow in networks of pressure vessels: Program TRIC [DE83-017121] N84-12431

EQUILIBRIUM
Three-dimensional equilibrium in quadrupole symmetric tandem mirrors in the paraxial limit (reduced MHD) [DE83-017840] N84-12940

ERBIUM
Temperature dependence of the electric-field gradient in Er metal [DE83-015564] N84-12989

ERGODIC PROCESS
Kingman's subadditive ergodic theorem [AD-A131795] N84-12801

EROSION
Solid impingement erosion mechanisms and characterization of erosion resistance of ductile metals [NASA-TM-83492] N84-12287

ERROR DETECTION CODES
Perkin-Elmer, Perkin-Elmer 3230 COBOL R07 (pre-release) [PB83-238600] N84-12766

ERRORS
Improving NDE (Non-destructive evaluation) capability through multiple inspection with application to gas turbine engine disks [AD-A131762] N84-12509

ESTIMATES
Estimation of uncertainty in coal resources [DE83-902538] N84-12620
Asymptotic maximal deviation of m-smoothers [AD-A131906] N84-12799

EULER EQUATIONS OF MOTION
Vortex flow simulations past wings using the Euler-equations N84-12118
Numerical solutions of the Euler equations simulating vortex flows around wings N84-12120

EUROPE
Use of remote sensing methods for the ecological mapping project of the European community N84-12580
Considerations on a permanent inventory and monitoring system for European forests N84-12582

EUROPEAN AIRBUS
Ground and inflight operational effects of APU's N84-12182

EUTECTICS
Stress production and relief in the gold/silicon eutectic die-attach process [DE83-015230] N84-12400

EVALUATION
Two types of values and their assessment by the collective interest [DE83-012064] N84-13031

EVENTS
Periodicities in the occurrence of aurora as indicators of solar variability N84-13093

EVOKED RESPONSE (PSYCHOPHYSIOLOGY)
Utility of the cortical evoked response as a measure of photographic image quality [AD-A131679] N84-12455

EVOLUTION (DEVELOPMENT)
Dynamical evolution of substucture in molecular clouds N84-13043
The chemical evolution of the coma of comet P/Stephan-Oterma N84-13055

EXCITATION
Unipolar machine with superconductive excitation winding [AD-A131820] N84-12383
Experiments to study the feasibility of making an X-ray laser at the Novette laser facility [DE83-015615] N84-12476
RF conditioned dc discharges for excitation of rare gas halide lasers [DE83-016537] N84-12479
Absolute collisional excitation cross section measurements using crossed molecular beams [AD-A132038] N84-12830
Study of excited state energy transfer processes [AD-A131777] N84-12837

EXERCISE PHYSIOLOGY
A laboratory comparison of portable cooling systems for workers exposed to two levels of heat stress [AD-A131848] N84-12423
Effects of pulsed microwaves at 1.28 and 5.62 GHz on Rhesus monkeys (Macaca mulatta) performing an exercise task at three levels of work [AD-A132057] N84-12704
A restraint chair with rowing-like movement for exposing exercising nonhuman primates to microwave irradiation [AD-A132047] N84-12705

EXHAUST EMISSION
A study of the relationship between exhaust emissions and fuel economy [PB83-235564] N84-12506

EXHAUST GASES
Infrared characteristics of gas plumes [AD-A131796] N84-12269

EXHAUST SYSTEMS
Use of the one-dimensional theory of the filament of flow for the interpretation and synthesis of mufflers in exhaust pipes of internal combustion engines [REPT-81.4] N84-12494

EXHAUST VELOCITY
Investigation of a pulsed electrothermal thruster [NASA-CR-168266] N84-12227

EXOBIOLOGY
Aerospace Medicine and Biology: A continuing bibliography with indexes (supplement 250) [NASA-SP-7011(250)] N84-12712

EXPANDABLE STRUCTURES
Seamless collapsible fuel tanks [AD-A131933] N84-12496

EXPERIMENT DESIGN
Low gravity experiment for studying a rotating fluid having a free surface [NASA-CR-170923] N84-12413

EXPLOSIONS
Initial decay of flow properties of planar, cylindrical and spherical blast waves [UTIAS-TN-244] N84-12416

EXPLOSIVE DEVICES
Using an X-ray-sensitive vidicon and remote-control stage mechanism to obtain critical radiographic alignment of small explosive devices [DE83-012846] N84-12326

EXPONENTS
On Waring's problem g (4) or = 20 N84-12781

EXTERNAL STORES
External stores interference N84-12083

EXTINCTION
Optical extinction coefficients beneath marine stratus clouds. Comparison of coefficients calculated from observed aerosol spectra with coefficients specified by the Navy aerosol model [AD-A132011] N84-12685

EXTRAPOLATION
Weighted nonparametric tail estimation procedures [DE83-017870] N84-12804

EXTREMELY HIGH FREQUENCIES
Dielectric loss measurement at millimetre wave frequencies using an untuned cavity [RSRE-3597] N84-12379
Observations and classifications with a 35/94 GHz radiometer of terrain near Motala, Sweden, July 1982 [FOA-C-30325-E1,E3] N84-12630

EXTREMELY LOW FREQUENCIES
Eruption of permanent dentition in rhesus monkeys exposed to ELF (Extremely low frequency) fields [AD-A132065] N84-12703

EYE (ANATOMY)
An age comparison of the vestibulo-ocular counterroll reflex [AD-A132064] N84-12716
Vestibulo-ocular reflex gain in man during active versus passive oscillation and the influence of voluntary gaze-control tasks [AD-A132006] N84-12717

F

F-4 AIRCRAFT
Development and flight test of an active flutter suppression system for the F-4F with stores. Part 3. Flight demonstration of the active flutter suppression system [AD-A131972] N84-12191

F-16 AIRCRAFT
F-16 Penguin anti-ship missile integration N84-12059

FABRICATION
A balloon design for 9000 pounds at 90,000 feet: Recommendations based on heavy-load balloon history [AD-A131987] N84-12093
Walk-through survey report: Control technology for integrated circuit fabrication, Xerox Corporation, El Segundo, California [PB83-239053] N84-12333
Seamless collapsible fuel tanks [AD-A131933] N84-12496
Ultra low loss optical fiber cable assemblies, volume 1 [AD-A132007] N84-12892
Fabrication and properties of multilayer structures [AD-A131934] N84-12969
A program of research on microfabrication techniques for VLSI magnetic devices [AD-A131706] N84-12978

FABRY-PEROT INTERFEROMETERS
OI 630.0 nm optical measurements of neutral winds, temperatures and airglow enhancements during the BIME program [AD-A131695] N84-12671
Ultrasensitive optical rotation and refractive-index measurements [DE83-018078] N84-12903

FACTOR ANALYSIS
The analysis of crack growth data with application to trip steel
[AD-A132021] N84-12535
FACTORIAL DESIGN
On the performance of two-stage group screening experiments
[AD-A131970] N84-12807
FADDEEV EQUATIONS
Minimal unitary (covariant) scattering theory
[DE83-014896] N84-12849
Covariant theory with a confined quantum
[DE83-014897] N84-12850
FAILURE
Development in reliability models and methods
[DE83-014683] N84-12511
FAILURE ANALYSIS
Review of aircraft crash structural response research
[AD-A131696] N84-12160
Replacement of PBNA in HB and HC polymers used in SRM propellant and liner
[NASA-CR-170936] N84-12311
Failure processes in elastomers at or near a rigid spherical inclusion
[AD-A132060] N84-12314
FAILURE MODES
Multiplane finite element method: Applications to fiber reinforced material N84-12261
FALLING
Bibliography of coefficient of friction literature relating to slip type accidents --- slipping accidents
[PB83-243626] N84-12334
FALLING SPHERES
Topically classified bibliography on shapes of falling drops, drops in electric fields and related topics
[AD-A131134] N84-12417
FAR FIELDS
The effect of wing tip devices on the far-field wake of a Paris Aircraft N84-12131
FAR ULTRAVIOLET RADIATION
Studies of collisional and nonlinear radiative processes for development of coherent UV and XUV sources
[AD-A131837] N84-12467
FARMLANDS
Relating spatial patterns in image data to scene characteristics N84-12573
FATIGUE (BIOLOGY)
Physical fitness as a moderator of cognitive degradation during sleep deprivation
[AD-A131962] N84-12718
Experimental studies relating environmental lighting and flicker to visual fatigue in VDT operators
[DE83-016316] N84-12738
FATIGUE (MATERIALS)
Composite structural materials
[NASA-CR-174597] N84-12257
Fatigue of fiber composites
[FFA-TN-1983-30] N84-12260
Accelerated compatibility testing using corrosion fatigue techniques
[DE83-015104] N84-12296
A review of Australian investigations on aeronautical fatigue during the period April 1981 to March 1983
[AD-A130968] N84-12532
Inference of fatigue-crack closure stresses from ultrasonic-transmission measurements
[DE83-017684] N84-12547
Evaluation of the crack gage as an advanced individual aircraft tracking concept N84-12551
FATIGUE LIFE
Fatigue of fiber composites
[FFA-TN-1983-30] N84-12260
FATIGUE TESTS
A review of Australian investigations on aeronautical fatigue during the period April 1981 to March 1983
[AD-A130968] N84-12532
FAULT TOLERANCE
A fault-tolerant distributed computer network design and analysis for an integrated flight control system N84-12189
FEASIBILITY ANALYSIS
A simulator evaluation of an automatic terminal approach system N84-12037
L band satellite communication experiment in the Antartic
[ESA-TT-805] N84-12356
A thousand TeV in the center of mass: Introduction to high-energy storage rings
[DE83-015649] N84-12855
FEED SYSTEMS
Constant-output atomizer --- Inhalation therapy and aerosol research
[NASA-CASE-MFS-25631-1] N84-12406
FEEDBACK CONTROL
Development of instrumentation for monitoring carbon fiber emission
[PB83-233726] N84-12460
FERRIC IONS
Iron charge states observed in the solar wind N84-13112
Spatial variation of iron abundance in the high speed solar wind, 1972 to 1976 N84-13113
FERROMAGNETIC MATERIALS
Muon spin relaxation in ferromagnetic PdMn
[DE83-012659] N84-12979
FERROMAGNETISM
Universality and fractal dimension of mode locking structure in systems with competing periodicities
[DE83-017352] N84-12545
FIBER COMPOSITES
Fatigue of fiber composites
[FFA-TN-1983-30] N84-12260
FIBER OPTICS
Prototype fiber optic system to remote TRACALS radar
[AD-A132073] N84-12341
Novel optical pin using microballoons
[DE83-015222] N84-12391
Real-time attenuation of heated optical fibers in a nuclear reactor
[DE83-015141] N84-12873
Ultra low loss optical fiber cable assemblies, volume 2
[AD-A132008] N84-12891
Ultra low loss optical fiber cable assemblies, volume 1
[AD-A132007] N84-12892
Evaluation of multicomponent fluoride glass candidates for double crucible drawn optical fiber
[AD-A131932] N84-12893
Process, product, and waste-stream monitoring with fiber optics
[DE83-01102] N84-12899
Atenuation measurements between 840 and 1620 nm on an optical cable in Berlin
[FI-465-TBR-22] N84-12906
Economic study of long distance optical fibre links
[FUB-38-1982] N84-12908
FIBER REINFORCED COMPOSITES
Review of aircraft crash structural response research
[AD-A131696] N84-12160
Composite structural materials
[NASA-CR-174597] N84-12257
Multiplane finite element method: Applications to fiber reinforced material N84-12261
FIELD EFFECT TRANSISTORS
Unipolar machine with superconductive excitation winding
[AD-A131820] N84-12383
The study of thin films on semi-insulating gallium arsenide by ellipsometry
[AD-A131844] N84-12972
FIELD OF VIEW
Electron beam trajectory in a photometer field of view
[AD-A131949] N84-12831
FIELD THEORY (PHYSICS)
Commensurability, chaos, and the devil's staircase
[DE83-013280] N84-12987
FIGHTER AIRCRAFT
Some aspects of flight trajectory control in future avionic systems for combat aircraft N84-12066
Special Course on Subsonic/Transonic Aerodynamic Interference for Aircraft
[AGARD-R-712] N84-12072
Subsonic/transonic viscous interactions N84-12075
Transonic configuration design (fighter) N84-12082
Experimental investigation of forebody and wing leading-edge vortex interactions at high angles of attack N84-12110
Augmentation of fighter-aircraft performance by spanwise blowing over the wing leading edge N84-12133
Secondary power systems for fighter aircraft experiences today and requirements for a next generation N84-12171
Super integrated power unit for fighter aircraft N84-12183
FILE MAINTENANCE (COMPUTERS)
Review of the ANSI metafile and virtual device interface standardization activities
[DE83-015925] N84-12737
Praxis language environment: Distribution-package description
[DE83-017546] N84-12750
DRAMIN: Transferring data from the Applicon graphic system to A DRAM input file user guide
[DE83-018235] N84-12753
FILM CONDENSATION
Numerical solution of the two-phase, three dimensional boundary layer in laminar film condensation over a curved surface N84-12442
FILMS
Tailoring polymer films for solar-collection use, phase 1
[DE83-018117] N84-12640
FILTRATION
Method for treating wastewater using microorganisms and vascular aquatic plants
[NASA-CASE-NSTL-10] N84-12654
FINANCIAL MANAGEMENT
Develop a normative or descriptive model of the international/domestic civil aviation industry. Volume 1: Executive summary
[AD-A131876] N84-12053
Activities report of the aerospace industry in West Germany N84-12139
Activities report of the aerospace industry in West Germany N84-12140
FINITE DIFFERENCE THEORY
Computational methods for subsonic and transonic aerodynamic design N84-12074
Vortex flow simulations past wings using the Euler-equations N84-12118
Numerical solution of the two-phase, three dimensional boundary layer in laminar film condensation over a curved surface N84-12442
Interaction of stress waves and cracks using a second order accurate finite difference method N84-12522
GRIDPACK: Toward unification of general grid programming
[AD-A131692] N84-12746
FINITE ELEMENT METHOD
Multiplane finite element method: Applications to fiber reinforced material N84-12261
Stress production and relief in the gold/silicon eutectic die-attach process
[DE83-015230] N84-12400
Analytical prediction of aerothermal environment in a wing-elevon cove --- space shuttle orbiter
[NASA-TM-85711] N84-12412
Numerical simulation of plastic fluids
[DE83-007911] N84-12424
Practical computation of multidimensional thermal flows in a gas centrifuge
[DE83-005697] N84-12426
Buckled plate vibrations, large amplitude vibrations and nonlinear flutter of elastic plates using high-order triangular finite elements N84-12523
A comparison of finite-element predictions and experimental data for the forced response of the DOE 100 kW vertical-axis wind turbine
[DE83-012624] N84-12537
Adaptive finite element methods for parabolic partial differential equations
[NASA-CR-174490] N84-12727
Using PAFEC as a preprocessor for COSMIC/NASTRAN
[DE83-017179] N84-12755
Design, development and use of the finite element machine
[NASA-CR-172250] N84-12777
A thin-walled beam finite element
[TT-8302] N84-12779
Lecture notes for contact-impact algorithms for large-deformation finite-element analysis
[DE83-013039] N84-12789
FINS
Some results from a programme of research into the structure of vortex flow fields around missile shapes N84-12111
FIRE CONTROL
Integration of Fire Control, Flight Control and Propulsion Control Systems
[AGARD-CP-349] N84-12056
Integration of fire, flight and propulsion control systems: An overview, retrospective and prospective N84-12057
Hypervelocity missile: Based on the concept of aircraft/missile integration for maximum firepower N84-12058
F-16 Penguin anti-ship missile integration N84-12059
Integration of fire control, navigation system and head up display N84-12060
A nonlinear control law for piloting aircraft in the air-to-ground attack phase N84-12071
FIRES
Correlation of laboratory-scale fire test methods for seat blocking layer materials with large-scale test results
[AD-A131666] N84-12138
FISCHER-TROPSCH PROCESS
New approach to the generation of metal-bearing, medium-pore, shape-selective zeolites for Fischer-Tropsch catalysis: Spectroscopic studies of zeolites
[DE83-014344] N84-12254
FISHERIES
Introductory studies of natural contamination and manmade pollution in Danish waters N84-12608

FIXED WINGS
Application of the small body pressure transducer [AD-A131733] N84-12454
FLAME PROPAGATION
Flame acceleration mechanisms under conditions of partial confinement [PB83-244012] N84-12328
Theoretical and experimental investigation of turbulent premixed flames N84-12409
FLAME RETARDANTS
Polymers of phosphonylmethyl-2,4- and -2,6-diamino benzenes and the like [NASA-ARC-11506-1] N84-12313
FLAME TEMPERATURE
Laser spectroscopy of propellant-like flames [AD-A132042] N84-12267
FLAMES
Soot formation from polycyclic aromatics [DE83-009750] N84-12271
FLANGES
Hermetically sealed microminiature multisocket connector [DE83-017484] N84-12503
FLAT PLATES
Aspects of second- and third-order panel methods demonstrated for the two-dimensional flat plate problem [NLR-TR-81074-U] N84-12433
FLEXIBILITY
Control of flexible spacecraft by optimal model following N84-12222
FLEXING
Unidirectional flexural pivot [NASA-CASE-GSC-12622-1] N84-12492
FLICKER
Experimental studies relating environmental lighting and flicker to visual fatigue in VDT operators [DE83-016316] N84-12738
FLIGHT CHARACTERISTICS
Simulator study of flight characteristics of a large twin-fuselage cargo transport airplane during approach and landing [NASA-TP-2183] N84-12190
FLIGHT CONTROL
Controls, Displays, and Information Transfer for General Aviation IFR Operations [NASA-CP-2279] N84-12029
Analysis of general aviation single-pilot IFR incident data obtained from the NASA Aviation Safety Reporting System N84-12033
Integration of Fire Control, Flight Control and Propulsion Control Systems [AGARD-CP-349] N84-12056
Integration of fire, flight and propulsion control systems: An overview, retrospective and prospective N84-12057
Hypervelocity missile: Based on the concept of aircraft/missile integration for maximum firepower N84-12058
Integration of fire control, navigation system and head up display N84-12060
Application of flight controls technology to engine control systems N84-12061
Integrated powerplant control systems and potential performance benefits N84-12063
Full authority digital electronic engine controls and their integration with flight control systems in VSTOL aircraft N84-12064
Design and development of the multifunction flight control reference system N84-12065
Some aspects of flight trajectory control in future avionic systems for combat aircraft N84-12066
A diagnosis scheme for sensors of a flight control system using analytic redundancy N84-12067
The integration of flight and engine control for VSTOL aircraft N84-12070
A nonlinear control law for piloting aircraft in the air-to-ground attack phase N84-12071
Hydraulic generation of auxiliary power for the Mirage 2000 aircraft N84-12176
A fault-tolerant distributed computer network design and analysis for an integrated flight control system N84-12189
FLIGHT INSTRUMENTS
Single pilot IFR program overview and status N84-12030
Pilot controls and SPIRF flight N84-12038
Single pilot scanning behavior in simulated instrument flight N84-12041
FLIGHT PATHS
Airport capacity alternatives N84-12149
FLIGHT SAFETY
The National Airspace System N84-12146
Technology and the future evolution of the ATC system N84-12148
FLIGHT SIMULATION
Single pilot IFR program overview and status N84-12030
Single pilot scanning behavior in simulated instrument flight N84-12041
A simulator evaluation of a rate-enhanced instrument landing system display N84-12042
FLIGHT STABILITY TESTS
Development and flight test of an active flutter suppression system for the F-4F with stores. Part 3. Flight demonstration of the active flutter suppression system [AD-A131972] N84-12191
FLIGHT TESTS
Advanced symbology for general aviation approach to landing displays N84-12039
An overview of the demonstration advanced avionics system guest pilot evaluation conducted at Ames Research Center N84-12049
Flight tests for a strapdown system (MSS): The results of a special flight test [ESA-TT-818] N84-12153
Development and flight test of an active flutter suppression system for the F-4F with stores. Part 3. Flight demonstration of the active flutter suppression system [AD-A131972] N84-12191
Radar investigation of soils and sea (ERASME): C band helicopter-borne scatterometer. Application to soil moisture measurement N84-12588
FLOOD PLAINS
Major water conservation and reclamation projects in the Jianghan Plain and surroundings, Hubei Province, China — Landsat imagery N84-12593
FLOODS
Poststorm reconnaissance of Tropical Storm Chris [AD-A131948] N84-12688
FLORIDA
Identifying environmental features for land management decisions [E84-10016] N84-12556
FLOW CHARACTERISTICS
On the generation and subsequent development of spiral vortex flow over a swept-back wing N84-12105
Executive summary, aerothermal modeling program, phase 1 [NASA-CR-174602] N84-12263
Aerothermal modeling program, phase 1 [NASA-CR-168243-VOL-1] N84-12264
Aerothermal modeling program, phase 1 [NASA-CR-168243-VOL-2] N84-12265
Analytical prediction of aerothermal environment in a wing-elevon cove — space shuttle orbiter [NASA-TM-85711] N84-12412
Initial decay of flow properties of planar, cylindrical and spherical blast waves [UTIAS-TN-244] N84-12416
FLOW DISTRIBUTION
Acta Aeronautica et Astronautica Sinica [AD-A131828] N84-12055
An experimental investigation of separated three dimensional flow on general aviation twin-engine aircraft N84-12087
An experimental investigation of the vortex flow over delta and double-delta wings at low speed N84-12106
Laser velocimetry study of compressibility effects on the flow field of a delta wing N84-12108
Experimental investigation of forebody and wing leading-edge vortex interactions at high angles of attack N84-12110
Some results from a programme of research into the structure of vortex flow fields around missile shapes N84-12111
Separation and vortical-type flow around a prolate spheroid: Evaluation of relevant parameters N84-12113
On the generation of vortical flow at hypersonic speeds over elliptical cones N84-12114
Theoretical modelling of three-dimensional vortex flows in aerodynamics N84-12116
Vortex flow simulations past wings using the Euler-equations N84-12118
Combustion jet ignition N84-12186
Laser velocimeter measurements and analysis in turbulent flows with combustion, part 2 [AD-A131882] N84-12421
FLOW EQUATIONS
Calculation of unsteady flow in tubes of combustion engines with special regard to multiple branching [REPT-82.8] N84-12410
FLOW GEOMETRY
Magnetohydrodynamic modeling of coronal structure and expansion N84-13081
FLOW STABILITY
Vortex stability and breakdown N84-12122
The break-up mechanism of a streamwise directed vortex N84-12123
Vortex breakdown: A two-stage transition N84-12124
Experimentation with turbulent flows experiencing the effects of an adverse pressure gradient N84-12127
Waves on vortex cores and their relation to vortex breakdown N84-12128
Flame acceleration mechanisms under conditions of partial confinement [PB83-244012] N84-12328
FLOW THEORY
Use of the one-dimensional theory of the filament of flow for the interpretation and synthesis of mufflers in exhaust pipes of internal combustion engines [REPT-81.4] N84-12494
FLOW VELOCITY
Observational constraints on solar wind acceleration mechanisms N84-13078
FLOW VISUALIZATION
Instabilities in trailing vortices: Flow visualization using hot-wire anemometry N84-12103
Visualization of vortical type flows in three dimensions N84-12107
Viscous three-dimensional flow separations from high-wing propeller-turbine nacelle models N84-12115
Advanced diagnostics and instrumentation for chemically reactive flow systems [AD-A131814] N84-12251
FLOWMETERS
Helium-flow measurement using ultrasonic technique [DE83-017765] N84-12826
FLUID DYNAMICS
Aerodynamic design for overall vehicle performance N84-12077
Waves on vortex cores and their relation to vortex breakdown N84-12128
Space station attitude control system concept and requirements N84-12234
Rising bubbles [AD-A131572] N84-12418
Dense molecular thermodynamics [DE83-015216] N84-13006
Role of thermal conduction in the acceleration of the solar wind N84-13079
FLUID FLOW
Aerodynamics of Vortical Type Flows in Three Dimensions [AGARD-CP-342] N84-12099
Vortex breakdown: A two-stage transition N84-12124
A contribution to the problem of vortex breakdown N84-12125
Numerical simulation of vortex breakdown by the vortex-filament method N84-12126
Mechanical response of fluid-filled poroelastic solids N84-12525
On the growth of gravity-capillary waves by wind [KNMI-WR-83-10] N84-12698
FLUID MECHANICS
Special Course on Subsonic/Transonic Aerodynamic Interference for Aircraft [AGARD-R-712] N84-12072
Computational synergetics and innovation in wave, vortex, and plasma cloud dynamics [DE83-015252] N84-12928
FLUID-SOLID INTERACTIONS
Recent studies at NASA-Langley of vortical flows interacting with neighboring surfaces N84-12109
FLUIDIZED BED PROCESSORS
Fluidized bed gasification of biomass to methane [NASA-CASE-NPO-15903-1] N84-12635
FLUORESCENCE
Comparison of technologies for new energy-efficient lamps [DE83-015949] N84-12401
Chemiluminescence and laser induced fluorescence of boron atom reactions [AD-A131709] N84-12471
FLUORIDES
Evaluation of multicomponent fluoride glass candidates for double crucible drawn optical fiber [AD-A131932] N84-12893
FLUTTER
Development and flight test of an active flutter suppression system for the F-4F with stores. Part 3. Flight demonstration of the active flutter suppression system [AD-A131972] N84-12191
FLUTTER ANALYSIS
Aeroelastic analysis for propellers - mathematical formulations and program user's manual [NASA-CR-3729] N84-12530
FLUX (RATE)
Conceptual design of the high-flux VTA-2 test assembly for FMIT [DE83-017022] N84-12935
FLUX DENSITY
Assessment of potential for batteries in space applications N84-12246
Some comments on longevity by a technologist N84-12247

Quark-gluon plasma formation
[DE83-017742] N84-12861

FLYING PLATFORMS
Orbiting geophysics laboratory experiment
[AD-A131950] N84-12218

FLYWHEELS
Integrated Flywheel Technology, 1983
[NASA-CP-2290] N84-12228
Integrated Power/Attitude Control System (IPACS) N84-12229
GSFC flywheel status N84-12230
Overview of state-of-the-art flywheel technology N84-12231
Electrical power trade-offs N84-12232
Space station energy sizing N84-12233
The Boeing flywheel study N84-12235
Space station control requirements and flywheel system weights for combined momentum and energy storage N84-12236
Combined attitude control and energy storage N84-12237
IPACS attitude control technology considerations N84-12238
Flywheel electronics N84-12239
Advanced Control and Power System (ACAPS) technology program N84-12243
Power system considerations and test activities N84-12244
Some comments on longevity by a technologist N84-12247
New developments in composite-flywheel containment
[DE83-012583] N84-12497

FOCUSING
Design of doubly focusing, tunable (5 - 30 keV), wide-bandpass optics made from layered synthetic microstructures
[DE83-015492] N84-12897
Light-ion-beam fusion
[DE83-018263] N84-12944

FOKKER-PLANCK EQUATION
New soluble approximation to Fokker-Planck equations
[DE83-016210] N84-12791
Fokker-Planck equation in mirror research
[DE83-016568] N84-12932

FORBUSH DECREASES
Interplanetary perturbations associated with type 4 solar flares
[IFSI-82-6] N84-13129

FOREBODIES
Experimental investigation of forebody and wing leading-edge vortex interactions at high angles of attack N84-12110

FORECASTING
Develop a normative or descriptive model of the international/domestic civil aviation industry. Volume 1: Executive summary
[AD-A131876] N84-12053
Domestic scheduled air transport for the year 2000. Financial and capacity related effects of supply alternatives, considering, also, the cooperation with high speed rail transport services --- West Germany
[DFVLR-FB-83-03] N84-12141
Airport and air traffic control system. Executive summary N84-12144
Aviation growth scenarios N84-12147
Policy implications N84-12150
Why didn't Box-Jenkins win (again)?
[DE83-014043] N84-12802

FOREIGN BODIES
Vibration response of geometrically nonlinear elastic beams to pulse and impact loading
[NASA-CR-174495] N84-12527

FOREST MANAGEMENT
Considerations on a permanent inventory and monitoring system for European forests N84-12582
SAR 580: Images for agricultural and forest survey. First results in middle Belgium N84-12595
Inventory of Flemish forests using medium-scale Color Infrared (CIR) photography and CIR orthophotoplans as base for a forest management data bank N84-12614

FORESTS
Relating spatial patterns in image data to scene characteristics N84-12573
Remote Sensing Applications for Environmental Studies --- conferences
[ESA-SP-188] N84-12579
Considerations on a permanent inventory and monitoring system for European forests N84-12582
First results of the evaluations of the European SAR 580 data for agricultural and forestry purposes in test site D6, Freiburg (West Germany) N84-12599
Detecting long-term ecological effects in forests and food chains
[DE83-003469] N84-12655

FORMULAS
Polymers of phosphonylmethyl-2,4- and -2,6-diamino benzenes and the like
[NASA-ARC-11506-1] N84-12313

FORMULAS (MATHEMATICS)
The analysis of crack growth data with application to trip steel
[AD-A132021] N84-12535

FORTRAN
A generalized computer code for developing dynamic gas turbine engine models (DIGTEM)
[NASA-TM-83508] N84-12166
Assembly language graphics library (EGR1.LB) with Fortran interfacing
[PB83-239624] N84-12757
Compute. Sciences Corporation UNIVAC 1100/80 CSTS FORTRAN, release FTN148
[PB83-243428] N84-12763
On the performance of two-stage group screening experiments
[AD-A131970] N84-12807
The computerization of material safety data sheet information
[AD-A131992] N84-13021

FOULING
Structure of convective surface deposits and effect on MHD steam-plant design
[DE83-010757] N84-12931

FOURIER ANALYSIS
Acquisition, image and data compression
[AD-A131923] N84-12344
Nonlinear dynamics and control of a vibrating rectangular plate
[NASA-CR-172215] N84-12528

FOURIER TRANSFORMATION
Self-correction coil: Operation mechanism of self-correction coil
[DE83-016324] N84-12392
Acoustic pulse scattering from impedance covered cylinders
[AD-A131653] N84-12822

FRACTURE MECHANICS
Composite structural materials
[NASA-CR-174597] N84-12257
Strain rate effects on ductile/brittle transitions in steels
[DE83-016906] N84-12308
Interaction of a dislocation with a crack
[AD-A131912] N84-12536
Mechanics of fracture under high-rate stress loading
[DE83-013770] N84-12544
On the dynamic fracture of bars, beams and plates N84-12552
Elastic-plastic fracture of cylindrical shells containing part-through circumferential cracks N84-12553

FRACTURE STRENGTH
Single specimen J-integral testing
[DE83-016069] N84-12543

FRACTURES (MATERIALS)
Electron-microscope observation of crack propagation and a dislocation model of fracture
[DE83-014623] N84-12540

FRACTURING
Microearthquakes induced during hydraulic fracturing at the Fenton Hill HDR site: The 1982 experiments
[DE83-014191] N84-12672

FRAGMENTATION
Mechanics of fracture under high-rate stress loading
[DE83-013770] N84-12544
Statistical calculation of complete events in medium-energy nuclear collisions
[DE83-015951] N84-12847

FRAMES
Plastic deformations of a portable frame under short pulse loading on one column by an approximate method including effects of elasticity and plastic rate sensitivity N84-12521

FRANCE
Contribution of satellite remote sensing to knowledge of the littoral from the mouth of the Loire to that of the Gironde (France) N84-12584
Application of high resolution satellite data to coastal zones: SPOT simulations during ecological survey of the Britanny coast N84-12591
Interpretability of wetland on SEASAT-A imagery in the polderland of Flanders: A structural approach N84-12597
Actual state and recent evolution of the French coast observed by remote sensing using LANDSAT recordings N84-12606

FREE CONVECTION
Steady laminar natural convection in open rectangular cavities N84-12441
Automated data reduction for optical interferometric data
[DE83-012075] N84-12457

FREE ELECTRON LASERS
Subharmonic buncher for the Los Alamos free-electron laser oscillator experiment
[DE83-015220] N84-12474
Electron-beam diagnostics for the Los Alamos free-electron oscillator experiment
[DE83-017230] N84-12481
Evolution of long pulses in a tapered wiggler free-electron laser
[DE83-017235] N84-12484
The Los Alamos free-electron-laser oscillator experiment: Plans and present status
[DE83-017290] N84-12485
Free-electron-laser research
[DE83-016957] N84-12489

FREE ENERGY
Review of some recent theoretical calculations of phase transitions and comparisons with experimental results
[DE83-015863] N84-12983

FREE RADICALS
Free-radical and ion chemistry of volatile silanes, germanes, and phosphines
[DE83-016389] N84-12277

FREQUENCY MODULATION
The simulation of a Frequency Shift Keying (FSK) diversity system
[DFVLR-FB-83-22] N84-12363

FREQUENCY SHIFT KEYING
The simulation of a Frequency Shift Keying (FSK) diversity system
[DFVLR-FB-83-22] N84-12363

FRICTION
Piston-displacement equations of state for sodium, potassium, and rubidium metals to 20 kbar from 300 K to 4 K
[DE83-018079] N84-12252
Use of superposition in calculating cooling requirements for circuit cards containing arrays of electronic components
[DE83-016091] N84-12428
A numerical study on the evolution of tornadoes N84-12679

FRICTION FACTOR
Unidirectional flexural pivot
[NASA-CASE-GSC-12622-1] N84-12492

FUEL CELL POWER PLANTS
Solid-oxide fuel-cell performance
[DE83-017926] N84-12396

FUEL CELLS
Solid-oxide fuel-cell performance
[DE83-017926] N84-12396

FUEL COMBUSTION
Combustion of EDS mid-distillate and refined shale-oil residual fuel in a gas turbine with large single-combustion chamber
[DE83-017700] N84-12281

FUEL CONSUMPTION
A study of the relationship between exhaust emissions and fuel economy
[PB83-235564] N84-12506

FUEL FLOW
Numerical simulations of fuel droplet flows using a Lagrangian triangular mesh
[NASA-CR-166263] N84-12411

FUEL INJECTION
Evaluation of unthrottled combustion system options for light duty applications with future syncrude derived fuels
[DE83-017047] N84-12327

FUEL OILS
Short-term energy outlook. Volume 2. Methodology
[DE83-016853] N84-12648

FUEL PRODUCTION
Fluidized bed gasification of biomass to methane
[NASA-CASE-NPO-15903-1] N84-12635
Vehicle-emission characteristics using mechanically emulsified alcohol/diesel fuels
[DE83-016012] N84-12656

FUEL TANKS
Seamless collapsible fuel tanks
[AD-A131933] N84-12496

FUNCTIONAL ANALYSIS
A computer subroutine for evaluating polygamma functions for complex arguments
[AD-A131936] N84-12744

FUNCTIONAL DESIGN SPECIFICATIONS
Layout of a SAR sensor for Spacelab and satellite. Part 1: Design considerations for fundamental SAR parameters
[ESA-TT-802] N84-12224
Space station attitude control system concept and requirements N84-12234
Influence of the airframe on the performance of antennas for avionics N84-12372
Space reactors: Past, present and future
[DE83-011177] N84-12870

FUNCTIONAL INTEGRATION
The relations between the numerical control of the engine and other aircraft functions N84-12062
FUNCTIONS
Design and development of the multifunction flight control reference system N84-12065
FUSELAGES
Vertical drop test of a transport fuselage center section including the wheel wells [NASA-TM-85706] N84-12531
FUSION REACTORS
Lithium equation-of-state [DE83-017966] N84-12253
Advanced high-field coil designs: 20 Tesla [DE83-017368] N84-12397
Feasibility of a laser or charged-particle-beam fusion-reactor concept with direct electric generation by magnetic-flux compression [DE83-015735] N84-12482
Tokamak fusion reactors with less than full tritium breeding [DE83-016711] N84-12936
Summary of the MARS tandem-mirror reactor design [DE83-017293] N84-12939
Nuclear design of a very-low-activation fusion reactor [DE83-017470] N84-12949
FUSION WEAPONS
Pulsed power bibliography. Volume 2: Annotated bibliography [AD-A131753] N84-12468
Pulsed power bibliography. Volume 1: Indices [AD-A131752] N84-12469

G

GALACTIC CLUSTERS
Faint galaxies in the Coma cluster: Luminosity function and spatial distribution N84-13053
GALACTIC NUCLEI
Photon damping in cosmic-ray acceleration in active galactic nuclei [DE83-011320] N84-13133
GALACTIC RADIATION
Photon damping in cosmic-ray acceleration in active galactic nuclei [DE83-011320] N84-13133
GALACTIC STRUCTURE
Simulations of galaxy mergers N84-13054
GALAXIES
Spherical simulations of large scale structure in the universe N84-13052
Faint galaxies in the Coma cluster: Luminosity function and spatial distribution N84-13053
GALERKIN METHOD
Adaptive finite element methods for parabolic partial differential equations [NASA-CR-174490] N84-12727
GALILEAN SATELLITES
Galilean satellite geomorphology [NASA-CR-174574] N84-13057
GALLIUM ARSENIDES
Surface and interfacial properties of Ga(0.47) In(0.53) As alloys [AD-A131925] N84-12970
The study of thin films on semi-insulating gallium arsenide by ellipsometry [AD-A131844] N84-12972
Growth and characterization of InP and InGaAs films using the hydride VPE technique [AD-A131841] N84-12973
GAMMA FUNCTION
A computer subroutine for evaluating polygamma functions for complex arguments [AD-A131936] N84-12744
GAMMA RAY ASTRONOMY
Cross sections relevant to gamma-ray astronomy: Alpha-particle-induced reactions [DE83-015533] N84-13036
GAMMA RAY SPECTRA
Monte Carlo calculations of neutron and gamma-ray energy spectra for fusion-reactor shield design: Comparison with experiment [DE83-016932] N84-12956
Methods for deconvoluting and interpreting complex gammaand X-ray spectral regions [DE83-013585] N84-12991
GAMMA RAY SPECTROMETERS
Development of a segmented n-type germanium detector, and its application to astronomical gamma-ray spectroscopy [NASA-TM-85435] N84-13039
GAMMA RAYS
Formation of free hydrogen during radiolysis in a bed of clay [DE83-017724] N84-12275
Real-time attenuation of heated optical fibers in a nuclear reactor [DE83-015141] N84-12873
Cross sections relevant to gamma-ray astronomy: Alpha-particle-induced reactions [DE83-015533] N84-13038
GAPS
Analytical prediction of aerothermal environment in a wing-elevon cove --- space shuttle orbiter [NASA-TM-85711] N84-12412
GARNETS
The growth and measurement of single-crystal doped GGG (Gd3-xCaxGa5-xZrx012) [AD-A131875] N84-12971
A program of research on microfabrication techniques for VLSI magnetic devices [AD-A131706] N84-12978
GAS CHROMATOGRAPHY
Atmospheric-pressure argon afterglows as a detector for gas chromatography [DE83-017695] N84-12282
GAS DETECTORS
Atmospheric-pressure argon afterglows as a detector for gas chromatography [DE83-017695] N84-12282
GAS DISCHARGE TUBES
Power-loading effects in gas-discharge models [DE83-016504] N84-12393
GAS DYNAMICS
Practical computation of multidimensional thermal flows in a gas centrifuge [DE83-005697] N84-12426
The possibility of amplifying infrared radiation by high-pressure reacting gas [AD-A131086] N84-12890
GAS FLOW
A gas-flow tracing technique applicable to rotating systems boundary layer on a rotating disk [DE83-012761] N84-12425
Practical computation of multidimensional thermal flows in a gas centrifuge [DE83-005697] N84-12426
Zero-dimensional model of compressible gas flow in networks of pressure vessels: Program TRIC [DE83-017121] N84-12431
GAS LASERS
Semiconductor processing with excimer lasers [DE83-007509] N84-12477
RF conditioned dc discharges for excitation of rare gas halide lasers [DE83-016537] N84-12479
GAS TRANSPORT
Pulmonary dosimetry of nitrogen dioxide in animals and man [PB83-243394] N84-12711
GAS TURBINE ENGINES
Auxilliary power systems with gas turbines N84-12170
Small auxiliary power unit design constraints N84-12172
Executive summary, aerothermal modeling program, phase 1 [NASA-CR-174602] N84-12263
Aerothermal modeling program, phase 1 [NASA-CR-168243-VOL-1] N84-12264
Aerothermal modeling program, phase 1 [NASA-CR-168243-VOL-2] N84-12265
GAS TURBINES
Combustion of EDS mid-distillate and refined shale-oil residual fuel in a gas turbine with large single-combustion chamber [DE83-017700] N84-12281
Improving NDE (Non-destructive evaluation) capability through multiple inspection with application to gas turbine engine disks [AD-A131762] N84-12509
GAS-METAL INTERACTIONS
Chemical erosion of first-wall materials by atomic hydrogen at high temperatures [DE83-017161] N84-12962
GAS-SOLID INTERACTIONS
High temperature gas energy transfer [AD-A131782] N84-12836
GAS-SOLID INTERFACES
Study of vibrational energy transfer at a surface by a time-of-flight method [AD-A131798] N84-12833
GASEOUS DIFFUSION
A numerical model for diffusion of helium in a hydrogen plasma [REPT-83-147] N84-12964
GASES
The shock wave structure in one-component gas and in binary gas mixture [ISSN-0208-5658] N84-12407
GASIFICATION
Fluidized bed gasification of biomass to methane [NASA-CASE-NPO-15903-1] N84-12635
GAUGE THEORY
Progress in lattice gauge theory [DE83-014055] N84-12862
Physics at very high energies [DE83-012854] N84-12878
GELS
Multi-detector gel permeation chromatography and its application to the analysis of industrial samples [MQAD-808] N84-12283
GENERAL AVIATION AIRCRAFT
Single pilot IFR accident data analysis N84-12031
Study to determine the IFR operational profile and problems to the general aviation pilot N84-12032
Analysis of general aviation single-pilot IFR incident data obtained from the NASA Aviation Safety Reporting System N84-12033
Flight test validation of a design procedure for digital autopilots N84-12036
Pilot controls and SPIRF flight N84-12038
NASA Demonstration Advanced Avionics System (DAAS) N84-12046
An overview of the demonstration advanced avionics system guest pilot evaluation conducted at Ames Research Center N84-12049
An experimental investigation of separated three dimensional flow on general aviation twin-engine aircraft N84-12087
A study of wing-body aerodynamic interference of a light twin aircraft utilizing a panel method potential flow program N84-12134
Safety report: General aviation crashworthiness project, phase 1 [PB83-917004] N84-12142
GEODESY
Investigation of mathematical models to combine a terrestrial network with a satellite network --- geodesy [SER-C-274] N84-12554
GEODETIC COORDINATES
Investigation of mathematical models to combine a terrestrial network with a satellite network --- geodesy [SER-C-274] N84-12554
GEODETIC SATELLITES
Technique for producing a coherent sum of the data from P78-1, F2, and F4 satellites [AD-A131965] N84-12210
GEODETIC SURVEYS
Test and demonstration of Macrometer (TM) model V-1000 interferometric surveyor [PB83-239103] N84-12631
GEOGRAPHIC INFORMATION SYSTEMS
Mapping land use in Catalonia (Spain) --- using LANDSAT imagery N84-12613
GEOIDS
Accuracy of gravimetrically determined absolute and relative geoid heights [SER-A-97] N84-12661
GEOLOGICAL FAULTS
Compilation of selected faults and lineaments that may be relevant to a study of seismic activity in southern Nevada and part of adjacent California [DE83-017085] N84-12673
GEOLOGICAL SURVEYS
Compilation of selected faults and lineaments that may be relevant to a study of seismic activity in southern Nevada and part of adjacent California [DE83-017085] N84-12673
GEOMAGNETIC TAIL
Observation of multiple ion beams in the magnetotail low latitude boundary layer. Evidence for a double H+ population [IFSI-82-10] N84-12676
The structure of the plasma sheet-lobe boundary in the Earth's magnetotail [NASA-TM-85434] N84-13049
GEOMAGNETISM
Guidance of electromagnetic waves in the ionosphere and magnetosphere [IFSI-82-15] N84-12361
A comparison between GEOS 1 magnetic field measurements and some models of the geomagnetic field [IFSI-82-5] N84-12675
Solar wind variations in the 60-100 year period range: A review N84-13092
GEOMETRIC RECTIFICATION (IMAGERY)
Simulation aspects in the study of rectification of satellite scanner data N84-12571
Remote sensing and topographic maps --- belgium N84-12600
Rectification of multispectral scanner images [GEOWISS-MITT-24-1983] N84-12628

GEOMETRICAL ACOUSTICS
Numerical modeling techniques according to the wave equation and the ray method — in seismology [BMFT-FB-T-83-136] N84-12354
GEOMORPHOLOGY
Contribution of satellite remote sensing to knowledge of the littoral from the mouth of the Loire to that of the Gironde (France) N84-12584
Radar bathymetry : A review N84-12612
Galilean satellite geomorphology [NASA-CR-174574] N84-13057
Geomorphic studies of Mars N84-13063
GEOPHYSICS
Orbiting geophysics laboratory experiment [AD-A131950] N84-12218
Winds: Chapter 6, 1983 revision. Handbook of Geophysics and Space Environments [AD-A132018] N84-12683
GEOPOTENTIAL
Accuracy estimates of gravity potential differences between western Europe and United States through Lageos satellite laser ranging network [AD-A131838] N84-12669
GEOPOTENTIAL HEIGHT
Accuracy of gravimetrically determined absolute and relative geoid heights [SER-A-97] N84-12661
GEOS 1 SATELLITE
A comparison between GEOS 1 magnetic field measurements and some models of the geomagnetic field [IFSI-82-5] N84-12675
GEOTHERMAL RESOURCES
Alaska's mineral resources [DE83-016599] N84-12623
GERMANIUM
Development of a segmented n-type germanium detector, and its application to astronomical gamma-ray spectroscopy [NASA-TM-85435] N84-13039
GERMANIUM COMPOUNDS
Optical properties and correlation energy of defects in a-Ge:H [DE83-016697] N84-12993
GERMINATION
Phytochrome from green plants: Assay, purification, and characterization [DE83-017447] N84-12710
GESTALT THEORY
Interpretability of wetland on SEASAT-A imagery in the polderland of Flanders: A structural approach N84-12597
GIANT STARS
Problems of stellar evolution in star clusters of the Magellanic clouds N84-13051
Theory of winds in late-type evolved and pre-main-sequence stars N84-13085
GLASS
Thermal stress analysis of annular glass-to-metal seals under thermal shock N84-12408
Hermetically sealed microminiature multisocket connector [DE83-017484] N84-12503
Evaluation of multicomponent fluoride glass candidates for double crucible drawn optical fiber [AD-A131932] N84-12893
GLASS FIBERS
Evaluation of multicomponent fluoride glass candidates for double crucible drawn optical fiber [AD-A131932] N84-12893
GLIDERS
Composite structural materials [NASA-CR-174597] N84-12257
GLOBAL POSITIONING SYSTEM
High dynamic global positioning system receiver [NASA-CASE-NPO-16171-1-CU] N84-12151
GLUONS
Quark-gluon plasma formation [DE83-017742] N84-12861
GOLD
Stress production and relief in the gold/silicon eutectic die-attach process [DE83-015230] N84-12400
GOVERNMENTS
Two types of values and their assessment by the collective interest [DE83-012064] N84-13031
GRADIENT INDEX OPTICS
Atenuation measurements between 840 and 1620 nm on an optical cable in Berlin [FI-465-TBR-22] N84-12906
GRAIN BOUNDARIES
Grain-boundary cavitation and weld-underbead cracking in DOP-26 iridium alloy [DE83-015406] N84-12539
GRAINS
Ultraviolet extinction properties of grains in the interstellar medium N84-13131
GRANULAR MATERIALS
Effects of microstructure and pore fluids on the acoustic properties of granular materials [AD-A131983] N84-12668
GRAPHITE
Disparate changes in the physical properties of graphite [DE83-015986] N84-12321
GRAPHS (CHARTS)
Space station energy sizing N84-12233
GRAVIMETRY
Accuracy of gravimetrically determined absolute and relative geoid heights [SER-A-97] N84-12661
GRAVITATIONAL FIELDS
Accuracy estimates of gravity potential differences between western Europe and United States through Lageos satellite laser ranging network [AD-A131838] N84-12669
GRAVITATIONAL WAVE ANTENNAS
Analysis of some filtering and data analysis methods for gravitational wave antennas with resonant transducers [IFSI-82-11] N84-12359
Data analysis for gravitational wave antenna with resonant transducers [IFSI-82-12] N84-12360
GRAVITATIONAL WAVES
Correlation between two spacecraft in the Doppler detection of a gravitational background radiation [IFSI-83-7] N84-12362
GRAVITY WAVES
Rising bubbles [AD-A131572] N84-12418
A case study of gravity wave-convective storm interactions N84-12659
On the growth of gravity-capillary waves by wind [KNMI-WR-83-10] N84-12698
GREENLAND
Glaciological applications of LANDSAT images in connection with hydropower investigations in West Greenland N84-12598
GROUND EFFECT
The Tracked Wing In Ground-Effect (TWIG) N84-12155
Ground and inflight operational effects of APU's N84-12182
GROUND TRUTH
Quantile data analysis of image data N84-12565
GROUND WATER
Velocity plots and capture zones of pumping centers for ground-water investigations [DE83-016618] N84-12624
GROUND WAVE PROPAGATION
Physical modeling of EM propagation over nonhomgeneous terrain N84-12370
GROUND-AIR-GROUND COMMUNICATION
Weather data communication and utilization N84-12045
GROUP THEORY
On the performance of two-stage group screening experiments [AD-A131970] N84-12807
Progress in lattice gauge theory [DE83-014055] N84-12862
GROWTH
Silicide formation and Schottky barrier of rare-earth metals on SI [AD-A131750] N84-12975
GUIDANCE SENSORS
IPACS guidance navigation and control system considerations and test activities N84-12245
GULF OF MEXICO
Satellite remote sensing, environmental monitoring and the offshore oil and gas industries N84-12603
GUN PROPELLANTS
Laser spectroscopy of propellant-like flames [AD-A132042] N84-12267
GUSTS
Gust structure and gust statistics. Results from an analysis of atmospheric turbulence measurements by using conditional sampling technique [FFA-TN-1983-28] N84-12696
GYROSCOPE FLUIDS
Discussion of static pressure liquid-floated gyros [AD-A131874] N84-12451
GYROSCOPES
Discussion of static pressure liquid-floated gyros [AD-A131874] N84-12451

H

HADRONS
Hadronic multiplicity distributions: Example of a universal stochastic mechanism [DE83-015232] N84-12845
Hadron-hadron collider group [DE83-010704] N84-12865
Tau and B lifetime measurements from the MARK 2 [DE83-018219] N84-12879
HALIDES
RF conditioned dc discharges for excitation of rare gas halide lasers [DE83-016537] N84-12479
HAMILTONIAN FUNCTIONS
Hamiltonian for antisotropic bodies with defects [ISSN-0208-5658] N84-12966
HANDBOOKS
Winds: Chapter 6, 1983 revision. Handbook of Geophysics and Space Environments [AD-A132018] N84-12683
HARDWARE
Processing elements [AD-A131068] N84-12743
HARMONIC OSCILLATORS
Hadronic multiplicity distributions: Example of a universal stochastic mechanism [DE83-015232] N84-12845
HAZARDS
Hazards Control Department annual technology review, 1982 [DE83-015598] N84-12883
HEAD (ANATOMY)
Vestibulo-ocular reflex gain in man during active versus passive oscillation and the influence of voluntary gaze-control tasks [AD-A132006] N84-12717
HEAD-UP DISPLAYS
Integration of fire control, navigation system and head up display N84-12060
HEAT
A laboratory comparison of portable cooling systems for workers exposed to two levels of heat stress [AD-A131848] N84-12423
Effect of atropine on the exercise-heat performance of man [AD-A131843] N84-12719
Effectiveness in reducing heat stress of three conditioned-air cooling vests worn with and without cooling air supplied to a face piece [AD-A131975] N84-12726
HEAT CAPACITY MAPPING MISSION
Identifying environmental features for land management decisions [E84-10016] N84-12556
HEAT EXCHANGERS
Tailoring polymer films for solar-collection use, phase 1 [DE83-018117] N84-12640
Reliability and maintainability study of select solar-energy-system components in the National Solar Data Network [DE83-011974] N84-12647
New conformal solution theory [PB83-249441] N84-13008
HEAT FLUX
Determination of the uncertainty of experimental heat-flux calibrations [AD-A131918] N84-12450
Role of thermal conduction in the acceleration of the solar wind N84-13079
The collapse of the local, Spitzer-Haerm formulation and a global-local generalization for heat flow in an inhomogeneous, fully ionized plasma N84-13080
HEAT MEASUREMENT
Calorimeter operating system implemented on a Z-80 microcomputer in read only memory [DE83-016647] N84-12734
HEAT OF COMBUSTION
Correlation of laboratory-scale fire test methods for seat blocking layer materials with large-scale test results [AD-A131666] N84-12138
HEAT PUMPS
Performance of add-on-type heat pump water heaters using two different test methods [PB83-222703] N84-12332
Ground coupled heat-pump-system experimental results [DE83-014011] N84-12427
Thermochemical energy systems research [DE83-012132] N84-12644
Reliability and maintainability study of select solar-energy-system components in the National Solar Data Network [DE83-011974] N84-12647

HEAT SINKS
A laboratory comparison of portable cooling systems for workers exposed to two levels of heat stress
[AD-A131848] N84-12423
HEAT TRANSFER
Deposit formation and heat transfer in hydrocarbon rocket fuels
[NASA-CR-168277] N84-12225
Solid-oxide fuel-cell performance
[DE83-017926] N84-12396
Use of superposition in calculating cooling requirements for circuit cards containing arrays of electronic components
[DE83-016091] N84-12428
Convection in horizontal porous media with different end temperatures N84-12438
Numerical calculations of turbulent recirculating heat transfer beyond two-dimensional back-steps and sudden pipe expansions N84-12439
Transient heat transfer in superfluid helium, part 2
[DE83-015767] N84-12984
Superconductor stability, 1983: A review
[DE83-015506] N84-12990
HEAT TRANSFER COEFFICIENTS
Turbulent tube-flow heat transfer coefficients in the presence of flow imbalance in the tubes of a parallel array N84-12437
HEAT TRANSMISSION
Practical computation of multidimensional thermal flows in a gas centrifuge
[DE83-005697] N84-12426
Electrostatic waves and anomalous transport in the solar wind N84-13095
HEAT TREATMENT
Influence of heat-treatment and physicochemical properties on the electrochemical oxidation of carbon blacks in phosphoric acid
[DE83-017744] N84-12276
Evaluation of several high-strength copper sheet alloys
[DE83-015612] N84-12298
HEATING
Heating with wind energy, part B
[BMFT-FB-T-83-131-PT-B] N84-12651
Direct coronal heating from dissipation of magnetic field N84-13069
HEAVY IONS
High-sensitivity mass spectrometry with a tandem accelerator
[DE83-017914] N84-12274
Implications of heavy-ion-induced satellite X-ray emission. 1: Introduction
[DE83-015682] N84-12851
The 83-inch cyclotron reseach program
[DE83-015827] N84-12852
Electron capture and loss cross sections for collisions between heavy ions and hydrogen molecules, revised
[IPPJ-AM-28] N84-12914
Inertial fusion with low-energy heavy ions
[DE83-016709] N84-12934
Implications of heavy-ion-induced satellite X-ray emission. Part 2: Production of K and L X-rays by 0.9 to 2.6 MeV/u Ar ions in thick targets of V, Cu, Nb, Ta, and Pt
[DE83-015681] N84-12982
Interpreting the solar wind ionization state N84-13115
Acceleration of heavy ions in the solar wind N84-13118
Ultra-relativistic heavy ions and cosmic rays
[DE83-015881] N84-13134
HELICAL WINDINGS
Design of the Advanced Toroidal Facility (ATF-1)
[DE83-012641] N84-12923
HELICOPTER TAIL ROTORS
Study of an asymptotic method for helicopter rotor blade aerodynamic loads N84-12135
HELICOPTER WAKES
Helicopter rotor wake geometry and its influence in forward flight. Volume 1: Generalized wake geometry and wake effect on rotor airloads and performance
[NASA-CR-3726] N84-12090
Helicopter rotor wake geometry and its influence in forward flight. Volume 2: Wake geometry charts
[NASA-CR-3727] N84-12091
HELICOPTERS
Development of the basic methods needed to predict the aeroelastic behavior of helicopters N84-12811
Noise emission by helicopters N84-13007
HELIOS SATELLITES
Interplanetary Alfvenic fluctuations: A statistical study of the directional variations of the magnetic field N84-13076
HELIOS 1
The average solar wind in the inner heliosphere. Structures and slow variations N84-13105
HELIOS 2
The average solar wind in the inner heliosphere: Structures and slow variations N84-13105
HELIOSPHERE
Solar wind variations in the 60-100 year period range: A review N84-13092
Radial evolution of ion distribution functions N84-13094
Solar wind distrubances in th outer heliosphere caused by successive solar flares from the same active region N84-13104
The average solar wind in the inner heliosphere: Structures and slow variations N84-13105
Corotating shocks in inner heliosphere N84-13124
HELIUM
Self-pumping impurity by in-situ metal deposition
[DE83-017937] N84-12306
Helium damage in austenitic stainless steels
[DE83-017494] N84-12309
Satellite refrigerator compressors with the oil and moisture removal systems
[DE83-016079] N84-12502
Helium-flow measurement using ultrasonic technique
[DE83-017765] N84-12826
A numerical model for diffusion of helium in a hydrogen plasma
[REPT-83-147] N84-12964
The far infrared sky survey experiment
[AD-A131966] N84-13037
The interplanetary hydrogen and helium glow and the inferred interstellar gas properties N84-13109
Survey of He(+)/He(2+) abundance ratios in energetic particle events N84-13117
HELIUM IONS
The relative abundance of 3He(++) in the solar wind N84-13111
HELIUM ISOTOPES
Interpretation of 3He variations in the solar wind
[NASA-TM-85049] N84-13065
The relative abundance of 3He(++) in the solar wind N84-13111
HELIUM-NEON LASERS
Gauge block lasometer development
[DE83-016288] N84-12458
HERMETIC SEALS
Thermal stress analysis of annular glass-to-metal seals under thermal shock N84-12408
HERMITIAN POLYNOMIAL
Aspects of second- and third-order panel methods demonstrated for the two-dimensional flat plate problem
[NLR-TR-81074-U] N84-12433
HETERODYNING
Pulse signals in heterodyne and homodyne detection
[ESA-TT-809] N84-12357
HETEROJUNCTIONS
Liquid phase epitaxy of InP/In1-xGxAsyP1-y heterostructures. Part 3: Phase diagrams
[FI-65-TBR-20-PT-3] N84-13000
HIERARCHIES
Disjunctive programming and a hierarchy of relaxations for discrete optimization problems
[AD-A132004] N84-12784
HIGH ALTITUDE BALLOONS
Thin film strain transducer --- in-flight monitoring of balloon film strain
[NASA-WLP-10055-2] N84-12448
HIGH ENERGY INTERACTIONS
From accelerators to storage rings to ?
[DE83-011849] N84-12842
A thousand TeV in the center of mass: Introduction to high-energy storage rings
[DE83-015649] N84-12855
Theory of elementary particles
[DE83-015904] N84-12871
New facilities for the US high-energy physics program
[DE83-016589] N84-12876
Low energy nuclear physics and accelerator development
[DE83-013384] N84-12877
Physics at very high energies
[DE83-012854] N84-12878
Effect of RF structure on cumulative beam breakup
[DE83-017302] N84-12882
Longitudinal space-charge effects in bunched beams
[DE83-017305] N84-12888
HIGH FREQUENCIES
Techniques for locating a remote HF transmitter from single-site measurements
[AD-A132014] N84-12342
HIGH LEVEL LANGUAGES
High-level control programs at NSLS
[DE83-010935] N84-12754
HIGH PRESSURE
The possibility of amplifying infrared radiation by high-pressure reacting gas
[AD-A131086] N84-12890
HIGH RESOLUTION
High Resolution Imager (HRI) for the Roentgen Satellite (ROSAT) definition study
[NASA-CR-174598] N84-12223
Snow characterization instruments
[AD-A131984] N84-12687
The 83-inch cyclotron reseach program
[DE83-015827] N84-12852
Spectroscopic measurements of solar wind generation N84-13071
HIGH SPEED
Solar cycle variations of the solar wind N84-13089
HIGH TEMPERATURE
Corrosion behavior of Fe-Cr-Ni-Zr alloys in aggressive environments at high temperatures
[DE83-014735] N84-12297
Breakaway corrosion in mixed-gas environments
[DE83-014704] N84-12299
Solid-oxide fuel-cell performance
[DE83-017926] N84-12396
HIGH TEMPERATURE GAS COOLED REACTORS
Disparate changes in the physical properties of graphite
[DE83-015986] N84-12321
Creep and tensile properties of alloy 800H-Hastelloy X weldments
[DE83-017067] N84-12542
HIGH TEMPERATURE GASES
Hot gas APU starter for advanced aircraft applications N84-12178
Infrared characteristics of gas plumes
[AD-A131796] N84-12269
High temperature gas energy transfer
[AD-A131782] N84-12836
HIGH TEMPERATURE PLASMAS
Atomic processes in hot dense plasma
[IPPJ-AM-31] N84-12911
Bibliography on atomic processes in hot dense plasmas
[IPPJ-AM-29] N84-12913
HIGH VOLTAGES
Megavolt pulse transformer powered by a fast plate generator
[DE83-014189] N84-12384
HILSCH TUBES
Acoustic streaming as a mechanism of the Ranque-Hilsch effect N84-12088
HINGES
Plastic deformations of a portable frame under short pulse loading on one column by an approximate method including effects of elasticity and plastic rate sensitivity N84-12521
HISTORIES
A balloon design for 9000 pounds at 90,000 feet: Recommendations based on heavy-load balloon history
[AD-A131987] N84-12093
HOLDERS
Holding fixture for a hot stamping press
[NASA-CASE-GSC-12619-1] N84-12491
HOLES (ELECTRON DEFICIENCIES)
Hole trapping, recombination, and space charge in irradiated Sandia oxides
[DE83-015212] N84-12986
HOLMIUM
Novel interactions of the charge-balancing cations with framework defects and trapped hydrogen atoms in holmium-exchanged Y zeolites
[DE83-014204] N84-12839
HOMODYNE RECEPTION
Pulse signals in heterodyne and homodyne detection
[ESA-TT-809] N84-12357
HORIZONTAL FLIGHT
Helicopter rotor wake geometry and its influence in forward flight. Volume 1: Generalized wake geometry and wake effect on rotor airloads and performance
[NASA-CR-3726] N84-12090
HORIZONTAL ORIENTATION
Convection in horizontal porous media with different end temperatures N84-12438
HOT ELECTRONS
Initial assessment of the MHD stability of TMX-U
[DE83-016521] N84-12646
HOT PRESSING
Holding fixture for a hot stamping press
[NASA-CASE-GSC-12619-1] N84-12491
HOT-WIRE ANEMOMETERS
Instabilities in trailing vortices: Flow visualization using hot-wire anemometry N84-12103
HOVERING
V/STOL (Vertical/Short Takeoff and Landing) low speed and transition equivalent systems analysis
[AD-A131955] N84-12156
HUMAN BEHAVIOR
Search among queues
[AD-A131639] N84-12773

HUMAN BODY
Vestibulo-ocular reflex gain in man during active versus passive oscillation and the influence of voluntary gaze-control tasks
[AD-A132006] N84-12717
HUMAN FACTORS ENGINEERING
Proposed study to determine potential flight applications and human factors design guidelines of voice recognition/synthesis systems N84-12047
HUMAN PERFORMANCE
Biological clocks and shift work scheduling
[GPO-21-747] N84-12713
Effect of atropine on the exercise-heat performance of man
[AD-A131843] N84-12719
Coherence of appraisal and coping: Parachute jump effectiveness
[FOA-C-55058-H3] N84-12724
HUMIDITY
Optical extinction coefficients beneath marine stratus clouds. Comparison of coefficients calculated from observed aerosol spectra with coefficients specified by the Navy aerosol model
[AD-A132011] N84-12685
HURRICANES
Omega Dropwindsonde processing
[PB83-248773] N84-12700
HYDRAULIC EQUIPMENT
Auxiliary Power Systems
[AGARD-CP-352] N84-12168
Hydraulic generation of auxilliary power for the Mirage 2000 aircraft N84-12176
Spacecraft Vibration Testing Using Multi-Axis Hydraulic Vibration Systems — conferences
[ESA-SP-197] N84-12197
The hydraulic multiaxes vibrator: Its capabilities to simulate real mechanical environments and to verify aerospace structures N84-12198
Practical experience during installation of the large multiaxes vibration test facility SAMSON N84-12199
The development of a multi-axis hydraulic vibration test facility at the National Engineering Laboratory, Scotland N84-12200
Hydraulic actuators and associated components suited for multiaxis vibration systems — spacecraft testing N84-12201
Concept of a safety system for a servohydraulic test facility N84-12202
Mathematical modeling and simulation of multiaxis hydraulic test facilities N84-12204
Simulation of electro-servo-hydraulic actuator for high quality testing — of spacecraft N84-12206
HYDRAULIC JETS
Rapid runway repair program subtask 1.07 - rapid concrete cutting
[AD-A131771] N84-12195
HYDRAULICS
Microearthquakes induced during hydraulic fracturing at the Fenton Hill HDR site: The 1982 experiments
[DE83-014191] N84-12672
HYDRIDES
Growth and characterization of InP and InGaAs films using the hydride VPE technique
[AD-A131841] N84-12973
HYDROBALLISTICS
Water entry impact shock on flat faced cylindrical missiles
[AD-A131937] N84-12419
HYDROCARBON FUELS
Deposit formation and heat transfer in hydrocarbon rocket fuels
[NASA-CR-168277] N84-12225
HYDROCARBONS
Soot formation from polycyclic aromatics
[DE83-009750] N84-12271
HYDRODYNAMIC EQUATIONS
Formation of standing shocks in stellar winds and related astrophysical flows N84-13088
HYDRODYNAMICS
Lithium equation-of-state
[DE83-017988] N84-12253
Feasibility of a laser or charged-particle-beam fusion-reactor concept with direct electric generation by magnetic-flux compression
[DE83-015735] N84-12482
Using inner-shell X-rays as an ion-beam diagnostic
[DE83-017784] N84-12857
Hydrodynamic simulations of a combined hydrogen, helium thermonuclear runaway on a 10 km neutron star
[DE83-012658] N84-13047
Modeling of transient disturbances in coronal-streamer configurations N84-13119
HYDROELECTRICITY
Glaciological applications of LANDSAT images in connection with hydropower investigations in West Greenland N84-12598
HYDROGEN
Formation of free hydrogen during radiolysis in a bed of clay
[DE83-017724] N84-12275
Hydrogen-air detonations
[DE83-009289] N84-12278
Isotope dependence of the breakdown strength of gases
[DE83-017272] N84-12430
New developments and oppotunities for NMR in metal-hydrogen systems
[DE83-017696] N84-12864
Electron capture and loss cross sections for collisions between heavy ions and hydrogen molecules, revised
[IPPJ-AM-28] N84-12914
Chemical erosion of first-wall materials by atomic hydrogen at high temperatures
[DE83-017161] N84-12962
Hydrogen in MgO crystals thermochemically reduced at very high temperatures
[DE83-014058] N84-12981
The interplanetary hydrogen and helium glow and the inferred interstellar gas properties N84-13109
HYDROGEN ATOMS
Novel interactions of the charge-balancing cations with framework defects and trapped hydrogen atoms in holmium-exchanged Y zeolites
[DE83-014204] N84-12839
Cross sections for charge transfers of highly ionized ions in hydrogen atoms
[IPPJ-AM-30] N84-12912
HYDROGEN EMBRITTLEMENT
Hydrogen compatibility handbook for stainless steels
[DE83-017051] N84-12301
HYDROGEN IONS
Observation of multiple ion beams in the magnetotail low latitude boundary layer. Evidence for a double H+ population
[IFSI-82-10] N84-12676
The 100% alignment of hydrogen excited states in beam-foil spectroscopy
[DE83-017963] N84-12859
HYDROGEN PLASMA
A numerical model for diffusion of helium in a hydrogen plasma
[REPT-83-147] N84-12964
HYDROGENATION
Preparation of a design study for the construction of a 2 million tons/annum commercial scale hydrogenation plant
[BMFT-FB-T-83-135] N84-12652
HYDROMECHANICS
The 400 Hz generators evolution, effects on installation arrangements N84-12186
HYPERBOLIC DIFFERENTIAL EQUATIONS
Multidimensional explicit difference schemes for hyperbolic conservation laws
[NASA-CR-172254] N84-12778
HYPERCAPNIA
Naloxone does not affect ventilatory responses to hypoxia and hypercapnia in rats
[AD-A131836] N84-12708
HYPERFINE STRUCTURE
Theory of hyperfine anomalies in muonic atoms
[DE83-015392] N84-12872
HYPERSONIC FLOW
On the generation of vortical flow at hypersonic speeds over elliptical cones N84-12114
HYPOXIA
Naloxone does not affect ventilatory responses to hypoxia and hypercapnia in rats
[AD-A131836] N84-12708

I

ICE
Snow characterization instruments
[AD-A131984] N84-12687
ICE FORMATION
Construction of two wind turbines AEROMAN 11/11 for Indonesia
[BMFT-FB-T-82-143] N84-12505
Field and laboratory studies of ice nucleation in winter orographic clouds N84-12678
Proceedings of 1st International Workshop on Atmospheric Icing of Structures
[AD-A131869] N84-12690
ICE MAPPING
Glaciological applications of LANDSAT images in connection with hydropower investigations in West Greenland N84-12598
Field and laboratory studies of ice nucleation in winter orographic clouds N84-12678
ICE NUCLEI
Field and laboratory studies of ice nucleation in winter orographic clouds N84-12678
IGNITERS
Combustion jet ignition N84-12188
IGNITION
Combustion jet ignition N84-12188
ILLINOIS
Initial operation of the compressed air experiment at Pittsfield, Illinois
[DE83-016930] N84-12643
ILLUMINANCE
Model for illuminance on horizontal and vertical surfaces
[DE83-011973] N84-13127
Graphical method for determining interflected daylight in clear climates
[DE83-011989] N84-13128
IMAGE ANALYSIS
LANDSAT 4 investigations of thematic mapper and multispectral scanner applications
[E84-10006] N84-12555
Proceedings of the NASA Symposium on Mathematical Pattern Recognition and Image Analysis
[E83-10032] N84-12557
Estimating location parameters in a mixture model N84-12559
Multivariate density estimation and remote sensing N84-12560
An empirical Bayes approach to spatial analysis N84-12563
Quantile data analysis of image data N84-12565
Repeated-measures analysis of image data N84-12567
Image matching using generalized Hough transforms N84-12569
Analysis of subpixel registration accuracy N84-12570
Relating spatial patterns in image data to scene characteristics N84-12573
Shape from shading: An assessment N84-12574
The influence of sensor and flight parameters on texture in radar images N84-12575
Earth Resources Laboratory research and technology
[E84-10033] N84-12576
Measuring landscape information content and distribution on a SAR-580 image N84-12596
Interpretability of wetland on SEASAT-A imagery in the polderland of Flanders: A structural approach N84-12597
Remote sensing analysis of oil pollution in Augusta Bay, Sicily N84-12616
Pyramid methods in image analysis N84-12796
IMAGE CONTRAST
Utility of the cortical evoked response as a measure of photographic image quality
[AD-A131679] N84-12455
IMAGE INTENSIFIERS
High-speed videography combined with an x-ray image intensifier for dynamic radiography
[DE83-017233] N84-12905
IMAGE PROCESSING
Digital image registration by sequential analysis
[INPE-2940-PHE/429] N84-12446
LANDSAT 4 investigations of thematic mapper and multispectral scanner applications
[E84-10006] N84-12555
SAR speckle noise reduction using Wiener filter N84-12568
Progress in the scene-to-map registration investigation N84-12572
Earth Resources Laboratory research and technology
[E84-10033] N84-12576
Glaciological applications of LANDSAT images in connection with hydropower investigations in West Greenland N84-12598
Rectification of multispectral scanner images
[GEOWISS-MITT-24-1983] N84-12628
Evaluation of automated imagery analysis algorithms for use in the three-dimensional nephanalysis model at AFGWC (Air Force Global Weather Central)
[AD-A131986] N84-12686
Galilean satellite geomorphology
[NASA-CR-174574] N84-13057
IMAGE RESOLUTION
Pyramid methods in image analysis N84-12796
IMAGING TECHNIQUES
Variations in task and the ideal observer
[DE83-015394] N84-12723
Representations for reasoning about change
[AD-A131649] N84-12772
Survey of flash X-ray techniques and applications
[DE83-017234] N84-12904
IMPACT DAMAGE
Vibration response of geometrically nonlinear elastic beams to pulse and impact loading
[NASA-CR-174495] N84-12527

IMPACT LOADS
Water entry impact shock on flat faced cylindrical missiles
[AD-A131937] N84-12419
Vertical drop test of a transport fuselage center section including the wheel wells
[NASA-TM-85706] N84-12531
IMPACT TESTS
Aircraft transparency testing methodology and evaluation criteria. Part 2: Methodology development for improved durability
[AD-A131928] N84-12157
Aircraft transparency testing methodology and evaluation criteria. Part 1: Test methods and information analysis
[AD-A131927] N84-12158
Alternate T-38 transparency development. Part 4: Parametric studies
[AD-A131904] N84-12159
Flightline thermal environment testing of F-111 transparencies
[AD-A131642] N84-12163
A pressure-shear experiment for studying the dynamic plastic responses of metals at shear strain rates of 10 to the 5th power s(-1) N84-12519
IMPEDANCE
Physical modeling of EM propagation over nonhomgeneous terrain N84-12370
IMPINGEMENT
Solid impingement erosion mechanisms and characterization of erosion resistance of ductile metals
[NASA-TM-83492] N84-12287
IMPLOSIONS
Inertial effects in laser-driven ablation
[DE83-016941] N84-12478
IMPURITIES
Self-pumping impurity by in-situ metal deposition
[DE83-017937] N84-12306
INCENTIVES
Revitalization: An organizational program for the individual
[DE83-014949] N84-13013
INCOHERENT SCATTER RADAR
Speed-dependent collision effects on radar back-scattering from the ionosphere --- incoherent scatter radar
[NASA-CR-173077] N84-12336
INCOMPRESSIBLE FLOW
Stability of a pair of stationary vortices in the leeward side of a cylinder in a potential flowfield
[AD-A131917] N84-12095
Computational vortex flow aerodynamics N84-12117
Simulation of turbulent flows with a point vortex method N84-12119
Steady and unsteady flow models for airfoils with spoiler N84-12136
Computation of turbulent flows over backward-facing step
[NASA-TM-85851] N84-12414
INDEXES (DOCUMENTATION)
Source header list, supplement 1
[AD-A131800] N84-13024
Permuted medical subject headings, 1984
[PB83-234781] N84-13027
Medical subject headings, tree structures, 1984
[PB83-223164] N84-13028
Medical Subject Headings, Annotated Alphabetic List, 1984
[PB83-223156] N84-13029
INDICATING INSTRUMENTS
Snow characterization instruments
[AD-A131984] N84-12687
INDIUM
Predevelopment of IR-CCD components
[BMFT-FB-T-83-133] N84-13001
INDIUM ARSENIDES
Surface and interfacial properties of Ga(0.47) In(0.53) As alloys
[AD-A131925] N84-12970
INDIUM PHOSPHIDES
Growth and characterization of InP and InGaAs films using the hydride VPE technique
[AD-A131841] N84-12973
INDUSTRIAL ENERGY
Innovative industrial-materials processes --- potential for energy conservation
[DE83-016784] N84-12649
INDUSTRIAL SAFETY
Concept of a safety system for a servohydraulic test facility N84-12202
Walk-through survey report: Control technology for integrated circuit fabrication, Xerox Corporation, El Segundo, California
[PB83-239053] N84-12333
Hazards Control Department annual technology review, 1982
[DE83-015598] N84-12683
INELASTIC COLLISIONS
Study of excited state energy transfer processes
[AD-A131777] N84-12837
New statistical and non-statistical effects in deep inelastic heavy-ion collisions
[DE83-015732] N84-12885
INELASTIC SCATTERING
Electron-ion collisions
[DE83-017211] N84-12867
INELASTIC STRESS
Cumulative damage in components of steel structures under cyclic inelastic loading N84-12550
INERTIA PRINCIPLE
Magnetic bearings for inertial energy storage N84-12242
INERTIAL CONFINEMENT FUSION
Rotating and propagating LIB stabilized by self-induced magnetic field
[IPPJ-840] N84-12916
Inertial fusion with low-energy heavy ions
[DE83-016709] N84-12934
Ion stopping in heated targets
[DE83-017800] N84-12941
Light-ion-beam fusion
[DE83-018263] N84-12944
INERTIAL FUSION (REACTOR)
Lithium equation-of-state
[DE83-017988] N84-12253
Diagnosing the ion beam on the applied-B diode
[DE83-017822] N84-12943
INERTIAL NAVIGATION
Integration of fire control, navigation system and head up display N84-12060
INFLATABLE STRUCTURES
Load deflection characteristics of inflated structures
[NASA-CR-174585] N84-12028
Inflatable device for installing strain gage bridges
[NASA-CASE-FRC-11068-1] N84-12443
INFORMATION DISSEMINATION
The SPOT distribution system N84-12615
INFORMATION MANAGEMENT
A study of critical factors affecting the development of performance measures in evaluating bibliographic information retrieval systems N84-13030
INFORMATION RETRIEVAL
Development of a unique Physical Metrology Laboratory Recall System
[DE83-017415] N84-12767
The computerization of material safety data sheet information
[AD-A131992] N84-13021
Information retrieval research support
[AD-A131990] N84-13022
A study of critical factors affecting the development of performance measures in evaluating bibliographic information retrieval systems N84-13030
INFORMATION SYSTEMS
Development of a data base for carbon dioxide releases resulting from conversion of land to agricultural uses
[DE83-015728] N84-12626
The computerization of material safety data sheet information
[AD-A131992] N84-13021
Information resources management plan
[AD-A131964] N84-13023
Source header list, supplement 1
[AD-A131800] N84-13024
Information processing for the infrared balloon telescope Goldener Drache
[MPE-38] N84-13035
INFORMATION THEORY
Measuring landscape information content and distribution on a SAR-580 image N84-12596
GRIDPACK: Toward unification of general grid programming
[AD-A131692] N84-12746
Using structural and functional information in diagnostic design
[AD-A131859] N84-12769
INFRARED ABSORPTION
Amorphous silicon-carbon films
[DE83-018077] N84-12259
INFRARED ASTRONOMY SATELLITE
NASA Facts: IRAS - Mapping the Infrared Sky
[NASA-FACTS-139] N84-13036
INFRARED DETECTORS
Predevelopment of IR-CCD components
[BMFT-FB-T-83-133] N84-13001
INFRARED IMAGERY
Noise reduction and segmentation of IR images using CO-median filters
[RSRE-3582] N84-12378
INFRARED LASERS
Laser journal (selected articles)
[AD-A131886] N84-12465
Infrared-laser spectroscopy using a long-pathlength absorption cell
[DE83-014197] N84-12480
INFRARED RADIATION
Absolute collisional excitation cross section measurements using crossed molecular beams
[AD-A132038] N84-12830
Novel techniques for enhanced reflectivity infrared mirrors
[AD-A131924] N84-12894
INFRARED SIGNATURES
Absolute collisional excitation cross section measurements using crossed molecular beams
[AD-A132038] N84-12830
INFRARED SPECTRA
Infrared characteristics of gas plumes
[AD-A131796] N84-12269
NASA Facts: IRAS - Mapping the Infrared Sky
[NASA-FACTS-139] N84-13036
INFRARED SPECTROSCOPY
Infrared characteristics of gas plumes
[AD-A131796] N84-12269
Laser journal (selected articles)
[AD-A131886] N84-12465
INFRARED TELESCOPES
Information processing for the infrared balloon telescope Goldener Drache
[MPE-38] N84-13035
The far infrared sky survey experiment
[AD-A131966] N84-13037
INFRARED WINDOWS
Observation of the Earth in the middle infrared
[ESA-TT-790] N84-12629
INHIBITORS
Combined effects of ionizing radiation and anticholinesterase exposure on rodent motor performance
[AD-A131847] N84-12707
INHOMOGENEITY
Investigation of inhomogeneity in ceramic reactor materials using laser-localized emission spectroscopy
[JUEL-1834] N84-12323
INLETS (TOPOGRAPHY)
Sediment transport in a tidal inlet
[PB83-242271] N84-12632
INORGANIC CHEMISTRY
Applications of molecular quantum mechanics to problems in chemistry
[DE83-015943] N84-13003
INSOLATION
Review of potential satellite techniques for mesoscale mapping of insolation
[DE83-011998] N84-12622
Model for illuminance on horizontal and vertical surfaces
[DE83-011973] N84-13127
Graphical method for determining interflected daylight in clear climates
[DE83-011989] N84-13128
INSPECTION
Improving NDE (Non-destructive evaluation) capability through multiple inspection with application to gas turbine engine disks
[AD-A131762] N84-12509
Nondestructive evaluation publications, 1981
[PB83-239574] N84-12517
INSTALLING
Inflatable device for installing strain gage bridges
[NASA-CASE-FRC-11068-1] N84-12443
INSTRUMENT ERRORS
Flight tests for a strapdown system (MSS): The results of a special flight test
[ESA-TT-818] N84-12153
INSTRUMENT FLIGHT RULES
Controls, Displays, and Information Transfer for General Aviation IFR Operations
[NASA-CP-2279] N84-12029
Single pilot IFR program overview and status N84-12030
Single pilot IFR accident data analysis N84-12031
Study to determine the IFR operational profile and problems to the general aviation pilot N84-12032
Analysis of general aviation single-pilot IFR incident data obtained from the NASA Aviation Safety Reporting System N84-12033
A summary and integration of research concerning single pilot IFR operational problems N84-12034
General aviation single pilot IFR autopilot study N84-12035
Flight test validation of a design procedure for digital autopilots N84-12036
A simulator evaluation of an automatic terminal approach system N84-12037

Pilot controls and SPIRF flight N84-12038
Advanced symbology for general aviation approach to landing displays N84-12039
A flight investigation of simulated data link communications during single-pilot IFR flight N84-12046
Proposed study to determine potential flight applications and human factors design guidelines of voice recognition/synthesis systems N84-12047

INSTRUMENT LANDING SYSTEMS
A simulator evaluation of a rate-enhanced instrument landing system display N84-12042

INSTRUMENT ORIENTATION
Simulation aspects in the study of rectification of satellite scanner data N84-12571

INSTRUMENTS
Development of instrumentation for monitoring carbon fiber emission
[PB83-233726] N84-12460

INSULATORS
Development of materials for open-cycle MHD
[DE83-016334] N84-12926

INTEGERS
On Waring's problem g (4) or = 20 N84-12781

INTEGRAL EQUATIONS
Transition flow ion transport via integral Boltzmann equation
[UTIAS-269] N84-12828

INTEGRAL TRANSFORMATIONS
Reduction of structural complexity in evaluating convolutions by polynomial transforms
[FUB-59-1981] N84-12794

INTEGRATED CIRCUITS
Walk-through survey report: Control technology for integrated circuit fabrication, Xerox Corporation, El Segundo, California
[PB83-239053] N84-12333
Alternative transmission media for third-generation interface standards
[PB83-238345] N84-12365
Development of instrumentation for monitoring carbon fiber emission
[PB83-233726] N84-12460

INTEGRATED ENERGY SYSTEMS
Super integrated power unit for fighter aircraft N84-12183
IPACS attitude control technology considerations N84-12238
Flywheel electronics N84-12239
IPACS electronics: Comments on the original design and current efforts at Langley Research Center N84-12240
Power system considerations and test activities N84-12244
IPACS guidance navigation and control system considerations and test activities N84-12245

INTERACTIONS
Laser interaction with metallic surfaces
[AD-A126269] N84-12464
Simulations of galaxy mergers N84-13054

INTERFACES
Geometries for roughness shapes in laminar flow
[NASA-CASE-LAR-13255-1] N84-12092
Spacecraft interface design and its impact on operational support
[ESA-STR-211] N84-12220
Inference of fatigue-crack closure stresses from ultrasonic-transmission measurements
[DE83-017684] N84-12547
Review of the ANSI metafile and virtual device interface standardization activities
[DE83-015925] N84-12737
Using PAFEC as a preprocessor for COSMIC/NASTRAN
[DE83-017179] N84-12755

INTERFACIAL TENSION
Numerical simulations of fuel droplet flows using a Lagrangian triangular mesh
[NASA-CR-168263] N84-12411

INTERFERENCE DRAG
Engine/airframe interference drag at cruise conditions, using propulsion simulation
[NLR-TR-82012-U] N84-12098

INTERFEROMETERS
Gauge block lasometer development
[DE83-018288] N84-12458

INTERFEROMETRY
Automated data reduction for optical interferometric data
[DE83-012075] N84-12457
Test and demonstration of Micrometer (TM) model V-1000 interferometric surveyor
[PB83-239103] N84-12631

INTERNAL COMBUSTION ENGINES
Evaluation of unthrottled combustion system options for light duty applications with future syncrude derived fuels
[DE83-017047] N84-12327
Calculation of unsteady flow in tubes of combustion engines with special regard to multiple branching
[REPT-82.8] N84-12410
Use of the one-dimensional theory of the filament of flow for the interpretation and synthesis of mufflers in exhaust pipes of internal combustion engines
[REPT-81.4] N84-12494
Controlled combustion engine evaluation
[DE83-011245] N84-12499

INTERNAL WAVES
Radar bathymetry : A review N84-12612

INTERNATIONAL COOPERATION
Use of remote sensing methods for the ecological mapping project of the European community N84-12580
Remote sensing applied to marine pollution control N84-12607
Proceedings of 1st International Workshop on Atmospheric Icing of Structures
[AD-A131869] N84-12690

INTERNATIONAL MAGNETOSPHERIC STUDY
GSE for balloon-borne I.M.S.: Decommutator and D/A units
[AD-A131845] N84-12452

INTERNATIONAL SUN EARTH EXPLORER 3
Solar cycle variations in the interplanetary magnetic field N84-13091
Measurement of macroscopic plasma parameters with a radio experiment: Interpretation of the quasi-thermal noise spectrum observed in the solar wind N84-13096
Radio evidence for interplanetary streamers in the range 10-170 solar radii N84-13103

INTERPLANETARY DUST
Minor constituents in the solar wind originating from plasma-dust interactions N84-13116

INTERPLANETARY GAS
The interplanetary hydrogen and helium glow and the inferred interstellar gas properties N84-13109

INTERPLANETARY MAGNETIC FIELDS
Radial variations of large-scale magnetohydrodynamic fluctuations in the solar wind
[NASA-TM-85116] N84-13045
Interplanetary Alfvenic fluctuations: A statistical study of the directional variations of the magnetic field
[IFSI-82-14] N84-13050
The effect of the solar field reversal on the modulation of galactic cosmic rays N84-13101
The radial evolution of the solar wind, 1-10 AU N84-13106
Spatial dependences in the distant solar wind: Pioneers 10 and 11 N84-13107
Interplanetary perturbations associated with type 4 solar flares
[IFSI-82-6] N84-13129

INTERPLANETARY MEDIUM
Radio scintillations at large elongation angles: Contributions of waves versus discontinuities
[IFSI-82-4] N84-12358
Interplanetary Alfvenic fluctuations: A statistical study of the directional variations of the magnetic field N84-13076
Electron heating at interplanetary shocks N84-13098
Interplanetary scintillation observations of the solar wind close to the Sun and out of the ecliptic N84-13102
Radio evidence for interplanetary streamers in the range 10-170 solar radii N84-13103
Associations between coronal mass ejections and interplanetary shocks N84-13121
Velocity profiles of interplanetary shocks N84-13122
Plasma properties of driver gas following interplanetary shocks observed by ISEE-3 N84-13123
Corotating shocks in inner heliosphere N84-13124
On the field configuration in magnetic clouds N84-13125

INTERPLANETARY SPACE
Multiple spacecraft observations of interplanetary shocks: Characteristics of the upstream ULF turbulence N84-13097
Interplanetary perturbations associated with type 4 solar flares
[IFSI-82-6] N84-13129

INTERPROCESSOR COMMUNICATION
Trends in the development of teleinformatics
[AD-A131067] N84-12338
Network design tool for EHF satellite communications networks
[AD-A131812] N84-12349
Design and implementation of a preprocessing system for a sodium lidar
[NASA-CR-174593] N84-12462
Procedures for the transfer of data files between the BRL CYBER computer system and the IBD Hewlett-Packard minicomputer network
[AD-A132063] N84-12731

INTERSTELLAR EXTINCTION
Ultraviolet extinction properties of grains in the interstellar medium N84-13131

INTERSTELLAR GAS
A study of depletion in low-velocity diffuse interstellar gas N84-13042
Theory of interstellar medium diagnostics N84-13108
The interplanetary hydrogen and helium glow and the inferred interstellar gas properties N84-13109

INTERSTELLAR MASERS
The excitation of SiO in circumstellar envelopes N84-13041

INTERSTELLAR MATTER
Ultraviolet extinction properties of grains in the interstellar medium N84-13131

INTERSTELLAR RADIATION
The interplanetary hydrogen and helium glow and the inferred interstellar gas properties N84-13109

INTERSTELLAR SPACE
The far infrared sky survey experiment
[AD-A131966] N84-13037

INVENTORIES
Estimation of uncertainty in coal resources
[DE83-902538] N84-12620
Inventory of numeric data for carbon dioxide research
[DE83-017571] N84-12657

INVERSE SCATTERING
Effects of dissipation in one-dimensional inverse problems
[DE83-017692] N84-12353
Inverse born approximation: Exact determination of shape of convex voids
[DE83-017685] N84-12512
The effect of noisy reflection data on an inverse method for determining the structure of a layered ocean bottom
[AD-A131976] N84-12820

INVISCID FLOW
Stability of a pair of stationary vortices in the leeward side of a cylinder in a potential flowfield
[AD-A131917] N84-12095

ION ACCELERATORS
High-sensitivity mass spectrometry with a tandem accelerator
[DE83-017914] N84-12274

ION ATOM INTERACTIONS
Cross sections for charge transfers of highly ionized ions in hydrogen atoms
[IPPJ-AM-30] N84-12912

ION BEAMS
Selective laser ionization for mass-spectral isotopic analysis
[DE83-017303] N84-12483
Observation of multiple ion beams in the magnetotail low latitude boundary layer. Evidence for a double H+ population
[IFSI-82-10] N84-12676
Using inner-shell X-rays as an ion-beam diagnostic
[DE83-017784] N84-12857
Beam-target interaction of intense ion beams: Theory and experiment
[DE83-018264] N84-12858
Magnetic trapping of intense ion beams
[DE83-017356] N84-12866
Rotating and propagating LIB stabilized by self-induced magnetic field
[IPPJ-640] N84-12916
Inertial fusion with low-energy heavy ions
[DE83-016709] N84-12934
Ion stopping in heated targets
[DE83-017800] N84-12941
Diagnosing the ion beam on the applied-B diode
[DE83-017822] N84-12943
Light-ion-beam fusion
[DE83-018263] N84-12944
Proceedings of the Workshop on Ion Mixing and Surface Layer Alloying
[DE83-015354] N84-12994
Spectral analysis of magnetohydrodynamic fluctuations near interplanetary schocks
[NASA-TM-85119] N84-13044

ION CHARGE
Iron charge states observed in the solar wind N84-13112
Mixed solar wind originating from coronal regions of different temperatures N84-13114
Interpreting the solar wind ionization state N84-13115

ION CONCENTRATION
Solar wind minor ions: Recent observations N84-13110
The relative abundance of 3He(++)-in the solar wind N84-13111

Spatial variation of iron abundance in the high speed solar wind, 1972 to 1976 N84-13113

ION CURRENTS
Ionic conductivity in lithium hexaoxometallate solid solutions
[AD-A131842] N84-12250
Defect interactions at high concentrations in solid oxide electrolytes
[DE83-016849] N84-12992

ION DISTRIBUTION
Observation of multiple ion beams in the magnetotail low latitude boundary layer. Evidence for a double H+ population
[IFSI-82-10] N84-12676

ION IMPLANTATION
Semiconductor processing with excimer lasers
[DE83-007509] N84-12477
Proceedings of the Workshop on Ion Mixing and Surface Layer Alloying
[DE83-015354] N84-12994
Physics of ion implantation: Ion-cascade processes and physical state of the implanted solid
[DE83-017152] N84-12998

ION IRRADIATION
Radiation damage and phase instability in irradiated stainless steel
[DE83-017190] N84-12303

ION PUMPS
Thermal barriers: Their purpose and functioning
[DE83-017365] N84-12954

ION RECOMBINATION
Ion-ion recombination rate in the EMP source region
[AD-A131148] N84-12339

ION SOURCES
High-sensitivity mass spectrometry with a tandem accelerator
[DE83-017914] N84-12274
Magnetic trapping of intense ion beams
[DE83-017356] N84-12866
Developing a 500-eV proton beam
[DE83-012781] N84-12880
Applied-B ion diode experiments on PBFA 1
[DE83-017792] N84-12942
Ampfion hybrid diodes on hydramite and PBFA-1
[DE83-017824] N84-12945

IONIC COLLISIONS
Transition flow ion transport via integral Boltzmann equation
[UTIAS-269] N84-12828
Electron-ion collisions
[DE83-017211] N84-12867
Cross sections for charge transfers of highly ionized ions in hydrogen atoms
[IPPJ-AM-30] N84-12912
Electron capture and loss cross sections for collisions between heavy ions and hydrogen molecules, revised
[IPPJ-AM-28] N84-12914
Ultra-relativistic heavy ions and cosmic rays
[DE83-015881] N84-13134

IONIZATION
Selective laser ionization for mass-spectral isotopic analysis
[DE83-017303] N84-12483
Using inner-shell X-rays as an ion-beam diagnostic
[DE83-017784] N84-12857
Ion stopping in heated targets
[DE83-017800] N84-12941
Mixed solar wind originating from coronal regions of different temperatures N84-13114
Interpreting the solar wind ionization state N84-13115

IONIZATION CROSS SECTIONS
Electron capture and loss cross sections for collisions between heavy ions and hydrogen molecules, revised
[IPPJ-AM-28] N84-12914

IONIZING RADIATION
Combined effects of ionizing radiation and anticholinesterase exposure on rodent motor performance
[AD-A131847] N84-12707

IONOSPHERE
Techniques for locating a remote HF transmitter from single-site measurements
[AD-A132014] N84-12342
Activities report on ionospheric observation
[UIO-AR-83-05] N84-12674
Beam plasma turbulence study
[AD-A131946] N84-12917

IONOSPHERIC DISTURBANCES
Activities report on ionospheric observation
[UIO-AR-83-05] N84-12674

IONOSPHERIC HEATING
Activities report on ionospheric observation
[UIO-AR-83-05] N84-12674

IONOSPHERIC PROPAGATION
Guidance of electromagnetic waves in the ionosphere and magnetosphere
[IFSI-82-15] N84-12361

IONOSPHERIC SOUNDING
Speed-dependent collision effects on radar back-scattering from the ionosphere --- incoherent scatter radar
[NASA-CR-173077] N84-12336

IONS
Transition flow ion transport via integral Boltzmann equation
[UTIAS-269] N84-12828
Solar wind minor ions: Recent observations N84-13110
Minor constituents in the solar wind originating from plasma-dust interactions N84-13116

IRIDIUM
Grain-boundary cavitation and weld-underbead cracking in DOP-26 iridium alloy
[DE83-015406] N84-12539

IRON
Comparison of damage microstructures in neutron-irradiated vanadium and iron
[DE83-017189] N84-12304
Charge characteristics of Ni/Fe traction cells
[DE83-014205] N84-12389
Spatial variation of iron abundance in the high speed solar wind, 1972 to 1976 N84-13113

IRON ALLOYS
Corrosion behavior of Fe-Cr-Ni-Zr alloys in aggressive environments at high temperatures
[DE83-014735] N84-12297
Single specimen J-integral testing
[DE83-016069] N84-12543

IRRADIATION
Beam-target interaction of intense ion beams: Theory and experiment
[DE83-018264] N84-12858
The growth and measurement of single-crystal doped GGG (Gd3-xCaxGa5-xZrx012)
[AD-A131875] N84-12971

ISOTHERMAL PROCESSES
Revised isothermal analysis program for Stirling engines
[DE83-017276] N84-12504

ISOTOPE EFFECT
Isotope dependence of the breakdown strength of gases
[DE83-017272] N84-12430

ISOTOPE SEPARATION
Research activities in materials and molecular research
[DE83-015005] N84-12255
Solid state copper vapor laser modulator
[DE83-015837] N84-12475
Selective laser ionization for mass-spectral isotopic analysis
[DE83-017303] N84-12483

ITERATION
Galilean satellite geomorphology
[NASA-CR-174574] N84-13057

J

JET ENGINE FUELS
A jet fuel starter for lowest system life cycle cost N84-12179

JETS
Jet production and high p/sub T/ phenomena in photon-photon reactions
[DE83-016397] N84-12868

JETSTREAM AIRCRAFT
The effects of wing tip devices on the performance of the BAe Jetstream N84-12130

JOINTS (JUNCTIONS)
System identification of structures with joint rotation N84-12330

JUPITER (PLANET)
Jupiter Data Analysis Program: Analysis of Voyager wideband plasma wave observations
[NASA-CR-174575] N84-13058
Comment on the observed plasma densities in Jupiter's distant magnetotail (wake); a possible explanation
[IFSI-83-2] N84-13062

K

KANSAS
Progress in the scene-to-map registration investigation N84-12572

KEROSENE
Numerical simulations of fuel droplet flows using a Lagrangian triangular mesh
[NASA-CR-168263] N84-12411

KINEMATICS
Erosive particle kinematics in the turbulent combustion boundary layer contacting a solid wall
[DE83-010594] N84-12272

KINETIC ENERGY
Annular Momentum Control Device (AMCD) N84-12241
Magnetic bearings for inertial energy storage N84-12242
Feasibility of a laser or charged-particle-beam fusion-reactor concept with direct electric generation by magnetic-flux compression
[DE83-015735] N84-12482

KINETICS
Strong coupling effects on bound states in plasmas
[AD-A131661] N84-12918

KLEIN-GORDON EQUATION
On space-time means and everywhere defined scattering operators for nonlinear Klein-Gordon equations
[CTH-MATH-1983-13-PREPRINT] N84-12793

KNUDSEN FLOW
The collapse of the local, Spitzer-Haerm formulation and a global-local generalization for heat flow in an inhomogeneous, fully ionized plasma N84-13080

KRYPTON
Kinetics of growth and decay of excited rare-gas atoms and molecules in the pulse radiolysis of pure rare gases and of mixtures of rare gases with molecular quenching agents
[DE83-017016] N84-12856

L

LAGEOS (SATELLITE)
Accuracy estimates of gravity potential differences between western Europe and United States through Lageos satellite laser ranging network
[AD-A131838] N84-12669

LAKE ICE
Predicting lake ice decay
[AD-A132012] N84-12618

LAKES
Limnology, second edition
[DE83-016792] N84-12627
World-wide sea-surface temperatures
[AD-A131892] N84-12689

LAMINAR BOUNDARY LAYER
Unsteady compressible laminar boundary-layer flow within an expansion wave
[AD-A131889] N84-12420
Numerical solution of the two-phase, three dimensional boundary layer in laminar film condensation over a curved surface N84-12442

LAMINAR FLOW
Transonic airfoil development N84-12076
Steady laminar natural convection in open rectangular cavities N84-12441
Effects of pressure-drop correlations on Stirling-engine predicted performance
[DE83-017279] N84-12501

LAMINAR FLOW AIRFOILS
Geometries for roughness shapes in laminar flow
[NASA-CASE-LAR-13255-1] N84-12092

LAMINAR HEAT TRANSFER
Unsteady compressible laminar boundary-layer flow within an expansion wave
[AD-A131889] N84-12420
Numerical solution of the two-phase, three dimensional boundary layer in laminar film condensation over a curved surface N84-12442

LAMINATES
Three-dimensional analysis of composite plates with material nonlinearity
[AD-A131884] N84-12258
Vibration response of geometrically nonlinear elastic beams to pulse and impact loading
[NASA-CR-174495] N84-12527

LAND MANAGEMENT
Monitoring of renewable resources (a land information system for Europe) --- remote sensing N84-12581
Inventoring and monitoring of landscape as a natural and cultural resource N84-12594
SAR 580: Images for agricultural and forest survey. First results in middle Belgium N84-12595

LAND USE
Earth Resources Laboratory research and technology
[E84-10033] N84-12576
Remote Sensing Applications for Environmental Studies --- conferences
[ESA-SP-188] N84-12579

SPOT potential applications: An overview of the results of the simulation campaigns N84-12587
Actual state and recent evolution of the French coast observed by remote sensing using LANDSAT recordings N84-12606
Mapping land use in Catalonia (Spain) --- using LANDSAT imagery N84-12613
Development of a data base for carbon dioxide releases resulting from conversion of land to agricultural uses [DE83-015728] N84-12626
Arizona State science, engineering and technology process [PB83-237107] N84-13016
Actitities report on the projet DESBOD --- geographical data acquisition [REPT-5] N84-13025

LANDFORMS
Geomorphic studies of Mars N84-13063

LANDING AIDS
Advanced symbology for general aviation approach to landing displays N84-12039

LANDSAT 4
LANDSAT 4 investigations of thematic mapper and multispectral scanner applications [E84-10006] N84-12555

LAP JOINTS
Some considerations of the efficiency of sewn lap joints in a nylon webbing [RAE-TR-83009] N84-12310

LARGE SPACE STRUCTURES
Control of flexible spacecraft by optimal model following N84-12222
Study of auxiliary propulsion requirements for large space systems. Volume 1: Executive summary [NASA-CR-168193] N84-12226

LARGE SPACE TELESCOPE
Shuttle measured contaminant environment and modeling for payloads. Preliminary assessment of the space telescope environment in the shuttle bay [NASA-TM-85111] N84-12216

LASER APPLICATIONS
Laser velocimeter measurements and analysis in turbulent flows with combustion, part 2 [AD-A131882] N84-12421
Laser activated MTOS microwave device [NASA-NPO-16112-1] N84-12463
Semiconductors investigated by time resolved raman absorption and photoluminescence spectroscopy using femtosecond and picosecond laser techniques [AD-A131860] N84-12466

LASER CAVITIES
Laser journal (selected articles) [AD-A131886] N84-12465
Semiconductors investigated by time resolved raman absorption and photoluminescence spectroscopy using femtosecond and picosecond laser techniques [AD-A131860] N84-12466

LASER DAMAGE
Damage thresholds of thin film materials and high reflectors at 248 nm [DE83-012663] N84-12472
Characterization by X-ray topography of laser-induced damage in potassium dihydrogen phosphate crystals [DE83-012045] N84-12985

LASER DOPPLER VELOCIMETERS
Laser velocimetry study of compressibility effects on the flow field of a delta wing N84-12108
Soot formation from polycyclic aromatics [DE83-009750] N84-12271

LASER GYROSCOPES
Evaluation of the stochastic drift of rate integrating gyros as preparation for the analysis of laser gyro drift measurements [DFVLR-MITT-83-04] N84-12449

LASER HEATING
Semiconductor processing with excimer lasers [DE83-007509] N84-12477

LASER MATERIALS
Laser interaction with metallic surfaces [AD-A126269] N84-12464

LASER OUTPUTS
Laser journal (selected articles) [AD-A131886] N84-12465
Windows and mirrors needed for a laser-driven photoneutralizer [DE83-013582] N84-12473
Inertial effects in laser-driven ablation [DE83-016941] N84-12478

LASER PLASMAS
Time-resolved spectral measurements above 80 A [DE83-015616] N84-12933

LASER PUMPING
RF conditioned dc discharges for excitation of rare gas halide lasers [DE83-016537] N84-12479
Ukrainian Physics Journal (selected articles) [AD-A131087] N84-12814

LASER RANGE FINDERS
Y03: Prequalification of surface treatment. Measurement of laser reflecting power --- Earth-Moon telemetry [ESA-TT-791] N84-12490
Retroreflector YO3: Study of the optical properties of protected mirrors --- Earth-Moon telemetry [ESA-TT-789] N84-12907

LASER SPECTROSCOPY
Laser spectroscopy of propellant-like flames [AD-A132042] N84-12267
Investigation of inhomogeneity in ceramic reactor materials using laser-localized emission spectroscopy [JUEL-1834] N84-12323
Laser physics and laser spectroscopy [AD-A131720] N84-12470
Infrared-laser spectroscopy using a long-pathlength absorption cell [DE83-014197] N84-12480

LASER STABILITY
Laser journal (selected articles) [AD-A131886] N84-12465

LASER TARGET INTERACTIONS
Y03: Prequalification of surface treatment. Measurement of laser reflecting power --- Earth-Moon telemetry [ESA-TT-791] N84-12490

LASER TARGETS
Inertial effects in laser-driven ablation [DE83-016941] N84-12478
Creation of ultra-high-pressure shocks by the collision of laser-accelerated disks: Experiment and theory [DE83-017366] N84-12486

LASER WEAPONS
Pulsed power bibliography. Volume 2: Annotated bibliography [AD-A131753] N84-12468
Pulsed power bibliography. Volume 1: Indices [AD-A131752] N84-12469

LASER WINDOWS
Windows and mirrors needed for a laser-driven photoneutralizer [DE83-013582] N84-12473

LASERS
Laser interaction with metallic surfaces [AD-A126269] N84-12464

LASING
Free-electron-laser research [DE83-016957] N84-12489

LATE STARS
Theory of winds in late-type evolved and pre-main-sequence stars N84-13085

LATITUDE
Variability of atmospheric density in the middle atmosphere [AD-A131985] N84-12667

LATTICE VIBRATIONS
Structure and vibrational spectra of a model of a-Si:H with periodic boundary conditions [DE83-015245] N84-12390

LAWS
IPACS attitude control technology considerations N84-12238
National Aeronautics and Space Act of 1958, as amended and related legislation [GPO-24-491] N84-13032

LAYERS
Fabrication and properties of multilayer structures [AD-A131934] N84-12969

LEAD ACID BATTERIES
Assessment of potential for batteries in space applications N84-12246
Comparative response of lead-acid and nickel-iron batteries to pulsed and constant-current loads [DE83-017939] N84-12395
Effect of antimony on lead-acid battery negative electrode [DE83-014680] N84-12404

LEAD TELLURIDES
Single Pb (1-x)Sn(x) Te crystal growth by vapor phase transport, with formation of a liquid/solid interface [INPE-2811-PRE/369] N84-12967

LEADING EDGE SWEEP
On the generation and subsequent development of spiral vortex flow over a swept-back wing N84-12105

LEADING EDGES
Geometries for roughness shapes in laminar flow [NASA-CASE-LAR-13255-1] N84-12092
Recent studies at NASA-Langley of vortical flows interacting with neighboring surfaces N84-12109
Experimental investigation of forebody and wing leading-edge vortex interactions at high angles of attack N84-12110
Computational vortex flow aerodynamics N84-12117
Boundary layer segmentation on sharp highly swept leading edges and its effects on secondary vortices N84-12132
Augmentation of fighter-aircraft performance by spanwise blowing over the wing leading edge N84-12133
Quasi-steady solar wind dynamics N84-13120

LEAKAGE
In-situ permeation tests of elastomeric O-ring seals [DE83-015622] N84-12318
The SSME seal test program: Leakage tests for helically-grooved seals [NASA-CR-170921] N84-12495
Transmission of fast neutrons from the Li(d,xn) reaction through thick iron [DE83-015975] N84-12884

LENSES
Performance analysis of a three-dimensional microwave lens in a cylindrical array scanning application [AD-A131891] N84-12345

LEVITATION
Containerless electromagnetic levitation melting of Cu-Fe and Ag-Ni alloys [NASA-TM-82553] N84-12288

LIBRARIES
Guidelines for the design of large modular scientific libraries in Ada [NPL-DITC-28/83] N84-12740
Environments and search paths for the software tools [DE83-016607] N84-12749
Perkin-Elmer, Perkin-Elmer 3230 COBOL R07 (pre-release) [PB83-236600] N84-12766
NBS (National Bureau of Standards) Workshop: Environmental Control for Archival Records Storage [PB83-242230] N84-13026
Permuted medical subject headings, 1984 [PB83-234781] N84-13027
Medical subject headings, tree structures, 1984 [PB83-223164] N84-13028

LIFE (DURABILITY)
Life prediction under stress corrosion conditions below K sub ISCC [DE83-018074] N84-12307

LIFE CYCLE COSTS
A jet fuel starter for lowest system life cycle cost N84-12179

LIFT
Dynamic-stall regulation of the Darrieus turbine [DE83-017994] N84-12097

LIFT DRAG RATIO
Recent studies at NASA-Langley of vortical flows interacting with neighboring surfaces N84-12109

LIGANDS
Measurements, in vivo, of parameters of the dopamine system [DE83-017964] N84-12709

LIGHT (VISIBLE RADIATION)
Fundamentals and techniques of nonimaging optics, volume 2 [DE83-015447] N84-12902

LIGHT ADAPTATION
Experimental studies relating environmental lighting and flicker to visual fatigue in VDT operators [DE83-016316] N84-12738

LIGHT EMISSION
Comparison of technologies for new energy-efficient lamps [DE83-015949] N84-12401
Luminosity enhancement in relativistic jets and altered luminosity functions for beamed objects [NASA-TM-85053] N84-12889

LIGHT IONS
Magnetic trapping of intense ion beams [DE83-017356] N84-12866
Rotating and propagating LIB stabilized by self-induced magnetic field [IPPJ-840] N84-12916
Light-ion-beam fusion [DE83-018263] N84-12944

LIGHT SCATTERING
Transport and relaxation processes in supercritical fluids [DE83-015966] N84-12432
Design and operation of a light-scattering device for sizing and velocimetry of large droplets [DE83-902641] N84-12456

LIGHT TRANSMISSION
Turbulence environment characterization [AD-A131815] N84-12692

LIGHTNING
The effects of channel tortuosity on electromagnetic radiations from lightning return strokes N84-12335

LIGNIN
Effect of antimony on lead-acid battery negative electrode
[DE83-014660] N84-12404
LIMITERS (FUSION REACTORS)
Self-pumping impurity by in-situ metal deposition
[DE83-017937] N84-12306
LIMNOLOGY
Limnology, second edition
[DE83-016792] N84-12627
LINE OF SIGHT
Luminosity enhancement in relativistic jets and altered luminosity functions for beamed objects
[NASA-TM-85053] N84-12889
LINE SPECTRA
Development of a continuous monitor for detection of toxic organic compounds
[PB83-234922] N84-12461
The winds and coronae of early-type stars N84-13086
Stellar winds driven by multi-line scattering N84-13087
LINEAR ACCELERATORS
Subharmonic buncher for the Los Alamos free-electron laser oscillator experiment
[DE83-015220] N84-12474
Monitoring of the Stanford Linac microbunches' position
[DE83-012712] N84-12640
Magnetic switching
[DE83-012952] N84-12841
University of Washington superconducting-booster project
[DE83-015689] N84-12846
New facilities for the US high-energy physics program
[DE83-016589] N84-12876
Effect of RF structure on cumulative beam breakup
[DE83-017302] N84-12882
Generation of monoenergetic positrons
[DE83-015535] N84-12887
Conceptual design of the high-flux VTA-2 test assembly for FMIT
[DE83-017022] N84-12935
LINEAR EQUATIONS
Rank modification method for certain singular systems of linear equations N84-12797
LINEAR PROGRAMMING
Acquisition, image and data compression
[AD-A131923] N84-12344
Disjunctive programming and a hierarchy of relaxations for discrete optimization problems
[AD-A132004] N84-12784
LINEAR SYSTEMS
Maximum likelihood estimation of linear dynamic system parameters
[AR-002-934] N84-12780
LINEARITY
Interaction of stress waves and cracks using a second order accurate finite difference method N84-12522
Electrostatic waves and anomalous transport in the solar wind N84-13095
LININGS
Replacement of PBNA in HB and HC polymers used in SRM propellant and liner
[NASA-CR-170936] N84-12311
LIQUID ATOMIZATION
Constant-output atomizer --- inhalation therapy and aerosol research
[NASA-CASE-MFS-25631-1] N84-12406
LIQUID HELIUM
Transient heat transfer in superfluid helium, part 2
[DE83-015767] N84-12984
LIQUID HYDROGEN
Analytical design of a liquid hydrogen fueled turbofan-ramjet engine for flight Mach numbers zero to five N84-12187
LIQUID PHASE EPITAXY
Liquid phase epitaxy of InP/In1-xGxAsyP1-y heterostructures. Part 3: Phase diagrams
[FI-65-TBR-20-PT-3] N84-13000
LIQUID PHASES
Electron-molecule interactions in gases and liquids: The electron-attachment process in gases and nonpolar liquids
[DE83-017205] N84-12863
LIQUID-SOLID INTERFACES
Measurements of ultrasonic scattering from near-surface flaws
[DE83-017693] N84-12827
Single Pb (1-x)Sn(x) Te crystal growth by vapor phase transport, with formation of a liquid/solid interface
[INPE-2811-PRE/369] N84-12967
LITHIUM
Lithium equation-of-state
[DE83-017988] N84-12253
Feasibility of a laser or charged-particle-beam fusion-reactor concept with direct electric generation by magnetic-flux compression
[DE83-015735] N84-12482
LITHIUM COMPOUNDS
Ionic conductivity in lithium hexaoxometallate solid solutions
[AD-A131842] N84-12250
LOAD DISTRIBUTION (FORCES)
Load deflection characteristics of inflated structures
[NASA-CR-174585] N84-12028
LOAD TESTS
The analysis of crack growth data with application to trip steel
[AD-A132021] N84-12535
LOADS (FORCES)
Effects of nonlinear loads on antennas and scatterers N84-12376
Bending of transversally loaded orthotropic rectangular and sector plates N84-12520
On the dynamic fracture of bars, beams and plates N84-12552
A model for stresses in circular magnets for toroidal fusion devices
[DE83-016535] N84-12937
LOCI
On sensitivity, compensation and the approach to the asymptotes in multivariable root-loci
[RR-222] N84-12795
LOGARITHMS
An iterated logarithm law result for extreme values from Gaussian sequences
[AD-A129559] N84-12798
LOGISTICS
Models of maintenance resources interaction: Peacetime operations
[AD-A131379] N84-13011
LONG RANGE WEATHER FORECASTING
Estimating long-term mean winds from short-term wind data
[DE83-017417] N84-12693
LONG TERM EFFECTS
Long term evaluation of the effects of shale oil produced JP-4 on aircraft construction materials
[AD-A131665] N84-12161
Estimating long-term mean winds from short-term wind data
[DE83-017417] N84-12693
LONGITUDINAL CONTROL
An integrated AFCS for the "PROFILE"-mode N84-12069
LOUISIANA
Progress in the scene-to-map registration investigation N84-12572
LOW SPEED
An experimental investigation of the vortex flow over delta and double-delta wings at low speed N84-12106
LOW TEMPERATURE PHYSICS
Thermal conductance measurements of pressed OFHC copper contacts at liquid helium temperatures
[NASA-TM-85861] N84-12809
LOWER BODY NEGATIVE PRESSURE
Lower body graduated negative pressure system
[NASA-CR-171717] N84-12725
LUBRICATING OILS
150 hour engine test of corrosion inhibited MIL-L-23699C oil
[AD-A131633] N84-12317
LUGS
Composite structural materials
[NASA-CR-174597] N84-12257
LUMINAIRES
Comparison of technologies for new energy-efficient lamps
[DE83-015949] N84-12401
LUMINANCE
The interplanetary hydrogen and helium glow and the inferred interstellar gas properties N84-13109
LUMINESCENCE
Hydrogen in MgO crystals thermochemically reduced at very high temperatures
[DE83-014058] N84-12981
LUMINOSITY
Luminosity enhancement in relativistic jets and altered luminosity functions for beamed objects
[NASA-TM-85053] N84-12889
Faint galaxies in the Coma cluster: Luminosity function and spatial distribution N84-13053
LUNAR EVOLUTION
Workshop on Pristine Highlands Rocks and the early History of the Moon
[NASA-CR-174584] N84-13059
Workshop on Pristine Highlands Rocks and the Early History of the Moon
[NASA-CR-174600] N84-13060
LUNAR GEOLOGY
Workshop on Pristine Highlands Rocks and the Early History of the Moon
[NASA-CR-174600] N84-13060
LUNAR RETROREFLECTORS
Y03: Prequalification of surface treatment. Measurement of laser reflecting power --- Earth-Moon telemetry
[ESA-TT-791] N84-12490
Retroreflector YO3: Study of the optical properties of protected mirrors --- Earth-Moon telemetry
[ESA-TT-789] N84-12907
LUNAR ROCKS
Workshop on Pristine Highlands Rocks and the early History of the Moon
[NASA-CR-174584] N84-13059
LUNGS
Pulmonary dosimetry of nitrogen dioxide in animals and man
[PB83-243394] N84-12711

M

MACHINE TOOLS
Holding fixture for a hot stamping press
[NASA-CASE-GSC-12619-1] N84-12491
Fabrication of machined optics for precision applications
[DE83-015720] N84-12900
MACHINE TRANSLATION
Prerequisites for deriving formal specifications from natural language requirements
[AD-A131722] N84-12771
MAGELLANIC CLOUDS
Problems of stellar evolution in star clusters of the Magellanic clouds N84-13051
MAGNESIUM OXIDES
Hydrogen in MgO crystals thermochemically reduced at very high temperatures
[DE83-014058] N84-12981
MAGNET COILS
Self-correction coil: Operation mechanism of self-correction coil
[DE83-016324] N84-12392
Comparative evaluation of existing concepts for a 10-tesla FED toroidal field coil
[DE83-012817] N84-12815
A model for stresses in circular magnets for toroidal fusion devices
[DE83-016535] N84-12937
MAGNETIC BEARINGS
GSFC flywheel status N84-12230
Magnetic bearings for inertial energy storage N84-12242
MAGNETIC COILS
Advanced high-field coil designs: 20 Tesla
[DE83-017368] N84-12397
Design of the Advanced Toroidal Facility (ATF-1)
[DE83-012641] N84-12923
Operational studies and expected performance of superconducting quadrupole magnets in the first stages of secondary beams
[DE83-016734] N84-12999
MAGNETIC COMPRESSION
Feasibility of a laser or charged-particle-beam fusion-reactor concept with direct electric generation by magnetic-flux compression
[DE83-015735] N84-12482
MAGNETIC DIPOLES
Multidipole magnetic fields for plasma confinement
[DE83-016014] N84-12960
MAGNETIC DISKS
Creation of ultra-high-pressure shocks by the collision of laser-accelerated disks: Experiment and theory
[DE83-017366] N84-12486
MAGNETIC EFFECTS
On the field configuration in magnetic clouds N84-13125
MAGNETIC FIELD CONFIGURATIONS
Fokker-Planck equation in mirror research
[DE83-016568] N84-12932
Three-dimensional equilibrium in quadrupole symmetric tandem mirrors in the paraxial limit (reduced MHD)
[DE83-017840] N84-12940
Multidipole magnetic fields for plasma confinement
[DE83-016014] N84-12960
Effect of magnetic bending on the high-frequency stability of the ELMO Bumpy Torus
[DE83-017177] N84-12961
Interplanetary Alfvenic fluctuations: A statistical study of the directional variations of the magnetic field
[IFSI-82-14] N84-13050
Solar Wind Five
[NASA-CP-2280] N84-13067

Observations of hydromagnetic turbulence in the solar wind N84-13074

MAGNETIC FIELDS

Techniques for locating a remote HF transmitter from single-site measurements
[AD-A132014] N84-12342

Synchronous generators with superconductive excitation windings
[AD-A131832] N84-12382

A high-performance digital triggering system for phase-controlled rectifiers
[DE83-012217] N84-12386

Problem of magnet ramping
[DE83-014054] N84-12399

Storage of energy in magnetic field of superconductive coils
[AD-A131898] N84-12636

Eruption of permanent dentition in rhesus monkeys exposed to ELF (Extremely low frequency) fields
[AD-A132065] N84-12703

Dissipative instabilities of magnetic neutral layers with velocity shear
[IFSI-82-13] N84-12965

Direct coronal heating from dissipation of magnetic field N84-13069

Solar cycle variations of the solar wind N84-13089

Solar cycle evolution of the solar wind in three dimensions N84-13090

Solar cycle variations in the interplanetary magnetic field N84-13091

Plasma properties of driver gas following interplanetary shocks observed by ISEE-3 N84-13123

MAGNETIC FILMS

A program of research on microfabrication techniques for VLSI magnetic devices
[AD-A131706] N84-12978

MAGNETIC INDUCTION

Steam turbine as unipolar generator
[AD-A131142] N84-12498

MAGNETIC MATERIALS

Anisotropy and microstructure of Sm2(Co, Fe, Cu, Zr)17 magnetic materials
[AD-A131961] N84-12291

MAGNETIC MIRRORS

Initial assessment of the MHD stability of TMX-U
[DE83-016521] N84-12646

Magnetic trapping of intense ion beams
[DE83-017356] N84-12866

Summary of the MARS tandem-mirror reactor design
[DE83-017293] N84-12939

Three-dimensional equilibrium in quadrupole symmetric tandem mirrors in the paraxial limit (reduced MHD)
[DE83-017840] N84-12940

Vacuum measurements on the tandem mirror experiment upgrade (TMX-U) fusion experiment
[DE83-017836] N84-12946

Status of tandem-mirror confinement
[DE83-017369] N84-12948

Drift wave studies in a linear multiple mirror
[DE83-016881] N84-12951

Thermal barriers: Their purpose and functioning
[DE83-017365] N84-12954

TMX-U experimental results
[DE83-016790] N84-12955

Thermal performance of the MFTF magnets
[DE83-016275] N84-12988

MAGNETIC MOMENTS

Radial evolution of ion distribution functions N84-13094

MAGNETIC PROPERTIES

Progress in developing repetitive pulse systems utilizing inductive energy storage
[DE83-015167] N84-12388

On the field configuration in magnetic clouds N84-13125

MAGNETIC SUSPENSION

Performance measurements of a pilot superconducting solenoid model core for a wind tunnel magnetic suspension and balance system
[NASA-CR-172243] N84-12192

MAGNETIC SWITCHING

Magnetic switching
[DE83-012952] N84-12841

MAGNETICALLY TRAPPED PARTICLES

Magnetic trapping of intense ion beams
[DE83-017356] N84-12866

MAGNETIZATION

Steam turbine as unipolar generator
[AD-A131142] N84-12498

MAGNETOHYDRODYNAMIC FLOW

Theory of hydromagnetic turbulence N84-13077

Observational constraints on solar wind acceleration mechanisms N84-13078

Magnetohydrodynamic modeling of coronal structure and expansion N84-13081

Plasma properties of driver gas following interplanetary shocks observed by ISEE-3 N84-13123

MAGNETOHYDRODYNAMIC GENERATORS

Development of materials for open-cycle MHD
[DE83-016334] N84-12926

Structure of convective surface deposits and effect on MHD steam-plant design
[DE83-010757] N84-12931

MAGNETOHYDRODYNAMIC STABILITY

Longitudinal space-charge effects in bunched beams
[DE83-017305] N84-12888

Magnetohydrodynamic equilibrium and stability of spheromak plasma in flux conserver
[IPPJ-642] N84-12909

Instabilities in cylindrical plasma liners imploded by high magnetic fields
[DE83-013640] N84-12921

Theoretical studies of fusion physics. Volume 2: Appendices
[DE83-010371] N84-12925

Drift wave studies in a linear multiple mirror
[DE83-016881] N84-12951

Effect of magnetic bending on the high-frequency stability of the ELMO Bumpy Torus
[DE83-017177] N84-12961

Dissipative instabilities of magnetic neutral layers with velocity shear
[IFSI-82-13] N84-12965

Superconducting stability, 1983: A review
[DE83-017262] N84-12995

MAGNETOHYDRODYNAMIC TURBULENCE

Solar Wind Five
[NASA-CP-2280] N84-13067

HRTS observations of the fine structure and dynamics of the solar chromosphere and transition zone N84-13070

Magnetohydrodynamic turbulence in the solar wind N84-13073

Observations of hydromagnetic turbulence in the solar wind N84-13074

MAGNETOHYDRODYNAMIC WAVES

Radio scintillations at large elongation angles: Contributions of waves versus discontinuities
[IFSI-82-4] N84-12358

Observations of soft X-ray fluctuations with an imaging array on TEXT
[DE83-018118] N84-12938

Spectral analysis of magnetohydrodynamic fluctuations near interplanetary schocks
[NASA-TM-85119] N84-13044

Coronal heating by waves N84-13068

Alfven solitons in the solar wind N84-13075

Interplanetary Alfvenic fluctuations: A statistical study of the directional variations of the magnetic field N84-13076

MAGNETOHYDRODYNAMICS

Initial assessment of the MHD stability of TMX-U
[DE83-016521] N84-12646

Boundary-integral simulations of rayleigh-taylor instability in ideal magnetohydrodynamics
[AD-A131667] N84-12920

A 2-D skin-current toroidal-MHD-equilibrium code
[DE83-016916] N84-12929

Variational-moment method for computing magnetohydrodynamic equilibria
[DE83-017477] N84-12957

Radial variations of large-scale magnetohydrodynamic fluctuations in the solar wind
[NASA-TM-85116] N84-13045

Modeling of transient disturbances in coronal-streamer configurations N84-13119

On the field configuration in magnetic clouds N84-13125

MAGNETOMETERS

Low energy electron magnetometer using a monoenergetic electron beam
[NASA-CASE-LAR-12706-1] N84-12444

MAGNETOSPHERE

Guidance of electromagnetic waves in the ionosphere and magnetosphere
[IFSI-82-15] N84-12361

Magnetospheric plasma studies using data from the dynamics high and low altitude plasma instruments
[AD-A131793] N84-12670

Beam plasma turbulence study
[AD-A131946] N84-12917

Comment on the observed plasma densities in Jupiter's distant magnetotail (wake); a possible explanation
[IFSI-83-2] N84-13062

Measurement of macroscopic plasma parameters with a radio experiment: Interpretation of the quasi-thermal noise spectrum observed in the solar wind N84-13096

MAGNETRON SPUTTERING

Corrosion resistant coating
[NASA-NPO-15928-1] N84-12289

MAGNETS

Development of a continuous monitor for detection of toxic organic compounds
[PB83-234922] N84-12461

MAINE

Snow cover and meteorology at Allagash, Maine, 1977 - 1980
[AD-A132013] N84-12684

MAINTAINABILITY

Reliability and maintainability study of select solar-energy-system components in the National Solar Data Network
[DE83-011974] N84-12647

MAINTENANCE

Effects of integrated maintenance on the definitions of onboard equipments --- Mirage 2000 aircraft N84-12068

MAN ENVIRONMENT INTERACTIONS

Introductory studies of natural contamination and manmade pollution in Danish waters N84-12608

MAN MACHINE SYSTEMS

A comparison of manual and vocal response modes for the control of aircraft subsystems
[AD-A132048] N84-12152

Automated reasoning in man-machine control systems
[DE83-014307] N84-12774

MANAGEMENT INFORMATION SYSTEMS

Office automation management guide
[AD-A131770] N84-13012

MANAGEMENT METHODS

Quality is not a dirty word
[DE83-012166] N84-12510

Information resources management plan
[AD-A131964] N84-13023

MANAGEMENT PLANNING

Develop a normative or descriptive model of the international/domestic civil aviation industry, volume 3
[AD-A131878] N84-12051

Develop a normative or descriptive model of the international/domestic civil aviation industry, volume 2
[AD-A131877] N84-12052

Develop a normative or descriptive model of the international/domestic civil aviation industry. Volume 1: Executive summary
[AD-A131876] N84-12053

Ris assessment techniques: A handbook for program management personnel
[AD-A131596] N84-13010

Office automation management guide
[AD-A131770] N84-13012

Management of QA in an R and D organization
[DE83-016924] N84-13014

Arizona State science, engineering and technology process
[PB83-237107] N84-13016

Information resources management plan
[AD-A131964] N84-13023

MANAGEMENT SYSTEMS

Design and development of the multifunction flight control reference system N84-12065

MANGANESE

Analysis of the world distribution of metal-rich subsea manganese nodules
[USGS-CIRC-886] N84-12577

MANGANESE ALLOYS

Formation of surface layers during oxidation of a Fe-Mn-Si alloy
[DE83-009495] N84-12302

MANUAL CONTROL

A comparison of manual and vocal response modes for the control of aircraft subsystems
[AD-A132048] N84-12152

MANUALS

Praxis language environment: Distribution-package description
[DE83-017546] N84-12750

Integrated Cuing Requirements (ICR) study: Demonstration data base and users guide
[AD-A131119] N84-13019

MAPPING

OI 630.0 nm optical measurements of neutral winds, temperatures and airglow enhancements during the BIME program
[AD-A131695] N84-12671

PLT: A multipurpose plotting package
[DE83-018261] N84-12735

NASA Facts: IRAS - Mapping the Infrared Sky
[NASA-FACTS-139] N84-13036

MAPS

Wind-speed extremes in the Northern Hemisphere, 30 through 60 km
[AD-A132019] N84-12682

MARINE ENVIRONMENTS
The dependence of the radar modulation transfer function on environmental conditions and wave parameters
[AD-A131858] N84-12348
Remote sensing applied to marine pollution control N84-12607
Optical extinction coefficients beneath marine stratus clouds. Comparison of coefficients calculated from observed aerosol spectra with coefficients specified by the Navy aerosol model
[AD-A132011] N84-12685

MARKET RESEARCH
Search among queues
[AD-A131639] N84-12773

MARKETING
The SPOT distribution system N84-12615
Search among queues
[AD-A131639] N84-12773

MARKOV CHAINS
Mixture models for dependent observations N84-12562

MARS SURFACE
Geomorphic studies of Mars N84-13063

MASS DISTRIBUTION
Associations between coronal mass ejections and interplanetary shocks N84-13121

MASS FLOW
Helium-flow measurement using ultrasonic technique
[DE83-017765] N84-12826

MASS SPECTROMETERS
Operation of the Brookhaven MPS Facility
[DE83-015383] N84-12896

MASS SPECTROSCOPY
High-sensitivity mass spectrometry with a tandem accelerator
[DE83-017914] N94-12274
Laser physics and laser spectroscopy
[AD-A131720] N84-12470
Selective laser ionization for mass-spectral isotopic analysis
[DE83-017303] N84-12483

MASS TRANSFER
New statistical and non-statistical effects in deep inelastic heavy-ion collisions
[DE83-015732] N84-12885

MATCHING
Image matching using generalized Hough transforms N84-12569
Analysis of subpixel registration accuracy N84-12570

MATERIALS HANDLING
Innovative industrial-materials processes — potential for energy conservation
[DE83-016784] N84-12649
PATRAM '83: 7th International Symposium on Packaging and Transportation of Radioactive Materials, summaries
[DE83-012390] N84-12681

MATERIALS RECOVERY
Advanced technologies for the recovery, disposal, and reuse of carbon dioxide for atmospheric control
[DE83-016371] N84-12256

MATHEMATICAL MODELS
Mathematical modeling and simulation of multiaxis hydraulic test facilities N84-12204
Numerical modeling techniques according to the wave equation and the ray method — in seismology
[BMFT-FB-T-83-136] N84-12354
Scale modelling and full scale measurement techniques with particular reference to antennas in their operational environments N84-12368
Physical modeling of EM propagation over nonhomgeneous terrain N84-12370
Numerical modeling techniques for antennas N84-12373
Numerical modeling techniques for half-space (ground) problems N84-12374
Numerical modelling methods for predicting antenna performance on aircraft N84-12375
Optimization of ultrasonic flaw detection in railroad rail
[PB83-236919] N84-12518
Cumulative damage in components of steel structures under cyclic inelastic loading N84-12550
Autoregressive models for use in scene segmentation N84-12561
Simulation aspects in the study of rectification of satellite scanner data N84-12571
A comparison between GEOS 1 magnetic field measurements and some models of the geomagnetic field
[IFSI-82-5] N84-12675
Second order partial differential equations of mixed type N84-12775
Deterministic models in mathematical demography: An investigation of stable population theory including an analysis of the population statistics of Denmark N84-12806
Double porosity model for acoustic wave propagation in fractured-porous rock
[DE83-017823] N84-12823
Beam-target interaction of intense ion beams: Theory and experiment
[DE83-018264] N84-12858
Atomic processes in hot dense plasma
[IPPJ-AM-31] N84-12911
Computational synergetics and innovation in wave, vortex, and plasma cloud dynamics
[DE83-015252] N84-12928
A model for stresses in circular magnets for toroidal fusion devices
[DE83-016535] N84-12937
Detailed modeling of microwave energy deposition in EBT devices
[DE83-017496] N84-12952
A numerical model for diffusion of helium in a hydrogen plasma
[REPT-83-147] N84-12964
Models of maintenance resources interaction: Peacetime operations
[AD-A131379] N84-13011
Theory of hydromagnetic turbulence N84-13077
Magnetohydrodynamic modeling of coronal structure and expansion N84-13081

MATRICES (MATHEMATICS)
Limit theorems for the eigenvalues of product of two random matrices
[AD-A131682] N84-12787

MATRIX MATERIALS
Fatigue of fiber composites
[FFA-TN-1983-30] N84-12260

MAXIMA
An iterated logarithm law result for extreme values from Gaussian sequences
[AD-A129559] N84-12798

MAXIMUM LIKELIHOOD ESTIMATES
Discrimination relative to measures of non-normality N84-12566
Effect of noise in the three-parameter logistic model
[AD-A131867] N84-12721
Maximum likelihood estimation of linear dynamic system parameters
[AR-002-934] N84-12780

MAXWELL EQUATION
The effects of channel tortuosity on electromagnetic radiations from lightning return strokes N84-12335
A model for chorus associated electrostatic bursts
[NASA-CR-174489] N84-12832

MEAN
Wind-speed extremes in the Northern Hemisphere, 30 through 60 km
[AD-A132019] N84-12682

MEASURING INSTRUMENTS
Visual accommodation trainer-tester
[NASA-CASE-ARC-11426-1] N84-12193
Design and operation of a light-scattering device for sizing and velocimetry of large droplets
[DE83-902641] N84-12456
Evaluation of the crack gage as an advanced individual aircraft tracking concept N84-12551

MECHANICAL DEVICES
Robotics: An introduction to today's robot and future trends
[AD-A132070] N84-12768

MECHANICAL PROPERTIES
Mechanical property evaluation of P/M (Powder-Metallurgy) aluminum 7090-T7E71 plate
[AD-A132058] N84-12290
Mechanical behavior of sea ice
[AD-A131852] N84-12619

MEDICAL SCIENCE
Permuted medical subject headings, 1984
[PB83-234781] N84-13027
Medical subject headings, tree structures, 1984
[PB83-223164] N84-13028
Medical Subject Headings, Annotated Alphabetic List, 1984
[PB83-223156] N84-13029

MEDITERRANEAN SEA
Marine remote sensing activities of the Joint Research Center, Ispra, Italy N84-12586
Remote sensing analysis of oil pollution in Augusta Bay, Sicily N84-12616

MELTING
Predicting lake ice decay
[AD-A132012] N84-12618

MEMBRANES
Novel composite membranes
[PB83-243170] N84-12284

MENTAL PERFORMANCE
Physical fitness as a moderator of cognitive degradation during sleep deprivation
[AD-A131962] N84-12718

MERCURY CADMIUM TELLURIDES
HgCdTe surface study program
[AD-A132071] N84-12266

MESONS
Proceedings of the 16th LAMPF Users-Group Meeting
[DE83-013215] N84-12488

MESOSCALE PHENOMENA
Numerical simulation of convective scaling N84-12660

METAL FILMS
Polymer degradation on reflecting metal films: Fourier transform infrared (FTIR) reflection-absorbance studies
[DE83-012129] N84-12641
Sputtered C-axis inclined piezoelectric films and shear-wave resonators
[DE83-017253] N84-12997

METAL MATRIX COMPOSITES
Cold sintering: A new powder consolidation process
[AD-A131687] N84-12292

METAL OXIDE SEMICONDUCTORS
Laser activated MTOS microwave device
[NASA-NPO-16112-1] N84-12463
Hole trapping, recombination, and space charge in irradiated Sandia oxides
[DE83-015212] N84-12986
Applications of analog Change Coupled Devices (CCD's)
[BMFT-FB-T-83-141] N84-13002

METAL PARTICLES
Structural characterization of dispersed metal catalysts
[DE83-017145] N84-12305

METAL PLATES
Mechanical property evaluation of P/M (Powder-Metallurgy) aluminum 7090-T7E71 plate
[AD-A132058] N84-12290

METAL SURFACES
Self-pumping impurity by in-situ metal deposition
[DE83-017937] N84-12306
Research and development for investigations of metallic adsorptions on metal surfaces by optical techniques complemented by dc resistivity and auger spectroscopy
[AD-A131739] N84-12351
Laser interaction with metallic surfaces
[AD-A126269] N84-12464
International Conference on Vibrations at Surfaces (3rd)
[AD-A131794] N84-12834

METAL VAPOR LASERS
Solid state copper vapor laser modulator
[DE83-015837] N84-12475

METAL WORKING
Holding fixture for a hot stamping press
[NASA-CASE-GSC-12619-1] N84-12491

METALLIC GLASSES
Chemical properties of metallic glasses
[DE83-017353] N84-12322

METALLOGRAPHY
Mechanical property evaluation of P/M (Powder-Metallurgy) aluminum 7090-T7E71 plate
[AD-A132058] N84-12290

METALS
Evaluation of the kinematic variable (back stress) response of metals
[DE83-008381] N84-12293
Elastic-wave inverse scattering in non-destructive evaluation
[DE83-017683] N84-12513
A pressure-shear experiment for studying the dynamic plastic responses of metals at shear strain rates of 10 to the 5th power s(-1) N84-12519
New developments and oppotunities for NMR in metal-hydrogen systems
[DE83-017696] N84-12864

METASTABLE STATE
Superconductor stability, 1983: A review
[DE83-015506] N84-12990
Proceedings of the Workshop on Ion Mixing and Surface Layer Alloying
[DE83-015354] N84-12994

METEOROLOGICAL BALLOONS
Thin film strain transducer — in-flight monitoring of balloon film strain
[NASA-WLP-10055-2] N84-12448

METEOROLOGICAL PARAMETERS
Pilot controls and SPIRF flight N84-12038
Wind-speed extremes in the Northern Hemisphere, 30 through 60 km
[AD-A132019] N84-12682
Winds: Chapter 6, 1983 revision. Handbook of Geophysics and Space Environments
[AD-A132018] N84-12683

Snow cover and meteorology at Allagash, Maine, 1977 - 1980
[AD-A132013] N84-12684
Optical extinction coefficients beneath marine stratus clouds. Comparison of coefficients calculated from observed aerosol spectra with coefficients specified by the Navy aerosol model
[AD-A132011] N84-12685
Proceedings of 1st International Workshop on Atmospheric Icing of Structures
[AD-A131869] N84-12690
Climate of Phoenix, Arizona (revised)
[PB83-246801] N84-12699

METEOROLOGICAL RADAR
Radar meteorology in cloud physics and radio wave propagation research
[ESA-TT-806] N84-12695

METEOROLOGICAL SATELLITES
US weather satellites and services
[GPO-25-753] N84-12208

METHANATION
Fluidized bed gasification of biomass to methane
[NASA-CASE-NPO-15903-1] N84-12635

METHANE
Fluidized bed gasification of biomass to methane
[NASA-CASE-NPO-15903-1] N84-12635

METHOD OF MOMENTS
Variational-moment method for computing magnetohydrodynamic equilibria
[DE83-017477] N84-12957

METHYL ALCOHOLS
Reduction of CO2 to methanol and methane by photo and dark reactions on semiconductor electrodes
[PB83-249490] N84-12329
Optimum engine for methanol utilization
[PB83-239459] N84-12507

METHYL COMPOUNDS
Thermolysis of 4-methyl-4-phenyl malonyl peroxide: A new oxygen dependent chemiluminescent reaction
[AD-A131863] N84-12268
Polymers of phosphonylmethyl-2,4- and -2,6-diamino benzenes and the like
[NASA-ARC-11506-1] N84-12313
Radiolysis of resist polymers. 1: Poly(methyl-alpha-haloacrylates) and copolymers with methylmethacrylate
[AD-A131864] N84-12315

METROLOGY
Fabrication of machined optics for precision applications
[DE83-015720] N84-12900

MICROBALLOONS
Novel optical pin using microballoons
[DE83-015222] N84-12391

MICROCLIMATOLOGY
The synthesized climatic function map N84-12617

MICROPROCESSORS
A generalized computer code for developing dynamic gas turbine engine models (DIGTEM)
[NASA-TM-83508] N84-12166
Implementing microprocessor technology in aircraft electrical power generating system control N84-12185
Problem of magnet ramping
[DE83-014054] N84-12399
Calorimeter operating system implemented on a Z-80 microcomputer in read only memory
[DE83-016647] N84-12734
The AXIS test box software report
[RSRE-3585] N84-12741

MICROSTRUCTURE
Research activities in materials and molecular research
[DE83-015005] N84-12255
Anisotropy and microstructure of Sm2(Co, Fe, Cu, Zr)17 magnetic materials
[AD-A131961] N84-12291
Evaluation of several high-strength copper sheet alloys
[DE83-015612] N84-12298
Microstructural origins of hot spots in RDX explosive and several reference inert materials
[AD-A132056] N84-12325
Hermetically sealed microminiature multisocket connector
[DE83-017484] N84-12503
Mechanical response of fluid-filled poroelastic solids N84-12525
Effects of microstructure and pore fluids on the acoustic properties of granular materials
[AD-A131983] N84-12668
Physics of ion implantation: Ion-cascade processes and physical state of the implanted solid
[DE83-017152] N84-12998

MICROWAVE ANTENNAS
Performance analysis of a three-dimensional microwave lens in a cylindrical array scanning application
[AD-A131891] N84-12345

MICROWAVE INTERFEROMETERS
The Owens Valley frequency-agile interferometer
[AD-A131825] N84-12453

MICROWAVE PROBES
Non-destructive testing of non-metallic materials using microwaves
[DRIC-T-6974] N84-12508

MICROWAVE RADIOMETERS
Passive radiometry and other remote sensing data interpretation for oil slick thickness assessment, in an experimental case N84-12609
Observations and classifications with a 35/94 GHz radiometer of terrain near Motala, Sweden, July 1982
[FOA-C-30325-E1,E3] N84-12630

MICROWAVES
Effects of pulsed microwaves at 1.28 and 5.62 GHz on Rhesus monkeys (Macaca mulatta) performing an exercise task at three levels of work
[AD-A132057] N84-12704
A restraint chair with rowing-like movement for exposing exercising nonhuman primates to microwave irradiation
[AD-A132047] N84-12705
Effect of pulsed 5.62 GHz microwaves on squirrel monkeys (Saimiri sciureus) performing a repeated acquisition task
[AD-A132045] N84-12706
Theoretical aspects of throat-launch microwave heating in EBT-S
[DE83-015762] N84-12875
Detailed modeling of microwave energy deposition in EBT devices
[DE83-017496] N84-12952

MIDDLE ATMOSPHERE
Variability of atmospheric density in the middle atmosphere
[AD-A131985] N84-12667

MILITARY OPERATIONS
Physical fitness as a moderator of cognitive degradation during sleep deprivation
[AD-A131962] N84-12718

MILITARY TECHNOLOGY
AFWAL FY82 technical accomplishments
[AD-A131839] N84-12054

MIMAS
The Mimas ghost revisited: An analysis of the electron flux and electron microsignatures observed in the vicinity of Mimas at Saturn
[NASA-CR-174596] N84-13056

MINERAL DEPOSITS
Estimation of uncertainty in coal resources
[DE83-902538] N84-12620
Alaska's mineral resources
[DE83-016599] N84-12623

MINES (EXCAVATIONS)
Use of aircraft imagery in evaluating ground stability at open-pit uranium mines in Gas Hills, Wyoming
[DE83-903011] N84-12621

MINICOMPUTERS
Procedures for the transfer of data files between the BRL CYBER computer system and the IBD Hewlett-Packard minicomputer network
[AD-A132063] N84-12731

MINIMA
User's guide for SOL/QPSOL: A FORTRAN package for quadratic programming
[DE83-016990] N84-12752

MINORITIES
Racial bias and predictive validity in testing for selection
[AD-A131830] N84-12722

MIRAGE AIRCRAFT
Effects of integrated maintenance on the definitions of onboard equipments --- Mirage 2000 aircraft N84-12068
Hydraulic generation of auxilliary power for the Mirage 2000 aircraft N84-12176

MIRROR FUSION
Advanced high-field coil designs: 20 Tesla
[DE83-017368] N84-12397
Summary of the MARS tandem-mirror reactor design
[DE83-017293] N84-12939
Vacuum measurements on the tandem mirror experiment upgrade (TMX-U) fusion experiment
[DE83-017836] N84-12946
Status of tandem-mirror confinement
[DE83-017369] N84-12948
Thermal barriers: Their purpose and functioning
[DE83-017365] N84-12954
TMX-U experimental results
[DE83-016790] N84-12955
Thermal performance of the MFTF magnets
[DE83-016275] N84-12988

MIRRORS
High Resolution Imager (HRI) for the Roentgen Satellite (ROSAT) definition study
[NASA-CR-174598] N84-12223
Windows and mirrors needed for a laser-driven photoneutralizer
[DE83-013582] N84-12473
Novel techniques for enhanced reflectivity infrared mirrors
[AD-A131924] N84-12894
Development of a portable specular reflectometer for monitoring solar-mirror materials
[DE83-016065] N84-12901
Fokker-Planck equation in mirror research
[DE83-016568] N84-12932

MISSILES
Some results from a programme of research into the structure of vortex flow fields around missile shapes N84-12111
Water entry impact shock on flat faced cylindrical missiles
[AD-A131937] N84-12419

MISSISSIPPI
Progress in the scene-to-map registration investigation N84-12572

MIXING LENGTH FLOW THEORY
Turbulence modelling: A state-of-the-art review
[CFD/83/3] N84-12435

MODE (STATISTICS)
Quality control and sample comparison by differential modal analysis
[MBB-BB-543-83-OE] N84-12514

MODEMS
Telecommunications (selected articles)
[AD-A131872] N84-12346

MODULATION
New soluble approximation to Fokker-Planck equations
[DE83-016210] N84-12791
The effect of the solar field reversal on the modulation of galactic cosmic rays N84-13101

MODULATION TRANSFER FUNCTION
The dependence of the radar modulation transfer function on environmental conditions and wave parameters
[AD-A131858] N84-12348

MODULES
Analysis of the world distribution of metal-rich subsea manganese nodules
[USGS-CIRC-886] N84-12577

MODULUS OF ELASTICITY
Failure processes in elastomers at or near a rigid spherical inclusion
[AD-A132060] N84-12314
An interactive computer program for analysis of ultrasonic modulus data on anistropic materials
[NPL-DMA(A)88] N84-12526
Effects of microstructure and pore fluids on the acoustic properties of granular materials
[AD-A131983] N84-12668

MOISTURE
Composite structural materials
[NASA-CR-174597] N84-12257
The effect of moisture on the physical and durability properties of methyl methacrylate polymer concrete
[DE83-016733] N84-12541

MOLECULAR CHAINS
Investigation of the statistical mechanics of linear polymers for various physical conditions
[JUEL-1832] N84-12324

MOLECULAR CLOUDS
Dynamical evolution of substucture in molecular clouds N84-13043

MOLECULAR COLLISIONS
The shock wave structure in one-component gas and in binary gas mixture
[ISSN-0208-5858] N84-12407
Study of vibrational energy transfer at a surface by a time-of-flight method
[AD-A131798] N84-12833
Electron capture and loss cross sections for collisions between heavy ions and hydrogen molecules, revised
[IPPJ-AM-28] N84-12914

MOLECULAR ENERGY LEVELS
Study of vibrational energy transfer at a surface by a time-of-flight method
[AD-A131798] N84-12833

MOLECULAR EXCITATION
Kinetics of growth and decay of excited rare-gas atoms and molecules in the pulse radiolysis of pure rare gases and of mixtures of rare gases with molecular quenching agents
[DE83-017016] N84-12856
The excitation of SiO in circumstellar envelopes N84-13041

MOLECULAR INTERACTIONS
New materials for organic photovoltaic cells
[DE83-016845] N84-12645
High temperature gas energy transfer
[AD-A131782] N84-12836
Electron-molecule interactions in gases and liquids: The electron-attachment process in gases and nonpolar liquids
[DE83-017205] N84-12863
MOLECULAR OSCILLATIONS
Study of vibrational energy transfer at a surface by a time-of-flight method
[AD-A131798] N84-12833
International Conference on Vibrations at Surfaces (3rd)
[AD-A131794] N84-12834
MOLECULAR RELAXATION
Kinetics of growth and decay of excited rare-gas atoms and molecules in the pulse radiolysis of pure rare gases and of mixtures of rare gases with molecular quenching agents
[DE83-017016] N84-12856
MOLECULAR STRUCTURE
Structure and vibrational spectra of a model of a-Si:H with periodic boundary conditions
[DE83-015245] N84-12390
Studies of the correlation of electrode kinetics with molecular structure
[AD-A131704] N84-12838
Solitons and polarons in quasi-one dimensional conducting polymers and related materials
[DE83-015233] N84-12853
MOLECULES
Dense molecular thermodynamics
[DE83-015216] N84-13006
MOLYBDENUM
Miniature charpy-impact test results for the irradiated ferritic alloys HT-9 and modified 9Cr-1Mo
[DE83-016935] N84-12300
MOMENTUM
Stellar winds driven by multi-line scattering N84-13087
Formation of standing shocks in stellar winds and related astrophysical flows N84-13088
MOMENTUM THEORY
A contribution to the problem of vortex breakdown N84-12125
Annular Momentum Control Device (AMCD) N84-12241
MOMENTUM TRANSFER
Space station control requirements and flywheel system weights for combined momentum and energy storage N84-12236
MONITORS
Development of a continuous monitor for detection of toxic organic compounds
[PB83-234922] N84-12461
MONOCHROMATIC RADIATION
Ultrasensitive optical rotation and refractive-index measurements
[DE83-018078] N84-12903
MONOCHROMATORS
Generation of monoenergetic positrons
[DE83-015535] N84-12887
Design of doubly focusing, tunable (5 - 30 keV), wide-bandpass optics made from layered synthetic microstructures
[DE83-015492] N84-12897
MONOPULSE ANTENNAS
Simultaneous nulling in the sum and difference patterns of a monopulse antenna
[AD-A131865] N84-12347
MONSOONS
Mechanisms of monsoonal cyclogenesis N84-12680
MONTE CARLO METHOD
Monte Carlo computer simulation program (MCHP) supporting a covariance analysis using the STANHP program
[DFVLR-MITT-83-06] N84-12756
An alternative to the Monte Carlo estimation of network reliability
[AD-A131849] N84-12800
Estimation of the ridge constant: An approach based on the condition index
[DE83-017955] N84-12805
Vectorized Monte Carlo photon transport
[DE83-014807] N84-12843
Monte Carlo calculations of neutron and gamma-ray energy spectra for fusion-reactor shield design: Comparison with experiment
[DE83-016932] N84-12956
MORPHOLOGY
Dynamical evolution of substucture in molecular clouds N84-13043
MOTION PERCEPTION
Integrated Cuing Requirements (ICR) study: Demonstration data base and users guide
[AD-A131119] N84-13019
MOTOR VEHICLES
Optimum engine for methanol utilization
[PB83-239459] N84-12507
Ragone characteristics of aqueous mobile batteries and their application in projecting ranges of electric vehicles
[DE83-014701] N84-12642
MOUNTAINS
A subsynoptic environment associated with two inter-mountain severe thunderstorm events
[DE83-014498] N84-12694
MOUNTING
Inflatable device for installing strain gage bridges
[NASA-CASE-FRC-11068-1] N84-12443
MUFFLERS
Use of the one-dimensional theory of the filament of flow for the interpretation and synthesis of mufflers in exhaust pipes of internal combustion engines
[REPT-81.4] N84-12494
MULTICHANNEL COMMUNICATION
Research in net management techniques for tactical data networks
[AD-A131674] N84-12352
Ultra low loss optical fiber cable assemblies, volume 2
[AD-A132008] N84-12891
Ultra low loss optical fiber cable assemblies, volume 1
[AD-A132007] N84-12892
MULTIPHASE FLOW
Turbulence modelling: A state-of-the-art review
[CFD/83/3] N84-12435
MULTIPLE ACCESS
Acquisition, image and data compression
[AD-A131923] N84-12344
Processing elements
[AD-A131068] N84-12743
MULTIPOLAR FIELDS
Multidipole magnetic fields for plasma confinement
[DE83-016014] N84-12960
MULTISPECTRAL BAND CAMERAS
Remote sensing using the airborne MEIS 2 multidetector electro optical imaging scanner N84-12592
MULTISPECTRAL BAND SCANNERS
LANDSAT 4 investigations of thematic mapper and multispectral scanner applications
[E84-10006] N84-12555
The modular optoelectronic scanner (MOMS) on STS-7, June 83 N84-12589
Rectification of multispectral scanner images
[GEOWISS-MITT-24-1983] N84-12628
MULTISPECTRAL PHOTOGRAPHY
The use of airborne thematic mapper simulation data for the estimation and mapping of Green Leaf Area Index (GLAI) N84-12602
MULTIVARIATE STATISTICAL ANALYSIS
Multivariate density estimation and remote sensing N84-12560
Autoregressive models for use in scene segmentation N84-12561
Limit theorems for the eigenvalues of product of two random matrices
[AD-A131682] N84-12787
MUON SPIN ROTATION
Theory of hyperfine anomalies in muonic atoms
[DE83-015392] N84-12872
MUONS
Muon spin relaxation in ferromagnetic PdMn
[DE83-012659] N84-12979
MYOPIA
Visual accommodation trainer-tester
[NASA-CASE-ARC-11426-1] N84-12193

N

N-TYPE SEMICONDUCTORS
Development of a segmented n-type germanium detector, and its application to astronomical gamma-ray spectroscopy
[NASA-TM-85435] N84-13039
NACELLES
Viscous three-dimensional flow separations from high-wing propeller-turbine nacelle models N84-12115
NASA PROGRAMS
NASA patent abstracts bibiliography. Section 1: Abstracts. A continuing bibliography
[NASA-SP-7039(23)] N84-13017
NASA Patent Abstracts Bibliography. Section 2: Indexes. A continuing bibliography (supplement 23)
[NASA-SP-7039(23)] N84-13018
National Aeronautics and Space Act of 1958, as amended and related legislation
[GPO-24-491] N84-13032
Spinoff, 1983
[NASA-TM-85475] N84-13033
NATIONAL AIRSPACE UTILIZATION SYSTEM
Airport and air traffic control system. Introduction and overview N84-12145
The National Airspace System N84-12146
Aviation growth scenarios N84-12147
Policy implications N84-12150
NATURAL GAS
Alaska's mineral resources
[DE83-016599] N84-12623
NATURAL GAS EXPLORATION
Geologic study of the Wind River Basin, Fremont and Natrona Counties, central Wyoming
[PB83-254912] N84-12677
NATURAL LANGUAGE (COMPUTERS)
Representations for reasoning about change
[AD-A131649] N84-12772
NAVIER-STOKES EQUATION
On the generation of vortical flow at hypersonic speeds over elliptical cones N84-12114
Acta Mechanica Sinica (selected articles)
[AD-A131871] N84-12422
NEODYMIUM LASERS
Experiments to study the feasibility of making an X-ray laser at the Novette laser facility
[DE83-015615] N84-12476
NEPHANALYSIS
Evaluation of automated imagery analysis algorithms for use in the three-dimensional nephanalysis model at AFGWC (Air Force Global Weather Central)
[AD-A131986] N84-12686
NERVES
Measurements, in vivo, of parameters of the dopamine system
[DE83-017964] N84-12709
NERVOUS SYSTEM
Measurements, in vivo, of parameters of the dopamine system
[DE83-017964] N84-12709
NETHERLANDS
Interpretability of wetland on SEASAT-A imagery in the polderland of Flanders: A structural approach N84-12597
NETWORK ANALYSIS
An alternative to the Monte Carlo estimation of network reliability
[AD-A131849] N84-12800
NEUTRAL BEAMS
Efficient radiation-hardened, 400- and 800-keV neutral-beam injection systems
[DE83-015691] N84-12886
Operational studies and expected performance of superconducting quadrupole magnets in the first stages of secondary beams
[DE83-016734] N84-12999
NEUTRAL GASES
Theory of interstellar medium diagnostics N84-13108
NEUTRAL SHEETS
Dissipative instabilities of magnetic neutral layers with velocity shear
[IFSI-82-13] N84-12965
NEUTRINOS
Research in theoretical physics
[DE83-0166222] N84-13004
NEUTRON DIFFRACTION
Phonon dispersion of transverse basal-plane modes in alkali-graphite compounds
[DE83-003910] N84-12273
NEUTRON IRRADIATION
Comparison of damage microstructures in neutron-irradiated vanadium and iron
[DE83-017189] N84-12304
Spallation and 14-MeV neutron irradiation of stabilized NbTi superconductors
[DE83-017973] N84-12394
Real-time attenuation of heated optical fibers in a nuclear reactor
[DE83-015141] N84-12873
Monte Carlo calculations of neutron and gamma-ray energy spectra for fusion-reactor shield design: Comparison with experiment
[DE83-016932] N84-12956
NEUTRON SPECTRA
Transmission of fast neutrons from the Li(d,xn) reaction through thick iron
[DE83-015975] N84-12884
Monte Carlo calculations of neutron and gamma-ray energy spectra for fusion-reactor shield design: Comparison with experiment
[DE83-016932] N84-12956
NEUTRON STARS
Hydrodynamic simulations of a combined hydrogen, helium thermonuclear runaway on a 10 km neutron star
[DE83-012658] N84-13047

NEVADA
Compilation of selected faults and lineaments that may be relevant to a study of seismic activity in southern Nevada and part of adjacent California
[DE83-017085] N84-12673
NICKEL
Charge characteristics of Ni/Fe traction cells
[DE83-014205] N84-12389
NICKEL ALLOYS
Corrosion behavior of Fe-Cr-Ni-Zr alloys in aggressive environments at high temperatures
[DE83-014735] N84-12297
Formation of surface layers during oxidation of a Fe-Mn-Si alloy
[DE83-009495] N84-12302
NICKEL ZINC BATTERIES
Diffusion mass transfer of KOH through Ni/Zn battery membrane separators
[DE83-014551] N84-12387
Ragone characteristics of aqueous mobile batteries and their application in projecting ranges of electric vehicles
[DE83-014701] N84-12642
NICKEL-IRON BATTERIES
Comparative response of lead-acid and nickel-iron batteries to pulsed and constant-current loads
[DE83-017939] N84-12395
Ragone characteristics of aqueous mobile batteries and their application in projecting ranges of electric vehicles
[DE83-014701] N84-12642
NIOBIUM ALLOYS
Degradation of shape memory effect
[DE83-016586] N84-12295
Spallation and 14-MeV neutron irradiation of stabilized NbTi superconductors
[DE83-017973] N84-12394
NOCTURNAL VARIATIONS
Identifying environmental features for land management decisions
[E84-10016] N84-12556
NOISE (SOUND)
The effects of small noise on implicitly defined non-linear dynamical systems
[AD-A131632] N84-12808
NOISE INTENSITY
The effects of small noise on implicitly defined non-linear dynamical systems
[AD-A131632] N84-12808
NOISE METERS
Ride quality meter
[NASA-CASE-LAR-12882-1] N84-12445
NOISE POLLUTION
Noise emission by helicopters N84-13007
NOISE REDUCTION
Technique for producing a coherent sum of the data from P78-1, F2, and F4 satellites
[AD-A131965] N84-12210
Noise reduction and segmentation of IR images using CO-median filters
[RSRE-3582] N84-12378
SAR speckle noise reduction using Wiener filter N84-12568
NOISE SPECTRA
Optimum reception in non-Gaussian electromagnetic interference environments. Part 2: Optimum and suboptimum threshold signal detection in class A and B noise
[PB83-241141] N84-12364
Large-area mercuric iodide photodectors
[DE83-013035] N84-12898
Measurement of macroscopic plasma parameters with a radio experiment: Interpretation of the quasi-thermal noise spectrum observed in the solar wind N84-13096
NONDESTRUCTIVE TESTS
Non-destructive testing of non-metallic materials using microwaves
[DRIC-T-6974] N84-12508
Improving NDE (Non-destructive evaluation) capability through multiple inspection with application to gas turbine engine disks
[AD-A131762] N84-12509
Inverse born approximation: Exact determination of shape of convex voids
[DE83-017685] N84-12512
An X-ray radiography study of delamination growth in notched carbon/epoxy laminates
[FFA-TN-1983-29] N84-12516
Nondestructive evaluation publications, 1981
[PB83-239574] N84-12517
NONLINEAR EQUATIONS
Computational methods for subsonic and transonic aerodynamic design N84-12074
Crank-Nicholson difference schemes for solving coupled systems of nonlinear diffusion equations
[IPP-6/223] N84-12776
Dynasty 2: A nonlinear implicit code for relativistic electron beam tracking studies
[AD-A131592] N84-12829
NONLINEAR SYSTEMS
A nonlinear control law for piloting aircraft in the air-to-ground attack phase N84-12071
Nonlinear dynamics and control of a vibrating rectangular plate
[NASA-CR-172215] N84-12528
The effects of small noise on implicitly defined non-linear dynamical systems
[AD-A131632] N84-12808
Nonlinear force on an unpolarized relativistic test particle to second order in the total field in a nonequilibrium beam-plasma system
[AD-A131631] N84-12919
NONLINEARITY
Studies of collisional and nonlinear radiative processes for development of coherent UV and XUV sources
[AD-A131837] N84-12467
Some bifurcation topics in non-linear elastostatics N84-12524
Computational synergetics and innovation in wave, vortex, and plasma cloud dynamics
[DE83-015252] N84-12928
Magnetohydrodynamic turbulence in the solar wind N84-13073
Alfven solitons in the solar wind N84-13075
NONPARAMETRIC STATISTICS
Multivariate density estimation and remote sensing N84-12560
Asymptotic maximal deviation of m-smoothers
[AD-A131906] N84-12799
Weighted nonparametric tail estimation procedures
[DE83-017870] N84-12804
NORMAL DENSITY FUNCTIONS
Mixture models for dependent observations N84-12562
NORMAL SHOCK WAVES
Interaction between a shock-wave and a vortex flow N84-12104
NORMALITY
Discrimination relative to measures of non-normality N84-12566
NORTH SEA
Marine remote sensing activities of the Joint Research Center, Ispra, Italy N84-12586
Satellite remote sensing, environmental monitoring and the offshore oil and gas industries N84-12603
Application of remote sensing for studies, mapping and forecasting of eddies on the Norwegian continental shelf N84-12605
NORTHERN HEMISPHERE
Wind-speed extremes in the Northern Hemisphere, 30 through 60 km
[AD-A132019] N84-12682
NORTHERN SKY
A search for radio pulsars in the Northern sky: Discovery of a pulsar in a unique binary system N84-13040
NOVAE
Boundary layers in cataclysmic variables: The HEAO-1 X-ray constraints
[NASA-TM-85112] N84-13046
NUCLEAR BINDING ENERGY
Covariant theory with a confined quantum
[DE83-014897] N84-12850
NUCLEAR FUSION
Research activities in materials and molecular research
[DE83-015005] N84-12255
Theoretical studies of fusion physics. Volume 1: Summary
[DE83-010378] N84-12924
Nuclear design of a very-low-activation fusion reactor
[DE83-017470] N84-12949
NUCLEAR MAGNETIC RESONANCE
New developments and oppotunities for NMR in metal-hydrogen systems
[DE83-017696] N84-12864
NUCLEAR MODELS
Ultra-relativistic heavy ions and cosmic rays
[DE83-015881] N84-13134
NUCLEAR PHYSICS
Proceedings of the 16th LAMPF Users-Group Meeting
[DE83-013215] N84-12488
The 83-inch cyclotron reseach program
[DE83-015827] N84-12852
Low energy nuclear physics and accelerator development
[DE83-013384] N84-12877
NUCLEAR POWER PLANTS
Analytical response of concrete structures subjected to high temperatures
[DE83-009625] N84-12538
Automated reasoning in man-machine control systems
[DE83-014307] N84-12774
NUCLEAR RADIATION
Vectorized Monte Carlo photon transport
[DE83-014807] N84-12843
NUCLEAR REACTIONS
Statistical calculation of complete events in medium-energy nuclear collisions
[DE83-015951] N84-12847
NUCLEAR REACTORS
Comparative evaluation of existing concepts for a 10-tesla FED toroidal field coil
[DE83-012817] N84-12815
NUCLEAR STRUCTURE
Low energy nuclear physics and accelerator development
[DE83-013384] N84-12877
NUCLEON-NUCLEON INTERACTIONS
Nucleon-nucleon interactions and polarized-beam (both proton and antiproton) facilities at LAMPF 2
[DE83-017215] N84-12860
NULL ZONES
Simultaneous nulling in the sum and difference patterns of a monopulse antenna
[AD-A131865] N84-12347
NUMERICAL ANALYSIS
Vortex breakdown: A two-stage transition N84-12124
Numerical simulation of vortex breakdown by the vortex-filament method N84-12126
Numerical analysis of stable crack growth in elastic-plastic materials in small scale and general yielding N84-12549
Numerical simulation of convective scaling N84-12660
Guidelines for the design of large modular scientific libraries in Ada
[NPL-DITC-28/83] N84-12740
Effect of magnetic bending on the high-frequency stability of the ELMO Bumpy Torus
[DE83-017177] N84-12961
NUMERICAL CONTROL
The relations between the numerical control of the engine and other aircraft functions N84-12062
Microprocessor-based control system for flowing-electrolyte zinc-bromine battery systems
[DE83-012506] N84-12403
NUMERICAL FLOW VISUALIZATION
Simulation of turbulent flows with a point vortex method N84-12119
Numerical solutions of the Euler equations simulating vortex flows around wings N84-12120
NUMERICAL INTEGRATION
The effect of noisy reflection data on an inverse method for determining the structure of a layered ocean bottom
[AD-A131976] N84-12820
Boundary-integral simulations of rayleigh-taylor instability in ideal magnetohydrodynamics
[AD-A131667] N84-12920
Multiple transonic solutions and a new class of shock transitions in solar and stellar winds N84-13063
NYLON (TRADEMARK)
Some considerations of the efficiency of sewn lap joints in a nylon webbing
[RAE-TR-83009] N84-12310

O

O RING SEALS
In-situ permeation tests of elastomeric O-ring seals
[DE83-015622] N84-12318
OBSERVATION
Variations in task and the ideal observer
[DE83-015394] N84-12723
OCEAN BOTTOM
Radar bathymetry : A review N84-12812
Turn-around loss for oceanic sound on a bottom slope
[AUWE-TN-705/83] N84-12818
The effect of noisy reflection data on an inverse method for determining the structure of a layered ocean bottom
[AD-A131976] N84-12820
OCEAN CURRENTS
Adjustment in the oceans: The long-period tides and coastal upwelling N84-12702
OCEAN DYNAMICS
Contributions of remote sensing satellite tracking techniques to marine environment monitoring and marine applications N84-12585
OCEAN SURFACE
Contributions of remote sensing satellite tracking techniques to marine environment monitoring and marine applications N84-12585
OCEAN TEMPERATURE
Contributions of remote sensing satellite tracking techniques to marine environment monitoring and marine applications N84-12585

World-wide sea-surface temperatures
[AD-A131892] N84-12689
OCEANOGRAPHIC PARAMETERS
Remote Sensing Applications for Environmental Studies — conferences
[ESA-SP-188] N84-12579
Contributions of remote sensing satellite tracking techniques to marine environment monitoring and marine applications N84-12585
Australian Oceanographic Data Centre bulletin 16
[AD-A132002] N84-12701
OCEANOGRAPHY
Australian Oceanographic Data Centre bulletin 16
[AD-A132002] N84-12701
OCEANS
Adjustment in the oceans: The long-period tides and coastal upwelling N84-12702
Transverse horizontal coherence and low-frequency array gain limits in the deep ocean
[AD-A131916] N84-12821
OFFSHORE PLATFORMS
Satellite remote sensing, environmental monitoring and the offshore oil and gas industries N84-12603
OIL POLLUTION
The Istituto di Ricerca sulle Onde Elettromagnetiche (IROE)-lidar remote sensing of the environment N84-12590
Satellite remote sensing, environmental monitoring and the offshore oil and gas industries N84-12603
Remote sensing applied to marine pollution control N84-12607
Introductory studies of natural contamination and manmade pollution in Danish waters N84-12608
Passive radiometry and other remote sensing data interpretation for oil slick thickness assessment, in an experimental case N84-12609
Remote sensing analysis of oil pollution in Augusta Bay, Sicily N84-12616
OIL SLICKS
Marine remote sensing activities of the Joint Research Center, Ispra, Italy N84-12586
OILS
Discussion of static pressure liquid-floated gyros
[AD-A131874] N84-12451
Alaska's mineral resources
[DE83-016599] N84-12623
ON-LINE SYSTEMS
Procedures for the transfer of data files between the BRL CYBER computer system and the IBD Hewlett-Packard minicomputer network
[AD-A132063] N84-12731
OPERATIONS
Vehicle-emission characteristics using mechanically emulsified alcohol/diesel fuels
[DE83-016012] N84-12656
OPERATORS (MATHEMATICS)
On space-time means and everywhere defined scattering operators for nonlinear Klein-Gordon equations
[CTH-MATH-1983-13-PREPRINT] N84-12793
OPTICAL DATA PROCESSING
Turbulence environment characterization
[AD-A131815] N84-12692
OPTICAL EQUIPMENT
Prototype fiber optic system to remote TRACALS radar
[AD-A132073] N84-12341
Fabrication of machined optics for precision applications
[DE83-015720] N84-12900
OPTICAL MEASUREMENT
OI 630.0 nm optical measurements of neutral winds, temperatures and airglow enhancements during the BIME program
[AD-A131695] N84-12671
OPTICAL PROPERTIES
Amorphous silicon-carbon films
[DE83-016077] N84-12259
Photothermal displacement spectroscopy of surfaces and thin films
[DE83-015957] N84-12279
New materials for organic photovoltaic cells
[DE83-016845] N84-12645
Ultra low loss optical fiber cable assemblies, volume 2
[AD-A132008] N84-12891
Ultra low loss optical fiber cable assemblies, volume 1
[AD-A132007] N84-12892
Novel method for the study of optical properties of surfaces
[DE83-012899] N84-12895
The growth and measurement of single-crystal doped GGG (Gd3-xCaxGa5-xZrx012)
[AD-A131875] N84-12971
Optical properties and correlation energy of defects in a-Ge:H
[DE83-016697] N84-12993
OPTICAL RADAR
Design and implementation of a preprocessing system for a sodium lidar
[NASA-CR-174593] N84-12462
The Istituto di Ricerca sulle Onde Elettromagnetiche (IROE)-lidar remote sensing of the environment N84-12590
OPTICAL REFLECTION
Retroreflector YO3: Study of the optical properties of protected mirrors — Earth-Moon telemetry
[ESA-TT-789] N84-12907
OPTIMIZATION
Subsonic/Transonic Aerodynamic Interference for Aircraft: Introductory remarks N84-12073
Application of computational procedures in aerodynamic design N84-12078
Optimization of engine power offtake by secondary power system design N84-12177
Optimization of ultrasonic flaw detection in railroad rail
[PB83-236919] N84-12518
User's guide for SOL/NPSOL: A FORTRAN package for nonlinear programming
[DE83-016903] N84-12751
User's guide for SOL/QPSOL: A FORTRAN package for quadratic programming
[DE83-016990] N84-12752
Disjunctive programming and a hierarchy of relaxations for discrete optimization problems
[AD-A132004] N84-12784
ORBITAL SPACE STATIONS
Study of multi-kilowatt solar arrays for Earth orbit applications
[NASA-CR-170839] N84-12634
ORGANIC CHEMISTRY
Applications of molecular quantum mechanics to problems in chemistry
[DE83-015943] N84-13003
ORGANIC COMPOUNDS
Development of a continuous monitor for detection of toxic organic compounds
[PB83-234922] N84-12461
ORGANIZATIONS
Source header list, supplement 1
[AD-A131800] N84-13024
OROGRAPHY
Field and laboratory studies of ice nucleation in winter orographic clouds N84-12678
ORTHOGONALITY
Geometries for roughness shapes in laminar flow
[NASA-CASE-LAR-13255-1] N84-12092
ORTHOTROPIC PLATES
Bending of transversally loaded orthotropic rectangular and sector plates N84-12520
OSCILLATIONS
Vestibulo-ocular reflex gain in man during active versus passive oscillation and the influence of voluntary gaze-control tasks
[AD-A132006] N84-12717
OSCILLATORS
Subharmonic buncher for the Los Alamos free-electron laser oscillator experiment
[DE83-015220] N84-12474
The Los Alamos free-electron-laser oscillator experiment: Plans and present status
[DE83-017290] N84-12485
OTS (ESA)
The OTS: Fifth year in orbit N84-12221
OVERVOLTAGE
Charge characteristics of Ni/Fe traction cells
[DE83-014205] N84-12389
OXIDATION
Influence of heat-treatment and physicochemical properties on the electrochemical oxidation of carbon blacks in phosphoric acid
[DE83-017744] N84-12276
Breakaway corrosion in mixed-gas environments
[DE83-014704] N84-12299
Formation of surface layers during oxidation of a Fe-Mn-Si alloy
[DE83-009495] N84-12302
OXIDATION-REDUCTION REACTIONS
Mechanisms and kinetics of diphthalocyanine electrode processes
[AD-A131726] N84-12270
OXIDE FILMS
Sputtered C-axis inclined piezoelectric films and shear-wave resonators
[DE83-017253] N84-12997
OXYGEN
Temporal variations of the anomalous oxygen component N84-13099

P

PACKAGING
In-situ permeation tests of elastomeric O-ring seals
[DE83-015622] N84-12318
PATRAM '83: 7th International Symposium on Packaging and Transportation of Radioactive Materials, summaries
[DE83-012390] N84-12881
PACKET SWITCHING
An introduction to the AXIS test box
[RSRE-3583] N84-12729
PAINTS
Assessment of energy-efficiency improvements for paint spray booths
[DE83-016680] N84-12320
PANEL METHOD (FLUID DYNAMICS)
Predicting aerodynamic characteristics of vortical flows on three-dimensional configurations using a surface-singularity panel method N84-12112
A study of wing-body aerodynamic interference of a light twin aircraft utilizing a panel method potential flow program N84-12134
Aspects of second- and third-order panel methods demonstrated for the two-dimensional flat plate problem
[NLR-TR-81074-U] N84-12433
PARABOLIC REFLECTORS
Development of mass-producible line-focus tracking concentrating solar collectors. Category 1: Collectors
[DE83-015629] N84-12639
PARACHUTE DESCENT
Recent advances in parachute technology
[RAE-TM-FS(F)-514] N84-12089
Coherence of appraisal and coping: Parachute jump effectiveness
[FOA-C-55058-H3] N84-12724
PARACHUTE FABRICS
Recent advances in parachute technology
[RAE-TM-FS(F)-514] N84-12089
PARALLEL FLOW
Turbulent tube-flow heat transfer coefficients in the presence of flow imbalance in the tubes of a parallel array N84-12437
Scale lengths in quasi-parallel shocks
[NASA-TM-85109] N84-12663
PARALLEL PROCESSING (COMPUTERS)
A model for the distributed storage and processing of large arrays
[NASA-CR-172252] N84-12742
Design, development and use of the finite element machine
[NASA-CR-172250] N84-12777
PARAMETER IDENTIFICATION
Estimating location parameters in a mixture model N84-12559
An empirical Bayes approach to spatial analysis N84-12563
PARTIAL DIFFERENTIAL EQUATIONS
Adaptive finite element methods for parabolic partial differential equations
[NASA-CR-174490] N84-12727
Second order partial differential equations of mixed type N84-12775
On differential equations of nonlocal elasticity and solutions of screw dislocation and surface waves
[AD-A131911] N84-12786
PARTICLE ACCELERATION
Acceleration of heavy ions in the solar wind N84-13118
Photon damping in cosmic-ray acceleration in active galactic nuclei
[DE83-011320] N84-13133
PARTICLE ACCELERATOR TARGETS
Implications of heavy-ion-induced satellite X-ray emission. Part 2: Production of K and L X-rays by 0.9 to 2.6 MeV/u Ar ions in thick targets of V, Cu, Nb, Ta, and Pt
[DE83-015681] N84-12982
PARTICLE ACCELERATORS
Nucleon-nucleon interactions and polarized-beam (both proton and antiproton) facilities at LAMPF 2
[DE83-017215] N84-12860
Low energy nuclear physics and accelerator development
[DE83-013384] N84-12877
New statistical and non-statistical effects in deep inelastic heavy-ion collisions
[DE83-015732] N84-12885
Applied-B ion diode experiments on PBFA 1
[DE83-017792] N84-12942
Diagnosing the ion beam on the applied-B diode
[DE83-017822] N84-12943

PARTICLE COLLISIONS
New results for transition probabilities in two-level systems: The large detuning regime
[AD-A131783] N84-12835
Statistical calculation of complete events in medium-energy nuclear collisions
[DE83-015951] N84-12847
Jet production and high p/sub T/ phenomena in photon-photon reactions
[DE83-016397] N84-12868
Operation of the Brookhaven MPS Facility
[DE83-015383] N84-12896
PARTICLE INTERACTIONS
Hadronic multiplicity distributions: Example of a universal stochastic mechanism
[DE83-015232] N84-12845
Tau and B lifetime measurements from the MARK 2
[DE83-018219] N84-12879
Cross sections relevant to gamma-ray astronomy: Alpha-particle-induced reactions
[DE83-015533] N84-13038
Measurement of macroscopic plasma parameters with a radio experiment: Interpretation of the quasi-thermal noise spectrum observed in the solar wind N84-13096
Survey of He(+)/He(2+) abundance ratios in energetic particle events N84-13117
PARTICLE SIZE DISTRIBUTION
Design and operation of a light-scattering device for sizing and velocimetry of large droplets
[DE83-902641] N84-12456
Mechanical response of fluid-filled poroelastic solids N84-12525
PARTICLE THEORY
Theory of elementary particles
[DE83-015904] N84-12871
PARTICLE TRAJECTORIES
Electron beam trajectory in a photometer field of view
[AD-A131949] N84-12831
PASSENGERS
Ride quality meter
[NASA-CASE-LAR-12882-1] N84-12445
PASSIVITY
Chemical properties of metallic glasses
[DE83-017353] N84-12322
PATENT POLICY
NASA patent abstracts bibiliography. Section 1: Abstracts. A continuing bibliography
[NASA-SP-7039(23)] N84-13017
NASA Patent Abstracts Bibliography. Section 2: Indexes. A continuing bibliography (supplement 23)
[NASA-SP-7039(23)] N84-13018
PATTERN RECOGNITION
Proceedings of the NASA Symposium on Mathematical Pattern Recognition and Image Analysis
[E83-10032] N84-12557
Autoregressive models for use in scene segmentation N84-12561
Image matching using generalized Hough transforms N84-12569
Relating spatial patterns in image data to scene characteristics N84-12573
First results of the evaluations of the European SAR 580 data for agricultural and forestry purposes in test site D6, Freiburg (West Germany) N84-12599
Mesocyclone detection and classification algorithm
[AD-A131826] N84-12691
PATTERN REGISTRATION
Image matching using generalized Hough transforms N84-12569
Analysis of subpixel registration accuracy N84-12570
Progress in the scene-to-map registration investigation N84-12572
PAVEMENTS
Detection of cavities under concrete pavement
[AD-A131851] N84-12331
PAYLOADS
A balloon design for 9000 pounds at 90,000 feet: Recommendations based on heavy-load balloon history
[AD-A131987] N84-12093
PEAT
Alaska's mineral resources
[DE83-016599] N84-12623
PENDULUMS
Universality and fractal dimension of mode locking structure in systems with competing periodicities
[DE83-017352] N84-12545
PERFORMANCE
Passive-solar performance: Summary of 1981-1982 class B results
[DE83-009407] N84-12650
PERFORMANCE PREDICTION
Overview of state-of-the-art flywheel technology N84-12231
Numerical modelling methods for predicting antenna performance on aircraft N84-12375
The SSME seal test program: Leakage tests for helically-grooved seals
[NASA-CR-170921] N84-12495
A study of critical factors affecting the development of performance measures in evaluating bibliographic information retrieval systems N84-13030
PERFORMANCE TESTS
Special Course on Subsonic/Transonic Aerodynamic Interference for Aircraft
[AGARD-R-712] N84-12072
Recent advances in parachute technology
[RAE-TM-FS(F)-514] N84-12089
Test operations procedure: Absolute altimeters
[AD-A131746] N84-12165
Performance of add-on-type heat pump water heaters using two different test methods
[PB83-222703] N84-12332
PERIODIC VARIATIONS
Interplanetary Alfvenic fluctuations: A statistical study of the directional variations of the magnetic field N84-13076
Periodicities in the occurrence of aurora as indicators of solar variability N84-13093
PERMAFROST
Handbook on the determination of the physical, thermal and mechanical properties of frozen soils
[NRC/CNR-TT-2064] N84-12578
PERMEABILITY
In-situ permeation tests of elastomeric O-ring seals
[DE83-015822] N84-12318
PERMITTIVITY
Effects of dissipation in one-dimensional inverse problems
[DE83-017692] N84-12353
PERSONNEL MANAGEMENT
Revitalization: An organizational program for the individual
[DE83-014949] N84-13013
PERTURBATION
First passage times in stochastic differential equations of mathematical physics and engineering
[AD-A131705] N84-12728
Temperature dependence of the electric-field gradient in Er metal
[DE83-015564] N84-12989
Superconducting stability, 1983: A review
[DE83-017262] N84-12995
PERTURBATION THEORY
New results for transition probabilities in two-level systems: The large detuning regime
[AD-A131783] N84-12835
PETROLEUM PRODUCTS
Long term evaluation of the effects of shale oil produced JP-4 on aircraft construction materials
[AD-A131665] N84-12161
PHASE DIAGRAMS
Liquid phase epitaxy of InP/In1-xGxAsyP1-y heterostructures. Part 3: Phase diagrams
[FI-65-TBR-20-PT-3] N84-13000
PHASE TRANSFORMATIONS
Degradation of shape memory effect
[DE83-016586] N84-12295
Quark-gluon plasma formation
[DE83-017742] N84-12861
Review of some recent theoretical calculations of phase transitions and comparisons with experimental results
[DE83-015863] N84-12983
PHASED ARRAYS
Simultaneous nulling in the sum and difference patterns of a monopulse antenna
[AD-A131865] N84-12347
PHENYLS
Thermolysis of 4-methyl-4-phenyl malonyl peroxide: A new oxygen dependent chemiluminescent reaction
[AD-A131863] N84-12268
PHOENIX (AZ)
Climate of Phoenix, Arizona (revised)
[PB83-246801] N84-12699
PHONONS
Phonon dispersion of transverse basal-plane modes in alkali-graphite compounds
[DE83-003910] N84-12273
Phonon-induced enhancements of the energy gap and critical current in superconducting aluminum
[DE83-015210] N84-12996
PHOSPHINES
Free-radical and ion chemistry of volatile silanes, germanes, and phosphines
[DE83-016389] N84-12277
PHOTOCHEMICAL REACTIONS
Free-radical and ion chemistry of volatile silanes, germanes, and phosphines
[DE83-016389] N84-12277
Time-resolved laser studies on the energy transfer and the configurational changes in bacteriohodopsin
[DE83-015708] N84-12487
Fourth International Conference on Photochemical Conversion and Storage of Solar Energy
[DE83-014760] N84-12638
PHOTODECOMPOSITION
Polymer degradation on reflecting metal films: Fourier transform infrared (FTIR) reflection-absorbance studies
[DE83-012129] N84-12641
PHOTODISSOCIATION
Novel techniques for enhanced reflectivity infrared mirrors
[AD-A131924] N84-12894
PHOTOELECTRIC EMISSION
HgCdTe surface study program
[AD-A132071] N84-12266
Coronal transients in FE XIV 5303A: First two-dimensional photoelectric ground-based observations N84-13072
PHOTOELECTRIC MATERIALS
Transactions of the Chinese Solar Energy Society (selected articles)
[AD-A131870] N84-12637
PHOTOELECTROCHEMICAL DEVICES
Photoelectrochemical electrodes
[NASA-CASE-NPO-15458-1] N84-12262
PHOTOGRAPHY
Utility of the cortical evoked response as a measure of photographic image quality
[AD-A131679] N84-12455
PHOTOINTERPRETATION
Proceedings of the NASA Symposium on Mathematical Pattern Recognition and Image Analysis
[E83-10032] N84-12557
Actual state and recent evolution of the French coast observed by remote sensing using LANDSAT recordings N84-12606
Variations in task and the ideal observer
[DE83-015384] N84-12723
PHOTOLUMINESCENCE
Semiconductors investigated by time resolved raman absorption and photoluminescence spectroscopy using femtosecond and picosecond laser techniques
[AD-A131860] N84-12466
PHOTOMAPPING
Inventory of Flemish forests using medium-scale Color Infrared (CIR) photography and CIR orthophotoplans as base for a forest management data bank N84-12614
PHOTOMETERS
Electron beam trajectory in a photometer field of view
[AD-A131949] N84-12831
Large-area mercuric iodide photodectors
[DE83-013035] N84-12698
Coronal transients in FE XIV 5303A: First two-dimensional photoelectric ground-based observations N84-13072
PHOTOMULTIPLIER TUBES
Evaluation of the Beijing Instrument Factory GDB-44F photomultiplier
[DE84-000849] N84-12398
PHOTONS
Vectorized Monte Carlo photon transport
[DE83-014807] N84-12843
Jet production and high p/sub T/ phenomena in photon-photon reactions
[DE83-016397] N84-12868
Photon damping in cosmic-ray acceleration in active galactic nuclei
[DE83-011320] N84-13133
PHOTOSYNTHESIS
Time-resolved laser studies on the energy transfer and the configurational changes in bacteriohodopsin
[DE83-015708] N84-12487
Fourth International Conference on Photochemical Conversion and Storage of Solar Energy
[DE83-014760] N84-12638
PHOTOVOLTAIC CELLS
New materials for organic photovoltaic cells
[DE83-016845] N84-12645
PHYSICAL CHEMISTRY
Applications of molecular quantum mechanics to problems in chemistry
[DE83-015943] N84-13003
PHYSICAL EXERCISE
Effect of atropine on the exercise-heat performance of man
[AD-A131843] N84-12719
PHYSICAL FITNESS
Physical fitness as a moderator of cognitive degradation during sleep deprivation
[AD-A131962] N84-12718
PHYSICAL OPTICS
Fundamentals and techniques of nonimaging optics, volume 2
[DE83-015447] N84-12902

PHYSIOLOGICAL EFFECTS
Physical fitness as a moderator of cognitive degradation during sleep deprivation
[AD-A131962] N84-12718
Effect of atropine on the exercise-heat performance of man
[AD-A131843] N84-12719
PHYSIOLOGICAL RESPONSES
Effects of pulsed microwaves at 1.28 and 5.62 GHz on Rhesus monkeys (Macaca mulatta) performing an exercise task at three levels of work
[AD-A132057] N84-12704
A restraint chair with rowing-like movement for exposing exercising nonhuman primates to microwave irradiation
[AD-A132047] N84-12705
Combined effects of ionizing radiation and anticholinesterase exposure on rodent motor performance
[AD-A131847] N84-12707
Naloxone does not affect ventilatory responses to hypoxia and hypercapnia in rats
[AD-A131836] N84-12708
PHYTOTRONS
Phytochrome from green plants: Assay, purification, and characterization
[DE83-017447] N84-12710
PIEZOELECTRICITY
Sputtered C-axis inclined piezoelectric films and shear-wave resonators
[DE83-017253] N84-12997
PILOT ERROR
Single pilot IFR program overview and status N84-12030
General aviation single pilot IFR autopilot study N84-12035
PILOT PERFORMANCE
Single pilot IFR program overview and status N84-12030
Study to determine the IFR operational profile and problems to the general aviation pilot N84-12032
Analysis of general aviation single-pilot IFR incident data obtained from the NASA Aviation Safety Reporting System N84-12033
Pilot response with conventional displays N84-12040
Single pilot scanning behavior in simulated instrument flight N84-12041
Display research: Pilot response with the "follow-me" box display N84-12043
A comparison of manual and vocal response modes for the control of aircraft subsystems
[AD-A132048] N84-12152
PILOT TRAINING
Controls, Displays, and Information Transfer for General Aviation IFR Operations
[NASA-CP-2279] N84-12029
PILOTLESS AIRCRAFT
Controls, Displays, and Information Transfer for General Aviation IFR Operations
[NASA-CP-2279] N84-12029
PILOTS (PERSONNEL)
A summary and integration of research concerning single pilot IFR operational problems N84-12034
Pilot controls and SPIRF flight N84-12038
PINCH EFFECT
Rotating and propagating LIB stabilized by self-induced magnetic field
[IPPJ-640] N84-12916
PIONEER 10 SPACE PROBE
Spatial dependences in the distant solar wind: Pioneers 10 and 11 N84-13107
PIONEER 11 SPACE PROBE
Spatial dependences in the distant solar wind: Pioneers 10 and 11 N84-13107
PIONS
Experiments on the nuclear interactions of pions
[DE83-016265] N84-12844
PIPE FLOW
Turbulent tube-flow heat transfer coefficients in the presence of flow imbalance in the tubes of a parallel array N84-12437
PITS (EXCAVATIONS)
Use of aircraft imagery in evaluating ground stability at open-pit uranium mines in Gas Hills, Wyoming
[DE83-903011] N84-12621
PIVOTS
Unidirectional flexural pivot
[NASA-CASE-GSC-12622-1] N84-12492
PLANE WAVES
Effects of dissipation in one-dimensional inverse problems
[DE83-017692] N84-12353
PLANETARY ATMOSPHERES
Activities report of the Laboratory of Environmental Physics and Chemistry N84-12963
Conference on Planetary Volatiles
[NASA-CR-174583] N84-13061
PLANETARY EVOLUTION
Conference on Planetary Volatiles
[NASA-CR-174583] N84-13061
PLANKTON
Two different aspects of phytoplankton bloom seen by satellite (CZCS) in the western English Channel — coastal zone color scanner (CZCS) N84-12604
Introductory studies of natural contamination and manmade pollution in Danish waters N84-12608
PLASMA ACCELERATION
Observational constraints on solar wind acceleration mechanisms N84-13078
Role of thermal conduction in the acceleration of the solar wind N84-13079
Observational evidence for solar wind acceleration at the base of coronal holes N84-13082
PLASMA CLOUDS
On the field configuration in magnetic clouds N84-13125
PLASMA CONTROL
Spallation and 14-MeV neutron irradiation of stabilized NbTi superconductors
[DE83-017973] N84-12394
Initial assessment of the MHD stability of TMX-U
[DE83-016521] N84-12646
Recent results in the Los Alamos compact torus program
[DE83-014147] N84-12930
Fokker-Planck equation in mirror research
[DE83-016568] N84-12932
Status of tandem-mirror confinement
[DE83-017369] N84-12948
Constraints on the scale of toroidal-fusion experiments with application to the design of a helical-axis stellarator
[DE83-016812] N84-12950
Thermal barriers: Their purpose and functioning
[DE83-017365] N84-12954
TMX-U experimental results
[DE83-016790] N84-12955
Multidipole magnetic fields for plasma confinement
[DE83-016014] N84-12960
PLASMA DENSITY
Comment on the observed plasma densities in Jupiter's distant magnetotail (wake); a possible explanation
[IFSI-83-2] N84-13062
PLASMA DIAGNOSTICS
Performance of antennas in plasma N84-12377
Atomic processes in hot dense plasma
[IPPJ-AM-31] N84-12911
Bibliography on atomic processes in hot dense plasmas
[IPPJ-AM-29] N84-12913
Real-time diagnostic-data-acquisition system for the Doublet 3 Tokamak fusion experiment
[DE83-015871] N84-12927
Time-resolved spectral measurements above 80 A
[DE83-015616] N84-12933
TFTR alpha extraction and measurement project
[DE83-018120] N84-12947
Theory of interstellar medium diagnostics N84-13108
PLASMA DRIFT
Drift wave studies in a linear multiple mirror
[DE83-016881] N84-12951
PLASMA DYNAMICS
Magnetospheric plasma studies using data from the dynamics high and low altitude plasma instruments
[AD-A131793] N84-12670
PLASMA EQUILIBRIUM
Magnetohydrodynamic equilibrium and stability of spheromak plasma in flux conserver
[IPPJ-642] N84-12909
A 2-D skin-current toroidal-MHD-equilibrium code
[DE83-016916] N84-12929
Reversed-field pinch large aspect ratio equilibrium
[DE83-016771] N84-12953
Variational-moment method for computing magnetohydrodynamic equilibria
[DE83-017477] N84-12957
PLASMA GENERATORS
Spectroscopic measurements of solar wind generation N84-13071
PLASMA HEATING
Theoretical aspects of throat-launch microwave heating in EBT-S
[DE83-015762] N84-12875
Electron heating at interplanetary shocks N84-13098
PLASMA INTERACTIONS
Magnetospheric plasma studies using data from the dynamics high and low altitude plasma instruments
[AD-A131793] N84-12670
Theory of interstellar medium diagnostics N84-13108
Minor constituents in the solar wind originating from plasma-dust interactions N84-13116
PLASMA JETS
Baryon-antibaryon angular correlations in quark jets
[DE83-015923] N84-12854
PLASMA LIFETIME
Tau and B lifetime measurements from the MARK 2
[DE83-018219] N84-12879
PLASMA PHYSICS
Radial evolution of ion distribution functions N84-13094
Measurement of macroscopic plasma parameters with a radio experiment: Interpretation of the quasi-thermal noise spectrum observed in the solar wind N84-13096
PLASMA PUMPING
Self-pumping impurity by in-situ metal deposition
[DE83-017937] N84-12306
PLASMA TURBULENCE
Beam plasma turbulence study
[AD-A131946] N84-12917
Nonlinear force on an unpolarized relativistic test particle to second order in the total field in a nonequilibrium beam-plasma system
[AD-A131631] N84-12919
Theory of hydromagnetic turbulence N84-13077
PLASMA WAVES
Beam plasma turbulence study
[AD-A131946] N84-12917
Jupiter Data Analysis Program: Analysis of Voyager wideband plasma wave observations
[NASA-CR-174575] N84-13058
PLASMA-ELECTROMAGNETIC INTERACTION
Propagation and absorption of electromagnetic waves in fully relativistic plasmas
[DE83-017246] N84-12959
The structure of the plasma sheet-lobe boundary in the Earth's magnetotail
[NASA-TM-85434] N84-13049
PLASMAS (PHYSICS)
Quark-gluon plasma formation
[DE83-017742] N84-12861
Detailed modeling of microwave energy deposition in EBT devices
[DE83-017496] N84-12952
The collapse of the local, Spitzer-Haerm formulation and a global-local generalization for heat flow in an inhomogeneous, fully ionized plasma N84-13080
PLASMASPHERE
Magnetospheric plasma studies using data from the dynamics high and low altitude plasma instruments
[AD-A131793] N84-12670
PLASTIC DEFORMATION
Cold sintering: A new powder consolidation process
[AD-A131687] N84-12292
Microstructural origins of hot spots in RDX explosive and several reference inert materials
[AD-A132056] N84-12325
Plastic deformations of a portable frame under short pulse loading on one column by an approximate method including effects of elasticity and plastic rate sensitivity N84-12521
The Dugdale model for the compact specimen
[NASA-TM-85714] N84-12529
Hamiltonian for antisotropic bodies with defects
[ISSN-0208-5658] N84-12966
PLASTIC FLOW
Numerical simulation of plastic fluids
[DE83-007911] N84-12424
PLASTIC PROPERTIES
Evaluation of the kinematic variable (back stress) response of metals
[DE83-008381] N84-12293
A pressure-shear experiment for studying the dynamic plastic responses of metals at shear strain rates of 10 to the 5th power s(-1) N84-12519
Yield surface for bars including warping restraint
[AD-A131393] N84-12533
Endochronic theory of dynamic viscoplasticity
[DE83-017531] N84-12546
Numerical analysis of stable crack growth in elastic-plastic materials in small scale and general yielding N84-12549
PLASTICS
The performance of the perfluorocarbon liquid/plastic-film capacitor technology in pulse-power service. A current status report
[DE83-014606] N84-12402
The effect of moisture on the physical and durability properties of methyl methacrylate polymer concrete
[DE83-016733] N84-12541
PLATES (STRUCTURAL MEMBERS)
Buckled plate vibrations, large amplitude vibrations and nonlinear flutter of elastic plates using high-order triangular finite elements N84-12523
Some bifurcation topics in non-linear elastostatics N84-12524
On the dynamic fracture of bars, beams and plates N84-12552

PLOTTING
Technique for producing a coherent sum of the data from P78-1, F2, and F4 satellites
[AD-A131965] N84-12210
PLT: A multipurpose plotting package
[DE83-016261] N84-12735
PLUGGING
Status of tandem-mirror confinement
[DE83-017369] N84-12948
Thermal barriers: Their purpose and functioning
[DE83-017365] N84-12954
TMX-U experimental results
[DE83-016790] N84-12955
PLUMES
Infrared characteristics of gas plumes
[AD-A131796] N84-12269
A study of coherent structures in the near-neutral marine atmospheric boundary layer N84-12658
Absolute collisional excitation cross section measurements using crossed molecular beams
[AD-A132038] N84-12830
PNEUMATIC EQUIPMENT
Auxiliary Power Systems
[AGARD-CP-352] N84-12168
Inflatable device for installing strain gage bridges
[NASA-CASE-FRC-11068-1] N84-12443
POLARIMETERS
Ultrasensitive optical rotation and refractive-index measurements
[DE83-018078] N84-12903
POLARITY
Montoring of the Stanford Linac microbunches' position
[DE83-012712] N84-12840
The effect of the solar field reversal on the modulation of galactic cosmic rays N84-13101
POLARIZATION (SPIN ALIGNMENT)
Nucleon-nucleon interactions and polarized-beam (both proton and antiproton) facilities at LAMPF 2
[DE83-017215] N84-12860
Theory of elementary particles
[DE83-015904] N84-12871
POLARIZATION (WAVES)
Theoretical aspects of throat-launch microwave heating in EBT-S
[DE83-015762] N84-12875
POLARIZATION CHARACTERISTICS
Time-resolved laser studies on the energy transfer and the configurational changes in bacteriohodopsin
[DE83-015708] N84-12487
POLES (SUPPORTS)
Interaction of antennas with masts under special consideration of the sensitivity and nonlinear effects in ship borne receiving systems N84-12371
POLICIES
Two types of values and their assessment by the collective interest
[DE83-012064] N84-13031
POLLUTION CONTROL
Remote sensing applied to marine pollution control N84-12607
POLLUTION MONITORING
Marine remote sepsing activities of the Joint Research Center, Ispra, Italy N84-12586
Introductory studies of natural contamination and manmade pollution in Danish waters N84-12608
Passive radiometry and other remote sensing data interpretation for oil slick thickness assessment, in an experimental case N84-12609
POLOIDAL FLUX
Magnetohydrodynamic equilibrium and stability of spheromak plasma in flux conserver
[IPPJ-642] N84-12909
Ripple-reduction poloidal-field coils for Tokamak reactors
[DE83-009532] N84-12922
POLYACETYLENE
Solitons and polarons in quasi-one dimensional conducting polymers and related materials
[DE83-015233] N84-12853
POLYCARBONATES
The performance of the perfluorocarbon liquid/plastic-film capacitor technology in pulse-power service. A current status report
[DE83-014606] N84-12402
POLYCRYSTALS
Generation of monoenergetic positrons
[DE83-015535] N84-12887
POLYMERIC FILMS
Polymer degradation on reflecting metal films: Fourier transform infrared (FTIR) reflection-absorbance studies
[DE83-012129] N84-12641
POLYMERIZATION
Replacement of PBNA in HB and HC polymers used in SRM propellant and liner
[NASA-CR-170936] N84-12311
Polymers of phosphonylmethyl-2,4- and -2,6-diamino benzenes and the like
[NASA-ARC-11505-1] N84-12313
Solitons and polarons in quasi-one dimensional conducting polymers and related materials
[DE83-015233] N84-12853
POLYMERS
Investigation of the statistical mechanics of linear polymers for various physical conditions
[JUEL-1832] N84-12324
Tailoring polymer films for solar-collection use, phase 1
[DE83-018117] N84-12640
POLYNOMIALS
Reduction of structural complexity in evaluating convolutions by polynomial transforms
[FUB-59-1981] N84-12794
PONDS
Predicting lake ice decay
[AD-A132012] N84-12618
POPULATION THEORY
Deterministic models in mathematical demography: An investigation of stable population theory including an analysis of the population statistics of Denmark N84-12806
POROSITY
Mechanical response of fluid-filled poroelastic solids N84-12525
Effects of microstructure and pore fluids on the acoustic properties of granular materials
[AD-A131983] N84-12668
POROUS MATERIALS
Convection in horizontal porous media with different end temperatures N84-12438
Double porosity model for acoustic wave propagation in fractured-porous rock
[DE83-017823] N84-12823
POSITRONS
Measurements, in vivo, of parameters of the dopamine system
[DE83-017964] N84-12709
POTASSIUM
Piston-displacement equations of state for sodium, potassium, and rubidium metals to 20 kbar from 300 K to 4 K
[DE83-018079] N84-12252
POTASSIUM COMPOUNDS
Phonon dispersion of transverse basal-plane modes in alkali-graphite compounds
[DE83-003910] N84-12273
POTASSIUM HYDROXIDES
Diffusion mass transfer of KOH through Ni/Zn battery membrane separators
[DE83-014551] N84-12387
POTASSIUM PHOSPHATES
Characterization by X-ray topography of laser-induced damage in potassium dihydrogen phosphate crystals
[DE83-012045] N84-12985
POTENTIAL FLOW
The treatment of convected vortices in compressible potential flow N84-12121
The Tracked Wing In Ground-Effect (TWIG) N84-12155
POWDER METALLURGY
Mechanical property evaluation of P/M (Powder-Metallurgy) aluminum 7090-T7E71 plate
[AD-A132058] N84-12290
Cold sintering: A new powder consolidation process
[AD-A131687] N84-12292
POWDERED ALUMINUM
Mechanical property evaluation of P/M (Powder-Metallurgy) aluminum 7090-T7E71 plate
[AD-A132058] N84-12290
POWER
Super integrated power unit for fighter aircraft N84-12183
POWER CONDITIONING
Integrated Power/Attitude Control System (IPACS) N84-12229
IPACS attitude control technology considerations N84-12238
IPACS electronics: Comments on the original design and current efforts at Langley Research Center N84-12240
Advanced Control and Power System (ACAPS) technology program N84-12243
Power system considerations and test activities N84-12244
IPACS guidance navigation and control system considerations and test activities N84-12245
POWER EFFICIENCY
Optimization of engine power offtake by secondary power system design N84-12177
APU operational efficiency N84-12181
POWER REACTORS
Development in reliability models and methods
[DE83-014683] N84-12511
POWER SUPPLIES
High-average-power rep rate systems
[DE83-013769] N84-12385
Problem of magnet ramping
[DE83-014054] N84-12399
PRECIPITATION (METEOROLOGY)
Climate of Phoenix, Arizona (revised)
[PB83-246801] N84-12699
PREDICTION ANALYSIS TECHNIQUES
Improved wave drag predictions using modified linear theory
[NASA-CR-174494] N84-12096
Calculation of forced response to base excitation using experimentally derived modal participation factors N84-12205
Erosive particle kinematics in the turbulent combustion boundary layer contacting a solid wall
[DE83-010594] N84-12272
Prediction of dynamic effects due to vehicles crossing military bridges
[ISVR-TR-120] N84-12548
Predicting lake ice decay
[AD-A132012] N84-12618
Effects of microstructure and pore fluids on the acoustic properties of granular materials
[AD-A131983] N84-12668
Coherence of appraisal and coping: Parachute jump effectiveness
[FOA-C-55058-H3] N84-12724
Development of the basic methods needed to predict the aeroelastic behavior of helicopters N84-12811
Transverse horizontal coherence and low-frequency array gain limits in the deep ocean
[AD-A131916] N84-12821
Using inner-shell X-rays as an ion-beam diagnostic
[DE83-017784] N84-12857
PREDICTIONS
Improved wave drag predictions using modified linear theory
[NASA-CR-174494] N84-12096
Predicting aerodynamic characteristics of vortical flows on three-dimensional configurations using a surface-singularity panel method N84-12112
Soot formation from polycyclic aromatics
[DE83-009750] N84-12271
Life prediction under stress corrosion conditions below K sub ISCC
[DE83-018074] N84-12307
Racial bias and predictive validity in testing for selection
[AD-A131830] N84-12722
PRELAUNCH SUMMARIES
STS-9 Spacelab 1 press kit
[PB3-10209] N84-12214
PREMIXED FLAMES
Laser spectroscopy of propellant-like flames
[AD-A132042] N84-12267
Theoretical and experimental investigation of turbulent premixed flames N84-12409
PRESSURE DROP
Effects of pressure-drop correlations on Stirling-engine predicted performance
[DE83-017279] N84-12501
PRESSURE GAGES
Novel optical pin using microballoons
[DE83-015222] N84-12391
PRESSURE GRADIENTS
A contribution to the problem of vortex breakdown N84-12125
Experimentation with turbulent flows experiencing the effects of an adverse pressure gradient N84-12127
Quasi-steady solar wind dynamics N84-13120
PRESSURE MEASUREMENT
Vacuum measurements on the tandem mirror experiment upgrade (TMX-U) fusion experiment
[DE83-017836] N84-12946
PRESSURE REDUCTION
Assessment of TRAC-PF1 and RELAP5/MOD1 codes with GE large-vessel blowdown test
[DE83-015384] N84-12874
PRESSURE SENSORS
Application of the small body pressure transducer
[AD-A131733] N84-12454
PRESSURE SUITS
Lower body graduated negative pressure system
[NASA-CR-171717] N84-12725
PRESSURE VESSELS
Zero-dimensional model of compressible gas flow in networks of pressure vessels: Program TRIC
[DE83-017121] N84-12431

PRIMARY COSMIC RAYS
Evolution of the ultra high energy cosmic ray spectron by transport equation
[DE83-013711] N84-13132
PROBABILITY DENSITY FUNCTIONS
Estimating location parameters in a mixture model N84-12559
PROBABILITY DISTRIBUTION FUNCTIONS
An empirical Bayes approach to spatial analysis N84-12563
PROBABILITY THEORY
Improving NDE (Non-destructive evaluation) capability through multiple inspection with application to gas turbine engine disks
[AD-A131762] N84-12509
Analysis of subpixel registration accuracy N84-12570
Asymptotic maximal deviation of m-smoothers
[AD-A131906] N84-12799
An alternative to the Monte Carlo estimation of network reliability
[AD-A131849] N84-12800
Kingman's subadditive ergodic theorem
[AD-A131795] N84-12801
Weighted nonparametric tail estimation procedures
[DE83-017870] N84-12804
New results for transition probabilities in two-level systems: The large detuning regime
[AD-A131783] N84-12835
PROBLEM SOLVING
User's guide for SOL/NPSOL: A FORTRAN package for nonlinear programming
[DE83-016903] N84-12751
User's guide for SOL/QPSOL: A FORTRAN package for quadratic programming
[DE83-016990] N84-12752
Design, development and use of the finite element machine
[NASA-CR-172250] N84-12777
Multidimensional explicit difference schemes for hyperbolic conservation laws
[NASA-CR-172254] N84-12778
Disjunctive programming and a hierarchy of relaxations for discrete optimization problems
[AD-A132004] N84-12784
Pyramid methods in image analysis N84-12796
Dynasty 2: A nonlinear implicit code for relativistic electron beam tracking studies
[AD-A131592] N84-12829
Information resources management plan
[AD-A131964] N84-13023
PROCEDURES
Guide to agricultural meteorological practices, second edition
[WMO-134] N84-12697
PROCESS CONTROL (INDUSTRY)
Walk-through survey report: Control technology for integrated circuit fabrication, Xerox Corporation, El Segundo, California
[PB83-239053] N84-12333
PRODUCT DEVELOPMENT
Overview of state-of the-art flywheel technology N84-12231
Spinoff, 1983
[NASA-TM-85475] N84-13033
PRODUCTION
Development of mass-producible line-focus tracking concentrating solar collectors. Category 1: Collectors
[DE83-015629] N84-12639
PRODUCTIVITY
Limnology, second edition
[DE83-016792] N84-12627
Revitalization: An organizational program for the individual
[DE83-014949] N84-13013
PROFILES
Some aspects of flight trajectory control in future avionic systems for combat aircraft N84-12066
An integrated AFCS for the "PROFILE"-mode N84-12069
PROGRAM VERIFICATION (COMPUTERS)
Northern Telecom, Incorporated NTI-585 ACOBOL/3 release 3 (COBOL technical report)
[PB83-241521] N84-12758
Northern Telecom Incorporated NTI-585 XCOBOL, release 3
[PB83-241539] N84-12759
Northern Telecom, Incorporated NTI-585 XCOBOL, release 3 (COBOL technical report)
[PB83-241547] N84-12760
Digital Equipment Corporation VAX 11/750, VAL-11 COBOL version 2.2
[PB83-241588] N84-12761
NCR Corporation NCR 9300 ITX-BASIC release 1.1
[PB83-243410] N84-12762
Computer Sciences Corporation UNIVAC 1100/80 CSTS FORTRAN, release FTN148
[PB83-243428] N84-12763
Digital Equipment Corporation, PDP-11/44 COBOL-81 version 2.0
[PB83-247734] N84-12764
Digital Equipment Corporation COBOL-81 version 2.0 (COBOL technical report)
[PB83-247742] N84-12765
PROGRAMMING LANGUAGES
Comments on ISO/TC 97/SC 18/WG3 N120
[DE83-011391] N84-12748
Praxis language environment: Distribution-package description
[DE83-017546] N84-12750
PROJECT MANAGEMENT
Overview of state-of-the-art flywheel technology N84-12231
Ris assessment techniques: A handbook for program management personnel
[AD-A131596] N84-13010
Management of QA in an R and D organization
[DE83-016924] N84-13014
PROJECTILES
A theoretical and experimental investigation of a transonic projectile flow field
[AD-A131938] N84-12094
PROLATE SPHEROIDS
Separation and vortical-type flow around a prolate spheroid: Evaluation of relevant parameters N84-12113
PROPELLANT TANKS
Space Shuttle external interference heating test
[AD-A131686] N84-12215
PROPELLANTS
Replacement of PBNA in HB and HC polymers used in SRM propellant and liner
[NASA-CR-170936] N84-12311
PROPELLERS
Aeroelastic analysis for propellers - mathematical formulations and program user's manual
[NASA-CR-3729] N84-12530
PROPULSION SYSTEM CONFIGURATIONS
AFWAL FY82 technical accomplishments
[AD-A131839] N84-12054
Space Shuttle propulsion parameter estimation using optimal estimation techniques, volume 1
[NASA-CR-170935] N84-12213
Alternate propulsion energy sources
[AD-A131939] N84-12249
PROPULSION SYSTEM PERFORMANCE
AFWAL FY82 technical accomplishments
[AD-A131839] N84-12054
Ground and inflight operational effects of APU's N84-12182
Journal of the Chinese Society of Astronautics (selected articles)
[AD-A131881] N84-12212
PROTECTIVE CLOTHING
A laboratory comparison of portable cooling systems for workers exposed to two levels of heat stress
[AD-A131848] N84-12423
Effectiveness in reducing heat stress of three conditioned-air cooling vests worn with and without cooling air supplied to a face piece
[AD-A131975] N84-12726
PROTECTIVE COATINGS
Corrosion resistant coating
[NASA-NPO-15928-1] N84-12289
Damage thresholds of thin film materials and high reflectors at 248 nm
[DE83-012663] N84-12472
PROTON BEAMS
Using inner-shell X-rays as an ion-beam diagnostic
[DE83-017784] N84-12857
Nucleon-nucleon interactions and polarized-beam (both proton and antiproton) facilities at LAMPF 2
[DE83-017215] N84-12860
Developing a 500-eV proton beam
[DE83-012781] N84-12880
Applied-B ion diode experiments on PBFA 1
[DE83-017792] N84-12942
Operational studies and expected performance of superconducting quadrupole magnets in the first stages of secondary beams
[DE83-016734] N84-12999
PROTONS
Temporal variations of the anomalous oxygen component N84-13099
PSYCHOLOGICAL EFFECTS
Effects of pulsed microwaves at 1.28 and 5.62 GHz on Rhesus monkeys (Macaca mulatta) performing an exercise task at three levels of work
[AD-A132057] N84-12704
A restraint chair with rowing-like movement for exposing exercising nonhuman primates to microwave irradiation
[AD-A132047] N84-12705
Effect of pulsed 5.62 GHz microwaves on squirrel monkeys (Saimiri sciureus) performing a repeated acquisition task
[AD-A132045] N84-12706
PSYCHOLOGICAL FACTORS
Revitalization: An organizational program for the individual
[DE83-014949] N84-13013
PSYCHOLOGICAL TESTS
Effect of noise in the three-parameter logistic model
[AD-A131867] N84-12721
Racial bias and predictive validity in testing for selection
[AD-A131830] N84-12722
PULMONARY FUNCTIONS
Pulmonary dosimetry of nitrogen dioxide in animals and man
[PB83-243394] N84-12711
PULSARS
A search for radio pulsars in the Northern sky: Discovery of a pulsar in a unique binary system N84-13040
PULSE COMMUNICATION
A flight investigation of simulated data link communications during single-pilot IFR flight N84-12046
Satellite communication, part 1
[INPE-2893-PRE/417] N84-12337
PULSE GENERATORS
Megavolt pulse transformer powered by a fast plate generator
[DE83-014189] N84-12384
Solid state copper vapor laser modulator
[DE83-015837] N84-12475
Montoring of the Stanford Linac microbunches' position
[DE83-012712] N84-12840
Magnetic switching
[DE83-012952] N84-12841
PULSE MODULATION
Solid state copper vapor laser modulator
[DE83-015837] N84-12475
PULSED JET ENGINES
Investigation of a pulsed electrothermal thruster
[NASA-CR-168266] N84-12227
PULSED LASERS
Pulsed power bibliography. Volume 2: Annotated bibliography
[AD-A131753] N84-12468
Pulsed power bibliography. Volume 1: Indices
[AD-A131752] N84-12469
PULSED RADIATION
Pulse signals in heterodyne and homodyne detection
[ESA-TT-809] N84-12357
PULSES
High-average-power rep rate systems
[DE83-013769] N84-12385
Comparative response of lead-acid and nickel-iron batteries to pulsed and constant-current loads
[DE83-017939] N84-12395
Evolution of long pulses in a tapered wiggler free-electron laser
[DE83-017235] N84-12484
PUMPS
Microprocessor-based control system for flowing-electrolyte zinc-bromine battery systems
[DE83-012506] N84-12403
PUSHBROOM SENSOR MODES
The modular optoelectronic scanner (MOMS) on STS-7, June 83 N84-12589
Remote sensing using the airborne MEIS 2 multidetector electro optical imaging scanner N84-12592
PYROLYSIS
Soot formation from polycyclic aromatics
[DE83-009750] N84-12271
PYROLYTIC GRAPHITE
A multistage spent particle collector and a method for making same
[NASA-LEW-13914-1] N84-12447

Q

QUADRATIC PROGRAMMING
User's guide for SOL/NPSOL: A FORTRAN package for nonlinear programming
[DE83-016903] N84-12751
User's guide for SOL/QPSOL: A FORTRAN package for quadratic programming
[DE83-016990] N84-12752
QUADRUPOLES
Three-dimensional equilibrium in quadrupole symmetric tandem mirrors in the paraxial limit (reduced MHD)
[DE83-017840] N84-12940

Operational studies and expected performance of superconducting quadrupole magnets in the first stages of secondary beams
[DE83-016734] N84-12999

QUALITY CONTROL
Quality is not a dirty word
[DE83-012166] N84-12510
Quality control and sample comparison by differential modal analysis
[MBB-BB-543-83-OE] N84-12514
Development of an ultrasonic testing procedure for electron beam welded parts for aerospace applications
[BMFT-FB-W-72-011] N84-12515
Management of QA in an R and D organization
[DE83-018924] N84-13014

QUANTILES
Quantile data analysis of image data N84-12565

QUANTUM CHROMODYNAMICS
Quark-gluon plasma formation
[DE83-017742] N84-12861
Hadron-hadron collider group
[DE83-010704] N84-12865
Physics at very high energies
[DE83-012854] N84-12878
Research in theoretical physics
[DE83-0166222] N84-13004

QUANTUM MECHANICS
Applications of molecular quantum mechanics to problems in chemistry
[DE83-015943] N84-13003

QUANTUM NUMBERS
Progress in lattice gauge theory
[DE83-014055] N84-12862

QUARK PARTON MODEL
Covariant theory with a confined quantum
[DE83-014897] N84-12850
Baryon-antibaryon angular correlations in quark jets
[DE83-015923] N84-12854
Theory of elementary particles
[DE83-015904] N84-12871

QUARKS
Quark-gluon plasma formation
[DE83-017742] N84-12861
Progress in lattice gauge theory
[DE83-014055] N84-12862
Jet production and high p/sub T/ phenomena in photon-photon reactions
[DE83-016397] N84-12868
Tau and B lifetime measurements from the MARK 2
[DE83-018219] N84-12879

QUARTZ CRYSTALS
Radiation-induced transient acoustic loss in quartz crystals
[DE83-012626] N84-12980

QUENCHING
Comparative evaluation of existing concepts for a 10-tesla FED toroidal field coil
[DE83-012817] N84-12815

QUEUEING THEORY
Software voting in asynchronous NMR (N-Modular Redundancy) computer structures
[NASA-CR-174488] N84-12732
Search among queues
[AD-A131639] N84-12773
Rank modification method for certain singular systems of linear equations N84-12797

R

RADAR
The dependence of the radar modulation transfer function on environmental conditions and wave parameters
[AD-A131858] N84-12348

RADAR EQUIPMENT
Prototype fiber optic system to remote TRACALS radar
[AD-A132073] N84-12341

RADAR GEOLOGY
Radar bathymetry : A review N84-12612

RADAR IMAGERY
SAR speckle noise reduction using Wiener filter N84-12568
The influence of sensor and flight parameters on texture in radar images N84-12575
SAR 580: Images for agricultural and forest survey. First results in middle Belgium N84-12595
Measuring landscape information content and distribution on a SAR-580 image N84-12596
Interpretability of wetland on SEASAT-A imagery in the polderland of Flanders: A structural approach N84-12597
First results of the evaluations of the European SAR 580 data for agricultural and forestry purposes in test site D6, Freiburg (West Germany) N84-12599

RADAR PHOTOGRAPHY
Interpretability of wetland on SEASAT-A imagery in the polderland of Flanders: A structural approach N84-12597

RADAR SCANNING
Detection of cavities under concrete pavement
[AD-A131851] N84-12331

RADAR SCATTERING
Effects of nonlinear loads on antennas and scatterers N84-12376
Radar investigation of soils and sea (ERASME): C band helicopter-borne scatterometer. Application to soil moisture measurement N84-12588

RADAR TRACKING
Observations of the upper troposphere and lower stratosphere using the urbana coherent-scatter radar
[NASA-CR-174594] N84-12664

RADAR TRANSMISSION
La Recherche Aerospatiale, Bimonthly Bulletin, no. 1983-1/212, January-February 1983
[ESA-TT-814] N84-12810

RADIAL VELOCITY
Radial evolution of ion distribution functions N84-13094

RADIANCE
Normalization of water-leaving radiance obtained from the Coastal Zone Colour Scanner (CZCS) data N84-12610

RADIANT HEATING
Theoretical aspects of throat-launch microwave heating in EBT-S
[DE83-015762] N84-12875

RADIATION COUNTERS
TFTR alpha extraction and measurement project
[DE83-018120] N84-12947
Methods for deconvoluting and interpreting complex gammaand X-ray spectral regions
[DE83-013585] N84-12991
Development of a segmented n-type germanium detector, and its application to astronomical gamma-ray spectroscopy
[NASA-TM-85435] N84-13039

RADIATION DAMAGE
Radiation damage and phase instability in irradiated stainless steel
[DE83-017190] N84-12303
Comparison of damage microstructures in neutron-irradiated vanadium and iron
[DE83-017189] N84-12304
Radiolysis of resist polymers. 1: Poly(methyl-alpha-haloacrylates) and copolymers with methylmethacrylate
[AD-A131864] N84-12315

RADIATION EFFECTS
Miniature charpy-impact test results for the irradiated ferritic alloys HT-9 and modified 9Cr-1Mo
[DE83-016935] N84-12300
Effects of pulsed microwaves at 1.28 and 5.62 GHz on Rhesus monkeys (Macaca mulatta) performing an exercise task at three levels of work
[AD-A132057] N84-12704
Effect of pulsed 5.62 GHz microwaves on squirrel monkeys (Saimiri sciureus) performing a repeated acquisition task
[AD-A132045] N84-12706
Radiation-induced transient acoustic loss in quartz crystals
[DE83-012626] N84-12980
Hole trapping, recombination, and space charge in irradiated Sandia oxides
[DE83-015212] N84-12986

RADIATION HARDENING
Efficient radiation-hardened, 400- and 800-keV neutral-beam injection systems
[DE83-015691] N84-12886

RADIATION PROTECTION
Engineering hot-cell windows for radiation protection --- for remote handling of radioactive materials
[DE83-014675] N84-12319
Hazards Control Department annual technology review, 1982
[DE83-015598] N84-12883

RADIATION SHIELDING
Engineering hot-cell windows for radiation protection --- for remote handling of radioactive materials
[DE83-014675] N84-12319
Transmission of fast neutrons from the Li(d,xn) reaction through thick iron
[DE83-015975] N84-12884
Monte Carlo calculations of neutron and gamma-ray energy spectra for fusion-reactor shield design: Comparison with experiment
[DE83-016932] N84-12956

RADIATION TOLERANCE
A restraint chair with rowing-like movement for exposing exercising nonhuman primates to microwave irradiation
[AD-A132047] N84-12705
Effect of pulsed 5.62 GHz microwaves on squirrel monkeys (Saimiri sciureus) performing a repeated acquisition task
[AD-A132045] N84-12706

RADIATION TRANSPORT
Monte Carlo calculations of neutron and gamma-ray energy spectra for fusion-reactor shield design: Comparison with experiment
[DE83-016932] N84-12956

RADIATIVE HEAT TRANSFER
Determination of the uncertainty of experimental heat-flux calibrations
[AD-A131918] N84-12450

RADIO ASTRONOMY
A search for radio pulsars in the Northern sky: Discovery of a pulsar in a unique binary system N84-13040

RADIO BEACONS
Technology and the future evolution of the ATC system N84-12148

RADIO BURSTS
Velocity profiles of interplanetary shocks N84-13122

RADIO COMMUNICATION
Weather data communication and utilization N84-12045

RADIO EQUIPMENT
Influence of the airframe on the performance of antennas for avionics N84-12372

RADIO FREQUENCY HEATING
Electron-cyclotron-heating experiments in Tokamaks and stellarators
[DE83-017210] N84-12958

RADIO INTERFEROMETERS
Test and demonstration of Macrometer (TM) model V-1000 interferometric surveyor
[PB83-239103] N84-12631

RADIO TELEMETRY
Preliminary data processing plan for the thermal plasma experiment on the HILAT satellite
[AD-A132017] N84-12209

RADIO TRANSMISSION
Radar meteorology in cloud physics and radio wave propagation research
[ESA-TT-808] N84-12695

RADIO TRANSMITTERS
Techniques for locating a remote HF transmitter from single-site measurements
[AD-A132014] N84-12342

RADIO WAVES
Radio scintillations at large elongation angles: Contributions of waves versus discontinuities
[IFSI-82-4] N84-12358

RADIOACTIVE DECAY
Experiments on the nuclear interactions of pions
[DE83-016285] N84-12944

RADIOACTIVE MATERIALS
In-situ permeation tests of elastomeric O-ring seals
[DE83-015622] N84-12318
Engineering hot-cell windows for radiation protection --- for remote handling of radioactive materials
[DE83-014675] N84-12319
PATRAM '83: 7th International Symposium on Packaging and Transportation of Radioactive Materials, summaries
[DE83-012390] N84-12881

RADIOACTIVE WASTES
Research activities in materials and molecular research
[DE83-015005] N84-12255

RADIOACTIVITY
Nuclear design of a very-low-activation fusion reactor
[DE83-017470] N84-12949

RADIOBIOLOGY
Eruption of permanent dentition in rhesus monkeys exposed to ELF (Extremely low frequency) fields
[AD-A132065] N84-12703

RADIOGRAPHY
Using an X-ray-sensitive vidicon and remote-control stage mechanism to obtain critical radiographic alignment of small explosive devices
[DE83-012846] N84-12326
Variations in task and the ideal observer
[DE83-015394] N84-12723
Survey of flash X-ray techniques and applications
[DE83-017234] N84-12904

RADIOISOTOPE BATTERIES
Space nuclear safety program
[DE83-014070] N84-12869

RADIOLYSIS
Formation of free hydrogen during radiolysis in a bed of clay
[DE83-017724] N84-12275

Radiolysis of resist polymers. 1: Poly(methyl-alpha-haloacrylates) and copolymers with methylmethacrylate
[AD-A131864] N84-12315

RAILGUN ACCELERATORS
Progress in developing repetitive pulse systems utilizing inductive energy storage
[DE83-015167] N84-12388

RAILS
Optimization of ultrasonic flaw detection in railroad rail
[PB83-236919] N84-12518

RAMAN SPECTROSCOPY
Laser spectroscopy of propellant-like flames
[AD-A132042] N84-12267

RAMJET ENGINES
Analytical design of a liquid hydrogen fueled turbofan-ramjet engine for flight Mach numbers zero to five N84-12187

RANDOM SAMPLING
Quality control and sample comparison by differential modal analysis
[MBB-BB-543-83-OE] N84-12514
TRAN-STAT (statistics for environmental studies). Issue no. 24: Field sampling designs, simple random and stratified random sampling
[DE83-016826] N84-12803

RANDOM VARIABLES
Limit theorems for the eigenvalues of product of two random matrices
[AD-A131682] N84-12787

RANGEFINDING
Accuracy estimates of gravity potential differences between western Europe and United States through Lageos satellite laser ranging network
[AD-A131838] N84-12669

RANKING
An iterated logarithm law result for extreme values from Gaussian sequences
[AD-A129559] N84-12798

RARE EARTH COMPOUNDS
Mechanisms and kinetics of diphthalocyanine electrode processes
[AD-A131726] N84-12270

RAYLEIGH SCATTERING
Investigation of the Rayleigh critical angle phenomenon for the characterization of surface properties
[AD-A131530] N84-12340
Instabilities in cylindrical plasma liners imploderl by high magnetic fields
[DE83-013640] N84-12921

RDX
Microstructural origins of hot spots in RDX explosive and several reference inert materials
[AD-A132056] N84-12325

REACTION KINETICS
Chemiluminescence and laser induced fluorescence of boron atom reactions
[AD-A131709] N84-12471
Ukrainian Physics Journal (selected articles)
[AD-A131087] N84-12814
Studies of the correlation of electrode kinetics with molecular structure
[AD-A131704] N84-12838
Statistical calculation of complete events in medium-energy nuclear collisions
[DE83-015951] N84-12847
The possibility of amplifying infrared radiation by high-pressure reacting gas
[AD-A131086] N84-12890

REACTOR CORES
Disparate changes in the physical properties of graphite
[DE83-015986] N84-12321

REACTOR DESIGN
Tokamak fusion reactors with less than full tritium breeding
[DE83-016711] N84-12936
Summary of the MARS tandem-mirror reactor design
[DE83-017293] N84-12939
Nuclear design of a very-low-activation fusion reactor
[DE83-017470] N84-12949
Constraints on the scale of toroidal-fusion experiments with application to the design of a helical-axis stellarator
[DE83-016812] N84-12950

REACTOR MATERIALS
Miniature charpy-impact test results for the irradiated ferritic alloys HT-9 and modified 9Cr-1Mo
[DE83-016935] N84-12300
Disparate changes in the physical properties of graphite
[DE83-015986] N84-12321
Investigation of inhomogeneity in ceramic reactor materials using laser-localized emission spectroscopy
[JUEL-1834] N84-12323
Creep and tensile properties of alloy 800H-Hastelloy X weldments
[DE83-017067] N84-12542
Real-time attenuation of heated optical fibers in a nuclear reactor
[DE83-015141] N84-12873
Tokamak fusion reactors with less than full tritium breeding
[DE83-016711] N84-12936
Monte Carlo calculations of neutron and gamma-ray energy spectra for fusion-reactor shield design: Comparison with experiment
[DE83-016932] N84-12956
Chemical erosion of first-wall materials by atomic hydrogen at high temperatures
[DE83-017161] N84-12962

REACTOR SAFETY
Hydrogen-air detonations
[DE83-009289] N84-12278
Development in reliability models and methods
[DE83-014683] N84-12511
Space nuclear safety program
[DE83-014070] N84-12869
Real-time attenuation of heated optical fibers in a nuclear reactor
[DE83-015141] N84-12873
Assessment of TRAC-PF1 and RELAP5/MOD1 codes with GE large-vessel blowdown test
[DE83-015384] N84-12874
Hazards Control Department annual technology review, 1982
[DE83-015598] N84-12883

REACTOR TECHNOLOGY
Development in reliability models and methods
[DE83-014683] N84-12511
Space reactors: Past, present and future
[DE83-011177] N84-12870

READ-ONLY MEMORY DEVICES
Calorimeter operating system implemented on a Z-80 microcomputer in read only memory
[DE83-016647] N84-12734

READOUT
Operation of the Brookhaven MPS Facility
[DE83-015383] N84-12896

REAL TIME OPERATION
A generalized computer code for developing dynamic gas turbine engine models (DIGTEM)
[NASA-TM-83508] N84-12166
The use of a formal simulator to verify a simple real time control program
[AD-A131732] N84-12745

REATTACHED FLOW
Computation of turbulent flows over backward-facing step
[NASA-TM-85851] N84-12414

RECEIVERS
High dynamic global positioning system receiver
[NASA-CASE-NPO-16171-1-CU] N84-12151
Test and demonstration of Macrometer (TM) model V-1000 interferometric surveyor
[PB83-239103] N84-12631

RECOMBINATION COEFFICIENT
Ion-ion recombination rate in the EMP source region
[AD-A131148] N84-12339

RECOMBINATION REACTIONS
Ukrainian Physics Journal (selected articles)
[AD-A131087] N84-12814

RECONNAISSANCE
Poststorm reconnaissance of Tropical Storm Chris
[AD-A131948] N84-12688

RECTANGULAR PLATES
Bending of transversally loaded orthotropic rectangular and sector plates N84-12520
Nonlinear dynamics and control of a vibrating rectangular plate
[NASA-CR-172215] N84-12528

RECTIFIERS
A high-performance digital triggering system for phase-controlled rectifiers
[DE83-012217] N84-12386

REDUCED GRAVITY
Low gravity experiment for studying a rotating fluid having a free surface
[NASA-CR-170923] N84-12413

REDUCTION (CHEMISTRY)
Reduction of CO2 to methanol and methane by photo and dark reactions on semiconductor electrodes
[PB83-249490] N84-12329
Hydrogen in MgO crystals thermochemically reduced at very high temperatures
[DE83-014058] N84-12981

REDUNDANCY
Design and development of the multifunction flight control reference system N84-12065
A diagnosis scheme for sensors of a flight control system using analytic redundancy N84-12067

REFERENCE SYSTEMS
Design and development of the multifunction flight control reference system N84-12065

REFINING
Innovative industrial-materials processes --- potential for energy conservation
[DE83-016784] N84-12649

REFLECTANCE
Research and development for investigations of metallic adsorptions on metal surfaces by optical techniques complemented by dc resistivity and auger spectroscopy
[AD-A131739] N84-12351
Graphical method for determining interflected daylight in clear climates
[DE83-011989] N84-13128

REFLECTOMETERS
Development of a portable specular reflectometer for monitoring solar-mirror materials
[DE83-016065] N84-12901

REFLEXES
Vestibulo-ocular reflex gain in man during active versus passive oscillation and the influence of voluntary gaze-control tasks
[AD-A132006] N84-12717

REFRACTORY COATINGS
Chemical erosion of first-wall materials by atomic hydrogen at high temperatures
[DE83-017161] N84-12962

REFRACTORY MATERIALS
Fabrication and properties of multilayer structures
[AD-A131934] N84-12969

REFRIGERATING MACHINERY
Satellite refrigerator compressors with the oil and moisture removal systems
[DE83-016079] N84-12502

REGENERATIVE COOLING
Improved Two-Dimensional Kinetics (TDK) computer program
[NASA-CR-170922] N84-12248

REGENERATIVE FUEL CELLS
The Boeing flywheel study N84-12235

REGENERATORS
Effects of pressure-drop correlations on Stirling-engine predicted performance
[DE83-017279] N84-12501

REGRESSION ANALYSIS
Estimation of the ridge constant: An approach based on the condition index
[DE83-017955] N84-12805
Models of maintenance resources interaction: Peacetime operations
[AD-A131379] N84-13011

REGULATIONS
Develop a normative or descriptive model of the international/domestic civil aviation industry, volume 3
[AD-A131878] N84-12051
Develop a normative or descriptive model of the international/domestic civil aviation industry, volume 2
[AD-A131877] N84-12052
Develop a normative or descriptive model of the international/domestic civil aviation industry. Volume 1: Executive summary
[AD-A131876] N84-12053

REINFORCED PLASTICS
Non-destructive testing of non-metallic materials using microwaves
[DRIC-T-6974] N84-12508

RELATIVISTIC EFFECTS
Implications of heavy-ion-induced satellite X-ray emission. Part 2: Production of K and L X-rays by 0.9 to 2.6 MeV/u Ar ions in thick targets of V, Cu, Nb, Ta, and Pt
[DE83-015681] N84-12982

RELATIVISTIC ELECTRON BEAMS
Dynasty 2: A nonlinear implicit code for relativistic electron beam tracking studies
[AD-A131592] N84-12829
Theoretical studies of fusion physics. Volume 1: Summary
[DE83-010378] N84-12924
Theoretical studies of fusion physics. Volume 2: Appendices
[DE83-010371] N84-12925

RELATIVISTIC PARTICLES
Ultra-relativistic heavy ions and cosmic rays
[DE83-015881] N84-13134

RELATIVISTIC PLASMAS
Propagation and absorption of electromagnetic waves in fully relativistic plasmas
[DE83-017246] N84-12959

RELAXATION METHOD (MATHEMATICS)
Structure and vibrational spectra of a model of a-Si:H with periodic boundary conditions
[DE83-015245] N84-12390

Disjunctive programming and a hierarchy of relaxations for discrete optimization problems
[AD-A132004] N84-12784

RELIABILITY
A diagnosis scheme for sensors of a flight control system using analytic redundancy N84-12067
Nondestructive evaluation publications, 1981
[PB83-239574] N84-12517
Reliability and maintainability study of select solar-energy-system components in the National Solar Data Network
[DE83-011974] N84-12647
Survey of flash X-ray techniques and applications
[DE83-017234] N84-12904

RELIABILITY ANALYSIS
Initial operation of the compressed air experiment at Pittsfield, Illinois
[DE83-016930] N84-12643
A study of critical factors affecting the development of performance measures in evaluating bibliographic information retrieval systems N84-13030

REMOTE CONTROL
Using an X-ray-sensitive vidicon and remote-control stage mechanism to obtain critical radiographic alignment of small explosive devices
[DE83-012846] N84-12326

REMOTE HANDLING
Engineering hot-cell windows for radiation protection --- for remote handling of radioactive materials
[DE83-014675] N84-12319

REMOTE SENSING
Earth Resources Laboratory research and technology
[E84-10033] N84-12576
An operational remote sensing methodology for the detection, inventory and environmental monitoring of waste disposal sites N84-12601
Passive radiometry and other remote sensing data interpretation for oil slick thickness assessment, in an experimental case N84-12609
Observation of the Earth in the middle infrared
[ESA-TT-790] N84-12629

REMOTE SENSORS
Layout of a SAR sensor for Spacelab and satellite. Part 1: Design considerations for fundamental SAR parameters
[ESA-TT-802] N84-12224
Earth Resources Laboratory research and technology
[E84-10033] N84-12576
Remote sensing instruments for trace species measurements in the troposphere and stratosphere: A review N84-12583
Contributions of remote sensing satellite tracking techniques to marine environment monitoring and marine applications N84-12585
Remote sensing using the airborne MEIS 2 multidetector electro optical imaging scanner N84-12592

REQUIREMENTS
Auxiliary power requirements: Their role in aircraft performance N84-12169
Secondary power systems for fighter aircraft experiences today and requirements for a next generation N84-12171

RESEARCH
USAF/SCEEE summary faculty research program (1982) research reports, volume 2
[AD-A130770] N84-13009

RESEARCH AND DEVELOPMENT
Earth Resources Laboratory research and technology
[E84-10033] N84-12576
Portrait of the Max-Planck research organization and its institutes N84-13015

RESEARCH FACILITIES
Proceedings of the 16th LAMPF Users-Group Meeting
[DE83-013215] N84-12488
Portrait of the Max-Planck research organization and its institutes N84-13015

RESEARCH MANAGEMENT
Portrait of the Max-Planck research organization and its institutes N84-13015
Information retrieval research support
[AD-A131990] N84-13022

RESIDENTIAL ENERGY
Passive-solar performance: Summary of 1981-1982 class B results
[DE83-009407] N84-12650
Empirical validation of computer models for passive-solar residences
[DE83-016887] N84-13005

RESONANCE
Selective laser ionization for mass-spectral isotopic analysis
[DE83-017303] N84-12483

RESONATORS
Analysis of some filtering and data analysis methods for gravitational wave antennas with resonant transducers
[IFSI-82-11] N84-12359
Data analysis for gravitational wave antenna with resonant transducers
[IFSI-82-12] N84-12360
Sputtered C-axis inclined piezoelectric films and shear-wave resonators
[DE83-017253] N84-12997

RETROFITTING
A graphics subsystem retrofit design for the bladed-disk data acquisition system
[NASA-TM-83510] N84-12730

REVERSE FIELD PINCH
Recent results in the Los Alamos compact torus program
[DE83-014147] N84-12930
Reversed-field pinch large aspect ratio equilibrium
[DE83-016771] N84-12953

REVERSE OSMOSIS
Novel composite membranes
[PB83-243170] N84-12284

RIDING QUALITY
Ride quality meter
[NASA-CASE-LAR-12882-1] N84-12445

RIGID STRUCTURES
Test report for MSFC test 83-2. Pressure scaled water impact test of a 12.5 inch diameter model of the Space Shuttle Solid Rocket booster filament wound case and external TVC pod
[NASA-CR-174601] N84-12217
Yield surface for bars including warping restraint
[AD-A131393] N84-12533

RING LASERS
Laser journal (selected articles)
[AD-A131886] N84-12465

RING STRUCTURES
A multistage spent particle collector and a method for making same
[NASA-LEW-13914-1] N84-12447

RISK
Ris assessment techniques: A handbook for program management personnel
[AD-A131596] N84-13010

ROADWAY POWERED VEHICLES
The Tracked Wing In Ground-Effect (TWIG) N84-12155

ROBOTICS
Robotics: An introduction to today's robot and future trends
[AD-A132070] N84-12768

ROBOTS
Robotics: An introduction to today's robot and future trends
[AD-A132070] N84-12768

ROCKET ENGINE CONTROL
Journal of the Chinese Society of Astronautics (selected articles)
[AD-A131881] N84-12212

ROCKET LAUNCHING
From launching carrier rockets towards the Pacific on the accomplishments and problems of electronic technologies in our country
[AD-A131088] N84-12380

ROCKET SOUNDING
Speed-dependent collision effects on radar back-scattering from the ionosphere --- incoherent scatter radar
[NASA-CR-173077] N84-12336

ROCKET THRUST
Investigation of a pulsed electrothermal thruster
[NASA-CR-168266] N84-12227

RODENTS
Combined effects of ionizing radiation and anticholinesterase exposure on rodent motor performance
[AD-A131847] N84-12707

RODS
Some bifurcation topics in non-linear elastostatics N84-12524

ROOTS OF EQUATIONS
On sensitivity, compensation and the approach to the asymptotes in multivariable root-loci
[RR-222] N84-12795

ROSAT MISSION
High Resolution Imager (HRI) for the Roentgen Satellite (ROSAT) definition study
[NASA-CR-174598] N84-12223

ROTARY WING AIRCRAFT
Application of the small body pressure transducer
[AD-A131733] N84-12454

ROTARY WINGS
Helicopter rotor wake geometry and its influence in forward flight. Volume 1: Generalized wake geometry and wake effect on rotor airloads and performance
[NASA-CR-3726] N84-12090
Helicopter rotor wake geometry and its influence in forward flight. Volume 2: Wake geometry charts
[NASA-CR-3727] N84-12091
Design considerations for bearingless rotor hubs
[AD-A131660] N84-12162

ROTATING DISKS
A gas-flow tracing technique applicable to rotating systems boundary layer on a rotating disk
[DE83-012761] N84-12425

ROTATING FLUIDS
Low gravity experiment for studying a rotating fluid having a free surface
[NASA-CR-170923] N84-12413
The AGCE related studies of baroclinic flows in spherical geometry
[NASA-CR-170934] N84-12415

ROTATING SHAFTS
Vertical shaft windmill
[NASA-CASE-LAR-12923-1] N84-12493

ROTATION
The effect of coordinate system rotation on spherical harmonic expansions: A numerical method
[AD-A131974] N84-12785

ROTOR AERODYNAMICS
Aeroelastic analysis for propellers - mathematical formulations and program user's manual
[NASA-CR-3729] N84-12530

RUBIDIUM
Piston-displacement equations of state for sodium, potassium, and rubidium metals to 20 kbar from 300 K to 4 K
[DE83-018079] N84-12252
Phonon dispersion of transverse basal-plane modes in alkali-graphite compounds
[DE83-003910] N84-12273
Equations of state for the alkali metals, with generalizations to NaCl
[DE83-018075] N84-12280

RUNWAYS
Rapid runway repair program subtask 1.07 - rapid concrete cutting
[AD-A131771] N84-12195

S

S MATRIX THEORY
Considerations of the three-wave interactions
[IPPJ-641] N84-12915

S WAVES
Sputtered C-axis inclined piezoelectric films and shear-wave resonators
[DE83-017253] N84-12997

SAFETY
Controls, Displays, and Information Transfer for General Aviation IFR Operations
[NASA-CP-2279] N84-12029
Single pilot IFR program overview and status N84-12030
Analysis of general aviation single-pilot IFR incident data obtained from the NASA Aviation Safety Reporting System N84-12033
A summary and integration of research concerning single pilot IFR operational problems N84-12034
Safety report: General aviation crashworthiness project, phase 1
[PB83-917004] N84-12142

SAFETY FACTORS
US weather satellites and services
[GPO-25-753] N84-12208

SAMARIUM COMPOUNDS
Anisotropy and microstructure of Sm2(Co, Fe, Cu, Zr)17 magnetic materials
[AD-A131961] N84-12291

SAMPLING
Initial operation of the compressed air experiment at Pittsfield, Illinois
[DE83-016930] N84-12643
Detecting long-term ecological effects in forests and food chains
[DE83-003469] N84-12655

SANDS
Non-destructive testing of non-metallic materials using microwaves
[DRIC-T-6974] N84-12508

SATELLITE GROUND SUPPORT
Spacecraft interface design and its impact on operational support
[ESA-STR-211] N84-12220

SATELLITE IMAGERY
Digital image registration by sequential analysis
[INPE-2940-PHE/429] N84-12446
Relative elevation determination from LANDSAT imagery N84-12558
The SPOT distribution system N84-12615
SATELLITE INSTRUMENTS
High Resolution Imager (HRI) for the Roentgen Satellite (ROSAT) definition study
[NASA-CR-174598] N84-12223
SATELLITE NETWORKS
Network design tool for EHF satellite communications networks
[AD-A131812] N84-12349
Investigation of mathematical models to combine a terrestrial network with a satellite network --- geodesy
[SER-C-274] N84-12554
Monitoring of renewable resources (a land information system for Europe) --- remote sensing N84-12581
Accuracy estimates of gravity potential differences between western Europe and United States through Lageos satellite laser ranging network
[AD-A131638] N84-12669
SATELLITE OBSERVATION
System definition Roentgensatellit, phase B 1.2
[BMFT-FB-W-83-010] N84-12219
Monitoring of renewable resources (a land information system for Europe) --- remote sensing N84-12581
SATELLITE TRANSMISSION
Phase A study for a test satellite for propagation and transmission experiments in the 20/30 GHz frequency band
[BMFT-FB-W-83-009] N84-12355
L band satellite communication experiment in the Antartic
[ESA-TT-805] N84-12356
SATELLITE-BORNE INSTRUMENTS
System definition Roentgensatellit, phase B 1.2
[BMFT-FB-W-83-010] N84-12219
Layout of a SAR sensor for Spacelab and satellite. Part 1: Design considerations for fundamental SAR parameters
[ESA-TT-802] N84-12224
SCALING
Corrosion behavior of Fe-Cr-Ni-Zr alloys in aggressive environments at high temperatures
[DE83-014735] N84-12297
SCALING LAWS
Numerical simulation of convective scaling N84-12660
Study of excited state energy transfer processes
[AD-A131777] N84-12837
Constraints on the scale of toroidal-fusion experiments with application to the design of a helical-axis stellarator
[DE83-016812] N84-12950
SCANNERS
Performance analysis of a three-dimensional microwave lens in a cylindrical array scanning application
[AD-A131891] N84-12345
SCANNING
Pilot response with conventional displays N84-12040
Single pilot scanning behavior in simulated instrument flight N84-12041
SCATTERING
Elastic-wave inverse scattering in non-destructive evaluation
[DE83-017683] N84-12513
Minimal unitary (covariant) scattering theory
[DE83-014896] N84-12849
Jet production and high p/sub T/ phenomena in photon-photon reactions
[DE83-016397] N84-12868
SCATTERING AMPLITUDE
Analytic diffraction corrections to ultrasonic scattering measurements
[DE83-016080] N84-12825
SCATTERING CROSS SECTIONS
Implications of heavy-ion-induced satellite X-ray emission. Part 2: Production of K and L X-rays by 0.9 to 2.6 MeV/u Ar ions in thick targets of V, Cu, Nb, Ta, and Pt
[DE83-015681] N84-12982
SCATTERING FUNCTIONS
On space-time means and everywhere defined scattering operators for nonlinear Klein-Gordon equations
[CTH-MATH-1983-13-PREPRINT] N84-12793
SCATTEROMETERS
Radar investigation of soils and sea (ERASME): C band helicopter-borne scatterometer. Application to soil moisture measurement N84-12588
SCENE ANALYSIS
Relative elevation determination from LANDSAT imagery N84-12558
Autoregressive models for use in scene segmentation N84-12561
Relating spatial patterns in image data to scene characteristics N84-12573
Shape from shading: An assessment N84-12574
Measuring landscape information content and distribution on a SAR-580 image N84-12596
Interpretability of wetland on SEASAT-A imagery in the polderland of Flanders: A structural approach N84-12597
Mapping land use in Catalonia (Spain) --- using LANDSAT imagery N84-12613
SCHEDULING
Biological clocks and shift work scheduling
[GPO-21-747] N84-12713
SCHOTTKY DIODES
Transactions of the Chinese Solar Energy Society (selected articles)
[AD-A131870] N84-12637
Silicide formation and Schottky barrier of rare-earth metals on Si
[AD-A131750] N84-12975
Silicide formation and Schottky barrier of rare-earth metals on Si
[AD-A131749] N84-12976
Silicide formation and Schottky barrier of rare-earth metals on Si
[AD-A131748] N84-12977
SCINTILLATION
Preliminary data processing plan for the thermal plasma experiment on the HILAT satellite
[AD-A132017] N84-12209
Radio scintillations at large elongation angles: Contributions of waves versus discontinuities
[IFSI-82-4] N84-12358
Solar cycle evolution of the solar wind in three dimensions N84-13090
Interplanetary scintillation observations of the solar wind close to the Sun and out of the ecliptic N84-13102
SCREW DISLOCATIONS
On differential equations of nonlocal elasticity and solutions of screw dislocation and surface waves
[AD-A131911] N84-12786
SEA ICE
Contributions of remote sensing satellite tracking techniques to marine environment monitoring and marine applications N84-12585
Mechanical behavior of sea ice
[AD-A131852] N84-12619
SEA LEVEL
On the wind stress - sea level power law
[AD-A132035] N84-12681
SEA ROUGHNESS
Application of remote sensing for studies, mapping and forecasting of eddies on the Norwegian continental shelf N84-12605
SEA WATER
Novel composite membranes
[PB83-243170] N84-12284
Operational utilization of remote sensing in a study of the impact of disposal of urban waste at sea N84-12611
SEALS (STOPPERS)
The SSME seal test program: Leakage tests for helically-grooved seals
[NASA-CR-170921] N84-12495
SEARCH PROFILES
Environments and search paths for the software tools
[DE83-016607] N84-12749
Development of a unique Physical Metrology Laboratory Recall System
[DE83-017415] N84-12767
A study of critical factors affecting the development of performance measures in evaluating bibliographic information retrieval systems N84-13030
SEATS
Correlation of laboratory-scale fire test methods for seat blocking layer materials with large-scale test results
[AD-A131666] N84-12138
A restraint chair with rowing-like movement for exposing exercising nonhuman primates to microwave irradiation
[AD-A132047] N84-12705
SEDIMENT TRANSPORT
Sediment transport in a tidal inlet
[PB83-242271] N84-12632
SEDIMENTS
The effect of noisy reflection data on an inverse method for determining the structure of a layered ocean bottom
[AD-A131976] N84-12820
SEGMENTS
Noise reduction and segmentation of IR images using CO-median filters
[RSRE-3582] N84-12378
SEISMIC WAVES
Numerical modeling techniques according to the wave equation and the ray method --- in seismology
[BMFT-FB-T-83-136] N84-12354
Description of an automatic seismic measurements package: Analysis and design goals
[AD-A132067] N84-12666
Velocity profiles of interplanetary shocks N84-13122
SELF CONSISTENT FIELDS
Applications of molecular quantum mechanics to problems in chemistry
[DE83-015943] N84-13003
SEMICONDUCTOR DEVICES
Methods for deconvoluting and interpreting complex gammaand X-ray spectral regions
[DE83-013585] N84-12991
SEMICONDUCTORS (MATERIALS)
Semiconductors investigated by time resolved raman absorption and photoluminescence spectroscopy using femtosecond and picosecond laser techniques
[AD-A131860] N84-12466
Semiconductor processing with excimer lasers
[DE83-007509] N84-12477
Surface and interfacial properties of Ga(0.47) In(0.53) As alloys
[AD-A131925] N84-12970
Clustering and ordering in 3-5 alloys
[AD-A131785] N84-12974
Liquid phase epitaxy of InP/In1-xGxAsyP1-y heterostructures. Part 3: Phase diagrams
[FI-65-TBR-20-PT-3] N84-13000
SENSORIMOTOR PERFORMANCE
Coherence of appraisal and coping: Parachute jump effectiveness
[FOA-C-55058-H3] N84-12724
SENSORS
A diagnosis scheme for sensors of a flight control system using analytic redundancy N84-12067
Evaluation of a total energy-rate sensor on a transport airplane
[NASA-TP-2212] N84-12164
Technique for producing a coherent sum of the data from P78-1, F2, and F4 satellites
[AD-A131965] N84-12210
SENSORY PERCEPTION
Coherence of appraisal and coping: Parachute jump effectiveness
[FOA-C-55058-H3] N84-12724
Integrated Cuing Requirements (ICR) study: Demonstration data base and users guide
[AD-A131119] N84-13019
SEPARATED FLOW
An experimental investigation of separated three dimensional flow on general aviation twin-engine aircraft N84-12087
On issues concerning flow separation and vortical flows in three dimensions N84-12100
The vortex skeleton model for three-dimensional steady flows N84-12101
Separation and vortical-type flow around a prolate spheroid: Evaluation of relevant parameters N84-12113
Viscous three-dimensional flow separations from high-wing propeller-turbine nacelle models N84-12115
Steady and unsteady flow models for airfoils with spoiler N84-12136
SEPARATORS
Diffusion mass transfer of KOH through Ni/Zn battery membrane separators
[DE83-014551] N84-12387
SEQUENTIAL ANALYSIS
Digital image registration by sequential analysis
[INPE-2940-PHE/429] N84-12446
Coherence of appraisal and coping: Parachute jump effectiveness
[FOA-C-55058-H3] N84-12724
An iterated logarithm law result for extreme values from Gaussian sequences
[AD-A129559] N84-12798
SERIES EXPANSION
Study of an asymptotic method for helicopter rotor blade aerodynamic loads N84-12135
SERVOCONTROL
Hydraulic generation of auxilliary power for the Mirage 2000 aircraft N84-12176
SERVOMECHANISMS
Concept of a safety system for a servohydraulic test facility N84-12202
Simulation of electro-servo-hydraulic actuator for high quality testing --- of spacecraft N84-12206
Robotics: An introduction to today's robot and future trends
[AD-A132070] N84-12768
SET THEORY
Disjunctive programming and a hierarchy of relaxations for discrete optimization problems
[AD-A132004] N84-12784

SEWAGE
Operational utilization of remote sensing in a study of the impact of disposal of urban waste at sea
N84-12611
SEWAGE TREATMENT
Method for treating wastewater using microorganisms and vascular aquatic plants
[NASA-CASE-NSTL-10] N84-12654
SEWING
Some considerations of the efficiency of sewn lap joints in a nylon webbing
[RAE-TR-83009] N84-12310
SHALE OIL
Long term evaluation of the effects of shale oil produced JP-4 on aircraft construction materials
[AD-A131665] N84-12161
Combustion of EDS mid-distillate and refined shale-oil residual fuel in a gas turbine with large single-combustion chamber
[DE83-017700] N84-12281
SHALLOW WATER
Radar bathymetry : A review N84-12612
Short-range acoustic intensity vectors of the Pekeris shallow water model
[AMTE(N)-TM-83065] N84-12819
SHAPE MEMORY ALLOYS
Degradation of shape memory effect
[DE83-016586] N84-12295
SHAPES
Topically classified bibliography on shapes of falling drops, drops in electric fields and related topics
[AD-A131134] N84-12417
Inverse born approximation: Exact determination of shape of convex voids
[DE83-017685] N84-12512
Shape from shading: An assessment N84-12574
An investigation of geometric radar shapes for stereotyping
[AD-A131120] N84-13020
Radial evolution of ion distribution functions
N84-13094
SHARP LEADING EDGES
An experimental investigation of the vortex flow over delta and double-delta wings at low speed N84-12106
SHEAR
Piston-displacement equations of state for sodium, potassium, and rubidium metals to 20 kbar from 300 K to 4 K
[DE83-018079] N84-12252
SHEAR STRESS
Computation of three-dimensional unsteady flow in rigid and deformable curved tubes N84-12440
A pressure-shear experiment for studying the dynamic plastic responses of metals at shear strain rates of 10 to the 5th power s(-1) N84-12519
SHELLS (STRUCTURAL FORMS)
Submerged shock response of a linearly elastic shell of revolution containing internal structure. User's manual for the ELSHOK code
[AD-A131282] N84-12534
SHIPS
Interaction of antennas with masts under special consideration of the sensitivity and nonlinear effects in ship borne receiving systems N84-12371
SHIVA LASER SYSTEM
Creation of ultra-high-pressure shocks by the collision of laser-accelerated disks: Experiment and theory
[DE83-017366] N84-12486
SHOCK FRONTS
Initial decay of flow properties of planar, cylindrical and spherical blast waves
[UTIAS-TN-244] N84-12416
SHOCK TUBES
Experimental and computational modeling of rarefaction wave eliminators suitable for the BRL 2.44 m shock tube
[AD-A131894] N84-12194
SHOCK WAVE INTERACTION
Interaction between a shock-wave and a vortex flow
N84-12104
SHOCK WAVE PROFILES
Velocity profiles of interplanetary shocks N84-13122
SHOCK WAVE PROPAGATION
Formation of standing shocks in stellar winds and related astrophysical flows N84-13088
Plasma properties of driver gas following interplanetary shocks observed by ISEE-3 N84-13123
Corotating shocks in inner heliosphere N84-13124
SHOCK WAVES
Experimental and computational modeling of rarefaction wave eliminators suitable for the BRL 2.44 m shock tube
[AD-A131894] N84-12194
Novel optical pin using microballoons
[DE83-015222] N84-12391
The shock wave structure in one-component gas and in binary gas mixture
[ISSN-0208-5658] N84-12407
Initial decay of flow properties of planar, cylindrical and spherical blast waves
[UTIAS-TN-244] N84-12416
Scale lengths in quasi-parallel shocks
[NASA-TM-85109] N84-12663
Theoretical and experimental studies of shock-compressed benzene and polybutene
[DE83-015884] N84-12816
Multiple transonic solutions and a new class of shock transitions in solar and stellar winds N84-13083
Solar cycle variations of the solar wind N84-13089
Multiple spacecraft observations of interplanetary shocks: Characteristics of the upstream ULF turbulence
N84-13097
Electron heating at interplanetary shocks N84-13098
SHORT CIRCUIT CURRENTS
Orbiting wire as a dynamo: Auxiliary power possibilites for space platforms
[IFSI-83-3] N84-12653
SHUTTLE PALLET SATELLITES
The modular optoelectronic scanner (MOMS) on STS-7, June 83 N84-12589
SIDEBANDS
Effects of nonlinear loads on antennas and scatterers
N84-12376
SIGNAL ANALYSIS
Analysis of some filtering and data analysis methods for gravitational wave antennas with resonant transducers
[IFSI-82-11] N84-12359
Data analysis for gravitational wave antenna with resonant transducers
[IFSI-82-12] N84-12360
La Recherche Aerospatiale, Bimonthly Bulletin, no. 1983-1/212, January-February 1983
[ESA-TT-814] N84-12810
SIGNAL DETECTION
Optimum reception in non-Gaussian electromagnetic interference environments. Part 2: Optimum and suboptimum threshold signal detection in class A and B noise
[PB83-241141] N84-12364
Description of an automatic seismic measurements package: Analysis and design goals
[AD-A132067] N84-12666
SIGNAL DISTORTION
Interaction of antennas with masts under special consideration of the sensitivity and nonlinear effects in ship borne receiving systems N84-12371
SIGNAL PROCESSING
The dependence of the radar modulation transfer function on environmental conditions and wave parameters
[AD-A131858] N84-12348
Optimum reception in non-Gaussian electromagnetic interference environments. Part 2: Optimum and suboptimum threshold signal detection in class A and B noise
[PB83-241141] N84-12364
Center for electronics and electrical engineering technical progress bulletin covering signals and systems program, April 1982 - September 1982
[PB83-241158] N84-12405
Utility of the cortical evoked response as a measure of photographic image quality
[AD-A131679] N84-12455
Description of an automatic seismic measurements package: Analysis and design goals
[AD-A132067] N84-12666
Microearthquakes induced during hydraulic fracturing at the Fenton Hill HDR site: The 1982 experiments
[DE83-014191] N84-12672
High-speed videography combined with an x-ray image intensifier for dynamic radiography
[DE83-017233] N84-12905
SIGNAL TO NOISE RATIOS
On the performance of two-stage group screening experiments
[AD-A131970] N84-12807
SIGNATURE ANALYSIS
The Mimas ghost revisited: An analysis of the electron flux and electron microsignatures observed in the vicinity of Mimas at Saturn
[NASA-CR-174596] N84-13056
SILANES
Amorphous silicon-carbon films
[DE83-018077] N84-12259
Free-radical and ion chemistry of volatile silanes, germanes, and phosphines
[DE83-016389] N84-12277
Structure and vibrational spectra of a model of a-Si:H with periodic boundary conditions
[DE83-015245] N84-12390
The effect of moisture on the physical and durability properties of methyl methacrylate polymer concrete
[DE83-016733] N84-12541
SILICIDES
Silicide formation and Schottky barrier of rare-earth metals on Si
[AD-A131750] N84-12975
Silicide formation and Schottky barrier of rare-earth metals on Si
[AD-A131749] N84-12976
Silicide formation and Schottky barrier of rare-earth metals on Si
[AD-A131748] N84-12977
SILICON
Stress production and relief in the gold/silicon eutectic die-attach process
[DE83-015230] N84-12400
Silicide formation and Schottky barrier of rare-earth metals on Si
[AD-A131750] N84-12975
Silicide formation and Schottky barrier of rare-earth metals on Si
[AD-A131749] N84-12976
Silicide formation and Schottky barrier of rare-earth metals on Si
[AD-A131748] N84-12977
Predevelopment of IR-CCD components
[BMFT-FB-T-83-133] N84-13001
SILICON ALLOYS
Formation of surface layers during oxidation of a Fe-Mn-Si alloy
[DE83-009495] N84-12302
SILICON CARBIDES
Amorphous silicon-carbon films
[DE83-018077] N84-12259
Fabrication and properties of multilayer structures
[AD-A131934] N84-12969
SILICON DIOXIDE
Hole trapping, recombination, and space charge in irradiated Sandia oxides
[DE83-015212] N84-12986
SILICON OXIDES
Fabrication and properties of multilayer structures
[AD-A131934] N84-12969
The excitation of SiO in circumstellar envelopes
N84-13041
SILVER
Research and development for investigations of metallic adsorptions on metal surfaces by optical techniques complemented by dc resistivity and auger spectroscopy
[AD-A131739] N84-12351
SIMULATION
A flight investigation of simulated data link communications during single-pilot IFR flight
N84-12046
Numerical simulation of vortex breakdown by the vortex-filament method N84-12126
SPOT potential applications: An overview of the results of the simulation campaigns N84-12587
SINGLE CRYSTALS
Microstructural origins of hot spots in RDX explosive and several reference inert materials
[AD-A132056] N84-12325
Investigation of the Rayleigh critical angle phenomenon for the characterization of surface properties
[AD-A131530] N84-12340
Generation of monoenergetic positrons
[DE83-015535] N84-12687
Single Pb (1-x)Sn(x) Te crystal growth by vapor phase transport, with formation of a liquid/solid interface
[INPE-2811-PRE/369] N84-12967
The growth and measurement of single-crystal doped GGG (Gd3-xCaxGa5-xZrx012)
[AD-A131875] N84-12971
Temperature dependence of the electric-field gradient in Er metal
[DE83-015564] N84-12989
SINGULARITY (MATHEMATICS)
Rank modification method for certain singular systems of linear equations N84-12797
SINTERING
Cold sintering: A new powder consolidation process
[AD-A131687] N84-12292
SITE SELECTION
Compilation of selected faults and lineaments that may be relevant to a study of seismic activity in southern Nevada and part of adjacent California
[DE83-017085] N84-12673
SKIN FRICTION
Transonic airfoil development N84-12076
SKY
The far infrared sky survey experiment
[AD-A131966] N84-13037
SKY BRIGHTNESS
Model for illuminance on horizontal and vertical surfaces
[DE83-011973] N84-13127

Graphical method for determining interflected daylight in clear climates
[DE83-011969] N84-13128
SLEEP DEPRIVATION
Physical fitness as a moderator of cognitive degradation during sleep deprivation
[AD-A131962] N84-12718
SLENDER BODIES
Vortical flow management for improved configuration aerodynamics: Recent experiences N84-12129
SLIDING
Bibliography of coefficient of friction literature relating to slip type accidents --- slipping accidents
[PB83-243626] N84-12334
SLOPES
Turn-around loss for oceanic sound on a bottom slope
[AUWE-TN-705/83] N84-12618
SNOW
Snow cover and meteorology at Allagash, Maine, 1977 - 1980
[AD-A132013] N84-12684
Snow characterization instruments
[AD-A131984] N84-12687
SNOW COVER
Snow cover and meteorology at Allagash, Maine, 1977 - 1980
[AD-A132013] N84-12684
SOCIAL FACTORS
To quench our thirst: The present and future status of freshwater resources of the United States, part 3
[DE83-016791] N84-12625
SODIUM
Piston-displacement equations of state for sodium, potassium, and rubidium metals to 20 kbar from 300 K to 4 K
[DE83-016079] N84-12252
SODIUM CHLORIDES
Equations of state for the alkali metals, with generalizations to NaCl
[DE83-016075] N84-12280
SOIL MAPPING
Actitities report on the projet DESBOD --- geographical data acquisition
[REPT-5] N84-13025
SOIL MECHANICS
Handbook on the determination of the physical, thermal and mechanical properties of frozen soils
[NRC/CNR-TT-2064] N84-12578
SOIL MOISTURE
Identifying environmental features for land management decisions
[E84-10016] N84-12556
Handbook on the determination of the physical, thermal and mechanical properties of frozen soils
[NRC/CNR-TT-2064] N84-12578
Radar investigation of soils and sea (ERASME): C band helicopter-borne scatterometer. Application to soil moisture measurement N84-12588
SOILS
Lecture notes for contact-impact algorithms for large-deformation finite-element analysis
[DE83-013039] N84-12789
SOLAR ACTIVITY
Interpretation of 3He variations in the solar wind
[NASA-TM-85049] N84-13065
Solar cycle variations of the solar wind N84-13089
Periodicities in the occurrence of aurora as indicators of solar variability N84-13093
SOLAR ACTIVITY EFFECTS
Observations of hydromagnetic turbulence in the solar wind N84-13074
Solar wind distrubances in th outer heliosphere caused by successive solar flares from the same active region N84-13104
Corotating shocks in inner heliosphere N84-13124
SOLAR ARRAYS
Study of multi-kilowatt solar arrays for Earth orbit applications
[NASA-CR-170939] N84-12634
SOLAR ATMOSPHERE
The Owens Valley frequency-agile interferometer
[AD-A131825] N84-12453
SOLAR CELLS
Transactions of the Chinese Solar Energy Society (selected articles)
[AD-A131870] N84-12637
SOLAR COLLECTORS
Study of multi-kilowatt solar arrays for Earth orbit applications
[NASA-CR-170939] N84-12634
Tailoring polymer films for solar-collection use, phase 1
[DE83-018117] N84-12640
Fundamentals and techniques of nonimaging optics, volume 2
[DE83-015447] N84-12902
SOLAR COOLING
Reliability and maintainability study of select solar-energy-system components in the National Solar Data Network
[DE83-011974] N84-12647
SOLAR CORONA
Solar Wind Five
[NASA-CP-2280] N84-13067
Coronal heating by waves N84-13068
Direct coronal heating from dissipation of magnetic field N84-13069
Spectroscopic measurements of solar wind generation N84-13071
Coronal transients in FE XIV 5303A: First two-dimensional photoelectric ground-based observations N84-13072
Magnetohydrodynamic modeling of coronal structure and expansion N84-13081
Mixed solar wind originating from coronal regions of different temperatures N84-13114
Interpreting the solar wind ionization state N84-13115
Modeling of transient disturbances in coronal-streamer configurations N84-13119
Velocity profiles of interplanetary shocks N84-13122
The behavior of the cosmic ray equatorial anisotropy inside fast solar wind streams ejected by coronal holes
[IFSI-82-16] N84-13130
SOLAR COSMIC RAYS
The behavior of the cosmic ray equatorial anisotropy inside fast solar wind streams ejected by coronal holes
[IFSI-82-16] N84-13130
SOLAR CYCLES
Solar cycle variations of the solar wind N84-13089
Solar cycle evolution of the solar wind in three dimensions N84-13090
Solar cycle variations in the interplanetary magnetic field N84-13091
Solar wind variations in the 60-100 year period range: A review N84-13092
Periodicities in the occurrence of aurora as indicators of solar variability N84-13093
The effect of the solar field reversal on the modulation of galactic cosmic rays N84-13101
The average solar wind in the inner heliosphere: Structures and slow variations N84-13105
SOLAR DIAMETER
Preliminary studies of Solar Advance Observatory and Solar Beacon Facility
[NASA-CR-170937] N84-13066
SOLAR ENERGY
Ground coupled heat-pump-system experimental results
[DE83-014011] N84-12427
Thermochemical energy systems research
[DE83-012132] N84-12644
Empirical validation of computer models for passive-solar residences
[DE83-016887] N84-13005
SOLAR ENERGY CONVERSION
Photoelectrochemical electrodes
[NASA-CASE-NPO-15458-1] N84-12262
Reduction of CO2 to methanol and methane by photo and dark reactions on semiconductor electrodes
[PB83-249490] N84-12329
Transactions of the Chinese Solar Energy Society (selected articles)
[AD-A131870] N84-12637
Fourth International Conference on Photochemical Conversion and Storage of Solar Energy
[DE83-014760] N84-12638
SOLAR FLARES
The Owens Valley frequency-agile interferometer
[AD-A131825] N84-12453
Solar wind distrubances in th outer heliosphere caused by successive solar flares from the same active region N84-13104
Modeling of transient disturbances in coronal-streamer configurations N84-13119
Associations between coronal mass ejections and interplanetary shocks N84-13121
Interplanetary perturbations associated with type 4 solar flares
[IFSI-82-6] N84-13129
SOLAR FLUX DENSITY
Associations between coronal mass ejections and interplanetary shocks N84-13121
SOLAR HEATING
Reliability and maintainability study of select solar-energy-system components in the National Solar Data Network
[DE83-011974] N84-12647
Passive-solar performance: Summary of 1981-1982 class B results
[DE83-009407] N84-12650
SOLAR MAGNETIC FIELD
Spatial dependences in the distant solar wind: Pioneers 10 and 11 N84-13107
SOLAR OBSERVATORIES
Preliminary studies of Solar Advance Observatory and Solar Beacon Facility
[NASA-CR-170937] N84-13066
SOLAR ORBITS
Quasi-steady solar wind dynamics N84-13120
SOLAR PHYSICS
Activities report of the Institute of Astronomy and Astrophysics N84-13048
SOLAR POWERED AIRCRAFT
Solar powered aircraft
[NASA-CASE-LAR-12615-1] N84-12154
SOLAR RADIO BURSTS
Radio evidence for interplanetary streamers in the range 10-170 solar radii N84-13103
SOLAR REFLECTORS
Polymer degradation on reflecting metal films: Fourier transform infrared (FTIR) reflection-absorbance studies
[DE83-012129] N84-12641
Development of a portable specular reflectometer for monitoring solar-mirror materials
[DE83-016065] N84-12901
SOLAR SPECTROMETERS
Observational evidence for solar wind acceleration at the base of coronal holes N84-13082
SOLAR STORMS
Radio evidence for interplanetary streamers in the range 10-170 solar radii N84-13103
SOLAR WIND
Radial variations of large-scale magnetohydrodynamic fluctuations in the solar wind
[NASA-TM-85116] N84-13045
Interpretation of 3He variations in the solar wind
[NASA-TM-85049] N84-13065
Solar Wind Five
[NASA-CP-2280] N84-13067
Coronal heating by waves N84-13068
HRTS observations of the fine structure and dynamics of the solar chromosphere and transition zone N84-13070
Spectroscopic measurements of solar wind generation N84-13071
Magnetohydrodynamic turbulence in the solar wind N84-13073
Alfven solitons in the solar wind N84-13075
Theory of hydromagnetic turbulence N84-13077
Observational constraints on solar wind acceleration mechanisms N84-13078
Role of thermal conduction in the acceleration of the solar wind N84-13079
The collapse of the local, Spitzer-Haerm formulation and a global-local generalization for heat flow in an inhomogeneous, fully ionized plasma N84-13080
Observational evidence for solar wind acceleration at the base of coronal holes N84-13082
Solar cycle variations of the solar wind N84-13089
Solar cycle evolution of the solar wind in three dimensions N84-13090
Solar cycle variations in the interplanetary magnetic field N84-13091
Solar wind variations in the 60-100 year period range: A review N84-13092
Radial evolution of ion distribution functions N84-13094
Electrostatic waves and anomalous transport in the solar wind N84-13095
Measurement of macroscopic plasma parameters with a radio experiment: Interpretation of the quasi-thermal noise spectrum observed in the solar wind N84-13096
Interplanetary scintillation observations of the solar wind close to the Sun and out of the ecliptic N84-13102
Solar wind distrubances in th outer heliosphere caused by successive solar flares from the same active region N84-13104
The average solar wind in the inner heliosphere: Structures and slow variations N84-13105
The radial evolution of the solar wind, 1-10 AU N84-13106
Spatial dependences in the distant solar wind: Pioneers 10 and 11 N84-13107
Solar wind minor ions: Recent observations N84-13110
The relative abundance of 3He(++) in the solar wind N84-13111
Iron charge states observed in the solar wind N84-13112
Spatial variation of iron abundance in the high speed solar wind, 1972 to 1976 N84-13113
Mixed solar wind originating from coronal regions of different temperatures N84-13114
Interpreting the solar wind ionization state N84-13115

Minor constituents in the solar wind originating from plasma-dust interactions N84-13116
Acceleration of heavy ions in the solar wind N84-13118
Quasi-steady solar wind dynamics N84-13120
Plasma properties of driver gas following interplanetary shocks observed by ISEE-3 N84-13123
Corotating shocks in inner heliosphere N84-13124
Interaction of the plasma tail of comet Bradfield 1979L on 1980 February 6 with a possibly flare-generated solar-wind disturbance N84-13126
The behavior of the cosmic ray equatorial anisotropy inside fast solar wind streams ejected by coronal holes [IFSI-82-16] N84-13130

SOLAR WIND VELOCITY
Multiple transonic solutions and a new class of shock transitions in solar and stellar winds N84-13083
The average solar wind in the inner heliosphere: Structures and slow variations N84-13105
The radial evolution of the solar wind, 1-10 AU N84-13106
Interaction of the plasma tail of comet Bradfield 1979L on 1980 February 6 with a possibly flare-generated solar-wind disturbance N84-13126

SOLENOIDS
Performance measurements of a pilot superconducting solenoid model core for a wind tunnel magnetic suspension and balance system [NASA-CR-172243] N84-12192
The 12-T solenoid-design options for the MFTF-B upgrade [DE83-016646] N84-12817

SOLID ELECTROLYTES
Solid-oxide fuel-cell performance [DE83-017926] N84-12396
Defect interactions at high concentrations in solid oxide electrolytes [DE83-016849] N84-12992

SOLID PROPELLANT COMBUSTION
Combustion modeling of composite solid propellants N84-12285

SOLID SOLUTIONS
Ionic conductivity in lithium hexaoxometallate solid solutions [AD-A131842] N84-12250

SOLID STATE DEVICES
Large-area mercuric iodide photodectors [DE83-013035] N84-12898

SOLID-SOLID INTERFACES
Surface and interfacial properties of Ga(0.47) In(0.53) As alloys [AD-A131925] N84-12970

SOLIDIFICATION
Materials processing in space program tasks-supplement [NASA-TM-82548] N84-12196
Solidification of aluminum and aluminum alloys at high levels of undercooling N84-12286
Containerless electromagnetic levitation melting of Cu-Fe and Ag-Ni alloys [NASA-TM-82553] N84-12288

SOLIDS
Mechanical response of fluid-filled poroelastic solids N84-12525
Physics of ion implantation: Ion-cascade processes and physical state of the implanted solid [DE83-017152] N84-12998

SOLITARY WAVES
Solitons and polarons in quasi-one dimensional conducting polymers and related materials [DE83-015233] N84-12853
Considerations of the three-wave interactions [IPPJ-641] N84-12915
Computational synergetics and innovation in wave, vortex, and plasma cloud dynamics [DE83-015252] N84-12928
Commensurability, chaos, and the devil's staircase [DE83-013280] N84-12987
Alfven solitons in the solar wind N84-13075

SOLUTIONS
Method and apparatus for minimizing convection during crystal growth from solution [NASA-CASE-NPO-15811-1] N84-12968

SOOT
Soot formation from polycyclic aromatics [DE83-009750] N84-12271
Structure of convective surface deposits and effect on MHD steam-plant design [DE83-010757] N84-12931

SOUND AMPLIFICATION
Transverse horizontal coherence and low-frequency array gain limits in the deep ocean [AD-A131916] N84-12821

SOUND FIELDS
Transverse horizontal coherence and low-frequency array gain limits in the deep ocean [AD-A131916] N84-12821

SOUND PROPAGATION
Turn-around loss for oceanic sound on a bottom slope [AUWE-TN-705/83] N84-12818
Short-range acoustic intensity vectors of the Pekeris shallow water model [AMTE(N)-TM-83065] N84-12819

SOUND TRANSMISSION
Transverse horizontal coherence and low-frequency array gain limits in the deep ocean [AD-A131916] N84-12821

SOUND WAVES
Acoustic pulse scattering from impedance covered cylinders [AD-A131653] N84-12822
Double porosity model for acoustic wave propagation in fractured-porous rock [DE83-017823] N84-12823

SOUNDING ROCKETS
Engineering services in support of the AFGL sounding rocket program [AD-A131929] N84-12211

SOURCES
Source header list, supplement 1 [AD-A131800] N84-13024

SPACE CHARGE
Developing a 500-eV proton beam [DE83-012781] N84-12880
Longitudinal space-charge effects in bunched beams [DE83-017305] N84-12888
Hole trapping, recombination, and space charge in irradiated Sandia oxides [DE83-015212] N84-12986

SPACE HEATING (BUILDINGS)
Passive-solar performance: Summary of 1981-1982 class B results [DE83-009407] N84-12650

SPACE LABORATORIES
Orbiting geophysics laboratory experiment [AD-A131950] N84-12218

SPACE OBSERVATIONS (FROM EARTH)
A search for radio pulsars in the Northern sky: Discovery of a pulsar in a unique binary system N84-13040

SPACE PLASMAS
Theory of hydromagnetic turbulence N84-13077
Theory of interstellar medium diagnostics N84-13108

SPACE POWER UNIT REACTORS
Space reactors: Past, present and future [DE83-011177] N84-12870

SPACE PROCESSING
Materials processing in space program tasks-supplement [NASA-TM-82548] N84-12196

SPACE SHUTTLE BOOSTERS
Space Shuttle external interference heating test [AD-A131688] N84-12215

SPACE SHUTTLE MAIN ENGINE
The SSME seal test program: Leakage tests for helically-grooved seals [NASA-CR-170921] N84-12495

SPACE SHUTTLE ORBITERS
Analytical prediction of aerothermal environment in a wing-elevon cove --- space shuttle orbiter [NASA-TM-85711] N84-12412

SPACE SHUTTLE PAYLOADS
Shuttle measured contaminant environment and modeling for payloads. Preliminary assessment of the space telescope environment in the shuttle bay [NASA-TM-85111] N84-12216
Performance of antennas in plasma N84-12377

SPACE SHUTTLE UPPER STAGE D
Phase A study for a test satellite for propagation and transmission experiments in the 20/30 GHz frequency band [BMFT-FB-W-83-009] N84-12355

SPACE SHUTTLES
Space Shuttle propulsion parameter estimation using optimal estimation techniques, volume 1 [NASA-CR-170935] N84-12213
Test report for MSFC test 83-2. Pressure scaled water impact test of a 12.5 inch diameter model of the Space Shuttle Solid Rocket booster filament wound case and external TVC pod [NASA-CR-174601] N84-12217
Study of auxiliary propulsion requirements for large space systems. Volume 1: Executive summary [NASA-CR-168193] N84-12226

SPACE STATIONS
Integrated Flywheel Technology, 1983 [NASA-CP-2290] N84-12228
Space station attitude control system concept and requirements N84-12234
Space station control requirements and flywheel system weights for combined momentum and energy storage N84-12236
Advanced Control and Power System (ACAPS) technology program N84-12243

SPACE TRANSPORTATION SYSTEM 9 FLIGHT
STS-9 Spacelab 1 press kit [P83-10209] N84-12214

SPACE-TIME FUNCTIONS
On space-time means and everywhere defined scattering operators for nonlinear Klein-Gordon equations [CTH-MATH-1983-13-PREPRINT] N84-12793
Random eddies in wakes and mixing layers --- wind tunnel tests N84-12813
Magnetohydrodynamic turbulence in the solar wind N84-13073

SPACEBORNE EXPERIMENTS
Phase A study for a test satellite for propagation and transmission experiments in the 20/30 GHz frequency band [BMFT-FB-W-83-009] N84-12355

SPACECRAFT CONFIGURATIONS
Space station attitude control system concept and requirements N84-12234

SPACECRAFT CONTROL
Spacecraft interface design and its impact on operational support [ESA-STR-211] N84-12220

SPACECRAFT DESIGN
System definition Roentgensatellit, phase B 1.2 [BMFT-FB-W-83-010] N84-12219
Spacecraft interface design and its impact on operational support [ESA-STR-211] N84-12220
Space station attitude control system concept and requirements N84-12234

SPACECRAFT ENVIRONMENTS
Shuttle measured contaminant environment and modeling for payloads. Preliminary assessment of the space telescope environment in the shuttle bay [NASA-TM-85111] N84-12216

SPACECRAFT LAUNCHING
Study of auxiliary propulsion requirements for large space systems. Volume 1: Executive summary [NASA-CR-168193] N84-12226

SPACECRAFT PERFORMANCE
The OTS: Fifth year in orbit N84-12221

SPACECRAFT POWER SUPPLIES
GSFC flywheel status N84-12230
Electrical power trade-offs N84-12232
Space station energy sizing N84-12233
Study of multi-kilowatt solar arrays for Earth orbit applications [NASA-CR-170939] N84-12634
Orbiting wire as a dynamo: Auxiliary power possibilites for space platforms [IFSI-83-3] N84-12653

SPACECRAFT PROPULSION
Space Shuttle propulsion parameter estimation using optimal estimation techniques, volume 1 [NASA-CR-170935] N84-12213
Study of auxiliary propulsion requirements for large space systems. Volume 1: Executive summary [NASA-CR-168193] N84-12226

SPACECRAFT STRUCTURES
Spacecraft Vibration Testing Using Multi-Axis Hydraulic Vibration Systems --- conferences [ESA-SP-197] N84-12197
Simulation of electro-servo-hydraulic actuator for high quality testing --- of spacecraft N84-12206

SPACECRAFT TRACKING
Correlation between two spacecraft in the Doppler detection of a gravitational background radiation [IFSI-83-7] N84-12362

SPACELAB
STS-9 Spacelab 1 press kit [P83-10209] N84-12214

SPACELAB PAYLOADS
System definition Roentgensatellit, phase B 1.2 [BMFT-FB-W-83-010] N84-12219
Layout of a SAR sensor for Spacelab and satellite. Part 1: Design considerations for fundamental SAR parameters [ESA-TT-802] N84-12224

SPAIN
Mapping land use in Catalonia (Spain) --- using LANDSAT imagery N84-12613

SPALLATION
Spallation and 14-MeV neutron irradiation of stabilized NbTi superconductors [DE83-017973] N84-12394

SPANWISE BLOWING
Augmentation of fighter-aircraft performance by spanwise blowing over the wing leading edge N84-12133

SPARK IGNITION
Evaluation of unthrottled combustion system options for light duty applications with future syncrude derived fuels [DE83-017047] N84-12327
SPATIAL DISTRIBUTION
An empirical Bayes approach to spatial analysis N84-12563
Relating spatial patterns in image data to scene characteristics N84-12573
Transverse horizontal coherence and low-frequency array gain limits in the deep ocean [AD-A131916] N84-12821
Faint galaxies in the Coma cluster: Luminosity function and spatial distribution N84-13053
Spatial variation of iron abundance in the high speed solar wind, 1972 to 1976 N84-13113
SPATIAL FILTERING
Noise reduction and segmentation of IR images using CO-median filters [RSRE-3582] N84-12378
SPECIFICATIONS
A balloon design for 9000 pounds at 90,000 feet: Recommendations based on heavy-load balloon history [AD-A131987] N84-12093
Prerequisites for deriving formal specifications from natural language requirements [AD-A131722] N84-12771
SPECKLE PATTERNS
SAR speckle noise reduction using Wiener filter N84-12568
SPECTRA
Structure and vibrational spectra of a model of a-Si:H with periodic boundary conditions [DE83-015245] N84-12390
SPECTRAL RECONNAISSANCE
The use of airborne thematic mapper simulation data for the estimation and mapping of Green Leaf Area Index (GLAI) N84-12602
Operational utilization of remote sensing in a study of the impact of disposal of urban waste at sea N84-12611
SPECTRAL SIGNATURES
Quantile data analysis of image data N84-12565
SPECTROSCOPIC ANALYSIS
Spectroscopic measurements of solar wind generation N84-13071
SPECTROSCOPY
Photothermal displacement spectroscopy of surfaces and thin films [DE83-015957] N84-12279
International Conference on Vibrations at Surfaces (3rd) [AD-A131794] N84-12834
Novel method for the study of optical properties of surfaces [DE83-012899] N84-12895
SPECTRUM ANALYSIS
Research and development for investigations of metallic adsorptions on metal surfaces by optical techniques complemented by dc resistivity and auger spectroscopy [AD-A131739] N84-12351
Maximum likelihood estimation of linear dynamic system parameters [AR-002-934] N84-12780
Spectral analysis of magnetohydrodynamic fluctuations near interplanetary schocks [NASA-TM-85119] N84-13044
SPECULAR REFLECTION
Development of a portable specular reflectometer for monitoring solar-mirror materials [DE83-016065] N84-12901
SPEECH RECOGNITION
Proposed study to determine potential flight applications and human factors design guidelines of voice recognition/synthesis systems N84-12047
SPHERICAL HARMONICS
The effect of coordinate system rotation on spherical harmonic expansions: A numerical method [AD-A131974] N84-12785
SPHERICAL SHELLS
The AGCE related studies of baroclinic flows in spherical geometry [NASA-CR-170934] N84-12415
SPHEROMAKS
Magnetohydrodynamic equilibrium and stability of spheromak plasma in flux conserver [IPPJ-642] N84-12909
Recent results in the Los Alamos compact torus program [DE83-014147] N84-12930
SPIN DYNAMICS
Theory of hyperfine anomalies in muonic atoms [DE83-015392] N84-12872
SPIN-LATTICE RELAXATION
Muon spin relaxation in ferromagnetic PdMn [DE83-012659] N84-12979
SPLINE FUNCTIONS
Aspects of second- and third-order panel methods demonstrated for the two-dimensional flat plate problem [NLR-TR-81074-U] N84-12433
Spline classification methods N84-12564
SPOILERS
Steady and unsteady flow models for airfoils with spoiler N84-12136
SPOT (FRENCH SATELLITE)
SPOT potential applications: An overview of the results of the simulation campaigns N84-12587
Application of high resolution satellite data to coastal zones: SPOT simulations during ecological survey of the Britanny coast N84-12591
The SPOT distribution system N84-12615
SPRAY CHARACTERISTICS
Constant-output atomizer --- inhalation therapy and aerosol research [NASA-CASE-MFS-25631-1] N84-12406
SPRAYED COATINGS
Development of strain tolerant thermal barrier coating systems, tasks 1 - 3 [NASA-CR-168251] N84-12312
SPRAYING
Assessment of energy-efficiency improvements for paint spray booths [DE83-016680] N84-12320
SPRINGS (ELASTIC)
Unidirectional flexural pivot [NASA-CASE-GSC-12622-1] N84-12492
SPUTTERING
Novel techniques for enhanced reflectivity infrared mirrors [AD-A131924] N84-12894
Fabrication and properties of multilayer structures [AD-A131934] N84-12969
Proceedings of the Workshop on Ion Mixing and Surface Layer Alloying [DE83-015354] N84-12994
Sputtered C-axis inclined piezoelectric films and shear-wave resonators [DE83-017253] N84-12997
SQUARES (MATHEMATICS)
On Waring's problem g (4) or = 20 N84-12781
STABILITY
Use of aircraft imagery in evaluating ground stability at open-pit uranium mines in Gas Hills, Wyoming [DE83-903011] N84-12621
Initial operation of the compressed air experiment at Pittsfield, Illinois [DE83-016930] N84-12643
Initial assessment of the MHD stability of TMX-U [DE83-016521] N84-12646
STABILIZATION
Rotating and propagating LIB stabilized by self-induced magnetic field [IPPJ-640] N84-12916
STAGNATION POINT
A contribution to the problem of vortex breakdown N84-12125
STAINLESS STEELS
Hydrogen compatibility handbook for stainless steels [DE83-017051] N84-12301
Radiation damage and phase instability in irradiated stainless steel [DE83-017190] N84-12303
STAMPING
Holding fixture for a hot stamping press [NASA-CASE-GSC-12619-1] N84-12491
STANDARD DEVIATION
Wind-speed extremes in the Northern Hemisphere, 30 through 60 km [AD-A132019] N84-12682
STANDARDIZATION
Review of the ANSI metafile and virtual device interface standardization activities [DE83-015925] N84-12737
Environments and search paths for the software tools [DE83-016607] N84-12749
STANDARDS
Alternative transmission media for third-generation interface standards [PB83-238345] N84-12365
International Telecommunication Standards: Issues and Implications for the '80's [PB83-241471] N84-12366
Comments on ISO/TC 97/SC 18/WG3 N120 [DE83-011391] N84-12748
STANDING WAVES
Rising bubbles [AD-A131572] N84-12418
STAR CLUSTERS
Problems of stellar evolution in star clusters of the Magellanic clouds N84-13051
STARTING
Auxilliary power systems with gas turbines N84-12170
STATIC PRESSURE
Discussion of static pressure liquid-floated gyros [AD-A131874] N84-12451
Application of the small body pressure transducer [AD-A131733] N84-12454
The SSME seal test program: Leakage tests for helically-grooved seals [NASA-CR-170921] N84-12495
STATISTICAL ANALYSIS
Single pilot IFR accident data analysis N84-12031
A summary and integration of research concerning single pilot IFR operational problems N84-12034
Proceedings of the NASA Symposium on Mathematical Pattern Recognition and Image Analysis [E83-10032] N84-12557
Estimation of uncertainty in coal resources [DE83-902538] N84-12620
On the wind stress - sea level power law [AD-A132035] N84-12681
Gust structure and gust statistics. Results from an analysis of atmospheric turbulence measurements by using conditional sampling technique [FFA-TN-1983-28] N84-12696
Weak and strong law results for a function of the spacings [AD-A130705] N84-12782
TRAN-STAT (statistics for environmental studies). Issue no. 24: Field sampling designs, simple random and stratified random sampling [DE83-016826] N84-12803
Interplanetary Alfvenic fluctuations: A statistical study of the directional variations of the magnetic field [IFSI-82-14] N84-13050
STATISTICAL DISTRIBUTIONS
Estimating location parameters in a mixture model N84-12559
Mixture models for dependent observations N84-12562
Effect of noise in the three-parameter logistic model [AD-A131867] N84-12721
STATISTICAL MECHANICS
Investigation of the statistical mechanics of linear polymers for various physical conditions [JUEL-1832] N84-12324
Progress in lattice gauge theory [DE83-014055] N84-12862
STEADY FLOW
Stability of a pair of stationary vortices in the leeward side of a cylinder in a potential flowfield [AD-A131917] N84-12095
The vortex skeleton model for three-dimensional steady flows N84-12101
Steady and unsteady flow models for airfoils with spoiler N84-12136
The AGCE related studies of baroclinic flows in spherical geometry [NASA-CR-170934] N84-12415
STEADY STATE
Effect of RF structure on cumulative beam breakup [DE83-017302] N84-12882
A steady-state axisymmetric toroidal system [IPPJ-643] N84-12910
STEAM
Creep and tensile properties of alloy 800H-Hastelloy X weldments [DE83-017067] N84-12542
STEAM TURBINES
Steam turbine as unipolar generator [AD-A131142] N84-12498
STEEL STRUCTURES
Cumulative damage in components of steel structures under cyclic inelastic loading N84-12550
STEELS
Research activities in materials and molecular research [DE83-015005] N84-12255
Study of chromium-free and chromium-reduced steels [DE83-016717] N84-12294
Strain rate effects on ductile/brittle transitions in steels [DE83-016906] N84-12308
The analysis of crack growth data with application to trip steel [AD-A132021] N84-12535
STELLAR ATMOSPHERES
Activities report of the Institute of Astronomy and Astrophysics N84-13048
Observation of winds in cool stars N84-13084
STELLAR CORONAS
The winds and coronae of early-type stars N84-13086

STELLAR ENVELOPES
The excitation of SiO in circumstellar envelopes N84-13041
STELLAR EVOLUTION
Problems of stellar evolution in star clusters of the Magellanic clouds N84-13051
STELLAR MASS
Associations between coronal mass ejections and interplanetary shocks N84-13121
STELLAR MASS ACCRETION
Hydrodynamic simulations of a combined hydrogen, helium thermonuclear runaway on a 10 km neutron star [DE83-012658] N84-13047
STELLAR STRUCTURE
Activities report of the Institute of Astronomy and Astrophysics N84-13048
STELLAR WINDS
Multiple transonic solutions and a new class of shock transitions in solar and stellar winds N84-13083
Observation of winds in cool stars N84-13084
Theory of winds in late-type evolved and pre-main-sequence stars N84-13085
The winds and coronae of early-type stars N84-13086
Stellar winds driven by multi-line scattering N84-13087
Formation of standing shocks in stellar winds and related astrophysical flows N84-13088
STELLARATORS
Constraints on the scale of toroidal-fusion experiments with application to the design of a helical-axis stellarator [DE83-016812] N84-12950
Electron-cyclotron-heating experiments in Tokamaks and stellarators [DE83-017210] N84-12958
STIFFNESS
An interactive computer program for analysis of ultrasonic modulus data on anistropic materials [NPL-DMA(A)68] N84-12526
Lecture notes for contact-impact algorithms for large-deformation finite-element analysis [DE83-013039] N84-12789
STIFFNESS MATRIX
A thin-walled beam finite element [TT-8302] N84-12779
STIMULATED EMISSION DEVICES
Experiments to study the feasibility of making an X-ray laser at the Novette laser facility [DE83-015615] N84-12476
STIRLING CYCLE
Dynamic analysis of the fluidyne [DE83-017283] N84-12500
Effects of pressure-drop correlations on Stirling-engine predicted performance [DE83-017279] N84-12501
Revised isothermal analysis program for Stirling engines [DE83-017276] N84-12504
STOCHASTIC PROCESSES
Evaluation of the stochastic drift of rate integrating gyros as preparation for the analysis of laser gyro drift measurements [DFVLR-MITT-83-04] N84-12449
First passage times in stochastic differential equations of mathematical physics and engineering [AD-A131705] N84-12728
An iterated logarithm law result for extreme values from Gaussian sequences [AD-A129559] N84-12798
The effects of small noise on implicitly defined non-linear dynamical systems [AD-A131632] N84-12808
STOPPING
Ion stopping in heated targets [DE83-017800] N84-12941
STOPPING POWER
Beam-target interaction of intense ion beams: Theory and experiment [DE83-018264] N84-12858
STORAGE BATTERIES
Assessment of potential for batteries in space applications N84-12246
STORAGE RINGS (PARTICLE ACCELERATORS)
A high-performance digital triggering system for phase-controlled rectifiers [DE83-012217] N84-12386
High-level control programs at NSLS [DE83-010935] N84-12754
From accelerators to storage rings to ? [DE83-011849] N84-12842
A thousand TeV in the center of mass: Introduction to high-energy storage rings [DE83-015649] N84-12855
Hadron-hadron collider group [DE83-010704] N84-12865
New facilities for the US high-energy physics program [DE83-016589] N84-12876
STORAGE STABILITY
Transactions of the Chinese Solar Energy Society (selected articles) [AD-A131870] N84-12637
STORMS (METEOROLOGY)
A case study of gravity wave-convective storm interactions N84-12659
Climate of Phoenix, Arizona (revised) [PB83-246801] N84-12699
STRAIN GAGES
Inflatable device for installing strain gage bridges [NASA-CASE-FRC-11068-1] N84-12443
Thin film strain transducer --- in-flight monitoring of balloon film strain [NASA-WLP-10055-2] N84-12448
Transient temperature response of strain gages, revision 1 [DE83-017514] N84-12459
STRAIN RATE
Strain rate effects on ductile/brittle transitions in steels [DE83-016906] N84-12308
A pressure-shear experiment for studying the dynamic plastic responses of metals at shear strain rates of 10 to the 5th power s(-1) N84-12519
Endochronic theory of dynamic viscoplasticity [DE83-017531] N84-12546
STRAPDOWN INERTIAL GUIDANCE
Flight tests for a strapdown system (MSS): The results of a special flight test [ESA-TT-818] N84-12153
STRATIGRAPHY
Geologic study of the Wind River Basin, Fremont and Natrona Counties, central Wyoming [PB83-254912] N84-12677
STRATOSPHERE
Remote sensing instruments for trace species measurements in the troposphere and stratosphere: A review N84-12583
Observations of the upper troposphere and lower stratosphere using the urbana coherent-scatter radar [NASA-CR-174594] N84-12664
STRATUS CLOUDS
Optical extinction coefficients beneath marine stratus clouds. Comparison of coefficients calculated from observed aerosol spectra with coefficients specified by the Navy aerosol model [AD-A132011] N84-12685
STREAK PHOTOGRAPHY
Time-resolved spectral measurements above 80 A [DE83-015616] N84-12933
STREAM FUNCTIONS (FLUIDS)
The break-up mechanism of a streamwise directed vortex N84-12123
STREAMS
Snowy Range Observatory: Climatological and streamflow data report 1982 [PB83-243147] N84-12633
STRESS (PHYSIOLOGY)
A laboratory comparison of portable cooling systems for workers exposed to two levels of heat stress [AD-A131848] N84-12423
Physical fitness as a moderator of cognitive degradation during sleep deprivation [AD-A131962] N84-12718
Effect of atropine on the exercise-heat performance of man [AD-A131843] N84-12719
Effectiveness in reducing heat stress of three conditioned-air cooling vests worn with and without cooling air supplied to a face piece [AD-A131975] N84-12726
STRESS ANALYSIS
Thermal stress analysis of annular glass-to-metal seals under thermal shock N84-12408
Analytical response of concrete structures subjected to high temperatures [DE83-009625] N84-12538
Mechanics of fracture under high-rate stress loading [DE83-013770] N84-12544
Design, development and use of the finite element machine [NASA-CR-172250] N84-12777
Lecture notes for contact-impact algorithms for large-deformation finite-element analysis [DE83-013039] N84-12789
STRESS CONCENTRATION
A study of coherent structures in the near-neutral marine atmospheric boundary layer N84-12658
STRESS CORROSION CRACKING
Life prediction under stress corrosion conditions below K sub ISCC [DE83-018074] N84-12307
Interaction of stress waves and cracks using a second order accurate finite difference method N84-12522
STRESS INTENSITY FACTORS
The Dugdale model for the compact specimen [NASA-TM-85714] N84-12529
STRESS RELAXATION
Stress production and relief in the gold/silicon eutectic die-attach process [DE83-015230] N84-12400
STRESSES
Inference of fatigue-crack closure stresses from ultrasonic-transmission measurements [DE83-017684] N84-12547
On the wind stress - sea level power law [AD-A132035] N84-12681
STRONGLY COUPLED PLASMAS
Strong coupling effects on bound states in plasmas [AD-A131661] N84-12918
STRUCTURAL ANALYSIS
On the structure of the turbulent vortex N84-12102
Control of flexible spacecraft by optimal model following N84-12222
Evaluation of the kinematic variable (back stress) response of metals [DE83-008381] N84-12293
Analytical response of concrete structures subjected to high temperatures [DE83-009625] N84-12538
Design, development and use of the finite element machine [NASA-CR-172250] N84-12777
A thin-walled beam finite element [TT-8302] N84-12779
STRUCTURAL BASINS
Geologic study of the Wind River Basin, Fremont and Natrona Counties, central Wyoming [PB83-254912] N84-12677
STRUCTURAL DESIGN
Evaluation of the kinematic variable (back stress) response of metals [DE83-008381] N84-12293
New conformal solution theory [PB83-249441] N84-13008
STRUCTURAL DESIGN CRITERIA
Geometries for roughness shapes in laminar flow [NASA-CASE-LAR-13255-1] N84-12092
Acta Mechanica Sinica (selected articles) [AD-A131871] N84-12422
Lower body graduated negative pressure system [NASA-CR-171717] N84-12725
The 12-T solenoid-design options for the MFTF-B upgrade [DE83-016646] N84-12817
University of Washington superconducting-booster project [DE83-015689] N84-12846
A thousand TeV in the center of mass: Introduction to high-energy storage rings [DE83-015649] N84-12855
Ripple-reduction poloidal-field coils for Tokamak reactors [DE83-009532] N84-12922
Design of the Advanced Toroidal Facility (ATF-1) [DE83-012641] N84-12923
STRUCTURAL MEMBERS
Review of aircraft crash structural response research [AD-A131696] N84-12160
STRUCTURAL PROPERTIES (GEOLOGY)
Use of aircraft imagery in evaluating ground stability at open-pit uranium mines in Gas Hills, Wyoming [DE83-903011] N84-12621
Geologic study of the Wind River Basin, Fremont and Natrona Counties, central Wyoming [PB83-254912] N84-12677
STRUCTURAL STABILITY
System identification of structures with joint rotation N84-12330
Development of the basic methods needed to predict the aeroelastic behavior of helicopters N84-12811
STRUCTURAL VIBRATION
Present trends in structural analysis at ONERA N84-12812
SUBMERGED BODIES
Yield surface for bars including warping restraint [AD-A131393] N84-12533
SUBROUTINE LIBRARIES (COMPUTERS)
Guidelines for the design of large modular scientific libraries in Ada [NPL-DITC-28/83] N84-12740
Assembly language graphics library (EGR1.LB) with Fortran interfacing [PB83-239624] N84-12757
SUBROUTINES
A computer subroutine for evaluating polygamma functions for complex arguments [AD-A131936] N84-12744

User's guide for SOL/NPSOL: A FORTRAN package for nonlinear programming
[DE83-016903] N84-12751
User's guide for SOL/QPSOL: A FORTRAN package for quadratic programming
[DE83-016990] N84-12752

SUBSONIC FLOW
Special Course on Subsonic/Transonic Aerodynamic Interference for Aircraft
[AGARD-R-712] N84-12072
Subsonic/Transonic Aerodynamic Interference for Aircraft: Introductory remarks N84-12073
Subsonic/transonic viscous interactions N84-12075
Theoretical modelling of three-dimensional vortex flows in aerodynamics N84-12116

SUBSTITUTES
Domestic scheduled air transport for the year 2000. Financial and capacity related effects of supply alternatives, considering, also, the cooperation with high speed rail transport services — West Germany
[DFVLR-FB-83-03] N84-12141

SULFATION
Breakaway corrosion in mixed-gas environments
[DE83-014704] N84-12299

SULFONES
The performance of the perfluorocarbon liquid/plastic-film capacitor technology in pulse-power service. A current status report
[DE83-014606] N84-12402

SULFUR FLUORIDES
Transport and relaxation processes in supercritical fluids
[DE83-015966] N84-12432

SUMS
Technique for producing a coherent sum of the data from P78-1, F2, and F4 satellites
[AD-A131965] N84-12210
On Waring's problem g (4) or = 20 N84-12781

SUNSPOTS
Solar cycle variations in the interplanetary magnetic field N84-13091

SUPERCONDUCTING MAGNETS
Self-correction coil: Operation mechanism of self-correction coil
[DE83-016324] N84-12392
Advanced high-field coil designs: 20 Tesla
[DE83-017368] N84-12397
Comparative evaluation of existing concepts for a 10-tesla FED toroidal field coil
[DE83-012817] N84-12815
The 12-T solenoid-design options for the MFTF-B upgrade
[DE83-016646] N84-12817
Ripple-reduction poloidal-field coils for Tokamak reactors
[DE83-009532] N84-12922
Thermal performance of the MFTF magnets
[DE83-016275] N84-12988
Superconductor stability, 1983: A review
[DE83-015506] N84-12990
Operational studies and expected performance of superconducting quadrupole magnets in the first stages of secondary beams
[DE83-016734] N84-12999

SUPERCONDUCTIVITY
Synchronous generators with superconductive excitation windings
[AD-A131832] N84-12382
Unipolar machine with superconductive excitation winding
[AD-A131820] N84-12383

SUPERCONDUCTORS
Spallation and 14-MeV neutron irradiation of stabilized NbTi superconductors
[DE83-017973] N84-12394
Storage of energy in magnetic field of superconductive coils
[AD-A131898] N84-12636
University of Washington superconducting-booster project
[DE83-015689] N84-12846
Superconducting stability, 1983: A review
[DE83-017262] N84-12995
Phonon-induced enhancements of the energy gap and critical current in superconducting aluminum
[DE83-015210] N84-12996

SUPERCRITICAL FLOW
Transonic airfoil development N84-12076

SUPERCRITICAL WINGS
Transonic airfoil development N84-12076
Transonic empirical configuration design process N84-12079

SUPERFLUIDITY
Transient heat transfer in superfluid helium, part 2
[DE83-015767] N84-12984
The far infrared sky survey experiment
[AD-A131968] N84-13037

SUPERGIANT STARS
Theory of winds in late-type evolved and pre-main-sequence stars N84-13085

SUPERHIGH FREQUENCIES
Phase A study for a test satellite for propagation and transmission experiments in the 20/30 GHz frequency band
[BMFT-FB-W-83-009] N84-12355
Radar investigation of soils and sea (ERASME): C band helicopter-borne scatterometer. Application to soil moisture measurement N84-12588

SUPPRESSORS
Development and flight test of an active flutter suppression system for the F-4F with stores. Part 3. Flight demonstration of the active flutter suppression system
[AD-A131972] N84-12191

SURFACE FINISHING
Y03: Prequalification of surface treatment. Measurement of laser reflecting power — Earth-Moon telemetry
[ESA-TT-791] N84-12490
Fabrication of machined optics for precision applications
[DE83-015720] N84-12900

SURFACE PROPERTIES
HgCdTe surface study program
[AD-A132071] N84-12266
Photothermal displacement spectroscopy of surfaces and thin films
[DE83-015957] N84-12279
Formation of surface layers during oxidation of a Fe-Mn-Si alloy
[DE83-009495] N84-12302
Investigation of the Rayleigh critical angle phenomenon for the characterization of surface properties
[AD-A131530] N84-12340
Novel method for the study of optical properties of surfaces
[DE83-012899] N84-12895
Surface and interfacial properties of Ga(0.47) In(0.53) As alloys
[AD-A131925] N84-12970
Physics of ion implantation: Ion-cascade processes and physical state of the implanted solid
[DE83-017152] N84-12998

SURFACE REACTIONS
HgCdTe surface study program
[AD-A132071] N84-12266
Laser interaction with metallic surfaces
[AD-A126269] N84-12464
Study of vibrational energy transfer at a surface by a time-of-flight method
[AD-A131798] N84-12833
International Conference on Vibrations at Surfaces (3rd)
[AD-A131794] N84-12834

SURFACE ROUGHNESS
Transonic airfoil development N84-12076
A numerical study on the evolution of tornadoes N84-12679

SURFACE ROUGHNESS EFFECTS
Thermal conductance measurements of pressed OFHC copper contacts at liquid helium temperatures
[NASA-TM-85861] N84-12809

SURFACE STABILITY
Yield surface for bars including warping restraint
[AD-A131393] N84-12533

SURFACE TEMPERATURE
Identifying environmental features for land management decisions
[E84-10016] N84-12556
The synthesized climatic function map N84-12617
World-wide sea-surface temperatures
[AD-A131892] N84-12689

SURFACE WAVES
On differential equations of nonlocal elasticity and solutions of screw dislocation and surface waves
[AD-A131911] N84-12786

SURGES
Modeling of transient disturbances in coronal-streamer configurations N84-13119

SWEPT WINGS
Subsonic/transonic viscous interactions N84-12075
Vortical flow management for improved configuration aerodynamics: Recent experiences N84-12129

SWEPTBACK WINGS
On the generation and subsequent development of spiral vortex flow over a swept-back wing N84-12105

SWIMMING POOL REACTORS
Real-time attenuation of heated optical fibers in a nuclear reactor
[DE83-015141] N84-12873

SWITCHES
High-average-power rep rate systems
[DE83-013769] N84-12385
Progress in developing repetitive pulse systems utilizing inductive energy storage
[DE83-015167] N84-12388
Power-loading effects in gas-discharge models
[DE83-016504] N84-12393

SYMBOLS
Advanced symbology for general aviation approach to landing displays N84-12039
An investigation of geometric radar shapes for stereotyping
[AD-A131120] N84-13020

SYMMETRY
Relative symmetries of differential equations
[DE83-015231] N84-12790
A steady-state axisymmetric toroidal system
[IPPJ-643] N84-12910

SYNCHRONISM
Software voting in asynchronous NMR (N-Modular Redundancy) computer structures
[NASA-CR-174488] N84-12732

SYNCHROTRON RADIATION
Uses of synchrotron radiation
[DE83-014431] N84-12720
Design of doubly focusing, tunable (5 - 30 keV), wide-bandpass optics made from layered synthetic microstructures
[DE83-015492] N84-12897

SYNOPTIC METEOROLOGY
Mechanisms of monsoonal cyclogenesis N84-12680
A subsynoptic environment associated with two inter-mountain severe thunderstorm events
[DE83-014498] N84-12694

SYNTHESIS (CHEMISTRY)
New approach to the generation of metal-bearing, medium-pore, shape-selective zeolites for Fischer-Tropsch catalysis: Spectroscopic studies of zeolites
[DE83-014344] N84-12254

SYNTHETIC APERTURE RADAR
Layout of a SAR sensor for Spacelab and satellite. Part 1: Design considerations for fundamental SAR parameters
[ESA-TT-802] N84-12224
SAR speckle noise reduction using Wiener filter N84-12568
SAR 580: Images for agricultural and forest survey. First results in middle Belgium N84-12595
Measuring landscape information content and distribution on a SAR-580 image N84-12596
First results of the evaluations of the European SAR 580 data for agricultural and forestry purposes in test site D6, Freiburg (West Germany) N84-12599

SYNTHETIC FUELS
Evaluation of unthrottled combustion system options for light duty applications with future syncrude derived fuels
[DE83-017047] N84-12327

SYSTEMS ANALYSIS
Network design tool for EHF satellite communications networks
[AD-A131812] N84-12349
Center for electronics and electrical engineering technical progress bulletin covering signals and systems program, April 1982 - September 1982
[PB83-241158] N84-12405

SYSTEMS ENGINEERING
Control of multiaxis vibration systems N84-12203
Engineering services in support of the AFGL sounding rocket program
[AD-A131929] N84-12211
Center for electronics and electrical engineering technical progress bulletin covering signals and systems program, April 1982 - September 1982
[PB83-241158] N84-12405
Design and implementation of a preprocessing system for a sodium lidar
[NASA-CR-174593] N84-12462
Computational tool for the design of ultrasonic systems
[DE83-018092] N84-12824
Efficient radiation-hardened, 400- and 800-keV neutral-beam injection systems
[DE83-015691] N84-12886
Conceptual design of the high-flux VTA-2 test assembly for FMIT
[DE83-017022] N84-12935

SYSTEMS INTEGRATION
Integration of Fire Control, Flight Control and Propulsion Control Systems
[AGARD-CP-349] N84-12056
F-16 Penguin anti-ship missile integration N84-12059
Integration of fire control, navigation system and head up display N84-12060
The relations between the numerical control of the engine and other aircraft functions N84-12062

Integrated powerplant control systems and potential performance benefits N84-12063
Full authority digital electronic engine controls and their integration with flight control systems in VSTOL aircraft N84-12064
Design and development of the multifunction flight control reference system N84-12065
Some aspects of flight trajectory control in future avionic systems for combat aircraft N84-12066
A diagnosis scheme for sensors of a flight control system using analytic redundancy N84-12067
Effects of integrated maintenance on the definitions of onboard equipments --- Mirage 2000 aircraft N84-12068
An integrated AFCS for the "PROFILE"-mode N84-12069
The integration of flight and engine control for VSTOL aircraft N84-12070
A nonlinear control law for piloting aircraft in the air-to-ground attack phase N84-12071
Integrated Flywheel Technology, 1983 [NASA-CP-2290] N84-12228
Integrated Power/Attitude Control System (IPACS) N84-12229
The Boeing flywheel study N84-12235
Combined attitude control and energy storage N84-12237

SYSTEMS MANAGEMENT
Integrated powerplant control systems and potential performance benefits N84-12063

SYSTEMS SIMULATION
Simulation of electro-servo-hydraulic actuator for high quality testing --- of spacecraft N84-12206
The simulation of a Frequency Shift Keying (FSK) diversity system [DFVLR-FB-83-22] N84-12363
Nonlinear dynamics and control of a vibrating rectangular plate [NASA-CR-172215] N84-12528

T

T TAURI STARS
Theory of winds in late-type evolved and pre-main-sequence stars N84-13085

T-38 AIRCRAFT
Alternate T-38 transparency development. Part 4: Parametric studies [AD-A131904] N84-12159

TABLES (DATA)
Extent of hearing loss among Army aviators at Fort Rucker, Alabama [AD-A132069] N84-12714

TARGETS
Beam-target interaction of intense ion beams: Theory and experiment [DE83-018264] N84-12858
Ion stopping in heated targets [DE83-017800] N84-12941

TASKS
Vestibulo-ocular reflex gain in man during active versus passive oscillation and the influence of voluntary gaze-control tasks [AD-A132006] N84-12717

TAYLOR INSTABILITY
Boundary-integral simulations of rayleigh-taylor instability in ideal magnetohydrodynamics [AD-A131667] N84-12920
Instabilities in cylindrical plasma liners imploded by high magnetic fields [DE83-013640] N84-12921

TECHNOLOGY ASSESSMENT
Airport and air traffic control system [OTA-STI-175] N84-12143
Auxiliary power requirements: Their role in aircraft performance N84-12169
The OTS: Fifth year in orbit N84-12221
Some comments on longevity by a technologist N84-12247
Arizona State science, engineering and technology process [PB83-237107] N84-13016

TECHNOLOGY TRANSFER
Spinoff, 1983 [NASA-TM-85475] N84-13033

TECHNOLOGY UTILIZATION
Spinoff, 1983 [NASA-TM-85475] N84-13033

TEETH
Eruption of permanent dentition in rhesus monkeys exposed to ELF (Extremely low frequency) fields [AD-A132065] N84-12703

TELECOMMUNICATION
Trends in the development of teleinformatics [AD-A131067] N84-12338
Telecommunications (selected articles) [AD-A131872] N84-12346
Research in net management techniques for tactical data networks [AD-A131674] N84-12352
Alternative transmission media for third-generation interface standards [PB83-238345] N84-12365
International Telecommunication Standards: Issues and Implications for the '80's [PB83-241471] N84-12366

TELEMETRY
Y03: Prequalification of surface treatment. Measurement of laser reflecting power --- Earth-Moon telemetry [ESA-TT-791] N84-12490
Retroreflector YO3: Study of the optical properties of protected mirrors --- Earth-Moon telemetry [ESA-TT-789] N84-12907

TELEPHONY
Telecommunications (selected articles) [AD-A131872] N84-12346

TELLURIUM
The relative abundances of Sn, Te, Xe, Ba and Ce [NASA-CR-174599] N84-13064

TEMPERATURE CONTROL
Conceptual design of the high-flux VTA-2 test assembly for FMIT [DE83-017022] N84-12935
Method and apparatus for minimizing convection during crystal growth from solution [NASA-CASE-NPO-15811-1] N84-12968

TEMPERATURE DEPENDENCE
Transient temperature response of strain gages, revision 1 [DE83-017514] N84-12459

TEMPERATURE DISTRIBUTION
Microstructural origins of hot spots in RDX explosive and several reference inert materials [AD-A132056] N84-12325
Transient heat transfer in superfluid helium, part 2 [DE83-015767] N84-12984

TEMPERATURE EFFECTS
Degradation of shape memory effect [DE83-016586] N84-12295
New conformal solution theory [PB83-249441] N84-13008

TEMPERATURE MEASUREMENT
Process, product, and waste-stream monitoring with fiber optics [DE83-01102] N84-12899

TENSILE STRENGTH
Failure processes in elastomers at or near a rigid spherical inclusion [AD-A132060] N84-12314

TENSILE STRESS
Failure processes in elastomers at or near a rigid spherical inclusion [AD-A132060] N84-12314

TENSILE TESTS
Aircraft transparency testing methodology and evaluation criteria. Part 1: Test methods and information analysis [AD-A131927] N84-12158

TERMINOLOGY
Permuted medical subject headings, 1984 [PB83-234781] N84-13027
Medical subject headings, tree structures, 1984 [PB83-223164] N84-13028
Medical Subject Headings, Annotated Alphabetic List, 1984 [PB83-223156] N84-13029

TERNARY ALLOYS
Surface and interfacial properties of Ga(0.47) In(0.53) As alloys [AD-A131925] N84-12970

TERRAIN
Calculation of ground wave attenuation over irregular, inhomogeneous, layered media using PROGRAM WAGNER N84-12369
Inventoring and monitoring of landscape as a natural and cultural resource N84-12594
Measuring landscape information content and distribution on a SAR-580 image N84-12596

TERRAIN ANALYSIS
Observations and classifications with a 35/94 GHz radiometer of terrain near Motala, Sweden, July 1982 [FOA-C-30325-E1,E3] N84-12630

TEST FACILITIES
IPACS guidance navigation and control system considerations and test activities N84-12245
Low gravity experiment for studying a rotating fluid having a free surface [NASA-CR-170923] N84-12413
Conceptual design of the high-flux VTA-2 test assembly for FMIT [DE83-017022] N84-12935

TEST STANDS
The hydraulic multiaxes vibrator: Its capabilities to simulate real mechanical environments and to verify aerospace structures N84-12198
Practical experience during installation of the large multiaxes vibration test facility SAMSON N84-12199
The development of a multi-axis hydraulic vibration test facility at the National Engineering Laboratory, Scotland N84-12200
Concept of a safety system for a servohydraulic test facility N84-12202
Mathematical modeling and simulation of multiaxis hydraulic test facilities N84-12204
Simulation of mechanical cross coupling of multiaxes vibration facilities N84-12207

TEXAS
Poststorm reconnaissance of Tropical Storm Chris [AD-A131948] N84-12686

TEXTURES
The influence of sensor and flight parameters on texture in radar images N84-12575

THEMATIC MAPPING
Earth Resources Laboratory research and technology [E84-10033] N84-12576
Remote Sensing Applications for Environmental Studies --- conferences [ESA-SP-188] N84-12579
Use of remote sensing methods for the ecological mapping project of the European community N84-12580
SPOT potential applications: An overview of the results of the simulation campaigns N84-12587
Major water conservation and reclamation projects in the Jianghan Plain and surroundings, Hubei Province, China --- Landsat imagery N84-12593
Inventoring and monitoring of landscape as a natural and cultural resource N84-12594
SAR 580: Images for agricultural and forest survey. First results in middle Belgium N84-12595
Remote sensing and topographic maps --- belgium N84-12600
The use of airborne thematic mapper simulation data for the estimation and mapping of Green Leaf Area Index (GLAI) N84-12602
Application of remote sensing for studies, mapping and forecasting of eddies on the Norwegian continental shelf N84-12605
Mapping land use in Catalonia (Spain) --- using LANDSAT imagery N84-12613
Inventory of Flemish forests using medium-scale Color Infrared (CIR) photography and CIR orthophotoplans as base for a forest management data bank N84-12614
Actitities report on the projet DESBOD --- geographical data acquisition [REPT-5] N84-13025

THEOREMS
Kingman's subadditive ergodic theorem [AD-A131795] N84-12801

THEORETICAL PHYSICS
Research in theoretical physics [DE83-0166222] N84-13004

THERMAL CONTROL COATINGS
Development of strain tolerant thermal barrier coating systems, tasks 1 - 3 [NASA-CR-168251] N84-12312
Y03: Prequalification of surface treatment. Measurement of laser reflecting power --- Earth-Moon telemetry [ESA-TT-791] N84-12490
Retroreflector YO3: Study of the optical properties of protected mirrors --- Earth-Moon telemetry [ESA-TT-789] N84-12907

THERMAL DEGRADATION
Flightline thermal environment testing of F-111 transparencies [AD-A131642] N84-12163

THERMAL ENVIRONMENTS
Flightline thermal environment testing of F-111 transparencies [AD-A131642] N84-12163
Analytical prediction of aerothermal environment in a wing-elevon cove --- space shuttle orbiter [NASA-TM-85711] N84-12412

THERMAL MAPPING
Identifying environmental features for land management decisions [E84-10016] N84-12556
Two different aspects of phytoplankton bloom seen by satellite (CZCS) in the western English Channel --- coastal zone color scanner (CZCS) N84-12604
Remote sensing analysis of oil pollution in Augusta Bay, Sicily N84-12616
The synthesized climatic function map N84-12617

THERMAL PLASMAS
Preliminary data processing plan for the thermal plasma experiment on the HILAT satellite
[AD-A132017] N84-12209
THERMAL RESISTANCE
Thermal conductance measurements of pressed OFHC copper contacts at liquid helium temperatures
[NASA-TM-85861] N84-12809
THERMAL SHOCK
Thermal stress analysis of annular glass-to-metal seals under thermal shock N84-12408
THERMAL STABILITY
Evaluation of several high-strength copper sheet alloys
[DE83-015612] N84-12298
THERMAL STRESSES
Thermal stress analysis of annular glass-to-metal seals under thermal shock N84-12408
Analytical response of concrete structures subjected to high temperatures
[DE83-009625] N84-12538
Space nuclear safety program
[DE83-014070] N84-12869
THERMOCHEMISTRY
Thermolysis of 4-methyl-4-phenyl malonyl peroxide: A new oxygen dependent chemiluminescent reaction
[AD-A131863] N84-12268
Thermochemical energy systems research
[DE83-012132] N84-12644
THERMODYNAMIC PROPERTIES
Photothermal displacement spectroscopy of surfaces and thin films
[DE83-015957] N84-12279
Thermal performance of the MFTF magnets
[DE83-016275] N84-12988
Dense molecular thermodynamics
[DE83-015216] N84-13006
The far infrared sky survey experiment
[AD-A131966] N84-13037
THERMODYNAMICS
New conformal solution theory
[PB83-249441] N84-13008
THERMOLUMINESCENCE
Transmission of fast neutrons from the Li(d,xn) reaction through thick iron
[DE83-015975] N84-12884
THERMONUCLEAR REACTIONS
Hydrodynamic simulations of a combined hydrogen, helium thermonuclear runaway on a 10 km neutron star
[DE83-012658] N84-13047
THERMOSPHERE
Properties of the neutral density and composition in the thermosphere
[AD-A131557] N84-12665
OI 630.0 nm optical measurements of neutral winds, temperatures and airglow enhancements during the BIME program
[AD-A131695] N84-12671
THICK PLATES
Three-dimensional analysis of composite plates with material nonlinearity
[AD-A131884] N84-12258
THIN FILMS
Amorphous silicon-carbon films
[DE83-018077] N84-12259
Photothermal displacement spectroscopy of surfaces and thin films
[DE83-015957] N84-12279
Corrosion resistant coating
[NASA-NPO-15928-1] N84-12289
Thin film strain transducer --- in-flight monitoring of balloon film strain
[NASA-WLP-10055-2] N84-12448
Laser activated MTOS microwave device
[NASA-NPO-16112-1] N84-12463
Damage thresholds of thin film materials and high reflectors at 248 nm
[DE83-012663] N84-12472
Novel techniques for enhanced reflectivity infrared mirrors
[AD-A131924] N84-12894
Novel method for the study of optical properties of surfaces
[DE83-012899] N84-12895
Fabrication and properties of multilayer structures
[AD-A131934] N84-12969
The study of thin films on semi-insulating gallium arsenide by ellipsometry
[AD-A131844] N84-12972
Growth and characterization of InP and InGaAs films using the hydride VPE technique
[AD-A131841] N84-12973
A program of research on microfabrication techniques for VLSI magnetic devices
[AD-A131706] N84-12978
Phonon-induced enhancements of the energy gap and critical current in superconducting aluminum
[DE83-015210] N84-12996
THIN LAYER CHROMATOGRAPHY
Multi-detector gel permeation chromatography and its application to the analysis of industrial samples
[MQAD-808] N84-12283
THIN WALLS
A thin-walled beam finite element
[TT-8302] N84-12779
THREE BODY PROBLEM
Minimal unitary (covariant) scattering theory
[DE83-014896] N84-12849
Covariant theory with a confined quantum
[DE83-014897] N84-12850
THREE DIMENSIONAL BOUNDARY LAYER
Numerical solution of the two-phase, three dimensional boundary layer in laminar film condensation over a curved surface N84-12442
THREE DIMENSIONAL COMPOSITES
Multiplane finite element method: Applications to fiber reinforced material N84-12261
THREE DIMENSIONAL FLOW
An experimental investigation of separated three dimensional flow on general aviation twin-engine aircraft N84-12087
Aerodynamics of Vortical Type Flows in Three Dimensions
[AGARD-CP-342] N84-12099
On issues concerning flow separation and vortical flows in three dimensions N84-12100
The vortex skeleton model for three-dimensional steady flows N84-12101
Visualization of vortical type flows in three dimensions N84-12107
Viscous three-dimensional flow separations from high-wing propeller-turbine nacelle models N84-12115
Theoretical modelling of three-dimensional vortex flows in aerodynamics N84-12116
Flame acceleration mechanisms under conditions of partial confinement
[PB83-244012] N84-12328
The Performance of Antennas in Their Operational Environment
[AGARD-LS-131] N84-12367
Numerical solution of the three-dimensional unsteady Euler equations
[AD-A132034] N84-12783
Solar cycle evolution of the solar wind in three dimensions N84-13090
THRUST CONTROL
Journal of the Chinese Society of Astronautics (selected articles)
[AD-A131881] N84-12212
THUNDERSTORMS
A subsynoptic environment associated with two inter-mountain severe thunderstorm events
[DE83-014498] N84-12694
TIDES
Sediment transport in a tidal inlet
[PB83-242271] N84-12632
Adjustment in the oceans: The long-period tides and coastal upwelling N84-12702
TIMBER IDENTIFICATION
First results of the evaluations of the European SAR 580 data for agricultural and forestry purposes in test site D6, Freiburg (West Germany) N84-12599
TIMBER INVENTORY
Considerations on a permanent inventory and monitoring system for European forests N84-12582
Inventory of Flemish forests using medium-scale Color Infrared (CIR) photography and CIR orthophotoplans as base for a forest management data bank N84-12614
TIME DEPENDENCE
Numerical solutions of the Euler equations simulating vortex flows around wings N84-12120
Quasi-steady solar wind dynamics N84-13120
TIME DIVISION MULTIPLEXING
High dynamic global positioning system receiver
[NASA-CASE-NPO-16171-1-CU] N84-12151
TIME SERIES ANALYSIS
Why didn't Box-Jenkins win (again)?
[DE83-014043] N84-12802
TIN
The relative abundances of Sn, Te, Xe, Ba and Ce
[NASA-CR-174599] N84-13064
TIN TELLURIDES
Single Pb (1-x)Sn(x) Te crystal growth by vapor phase transport, with formation of a liquid/solid interface
[INPE-2811-PRE/369] N84-12967
TITANIUM
Measurements of ultrasonic scattering from near-surface flaws
[DE83-017693] N84-12827
TITANIUM ALLOYS
Spallation and 14-MeV neutron irradiation of stabilized NbTi superconductors
[DE83-017973] N84-12394
TOKAMAK DEVICES
Comparative evaluation of existing concepts for a 10-tesla FED toroidal field coil
[DE83-012817] N84-12815
Efficient radiation-hardened, 400- and 800-keV neutral-beam injection systems
[DE83-015691] N84-12886
A steady-state axisymmetric toroidal system
[IPPJ-643] N84-12910
Ripple-reduction poloidal-field coils for Tokamak reactors
[DE83-009532] N84-12922
Real-time diagnostic-data-acquisition system for the Doublet 3 Tokamak fusion experiment
[DE83-015871] N84-12927
Tokamak fusion reactors with less than full tritium breeding
[DE83-016711] N84-12936
Observations of soft X-ray fluctuations with an imaging array on TEXT
[DE83-018118] N84-12938
TFTR alpha extraction and measurement project
[DE83-018120] N84-12947
Nuclear design of a very-low-activation fusion reactor
[DE83-017470] N84-12949
Electron-cyclotron-heating experiments in Tokamaks and stellarators
[DE83-017210] N84-12958
TOLERANCES (PHYSIOLOGY)
Effects of pulsed microwaves at 1.28 and 5.62 GHz on Rhesus monkeys (Macaca mulatta) performing an exercise task at three levels of work
[AD-A132057] N84-12704
TOLUENE
Transport and relaxation processes in supercritical fluids
[DE83-015966] N84-12432
TOMOGRAPHY
Measurements, in vivo, of parameters of the dopamine system
[DE83-017964] N84-12709
TOPOGRAPHY
Relative elevation determination from LANDSAT imagery N84-12558
Inventoring and monitoring of landscape as a natural and cultural resource N84-12594
Measuring landscape information content and distribution on a SAR-580 image N84-12596
Remote sensing and topographic maps --- belgium N84-12600
Characterization by X-ray topography of laser-induced damage in potassium dihydrogen phosphate crystals
[DE83-012045] N84-12985
Actitities report on the projet DESBOD --- geographical data acquisition
[REPT-5] N84-13025
TOPOLOGY
Formation of standing shocks in stellar winds and related astrophysical flows N84-13088
TORNADOES
A numerical study on the evolution of tornadoes N84-12679
TOROIDAL PLASMAS
The 12-T solenoid-design options for the MFTF-B upgrade
[DE83-016646] N84-12817
A steady-state axisymmetric toroidal system
[IPPJ-643] N84-12910
A 2-D skin-current toroidal-MHD-equilibrium code
[DE83-016916] N84-12929
Recent results in the Los Alamos compact torus program
[DE83-014147] N84-12930
A model for stresses in circular magnets for toroidal fusion devices
[DE83-016535] N84-12937
TOROIDAL SHELLS
Design of the Advanced Toroidal Facility (ATF-1)
[DE83-012641] N84-12923
TOROIDS
A 2-D skin-current toroidal-MHD-equilibrium code
[DE83-016916] N84-12929
TORUSES
Load deflection characteristics of inflated structures
[NASA-CR-174585] N84-12028
TOXICITY
Development of a continuous monitor for detection of toxic organic compounds
[PB83-234922] N84-12461

TRACE ELEMENTS
Remote sensing instruments for trace species measurements in the troposphere and stratosphere: A review N84-12583
TRACING
A gas-flow tracing technique applicable to rotating systems boundary layer on a rotating disk [DE83-012761] N84-12425
TRACKING (POSITION)
Tracking theory for airborne surveillance radars [AD-A131792] N84-12350
Vestibulo-ocular reflex gain in man during active versus passive oscillation and the influence of voluntary gaze-control tasks [AD-A132006] N84-12717
Dynasty 2: A nonlinear implicit code for relativistic electron beam tracking studies [AD-A131592] N84-12829
TRADEOFFS
Control/display trade-off study for single-pilot instrument flight rule operations N84-12044
TRAILING EDGES
On the structure of the turbulent vortex N84-12102
Instabilities in trailing vortices: Flow visualization using hot-wire anemometry N84-12103
TRAINING DEVICES
Visual accommodation trainer-tester [NASA-CASE-ARC-11426-1] N84-12193
TRAJECTORIES
Some aspects of flight trajectory control in future avionic systems for combat aircraft N84-12066
TRAJECTORY MEASUREMENT
La Recherche Aerospatiale, Bimonthly Bulletin, no. 1983-1/212, January-February 1983 [ESA-TT-814] N84-12810
TRANSDUCERS
Thin film strain transducer --- in-flight monitoring of balloon film strain [NASA-WLP-10055-2] N84-12448
TRANSFER FUNCTIONS
The effect of coordinate system rotation on spherical harmonic expansions: A numerical method [AD-A131974] N84-12785
On sensitivity, compensation and the approach to the asymptotes in multivariable root-loci [RR-222] N84-12795
TRANSFORMATIONS (MATHEMATICS)
Image matching using generalized Hough transforms N84-12569
Kingman's subadditive ergodic theorem [AD-A131795] N84-12801
TRANSFORMERS
Megavolt pulse transformer powered by a fast plate generator [DE83-014189] N84-12384
TRANSIENT RESPONSE
Submerged shock response of a linearly elastic shell of revolution containing internal structure. User's manual for the ELSHOK code [AD-A131282] N84-12534
TRANSITION FLOW
Vortex breakdown: A two-stage transition N84-12124
TRANSITION PROBABILITIES
New results for transition probabilities in two-level systems: The large detuning regime [AD-A131783] N84-12835
TRANSITION TEMPERATURE
Strain rate effects on ductile/brittle transitions in steels [DE83-016906] N84-12308
TRANSMISSION LINES
Prototype fiber optic system to remote TRACALS radar [AD-A132073] N84-12341
Ultra low loss optical fiber cable assemblies, volume 2 [AD-A132008] N84-12891
Ultra low loss optical fiber cable assemblies, volume 1 [AD-A132007] N84-12892
TRANSMISSION LOSS
Ultra low loss optical fiber cable assemblies, volume 2 [AD-A132008] N84-12891
Ultra low loss optical fiber cable assemblies, volume 1 [AD-A132007] N84-12892
TRANSMITTERS
Interaction of antennas with masts under special consideration of the sensitivity and nonlinear effects in ship borne receiving systems N84-12371
Effects of nonlinear loads on antennas and scatterers N84-12376
TRANSONIC FLIGHT
Transonic configuration design N84-12081
Transonic configuration design (fighter) N84-12082
TRANSONIC FLOW
Special Course on Subsonic/Transonic Aerodynamic Interference for Aircraft [AGARD-R-712] N84-12072
Subsonic/Transonic Aerodynamic Interference for Aircraft: Introductory remarks N84-12073
Subsonic/transonic viscous interactions N84-12075
Transonic empirical configuration design process N84-12079
A theoretical and experimental investigation of a transonic projectile flow field [AD-A131938] N84-12094
Results of a new version of the LTRAN2-NLR (LTRANV) for unsteady viscous transonic flow computations [NLR-TR-81078-U] N84-12434
Second order partial differential equations of mixed type N84-12775
Multiple transonic solutions and a new class of shock transitions in solar and stellar winds N84-13083
TRANSPORT AIRCRAFT
Computational vortex flow aerodynamics N84-12117
Evaluation of a total energy-rate sensor on a transport airplane [NASA-TP-2212] N84-12164
Auxiliary power units for wide-body aircraft N84-12174
TRANSPORT THEORY
A revised two-equation model of turbulence [CFD/83/5] N84-12436
Transition flow ion transport via integral Boltzmann equation [UTIAS-269] N84-12828
Vectorized Monte Carlo photon transport [DE83-014807] N84-12843
Evolution of the ultra high energy cosmic ray spectron by transport equation [DE83-013711] N84-13132
TRANSPORTATION
PATRAM '83: 7th International Symposium on Packaging and Transportation of Radioactive Materials, summaries [DE83-012390] N84-12881
TRAPPING
Magnetic trapping of intense ion beams [DE83-017356] N84-12866
Hole trapping, recombination, and space charge in irradiated Sandia oxides [DE83-015212] N84-12986
TRAVELING WAVES
Waves on vortex cores and their relation to vortex breakdown N84-12128
TRITIUM
Tokamak fusion reactors with less than full tritium breeding [DE83-016711] N84-12936
TROMBE WALLS
Empirical validation of computer models for passive-solar residences [DE83-016887] N84-13005
TROPICAL STORMS
Poststorm reconnaissance of Tropical Storm Chris [AD-A131948] N84-12688
TROPOSPHERE
Remote sensing instruments for trace species measurements in the troposphere and stratosphere: A review N84-12583
Observations of the upper troposphere and lower stratosphere using the urbana coherent-scatter radar [NASA-CR-174594] N84-12664
TURBINE BLADES
Development of strain tolerant thermal barrier coating systems, tasks 1 - 3 [NASA-CR-168251] N84-12312
Vertical shaft windmill [NASA-CASE-LAR-12923-1] N84-12493
A graphics subsystem retrofit design for the bladed-disk data acquisition system [NASA-TM-83510] N84-12730
TURBINE ENGINES
A generalized computer code for developing dynamic gas turbine engine models (DIGTEM) [NASA-TM-83508] N84-12166
Progress on ultrasonic flaw sizing in turbine-engine rotor components: Bore and web geometries [DE83-018081] N84-12167
TURBOFAN ENGINES
Analytical design of a liquid hydrogen fueled turbofan-ramjet engine for flight Mach numbers zero to five N84-12187
TURBOJET ENGINES
A graphics subsystem retrofit design for the bladed-disk data acquisition system [NASA-TM-83510] N84-12730
TURBOMACHINE BLADES
Development of an ultrasonic testing procedure for electron beam welded parts for aerospace applications [BMFT-FB-W-72-011] N84-12515
TURBULENCE
Acoustic streaming as a mechanism of the Ranque-Hilsch effect N84-12088
Theoretical modelling of three-dimensional vortex flows in aerodynamics N84-12116
Executive summary, aerothermal modeling program, phase 1 [NASA-CR-174602] N84-12263
Solar cycle variations in the interplanetary magnetic field N84-13091
TURBULENT BOUNDARY LAYER
Transonic airfoil development N84-12076
A theoretical and experimental investigation of a transonic projectile flow field [AD-A131938] N84-12094
Erosive particle kinematics in the turbulent combustion boundary layer contacting a solid wall [DE83-010594] N84-12272
TURBULENT DIFFUSION
A study of coherent structures in the near-neutral marine atmospheric boundary layer N84-12658
TURBULENT FLOW
On the structure of the turbulent vortex N84-12102
Simulation of turbulent flows with a point vortex method N84-12119
Vortex stability and breakdown N84-12122
Experimentation with turbulent flows experiencing the effects of an adverse pressure gradient N84-12127
Waves on vortex cores and their relation to vortex breakdown N84-12128
Advanced diagnostics and instrumentation for chemically reactive flow systems [AD-A131814] N84-12251
Theoretical and experimental investigation of turbulent premixed flames N84-12409
Computation of turbulent flows over backward-facing step [NASA-TM-85851] N84-12414
Turbulence modelling: A state-of-the-art review [CFD/83/3] N84-12435
A revised two-equation model of turbulence [CFD/83/5] N84-12436
Turbulent tube-flow heat transfer coefficients in the presence of flow imbalance in the tubes of a parallel array N84-12437
Numerical calculations of turbulent recirculating heat transfer beyond two-dimensional back-steps and sudden pipe expansions N84-12439
The SSME seal test program: Leakage tests for helically-grooved seals [NASA-CR-170921] N84-12495
TURBULENT MIXING
Turbulence modelling: A state-of-the-art review [CFD/83/3] N84-12435
Random eddies in wakes and mixing layers --- wind tunnel tests N84-12813
TURBULENT WAKES
Acoustic streaming as a mechanism of the Ranque-Hilsch effect N84-12088
TWO DIMENSIONAL BOUNDARY LAYER
Improved Two-Dimensional Kinetics (TDK) computer program [NASA-CR-170922] N84-12248
TWO DIMENSIONAL FLOW
Improved Two-Dimensional Kinetics (TDK) computer program [NASA-CR-170922] N84-12248
Numerical calculations of turbulent recirculating heat transfer beyond two-dimensional back-steps and sudden pipe expansions N84-12439
Coronal transients in FE XIV 5303A: First two-dimensional photoelectric ground-based observations N84-13072

U

ULTRAHIGH FREQUENCIES
L band satellite communication experiment in the Antartic [ESA-TT-805] N84-12356
ULTRAHIGH VACUUM
Materials processing in space program tasks-supplement [NASA-TM-82548] N84-12196
ULTRASONIC FLAW DETECTION
Optimization of ultrasonic flaw detection in railroad rail [PB83-236919] N84-12518
Analytic diffraction corrections to ultrasonic scattering measurements [DE83-018080] N84-12825

Measurements of ultrasonic scattering from near-surface flaws
[DE83-017693] N84-12827

ULTRASONIC RADIATION
Progress on ultrasonic flaw sizing in turbine-engine rotor components: Bore and web geometries
[DE83-018081] N84-12167
Rising bubbles
[AD-A131572] N84-12418

ULTRASONIC TESTS
Elastic-wave inverse scattering in non-destructive evaluation
[DE83-017683] N84-12513
Development of an ultrasonic testing procedure for electron beam welded parts for aerospace applications
[BMFT-FB-W-72-011] N84-12515
An interactive computer program for analysis of ultrasonic modulus data on anistropic materials
[NPL-DMA(A)68] N84-12526

ULTRASONIC WAVE TRANSDUCERS
Computational tool for the design of ultrasonic systems
[DE83-018092] N84-12824
Helium-flow measurement using ultrasonic technique
[DE83-017765] N84-12826

ULTRAVIOLET LASERS
Laser physics and laser spectroscopy
[AD-A131720] N84-12470

ULTRAVIOLET RADIATION
Studies of collisional and nonlinear radiative processes for development of coherent UV and XUV sources
[AD-A131837] N84-12467
Ultraviolet extinction properties of grains in the interstellar medium N84-13131

UNDERWATER ACOUSTICS
Turn-around loss for oceanic sound on a bottom slope
[AUWE-TN-705/83] N84-12818
Short-range acoustic intensity vectors of the Pekeris shallow water model
[AMTE(N)-TM-83065] N84-12819
The effect of noisy reflection data on an inverse method for determining the structure of a layered ocean bottom
[AD-A131978] N84-12820
Transverse horizontal coherence and low-frequency array gain limits in the deep ocean
[AD-A131916] N84-12821

UNDERWATER RESOURCES
Analysis of the world distribution of metal-rich subsea manganese nodules
[USGS-CIRC-886] N84-12577

UNDERWATER STRUCTURES
Submerged shock response of a linearly elastic shell of revolution containing internal structure. User's manual for the ELSHOK code
[AD-A131282] N84-12534

UNIVERSE
Spherical simulations of large scale structure in the universe N84-13052

UNIVERSITIES
USAF/SCEEE summary faculty research program (1982) research reports, volume 2
[AD-A130770] N84-13009
Arizona State science, engineering and technology process
[PB83-237107] N84-13016
Source header list, supplement 1
[AD-A131800] N84-13024

UNSTEADY FLOW
Steady and unsteady flow models for airfoils with spoiler N84-12136
Calculation of unsteady flow in tubes of combustion engines with special regard to multiple branching
[REPT-82.8] N84-12410
Results of a new version of the LTRAN2-NLR (LTRANV) for unsteady viscous transonic flow computations
[NLR-TR-81078-U] N84-12434
Computation of three-dimensional unsteady flow in rigid and deformable curved tubes N84-12440
Numerical solution of the three-dimensional unsteady Euler equations
[AD-A132034] N84-12783

UPWELLING WATER
Adjustment in the oceans: The long-period tides and coastal upwelling N84-12702

URANIUM
Use of aircraft imagery in evaluating ground stability at open-pit uranium mines in Gas Hills, Wyoming
[DE83-903011] N84-12621
Alaska's mineral resources
[DE83-016599] N84-12623

URANIUM ALLOYS
Degradation of shape memory effect
[DE83-016586] N84-12295

URBAN PLANNING
SPOT potential applications: An overview of the results of the simulation campaigns N84-12587

USER MANUALS (COMPUTER PROGRAMS)
Calculation of ground wave attenuation over irregular, inhomogeneous, layered media using PROGRAM WAGNER N84-12369
Aeroelastic analysis for propellers - mathematical formulations and program user's manual
[NASA-CR-3729] N84-12530
Submerged shock response of a linearly elastic shell of revolution containing internal structure. User's manual for the ELSHOK code
[AD-A131282] N84-12534
A computer subroutine for evaluating polygamma functions for complex arguments
[AD-A131936] N84-12744
User's guide for SOL/NPSOL: A FORTRAN package for nonlinear programming
[DE83-016903] N84-12751
User's guide for SOL/QPSOL: A FORTRAN package for quadratic programming
[DE83-016990] N84-12752

USER REQUIREMENTS
Airport and air traffic control system. Executive summary N84-12144
The Boeing flywheel study N84-12235
Telecommunications (selected articles)
[AD-A131872] N84-12346
Computer system design environment software development plan
[AD-A131651] N84-12747

UTILITIES
Integrated powerplant control systems and potential performance benefits N84-12063

V

V/STOL AIRCRAFT
V/STOL (Vertical/Short Takeoff and Landing) low speed and transition equivalent systems analysis
[AD-A131955] N84-12156

VACUUM SYSTEMS
Vacuum measurements on the tandem mirror experiment upgrade (TMX-U) fusion experiment
[DE83-017836] N84-12946

VALENCE
Implications of heavy-ion-induced satellite X-ray emission. 1: Introduction
[DE83-015682] N84-12851

VALVES
Microprocessor-based control system for flowing-electrolyte zinc-bromine battery systems
[DE83-012506] N84-12403
Controlled combustion engine evaluation
[DE83-011245] N84-12499
Two types of values and their assessment by the collective interest
[DE83-012064] N84-13031

VANADIUM
Comparison of damage microstructures in neutron-irradiated vanadium and iron
[DE83-017189] N84-12304

VANES
Hot gas APU starter for advanced aircraft applications N84-12178

VAPOR DEPOSITION
Novel techniques for enhanced reflectivity infrared mirrors
[AD-A131924] N84-12894

VAPOR PHASES
Chemiluminescence and laser induced fluorescence of boron atom reactions
[AD-A131709] N84-12471
Electron-molecule interactions in gases and liquids: The electron-attachment process in gases and nonpolar liquids
[DE83-017205] N84-12863

VARIABLE THRUST
Journal of the Chinese Society of Astronautics (selected articles)
[AD-A131881] N84-12212

VARIATIONAL PRINCIPLES
Present trends in structural analysis at ONERA N84-12812

VARIATIONS
Observations of soft X-ray fluctuations with an imaging array on TEXT
[DE83-018118] N84-12938
Solar cycle variations of the solar wind N84-13089
Solar cycle variations in the interplanetary magnetic field N84-13091
Solar wind variations in the 60-100 year period range: A review N84-13092
Temporal variations of the anomalous oxygen component N84-13099
Voyager measurements of the energy spectrum, charge composition, and long term temporal variations of the anomalous components in 1977-1982 N84-13100

VECTORS (MATHEMATICS)
Dynamic analysis of the fluidyne
[DE83-017283] N84-12500
Vectorized Monte Carlo photon transport
[DE83-014807] N84-12843

VEGETATIVE INDEX
The use of airborne thematic mapper simulation data for the estimation and mapping of Green Leaf Area Index (GLAI) N84-12602

VELOCITY COUPLING
Combustion modeling of composite solid propellants N84-12285

VELOCITY DISTRIBUTION
The break-up mechanism of a streamwise directed vortex N84-12123
Transition flow ion transport via integral Boltzmann equation
[UTIAS-269] N84-12828
Dissipative instabilities of magnetic neutral layers with velocity shear
[IFSI-82-13] N84-12965

VELOCITY MEASUREMENT
Laser velocimeter measurements and analysis in turbulent flows with combustion, part 2
[AD-A131882] N84-12421
An interactive computer program for analysis of ultrasonic modulus data on anistropic materials
[NPL-DMA(A)68] N84-12526
Effects of microstructure and pore fluids on the acoustic properties of granular materials
[AD-A131983] N84-12668

VENTILATION
Effectiveness in reducing heat stress of three conditioned-air cooling vests worn with and without cooling air supplied to a face piece
[AD-A131975] N84-12726

VERTICAL ORIENTATION
Vertical shaft windmill
[NASA-CASE-LAR-12923-1] N84-12493

VERTICAL TAKEOFF AIRCRAFT
The integration of flight and engine control for VSTOL aircraft N84-12070

VERY HIGH FREQUENCIES
Physical modeling of EM propagation over nonhomgeneous terrain N84-12370

VERY LARGE SCALE INTEGRATION
A program of research on microfabrication techniques for VLSI magnetic devices
[AD-A131706] N84-12978

VERY LOW FREQUENCIES
Physical modeling of EM propagation over nonhomgeneous terrain N84-12370

VESTIBULAR TESTS
Vestibulo-ocular reflex gain in man during active versus passive oscillation and the influence of voluntary gaze-control tasks
[AD-A132006] N84-12717

VESTIBULES
An age comparison of the vestibulo-ocular counterroll reflex
[AD-A132064] N84-12716

VESTS
Effectiveness in reducing heat stress of three conditioned-air cooling vests worn with and without cooling air supplied to a face piece
[AD-A131975] N84-12726

VIBRATION
Development and flight test of an active flutter suppression system for the F-4F with stores. Part 3. Flight demonstration of the active flutter suppression system
[AD-A131972] N84-12191
Quality control and sample comparison by differential modal analysis
[MBB-BB-543-83-OE] N84-12514
International Conference on Vibrations at Surfaces (3rd)
[AD-A131794] N84-12834

VIBRATION METERS
Ride quality meter
[NASA-CASE-LAR-12882-1] N84-12445

VIBRATION SIMULATORS
The hydraulic multiaxes vibrator: Its capabilities to simulate real mechanical environments and to verify aerospace structures N84-12198
Practical experience during installation of the large multiaxes vibration test facility SAMSON N84-12199
The development of a multi-axis hydraulic vibration test facility at the National Engineering Laboratory, Scotland N84-12200
Hydraulic actuators and associated components suited for multiaxis vibration systems --- spacecraft testing N84-12201

Concept of a safety system for a servohydraulic test facility N84-12202
Control of multiaxis vibration systems N84-12203
Mathematical modeling and simulation of multiaxis hydraulic test facilities N84-12204
Simulation of mechanical cross coupling of multiaxes vibration facilities N84-12207

VIBRATION TESTS
Spacecraft Vibration Testing Using Multi-Axis Hydraulic Vibration Systems --- conferences [ESA-SP-197] N84-12197
Practical experience during installation of the large multiaxes vibration test facility SAMSON N84-12199
The development of a multi-axis hydraulic vibration test facility at the National Engineering Laboratory, Scotland N84-12200

VIDEO EQUIPMENT
High-speed videography combined with an x-ray image intensifier for dynamic radiography [DE83-017233] N84-12905

VIRGO GALACTIC CLUSTER
Spherical simulations of large scale structure in the universe N84-13052

VISCOELASTICITY
Crustal deformation, the earthquake cycle, and models of viscoelastic flow in the asthenosphere [NASA-TM-85117] N84-12662

VISCOSITY
Numerical simulations of fuel droplet flows using a Lagrangian triangular mesh [NASA-CR-168263] N84-12411
Dissipative instabilities of magnetic neutral layers with velocity shear [IFSI-82-13] N84-12965

VISCOUS FLOW
Subsonic/Transonic Aerodynamic Interference for Aircraft: Introductory remarks N84-12073
Subsonic/transonic viscous interactions N84-12075
Viscous three-dimensional flow separations from high-wing propeller-turbine nacelle models N84-12115
Rising bubbles [AD-A131572] N84-12418
Results of a new version of the LTRAN2-NLR (LTRANV) for unsteady viscous transonic flow computations [NLR-TR-81078-U] N84-12434

VISIBLE SPECTRUM
Advanced diagnostics and instrumentation for chemically reactive flow systems [AD-A131814] N84-12251

VISION
Figural aftereffects: An explanation in terms of multiple mechanisms in the human visual system [AD-A132066] N84-12715
Vestibulo-ocular reflex gain in man during active versus passive oscillation and the influence of voluntary gaze-control tasks [AD-A132006] N84-12717

VISUAL FIELDS
Visual accommodation trainer-tester [NASA-CASE-ARC-11426-1] N84-12193

VISUAL PERCEPTION
Pilot response with conventional displays N84-12040
Figural aftereffects: An explanation in terms of multiple mechanisms in the human visual system [AD-A132066] N84-12715
Experimental studies relating environmental lighting and flicker to visual fatigue in VDT operators [DE83-016316] N84-12738

VISUAL STIMULI
Figural aftereffects: An explanation in terms of multiple mechanisms in the human visual system [AD-A132066] N84-12715
Experimental studies relating environmental lighting and flicker to visual fatigue in VDT operators [DE83-016316] N84-12738

VOICE COMMUNICATION
Proposed study to determine potential flight applications and human factors design guidelines of voice recognition/synthesis systems N84-12047

VOICE CONTROL
A comparison of manual and vocal response modes for the control of aircraft subsystems [AD-A132048] N84-12152

VOID RATIO
The Dugdale model for the compact specimen [NASA-TM-85714] N84-12529

VOIDS
Detection of cavities under concrete pavement [AD-A131851] N84-12331
Inverse born approximation: Exact determination of shape of convex voids [DE83-017685] N84-12512
Measurements of ultrasonic scattering from near-surface flaws [DE83-017693] N84-12827

VOLATILITY
Conference on Planetary Volatiles [NASA-CR-174583] N84-13061

VON KARMAN EQUATION
A gas-flow tracing technique applicable to rotating systems boundary layer on a rotating disk [DE83-012761] N84-12425

VORTEX BREAKDOWN
Interaction between a shock-wave and a vortex flow N84-12104
Vortex stability and breakdown N84-12122
The break-up mechanism of a streamwise directed vortex N84-12123
Vortex breakdown: A two-stage transition N84-12124
A contribution to the problem of vortex breakdown N84-12125
Numerical simulation of vortex breakdown by the vortex-filament method N84-12126
Experimentation with turbulent flows experiencing the effects of an adverse pressure gradient N84-12127
Waves on vortex cores and their relation to vortex breakdown N84-12128

VORTEX FILAMENTS
Numerical simulation of vortex breakdown by the vortex-filament method N84-12126

VORTEX FLAPS
Instabilities in trailing vortices: Flow visualization using hot-wire anemometry N84-12103

VORTEX GENERATORS
On the generation and subsequent development of spiral vortex flow over a swept-back wing N84-12105
Vortex stability and breakdown N84-12122

VORTEX SHEDDING
Flame acceleration mechanisms under conditions of partial confinement [PB83-244012] N84-12328

VORTICES
Acoustic streaming as a mechanism of the Ranque-Hilsch effect N84-12088
Stability of a pair of stationary vortices in the leeward side of a cylinder in a potential flowfield [AD-A131917] N84-12095
Dynamic-stall regulation of the Darrieus turbine [DE83-017994] N84-12097
Aerodynamics of Vortical Type Flows in Three Dimensions [AGARD-CP-342] N84-12099
On issues concerning flow separation and vortical flows in three dimensions N84-12100
On the structure of the turbulent vortex N84-12102
Interaction between a shock-wave and a vortex flow N84-12104
On the generation and subsequent development of spiral vortex flow over a swept-back wing N84-12105
An experimental investigation of the vortex flow over delta and double-delta wings at low speed N84-12106
Visualization of vortical type flows in three dimensions N84-12107
Laser velocimetry study of compressibility effects on the flow field of a delta wing N84-12108
Recent studies at NASA-Langley of vortical flows interacting with neighboring surfaces N84-12109
Experimental investigation of forebody and wing leading-edge vortex interactions at high angles of attack N84-12110
Some results from a programme of research into the structure of vortex flow fields around missile shapes N84-12111
Predicting aerodynamic characteristics of vortical flows on three-dimensional configurations using a surface-singularity panel method N84-12112
Separation and vortical-type flow around a prolate spheroid: Evaluation of relevant parameters N84-12113
Theoretical modelling of three-dimensional vortex flows in aerodynamics N84-12116
Computational vortex flow aerodynamics N84-12117
Simulation of turbulent flows with a point vortex method N84-12119
Vortical flow management for improved configuration aerodynamics: Recent experiences N84-12129
Boundary layer segmentation on sharp highly swept leading edges and its effects on secondary vortices N84-12132
La Recherche Aerospatiale, Bimonthly Bulletin, no. 1983-1/212, January-February 1983 [ESA-TT-814] N84-12810
Random eddies in wakes and mixing layers --- wind tunnel tests N84-12813

VORTICITY
Computational vortex flow aerodynamics N84-12117

VOYAGER PROJECT
Jupiter Data Analysis Program: Analysis of Voyager wideband plasma wave observations [NASA-CR-174575] N84-13058

VOYAGER 1 SPACECRAFT
Temporal variations of the anomalous oxygen component N84-13099
Voyager measurements of the energy spectrum, charge composition, and long term temporal variations of the anomalous components in 1977-1982 N84-13100

VOYAGER 2 SPACECRAFT
Temporal variations of the anomalous oxygen component N84-13099
Voyager measurements of the energy spectrum, charge composition, and long term temporal variations of the anomalous components in 1977-1982 N84-13100

W

WAKES
Random eddies in wakes and mixing layers --- wind tunnel tests N84-12813

WALLS
Load deflection characteristics of inflated structures [NASA-CR-174585] N84-12028
Chemical erosion of first-wall materials by atomic hydrogen at high temperatures [DE83-017161] N84-12962

WASTE DISPOSAL
Advanced technologies for the recovery, disposal, and reuse of carbon dioxide for atmospheric control [DE83-016371] N84-12256
An operational remote sensing methodology for the detection, inventory and environmental monitoring of waste disposal sites N84-12601
Operational utilization of remote sensing in a study of the impact of disposal of urban waste at sea N84-12611
Preparation of a design study for the construction of a 2 million tons/annum commercial scale hydrogenation plant [BMFT-FB-T-83-135] N84-12652

WASTE TREATMENT
Research activities in materials and molecular research [DE83-015005] N84-12255

WASTE WATER
Method for treating wastewater using microorganisms and vascular aquatic plants [NASA-CASE-NSTL-10] N84-12654
Process, product, and waste-stream monitoring with fiber optics [DE83-01102] N84-12899

WATER
Geomorphic studies of Mars N84-13063

WATER COLOR
Two different aspects of phytoplankton bloom seen by satellite (CZCS) in the western English Channel --- coastal zone color scanner (CZCS) N84-12604
Normalization of water-leaving radiance obtained from the Coastal Zone Colour Scanner (CZCS) data N84-12610

WATER FLOW
Snowy Range Observatory: Climatological and streamflow data report 1982 [PB83-243147] N84-12633

WATER HEATING
Performance of add-on-type heat pump water heaters using two different test methods [PB83-222703] N84-12332

WATER LANDING
Water entry impact shock on flat faced cylindrical missiles [AD-A131937] N84-12419

WATER MANAGEMENT
Major water conservation and reclamation projects in the Jianghan Plain and surroundings, Hubei Province, China --- Landsat imagery N84-12593

WATER POLLUTION
Marine remote sensing activities of the Joint Research Center, Ispra, Italy N84-12586
Remote sensing applied to marine pollution control N84-12607
Velocity plots and capture zones of pumping centers for ground-water investigations [DE83-016618] N84-12624
To quench our thirst: The present and future status of freshwater resources of the United States, part 3 [DE83-016791] N84-12625

WATER QUALITY
Operational utilization of remote sensing in a study of the impact of disposal of urban waste at sea N84-12611

WATER RECLAMATION
Major water conservation and reclamation projects in the Jianghan Plain and surroundings, Hubei Province, China --- Landsat imagery N84-12593

WATER RESOURCES
LANDSAT 4 investigations of thematic mapper and multispectral scanner applications
[E84-10006] N84-12555
Velocity plots and capture zones of pumping centers for ground-water investigations
[DE83-016618] N84-12624
To quench our thirst: The present and future status of freshwater resources of the United States, part 3
[DE83-016791] N84-12625

WATER TREATMENT
Method for treating wastewater using microorganisms and vascular aquatic plants
[NASA-CASE-NSTL-10] N84-12654

WATER WAVES
The dependence of the radar modulation transfer function on environmental conditions and wave parameters
[AD-A131858] N84-12348
On the growth of gravity-capillary waves by wind
[KNMI-WR-83-10] N84-12698

WATERSHEDS
Snow cover and meteorology at Allagash, Maine, 1977 - 1980
[AD-A132013] N84-12684

WAVE ATTENUATION
Calculation of ground wave attenuation over irregular, inhomogeneous, layered media using PROGRAM WAGNER N84-12369
Real-time attenuation of heated optical fibers in a nuclear reactor
[DE83-015141] N84-12873
Atenuation measurements between 840 and 1620 nm on an optical cable in Berlin
[FI-465-TBR-22] N84-12906

WAVE DRAG
Improved wave drag predictions using modified linear theory
[NASA-CR-174494] N84-12096

WAVE EQUATIONS
Improved wave drag predictions using modified linear theory
[NASA-CR-174494] N84-12096
Numerical modeling techniques according to the wave equation and the ray method — in seismology
[BMFT-FB-T-83-136] N84-12354
Considerations of the three-wave interactions
[IPPJ-641] N84-12915

WAVE FUNCTIONS
The 100% alignment of hydrogen excited states in beam-foil spectroscopy
[DE83-017963] N84-12859
Progress in lattice gauge theory
[DE83-014055] N84-12862

WAVE INTERACTION
Considerations of the three-wave interactions
[IPPJ-641] N84-12915

WAVE PACKETS
A model for chorus associated electrostatic bursts
[NASA-CR-174489] N84-12832

WAVE PROPAGATION
Vortex stability and breakdown N84-12122
The Performance of Antennas in Their Operational Environment
[AGARD-LS-131] N84-12367
Scale modelling and full scale measurement techniques with particular reference to antennas in their operational environments N84-12368
Performance of antennas in plasma N84-12377
Use of the one-dimensional theory of the filament of flow for the interpretation and synthesis of mufflers in exhaust pipes of internal combustion engines
[REPT-81.4] N84-12494
Optimization of ultrasonic flaw detection in railroad rail
[PB83-236919] N84-12518
Radar meteorology in cloud physics and radio wave propagation research
[ESA-TT-808] N84-12695
On the growth of gravity-capillary waves by wind
[KNMI-WR-83-10] N84-12698
Double porosity model for acoustic wave propagation in fractured-porous rock
[DE83-017823] N84-12823
Analytic diffraction corrections to ultrasonic scattering measurements
[DE83-018060] N84-12825
Multiple spacecraft observations of interplanetary shocks: Characteristics of the upstream ULF turbulence N84-13097

WAVE REFLECTION
The effect of noisy reflection data on an inverse method for determining the structure of a layered ocean bottom
[AD-A131976] N84-12820

WAVEFORMS
The effects of channel tortuosity on electromagnetic radiations from lightning return strokes N84-12335

WAVEGUIDES
Guidance of electromagnetic waves in the ionosphere and magnetosphere
[IFSI-82-15] N84-12361

WEAPON SYSTEMS
Hypervelocity missile: Based on the concept of aircraft/missile integration for maximum firepower N84-12058
F-16 Penguin anti-ship missile integration N84-12059

WEATHER
Weather data communication and utilization N84-12045

WEATHER FORECASTING
A summary and integration of research concerning single pilot IFR operational problems N84-12034
Mesocyclone detection and classification algorithm
[AD-A131826] N84-12691
A subsynoptic environment associated with two inter-mountain severe thunderstorm events
[DE83-014498] N84-12694

WEBS (SHEETS)
Some considerations of the efficiency of sewn lap joints in a nylon webbing
[RAE-TR-83009] N84-12310

WEIGHT REDUCTION
Some trends in airship technology developments
[AGARD-R-717] N84-12050

WELLS
Velocity plots and capture zones of pumping centers for ground-water investigations
[DE83-016618] N84-12624

WEST GERMANY
First results of the evaluations of the European SAR 580 data for agricultural and forestry purposes in test site D6, Freiburg (West Germany) N84-12599
The synthesized climatic function map N84-12617
Heating with wind energy, part B
[BMFT-FB-T-83-131-PT-B] N84-12651

WETLANDS
Identifying environmental features for land management decisions
[E84-10016] N84-12556
Interpretability of wetland on SEASAT-A imagery in the polderland of Flanders: A structural approach N84-12597

WHISTLERS
Multiple spacecraft observations of interplanetary shocks: Characteristics of the upstream ULF turbulence N84-13097

WIENER FILTERING
Analysis of some filtering and data analysis methods for gravitational wave antennas with resonant transducers
[IFSI-82-11] N84-12359
SAR speckle noise reduction using Wiener filter N84-12568

WIGGLER MAGNETS
Evolution of long pulses in a tapered wiggler free-electron laser
[DE83-017235] N84-12484

WIND (METEOROLOGY)
On the wind stress - sea level power law
[AD-A132035] N84-12681
Snow cover and meteorology at Allagash, Maine, 1977 - 1980
[AD-A132013] N84-12684
Estimating long-term mean winds from short-term wind data
[DE83-017417] N84-12693
Adjustment in the oceans: The long-period tides and coastal upwelling N84-12702

WIND EFFECTS
On the growth of gravity-capillary waves by wind
[KNMI-WR-83-10] N84-12698

WIND MEASUREMENT
Construction of two wind turbines AEROMAN 11/11 for Indonesia
[BMFT-FB-T-83-143] N84-12505
Estimating long-term mean winds from short-term wind data
[DE83-017417] N84-12693

WIND PROFILES
Winds: Chapter 6, 1983 revision. Handbook of Geophysics and Space Environments
[AD-A132018] N84-12683

WIND SHEAR
Evaluation of a total energy-rate sensor on a transport airplane
[NASA-TP-2212] N84-12164

WIND TUNNEL APPARATUS
Engine/airframe interference drag at cruise conditions, using propulsion simulation
[NLR-TR-82012-U] N84-12098

WIND TUNNEL MODELS
Engine/airframe interference drag at cruise conditions, using propulsion simulation
[NLR-TR-82012-U] N84-12098

WIND TUNNEL TESTS
Subsonic/Transonic Aerodynamic Interference for Aircraft: Introductory remarks N84-12073
Engine/airframe interference drag at cruise conditions, using propulsion simulation
[NLR-TR-82012-U] N84-12098
An experimental investigation of the vortex flow over delta and double-delta wings at low speed N84-12106
Recent studies at NASA-Langley of vortical flows interacting with neighboring surfaces N84-12109
Application of the small body pressure transducer
[AD-A131733] N84-12454
Random eddies in wakes and mixing layers — wind tunnel tests N84-12813

WIND TUNNELS
Performance measurements of a pilot superconducting solenoid model core for a wind tunnel magnetic suspension and balance system
[NASA-CR-172243] N84-12192
Acta Mechanica Sinica (selected articles)
[AD-A131871] N84-12422

WIND TURBINES
Construction of two wind turbines AEROMAN 11/11 for Indonesia
[BMFT-FB-T-83-143] N84-12505
A comparison of finite-element predictions and experimental data for the forced response of the DOE 100 kW vertical-axis wind turbine
[DE83-012624] N84-12537
Heating with wind energy, part B
[BMFT-FB-T-83-131-PT-B] N84-12651

WIND VELOCITY
Wind-speed extremes in the Northern Hemisphere, 30 through 60 km
[AD-A132019] N84-12682
Optical extinction coefficients beneath marine stratus clouds. Comparison of coefficients calculated from observed aerosol spectra with coefficients specified by the Navy aerosol model
[AD-A132011] N84-12685
Solar cycle evolution of the solar wind in three dimensions N84-13090
Radial evolution of ion distribution functions N84-13094

WIND VELOCITY MEASUREMENT
Contributions of remote sensing satellite tracking techniques to marine environment monitoring and marine applications N84-12585

WINDING
Unipolar machine with superconductive excitation winding
[AD-A131820] N84-12383

WINDMILLS (WINDPOWERED MACHINES)
Vertical shaft windmill
[NASA-CASE-LAR-12923-1] N84-12493

WINDOWS (APERTURES)
Engineering hot-cell windows for radiation protection — for remote handling of radioactive materials
[DE83-014675] N84-12319

WINDPOWER UTILIZATION
Heating with wind energy, part B
[BMFT-FB-T-83-131-PT-B] N84-12651

WINDPOWERED GENERATORS
Construction of two wind turbines AEROMAN 11/11 for Indonesia
[BMFT-FB-T-83-143] N84-12505

WINDSHIELDS
Aircraft transparency testing methodology and evaluation criteria. Part 2: Methodology development for improved durability
[AD-A131928] N84-12157
Aircraft transparency testing methodology and evaluation criteria. Part 1: Test methods and information analysis
[AD-A131927] N84-12158
Alternate T-38 transparency development. Part 4: Parametric studies
[AD-A131904] N84-12159

WING NACELLE CONFIGURATIONS
The treatment of convected vortices in compressible potential flow N84-12121

WING ROOTS
Solar powered aircraft
[NASA-CASE-LAR-12615-1] N84-12154

WING TIP VORTICES
Helicopter rotor wake geometry and its influence in forward flight. Volume 1: Generalized wake geometry and wake effect on rotor airloads and performance
[NASA-CR-3726] N84-12090

WING TIPS
Predicting aerodynamic characteristics of vortical flows on three-dimensional configurations using a surface-singularity panel method N84-12112
The effects of wing tip devices on the performance of the BAe Jetstream N84-12130
The effect of wing tip devices on the far-field wake of a Paris Aircraft N84-12131
WINGS
Transonic configuration design N84-12081
Predicting aerodynamic characteristics of vortical flows on three-dimensional configurations using a surface-singularity panel method N84-12112
Analytical prediction of aerothermal environment in a wing-elevon cove --- space shuttle orbiter [NASA-TM-85711] N84-12412
WINTER
Field and laboratory studies of ice nucleation in winter orographic clouds N84-12678
WOLF-RAYET STARS
Stellar winds driven by multi-line scattering N84-13087
WORK
Biological clocks and shift work scheduling [GPO-21-747] N84-12713
WORKLOADS (PSYCHOPHYSIOLOGY)
Effect of pulsed 5.62 GHz microwaves on squirrel monkeys (Saimiri sciureus) performing a repeated acquisition task [AD-A132045] N84-12706
WORLD METEOROLOGICAL ORGANIZATION
Guide to agricultural meteorological practices, second edition [WMO-134] N84-12697
WYOMING
Use of aircraft imagery in evaluating ground stability at open-pit uranium mines in Gas Hills, Wyoming [DE83-903011] N84-12621
Snowy Range Observatory: Climatological and streamflow data report 1982 [PB83-243147] N84-12633
Geologic study of the Wind River Basin, Fremont and Natrona Counties, central Wyoming [PB83-254912] N84-12677

X

X RAY ANALYSIS
An X-ray radiography study of delamination growth in notched carbon/epoxy laminates [FFA-TN-1983-29] N84-12516
X RAY ASTRONOMY
High Resolution Imager (HRI) for the Roentgen Satellite (ROSAT) definition study [NASA-CR-174598] N84-12223
X RAY FLUORESCENCE
Uses of synchrotron radiation [DE83-014431] N84-12720
X RAY IMAGERY
Survey of flash X-ray techniques and applications [DE83-017234] N84-12904
High-speed videography combined with an x-ray image intensifier for dynamic radiography [DE83-017233] N84-12905
X RAY INSPECTION
An X-ray radiography study of delamination growth in notched carbon/epoxy laminates [FFA-TN-1983-29] N84-12516
Characterization by X-ray topography of laser-induced damage in potassium dihydrogen phosphate crystals [DE83-012045] N84-12985
X RAY LASERS
Experiments to study the feasibility of making an X-ray laser at the Novette laser facility [DE83-015615] N84-12476
X RAY SOURCES
Uses of synchrotron radiation [DE83-014431] N84-12720
X RAY SPECTRA
Implications of heavy-ion-induced satellite X-ray emission. 1: Introduction [DE83-015682] N84-12851
Observations of soft X-ray fluctuations with an imaging array on TEXT [DE83-018118] N84-12938
Implications of heavy-ion-induced satellite X-ray emission. Part 2: Production of K and L X-rays by 0.9 to 2.6 MeV/u Ar ions in thick targets of V, Cu, Nb, Ta, and Pt [DE83-015681] N84-12982
Methods for deconvoluting and interpreting complex gammaand X-ray spectral regions [DE83-013585] N84-12991
X RAY TELESCOPES
System definition Roentgensatellit, phase B 1.2 [BMFT-FB-W-83-010] N84-12219
X RAYS
Using an X-ray-sensitive vidicon and remote-control stage mechanism to obtain critical radiographic alignment of small explosive devices [DE83-012846] N84-12326
Using inner-shell X-rays as an ion-beam diagnostic [DE83-017784] N84-12857
Boundary layers in cataclysmic variables: The HEAO-1 X-ray constraints [NASA-TM-85112] N84-13046
XENON
The relative abundances of Sn, Te, Xe, Ba and Ce [NASA-CR-174599] N84-13064

Y

YIELD
Numerical simulation of plastic fluids [DE83-007911] N84-12424
YTTRIUM OXIDES
Y03: Prequalification of surface treatment. Measurement of laser reflecting power --- Earth-Moon telemetry [ESA-TT-791] N84-12490
Retroreflector YO3: Study of the optical properties of protected mirrors --- Earth-Moon telemetry [ESA-TT-789] N84-12907
Defect interactions at high concentrations in solid oxide electrolytes [DE83-016849] N84-12992

Z

ZEOLITES
New approach to the generation of metal-bearing, medium-pore, shape-selective zeolites for Fischer-Tropsch catalysis: Spectroscopic studies of zeolites [DE83-014344] N84-12254
Novel interactions of the charge-balancing cations with framework defects and trapped hydrogen atoms in holmium-exchanged Y zeolites [DE83-014204] N84-12839
ZINC-BROMIDE BATTERIES
Microprocessor-based control system for flowing-electrolyte zinc-bromine battery systems [DE83-012506] N84-12403
ZODIACAL DUST
Minor constituents in the solar wind originating from plasma-dust interactions N84-13116

PERSONAL AUTHOR INDEX

Typical Personal Author Index Listing

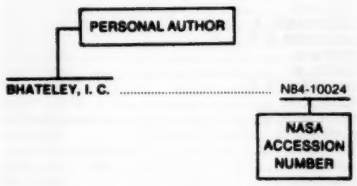

Listings in this index are arranged alphabetically by personal author. The NASA accession number denotes the number by which the citation is identified.

A

ABARCAR, R. N84-12649
ABBASCHIAN, G. J. N84-12288
ABBOTT, N. J. N84-12496
ABELES, F. N84-12351
ACKERMAN, J. P. N84-12396
ACUNA, M. H. N84-13044
ADAMS, B. B. N84-12821
ADAMS, J. J. N84-12040
N84-12043
ADAMS, L. M. N84-12777
ADAMS, O. B. N84-12923
ADAMS, P. H. N84-12459
ADEN, T. C. N84-12058
ADLASOR, M. N84-12328
AGAHI, M. N84-12775
AKASOFU, S. I. N84-13104
AL-SHEIKH, A. M. S. N84-12779
ALANSARI, A. R. A. J. N84-12442
ALBRIGHT, J. N. N84-12672
ALCORN, J. S. N84-12815
ALFANO, R. R. N84-12466
ALIYEVSKIY, B. L. N84-12381
ALLEN, S. L. N84-12955
ALLES, W. N84-12069
ALLISON, L. J. N84-12657
ALLSUP, J. R. N84-12656
ALSHITE, V. I. N84-12966
ALTROCK, R. C. N84-13072
ALVAREZ, R. A. N84-12887
AMATA, E. N84-12675
AMER, N. M. N84-12279
N84-12895
N84-12993
AN, C. Y. N84-12967
ANAND, V. R. N84-12135
ANDERSON, M. S. N84-12252
N84-12280
ANDERSON, N. P. N84-12312
ANDERSON, O. A. N84-12886
ANDERSON, R. J. N84-12945
ANDREWS, G. L. N84-12694
ANGELO, J. A. N84-12870
ANGELO, P. N84-13008
ANKENBRANDT, C. N84-12865
ANSELL, G. S. N84-12257
ANTROP, M. N84-12594
AOKI, T. N84-12916
APPLETON, B. S. N84-12719
ARBIOL, R. N84-12613
ARENZ, R. W. N84-12316
ARETZ, A. J. N84-12152
ARLOTTO, J. J. N84-13022
ARMSTRONG, R. W. N84-12325
ARMSTRONG, W. T. N84-12930
ARVIZU, D. E. N84-12428
ASBRIDGE, J. R. N84-13098
N84-13123
ASHBY, C. I. H. N84-12962
ASHTON, G. D. N84-12618
ASIALA, C. F. N84-13011
ATLAN, P. N84-12176
AUBLE, R. L. N84-12982
AUBREY, D. G. N84-12632
AYERS, W. B., JR. N84-12620
AZZAZY, M. T. F. N84-12409

B

BABCOCK, W. C. N84-12284
BABU, G. N. N84-12315
BACCHIALONI, F. L. N84-12218
BACHOR, E. N84-12219
BAGANOFF, D. N84-12251
BAGRASH, F. M. N84-12715
BAHIMAN, H. N84-12492
BAIL, I. N84-12263
BAILEY, I. L. N84-12738
BAK, P. N84-12545
N84-12967
BAKER, G. R. N84-12920
BALAS, E. N84-12784
BALASUBRAMANIAN, R. N84-12781
BALDWIN, D. E. N84-12948
N84-12954
BALL, I. N84-12264
N84-12265
BALMAIN, K. G. N84-12377
BALSIGER, H. N84-12676
N84-13049
BALTAY, C. N84-12865
BAME, S. J. N84-13097
N84-13098
N84-13110
N84-13113
N84-13123
N84-13126
BANDEIRA, I. N. N84-12967
BANKS, P. N. N84-13026
BARBEE, T. W., JR. N84-12897
N84-12969
BARCHET, W. R. N84-12693
BARFIELD, J. N. N84-12670
BARISANO, E. N84-12595
BARKER, R. N84-13019
BARLING, G. M. N84-12060
BARNES, A. N84-13107
BARNES, C. W. N84-12930
BARNES, D. C. N84-12930
BARNES, J. N84-12739
BARNES, J. M. N84-12956
BARNES, J. W. N84-12620
BARNES, R. G. N84-12864
BARON, A. N84-12132
BARR, A. N84-12770
BARRETT, M. N84-12220
BARSS, R. P. N84-12284
BARTHEL, J. R. N84-12837
BARTHOLOME, E. N84-12595
BARTL, A. N84-12854
BARTON, J. M. N84-12783
BARTSCH, N. N84-12224
BARTSCH, R. R. N84-12930
BASU, R. N84-12559
BATCHELOR, D. B. N84-12875
N84-12952
N84-12959
BATEMAN, G. N84-12922
BATES, J. L. N84-12926
BATES, R. E. N84-12684
BAUDRY, T. V. N84-12755
BAUER, C. L. N84-12978
BAUER, M. A. N84-12620
BAUMGARTEN, J. R. N84-12028
BAUN, W. L. N84-12972
BAVASSANO, B. N84-13050
N84-13076
BAXTER, D. J. N84-12297
N84-12299
BEAL, R. B. N84-12254
BECKER, K. E. N84-12341
BECKMAN, B. C. N84-13053
BEDER, E. C. N84-12183
BEEUWKES, R., JR. N84-12535
BEEZHOLD, W. N84-12666
BEHL, Y. K. N84-12336
BELCASTRO, C. M. N84-12164
BELLOWS, R. J. N84-12403
BELROSE, J. S. N84-12368
BEMESDERFER, J. N84-12468
N84-12469
BENAQE, J. F., JR. N84-12680
BENEDICK, W. B. N84-12278
BENJAMIN, R. F. N84-12391
BENTLEY, J. N84-12305
BERENSTEIN, C. A. N84-12570
BERGER, M. H. N84-12426
BERGERON, H. P. N84-12029
N84-12033
N84-12035
N84-12047
BERMAN, P. R. N84-12835
BERMAN, S. M. N84-12738
BERNARD, R. N84-12588
BERNERT, J. N84-12652
BERRY, H. G. N84-12859
BERRY, R. N84-12263
N84-12264
N84-12265
BERTHEL, R. O. N84-12687
BERTONI, E. A. N84-12682
BERTOTTI, B. N84-12358
N84-12362
BEST, F. R. N84-12456
BEY, K. S. N84-12412
BEYER, R. A. N84-12267
BIELAWA, R. L. N84-12530
BIENIEK, M. P. N84-12533
BILDERBACK, D. H. N84-12897
BIONDI, M. A. N84-12671
BIRD, G. R. N84-12645
BIRX, D. L. N84-12841
BIWER, R. N84-12389
BIWER, T. L. N84-12395
BJORKEN, J. D. N84-12855
BLASZYK, J. N84-12346
BLEY, J. A., JR. N84-12703
BLINK, J. A. N84-12253
BLITZ, A. L. N84-12350
BLOM, A. F. N84-12260
N84-12516
BLOOM, L. R. N84-12365
BOBROWICZ, F. W. N84-12643
BOCCARA, A. C. N84-12279
BOCHSLER, P. N84-13065
N84-13111
N84-13114
BODANSKY, D. N84-13038
BODECHTEL, J. N84-12580
N84-12589
BOESSMANN, D. N84-13021
BOESSWETTER, C. N84-12224
BOLAND, A. J. N84-12340
BOLSTAD, J. O. N84-12873
BONAVENTURA, G. N84-12908
BOORSTYN, R. N84-12352
BOOY, A. N84-12173
BOPP, W. B. N84-12753
BORENSZTEIN, Y. N84-12351
BOSLOUGH, M. N84-12816
BOSSI, R. H. N84-12326
BOUGERET, J. L. N84-13103
BOUSMAN, W. G. N84-12162
BOWEN, R. W. N84-12577
BOWERS, J. N84-12747
BOWHILL, S. A. N84-12664
BOWMAN, C. T. N84-12251
BOYD, R. D. N84-12457
BOYER, R. S. N84-12745
BOZOKI, E. S. N84-12399
N84-12754
BRADBURY, J. N. N84-12488
BRADLEY, A. N84-12738
BRADY, F. P. N84-12884
BRANDON, L. N84-12238
BRANDT, A. N84-12746

BRANDT, H. E. N84-12919
BRANDT, J. C. N84-13126
BRATOS, M. N84-12407
BRAU, C. A. N84-12485
BRAY, D. E. N84-12516
BRECKON, T. N84-12749
BRENNER, P. N84-12793
BRESNAHAN, P. A. N84-12284
BREWER, J. M. N84-13013
BRIESMEISTER, R. A. N84-12480
BRIGGS, J. N84-12739
BRITCHER, C. P. N84-12192
BRODERSEN, E. N84-12059
BRONISZ, S. E. N84-12869
BROOKS, A. L. N84-12656
BROOKS, J. N. N84-12306
BROUGH, A. W. J. N84-12283
BROWN, B. S. N84-12394
BROWN, G. J. N84-12349
BROWN, L. J., JR. N84-12138
BROWN, N. J. N84-12900
BRYANT, L. E., JR. N84-12904
N84-12905
BRYANT, W. H. N84-12036
N84-12039
BSCHORR, O. N84-12514
BUCHANAN, H. J. N84-12245
BUCK, O. N84-12307
N84-12547
BUCKHAM, R. C. N84-12673
BUCKINGHAM, A. C. N84-12272
BUCKLEY, D. H. N84-12287
BUDEN, D. N84-12870
BULLOCK, K. N84-12404
BULMASH, G. N84-12194
BUNTING, J. T. N84-12686
BURCHETT, S. N. N84-12400
BURKE, G. J. N84-12374
BURKE, W. R. N84-12197
BURLAGA, L. F. N84-12663
N84-13045
BURNS, E. J. T. N84-12857
N84-12942
N84-12943
BURNS, F. B. N84-12318
BURRELL, J. P. N84-13024
BURTON, R. L. N84-12227
BUTTRAM, M. N84-12385
BYER, R. L. N84-12251
N84-12470
BYRAM, T. R. N84-12111

C

CAIRD, R. S. N84-12384
CALDERON, M. O. N84-12946
CALLAS, G. P. N84-12049
CALLISON, R. D. N84-12603
CALMELS, P. N84-12170
CALTABIANO, T. N84-12616
CAMAGNI, S. N84-12586
CAMARASA, J. M. N84-12613
CAMPBELL, D. K. N84-12853
CAMPBELL, E. M. N84-12486
CAMPBELL, J. F. N84-12109
CAMPBELL, N. A. N84-12603
CANDIDI, M. N84-12675
N84-12676
N84-13049
CANE, H. V. N84-13122
CANFIELD, D. N84-12329
CANNON, C. Y. N84-12767
CANTWELL, B. J. N84-12251
CAPPELLINI, V. N84-12590
CARLONE, C. N84-12259
CARLSSON, L. N84-12516
CARLSTEDT, L. N84-12724
CARNES, B. A. ..... N8 :-12805
CARNEY, R. R. N84-12730
CARNIGLIA, C. K. N84-12472
CARPENTER, C. G. N84-12156
CARR, D. B. N84-12804
CARRUTHERS, P. N84-12845
CARTER, L. L. N84-12884
CARTER, R. J. N84-13020
CARTON, J. A. N84-12702
CASKEY, G. R., JR. N84-12301
N84-12309
CASPER, T. A. N84-12955
CASSINELLI, J. P. N84-13066
CASTAGNOLI, F. N84-12590
CASTANEDA, C. M. N84-12884
CASTELLANI, A. N84-12050
CEGLIO, N. N84-12933
CENIVAL, M. N84-12174
CERNI, D. M. N84-12366
CHAMBERLIN, E. P. N84-12880
CHAMBERS, M. J. N84-12767
CHAN, Y. L. N84-12441
CHANG, J. N84-12943
CHANG, L. M. N84-12420
CHANG, L. S. N84-12403
CHANG, T. N84-12917
CHANNELL, P. J. N84-12882
N84-12888
CHAPMAN, G. C. N84-12034
CHEN, D. Y. N84-12188
CHEN, N. C. J. N84-12501
CHEN, S. H. N84-12456
CHEN, W. Y. N84-12815
CHEN, Y. N84-12981
CHEN, Y. P. N84-13008
CHENETTE, D. L. N84-13056
CHENG, E. T. N84-12949
CHENG, J. P. N84-12506
CHENG, L. J. N84-12477
CHENG, W. S. N84-12440
CHENGTIAN, L. N84-12971
CHERVENAK, J. G. N84-12339
CHI, R. M. N84-12530
CHIDLAW, M. B. N84-12284
CHIEN, J. C. W. N84-12315
CHILDS, D. W. N84-12495
CHIN-HO, L. N84-12519
CHOW, L. S. H. N84-12931
CHRIEN, R. E. N84-12930
CHRISTENSEN, D. G. N84-12046
CHRISTIANSEN, P. N84-13002
CHRISTIANSON, C. C. N84-12395
N84-12642
CHRISTIE, W. H. N84-12477
CHRISTOPHOROU, L. G. N84-12430
N84-12863
CHU, J. Q. N84-12088
CLARK, C. F. N84-12316
CLARK, G. L. N84-12431
CLARK, L. G. N84-12455
CLAUSER, J. F. N84-12955
CLAYTON, K. I. N84-12157
N84-12158
CLEVENSON, S. A. N84-12445
CLINE, T. L. N84-13039
CLOWER, C. A. N84-12955
COCHRAN, A. L. N84-13055
COCHRANE, J. C. N84-12930
CODY, W. J. N84-13011
COENSGEN, F. H. N84-12955
COFFEY, C. S. N84-12325
COHEN, H. A. N84-12831
COHEN, S. C. N84-12662
COLE, A. E. N84-12683
COLEMAN, H. P. N84-12345
COLES, W. A. N84-13090
COLGATE, S. A. N84-13133
COLLINS, D. R. N84-12873
COOK, C. E. N84-12443
COOK, E. N84-12841
COOK, G. M. N84-12387
COONROD, J. N84-12929
COOPER, B. M. N84-12327
COOPER, R. K. N84-12882
COOPER, W. S. N84-12886
COPLAN, M. A. N84-13065
N84-13111
COPPA, A. P. N84-12497
COPPI, B. N84-12917
COPPIN, P. R. N84-12614
CORDTS, R. E. N84-12707
CORNISH, D. N. N84-12397
CORNWELL, L. R. N84-12518
CORONES, J. P. N84-12353
CORP, D. N84-12642
CORRELL, D. L. N84-12955
CORY, J. N84-12205
COSTON, V. A. N84-12510
COTTATELLUCCI, G. N84-12908
COULTER, G. A. N84-12194
COURTNEY, J. C. N84-12319
COUTOIS, M. N84-12068
COUTURIER, P. N84-13096
COWING, T. N84-12650
COX, E. N84-12211
COX, F. W. N84-12656
COYLE, J. M. N84-12727
CRACKNELL, A. P. N84-12603
CRAIN, W. K. N84-12215
CRAMER, J. G. N84-12846
CRANDALL, D. H. N84-12867
CREEDON, J. F. N84-12164
CREMA, L. B. N84-12050
CREUTZ, M. N84-12862
CROOKER, N. U. N84-13089
CROW, J. T. N84-12942
N84-12943
N84-12945
CUMMINGS, A. C. N84-13099
N84-13100
CUMMINS, W. F. N84-12955
CUO, F. N84-12584
CURRAN, P. N84-12602
CZANDERNA, A. W. N84-12641
CZINK, F. N84-12651

D

DABROWSKI, A. N84-12898
DADDAZIO, R. P. N84-12533
DAFNI, E. N84-12989
DAINO, B. N84-12908
DALDER, E. N. C. N84-12298
DALE, J. M. N84-12887
DAMASHEK, M. N84-13040
DAMM, C. C. N84-12955
DANBERG, J. E. N84-12094
DANG, L. D. N84-12248
DANIELE, C. J. N84-12166
DARCIE, T. E. N84-12828
DAT, R. N84-12811
DAVE, S. M. N84-12499
DAVID, T. D. N84-12703
DAVIDOVITS, P. N84-12471
DAVIS, G. A. N84-12974
DAVIS, L. S. N84-12569
DAVIS, R. N84-12772
DAVIS, S. F. N84-12727
DAVIS, W. E. N84-12693
DAVISON, M. E. N84-12353
DEA, J. Y. N84-12406
DEAL, P. L. N84-12190
DEANGELIS, R. J. N84-12305
DEARS, W. N84-12195
DEBARBIERI, O. N84-12776
DEGROOF, H. N84-12596
DEGROOT, A. J. N84-12750
DEJESUS, O. T. N84-12709
DELANEY, J. R. N84-12350
DELERY, J. N84-12104
DELORGE, J. N84-12704
N84-12705
N84-12706
DELUCA, W. H. N84-12389
N84-12395
DEMARCHIS, G. N84-12908
DEMASTUS, H. L. N84-13072
DEMPSEY, T. K. N84-12445
DENARD, J. C. N84-12840
DENEMARK, D. L. N84-12051
N84-12052
N84-12053
DENERY, D. G. N84-12049
DENK, S. V. N84-12419
DENNIS, D. R. N84-12089
DENSKAT, K. U. N84-13074
DENTREMONT, R. P. N84-12686
DEPONTE, S. N84-12132
DERE, K. P. N84-13070
DEROOVER, B. N84-12614
DESCLAUX, J. P. N84-12872
DESHPANDE, N. N84-12871
DEWILDE, M. A. N84-12267
DEWISPELAERE, W. M. N84-12614
DEWOLF, W. B. N84-12098
DIAMOND, C. N84-12716
DIBBLE, W. N84-12969
DIEBOLD, R. N84-12865
DIEGLE, R. B. N84-12322
DIMAGGIO, F. D. N84-12533
DIMSDALE, J. S. N84-12330
DINERSTEIN, R. N84-12709
DINGUIRARD, M. N84-12490
N84-12629
N84-12907
DOBROTT, D. N84-12953
DOBROWOLNY, M. N84-12358
N84-12361
N84-12965
DODDS, S. A. N84-12979
DOHERTY, T. J. N84-12643
DOHREN, H. N84-12652
DOMACK, C. S. N84-12092
DONALDSON, R. J., JR. N84-12691
DONALDSON, R. R. N84-12900
DONATH, R. C. N84-12509
DOORNBOS, G. N84-12098
DOUKAS, A. G. N84-12466
DOW, D. D. N84-12572

DOWLING, T. N84-12739
DOWNEY, S. W. N84-12483
DOWNING, D. J. N84-12802
DOWNING, D. R. N84-12038
DREIKE, P. L. N84-12941
N84-12942
N84-12943
DRESNER, L. N84-12984
N84-12990
N84-12995
DRUCE, R. L. N84-12468
N84-12489
DSILVA, A. P. N84-12282
DUCHENNE, B. N84-12490
DUCHOSSOIS, G. N84-12585
DUECHS, D. N84-12776
DUES, J. N. N84-12161
DUFF, R. E. N84-12837
DUFFY, J. M. N84-12750
DUFFY, J. W. N84-12046
DUFOURMONT, H. N84-12597
DUM, C. T. N84-13095
DUMANISMODAN, A. N84-12551
DUNDORE, D. M. N84-12821
DUPOUY, C. N84-12604
DUPREE, A. K. N84-13084
DUPUY, J. D. N84-12615
DWYER, J. F. N84-12093
DYER, P. N84-13038
DYMOND, L. H. N84-12051
N84-12052
N84-12053

E

EBIHARA, B. T. N84-12447
ECCLES, E. S. N84-12064
ECKERT, E. W. N84-12169
ECKHARDT, K. N84-12198
EDINGER, L. N84-12065
EDWARDS, R. A. N84-12063
EGGER, H. N84-12467
EGGER, T. J. N84-12757
EGLEM, M. N84-12174
EGOLF, T. A. N84-12090
N84-12091
EICHMANN, G. N84-12344
EICHTEN, E. N84-12865
EIDENT, C. J. N84-13021
EINSTEIN, T. H. N84-12343
EL-SAYED, M. A. N84-12487
ELAM, F. M. N84-12236
ELBAN, W. L. N84-12325
ELLINGHAUS, A. R. N84-12652
ELNADI, A. M. N84-12961
ELSPASS, C. E. N84-12403
ENGEL, H. N84-12211
ENGLAND, A. C. N84-12958
ERAUD, M. Y. N84-12715
ERICKSON, D. J. N84-12384
ERICKSON, G. E. N84-12110
ERICKSON, P. A. N84-12753
ERIKSEN, T. N84-12275
ERIKSSON, L. E. N84-12120
ERINGEN, A. C. N84-12536
N84-12786
ERLANDSON, R. E. N84-12496
ESCUDIER, M. P. N84-12124
ETHRIDGE, E. C. N84-12288
ETKIN, A. N84-12898
EVANGELOU, P. N84-12114
EVANS, K., JR. N84-12936
EYCHNER, D. M. N84-12805
EZELL, C. N84-12705
EZZAT, H. A. N84-12553

F

FAHR, H. J. N84-13108
FAILOR, B. H. N84-12955
FAINBERG, J. N84-13103
FAIRBAIRN, J. N84-12200
FANG, T. M. N84-12960
FARNSWORTH, A. V., JR. N84-12858
FARRELL, K. N84-12304
FARRELL, R. N84-13019
FARRELLY, B. A. N84-12605
FASSEL, V. A. N84-12282
FEE, D. C. N84-12396
FEINBERG, B. N84-12929
FELDMAN, H. A. N84-12708
FELDMAN, W. C. N84-13098
N84-13123
FELL, M. J. N84-12130
FENCL, V. N84-12708
FERGUSON, K. R. N84-12319
FESSENDEN, T. J. N84-12848
FEYNMAN, J. N84-13092
FIDLER, J. N84-12291
FIEDLER, C. J. N84-12547
FINK, J. A. N84-12886
FINK, J. H. N84-12473
FIRESTONE, R. F. N84-12856
FISHER, K. J. N84-12843
FISHMAN, G. S. N84-12800
FITZPATRICK, G. L. N84-12340
FLAHERTY, J. E. N84-12727
FLOR, T. H. N84-12688
FOLEY, K. J. N84-12896
FONSECA, G. F. N84-12726
FONTANA, J. J. N84-12541
FORD, F. E. N84-12246
FORD, H. N84-12714
FORMISANO, V. N84-13049
FORTE, V. A., JR. N84-12708
FORWARD, R. L. N84-12249
FOURNIER, D. N84-12279
FOUSER, J. P. N84-12640
FOWLER, C. M. N84-12384
FRAEDRICH, W. M. N84-12057
FRANCKO, D. A. N84-12625
FRANKENBACH, K. N84-12219
FRANKLIN, J. N84-12700
FRANTZ, B. N84-12488
N84-12489
FRASER, J. S. N84-12474
N84-12481
N84-12485
FRAYSSE, G. N84-12581
FREDRICKSON, D. N84-12642
FREEDMAN, A. N84-12830
FREEMAN, A. J. N84-12872
FREEMAN, B. L. N84-12384
FREESE, J. M. N84-12901
FRENKLACH, M. N84-12271
FRESE, K. W., JR. N84-12329
FRIEDMAN, A. M. N84-12709
FRIEND, D. B. N84-13087
FRITTS, M. J. N84-12411
FRONCZEK, C. J. N84-12631
FRORIEP, R. N84-12756
FROST, V. S. N84-12575
FUERSTENAU, N. N84-12449
FYFE, D. E. N84-12411

G

GABEL, R. A. N84-12708
GABLER, L. N84-13001
GALBRAITH, L. D. N84-12178
GALLIDEPARATESI, S. N84-12586
GALVIN, A. B. N84-13112
GANGWANI, S. T. N84-12530
GARBINCIUS, P. H. N84-12999
GARDNER, M. E. N84-12665
GARN, W. B. N84-12384
GARTLING, D. K. N84-12424
GAY, E. N84-12642
GAZIS, P. R. N84-13106
GEBHARDT, P. N84-13002
GEHRELS, N. N84-13039
GEISS, J. N84-13065
N84-13111
GELLES, D. S. N84-12300
GENT, A. N. N84-12314
GEORGE, R. E. N84-12454
GERACI, A. L. N84-12616
GERDIN, G. A. N84-12947
GERWIN, R. N84-13015
GHIELMETTI, A. N84-12676
N84-13049
GHIGLIA, D. C. N84-12457
GIBBONS, L. C. N84-12687
GILBERT, R. O. N84-12803
GILBERT, W. P. N84-12110
GILDEN, D. L. N84-13043
GILL, P. E. N84-12751
N84-12752
GILLIGAN, J. G. N84-12936
GILLOT, R. N84-12586
GINEVAN, M. E. N84-12805
GIOVANETTI, A. J. N84-12225
GIST, G. A. N84-12979
GIUDICI, B. N84-12232
GLANTSCHNIG, W. J. N84-12456
GLAZER, A. N84-12773
GLIATTI, E. L. N84-12455
GLOECKLER, G. N84-13112
N84-13117
GLUCKSTERN, R. L. N84-12882
GOERG, K. A. N84-12410
GOFORTH, J. H. N84-12384
GOLAY, M. W. N84-12456
GOLDBERG, D. A. N84-12886
GOLDFINGER, R. C. N84-12875
N84-12952
N84-12959
GOLDSACK, S. N84-12739
GOLDSTEIN, B. E. N84-13101
GOLDSTEIN, H. N84-13125
GOLDSTEIN, J. C. N84-12484
GOLDSTEIN, J. D. N84-12785
GOLDSTEIN, M. L. N84-13044
N84-13045
N84-13073
GOLDSTEIN, S. A. N84-12227
GONCZY, J. D. N84-12999
GOODYER, M. J. N84-12192
GOORAY, A. M. N84-12439
GOOSSENS, R. E. N84-12814
GORDON, B. M. N84-12720
GORDON, H. N84-12865
GOSLING, J. T. N84-13097
N84-13098
N84-13123
GOSS, L. D. N84-12664
GOTTLIEB, J. J. N84-12418
GOULD, R. D. N84-12421
GOWDEY, J. C. N84-12240
GRABBE, C. L. N84-12832
GRADY, D. N84-12544
GRAHAM, G. H. N84-12097
GRAHAM, J. A. N84-12711
GRANA, D. C. N84-12493
GRANNIS, P. N84-12865
GRANTHAM, D. D. N84-12683
GRANTHAM, W. D. N84-12190
GRAY, E. M. N84-12366
GRAY, T. A. N84-12167
N84-12825
N84-12827
GRAY, W. H. N84-12755
GREEN, M. W. N84-12745
GREENBLATT, M. N84-12250
GREENHOUSE, D. S. N84-12738
GREENSTADT, E. W. N84-12663
GREENWOOD, W. N84-12211
GRELLIER, M. N84-12629
GRIFFIN, F. P. N84-12501
GRIFFITH, R. V. N84-12883
GRINER, T. N84-12704
GRINGORTEN, I. I. N84-12683
GROOM, N. J. N84-12228
N84-12241
N84-12243
GROSSINGER, R. N84-12291
GRUENINGER, W. N84-12661
GRZEDZIELSKI, S. N84-13062
GU, Z. P. N84-12300
GUEDRY, F. E., JR. N84-12717
GUENTHER, A. H. N84-12468
N84-12469
GUINAN, M. W. N84-12394
GUIRAO, C. N84-12278
GUMBEL, H. N84-12639
GUNNINK, R. N84-12991
GUNTON, D. J. N84-12379
GUOAN, Z. N84-12451
GUSEMAN, L. F., JR. N84-12557
N84-12564
GUTMANAS, E. Y. N84-12292
GUZMAN, A. N84-12978
GYULASSY, M. N84-12861

H

HAAJIZADEH, M. N84-12438
HABBAL, S. R. N84-13083
N84-13088
HABERL, S. N84-12617
HADEISHI, T. N84-12461
HAERDLE, W. N84-12799
HAGELSTEIN, P. N84-12476
HAGGERTY, J. J. N84-13033
HAHN, H. N84-12202
N84-12204
N84-12206
N84-12207
HAHN, P. N84-12394
HAINES, A. B. N84-12080
N84-12083
HAIRUN, L. N84-12971
HAJELA, D. P. N84-12669
HAKAMADA, K. N84-13104

HALLQUIST, J. O. N84-12789
HAMANN, R. N84-12211
HAMEISTER, R. N84-13011
HAMSCHER, W. N84-12769
HAN, A. D. N84-12523
HAND, C. N84-12891
N84-12892
HANE, G. J. N84-12649
HANG, T. N84-13008
HANSEN, A. F. N84-12417
HANSEN, P. N84-12608
HANSEN, V. N84-12608
HANSON, A. G. N84-12365
HANSON, G. G. N84-12879
HANSON, K. M. N84-12723
HANSON, R. K. N84-12251
HARALICK, R. M. N84-12558
HARDIS, J. N84-12859
HARDY, G. H. N84-12043
HARIK, I. E. N84-12520
HARNED, D. S. N84-12930
HARRACH, R. J. N84-12478
HARRIS, D. F. N84-12031
HARRIS, G. A. N84-12703
HARRIS, J. E. N84-12332
HARRIS, R. P. N84-12491
HARROD, W. J. N84-12797
HART, T. T. N84-12472
HARTINELLI, G. N84-12794
HARVEY, J. K. N84-12103
HASER, L. N84-13035
HASSAN, A. A. N84-12092
HASSAN, H. F. N84-12961
HASSIN, R. N84-12773
HAUPT, R. J. N84-12141
HAUPT, R. L. N84-12347
HAUSER, S. G. N84-12649
HAUSMANN, W. N84-12171
HAWKINS, R. S. N84-12686
HAWKINS, S. N84-12841
HAYDUK, R. J. N84-12531
HAYES, E. N84-12642
HEATON, G. N84-12476
HECK, B. N84-12661
HEELIS, R. A. N84-12209
HEFFNER, R. H. N84-12979
HEITMANN, W. N84-12906
HELD, D. N. N84-12568
HELLBAUM, R. F. N84-12164
HENINS, I. N84-12930
HENNING, W. N84-12274
HENRY, C. L. N84-12731
HERCZYNSKI, R. N84-12407
HERMAN, C. N84-12570
HERSTEIN, P. D. N84-12820
HEWETT, D. W. N84-12930
HEYDORN, R. P. N84-12559
HICKMAN, R. B. N84-12397
HILDEBRAND, B. P. N84-12340
HILDEBRANDT, G. N84-12582
HILKO, B. K. N84-12227
HILL, C. T. N84-13132
HILLMAN, D. E. N84-12283
HINDS, W. T. N84-12655
HINTON, D. A. N84-12037
N84-12042
HIRANO, K. N84-12910
HIRSCH, G. N84-12199
HIRSCHFELD, T. N84-12899
HITZEL, S. N84-12120
HOANG, S. N84-13096
HOARD, R. W. N84-12397
HOBLITZELL, R. N84-12326
HODGES, G. S. N84-12184
HODGKINSON, J. N84-12156
HODUL, D. T. N84-12254
HOEIJMAKERS, H. W. M. N84-12117
N84-12433
HOENLINGER, H. N84-12191
HOFF, R. S., JR. N84-12054
HOFFMAN, G. L., JR. N84-13052
HOFFMAN, H. N84-12237
HOFFMANN, W. N84-12652
HOH, R. N84-12044
HOLDERER, O. C. N84-12413
HOLEMAN, E. G. N84-12210
HOLIAN, B. L. N84-13006
HOLLWEG, J. V. N84-13068
HOLMES, B. J. N84-12092
HOLTZ, B. N84-13015
HOLTZMAN, J. C. N84-12575
HOLZAPFEL, G. N84-12652
HONG, T. H. N84-12796
HONIG, E. M. N84-12388
HOOSE, W. N84-12181
HOPFINGER, E. J. N84-12128
HOPKINS, G. R. N84-12949
HOPKINS, J. R. N84-12177
HORNSTRA, F. N84-12395
N84-12642
HORNUNG, E. N84-12198
HORNUNG, H. G. N84-12101
HOROWITZ, E. N84-12104
HORTON, L. L. N84-12304
HOSENBALL, S. N. N84-13032
HOSOYAMA, K. N84-12392
HOTHEM, L. D. N84-12631
HOTOP, H. J. N84-12153
HOUWINK, R. N84-12434
HOVESTADT, D. N84-13112
N84-13117
HOWARD, K. L. N84-12205
HOWARD, R. A. N84-13121
HOWARD, W. M. N84-12478
HOWELL, R. H. N84-12887
HSIEH, S. J. N84-12974
HSU, D. K. N84-12827
HSU, S. L. N84-12315
HU, F. P. N84-12569
HU, W. L. N84-12300
HUBERSON, S. N84-12119
HUESCHEN, R. M. N84-12164
HUGHES, R. C. N84-12986
HUI, B. N84-12829
HULETT, L. D., JR. N84-12887
N84-12982
HULL, J. A. N84-12365
HULSTROM, R. L. N84-12622
HUND, T. D. N84-12400
HUNT, A. L. N84-12946
HUNTER, K. C. N84-13127
N84-13128
HURD, W. J. N84-12151
HURFORD, G. J. N84-12453
HUSSEY, T. W. N84-12921
HUTTSELL, L. J. N84-12191
HWANG, V. N84-12569
HYUN, J. M. N84-12415

I

ICE, G. E. N84-12897
IESS, L. N84-12358
N84-12362
ILEGBUSI, J. O. N84-12436
IM, B. J. N84-12097
IMPAGLIAZZO, J. N84-12806
INGE, S. V., JR. N84-12493
INGER, G. R. N84-12094
INTEMANN, P. R. N84-13031
IPAVICH, F. M. N84-13112
ISENBERG, P. A. N84-13118
ITON, L. E. N84-12254
N84-12839
IUCCI, N. N84-13129
N84-13130
IWANCZYK, J. N84-12898

J

JACQUES, C. N84-12186
JAGERS, P. N84-12792
JAMES, D. R. N84-12430
JANKOWSKI, R. N84-12346
JANSA, J. N84-12628
JASKOLLA, F. N84-12580
JEANROND, H. N84-12739
JELL, R. M. N84-12717
JENSEN, K. A. N84-13046
JENSEN, M. H. N84-12987
JERNIGAN, T. C. N84-12923
JIANG, D. P. W. N84-12189
JIANG, X. N84-12637
JO, J. H. N84-12874
JOHANNESSEN, J. A. N84-12605
JOHANNESSEN, O. M. N84-12605
JOHNSON, B. L., SR. N84-12425
JOHNSON, D. J. N84-12941
N84-12942
N84-12943
JOHNSON, D. L. N84-12884
JOHNSON, J. D. N84-13006
JOHNSON, K. N84-12263
N84-12264
N84-12265
JOHNSON, M. L. N84-12884
JOHNSON, R. L. N84-12923
JOHNSON, R. M. N84-12138
JOHNSON, S. A. N84-12530
JOHNSON, T. R. N84-12931
JOHNSON, W. B. N84-13026
JONAS, J. N84-12432
JONES, G. N84-12175
JONES, J. H. N84-12333
JONES, W. B. N84-12293
JOO, T. H. N84-12568
JORGENSON, W. E. N84-12178
JOST, G. S. N84-12532
JOYCE, B. E. N84-12719
JUDGE, D. L. N84-13109
JUNG, J. N84-12936

K

KAGAWA, T. N84-12911
N84-12913
KAIER, U. N84-12651
KAINZ, W. N84-13025
KAISER, W. R. N84-12620
KALMAN, G. J. N84-12918
KAMITAKAHARA, W. A. N84-12273
KANAL, L. N. N84-12570
KANEKO, S. N84-12909
KANNBERG, L. D. N84-12643
KANTOR, A. J. N84-12667
N84-12682
N84-12683
KAO, C. N84-12422
KARASHIMA, S. N84-12911
N84-12913
KATO, T. N84-12911
N84-12912
N84-12913
N84-12914
KATSUBE, N. N84-12525
KAUFFMAN, R. N84-12476
KAUFFMAN, R. L. N84-12933
KAWATA, S. N84-12916
KAWATA, T. N84-12915
KECKLER, C. R. N84-12228
N84-12229
N84-12243
KEELY, J. F. N84-12624
KELLER, J. B. N84-12418
KELLER, J. J. N84-12124
KELLER, K. N84-12207
KELLY, A. L. N84-12999
KENDALL, P. W. N84-12647
KENIK, E. A. N84-12303
KENNEDY, J. M. N84-12538
KENYON, S. N84-13047
KEPPLER, H. N84-12672
KERR, G. L. N84-12633
KERSHENBAUM, A. N84-12352
KESSLER, R. N84-12599
KEYES, J. J., JR. N84-12425
KEYSER, G. L., JR. N84-12190
KHANNA, S. K. N84-12289
KHAVARAN, A. N84-12822
KIATCHENKO, N. N84-12817
KIDD, C. T. N84-12450
KIJAK, S. N84-12346
KIM, H. J. N84-12982
KIM, J. N84-12414
KIM, K. C. N84-12480
KIM, N. N84-12620
KIM, S. B. N84-12938
KIM, S. H. N84-12999
KING, J. F. N84-12542
KING, R. J. N84-12370
N84-12374
KING, W. N84-12302
KINGERY, C. N. N84-12194
KINOSHITA, K. N84-12276
KIRCHMAYR, H. N84-12291
KIROLOUS, H. A. N84-12961
KISTNER, O. C. N84-12989
KITCHEN, L. N84-12569
KITSON, S. T. N84-12111
KITTEL, P. N84-12809
KLAPPER, H. N84-12985
KLECKER, B. N84-13112
N84-13117
KLEINE-TEBBE, A. N84-12199
KNEPTON, J. N84-12704
N84-12705
N84-12706
KNOROVSKY, G. A. N84-12308
KNUDSEN, H. K. N84-12736
KNYSTAUTAS, R. N84-12278
KOCHANSKI, T. P. N84-12938
KOCHELAN, V. A. N84-12890
KOCHELAP, V. A. N84-12814
KOEHLER, D. R. N84-12980
KOENIG, K. N84-12783

KOHL, J. L. N84-13071
KOHLBACHER, G. N84-13002
KOK, J. N84-12740
KOKINI, K. N84-12408
KOLKA, M. A. N84-12719
KONNICK, P. J. N84-12503
KOOMEN, M. J. N84-13121
KORN, J. N84-12350
KOSTAL, H. N84-12563
KOTOWSKI, R. K. N84-12966
KOURTIDES, D. A. N84-12313
KOVACS, A. N84-12331
KOZUMA, R. N84-12211
KRAMER, M. A. N84-12896
KRAMER, M. J. N84-12662
KRAUSE, E. N84-12125
KREMER, K. N84-12324
KRENZ, D. N84-12206
KRENZ, G. N84-12081
N84-12085
KREPLIN, H. P. N84-12113
KRIEGER, C. I. N84-12999
KRIEGER, U. N84-12652
KRISHNAIAH, P. R. N84-12787
KRISTIANSEN, M. N84-12468
N84-12469
KROMBEL, K. E. N84-13064
KRUEGER, R. J. N84-12353
KRYDER, M. H. N84-12978
KRYSZTOFIAK, A. N84-12346
KUBIBNYY, Y. A. N84-12890
KUBINA, S. J. N84-12375
KUPERSHMIDT, B. A. N84-12790
KUPHAL, E. N84-13000
KUPPUSAMY, T. N84-12258
KURTH, W. S. N84-13058

L

LABELLE, S. N84-13034
LAI, S. T. N84-12831
LAIRSON, B. M. N84-12897
LAKIN, K. M. N84-12824
N84-12997
LAM, P. S. N84-12549
LAMAR, J. E. N84-12109
LAMMERZAHL, P. N84-12665
LAMPE, F. W. N84-12277
LAMPE, M. N84-12829
LANDGREBE, A. J. N84-12090
N84-12091
LANDIN, A. R. N84-12997
LANDMAN, L. C. N84-12506
LANDT, J. A. N84-12376
LANG, D. D. N84-12946
LANOU, R. N84-12865
LAO, L. L. N84-12957
LAPICKI, G. N84-12982
LASCHE, G. P. N84-12482
LATHAM, R. L. N84-12522
LAU, S. S. N84-12975
N84-12976
N84-12977
LAUER, D. T. N84-12555
LAUER, L. N84-12652
LAUG, M. N84-12629
LAVINE, D. N84-12570
LAW, R. D. N84-12311
LAWLESS, W. N. N84-12316
LAWLEY, A. N84-12292
LAZARUS, A. J. N84-13106
LEACH, D. D. N84-13038
LEATHERWOOD, J. D. N84-12445
LEAVITT, R. P. N84-12417
LEBEAU, S. E. N84-12286
LEBER, R. L. N84-12397
LEE, E. H. N84-12303
LEE, E. K. L. N84-12284
LEE, J. D. N84-12397
LEE, J. H. S. N84-12278
LEE, P. N84-12476
LEEPER, R. J. N84-12942
N84-12943
LEGENDRE, R. N84-12813
LEGORGEU, J. P. N84-12587
LEIBOVICH, S. N84-12122
LEIPELT, G. N84-12476
LEISHER, W. B. N84-12318
LELAND, T. W. N84-13008
LENCO, M. N84-12606
LEON, M. N84-12979
LEONARD, A. N84-12126
LEUCHTER, O. N84-12127
LEVEILLE, J. N84-12865
LEVENTHAL, M. N84-13039
LEVINE, L. N84-12719
LEVINE, M. A. N84-12929
LEVINTHAL, M. L. N84-12311
LEVY, C. N84-12552
LIAW, Y. P. N84-12335
LICHTENSTEIN, T. L. N84-12472
LIEBOWITZ, H. N84-12527
LIN, H. C. N84-12546
LIND, J. N84-12275
LINDE, M. N84-12696
LINDENMEIER, H. K. N84-12371
LINDESAY, J. V. N84-12849
LINDSEY, G. D. N84-12137
LIPINSKA, N. N84-12636
LIPINSKI, W. N84-12636
LO, C. C. N84-12398
LOBITZ, D. W. N84-12537
LOCKENOUR, J. L. N84-12061
LOESCHE, P. N84-12599
LOEWY, R. G. N84-12257
LOGAN, B. G. N84-12939
LOGEE, T. L. N84-12647
LONGACRE, R. S. N84-12896
LONGDON, N. N84-12579
LONGHI, J. N84-13059
N84-13060
LOODTS, J. N84-12600
LOPEZ-RIOS, T. N84-12351
LORENZ, S. N84-12185
LOUBERSAC, L. N84-12591
LOVE, R. N84-12455
LOVE, W. A. N84-12896
LOWDERMILK, W. H. N84-12472
LOY, S. L. N84-13011
LUCCI, A. D. N84-12183
LUCERO, J. P. N84-12904
LUDEMANN, W. N84-12298
LUDWIG, R. N84-12727
LULL, W. P. N84-13026
LUMPKIN, A. N84-12481
N84-12485
LUOHUI, Z. N84-12971
LUSK, E. L. N84-12774
LUTZ, T. J. N84-12543
LYNCH, J. E. N84-12843
LYON, J. F. N84-12923

M

MACCALLUM, C. J. N84-13039
MACEK, W. N84-13062
MACGREGOR, K. B. N84-13085
MACHLES, G. W. N84-12226
MADSON, C. A. N84-13026
MAHATO, B. N84-12404
MAHER, F. A. N84-13011
MAHONEY, A. R. N84-12901
MAJEWSKI, W. N84-12338
MAKOWSKI, M. A. N84-12951
MALACHESKY, P. A. N84-12403
MALIN, M. C. N84-13057
MALL, S. N84-12529
MALLOW, J. V. N84-12872
MALMGREN, A. N84-12608
MALOTA, F. N84-12357
MANGENEY, A. N84-12965
MANN, F. M. N84-12884
MANSER, R. N84-12191
MANSFIELD, J. L. N84-12893
MANSOUR, N. N. N84-12414
MARACCI, G. N84-12586
MARCHANT, D. D. N84-12926
MARCHERTAS, A. H. N84-12536
MARIANI, F. N84-13050
N84-13076
MARKAKIS, J. N84-12898
MARKEVICH, A. N84-12849
MARSCH, E. N84-13094
MARSHALL, R. P. N84-12643
MARTIN, G. L. N84-12092
MARTIN, J. J. N84-12980
MARTINI, W. R. N84-12504
MASCARENHAS, N. D. A. N84-12446
MASCHKE, A. W. N84-12934
MASERJIAN, J. N84-12463
MASKEW, B. N84-12112
MASON, J. D. N84-12748
MASSIN, J. M. N84-12607
MASTRANTONIO, G. N84-12653
MATHEW, D. N84-12620
MATHIS, R. A. N84-12430
MATHUR, N. C. N84-12374
MATKOWSKY, B. J. N84-12728
MATTAS, R. F. N84-12306
MATTHAEUS, W. H. N84-13073
MATTHEWS, A. J. N84-12687
MATTHEWS, D. L. N84-12476
MAULDIN, G. H. N84-12402
MAURO, C. A. N84-12607
MAXWORTHY, T. N84-12128
MAYO-WELLS, J. F. N84-12405
MAZUR, P. N84-12999
MAZURKIEWICZ, M. N84-12323
MCCALL, D. L. N84-12045
MCCLELLAN, R. O. N84-12656
MCCOLL, W. D. N84-12592
MCCORMICK, W. P. N84-12782
N84-12798
MCCOY, H. E. N84-12542
MCCOY, J. J. N84-12821
MCCRORY, R. L. N84-12920
MCDEVITT, N. T. N84-12972
MCFADDEN, B. L. N84-12183
MCFARLAND, R. H. N84-12045
MCGUIRE, E. J. N84-12857
N84-12858
MCHARG, B. B., JR. N84-12733
N84-12927
MCKELVEY, V. E. N84-12577
MCKINLAY, W. H. N84-12066
MCLAUGHLIN, D. E. N84-12979
MCLAUGHLIN, R. N84-12461
MCLEAN, E. A. N84-12486
MCLERRAN, L. N84-13134
MCNALLAN, M. J. N84-12302
MEDECKI, H. N84-12933
MEGIE, G. N84-12583
MEGOS, E. L. N84-13021
MEHL, W. N84-12586
MEHLHORN, T. A. N84-12858
N84-12941
MEHROTA, P. N84-12742
MEI-DONG, C. N84-13093
MEIER, H. U. N84-12113
MELHORN, T. A. N84-12866
MELITA, O. N84-12579
MELLOR, M. N84-12619
MENDEL, C. W., JR. N84-12945
MENDILLO, M. N84-13093
MENL, B. N84-12185
MERCIER, O. L. N84-12071
METZ, P. D. N84-12427
MEYER-VERNET, N. N84-13096
MEYERS, K. A. N84-13042
MEZZANOTTE, D. A., JR. N84-12309
MICHELS, D. J. N84-13121
MIDDLETON, D. N84-12364
MIHLAN, G. J. N84-12333
MIKHAIL, E. M. N84-12571
MIKROYANNIDIS, J. A. N84-12313
MILAM, D. N84-12472
N84-12985
MILANOVICH, F. P. N84-12899
MILLAUD, J. N84-12461
MILLER, C. M. N84-12483
MILLER, D. J. N84-12457
MILLER, E. J. N84-12711
MILLER, E. K. N84-12373
N84-12374
MILLER, J. N84-12244
MILLER, J. M. N84-12334
MILLER, M. G. N84-12692
MILLER, P. A. N84-12945
MILLER, P. D., JR. N84-12887
MILNER, W. T. N84-12962
MINEHART, R. C. N84-12844
MINSK, L. D. N84-12690
MIRICK, P. H. N84-12162
MITCHELL, A. C. N84-12818
MITCHELL, D. G. N84-13113
MITCHELL, R. I. N84-12333
MITCHUM, G. T. N84-12581
MITTMANN, J. N84-12514
MIX, L. P. N84-12942
N84-12943
MIYANAGA, N. N84-12913
MOAK, C. D. N84-12887
MOATS, R. K. N84-12195
MOCCI, U. N84-12908
MOFFAT, R. J. N84-12428
N84-12429
MOHLIN, T. N84-12516
MOHSEN, M. N84-12969
MOIN, P. N84-12414
MOLKI, M. N84-12437
MONAGHAN, R. C. N84-12443
MONGIA, H. N84-12263
N84-12264
N84-12265
MONTANEGRO, C. N84-12739
MONTGOMERY, A. N84-12739

MONTGOMERY, D. N84-13077
MONTRY, G. R. N84-12857
MOORE, J. S. N84-12745
MORANDI, M. N84-12590
MORAWITZ, H. N84-12834
MORDFIN, L. N84-12517
MORETTO, L. G. N84-12885
MOREY, R. M. N84-12331
MORGAN, W. C. N84-12321
MORGEN, P. N84-12266
MORRIS, C. N. N84-12563
MORRIS, T. W. N84-12896
MORRISON, C. A. N84-12417
MORTON, P. L. N84-12489
MORY, M. N84-12128
MOSE, K. N84-12180
MOSHER, A. N84-12878
MOSLEY, W. C., JR. N84-12539
MUHLHAUSER, K. H. N84-13121
MUIRHEAD, K. N84-12603
MULLER, M. W. N84-12974
MURAKAMI, H. N84-12916
MURDOCK, T. L. N84-13037
MURRAY, W. N84-12751
N84-12752
MUSSMAN, D. N84-12191
MYDOSH, J. A. N84-12979
MYERS, E. T. N84-12711

N

NAGEL, L. N84-12969
NAIZHI, B. N84-12971
NAJM, M. N84-12518
NAKAI, Y. N84-12912
N84-12914
NAKAMURA, Y. N84-12126
NANDA, A. N84-12258
NARAGHI, M. N84-12561
NARAYAN, J. N84-12477
NARULA, A. N84-12315
NASH, R. A. N84-12159
NATESAN, K. N84-12297
N84-12299
NAUMANN, K. H. N84-13008
NEEDHAM, J. R. N84-12327
NEEK, D. N84-12859
NELSON, B. E. N84-12923
NERMAN, O. N84-12792
NERSESOVA, A. Z. N84-12578
NEUBAUER, F. M. N84-13074
NEUGEBAUER, M. N84-13067
N84-13078
NEVILLE, R. A. N84-12592
NEWKIRK, H. N84-12985
NEWMAN, J. C., JR. N84-12529
NEWNAM, B. E. N84-12485
NEWTON, H. J. N84-12567
NEXSEN, W. E. N84-12646
N84-12946
NIAN-ZU, D. N84-13093
NICAISE, P. D. N84-12234
NICHOLSON, M. M. N84-12270
NICKEL, H. N84-12323
NICKERSON, G. R. N84-12248
NICKLOW, R. M. N84-12273
NICKUM, J. D. N84-12045
NICOLET, M. A. N84-12994
NIEDNER, M. B., JR. N84-13126
NIELSEN, A. N84-12608
NIETUBICZ, C. J. N84-12094
NIEUWENHUYS, G. J. N84-12979
NILAND, R. A. N84-12929
NISSEN, J. C. D. N84-12739
NIU, K. N84-12916
NIX, R. G. N84-12644
NOCI, G. N84-13071
NOGAR, N. S. N84-12483
NOLA, F. N84-12239
NOMURA, E. N84-12250
NOONKESTER, V. R. N84-12685
NORMAN, E. B. N84-13038
NORRISJONES, S. R. N84-12327
NORVELL, S. N84-12349
NOTERDAEME, J. M. N84-12937
N84-12950
NOWICK, A. S. N84-12992
NOYES, H. P. N84-12650
NUNNALLY, W. C. N84-12402
NUNNELEY, S. A. N84-12423
NUR, A. N84-12668
NUTT, K. W. N84-12215

O

OBARA, C. J. N84-12092
OBENSCHAIN, S. P. N84-12486
OBRIEN, J. E. N84-13032
OCONNELL, R. N84-13061
ODONNELL, R. D. N84-12455
OERY, H. N84-12198
OGALLAGHER, J. J. N84-12902
OGILVIE, K. W. N84-13049
N84-13065
N84-13111
OH, J. M. N84-12302
OHR, S. M. N84-12540
OKEEFE, J. M. N84-12205
OKELLEY, G. D. N84-12982
OLBERT, S. N84-13079
N84-13080
OLER, J. W. N84-12097
OLEYNIKOV, Y. G. N84-12498
OLMSTEAD, M. A. N84-12279
N84-12895
OLOUGHLIN, J. P. N84-12468
N84-12469
OLSEN, J. N. N84-12858
N84-12941
OLSEN, R. E. N84-12386
OLSON, J. S. N84-12626
OLSONI, K. E. N84-12051
N84-12052
N84-12053
OLSZEWSKI, E. W. N84-13051
OLSZEWSKI, M. N84-12231
OMARAMRANI, A. N84-12136
OMENETTO, N. N84-12586
OPHIR, D. N84-12746
OPSAL, J. L. N84-12167
N84-12512
ORAN, E. S. N84-12411
ORFEI, R. N84-12675
ORMISTON, R. A. N84-12162
ORMSBEE, A. I. N84-12328
ORR, E. D. N84-12620
ORRALL, F. Q. N84-13082
ORSINI, S. N84-12676
N84-13049
ORSZAG, S. A. N84-12920
ORTALE, C. N84-12898
OSTOWARI, C. N84-12087
OSTROFF, A. J. N84-12164
OTT, R. H. N84-12369
OVENDEN, C. N84-13075
OVERTON, J. H. N84-12711
OWENS, D. H. N84-12795
OWOCKI, S. P. N84-13115
OXOBY, G. N84-12840

P

PACK, D. J. N84-12802
PACK, S. C. N84-12261
PADERES, F. C., JR. N84-12571
PAHL, D. A. N84-12178
PALACZ, M. N84-12346
PALLOTTINO, G. V. N84-12359
N84-12360
PALMER, L. B. N84-12821
PALMER, R. N84-12865
PANOFSKY, W. K. H. N84-12842
PANTANI, L. N84-12590
PARISI, M. N84-13129
N84-13130
PARK, B. N84-12314
PARK, J. E. N84-12425
PARKER, E. N. N84-13069
PARKER, J. F. N84-12046
PARKINSON, W. C. N84-12852
PARTIN, J. K. N84-12873
PARZEN, E. N84-12565
PASTRANA, G. N84-12850
PASZEK, W. N84-12382
N84-12383
PATTERSON, R. E. N84-12634
PATTINSON, N. P. N84-12070
PAWELEC, Z. N84-12383
PEAKE, D. J. N84-12100
PEARLSTEIN, L. D. N84-12940
PEARSON, C. F. N84-12672
PEDRINI, A. N84-12586
PEEK, J. M. N84-12858
PEELE, W. D. N84-13009
PEELING, S. M. N84-12378
PEKAR, S. I. N84-12814
PELLEGRIN, J. L. N84-12840

PENDLETON, W. K. N84-12468
N84-12469
PENDYALA, S. N84-12887
PENNINGTON, J. E. N84-12041
PENTECOST, E. N84-12196
PEOPLES, J. N84-12865
PEPIN, R. O. N84-13061
PERDZOCK, J. M. N84-12065
PEREIRA, J. A. G. N84-12446
PERKOWSKI, Z. N84-13135
PERRY, F. C. N84-12942
N84-12943
PERSEN, L. N. N84-12123
PETERS, C. N84-12562
PETERS, L. J. N84-12714
PETERSEN, A. N84-12111
PETERSON, E. M. N84-12048
PETTIT, R. B. N84-12901
PHILBRICK, C. R. N84-12665
PHILLION, D. W. N84-12486
PHILLIPS, W. H. N84-12154
PIAU, P. N84-12612
PICKLES, W. L. N84-12946
PICRAUX, S. T. N84-12994
N84-12998
PIEPER, G. W. N84-12788
PILKEY, R. D. N84-12458
PIPPI, I. N84-12590
PITCHFORD, L. C. N84-12393
PITTS, J. R. N84-12641
PIWONSKI, W. N84-12743
PIZZARELLO, F. A. N84-12270
PIZZELLA, G. N84-12360
PIZZO, V. J. N84-13120
PLANK, V. G. N84-12687
PLATNER, E. D. N84-12896
POA, D. S. N84-12387
POLL, D. I. A. N84-12105
POLLACK, J. G. N84-12716
POLLARD, M. N84-12461
POLYCHRONAKOS, V. A. N84-12896
POOR, S. N84-12841
PORTER, J. E. N84-12268
POST, R. F. N84-12932
POTENZA, J. N84-12645
POTTER, R. M. N84-12672
POTTERS, J. H. H. M. N84-12964
PRATT, T. W. N84-12742
PRICE, R. N84-12476
PRICE, R. H. N84-12486
PRICE, S. D. N84-13037
PROCTOR, F. H. N84-12679
PROFFER, W. J. N84-12837
PUCHER, M. N84-12171
PUMMER, H. N84-12467
PURCELL, J. N84-12815

Q

QADER, S. A. N84-12635
QUAIL, P. H. N84-12710
QUINTENZ, J. P. N84-12945
QUIRK, J. A. N84-12222

R

RAASCH, W. N84-12201
RABINOVITCH, B. S. N84-12833
N84-12836
RADCLIFF, J. A. N84-12341
RADICATI, B. N84-12590
RAFAILOVICH, M. H. N84-12989
RAHBEE, A. N84-12830
RAINER, F. N84-12472
RAINZINGER, M. N84-13025
RAMACHANDRAN, K. N84-12121
RAMAN, S. N84-12851
N84-12982
RAMBACH, D. N84-12062
RAND, J. L. N84-12448
RANDLE, R. J., JR. N84-12193
RANDRUP, J. N84-12847
RANJAN, R. N84-12307
RANLET, D. N84-12534
RAO, D. M. N84-12129
RAO, V. P. N84-12287
RAPHANEL, J. L. N84-12521
RASMUSSEN, D. A. N84-12875
N84-12952
RAVAIOLI, G. N84-12908
RAWL, D. E., JR. N84-12309
RAYBORN, G. H. N84-12444
RAYMOND, M. G. N84-12647
RAYNE, J. A. N84-12978

REAMS, W. N84-12541
REDDY, J. N. N84-12258
REE, F. H. N84-12816
REED, T. N. N84-12737
REEDER, M. J. N84-12137
REESE, J., JR. N84-12639
REFOLO, P. J. N84-12677
REGAZZI, J. J., III N84-13030
REGINATO, L. N84-12841
REICHERT, P. N84-12599
REILLY, M. H. N84-12342
REMBAUM, A. N84-12262
RENIE, J. P. N84-12285
RENKEN, J. H. N84-12182
RETTIE, I. H. N84-12077
N84-12084
REUCROFT, P. J. N84-12305
REVENAUGH, J. N84-12709
REYNOLDS, R. N84-12263
N84-12264
N84-12265
RHODES, C. K. N84-12467
RIAZUELO, S. N84-12174
RICE, G. W. N84-12282
RICE, R. R. N84-12233
N84-12235
RICH, F. J. N84-12209
RICHARDS, J. F. N84-12626
RICKETSON, D. S., JR. N84-12137
RICKETT, B. J. N84-13090
RICKMANN N84-13007
RIORDAN, C. J. N84-12622
RIPIN, B. H. N84-12486
RIPKEN, H. W. N84-13116
RISTOW, D. N84-12354
RIVEREAU, J. C. N84-12587
RIZZI, A. N84-12120
ROBBINS, C. L. N84-13127
N84-13128
ROBERTS, L. N84-12102
ROBERTS, M. P. N84-12620
ROBINSON, E. J. N84-12835
ROBINSON, S. E. N84-13041
ROCHEFORT, J. S. N84-12452
RODACY, P. J. N84-12318
RODGERS, C. N84-12172
RODRIGUEZ, G. E. N84-12228
N84-12230
ROELOF, E. C. N84-13113
ROGERS, D. C. N84-12678
ROHDE, R. W. N84-12293
ROMERO, J. L. N84-12864
ROMIER, A. N84-12170
ROSE, J. H. N84-12167
N84-12512
N84-12513
ROSEMEIER, R. G. N84-12325
ROSEN, M. D. N84-12486
ROSENBAUER, H. N84-13121
ROSENTHAL, S. E. N84-12945
ROSNER, R. N84-13083
N84-13088
ROSS, A. A. N84-12747
ROSS, M. N84-12983
ROSSBACHER, L. A. N84-13063
ROSSI, G. N84-12586
ROTHE, D. E. N84-12477
ROTHERMEL, J. N84-12660
ROTTMAN, G. J. N84-13082
ROTTY, R. M. N84-12626
ROZYCKI, A. N84-12382
N84-12383
RUBINSTEIN, F. R. N84-12401
RUBY, L. N84-12886
RUFFNER, G. N84-12185
RUMINER, K. N84-12488
RUNDE, C. P. N84-13032
RUPPEN, J. A. N84-12296
RUSCHAU, J. J. N84-12290
RUSSELL, C. T. N84-13097
RYALL, T. G. N84-12780
RYDER, D. E. N84-13014
RYDER, G. N84-13059
N84-13060
RYGE, P. N84-13039

S

SADEK, A. G. N84-12494
SADEK, H. S. I. N84-12416
SALERNO, L. J. N84-12809
SALFNER, P. N84-12515
SALOMON, M. N84-12133
SALZBRENNER, R. N84-12296
N84-12543
SALZER, D. T. N84-12356
SALZMAN, K. A. N84-12974
SAMEJIMA, F. N84-12721
SANDFORD, T. W. L. N84-12866
SANKRITHI, M. M. K. V. N84-12155
SANTORO, R. T. N84-12956
SANTORO, T. P. N84-13021
SARDESHMUKH, P. D. N84-12680
SARJEANT, W. J. N84-12402
SARKISYAN, R. M. N84-12578
SASTRY, S. N84-12808
SATTI, J. A. N84-12502
SAUERS, R. R. N84-12645
SAULYS, A. C. N84-12896
SAUNDERS, M. A. N84-12751
N84-12752
SAWKA, M. N. N84-12719
SAX, R. N84-12666
SCANLAN, R. M. N84-12397
SCHAEFER, H. F., III N84-13003
SCHILLACI, M. E. N84-12979
SCHILLING N84-13007
SCHILLING, D. L. N84-12344
SCHINAGEL, H. N84-13002
SCHISSEL, P. N84-12641
SCHLITTENHARDT, P. N84-12586
SCHMIDLI, R. J. N84-12699
SCHMIDT, A. N84-12203
SCHMIDT, J. N84-12841
SCHMIDT, W. N84-12120
SCHMITZ, B. W. N84-12178
SCHNACK, D. D. N84-12953
SCHNEIDER, G. N84-12355
SCHNEIDER, J. N84-12354
SCHNEPPLE, W. N84-12898
SCHOEVERS, H. W. C. L. N84-12173
SCHOLER, M. N84-13112
SCHONFELD, J. F. N84-12791
SCHRAMM, D. N. N84-13132
SCHROTH, A. N84-12695
SCHULTZ, J. H. N84-12817
SCHUMACHER, B. N84-12298
SCHUMAKER, L. L. N84-12564
SCHUSTER, G. B. N84-12268
SCHWARTZ, M. N. N84-12694
SCHWARTZ, S. J. N84-13075
SCHWENN, R. N84-13105
N84-13121
SCHWIND, R. G. N84-12429
SCIALDONE, J. J. N84-12216
SCOTT, D. W. N84-12560
SCUDDER, J. D. N84-12663
N84-13080
SCULLY, K. R. N84-12768
SEAB, C. G. N84-13131
SEABRIDGE, A. G. N84-12063
SEAGER, C. H. N84-12986
SEAMSTER, A. G. N84-13038
SEARCY, A. W. N84-12255
SEARS, M. P. N84-12735
SEBALD, A. V. N84-13005
SEBRING, D. L. N84-12065
SECHRIST, C. F., JR. N84-12462
SEEMANN, R. J. N84-12061
SEGALL, Z. N84-12732
SEGINER, A. N84-12133
SEIDEL, D. B. N84-12942
SEIZINGER, D. E. N84-12656
SELIGSON, D. N84-12996
SELLECK, C. B. N84-12735
SEVESTRE, C. N84-12810
SHAFER, R. A. N84-12889
SHAHA, O. N84-12982
SHALIT, B. N84-12724
SHANKS, H. R. N84-12259
SHANMUGAN, K. S. N84-12575
SHARMAN, P. W. N84-12779
SHAUGHNESSY, J. D. N84-12029
N84-12030
SHAW, D. E. N84-12082
SHAW, M. S. N84-13006
SHAW, W. J. N84-12658
SHEA, M. L. N84-13021
SHEBALIN, J. V. N84-12528
SHEELEY, N. R., JR. N84-13121
SHEFFIELD, R. L. N84-12481
N84-12485
SHEFFLER, K. D. N84-12312
SHEKELL, G. N84-12767
SHELTON, J. P. N84-12345
SHEPHERD, J. E. N84-12278
SHINE, E. P. N84-12566
SHIVANANDAN, K. N84-13037
SHLICHTA, P. J. N84-12968
SIDFORD, M. J. N84-12372
SIEBENECK, J. N84-13001
SIEBERS, D. L. N84-12429
SIECHAU, R. N84-12323
SIEGEL, E. N. N84-13032
SIEKHAUS, W. J. N84-12272
SIEWIOREK, D. N84-12732
SIGNORINI, C. N84-12675
SILBERMAN, J. N84-12266
SILVER, J. A. N84-12830
SIMCOCK, A. L. N84-12729
N84-12741
SIME, D. G. N84-13102
SIMMONS, R. G. N84-12772
SIMMONS, R. J. N84-12163
SIMO-MUERZA, J. C. N84-12524
SIMONEN, T. C. N84-12955
SINGH, J. J. N84-12444
SINGH, S. M. N84-12810
SINGH, S. N. N84-12095
SINHA, V. N84-12337
SIOMOS, K. N84-12863
SITES, J. R. N84-12894
SKALICKY, P. N84-12291
SKELTON, E. A. N84-12819
SKOU, N. N84-12609
SKUMANICH, A. N84-12993
SLAVIN, J. A. N84-13091
SLOOFF, J. W. N84-12074
N84-12078
SLUD, E. N84-12570
SLUTZ, S. A. N84-12942
N84-12943
SMITH, C. N84-12137
SMITH, C. W. N84-12419
SMITH, D. N84-12985
SMITH, E. J. N84-13091
N84-13097
N84-13107
N84-13123
SMITH, G. B. N84-12574
SMITH, G. E. N84-12443
SMITH, J. H. B. N84-12116
SMITH, M. N84-12841
SMITH, P. M. N84-12190
SMITH, R. N84-12179
SMITH, R. K. N84-12333
SMITH, R. P. N84-12999
SMITH, W. B. N84-12566
SMITH, W. W. N84-12226
SMYK, E. B. N84-12931
SNIPES, J. A. N84-12938
SOLIGNAC, J. L. N84-12127
SOLLID, J. E. N84-12485
SOMERVILLE, L. P. N84-12859
SONDERICKER, J. H. N84-12826
SOROKA, L. N84-12886
SPADACCINI, L. J. N84-12225
SPALART, P. R. N84-12126
SPALDING, D. B. N84-12435
SPARKS, C. J., JR. N84-12997
SPARKS, W. M. N84-13047
SPAULDING, A. D. N84-12364
SPEER, P. E. N84-12632
SPICER, W. E. N84-12266
SPILLMAN, J. J. N84-12130
N84-12131
SPIVAK, A. L. N84-12809
SPROUSE, G. D. N84-12989
SRINIVASAN, R. N84-12263
N84-12264
N84-12265
STAAHLBERGCARLSTEDT, B. N84-12724
STAHL, R. L. N84-12621
STANCIL, R. T. N84-12096
STANEK, R. P. N84-12999
STANTON, A. C. N84-12630
STANZIONE, T. N84-12455
STARRFIELD, S. N84-13047
STEELE, E. I. N84-13009
STEELE, J. M. N84-12801
STEFANUTTI, L. N84-12590
STEIGMANN, D. J. N84-12160
STEIN, W. E. N84-12481
N84-12485
STEINBERG, J. L. N84-13096
STEINBERG, M. N84-12256
STEINBROOK, R. A. N84-12708
STEINHOFF, J. N84-12121
STEINOLFSON, R. S. N84-13119
STEPHENS, D. G. N84-12445
STEVEN, A. N84-12269
STEVENSON, W. H. N84-12421
STOBIE, J. G. N84-12659
STOCK, P. N84-12617
STOCKWELL, C. W. N84-12717
STOFFER, G. R. N84-12715
STOKOWSKI, S. N84-12985

STONE, E. C. N84-13056
STONE, R. G. N84-13103
STORINI, M. N84-13129
N84-13130
STORM, D. W. N84-12846
STRAHLER, A. H. N84-12573
STRANGE, C. N84-12103
STRATTON, R. C. N84-12774
STREBE, J. N84-12404
STREHLOW, R. A. N84-12328
STRICKLAND, J. H. N84-12097
STUCKENBERG, N. N84-12067
STUDER, P. A. N84-12242
STUERMER, A. N84-13002
STURGES, W. N84-12681
STURM, B. N84-12586
STYGAR, W. A. N84-12943
SUCKOW, U. N84-13001
SUESS, S. T. N84-13081
SUISSE, D. C. N84-12311
SUKYS, R. N84-12452
SULLIVAN, W. N. N84-12537
SUN, J. N84-12363
SUN, Z. N84-12637
SUNYAR, A. W. N84-12969
SURYANARAYANAN, K. N84-12121
SUSINI, C. N84-12590
SUTTON, G. N84-12639
SUWANPRASERT, S. N84-12187
SVENSSON, B. N84-12630
SWAIN, D. W. N84-12675
SWAIN, J. N84-12985
SWANN, T. A. N84-12485
SWENSON, C. A. N84-12252
N84-12280
SWISHER, J. N84-12650
SYMM, G. T. N84-12740
SZETELA, E. J. N84-12225
SZOEKE, A. N84-12478

T

TABOR, J. E. N84-12843
TAELJEDALSHALIT, I. L. N84-12724
TAGUE, D. L. N84-12460
TAKIMOTO, A. N84-12909
TALLEY, B. N84-12488
TANABE, J. N84-12886
TATTELMAN, P. N84-12683
TAWARA, H. N84-12912
N84-12913
N84-12914
TEEGARDEN, B. J. N84-13039
TERRIAN, D. M. N84-12423
TEWALT, S. J. N84-12620
THAKOOR, A. N84-12289
THALLER, L. H. N84-12247
THATHACHAR, Y. T. N84-12969
THEATRE, J. N84-12600
THEIMER, O. H. N84-12336
THIELE, H. M. N84-12505
THOMAS, B. T. N84-13101
THOMAS, T. M. N84-12641
THOMPSON, D. C. N84-12900
THOMPSON, D. O. N84-12824
THOMPSON, H. D. N84-12421
THOMPSON, H. L., III N84-12718
THOMPSON, M. C. N84-12402
THOMPSON, P. B. N84-12923
THOMPSON, R. B. N84-12167
N84-12547
N84-12825
N84-12827
THOMSEN, H. H. N84-12598
THOMSON, D. J. N84-12820
THOMSON, W. G. N84-12134
THRESH, H. R. N84-12294
TIDMAN, D. A. N84-12227
TILL, S. M. N84-12592
TILLER, W. A. N84-12969
TIRSELL, G. N84-12476
TOBAK, M. N84-12100
TOBIAS, I. N84-12645
TOLLEY, H. D. N84-12804
TOSELLI, F. N84-12609
TOYNE, G. B. N84-12184
TRAINOR, R. J. N84-12816
TRAXLER, R. R. N84-12689
TRIFTSHAEUSER, W. N84-12887
TRUJILLO, A. A. N84-12318
TRURAN, J. W. N84-13047
TSANG, C. F. N84-12624
TSINGANOS, K. N84-13083
N84-13088
TSURUTANI, B. T. N84-13097
TUELLER, J. N84-13039
TUMMILLO, A. F. N84-12389
N84-12395
TURK, A. N84-13026
TURNER, W. C. N84-12946
TURNIPSEED, G. T. N84-12717
TUSZEWSKI, M. N84-12930

U

ULLMANN, J. L. N84-12884
UNDERWOOD, D. C. N84-12999
UNGERS, L. J. N84-12333
URRY, C. M. N84-12889

V

VAJDA, S. N84-12989
VALERIO, C. N84-12611
VALID, R. N84-12812
VANDAM, H. N84-13004
VANDEGRIEND, J. A. N84-12601
VANDENAVYLE, J. A. N84-12543
VANDENBOSCH, R. N84-12846
VANDERHOFF, J. A. N84-12267
VANDERLEEDEN, G. A. N84-12477
VANDERMEER, R. A. N84-12295
VANDEVENDER, J. P. N84-12944
N84-12945
VANE, C. R. N84-12851
N84-12982
VANGASTEL, K. N84-12698
VANGENDEREN, J. L. N84-12601
VANLEER, B. N84-12778
VANLINT, V. A. J. N84-12339
VANSANT, J. H. N84-12988
VANSTOKKOM, H. T. C. N84-12601
VASUDEVAN, R. N84-12534
VAURIO, J. K. N84-12511
VELTRI, P. N84-12965
VERDERBER, R. R. N84-12401
VERHAAGEN, N. G. N84-12106
VIDAL-MADJAR, D. N84-12588
VILLORESI, G. N84-13129
N84-13130
VILLUMSEN, J. V. N84-13054
VINAS, A. F. N84-13044
VINAS, O. N84-12613
VINT, A. N84-12086
VIRCHIS, V. J. N84-12548
VIRK, G. S. N84-12795
VOELZ, D. G. N84-12462
VOGEL, M. A. N84-12935
VOIGT, R. C. N84-12777
VOLLMERS, H. N84-12113
VONFINCKENSTEIN, K. N84-12776
VORROPOULOS, G. N84-12108
VU, B. D. N84-12071
VUYE, G. N84-12351
VYALOV, S. S. N84-12578

W

WADSWORTH, A. N84-12609
N84-12612
WAGNER, E. N84-12515
WAGNER, R. D. N84-12506
WALBERT, J. N. N84-12744
WALLACE, E. J. N84-12999
WALLIS, P. N84-12739
WALTER, W. T. N84-12464
WANG, C. N84-12476
WANG, F. D. N84-12195
WANG, J. S. N84-12997
WANG, S. N84-12558
WANG, S. G. N84-12422
WANG, Z. N84-12637
WARD, J. F. N84-12259
WARDLEY, M. N84-12602
WARNSTAEDT, C. N84-12652
WARREN, R. W. N84-12481
N84-12485
WATANABE, T. N84-12911
WATTS, J. A. N84-12657
WEAVER, M. J. N84-12838
WEBB, J. D. N84-12641
WEBB, M. N84-12310
WEBBER, W. R. N84-13099
N84-13100
WEBER, H. W. N84-12394
WEBER, T. N84-12171
WEBSTER, C. N84-12642
WEHRING, B. W. N84-12947
WEILAND, C. N84-12118
WEINERT, M. N84-12872
WEISCHEDEL, R. M. N84-12771
WEISLOGEL, S. N84-12032
WEISMULLER, T. P. N94-12270
WEISSMAN, D. E. N84-12348
WEITZMAN, R. A. N84-12722
WEITZNER, H. N84-12959
WELLIS, W. J. N84-12816
WENDT, J. F. N84-12108
WENGERT, J. N84-12476
WERLE, H. N84-12107
WERMES, N. N84-12868
WESCHE, T. A. N84-12633
WEST, B. S. N84-12157
N84-12158
N84-12159
WEST, C. D. N84-12500
WESTLIN, K. L. N84-13026
WESTON, D. E. N84-12818
WETZEL, J. R. N84-12734
WETZEL, R. G. N84-12625
N84-12627
WHANG, Y. C. N84-13124
WHEELER, C. D. N84-12896
WHEELER, G. L. N84-12689
WHEELER, T. G. N84-12707
WHITCOMB, R. T. N84-12076
N84-12079
WHITE, F. A. N84-12444
WHITLOCK, R. R. N84-12486
WHITSON, J. C. N84-12961
WIBERLEY, S. E. N84-12257
WICHMANN, B. A. N84-12739
N84-12740
WICKENS, R. H. N84-12115
WIDNER, M. M. N84-12945
WIEDER, H. H. N84-12970
WIELER, J. G. N84-12691
WIENCEK, T. C. N84-12294
WILKINS, D. N84-12220
WILKINSON, D. N84-12404
WILKINSON, G. T. N84-12269
WILLIAMS, D. E. N84-12602
WILLIAMS, H. E. N84-12880
WILLIAMS, J. A. N84-12183
WILLIAMS, M. S. N84-12531
WILLIAMS, R. M. N84-12262
N84-12289
WILLIAMS, S. N84-12840
WILLIAMS, T. A. N84-12649
WILLSKY, A. S. N84-12350
WILSON, B. G. N84-12317
WILSON, C. H. N84-12620
WILSON, J. A. N84-12266
WILSON, R. K. N84-12823
WILT, B. H. N84-12161
WIMMER, W. N84-12220
WINER, K. N84-12390
WINSOR, N. K. N84-12227
WINSTON, J. G. N84-12485
WINSTON, R. N84-12902
WINTER, D. T. N84-12740
WITHBROE, G. L. N84-13071
WITMER, E. A. N84-12160
WITTIG, G. N84-12508
WOLDAI, I. N84-12593
WOLF, W. N84-13002
WOLFE, C. M. N84-12974
WOLFRAM, A. P. N84-12224
WOLVERTON, B. C. N84-12654
WONG, V. N84-12639
WOOD, G. M. N84-12444
WOODCOCK, C. E. N84-12573
WOODRUFF, G. L. N84-12884
WOODS, J. E. N84-13026
WOOLF, A. N84-12526
WOOTEN, F. N84-12390
WORMLEY, S. J. N84-12824
WRIGHT, M. H. N84-12751
N84-12752
WRIGHT, N. A. N84-12577
WRIGHT, T. P. N84-12866
WU, S. T. N84-13066
WUEST, P. N84-12069

X

XIONG, S. N84-12637

Y

YAMAGUCHI, N. N84-12913
YAMAMOTO, K. N84-12913
YANG, J. N. N84-12509

YAO, N. P. N84-12387
N84-12389
N84-12395
N84-12642
YEUNG, E. S. N84-12903
YIE, G. G. N84-12195
YIN, W. N84-12637
YIN, Y. Q. N84-12787
YIP, T. W. G. N84-12328
YOKOSAWA, A. N84-12860
YONEI, K. N84-12913
YOO, K. C. N84-12325
YORK, G. N84-12732
YOSHIHARA, H. N84-12073
N84-12075
YOUNG, E. N84-12398
YOUNG, F. C. N84-12858
YOUNG, J. P. N84-12982
YOUNG, J. T. N84-12065
YOUNG, R. T. N84-12477
YUAN, W. N84-12833
YUZHEN, Z. N84-12971

Z

ZABEL, H. N84-12273
ZABUSKY, N. J. N84-12928
ZAPATA, C. A. N84-13071
ZATSARNAYA, A. G. N84-12578
ZBASNIK, J. P. N84-12397
ZHEN-JIN, Z. N84-13093
ZHOU, Z. N84-12554
ZIESKE, P. L. N84-12692
ZIOCK, K. O. H. N84-12844
ZOHREI, M. N84-12550
ZWICK, S. A. N84-12396
ZWICKL, R. D. N84-13098
N84-13123
N84-13126

Typical Corporate Source Index Listing

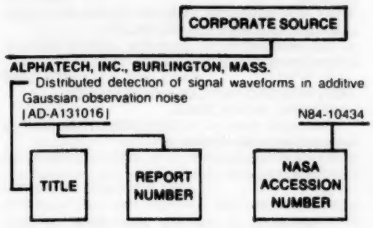

Listings in this index are arranged alphabetically by corporate source. The title of the document provides the user with a brief description of the subject matter. The report number helps to indicate the type of document cited (e.g., NASA report, translation, NASA contractor report). The NASA accession number denotes the number by which the citation is identified. The titles are arranged under each corporate source in ascending accession number order.

A

ABG-SEMCA S.A., TOULOUSE (FRANCE).
Auxiliary power units for wide-body aircraft
N84-12174

ACUREX CORP., MOUNTAIN VIEW, CALIF.
Development of mass-producible line-focus tracking concentrating solar collectors. Category 1: Collectors
[DE83-015629] N84-12639

ADELPHI UNIV., GARDEN CITY, N. Y.
Deterministic models in mathematical demography: An investigation of stable population theory including an analysis of the population statistics of Denmark
N84-12806

ADMIRALTY MARINE TECHNOLOGY ESTABLISHMENT, TEDDINGTON (ENGLAND).
Short-range acoustic intensity vectors of the Pekeris shallow water model
[AMTE(N)-TM-83065] N84-12819

ADMIRALTY UNDERWATER WEAPONS ESTABLISHMENT, PORTLAND (ENGLAND).
Turn-around loss for oceanic sound on a bottom slope
[AUWE-TN-705/83] N84-12818

ADVISORY GROUP FOR AEROSPACE RESEARCH AND DEVELOPMENT, NEUILLY-SUR-SEINE (FRANCE).
Some trends in airship technology developments
[AGARD-R-717] N84-12050
Integration of Fire Control, Flight Control and Propulsion Control Systems
[AGARD-CP-349] N84-12056
Special Course on Subsonic/Transonic Aerodynamic Interference for Aircraft
[AGARD-R-712] N84-12072
Aerodynamics of Vortical Type Flows in Three Dimensions
[AGARD-CP-342] N84-12099
Auxiliary Power Systems
[AGARD-CP-352] N84-12168
The Performance of Antennas in Their Operational Environment
[AGARD-LS-131] N84-12367

AEG-TELEFUNKEN, ULM (WEST GERMANY).
Applications of analog Change Coupled Devices (CCD's)
[BMFT-FB-T-83-141] N84-13002

AERONAUTICAL RESEARCH INST. OF SWEDEN, BROMMA.
Numerical solutions of the Euler equations simulating vortex flows around wings N84-12120

AERONAUTICAL RESEARCH INST. OF SWEDEN, STOCKHOLM.
Fatigue of fiber composites
[FFA-TN-1983-30] N84-12260
An X-ray radiography study of delamination growth in notched carbon/epoxy laminates
[FFA-TN-1983-29] N84-12516
Gust structure and gust statistics. Results from an analysis of atmospheric turbulence measurements by using conditional sampling technique
[FFA-TN-1983-28] N84-12696

AERONAUTICAL RESEARCH LABS., MELBOURNE (AUSTRALIA).
A review of Australian investigations on aeronautical fatigue during the period April 1981 to March 1983
[AD-A130968] N84-12532
Maximum likelihood estimation of linear dynamic system parameters
[AR-002-934] N84-12780

AEROSPACE CORP., EL SEGUNDO, CALIF.
The Mimas ghost revisited: An analysis of the electron flux and electron microsignatures observed in the vicinity of Mimas at Saturn
[NASA-CR-174596] N84-13056

AIR FORCE ARMAMENT LAB., EGLIN AFB, FLA.
Hypervelocity missile: Based on the concept of aircraft/missile integration for maximum firepower
N84-12058

AIR FORCE FLIGHT DYNAMICS LAB., WRIGHT-PATTERSON AFB, OHIO.
Design and development of the multifunction flight control reference system N84-12065

AIR FORCE GEOPHYSICS LAB., HANSCOM AFB, MASS.
A balloon design for 9000 pounds at 90,000 feet: Recommendations based on heavy-load balloon history
[AD-A131987] N84-12093
Preliminary data processing plan for the thermal plasma experiment on the HILAT satellite
[AD-A132017] N84-12209
Orbiting geophysics laboratory experiment
[AD-A131950] N84-12218
Properties of the neutral density and composition in the thermosphere
[AD-A131557] N84-12665
Variability of atmospheric density in the middle atmosphere
[AD-A131965] N84-12667
Wind-speed extremes in the Northern Hemisphere, 30 through 60 km
[AD-A132019] N84-12682
Winds: Chapter 6, 1983 revision. Handbook of Geophysics and Space Environments
[AD-A132018] N84-12683
Evaluation of automated imagery analysis algorithms for use in the three-dimensional nephanalysis model at AFGWC (Air Force Global Weather Central)
[AD-A131966] N84-12686
Snow characterization instruments
[AD-A131984] N84-12687
Absolute collisional excitation cross section measurements using crossed molecular beams
[AD-A132038] N84-12830
Electron beam trajectory in a photometer field of view
[AD-A131949] N84-12831
The far infrared sky survey experiment
[AD-A131968] N84-13037

AIR FORCE SYSTEMS COMMAND, WRIGHT-PATTERSON AFB, OHIO.
Acta Aeronautica et Astronautica Sinica
[AD-A131828] N84-12055
Journal of the Chinese Society of Astronautics (selected articles)
[AD-A131881] N84-12212
Trends in the development of teleinformatics
[AD-A131067] N84-12338
Telecommunications (selected articles)
[AD-A131872] N84-12346
From launching carrier rockets towards the Pacific on the accomplishments and problems of electronic technologies in our country
[AD-A131088] N84-12380
Scientific-Technical Conference on Acyclic Electric Machines
[AD-A131880] N84-12381
Synchronous generators with superconductive excitation windings
[AD-A131832] N84-12382
Unipolar machine with superconductive excitation winding
[AD-A131820] N84-12383
Acta Mechanica Sinica (selected articles)
[AD-A131871] N84-12422
Discussion of static pressure liquid-floated gyros
[AD-A131874] N84-12451
Laser journal (selected articles)
[AD-A131886] N84-12465
Steam turbine as unipolar generator
[AD-A131142] N84-12498
Storage of energy in magnetic field of superconductive coils
[AD-A131896] N84-12636
Transactions of the Chinese Solar Energy Society (selected articles)
[AD-A131870] N84-12637
Processing elements
[AD-A131068] N84-12743
Ukrainian Physics Journal (selected articles)
[AD-A131067] N84-12814
The possibility of amplifying infrared radiation by high-pressure reacting gas
[AD-A131066] N84-12890
The growth and measurement of single-crystal doped GGG (Gd3-xCaxGa5-xZn012)
[AD-A131875] N84-12971
Horizons of technology (selected articles)
[AD-A131897] N84-13135

AIR FORCE WEAPONS LAB., KIRTLAND AFB, N. MEX.
Pulsed power bibliography. Volume 2: Annotated bibliography
[AD-A131753] N84-12468
Pulsed power bibliography. Volume 1: Indices
[AD-A131752] N84-12469

AIR FORCE WRIGHT AERONAUTICAL LABS., WRIGHT-PATTERSON AFB, OHIO.
AFWAL FY82 technical accomplishments
[AD-A131639] N84-12054
A comparison of manual and vocal response modes for the control of aircraft subsystems
[AD-A132048] N84-12152
Flightline thermal environment testing of F-111 transparencies
[AD-A131642] N84-12163
Development and flight test of an active flutter suppression system for the F-4F with stores. Part 3. Flight demonstration of the active flutter suppression system
[AD-A131972] N84-12191
Utility of the cortical evoked response as a measure of photographic image quality
[AD-A131679] N84-12455
Improving NDE (Non-destructive evaluation) capability through multiple inspection with application to gas turbine engine disks
[AD-A131762] N84-12509
The study of thin films on semi-insulating gallium arsenide by ellipsometry
[AD-A131844] N84-12972

AIRCRAFT RESEARCH ASSOCIATION LTD., BEDFORD (ENGLAND).
Aerodynamic interference: A general overview
N84-12080
External stores interference N84-12083

AKRON UNIV., OHIO.
Failure processes in elastomers at or near a rigid spherical inclusion
[AD-A132060] N84-12314

ALABAMA UNIV., HUNTSVILLE.
Preliminary studies of Solar Advance Observatory and Solar Beacon Facility
[NASA-CR-170937] N84-13066

ALASKA UNIV., FAIRBANKS.
Solar wind distrubances in th outer heliosphere caused by successive solar flares from the same active region
N84-13104

ALBANY INTERNATIONAL CORP., DEDHAM, MASS.
Seamless collapsible fuel tanks
[AD-A131933] N84-12496

ALPHATECH, INC., BURLINGTON, MASS.
Tracking theory for airborne surveillance radars
[AD-A131792] N84-12350
AMES LAB., IOWA.
Progress on ultrasonic flaw sizing in turbine-engine rotor components: Bore and web geometries
[DE83-018081] N84-12167
Piston-displacement equations of state for sodium, potassium, and rubidium metals to 20 kbar from 300 K to 4 K
[DE83-018079] N84-12252
Amorphous silicon-carbon films
[DE83-018077] N84-12259
Phonon dispersion of transverse basal-plane modes in alkali-graphite compounds
[DE83-003910] N84-12273
Equations of state for the alkali metals, with generalizations to NaCl
[DE83-018075] N84-12280
Atmospheric-pressure argon afterglows as a detector for gas chromatography
[DE83-017695] N84-12282
Life prediction under stress corrosion conditions below K sub ISCC
[DE83-018074] N84-12307
Effects of dissipation in one-dimensional inverse problems
[DE83-017692] N84-12353
Inverse born approximation: Exact determination of shape of convex voids
[DE83-017685] N84-12512
Elastic-wave inverse scattering in non-destructive evaluation
[DE83-017683] N84-12513
Inference of fatigue-crack closure stresses from ultrasonic-transmission measurements
[DE83-017684] N84-12547
Computational tool for the design of ultrasonic systems
[DE83-018092] N84-12824
Analytic diffraction corrections to ultrasonic scattering measurements
[DE83-018080] N84-12825
Measurements of ultrasonic scattering from near-surface flaws
[DE83-017693] N84-12827
New developments and oppotunities for NMR in metal-hydrogen systems
[DE83-017696] N84-12864
Ultrasensitive optical rotation and refractive-index measurements
[DE83-018078] N84-12903
Sputtered C-axis inclined piezoelectric films and shear-wave resonators
[DE83-017253] N84-12997
ANALYTIC SCIENCES CORP., READING, MASS.
The effect of coordinate system rotation on spherical harmonic expansions: A numerical method
[AD-A131974] N84-12785
ANALYTICAL METHODS, INC., BELLEVUE, WASH.
Predicting aerodynamic characteristics of vortical flows on three-dimensional configurations using a surface-singularity panel method N84-12112
ANALYTICAL SYSTEMS ENGINEERING CORP., BURLINGTON, MASS.
Engineering services in support of the AFGL sounding rocket program
[AD-A131929] N84-12211
ANRADEX LTD., SAN FRANCISCO, CALIF.
Tailoring polymer films for solar-collection use, phase 1
[DE83-018117] N84-12640
APPLIED PHYSICS LAB., JOHNS HOPKINS UNIV., LAUREL, MD.
Spatial variation of iron abundance in the high speed solar wind, 1972 to 1976 N84-13113
ARGONNE NATIONAL LAB., IDAHO FALLS, IDAHO.
Automated reasoning in man-machine control systems
[DE83-014307] N84-12774
ARGONNE NATIONAL LAB., ILL.
New approach to the generation of metal-bearing, medium-pore, shape-selective zeolites for Fischer-Tropsch catalysis: Spectroscopic studies of zeolites
[DE83-014344] N84-12254
High-sensitivity mass spectrometry with a tandem accelerator
[DE83-017914] N84-12274
Study of chromium-free and chromium-reduced steels
[DE83-016717] N84-12294
Corrosion behavior of Fe-Cr-Ni-Zr alloys in aggressive environments at high temperatures
[DE83-014735] N84-12297
Breakaway corrosion in mixed-gas environments
[DE83-014704] N84-12299
Self-pumping impurity by in-situ metal deposition
[DE83-017937] N84-12306
Engineering hot-cell windows for radiation protection
[DE83-014675] N84-12319
Diffusion mass transfer of KOH through Ni/Zn battery membrane separators
[DE83-014551] N84-12387
Charge characteristics of Ni/Fe traction cells
[DE83-014205] N84-12389
Spallation and 14-MeV neutron irradiation of stabilized NbTi superconductors
[DE83-017973] N84-12394
Comparative response of lead-acid and nickel-iron batteries to pulsed and constant-current loads
[DE83-017939] N84-12395
Solid-oxide fuel-cell performance
[DE83-017926] N84-12396
Development in reliability models and methods
[DE83-014683] N84-12511
Analytical response of concrete structures subjected to high temperatures
[DE83-009625] N84-12538
Endochronic theory of dynamic viscoplasticity
[DE83-017531] N84-12546
Ragone characteristics of aqueous mobile batteries and their application in projecting ranges of electric vehicles
[DE83-014701] N84-12642
Measurements, in vivo, of parameters of the dopamine system
[DE83-017964] N84-12709
Applied mathematical sciences research at Argonne
[DE83-3014268] N84-12788
Estimation of the ridge constant: An approach based on the condition index
[DE83-017955] N84-12805
Novel interactions of the charge-balancing cations with framework defects and trapped hydrogen atoms in holmium-exchanged Y zeolites
[DE83-014204] N84-12839
The 100% alignment of hydrogen excited states in beam-foil spectroscopy
[DE83-017963] N84-12859
Nucleon-nucleon interactions and polarized-beam (both proton and antiproton) facilities at LAMPF 2
[DE83-017215] N84-12860
Hadron-hadron collider group
[DE83-010704] N84-12865
Structure of convective surface deposits and effect on MHD steam-plant design
[DE83-010757] N84-12931
Tokamak fusion reactors with less than full tritium breeding
[DE83-016711] N84-12936
Energy use and range of electric vehicles in selected US Department of Energy sites
[DE83-015719] N84-13034
ARIZONA STATE OFFICE OF ECONCMIC PLANNING AND DEVELOPMENT, PHOENIX.
Arizona State science, engineering and technology process
[PB83-237107] N84-13016
ARIZONA STATE UNIV., TEMPE.
Hydrodynamic simulations of a combined hydrogen, helium thermonuclear runaway on a 10 km neutron star
[DE83-012658] N84-13047
Galilean satellite geomorphology
[NASA-CR-174574] N84-13057
ARMY AEROMEDICAL RESEARCH LAB., FORT RUCKER, ALA.
Extent of hearing loss among Army aviators at Fort Rucker, Alabama
[AD-A132069] N84-12714
ARMY COLD REGIONS RESEARCH AND ENGINEERING LAB., HANOVER, N. H.
Detection of cavities under concrete pavement
[AD-A131851] N84-12331
Predicting lake ice decay
[AD-A132012] N84-12618
Mechanical behavior of sea ice
[AD-A131852] N84-12619
Snow cover and meteorology at Allagash, Maine, 1977 - 1980
[AD-A132013] N84-12684
Proceedings of 1st International Workshop on Atmospheric Icing of Structures
[AD-A131869] N84-12690
ARMY COMMAND AND GENERAL STAFF COLL., FORT LEAVENWORTH, KANSAS.
Physical fitness as a moderator of cognitive degradation during sleep deprivation
[AD-A131962] N84-12718
ARMY ENGINEER WATERWAYS EXPERIMENT STATION, VICKSBURG, MISS.
Poststorm reconnaissance of Tropical Storm Chris
[AD-A131948] N84-12688
ARMY MATERIALS AND MECHANICS RESEARCH CENTER, WATERTOWN, MASS.
The analysis of crack growth data with application to trip steel
[AD-A132021] N84-12535
ARMY RESEARCH AND TECHNOLOGY LABS., MOFFETT FIELD, CALIF.
Design considerations for bearingless rotor hubs
[AD-A131660] N84-12162
Application of the small body pressure transducer
[AD-A131733] N84-12454
ARMY RESEARCH INST. FOR THE BEHAVIORAL AND SOCIAL SCIENCES, ARLINGTON, VA.
An investigation of geometric radar shapes for stereotyping
[AD-A131120] N84-13020
ARMY RESEARCH INST. OF ENVIRONMENTAL MEDICINE, NATICK, MASS.
Naloxone does not affect ventilatory responses to hypoxia and hypercapnia in rats
[AD-A131836] N84-12708
Effect of atropine on the exercise-heat performance of man
[AD-A131843] N84-12719
Effectiveness in reducing heat stress of three conditioned-air cooling vests worn with and without cooling air supplied to a face piece
[AD-A131975] N84-12726
ARMY SAFETY CENTER, FORT RUCKER, ALA.
Lessons learned from FY82 US Army aviation mishaps
[AD-A131725] N84-12137
ARMY TEST AND EVALUATION COMMAND, ABERDEEN PROVING GROUND, MD.
Test operations procedure: Absolute altimeters
[AD-A131746] N84-12165
ARMY TROOP SUPPORT AND AVIATION MATERIEL READINESS COMMAND, CORPUS CHRISTI, TEX.
150 hour engine test of corrosion inhibited MIL-L-23699C oil
[AD-A131633] N84-12317
ARNOLD ENGINEERING DEVELOPMENT CENTER, ARNOLD AIR FORCE STATION, TENN.
Determination of the uncertainty of experimental heat-flux calibrations
[AD-A131918] N84-12450
Numerical solution of the three-dimensional unsteady Euler equations
[AD-A132034] N84-12783
AUSTRALIAN OCEANOGRAPHIC DATA CENTRE, NORTH SYDNEY.
Australian Oceanographic Data Centre bulletin 16
[AD-A132002] N84-12701
AUXILEC S.A., COLOMBUS (FRANCE).
The 400 Hz generators evolution, effects on installation arrangements N84-12186
AVCO-EVERETT RESEARCH LAB., MASS.
Turbulence environment characterization
[AD-A131815] N84-12692
AVIONS MARCEL DASSAULT, SAINT-CLOUD (FRANCE).
Effects of integrated maintenance on the definitions of onboard equipments N84-12068
Hydraulic generation of auxilliary power for the Mirage 2000 aircraft N84-12176

B

BALLISTIC RESEARCH LABS., ABERDEEN PROVING GROUND, MD.
A theoretical and experimental investigation of a transonic projectile flow field
[AD-A131938] N84-12094
Experimental and computational modeling of rarefaction wave eliminators suitable for the BRL 2.44 m shock tube
[AD-A131894] N84-12194
Laser spectroscopy of propellant-like flames
[AD-A132042] N84-12267
Unsteady compressible laminar boundary-layer flow within an expansion wave
[AD-A131889] N84-12420
Procedures for the transfer of data files between the BRL CYBER computer system and the IBD Hewlett-Packard minicomputer network
[AD-A132063] N84-12731
A computer subroutine for evaluating polygamma functions for complex arguments
[AD-A131936] N84-12744
BATTELLE COLUMBUS LABS., OHIO.
Walk-through survey report: Control technology for integrated circuit fabrication, Xerox Corporation, El Segundo, California.
[PB83-239053] N84-12333

BAYERISCHE AKADEMIE DER WISSENSCHAFTEN, MUNICH (WEST GERMANY).
Investigation of mathematical models to combine a terrestrial network with a satellite network
[SER-C-274] N84-12554
Accuracy of gravimetrically determined absolute and relative geoid heights
[SER-A-97] N84-12661
BDM CORP., MCLEAN, VA.
Rapid runway repair program subtask 1.07 - rapid concrete cutting
[AD-A131771] N84-12195
BELFOTOP P.V.B.A., WEMMEL (BELGIUM).
Inventory of Flemish forests using medium-scale Color Infrared (CIR) photography and CIR orthophotoplans as base for a forest management data bank N84-12614
BEND RESEARCH, INC., OREG.
Novel composite membranes
[PB83-243170] N84-12284
BERGEN UNIV. (NORWAY).
Application of remote sensing for studies, mapping and forecasting of eddies on the Norwegian continental shelf N84-12605
BERN UNIV. (SWITZERLAND).
Mixed solar wind originating from coronal regions of different temperatures N84-13114
BIOTECHNOLOGY, INC., FALLS CHURCH, VA.
A flight investigation of simulated data link communications during single-pilot IFR flight N84-12046
BODENSEEWERK GERAETETECHNIK G.M.B.H., UEBERLINGEN (WEST GERMANY).
An integrated AFCS for the "PROFILE"-mode N84-12069
BOEING AEROSPACE CO., SEATTLE, WASH.
Study of auxiliary propulsion requirements for large space systems. Volume 1: Executive summary
[NASA-CR-168193] N84-12226
Integrated Cuing Requirements (ICR) study: Demonstration data base and users guide
[AD-A131119] N84-13019
BOEING CO., SEATTLE, WASH.
Subsonic/Transonic Aerodynamic Interference for Aircraft: Introductory remarks N84-12073
Subsonic/transonic viscous interactions N84-12075
BOEING COMMERCIAL AIRPLANE CO., SEATTLE, WASH.
Aerodynamic design for overall vehicle performance N84-12077
Interference problems in aircraft design N84-12084
BONN UNIV. (WEST GERMANY).
Theory of interstellar medium diagnostics N84-13108
Minor constituents in the solar wind originating from plasma-dust interactions N84-13116
BOSTON COLL., CHESTNUT HILL, MASS.
Chemiluminescence and laser induced fluorescence of boron atom reactions
[AD-A131709] N84-12471
Strong coupling effects on bound states in plasmas
[AD-A131661] N84-12918
Solar wind variations in the 60-100 year period range: A review N84-13092
BRITISH AEROSPACE AIRCRAFT GROUP, BROUGH (ENGLAND).
The integration of flight and engine control for VSTOL aircraft N84-12070
Secondary power supplies for a small single engine combat aircraft N84-12175
BRITISH AEROSPACE AIRCRAFT GROUP, PRESTON (ENGLAND).
Transonic configuration design (fighter) N84-12082
Engine-airframe interference effects N84-12086
Optimization of engine power offtake by secondary power system design N84-12177
BRITISH AEROSPACE PUBLIC LTD. CO., LANCASHIRE (ENGLAND).
Integrated powerplant control systems and potential performance benefits N84-12063
BROOKHAVEN NATIONAL LAB., UPTON, N. Y.
Advanced technologies for the recovery, disposal, and reuse of carbon dioxide for atmospheric control
[DE83-016371] N84-12256
Formation of free hydrogen during radiolysis in a bed of clay
[DE83-017724] N84-12275
A high-performance digital triggering system for phase-controlled rectifiers
[DE83-012217] N84-12386
Problem of magnet ramping
[DE83-014054] N84-12399
Ground coupled heat-pump-system experimental results
[DE83-014011] N84-12427
The effect of moisture on the physical and durability properties of methyl methacrylate polymer concrete
[DE83-016733] N84-12541
Universality and fractal dimension of mode locking structure in systems with competing periodicities
[DE83-017352] N84-12545
Uses of synchrotron radiation
[DE83-014431] N84-12720
High-level control programs at NSLS
[DE83-010935] N84-12754
Helium-flow measurement using ultrasonic technique
[DE83-017765] N84-12826
Progress in lattice gauge theory
[DE83-014055] N84-12862
Hadron-hadron collider group
[DE83-010704] N84-12865
Assessment of TRAC-PF1 and RELAP5/MOD1 codes with GE large-vessel blowdown test
[DE83-015384] N84-12874
Operation of the Brookhaven MPS Facility
[DE83-015383] N84-12896
Inertial fusion with low-energy heavy ions
[DE83-016709] N84-12934
Commensurability, chaos, and the devil's staircase
[DE83-013280] N84-12987
Temperature dependence of the electric-field gradient in Er metal
[DE83-015564] N84-12989
BROWN BOVERI RESEARCH CENTER, BADEN (SWITZERLAND).
Vortex breakdown: A two-stage transition N84-12124
BROWN UNIV., PROVIDENCE, R. I.
A pressure-shear experiment for studying the dynamic plastic responses of metals at shear strain rates of 10 to the 5th power s(-1) N84-12519
Plastic deformations of a portable frame under short pulse loading on one column by an approximate method including effects of elasticity and plastic rate sensitivity N84-12521
Hadron-hadron collider group
[DE83-010704] N84-12865
BUNDESMINISTERIUM DER VERTEIDIGUNG, BONN (WEST GERMANY).
Auxiliary power requirements: Their role in aircraft performance N84-12169
BUNDESWEHR MUNICH UNIV., NEUBIBERG (WEST GERMANY).
Interaction of antennas with masts under special consideration of the sensitivity and nonlinear effects in ship borne receiving systems N84-12371
BURKES (T. R.), INC., LUBBOCK, TEX.
Solid state copper vapor laser modulator
[DE83-015837] N84-12475

C

CALIFORNIA INST. OF TECH., PASADENA.
The Owens Valley frequency-agile interferometer
[AD-A131825] N84-12453
The relative abundances of Sn, Te, Xe, Ba and Ce
[NASA-CR-174599] N84-13064
Temporal variations of the anomalous oxygen component N84-13099
Voyager measurements of the energy spectrum, charge composition, and long term temporal variations of the anomalous components in 1977-1982 N84-13100
CALIFORNIA UNIV., BERKELEY.
Combustion jet ignition N84-12188
System identification of structures with joint rotation N84-12330
Theoretical and experimental investigation of turbulent premixed flames N84-12409
Convection in horizontal porous media with different end temperatures N84-12438
Steady laminar natural convection in open rectangular cavities N84-12441
Some bifurcation topics in non-linear elastostatics N84-12524
Mechanical response of fluid-filled poroelastic solids N84-12525
Environments and search paths for the software tools
[DE83-016607] N84-12749
Second order partial differential equations of mixed type N84-12775
CALIFORNIA UNIV., BERKELEY. LAWRENCE BERKELEY LAB.
Research activities in materials and molecular research
[DE83-015005] N84-12255
Influence of heat-treatment and physicochemical properties on the electrochemical oxidation of carbon blacks in phosphoric acid
[DE83-017744] N84-12276
Photothermal displacement spectroscopy of surfaces and thin films
[DE83-015957] N84-12279
Self-correction coil: Operation mechanism of self-correction coil
[DE83-016324] N84-12392
Evaluation of the Beijing Instrument Factory GDB-44F photomultiplier
[DE84-000849] N84-12398
Comparison of technologies for new energy-efficient lamps
[DE83-015949] N84-12401
Development of a continuous monitor for detection of toxic organic compounds
[PB83-234922] N84-12461
Experimental studies relating environmental lighting and flicker to visual fatigue in VDT operators
[DE83-016316] N84-12736
Statistical calculation of complete events in medium-energy nuclear collisions
[DE83-015951] N84-12847
Quark-gluon plasma formation
[DE83-017742] N84-12861
New statistical and non-statistical effects in deep inelastic heavy-ion collisions
[DE83-015732] N84-12865
Efficient radiation-hardened, 400- and 800-keV neutral-beam injection systems
[DE83-015691] N84-12886
Novel method for the study of optical properties of surfaces
[DE83-012899] N84-12895
A 2-D skin-current toroidal-MHD-equilibrium code
[DE83-016916] N84-12929
Optical properties and correlation energy of defects in a-Ge:H
[DE83-016697] N84-12993
Phonon-induced enhancements of the energy gap and critical current in superconducting aluminum
[DE83-015210] N84-12996
Applications of molecular quantum mechanics to problems in chemistry
[DE83-015943] N84-13003
CALIFORNIA UNIV., DAVIS.
Transmission of fast neutrons from the Li(d,xn) reaction through thick iron
[DE83-015975] N84-12884
CALIFORNIA UNIV., IRVINE.
Modeling of transient disturbances in coronal-streamer configurations N84-13119
CALIFORNIA UNIV., LIVERMORE. LAWRENCE LIVERMORE LAB.
Lithium equation-of-state
[DE83-017988] N84-12253
Erosive particle kinematics in the turbulent combustion boundary layer contacting a solid wall
[DE83-010594] N84-12272
Evaluation of several high-strength copper sheet alloys
[DE83-015612] N84-12298
Using an X-ray-sensitive vidicon and remote-control stage mechanism to obtain critical radiographic alignment of small explosive devices
[DE83-012846] N84-12326
Physical modeling of EM propagation over nonhomgeneous terrain N84-12370
Numerical modeling techniques for antennas N84-12373
Numerical modeling techniques for half-space (ground) problems N84-12374
Structure and vibrational spectra of a model of a-Si:H with periodic boundary conditions
[DE83-015245] N84-12390
Advanced high-field coil designs: 20 Tesla
[DE83-017368] N84-12397
Damage thresholds of thin film materials and high reflectors at 248 nm
[DE83-012683] N84-12472
Windows and mirrors needed for a laser-driven photoneutralizer
[DE83-013582] N84-12473
Experiments to study the feasibility of making an X-ray laser at the Novette laser facility
[DE83-015615] N84-12476
Inertial effects in laser-driven ablation
[DE83-016941] N84-12478
Feasibility of a laser or charged-particle-beam fusion-reactor concept with direct electric generation by magnetic-flux compression
[DE83-015735] N84-12482
Creation of ultra-high-pressure shocks by the collision of laser-accelerated disks: Experiment and theory
[DE83-017366] N84-12486
Initial assessment of the MHD stability of TMX-U
[DE83-016521] N84-12646
Praxis language environment: Distribution-package description
[DE83-017546] N84-12750

Lecture notes for contact-impact algorithms for large-deformation finite-element analysis
[DE83-013039] N84-12789
Theoretical and experimental studies of shock-compressed benzene and polybutene
[DE83-015864] N84-12816
Magnetic switching
[DE83-012952] N84-12841
Measurements of the emittance and current density profile of the beam produced by the ATA injector
[DE83-016522] N84-12848
Hazards Control Department annual technology review, 1982
[DE83-015598] N84-12883
Generation of monoenergetic positrons
[DE83-015535] N84-12887
Process, product, and waste-stream monitoring with fiber optics
[DE83-01102] N84-12899
Fabrication of machined optics for precision applications
[DE83-015720] N84-12900
Recent results in the Los Alamos compact torus program
[DE83-014147] N84-12930
Fokker-Planck equation in mirror research
[DE83-016568] N84-12932
Time-resolved spectral measurements above 80 A
[DE83-015616] N84-12933
Summary of the MARS tandem-mirror reactor design
[DE83-017293] N84-12939
Three-dimensional equilibrium in quadrupole symmetric tandem mirrors in the paraxial limit (reduced MHD)
[DE83-017840] N84-12940
Vacuum measurements on the tandem mirror experiment upgrade (TMX-U) fusion experiment
[DE83-017836] N84-12946
Status of tandem-mirror confinement
[DE83-017369] N84-12948
Thermal barriers: Their purpose and functioning
[DE83-017385] N84-12954
TMX-U experimental results
[DE83-016790] N84-12955
Multidipole magnetic fields for plasma confinement
[DE83-016014] N84-12960
Review of some recent theoretical calculations of phase transitions and comparisons with experimental results
[DE83-015863] N84-12983
Characterization by X-ray topography of laser-induced damage in potassium dihydrogen phosphate crystals
[DE83-012045] N84-12985
Thermal performance of the MFTF magnets
[DE83-016275] N84-12988
Methods for deconvoluting and interpreting complex gammaand X-ray spectral regions
[DE83-013585] N84-12991
Revitalization: An organizational program for the individual
[DE83-014949] N84-13013

CALIFORNIA UNIV., LOS ANGELES.
Time-resolved laser studies on the energy transfer and the configurational changes in bacteriohodopsin
[DE83-015708] N84-12487
Solar cycle variations of the solar wind N84-13089
Multiple spacecraft observations of interplanetary shocks: Characteristics of the upstream ULF turbulence N84-13097

CALIFORNIA UNIV., SAN DIEGO.
Silicide formation and Schottky barrier of rare-earth metals on Si
[AD-A131750] N84-12975
Silicide formation and Schottky barrier of rare-earth metals on Si
[AD-A131749] N84-12976
Silicide formation and Schottky barrier of rare-earth metals on Si
[AD-A131748] N84-12977

CALIFORNIA UNIV., SAN DIEGO, LA JOLLA.
Surface and interfacial properties of Ga(0.47) In(0.53) As alloys
[AD-A131925] N84-12970
Empirical validation of computer models for passive-solar residences
[DE83-016887] N84-13005
Solar cycle evolution of the solar wind in three dimensions N84-13090

CALSPAN FIELD SERVICES, INC., ARNOLD AIR FORCE STATION, TENN.
Space Shuttle external interference heating test
[AD-A131688] N84-12215

CAMBRIDGE HYDRODYNAMICS, INC., MASS.
Boundary-integral simulations of rayleigh-taylor instability in ideal magnetohydrodynamics
[AD-A131667] N84-12920

CANADA CENTRE FOR REMOTE SENSING, OTTAWA (ONTARIO).
Remote sensing using the airborne MEIS 2 multidetector electro optical imaging scanner N84-12592

CANADA INST. FOR SCIENTIFIC AND TECHNICAL INFORMATION, OTTAWA (ONTARIO).
Handbook on the determination of the physical, thermal and mechanical properties of frozen soils
[NRC/CNR-TT-2064] N84-12578

CARNEGIE-MELLON UNIV., PITTSBURGH, PA.
Software voting in asynchronous NMR (N-Modular Redundancy) computer structures
[NASA-CR-174488] N84-12732
Disjunctive programming and a hierarchy of relaxations for discrete optimization problems
[AD-A132004] N84-12784
A program of research on microfabrication techniques for VLSI magnetic devices
[AD-A131706] N84-12978

CATANIA UNIV. (ITALY).
Remote sensing analysis of oil pollution in Augusta Bay, Sicily N84-12616

CATHOLIC UNIV. OF AMERICA, WASHINGTON, D.C.
Corotating shocks in inner heliosphere N84-13124

CENTEC CONSULTANTS, INC., RESTON, VA.
Assessment of energy-efficiency improvements for paint spray booths
[DE83-016680] N84-12320

CENTRE D'ETUDES TECHNIQUES DE L'EQUIPMENT, AIX-EN-PROVENCE (FRANCE).
Operational utilization of remote sensing in a study of the impact of disposal of urban waste at sea N84-12611

CENTRE DE RECHERCHES EN PHYSIQUE DE L'ENVIRONNEMENT, ISSY-LES-MOULINEAUX (FRANCE).
Radar investigation of soils and sea (ERASME): C band helicopter-borne scatterometer. Application to soil moisture measurement N84-12588

CENTRE NATIONAL DE LA RECHERCHE SCIENTIFIQUE, ORLEANS (FRANCE).
Activities report of the Laboratory of Environmental Physics and Chemistry N84-12963

CENTRE NATIONAL DE LA RECHERCHE SCIENTIFIQUE, VERRIERES-LE-BUISSON (FRANCE).
Remote sensing instruments for trace species measurements in the troposphere and stratosphere: A review N84-12583

CENTRE NATIONAL POUR L'EXPLOITATION DES OCEANS, BREST (FRANCE).
Application of high resolution satellite data to coastal zones: SPOT simulations during ecological survey of the Britanny coast N84-12591

CER CORP., LAS VEGAS, NEV.
Geologic study of the Wind River Basin, Fremont and Natrona Counties, central Wyoming
[PB83-254912] N84-12677

CHALMERS UNIV. OF TECHNOLOGY, GOTEBORG (SWEDEN).
Branching processes in periodically varying environment
[CTH-MATH-1983-12-PREPRINT] N84-12792
On space-time means and everywhere defined scattering operators for nonlinear Klein-Gordon equations
[CTH-MATH-1983-13-PREPRINT] N84-12793

CHICAGO UNIV., ILL.
Measurements, in vivo, of parameters of the dopamine system
[DE83-017964] N84-12709
Fundamentals and techniques of nonimaging optics, volume 2
[DE83-015447] N84-12902
Direct coronal heating from dissipation of magnetic field N84-13069

CHINESE ACADEMY OF SCIENCES, PEKING.
Periodicities in the occurrence of aurora as indicators of solar variability N84-13093

CHRYSLER CORP., NEW ORLEANS, LA.
Test report for MSFC test 83-2. Pressure scaled water impact test of a 12.5 inch diameter model of the Space Shuttle Solid Rocket booster filament wound case and external TVC pod
[NASA-CR-174601] N84-12217

CITY COLL. OF THE CITY UNIV. OF NEW YORK.
Acquisition, image and data compression
[AD-A131923] N84-12344
Semiconductors investigated by time resolved raman absorption and photoluminescence spectroscopy using femtosecond and picosecond laser techniques
[AD-A131860] N84-12466

CLARKSON COLL. OF TECHNOLOGY, POTSDAM, N.Y.
The AGCE related studies of baroclinic flows in spherical geometry
[NASA-CR-170934] N84-12415

COLLEGE OF WILLIAM AND MARY, WILLIAMSBURG, VA.
Theory of hydromagnetic turbulence N84-13077

COLORADO STATE UNIV., FORT COLLINS.
Novel techniques for enhanced reflectivity infrared mirrors
[AD-A131924] N84-12894
Growth and characterization of InP and InGaAs films using the hydride VPE technique
[AD-A131841] N84-12973

COLORADO UNIV., BOULDER.
Low energy nuclear physics and accelerator development
[DE83-013384] N84-12877
A study of depletion in low-velocity diffuse interstellar gas N84-13042
Observational evidence for solar wind acceleration at the base of coronal holes N84-13082
Ultraviolet extinction properties of grains in the interstellar medium N84-13131

COLUMBIA UNIV., NEW YORK.
Hadron-hadron collider group
[DE83-010704] N84-12865
Defect interactions at high concentrations in solid oxide electrolytes
[DE83-016849] N84-12992

COMMITTEE ON COMMERCE, SCIENCE, AND TRANSPORTATION (U. S. SENATE).
US weather satellites and services
[GPO-25-753] N84-12208

COMMITTEE ON SCIENCE AND TECHNOLOGY (U. S. HOUSE).
Biological clocks and shift work scheduling
[GPO-21-747] N84-12713
National Aeronautics and Space Act of 1958, as amended and related legislation
[GPO-24-491] N84-13032

COMMUNICATIONS RESEARCH CENTRE, OTTAWA (ONTARIO).
Scale modelling and full scale measurement techniques with particular reference to antennas in their operational environments N84-12368

COMMUNICATIONS SATELLITE CORP., CLARKSBURG, MD.
Calculation of ground wave attenuation over irregular, inhomogeneous, layered media using PROGRAM WAGNER N84-12369

CONCORDIA UNIV., LOYOLA CAMPUS, MONTREAL (QUEBEC).
Numerical modelling methods for predicting antenna performance on aircraft N84-12375

CONSIGLIO NAZIONALE DELLE RICERCHE, FLORENCE (ITALY).
The Istituto di Ricerca sulle Onde Elettromagnetiche (IROE)-lidar remote sensing of the environment N84-12590

CONSIGLIO NAZIONALE DELLE RICERCHE, FRASCATI (ITALY).
Interplanetary Alfvenic fluctuations: A statistical study of the directional variations of the magnetic field N84-13076

CORNELL UNIV., ITHACA, N.Y.
Vortex stability and breakdown N84-12122
Design of doubly focusing, tunable (5 - 30 keV), wide-bandpass optics made from layered synthetic microstructures
[DE83-015492] N84-12897
Spherical simulations of large scale structure in the universe N84-13052

CRANFIELD INST. OF TECH., BEDFORDSHIRE (ENGLAND).
On the generation and subsequent development of spiral vortex flow over a swept-back wing N84-12105
The effects of wing tip devices on the performance of the BAe Jetstream N84-12130
The effect of wing tip devices on the far-field wake of a Paris Aircraft N84-12131

D

DAVE (SHARAD M.), FARMINGTON HILLS, MICH.
Controlled combustion engine evaluation
[DE83-011245] N84-12499

DAYTON UNIV., OHIO.
Aircraft transparency testing methodology and evaluation criteria. Part 2: Methodology development for improved durability
[AD-A131928] N84-12157
Aircraft transparency testing methodology and evaluation criteria. Part 1: Test methods and information analysis
[AD-A131927] N84-12158
Alternate T-38 transparency development. Part 4: Parametric studies
[AD-A131904] N84-12159

Long term evaluation of the effects of shale oil produced JP-4 on aircraft construction materials
[AD-A131665] N84-12161
Mechanical property evaluation of P/M (Powder-Metallurgy) aluminum 7090-T7E71 plate
[AD-A132058] N84-12290

DEFENCE RESEARCH INFORMATION CENTRE, ORPINGTON (ENGLAND).
Non-destructive testing of non-metallic materials using microwaves
[DRIC-T-6974] N84-12508

DEFENSE TECHNICAL INFORMATION CENTER, ALEXANDRIA, VA.
Source header list, supplement 1
[AD-A131800] N84-13024

DELAWARE UNIV., NEWARK.
Prerequisites for deriving formal specifications from natural language requirements
[AD-A131722] N84-12771

DEPARTMENT OF ENERGY, BARTLESVILLE, OKLA.
Vehicle-emission characteristics using mechanically emulsified alcohol/diesel fuels
[DE83-016012] N84-12656

DEPARTMENT OF ENERGY, WASHINGTON, D. C.
New facilities for the US high-energy physics program
[DE83-016589] N84-12876

DESMATICS, INC., STATE COLLEGE, PA.
On the performance of two-stage group screening experiments
[AD-A131970] N84-12807

DEUTSCHE BUNDESPOST, DARMSTADT (WEST GERMANY).
Atenuation measurements between 840 and 1620 nm on an optical cable in Berlin
[FI-465-TBR-22] N84-12906
Liquid phase epitaxy of InP/In1-xGxAsyP1-y heterostructures. Part 3: Phase diagrams
[FI-65-TBR-20-PT-3] N84-13000

DEUTSCHE FORSCHUNGS- UND VERSUCHSANSTALT FUER LUFT- UND RAUMFAHRT, BRUNSWICK (WEST GERMANY).
A diagnosis scheme for sensors of a flight control system using analytic redundancy N84-12067
Evaluation of the stochastic drift of rate integrating gyros as preparation for the analysis of laser gyro drift measurements
[DFVLR-MITT-83-04] N84-12449

DEUTSCHE FORSCHUNGS- UND VERSUCHSANSTALT FUER LUFT- UND RAUMFAHRT, COLOGNE (WEST GERMANY).
Domestic scheduled air transport for the year 2000. Financial and capacity related effects of supply alternatives, considering, also, the cooperation with high speed rail transport services
[DFVLR-FB-83-03] N84-12141

DEUTSCHE FORSCHUNGS- UND VERSUCHSANSTALT FUER LUFT- UND RAUMFAHRT, GOETTINGEN (WEST GERMANY).
The vortex skeleton model for three-dimensional steady flows N84-12101
Separation and vortical-type flow around a prolate spheroid: Evaluation of relevant parameters N84-12113

DEUTSCHE FORSCHUNGS- UND VERSUCHSANSTALT FUER LUFT- UND RAUMFAHRT, OBERPFAFFENHOFEN (WEST GERMANY).
The simulation of a Frequency Shift Keying (FSK) diversity system
[DFVLR-FB-83-22] N84-12363
Monte Carlo computer simulation program (MCHP) supporting a covariance analysis using the STANHP program
[DFVLR-MITT-83-06] N84-12756

DEUTSCHE LUFTHANSA AKTIENGESELLSCHAFT, FRANKFURT AM MAIN (WEST GERMANY).
Activities report of the aerospace industry in West Germany N84-12139
Activities report of the aerospace industry in West Germany N84-12140

DORNIER-WERKE G.M.B.H., FRIEDRICHSHAFEN (WEST GERMANY).
Numerical solutions of the Euler equations simulating vortex flows around wings N84-12120
System definition Roentgensatellit, phase B 1.2
[BMFT-FB-W-83-010] N84-12219

DOWTY AND SMITH INDUSTRIES CONTROLS LTD., CHELTENHAM (ENGLAND).
Full authority digital electronic engine controls and their integration with flight control systems in VSTOL aircraft N84-12064

DREXEL UNIV., PHILADELPHIA, PA.
Cold sintering: A new powder consolidation process
[AD-A131687] N84-12292

DU PONT DE NEMOURS (E. I.) AND CO., AIKEN, S.C.
Hydrogen compatibility handbook for stainless steels
[DE83-017051] N84-12301
Helium damage in austenitic stainless steels
[DE83-017494] N84-12309
Grain-boundary cavitation and weld-underbead cracking in DOP-26 iridium alloy
[DE83-015406] N84-12539

DUKE UNIV., DURHAM, N. C.
Development of a data base for carbon dioxide releases resulting from conversion of land to agricultural uses
[DE83-015728] N84-12626

DUNDEE UNIV. (SCOTLAND).
Satellite remote sensing, environmental monitoring and the offshore oil and gas industries N84-12603
Normalization of water-leaving radiance obtained from the Coastal Zone Colour Scanner (CZCS) data N84-12610

DYNATEST, MUNICH (WEST GERMANY).
Control of multiaxis vibration systems N84-12203

E

ECOLE NORMALE SUPERIEURE, PARIS (FRANCE).
Contribution of satellite remote sensing to knowledge of the littoral from the mouth of the Loire to that of the Gironde (France) N84-12584

EDGERTON, GERMESHAUSEN AND GRIER, INC., GOLETA, CALIF.
Large-area mercuric iodide photodectors
[DE83-013035] N84-12898

ELECTRONICS ENGINEERING GROUP (1842ND), SCOTT AFB, ILL.
Prototype fiber optic system to remote TRACALS radar
[AD-A132073] N84-12341

EMMANUEL COLL., BOSTON, MASS.
Technique for producing a coherent sum of the data from P78-1, F2, and F4 satellites
[AD-A131965] N84-12210

ENERGIECONSULTING HEIDELBURG (WEST GERMANY).
Heating with wind energy, part B
[BMFT-FB-T-83-131-PT-B] N84-12651

ENERGY INFORMATION ADMINISTRATION, WASHINGTON, D.C.
Short-term energy outlook. Volume 2. Methodology
[DE83-016853] N84-12648

ENSCO, INC., SPRINGFIELD, VA.
Description of an automatic seismic measurements package: Analysis and design goals
[AD-A132087] N84-12666

ENVIRONMENTAL PROTECTION AGENCY, ADA, OKLA.
Velocity plots and capture zones of pumping centers for ground-water investigations
[DE83-016618] N84-12624

ENVIRONMENTAL PROTECTION AGENCY, ANN ARBOR, MICH.
A study of the relationship between exhaust emissions and fuel economy
[PB83-235564] N84-12506

ENVIRONMENTAL PROTECTION AGENCY, RESEARCH TRIANGLE PARK, N.C.
Pulmonary dosimetry of nitrogen dioxide in animals and man
[PB83-243394] N84-12711

ERNO RAUMFAHRTTECHNIK G.M.B.H., BREMEN (WEST GERMANY).
Phase A study for a test satellite for propagation and transmission experiments in the 20/30 GHz frequency band
[BMFT-FB-W-83-009] N84-12355

EROS DATA CENTER, SIOUX FALLS, S. DAK.
LANDSAT 4 investigations of thematic mapper and multispectral scanner applications
[E84-10006] N84-12555

EUROPEAN SPACE AGENCY, PARIS (FRANCE).
Flight tests for a strapdown system (MSS): The results of a special flight test
[ESA-TT-818] N84-12153
Spacecraft Vibration Testing Using Multi-Axis Hydraulic Vibration Systems
[ESA-SP-197] N84-12197
The OTS: Fifth year in orbit N84-12221
Layout of a SAR sensor for Spacelab and satellite. Part 1: Design considerations for fundamental SAR parameters
[ESA-TT-802] N84-12224
L band satellite communication experiment in the Antartic
[ESA-TT-805] N84-12356
Pulse signals in heterodyne and homodyne detection
[ESA-TT-809] N84-12357
Y03: Prequalification of surface treatment. Measurement of laser reflecting power
[ESA-TT-791] N84-12490

Remote Sensing Applications for Environmental Studies
[ESA-SP-188] N84-12579
Contributions of remote sensing satellite tracking techniques to marine environment monitoring and marine applications N84-12585
Two different aspects of phytoplankton bloom seen by satellite (CZCS) in the western English Channel N84-12604
Observation of the Earth in the middle infrared
[ESA-TT-790] N84-12629
Radar meteorology in cloud physics and radio wave propagation research
[ESA-TT-808] N84-12695
Retroreflector YO3: Study of the optical properties of protected mirrors
[ESA-TT-789] N84-12907

EUROPEAN SPACE OPERATIONS CENTER, DARMSTADT (WEST GERMANY).
Spacecraft interface design and its impact on operational support
[ESA-STR-211] N84-12220

EUROSENSE B.V., THE HAGUE (NETHERLANDS).
An operational remote sensing methodology for the detection, inventory and environmental monitoring of waste disposal sites N84-12601

EUROSENSE BELFOTOP G.M.B.H., HUERTH (WEST GERMANY).
The synthesized climatic function map N84-12617

EXXON RESEARCH AND ENGINEERING CO., BAYTON, TEX.
Combustion of EDS mid-distillate and refined shale-oil residual fuel in a gas turbine with large single-combustion chamber
[DE83-017700] N84-12281

EXXON RESEARCH AND ENGINEERING CO., LINDEN, N.J.
Microprocessor-based control system for flowing-electrolyte zinc-bromine battery systems
[DE83-012506] N84-12403

F

FEDERAL AVIATION ADMINISTRATION, ATLANTIC CITY, N.J.
Correlation of laboratory-scale fire test methods for seat blocking layer materials with large-scale test results
[AD-A131666] N84-12138

FEDERAL AVIATION ADMINISTRATION, WASHINGTON, D.C.
Information resources management plan
[AD-A131964] N84-13023

FEDERAL COMPILER TESTING CENTER, FALLS CHURCH, VA.
Northern Telecom, Incorporated NTI-585 ACOBOL/3 release 3 (COBOL technical report)
[PB83-241521] N84-12758
Northern Telecom Incorporated NTI-585 XCOBOL, release 3
[PB83-241539] N84-12759
Northern Telecom, Incorporated NTI-585 XCOBOL, release 3 (COBOL technical report)
[PB83-241547] N84-12760
Digital Equipment Corporation VAX 11/750, VAL-11 COBOL version 2.2
[PB83-241588] N84-12761
NCR Corporation NCR 9300 ITX-BASIC release 1.1
[PB83-243410] N84-12762
Computer Sciences Corporation UNIVAC 1100/80 CSTS FORTRAN, release FTN148
[PB83-243428] N84-12763
Digital Equipment Corporation, PDP-11/44 COBOL-81 version 2.0
[PB83-247734] N84-12764
Digital Equipment Corporation COBOL-81 version 2.0 (COBOL technical report)
[PB83-247742] N84-12765

FEDERAL GEODETIC CONTROL COMMITTEE, ROCKVILLE, MD.
Test and demonstration of Macrometer (TM) model V-1000 interferometric surveyor
[PB83-239103] N84-12631

FEDERAL MINISTRY FOR DEFENCE, BONN (WEST GERMANY).
Integration of fire, flight and propulsion control systems: An overview, retrospective and prospective N84-12057

FERMI NATIONAL ACCELERATOR LAB., BATAVIA, ILL.
Satellite refrigerator compressors with the oil and moisture removal systems
[DE83-016079] N84-12502
New soluble approximation to Fokker-Planck equations
[DE83-016210] N84-12791

A thousand TeV in the center of mass: Introduction to high-energy storage rings
[DE83-015649] N84-12855
Hadron-hadron collider group
[DE83-010704] N84-12865
Operational studies and expected performance of superconducting quadrupole magnets in the first stages of secondary beams
[DE83-016734] N84-12999
Evolution of the ultra high energy cosmic ray spectron by transport equation
[DE83-013711] N84-13132

FERRANTI LTD., EDINBURGH (SCOTLAND).
Some aspects of flight trajectory control in future avionic systems for combat aircraft N84-12066

FLORIDA STATE UNIV., TALLAHASSEE.
On the wind stress - sea level power law
[AD-A132035] N84-12681

FOM-INSTITUUT VOOR PLASMAFYSICA, JUTPHAAS (NETHERLANDS).
A numerical model for diffusion of helium in a hydrogen plasma
[REPT-83-147] N84-12964

FONDAZIONE UGO BORDONI, ROME (ITALY).
Reduction of structural complexity in evaluating convolutions by polynomial transforms
[FUB-59-1981] N84-12794
Economic study of long distance optical fibre links
[FUB-38-1982] N84-12908

FORWARD (ROBERT L.), OXNARD, CALIF.
Alternate propulsion energy sources
[AD-A131939] N84-12249

FREIBURG UNIV. (WEST GERMANY).
Considerations on a permanent inventory and monitoring system for European forests N84-12582
First results of the evaluations of the European SAR 580 data for agricultural and forestry purposes in test site D6, Freiburg (West Germany) N84-12599

G

GALILEO ELECTRO-OPTICS CORP., STURBRIDGE, MASS.
Evaluation of multicomponent fluoride glass candidates for double crucible drawn optical fiber
[AD-A131932] N84-12893

GARRETT TURBINE ENGINE CO., PHOENIX, ARIZ.
Executive summary, aerothermal modeling program, phase 1
[NASA-CR-174602] N84-12263
Aerothermal modeling program, phase 1
[NASA-CR-168243-VOL-1] N84-12264
Aerothermal modeling program, phase 1
[NASA-CR-168243-VOL-2] N84-12265

GENERAL ATOMIC CO., SAN DIEGO, CALIF.
Hardware and software configuration of the Doublet 3 diagnostic-data-acquisition computer system
[DE83-013427] N84-12733
Comparative evaluation of existing concepts for a 10-tesla FED toroidal field coil
[DE83-012817] N84-12815
Real-time diagnostic-data-acquisition system for the Doublet 3 Tokamak fusion experiment
[DE83-015871] N84-12927
Nuclear design of a very-low-activation fusion reactor
[DE83-017470] N84-12949
Variational-moment method for computing magnetohydrodynamic equilibria
[DE83-017477] N84-12957

GENERAL ELECTRIC CO., PHILADELPHIA, PA.
New developments in composite-flywheel containment
[DE83-012583] N84-12497

GEOLOGICAL SURVEY, ALEXANDRIA, VA.
Alaska's mineral resources
[DE83-016599] N84-12623

GEOLOGICAL SURVEY, DENVER, COLO.
Compilation of selected faults and lineaments that may be relevant to a study of seismic activity in southern Nevada and part of adjacent California
[DE83-017085] N84-12673

GEOLOGICAL SURVEY, WASHINGTON, D. C.
Analysis of the world distribution of metal-rich subsea manganese nodules
[USGS-CIRC-886] N84-12577

GEOLOGICAL SURVEY OF GREENLAND, COPENHAGEN (DENMARK).
Glaciological applications of LANDSAT images in connection with hydropower investigations in West Greenland N84-12598

GEORGE WASHINGTON UNIV., WASHINGTON, D.C.
Vibration response of geometrically nonlinear elastic beams to pulse and impact loading
[NASA-CR-174495] N84-12527

GEORGIA INST. OF TECH., ATLANTA.
Study of an asymptotic method for helicopter rotor blade aerodynamic loads N84-12135
Interaction of stress waves and cracks using a second order accurate finite difference method N84-12522
A case study of gravity wave-convective storm interactions N84-12659
Ripple-reduction poloidal-field coils for Tokamak reactors
[DE83-009532] N84-12922

GESELLSCHAFT FUER KOHLEVERFLUESSIGUNG M.B.H., SAARBRUECKEN (WEST GERMANY).
Preparation of a design study for the construction of a 2 million tons/annum commercial scale hydrogenation plant
[BMFT-FB-T-83-135] N84-12652

GHENT UNIV. (BELGIUM).
Inventoring and monitoring of landscape as a natural and cultural resource N84-12594
Measuring landscape information content and distribution on a SAR-580 image N84-12596
Interpretability of wetland on SEASAT-A imagery in the polderland of Flanders: A structural approach N84-12597

GRENOBLE UNIV. (FRANCE).
Waves on vortex cores and their relation to vortex breakdown N84-12128

GROUPEMENT POUR LE DEVELOPPEMENT DE LA TELEDETECTION AEROSPATIALE, TOULOUSE (FRANCE).
SPOT potential applications: An overview of the results of the simulation campaigns N84-12587
The SPOT distribution system N84-12615

GT-DEVICES, ALEXANDRIA, VA.
Investigation of a pulsed electrothermal thruster
[NASA-CR-168266] N84-12227

H

HANFORD ENGINEERING DEVELOPMENT LAB., RICHLAND, WASH.
Miniature charpy-impact test results for the irradiated ferritic alloys HT-9 and modified 9Cr-1Mo
[DE83-016935] N84-12300
Quality is not a dirty word
[DE83-012166] N84-12510
Conceptual design of the high-flux VTA-2 test assembly for FMIT
[DE83-017022] N84-12935

HARRY DIAMOND LABS., ADELPHI, MD.
Topically classified bibliography on shapes of falling drops, drops in electric fields and related topics
[AD-A131134] N84-12417
Nonlinear force on an unpolarized relativistic test particle to second order in the total field in a nonequilibrium beam-plasma system
[AD-A131631] N84-12919

HARVARD-SMITHSONIAN CENTER FOR ASTROPHYSICS, CAMBRIDGE, MASS.
Spectroscopic measurements of solar wind generation N84-13071
Multiple transonic solutions and a new class of shock transitions in solar and stellar winds N84-13083
Observation of winds in cool stars N84-13084
Formation of standing shocks in stellar winds and related astrophysical flows N84-13088
Interpreting the solar wind ionization state N84-13115

HEBREW UNIV., JERUSALEM (ISRAEL).
Fourth International Conference on Photochemical Conversion and Storage of Solar Energy
[DE83-014760] N84-12638

HELIONETICS, INC., SAN DIEGO, CALIF.
Semiconductor processing with excimer lasers
[DE83-007509] N84-12477

HONEYWELL, INC., ST. LOUIS PARK, MINN.
NASA Demonstration Advanced Avionics System (DAAS) N84-12048

HOUSTON UNIV., TEX.
Mixture models for dependent observations N84-12562

HOWARD UNIV., WASHINGTON, D. C.
Numerical calculations of turbulent recirculating heat transfer beyond two-dimensional back-steps and sudden pipe expansions N84-12439

HUBSCHRAUBERFLUGPLAZ DER US-ARMY, FRANKFURT AM MAIN (WEST GERMANY).
Noise emission by helicopters N84-13007

HULBURT (E. O.) CENTER FOR SPACE RESEARCH, WASHINGTON, D.C.
HRTS observations of the fine structure and dynamics of the solar chromosphere and transition zone N84-13070

HUNTER COLL., NEW YORK.
Relating spatial patterns in image data to scene characteristics N84-12573

I

IDAHO NATIONAL ENGINEERING LAB., IDAHO FALLS.
Real-time attenuation of heated optical fibers in a nuclear reactor
[DE83-015141] N84-12873

ILLINOIS UNIV., CHICAGO.
Formation of surface layers during oxidation of a Fe-Mn-Si alloy
[DE83-009495] N84-12302
Studies of collisional and nonlinear radiative processes for development of coherent UV and XUV sources
[AD-A131837] N84-12467

ILLINOIS UNIV., URBANA.
Thermolysis of 4-methyl-4-phenyl malonyl peroxide: A new oxygen dependent chemiluminescent reaction
[AD-A131863] N84-12268
Flame acceleration mechanisms under conditions of partial confinement
[PB83-244012] N84-12328
Transport and relaxation processes in supercritical fluids
[DE83-015966] N84-12432
Design and implementation of a preprocessing system for a sodium lidar
[NASA-CR-174593] N84-12462
Observations of the upper troposphere and lower stratosphere using the urbana coherent-scatter radar
[NASA-CR-174594] N84-12664
TFTR alpha extraction and measurement project
[DE83-018120] N84-12947

ILLINOIS UNIV., URBANA-CHAMPAIGN.
Numerical analysis of stable crack growth in elastic-plastic materials in small scale and general yielding N84-12549

IMPERIAL COLL. OF SCIENCE AND TECHNOLOGY, LONDON (ENGLAND).
Instabilities in trailing vortices: Flow visualization using hot-wire anemometry N84-12103
Turbulence modelling: A state-of-the-art review
[CFD/83/3] N84-12435
A revised two-equation model of turbulence
[CFD/83/5] N84-12436

INDUSTRIEANLAGEN-BETRIEBSGESELLSCHAFT M.B.H., OTTOBRUNN (WEST GERMANY).
Hydraulic actuators and associated components suited for multiaxis vibration systems N84-12201
Concept of a safety system for a servohydraulic test facility N84-12202
Mathematical modeling and simulation of multiaxis hydraulic test facilities N84-12204
Simulation of electro-servo-hydraulic actuator for high quality testing N84-12206
Simulation of mechanical cross coupling of multiaxes vibration facilities N84-12207

INFORMATION SPECTRUM, INC., ARLINGTON, VA.
Ris assessment techniques: A handbook for program management personnel
[AD-A131596] N84-13010

INSTITUT FRANCAIS DU PETROLE, RUEIL-MALMAISON.
Radar bathymetry : A review N84-12612

INSTITUT GEOGRAPHIQUE NATIONAL, BRUSSELS (BELGIUM).
Remote sensing and topographic maps N84-12600

INSTITUTE FOR TELECOMMUNICATION SCIENCES, BOULDER, COLO.
Optimum reception in non-Gaussian electromagnetic interference environments. Part 2: Optimum and suboptimum threshold signal detection in class A and B noise
[PB83-241141] N84-12364
Alternative transmission media for third-generation interface standards
[PB83-238345] N84-12365

INSTITUTO DE PESQUISAS ESPACIAIS, SAO JOSE DOS CAMPOS (BRAZIL).
Satellite communication, part 1
[INPE-2893-PRE/417] N84-12337
Digital image registration by sequential analysis
[INPE-2940-PHE/429] N84-12446
Single Pb (1-x)Sn(x) Te crystal growth by vapor phase transport, with formation of a liquid/solid interface
[INPE-2811-PRE/369] N84-12967

INTERNATIONAL INST. FOR AERIAL SURVEY AND EARTH SCIENCES, ENSCHEDE (NETHERLANDS).
Major water conservation and reclamation projects in the Jianghan Plain and surroundings, Hubei Province, China N84-12593

IOWA STATE UNIV. OF SCIENCE AND TECHNOLOGY, AMES.
Load deflection characteristics of inflated structures [NASA-CR-174585] N84-12028
IOWA UNIV., IOWA CITY.
A model for chorus associated electrostatic bursts [NASA-CR-174489] N84-12832
Jupiter Data Analysis Program: Analysis of Voyager wideband plasma wave observations [NASA-CR-174575] N84-13058
ISTITUTO DI RICERCA E TECNOLOGIA PER LO STUDIO DEL PLASMA NELLO SPAZIO, FRASCATI (ITALY).
Radio scintillations at large elongation angles: Contributions of waves versus discontinuities [IFSI-82-4] N84-12358
Analysis of some filtering and data analysis methods for gravitational wave antennas with resonant transducers [IFSI-82-11] N84-12359
Data analysis for gravitational wave antenna with resonant transducers [IFSI-82-12] N84-12360
Guidance of electromagnetic waves in the ionosphere and magnetosphere [IFSI-82-15] N84-12361
Correlation between two spacecraft in the Doppler detection of a gravitational background radiation [IFSI-83-7] N84-12362
Orbiting wire as a dynamo: Auxiliary power possibilites for space platforms [IFSI-83-3] N84-12653
A comparison between GEOS 1 magnetic field measurements and some models of the geomagnetic field [IFSI-82-5] N84-12675
Observation of multiple ion beams in the magnetotail low latitude boundary layer. Evidence for a double H+ population [IFSI-82-10] N84-12676
Dissipative instabilities of magnetic neutral layers with velocity shear [IFSI-82-13] N84-12965
The structure of the plasma sheet-lobe boundary in the Earth's magnetotail [NASA-TM-85434] N84-13049
Interplanetary Alfvenic fluctuations: A statistical study of the directional variations of the magnetic field [IFSI-82-14] N84-13050
Comment on the observed plasma densities in Jupiter's distant magnetotail (wake); a possible explanation [IFSI-83-2] N84-13062
Interplanetary perturbations associated with type 4 solar flares [IFSI-82-6] N84-13129
The behavior of the cosmic ray equatorial anisotropy inside fast solar wind streams ejected by coronal holes [IFSI-82-16] N84-13130
ITT ELECTRO-OPTICAL PRODUCTS DIV., ROANOKE, VA.
Ultra low loss optical fiber cable assemblies, volume 2 [AD-A132008] N84-12891
Ultra low loss optical fiber cable assemblies, volume 1 [AD-A132007] N84-12892

J

JAYCOR, DEL MAR, CALIF.
Recent results in the Los Alamos compact torus program [DE83-014147] N84-12930
JAYCOR, SAN DIEGO, CALIF.
Theoretical studies of fusion physics. Volume 1: Summary [DE83-010378] N84-12924
Theoretical studies of fusion physics. Volume 2: Appendices [DE83-010371] N84-12925
JET PROPULSION LAB., CALIFORNIA INST. OF TECH., PASADENA.
Photoelectrochemical electrodes [NASA-CASE-NPO-15458-1] N84-12262
Corrosion resistant coating [NASA-NPO-15928-1] N84-12289
Laser activated MTOS microwave device [NASA-NPO-16112-1] N84-12463
Autoregressive models for use in scene segmentation N84-12561
SAR speckle noise reduction using Wiener filter N84-12568
Fluidized bed gasification of biomass to methane [NASA-CASE-NPO-15903-1] N84-12635
Method and apparatus for minimizing convection during crystal growth from solution [NASA-CASE-NPO-15811-1] N84-12968
Solar Wind Five [NASA-CP-2280] N84-13067
Observational constraints on solar wind acceleration mechanisms N84-13078
Solar cycle variations in the interplanetary magnetic field N84-13091
The effect of the solar field reversal on the modulation of galactic cosmic rays N84-13101
JOHNSON CONTROLS, INC., MILWAUKEE, WIS.
Effect of antimony on lead-acid battery negative electrode [DE83-014680] N84-12404
JOINT RESEARCH CENTRE OF THE EUROPEAN COMMUNITIES, ISPRA (ITALY).
Monitoring of renewable resources (a land information system for Europe) N84-12581
Marine remote sensing activities of the Joint Research Center, Ispra, Italy N84-12586

K

KANSAS UNIV., LAWRENCE.
Pilot controls and SPIRF flight N84-12038
A fault-tolerant distributed computer network design and analysis for an integrated flight control system N84-12189
KANSAS UNIV. CENTER FOR RESEARCH, INC., LAWRENCE.
The influence of sensor and flight parameters on texture in radar images N84-12575
KENTRON INTERNATIONAL, INC., HAMPTON, VA.
Nonlinear dynamics and control of a vibrating rectangular plate [NASA-CR-172215] N84-12528
KENTUCKY UNIV., LEXINGTON.
Stability of a pair of stationary vortices in the leeward side of a cylinder in a potential flowfield [AD-A131917] N84-12095
Structural characterization of dispersed metal catalysts [DE83-017145] N84-12305
KERNFORSCHUNGSANLAGE, JUELICH (WEST GERMANY).
Investigation of inhomogeneity in ceramic reactor materials using laser-localized emission spectroscopy [JUEL-1834] N84-12323
Investigation of the statistical mechanics of linear polymers for various physical conditions [JUEL-1832] N84-12324
KHD LUFTFAHRTTECHNIK G.M.B.H., OBERURSEL (WEST GERMANY).
Secondary power systems for fighter aircraft experiences today and requirements for a next generation N84-12171
KLM ROYAL DUTCH AIRLINES, AMSTERDAM (NETHERLANDS).
APU in commercial airline operation N84-12173

L

LAKE SHORE CRYOTRONICS, INC., WESTERVILLE, OHIO.
Enthalpy - improved dielectric insulation for superconducting wires [AD-A131857] N84-12316
LANGUAGE SERVICES, KNOXVILLE, TENN.
Formation of free hydrogen during radiolysis in a bed of clay [DE83-017724] N84-12275
LEHIGH UNIV., BETHLEHEM, PA.
Elastic-plastic fracture of cylindrical shells containing part-through circumferential cracks N84-12553
LINCOLN LAB., MASS. INST. OF TECH., LEXINGTON.
Effect of frequency-averaging on estimation of clutter statistics used in setting CFAR detection thresholds [AD-A131947] N84-12343
LNK CORP., SILVER SPRING, MD.
Analysis of subpixel registration accuracy N84-12570
LOS ALAMOS SCIENTIFIC LAB., N. MEX.
Effects of nonlinear loads on antennas and scatterers N84-12376
Megavolt pulse transformer powered by a fast plate generator [DE83-014189] N84-12384
Progress in developing repetitive pulse systems utilizing inductive energy storage [DE83-015167] N84-12388
Novel optical pin using microballoons [DE83-015222] N84-12391
Subharmonic buncher for the Los Alamos free-electron laser oscillator experiment [DE83-015220] N84-12474
Infrared-laser spectroscopy using a long-pathlength absorption cell [DE83-014197] N84-12480
Electron-beam diagnostics for the Los Alamos free-electron oscillator experiment [DE83-017230] N84-12481
Selective laser ionization for mass-spectral isotopic analysis [DE83-017303] N84-12483
Evolution of long pulses in a tapered wiggler free-electron laser [DE83-017235] N84-12484
The Los Alamos free-electron-laser oscillator experiment: Plans and present status [DE83-017290] N84-12485
Proceedings of the 16th LAMPF Users-Group Meeting [DE83-013215] N84-12488
Microearthquakes induced during hydraulic fracturing at the Fenton Hill HDR site: The 1982 experiments [DE83-014191] N84-12672
Variations in task and the ideal observer [DE83-015394] N84-12723
Linked state machines [DE83-4000123] N84-12736
Review of the ANSI metafile and virtual device interface standardization activities [DE83-015925] N84-12737
Vectorized Monte Carlo photon transport [DE83-014807] N84-12843
Hadronic multiplicity distributions: Example of a universal stochastic mechanism [DE83-015232] N84-12845
Solitons and polarons in quasi-one dimensional conducting polymers and related materials [DE83-015233] N84-12853
Space nuclear safety program [DE83-014070] N84-12869
Space reactors: Past, present and future [DE83-011177] N84-12870
Developing a 500-eV proton beam [DE83-012781] N84-12880
Effect of RF structure on cumulative beam breakup [DE83-017302] N84-12882
Longitudinal space-charge effects in bunched beams [DE83-017305] N84-12888
Survey of flash X-ray techniques and applications [DE83-017234] N84-12904
High-speed videography combined with an x-ray image intensifier for dynamic radiography [DE83-017233] N84-12905
Computational synergetics and innovation in wave, vortex, and plasma cloud dynamics [DE83-015252] N84-12928
Recent results in the Los Alamos compact torus program [DE83-014147] N84-12930
Muon spin relaxation in ferromagnetic PdMn [DE83-012659] N84-12979
Dense molecular thermodynamics [DE83-015216] N84-13006
Electron heating at interplanetary shocks N84-13098
Solar wind minor ions: Recent observations N84-13110
Plasma properties of driver gas following interplanetary shocks observed by ISEE-3 N84-13123
Interaction of the plasma tail of comet Bradfield 1979L on 1980 February 6 with a possibly flare-generated solar-wind disturbance N84-13126
Photon damping in cosmic-ray acceleration in active galactic nuclei [DE83-011320] N84-13133
LOUGHBOROUGH UNIV. OF TECHNOLOGY (ENGLAND).
A thin-walled beam finite element [TT-8302] N84-12779
LOUISIANA STATE UNIV., BATON ROUGE.
Soot formation from polycyclic aromatics [DE83-009750] N84-12271
LUFTHANSA G.M.B.H., HAMBURG (WEST GERMANY).
Cost efficient on board power for airline operation N84-12180
LUNAR AND PLANETARY INST., HOUSTON, TEX.
Workshop on Pristine Highlands Rocks and the early History of the Moon [NASA-CR-174584] N84-13059
Workshop on Pristine Highlands Rocks and the Early History of the Moon [NASA-CR-174600] N84-13060
Conference on Planetary Volatiles [NASA-CR-174583] N84-13061

M

MARCONI AVIONICS LTD., ROCHESTER (ENGLAND).
Integration of fire control, navigation system and head up display N84-12060

MARTINI ENGINEERING, RICHLAND, WASH.
Revised isothermal analysis program for Stirling engines
[DE83-017276] N84-12504
MARYLAND UNIV., COLLEGE PARK.
Microstructural origins of hot spots in RDX explosive and several reference inert materials
[AD-A132056] N84-12325
Image matching using generalized Hough transforms N84-12569
Pyramid methods in image analysis N84-12796
Iron charge states observed in the solar wind N84-13112
MASCHINENFABRIK AUGSBURG-NUERNBERG A.G., MUNICH (WEST GERMANY).
Construction of two wind turbines AEROMAN 11/11 for Indonesia
[BMFT-FB-T-83-143] N84-12505
Development of an ultrasonic testing procedure for electron beam welded parts for aerospace applications
[BMFT-FB-W-72-011] N84-12515
MASSACHUSETTS INST. OF TECH., CAMBRIDGE.
Review of aircraft crash structural response research
[AD-A131696] N84-12160
Design and operation of a light-scattering device for sizing and velocimetry of large droplets
[DE83-902641] N84-12456
Using structural and functional information in diagnostic design
[AD-A131859] N84-12769
Representations for reasoning about change
[AD-A131649] N84-12772
The effects of small noise on implicitly defined non-linear dynamical systems
[AD-A131632] N84-12808
The 12-T solenoid-design options for the MFTF-B upgrade
[DE83-016646] N84-12817
Study of excited state energy transfer processes
[AD-A131777] N84-12837
Beam plasma turbulence study
[AD-A131946] N84-12917
A model for stresses in circular magnets for toroidal fusion devices
[DE83-016535] N84-12937
Constraints on the scale of toroidal-fusion experiments with application to the design of a helical-axis stellarator
[DE83-016812] N84-12950
Role of thermal conduction in the acceleration of the solar wind N84-13079
The radial evolution of the solar wind, 1-10 AU N84-13106
MASSACHUSETTS UNIV., AMHERST.
Radiolysis of resist polymers. 1: Poly(methyl-alpha-haloacrylates) and copolymers with methylmethacrylate
[AD-A131864] N84-12315
A search for radio pulsars in the Northern sky: Discovery of a pulsar in a unique binary system N84-13040
The excitation of SiO in circumstellar envelopes N84-13041
MATERIALS QUALITY ASSURANCE DIRECTORATE, LONDON (ENGLAND).
Multi-detector gel permeation chromatography and its application to the analysis of industrial samples
[MQAD-808] N84-12283
MAX-PLANCK-GESELLSCHAFT ZUER FOERDERUNG DER WISSENSCHAFT E.V., GARCHING (WEST GERMANY).
Portrait of the Max-Planck research organization and its institutes N84-13015
MAX-PLANCK-INSTITUT FUER AERONOMIE, KATLENBURG-LINDAU (WEST GERMANY).
Radial evolution of ion distribution functions N84-13094
The average solar wind in the inner heliosphere: Structures and slow variations N84-13105
Associations between coronal mass ejections and interplanetary shocks N84-13121
On the field configuration in magnetic clouds N84-13125
MAX-PLANCK-INSTITUT FUER PHYSIK UND ASTROPHYSIK, GARCHING (WEST GERMANY).
Information processing for the infrared balloon telescope Goldener Drache
[MPE-38] N84-13035
Electrostatic waves and anomalous transport in the solar wind N84-13095
Iron charge states observed in the solar wind N84-13112
Survey of He(+)/He(2+) abundance ratios in energetic particle events N84-13117
MAX-PLANCK-INSTITUT FUER PLASMAPHYSIK, GARCHING (WEST GERMANY).
Crank-Nicholson difference schemes for solving coupled systems of nonlinear diffusion equations
[IPP-6/223] N84-12776
MCDONNELL AIRCRAFT CO., ST. LOUIS, MO.
V/STOL (Vertical/Short Takeoff and Landing) low speed and transition equivalent systems analysis
[AD-A131955] N84-12156
MCDONNELL-DOUGLAS ASTRONAUTICS CO., ST. LOUIS, MO.
Models of maintenance resources interaction: Peacetime operations
[AD-A131379] N84-13011
MCGILL UNIV., MONTREAL (QUEBEC).
Hydrogen-air detonations
[DE83-009289] N84-12278
MESSERSCHMITT-BOELKOW-BLOHM/ENTWICKLUNG SPRING NORD, BREMEN (WEST GERMANY).
Transonic configuration design N84-12081
Engine/airframe interference N84-12085
MESSERSCHMITT-BOELKOW-BLOHM G.M.B.H., HAMBURG (WEST GERMANY).
APU operational efficiency N84-12181
MESSERSCHMITT-BOELKOW-BLOHM G.M.B.H., OTTOBRUNN (WEST GERMANY).
Vortex flow simulations past wings using the Euler-equations N84-12118
Development and flight test of an active flutter suppression system for the F-4F with stores. Part 3. Flight demonstration of the active flutter suppression system
[AD-A131972] N84-12191
Quality control and sample comparison by differential modal analysis
[MBB-BB-543-83-OE] N84-12514
METROPOLITAN COLL. OF TECHNOLOGY, TOKYO (JAPAN).
Rotating and propagating LIB stabilized by self-induced magnetic field
[IPPJ-640] N84-12916
MICHIGAN STATE UNIV., EAST LANSING.
Studies of the correlation of electrode kinetics with molecular structure
[AD-A131704] N84-12838
MICHIGAN STATE UNIV., HICKORY CORNERS.
Limnology, second edition
[DE83-016792] N84-12627
MICHIGAN UNIV., ANN ARBOR.
Bibliography of coefficient of friction literature relating to slip type accidents
[PB83-243626] N84-12334
To quench our thirst: The present and future status of freshwater resources of the United States, part 3
[DE83-016791] N84-12625
Relative symmetries of differential equations
[DE83-015231] N84-12790
The 83-inch cyclotron reseach program
[DE83-015827] N84-12852
Hadron-hadron collider group
[DE83-010704] N84-12865
MIDWEST RESEARCH INST., GOLDEN, COLO.
Review of potential satellite techniques for mesoscale mapping of insolation
[DE83-011998] N84-12622
Polymer degradation on reflecting metal films: Fourier transform infrared (FTIR) reflection-absorbance studies
[DE83-012129] N84-12641
Thermochemical energy systems research
[DE83-012132] N84-12644
Passive-solar performance: Summary of 1981-1982 class B results
[DE83-009407] N84-12650
Model for illuminance on horizontal and vertical surfaces
[DE83-011973] N84-13127
Graphical method for determining interflected daylight in clear climates
[DE83-011989] N84-13128
MINE SAFETY AND HEALTH ADMINISTRATION, DENVER, COLO.
Use of aircraft imagery in evaluating ground stability at open-pit uranium mines in Gas Hills, Wyoming
[DE83-903011] N84-12621
MINISTERE DE L'ENVIRONMENT ET DU CADRE DE VIE, NEUILLY (FRANCE).
Actual state and recent evolution of the French coast observed by remote sensing using LANDSAT recordings N84-12606
Remote sensing applied to marine pollution control N84-12607
MINISTRY OF NATIONAL DEFENCE, ATHENS (GREECE).
On the generation of vortical flow at hypersonic speeds over elliptical cones N84-12114
MINNESOTA UNIV., MINNEAPOLIS.
Turbulent tube-flow heat transfer coefficients in the presence of flow imbalance in the tubes of a parallel array N84-12437
MISSION RESEARCH CORP., SAN DIEGO, CALIF.
Ion-ion recombination rate in the EMP source region
[AD-A131148] N84-12339
MONSANTO RESEARCH CORP., MIAMISBURG, OHIO.
Calorimeter operating system implemented on a Z-80 microcomputer in read only memory
[DE83-016647] N84-12734

N

NAGOYA UNIV. (JAPAN).
Magnetohydrodynamic equilibrium and stability of spheromak plasma in flux conserver
[IPPJ-642] N84-12909
A steady-state axisymmetric toroidal system
[IPPJ-643] N84-12910
Atomic processes in hot dense plasma
[IPPJ-AM-31] N84-12911
Cross sections for charge transfers of highly ionized ions in hydrogen atoms
[IPPJ-AM-30] N84-12912
Bibliography on atomic processes in hot dense plasmas
[IPPJ-AM-29] N84-12913
Electron capture and loss cross sections for collisions between heavy ions and hydrogen molecules, revised
[IPPJ-AM-28] N84-12914
Considerations of the three-wave interactions
[IPPJ-641] N84-12915
Rotating and propagating LIB stabilized by self-induced magnetic field
[IPPJ-640] N84-12916
NATIONAL ACADEMY OF SCIENCES - NATIONAL RESEARCH COUNCIL, WASHINGTON, D. C.
Polymers of phosphonylmethyl-2,4- and -2,6-diamino benzenes and the like
[NASA-ARC-11506-1] N84-12313
NATIONAL AERONAUTICAL ESTABLISHMENT, OTTAWA (ONTARIO).
Viscous three-dimensional flow separations from high-wing propeller-turbine nacelle models N84-12115
NATIONAL AERONAUTICS AND SPACE ADMINISTRATION, WASHINGTON, D. C.
Aeronautical Engineering: A continuing bibliography with indexes (supplement 166)
[NASA-SP-7037(166)] N84-12027
STS-9 Spacelab 1 press kit
[P83-10209] N84-12214
Containerless electromagnetic levitation melting of Cu-Fe and Ag-Ni alloys
[NASA-TM-82553] N84-12288
Aerospace Medicine and Biology: A continuing bibliography with indexes (supplement 250)
[NASA-SP-7011(250)] N84-12712
NASA patent abstracts bibiliography. Section 1: Abstracts. A continuing bibliography
[NASA-SP-7039(23)] N84-13017
NASA Patent Abstracts Bibliography. Section 2: Indexes. A continuing bibliography (supplement 23)
[NASA-SP-7039(23)] N84-13018
National Aeronautics and Space Act of 1958, as amended and related legislation
[GPO-24-491] N84-13032
Spinoff, 1983
[NASA-TM-85475] N84-13033
NASA Facts: IRAS - Mapping the Infrared Sky
[NASA-FACTS-139] N84-13036
NATIONAL AERONAUTICS AND SPACE ADMINISTRATION. AMES RESEARCH CENTER, MOFFETT FIELD, CALIF.
An overview of the demonstration advanced avionics system guest pilot evaluation conducted at Ames Research Center N84-12049
On issues concerning flow separation and vortical flows in three dimensions N84-12100
Numerical simulation of vortex breakdown by the vortex-filament method N84-12126
Augmentation of fighter-aircraft performance by spanwise blowing over the wing leading edge N84-12133
Visual accommodation trainer-tester
[NASA-CASE-ARC-11426-1] N84-12193
Polymers of phosphonylmethyl-2,4- and -2,6-diamino benzenes and the like
[NASA-ARC-11506-1] N84-12313
Computation of turbulent flows over backward-facing step
[NASA-TM-85851] N84-12414
Thermal conductance measurements of pressed OFHC copper contacts at liquid helium temperatures
[NASA-TM-85861] N84-12809

Spatial dependences in the distant solar wind: Pioneers 10 and 11 N84-13107

NATIONAL AERONAUTICS AND SPACE ADMINISTRATION. EARTH RESOURCES LABS., BAY ST. LOUIS, MISS.

Earth Resources Laboratory research and technology [E84-10033] N84-12576

NATIONAL AERONAUTICS AND SPACE ADMINISTRATION. FLIGHT RESEARCH CENTER, EDWARDS, CALIF.

Inflatable device for installing strain gage bridges [NASA-CASE-FRC-11068-1] N84-12443

NATIONAL AERONAUTICS AND SPACE ADMINISTRATION. GODDARD SPACE FLIGHT CENTER, GREENBELT, MD.

Shuttle measured contaminant environment and modeling for payloads. Preliminary assessment of the space telescope environment in the shuttle bay [NASA-TM-85111] N84-12216

GSFC flywheel status N84-12230

Combined attitude control and energy storage N84-12237

Magnetic bearings for inertial energy storage N84-12242

Assessment of potential for batteries in space applications N84-12246

Holding fixture for a hot stamping press [NASA-CASE-GSC-12619-1] N84-12491

Unidirectional flexural pivot [NASA-CASE-GSC-12622-1] N84-12492

Crustal deformation, the earthquake cycle, and models of viscoelastic flow in the asthenosphere [NASA-TM-85117] N84-12662

Scale lengths in quasi-parallel shocks [NASA-TM-85109] N84-12663

Luminosity enhancement in relativistic jets and altered luminosity functions for beamed objects [NASA-TM-85053] N84-12889

Development of a segmented n-type germanium detector, and its application to astronomical gamma-ray spectroscopy [NASA-TM-85435] N84-13039

Spectral analysis of magnetohydrodynamic fluctuations near interplanetary schocks [NASA-TM-85119] N84-13044

Radial variations of large-scale magnetohydrodynamic fluctuations in the solar wind [NASA-TM-85116] N84-13045

Boundary layers in cataclysmic variables: The HEAO-1 X-ray constraints [NASA-TM-85112] N84-13046

The structure of the plasma sheet-lobe boundary in the Earth's magnetotail [NASA-TM-85434] N84-13049

Interpretation of 3He variations in the solar wind [NASA-TM-85049] N84-13065

Magnetohydrodynamic turbulence in the solar wind N84-13073

The collapse of the local, Spitzer-Haerm formulation and a global-local generalization for heat flow in an inhomogeneous, fully ionized plasma N84-13080

Radio evidence for interplanetary streamers in the range 10-170 solar radii N84-13103

The relative abundance of 3He(++) in the solar wind N84-13111

Velocity profiles of interplanetary shocks N84-13122

Interaction of the plasma tail of comet Bradfield 1979L on 1980 February 6 with a possibly flare-generated solar-wind disturbance N84-13126

NATIONAL AERONAUTICS AND SPACE ADMINISTRATION. LYNDON B. JOHNSON SPACE CENTER, HOUSTON, TEX.

Space station energy sizing N84-12233

The Boeing flywheel study N84-12235

Space station control requirements and flywheel system weights for combined momentum and energy storage N84-12236

Estimating location parameters in a mixture model N84-12559

NATIONAL AERONAUTICS AND SPACE ADMINISTRATION. LANGLEY RESEARCH CENTER, HAMPTON, VA.

Controls, Displays, and Information Transfer for General Aviation IFR Operations [NASA-CP-2279] N84-12029

Single pilot IFR program overview and status N84-12030

Analysis of general aviation single-pilot IFR incident data obtained from the NASA Aviation Safety Reporting System N84-12033

General aviation single pilot IFR autopilot study N84-12035

Flight test validation of a design procedure for digital autopilots N84-12036

A simulator evaluation of an automatic terminal approach system N84-12037

Advanced symbology for general aviation approach to landing displays N84-12039

Pilot response with conventional displays N84-12040

Single pilot scanning behavior in simulated instrument flight N84-12041

A simulator evaluation of a rate-enhanced instrument landing system display N84-12042

Display research: Pilot response with the "follow-me" box display N84-12043

Proposed study to determine potential flight applications and human factors design guidelines of voice recognition/synthesis systems N84-12047

Transonic airfoil development N84-12076

Transonic empirical configuration design process N84-12079

Geometries for roughness shapes in laminar flow [NASA-CASE-LAR-13255-1] N84-12092

Recent studies at NASA-Langley of vortical flows interacting with neighboring surfaces N84-12109

Experimental investigation of forebody and wing leading-edge vortex interactions at high angles of attack N84-12110

Solar powered aircraft [NASA-CASE-LAR-12615-1] N84-12154

Evaluation of a total energy-rate sensor on a transport airplane [NASA-TP-2212] N84-12164

Simulator study of flight characteristics of a large twin-fuselage cargo transport airplane during approach and landing [NASA-TP-2183] N84-12190

Integrated Flywheel Technology, 1983 [NASA-CP-2290] N84-12228

Integrated Power/Attitude Control System (IPACS) N84-12229

IPACS electronics: Comments on the original design and current efforts at Langley Research Center N84-12240

Annular Momentum Control Device (AMCD) N84-12241

Advanced Control and Power System (ACAPS) technology program N84-12243

Analytical prediction of aerothermal environment in a wing-elevon cove [NASA-TM-85711] N84-12412

Low energy electron magnetometer using a monoenergetic electron beam [NASA-CASE-LAR-12706-1] N84-12444

Ride quality meter [NASA-CASE-LAR-12882-1] N84-12445

Vertical shaft windmill [NASA-CASE-LAR-12923-1] N84-12493

The Dugdale model for the compact specimen [NASA-TM-85714] N84-12529

Vertical drop test of a transport fuselage center section including the wheel wells [NASA-TM-85706] N84-12531

A model for the distributed storage and processing of large arrays [NASA-CR-172252] N84-12742

Design, development and use of the finite element machine [NASA-CR-172250] N84-12777

NATIONAL AERONAUTICS AND SPACE ADMINISTRATION. LEWIS RESEARCH CENTER, CLEVELAND, OHIO.

A generalized computer code for developing dynamic gas turbine engine models (DIGTEM) [NASA-TM-83508] N84-12166

Some comments on longevity by a technologist N84-12247

Solid impingement erosion mechanisms and characterization of erosion resistance of ductile metals [NASA-TM-83492] N84-12287

A multistage spent particle collector and a method for making same [NASA-LEW-13914-1] N84-12447

A graphics subsystem retrofit design for the bladed-disk data acquisition system [NASA-TM-83510] N84-12730

NATIONAL AERONAUTICS AND SPACE ADMINISTRATION. MARSHALL SPACE FLIGHT CENTER, HUNTSVILLE, ALA.

Materials processing in space program tasks-supplement [NASA-TM-82548] N84-12196

Electrical power trade-offs N84-12232

Space station attitude control system concept and requirements N84-12234

IPACS attitude control technology considerations N84-12238

Flywheel electronics N84-12239

Power system considerations and test activities N84-12244

IPACS guidance navigation and control system considerations and test activities N84-12245

Constant-output atomizer [NASA-CASE-MFS-25631-1] N84-12406

NATIONAL AERONAUTICS AND SPACE ADMINISTRATION. NATIONAL SPACE TECHNOLOGY LABS., BAY SAINT LOUIS, MISS.

Progress in the scene-to-map registration investigation N84-12572

Method for treating wastewater using microorganisms and vascular aquatic plants [NASA-CASE-NSTL-10] N84-12654

NATIONAL AERONAUTICS AND SPACE ADMINISTRATION. PASADENA OFFICE, CALIF.

High dynamic global positioning system receiver [NASA-CASE-NPO-16171-1-CU] N84-12151

Photoelectrochemical electrodes [NASA-CASE-NPO-15458-1] N84-12262

Corrosion resistant coating [NASA-NPO-15928-1] N84-12289

Laser activated MTOS microwave device [NASA-NPO-16112-1] N84-12463

Fluidized bed gasification of biomass to methane [NASA-CASE-NPO-15903-1] N84-12835

Method and apparatus for minimizing convection during crystal growth from solution [NASA-CASE-NPO-15811-1] N84-12968

NATIONAL AERONAUTICS AND SPACE ADMINISTRATION. WALLOPS FLIGHT CENTER, WALLOPS ISLAND, VA.

Thin film strain transducer [NASA-WLP-10055-2] N84-12448

NATIONAL AEROSPACE LAB., AMSTERDAM (NETHERLANDS).

Computational methods for subsonic and transonic aerodynamic design N84-12074

Application of computational procedures in aerodynamic design N84-12078

Engine/airframe interference drag at cruise conditions, using propulsion simulation [NLR-TR-82012-U] N84-12098

Computational vortex flow aerodynamics N84-12117

Aspects of second- and third-order panel methods demonstrated for the two-dimensional flat plate problem [NLR-TR-81074-U] N84-12433

Results of a new version of the LTRAN2-NLR (LTRANV) for unsteady viscous transonic flow computations [NLR-TR-81078-U] N84-12434

NATIONAL BUREAU OF STANDARDS, WASHINGTON, D.C.

Performance of add-on-type heat pump water heaters using two different test methods [PB83-222703] N84-12332

Center for electronics and electrical engineering technical progress bulletin covering signals and systems program, April 1982 - September 1982 [PB83-241158] N84-12405

Nondestructive evaluation publications, 1981 [PB83-239574] N84-12517

NATIONAL CENTER FOR ATMOSPHERIC RESEARCH, BOULDER, COLO.

Theory of winds in late-type evolved and pre-main-sequence stars N84-13085

Stellar winds driven by multi-line scattering N84-13087

Interplanetary scintillation observations of the solar wind close to the Sun and out of the ecliptic N84-13102

Quasi-steady solar wind dynamics N84-13120

NATIONAL ENGINEERING LAB., EAST KILBRIDE (SCOTLAND).

The development of a multi-axis hydraulic vibration test facility at the National Engineering Laboratory, Scotland N84-12200

NATIONAL LIBRARY OF MEDICINE, BETHESDA, MD.

Permuted medical subject headings, 1984 [PB83-234781] N84-13027

Medical subject headings, tree structures, 1984 [PB83-223164] N84-13028

Medical Subject Headings, Annotated Alphabetic List, 1984 [PB83-223156] N84-13029

NATIONAL OCEANIC AND ATMOSPHERIC ADMINISTRATION, BOULDER, COLO.

Magnetohydrodynamic modeling of coronal structure and expansion N84-13081

NATIONAL OCEANIC AND ATMOSPHERIC ADMINISTRATION, MIAMI, FLA.

Omega Dropwindsonde processing [PB83-248773] N84-12700

NATIONAL PHYSICAL LAB., TEDDINGTON (ENGLAND).

An interactive computer program for analysis of ultrasonic modulus data on anistropic materials [NPL-DMA(A)68] N84-12526

Ada-Europe guidelines for the portability of Ada programs, second edition [NPL-DITC-27/83] N84-12739

Guidelines for the design of large modular scientific libraries in Ada
[NPL-DITC-28/83] N84-12740

NATIONAL SCIENCE FOUNDATION, WASHINGTON, D.C.
International Conference on Vibrations at Surfaces (3rd)
[AD-A131794] N84-12834

NATIONAL TELECOMMUNICATIONS AND INFORMATION ADMINISTRATION, WASHINGTON, D.C.
International Telecommunication Standards: Issues and Implications for the '80's
[PB83-241471] N84-12366

NATIONAL TRANSPORTATION SAFETY BOARD, WASHINGTON, D. C.
Safety report: General aviation crashworthiness project, phase 1
[PB83-917004] N84-12142

NATIONAL WEATHER SERVICE, KANSAS CITY, MO.
Assembly language graphics library (EGR1.LB) with Fortran interfacing
[PB83-239624] N84-12757

NATIONAL WEATHER SERVICE, SALT LAKE CITY, UTAH.
Climate of Phoenix, Arizona (revised)
[PB83-246801] N84-12699

NAVAL AEROSPACE MEDICAL RESEARCH LAB., PENSACOLA, FLA.
Eruption of permanent dentition in rhesus monkeys exposed to ELF (Extremely low frequency) fields
[AD-A132085] N84-12703
Effects of pulsed microwaves at 1.26 and 5.62 GHz on Rhesus monkeys (Macaca mulatta) performing an exercise task at three levels of work
[AD-A132057] N84-12704
A restraint chair with rowing-like movement for exposing exercising nonhuman primates to microwave irradiation
[AD-A132047] N84-12705
Effect of pulsed 5.62 GHz microwaves on squirrel monkeys (Saimiri sciureus) performing a repeated acquisition task
[AD-A132045] N84-12706
Figural aftereffects: An explanation in terms of multiple mechanisms in the human visual system
[AD-A132066] N84-12715
An age comparison of the vestibulo-ocular counterroll reflex
[AD-A132064] N84-12716
Vestibulo-ocular reflex gain in man during active versus passive oscillation and the influence of voluntary gaze-control tasks
[AD-A132008] N84-12717

NAVAL OCEAN SYSTEMS CENTER, SAN DIEGO, CALIF.
Network design tool for EHF satellite communications networks
[AD-A131812] N84-12349
Optical extinction coefficients beneath marine stratus clouds. Comparison of coefficients calculated from observed aerosol spectra with coefficients specified by the Navy aerosol model
[AD-A132011] N84-12685

NAVAL POSTGRADUATE SCHOOL, MONTEREY, CALIF.
Racial bias and predictive validity in testing for selection
[AD-A131830] N84-12722
Computer system design environment software development plan
[AD-A131651] N84-12747

NAVAL RESEARCH LAB., WASHINGTON, D. C.
Techniques for locating a remote HF transmitter from single-site measurements
[AD-A132014] N84-12342
Performance analysis of a three-dimensional microwave lens in a cylindrical array scanning application
[AD-A131891] N84-12345
Numerical simulations of fuel droplet flows using a Lagrangian triangular mesh
[NASA-CR-168263] N84-12411
RF conditioned dc discharges for excitation of rare gas halide lasers
[DE83-016537] N84-12479
Creation of ultra-high-pressure shocks by the collision of laser-accelerated disks: Experiment and theory
[DE83-017366] N84-12486
Transverse horizontal coherence and low-frequency array gain limits in the deep ocean
[AD-A131916] N84-12621
Dynasty 2: A nonlinear implicit code for relativistic electron beam tracking studies
[AD-A131592] N84-12629
Associations between coronal mass ejections and interplanetary shocks N84-13121

NAVAL SHIP RESEARCH AND DEVELOPMENT CENTER, BETHESDA, MD.
Robotics: An introduction to today's robot and future trends
[AD-A132070] N84-12768

NAVAL SUBMARINE MEDICAL RESEARCH LAB., GROTON, CONN.
The computerization of material safety data sheet information
[AD-A131992] N84-13021

NAVAL SURFACE WEAPONS CENTER, WHITE OAK, MD.
Microstructural origins of hot spots in RDX explosive and several reference inert materials
[AD-A132056] N84-12325
Water entry impact shock on flat faced cylindrical missiles
[AD-A131937] N84-12419

NAVAL UNDERWATER SYSTEMS CENTER, NEW LONDON, CONN.
The effect of noisy reflection data on an inverse method for determining the structure of a layered ocean bottom
[AD-A131976] N84-12820

NEVADA UNIV. SYSTEM, RENO.
Constant-output atomizer
[NASA-CASE-MFS-25631-1] N84-12406

NEW HAMPSHIRE UNIV., DURHAM.
Coronal heating by waves N84-13068
Acceleration of heavy ions in the solar wind N84-13118

NEW MEXICO STATE UNIV., LAS CRUCES.
Speed-dependent collision effects on radar back-scattering from the ionosphere
[NASA-CR-173077] N84-12336

NEW YORK UNIV., NEW YORK.
New results for transition probabilities in two-level systems: The large detuning regime
[AD-A131783] N84-12835

NORTH CAROLINA STATE UNIV., RALEIGH.
Numerical solution of the two-phase, three dimensional boundary layer in laminar film condensation over a curved surface N84-12442

NORTH CAROLINA UNIV., CHAPEL HILL.
Weak and strong law results for a function of the spacings
[AD-A130705] N84-12782
An iterated logarithm law result for extreme values from Gaussian sequences
[AD-A129559] N84-12798
Asymptotic maximal deviation of m-smoothers
[AD-A131906] N84-12799
An alternative to the Monte Carlo estimation of network reliability
[AD-A131849] N84-12800
Research in theoretical physics
[DE83-0166222] N84-13004

NORTHEASTERN UNIV., BOSTON, MASS.
GSE for balloon-borne I.M.S.: Decommutator and D/A units
[AD-A131845] N84-12452

NORTHROP CORP., HAWTHORNE, CALIF.
Application of flight controls technology to engine control systems N84-12061

NORTHWESTERN UNIV., EVANSTON, ILL.
First passage times in stochastic differential equations of mathematical physics and engineering
[AD-A131705] N84-12728
Theory of hyperfine anomalies in muonic atoms
[DE83-015392] N84-12872

NORWEGIAN DEFENCE RESEARCH ESTABLISHMENT, KJELLER.
F-16 Penguin anti-ship missile integration N84-12059

O

OAK RIDGE GASEOUS DIFFUSION PLANT, TENN.
A gas-flow tracing technique applicable to rotating systems boundary layer on a rotating disk
[DE83-012761] N84-12425
Practical computation of multidimensional thermal flows in a gas centrifuge
[DE83-005697] N84-12426

OAK RIDGE NATIONAL LAB., TENN.
Overview of state-of-the-art flywheel technology N84-12231
Radiation damage and phase instability in irradiated stainless steel
[DE83-017190] N84-12303
Comparison of damage microstructures in neutron-irradiated vanadium and iron
[DE83-017189] N84-12304
Isotope dependence of the breakdown strength of gases
[DE83-017272] N84-12430
Dynamic analysis of the fluidyne
[DE83-017283] N84-12500
Effects of pressure-drop correlations on Stirling-engine predicted performance
[DE83-017279] N84-12501
Electron-microscope observation of crack propagation and a dislocation model of fracture
[DE83-014623] N84-12540
Creep and tensile properties of alloy 800H-Hastelloy X weldments
[DE83-017067] N84-12542
Inventory of numeric data for carbon dioxide research
[DE83-017571] N84-12657
Comments on ISO/TC 97/SC 18/WG3 N120
[DE83-011391] N84-12748
Using PAFEC as a preprocessor for COSMIC/NASTRAN
[DE83-017179] N84-12755
Why didn't Box-Jenkins win (again)?
[DE83-014043] N84-12802
Implications of heavy-ion-induced satellite X-ray emission. 1: Introduction
[DE83-015682] N84-12851
Electron-molecule interactions in gases and liquids: The electron-attachment process in gases and nonpolar liquids
[DE83-017205] N84-12863
Electron-ion collisions
[DE83-017211] N84-12867
Theoretical aspects of throat-launch microwave heating in EBT-S
[DE83-015762] N84-12875
PATRAM '83: 7th International Symposium on Packaging and Transportation of Radioactive Materials, summaries
[DE83-012390] N84-12881
Generation of monoenergetic positrons
[DE83-015535] N84-12887
Design of the Advanced Toroidal Facility (ATF-1)
[DE83-012641] N84-12923
Detailed modeling of microwave energy deposition in EBT devices
[DE83-017496] N84-12952
Monte Carlo calculations of neutron and gamma-ray energy spectra for fusion-reactor shield design: Comparison with experiment
[DE83-016932] N84-12956
Electron-cyclotron-heating experiments in Tokamaks and stellarators
[DE83-017210] N84-12958
Propagation and absorption of electromagnetic waves in fully relativistic plasmas
[DE83-017246] N84-12959
Effect of magnetic bending on the high-frequency stability of the ELMO Bumpy Torus
[DE83-017177] N84-12961
Hydrogen in MgO crystals thermochemically reduced at very high temperatures
[DE83-014058] N84-12981
Implications of heavy-ion-induced satellite X-ray emission. Part 2: Production of K and L X-rays by 0.9 to 2.6 MeV/u Ar ions in thick targets of V, Cu, Nb, Ta, and Pt
[DE83-015681] N84-12982
Transient heat transfer in superfluid helium, part 2
[DE83-015767] N84-12984
Superconductor stability, 1983: A review
[DE83-015506] N84-12990
Superconducting stability, 1983: A review
[DE83-017262] N84-12995
Two types of values and their assessment by the collective interest
[DE83-012064] N84-13031

OAK RIDGE Y-12 PLANT, TENN.
Degradation of shape memory effect
[DE83-016586] N84-12295

OBSERVATOIRE DE PARIS-MEUDON (FRANCE).
Measurement of macroscopic plasma parameters with a radio experiment: Interpretation of the quasi-thermal noise spectrum observed in the solar wind N84-13096

OFFICE NATIONAL D'ETUDES ET DE RECHERCHES AEROSPATIALES, PARIS (FRANCE).
A nonlinear control law for piloting aircraft in the air-to-ground attack phase N84-12071
Interaction between a shock-wave and a vortex flow N84-12104
Visualization of vortical type flows in three dimensions N84-12107
Simulation of turbulent flows with a point vortex method N84-12119
Experimentation with turbulent flows experiencing the effects of an adverse pressure gradient N84-12127
La Recherche Aerospatiale, Bimonthly Bulletin, no. 1983-1/212, January-February 1983
[ESA-TT-814] N84-12810

Development of the basic methods needed to predict the aeroelastic behavior of helicopters N84-12811
Present trends in structural analysis at ONERA N84-12812
Random eddies in wakes and mixing layers N84-12813

OFFICE OF SOFTWARE DEVELOPMENT, FALLS CHURCH, VA.
Perkin-Elmer, Perkin-Elmer 3230 COBOL R07 (pre-release)
[PB83-238600] N84-12766

OFFICE OF TECHNOLOGY ASSESSMENT, WASHINGTON, D.C.
Airport and air traffic control system
[OTA-STI-175] N84-12143
Airport and air traffic control system. Executive summary N84-12144
Airport and air traffic control system. Introduction and overview N84-12145
The National Airspace System N84-12146
Aviation growth scenarios N84-12147
Technology and the future evolution of the ATC system N84-12148
Airport capacity alternatives N84-12149
Policy implications N84-12150

OHIO STATE UNIV., COLUMBUS.
Study to determine the IFR operational profile and problems to the general aviation pilot N84-12032
A summary and integration of research concerning single pilot IFR operational problems N84-12034
Accuracy estimates of gravity potential differences between western Europe and United States through Lageos satellite laser ranging network
[AD-A131838] N84-12669
Kinetics of growth and decay of excited rare-gas atoms and molecules in the pulse radiolysis of pure rare gases and of mixtures of rare gases with molecular quenching agents
[DE83-017016] N84-12856

OHIO UNIV., ATHENS.
Weather data communication and utilization N84-12045

OKLAHOMA UNIV., NORMAN.
Three-dimensional analysis of composite plates with material nonlinearity
[AD-A131884] N84-12258
The effects of channel tortuosity on electromagnetic radiations from lightning return strokes N84-12335

OPTICAL COATING LAB., INC., SANTA ROSA, CALIF.
Damage thresholds of thin film materials and high reflectors at 248 nm
[DE83-012663] N84-12472

OREGON UNIV., EUGENE.
Theory of elementary particles
[DE83-015904] N84-12871

P

PACIFIC NORTHWEST LAB., RICHLAND, WASH.
Disparate changes in the physical properties of graphite
[DE83-015986] N84-12321
Initial operation of the compressed air experiment at Pittsfield, Illinois
[DE83-016930] N84-12643
Innovative industrial-materials processes
[DE83-016784] N84-12649
Detecting long-term ecological effects in forests and food chains
[DE83-003469] N84-12655
Estimating long-term mean winds from short-term wind data
[DE83-017417] N84-12693
A subsynoptic environment associated with two inter-mountain severe thunderstorm events
[DE83-014498] N84-12694
TRAN-STAT (statistics for environmental studies). Issue no. 24: Field sampling designs, simple random and stratified random sampling
[DE83-016826] N84-12803
Weighted nonparametric tail estimation procedures
[DE83-017870] N84-12804
Development of materials for open-cycle MHD
[DE83-016334] N84-12926
Management of QA in an R and D organization
[DE83-016924] N84-13014

PARIS XI UNIV., ORSAY (FRANCE).
Research and development for investigations of metallic adsorptions on metal surfaces by optical techniques complemented by dc resistivity and auger spectroscopy
[AD-A131739] N84-12351

PENNSYLVANIA STATE UNIV., UNIVERSITY PARK.
Free-radical and ion chemistry of volatile silanes, germanes, and phosphines
[DE83-016389] N84-12277
Acoustic pulse scattering from impedance covered cylinders
[AD-A131653] N84-12822

PENNSYLVANIA UNIV., PHILADELPHIA.
Hadron-hadron collider group
[DE83-010704] N84-12865

PITTSBURGH UNIV., PA.
Computation of three-dimensional unsteady flow in rigid and deformable curved tubes N84-12440
OI 630.0 nm optical measurements of neutral winds, temperatures and airglow enhancements during the BIME program
[AD-A131695] N84-12671
Limit theorems for the eigenvalues of product of two random matrices
[AD-A131682] N84-12787

POLISH ACADEMY OF SCIENCES, WARSAW.
The shock wave structure in one-component gas and in binary gas mixture
[ISSN-0208-5658] N84-12407
Hamiltonian for antisotropic bodies with defects
[ISSN-0208-5658] N84-12966

POLITECNICO DI MILANO (ITALY).
Boundary layer segmentation on sharp highly swept leading edges and its effects on secondary vortices N84-12132

POLYTECHNIC INST. OF NEW YORK, BROOKLYN.
Research in net management techniques for tactical data networks
[AD-A131674] N84-12352

POLYTECHNIC INST. OF NEW YORK, FARMINGDALE.
Laser interaction with metallic surfaces
[AD-A126269] N84-12464

PRAKLA-SEISMOS G.M.B.H., HANNOVER (WEST GERMANY).
Numerical modeling techniques according to the wave equation and the ray method
[BMFT-FB-T-83-136] N84-12354

PRATT AND WHITNEY AIRCRAFT GROUP, EAST HARTFORD, CONN.
Development of strain tolerant thermal barrier coating systems, tasks 1 - 3
[NASA-CR-168251] N84-12312

PRECISION DEVICES LTD., HUNTSVILLE, ALA.
Low gravity experiment for studying a rotating fluid having a free surface
[NASA-CR-170923] N84-12413

PRINCETON UNIV., N. J.
The Tracked Wing In Ground-Effect (TWIG) N84-12155
Interaction of a dislocation with a crack
[AD-A131912] N84-12536
Mechanisms of monsoonal cyclogenesis N84-12680
Adjustment in the oceans: The long-period tides and coastal upwelling N84-12702
On differential equations of nonlocal elasticity and solutions of screw dislocation and surface waves
[AD-A131911] N84-12786
Faint galaxies in the Coma cluster: Luminosity function and spatial distribution N84-13053
Geomorphic studies of Mars N84-13063

PURDUE UNIV., LAFAYETTE, IND.
Combustion modeling of composite solid propellants N84-12285
Laser velocimeter measurements and analysis in turbulent flows with combustion, part 2
[AD-A131882] N84-12421
Buckled plate vibrations, large amplitude vibrations and nonlinear flutter of elastic plates using high-order triangular finite elements N84-12523
Evaluation of the crack gage as an advanced individual aircraft tracking concept N84-12551
Simulation aspects in the study of rectification of satellite scanner data N84-12571
Numerical simulation of convective scaling N84-12660

Q

QUEEN MARY COLL., LONDON (ENGLAND).
Alfven solitons in the solar wind N84-13075

R

RENSSELAER POLYTECHNIC INST., TROY, N. Y.
Composite structural materials
[NASA-CR-174597] N84-12257
Adaptive finite element methods for parabolic partial differential equations
[NASA-CR-174490] N84-12727

RESEARCH INST. OF NATIONAL DEFENCE, LINKOEPING (SWEDEN).
Observations and classifications with a 35/94 GHz radiometer of terrain near Motala, Sweden, July 1982
[FOA-C-30325-E1,E3] N84-12630

RESEARCH INST. OF NATIONAL DEFENCE, STOCKHOLM (SWEDEN).
Coherence of appraisal and coping: Parachute jump effectiveness
[FOA-C-55058-H3] N84-12724

RICARDO & CO., ENGINEERS (1927) LTD., SHOREHAM-BY-SEA (ENGLAND).
Evaluation of unthrottled combustion system options for light duty applications with future syncrude derived fuels
[DE83-017047] N84-12327
Optimum engine for methanol utilization
[PB83-239459] N84-12507

RICE UNIV., HOUSTON, TEX.
Multivariate density estimation and remote sensing N84-12560
New conformal solution theory
[PB83-249441] N84-13008

ROCKEFELLER UNIV., NEW YORK.
Hadron-hadron collider group
[DE83-010704] N84-12865

ROCKET RESEARCH CORP., REDMOND, WASH.
Hot gas APU starter for advanced aircraft applications N84-12178

ROCKETDYNE, CANOGA PARK, CALIF.
Super integrated power unit for fighter aircraft N84-12183

ROCKWELL INTERNATIONAL CORP., ANAHEIM, CALIF.
Mechanisms and kinetics of diphthalocyanine electrode processes
[AD-A131726] N84-12270

ROCKWELL INTERNATIONAL CORP., GOLDEN, COLO.
Development of a unique Physical Metrology Laboratory Recall System
[DE83-017415] N84-12767

ROLLS-ROYCE LTD., BRISTOL (ENGLAND).
All-electric accessory drive systems: Implications on engine design and performance N84-12184

ROME AIR DEVELOPMENT CENTER, GRIFFISS AFB, N.Y.
Simultaneous nulling in the sum and difference patterns of a monopulse antenna
[AD-A131865] N84-12347

ROYAL AIRCRAFT ESTABLISHMENT, BEDFORD (ENGLAND).
Some results from a programme of research into the structure of vortex flow fields around missile shapes N84-12111

ROYAL AIRCRAFT ESTABLISHMENT, FARNBOROUGH (ENGLAND).
Recent advances in parachute technology
[RAE-TM-FS(F)-514] N84-12089
Theoretical modelling of three-dimensional vortex flows in aerodynamics N84-12116
Some considerations of the efficiency of sewn lap joints in a nylon webbing
[RAE-TR-83009] N84-12310
Influence of the airframe on the performance of antennas for avionics N84-12372

ROYAL NETHERLANDS METEOROLOGICAL INST., DE BILT.
On the growth of gravity-capillary waves by wind
[KNMI-WR-83-10] N84-12698

ROYAL SIGNALS AND RADAR ESTABLISHMENT, MALVERN (ENGLAND).
Noise reduction and segmentation of IR images using CO-median filters
[RSRE-3582] N84-12378
Dielectric loss measurement at millimetre wave frequencies using an untuned cavity
[RSRE-3597] N84-12379
An introduction to the AXIS test box
[RSRE-3583] N84-12729
The AXIS test box software report
[RSRE-3585] N84-12741

RUHR UNIV., BOCHUM (WEST GERMANY).
Calculation of unsteady flow in tubes of combustion engines with special regard to multiple branching
[REPT-82.8] N84-12410
Use of the one-dimensional theory of the filament of flow for the interpretation and synthesis of mufflers in exhaust pipes of internal combustion engines
[REPT-81.4] N84-12494

RUTGERS - THE STATE UNIV., NEW BRUNSWICK, N. J.
Ionic conductivity in lithium hexaoxometallate solid solutions
[AD-A131842] N84-12250
A study of critical factors affecting the development of performance measures in evaluating bibliographic information retrieval systems N84-13030

RUTGERS UNIV., NEW BRUNSWICK, N. J.
New materials for organic photovoltaic cells
[DE83-016845] N84-12645

S

SACRAMENTO PEAK OBSERVATORY, SUNSPOT, N. MEX.
Coronal transients in FE XIV 5303A: First two-dimensional photoelectric ground-based observations N84-13072

SANDIA LABS., ALBUQUERQUE, N. MEX.
Evaluation of the kinematic variable (back stress) response of metals
[DE83-006381] N84-12293
Accelerated compatibility testing using corrosion fatigue techniques
[DE83-015104] N84-12296
Strain rate effects on ductile/brittle transitions in steels
[DE83-016906] N84-12308
In-situ permeation tests of elastomeric O-ring seals
[DE83-015622] N84-12318
Chemical properties of metallic glasses
[DE83-017353] N84-12322
High-average-power rep rate systems
[DE83-013769] N84-12385
Power-loading effects in gas-discharge models
[DE83-016504] N84-12393
Stress production and relief in the gold/silicon eutectic die-attach process
[DE83-015230] N84-12400
The performance of the perfluorocarbon liquid/plastic-film capacitor technology in pulse-power service. A current status report
[DE83-014806] N84-12402
Numerical simulation of plastic fluids
[DE83-007911] N84-12424
Use of superposition in calculating cooling requirements for circuit cards containing arrays of electronic components
[DE83-016091] N84-12428
Experimental mixed-convection heat transfer from a large, vertical surface in a horizontal flow
[DE83-016419] N84-12429
Automated data reduction for optical interferometric data
[DE83-012075] N84-12457
Transient temperature response of strain gages, revision 1
[DE83-017514] N84-12459
Hermetically sealed microminiature multisocket connector
[DE83-017484] N84-12503
A comparison of finite-element predictions and experimental data for the forced response of the DOE 100 kW vertical-axis wind turbine
[DE83-012624] N84-12537
Single specimen J-integral testing
[DE83-016069] N84-12543
Mechanics of fracture under high-rate stress loading
[DE83-013770] N84-12544
PLT: A multipurpose plotting package
[DE83-018261] N84-12735
DRAMIN: Transferring data from the Applicon graphic system to A DRAM input file user guide
[DE83-018235] N84-12753
Double porosity model for acoustic wave propagation in fractured-porous rock
[DE83-017823] N84-12823
Using inner-shell X-rays as an ion-beam diagnostic
[DE83-017784] N84-12857
Beam-target interaction of intense ion beams: Theory and experiment
[DE83-018264] N84-12858
Magnetic trapping of intense ion beams
[DE83-017356] N84-12866
Development of a portable specular reflectometer for monitoring solar-mirror materials
[DE83-016065] N84-12901
Instabilities in cylindrical plasma liners imploded by high magnetic fields
[DE83-013640] N84-12921
Ion stopping in heated targets
[DE83-017800] N84-12941
Applied-B ion diode experiments on PBFA 1
[DE83-017792] N84-12942
Diagnosing the ion beam on the applied-B diode
[DE83-017822] N84-12943
Light-ion-beam fusion
[DE83-018263] N84-12944
Amplion hybrid diodes on hydramite and PBFA-1
[DE83-017824] N84-12945
Chemical erosion of first-wall materials by atomic hydrogen at high temperatures
[DE83-017161] N84-12962
Radiation-induced transient acoustic loss in quartz crystals
[DE83-012626] N84-12980
Hole trapping, recombination, and space charge in irradiated Sandia oxides
[DE83-015212] N84-12986
Proceedings of the Workshop on Ion Mixing and Surface Layer Alloying
[DE83-015354] N84-12994
Physics of ion implantation: Ion-cascade processes and physical state of the implanted solid
[DE83-017152] N84-12998

SANDIA LABS., LIVERMORE, CALIF.
Zero-dimensional model of compressible gas flow in networks of pressure vessels: Program TRIC
[DE83-017121] N84-12431
Gauge block isometer development
[DE83-018288] N84-12458

SANTA BARBARA RESEARCH CENTER, GOLETA, CALIF.
HgCdTe surface study program
[AD-A132071] N84-12266

SCHOOL OF AEROSPACE MEDICINE, BROOKS AFB, TEX.
A laboratory comparison of portable cooling systems for workers exposed to two levels of heat stress
[AD-A131848] N84-12423
Combined effects of ionizing radiation and anticholinesterase exposure on rodent motor performance
[AD-A131847] N84-12707

SCIENCE APPLICATIONS, INC., LA JOLLA, CALIF.
Reversed-field pinch large aspect ratio equilibrium
[DE83-016771] N84-12953

SDRC ENGINEERING SERVICES LTD., HERTS (ENGLAND).
Calculation of forced response to base excitation using experimentally derived modal participation factors N84-12205

SHEFFIELD UNIV. (ENGLAND).
The use of airborne thematic mapper simulation data for the estimation and mapping of Green Leaf Area Index (GLAI) N84-12602
On sensitivity, compensation and the approach to the asymptotes in multivariable root-loci
[RR-222] N84-12795

SMITHSONIAN ASTROPHYSICAL OBSERVATORY, CAMBRIDGE, MASS.
High Resolution Imager (HRI) for the Roentgen Satellite (ROSAT) definition study
[NASA-CR-174598] N84-12223

SOCIETE MICROTURBO, TOULOUSE (FRANCE).
Auxilliary power systems with gas turbines N84-12170

SOCIETE NATIONALE D'ETUDES ET DE CONSTRUCTION DE MOTEURS D'AVIATION, MOISSY-CRAMAYEL (FRANCE).
The relations between the numerical control of the engine and other aircraft functions N84-12062

SOFTWARE AND ENGINEERING ASSOCIATES, INC., SANTA ANA HEIGHTS, CALIF.
Improved Two-Dimensional Kinetics (TDK) computer program
[NASA-CR-170922] N84-12248

SOLAR TURBINES INTERNATIONAL, SAN DIEGO, CALIF.
Small auxiliary power unit design constraints N84-12172

SOUTH AUSTRALIAN INST. OF TECH., ADELAIDE.
Infrared characteristics of gas plumes
[AD-A131796] N84-12269

SOUTHAMPTON UNIV. (ENGLAND).
Performance measurements of a pilot superconducting solenoid model core for a wind tunnel magnetic suspension and balance system
[NASA-CR-172243] N84-12192
Prediction of dynamic effects due to vehicles crossing military bridges
[ISVR-TR-120] N84-12548

SOUTHEASTERN CENTER FOR ELECTRICAL ENGINEERING EDUCATION, INC., ST. CLOUD, FLA.
USAF/SCEEE summary faculty research program (1982) research reports, volume 2
[AD-A130770] N84-13009

SOUTHWEST RESEARCH INST., SAN ANTONIO, TEX.
Thin film strain transducer
[NASA-WLP-10055-2] N84-12448
Magnetospheric plasma studies using data from the dynamics high and low altitude plasma instruments
[AD-A131793] N84-12670

SPECTRON DEVELOPMENT LABS, INC., SEATTLE, WASH.
Investigation of the Rayleigh critical angle phenomenon for the characterization of surface properties
[AD-A131530] N84-12340

SPECTRUM TECHNOLOGY, INC., VIRGINIA BEACH, VA.
Single pilot IFR accident data analysis N84-12031

SRI INTERNATIONAL CORP., MENLO PARK, CALIF.
Reduction of CO2 to methanol and methane by photo and dark reactions on semiconductor electrodes
[PB83-249490] N84-12329
Shape from shading: An assessment N84-12574

STANFORD LINEAR ACCELERATOR CENTER, CALIF.
Free-electron-laser research
[DE83-016957] N84-12489
Montoring of the Stanford Linac microbunches' position
[DE83-012712] N84-12840
From accelerators to storage rings to ?
[DE83-011849] N84-12842
Minimal unitary (covariant) scattering theory
[DE83-014896] N84-12849
Covariant theory with a confined quantum
[DE83-014897] N84-12850
Baryon-antibaryon angular correlations in quark jets
[DE83-015923] N84-12854
Jet production and high p/sub T/ phenomena in photon-photon reactions
[DE83-016397] N84-12868
Physics at very high energies
[DE83-012854] N84-12878
Tau and B lifetime measurements from the MARK 2
[DE83-018219] N84-12879

STANFORD UNIV., CALIF.
On the structure of the turbulent vortex N84-12102
Steady and unsteady flow models for airfoils with spoiler N84-12136
Control of flexible spacecraft by optimal model following N84-12222
Advanced diagnostics and instrumentation for chemically reactive flow systems
[AD-A131814] N84-12251
Rising bubbles
[AD-A131572] N84-12413
Laser physics and laser spectroscopy
[AD-A131720] N84-12470
Cumulative damage in components of steel structures under cyclic inelastic loading N84-12550
On the dynamic fracture of bars, beams and plates N84-12552
Effects of microstructure and pore fluids on the acoustic properties of granular materials
[AD-A131983] N84-12668
User's guide for SOL/NPSOL: A FORTRAN package for nonlinear programming
[DE83-016903] N84-12751
User's guide for SOL/QPSOL: A FORTRAN package for quadratic programming
[DE83-016990] N84-12752
Artificial intelligence: Cognition as computation
[AD-A131804] N84-12770
Search among queues
[AD-A131639] N84-12773
Kingman's subadditive ergodic theorem
[AD-A131795] N84-12801
Fabrication and properties of multilayer structures
[AD-A131934] N84-12969

STATE UNIV. OF NEW YORK, STONY BROOK.
Hadron-hadron collider group
[DE83-010704] N84-12865

SUNDSTRAND ADVANCED TECHNOLOGY GROUP, ROCKFORD, ILL.
Implementing microprocessor technology in aircraft electrical power generating system control N84-12185

SYNERGY, INC., WASHINGTON, D. C.
Develop a normative or descriptive model of the international/domestic civil aviation industry, volume 3
[AD-A131878] N84-12051
Develop a normative or descriptive model of the international/domestic civil aviation industry, volume 2
[AD-A131877] N84-12052
Develop a normative or descriptive model of the international/domestic civil aviation industry. Volume 1: Executive summary
[AD-A131876] N84-12053

SYRACUSE UNIV., N. Y.
Multiplane finite element method: Applications to fiber reinforced material N84-12261
Thermal stress analysis of annular glass-to-metal seals under thermal shock N84-12408

SYRACUSE UNIV., UTICA, N. Y.
Information retrieval research support
[AD-A131990] N84-13022

SYSTEMS AND APPLIED SCIENCES CORP., HAMPTON, VA.
Mesocyclone detection and classification algorithm [AD-A131826] N84-12691
SYSTEMS DYNAMICS, INC., GAINESVILLE, FLA.
Space Shuttle propulsion parameter estimation using optimal estimation techniques, volume 1 [NASA-CR-170935] N84-12213
SYSTEMS TECHNOLOGY, INC., HAWTHORNE, CALIF.
Control/display trade-off study for single-pilot instrument flight rule operations N84-12044

T

TATA INST. OF FUNDAMENTAL RESEARCH, BOMBAY (INDIA).
On Waring's problem g (4) or = 20 N84-12781
TECHNICAL UNIV. OF DENMARK, LYNGBY.
Introductory studies of natural contamination and manmade pollution in Danish waters N84-12608
Passive radiometry and other remote sensing data interpretation for oil slick thickness assessment, in an experimental case N84-12609
TECHNISCHE HOCHSCHULE, AACHEN (WEST GERMANY).
A contribution to the problem of vortex breakdown N84-12125
The hydraulic multiaxes vibrator: Its capabilities to simulate real mechanical environments and to verify aerospace structures N84-12198
Practical experience during installation of the large multiaxes vibration test facility SAMSON N84-12199
TECHNISCHE HOGESCHOOL, DELFT (NETHERLANDS).
An experimental investigation of the vortex flow over delta and double-delta wings at low speed N84-12106
Multidimensional explicit difference schemes for hyperbolic conservation laws [NASA-CR-172254] N84-12778
TECHNISCHE UNIV., BRUNSWICK (WEST GERMANY).
Observations of hydromagnetic turbulence in the solar wind N84-13074
TECHNISCHE UNIV., GRAZ (AUSTRIA).
Actitities report on the projet DESBOD [REPT-5] N84-13025
TECHNISCHE UNIV., MUNICH (WEST GERMANY).
High-sensitivity mass spectrometry with a tandem accelerator [DE83-017914] N84-12274
TECHNISCHE UNIV., VIENNA (AUSTRIA).
Anisotropy and microstructure of Sm2(Co, Fe, Cu, Zr)17 magnetic materials [AD-A131961] N84-12291
Rectification of multispectral scanner images [GEOWISS-MITT-24-1983] N84-12628
TECHNISCHE UNIV. MUNICH, GARCHING (WEST GERMANY).
Use of remote sensing methods for the ecological mapping project of the European community N84-12580
The modular optoelectronic scanner (MOMS) on STS-7, June 83 N84-12589
TELEDYNE CAE, TOLEDO, OHIO.
A jet fuel starter for lowest system life cycle cost N84-12179
TENNESSEE UNIV., KNOXVILLE.
Acoustic streaming as a mechanism of the Ranque-Hilsch effect N84-12088
Effect of noise in the three-parameter logistic model [AD-A131867] N84-12721
Rank modification method for certain singular systems of linear equations N84-12797
TENNESSEE UNIV. SPACE INST., TULLAHOMA.
The treatment of convected vortices in compressible potential flow N84-12121
TEXAS A&M UNIV., COLLEGE STATION.
The SSME seal test program: Leakage tests for helically-grooved seals [NASA-CR-170921] N84-12495
Optimization of ultrasonic flaw detection in railroad rail [PB83-236919] N84-12518
Proceedings of the NASA Symposium on Mathematical Pattern Recognition and Image Analysis [E83-10032] N84-12557
Spline classification methods . N84-12564
Quantile data analysis of image data N84-12565
Discrimination relative to measures of non-normality N84-12566
Repeated-measures analysis of image data N84-12567
A numerical study on the evolution of tornadoes N84-12679
TEXAS TECHNOLOGICAL UNIV., LUBBOCK.
Dynamic-stall regulation of the Darrieus turbine [DE83-017994] N84-12097
TEXAS UNIV., AUSTIN.
An empirical Bayes approach to spatial analysis N84-12563
Estimation of uncertainty in coal resources [DE83-902538] N84-12620
The use of a formal simulator to verify a simple real time control program [AD-A131732] N84-12745
Observations of soft X-ray fluctuations with an imaging array on TEXT [DE83-018118] N84-12938
Dynamical evolution of substucture in molecular clouds N84-13043
The chemical evolution of the coma of comet P/Stephan-Oterma N84-13055
THIOKOL CORP., BRIGHAM CITY, UTAH.
Replacement of PBNA in HB and HC polymers used in SRM propellant and liner [NASA-CR-170936] N84-12311
TORONTO UNIV., DOWNSVIEW (ONTARIO).
Transition flow ion transport via integral Boltzmann equation [UTIAS-269] N84-12828
TORONTO UNIV. (ONTARIO).
Performance of antennas in plasma N84-12377
Initial decay of flow properties of planar, cylindrical and spherical blast waves [UTIAS-TN-244] N84-12416
TRONDHEIM UNIV. (NORWAY).
The break-up mechanism of a streamwise directed vortex N84-12123
TRW DEFENSE AND SPACE SYSTEMS GROUP, REDONDO BEACH, CALIF.
Development of instrumentation for monitoring carbon fiber emission [PB83-233726] N84-12460
TRW SPACE TECHNOLOGY LABS., REDONDO BEACH, CALIF.
Study of multi-kilowatt solar arrays for Earth orbit applications [NASA-CR-170939] N84-12634

U

UNITED TECHNOLOGIES CORP., EAST HARTFORD, CONN.
Helicopter rotor wake geometry and its influence in forward flight. Volume 1: Generalized wake geometry and wake effect on rotor airloads and performance [NASA-CR-3726] N84-12090
Deposit formation and heat transfer in hydrocarbon rocket fuels [NASA-CR-168277] N84-12225
UNITED TECHNOLOGIES RESEARCH CENTER, EAST HARTFORD, CONN.
Helicopter rotor wake geometry and its influence in forward flight. Volume 2: Wake geometry charts [NASA-CR-3727] N84-12091
Aeroelastic analysis for propellers - mathematical formulations and program user's manual [NASA-CR-3729] N84-12530
UNIVERSIDAD POLITECNICA DE BARCELONA (SPAIN).
Mapping land use in Catalonia (Spain) N84-12613
UNIVERSITE CATHOLIQUE DE LOUVAIN (BELGIUM).
SAR 580: Images for agricultural and forest survey. First results in middle Belgium N84-12595
UNIVERSITY OF SOUTHERN CALIFORNIA, LOS ANGELES.
The interplanetary hydrogen and helium glow and the inferred interstellar gas properties N84-13109
UNIVERSITY OF SOUTHERN CALIFORNIA, MARINA DEL REY.
Large-area mercuric iodide photodectors [DE83-013035] N84-12898
UNIVERSITY OF SOUTHERN MISSISSIPPI, HATTIESBURG.
Low energy electron magnetometer using a monoenergetic electron beam [NASA-CASE-LAR-12706-1] N84-12444
UPPSALA IONOSPHERIC OBSERVATORY (SWEDEN).
Activities report on ionospheric observation [UIO-AR-83-05] N84-12674
UTAH UNIV., SALT LAKE CITY.
Identifying environmental features for land management decisions [E84-10016] N84-12556

V

VALVO G.M.B.H., HAMBURG (WEST GERMANY).
Predevelopment of IR-CCD components [BMFT-FB-T-83-133] N84-13001
VEREINIGTE FLUGTECHNISCHE WERKE G.M.B.H., BREMEN (WEST GERMANY).
Ground and inflight operational effects of APU's N84-12182
VIGYAN RESEARCH ASSOCIATES, INC., HAMPTON, VA.
Vortical flow management for improved configuration aerodynamics: Recent experiences N84-12129
VIRGINIA POLYTECHNIC INST. AND STATE UNIV., BLACKSBURG.
Relative elevation determination from LANDSAT imagery N84-12558
VIRGINIA UNIV., CHARLOTTESVILLE.
Experiments on the nuclear interactions of pions [DE83-016285] N84-12844
VITRO LABS., SILVER SPRING, MD.
Reliability and maintainability study of select solar-energy-system components in the National Solar Data Network [DE83-011974] N84-12647
VON KARMAN INST. FOR FLUID DYNAMICS, RHODE-SAINT-GENESE (BELGIUM).
Laser velocimetry study of compressibility effects on the flow field of a delta wing N84-12108
VOUGHT CORP., DALLAS, TEX.
Improved wave drag predictions using modified linear theory [NASA-CR-174494] N84-12096

W

WASHINGTON UNIV., SEATTLE.
A study of coherent structures in the near-neutral marine atmospheric boundary layer N84-12658
Study of vibrational energy transfer at a surface by a time-of-flight method [AD-A131798] N84-12833
High temperature gas energy transfer [AD-A131782] N84-12836
University of Washington superconducting-booster project [DE83-015689] N84-12848
Clustering and ordering in 3-5 alloys [AD-A131785] N84-12974
Cross sections relevant to gamma-ray astronomy: Alpha-particle-induced reactions [DE83-015533] N84-13038
Problems of stellar evolution in star clusters of the Magellanic clouds N84-13051
Ultra-relativistic heavy ions and cosmic rays [DE83-015881] N84-13134
WAYNE STATE UNIV., DETROIT, MICH.
Bending of transversally loaded orthotropic rectangular and sector plates N84-12520
WEATHER WING (5TH), LANGLEY AFB, VA.
World-wide sea-surface temperatures [AD-A131892] N84-12689
WEIDLINGER ASSOCIATES, NEW YORK, N.Y.
Yield surface for bars including warping restraint [AD-A131393] N84-12533
Submerged shock response of a linearly elastic shell of revolution containing internal structure. User's manual for the ELSHOK code [AD-A131282] N84-12534
WEISSMAN (DAVID E.), NORTHPORT, N.Y.
The dependence of the radar modulation transfer function on environmental conditions and wave parameters [AD-A131858] N84-12348
WEIZMANN INST. OF SCIENCE, REHOVOTH (ISRAEL).
GRIDPACK: Toward unification of general grid programming [AD-A131892] N84-12748
WESTINGHOUSE HANFORD CO., RICHLAND, WASH.
Transmission of fast neutrons from the Li(d,xn) reaction through thick iron [DE83-015975] N84-12884
WHITMORE ENTERPRISES, SAN ANTONIO, TEX.
Lower body graduated negative pressure system [NASA-CR-171717] N84-12725
WICHITA STATE UNIV., KANS.
An experimental investigation of separated three dimensional flow on general aviation twin-engine aircraft N84-12087
A study of wing-body aerodynamic interference of a light twin aircraft utilizing a panel method potential flow program N84-12134
Analytical design of a liquid hydrogen fueled turbofan-ramjet engine for flight Mach numbers zero to five N84-12187
WISCONSIN UNIV., MADISON.
Solidification of aluminum and aluminum alloys at high levels of undercooling N84-12286

Phytochrome from green plants: Assay, purification, and characterization
[DE83-017447] N84-12710
Drift wave studies in a linear multiple mirror
[DE83-016881] N84-12951
The winds and coronae of early-type stars
N84-13086

WOODS HOLE OCEANOGRAPHIC INSTITUTION, MASS.
Sediment transport in a tidal inlet
[PB83-242271] N84-12632

WOODS (JAMES E.), AMES, IOWA.
NBS (National Bureau of Standards) Workshop: Environmental Control for Archival Records Storage
[PB83-242230] N84-13026

WORLD METEOROLOGICAL ORGANIZATION, GENEVA (SWITZERLAND).
Guide to agricultural meteorological practices, second edition
[WMO-134] N84-12697

WUERZBURG UNIV. (WEST GERMANY).
Activities report of the Institute of Astronomy and Astrophysics N84-13048

WYOMING UNIV., LARAMIE.
Snowy Range Observatory: Climatological and streamflow data report 1982
[PB83-243147] N84-12633
Field and laboratory studies of ice nucleation in winter orographic clouds N84-12678

Y

YALE UNIV., NEW HAVEN, CONN.
Simulations of galaxy mergers N84-13054

YOUNG (ARTHUR) AND CO., WASHINGTON, D. C.
Office automation management guide
[AD-A131770] N84-13012

CONTRACT NUMBER INDEX

Typical Contract Number Index Listing

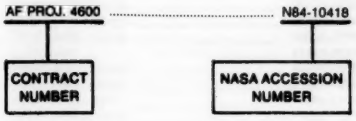

Listings in this index are arranged alphanumerically by contract number. Under each contract number the NASA accession numbers denoting documents that have been produced as a result of research done under that contract are arranged in ascending order. The NASA accession number denotes the number by which the citation is identified.

AF PROJ. 3G10 ..... N84-12343
AF PROJ. 317J N84-12894
AF PROJ. 1710 ..... N84-13011
AF PROJ. 1926 ..... N84-12159
N84-12163
AF PROJ. 2127 ..... N84-12211
AF PROJ. 2202 ..... N84-12159
AF PROJ. 2301 ..... N84-12316
N84-12467
N84-12470
N84-12837
N84-12918
N84-13009
AF PROJ. 2303 ..... N84-12270
N84-12471
N84-12830
N84-12838
N84-12972
AF PROJ. 2304 ..... N84-12418
N84-12728
N84-12771
N84-12798
N84-12799
N84-12808
AF PROJ. 2305 ..... N84-12344
N84-12466
N84-12978
AF PROJ. 2306 ..... N84-12340
N84-12974
AF PROJ. 2307 ..... N84-12095
N84-12509
AF PROJ. 2308 ..... N84-12251
N84-12421
AF PROJ. 2309 ..... N84-12669
AF PROJ. 2310 ..... N84-12452
N84-12671
AF PROJ. 2311 ..... N84-12453
AF PROJ. 2401 ..... N84-12191
AF PROJ. 2402 ..... N84-12157
N84-12158
AF PROJ. 2403 ..... N84-12152
AF PROJ. 2418 ..... N84-12290
AF PROJ. 2421 ..... N84-12161
AF PROJ. 2646 ..... N84-12692
AF PROJ. 2673 ..... N84-12195
AF PROJ. 2729 ..... N84-12423
AF PROJ. 3201 ..... N84-12785
AF PROJ. 5581 ..... N84-13022
AF PROJ. 6114 ..... N84-13019
AF PROJ. 6670 ..... N84-12667
N84-12682
N84-12683
N84-12686
N84-12687
N84-12691
AF PROJ. 6690 ..... N84-12665
AF PROJ. 7601 ..... N84-12209
N84-12210
N84-12917
AF PROJ. 7659 ..... N84-12093
N84-12218
AF PROJ. 7661 ..... N84-12670
N84-12831
AF PROJ. 7757 ..... N84-12707
AF PROJ. 8809 ..... N84-12920
AF PROJ. 9749 ..... N84-12727
AF PROJ. 9993 ..... N84-12468
N84-12469
AF-AFOSR-034-79 ..... N84-12418
AF-AFOSR-0055-82 ..... N84-12671
AF-AFOSR-0061-80 ..... N84-12471
AF-AFOSR-0067-81 ..... N84-12837
AF-AFOSR-0079-80 ..... N84-12466
AF-AFOSR-0091-81 ..... N84-12918
AF-AFOSR-0130-79 ..... N84-12467
AF-AFOSR-0169-81 ..... N84-12344
AF-AFOSR-0190-80 ..... N84-12771
AF-AFOSR-0231-82 ..... N84-12974
AF-AFOSR-0271-80 ..... N84-12838
AF-AFOSR-0284-80 ..... N84-12978
AF-AFOSR-3602-78 ..... N84-12728
AF-AFOSR-0258-82 ..... N84-12808
AFOSR-ISSA-82-00029 ..... N84-12834
ARPA ORDER 2551 ..... N84-12666
ARPA ORDER 3011 ..... N84-12975
N84-12976
N84-12977
ARPA ORDER 3391 ..... N84-12343
ARPA ORDER 3706 ..... N84-12969
ARPA ORDER 3985 ..... N84-12266
ARPA ORDER 4109 ..... N84-12340
AT(29-2)-474 ..... N84-12673
BMFT-RV-14-B8/74 ..... N84-13117
BMFT-RV14-B8/74 ..... N84-13112
DA PROJ. RR04204 ..... N84-12721
DA PROJ. 1L1-61101-A-91A N84-12417
DA PROJ. 1L1-61102-AH-42 ..... N84-12535
DA PROJ. 1L1-61102-AH-43 ..... N84-12094
N84-12267
N84-12420
DA PROJ. 1L1-61102-AH-48 ..... N84-12352
DA PROJ. 1L1-62618-AH-80 ..... N84-12194
N84-12731
N84-12744
DA PROJ. 1L1-161101-A-91-A N84-12919
DA PROJ. 1T1-61102-BH-57 ..... N84-12291
N84-12351
N84-12746
DA PROJ. 2Q7-62722-A-765 ..... N84-13020
DA PROJ. 3E1-62777-A-878 ..... N84-12714
N84-12726
DA PROJ. 3M1-61102-BS-10 ..... N84-12708
DA PROJ. 3M1-62734-A-875 ..... N84-12719
DA PROJ. 4600 ..... N84-12347
DA PROJ. 7670 ..... N84-13037
DAAB07-78-C-2922 ..... N84-12891
N84-12892
DAAG29-78-G-0057 ..... N84-12094
DAAG29-79-C-0110 ..... N84-12752
DAAG29-81-C-0032 ..... N84-12112
DAAG29-81-K-156 ..... N84-12751
DAAG29-81-K-0004 ..... N84-12632
DAAG29-82-K-0197 ..... N84-12727
DAAK70-80-C-0045 ..... N84-12496
DAAK80-80-K-0579 ..... N84-12352
DAJA37-79-C-0504 ..... N84-12746
DAJA37-79-C-0516 ..... N84-12351
DAJA37-82-C-0050 ..... N84-12291
DARPA ORDER 2646 ..... N84-12692
DARPA ORDER 3343 ..... N84-12895
DARPA ORDER 4395 ..... N84-12829
DASG60-80-C-0057 ..... N84-12732
DE-AC01-80CS-40402 ..... N84-12320
DE-AC01-80CS-50021 ..... N84-12327
DE-AC02-76CH-00016 ..... N84-12256
N84-12275
N84-12386
N84-12399
N84-12541
N84-12545
N84-12720
N84-12754
N84-12826
N84-12862
N84-12872
N84-12874
N84-12896
N84-12934
N84-12987
N84-12989
DE-AC02-76CH-03000 ..... N84-12502
N84-12791
N84-12855
N84-12999
N84-13132
DE-AC02-76ER-01116 ..... N84-12856
DE-AC02-76ER-01198 ..... N84-12273
DE-AC02-76ER-02167 ..... N84-12852
DE-AC02-76ER-03416 ..... N84-12277
DE-AC02-76ET-51001 ..... N84-12733
DE-AC02-76ET-53051 ..... N84-12951
DE-AC02-76EV-01599 ..... N84-12625
N84-12627
DE-AC02-77CH-00178 ..... N84-12622
N84-12641
N84-12644
N84-12647
N84-12650
N84-13127
N84-13128
DE-AC02-78ER-04693 ..... N84-12992
DE-AC02-78ET-51013 ..... N84-12817
N84-12937
N84-12950
DE-AC02-79ER-10463 ..... N84-12645
DE-AC02-80CS-30260 ..... N84-13005
DE-AC02-80ER-10575 ..... N84-12902
DE-AC02-81ER-10903 ..... N84-12710
DE-AC02-81ER-40014 ..... N84-12877
DE-AC02-83ER-53147 ..... N84-12947
DE-AC03-76SF-00098 ..... N84-12255
N84-12276
N84-12279
N84-12392
N84-12398
N84-12401
N84-12738
N84-12749
N84-12847
N84-12861
N84-12885
N84-12886
N84-12895
N84-12929
N84-12993
N84-12996
N84-13003
DE-AC03-76SF-00326 ..... N84-12752
DE-AC03-76SF-00515 ..... N84-12489
N84-12840
N84-12842
N84-12849
N84-12850
N84-12854
N84-12868
N84-12878
N84-12879
DE-AC03-80ER-53092 ..... N84-12924
N84-12925
DE-AC03-81ER-53113 ..... N84-12953
DE-AC03-82SF-11593 ..... N84-12640
DE-AC04-76DP-00053 ..... N84-12734
DE-AC04-76DP-00789 ..... N84-12097
N84-12278
N84-12293
N84-12296
N84-12308
N84-12318
N84-12322
N84-12385
N84-12393
N84-12400
N84-12402
N84-12403
N84-12428
N84-12429
N84-12431

N84-12457
N84-12458
N84-12459
N84-12503
N84-12543
N84-12544
N84-12735
N84-12753
N84-12823
N84-12857
N84-12858
N84-12866
N84-12901
N84-12921
N84-12941
N84-12942
N84-12943
N84-12944
N84-12945
N84-12962
N84-12980
N84-12986
N84-12994
N84-12998
DE-AC04-76DP-03533 N84-12767
DE-AC04-76DP-000789 N84-13039
DE-AC05-76OR-00033 N84-12626
DE-AC06-76ET-53043 N84-12938
DE-AC06-76FF-02170 N84-12300
N84-12510
N84-12884
N84-12935
DE-AC06-76RL-01830 N84-12321
N84-12843
N84-12849
N84-12855
N84-12893
N84-12894
N84-12903
N84-12904
N84-12926
N84-13014
DE-AC06-81ER-40048 N84-12848
N84-13038
N84-13134
DE-AC07-76ID-01570 N84-12873
DE-AC08-83NV-10262 N84-12898
DE-AC09-76SR-00001 N84-12301
N84-12309
N84-12539
DE-AI01-82NE-50004 N84-12479
DE-AI08-76DP-00474 N84-12673
DE-AM03-76SF-00326 N84-12751
DE-AS05-76ER-04043 N84-12844
DE-AS05-76ET-52025 N84-12922
DE-AS05-76ER-10448 N84-13004
DE-AS06-82ER-12096 N84-12305
DE-AT03-76ER-70279 N84-12487
DE-AT03-76ER-72018 N84-12751
N84-12752
DE-AT03-76ET-51011 N84-12815
N84-12927
N84-12949
N84-12957
DE-AT06-76ER-70004 N84-12871
DE-FC04-80CS-30284 N84-12639
DE-FC05-77ET-10069 N84-12281
DE-FG01-81CS-16040 N84-12469
DE-FG02-81ER-10961 N84-12636
DE-FG22-80PC-30247 N84-12271
DE-FG22-82PC-50800 N84-12432
DI-14-34-0001-1449 N84-12284
DI-14-34-0001-2154 N84-12633
DNA PROJ. X99-QAXV N84-12339
DNA PROJ. Y99-QAXS N84-12534
DNA001-81-C-0048 N84-12533
N84-12534
DNA001-81-C-0175 N84-12339
DRET-82-468 N84-12128
DTRS56-80-C-00032 N84-12518
EG-C-01-4042 N84-13127
EG-77-C-01-4042 N84-12822
N84-12841
N84-12844
N84-12847
N84-13128
EPA-IAG-AD-80-F-2A008 N84-12461
EPA-68-02-3273 N84-12460
EPA-68-03-1647 N84-12507
EPRI PROJ. 1367-1 N84-12620
ESA-81-IG-28-R3-81 N84-12207
ESA-3807/78/NL-HP(SC) N84-12202
ESA-3879/79/NL-MB N84-12204
ESA-5179/82/NL-PP(SC) N84-12204
FFA PROJ. HU-2302 N84-12260
FMV-F-FL-82223-80-001-21-001 N84-12260
FMV-F-FL-82223-80-183-21-001 N84-12516
F04611-83-C-0013 N84-12249
F08606-80-C-0021 N84-12666
F08635-80-C-0206 N84-12195
F19628-79-C-0152 N84-12917
F19628-80-C-0002 N84-12343
F19628-80-C-0125 N84-12211
F19628-81-C-0073 N84-12693
F19628-81-C-0162 N84-12452
F19628-81-K-0024 N84-13104
F19628-81-K-0051 N84-13093
F19628-82-C-0023 N84-12691
F19628-82-K-0015 N84-13090
F19628-82-K-0022 N84-12669
F19628-82-K-0024 N84-12670
F19628-82-K-0033 N84-12453
F19628-82-K-0039 N84-12210
F19628-83-C-0053 N84-12785
F29601-82-C-0036 N84-12920
F29601-82-K-0009 N84-12894
F30602-76-C-0054 N84-12692
F30602-79-C-0195 N84-13022
F33615-76-C-2148 N84-12178
F33615-76-C-3103 N84-12159
F33615-77-C-0074 N84-13011
F33615-77-C-5155 N84-12160
F33615-79-C-0014 N84-13019
F33615-79-C-3030 N84-12095
F33615-80-C-2022 N84-12316
F33615-80-C-3401 N84-12159
F33615-81-C-3421 N84-12157
N84-12158
F33615-81-K-2003 N84-12421
F33615-82-C-5039 N84-12161
N84-12290
F33657-76-C-2055 N84-12179
F49620-79-C-0131 N84-12771
F49620-80-C-0060 N84-12270
F49620-80-C-0091 N84-12251
F49620-81-C-0040 N84-12340
F49620-81-C-0047 N84-12470
F49620-82-C-0009 N84-12782
N84-12798
N84-12799
F49620-82-C-0035 N84-13009
F49620-82-K-0001 N84-12787
F49642-81-C-0237 N84-12051
N84-12052
N84-12053
F58524 N84-13021
GA PROJ. 3235 N84-12815
N84-12949
GA PROJ. 3344 N84-12927
MDA903-79-C-0690 N84-13012
MDA903-80-C-0496 N84-12266
MDA903-81-C-0348 N84-12975
N84-12976
N84-12977
MDA903-81-C-0484 N84-12969
MDA903-82-G-0055 N84-13010
MDA903-83-C-0027 N84-12574
MIPR-CES-82-3 N84-12331
MIPR-CES-82-3A N84-12331
M0100PN N84-13021
NAGW-76 N84-13068
N84-13118
NAGW-79 N84-13083
N84-13088
NAGW-95 N84-12556
NAGW-139 N84-13057
NAGW-200 N84-13099
N84-13100
NAGW-249 N84-13083
N84-13088
N84-13115
NAGW-264 N84-13113
NAGW-337 N84-13058
NAGW-365 N84-12223
NAG1-158 N84-12527
NAG1-198 N84-12732
NAG5-87 N84-13084
NAG5-130 N84-13118
NAG5-613 N84-13071
NAMRL PROJ. F51524 N84-12706
NAMRL PROJ. F58524 N84-12704
N84-12705
NAMRL PROJ. F58526 N84-12716
NAMRL PROJ. M0096PN N84-12703
NASA ORDER S-10757-C N84-12555
NASA ORDER S-50664-A N84-13097
NASW-3389 N84-13080
NAS1-14568 N84-12090
N84-12091
NAS1-15810 N84-12778
NAS1-16000 N84-12528
NAS1-16617 N84-12110
NAS1-17070 N84-12727
N84-12742
N84-12777
NAS1-17130 N84-12742
N84-12777
NAS2-5472 N84-13111
NAS2-8786 N84-12112
NAS3-22548 N84-12312
NAS3-22753 N84-12530
NAS3-23248 N84-12226
NAS3-23344 N84-12225
NAS3-23523 N84-12263
N84-12265
NAS3-23779 N84-12227
NAS5-20062 N84-13117
NAS5-26739 N84-13112
NAS5-26819 N84-12832
NAS5-27752 N84-13097
NAS7-100 N84-12151
N84-12289
N84-12463
N84-12635
N84-12968
N84-13078
N84-13097
N84-13101
N84-13107
N84-13123
NAS7-918 N84-13099
N84-13100
NAS8-30490 N84-12311
NAS8-33716 N84-12495
NAS8-34131 N84-12634
NAS8-34573 N84-13066
NAS8-34750 N84-12415
NAS8-35017 N84-12217
NAS8-35046 N84-12248
NAS8-35324 N84-12213
NAS8-35481 N84-12413
NAS9-16664 N84-12557
N84-12573
N84-12574
NAS9-16810 N84-12725
NA79AA-D-00102 N84-12632
NA80AA-D-00077 N84-12632
NE-5061-015 N84-12696
NE-5061-016 N84-12696
NERC-MSS-82 N84-12602
NGL-14-001-001 N84-13069
NGL-33-018-003 N84-12257
NGR-05-002-016 N84-13100
NGR-05-002-160 N84-13056
N84-13064
N84-13099
NGR-12-001-011 N84-13082
NOSC PROJ. F59551 N84-12685
NR PROJ. 042-467 N84-12807
NR PROJ. 047-607 N84-12784
NR PROJ. 064-410 N84-12536
N84-12786
NR PROJ. 083-231 N84-12681
NR PROJ. 092-549 N84-12833
N84-12836
NR PROJ. 659-797 N84-12325
NR PROJ. 659-798 N84-12325
NSF AST-80-19874 N84-13087
NSF ATM-81-1753 N84-13092
NSF ATM-81-19302 N84-13124
NSF ATM-81-20455 N84-13089
NSF ATM-81-21723 N84-12671
NSF ATM-82-09603 N84-13090
NSF CME-79-19817 N84-12122
NSF DMR-79-21210 N84-12302
NSF ECS-80-12974 N84-12751
N84-12752
NSF ECS-81-2070 N84-12732
NSF ISP-80-19800 N84-13016
NSF MCS-78-00783 N84-12742
NSF MCS-79-26009 N84-12751
NSF MCS-82-02259 N84-12782
NSF MCS-82-02943 N84-12745
NSF MS-79-26009 N84-12752
NSF-79-06337 N84-12428
NSG-1605 N84-12028
NSG-5178 N84-13082
NSG-7416 N84-13077
NSG-7422 N84-13124
NSG-7506 N84-12664
NSG-7523 N84-12192
NSG-7622 N84-12336
NUSC PROJ. A65000 N84-12820
N00014-75-C-0201 N84-12681
N00014-75-C-0267 N84-12751
N84-12752
N00014-75-C-0690 N84-12833
N84-12836

N00014-76-C-0016 ..... N84-12832
N00014-76-C-0240 ..... N84-12536
N84-12786
N00014-76-C-0302 ..... N84-12800
N00014-76-C-0408 ..... N84-12314
N00014-76-C-0475 ..... N84-12801
N00014-76-C-0745 ..... N84-12268
N00014-77-C-0390 ..... N84-12668
N00014-77-C-0553 ..... N84-12835
N00014-78-C-0128 ..... N84-12112
N00014-78-C-0647 ..... N84-12258
N00014-78-C-0678 ..... N84-12464
N00014-79-C-0302 ..... N84-12770
N00014-79-C-0650 ..... N84-12807
N00014-79-C-0685 ..... N84-12773
N00014-80-C-0505 ..... N84-12769
N84-12772
N00014-81-C-0569 ..... N84-12721
N00014-81-K-0039 ..... N84-12292
N00014-81-K-0611 ..... N84-12315
N00014-81-K-0634 ..... N84-12745
N00014-82-C-0354 ..... N84-12112
N00014-82-K-0084 ..... N84-12128
N00014-82-K-0263 ..... N84-12325
N00014-82-K-0317 ..... N84-12250
N00014-82-K-0329 ..... N84-12784
N00014-82-WR-20129 ..... N84-12325
N00014-83-G-0057 ..... N84-12994
N00014-83-M-0081 ..... N84-12348
N00019-81-C-0182 ..... N84-12350
N00019-81-C-0425 ..... N84-12973
N00019-82-C-0204 ..... N84-12970
N00024-79-C-6043 ..... N84-12822
N00024-83-C-5301 ..... N84-13113
N00167-82-C-0023 ..... N84-12096
N60921-83-WR-W0088 ..... N84-12829
N62269-81-C-0726 ..... N84-12156
RR01107 ..... N84-12835
RR01108 ..... N84-12821
RR02402OD N84-12325
RR0210543 ..... N84-12345
SRC-GR/B/79455 ..... N84-12795
SR0230100 ..... N84-12419
W-31-109-ENG-38 ..... N84-12254
N84-12274
N84-12294
N84-12297
N84-12299
N84-12302
N84-12306
N84-12319
N84-12387
N84-12389
N84-12394
N84-12395
N84-12396
N84-12404
N84-12511
N84-12546
N84-12642
N84-12709
N84-12774
N84-12788
N84-12805
N84-12839
N84-12859
N84-12860
N84-12865
N84-12931
N84-12936
N84-13034
W-7405-ENG-26 ..... N84-12273
N84-12295
N84-12303
N84-12304
N84-12305
N84-12425
N84-12426
N84-12427
N84-12430
N84-12477
N84-12497
N84-12500
N84-12501
N84-12504
N84-12540
N84-12542
N84-12626
N84-12657
N84-12748
N84-12755
N84-12802
N84-12851
N84-12863
N84-12867
N84-12875
N84-12881
N84-12887
N84-12897
N84-12923
N84-12952
N84-12956
N84-12958
N84-12959
N84-12961
N84-12981
N84-12982
N84-12984
N84-12990
N84-12995
N84-13031
W-7405-ENG-36 ..... N84-12384
N84-12388
N84-12474
N84-12480
N84-12481
N84-12483
N84-12484
N84-12485
N84-12488
N84-12672
N84-12723
N84-12736
N84-12737
N84-12790
N84-12843
N84-12845
N84-12853
N84-12869
N84-12870
N84-12880
N84-12882
N84-12888
N84-12904
N84-12905
N84-12928
N84-12930
N84-12979
N84-13006
N84-13047
N84-13133
W-7405-ENG-48 ..... N84-12253
N84-12272
N84-12298
N84-12326
N84-12370
N84-12373
N84-12374
N84-12390
N84-12397
N84-12472
N84-12473
N84-12475
N84-12476
N84-12478
N84-12482
N84-12486
N84-12646
N84-12750
N84-12789
N84-12816
N84-12841
N84-12848
N84-12883
N84-12899
N84-12900
N84-12932
N84-12933
N84-12939
N84-12940
N84-12946
N84-12948
N84-12954
N84-12960
N84-12983
N84-12985
N84-12991
N84-13013
W-7405-ENG-82 ..... N84-12167
N84-12252
N84-12259
N84-12273
N84-12280
N84-12282
N84-12307
N84-12353
N84-12512
N84-12513
N84-12547
N84-12824
N84-12825
N84-12827
N84-12864
N84-12903
N84-12997
W-47505-ENG-48 ..... N84-12968
505-31-53-10 ..... N84-12192
505-33-23-02 ..... N84-12529
505-33-52 ..... N84-12730
505-33-53-05 ..... N84-12531
505-34-03-03 ..... N84-12190
505-35-23-31 ..... N84-12029
505-40-5B N84-12166
506-52-49 ..... N84-12248
506-53-53 ..... N84-12412
506-57-13-10 ..... N84-12226
534-04-13-54 ..... N84-12164

REPORT / ACCESSION NUMBER INDEX

Typical Report / Accession Number Index Listing

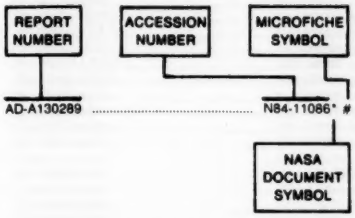

Listings in this index are arranged alphanumerically by report number. The NASA accession number denotes the number by which the citation is identified. An asterisk (*) indicates that the item is a NASA report. A pound sign (#) indicates that the item is available on microfiche.

A-9508 ..... N84-12414* #
A-9542 ..... N84-12809* #

ACC-67227 ..... N84-12818

AD-A126269 ..... N84-12484 #
AD-A129559 ..... N84-12798 #
AD-A130705 ..... N84-12782 #
AD-A130770 ..... N84-13009 #
AD-A130968 ..... N84-12532 #
AD-A131067 ..... N84-12336 #
AD-A131068 ..... N84-12743 #
AD-A131086 ..... N84-12890 #
AD-A131087 ..... N84-12814 #
AD-A131088 ..... N84-12380 #
AD-A131119 ..... N84-13019 #
AD-A131120 ..... N84-13020 #
AD-A131134 ..... N84-12417 #
AD-A131142 ..... N84-12498 #
AD-A131148 ..... N84-12339 #
AD-A131282 ..... N84-12534 #
AD-A131379 ..... N84-13011 #
AD-A131393 ..... N84-12533 #
AD-A131530 ..... N84-12340 #
AD-A131557 ..... N84-12665 #
AD-A131572 ..... N84-12418 #
AD-A131592 ..... N84-12829 #
AD-A131596 ..... N84-13010 #
AD-A131631 ..... N84-12919 #
AD-A131632 ..... N84-12808 #
AD-A131633 ..... N84-12317 #
AD-A131634 ..... N84-12096* #
AD-A131639 ..... N84-12773 #
AD-A131642 ..... N84-12163 #
AD-A131649 ..... N84-12772 #
AD-A131651 ..... N84-12747 #
AD-A131653 ..... N84-12822 #
AD-A131660 ..... N84-12162 #
AD-A131661 ..... N84-12918 #
AD-A131665 ..... N84-12161 #
AD-A131666 ..... N84-12138 #
AD-A131667 ..... N84-12920 #
AD-A131674 ..... N84-12352 #
AD-A131679 ..... N84-12455 #
AD-A131682 ..... N84-12787 #
AD-A131687 ..... N84-12292 #
AD-A131688 ..... N84-12215 #
AD-A131692 ..... N84-12746 #
AD-A131695 ..... N84-12671 #
AD-A131696 ..... N84-12160 #
AD-A131704 ..... N84-12838 #
AD-A131705 ..... N84-12726 #
AD-A131706 ..... N84-12978 #
AD-A131709 ..... N84-12471 #
AD-A131720 ..... N84-12470 #
AD-A131722 ..... N84-12771 #
AD-A131725 ..... N84-12137 #
AD-A131726 ..... N84-12270 #
AD-A131732 ..... N84-12745 #
AD-A131733 ..... N84-12454 #
AD-A131739 ..... N84-12351 #
AD-A131746 ..... N84-12165 #
AD-A131748 ..... N84-12977 #
AD-A131749 ..... N84-12976 #
AD-A131750 ..... N84-12975 #
AD-A131752 ..... N84-12469 #
AD-A131753 ..... N84-12468 #
AD-A131762 ..... N84-12509 #
AD-A131770 ..... N84-13012 #
AD-A131771 ..... N84-12195 #
AD-A131777 ..... N84-12837 #
AD-A131782 ..... N84-12836 #
AD-A131783 ..... N84-12835 #
AD-A131785 ..... N84-12974 #
AD-A131792 ..... N84-12350 #
AD-A131793 ..... N84-12670 #
AD-A131794 ..... N84-12834 #
AD-A131795 ..... N84-12801 #
AD-A131796 ..... N84-12269 #
AD-A131798 ..... N84-12833 #
AD-A131800 ..... N84-13024 #
AD-A131804 ..... N84-12770 #
AD-A131812 ..... N84-12349 #
AD-A131814 ..... N84-12251 #
AD-A131815 ..... N84-12692 #
AD-A131820 ..... N84-12383 #
AD-A131824 ..... N84-12727* #
AD-A131825 ..... N84-12453 #
AD-A131826 ..... N84-12691 #
AD-A131828 ..... N84-12055 #
AD-A131830 ..... N84-12722 #
AD-A131832 ..... N84-12382 #
AD-A131836 ..... N84-12708 #
AD-A131837 ..... N84-12467 #
AD-A131838 ..... N84-12669 #
AD-A131839 ..... N84-12054 #
AD-A131841 ..... N84-12973 #
AD-A131842 ..... N84-12250 #
AD-A131843 ..... N84-12719 #
AD-A131844 ..... N84-12972 #
AD-A131845 ..... N84-12452 #
AD-A131847 ..... N84-12707 #
AD-A131848 ..... N84-12423 #
AD-A131849 ..... N84-12800 #
AD-A131851 ..... N84-12331 #
AD-A131852 ..... N84-12619 #
AD-A131857 ..... N84-12316 #
AD-A131858 ..... N84-12348 #
AD-A131859 ..... N84-12769 #
AD-A131860 ..... N84-12466 #
AD-A131863 ..... N84-12268 #
AD-A131864 ..... N84-12315 #
AD-A131865 ..... N84-12347 #
AD-A131867 ..... N84-12721 #
AD-A131868 ..... N84-12832* #
AD-A131869 ..... N84-12690 #
AD-A131870 ..... N84-12837 #
AD-A131871 ..... N84-12422 #
AD-A131872 ..... N84-12346 #
AD-A131874 ..... N84-12451 #
AD-A131875 ..... N84-12971 #
AD-A131876 ..... N84-12053 #
AD-A131877 ..... N84-12052 #
AD-A131878 ..... N84-12051 #
AD-A131880 ..... N84-12381 #
AD-A131881 ..... N84-12212 #
AD-A131882 ..... N84-12421 #
AD-A131884 ..... N84-12258 #
AD-A131886 ..... N84-12465 #
AD-A131889 ..... N84-12420 #
AD-A131891 ..... N84-12345 #
AD-A131892 ..... N84-12689 #
AD-A131894 ..... N84-12194 #
AD-A131897 ..... N84-13135 #
AD-A131898 ..... N84-12636 #
AD-A131900 ..... N84-12732* #
AD-A131904 ..... N84-12159 #
AD-A131906 ..... N84-12799 #
AD-A131911 ..... N84-12786 #
AD-A131912 ..... N84-12536 #
AD-A131916 ..... N84-12821 #
AD-A131917 ..... N84-12095 #
AD-A131918 ..... N84-12450 #
AD-A131923 ..... N84-12344 #
AD-A131924 ..... N84-12894 #
AD-A131925 ..... N84-12970 #
AD-A131927 ..... N84-12158 #
AD-A131928 ..... N84-12157 #
AD-A131929 ..... N84-12211 #
AD-A131932 ..... N84-12893 #
AD-A131933 ..... N84-12496 #
AD-A131934 ..... N84-12969 #
AD-A131936 ..... N84-12744 #
AD-A131937 ..... N84-12419 #
AD-A131938 ..... N84-12094 #
AD-A131939 ..... N84-12249 #
AD-A131946 ..... N84-12917 #
AD-A131947 ..... N84-12343 #
AD-A131948 ..... N84-12686 #
AD-A131949 ..... N84-12831 #
AD-A131950 ..... N84-12218 #
AD-A131955 ..... N84-12156 #
AD-A131961 ..... N84-12291 #
AD-A131962 ..... N84-12718 #
AD-A131964 ..... N84-13023 #
AD-A131965 ..... N84-12210 #
AD-A131966 ..... N84-13037 #
AD-A131970 ..... N84-12807 #
AD-A131972 ..... N84-12191 #
AD-A131974 ..... N84-12785 #
AD-A131975 ..... N84-12726 #
AD-A131976 ..... N84-12820 #
AD-A131983 ..... N84-12668 #
AD-A131984 ..... N84-12667 #
AD-A131985 ..... N84-12667 #
AD-A131986 ..... N84-12666 #
AD-A131987 ..... N84-12093 #
AD-A131990 ..... N84-13022 #
AD-A131992 ..... N84-13021 #
AD-A132002 ..... N84-12701 #
AD-A132004 ..... N84-12784 #
AD-A132006 ..... N84-12717 #
AD-A132007 ..... N84-12892 #
AD-A132008 ..... N84-12891 #
AD-A132011 ..... N84-12685 #
AD-A132012 ..... N84-12818 #
AD-A132013 ..... N84-12684 #
AD-A132014 ..... N84-12342 #
AD-A132017 ..... N84-12209 #
AD-A132018 ..... N84-12683 #
AD-A132019 ..... N84-12682 #
AD-A132021 ..... N84-12535 #
AD-A132034 ..... N84-12783 #
AD-A132035 ..... N84-12681 #
AD-A132036 ..... N84-12830 #
AD-A132042 ..... N84-12267 #
AD-A132045 ..... N84-12708 #
AD-A132047 ..... N84-12705 #
AD-A132048 ..... N84-12152 #
AD-A132056 ..... N84-12325 #
AD-A132057 ..... N84-12704 #
AD-A132058 ..... N84-12290 #
AD-A132060 ..... N84-12314 #
AD-A132063 ..... N84-12731 #
AD-A132064 ..... N84-12716 #
AD-A132065 ..... N84-12703 #
AD-A132066 ..... N84-12715 #
AD-A132067 ..... N84-12666 #
AD-A132069 ..... N84-12714 #
AD-A132070 ..... N84-12768 #
AD-A132071 ..... N84-12266 #
AD-A132073 ..... N84-12341 #

AD-E000538 ..... N84-12345 #
AD-E301203 ..... N84-12339 #
AD-E750775 ..... N84-12215 #
AD-E750775 ..... N84-12292 #
AD-E750778 ..... N84-12314 #
AD-E750837 ..... N84-12291 #
AD-E750837 ..... N84-12718 #
AD-E850385 ..... N84-12689 #
AD-E850386 ..... N84-12496 #
AD-E850386 ..... N84-12969 #
AD-E850387 ..... N84-12268 #
AD-E850387 ..... N84-12315 #
AD-E850387 ..... N84-12346 #
AD-E850387 ..... N84-12347 #

AD-E850387 ..... N84-12422 #
AD-E850387 ..... N84-12637 #
AD-E850387 ..... N84-12690 #
AD-E850387 ..... N84-12721 #
AD-E850387 ..... N84-12832* #
AD-E950422 ..... N84-12258 #
AD-E950422 ..... N84-12465 #

AD-F000018 ..... N84-12093 #
AD-F000018 ..... N84-12667 #
AD-F000018 ..... N84-12668 #
AD-F000018 ..... N84-12686 #
AD-F000018 ..... N84-12687 #
AD-F000018 ..... N84-12726 #
AD-F000018 ..... N84-12820 #
AD-F300292 ..... N84-12194 #
AD-F300295 ..... N84-12094 #
AD-F300296 ..... N84-12420 #
AD-F300298 ..... N84-12744 #
AD-F500193 ..... N84-12419 #
AD-F630058 ..... N84-12636 #
AD-F630058 ..... N84-12732* #
AD-F630058 ..... N84-13135 #

AEDC-TR-83-13 ..... N84-12450 #
AEDC-TR-83-22 ..... N84-12783 #

AEDC-TSR-83-V2 ..... N84-12215 #

AFESC/ESL-TR-83-09 ..... N84-12195 #

AFGL-ERP-817 ..... N84-12686 #
AFGL-ERP-823 ..... N84-12682 #
AFGL-ERP-824 ..... N84-12831 #
AFGL-ERP-826 ..... N84-13037 #
AFGL-ERP-829 ..... N84-12830 #
AFGL-ERP-830 ..... N84-12667 #
AFGL-ERP-831 ..... N84-12683 #

AFGL-IP-315 ..... N84-12093 #
AFGL-IP-316 ..... N84-12687 #
AFGL-IP-317 ..... N84-12209 #

AFGL-SR-234 ..... N84-12218 #

AFGL-TR-82-0397 ..... N84-12686 #
AFGL-TR-83-0006 ..... N84-12785 #
AFGL-TR-83-0029 ..... N84-12682 #
AFGL-TR-83-0045 ..... N84-12831 #
AFGL-TR-83-0055 ..... N84-13037 #
AFGL-TR-83-0062 ..... N84-12093 #
AFGL-TR-83-0063 ..... N84-12687 #
AFGL-TR-83-0078 ..... N84-12830 #
AFGL-TR-83-0079 ..... N84-12667 #
AFGL-TR-83-0080 ..... N84-12683 #
AFGL-TR-83-0083 ..... N84-12218 #
AFGL-TR-83-0091 ..... N84-12209 #
AFGL-TR-83-0095 ..... N84-12452 #
AFGL-TR-83-0108 ..... N84-12453 #
AFGL-TR-83-0125 ..... N84-12917 #
AFGL-TR-83-0127 ..... N84-12211 #
AFGL-TR-83-0130 ..... N84-12210 #
AFGL-TR-83-0132 ..... N84-12669 #
AFGL-TR-83-0134 ..... N84-12670 #
AFGL-TR-83-0160 ..... N84-12665 #
AFGL-TR-83-0166 ..... N84-12691 #

AFHRL-TP-82-25(2) ..... N84-13019 #

AFHRL-TR-82-19 ..... N84-13011 #

AFOSR-83-0505TR ..... N84-12344 #
AFOSR-83-0510TR ..... N84-12798 #
AFOSR-83-0614TR ..... N84-13009 #
AFOSR-83-0619TR ..... N84-12837 #
AFOSR-83-0627TR ..... N84-12782 #
AFOSR-83-0637TR ..... N84-12918 #
AFOSR-83-0647TR ..... N84-12834 #
AFOSR-83-0666TR ..... N84-12808 #
AFOSR-83-0676TR ..... N84-12416 #
AFOSR-83-0678TR ..... N84-12340 #
AFOSR-83-0685TR ..... N84-12978 #
AFOSR-83-0687TR ..... N84-12771 #
AFOSR-83-0688TR ..... N84-12799 #
AFOSR-83-0689TR ..... N84-12727* #
AFOSR-83-0693TR ..... N84-12728 #
AFOSR-83-0694TR ..... N84-12466 #
AFOSR-83-0697TR ..... N84-12787 #
AFOSR-83-0705TR ..... N84-12251 #
AFOSR-83-0711TR ..... N84-12671 #
AFOSR-83-0713TR ..... N84-12467 #
AFOSR-83-0715TR ..... N84-12974 #
AFOSR-83-0717TR ..... N84-12471 #
AFOSR-83-0720TR ..... N84-12838 #
AFOSR-83-0721TR ..... N84-12270 #
AFOSR-83-0733TR ..... N84-12470 #

AFRPL-TR-83-039 ..... N84-12249 #

AFWAL-TR-80-3132-PT-4 ..... N84-12159 #
AFWAL-TR-82-2056 ..... N84-12316 #
AFWAL-TR-82-2076-PT-2 ..... N84-12421 #
AFWAL-TR-82-3040-PT-3 ..... N84-12191 #
AFWAL-TR-82-4111 ..... N84-12509 #
AFWAL-TR-83-0001 ..... N84-12054 #
AFWAL-TR-83-1025 ..... N84-12455 #
AFWAL-TR-83-3005 ..... N84-12152 #
AFWAL-TR-83-3045-PT-1 ..... N84-12158 #
AFWAL-TR-83-3045-PT-2 ..... N84-12157 #
AFWAL-TR-83-3062 ..... N84-12163 #
AFWAL-TR-83-3067 ..... N84-12095 #
AFWAL-TR-83-4034 ..... N84-12972 #
AFWAL-TR-83-4046 ..... N84-12161 #
AFWAL-TR-83-4074 ..... N84-12290 #

AFWL-TR-83-12 ..... N84-12920 #
AFWL-TR-83-13 ..... N84-12894 #
AFWL-TR-83-74-VOL-1 ..... N84-12469 #
AFWL-TR-83-74-VOL-2 ..... N84-12468 #

AGARD-CP-342 ..... N84-12099 #
AGARD-CP-349 ..... N84-12056 #
AGARD-CP-352 ..... N84-12168 #

AGARD-LS-131 ..... N84-12367 #

AGARD-R-712 ..... N84-12072 #
AGARD-R-717 ..... N84-12050 #

AI-MEMO-702 ..... N84-12772 #

AI-TR-707 ..... N84-12769 #

AMMRC-TR-83-14 ..... N84-12535 #

AMTE(N)-TM-83065 ..... N84-12619

ANL-HEP-CP-83-22 ..... N84-12865 #

ANL-82-43 ..... N84-12294 #
ANL-83-31 ..... N84-12788 #
ANL-83-59 ..... N84-12546 #

ANL/FPP/TM-169 ..... N84-12936 #

ANL/OEPM-83-4 ..... N84-12387 #

APR-1 ..... N84-12325 #

APS-89 ..... N84-12953 #

AR-2 ..... N84-12328 #
AR-302-934 ..... N84-12780 #
AR-111 ..... N84-12664* #
AR-112 ..... N84-12462* #

ARBRL-IMR-712 ..... N84-12094 #

ARBRL-MR-03291 ..... N84-12094 #
ARBRL-MR-03296 ..... N84-12731 #

ARBRL-TR-02503 ..... N84-12194 #
ARBRL-TR-02507 ..... N84-12267 #
ARBRL-TR-02510 ..... N84-12744 #
ARBRL-TR-02511 ..... N84-12420 #

ARI-TR-570 ..... N84-13020 #

ARL-STRUC-TM-359 ..... N84-12532 #

ARL-STRUC-395 ..... N84-12780 #

ARL/PSU/TM-83-100 ..... N84-12822 #

ASECR-83-126 ..... N84-12211 #

ASRL-TR-198-1 ..... N84-12160 #

ATR-83(9990)-3 ..... N84-13056* #

AUWE-TN-705/83 ..... N84-12818

BDM/W-82-770-TR ..... N84-12195 #

BMFT-FB-T-83-131-PT-B ..... N84-12651 #
BMFT-FB-T-83-133 ..... N84-13001 #
BMFT-FB-T-83-135 ..... N84-12652 #
BMFT-FB-T-83-136 ..... N84-12354 #
BMFT-FB-T-83-141 ..... N84-13002 #
BMFT-FB-T-83-143 ..... N84-12505 #

BMFT-FB-W-72-011 ..... N84-12515 #
BMFT-FB-W-83-009 ..... N84-12355 #

BMFT-FB-W-83-010 ..... N84-12219 #

BNL-NUREG-33352 ..... N84-12874 #

BNL-TR-1000 ..... N84-12275 #

BNL-32775 ..... N84-12934 #
BNL-32777 ..... N84-12386 #
BNL-33117 ..... N84-12987 #
BNL-33143 ..... N84-12720 #
BNL-33326 ..... N84-12896 #
BNL-33376 ..... N84-12989 #
BNL-33379 ..... N84-12872 #
BNL-33420 ..... N84-12541 #
BNL-33441 ..... N84-12256 #
BNL-33493 ..... N84-12545 #
BNL-33591 ..... N84-12826 #
BNL-33649 ..... N84-12862 #
BNL-33651 ..... N84-12399 #
BNL-33652 ..... N84-12754 #

BR85803 ..... N84-12283 #
BR88457 ..... N84-12310
BR88700 ..... N84-12089
BR88807 ..... N84-12508
BR88862 ..... N84-12818
BR89151 ..... N84-12729
BR89152 ..... N84-12741
BR89248 ..... N84-12379
BR89250 ..... N84-12378

C-11 ..... N84-12908 #

CECOM-80-0579-3 ..... N84-12352 #

CECOM/DRSEL-TR-78-2922F-1 ..... N84-12892 #
CECOM/DRSEL-TR-78-2922F-2 ..... N84-12891 #

CERT-2/6035-DERO ..... N84-12490 #
CERT-5/6026-DERO ..... N84-12907 #
CERT-9/6026-DERO ..... N84-12629 #

CFD/83/3 ..... N84-12435 #
CFD/83/5 ..... N84-12436 #

CMU-CS-83-128 ..... N84-12732* #

CONF-820839-9 ..... N84-12897 #
CONF-820897 ..... N84-12878 #
CONF-820898-3 ..... N84-12295 #
CONF-821108-30 ..... N84-12815 #
CONF-821185-2 ..... N84-12273 #
CONF-821191 ..... N84-12488 #
CONF-821194-1 ..... N84-12472 #
CONF-830109-1 ..... N84-12853 #
CONF-830109-3 ..... N84-12477 #
CONF-830135-3 ..... N84-13047 #
CONF-830141-4 ..... N84-12823 #
CONF-830210-20 ..... N84-12959 #
CONF-830311-143 ..... N84-12840 #
CONF-830311-148 ..... N84-12386 #
CONF-830311-153 ..... N84-12842 #
CONF-830311-187 ..... N84-12934 #
CONF-830317-3 ..... N84-12309 #
CONF-830378-1 ..... N84-12790 #
CONF-830384-1 ..... N84-12885 #
CONF-830384-2 ..... N84-12274 #
CONF-830385-1 ..... N84-12543 #
CONF-830386-2 ..... N84-12282 #
CONF-830406-63 ..... N84-12923 #
CONF-830406-94 ..... N84-12886 #
CONF-830406-109 ..... N84-12949 #
CONF-830420-5 ..... N84-12353 #
CONF-830430-2 ..... N84-12326 #
CONF-830455-6 ..... N84-12979 #
CONF-830455-8 ..... N84-12872 #
CONF-830468 ..... N84-12994 #
CONF-830475-2 ..... N84-12510 #
CONF-830492-1 ..... N84-12748 #
CONF-830503-3 ..... N84-12497 #
CONF-830508-23 ..... N84-12302 #
CONF-830528-SUMM. ..... N84-12881 #
CONF-830528-50 ..... N84-12318 #
CONF-830535-3 ..... N84-13014 #
CONF-830538-17 ..... N84-12884 #
CONF-830561-3 ..... N84-12624 #
CONF-830569-2 ..... N84-12476 #
CONF-830580-2 ..... N84-12873 #
CONF-830582-4 ..... N84-12789 #
CONF-830590-2 ..... N84-12958 #
CONF-830591-1 ..... N84-12880 #
CONF-830606-10 ..... N84-12921 #
CONF-830606-12 ..... N84-12384 #
CONF-830621-10 ..... N84-12841 #
CONF-830621-23 ..... N84-12385 #
CONF-830621-33 ..... N84-12388 #

CONF-830631-6 ..... N84-12537 #
CONF-830640-6 ..... N84-12427 #
CONF-830642-1 ..... N84-12425 #
CONF-830659-12 ..... N84-12300 #
CONF-830674-4 ..... N84-12861 #
CONF-830680-2 ..... N84-12540 #
CONF-830682-2 ..... N84-12802 #
CONF-830689-1 ..... N84-12845 #
CONF-830689-2 ..... N84-12854 #
CONF-830693-1 ..... N84-12474 #
CONF-830693-2 ..... N84-12481 #
CONF-830694-1 ..... N84-13003 #
CONF-830711-6 ..... N84-12321 #
CONF-830714-12 ..... N84-12986 #
CONF-830718-1 ..... N84-12896 #
CONF-830718-6 ..... N84-12879 #
CONF-830719-16 ..... N84-13006 #
CONF-830719-23 ..... N84-12816 #
CONF-830719-26 ..... N84-12983 #
CONF-830719-44-REV-1 ..... N84-12478 #
CONF-830719-49 ..... N84-12486 #
CONF-830719-51 ..... N84-12280 #
CONF-830756-6 ..... N84-12839 #
CONF-830758-1 ..... N84-12875 #
CONF-830763-8 ..... N84-12391 #
CONF-830763-15 ..... N84-12252 #
CONF-830770-2 ..... N84-12887 #
CONF-830772-2 ..... N84-12851 #
CONF-830772-4 ..... N84-12982 #
CONF-830776-1-PT-2 ..... N84-12984 #
CONF-830776-2 ..... N84-12990 #
CONF-830779-1 ..... N84-12989 #
CONF-830787-2 ..... N84-12998 #
CONF-830792-1 ..... N84-12749 #
CONF-830795-3 ..... N84-12306 #
CONF-830796-1 ..... N84-12545 #
CONF-830798-1 ..... N84-12860 #
CONF-830803-1 ..... N84-12426 #
CONF-830803-4 ..... N84-12424 #
CONF-830805-6 ..... N84-12293 #
CONF-830805-9 ..... N84-12538 #
CONF-830810-2 ..... N84-12393 #
CONF-830811-2 ..... N84-12827 #
CONF-830811-5 ..... N84-12512 #
CONF-830811-9 ..... N84-12167 #
CONF-830811-10 ..... N84-12825 #
CONF-830811-12 ..... N84-12307 #
CONF-830811-14 ..... N84-12824 #
CONF-830812-4 ..... N84-12870 #
CONF-830812-34 ..... N84-12389 #
CONF-830812-45 ..... N84-12649 #
CONF-830812-49 ..... N84-12500 #
CONF-830812-51 ..... N84-12504 #
CONF-830812-52 ..... N84-12501 #
CONF-830815-9 ..... N84-12539 #
CONF-830820-2 ..... N84-12308 #
CONF-830822-5 ..... N84-12882 #
CONF-830822-6 ..... N84-12888 #
CONF-830822-15 ..... N84-12999 #
CONF-830822-16 ..... N84-12489 #
CONF-830830-2 ..... N84-13133 #
CONF-830830-4 ..... N84-13132 #
CONF-830841-3 ..... N84-12988 #
CONF-830841-4 ..... N84-12995 #
CONF-830841-11 ..... N84-12397 #
CONF-830841-13 ..... N84-12394 #
CONF-830841-16 ..... N84-12826 #
CONF-830862-2 ..... N84-12850 #
CONF-830862-3 ..... N84-12849 #
CONF-830871-6 ..... N84-12304 #
CONF-830871-8 ..... N84-12303 #
CONF-830874-8 ..... N84-12933 #
CONF-830874-16 ..... N84-12641 #
CONF-830874-17 ..... N84-12901 #
CONF-830874-20 ..... N84-12904 #
CONF-830874-21 ..... N84-12905 #
CONF-830874-25 ..... N84-12903 #
CONF-830888-8 ..... N84-12322 #
CONF-830895-1 ..... N84-12390 #
CONF-830895-4 ..... N84-12993 #
CONF-830895-7 ..... N84-12259 #
CONF-830899-3 ..... N84-12805 #
CONF-830906-1 ..... N84-12931 #
CONF-830908-2 ..... N84-12930 #
CONF-830908-5 ..... N84-12948 #
CONF-830909-2 ..... N84-12932 #
CONF-830909-4 ..... N84-12955 #
CONF-830909-5 ..... N84-12954 #
CONF-830909-7 ..... N84-12940 #
CONF-830909-8 ..... N84-12939 #
CONF-830911-2 ..... N84-12866 #
CONF-830911-5 ..... N84-12943 #
CONF-830911-7 ..... N84-12942 #
CONF-830911-8 ..... N84-12944 #
CONF-830911-9 ..... N84-12945 #
CONF-830911-10 ..... N84-12941 #
CONF-830911-11 ..... N84-12858 #
CONF-830911-12 ..... N84-12857 #
CONF-830926-1 ..... N84-12457 #
CONF-830927-1-REV-1 ..... N84-12985 #
CONF-830929-5 ..... N84-13128 #
CONF-830936-2 ..... N84-12859 #
CONF-830942-2 ..... N84-12962 #
CONF-830974-3 ..... N84-12644 #
CONF-830975-3 ..... N84-12544 #
CONF-831003-1 ..... N84-12278 #
CONF-831015-1 ..... N84-13039* #
CONF-831015-2 ..... N84-12898 #
CONF-831020-1 ..... N84-13034 #
CONF-831020-2 ..... N84-12395 #
CONF-831025-1 ..... N84-12480 #
CONF-831041-2 ..... N84-12672 #
CONF-831047-1 ..... N84-12991 #
CONF-831047-7 ..... N84-12774 #
CONF-831047-27 ..... N84-12319 #
CONF-831047-35 ..... N84-12511 #
CONF-831063-3 ..... N84-12256 #
CONF-831070-4 ..... N84-12401 #
CONF-831086-1 ..... N84-12403 #
CONF-831086-2 ..... N84-12299 #
CONF-831086-3 ..... N84-12642 #
CONF-831086-4 ..... N84-12297 #
CONF-831086-5 ..... N84-12404 #
CONF-831096-1 ..... N84-13013 #
CONF-831182-1 ..... N84-12503 #
CONF-831476-6 ..... N84-12874 #
CONF-8205188-1 ..... N84-12980 #
CONF-8206120-9 ..... N84-12865 #
CONF-8206201-DRAFT ..... N84-12981 #
CONF-8206212-1 ..... N84-12855 #
CONF-8206219-1-DRAFT ..... N84-12867 #
CONF-8208106-ABSTS ..... N84-12638 #
CONF-8208146-1 ..... N84-12895 #
CONF-8210106-5 ..... N84-12720 #
CONF-8301059-4 ..... N84-12272 #
CONF-8304104-2 ..... N84-12847 #
CONF-8304105-4 ..... N84-12846 #
CONF-8304110-3 ..... N84-12868 #
CONF-8304111-1 ..... N84-12723 #
CONF-8304113-1 ..... N84-12279 #
CONF-8304117-1 ..... N84-12900 #
CONF-8304122-1 ..... N84-12547 #
CONF-8305110-1 ..... N84-12928 #
CONF-8305123-1 ..... N84-13134 #
CONF-8305125-1 ..... N84-12791 #
CONF-8305127-1 ..... N84-12961 #
CONF-8305128-1 ..... N84-12755 #
CONF-8306120-1 ..... N84-12997 #
CONF-8306121-2 ..... N84-12484 #
CONF-8306121-3 ..... N84-12485 #
CONF-8306122-1 ..... N84-12709 #
CONF-8306125-1 ..... N84-12862 #
CONF-8308102-1 ..... N84-12643 #
CONF-8308104-1 ..... N84-12738 #
CONF-8308108-1 ..... N84-12430 #
CONF-8308112-2 ..... N84-12863 #
CONF-8308114-1 ..... N84-12483 #
CONF-8308116-1 ..... N84-12276 #
CONF-8308120-1 ..... N84-12396 #
CONF-8309103-7 ..... N84-12946 #
CONF-8309134-1 ..... N84-12541 #
CONF-8309135-1 ..... N84-12513 #
CONF-8309136-1 ..... N84-12864 #
CONF-8309137-1 ..... N84-12957 #
CONF-8309144-1 ..... N84-12754 #
CONF-8309144-2 ..... N84-12399 #
CONF-8310102-1 ..... N84-12899 #
CONF-8310108-1 ..... N84-12400 #
CONF-8310111-1 ..... N84-12296 #
CONF-8310115-1 ..... N84-12694 #
CONF-8310120-1 ..... N84-12254 #
CONF-8310129-1 ..... N84-12298 #
CONF-8310130-1 ..... N84-12737 #
CONF-8310135-2 ..... N84-12402 #

COO-1599-233 ..... N84-12625 #
COO-1599-234 ..... N84-12627 #
COO-1599-235-PT-3 ..... N84-12625 #
COO-1599-235-PT-4 ..... N84-12627 #

CRREL-MONO-83-1 ..... N84-12619 #

CRREL-SR-83-17 ..... N84-12690 #
CRREL-SR-83-19 ..... N84-12618 #
CRREL-SR-83-20 ..... N84-12684 #

CRREL-83-18 ..... N84-12331 #

CTH-MATH-1983-12-PREPRINT ..... N84-12792 #
CTH-MATH-1983-13-PREPRINT ..... N84-12793 #

C83-522/201 ..... N84-12270 #

DCN-1-3-ES-26516 ..... N84-12413* #

DEW-83-1 ..... N84-12348 #

DE83-01102 ..... N84-12899 #
DE83-003469 ..... N84-12655 #
DE83-003910 ..... N84-12273 #
DE83-005697 ..... N84-12426 #
DE83-007509 ..... N84-12477 #
DE83-007911 ..... N84-12424 #
DE83-008381 ..... N84-12293 #
DE83-009289 ..... N84-12278 #
DE83-009407 ..... N84-12650 #
DE83-009495 ..... N84-12302 #
DE83-009532 ..... N84-12922 #
DE83-009625 ..... N84-12538 #
DE83-009750 ..... N84-12271 #
DE83-010371 ..... N84-12925 #
DE83-010378 ..... N84-12924 #
DE83-010594 ..... N84-12272 #
DE83-010704 ..... N84-12865 #
DE83-010757 ..... N84-12931 #
DE83-010935 ..... N84-12754 #
DE83-011177 ..... N84-12870 #
DE83-011245 ..... N84-12499 #
DE83-011315 ..... N84-13039* #
DE83-011320 ..... N84-13133 #
DE83-011391 ..... N84-12748 #
DE83-011849 ..... N84-12842 #
DE83-011973 ..... N84-13127 #
DE83-011974 ..... N84-12647 #
DE83-011989 ..... N84-13128 #
DE83-011998 ..... N84-12622 #
DE83-012045 ..... N84-12985 #
DE83-012064 ..... N84-13031 #
DE83-012075 ..... N84-12457 #
DE83-012129 ..... N84-12641 #
DE83-012132 ..... N84-12644 #
DE83-012168 ..... N84-12510 #
DE83-012217 ..... N84-12386 #
DE83-012390 ..... N84-12881 #
DE83-012506 ..... N84-12403 #
DE83-012583 ..... N84-12497 #
DE83-012624 ..... N84-12537 #
DE83-012626 ..... N84-12980 #
DE83-012641 ..... N84-12923 #
DE83-012658 ..... N84-13047 #
DE83-012659 ..... N84-12979 #
DE83-012663 ..... N84-12472 #
DE83-012712 ..... N84-12840 #
DE83-012761 ..... N84-12425 #
DE83-012781 ..... N84-12880 #
DE83-012817 ..... N84-12815 #
DE83-012846 ..... N84-12326 #
DE83-012854 ..... N84-12878 #
DE83-012899 ..... N84-12895 #
DE83-012952 ..... N84-12841 #
DE83-013035 ..... N84-12898 #
DE83-013039 ..... N84-12789 #
DE83-013215 ..... N84-12488 #
DE83-013280 ..... N84-12987 #
DE83-013384 ..... N84-12877 #
DE83-013427 ..... N84-12733 #
DE83-013582 ..... N84-12473 #
DE83-013585 ..... N84-12991 #
DE83-013640 ..... N84-12921 #
DE83-013711 ..... N84-13132 #
DE83-013769 ..... N84-12385 #
DE83-013770 ..... N84-12544 #
DE83-014011 ..... N84-12427 #
DE83-014043 ..... N84-12802 #
DE83-014054 ..... N84-12399 #
DE83-014055 ..... N84-12862 #
DE83-014058 ..... N84-12981 #
DE83-014070 ..... N84-12869 #
DE83-014147 ..... N84-12930 #
DE83-014189 ..... N84-12384 #
DE83-014191 ..... N84-12672 #
DE83-014197 ..... N84-12480 #
DE83-014204 ..... N84-12839 #
DE83-014205 ..... N84-12389 #
DE83-014307 ..... N84-12774 #
DE83-014344 ..... N84-12254 #
DE83-014431 ..... N84-12720 #
DE83-014498 ..... N84-12694 #
DE83-014551 ..... N84-12387 #
DE83-014606 ..... N84-12402 #
DE83-014623 ..... N84-12540 #
DE83-014675 ..... N84-12319 #
DE83-014680 ..... N84-12404 #
DE83-014683 ..... N84-12511 #
DE83-014701 ..... N84-12642 #
DE83-014704 ..... N84-12299 #
DE83-014735 ..... N84-12297 #
DE83-014760 ..... N84-12638 #
DE83-014807 ..... N84-12843 #

DE83-014896 ..... N84-12849 #
DE83-014897 ..... N84-12850 #
DE83-014949 ..... N84-13013 #
DE83-015005 ..... N84-12255 #
DE83-015104 ..... N84-12296 #
DE83-015141 ..... N84-12873 #
DE83-015167 ..... N84-12388 #
DE83-015210 ..... N84-12996 #
DE83-015212 ..... N84-12986 #
DE83-015216 ..... N84-13006 #
DE83-015220 ..... N84-12474 #
DE83-015222 ..... N84-12391 #
DE83-015230 ..... N84-12400 #
DE83-015231 ..... N84-12790 #
DE83-015232 ..... N84-12845 #
DE83-015233 ..... N84-12853 #
DE83-015245 ..... N84-12390 #
DE83-015252 ..... N84-12926 #
DE83-015354 ..... N84-12994 #
DE83-015363 ..... N84-12896 #
DE83-015384 ..... N84-12874 #
DE83-015392 ..... N84-12872 #
DE83-015394 ..... N84-12723 #
DE83-015406 ..... N84-12539 #
DE83-015447 ..... N84-12902 #
DE83-015492 ..... N84-12897 #
DE83-015506 ..... N84-12990 #
DE83-015533 ..... N84-13038 #
DE83-015535 ..... N84-12887 #
DE83-015564 ..... N84-12989 #
DE83-015596 ..... N84-12883 #
DE83-015612 ..... N84-12298 #
DE83-015615 ..... N84-12476 #
DE83-015616 ..... N84-12933 #
DE83-015622 ..... N84-12318 #
DE83-015629 ..... N84-12639 #
DE83-015649 ..... N84-12855 #
DE83-015681 ..... N84-12982 #
DE83-015682 ..... N84-12851 #
DE83-015689 ..... N84-12846 #
DE83-015691 ..... N84-12886 #
DE83-015706 ..... N84-12487 #
DE83-015719 ..... N84-13034 #
DE83-015720 ..... N84-12900 #
DE83-015728 ..... N84-12626 #
DE83-015732 ..... N84-12885 #
DE83-015735 ..... N84-12482 #
DE83-015762 ..... N84-12875 #
DE83-015767 ..... N84-12984 #
DE83-015827 ..... N84-12652 #
DE83-015837 ..... N84-12475 #
DE83-015863 ..... N84-12983 #
DE83-015871 ..... N84-12927 #
DE83-015881 ..... N84-13134 #
DE83-015884 ..... N84-12816 #
DE83-015904 ..... N84-12871 #
DE83-015923 ..... N84-12854 #
DE83-015925 ..... N84-12737 #
DE83-015943 ..... N84-13003 #
DE83-015949 ..... N84-12401 #
DE83-015951 ..... N84-12847 #
DE83-015957 ..... N84-12279 #
DE83-015966 ..... N84-12432 #
DE83-015975 ..... N84-12884 #
DE83-015986 ..... N84-12321 #
DE83-016012 ..... N84-12656 #
DE83-016014 ..... N84-12960 #
DE83-016065 ..... N84-12901 #
DE83-016069 ..... N84-12543 #
DE83-016079 ..... N84-12502 #
DE83-016091 ..... N84-12428 #
DE83-016210 ..... N84-12791 #
DE83-016275 ..... N84-12988 #
DE83-016295 ..... N84-12844 #
DE83-016316 ..... N84-12738 #
DE83-016324 ..... N84-12392 #
DE83-016334 ..... N84-12926 #
DE83-016371 ..... N84-12256 #
DE83-016389 ..... N84-12277 #
DE83-016397 ..... N84-12868 #
DE83-016419 ..... N84-12429 #
DE83-016504 ..... N84-12393 #
DE83-016521 ..... N84-12646 #
DE83-016522 ..... N84-12848 #
DE83-016535 ..... N84-12937 #
DE83-016537 ..... N84-12479 #
DE83-016568 ..... N84-12932 #
DE83-016586 ..... N84-12295 #
DE83-016589 ..... N84-12876 #
DE83-016599 ..... N84-12623 #
DE83-016607 ..... N84-12749 #
DE83-016618 ..... N84-12624 #
DE83-016646 ..... N84-12817 #
DE83-016647 ..... N84-12734 #
DE83-016660 ..... N84-12320 #
DE83-016697 ..... N84-12993 #
DE83-016709 ..... N84-12934 #
DE83-016711 ..... N84-12936 #
DE83-016717 ..... N84-12294 #
DE83-016733 ..... N84-12541 #
DE83-016734 ..... N84-12999 #
DE83-016771 ..... N84-12953 #
DE83-016784 ..... N84-12649 #
DE83-016790 ..... N84-12955 #
DE83-016791 ..... N84-12625 #
DE83-016792 ..... N84-12627 #
DE83-016812 ..... N84-12950 #
DE83-016826 ..... N84-12803 #
DE83-016845 ..... N84-12645 #
DE83-016849 ..... N84-12992 #
DE83-016853 ..... N84-12648 #
DE83-016881 ..... N84-12951 #
DE83-016887 ..... N84-13005 #
DE83-016903 ..... N84-12751 #
DE83-016906 ..... N84-12308 #
DE83-016916 ..... N84-12929 #
DE83-016924 ..... N84-13014 #
DE83-016930 ..... N84-12643 #
DE83-016932 ..... N84-12956 #
DE83-016935 ..... N84-12300 #
DE83-016941 ..... N84-12478 #
DE83-016957 ..... N84-12489 #
DE83-016990 ..... N84-12752 #
DE83-017016 ..... N84-12856 #
DE83-017022 ..... N84-12935 #
DE83-017047 ..... N84-12327 #
DE83-017051 ..... N84-12301 #
DE83-017067 ..... N84-12542 #
DE83-017085 ..... N84-12673 #
DE83-017121 ..... N84-12431 #
DE83-017145 ..... N84-12305 #
DE83-017152 ..... N84-12998 #
DE83-017161 ..... N84-12962 #
DE83-017177 ..... N84-12961 #
DE83-017179 ..... N84-12755 #
DE83-017189 ..... N84-12304 #
DE83-017190 ..... N84-12303 #
DE83-017205 ..... N84-12863 #
DE83-017210 ..... N84-12958 #
DE83-017211 ..... N84-12867 #
DE83-017215 ..... N84-12860 #
DE83-017230 ..... N84-12481 #
DE83-017233 ..... N84-12905 #
DE83-017234 ..... N84-12904 #
DE83-017235 ..... N84-12484 #
DE83-017246 ..... N84-12959 #
DE83-017253 ..... N84-12997 #
DE83-017262 ..... N84-12995 #
DE83-017272 ..... N84-12430 #
DE83-017276 ..... N84-12504 #
DE83-017279 ..... N84-12501 #
DE83-017283 ..... N84-12500 #
DE83-017290 ..... N84-12485 #
DE83-017293 ..... N84-12939 #
DE83-017302 ..... N84-12882 #
DE83-017303 ..... N84-12483 #
DE83-017305 ..... N84-12888 #
DE83-017352 ..... N84-12545 #
DE83-017353 ..... N84-12322 #
DE83-017356 ..... N84-12866 #
DE83-017365 ..... N84-12954 #
DE83-017366 ..... N84-12486 #
DE83-017368 ..... N84-12397 #
DE83-017369 ..... N84-12948 #
DE83-017415 ..... N84-12767 #
DE83-017417 ..... N84-12693 #
DE83-017447 ..... N84-12710 #
DE83-017470 ..... N84-12949 #
DE83-017477 ..... N84-12957 #
DE83-017484 ..... N84-12503 #
DE83-017494 ..... N84-12309 #
DE83-017496 ..... N84-12952 #
DE83-017514 ..... N84-12459 #
DE83-017531 ..... N84-12546 #
DE83-017546 ..... N84-12750 #
DE83-017571 ..... N84-12657 #
DE83-017683 ..... N84-12513 #
DE83-017684 ..... N84-12547 #
DE83-017685 ..... N84-12512 #
DE83-017692 ..... N84-12353 #
DE83-017693 ..... N84-12827 #
DE83-017695 ..... N84-12282 #
DE83-017696 ..... N84-12864 #
DE83-017700 ..... N84-12281 #
DE83-017724 ..... N84-12275 #
DE83-017742 ..... N84-12861 #
DE83-017744 ..... N84-12276 #
DE83-017765 ..... N84-12826 #
DE83-017784 ..... N84-12857 #
DE83-017792 ..... N84-12942 #
DE83-017800 ..... N84-12941 #
DE83-017822 ..... N84-12943 #
DE83-017823 ..... N84-12823 #
DE83-017824 ..... N84-12945 #
DE83-017836 ..... N84-12946 #
DE83-017840 ..... N84-12940 #
DE83-017870 ..... N84-12804 #
DE83-017914 ..... N84-12274 #
DE83-017926 ..... N84-12396 #
DE83-017937 ..... N84-12306 #
DE83-017939 ..... N84-12395 #
DE83-017955 ..... N84-12805 #
DE83-017963 ..... N84-12859 #
DE83-017964 ..... N84-12709 #
DE83-017973 ..... N84-12394 #
DE83-017988 ..... N84-12253 #
DE83-017994 ..... N84-12097 #
DE83-018074 ..... N84-12307 #
DE83-018075 ..... N84-12280 #
DE83-018077 ..... N84-12259 #
DE83-018078 ..... N84-12903 #
DE83-018079 ..... N84-12252 #
DE83-018080 ..... N84-12825 #
DE83-018081 ..... N84-12167 #
DE83-018092 ..... N84-12824 #
DE83-018117 ..... N84-12640 #
DE83-018118 ..... N84-12938 #
DE83-018120 ..... N84-12947 #
DE83-018219 ..... N84-12879 #
DE83-018235 ..... N84-12753 #
DE83-018261 ..... N84-12735 #
DE83-018263 ..... N84-12944 #
DE83-018264 ..... N84-12858 #
DE83-018288 ..... N84-12458 #
DE83-902538 ..... N84-12620 #
DE83-902641 ..... N84-12456 #
DE83-903011 ..... N84-12621 #
DE83-0166222 ..... N84-13004 #
DE83-3014268 ..... N84-12788 #
DE83-4000123 ..... N84-12736 #
DE84-000849 ..... N84-12398 #

DFVLR-FB-82-24 ..... N84-12356 #
DFVLR-FB-83-03 ..... N84-12141 #
DFVLR-FB-83-22 ..... N84-12363 #

DFVLR-MANUSKRIPT-8A-PT-1 ..... N84-12224 #

DFVLR-MITT-82-09 ..... N84-12695 #
DFVLR-MITT-82-13 ..... N84-12357 #
DFVLR-MITT-83-02 ..... N84-12153 #
DFVLR-MITT-83-04 ..... N84-12449 #
DFVLR-MITT-83-06 ..... N84-12756 #

DNA-TR-81-83 ..... N84-12339 #
DNA-TR-81-121 ..... N84-12533 #
DNA-TR-81-184 ..... N84-12534 #

DOE/BETC-RI-83/4 ..... N84-12656 #

DOE/CS-15040/T1 ..... N84-12499 #
DOE/CS-30260/1 ..... N84-13005 #
DOE/CS-30264/T1 ..... N84-12639 #
DOE/CS-40402/16 ..... N84-12320 #
DOE/CS-50021/3 ..... N84-12327 #

DOE/EIA-0202(83/2Q)-2 ..... N84-12648 #

DOE/ER-0169 ..... N84-12876 #
DOE/ER-0403/43 ..... N84-12844 #
DOE/ER-01116/36 ..... N84-12856 #
DOE/ER-01198/1394 ..... N84-12273 #
DOE/ER-02167/T1 ..... N84-12852 #
DOE/ER-03416/T1 ..... N84-12277 #
DOE/ER-04693/T4 ..... N84-12992 #
DOE/ER-10448/1 ..... N84-13004 #
DOE/ER-10463/1 ..... N84-12645 #
DOE/ER-10575/T1 ..... N84-12902 #
DOE/ER-10903/4 ..... N84-12710 #
DOE/ER-10961/1 ..... N84-12638 #
DOE/ER-12098/1 ..... N84-12305 #
DOE/ER-40014/T1 ..... N84-12877 #
DOE/ER-40048/61 ..... N84-13038 #
DOE/ER-40048/62-L3 ..... N84-12846 #
DOE/ER-53092/T6-VOL-1-SUMM ..... N84-12924 #
DOE/ER-53092/T6-VOL-2-APP ..... N84-12925 #
DOE/ER-53147/1 ..... N84-12947 #
DOE/ER-70004/351 ..... N84-12871 #

DOE/ET-10069/T41 ..... N84-12281 #
DOE/ET-51013/70 ..... N84-12937 #
DOE/ET-51013/88 ..... N84-12950 #
DOE/ET-51013/91 ..... N84-12817 #
DOE/ET-53043/6 ..... N84-12938 #
DOE/ET-53051/57 ..... N84-12951 #

DOE/EV-01599-235-PT-4 ..... N84-12627 #
DOE/EV-01599/235-PT-3 ..... N84-12625 #

DOE/NBM-3012064 ..... N84-13031 #

DOE/NE-50004/T1 ..... N84-12479 #

DOE/PC-30247/T4 ..... N84-12271 #
DOE/PC-50800/T3 ..... N84-12432 #

DOE/SF-115393/T1 ..... N84-12640 #

DOT/RSPA/DMA-50/83/18 ..... N84-12518 #

DP-MS-82-55 ..... N84-12309 #
DP-MS-82-103 ..... N84-12539 #

DP-1643 ..... N84-12301 #

DRIC-T-6974 ..... N84-12508

DTIC/TR/83/3-SUPPL-1 ..... N84-13024 #

DTNSRDC/ASED-CR-1-83 ..... N84-12096* #

DTNSRDC/CMLD-83-20 ..... N84-12768 #

D180-27728-1 ..... N84-12226* #

E&MA-82-176 ..... N84-12253 #

E-1760 ..... N84-12730* #
E-1823 ..... N84-12287* #
E-1853 ..... N84-12166* #

EEB-L-83-05 ..... N84-12738 #

EGG-M-06683 ..... N84-12873 #

EPA-460/3-83-005 ..... N84-12507 #
EPA-600/D-83-091 ..... N84-12711 #
EPA-600/3-83-056 ..... N84-12460 #
EPA-600/4-83-034 ..... N84-12461 #

EPA/AA/CTAB/TA/83-2 ..... N84-12506 #

EPRI-CS-3098 ..... N84-12456 #

EPRI-EA-3133 ..... N84-12620 #

ESA-SP-188 ..... N84-12579 #
ESA-SP-197 ..... N84-12197 #

ESA-STR-211 ..... N84-12220 #

ESA-TT-789 ..... N84-12907 #
ESA-TT-790 ..... N84-12629 #
ESA-TT-791 ..... N84-12490 #
ESA-TT-802 ..... N84-12224 #
ESA-TT-805 ..... N84-12356 #
ESA-TT-808 ..... N84-12695 #
ESA-TT-809 ..... N84-12357 #
ESA-TT-814 ..... N84-12810 #
ESA-TT-818 ..... N84-12153 #
ESA-TT-827 ..... N84-12449 #

ESD-TR-83-031 ..... N84-12343 #

E83-10032 ..... N84-12557* #
E84-10006 ..... N84-12555* #
E84-10016 ..... N84-12556* #
E84-10033 ..... N84-12576* #

FAA-CT-82-152 ..... N84-12160 #
FAA-CT-83-29 ..... N84-12138 #

FERMILAB-CONF-82/55-THY ..... N84-12855 #
FERMILAB-CONF-83/32-THY ..... N84-13132 #
FERMILAB-CONF-83/45-THY ..... N84-12791 #

FERMILAB/TM-1198 ..... N84-12502 #
FERMILAB/TM-1202 ..... N84-12999 #

FFA-TN-1983-28 ..... N84-12696 #
FFA-TN-1983-29 ..... N84-12516 #
FFA-TN-1983-30 ..... N84-12260 #

FGCC-IS-83-2 ..... N84-12631 #

FI-65-TBR-20-PT-3 ..... N84-13000 #
FI-465-TBR-22 ..... N84-12906 #

FOA-C-30325-E1,E3 ..... N84-12630 #
FOA-C-55058-H3 ..... N84-12724 #

FTD-ID(RS)T-0015-83 ..... N84-12451 #
FTD-ID(RS)T-0266-83 ..... N84-12055 #
FTD-ID(RS)T-0284-83 ..... N84-12422 #
FTD-ID(RS)T-0398-83 ..... N84-12498 #
FTD-ID(RS)T-0507-83 ..... N84-12814 #
FTD-ID(RS)T-0518-83 ..... N84-12380 #
FTD-ID(RS)T-0569-83 ..... N84-12890 #
FTD-ID(RS)T-0603-83 ..... N84-12465 #
FTD-ID(RS)T-0716-83 ..... N84-12743 #
FTD-ID(RS)T-0721-83 ..... N84-12381 #
FTD-ID(RS)T-0817-83 ..... N84-13135 #
FTD-ID(RS)T-0818-83 ..... N84-12346 #
FTD-ID(RS)T-0854-83 ..... N84-12338 #
FTD-ID(RS)T-0898-83 ..... N84-12212 #
FTD-ID(RS)T-1067-83 ..... N84-12637 #
FTD-ID(RS)T-1086-83 ..... N84-12383 #
FTD-ID(RS)T-1087-83 ..... N84-12382 #
FTD-ID(RS)T-1090-83 ..... N84-12971 #
FTD-ID(RS)T-1094-83 ..... N84-12636 #

FUB-38-1982 ..... N84-12908 #
FUB-59-1981 ..... N84-12794 #

GA-A-16923 ..... N84-12815 #
GA-A-17012 ..... N84-12949 #
GA-A-17031 ..... N84-12733 #
GA-A-17059 ..... N84-12927 #
GA-A-17188 ..... N84-12957 #

GARRETT-21-4742-1 ..... N84-12264* #
GARRETT-21-4742-2 ..... N84-12265* #
GARRETT-21-4766 ..... N84-12263* #

GEOWISS-MITT-24-1983 ..... N84-12628 #

GPO-21-747 ..... N84-12713 #
GPO-24-491 ..... N84-13032 #
GPO-25-753 ..... N84-12208 #

GRI-81/0025.7 ..... N84-12677 #
GRI-81/0051 ..... N84-13008 #
GRI-81/0162 ..... N84-12329 #
GRI-82/0054 ..... N84-12328 #

GSFC-921 ..... N84-12662* #

GTD-83-10 ..... N84-12227* #

GTFR-37 ..... N84-12922 #

G80143 ..... N84-12496 #

HDL-SR-83-8 ..... N84-12417 #

HDL-TR-1995 ..... N84-12919 #

HEDL-SA-2723-FP ..... N84-12884 #
HEDL-SA-2890-FP ..... N84-12510 #

HEDL-TME-83-19 ..... N84-12935 #

HEDL-21-2788-FP ..... N84-12300 #

ICASE-83-56 ..... N84-12777* #
ICASE-83-59 ..... N84-12742* #
ICASE-83-61 ..... N84-12778* #

ICSCA-CMP-29 ..... N84-12745 #

IFSI-82-4 ..... N84-12358 #
IFSI-82-5 ..... N84-12675 #
IFSI-82-6 ..... N84-13129 #
IFSI-82-9 ..... N84-13049* #
IFSI-82-10 ..... N84-12676 #
IFSI-82-11 ..... N84-12359 #
IFSI-82-12 ..... N84-12360 #
IFSI-82-13 ..... N84-12965 #
IFSI-82-14 ..... N84-13050 #
IFSI-82-15 ..... N84-12361 #
IFSI-82-16 ..... N84-13130 #
IFSI-83-2 ..... N84-13062 #
IFSI-83-3 ..... N84-12653 #
IFSI-83-7 ..... N84-12362 #

INPE-2811-PRE/369 ..... N84-12967 #
INPE-2893-PRE/417 ..... N84-12337 #
INPE-2940-PHE/429 ..... N84-12446 #

IOE/CE-83-01 ..... N84-12334 #

IPP-6/223 ..... N84-12776

IPPJ-AM-28 ..... N84-12914 #
IPPJ-AM-29 ..... N84-12913 #
IPPJ-AM-30 ..... N84-12912 #
IPPJ-AM-31 ..... N84-12911 #

IPPJ-640 ..... N84-12916 #
IPPJ-641 ..... N84-12915 #
IPPJ-642 ..... N84-12909 #
IPPJ-643 ..... N84-12910 #

IPR-2 ..... N84-12918 #

IR-2 ..... N84-12740

IS-M-428 ..... N84-12997 #
IS-M-433 ..... N84-12513 #
IS-M-434 ..... N84-12353 #
IS-M-435 ..... N84-12864 #
IS-M-436 ..... N84-12282 #
IS-M-438 ..... N84-12547 #
IS-M-440 ..... N84-12512 #
IS-M-445 ..... N84-12167 #
IS-M-446 ..... N84-12825 #
IS-M-447 ..... N84-12827 #
IS-M-450 ..... N84-12259 #
IS-M-452 ..... N84-12903 #
IS-M-453 ..... N84-12252 #
IS-M-454 ..... N84-12280 #
IS-M-455 ..... N84-12307 #
IS-M-460 ..... N84-12824 #

ISBN-0-03-057913-9 ..... N84-12627 #
ISBN-0-472-08037-7 ..... N84-12625 #
ISBN-0-472-10032-7 ..... N84-12626 #
ISBN-3-7696-8179-7 ..... N84-12661
ISBN-3-7696-9326-4 ..... N84-12554
ISBN-92-63-12134-6 ..... N84-12697 #
ISBN-92-835-0332-5 ..... N84-12072 #
ISBN-92-835-0334-1 ..... N84-12099 #
ISBN-92-835-0335-X ..... N84-12056 #
ISBN-92-835-0339-2 ..... N84-12168 #
ISBN-92-835-1458-0 ..... N84-12050 #
ISBN-92-835-1461-0 ..... N84-12367 #

ISI-V-3836-05 ..... N84-13010 #

ISSN-0065-5309 ..... N84-12661
ISSN-0065-5325 ..... N84-12554
ISSN-0077-5606 ..... N84-12578 #
ISSN-0082-5255 ..... N84-12828 #
ISSN-0082-5263 ..... N84-12416 #
ISSN-0143-7313 ..... N84-12526
ISSN-0170-1339 ..... N84-12219 #
ISSN-0170-1339 ..... N84-12355 #
ISSN-0170-1339 ..... N84-12515 #
ISSN-0208-5658 ..... N84-12407 #
ISSN-0208-5658 ..... N84-12966 #
ISSN-0262-5369 ..... N84-12739
ISSN-0262-5369 ..... N84-12740
ISSN-0340-7608 ..... N84-12354 #
ISSN-0340-7608 ..... N84-12505 #
ISSN-0340-7608 ..... N84-12651 #
ISSN-0340-7608 ..... N84-12652 #
ISSN-0340-7608 ..... N84-13001 #
ISSN-0340-7608 ..... N84-13002 #
ISSN-0340-8922 ..... N84-13035
ISSN-0347-2809 ..... N84-12792 #
ISSN-0347-2809 ..... N84-12793 #
ISSN-0347-3708 ..... N84-12630 #
ISSN-0347-7665 ..... N84-12724 #
ISSN-0349-2702 ..... N84-12674 #
ISSN-0366-0885 ..... N84-12323 #
ISSN-0379-6566 ..... N84-12197 #
ISSN-0379-6566 ..... N84-12579 #
ISSN-0568-0581 ..... N84-12462* #
ISSN-0568-0581 ..... N84-12684* #
ISSN-00379-4067 ..... N84-12220 #

ISU-ERI-A84414 ..... N84-12028* #

ISVR-TR-120 ..... N84-12548 #

ITT-80-22-07-VOL-1 ..... N84-12892 #
ITT-80-22-07-VOL-2 ..... N84-12891 #

JUEL-1832 ..... N84-12324 #
JUEL-1834 ..... N84-12323 #

K/OA-5325 ..... N84-12426 #

K/TS-10-997 ..... N84-12425 #

KNMI-WR-83-10 ..... N84-12698 #

L-75 ..... N84-12738 #
L-15461 ..... N84-12164* #
L 15505 ..... N84-12190* #
L-15649 ..... N84-12029* #
L-15707 ..... N84-12228* #

LA-UR-83-1048 ..... N84-13133 #
LA-UR-83-1210 ..... N84-12870 #
LA-UR-83-1405 ..... N84-12979 #
LA-UR-83-1406 ..... N84-13047 #

LA-UR-83-1466 ..... N84-12680 #
LA-UR-83-1568 ..... N84-12460 #
LA-UR-83-1585 ..... N84-12388 #
LA-UR-83-1671 ..... N84-12384 #
LA-UR-83-1678 ..... N84-12672 #
LA-UR-83-1898 ..... N84-12930 #
LA-UR-83-1991 ..... N84-12928 #
LA-UR-83-2039 ..... N84-12853 #
LA-UR-83-2041 ..... N84-12845 #
LA-UR-83-2045 ..... N84-12790 #
LA-UR-83-2147 ..... N84-12391 #
LA-UR-83-2151 ..... N84-12474 #
LA-UR-83-2186 ..... N84-12723 #
LA-UR-83-2232 ..... N84-13006 #
LA-UR-83-2257 ..... N84-12737 #
LA-UR-83-2317 ..... N84-12682 #
LA-UR-83-2319 ..... N84-12483 #
LA-UR-83-2339 ..... N84-12868 #
LA-UR-83-2383 ..... N84-12481 #
LA-UR-83-2389 ..... N84-12905 #
LA-UR-83-2400 ..... N84-12904 #
LA-UR-83-2411 ..... N84-12484 #
LA-UR-83-2443 ..... N84-12485 #

LA-9752-MS ..... N84-12843 #
LA-9767-C ..... N84-12488 #
LA-9770-MS ..... N84-12736 #
LA-9794-PR ..... N84-12869 #

LBL-10070 ..... N84-12929 #
LBL-15066 ..... N84-12886 #
LBL-15150 ..... N84-12255 #
LBL-15545 ..... N84-12279 #
LBL-15743 ..... N84-12895 #
LBL-15762 ..... N84-13003 #
LBL-15877 ..... N84-12847 #
LBL-16101 ..... N84-12624 #
LBL-16225 ..... N84-12401 #
LBL-16248 ..... N84-12398 #
LBL-16290 ..... N84-12996 #
LBL-16295 ..... N84-12861 #
LBL-16299 ..... N84-12738 #
LBL-16304 ..... N84-12392 #
LBL-16371 ..... N84-12865 #
LBL-16445 ..... N84-12749 #
LBL-16454 ..... N84-12993 #
LBL-16514 ..... N84-12276 #

LC-81-53073 ..... N84-12627 #
LC-82-600335 ..... N84-12577 #
LC-82-600545 ..... N84-12143 #
LC-83-1071 ..... N84-12625 #

LIDS-P-1249 ..... N84-12808 #

LPI-TR-83-01 ..... N84-13061* #
LPI-TR-83-02 ..... N84-13059* #
LPI-TR-83-02 ..... N84-13060* #

MBB-BB-543-83-OE ..... N84-12514 #

MLM-3085 ..... N84-12734 #

MMS-1523 ..... N84-12799 #

MPE-38 ..... N84-13035

MQAD-808 ..... N84-12283 #

MRC/SD-R-96 ..... N84-12339 #

MRDP-8297-1 ..... N84-12317 #

MSHA/IR-1131 ..... N84-12621 #

MSRR-492 ..... N84-12784 #

NADC-81104-60 ..... N84-12156 #

NAMRL-MONOGRAPH-30 ..... N84-12715 #

NAMRL-1290 ..... N84-12717 #
NAMRL-1291 ..... N84-12706 #
NAMRL-1292 ..... N84-12716 #
NAMRL-1293 ..... N84-12704 #
NAMRL-1295 ..... N84-12703 #
NAMRL-1298 ..... N84-12705 #

NAS 1.15:82548 ..... N84-12196* #
NAS 1.15:82553 ..... N84-12288* #
NAS 1.15:83492 ..... N84-12287* #
NAS 1.15:83508 ..... N84-12166* #
NAS 1.15:83510 ..... N84-12730* #
NAS 1.15:85049 ..... N84-13065* #
NAS 1.15:85053 ..... N84-12869* #
NAS 1.15:85109 ..... N84-12663* #

NAS 1.15:85111 ..... N84-12216* #
NAS 1.15:85112 ..... N84-13046* #
NAS 1.15:85116 ..... N84-13045* #
NAS 1.15:85117 ..... N84-12662* #
NAS 1.15:85119 ..... N84-13044* #
NAS 1.15:85434 ..... N84-13049* #
NAS 1.15:85435 ..... N84-13039* #
NAS 1.15:85475 ..... N84-13033* #
NAS 1.15:85476 ..... N84-12576* #
NAS 1.15:85706 ..... N84-12531* #
NAS 1.15:85711 ..... N84-12412* #
NAS 1.15:85714 ..... N84-12529* #
NAS 1.15:85851 ..... N84-12414* #
NAS 1.15:85861 ..... N84-12809* #
NAS 1.20:139 ..... N84-13036* #
NAS 1.21:7011(250) N84-12712*
NAS 1.21:7037(166) N84-12027*
NAS 1.21:7039(23) N84-13017*
NAS 1.21:7039(23) N84-13018*
NAS 1.26:3726 ..... N84-12090* #
NAS 1.26:3727 ..... N84-12091* #
NAS 1.26:3729 ..... N84-12530* #
NAS 1.26:168193 ..... N84-12226* #
NAS 1.26:168243-VOL-1 ..... N84-12264* #
NAS 1.26:168243-VOL-2 ..... N84-12265* #
NAS 1.26:168251 ..... N84-12312* #
NAS 1.26:168263 ..... N84-12411* #
NAS 1.26:168266 ..... N84-12227* #
NAS 1.26:168277 ..... N84-12225* #
NAS 1.26:170921 ..... N84-12495* #
NAS 1.26:170922 ..... N84-12248* #
NAS 1.26:170923 ..... N84-12413* #
NAS 1.26:170934 ..... N84-12415* #
NAS 1.26:170935 ..... N84-12213* #
NAS 1.26:170936 ..... N84-12311* #
NAS 1.26:170937 ..... N84-13066* #
NAS 1.26:170939 ..... N84-12634* #
NAS 1.26:171696 ..... N84-12557* #
NAS 1.26:171717 ..... N84-12725* #
NAS 1.26:172215 ..... N84-12526* #
NAS 1.26:172243 ..... N84-12192* #
NAS 1.26:172250 ..... N84-12777* #
NAS 1.26:172252 ..... N84-12742* #
NAS 1.26:172254 ..... N84-12778* #
NAS 1.26:173077 ..... N84-12336* #
NAS 1.26:174488 ..... N84-12732* #
NAS 1.26:174489 ..... N84-12832* #
NAS 1.26:174494 ..... N84-12096* #
NAS 1.26:174495 ..... N84-12527* #
NAS 1.26:174521 ..... N84-12555* #
NAS 1.26:174543 ..... N84-12556* #
NAS 1.26:174574 ..... N84-13057* #
NAS 1.26:174575 ..... N84-13058* #
NAS 1.26:174583 ..... N84-13061* #
NAS 1.26:174584 ..... N84-13059* #
NAS 1.26:174585 ..... N84-12028* #
NAS 1.26:174593 ..... N84-12462* #
NAS 1.26:174594 ..... N84-12664* #
NAS 1.26:174596 ..... N84-13056* #
NAS 1.26:174597 ..... N84-12257* #
NAS 1.26:174598 ..... N84-12223* #
NAS 1.26:174599 ..... N84-13064* #
NAS 1.26:174600 ..... N84-13060* #
NAS 1.26:174601 ..... N84-12217* #
NAS 1.26:174602 ..... N84-12263* #
NAS 1.55:2279 ..... N84-12029* #
NAS 1.55:2280 ..... N84-13067* #
NAS 1.55:2290 ..... N84-12228* #
NAS 1.60:2183 ..... N84-12190* #
NAS 1.60:2212 ..... N84-12164* #

NASA-ARC-11506-1 ..... N84-12313* #

NASA-CASE-ARC-11426-1 ..... N84-12193* #

NASA-CASE-FRC-11068-1 ..... N84-12443*

NASA-CASE-GSC-12619-1 ..... N84-12491*
NASA-CASE-GSC-12622-1 ..... N84-12492*

NASA-CASE-LAR-12615-1 ..... N84-12154*
NASA-CASE-LAR-12706-1 ..... N84-12444*
NASA-CASE-LAR-12882-1 ..... N84-12445*
NASA-CASE-LAR-12923-1 ..... N84-12493*
NASA-CASE-LAR-13255-1 ..... N84-12092* #

NASA-CASE-LEW-13914-1 ..... N84-12447* #

NASA-CASE-MFS-25631-1 ..... N84-12406*

NASA-CASE-NPO-15458-1 ..... N84-12262*
NASA-CASE-NPO-15811-1 ..... N84-12968* #
NASA-CASE-NPO-15903-1 ..... N84-12635* #
NASA-CASE-NPO-15928-1 ..... N84-12289* #
NASA-CASE-NPO-16112-1 ..... N84-12463* #
NASA-CASE-NPO-16171-1-CU ..... N84-12151* #

NASA-CASE-NSTL-10 ..... N84-12654*

NASA-CP-2279 ..... N84-12029* #
NASA-CP-2280 ..... N84-13067* #
NASA-CP-2290 ..... N84-12228* #

NASA-CR-3726 ..... N84-12090* #
NASA-CR-3727 ..... N84-12091* #
NASA-CR-3729 ..... N84-12530* #
NASA-CR-168193 ..... N84-12226* #
NASA-CR-168243-VOL-1 ..... N84-12264* #
NASA-CR-168243-VOL-2 ..... N84-12265* #
NASA-CR-168251 ..... N84-12312* #
NASA-CR-168263 ..... N84-12411* #
NASA-CR-168266 ..... N84-12227* #
NASA-CR-168277 ..... N84-12225* #
NASA-CR-170921 ..... N84-12495* #
NASA-CR-170922 ..... N84-12248* #
NASA-CR-170923 ..... N84-12413* #
NASA-CR-170934 ..... N84-12415* #
NASA-CR-170935 ..... N84-12213* #
NASA-CR-170936 ..... N84-12311* #
NASA-CR-170937 ..... N84-13066* #
NASA-CR-170939 ..... N84-12634* #
NASA-CR-171696 ..... N84-12557* #
NASA-CR-171717 ..... N84-12725* #
NASA-CR-172215 ..... N84-12526* #
NASA-CR-172243 ..... N84-12192* #
NASA-CR-172250 ..... N84-12777* #
NASA-CR-172252 ..... N84-12742* #
NASA-CR-172254 ..... N84-12778* #
NASA-CR-173077 ..... N84-12336* #
NASA-CR-174488 ..... N84-12732* #
NASA-CR-174489 ..... N84-12832* #
NASA-CR-174490 ..... N84-12727* #
NASA-CR-174494 ..... N84-12096* #
NASA-CR-174495 ..... N84-12527* #
NASA-CR-174521 ..... N84-12555* #
NASA-CR-174543 ..... N84-12556* #
NASA-CR-174574 ..... N84-13057* #
NASA-CR-174575 ..... N84-13058* #
NASA-CR-174583 ..... N84-13061* #
NASA-CR-174584 ..... N84-13059* #
NASA-CR-174585 ..... N84-12028* #
NASA-CR-174593 ..... N84-12462* #
NASA-CR-174594 ..... N84-12664* #
NASA-CR-174596 ..... N84-13056* #
NASA-CR-174597 ..... N84-12257* #
NASA-CR-174598 ..... N84-12223* #
NASA-CR-174599 ..... N84-13064* #
NASA-CR-174600 ..... N84-13060* #
NASA-CR-174601 ..... N84-12217* #
NASA-CR-174602 ..... N84-12263* #

NASA-FACTS-139 ..... N84-13036* #

NASA-SP-7011(250) N84-12712*
NASA-SP-7037(166) N84-12027*
NASA-SP-7039(23) N84-13017*
NASA-SP-7039(23) N84-13018*

NASA-TM-82548 ..... N84-12196* #
NASA-TM-82553 ..... N84-12288* #
NASA-TM-83492 ..... N84-12287* #
NASA-TM-83508 ..... N84-12166* #
NASA-TM-83510 ..... N84-12730* #
NASA-TM-85049 ..... N84-13065* #
NASA-TM-85053 ..... N84-12869* #
NASA-TM-85109 ..... N84-12663* #
NASA-TM-85111 ..... N84-12216* #
NASA-TM-85112 ..... N84-13046* #
NASA-TM-85116 ..... N84-13045* #
NASA-TM-85117 ..... N84-12662* #
NASA-TM-85119 ..... N84-13044* #
NASA-TM-85434 ..... N84-13049* #
NASA-TM-85435 ..... N84-13039* #
NASA-TM-85475 ..... N84-13033* #
NASA-TM-85476 ..... N84-12576* #
NASA-TM-85706 ..... N84-12531* #
NASA-TM-85711 ..... N84-12412* #
NASA-TM-85714 ..... N84-12529* #
NASA-TM-85851 ..... N84-12414* #
NASA-TM-85861 ..... N84-12809* #

NASA-TP-2183 ..... N84-12190* #
NASA-TP-2212 ..... N84-12164* #

NASA-WLP-10055-2 ..... N84-12448* #

NBS-GCR-83-438 ..... N84-13026 #

NBSIR-83-2719-2 ..... N84-12405 #
NBSIR-83-2723 ..... N84-12332 #
NBSIR-83-2741 ..... N84-12517 #

NLM-MED-83-02-REV ..... N84-13029 #
NLM-MED-83-03 ..... N84-13028 #
NLM-MED-83-04 ..... N84-13027 #

NLR-TR-81074-U ..... N84-12433 #
NLR-TR-81078-U ..... N84-12434 #
NLR-TR-82012-U ..... N84-12098 #

NOAA-NWS-CRCP-9 ..... N84-12757 #

NOAA-TM-ERL-AOML-54 ..... N84-12700 #

NOAA-TM-NWS-WR-177-REV ..... N84-12699 #

NOAA-83072201 ..... N84-12631 #
NOAA-83072601 ..... N84-12757 #
NOAA-83080101 ..... N84-12632 #
NOAA-83081107 ..... N84-12700 #

NOSC/TD-587 ..... N84-12685 #

NOSC/TR-839 ..... N84-12349 #

NPL-DITC-27/83 ..... N84-12739
NPL-DITC-28/83 ..... N84-12740

NPL-DMA(A)68 ..... N84-12526

NPS52-83-009 ..... N84-12747 #
NPS54-83-008 ..... N84-12722 #

NRC/CNR-TT-2064 ..... N84-12578 #

NRL-MR-5138 ..... N84-12829 #
NRL-MR-5145 ..... N84-12342 #

NRL-8695 ..... N84-12821 #
NRL-8713 ..... N84-12345 #

NR092-549-TR27 ..... N84-12833 #

NSF-ISP-83004 ..... N84-13016 #

NSMRL-MR-83-4 ..... N84-13021 #

NSWC-MP-83-116 ..... N84-12325 #

NSWC/TR-82-436 ..... N84-12419 #

NTIA-SP-83-15 ..... N84-12366 #

NTIA/REPT-83-120 ..... N84-12364 #
NTIA/REPT-83-121 ..... N84-12365 #

NTSB/SR-83/01 ..... N84-12142 #

NUSC-TD-6947 ..... N84-12820 #

ORAU/IEA-82-10(M) ..... N84-12626 #

ORNL-TM-8801 ..... N84-12626 #

ORNL/CDIC-1 ..... N84-12657 #

ORNL/TM-8707 ..... N84-12956 #
ORNL/TM-8728 ..... N84-12542 #
ORNL/TM-8770 ..... N84-12952 #

OSD/FSTC-83/176 ..... N84-12762 #
OSD/FSTC-83/180 ..... N84-12763 #
OSD/FSTC-83/186 ..... N84-12758 #
OSD/FSTC-83/187 ..... N84-12759 #
OSD/FSTC-83/188 ..... N84-12760 #
OSD/FSTC-83/200 ..... N84-12761 #
OSD/FSTC-83/202 ..... N84-12764 #
OSD/FSTC-83/203 ..... N84-12765 #
OSD/FSTC-83/205 ..... N84-12766 #

OSU/DGSS-345 ..... N84-12669 #

OTA-STI-175 ..... N84-12143 #

OWRT-A-030-WYO(1) ..... N84-12633 #

OWRT-C-10004-S(1449)(1) ..... N84-12284 #

PB83-222703 ..... N84-12332 #
PB83-223156 ..... N84-13029 #
PB83-223164 ..... N84-13028 #
PB83-233726 ..... N84-12460 #
PB83-234781 ..... N84-13027 #
PB83-234922 ..... N84-12461 #
PB83-235564 ..... N84-12506 #
PB83-236919 ..... N84-12518 #
PB83-237107 ..... N84-13016 #
PB83-238345 ..... N84-12365 #
PB83-238600 ..... N84-12766 #
PB83-239053 ..... N84-12333 #
PB83-239103 ..... N84-12631 #
PB83-239459 ..... N84-12507 #
PB83-239574 ..... N84-12517 #
PB83-239624 ..... N84-12757 #
PB83-241141 ..... N84-12364 #
PB83-241158 ..... N84-12405 #
PB83-241471 ..... N84-12366 #
PB83-241521 ..... N84-12758 #
PB83-241539 ..... N84-12759 #
PB83-241547 ..... N84-12760 #
PB83-241588 ..... N84-12761 #
PB83-242230 ..... N84-13026 #
PB83-242271 ..... N84-12632 #
PB83-243147 ..... N84-12633 #
PB83-243170 ..... N84-12284 #
PB83-243394 ..... N84-12711 #
PB83-243410 ..... N84-12762 #
PB83-243428 ..... N84-12763 #
PB83-243626 ..... N84-12334 #
PB83-244012 ..... N84-12328 #
PB83-246801 ..... N84-12699 #
PB83-247734 ..... N84-12764 #
PB83-247742 ..... N84-12765 #
PB83-248773 ..... N84-12700 #
PB83-249441 ..... N84-13008 #
PB83-249490 ..... N84-12329 #
PB83-254912 ..... N84-12677 #
PB83-917004 ..... N84-12142 #

PFC/RR-83-7 ..... N84-12937 #
PFC/RR-83-19 ..... N84-12950 #
PFC/RR-83-20 ..... N84-12817 #

PNL-SA-10382 ..... N84-13014 #
PNL-SA-10670 ..... N84-12655 #
PNL-SA-10923 ..... N84-12321 #
PNL-SA-11132 ..... N84-12643 #
PNL-SA-11167 ..... N84-12804 #
PNL-SA-11188 ..... N84-12694 #
PNL-SA-11354 ..... N84-12649 #
PNL-SA-11551 ..... N84-12803 #

PNL-4001-3 ..... N84-12926 #
PNL-4785 ..... N84-12693 #

POLY-MRI-1425-82 ..... N84-12464 #

PWA-5777-29 ..... N84-12312* #

P83-10209 ..... N84-12214* #

RADC-TR-82-274 ..... N84-12347 #
RADC-TR-83-120 ..... N84-13022 #
RADC-TR-83-131 ..... N84-12893 #

RAE-MAT/STRUCT-29 ..... N84-12310

RAE-TM-FS(F)-514 ..... N84-12089

RAE-TR-83009 ..... N84-12310

REPT-2-55110/2R-53299 ..... N84-12096* #
REPT-5 ..... N84-13025 #
REPT-5WW-TN-79/001 ..... N84-12689 #
REPT-5WW-TN-83/001 ..... N84-12689 #
REPT-81.4 ..... N84-12494
REPT-82.8 ..... N84-12410
REPT-82-2 ..... N84-12269 #
REPT-83-147 ..... N84-12964 #
REPT-115-12A ..... N84-12333 #
REPT-214 ..... N84-12681 #
REPT-1842-EEG/EEIT-TR-16-EZ ..... N84-12341 #
REPT-38172-6001-UE-00 ..... N84-12634* #

RFP-3500 ..... N84-12767 #

RR-82-2-ONR ..... N84-12721 #
RR-83-SM-9 ..... N84-12536 #
RR-83-SM-10 ..... N84-12786 #
RR-222 ..... N84-12795 #

RSRE-3582 ..... N84-12378
RSRE-3583 ..... N84-12729
RSRE-3585 ..... N84-12741
RSRE-3597 ..... N84-12379

R83-912666-58 ..... N84-12090* #
R83-912666-58 ..... N84-12091* #
R83-956152-10 ..... N84-12225* #

SAI-02383-468LJ ..... N84-12953 #

SAM-TR-83-14 ..... N84-12423 #
SAM-TR-83-30 ..... N84-12707 #
SAND-80-2689-REV-1 ..... N84-12459 #
SAND-82-0002 ..... N84-12428 #
SAND-82-1778C ..... N84-12293 #
SAND-82-1864C ..... N84-12278 #
SAND-82-2237C ..... N84-12316 #
SAND-82-2300C ..... N84-12457 #
SAND-82-2534C ..... N84-12537 #
SAND-82-2983C ..... N84-12980 #
SAND-83-0115C ..... N84-12966 #
SAND-83-0142C ..... N84-12543 #
SAND-83-0228C ..... N84-12385 #
SAND-83-0260C ..... N84-12402 #
SAND-83-0412C ..... N84-12400 #
SAND-83-0462C ..... N84-12424 #
SAND-83-0575C ..... N84-12945 #
SAND-83-0576C ..... N84-12986 #
SAND-83-0611C ..... N84-12942 #
SAND-83-0612C ..... N84-12943 #
SAND-83-0617C ..... N84-12857 #
SAND-83-0620C ..... N84-12941 #
SAND-83-0637 ..... N84-12735 #
SAND-83-0665C ..... N84-12503 #
SAND-83-0912C ..... N84-12901 #
SAND-83-0941C ..... N84-12962 #
SAND-83-1046C ..... N84-12996 #
SAND-83-1065C ..... N84-13039* #
SAND-83-1148C ..... N84-12544 #
SAND-83-1230 ..... N84-12994 #
SAND-83-1265 ..... N84-12753 #
SAND-83-1273C ..... N84-12322 #
SAND-83-1316C ..... N84-12858 #
SAND-83-1341C ..... N84-12921 #
SAND-83-1381C ..... N84-12296 #
SAND-83-1769C ..... N84-12393 #
SAND-83-1902C ..... N84-12823 #
SAND-83-1992C ..... N84-12944 #
SAND-83-2917C ..... N84-12308 #
SAND-83-7029 ..... N84-12097 #
SAND-83-7091C ..... N84-12403 #
SAND-83-8025 ..... N84-12458 #
SAND-83-8225 ..... N84-12429 #
SAND-83-8226 ..... N84-12431 #

SAR-44 ..... N84-12257* #

SAS-TR-81-03 ..... N84-12666 #

SATR-3 ..... N84-12352 #

SCIENTIFIC-1 ..... N84-12452 #

SDL-82-2188-14F ..... N84-12340 #

SEAL-3-83 ..... N84-12495* #

SER-A-97 ..... N84-12661

SER-C-274 ..... N84-12554

SERI/SP-281-1847 ..... N84-12650 #

SERI/STR-254-1848 ..... N84-12647 #

SERI/TP-234-2080 ..... N84-12644 #
SERI/TP-254-2027 ..... N84-13128 #
SERI/TP-255-2054 ..... N84-12641 #

SERI/TR-215-1824 ..... N84-12622 #
SERI/TR-254-1703 ..... N84-13127 #

SLAC-PUB-3163 ..... N84-12854 #

SLAC-259 ..... N84-12878 #

SN-54 ..... N84-12248* #

SOL-83-7 ..... N84-12752 #
SOL-83-12 ..... N84-12751 #

SR-1 ..... N84-12453 #
SR-1 ..... N84-12670 #
SR-1 ..... N84-12785 #
SR-2 ..... N84-12210 #
SR-3 ..... N84-12669 #

SRL-83-12 ..... N84-13064* #

SU-DMS-83-R-4 ..... N84-12969 #

SU-GL-3598 ..... N84-12470 #

SU-SLAC-PUB-3056 ..... N84-12840 #
SU-SLAC-PUB-3062 ..... N84-12842 #
SU-SLAC-PUB-3121 ..... N84-12868 #
SU-SLAC-PUB-3146 ..... N84-12850 #
SU-SLAC-PUB-3147 ..... N84-12849 #

SU-SLAC-PUB-3176 ..... N84-12489 #
SU-SLAC-PUB-3187 ..... N84-12879 #

SU-STAN-CS-82-956 ..... N84-12770 #

SU-STAN-HPP-82-20 ..... N84-12770 #

SU-TR-324 ..... N84-12801 #
SU-TR-406 ..... N84-12773 #

TM-SM-83-12 ..... N84-12217* #

TOP-6-2-013 ..... N84-12165 #

TR-1 ..... N84-12250 #
TR-1 ..... N84-12315 #
TR-29 ..... N84-12314 #
TR-29 ..... N84-12796 #
TR-30 ..... N84-12782 #
TR-34 ..... N84-12258 #
TR-58 ..... N84-12786 #
TR-59 ..... N84-12536 #
TR-82-39 ..... N84-12787 #
TR-113-9 ..... N84-12807 #
TR-142 ..... N84-12350 #

TT-60 ..... N84-12343 #
TT-8302 ..... N84-12779 #

TWR-13009 ..... N84-12311* #

U-OF-IOWA-83-23 ..... N84-12832* #

UCID-19788 ..... N84-12473 #
UCID-19832 ..... N84-12646 #
UCID-19839 ..... N84-12848 #
UCID-19852 ..... N84-12960 #
UCID-19890 ..... N84-12253 #
UCID-30196 ..... N84-12750 #

UCLA-34P278-39 ..... N84-12487 #

UCRL-15538 ..... N84-12475 #
UCRL-50007-82 ..... N84-12883 #
UCRL-53434 ..... N84-12482 #
UCRL-88178 ..... N84-12272 #
UCRL-88647 ..... N84-12841 #
UCRL-88682-REV-1 ..... N84-12478 #
UCRL-88696 ..... N84-12988 #
UCRL-88800 ..... N84-12816 #
UCRL-88811 ..... N84-12397 #
UCRL-88824-REV-1 ..... N84-12985 #
UCRL-88916 ..... N84-12946 #
UCRL-88919 ..... N84-12298 #
UCRL-88963 ..... N84-12326 #
UCRL-89026 ..... N84-12899 #
UCRL-89097 ..... N84-12472 #
UCRL-89157 ..... N84-12789 #
UCRL-89200 ..... N84-12932 #
UCRL-89266 ..... N84-12955 #
UCRL-89296 ..... N84-12939 #
UCRL-89364 ..... N84-12991 #
UCRL-89432 ..... N84-13013 #
UCRL-89444 ..... N84-12390 #
UCRL-89538 ..... N84-12933 #
UCRL-89541 ..... N84-12476 #
UCRL-89549 ..... N84-12983 #
UCRL-89674 ..... N84-12900 #
UCRL-89750 ..... N84-12486 #
UCRL-89767 ..... N84-12940 #
UCRL-89769 ..... N84-12954 #
UCRL-89771 ..... N84-12948 #

UDR-TR-82-25-PT-4 ..... N84-12159 #
UDR-TR-83-19 ..... N84-12290 #
UDR-TR-83-20 ..... N84-12161 #
UDR-TR-83-25-PT-1 ..... N84-12158 #
UDR-TR-83-25-PT-2 ..... N84-12157 #

UILU-ENG-83-2503 ..... N84-12664* #

UIO-AR-83-05 ..... N84-12674 #

UNC/ORSA/TR-83/2 ..... N84-12800 #

US-PATENT-APPL-SN-210498 ..... N84-12444*
US-PATENT-APPL-SN-225499 ..... N84-12491*
US-PATENT-APPL-SN-243684 ..... N84-12492*
US-PATENT-APPL-SN-263829 ..... N84-12154*
US-PATENT-APPL-SN-267179 ..... N84-12445*
US-PATENT-APPL-SN-308203 ..... N84-12406*
US-PATENT-APPL-SN-322314 ..... N84-12443*
US-PATENT-APPL-SN-335036 ..... N84-12654*
US-PATENT-APPL-SN-376306 ..... N84-12262*
US-PATENT-APPL-SN-383063 ..... N84-12493*
US-PATENT-APPL-SN-522629 ..... N84-12313* #
US-PATENT-APPL-SN-526741 ..... N84-12193* #
US-PATENT-APPL-SN-526770 ..... N84-12448* #
US-PATENT-APPL-SN-537615 ..... N84-12447* #
US-PATENT-APPL-SN-537616 ..... N84-12289* #
US-PATENT-APPL-SN-542232 ..... N84-12463* #
US-PATENT-APPL-SN-547171 ..... N84-12635* #
US-PATENT-APPL-SN-547175 ..... N84-12968* #
US-PATENT-APPL-SN-550681 ..... N84-12092* #
US-PATENT-APPL-SN-551536 ..... N84-12151* #

US-PATENT-CLASS-47-58 ..... N84-12654*
US-PATENT-CLASS-73-646 ..... N84-12445*
US-PATENT-CLASS-73-658 ..... N84-12445*
US-PATENT-CLASS-101-407BP N84-12491*
US-PATENT-CLASS-156-71 ..... N84-12443*
US-PATENT-CLASS-156-215 ..... N84-12443*
US-PATENT-CLASS-156-230 ..... N84-12443*
US-PATENT-CLASS-156-235 ..... N84-12443*
US-PATENT-CLASS-156-294 ..... N84-12443*
US-PATENT-CLASS-156-391 ..... N84-12443*
US-PATENT-CLASS-156-423 ..... N84-12443*
US-PATENT-CLASS-156-540 ..... N84-12443*
US-PATENT-CLASS-204-DIG.3 ..... N84-12262*
US-PATENT-CLASS-204-129 ..... N84-12262*
US-PATENT-CLASS-204-242 ..... N84-12262*
US-PATENT-CLASS-204-278 ..... N84-12262*
US-PATENT-CLASS-204-290R N84-12262*
US-PATENT-CLASS-210-151 ..... N84-12654*
US-PATENT-CLASS-210-602 ..... N84-12654*
US-PATENT-CLASS-210-605 ..... N84-12654*
US-PATENT-CLASS-210-617 ..... N84-12654*
US-PATENT-CLASS-239-426 ..... N84-12406*
US-PATENT-CLASS-244-13 ..... N84-12154*
US-PATENT-CLASS-244-45R N84-12154*
US-PATENT-CLASS-244-53R N84-12154*
US-PATENT-CLASS-244-55 ..... N84-12154*
US-PATENT-CLASS-244-91 ..... N84-12154*
US-PATENT-CLASS-269-3 ..... N84-12491*
US-PATENT-CLASS-308-2A N84-12492*
US-PATENT-CLASS-324-250 ..... N84-12444*
US-PATENT-CLASS-328-230 ..... N84-12444*
US-PATENT-CLASS-338-2 ..... N84-12443*
US-PATENT-CLASS-364-415 ..... N84-12445*
US-PATENT-CLASS-372-74 ..... N84-12444*
US-PATENT-CLASS-416-117 ..... N84-12493*
US-PATENT-CLASS-416-132B N84-12493*
US-PATENT-CLASS-427-443.2 ..... N84-12262*
US-PATENT-CLASS-429-111 ..... N84-12262*

US-PATENT-4,393,777 ..... N84-12491*
US-PATENT-4,405,184 ..... N84-12492*
US-PATENT-4,407,686 ..... N84-12443*
US-PATENT-4,413,522 ..... N84-12445*
US-PATENT-4,413,784 ..... N84-12406*
US-PATENT-4,414,080 ..... N84-12262*
US-PATENT-4,414,509 ..... N84-12444*
US-PATENT-4,415,133 ..... N84-12154*
US-PATENT-4,415,311 ..... N84-12493*
US-PATENT-4,415,450 ..... N84-12654*

USAARL-83-12 ..... N84-12714 #

USARIEM-M-42/83 ..... N84-12708 #

USARIEM-M41/83 ..... N84-12719 #

USARIEM-T-1/83 ..... N84-12726 #

USASC-TR-83-7 ..... N84-12137 #

USFS-CIRC-884 ..... N84-12623 #

USGS-CIRC-886 ..... N84-12577 #

USGS-474-11 ..... N84-12673 #

UTIAS-TN-244 ..... N84-12416 #

UTIAS-269 ..... N84-12828 #

UTRC83-6 ..... N84-12530* #

WES/MP/HL-83-5 ..... N84-12688 #

WHOI-TR-83-20 ..... N84-12632 #

WMO-134 ..... N84-12697 #

WP-69-82-83 ..... N84-12784 #

WU/SRL-59583-1 ..... N84-12974 #

W83-03675 ..... N84-12633 #
W83-03678 ..... N84-12284 #

Y/DV-203 ..... N84-12295 #

05423-F ..... N84-12466 #

U.S. GOVERNMENT PRINTING OFFICE: 1984—421-564/403

PUBLIC COLLECTIONS OF NASA DOCUMENTS

DOMESTIC

NASA distributes its technical documents and bibliographic tools to eleven special libraries located in the organizations listed below. Each library is prepared to furnish the public such services as reference assistance, interlibrary loans, photocopy service, and assistance in obtaining copies of NASA documents for retention.

CALIFORNIA
University of California, Berkeley
COLORADO
University of Colorado, Boulder
DISTRICT OF COLUMBIA
Library of Congress
GEORGIA
Georgia Institute of Technology, Atlanta
ILLINOIS
The John Crerar Library, Chicago
MASSACHUSETTS
Massachusetts Institute of Technology, Cambridge
MISSOURI
Linda Hall Library, Kansas City
NEW YORK
Columbia University, New York
OKLAHOMA
University of Oklahoma, Bizzell Library
PENNSYLVANIA
Carnegie Library of Pittsburgh
WASHINGTON
University of Washington, Seattle

NASA publications (those indicated by an '*' following the accession number) are also received by the following public and free libraries:

CALIFORNIA
Los Angeles Public Library
San Diego Public Library
COLORADO
Denver Public Library
CONNECTICUT
Hartford Public Library
MARYLAND
Enoch Pratt Free Library, Baltimore
MASSACHUSETTS
Boston Public Library
MICHIGAN
Detroit Public Library
MINNESOTA
Minneapolis Public Library and Information Center
NEW JERSEY
Trenton Public Library
NEW YORK
Brooklyn Public Library
Buffalo and Erie County Public Library
Rochester Public Library
New York Public Library
OHIO
Akron Public Library
Cincinnati and Hamilton County Public Library
Cleveland Public Library
Dayton Public Library
Toledo and Lucas County Public Library
TEXAS
Dallas Public Library
Fort Worth Public Library
WASHINGTON
Seattle Public Library
WISCONSIN
Milwaukee Public Library

An extensive collection of NASA and NASA-sponsored documents and aerospace publications available to the public for reference purposes is maintained by the American Institute of Aeronautics and Astronautics, Technical Information Service, 555 West 57th Street, 12th Floor, New York, New York 10019.

EUROPEAN

An extensive collection of NASA and NASA-sponsored publications is maintained by the British Library Lending Division, Boston Spa, Wetherby, Yorkshire, England. By virtue of arrangements other than with NASA, the British Library Lending Division also has available many of the non-NASA publications cited in *STAR*. European requesters may purchase facsimile copy of microfiche of NASA and NASA-sponsored documents, those identified by both the symbols '#' and '*', from: ESA - Information Retrieval Service, European Space Agency, 8-10 rue Mario-Nikis, 75738 Paris CEDEX 15, France.

National Aeronautics and
Space Administration

Washington, D.C.
20546

Official Business
Penalty for Private Use, $300

SPECIAL FOURTH CLASS MAIL
Book

Postage and Fees Paid
National Aeronautics and
Space Administration
NASA-451

10 1 STAR, 840216 S01733HU
UNIV OF MICHIGAN
HARLAN HATCHER LIBRARY
DOCUMENTS UNIT SERIALS DIV
ANN ARBOR MI 48109

OSTMASTER: If Undeliverable (Section 158
Postal Manual) Do Not Return